

## ATTACHMENT 1

### CHANNEL DESIGNS AND CROSS-SECTIONS

[illegible]

U. S. ARMY ENGINEER DISTRICT NEW YORK <a href="http://www.nan.usace.army.mil">http://www.nan.usace.army.mil</a>	DESIGNED BY: GSW		DATE:
	DWN BY: GSW	ODD BY:	SOLICITATION NO.:
CIVIL RESOURCES BRANCH ECOSYSTEM RESTORATION TEAM CEMAN-ENH	SUBMITTED BY: GSW		CONTRACT NO.:
	FILE NAME:		
	SIZE: ANSI D	PLOTTED BY:	PLT DATE: 9/19/2020

HUDSON RIVER CHANNEL  
IMPROVEMENTS PROJECT

AMBROSE CHANNEL

NEW YORK & NEW JERSEY HARBOR, USA

SHEET  
REFERENCE  
NUMBER



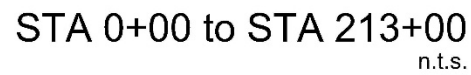
MAY 2009 NYD BORDER



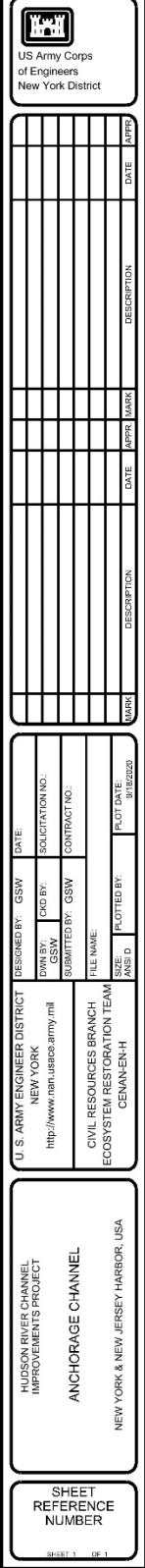
ALL DIMENSIONS/EXISTING CONDITIONS SHOWN SHALL BE CHECKED AND VERIFIED BY THE CONTRACTOR AT THE SITE. ANY DISCREPANCIES SHALL BE IMMEDIATELY REPORTED TO THE GOVERNMENT FOR CLARIFICATIONS. DRAWING SHALL NOT BE SCALED TO OBTAIN DIMENSIONS OR DISTANCES.

SHEET  
REFERENCE  
NUMBER

MAY 2009 NYD BORDER



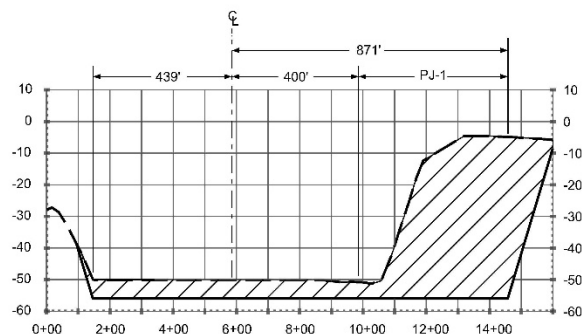
ALL DIMENSIONS/EXISTING CONDITIONS SHOWN SHALL BE CHECKED AND VERIFIED BY THE CONTRACTOR AT THE SITE. ANY DISCREPANCIES SHALL BE IMMEDIATELY REPORTED TO THE GOVERNMENT FOR CLARIFICATIONS. DRAWING SHALL NOT BE SCALED TO OBTAIN DIMENSIONS OR DISTANCES.



A

WARNING: THIS DOCUMENT MAY CONTAIN SENSITIVE SECURITY INFORMATION AND THEREFORE MUST BE TREATED AS A CONFIDENTIAL DOCUMENT. THE INFORMATION CONTAINED IN THIS DOCUMENT MUST BE MAINTAINED IN A CONFIDENTIAL MANNER TO PREVENT COMPROMISING HOMELAND SECURITY AS PROVIDED IN SECTION 214 OF THE HOMELAND SECURITY ACT OF 2002. NO PART OF THIS DOCUMENT SHALL BE REPRODUCED, RELEASED OR DISTRIBUTED WITHOUT THE EXPRESS WRITTEN PERMISSION OF THE UNITED STATES ARMY CORPS OF ENGINEERS, NEW YORK DISTRICT (USACE - NYD). UNAUTHORIZED REPRODUCTION, RELEASE OR DISTRIBUTION MAY RESULT IN CIVIL PENALTY OR OTHER ACTION BY USACE-NYD.

ALL DIMENSIONS/EXISTING CONDITIONS SHOWN SHALL BE CHECKED AND VERIFIED BY THE CONTRACTOR AT THE SITE, ANY DISCREPANCIES SHALL BE IMMEDIATELY REPORTED TO THE GOVERNMENT FOR CLARIFICATIONS. DRAWING SHALL NOT BE SCALED TO OBTAIN DIMENSIONS OR DISTANCES.



Typical Cross-Section  
STA 23+00

150 ft between PVSC  $\phi$  and approximate edge of excavation

(Stability of pipe to be more thoroughly examined during PED phase.)

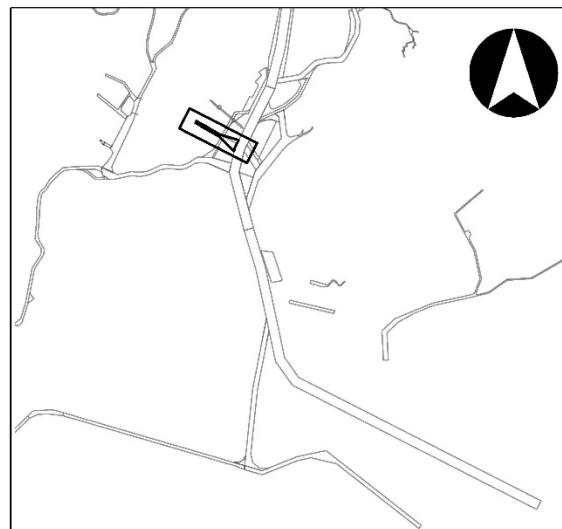
Channel to the west of PVSC pipe will not be deepened

Location of PVSC sewer main (n.t.s.)

- Proposed channel toe

- Existing channel toe

Areas to  
be excavated



US Army Corps  
of Engineers  
New York District

[illegible]

U. S. ARMY ENGINEER DISTRICT NEW YORK <a href="http://www.nan.usace.army.mil">http://www.nan.usace.army.mil</a>	DESIGNED BY: GSW		DATE:
	DRAWN BY: GSW	CHK BY:	SOLICITATION NO.:
CIVIL RESOURCES BRANCH ECOSYSTEM RESTORATION TEAM CENAN-ENH	SUBMITTED BY: GSW		CONTRACT NO.:
	FILE NAME:		
	DATE:	SIZE:	PLOT DATE:
	ANSI:	INCHES:	INCHES:

HUDSON RIVER CHANNEL  
IMPROVEMENTS PROJECT

PORT JERSEY CHANNEL

NEW YORK & NEW JERSEY HARBOR, L

SHEET  
REFERENCE  
NUMBER

SHEET 1 OF 1

MAY 2009 NYD BORDER



A

ALL DIMENSIONS/EXISTING CONDITIONS SHOWN SHALL BE CHECKED AND VERIFIED BY THE CONTRACTOR AT THE SITE. ANY DISCREPANCIES SHALL BE IMMEDIATELY REPORTED TO THE GOVERNMENT FOR CLARIFICATIONS. DRAWING SHALL NOT BE SCALED TO OBTAIN DIMENSIONS OR DISTANCES.



US Army Corps  
of Engineers  
New York District

[illegible]

U.S. ARMY ENGINEER DISTRICT NEW YORK http://www.nian.usace.army.mil	DESIGNED BY:	GSW	DATE:
	OWN BY:	GSW	SOLICITATION NO.:
	SUBMITTED BY:	GSW	CONTRACT NO.:
CIVIL RESOURCES BRANCH ECOSYSTEM RESTORATION TEAM CENAN-ENH	FILE NAME:		
	SIZE 405 D	PLOTTED BY:	PLOT DATE 5/13/2020

HUDSON RIVER CHANNEL  
IMPROVEMENTS PROJECT

KILL VAN KULL CHANNEL

NEW YORK & NEW JERSEY HARBOR, USA

**SHEET  
REFERENCE  
NUMBER**

MAY 2009 NYD BORDER



A

ALL DIMENSIONS/EXISTING CONDITIONS SHOWN SHALL BE CHECKED AND VERIFIED BY THE CONTRACTOR AT THE SITE. ANY DISCREPANCIES SHALL BE IMMEDIATELY REPORTED TO THE GOVERNMENT FOR CLARIFICATIONS. DRAWING SHALL NOT BE SCALED TO OBTAIN DIMENSIONS OR DISTANCES.

ALL DIMENSIONS/EXISTING CONDITIONS SHOWN SHALL BE CHECKED AND VERIFIED BY THE CONTRACTOR AT THE SITE. ANY DISCREPANCIES SHALL BE IMMEDIATELY REPORTED TO THE GOVERNMENT FOR CLARIFICATIONS. DRAWING SHALL NOT BE SCALED TO OBTAIN DIMENSIONS OR DISTANCES.

[illegible]

HUDSON RIVER CHANNEL  
IMPROVEMENTS PROJECT

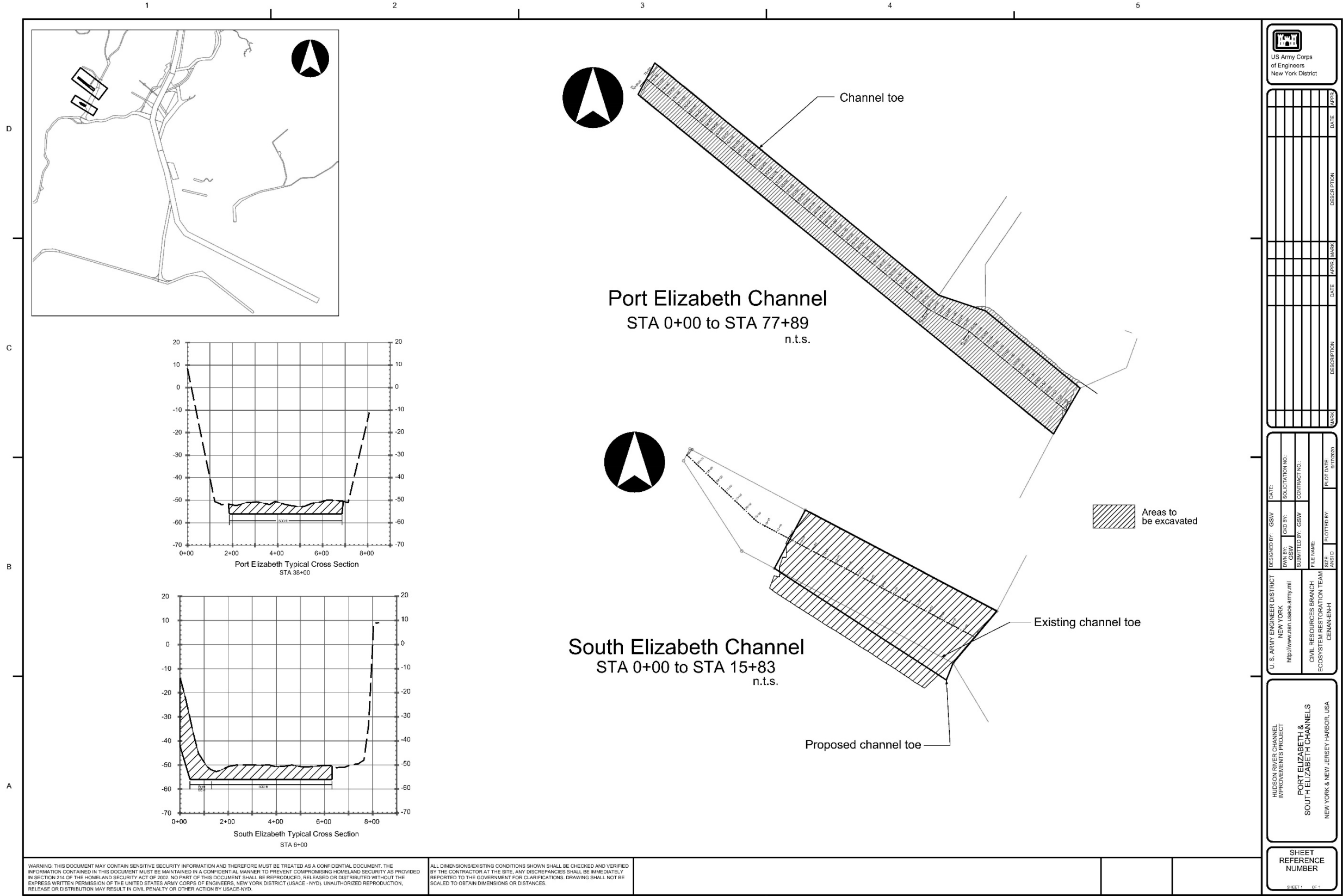
NEWARK BAY CHANNEL

NEW YORK & NEW JERSEY HARBOR, USA

**SHEET  
REFERENCE  
NUMBER**

D:\Telework coronavirus\Harbor\MicroStation\IDGN\Harbor\_final\_qtlys\_4-ft\_27Jul2020.dgn  
D:\Telework coronavirus\Harbor\MicroStation\Final Volumes\Pen Tables\NWK\_4ft.tbl

MAY 2009 NYO BORDER



THIS PAGE INTENTIONALLY  
LEFT BLANK

## ATTACHMENT 2

### PRELIMINARY QUANTITIES



Ambrose Channel

Total excavation volumes from MLLW=0 to the depth  
indicated

Channel Segment	Station		54 ft Volume (cy)	56 ft Volume (cy)	58 ft Volume (cy)	60 ft Volume (cy)
A	0	5000	-	-	-	-
B	5000	10000	-	-	-	-
C	10000	15000	-	40,901	258,688	601,183
D	15000	20000	1,502	163,862	734,028	1,408,763
E	20000	25000	10,923	51,373	178,724	397,140
F	25000	30000	90	13,653	93,524	279,229
G	30000	35000	829	10,165	47,180	118,427
H	35000	40000	67,883	104,272	164,970	254,424
I	40000	45000	98,438	133,075	176,633	230,799
J	45000	50000	-	-	848	2,781
K	50000	55000	4,216	37,430	207,593	491,950
L	55000	60000	17,522	147,649	515,009	1,018,791
M	60000	65000	16,811	280,834	935,792	1,699,169
N	65000	70000	86,984	252,249	996,910	1,762,902
O	70000	75000	442	79,261	747,414	1,505,023
P	75000	80000	3,187	21,252	123,288	332,222
Q	80000	85000	15,379	52,137	140,583	277,871
R	85000	90000	-	1,633	6,105	13,332
Total			324,207	1,389,742	5,327,290	10,394,005

54.0 ft is average as-built-elevation

### Volume above Grade

[illegible]

						Volume above Grade (cumulative)					
Channel	Reach	Reach-specific Geotech Notes	Design Depth	Total Area above Grade (ac)		Total	Contaminated sediment (non-HARS)	Non-contaminated sediment	Moderately hard Rock	Harder rock	Hardest rock
				SQ FT	ACRES						
ANCHORAGE	Anchorage A	Homgenous, Sand	52'	2,384,010	55	155,862		155,862			
			54'	4,828,752	111	319,326		319,326			
			56'	6,271,614	144	677,866		677,866			
			58'	10,419,552	239	1,148,042		1,148,042			
			60'	10,018,800	230	1,733,763		1,733,763			
	Anchorage B	Homgenous, Sand	52'	10,099,289	232	293,035		293,035			
			54'	12,617,525	290	986,034		986,034			
			56'	13,058,820	300	1,903,959		1,903,959			
			58'	13,500,115	310	2,881,035		2,881,035			
			60'	12,980,880	298	3,864,509		3,864,509			
	Anchorage Bend Lower	Homgenous, Sand	52'	2,484,011	57	107,653		107,653			
			54'	3,161,441	73	280,802		280,802			
			56'	4,403,408	101	513,926		513,926			
			58'	4,892,659	112	832,050		832,050			
			60'	4,704,480	108	1,183,652		1,183,652			
	Anchorage Bend Upper	Homgenous, Sand	52'	5,693,285	131	396,632		396,632			
			54'	7,039,872	162	814,769		814,769			
			56'	7,361,928	169	1,337,791		1,337,791			
			58'	7,610,803	175	1,875,601		1,875,601			
			60'	7,318,080	168	2,423,802		2,423,802			
	Anchorage C	Homgenous, Sand	52'	1,037,808	24	108,167		108,167			
			54'	2,239,559	51	193,337		193,337			
			56'	2,497,800	57	358,061		358,061			
			58'	2,582,237	59	541,553		541,553			
			60'	2,482,920	57	732,089		732,089			
	Anchorage AN-1	Homgenous, Sand	52'	3,678,178	84	291,820	291,820				
			54'	4,961,755	114	559,032	559,032				
			56'	5,083,152	117	910,839	910,839				
			58'	5,255,078	121	1,293,390	1,293,390				
			60'	5,052,960	116	1,625,612	1,625,612				

							Volume above Grade					
Channel	Reach	Reach-specific Geotech Notes	Pre-treatment notes	Design Depth	Total Area above Grade		Total	Contaminated sediment (non-HARS)	Non-contaminated sediment	Moderately hard Rock	Harder rock	Hardest rock
					SQ FT	ACRES						
ANCHORAGE	Port Jersey Channel			52'	4,226,376	97.02	750,482.00		750,482.00			
				54'	5,121,270	117.57	1,043,244.00		1,043,244.00			
				56'	5,040,420	115.71	1,419,227.00		1,419,227.00			
				58'	4,959,570	113.86	1,826,364.00		1,826,364.00			
				60'	4,878,720	112.00	2,251,355.00		2,251,355.00			
	Port Jersey Widening (PJ-1)	Holocene = Non-HARS Pleistocene = HARS		52'	1,560,960	35.83	1,621,049.00	1,222,756.58	398,292.42			
				54'	1,584,540	36.38	1,762,170.00	1,313,467.96	448,702.04			
				56'	1,608,120	36.92	1,898,719.38	1,440,831.13	457,888.25			
				58'	1,631,700	37.46	2,028,671.00	1,491,700.02	536,970.98			
				60'	1,655,280	38.00	2,140,526.00	1,563,649.00	576,877.00			

Kill Van Vull Channel	Design Depth	Total Area above Grade (sf)	Total Area above Grade (ac)	Total	Contaminated sediment	Non-contaminated sediment	Serpentinite HARDER	Schist HARDER	Shale NONE	Sandstone HARDEST	Gneiss	Diabase HARDEST	Glacial Till MODERATELY	Moderately hard Rock	Harder rock	Hardest rock
KVK A-0'	52'	10,494	0.24	2,411	-	2,411	-	-	-	-	-	-	-	-	-	-
	53.5'	24,972	0.57	2,411	-	2,411	-	-	-	-	-	-	-	-	-	-
	54'	30,919	0.71	2,411	-	2,411	-	-	-	-	-	-	-	-	-	-
	56'	46,810	1.07	2,411	-	2,411	-	-	-	-	-	-	-	-	-	-
	58'	56,054	1.29	2,411	-	2,411	-	-	-	-	-	-	-	-	-	-
	60'	60,204	1.38	2,411	-	2,411	-	-	-	-	-	-	-	-	-	-
KVK-A	52'	646,435	14.84	206,211	-	206,211	-	-	-	-	-	-	-	-	-	-
	53.5'	1,914,134	43.94	244,674	-	244,674	-	-	-	-	-	-	-	-	-	-
	54'	2,424,400	55.66	271,763	-	244,674	-	-	-	-	-	-	27,089	27,089	-	-
	56'	3,820,809	87.71	475,088	-	244,674	-	-	-	-	-	-	230,414	230,414	-	-
	58'	4,657,839	106.93	775,639	-	244,674	-	-	-	-	-	-	530,965	530,965	-	-
	60'	5,066,208	116.30	1,131,533	-	244,674	-	-	-	-	-	-	886,859	886,859	-	-
KVK-B	52'	354,440	8.14	78,882	-	78,882	-	-	-	-	-	-	-	-	-	-
	53.5'	502,799	11.54	95,311	-	95,311	-	-	-	-	-	-	-	-	-	-
	54'	744,986	17.10	102,248	-	95,311	904	3,326	-	-	-	-	2,707	2,707	4,230	-
	56'	1,174,192	26.96	173,502	-	95,311	10,535	39,495	-	-	-	-	28,161	28,161	50,030	-
	58'	1,165,246	26.75	264,338	-	95,311	23,151	86,735	-	-	-	-	59,141	59,141	109,886	-
	60'	1,156,300	26.54	355,351	-	95,311	35,913	134,067	-	-	-	-	90,060	90,060	169,980	-
KVK-C	52'	311,335	7.15	72,746	-	72,746	-	-	-	-	-	-	-	-	-	-
	53.5'	467,570	10.73	86,760	-	86,760	-	-	-	-	-	-	-	-	-	-
	54'	713,839	16.39	92,855	-	86,760	5,980	-	-	-	-	-	115	115	5,980	-
	56'	1,017,751	23.36	159,025	-	86,760	71,598	-	-	-	-	-	667	667	71,598	-
	58'	1,009,459	23.17	240,543	-	86,760	152,776	-	-	-	-	-	1,007	1,007	152,776	-
	60'	1,001,167	22.98	320,088	-	86,760	232,313	-	-	-	-	-	1,015	1,015	232,313	-
KVK-D	52'	579,887	13.29	124,011	-	124,011	-	-	-	-	-	-	-	-	-	-
	53.5'	1,292,115	29.66	151,720	-	151,720	-	-	-	-	-	-	-	-	-	-
	54'	1,949,801	44.76	167,812	-	151,720	12,201	-	-	-	-	-	3,891	3,891	12,201	-
	56'	2,679,958	61.52	328,367	-	151,720	140,029	-	-	-	-	-	36,618	36,618	140,029	-
	58'	2,653,420	60.91	532,838	-	151,720	306,665	-	-	-	-	-	74,453	74,453	306,665	-
	60'	2,626,882	60.30	740,411	-	151,720	475,829	-	-	-	-	-	112,862	112,862	475,829	-
KVK-E	52'	85,522	1.96	39,127	-	39,127	-	-	-	-	-	-	-	-	-	-
	53.5'	398,942	9.16	47,241	-	47,241	-	-	-	-	-	-	-	-	-	-
	54'	627,684	14.41	52,491	-	47,241	5,125	-	-	-	-	-	125	125	5,125	-
	56'	985,882	22.63	110,915	-	47,241	63,053	-	-	-	-	-	621	621	63,053	-
	58'	974,926	22.38	188,803	-	47,241	140,927	-	-	-	-	-	635	635	140,927	-
	60'	963,970	22.13	267,630	-	47,241	219,754	-	-	-	-	-	635	635	219,754	-
KVK-F	52'	124,128	2.85	92,484	-	92,484	-	-	-	-	-	-	-	-	-	-
	53.5'	576,495	13.23	99,884	-	99,884	-	-	-	-	-	-	-	-	-	-
	54'	1,066,985	24.49	106,822	-	99,884	2,709	-	-	-	-	-	4,229	4,229	2,709	-
	56'	2,149,325	49.34	240,803	-	99,884	57,285	-	-	-	-	-	83,634	83,634	57,285	-
	58'	2,224,151	51.06	432,405	-	99,884	136,910	-	-	-	-	-	195,611	195,611	136,910	-
	60'	2,193,119	50.35	630,935	-	99,884	219,415	-	-	-	-	-	311,636	311,636	219,415	-
KVK-G	52'	320,861	7.37	99,443	-	99,443	-	-	-	-	-	-	-	-	-	-
	53.5'	1,052,954	24.17	104,384	-	104,384	-	-	-	-	-	-	-	-	-	-
	54'	1,985,849	45.59	114,298	-	104,384	-	-	-	-	-	-	9,914	9,914	-	-
	56'	4,193,488	96.27	317,173	-	104,384	-	-	-	-	-	-	212,789	212,789	-	-
	58'	4,262,441	97.85	650,319	-	104,384	-	-	-	-	-	-	545,935	545,935	-	-
	60'	4,202,483	96.48	1,019,746	-	104,384	-	-	-	-	-	-	915,362	915,362	-	-
KVK-H	52'	766,351	17.59	98,424	-	98,424	-	-	-	-	-	-	-	-	-	-
	53.5'	828,586	19.02	106,417	-	106,417	-	-	-	-	-	-	-	-	-	-
	54'	2,455,947	56.38	117,751	-	106,417	-	-	-	-	-	-	11,334	11,334	-	-
	56'	4,295,360	98.61	349,017	-	106,417	-	-	-	-	-	-	242,600	242,600	-	-
	58'	4,234,400	97.21	675,887	-	106,417	-	-	-	-	-	-	569,470	569,470	-	-
	60'	4,173,440	95.81	1,009,171	-	106,417	-	-	-	-	-	-	902,754	902,754	-	-
KVK-I	52'	96,656	2.22	15,583	-	15,583	-	-	-	-	-	-	-	-	-	-
	53.5'	96,656	2.22	21,389	-	21,389	-	-	-	-	-	-	-	-	-	-
	54'	242,912	5.58	23,427	-	21,389	-	-	-	-	-	868	1,170	1,170	-	868
	56'	667,691	15.33	59,130	-	21,389	-	-	-	-	-	16,835	20,906	20,906	-	16,835
	58'	667,691	15.33	115,389	-	21,389	-	-	-	-	-	43,069	50,931	50,931	-	43,069
	60'	667,691	15.33	171,193	-	21,389	-	-	-	-	-	69,390	80,414	80,414	-	69,390
KVK-J	52'	221,499	5.08	40,268	-	40,268	-	-	-	-	-	-	-	-	-	-
	53.5'	221,499	5.08	41,343	-	41,343	-	-	-	-	-	-	-	-	-	-
	54'	276,873	6.36	46,334	-	41,343	-	-	-	-	-	4,991	-	-	-	4,991
	56'	678,083	15.57	126,342	-	41,343	-	-	-	-	-	84,999	-	-	-	84,999
	58'	1,725,330	39.61	258,286	-	41,343	-	-	-	-	-	216,943	-	-	-	216,943
	60'	1,725,330	39.61	392,943	-	41,343	-	-	-	-	-	351,600	-	-	-	351,600
KVK-K	52'	425,138	9.76	52,176	-	52,176	-	-	-	-	-	-	-	-	-	-
	53.5'	468,640	10.76	57,515	-	57,515	-	-	-	-	-	-	-	-	-	-
	54'	901,816	20.70	69,794	-	57,515	-	-	-	-	-	12,279.00	-	-	-	12,279
	56'	2,235,540	51.32	172,955	-	57,515	-	-	-	-	-	115,440.00	-	-	-	115,440
	58'	2,235,540	51.32	341,454	-	57,515	-	-	-	-	-	283,939.00	-	-	-	283,939
	60'	2,235,540	51.32	517,961	-	57,515	-	-	-	-	-	460,446.00	-	-	-	460,446
KVK-L	52'	535,796	12.30	45,543	-	45,543	-	-	-	-	-	-	-	-	-	-
	53.5'	669,745	15.38	50,136	-	50,136	-	-	-	-	-	-	-	-	-	-
	54'	1,070,081	24.57	78,763	-	50,136	-	-	-	-	-	28,627	-	-	-	28,627
	56'	1,951,324	44.80	182,679	-	50,136	-	-	-	-	-	132,543	-	-	-	132,543

Kill Van Vull Channel	Design Depth	Total Area above Grade (sf)	Total Area above Grade (ac)	Total	Contaminated sediment	Non-contaminated sediment	Serpentinite HARDER	Schist HARDER	Shale NONE	Sandstone HARDEST	Gneiss	Diabase HARDEST	Glacial Till MODERATELY	Moderately hard Rock	Harder rock	Hardest rock		
KVK-M	58'	1,951,324	44.80	328,818	50,136	-	-	-	-	-	-	278,682	-	-	-	278,682		
	60'	1,951,324	44.80	475,253	50,136	-	-	-	-	-	-	425,117	-	-	-	425,117		
	52'	755,938	17.35	40,723	40,723	-	-	-	-	-	-	-	-	-	-	-		
	53.5'	795,714	18.27	41,417	41,417	-	-	-	-	-	-	-	-	-	-	-		
	54'	884,127	20.30	51,067	41,417	-	-	-	-	2,780	-	2,235	4,635	-	4,635	-	5,015	
	56'	1,744,825	40.06	140,530	41,417	-	-	-	-	31,324	-	25,387	42,402	-	42,402	-	56,711	
	58'	1,744,825	40.06	269,970	41,417	-	-	-	-	75,108	-	60,936	92,509	-	92,509	-	136,044	
	60'	1,744,825	40.06	399,807	41,417	-	-	-	-	119,589	-	96,594	142,207	-	142,207	-	216,183	
	52'	18,770	0.43	1,045	1,045	-	-	-	-	-	-	-	-	-	-	-	-	
	53.5'	18,770	0.43	1,045	1,045	-	-	-	-	-	-	-	-	-	-	-	-	
KVK-M-0'	54'	22,686	0.52	1,263	1,045	-	-	-	-	218	-	-	-	-	-	-	218	
	56'	44,770	1.03	4,106	1,045	-	-	-	-	3,061	-	-	-	-	-	-	3,061	
	58'	44,770	1.03	7,425	1,045	-	-	-	-	6,380	-	-	-	-	-	-	6,380	
	60'	44,770	1.03	10,745	1,045	-	-	-	-	9,700	-	-	-	-	-	-	9,700	
	KVK-1 (Widening)	52'	931,006	21.37	181,614	14,644.00	131,798.00	35,172	-	-	-	-	-	-	-	-	35,172	-
		54'	959,626	22.03	234,808	14,644.00	177,822.00	42,342	-	-	-	-	-	-	-	-	42,342	-
56'		988,246	22.69	293,305	14,644.00	228,403.00	50,258	-	-	-	-	-	-	-	-	50,258	-	
58'		1,016,866	23.34	359,544	14,644.00	286,007.00	58,893	-	-	-	-	-	-	-	-	58,893	-	
60'		1,045,486	24.00	427,818	14,644.00	344,902.00	68,272	-	-	-	-	-	-	-	-	68,272	-	
KVK-3 (Widening)	52'	355,454	8.16	96,549	22,065.00	-	-	-	-	-	-	-	74,484.00	-	74,484	-	-	
	54'	380,354	8.73	96,549	22,065.00	-	-	-	-	-	-	-	74,484.00	-	74,484	-	-	
	56'	405,254	9.30	128,548	22,065.00	-	-	-	-	-	-	-	106,483.00	-	106,483	-	-	
	58'	430,154	9.87	162,809	22,065.00	-	-	-	-	-	-	-	140,744.00	-	140,744	-	-	
	60'	455,054	10.45	198,795	22,065.00	-	-	-	-	-	-	-	176,730.00	-	176,730	-	-	
KVK-4 (Widening)	52'	475,718	10.92	240,574	168,402.00	-	-	-	-	-	-	-	72,172.00	-	72,172	-	-	
	54'	493,088	11.32	240,574	168,402.00	-	-	-	-	-	-	-	72,172.00	-	72,172	-	-	
	56'	510,458	11.72	283,253	168,402.00	-	-	-	-	-	-	-	114,851.00	-	114,851	-	-	
	58'	527,828	12.12	329,464	168,402.00	-	-	-	-	-	-	-	161,062.00	-	161,062	-	-	
	60'	545,198	12.52	377,669	168,402.00	-	-	-	-	-	-	-	209,267.00	-	209,267	-	-	
KVK-5 (Widening)	52'	509,120	11.69	261,706	93,319.00	-	-	-	-	-	-	-	168,387.00	-	168,387	-	-	
	54'	531,320	12.20	261,706	93,319.00	-	-	-	-	-	-	-	168,387.00	-	168,387	-	-	
	56'	553,520	12.71	321,359	93,319.00	-	-	-	-	-	-	1,308	226,732.00	-	226,732	-	1,308	
	58'	575,720	13.22	399,060	93,319.00	-	-	-	-	-	-	17,207	288,534.00	-	288,534	-	17,207	
	60'	597,920	13.73	465,713	93,319.00	-	-	-	-	-	-	19,070	353,324.00	-	353,324	-	19,070	
KVK-2 (EFFICIENCY)	52'	708,647	16.27	409,929	55,902.00	-	-	-	-	-	-	-	354,027	-	354,027	-	-	
	54'	725,747	16.66	461,209	55,902.00	-	-	1,710	-	-	-	-	403,597	-	403,597	-	1,710	
	56'	742,847	17.05	510,418	55,902.00	-	-	9,044	-	-	-	-	445,472	-	445,472	-	9,044	
	58'	759,947	17.45	552,774	55,902.00	-	-	13,422	-	-	-	-	483,450	-	483,450	-	13,422	
	60'	777,047	17.84	590,742	55,902.00	-	-	16,352	-	-	-	-	518,488	-	518,488	-	16,352	

				Volume above Grade					
Reach	Area (sft)	Area (ac)	Design Depth	Total	Contaminated sediment (non-HARS) (Upland Disposal)	Non-contaminated sediment (HARS DISPOSAL)	Moderately hard Rock	Fractured Rock	Hardest rock
AK-A	495,828	11.38	-52	78,827	78,827				
	740,041	16.99	-54	178,247	141,450	5,018	14,217	14,217	3,345
	1,217,375	27.95	-56	299,367	141,450	5,018	14,217	14,217	124,465
	1,217,375	27.95	-58	423,865	141,450	5,018	14,217	14,217	248,963
	1,217,375	27.95	-60	551,272	141,450	5,018	14,217	14,217	376,370
AK-B	653,968	15.01	-52	95,496	95,496				
	976,072	22.41	-54	201,526	170,431	4,664	16,325	10,106	-
	976,072	22.41	-56	300,211	170,431	4,664	96,212	10,106	18,798
	976,072	22.41	-58	401,982	170,431	4,664	179,184	10,106	37,597
	976,072	22.41	-60	505,765	170,431	4,664	264,169	10,106	56,395
AK-C	855,878	19.65	-52	97,484	97,484				
	1,320,718	30.32	-54	231,881	200,873	4,651	16,279	10,078	-
	1,403,079	32.21	-56	375,083	200,873	4,651	159,481	10,078	-
	1,403,079	32.21	-58	524,924	200,873	4,651	309,323	10,078	-
	1,403,079	32.21	-60	677,960	200,873	4,651	462,358	10,078	-
AK-D	206,639	4.74	-52	27,547	27,547				
	303,881	6.98	-54	51,382	44,404	1,047	3,245	2,268	419
	354,339	8.13	-56	86,580	44,404	1,047	17,849	2,268	21,012
	354,339	8.13	-58	122,953	44,404	1,047	32,923	2,268	42,312
	354,339	8.13	-60	161,079	44,404	1,047	48,698	2,268	64,662
AK-E	175,905	4.04	-52	32,221	32,221				
	418,821	9.61	-54	92,656	72,615	3,006	8,518	6,513	2,004
	720,614	16.54	-56	164,105	72,615	3,006	8,518	6,513	73,454
	720,614	16.54	-58	241,048	72,615	3,006	8,518	6,513	150,396
	720,614	16.54	-60	320,123	72,615	3,006	8,518	6,513	229,471
AK-F	175,186	4.02	-52	40,556	40,556				
	417,109	9.58	-54	164,769	100,949	9,573	27,124	20,742	6,382
	1,045,887	24.01	-56	283,373	100,949	9,573	27,124	20,742	124,986
	1,152,873	26.47	-58	404,314	100,949	9,573	27,124	20,742	245,927
	1,152,873	26.47	-60	531,672	100,949	9,573	27,124	20,742	373,285
AK-G	42,945	0.99	-52	15,560	15,560				
	195,205	4.48	-54	142,508	142,508	-	-	-	-
	823,025	18.89	-56	223,177	142,508	-	-	-	80,669
	888,507	20.40	-58	309,566	142,508	-	-	-	167,058
	888,507	20.40	-60	397,412	142,508	-	-	-	254,904
AK-H	330,434	7.59	-52	35,723	35,723				
	493,186	11.32	-54	120,637	88,797	4,776	13,532	10,348	3,184
	981,464	22.53	-56	211,347	88,797	4,776	13,532	10,348	93,894
	981,464	22.53	-58	303,941	88,797	4,776	13,532	10,348	186,488
	981,464	22.53	-60	398,592	88,797	4,776	13,532	10,348	281,139
AK-1 (WIDENING)	959,905	22.04	-52	1,075,736	197,394	380,167	129,442	185,479	183,255
	976,609	22.42	-54	1,146,840	268,498	380,167	129,442	185,479	183,255
	993,229	22.80	-56	1,176,920	270,587	380,167	129,442	185,479	211,245
	1,009,849	23.18	-58	1,208,024	272,723	380,167	129,442	185,479	240,214
	1,026,469	23.56	-60	1,236,859	274,906	380,167	129,442	185,479	266,865
AK-2 (WIDENING)	2,144,329	49.23	-52	4,175,030	1,019,774		1,938,352	798,476	418,428
	2,659,129	61.05	-54	4,333,869	1,178,613		1,938,352	798,476	418,428
	2,710,159	62.22	-56	4,408,956	1,213,555		1,938,352	798,476	458,573
	2,761,189	63.39	-58	4,497,467	1,248,953		1,938,352	798,476	511,686
	2,812,219	64.56	-60	4,576,329	1,284,819		1,938,352	798,476	554,682

## Newark Bay Channel

Average as-built elevation assumed to be -53 ft

## Volume above Grade

Reach	Design Depth	Total Area above Grade (sf)	Total Area above Grade (ac)	Total	Contaminated sediment (Non-HARS Disposal)	Non-Contaminated Sediment (HARS Disposal)	Pleistocene Silt and Clay (Moderately Hard)	Other Rock (Hardest)	Serpentinite (Harder)	Sandstone (Hardest)	Diabase (Hardest)	Moderately hard Rock	Harder rock	Hardest rock
NWK-A	52'	1,972,320	45.28	236,335	236,335			-	-	-	-	-	-	-
	53	1,960,720	45.01	250,757	250,757			-	-	-	-	-	-	-
	54'	1,958,400	44.96	265,179	252,010		2,784.9	-	-	4,913	5,470	2,784.94	-	10,383.84
	56'	1,944,480	44.64	374,887	260,483		21,614.1	-	-	44,293	48,497	21,614.13	-	92,789.51
	58'	1,930,560	44.32	527,699	269,753		42,212.5	-	-	103,848	111,885	42,212.48	-	215,732.90
	60	1,916,640	44.00	690,614	277,566		59,576.6	-	-	171,227	182,244	59,576.57	-	353,470.98
NWK-B	52'	1,902,684	43.68	232,586	232,586	-		-	-	-	-	-	-	-
	53	1,886,534	43.31	260,524	260,524			-	-	-	-	-	-	-
	54'	1,883,304	43.23	288,462	260,524	3,169	16,901	-	-	7,868	-	16,901.07	-	7,867.98
	56'	1,863,924	42.79	402,364	260,524	15,574	83,059	-	-	43,208	-	83,058.94	-	43,207.50
	58'	1,844,544	42.34	535,608	260,524	29,131	155,363	-	-	90,590	-	155,363.19	-	90,590.21
	60'	1,825,164	41.90	670,874	260,524	42,129	224,687	-	-	143,534	-	224,686.80	-	143,534.42
NWK-C	52	4,509,192	103.52	442,831	442,831	-		-	-	-	-	-	-	-
	53	4,479,092	102.83	494,438	494,438			-	-	-	-	-	-	-
	54'	4,473,072	102.69	546,044	499,065	8,545	34,107	773	618	2,936	-	34,107.26	618	3,708.25
	56'	4,436,952	101.86	826,719	523,717	54,055	215,769	5,950	4,334	22,894	-	215,768.86	4,334	28,843.80
	58'	4,400,832	101.03	1,150,386	551,053	104,522	417,217	14,164	9,060	54,370	-	417,216.94	9,060	68,533.53
	60'	4,364,712	100.20	1,472,269	577,139	152,679	609,443	24,466	14,230	94,311	-	609,443.23	14,230	118,777.77
NWK-D	52'	4,988,268	114.51	565,634	565,634			-	-	-	-	-	-	-
	53	4,959,093	113.85	637,270	637,270			-	-	-	-	-	-	-
	54'	4,953,258	113.71	708,906	643,170		49,902	2,253	-	13,581	-	49,902.42	-	15,833.29
	56'	4,918,248	112.91	1,032,512	667,826		258,429	15,299	-	90,958	-	258,429.33	-	106,256.89
	58'	4,883,238	112.10	1,402,043	692,101		463,741	35,123	-	211,077	-	463,741.29	-	246,200.57
	60	4,848,228	111.30	1,827,293	716,482		669,943	61,158	-	379,710	-	669,943.25	-	440,868.03
NWK-E	52'	3,657,264	83.96	522,033	522,033			-	-	-	-	-	-	-
	53	3,634,039	83.43	588,684	588,684			-	-	-	-	-	-	-
	54'	3,629,394	83.32	655,333	611,876		43,457	-	-	-	-	43,457.10	-	-
	56'	3,601,524	82.68	863,971	684,479		179,492	-	-	-	-	179,492.14	-	-
	58'	3,573,654	82.04	1,112,075	770,816		341,259	-	-	-	-	341,258.93	-	-
	60'	3,545,784	81.40	1,376,567	862,855		513,712	-	-	-	-	513,711.59	-	-
NWK-F	52'	2,000,856	45.93	288,273	288,273			-	-	-	-	-	-	-
	53	1,988,756	45.66	324,620	324,620			-	-	-	-	-	-	-
	54'	1,986,336	45.60	360,967	337,524		22,188	-	-	-	1,255	22,188.20	-	1,255.03
	56'	1,971,816	45.27	442,692	366,305		71,678	-	-	4,709	-	71,678.49	-	4,709.15
	58'	1,957,296	44.93	548,478	402,923		134,643	-	-	10,912	-	134,643.26	-	10,911.56
	60'	1,942,776	44.60	672,449	445,397		206,732	-	-	-	20,320	206,732.29	-	20,320.41
NWK-G	52'	350,256	8.04	61,994	61,994			-	-	-	-	-	-	-
	53	346,256	7.95	76,239	76,239			-	-	-	-	-	-	-
	54'	345,456	7.93	90,484	84,486		5,998	-	-	-	-	5,997.89	-	-
	56'	340,656	7.82	120,704	101,982		18,722	-	-	-	-	18,722.11	-	-
	58'	335,856	7.71	153,994	121,255		32,739	-	-	-	-	32,738.95	-	-
	60'	331,056	7.60	185,064	139,243		45,821	-	-	-	-	45,821.05	-	-
NWK-1A	52	2,193,371	50.35	5,535,818	3,699,678	587,893	881,965	366,282				881,965.43	-	366,281.58
	54'	2,250,371	51.66	5,809,279	3,766,150	653,694	881,965	507,470				881,965.43	-	507,469.71
	56'	2,307,371	52.97	6,096,467	3,842,134	715,821	881,965	656,547				881,965.43	-	656,547.41
	58'	2,364,371	54.28	6,294,351	3,842,134	757,918	881,965	812,334				881,965.43	-	812,334.16
	60'	2,421,371	55.59	6,544,442	3,842,134	848,026	881,965	972,317				881,965.43	-	972,317.18
NWK-1B	52'	2,135,987	49.04	3,266,783	1,658,942	244,441	1,290,431	72,968				1,290,431.41	-	72,967.55
	54'	2,149,247	49.34	3,426,288	1,663,764	274,540	1,342,049	145,935				1,342,048.67	-	145,935.11
	56'	2,162,507	49.64	3,674,553	1,685,700	314,673	1,382,310	291,870				1,382,310.13	-	291,870.22
	58'	2,175,767	49.95	3,888,266	1,685,700	354,805	1,409,956	437,805				1,409,956.33	-	437,805.33
	60	2,189,027	50.25	4,051,284	1,685,700	364,838	1,417,006	583,740				1,417,006.11	-	583,740.43
NWK-2A	52'	1,757,168	40.34	3,596,100	639,751	303,431	2,302,193	350,725				2,302,193.13	-	350,725.32
	54'	1,776,668	40.79	3,769,122	647,018	307,708	2,329,151	485,246				2,329,150.93	-	485,245.77
	56'	1,796,168	41.23	4,116,924	663,731	333,602	2,494,221	625,370				2,494,221.27	-	625,369.64
	58'	1,815,668	41.68	4,113,119	661,551	315,854	2,368,062	767,652				2,368,061.89	-	767,652.29
	60'	1,835,168	42.13	4,290,940	668,818	319,927	2,389,022	913,174				2,389,021.58	-	913,173.84
NWK-2B	52'	527,494	12.11	1,463,912	487,511	94,060	620,016	262,325				620,015.56	-	262,324.63
	54'	548,194	12.58	1,544,203	494,778	98,338	645,226	305,861				645,225.99	-	305,861.41
	56'	568,894	13.06	1,803,274	511,491	124,232	813,131	354,420				813,130.59	-	354,419.99
	58'	589,594	13.54	1,708,737	509,311	106,484	687,597	405,345				687,596.80	-	405,345.01
	60'	610,294	14.01	1,794,105	516,578	110,557	707,836	459,135				707,836.50	-	459,134.52
NWK-2C	52'	442,134	10.15	966,590	211,796		749,972	4,822				749,972.36	-	4,821.76
	54'	449,094	10.31	1,013,791	214,026		792,565	7,200				792,565.47	-	7,200.42
	56'	456,054	10.47	1,061,489	216,256		835,159	10,075				835,158.58	-	10,074.64
	58'	463,014	10.63	1,109,682	218,486		877,752	13,444	-	-	-	877,751.69	-	13,444.42
	60'	469,974	10.79	1,158,370	220,716		915,145	22,510	-	-	-	915,144.80	-	22,509.76



Port Elizabeth Channel

53.0 ft is average as-built-elevation

Volume above Grade

Reach	Design Depth	Total Area above Grade (sf)	Total Area above Grade (ac)	Total	Contaminated sediment (UPLAND)	Non-contaminated sediment	Sandstone (REEF)	Other Rock (REEF)	Diabase (REEF)	Glacial Till (HARS DISPOSAL)	Pleistocene Silt and Clay (HARS DISPOSAL)	Moderately hard Rock	Harder rock	Hardest rock
South Eliz A	52'	873,492	20.05	49,791	49,791		-	-			-	-	-	-
	53'	863,949	19.83	56,458	100,153		-	-			-	-	-	-
	54'	854,406	19.61	129,216	110,162		7,274	2,302.81			9,477	9,477	-	9,576
	56'	835,320	19.18	188,166	126,577		27,665	8,906.49			25,018	25,018	-	36,571
	58'	816,234	18.74	247,190	138,588		54,435	17,776.22			36,391	36,391	-	72,211
	60	797,148	18.30	306,214	147,369		85,882	28,258.63			44,704	44,704	-	114,141
South Eliz A1	52'	80,208	1.84	165,379	165,379							-		-
	53'	85,428	1.96	180,217	172,493		4,055	771.74			2,897	2,897		4,827
	54'	90,648	2.08	195,054	179,496		8,241	1,568.29			5,749	5,749		9,809
	56'	101,088	2.32	221,853	189,877		18,482	3,517.40			9,976	9,976		22,000
	58'	111,528	2.56	251,545	198,237		33,544	6,383.80			13,380	13,380		39,928
	60	121,968	2.80	282,084	205,334		50,810	9,669.67			16,270	16,270		60,479
South Eliz PE-1 (EFFICIENCY)	52'	735,021	16.87	1,451,724	521,758			11,597		233,357	685,012	918,369		11,597
	54'	744,213	17.08	1,504,858	522,599			40,436		256,811	685,012	941,823		40,436
	56'	753,405	17.30	1,556,842	523,440			78,215		270,175	685,012	955,187		78,215
	58'	762,597	17.51	1,608,260	524,281			119,913		279,054	685,012	964,066		119,913
	60	771,789	17.72	1,658,700	525,122			163,793		284,773	685,012	969,785		163,793

Port Elizabeth Channel

(-53.5 ft is average as-built elevation)

Volume above Grade

Reach	Design Depth	Total Area above Grade (sf)	Total Area above Grade (ac)	Total	Contaminated sediment (UPLAND DISPOSAL)	Non-contaminated sediment (HARS DISPOSAL)	Other Rock (REEF DISPOSAL)	Recent Black Silt (UPLAND DISPOSAL)	Pleistocene Silt and Clay (HARS DISPOSAL)		Moderately hard Rock	Harder rock	Hardest rock
Eliz A	52'	1,290,240	29.62	88,027	88,027			-	-		-	-	-
	53.5'	1,273,725	29.24	120,208	120,208			-	-		-	-	-
	54'	1,270,422	29.16	133,139	127,721				5,418		5,418	-	-
	56'	1,250,604	28.71	205,906	169,998				35,908		35,908	-	-
	58'	1,230,786	28.25	298,696	223,908				74,788		74,788	-	-
	60'	1,210,968	27.80	400,709	283,177				117,532		117,532	-	-
Eliz B	52'	1,826,100	41.92	103,035	103,035.00				-				
	53.5'	1,795,050	41.21	124,161	124,161.00				-				
	54'	1,788,840	41.07	135,871	132,510.00				3,361		3,361		
	56'	1,751,580	40.21	240,970	207,445.00				33,525		33,525		
	58'	1,714,320	39.36	373,245	301,755.00				71,490		71,490		
	60'	1,677,060	38.50	508,673	398,314.00				110,359		110,359		
Eliz C	52'	930,180	21.35	71,151	71,151.00				-		-		
	53.5'	913,355	20.97	111,586	111,586.00				-		-		
	54'	909,990	20.89	117,858	113,389.00				4,469		4,469		
	56'	889,800	20.43	147,530	120,851.00				26,679		26,679		
	58'	869,610	19.96	270,689	128,539.00				142,150		142,150		
	60'	849,420	19.50	346,873	136,656.00				210,217		210,217		
Eliz-D	52'	704,568	16.17	68,299	68,299.00		-	-	-				
	53.5'	692,093	15.89	103,463	103,463.00		-	-	-				
	54'	689,598	15.83	115,434	110,965.00		4,469		-				4,469
	56'	674,628	15.49	164,269	137,590.00		26,679		-				26,679
	58'	659,658	15.14	213,715	160,798.00		52,917		-				52,917
	60'	644,688	14.80	260,638	180,934.00		79,704		-				79,704

THIS PAGE INTENTIONALLY  
LEFT BLANK

ATTACHMENT 3A

TSP QUANTITIES

4-FOOT DEEPENING

Ambrose 57 ft (Deepen by 4)

Ambrose Channel Reach	Reach-specific Geotech Notes	Pre-treatment notes	Design Depth	Total Area above Grade		Volume above Grade (cy)					
				Area (sf)	Area (ac)	Total Volume (cy)	Contaminated sediment (non-HARS)	Non-contaminated sediment	Moderately hard Rock	Harder rock	Hardest rock
A			57'	-	-	-		-			
B			57'	-	-	-		-			
C			57'	2,962,951.2	68.0	136,060		136,060.0			
D			57'	7,873,905.6	180.8	424,179		424,179.0			
E			57'	1,735,866.0	39.9	100,576		100,576.0			
F			57'	985,762.8	22.6	36,822		36,822.0			
G			57'	415,126.8	9.5	19,837		19,837.0			
H	Includes excavation of shoaling areas		57'	1,816,016.4	41.7	630,054		630,054.0			
I			57'	1,700,582.4	39.0	653,377		653,377.0			
J			57'	13,939.2	0.3	370		370.0			
K			57'	2,117,451.6	48.6	70,547		70,547.0			
L			57'	5,300,380.8	121.7	328,380		328,380.0			
M			57'	9,261,727.2	212.6	594,910		594,910.0			
N			57'	10,235,293.2	235.0	618,625		618,625.0			
O			57'	9,555,757.2	219.4	376,797		376,797.0			
P			57'	1,387,386.0	31.9	58,658		58,658.0			
Q			57'	1,190,494.8	27.3	88,086		88,086.0			
R			57'	8,276.4	0.2	180		180.0			

4,137,458

Anchorage 54 ft (Deepen by 4)

Anchorage Channel Reach	Reach-specific Geotech Notes	Pre-treatment notes	Design Depth	Total Area above Grade		Volume above Grade (cy)					
				Area (sf)	Area (ac)	Total Volume (cy)	Contaminated sediment (non-HARS)	Non-contaminated sediment	Moderately hard Rock	Harder rock	Hardest rock
A			54'	4,202,233	96	218,878		218,878			
B			54'	11,594,365	266	921,328		921,328			
BEND-L			54'	2,838,370	65	239,887		239,887			
BEND-U			54'	6,983,104	160	584,295		584,295			
C			54'	2,078,248	48	112,814		112,814			
AN-1			54'	4,203,104	96	473,667	473,667				

2,550,869

Port Jersey 56 ft (Deepen by 4)

				Volume Above Grade (cy)					
Port Jersey Reach	Design Depth	Total Area above Grade		Total (cy)	Contaminated sediment (non-HARS)	Non-contaminated sediment	Moderately hard Rock	Harder rock	Hardest rock
		SQ FT	ACRES						
Port Jersey channel	56'	4,857,811.2	111.52	896,184		896,184			
PJ-1	56'	2,010,294.0	46.15	1,847,751	1,324,143	523,608			

2,743,935

Kill Van Vull Channel 56 ft (Deepen by 4)  
(-53.5 ft is average as-built elevation)

(53.5 ft is average as-built elevation)																	Volume above Grade										Disposal Location Midpoint Coordinates			
Reach	Design Depth	Total Area above Grade (sf)	Total Area above Grade (ac)	Total	Contaminated sediment	Non-contaminated sediment	Serpentine HARDER	Schist HARDER	Shale NONE	Other Rock HARDEST	Gneiss	Diabase HARDEST	Glacial Till MODERATELY	Moderately hard Rock	Harder rock	Hardest rock	Disposal Description	Northing	Eastng	Additional Notes										
A	56"	3,920,490	90.8	336,909		264,436							72,473	72,473	-	-														
B	56"	1,186,574	27.24	122,492		70,728	17,328	64,903					13,532	13,532	82,232	-	-													
C	56"	1,012,334	23.24	107,760		12,787	94,973						-	-	94,973	-	-													
D	56"	2,750,814	63.15	255,951		5,504	250,447						-	-	250,447	-	-													
E	56"	976,615	22.42	76,831		7,135	69,696						-	-	69,696	-	-													
F	56"	2,193,692	50.36	145,563		2,817	99,123						43,623	43,623	99,123	-	-													
G	56"	6,276,107	98.12	279,617		22,423							257,194	257,194	-	-														
H	56"	6,315,054	99.06	314,553		15,676							298,877	298,877	-	-														
I	56"	727,452	16.70	46,750		3,809						3,168	39,773	39,773	-	-														
J	56"	1,775,941	40.77	111,979		2,473						85,628	23,878	23,878	-	-														
K	56"	2,272,961	52.18	151,485		14,245						137,240	-	-	137,240	-	-													
L	56"	1,964,992	45.11	159,400		25,852						104,812	28,696	28,696	-	-														
M	56"	1,778,555	40.83	126,127		17,669						2,027	306,451	306,451	-	-														
KVC-1	56"	835,045	19.2	228,670		94,145	8,794				11,516		114,214	114,214	8,794	11,516														
KVC-2	56"	463,914	10.65	157,320									157,320	157,320	-	-														
KVC-4	56"	561,053	12.88	277,029									277,029	277,029	-	-														
KVC-5	56"	669,517	15.37	339,136								5,759	333,377	333,377	-	5,759														



**Port Elizabeth Channel 56 ft (Deepen by 4)**  
 (-53.5 ft is average as-built elevation)

**Volume above Grad (cy)**

[illegible]

**South Elizabeth Channel 56 ft (Deepen by 4)**  
53.0 ft is average as-built-elevation

**Volume above Grade**

[illegible]

Average as-built elevation assumed to be -53.5 ft

[illegible]

THIS PAGE INTENTIONALLY  
LEFT BLANK

ATTACHMENT 3B

TSP QUANTITIES

5-FOOT DEEPENING

Ambrose Channel 58 ft (deepen by 5)

Ambrose Channel Reach	Reach-specific Geotech Notes	Pre-treatment notes	Design Depth	Total Area above Grade		Volume above Grade (cy)					
				Area (sf)	Area (ac)	Total Volume (cy)	Contaminated sediment (non-HARS)	Non-contaminated sediment	Moderately hard Rock	Harder rock	Hardest rock
A			58'	-	-	-		-			
B			58'	-	-	-		-			
C			58'	3,777,087.6	86.7	261,115		261,115.0			
D			58'	8,678,894.4	199.2	731,965		731,965.0			
E			58'	2,325,232.8	53.4	176,856		176,856.0			
F			58'	2,068,228.8	47.5	95,594		95,594.0			
G			58'	767,091.6	17.6	43,092		43,092.0			
H	Includes excavation of shoaling areas		58'	2,021,184.0	46.4	698,778		698,778.0			
I			58'	1,805,997.6	41.5	717,647		717,647.0			
J			58'	41,817.6	1.0	1,950		1,950.0			
K			58'	3,160,713.6	72.6	162,428		162,428.0			
L			58'	6,310,101.6	144.9	542,168		542,168.0			
M			58'	10,171,260.0	233.5	951,987		951,987.0			
N			58'	10,295,841.6	236.4	998,441		998,441.0			
O			58'	10,174,744.8	233.6	744,782		744,782.0			
P			58'	2,073,020.4	47.6	122,950		122,950.0			
Q			58'	1,538,103.6	35.3	138,652		138,652.0			
R			58'	16,117.2	0.4	663		663.0			

6,389,068

Anchorage Channel 55 ft (deepen by 5)

Anchorage Channel Reach	Reach-specific Geotech Notes	Pre-treatment notes	Design Depth	Total Area above Grade		Volume above Grade (cy)					
				Area (sf)	Area (ac)	Total Volume (cy)	Contaminated sediment (non-HARS)	Non-contaminated sediment	Moderately hard Rock	Harder rock	Hardest rock
A			55'	5,031,180	115.5	391,270		391,270			
B			55'	12,811,432	294.1	1,373,260		1,373,260			
BEND-L			55'	3,189,463	73.2	351,393		351,393			
BEND-U			55'	7,122,060	163.5	845,619		845,619			
C			55'	2,340,043	53.7	193,340		193,340			
AN-1			55'	5,066,464	116.3	645,444	645,444				

3,800,326

Port Jersey Channel 57 ft (Deepen by 5)

				Volume Above Grade (cy)					
Port Jersey Reach	Design Depth	Total Area above Grade		Total (cy)	Contaminated sediment (non-HARS)	Non-contaminated sediment	Moderately hard Rock	Harder rock	Hardest rock
		SQ FT	ACRES						
Port Jersey channel	57'	4,937,526.0	113.35	1,079,544		1,079,544			
PJ-1	57'	2,033,816.4	46.69	1,923,388	1,367,900	555,488			

3,002,932



Kill Van Vull Channel (-53.5 ft is average as-built elevation)

Kill Van Kull Channel		(-53.5 ft is average as-built elevation)		Volume above Grade												
Reach	Design Depth	Total Area above Grade (sf)	Total Area above Grade (ac)	Total	Contaminated sediment	Non-contaminated sediment	Serpentineite HARDER	Schist HARDER	Shale NONE	Other Rock HARDEST	Gneiss	Diabase HARDEST	Glacial Till MODERATELY	Moderately hard Rock	Harder rock	Hardest rock
A	57"	4,493,214	103.2	481,886		382,781							99,105	99,105	-	-
B	57"	1,188,317	27.28	166,541		47,673	17,687	64,545					36,636	36,636	82,232	-
C	57"	1,012,334	23.24	145,416		12,295	133,121								-	133,121
D	57"	2,750,814	63.15	359,961		5,504	354,457								-	354,457
E	57"	976,615	22.42	112,975		7,135	105,840								-	105,840
F	57"	2,193,682	50.36	227,963		2,817	132,164						92,982	92,982	132,164	-
G	57"	4,274,107	98.12	476,971		31,875							445,096	445,096	-	-
H	57"	4,315,054	99.06	474,742	15,676								459,066	459,066	-	-
I	57"	727,452	16.70	73,620	5,561							4,982	63,077	63,077	-	4,982
J	57"	1,775,941	40.77	177,579	2,473							137,156	37,950	37,950	-	137,156
K	57"	2,272,961	52.18	235,294	14,245							221,049		-	-	221,049
L	57"	1,964,992	45.11	231,943	25,852							162,003	44,088	44,088	-	162,003
M	57"	1,778,555	40.83	192,992	23,048							3,151	166,793	166,793	-	3,151
KVK-1	57"	835,045	19.2	258,045		105,660	11,244			12,928			128,212	128,212	11,244	12,928
KVK-3	57"	463,914	10.65	174,008									174,008	174,008	-	-
KVK-4	57"	561,053	12.88	298,655									298,655	298,655	-	-
KVK-5	57"	669,517	15.37	362,695								6,113	356,583	356,583	-	6,113
A KVK-1		617,245	14.2	175,745		75,163				9,213			91,369			
B KVK-1		113,692	2.61	56,498		23,339	1,928			2,861			28,371			
C KVK-1		46,609	1.07	23,137		6,970	6,841			854			8,472			
D KVK-1		57,499	1.32	2,665		189	2,476									
G KVK-3		463,914	10.65	174,008									174,008			
G KVK-4		11,326	0.26	2,786									2,786			
H KVK-4		549,727	12.62	295,869									295,869			
H KVK-5		510,959	11.73	281,202									281,202			
I KVK-5		135,036	3.10	73,343									73,343			
J KVK-5		23,522	0.54	8,150								6,113	2,038			

**Newark Bay Channel 57 ft (Deepen by 5)**  
 (-53.5 ft is average as-built elevation)

[illegible]

(-53.5 ft is average as-built elevation)

(-53.5 ft is average as-built elevation)

[illegible]

**South Elizabeth Channel 57 ft (Deepen by 5)**  
 (-53.5 ft is average as-built elevation)

**Volume above Grade**

[illegible]

THIS PAGE INTENTIONALLY  
LEFT BLANK

## ATTACHMENT 4

### ERDC/CHL SEDIMENTATION STUDY



**US Army Corps  
of Engineers®**  
Engineer Research and  
Development Center



## **New York/New Jersey Harbor Sedimentation Study**

Numerical Modeling of Hydrodynamics and Sediment Transport

Tate O. McAlpin, Joseph V. Letter, Jr., Mary Bryant,  
Anthony G. Emiren, Gary L. Brown, Gaurav Savant,  
Bryce W. Wisemiller, Jamal A. Sulayman, and Corey J. Trahan

August 2020



**The US Army Engineer Research and Development Center (ERDC)** solves the nation's toughest engineering and environmental challenges. ERDC develops innovative solutions in civil and military engineering, geospatial sciences, water resources, and environmental sciences for the Army, the Department of Defense, civilian agencies, and our nation's public good. Find out more at [www.erdclibrary.on.worldcat.org/discovery](http://www.erdclibrary.on.worldcat.org/discovery).

To search for other technical reports published by ERDC, visit the ERDC online library at [www.erdclibrary.on.worldcat.org/discovery](http://www.erdclibrary.on.worldcat.org/discovery).



# **New York/New Jersey Harbor Sedimentation Study**

## **Numerical Modeling of Hydrodynamics and Sediment Transport**

Tate O. McAlpin, Joseph V. Letter, Jr., Mary Bryant,  
Anthony G. Emiren, Gary L. Brown, and Gaurav Savant

*Coastal and Hydraulics Laboratory  
US Army Research and Development Center  
3909 Halls Ferry Road  
Vicksburg, MS 39180-6199*

Corey J. Trahan

*Information Technology Laboratory  
US Army Engineer Research and Development Center  
3909 Halls Ferry Road  
Vicksburg, MS 39180-6199*

Bryce W. Wisemiller and Jamal A. Sulayman

*US Army Corps of Engineers  
New York District  
26 Federal Plaza  
New York, NY 10278*

Final report

Approved for public release; distribution is unlimited

Prepared for US Army Corps of Engineers, New York District  
New York, NY 10278

Under Work Item Code 1J186F, "ERDC Sedimentation Modeling"

## Abstract

The New York/New Jersey Harbor (NYNJH) is a vital economic resource for both the local economy and the entire US economy due to the vast quantity of imports and exports handled by the numerous ports in this waterway. As with most ports, there is a significant, recurring expense associated with dredging the navigation channels to the authorized depths. In an effort to determine the impact of channel enlargements (“the project”) on dredging volumes, a numerical model study was performed. The advantage of a numerical model study is the ability to isolate individual system modifications and associated impacts in terms of dredging volumes. Five years (1985, 1995, 1996, 2011, and 2012) were simulated for both the with- and without-project conditions to determine the impact of the channel deepening on the dredging requirements for a wide range of meteorological conditions including storm events. The numerical model results were analyzed to provide insight into which locations will experience increased/decreased deposition and quantify the amount of increase/decrease for a given channel reach. The model results indicate a relatively minor increase in the total dredge volumes for the NYNJH with the increase being insignificant in comparison to the natural variability in dredge volumes across years.

**DISCLAIMER:** The contents of this report are not to be used for advertising, publication, or promotional purposes. Citation of trade names does not constitute an official endorsement or approval of the use of such commercial products. All product names and trademarks cited are the property of their respective owners. The findings of this report are not to be construed as an official Department of the Army position unless so designated by other authorized documents.

**DESTROY THIS REPORT WHEN NO LONGER NEEDED. DO NOT RETURN IT TO THE ORIGINATOR.**

# Contents

<b>Abstract.....</b>	<b>ii</b>
<b>Figures and Tables.....</b>	<b>vi</b>
<b>Preface .....</b>	<b>xxiv</b>
<b>1 Introduction .....</b>	<b>1</b>
Background.....	1
Objective .....	3
Approach .....	3
<b>2 Description of Hudson-Raritan Estuary.....</b>	<b>4</b>
History of navigation improvements.....	4
Previous analysis .....	4
Processes of importance .....	5
<i>Tidal energy .....</i>	<i>5</i>
<i>River inflows.....</i>	<i>5</i>
<i>Municipal wastewater treatment facility discharges .....</i>	<i>13</i>
<i>Ship traffic impacts.....</i>	<i>13</i>
<i>Salinity intrusion and baroclinic circulation .....</i>	<i>14</i>
<i>Sedimentation regimes .....</i>	<i>14</i>
<b>3 Technical Approach .....</b>	<b>17</b>
Hydrodynamics .....	17
Sediment transport .....	17
Wave energy.....	18
Meteorological impacts.....	18
Extreme events .....	19
Model simulation approach .....	19
<b>4 Numerical Models .....</b>	<b>21</b>
Adaptive Hydraulics (AdH).....	21
Sediment transport library (SEDLIB).....	22
STWAVE .....	22
<i>Code description .....</i>	<i>22</i>
<i>Execution .....</i>	<i>23</i>
Model coupling .....	24
<b>5 Model Development.....</b>	<b>26</b>
Mesh development.....	26
<i>Model domain .....</i>	<i>26</i>
<i>Mesh resolution .....</i>	<i>29</i>
<i>Bathymetric data.....</i>	<i>35</i>
Boundary conditions .....	40

<i>Riverine flows</i> .....	41
<i>Wastewater treatment facility flows</i> .....	59
<i>Tidal specification</i> .....	61
<i>Wind and pressure specification</i> .....	70
<i>Wave model offshore boundary spectra</i> .....	72
<i>Simulated sediment classes</i> .....	73
<i>Sediment bed initialization</i> .....	77
<b>6 Dredging History</b> .....	<b>93</b>
Dredging for the 45 ft project .....	93
<i>Lower New York Harbor</i> .....	93
<i>Upper Bay</i> .....	94
<i>Ambrose Channel</i> .....	94
Development of maintenance volumes by e4sciences.....	99
<b>7 Description of Project</b> .....	<b>101</b>
<b>8 Model Validation</b> .....	<b>104</b>
Model simulations .....	105
Sources of model uncertainty and consequences .....	105
Two-dimensional (2D) tidal harmonic comparisons .....	107
<i>Hudson River</i> .....	108
<i>East River and Long Island Sound</i> .....	111
<i>Staten Island</i> .....	113
<i>Hackensack River</i> .....	115
<i>Passaic River</i> .....	118
<i>Raritan River</i> .....	120
<i>Conclusion for tidal harmonic verification</i> .....	122
Three-dimensional (3D) hydrodynamic comparisons.....	122
<i>Quantitative comparisons</i> .....	122
<i>Qualitative comparisons</i> .....	135
Wave model validation .....	139
3D salinity transport comparisons .....	149
<i>Quantitative comparisons</i> .....	149
<i>Qualitative comparisons</i> .....	171
3D sediment transport comparisons .....	172
<i>Dredge volume comparisons</i> .....	172
<i>Sediment core comparisons</i> .....	178
<i>Qualitative sediment flux comparisons</i> .....	194
<b>9 With-Project and Without-Project Comparisons</b> .....	<b>198</b>
Lower Bay results .....	199
Newark Bay, Kill van Kull, and Upper Bay results.....	208
Arthur Kill and Raritan Bay results .....	217
Average dredge volumes for all reaches .....	225
Variation in dredge volumes for the simulated years.....	230

Wave impacts due to channel deepening.....	230
<b>10 Extreme Event Analysis .....</b>	<b>238</b>
<b>11 Sensitivity Simulations .....</b>	<b>246</b>
Sewage flow sensitivity.....	246
Diffusion specification sensitivity .....	246
Friction specification sensitivity.....	247
Wind wave sensitivity .....	247
Inflow sensitivity .....	247
Sea level rise sensitivity .....	247
Initial bed specification .....	247
Model results.....	248
<b>12 Conclusions .....</b>	<b>254</b>
<b>References.....</b>	<b>256</b>
<b>Appendix A: Ungauged Flows on the Hudson River.....</b>	<b>262</b>
<b>Appendix B: NOAA Tide Gauge Information.....</b>	<b>266</b>
<b>Appendix C: Sediment Core Comparisons.....</b>	<b>270</b>
<b>Appendix D: Results for 1985 .....</b>	<b>284</b>
<b>Appendix E: Results for 1996.....</b>	<b>310</b>
<b>Appendix F: Results for 2011.....</b>	<b>336</b>
<b>Appendix G: Results for 2012 .....</b>	<b>362</b>
<b>Appendix H: Difference Plots for the With- and Without-Project Bed Shears, Bottom Layer Salinity, Bottom Layer Fine Sediment Concentrations, and Bottom Layer Sand Concentrations.....</b>	<b>388</b>
<b>Unit Conversion Factors.....</b>	<b>419</b>
<b>Acronyms and Abbreviations.....</b>	<b>420</b>
<b>Report Documentation Page</b>	

# Figures and Tables

## Figures

Figure 1. Study area.....	2
Figure 2. River inflow locations. ....	7
Figure 3. River inflow locations, including the Hudson River. ....	8
Figure 4. Average daily river inflow statistics for the Hudson River at Green Island.....	9
Figure 5. Average daily river inflow statistics for the Hackensack River. ....	9
Figure 6. Average daily river inflow statistics for the Passaic River. ....	10
Figure 7. Average daily river inflow statistics for the Saddle River. ....	10
Figure 8. Average daily river inflow statistics for the Third River. ....	11
Figure 9. Average daily river inflow statistics for the Rahway River. ....	11
Figure 10. Average daily river inflow statistics for the Raritan River.....	12
Figure 11. Average daily river inflow statistics for the South River. ....	12
Figure 12. Average daily river inflow statistics for Lawrence Brook.....	13
Figure 13. Diagram of the solution steps.....	25
Figure 14. Model domain outlined with red line.....	26
Figure 15. NOAA model domain used for development of vertical tidal datum in New York area (NOAA 2008). ....	27
Figure 16. STWAVE model domain. ....	28
Figure 17. AdH numerical model mesh. ....	30
Figure 18. Mesh resolution in the NYNJH area. ....	31
Figure 19. Mesh resolution in the Upper Bay and Newark Bay area. ....	31
Figure 20. Vertical mesh resolution.....	32
Figure 21. Vertical mesh resolution in the study areas. ....	33
Figure 22. STWAVE domain indicated by black box overlaid on AdH domain. ....	35
Figure 23. Bathymetric model for 2004 from e4sciences.....	37
Figure 24. ADCIRC comprehensive model mesh resolution in the Delaware Bay to Nantucket area including New York Bight.....	38
Figure 25. ADCIRC comprehensive model depths, from -20 m mean sea level (MSL) (red) to 100 m (blue).....	38
Figure 26. AdH mesh bathymetry. ....	39
Figure 27. AdH without-project mesh bathymetry in the NYNJH.....	40
Figure 28. Annual river discharges for Hudson River for simulation years 1985, 1995, 1996, 2011, and 2012 compared to the minimum and maximum discharges. ....	41
Figure 29. Annual river discharges for Hackensack River for simulation years 1985, 1995, 1996, 2011, and 2012 compared to the minimum and maximum discharges. ....	42

Figure 30. Annual river discharges for Passaic River for simulation years 1985, 1995, 1996, 2011, and 2012 compared to the minimum and maximum discharges.....	42
Figure 31. Annual river discharges for Saddle River for simulation years 1985, 1995, 1996, 2011, and 2012 compared to the minimum and maximum discharges.....	43
Figure 32. Annual river discharges for Third River for simulation years 1985, 1995, 1996, 2011, and 2012 compared to the minimum and maximum discharges.....	43
Figure 33. Annual river discharges for Rahway River for simulation years 1985, 1995, 1996, 2011, and 2012 compared to the minimum and maximum discharges.....	44
Figure 34. Annual river discharges for Raritan River for simulation years 1985, 1995, 1996, 2011, and 2012 compared to the minimum and maximum discharges.....	44
Figure 35. Annual river discharges for Lawrence Brook for simulation years 1985, 1995, 1996, 2011, and 2012 compared to the minimum and maximum discharges.....	45
Figure 36. Annual river discharges for the South River for simulation years 1985, 1995, 1996, 2011, and 2012 compared to the minimum and maximum discharges.....	45
Figure 37. Cumulative frequency of average annual Hudson River discharge from 1947 through 2014 compared to model simulation years.....	46
Figure 38. Schematic of confluence of Mohawk River and Hudson River.....	49
Figure 39. Aerial Image of confluence of Mohawk and Hudson Rivers.....	50
Figure 40. Percentiles of sediment concentration for Hudson River at Waterford.....	51
Figure 41. Percentiles of sediment concentration for Mohawk River at Cohoes, NY.....	52
Figure 42. Estimation of 2011 SSC at Hudson River at Green Island via Equation 5.....	53
Figure 43. Estimation of 2012 SSC at Hudson River at Green Island via Equation 5.....	53
Figure 44. Relationship of flow-weighted suspended sediment concentration with nondimensional river discharge for the Hudson River at Green Island.....	54
Figure 45. Estimation of the SSC for 1985 using the regression shown in Figure 44.....	55
Figure 46. Estimation of the SSC for 1995 using the regression shown in Figure 44.....	55
Figure 47. Estimation of the SSC for 1996 using the regression shown in Figure 44.....	56
Figure 48. Secondary tributary SSC data as a function of the nondimensional river discharge.....	57
Figure 49. Time series of suspended sediment inflow boundary conditions for the 2012 simulation year.....	58

Figure 50. Grain size distribution used in the tributary inflows as a function of the nondimensional discharge. ....	59
Figure 51. Wastewater facility discharge locations. ....	60
Figure 52. ADCIRC East Coast tidal database model grid.....	62
Figure 53. Boundary condition locations (squares) for extraction of tidal harmonics from ADCIRC Tidal Database. ....	63
Figure 54. Variation of the nine ADCIRC tidal harmonic amplitudes along the AdH model boundary.....	64
Figure 55. Variation in the nine ADCIRC tidal harmonic phases along the AdH ocean tidal boundary. ....	64
Figure 56. Variation in the NOAA tidal harmonic amplitudes for the tidal constituents not included in the ADCIRC database. ....	65
Figure 57. Variation in the NOAA tidal harmonic phases for the tidal constituents not included in the ADCIRC database. ....	66
Figure 58. Comparison of tidal elevation time series in 1995 between Atlantic City, NJ, and Nantucket Island, MA, for the purpose of extracting the tidal residual series. ....	67
Figure 59. Details of the 1995 tidal time series for January. ....	67
Figure 60. Development of the residual tidal signal for AdH model.....	68
Figure 61. Result of using the combined ADCIRC and NOAA harmonics. The NOAA predicted tides at Sandy Hook are compared with the AdH model driven with harmonics only.....	69
Figure 62. Comparison of modeled versus observed tidal signal at Sandy Hook when driving the model with tidal harmonics and meteorological residuals. ....	69
Figure 63. Locations of WIS wind/pressure values in relation to the AdH model domain.....	71
Figure 64. Location of NDBC 44025. The gray point is the actual buoy location whereas the black point is the assigned location for the STWAVE model.....	73
Figure 65. SEDFLUME results for core sample in Newark Bay. ....	76
Figure 66. Sediment classifications developed by e4sciences and spatial variability within the harbor. ....	78
Figure 67. Example of the methodology used to approximate particle size distribution classifications provided by e4sciences (class number 2, clayey silt). ....	80
Figure 68. Particle size distribution approximations for all classifications developed by e4sciences. ....	81
Figure 69. Location of sediment characterization sampling from the combined LISSDB and ECSTDB sediment databases. The percent sand is color coded for each station. ....	82
Figure 70. Refinement of sediment class 1 for consistency between e4sciences and LISSDB/ECSTDB. ....	83
Figure 71. Refinement of sediment class 2 for consistency between e4sciences and LIS/ECST databases.....	84
Figure 72. Refinement of sediment class 3 for consistency between e4sciences and LIS/ECST databases.....	84



Figure 73. Refinement of sediment class 4 for consistency between e4sciences and LIS/ECST databases.....	85
Figure 74. Refinement of sediment class 5 for consistency between e4sciences and LIS/ECST databases.....	85
Figure 75. Refinement of sediment class 6 for consistency between e4sciences and LIS/ECST databases.....	86
Figure 76. Refinement of sediment class 7 for consistency between e4sciences and LIS/ECST databases.....	86
Figure 77. Refinement of sediment class 8 for consistency between e4sciences and LIS/ECST databases.....	87
Figure 78. Refinement of sediment class 9 for consistency between e4sciences and LIS/ECST databases.....	87
Figure 79. Refinement of sediment class 10 for consistency between e4sciences and LIS/ECST databases.....	88
Figure 80. Refinement of sediment class 11 for consistency between e4sciences and LIS/ECST databases.....	88
Figure 81. Refinement of sediment class 12 for consistency between e4sciences and LIS/ECST databases.....	89
Figure 82. Refinement of sediment class 13 for consistency between e4sciences and LIS/ECST databases.....	89
Figure 83. Summary of defined sediment classification distributions used in AdH numerical model.....	90
Figure 84. Sediment classifications used in the AdH numerical sediment transport model within the harbor (see color bars in Figure 66 and Figure 85). ....	91
Figure 85. Sediment classifications used in the AdH numerical sediment transport model within the harbor and Long Island Sound. ....	92
Figure 86. Commonly dredged channels for NYNJH.....	93
Figure 87. Navigation buoys for the 45 ft project. ....	95
Figure 88. Distribution of Ambrose Channel dredging for the 45 ft project (1940–1982).....	96
Figure 89. Average annual sedimentation rate derived from dredging volumes for 45 ft project.....	97
Figure 90. Prototype dredging frequencies, 1961–1984. ....	98
Figure 91. Without-project bathymetry. ....	102
Figure 92. With-project (channel deepening) bathymetry. ....	103
Figure 93. Location of NOAA tide stations with general tidal characteristics defined.....	108
Figure 94. Hudson River analysis locations.....	109
Figure 95. Tidal propagation for the times of high and low waters up the Hudson River for the low-flow tidal harmonic simulation. ....	110
Figure 96. Tidal range propagation up the Hudson River for the low-flow tidal harmonic simulation. ....	110
Figure 97. East River analysis locations. ....	111
Figure 98. Long Island sound analysis locations. ....	112

Figure 99. Tidal propagation for the times of high and low waters up the East River and through Long Island Sound for the low-flow tidal harmonic simulation.....	112
Figure 100. Tidal range propagation up the East River and through Long Island Sound for the low-flow tidal harmonic simulation.....	113
Figure 101. Staten Island analysis locations.....	114
Figure 102. Tidal propagation for the times of high and low waters around Staten Island through Kill van Kull and Arthur Kill for the low-flow tidal harmonic simulation.....	114
Figure 103. Tidal range propagation around Staten Island through Kill van Kull and Arthur Kill for the low-flow tidal harmonic simulation. ....	115
Figure 104. Hackensack River analysis locations.....	116
Figure 105. Tidal propagation for the times of high and low waters from Sandy Hook through Kill van Kull and up the Hackensack River for the low-flow tidal harmonic simulation. ....	117
Figure 106. Tide range profile from Sandy Hook through Kill van Kull and up the Hackensack River for the low-flow tidal harmonic simulation. ....	117
Figure 107. Passaic River analysis locations. ....	118
Figure 108. Tidal propagation for the times of high and low waters from Sandy Hook through Kill van Kull and up the Passaic River for the low-flow tidal harmonic simulation. ....	119
Figure 109. Tide range profile from Sandy Hook through Kill van Kull and up the Passaic River for the low-flow tidal harmonic simulation. ....	119
Figure 110. Raritan Bay/River analysis locations. ....	120
Figure 111. Tidal propagation for the times of high and low waters from Sandy Hook through Raritan Bay and up the Raritan River for the low-flow tidal harmonic simulation. ....	121
Figure 112. Tide range profile from Sandy Hook through Raritan Bay and up the Raritan River for the low-flow tidal harmonic simulation.....	121
Figure 113. Hydrodynamic validation locations. ....	123
Figure 114. Water surface elevation comparison plot for Atlantic City (1995). ....	124
Figure 115. Water surface elevation comparison plot for Bergen Point (1995).....	125
Figure 116. Water surface elevation comparison plot for Bridgeport (1995). ....	126
Figure 117. Water surface elevation comparison plot for Eatons Neck (1995).....	127
Figure 118. Water surface elevation comparison plot for Long Neck Point (1995).....	128
Figure 119. Water surface elevation comparison plot for Montauk (1995).....	129
Figure 120. Water surface elevation comparison plot for New London (1995). ....	130
Figure 121. Water surface elevation comparison plot for Sandy Hook (1995). ....	131
Figure 122. Water surface elevation comparison plot for The Battery (1995). ....	132
Figure 123. Water surface elevation comparison plot for Willets Point.....	133
Figure 124. Velocity comparison locations. ....	136
Figure 125. Location of ALSN6 and NDBC 44065.....	140
Figure 126. Time series of STWAVE results versus measurements at ALSN6 for 1995.....	141

Figure 127. Scatter plots for 1995 of significant wave height (top) and mean period (bottom). .....	142
Figure 128. Time series of STWAVE results versus measurements at ALSN6 for 1996. ....	143
Figure 129. Scatter plots for 1996 of significant wave height (top) and mean period (bottom). ....	144
Figure 130. Time series of STWAVE results versus measurements at NDBC 44065 for 2011.....	145
Figure 131. Scatter plots for 2011 of significant wave height (top) and mean period (bottom). ....	146
Figure 132. Time series of STWAVE results versus measurements at 44065 for 2012. ....	147
Figure 133. Scatter plots for 2012 of significant wave height (top) and mean period (bottom). ....	148
Figure 134. Salinity observation locations.....	150
Figure 135. Salinity distribution at BB4. ....	151
Figure 136. Salinity distribution at E2. ....	151
Figure 137. Salinity distribution at E4.....	152
Figure 138. Salinity distribution at E6. ....	152
Figure 139. Salinity distribution at E7. ....	153
Figure 140. Salinity distribution at E8. ....	153
Figure 141 Salinity distribution at E10. ....	154
Figure 142. Salinity distribution at E11.....	154
Figure 143. Salinity distribution at E14.....	155
Figure 144. Salinity distribution at E15.....	155
Figure 145. Salinity distribution at G2.....	156
Figure 146. Salinity distribution at H3.....	156
Figure 147. Salinity distribution at J1.....	157
Figure 148. Salinity distribution at J2.....	157
Figure 149. Salinity distribution at J3.....	158
Figure 150. Salinity distribution at J5.....	158
Figure 151. Salinity distribution at J5D. ....	159
Figure 152. Salinity distribution at J7. ....	159
Figure 153. Salinity distribution at J8.....	160
Figure 154. Salinity distribution J9A.....	160
Figure 155. Salinity distribution at J10. ....	161
Figure 156. Salinity distribution at J11. ....	161
Figure 157. Salinity distribution at K1. ....	162
Figure 158. Salinity distribution at K2.....	162
Figure 159. Salinity distribution at K3.....	163
Figure 160. Salinity distribution at K4.....	163

Figure 161. Salinity distribution at K5.....	164
Figure 162. Salinity distribution at K5A. ....	164
Figure 163. Salinity distribution at K6.....	165
Figure 164. Salinity distribution at K6.....	165
Figure 165. Salinity distribution at N3B. ....	166
Figure 166. Salinity distribution at N4.....	166
Figure 167. Salinity distribution at N5. ....	167
Figure 168. Salinity distribution at N6.....	167
Figure 169. Salinity distribution at N7. ....	168
Figure 170. Salinity distribution at N8.....	168
Figure 171. Salinity distribution at N9. ....	169
Figure 172. Salinity distribution at N9A. ....	169
Figure 173. Salinity distribution at N16. ....	170
Figure 174. Salinity distribution at PB2. ....	170
Figure 175. Salinity distribution at PB3.....	171
Figure 176. Stratification levels on the Hudson River.....	172
Figure 177. Dredge volume comparisons (without project versus historical rates). ....	174
Figure 178. Variation in dredge volumes for the five simulated years (model results).....	175
Figure 179. Statistics for the model range of dredging estimates. ....	176
Figure 180. Sediment core locations in Upper Bay.....	179
Figure 181. Sediment bed composition comparisons at Location A-2U for 2011 (top) and 2012 (bottom). ....	180
Figure 182. Sediment bed composition comparisons at Location E-1U for 2011 (top) and 2012 (bottom). ....	181
Figure 183. Sediment bed composition comparisons at Location E-4U for 2011 (top) and 2012 (bottom). ....	182
Figure 184. Sediment core locations in western Kill van Kull and southern Newark Bay.....	183
Figure 185. Sediment bed composition comparisons at Location W-4BU for 2011 (top) and 2012 (bottom). ....	184
Figure 186. Sediment bed composition comparisons at Location W-6AU for 2011 (top) and 2012 (bottom). ....	185
Figure 187. Sediment bed composition comparisons at Location W-3AU for 2011 (top) and 2012 (bottom). ....	186
Figure 188. Sediment core locations in Newark Bay.....	187
Figure 189. Sediment bed composition comparisons at Location MNB-3 for 2011 (top) and 2012 (bottom). ....	188
Figure 190. Sediment bed composition comparisons at Location MNB-4B for 2011 (top) and 2012 (bottom).....	189
Figure 191. Sediment bed composition comparisons at Location MNB-5A for 2011 (top) and 2012 (bottom).....	190

Figure 192. Sediment core locations in the Port Jersey channel.....	191
Figure 193. Sediment bed composition comparisons at Location PJ-1 for 2011 (top) and 2012 (bottom). ....	192
Figure 194. Sediment bed composition comparisons at Location PJ-4 for 2011 (top) and 2012 (bottom). ....	193
Figure 195. The black lines represent extracted sand transport locations. The lower black line is at the George Washington Bridge.....	195
Figure 196. Without-project (top) and with-project (bottom) average shear stresses, Pa (1995). ....	199
Figure 197. Without-project (top) and with-project (bottom) average bottom salinity, ppt (1995). ....	200
Figure 198. Without-project (top) and with-project (bottom) average fine sediment bottom concentrations, ppm (1995). ....	201
Figure 199. Without-project (top) and with-project (bottom) average sand bottom concentrations, ppm (1995). ....	202
Figure 200. Without-project (top) and with-project (bottom) bed displacement, m (1995). ....	203
Figure 201. Without-project (top) and with-project (bottom) fine-sediment accumulation, kg/m <sup>2</sup> (1995), ....	204
Figure 202. Without-project (top) and with-project (bottom) sand accumulation, kg/m <sup>2</sup> (1995). ....	205
Figure 203. Dredge with-project/without-project percent differences (1995). ....	206
Figure 204. Without-project (top) and with-project (bottom) average shear stresses, Pa (1995). ....	208
Figure 205. Without-project (top) and with-project (bottom) average bottom salinity, ppt (1995). ....	209
Figure 206. Without-project (top) and with-project (bottom) average fine bottom sediment concentrations, ppm (1995). ....	210
Figure 207. Without-project (top) and with-project (bottom) average sand bottom concentrations, ppm (1995). ....	211
Figure 208. Without-project (top) and with-project (bottom) bed displacement, m (1995). ....	212
Figure 209. Without-project (top) and with-project (bottom) fine sediment accumulation, kg/m <sup>2</sup> (1995). ....	213
Figure 210. Without-project (top) and with-project (bottom) sand accumulation, kg/m <sup>2</sup> (1995). ....	214
Figure 211. Dredge with-project/without-project percent differences (1995). ....	215
Figure 212. Without-project (top) and with-project (bottom) average shear stresses, Pa (1995). ....	217
Figure 213. Without-project (top) and with-project (bottom) average bottom salinity, ppt (1995). ....	218
Figure 214. Without-project (top) and with-project (bottom) average fine sediment bottom concentrations, ppm (1995). ....	219

Figure 215. Without-project (top) and with-project (bottom) average sand bottom concentrations, ppm (1995). .....	220
Figure 216. Without-project (top) and with-project (bottom) bed displacement, m (1995). .....	221
Figure 217. Without-project (top) and with-project (bottom) fine sediment accumulation, kg/m <sup>2</sup> (1995). .....	222
Figure 218. Without-project (top) and with-project (bottom) sand accumulation, kg/m <sup>2</sup> (1995). .....	223
Figure 219. Dredge with-project/without-project percent differences (1995). .....	224
Figure 220. Channel deepening in STWAVE domain. ....	231
Figure 221. Effect of channel deepening on mean significant wave height for 1985. ....	232
Figure 222. Effect of channel deepening on mean significant wave height for 1995. ....	232
Figure 223. Effect of channel deepening on mean significant wave height for 1996. ....	233
Figure 224. Effect of channel deepening on mean significant wave height for 2011. ....	233
Figure 225. Effect of channel deepening on mean significant wave height for 2012. ....	234
Figure 226. Effect of channel deepening on max significant wave height for 1985. ....	235
Figure 227. Effect of channel deepening on max significant wave height for 1995. ....	235
Figure 228. Effect of channel deepening on max significant wave height for 1996. ....	236
Figure 229. Effect of channel deepening on max significant wave height for 2011. ....	236
Figure 230. Effect of channel deepening on max significant wave height for 2012. ....	237
Figure 231. Three points to analyze for the duration of storm impacts on sediment concentrations. ....	238
Figure 232. Hudson River bottom water layer fine sediment concentrations. ....	239
Figure 233. Upper Bay bottom water layer fine sediment concentrations. ....	239
Figure 234. Newark Bay bottom water layer fine sediment concentrations. ....	240
Figure 235. Hurricane impacts of dredge volumes in the without-project configuration. ....	241
Figure 236. Hurricane impacts of dredge volumes in the with-project configuration. ....	242
Figure 237. With-project versus without-project hurricane impacts. ....	243
Figure 238. Sensitivity simulation results for 1995 for the without-project configuration. ....	252
Figure 239. Sensitivity simulation results for 1995 for the with-project configuration. ....	253

Figure 240. Additional tributary inflows below the Hudson River at Green Island for 1985. ....	263
Figure 241. Additional tributary inflows below the Hudson River at Green Island for 1995. ....	263
Figure 242. Additional tributary inflows below the Hudson River at Green Island for 1996. ....	264
Figure 243. Additional tributary inflows below the Hudson River at Green Island for 2011.....	264
Figure 244. Additional tributary inflows below the Hudson River at Green Island for 2012.....	265
Figure 245. Sediment bed composition comparisons at location A-1U for 2011 (top) and 2012 (bottom). ....	270
Figure 246. Sediment bed composition comparisons at location A-3U for 2011 (top) and 2012 (bottom). ....	271
Figure 247. Sediment bed composition comparisons at Location A-4U for 2011 (top) and 2012 (bottom). ....	272
Figure 248. Sediment bed composition comparisons at location A-5U for 2011 (top) and 2012 (bottom). ....	273
Figure 249. Sediment bed composition comparisons at location E-2U for 2011 (top) and 2012 (bottom). ....	274
Figure 250. Sediment bed composition comparisons at location E-3U for 2011 (top) and 2012 (bottom). ....	275
Figure 251. Sediment bed composition comparisons at location W-3BU for 2011 (top) and 2012 (bottom). ....	276
Figure 252. Sediment bed composition comparisons at location W-3U for 2011 (top) and 2012 (bottom). ....	277
Figure 253. Sediment bed composition comparisons at location W-4AU for 2011 (top) and 2012 (bottom). ....	278
Figure 254. Sediment bed composition comparisons at location W-4U for 2011 (top) and 2012 (bottom). ....	279
Figure 255. Sediment bed composition comparisons at location W-5AU for 2011 (top) and 2012 (bottom). ....	280
Figure 256. Sediment bed composition comparisons at location W-5BU for 2011 (top) and 2012 (bottom). ....	281
Figure 257. Sediment bed composition comparisons at location W-5U for 2011 (top) and 2012 (bottom). ....	282
Figure 258. Sediment bed composition comparisons at location W-6U for 2011 (top) and 2012 (bottom). ....	283
Figure 259. Without-project (top) and with-project (bottom) average shear stresses, Pa (1985). ....	284
Figure 260. Without-project (top) and with-project (bottom) average bottom salinity, ppt (1985). ....	285
Figure 261. Without-project (top) and with-project (bottom) average fine sediment bottom concentrations, ppm (1985). ....	286

Figure 262. Without-project (top) and with-project (bottom) average sand bottom concentrations, ppm (1985). .....	287
Figure 263. Without-project (top) and with-project (bottom) bed displacement, m (1985). .....	288
Figure 264. Without-project (top) and with-project (bottom) fine sediment accumulation, kg/m <sup>2</sup> (1985). .....	289
Figure 265. Without-project (top) and with-project (bottom) sand accumulation, kg/m <sup>2</sup> (1985). .....	290
Figure 266. Dredge with-project/without-project percent differences (1985). .....	291
Figure 267. Without-project (top) and with-project (bottom) average shear stresses, Pa (1985). .....	292
Figure 268. Without-project (top) and with-project (bottom) average bottom salinity, ppt (1985). .....	293
Figure 269. Without-project (top) and with-project (bottom) average fine sediment bottom concentrations, ppm (1985). .....	294
Figure 270. Without-project (top) and with-project (bottom) average sand bottom concentrations, ppm (1985). .....	295
Figure 271. Without-project (top) and with-project (bottom) bed displacement, m (1985). .....	296
Figure 272. Without-project (top) and with-project (bottom) fine sediment accumulation, kg/m <sup>2</sup> (1985). .....	297
Figure 273. Without-project (top) and with-project (bottom) sand accumulation, kg/m <sup>2</sup> (1985). .....	298
Figure 274. Dredge with-project/without-project percent differences (1985). .....	299
Figure 275. Without-project (top) and with-project (bottom) average shear stresses, Pa (1985). .....	301
Figure 276. Without-project (top) and with-project (bottom) average bottom salinity, ppt (1985). .....	302
Figure 277. Without-project (top) and with-project (bottom) average fine sediment bottom concentrations, ppm (1985). .....	303
Figure 278. Without-project (top) and with-project (bottom) average sand bottom concentrations, ppm (1985). .....	304
Figure 279. Without-project (top) and with-project (bottom) bed displacement, m (1985). .....	305
Figure 280. Without-project (top) and with-project (bottom) fine sediment accumulation, kg/m <sup>2</sup> (1985). .....	306
Figure 281. Without-project (top) and with-project (bottom) sand accumulation, kg/m <sup>2</sup> (1985). .....	307
Figure 282. Dredge with-project/without-project percent differences (1985). .....	308
Figure 283. Without-project (top) and with-project (bottom) average shear stresses, Pa (1996). .....	310
Figure 284. Without-project (top) and with-project (bottom) average bottom salinity, ppt (1996). .....	311



Figure 285. Without-project (top) and with-project (bottom) average fine sediment bottom concentrations, ppm (1996). .....	312
Figure 286. Without-project (top) and with-project (bottom) average sand bottom concentrations, ppm (1996). .....	313
Figure 287. Without-project (top) and with-project (bottom) bed displacement, m (1996). .....	314
Figure 288. Without-project (top) and with-project (bottom) fine sediment accumulation, kg/m <sup>2</sup> (1996). .....	315
Figure 289. Without-project (top) and with-project (bottom) sand accumulation, kg/m <sup>2</sup> (1996). .....	316
Figure 290. Dredge with-project/without-project percent differences (1996). .....	317
Figure 291. Without-project (top) and with-project (bottom) average shear stresses, Pa (1996). .....	318
Figure 292. Without-project (top) and with-project (bottom) average bottom salinity, ppt (1996). .....	319
Figure 293. Without-project (top) and with-project (bottom) average fine sediment bottom concentrations, ppm (1996). .....	320
Figure 294. Without-project (top) and with-project (bottom) average sand bottom concentrations, ppm (1996). .....	321
Figure 295. Without-project (top) and with-project (bottom) bed displacement, m (1996). .....	322
Figure 296. Without-project (top) and with-project (bottom) fine sediment accumulation, kg/m <sup>2</sup> (1996). .....	323
Figure 297. Without-project (top) and with-project (bottom) sand Accumulation, kg/m <sup>2</sup> (1996). .....	324
Figure 298. Dredge with-project/without-project percent differences (1996). .....	325
Figure 299. Without-project (top) and with-project (bottom) average shear stresses, Pa (1996). .....	327
Figure 300. Without-project (top) and with-project (bottom) average bottom salinity, ppt (1996). .....	328
Figure 301. Without-project (top) and with-project (bottom) average fine sediment bottom concentrations, ppm (1996). .....	329
Figure 302. Without-project (top) and with-project (bottom) average sand bottom concentrations, ppm (1996). .....	330
Figure 303. Without-project (top) and with-project (bottom) bed displacement, m (1996). .....	331
Figure 304. Without-project (top) and with-project (bottom) fine sediment accumulation, kg/m <sup>2</sup> (1996). .....	332
Figure 305. Without-project (top) and with-project (bottom) sand Accumulation, kg/m <sup>2</sup> (1996). .....	333
Figure 306. Dredge with-project/without-project percent differences (1996). .....	334
Figure 307. Without-project (top) and with-project (bottom) average shear stresses, Pa (2011). .....	336

Figure 308. Without-project (top) and with-project (bottom) average bottom salinity, ppt (2011).....	337
Figure 309. Without-project (top) and with-project (bottom) average fine sediment bottom concentrations, ppm (2011). ....	338
Figure 310. Without-project (top) and with-project (bottom) average sand bottom concentrations, ppm (2011). ....	339
Figure 311. Without-project (top) and with-project (bottom) bed displacement, m (2011).....	340
Figure 312. Without-project (top) and with-project (bottom) fine sediment accumulation, kg/m <sup>2</sup> (2011).....	341
Figure 313. Without-project (top) and with-project (bottom) sand accumulation, kg/m <sup>2</sup> (2011). ....	342
Figure 314. Dredge with-project/without-project percent differences (2011). ....	343
Figure 315. Without-project (top) and with-project (bottom) average shear stresses, Pa (2011). ....	344
Figure 316. Without-project (top) and with-project (bottom) average bottom salinity, ppt (2011).....	345
Figure 317. Without-project (top) and with-project (bottom) average fine sediment bottom concentrations, ppm (2011). ....	346
Figure 318. Without-project (top) and with-project (bottom) average sand bottom concentrations, ppm (2011). ....	347
Figure 319. Without-project (top) and with-project (bottom) bed displacement, m (2011). ....	348
Figure 320. Without-project (top) and with-project (bottom) fine sediment accumulation, kg/m <sup>2</sup> (2011).....	349
Figure 321. Without-project (top) and with-project (bottom) sand accumulation, kg/m <sup>2</sup> (2011). ....	350
Figure 322. Dredge with-project/without-project percent differences (2011).....	351
Figure 323. Without-project (top) and with-project (bottom) average shear stresses, Pa (2011). ....	353
Figure 324. Without-project (top) and with-project (bottom) average bottom salinity, ppt (2011).....	354
Figure 325. Without-project (top) and with-project (bottom) average fine sediment bottom concentrations, ppm (2011). ....	355
Figure 326. Without-project (top) and with-project (bottom) average sand bottom concentrations, ppm (2011). ....	356
Figure 327. Without-project (top) and with-project (bottom) bed displacement, m (2011). ....	357
Figure 328. . Without-project (top) and with-project (bottom) fine sediment accumulation, kg/m <sup>2</sup> (2011).....	358
Figure 329. Without-project (top) and with-project (bottom) sand accumulation, kg/m <sup>2</sup> (2011). ....	359
Figure 330. Dredge With-project/without-project percent differences (2011). ....	360

Figure 331. Without-project (top) and with-project (bottom) average shear stresses, Pa (2012). .....	362
Figure 332. Without-project (top) and with-project (bottom) average bottom salinity, ppt (2012). .....	363
Figure 333. Without-project (top) and with-project (bottom) average fine sediment bottom concentrations, ppm (2012), .....	364
Figure 334. Without-project (top) and with-project (bottom) average sand bottom concentrations, ppm (2012). .....	365
Figure 335. Without-project (top) and with-project (bottom) bed displacement, m (2012). .....	366
Figure 336. Without-project (top) and with-project (bottom) fine sediment accumulation, kg/m <sup>2</sup> (2012). .....	367
Figure 337. Without-project (top) and with-project (bottom) sand accumulation, kg/m <sup>2</sup> (2012). .....	368
Figure 338. Dredge with-project/without-project percent differences (2012). .....	369
Figure 339. Without-project (top) and with-project (bottom) average shear stresses, Pa (2012). .....	370
Figure 340. Without-project (top) and with-project (bottom) average bottom salinity, ppt (2012). .....	371
Figure 341. Without-project (top) and with-project (bottom) average fine sediment bottom concentrations, ppm (2012). .....	372
Figure 342. Without-project (top) and with-project (bottom) average sand bottom concentrations, ppm (2012). .....	373
Figure 343. Without-project (top) and with-project (bottom) bed displacement, m (2012). .....	374
Figure 344. Without-project (top) and with-project (bottom) fine sediment accumulation, kg/m <sup>2</sup> (2012). .....	375
Figure 345. Without-project (top) and with-project (bottom) sand accumulation, kg/m <sup>2</sup> (2012). .....	376
Figure 346. Dredge with-project/without-project percent differences (2012). .....	377
Figure 347. Without-project (top) and with-project (bottom) average shear stresses, Pa (2012). .....	379
Figure 348. Without-project (top) and with-project (bottom) average bottom salinity, ppt (2012). .....	380
Figure 349. Without-project (top) and with-project (bottom) average fine sediment bottom concentrations, ppm (2012). .....	381
Figure 350. Without-project (top) and with-project (bottom) average sand bottom concentrations, ppm (2012). .....	382
Figure 351. Without-project (top) and with-project (bottom) bed displacement, m (2012). .....	383
Figure 352. Without-project (top) and with-project (bottom) fine sediment accumulation, kg/m <sup>2</sup> (2012). .....	384
Figure 353. Without-project (top) and with-project (bottom) sand accumulation, kg/m <sup>2</sup> (2012). .....	385

Figure 354. Dredge with-project/without-project percent differences (2012).....	386
Figure 355. With-minus without-project average bed shear stresses (N/m <sup>2</sup> ) for 1985.....	388
Figure 356. With- minus without-project average bed shear stresses (N/m <sup>2</sup> ) for 1995.....	389
Figure 357. With- minus without-project average bed shear stresses (N/m <sup>2</sup> ) for 1996.....	389
Figure 358. With- minus without-project average bed shear stresses (N/m <sup>2</sup> ) for 2011.....	390
Figure 359. With- minus without-project average bed shear stresses (N/m <sup>2</sup> ) for 2012.....	390
Figure 360. With- minus without-project average bottom layer salinity values (ppt) for 1985.....	391
Figure 361. With- minus without-project average bottom layer salinity values (ppt) for 1995.....	391
Figure 362. With- minus without-project average bottom layer salinity values (ppt) for 1996.....	392
Figure 363. With- minus without-project average bottom layer salinity values (ppt) for 2011.....	392
Figure 364. With- minus without-project average bottom layer salinity values (ppt) for 2012.....	393
Figure 365. With- minus without-project average bottom layer fine sediment concentrations (ppm) for 1985.....	393
Figure 366. With- minus without-project average bottom layer fine sediment concentrations (ppm) for 1995.....	394
Figure 367. With- minus without-project average bottom layer fine sediment concentrations (ppm) for 1996.....	394
Figure 368. With- minus without-project average bottom layer fine sediment concentrations (ppm) for 2011.....	395
Figure 369. With- minus without-project average bottom layer fine sediment concentrations (ppm) for 2012.....	395
Figure 370. With- minus without-project average bottom layer sand concentrations (ppm) for 1985.....	396
Figure 371. With- minus without-project average bottom layer sand concentrations (ppm) for 1995.....	396
Figure 372. With- minus without-project average bottom layer sand concentrations (ppm) for 1996.....	397
Figure 373. With- minus without-project average bottom layer sand concentrations (ppm) for 2011.....	397
Figure 374. With- minus without-project average bottom layer sand concentrations (ppm) for 2012.....	398
Figure 375. With- minus without-project average bed shear stresses (N/m <sup>2</sup> ) for 1985.....	399
Figure 376. With- minus without-project average bed shear stresses (N/m <sup>2</sup> ) for 1995.....	399

Figure 377. With- minus without-project average bed shear stresses (N/m <sup>2</sup> ) for 1996.....	400
Figure 378. With- minus without-project average bed shear stresses (N/m <sup>2</sup> ) for 2011.....	400
Figure 379. With- minus without-project average bed shear stresses (N/m <sup>2</sup> ) for 2012.....	401
Figure 380. With- minus without-project average bottom layer salinity values (ppt) for 1985.....	401
Figure 381. With- minus without-project average bottom layer salinity values (ppt) for 1995.....	402
Figure 382. With- minus without-project average bottom layer salinity values (ppt) for 1996.....	402
Figure 383. With- minus without-project average bottom layer salinity values (ppt) for 2011.....	403
Figure 384. With- minus without-project average bottom layer salinity values (ppt) for 2012.....	403
Figure 385. With- minus without-project average bottom layer fine sediment concentrations (ppm) for 1985.....	404
Figure 386. With- minus without-project average bottom layer fine sediment concentrations (ppm) for 1995.....	404
Figure 387. With- minus without-project average bottom layer fine sediment concentrations (ppm) for 1996.....	405
Figure 388. With- minus without-project average bottom layer fine sediment concentrations (ppm) for 2011.....	405
Figure 389. With- minus without-project average bottom layer fine sediment concentrations (ppm) for 2012.....	406
Figure 390. With- minus without-project average bottom layer sand concentrations (ppm) for 1985.....	406
Figure 391. With- minus without-project average bottom layer sand concentrations (ppm) for 1995.....	407
Figure 392. With- minus without-project average bottom layer sand concentrations (ppm) for 1996.....	407
Figure 393. With- minus without-project average bottom layer sand concentrations (ppm) for 2011.....	408
Figure 394. With- minus without-project average bottom layer sand concentrations (ppm) for 2012.....	408
Figure 395. With- minus without-project average bed shear stresses (N/m <sup>2</sup> ) for 1985.....	409
Figure 396. With- minus without-project average bed shear stresses (N/m <sup>2</sup> ) for 1995.....	409
Figure 397. With- minus without-project average bed shear stresses (N/m <sup>2</sup> ) for 1996.....	410
Figure 398. With- minus without-project average bed shear stresses (N/m <sup>2</sup> ) for 2011.....	410

Figure 399. With- minus without-project average bed shear stresses (N/m <sup>2</sup> ) for 2012. ....	411
Figure 400. With- minus without-project average bottom layer salinity values (ppt) for 1985. ....	411
Figure 401. With- minus without-project average bottom layer salinity values (ppt) for 1995. ....	412
Figure 402. With- minus without-project average bottom layer salinity values (ppt) for 1996. ....	412
Figure 403. With- minus without-project average bottom layer salinity values (ppt) for 2011. ....	413
Figure 404. With- minus without-project average bottom layer salinity values (ppt) for 2012. ....	413
Figure 405. With- minus without-project average bottom layer fine sediment concentrations (ppm) for 1985. ....	414
Figure 406. With- minus without-project average bottom layer fine sediment concentrations (ppm) for 1995. ....	414
Figure 407. With- minus without-project average bottom layer fine sediment concentrations (ppm) for 1996. ....	415
Figure 408. With- minus without-project average bottom layer fine sediment concentrations (ppm) for 2011. ....	415
Figure 409. With- minus without-project average bottom layer fine sediment concentrations (ppm) for 2012. ....	416
Figure 410. With- minus without-project average bottom layer sand concentrations (ppm) for 1985. ....	416
Figure 411. With- minus without-project average bottom layer sand concentrations (ppm) for 1995. ....	417
Figure 412. With- minus without-project average bottom layer sand concentrations (ppm) for 1996. ....	417
Figure 413. With- minus without-project average bottom layer sand concentrations (ppm) for 2011. ....	418
Figure 414. With- minus without-project average bottom layer sand concentrations (ppm) for 2012. ....	418

## Tables

Table 1. STWAVE grid properties. ....	34
Table 2. Statistics of tributary inflows for simulation years (in cms) ....	47
Table 3. Return periods for mean annual Hudson River inflows for simulation years ....	48
Table 4. Wastewater treatment discharge locations and flow rates. ....	60
Table 5. Sediment classes used in sedimentation model. ....	74
Table 6. Cohesive sediment class properties. ....	75
Table 7. Noncohesive sediment class properties. ....	76

Table 8. Preliminary particle size of New York Harbor sediments (e4sciences 2018).	79
Table 9. Ambrose Channel maintenance for 45 ft channel (1940–1982) in thousands of cy/year.	95
Table 10. Dredging volume distributions by channel reach in cy (e4sciences 2015).	100
Table 11. Error metrics for water level comparisons.	134
Table 12. Velocity comparisons in m/s. Parenthesis indicates with-project values.	136
Table 13. Kill van Kull flow comparisons.	139
Table 14. Statistics for model estimations of annual dredging volumes in cy.	177
Table 15. Hudson River sediment loads for the simulated years.	194
Table 16. Sand transport up the Hudson River Estuary (negative indicates downward transport).	196
Table 17. Kill van Kull total sediment load for the simulated years.	197
Table 18. Passaic and Hackensack River total sediment load into Newark Bay for the simulated years.	197
Table 19. Dredge volumes in Lower Bay (1995).	206
Table 20. Dredge volumes in Newark Bay, Kill van Kull, and Upper Bay (1995).	216
Table 21. Dredge volumes for Arthur Kill and Raritan Bay (1995).	225
Table 22. Average annual dredge volumes in cy by reach over the five simulated years.	226
Table 23. Storm duration of influence on sediment transport.	240
Table 24. Hurricanes Gloria, Irene, and Sandy dredge volumes, cy.	244
Table 25. With-project sensitivity simulation results.	250
Table 26. Without-project sensitivity simulation results.	251
Table 27. NOAA tidal data.	266
Table 28. Dredge volumes for Lower Bay (1985).	291
Table 29. Dredge Volumes for Newark Bay, Kill van Kull, and Upper Bay (1985).	300
Table 30. Dredge Volumes for Arthur Kill (1985).	309
Table 31. Dredge volumes for Lower Bay (1996).	317
Table 32. Dredge volumes in Newark Bay, Kill van Kull, and Upper Bay (1996).	326
Table 33. Dredge volumes for Arthur Kill and Raritan Bay (1996).	335
Table 34. Dredge volumes for Lower Bay (2011).	343
Table 35. Dredge volumes for Newark Bay, Kill van Kull, and Upper Bay (2011).	352
Table 36. Dredge volumes for Arthur Kill and Raritan Bay (2011).	361
Table 37. Dredge volumes in Lower Bay (2012).	369
Table 38. Dredge volumes in Newark Bay, Kill van Kull, and Upper Bay (2012).	378

## Preface

The work documented in this report was conducted for the US Army Corps of Engineers, New York District, under the “ERDC Sedimentation Modeling” Work Item Code 1J186F. The New York District oversight was provided by Mr. Jamal A. Sulayman, and Mr. Bryce W. Wisemiller served as the Program Manager.

At the time of publication of this report, Mr. David P. May was Acting Chief, Riverine and Estuarine Engineering Branch; and Dr. Carey Talbot was Chief, Flood and Storm Protection Division. The Deputy Director of the US Army Engineer Research and Development Center, Coastal and Hydraulics Laboratory (ERDC-CHL), was Mr. Jeffery Eckstein, and the Director was Dr. Ty V. Wamsley.

Participants in the study included multiple branches and laboratories, with the primary work being completed within the Riverine and Estuarine Engineering Branch of ERDC-CHL.

The authors acknowledge the contributions of e4sciences in compiling bathymetric data, sediment data, and historical dredge volume information in addition to its thorough review and valuable consultation throughout this study. The authors specifically acknowledge the contributions of Dr. William Murphy III, Dr. W. Bruce Ward, and Dr. Daniel Rosales Roche.

COL Teresa A. Schlosser was the Commander of ERDC, and the Director was Dr. David W. Pittman.



# 1 Introduction

## Background

The New York/New Jersey Harbor (NYNJH) is a vital resource for both the local economies of New York and New Jersey as well as the entire US economy. The Port of New York and New Jersey is the third busiest port in the United States with approximately 60.9 million tons of bulk cargo at a value of almost 48 billion US dollars (PANYNJ 2010) with 5,000 ship arrivals per year (Caplow et al. 2003). The Port supports 279,200 jobs with wages of over 11 billion US dollars and contributes more than 19 billion US dollars to the New York/New Jersey gross regional product (PANYNJ 2010).

NYNJH includes numerous navigation channels and various ports resulting in a complex system of navigation channels extending from offshore, inland to the individual ports of call. Over the years, NYNJH has evolved continuously with numerous channels being deepened and widened to better facilitate navigational safety and efficiency. One such alteration is the latest harbor deepening project to a 50 ft\* channel depth (USACE 2007). The 50 ft harbor deepening project is considered the “with-project” condition analyzed in this study with the “pre-project” representing the conditions for the 45 ft channel configuration. While a typical Panamax containership could be accommodated by a 35 ft (10 m) channel, the new generation of post-Panamax containerships requires a channel depth between 42 and 52 ft (13–16 m) (Rodrigue 2004). This necessitates the deepening of the navigation channels to accommodate these larger vessels and maintain the Port of New York/New Jersey as one of the busiest ports in the United States.

The complexity of the system includes various important processes. These processes are critical to the overall circulation within the harbor, which are

---

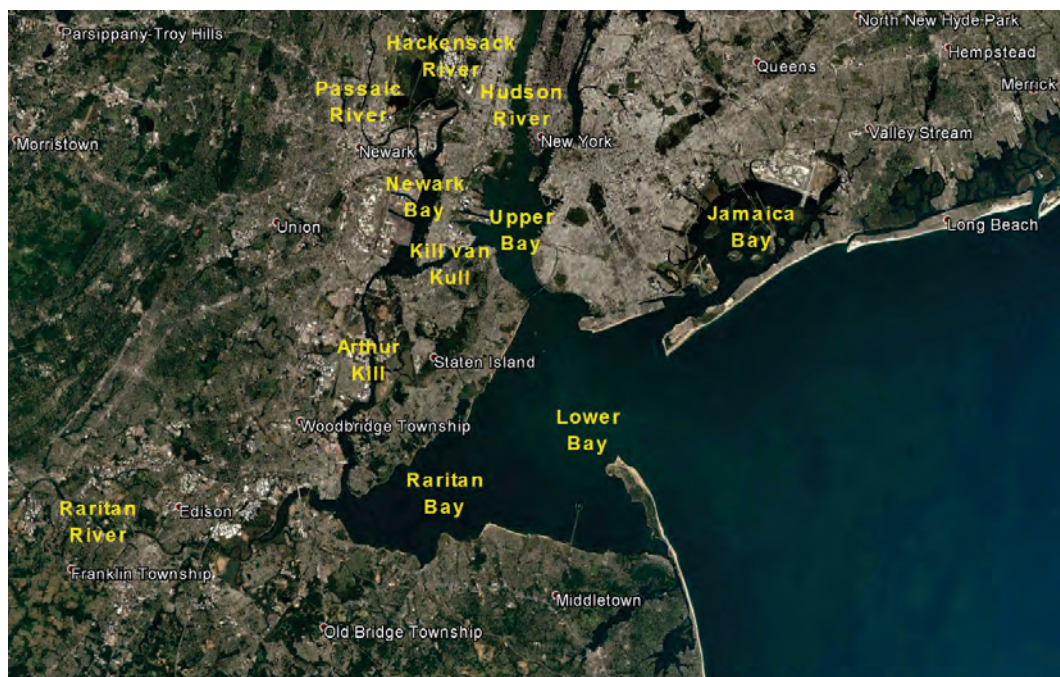
\* For a full list of the spelled-out forms of the units of measure used in this document, please refer to *US Government Publishing Office Style Manual*, 31st ed. (Washington, DC: US Government Publishing Office 2016), 248-52, <https://www.govinfo.gov/content/pkg/GPO-STYLEMANUAL-2016/pdf/GPO-STYLEMANUAL-2016.pdf>.

coupled strongly to the sediment transport and fate. Some of these include the following:

- numerous inflows (Hudson River, Passaic River, Hackensack River, Raritan River, etc.)
- large sewage outfalls
- complex hydrodynamic conditions with multiple flow pathways
- three-dimensional (3D) salinity transport
- cohesive and noncohesive sediment transport
- organic sediments with cohesive properties
- extreme storm events
- along-shore currents and sediment transport
- regular dredging operations
- deep-draft ship transit and associated bow waves.

Figure 1 provides a general study area map of the system. The inter-connectivity between the various areas and the general complexity of the system make accurate numerical modeling extremely challenging. This report will detail the numerical modeling completed as part of this study and associated results and conclusions.

Figure 1. Study area.



## **Objective**

The purpose of this study is to provide insight into the impact of the 50 ft channel deepening project on the dredging requirements in the NYNJH system as compared to the previously authorized 45 ft channel depth. The variability in the annual rate of dredging indicates significant natural variability due to irregularity in river flows and meteorological conditions. This is the primary motivation for the current numerical model study, which can isolate the navigation channel depth impacts by simulating the same conditions (tides, flows, winds, pressures, etc.) for both the pre- and post-deepening channel configurations. Analysis will include total dredge volume changes and the spatial variation in dredge requirements on a reach-by-reach basis. The resulting numerical model will also be available for future analysis for other projects as well, providing a means of evaluating system modifications in terms of hydrodynamics, salinity, and sediment transport.

## **Approach**

A 3D numerical model was developed for hydrodynamic, salinity, and sediment transport. Observational data were utilized to validate the model properly replicates the observed behavior in the real system. Five years (1985, 1995, 1996, 2011, and 2012) were simulated for both the pre- and post-deepened conditions to evaluate both the impact of the deepened navigation channels and the impact of the varying forcing conditions on yearly dredge volumes. The five years simulated high/low river flows along with large storm events (Hurricanes Gloria, Irene, and Sandy) providing a range of results for varying channel depths and forcing conditions.

## **2 Description of Hudson-Raritan Estuary**

### **History of navigation improvements**

The NYNJH has supported commercial shipping for over 300 years (Wakeman et al. 2007). After construction of the Erie Canal in 1825, NYNJH experienced phenomenal growth, becoming one of the leading ports in the United States (Parkman 1983). In the 1880s, the steady (and still ongoing) increases in ship sizes limited trans-Atlantic vessels to flood-tide transits into the harbor, necessitating the deepening of the main ship channel to 30 ft with a width of 1,000 ft (Parkman 1983). This quickly became inadequate and was again enlarged in 1899 with the construction of the Ambrose channel at a depth of 40 ft with a 2,000 ft width (Parkman 1983). During World War II, the Ambrose Channel was deepened to 45 ft along with improvements to the New York and New Jersey Channels that pass through Raritan and Newark Bays (Parkman 1983). Since then, navigation channels have been maintained and/or deepened throughout the estuary's rivers and bays, resulting in over 250 mi of established channels and berthing areas (USACE 2016). USACE (2007) provides a detailed listing of the historical deepening projects for the Kill van Kull, Arthur Kill, and Newark Bay channels. The latest authorized project included deepening of the main shipping channels within the harbor to a 50 ft depth with the exception of the Ambrose Channel, which was deepened to a 53 ft depth (CENAN 2007). The deepening was implemented in a consolidated approach with the previous authorization (45 ft depth) as detailed in USACE CENAN (2004) in an effort to reduce time and costs for completion. This study investigates the impact of this latest deepening project in terms of dredging requirements and associated changes in dredge volumes as compared to the previously authorized 45 ft channel configuration.

### **Previous analysis**

The importance of the NYNJH is illustrated by the numerous studies that have been completed to better understand this complex system. There have been many data collection efforts to understand the hydrodynamics, salinity, and sediment transport of the NYNJH and surrounding areas (Caplow et al. 2003; Chant 2006; Coch 2016; Clarke et al. 2015; Woodruff et al. 2001). These data collection efforts have provided much information about the system that has significantly improved the understanding of this

complex area. The data collected as part of these studies have also proved instrumental in improving the numerical models that have been utilized.

Some of the initial 3D hydrodynamic and salinity transport numerical modeling of the NYNJH system was documented in Blumberg et al. 1999. Additional subsequent studies have tended to focus on smaller spatial domains with increased model resolution. These studies have also shifted to incorporate sediment transport over smaller domains (Wakeman et al. 2007; Hellweger et al. 2004; Ralston and Geyer 2009). The study documented here attempts to model the hydrodynamics, salinity, and sediment transport over the entire NYNJH system and adjacent areas of importance.

## **Processes of importance**

Attempting to develop a numerical model of the sediment transport in the NYNJH system is an extremely challenging task due to the numerous processes impacting the sediment movement and deposition/erosion. These include hydrodynamic processes (tides, winds, pressure fields, riverine inflows, etc.) that will ultimately impact the salinity and sediment transport.

### **Tidal energy**

The NYNJH experiences semidiurnal tides with a mean tide range of approximately 5 ft. These tide ranges tend to dominate the hydrodynamic behavior in the system barring significant meteorological events. A 5 ft tide also equates to approximately 10% of the channel depth and equates to more than a 10% volume of water being overturned twice a day. This exchange of water can result in relatively high velocities in some locations like the Kill van Kull channel (surface velocities > 1.0 m/s).

### **River inflows**

The NYNJH system has several riverine freshwater inflows. The largest freshwater inflow impacting the system is the Hudson River. The Passaic, Raritan, and Hackensack flows are significantly smaller than that of the Hudson (based on US Geological Survey [USGS DOI 2020] surface water data at <https://waterdata.usgs.gov/nwis/sw?>). Additional smaller inflows were included in the modeling for thoroughness, including the Third River, Saddle River, South River, Rahway River, and Lawrence Brook. The

locations of these inflows are shown in Figure 2 and Figure 3. These stations have long periods of record allowing for extensive analysis of the seasonal flow behavior for these locations. The USGS provides daily minimum, maximum, and certain percent exceedance values for these locations for each day of the year. This information is plotted for these rivers in Figure 4 through Figure 12 to illustrate the seasonal variation in the riverine flows and also to illustrate the variability across years. Note that log plots cannot show 0.0 cfs discharges, so some minimum curves and even some of the lower percentile curves are not observed in the plots due to the very low discharges represented. The Hackensack River is a prime example of this.



Figure 2. River inflow locations.

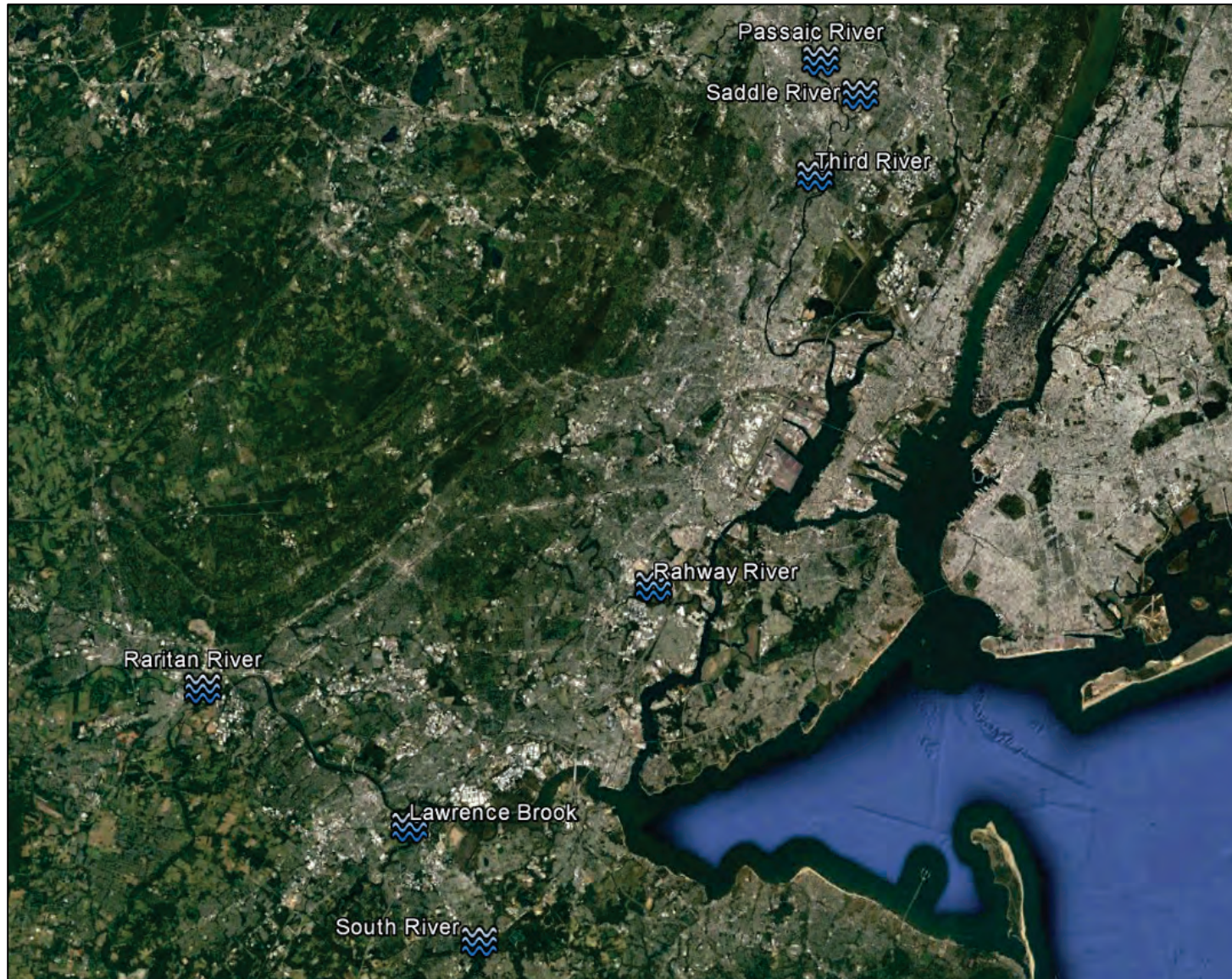




Figure 3. River inflow locations, including the Hudson River.

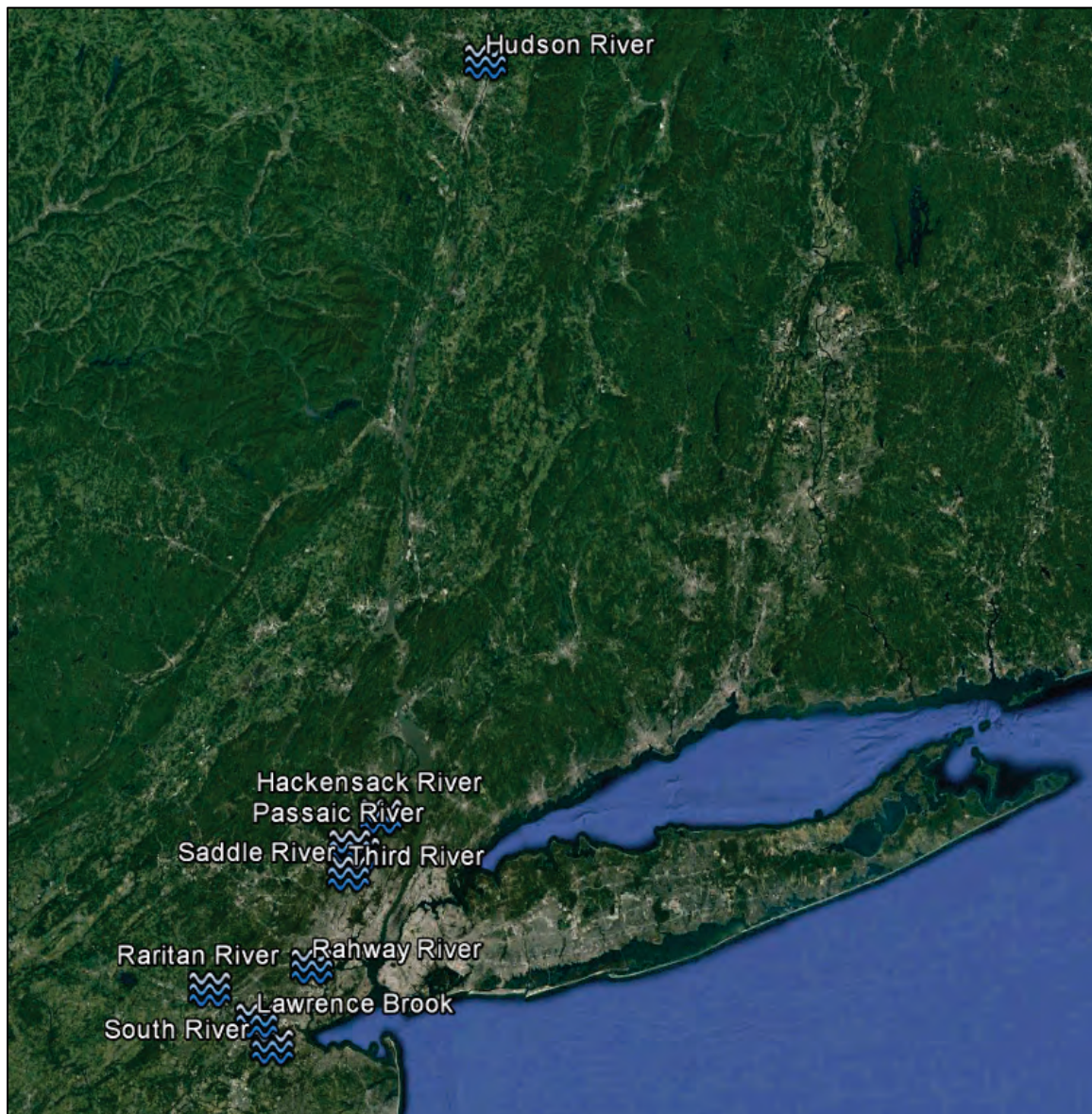




Figure 4. Average daily river inflow statistics for the Hudson River at Green Island.

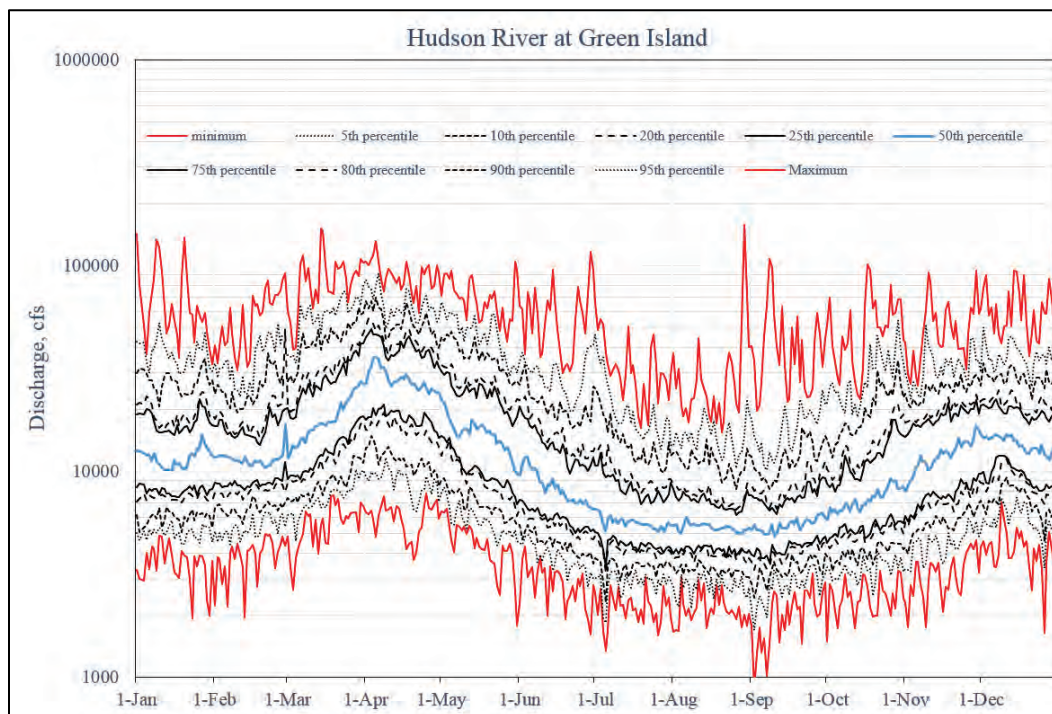


Figure 5. Average daily river inflow statistics for the Hackensack River.

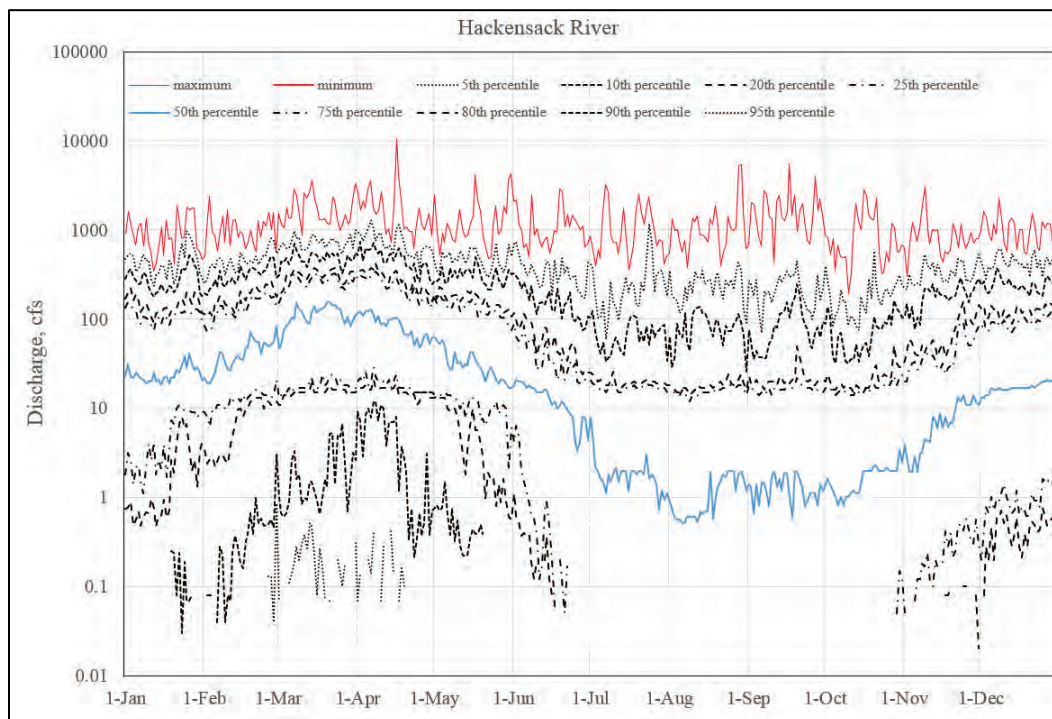


Figure 6. Average daily river inflow statistics for the Passaic River.

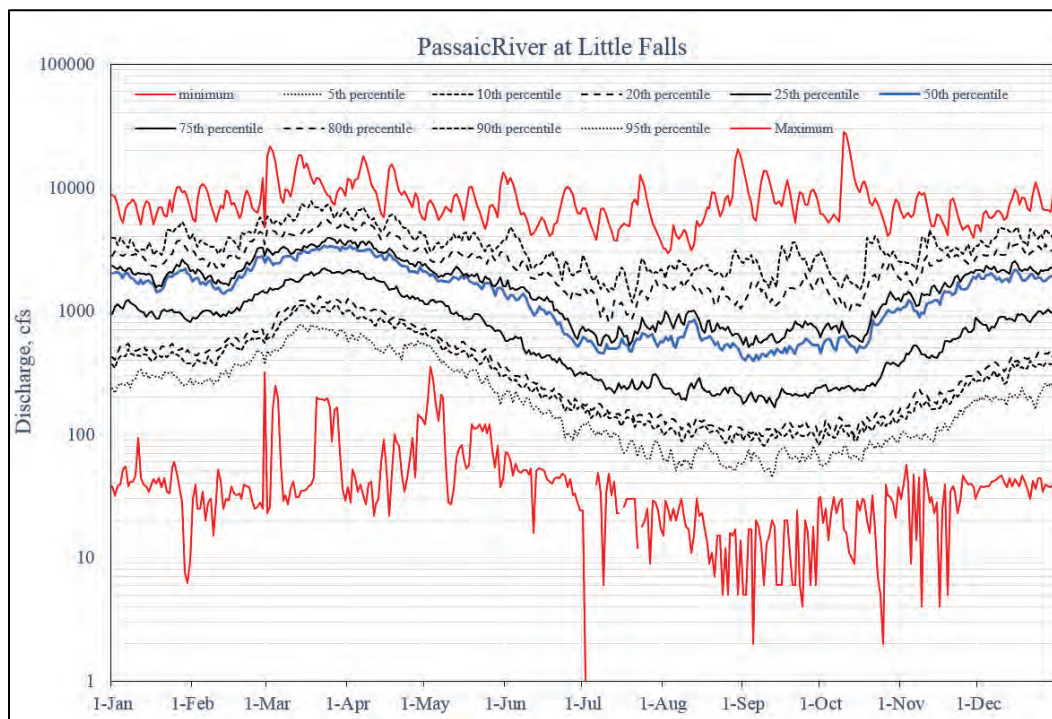


Figure 7. Average daily river inflow statistics for the Saddle River.

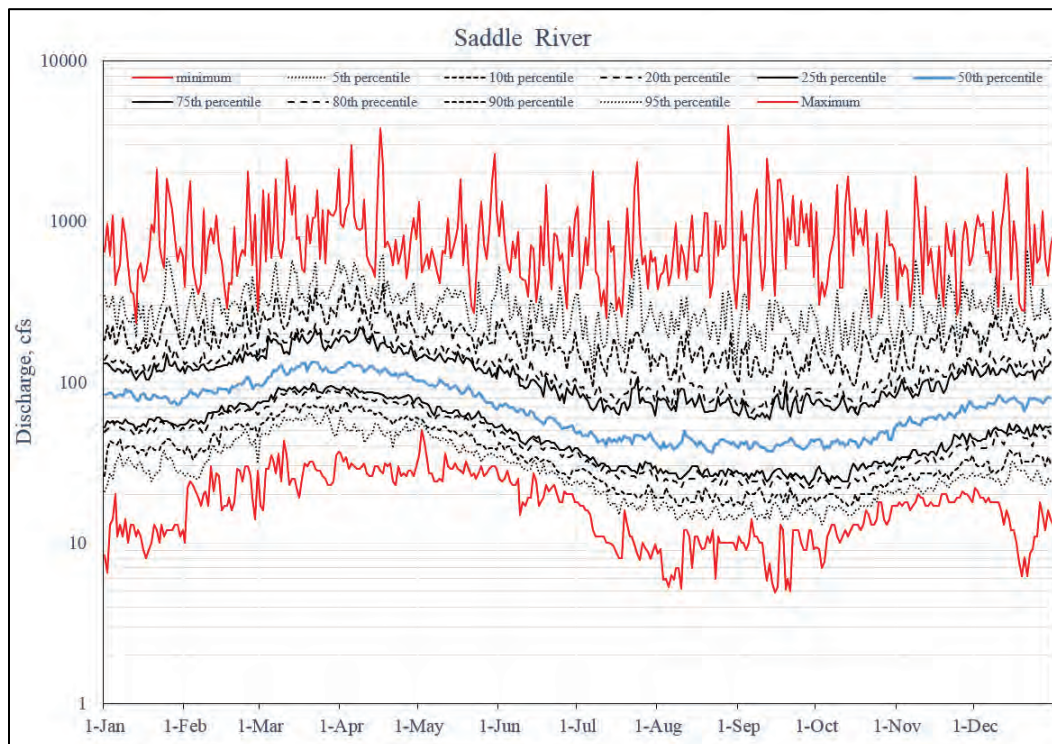




Figure 8. Average daily river inflow statistics for the Third River.

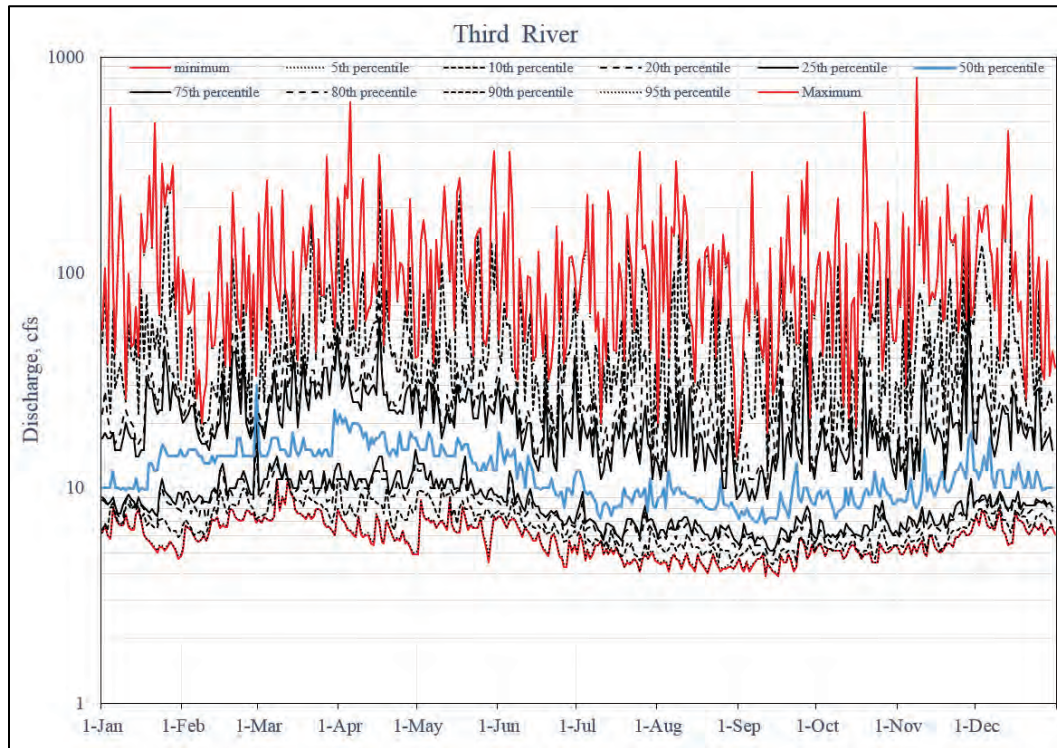


Figure 9. Average daily river inflow statistics for the Rahway River.

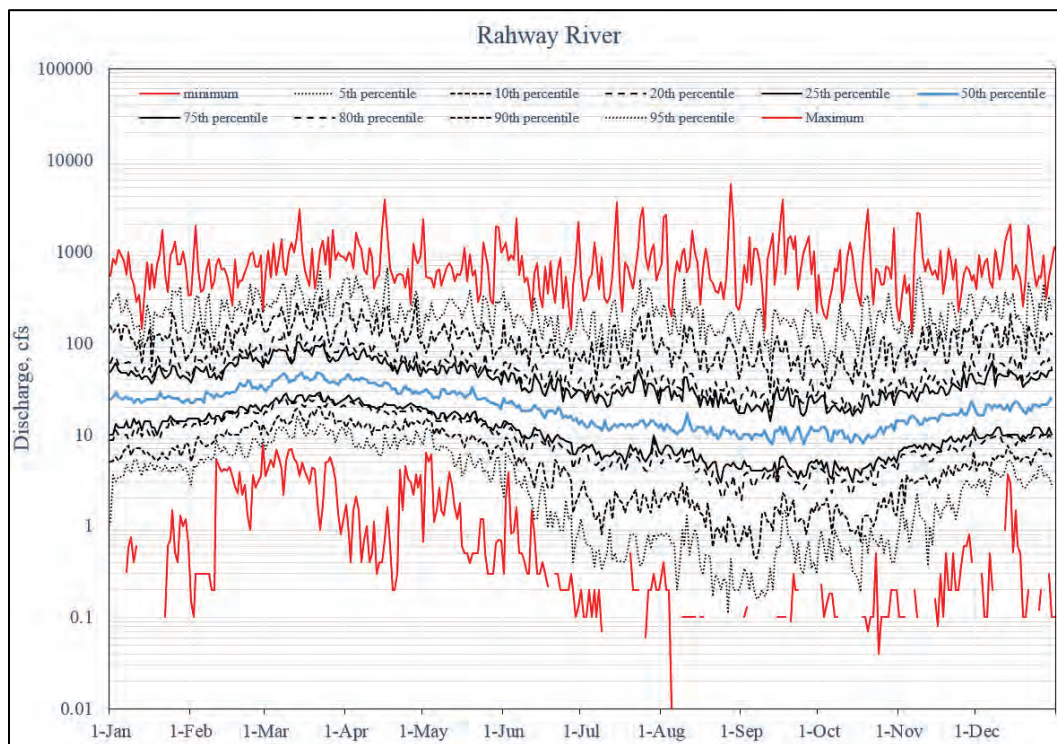


Figure 10. Average daily river inflow statistics for the Raritan River.

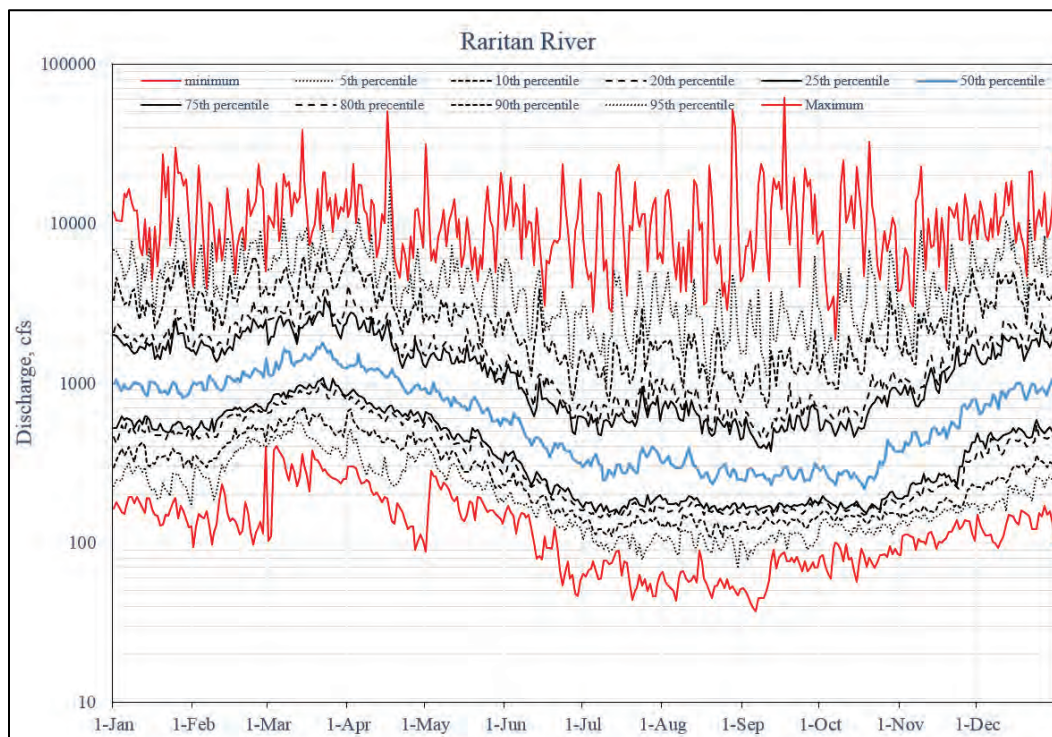


Figure 11. Average daily river inflow statistics for the South River.

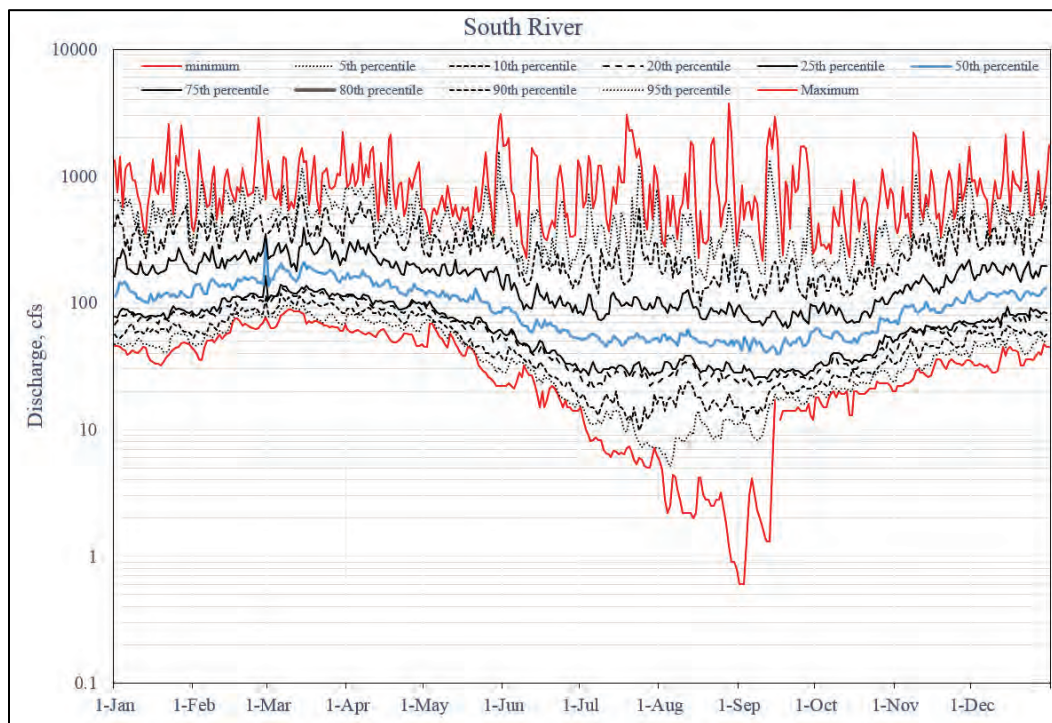
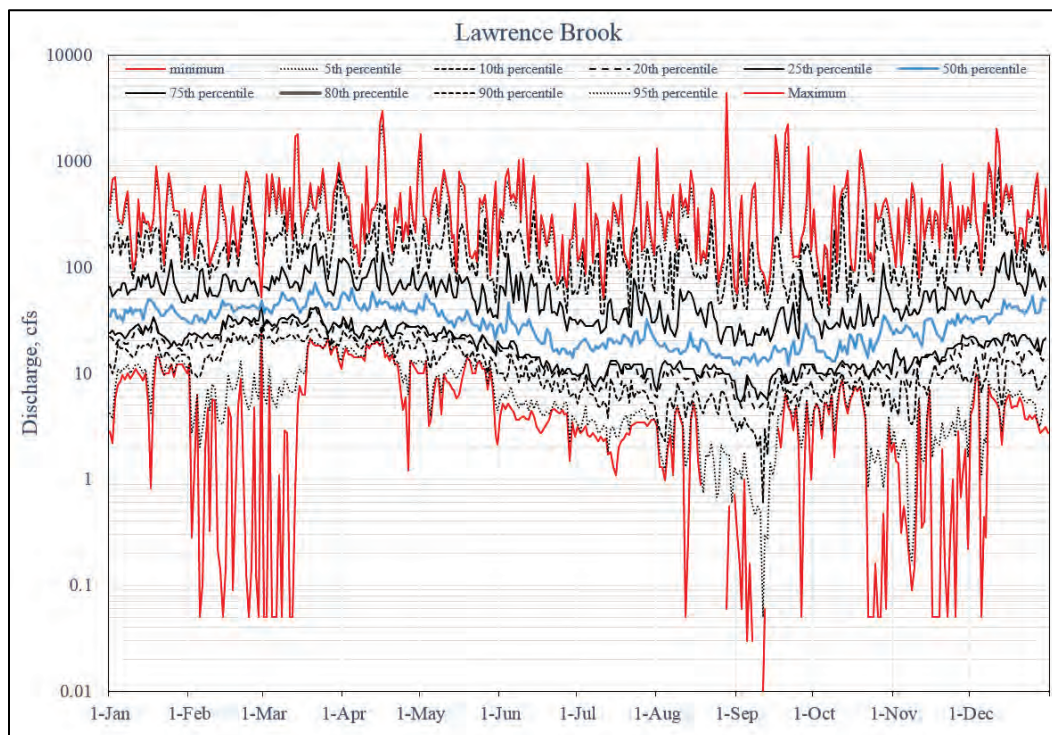




Figure 12. Average daily river inflow statistics for Lawrence Brook.



### Municipal wastewater treatment facility discharges

The New York/New Jersey area is a very densely populated region. As such, the discharges from Municipal Wastewater Treatment Facilities (MWWFs) can be significant. Therefore, it was deemed essential the numerical model account for the presence of these flows.

### Ship traffic impacts

The NYNJH system experiences a large volume of deep-draft navigation. The presence of these vessels can have a significant impact on the hydrodynamics and sediment suspension and transport. A vessel can create sediment resuspension due to the blockage of the channel, the propeller wash, and the bow wave generated during transit. Tate et al. (2014) investigated the impact of vessels for Galveston Bay and discovered that ship traffic is a significant contributor to the dredge volumes in the channel. The magnitude of the impact of ship traffic on the dredge volumes in the NYNJH system is unknown but should be recognized as a contributor to sediment resuspension and movement.

### **Salinity intrusion and baroclinic circulation**

The NYNJH is a partially mixed estuary that can transition from relatively high levels of stratification to completely mixed over short periods of time. The tide range (~5 ft) and currents increase the vertical mixing in the system and thereby prevent excessive levels of stratification (greater than 20 ppt), but stratification levels are high enough to create density driven circulation patterns. The salinity levels are highly dependent on the freshwater inflows, which can vary significantly during a given year.

### **Sedimentation regimes**

The NYNJH is a very complex area in terms of sediment transport. The system has areas of both cohesive (Newark Bay and portions of Upper Bay) and noncohesive (Lower Bay and portions of Upper Bay) sediment transport.

There are various hydrodynamic factors (flow pathways in the system, baroclinic circulation patterns, wind driven circulation patterns, etc.) that make it extremely challenging to accurately predict the sediment transport in the NYNJH system. This is in addition to the complex nature of sediment transport in general.

The Hudson River is essentially a sediment storage feature that provides a temporal delay in the delivery of upper basin sediment to the estuary. Geyer et al. (2001) reported that the greatest export of sediment from the Hudson River to the estuary occurs when peak river discharges coincides with spring tides. During neap tides, the sediment gets trapped within the river. Ralston and Geyer (2009) proposed that the greatest export of river sediment occurs at moderate flows while at extreme flows, the sediment delivery, which is cubic with discharge, overwhelms the capacity of the river to transport and gets trapped. Wall et al. (2008) suggested that the tributaries downstream of Troy (Hudson River inflow location in Figure 3) supply as much as 30%–40% of the sediment supply to the estuary.

The sedimentation environment of Newark Bay has been of particular interest over the past 4 decades because of the presence of contaminated sediments within the lower Passaic River and Newark Bay. Suszkowski (1978) did the first comprehensive analysis of the hydrodynamic and sedimentation environment of Newark Bay.

Chant et al. (2011) studied the sedimentation environment of the Passaic River. They found that the Passaic River has been depositional over the past 60 years but is approaching geomorphological equilibrium to the pre-dredging conditions. Although the net tidal sediment flux is upstream into the Passaic River from Newark Bay under normal tidal conditions, when salinity driven circulation is evident, episodic river flooding dominates the overall net flux with downstream transport. The result is a net sediment flux from the Passaic River into Newark Bay.

The primary sediment source for Newark Bay is from Upper Bay through Kill van Kull (Chant 2006; Sommerfield and Chant 2010) and estimated at approximately 100,000 tons per year. The Passaic and Hackensack Rivers supply approximately 17,000 and 5,000 tons per year, respectively.

Shrestha et al. (2014) developed a conceptual model of the hydrodynamics and sediment transport regime in Newark Bay. They concluded the following:

1. In the absence of strong wind forcing or large tidal gradients, the navigation channel displays classic estuarine, gravitational, two-layer circulation with a seaward surface flow of freshwater and a landward bottom flow of salt water. Without freshwater or atmospheric forcing, landward flow in the channels is balanced by seaward flow in the shallow tidal flats.
2. A counterclockwise residual circulation is most often observed around Staten Island, although this can reverse depending on the tidal and atmospheric forcing.
3. Low freshwater inputs or episodic wind and storm events can break down the classic estuarine circulation pattern generally observed in the bay.
4. The primary source of imported sediment to Newark Bay is the Kill van Kull, which may supply up to 140,000 MT/year.
5. By comparison, the Passaic and Hackensack Rivers supply approximately an order of magnitude less sediment to Newark Bay than the Kill van Kull, despite being the largest freshwater sources.
6. Under the existing dredged configuration, most of the sediment originating from the Kill van Kull is deposited within the southern half of Newark Bay; most of the sediment originating from the Passaic River is deposited within the northern half of the bay.

7. Long-term average sedimentation in Newark Bay, particularly within the dredged channels, is offset by rates of maintenance dredging.
8. The subtidal flats in Newark Bay have low deposition rates and appear to be in long-term equilibrium.
9. The extensive history of dredging and shoreline development that have taken place in the Newark Bay study area have resulted in changing historical circulation and sediment transport patterns. Historical transport patterns are likely quite different from current transport patterns.



### **3 Technical Approach**

#### **Hydrodynamics**

The hydrodynamics for the project were simulated using the 3D baroclinic version of the Adaptive Hydraulics (AdH) model (Savant et al. 2014). The model is based on the hydrostatic assumption and gradually varying flow. The governing momentum equations include terms for temporal variation (unsteady flow), advection, turbulent diffusion, bottom friction, vegetative friction, ice friction, Coriolis, wind stress, wave radiation stress, barometric pressure and pressure gradients, including density driven effects. Vertical turbulent diffusion is handled by Mellor-Yamada 2.0 (Mellor and Yamada 1982) closure with vertical mixing reduced based on Richardson number for cases of stratification (Savant 2015). The model also includes specification of rainfall and volumetric inflows (rivers, sewage discharges, etc.).

The hydrodynamic solution includes the simulation of salinity transport, which can induce density driven circulation patterns that are important to some critical aspects of sedimentation within the harbor.

#### **Sediment transport**

The sediment transport module within AdH is invoked by using the sediment transport algorithms of SEDLIB (Brown 2008a,b), which include cohesive and non-cohesive sedimentation processes. These processes are combined with the constituent transport solvers within AdH, with a constituent for each sediment size class simulated. The model includes both cohesive and noncohesive transport.

The current 3D version of AdH does not explicitly resolve bed load transport. It performs a total load calculation, and instead of distributing the total load between bedload and suspended load components, the total load is placed into suspension in the water column. Given the nature of bed material (large fall velocities), it is expected the bed material placed in suspension will quickly fall from suspension and return to the bed. This approach would tend to overestimate the transport of bed material in terms of travel distance and underestimate travel times, but given this is a tidally driven system, the overall impact is expected to be minimal. Sensitivity simulations with the two-dimensional (2D) version of AdH

(which includes bed-load transport) also indicated that bed-load transport was significantly less than the suspended load. Note that bed-load transport would only be important in sand-dominated areas. Cohesive sediment areas would not possess bed-load transport.

## **Wave energy**

The purpose of applying nearshore wave models is to describe quantitatively the change in wave parameters (wave height, period, direction, and spectral shape) between the offshore and the shoreline. As waves travel from the offshore through the surf zone, they shoal and break due to the shallower depths found in nearshore areas, leading to significant variations in wave conditions within relatively small areas. Offshore wave information obtained from wave buoys or global- or regional-scale wave hindcasts and forecasts is transformed through the nearshore coastal region using these models.

The nearshore wave model Steady-State spectral WAVE (STWAVE) was applied as part of the shoaling analysis for the navigation channel deepening in NYNJH. One STWAVE grid, previously developed as part of the North Atlantic Coast Comprehensive Study (NACCS), was updated for this modeling effort (Cialone et al. 2015).

To rigorously represent the hydrodynamic processes of the study area, tight two-wave coupling between AdH and STWAVE was facilitated with the CSTORM-MS, a physics-based modeling capability. During the two-way coupling process, AdH passes spatially variable water elevations, current velocities, and wind fields to STWAVE. When STWAVE completes its instance, it passes spatially variable wave radiation stress gradients to AdH to drive wave-induced water level changes (e.g., wave setup and setdown) and currents. These wave-generated currents can transport sediment onshore, offshore, and alongshore.

## **Meteorological impacts**

The impacts of meteorology on hydrodynamics and sedimentation processes within the harbor are addressed both directly and indirectly. The direct impacts are handled by specifying the wind and pressure field over the model domain to be used for the wind stresses on the water surface and the spatial variation in the barometric pressure within the hydrodynamic model. Indirect impacts are addressed by the wind-wave

generation calculations in STWAVE, which provide the radiation stress gradients that drive littoral currents to the AdH model. Indirect meteorological impacts are also included in the time-series boundary conditions for river discharges after major rainfall events and the associated induced suspended sediment influxes as well as the residual tidal signal across the open ocean boundary. Direct precipitation/evaporation within the harbor and drainage areas downstream of gaging stations were not included for this study. The tributary inflows are considered to be the primary response to precipitation. Local precipitation could result in some localized runoff and short-term variations in the salinity field but should have minimal effect on the long term model results.

### **Extreme events**

Major meteorological events such as tropical storms and winter storms (Nor'easters) were modeled directly within the AdH model. The tidal boundary forcing for extreme events was taken from the ADCIRC NACCS results and embedded in the tidal boundary specification.

### **Model simulation approach**

The conditions — hydrodynamic, salinity, and especially sediment — at a particular spatial location and time are impacted by the behavior prior to that time. Examples would be a large flow providing a significant amount of fine sediment to the system or a large storm event supplying coastal sand to the system. These types of events can result in system impacts for long periods of time and can significantly complicate efforts to replicate observations in the field. This study simulated five discrete years independently of each other. During these simulation time periods, the hydrodynamics, salinity, and sediment transport (including deposition and erosion) progress temporally with the bed elevations being updated during the simulation by erosional and depositional processes. The simulations were performed on the years independently to provide indicators of the relative shoaling intensity and potential dredging requirements. Since dredging activities prevent significant variations from the authorized depths, longer-term simulations could diverge from a realistic indicator of the dredging requirements as channel infilling could reduce depositional volumes.

The model simulations were completed with a probabilistic mindset. That is, given the deepened channel condition, what would be the sedimentation patterns during the next year for a range of potential forcing conditions? In general, the cumulative changes in erosion/deposition for multiple years would not be linear. As significant shoals form, the current velocities would be impacted, and nonlinear morphological changes could become important. However, the period of time for such significant changes is assumed to be much longer than the period between dredging cycles. Therefore, the linear superposition on the probabilistic yearly simulations is believed to be a valid indicator of the long-term dredging impacts for the deepening.

## 4 Numerical Models

### Adaptive Hydraulics (AdH)

AdH is a US Army Engineer Research and Development Center (ERDC) developed modular Finite Element Method code capable of simulating 2D (AdH-2DSW) and 3D (AdH-3DSW) Shallow Water (SW) flow, Reynolds Averaged Navier Stokes flow, Saturated and Unsaturated Groundwater flow, and Overland flow computations. Both AdH-2DSW and AdH-3DSW were used in the execution of this study.

AdH-2DSW is the depth-averaged module of the AdH code utilized for mass conservative vertically averaged hydrodynamic and transport computations for a wide variety of domains such as riverine flows, estuarine flows, dam and levee break flows, etc. (Savant et al. 2011; Tate et al. 2012; Savant and Berger 2012; Martin et al. 2011; McAlpin et al. 2013).

AdH-3DSW is the hydrostatic 3D module of the AdH code utilized for mass and momentum conservative hydrodynamic and transport computations in regions where the vertical distribution of velocities is sufficiently different such that the depth-averaged behavior is not equivalent to the 3D behavior of the system. AdH-3DSW represents a state of the art in the numerical simulation of 3D hydrostatic flows (Savant and Berger 2015) and a few of its features are the following:

1. Linear triangle-based meshing allows for an accurate representation of bathymetry.
2. Vertical meshing that is neither Sigma nor Z-grid based and hence is not encumbered by the drawbacks of either.
3. Run-time adaption in the horizontal and vertical allows for improved representation of hydrodynamics as well as transport.
4. Internal time-step size adaption allows for time-step changes to capture rapidly changing physics during run time.
5. Fluid and constituent mass are conserved.
6. Easy transition from the 2D realm to the 3D realm.
7. Availability of several turbulence options such as Mellor-Yamada (Level 2 and 2.5), K-e, and Smagorinski along with turbulence suppression options.

## Sediment transport library (SEDLIB)

SEDLIB is a sediment transport library developed at ERDC (Brown 2012a,b). It is capable of solving problems consisting of multiple grain sizes, cohesive and cohesionless sediment types, and multiple discrete bed layers. It calculates erosion and deposition processes simultaneously and simulates bed processes such as armoring, consolidation, and discrete depositional strata evolution.

The SEDLIB system is designed to link to any appropriate hydrodynamic code. The hydrodynamic code must be capable of performing advection-diffusion calculations for a constituent. SEDLIB interacts with the parent code by providing sources and sinks to the advection diffusion solver in the parent code. The sources and sinks are passed to the parent code via an explicit bed sediment flux for each grain class.

## STWAVE

STWAVE is a finite-difference, phase-averaged spectral wave code based on the wave action balance equation. STWAVE computes nearshore wave growth, propagation, and transformation, including refraction, shoaling, and breaking.

### Code description

The STWAVE code uses the governing equation for steady-state conservation of spectral wave action along a wave ray (Jonsson 1990):

$$(C_g)_i \frac{\partial}{\partial x_i} \frac{C C_g \cos(\alpha) E(\omega, \alpha)}{\omega} = \sum \frac{S}{\omega} \quad (1)$$

where:

- $C_g$  = group celerity
- $C$  = wave celerity
- $i$  = tensor notation for x- and y-coordinates
- $\alpha$  = wave orthogonal direction
- $E$  = wave energy density divided by the density of water  $\rho_w$  and the acceleration of gravity  $g$
- $\omega$  = angular frequency
- $S$  = energy source and sink terms.

The angular frequency is related to the wave number  $k$  by the dispersion relation

$$\omega^2 = gk \tanh(kd) \quad (2)$$

with celerity,  $C$ , and group celerity,  $C_g$ , given by

$$C = \frac{\omega}{k} \quad (3)$$

$$C_g = 0.5C \left[ 1 + \frac{2kd}{\sinh(2kd)} \right] \quad (4)$$

Source and sink mechanisms include surf-zone breaking in the form of the Miche criterion (Miche 1951), the flux of input energy due to wind (Resio 1988; Hasselmann et al. 1973), energy redistribution through wave-wave interactions (Resio and Perrie 1989) and whitecapping (Resio 1987, 1988), and energy losses due to bottom friction (Hasselmann et al. 1973; Padilla-Hernandez 2001; Holthuijsen 2007). Radiation stress gradients are calculated based on linear wave theory and provide wave forcing to external circulation models. The full equations for these source terms and additional technical details are provided in Massey et al. (2011a).

## Execution

STWAVE has two modes available, half-plane and full-plane. Half-plane allows wave energy to propagate only from the offshore towards the nearshore ( $\pm 87.5$  deg from the x-axis of the grid). In other words, all waves traveling in the negative x-direction, such as those generated by offshore blowing winds, are neglected. Full-plane allows wave transformation and generation on the full 360 deg plane. All simulations were executed in full-plane to allow a more complete representation of the wave climate affecting sediment transport.

The full-plane version of STWAVE uses an iterative solution process that requires user-defined convergence criteria to signal a suitable solution. Boundary spectra information is propagated from the boundary during the initial iterations. Once the initial stage converges, winds and water levels are added to the forcing, and this final stage iteratively executes until it also reaches a convergent state. The convergence criteria for both stages include the maximum number of iterations to perform per instance, the relative difference in significant wave height between iterations, and the minimum

percentage of cells that must satisfy the convergence criteria (i.e., have values less than the relative difference). Convergence parameters were selected based on a previous study by Massey et al. (2011a) in which the sensitivity of the solution to the final convergence criteria was examined. The relative difference was defined as 0.1 and 0.05 for the initial iterations and the final iterations, respectively. The minimum cell percentage was defined as 100.0 for the initial iterations and 99.8 for the final iterations. The maximum number of initial iterations to perform was 17 whereas the maximum number of final iterations was 22.

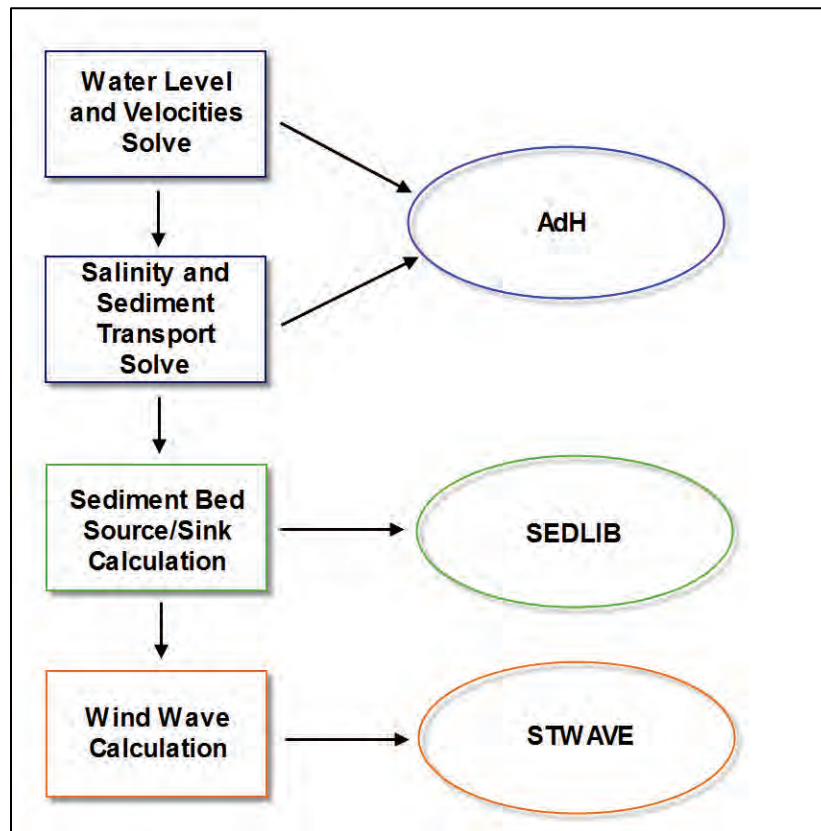
Full-plane requires considerably more memory with longer run times than half-plane. Thus, parallel computing was utilized to optimize the run time of the simulations. STWAVE was set up with parallel in-space execution whereby the computational grid was divided into different partitions in both the x and y directions, with each partition residing on a different computer processor. This application utilized 136 processors for the STWAVE solve.

## **Model coupling**

The simulation of the processes necessary for the sedimentation analysis within the harbor was accomplished by coupling of the hydrodynamics, sediment transport, salinity transport, and wave generation and propagation within a single computer simulation. The coupling involved specification of the wind fields generated as part of the Wave Information Study (WIS) (<http://wis.usace.army.mil/>). This linkage of the waves to the AdH hydrodynamics and sediment transport was accomplished using the CSTORM-MS system (Massey et al. 2011b). An overview of the solution process is provided in Figure 13. The AdH (hydrodynamics and transport) and SEDLIB (sediment source/sink calculation) are solved at each time-step in the order shown. The STWAVE calculation is performed every 3 hours to reduce the computational burden due to the wave generation and propagation calculations.



Figure 13. Diagram of the solution steps.



## 5 Model Development

### Mesh development

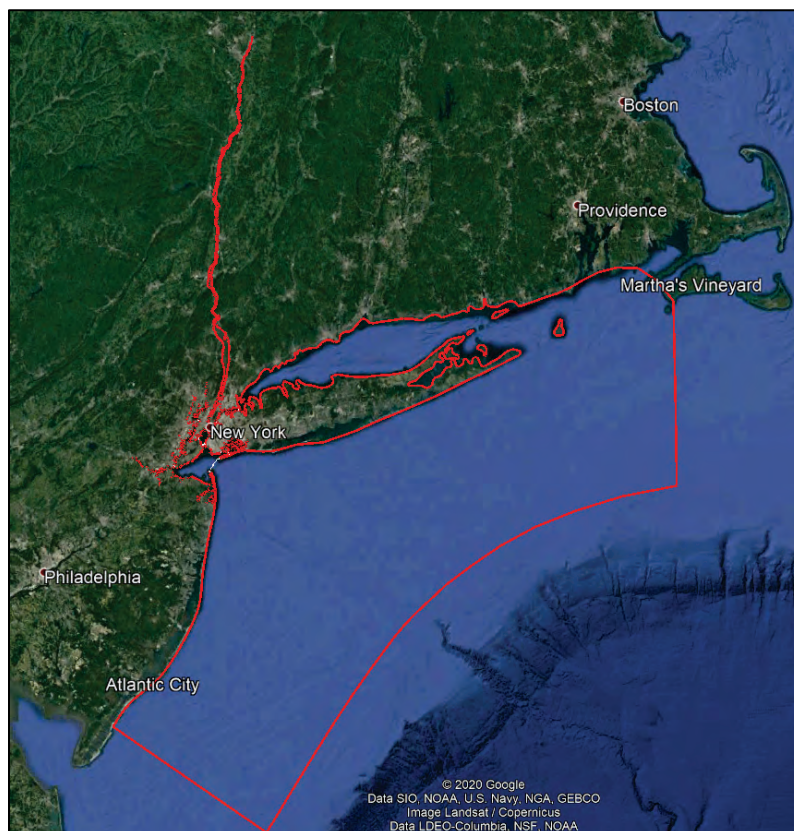
The numerical model requires a numerical model mesh for computations. The mesh specifies the model domain or computational area. It is imperative the model domain be large enough to prevent a prescribed result in the project area from the model boundary conditions. It is also important to include an appropriate level of model resolution and accurate bathymetric values to obtain useful model results.

### Model domain

*Hydrodynamic/salinity/sediment transport model*

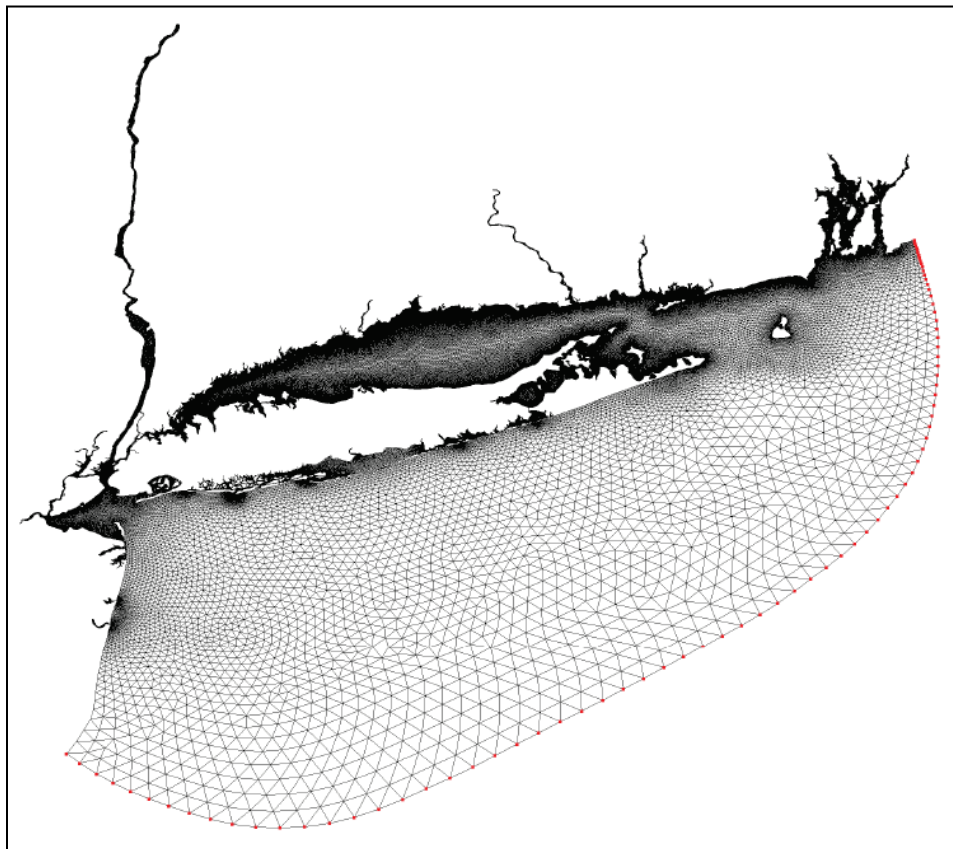
The numerical model domain for this study needs to be large enough to encompass the areas impacting the study area. For this complex system, that includes the previously discussed rivers along with the offshore areas. The model domain for this study is shown by the red line in Figure 14.

Figure 14. Model domain outlined with red line.



Previous studies completed at the ERDC Coastal and Hydraulics Laboratory consisted of a smaller domain due to computational constraints. This strategy began on the physical scale model of the harbor, when the domain was critical to the cost of construction. Previous numerical modeling efforts also included two tidal boundaries, one in the Long Island Sound and one offshore in the Atlantic Ocean. Proper specification of the phase variation between these two boundaries was an obvious source of error in the modeling but was unavoidable at the time for computational reasons. Given the advancements in numerical modeling and computational resources, this AdH model was able to avoid this complication. The choice of a proper model domain for this study area was reinforced by comparing the chosen AdH model domain to the domain utilized by National Oceanic and Atmospheric Administration (NOAA) (NOAA 2008) for its vertical tidal datum analysis (Figure 15). This model domain was also utilized by HydroQual (Blumberg et al. 1999; HydroQual 2008) model studies within the harbor and by pre-ERDC modeling of New York Bight (Scheffner et al. 1994), which was not focused within the harbor.

Figure 15. NOAA model domain used for development of vertical tidal datum in New York area (NOAA 2008).



### *Wave model*

The wave impacts are incorporated into the model by linking the hydrodynamic and salinity and sediment transport model to a wave model (STWAVE) using the CSTORM-MS system (Massey et al. 2011b). This linkage consists of passing flow information to the wave model with the wave model passing back wave radiation stress gradients, which impact the flow conditions. This information is needed only for locations where wind waves impact the study area. The STWAVE model does not solve on the same mesh as the AdH model and as such allows for the wave model domain to be reduced for computational savings. The domain of the wave model is shown by the red box in Figure 16.

Figure 16. STWAVE model domain.





## Mesh resolution

Excessive mesh resolution can result in extreme simulation times, and too little resolution can result in a reduction in the computational accuracy of the model results. Therefore, extreme care must be taken when choosing the spatial and vertical resolution in a numerical model. This issue is significantly reduced with AdH as it is an adaptive model whereby the resolution (horizontal and vertical) can be increased during the model simulation to better resolve the physics of the hydrodynamic and/or transported quantities. This added resolution is removed when no longer needed resulting in increased accuracy without significantly increasing the computational burden. However, the horizontal mesh resolution must be sufficient to capture all important features in the bathymetry, since horizontal adaption linearly interpolates the bottom elevation. The initial unadapted 3D mesh had approximately 220,000 nodes and approximately 750,000 elements.

### *Horizontal resolution*

AdH model meshes are unstructured allowing increased resolution in the study area with significantly less resolution in the offshore areas. This allows the AdH mesh to possess approximately 50 to 100 m nodal spacing in and near the ship channels with approximately 18 km nodal spacing at the tidal boundary. The numerical formulation of AdH does not have a constraint on the mesh dimensions, as with classical finite difference formulations. Structured meshes would either be forced to have more resolution offshore where it is not needed or less resolution in the study area where it is required. Figure 17, Figure 18, and Figure 19 show the AdH horizontal mesh resolution.

Figure 17. AdH numerical model mesh.

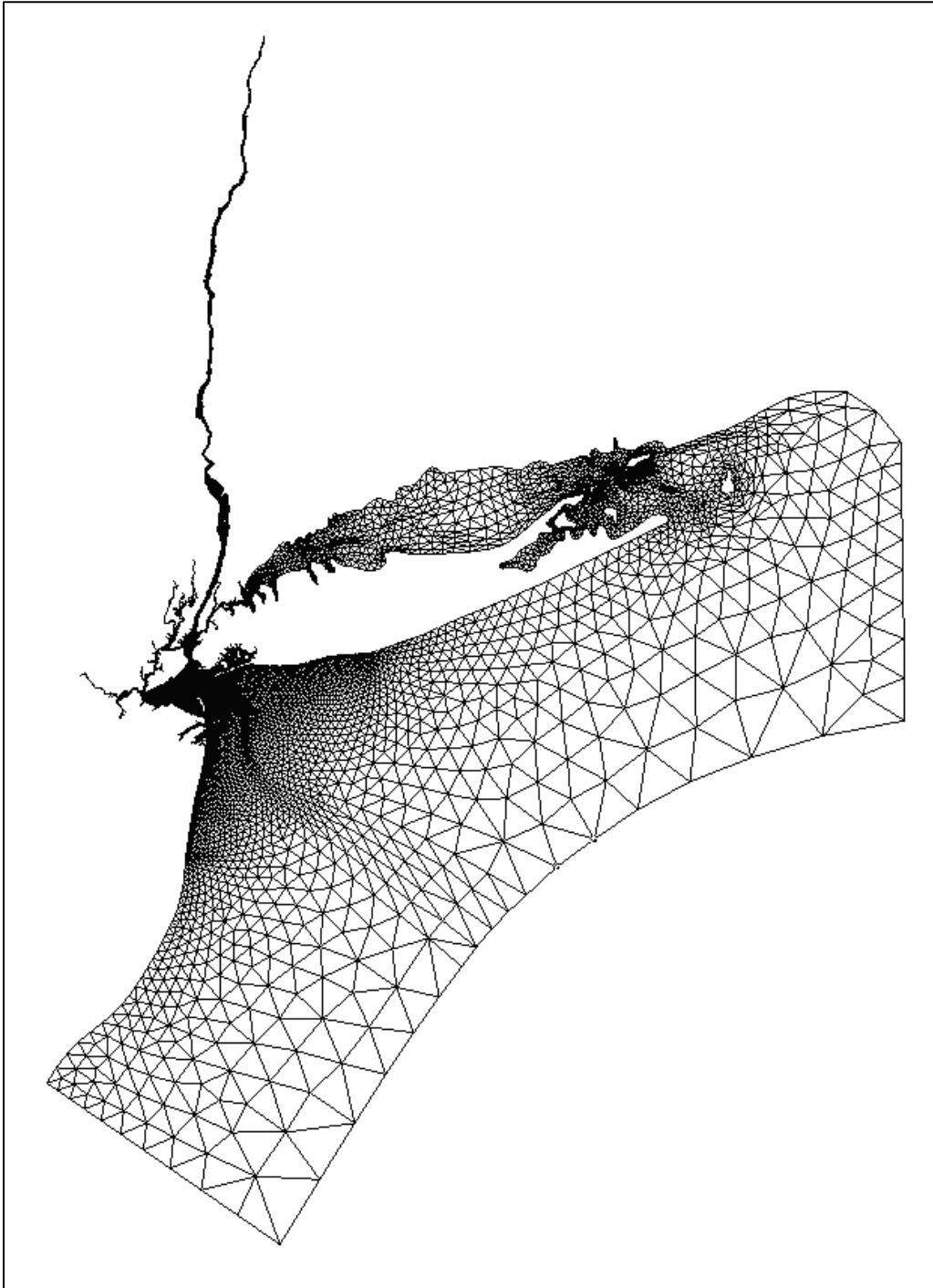


Figure 18. Mesh resolution in the NYNJH area.

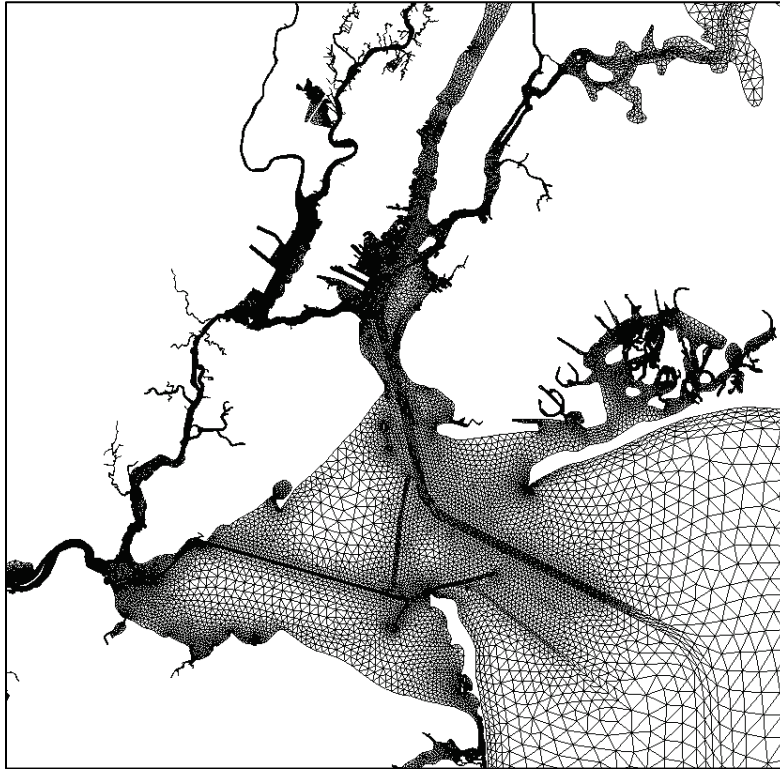
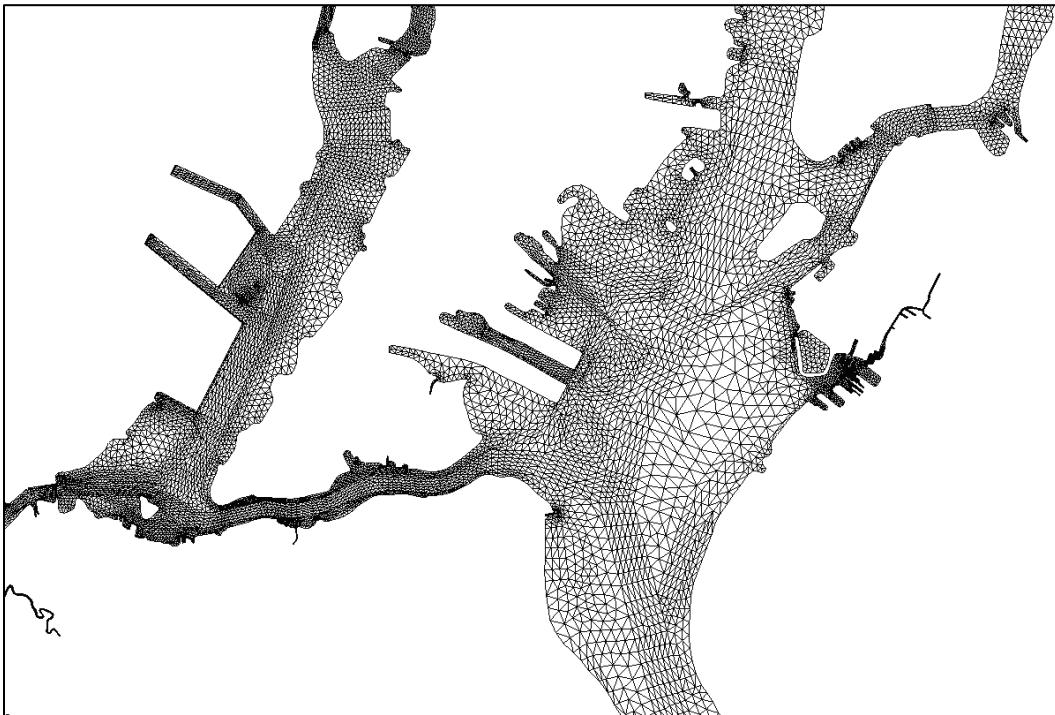


Figure 19. Mesh resolution in the Upper Bay and Newark Bay area.



### *Vertical resolution*

The vertical resolution is illustrated in Figure 20 and Figure 21. AdH is unstructured in the horizontal and columnar in the vertical with the ability for the user to specify the number of vertical layers spatially. The vertical resolution ranges from one layer (2 nodes) in shallow areas and areas outside the study area to as much as five layers (6 nodes) in the ship channels. The adaptive capability in AdH allows this resolution to increase as needed during the model simulation to better resolve the hydrodynamics, salinity and sediment transport.

Figure 20. Vertical mesh resolution.

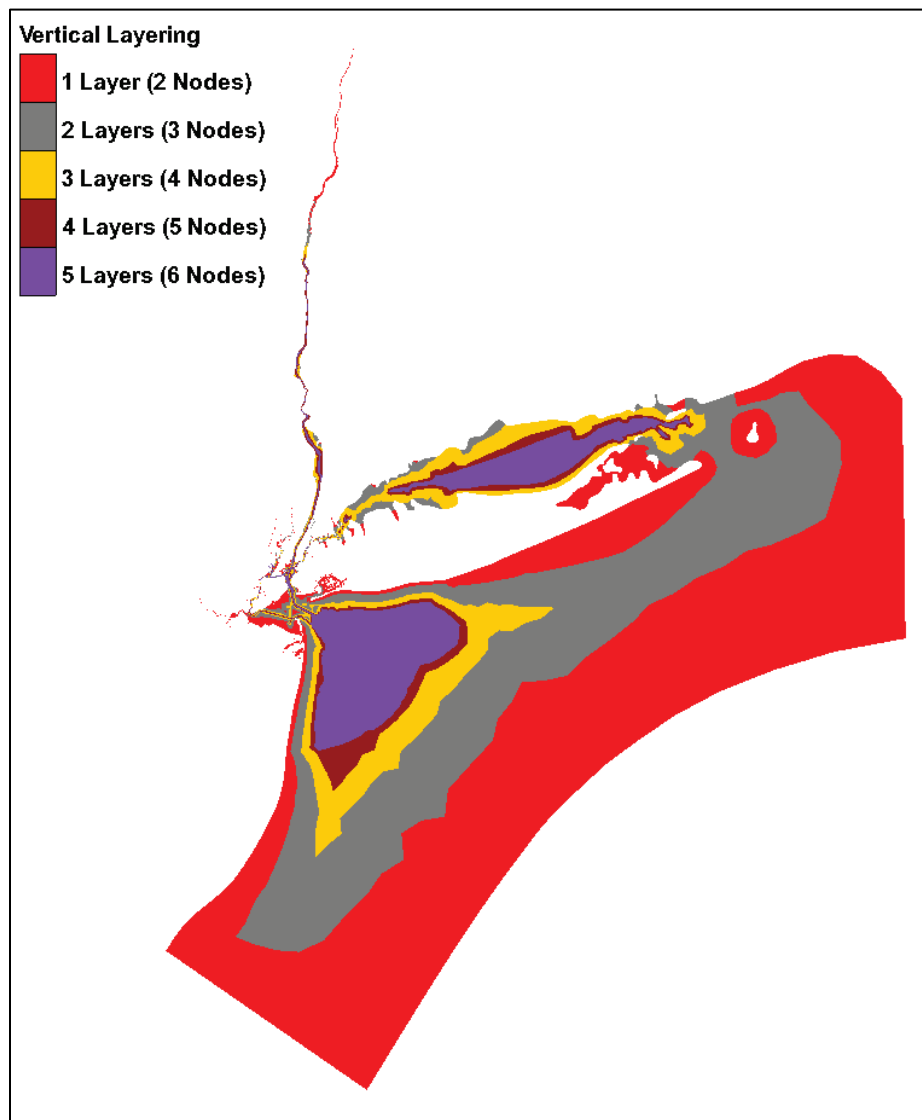
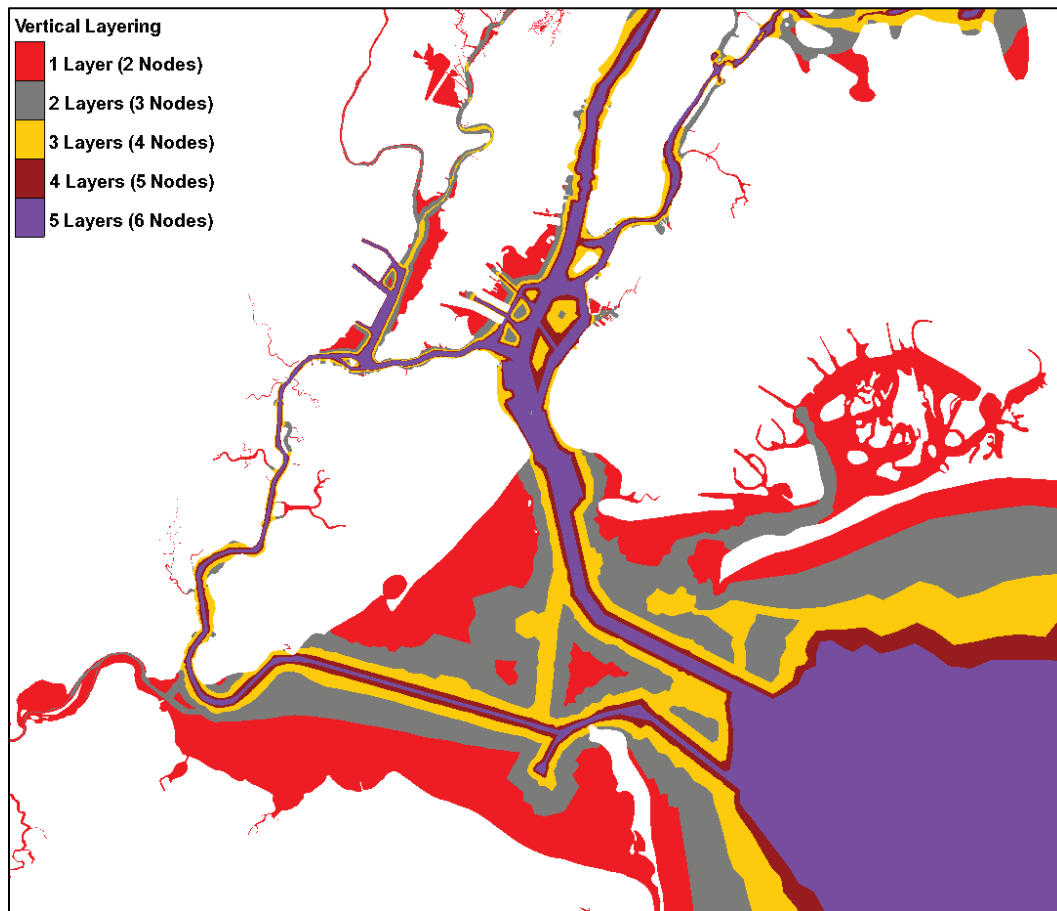




Figure 21. Vertical mesh resolution in the study areas.



### *Adaption*

The AdH numerical code has the capability to adapt the numerical mesh during the simulation to better resolve the hydrodynamics and transport. The adaption levels vary based on regions or material types. Supplemental areas (offshore areas and upstream areas on the rivers) were specified to have zero adaption as the near field accuracy of the model in these areas is not vital in obtaining accurate results in the study area. The regions in and near the ship channel were allowed to adapt each element twice; additional areas (shallower tidal flats and other off channel areas) were allowed to adapt once. As an example of the resolution possibilities with adaption, one level of adaption can result in both a doubling of the vertical resolution (e.g., from 5 layers to 10 layers) and also a doubling of the horizontal resolution. Additional discussion of the 3D adaption in AdH is provided in Savant et al. (2017).

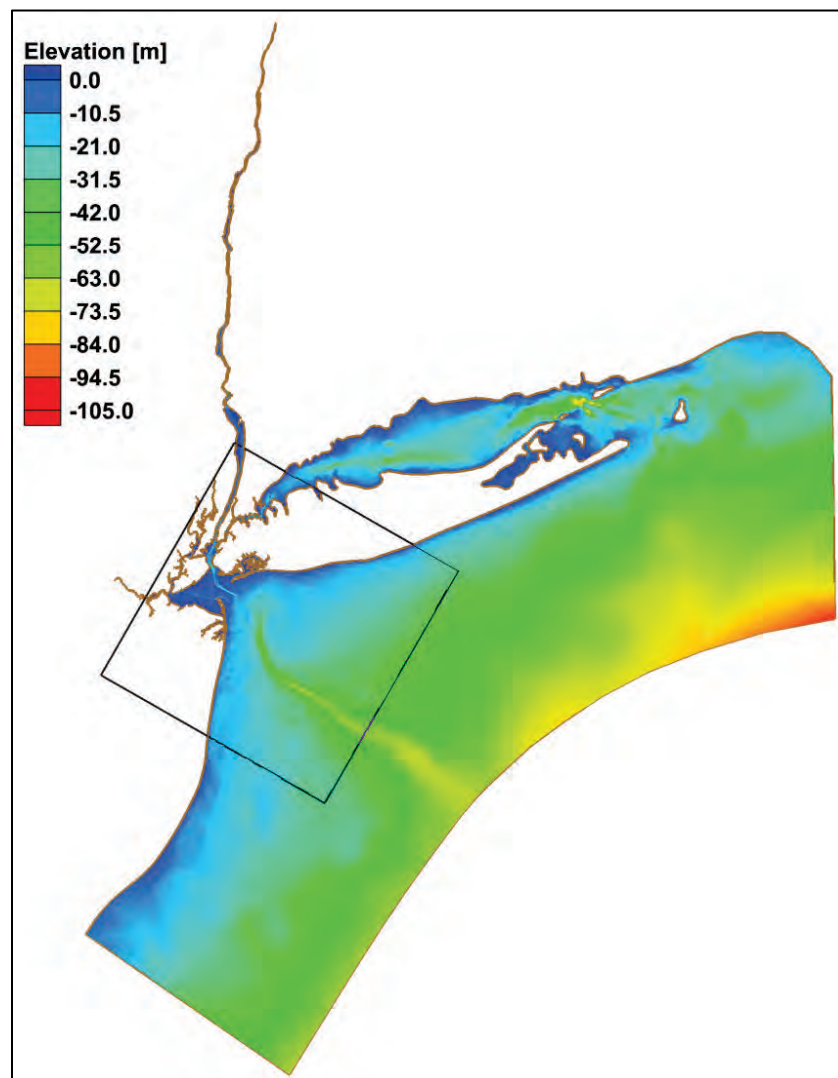
### *Wave model resolution*

STWAVE is formulated on a Cartesian grid, with the x-axis oriented in the cross-shore direction (I) and y-axis oriented alongshore (J), often parallel with the shoreline. Angles are measured counterclockwise with respect to the grid x-axis. The grid encompassing the study area was previously developed as part of the NACCS (Cialone et al. 2015). The grid was projected from Universal Transverse Mercator Zone 18 to State Plane Coordinate System New Jersey (FIPS 2900) to be consistent with the AdH projection. The grid properties are shown in Table 1, and the location of the STWAVE grid with respect to the AdH domain is shown in Figure 22. The grid's offshore boundary remained at approximately 40 m, the same as the NACCS. Wave interactions with the bed at this offshore extent are relatively small, particularly in comparison to the importance of wave generation by wind. The grid resolution of 200 m also remained the same as that defined in the NACCS. This resolution has demonstrated good agreements with measurements for the NACCS (e.g., Hurricanes Gloria, Sandy, and Irene) and previous studies of Hurricane Rita, Katrina, Gustav, and Ike (Dietrich et al. 2011; Hope et al. 2008; Bunya et al. 2010; Dietrich et al. 2010; Bender et al. 2013).

Table 1. STWAVE grid properties.

Projection	Grid Origin (x,y) (m)	Azimuth (deg)	$\Delta x \backslash \Delta y$ (m)	Number of Cells	
				I	J
State Plane 2900	297382.3, 195032.8	150.2	200.0	569	593

Figure 22. STWAVE domain indicated by black box overlaid on AdH domain.



### Bathymetric data

The accuracy of the model results is directly tied to the accuracy of the bathymetric data incorporated into the model. For this large model domain, multiple data sources were utilized in the specification of the bed elevations. The primary study area was specified utilizing data accumulated and merged by a district contractor (e4sciences\*; Please note: The footnote below will serve for all mentions of this unpublished document throughout this report.). The remaining data consisted of

---

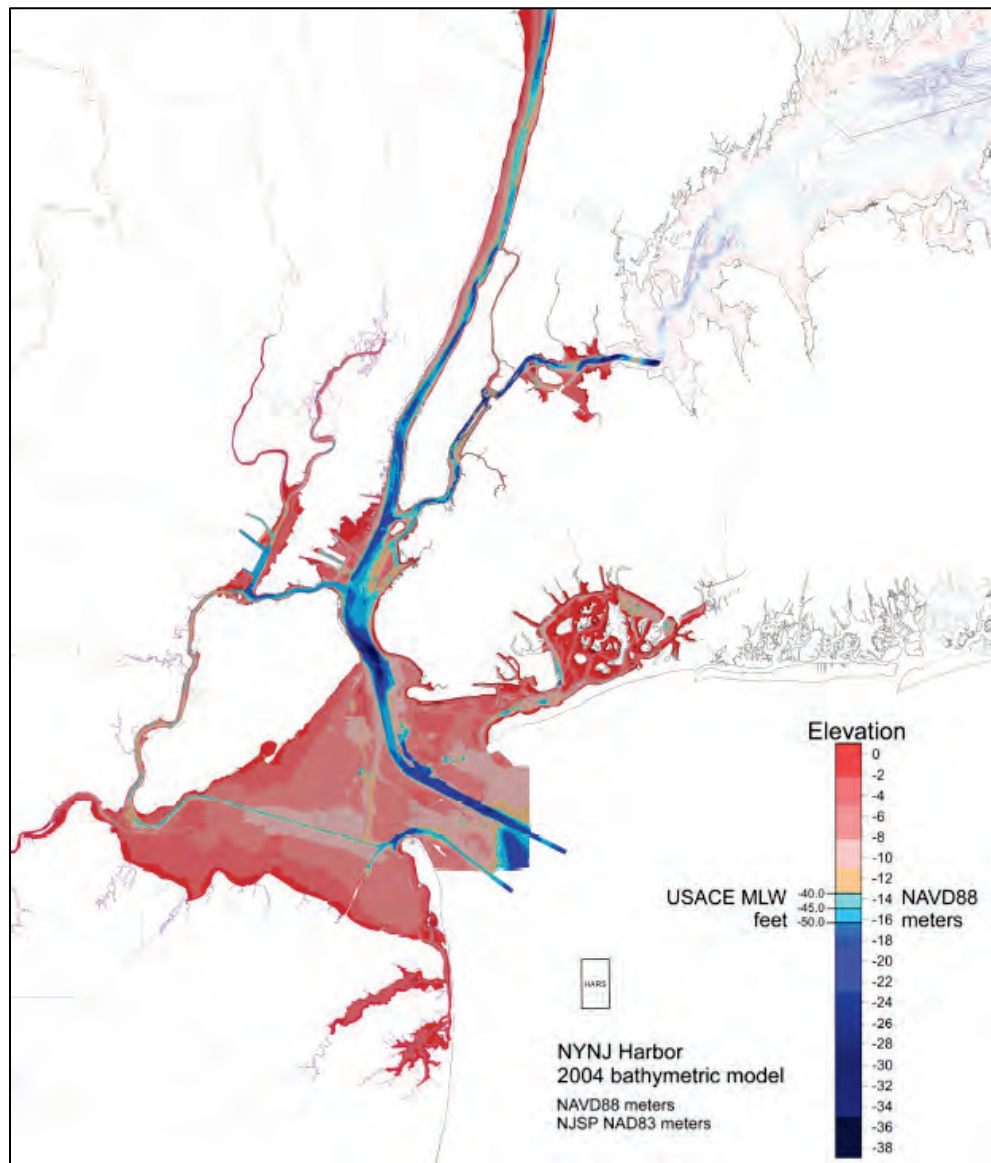
\* e4sciences. 2018. Unpublished report. Contract #W912DS-13-D-0002: Task Order #0004. *New York New Jersey Harbor Deepening Project Sedimentation Study*. Draft Report for the Department of the Army, New York District Corps of Engineers, April 2018.

offshore areas and was specified based on the data from the ADCIRC model utilized in the NACCS (Cialone et al. 2015).

*e4sciences bathymetric model*

e4sciences coalesced available data to create the most accurate representation of the NYNJH bathymetry for 2004 (Figure 23) and 2015. The vertical datum of the provided bathymetry was in meters, NAVD88. Initial model simulations were completed on the 2004 bathymetry dataset, but portions of the 50 ft NYNJH deepening project were already constructed in 2004, and therefore 2004 was not considered an appropriate without-project bathymetry set. As such, the 2004 bathymetry dataset provided by e4sciences was modified to remove any components of the project deepening already constructed in 2004. This was primarily limited to the Kill van Kull area. The with-project configuration is discussed more in subsequent chapters but primarily consisted of modifying the without-project bathymetry to incorporate the project deepening. Therefore, areas not altered due to the construction of the project are the same in both the with- and without-project bathymetry sets. This makes with-project versus without-project comparisons more appropriate as there are no mesh modifications outside the project deepening influencing the model results.

Figure 23. Bathymetric model for 2004 from e4sciences.



#### *ADCIRC bathymetric model*

The e4sciences dataset did not cover the entire model domain. Therefore, additional bathymetric data were required for the remaining areas of the mesh. The NACCS (Cialone et al. 2015) ADCIRC mesh was available for these outlying areas. The ADCIRC mesh resolution is provided in Figure 24. The bathymetric data associated with that mesh is shown in Figure 25.

Figure 24. ADCIRC comprehensive model mesh resolution in the Delaware Bay to Nantucket area including New York Bight.

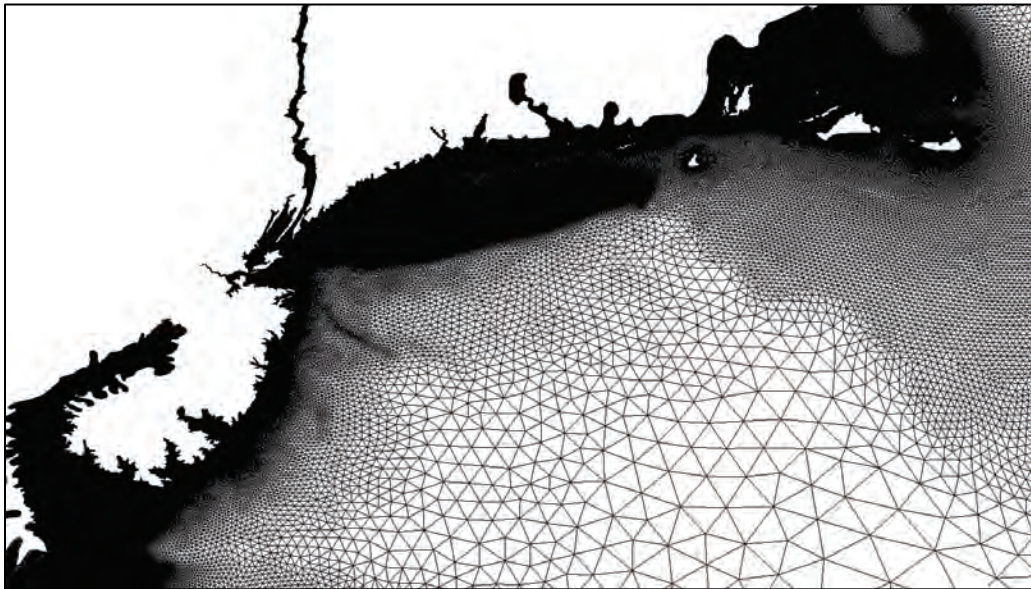
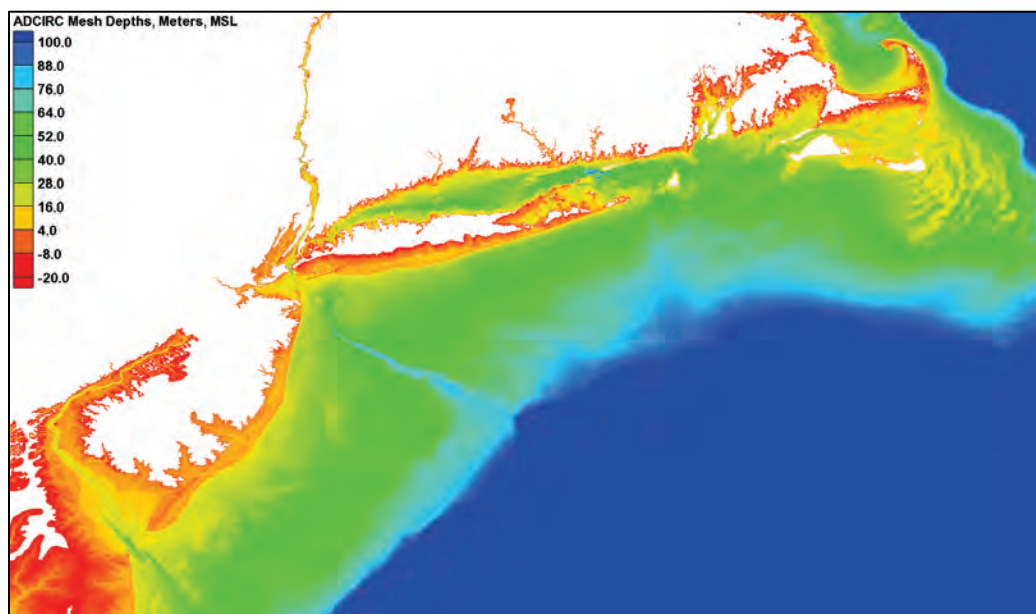


Figure 25. ADCIRC comprehensive model depths, from -20 m mean sea level (MSL) (red) to 100 m (blue).



#### *Adaptive hydraulics mesh bathymetry*

The two previously discussed datasets were converted to the same vertical and horizontal datums and combined with the e4sciences dataset having priority over the NACCS data. The resulting merged dataset was then incorporated into the numerical model mesh with any components of the



channel deepening being removed, resulting in the bathymetry shown in Figure 26 and Figure 27.

For consistency in coupling of the hydrodynamic model, the wave model and the NACCS offshore boundary conditions, the vertical datum for the AdH model was selected as MSL as defined at Sandy Hook.

Figure 26. AdH mesh bathymetry.

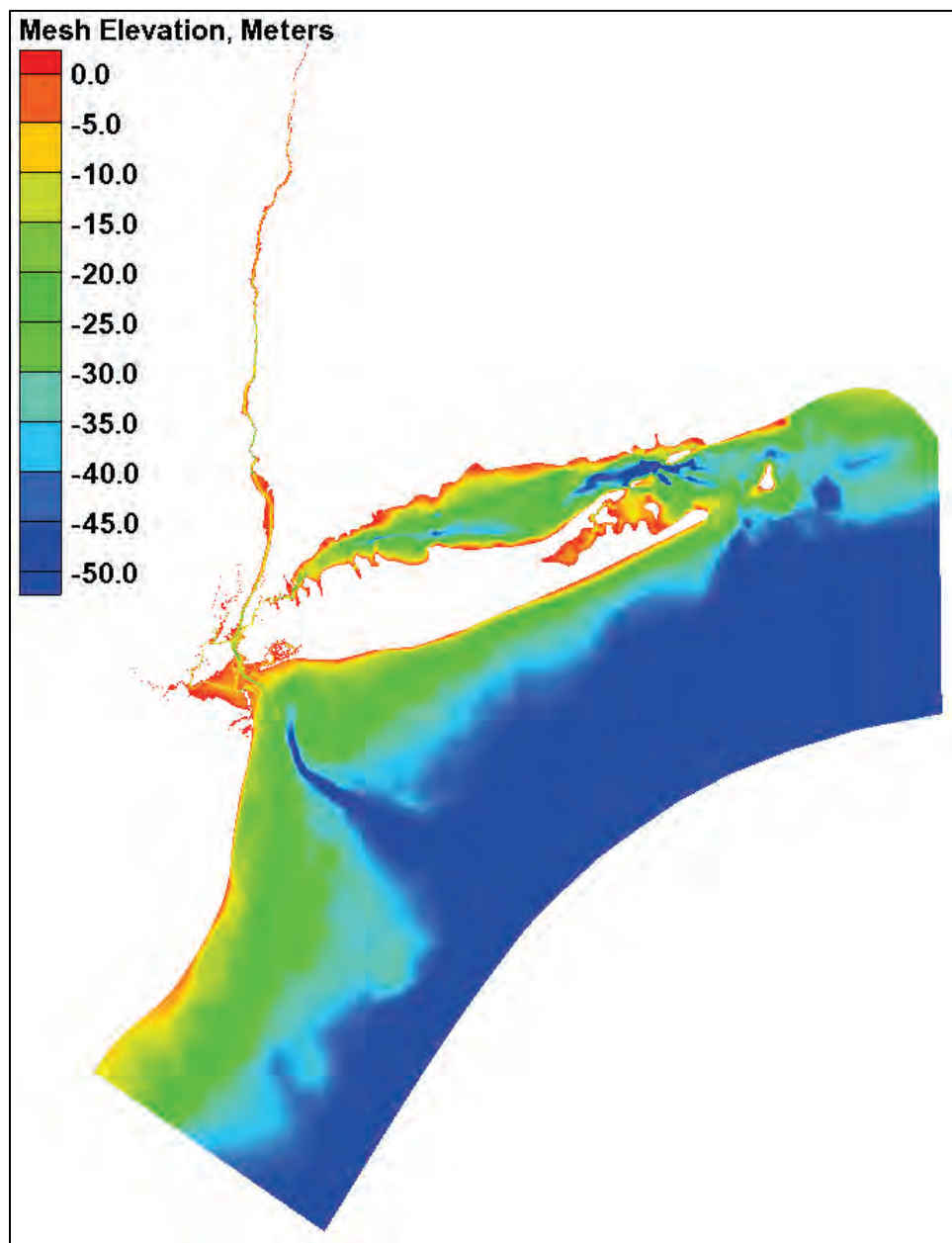
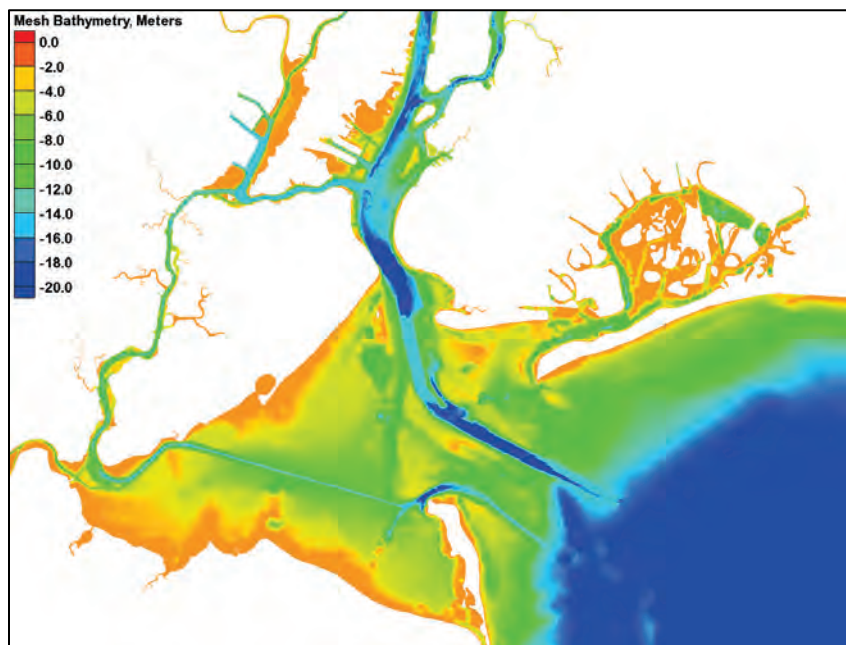


Figure 27. AdH without-project mesh bathymetry in the NYNJH.



*STWAVE mesh bathymetry*

The bathymetry was interpolated from the AdH mesh to populate the STWAVE domain with land based values obtained from the ADCIRC mesh.

## Boundary conditions

The purpose of the numerical model is to perform very complex computations that amount to balancing the water, salt, and each sediment size class over the complete domain of the model and report on the tendencies for various sediment classes to fall into the navigation channels. To perform those balances, the inflowing water, salt, and sediment must be defined as boundary time-series conditions at all tributary inflows and tidal boundaries.

Comparison of the numerical model to long-term field experience necessitates that the model be simulated for a sufficient variety of environmental forcing conditions to make the comparisons appropriate. This is particularly true for sedimentation results. Consequently, five specific calendar years (1985, 1995, 1996, 2011, and 2012) were chosen for model simulation to provide a range of hydrologic inflows and meteorological conditions, including both tropical and extra-tropical storms.



## Riverine flows

The time series for each tributary for the years simulated are presented in Figure 28 through Figure 36, along with the minimum and maximum daily flows during the year. Note that 0.0 values cannot be plotted on log plots. The Hackensack River in particular does not have a minimum line as the minimum flows are 0.0 cfs. The Hudson River is an order of magnitude larger than any of the remaining flows and as such tends to dominate the system. The mean annual discharges for the Hudson River for each of the five simulated years are compared to the cumulative frequency of the mean annual discharge derived from data for 1947 through 2014 in Figure 37. Calendar year 2011 was the year with the highest mean annual discharge (640 cms or 22,570 cfs) while 1995 was the lowest Hudson River discharge year. Table 2 shows the statistics for the included rivers for each of the five simulated years. Table 3 provides the mean flows for the Hudson River for the five simulated years along with an approximate return period for each year.

Figure 28. Annual river discharges for Hudson River for simulation years 1985, 1995, 1996, 2011, and 2012 compared to the minimum and maximum discharges.

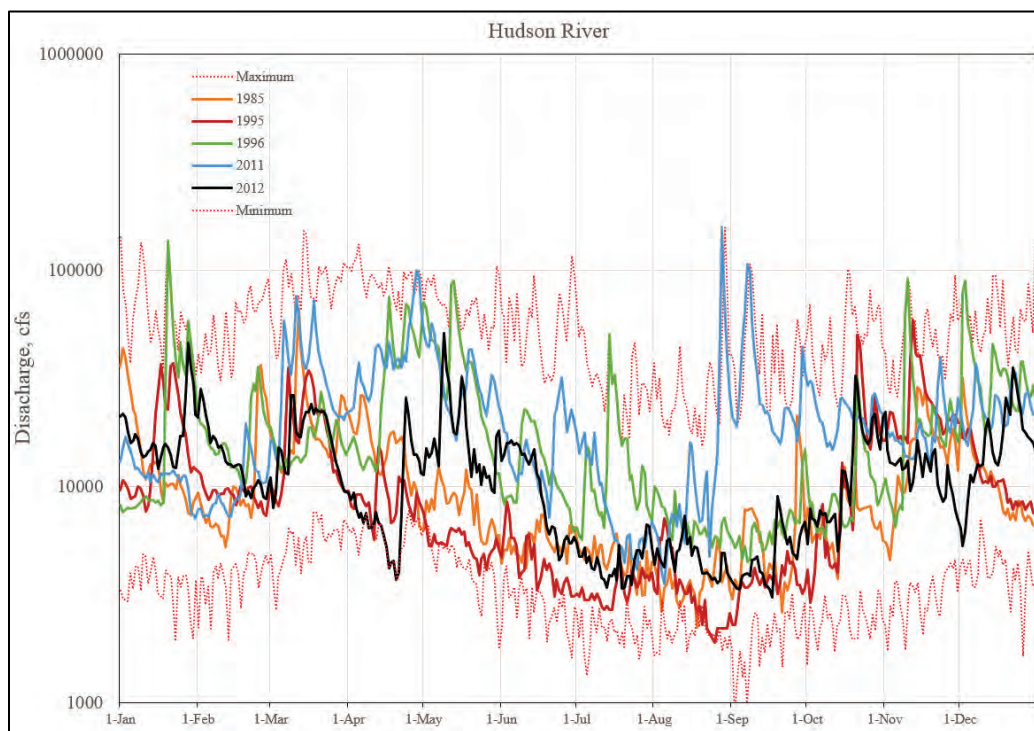


Figure 29. Annual river discharges for Hackensack River for simulation years 1985, 1995, 1996, 2011, and 2012 compared to the minimum and maximum discharges.

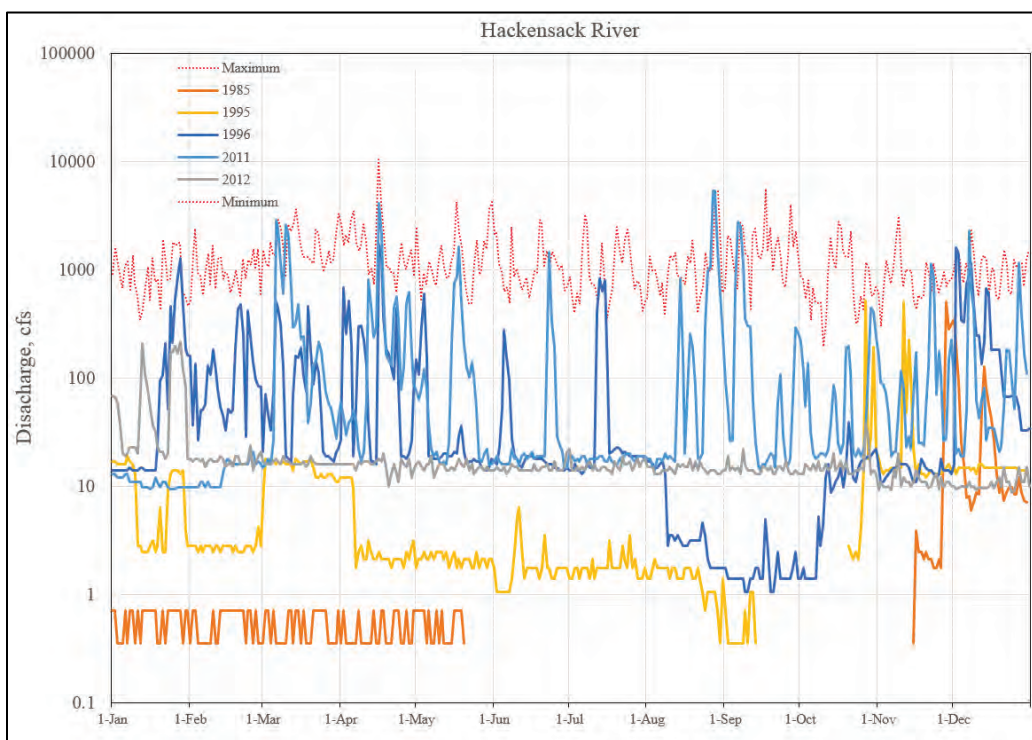


Figure 30. Annual river discharges for Passaic River for simulation years 1985, 1995, 1996, 2011, and 2012 compared to the minimum and maximum discharges.

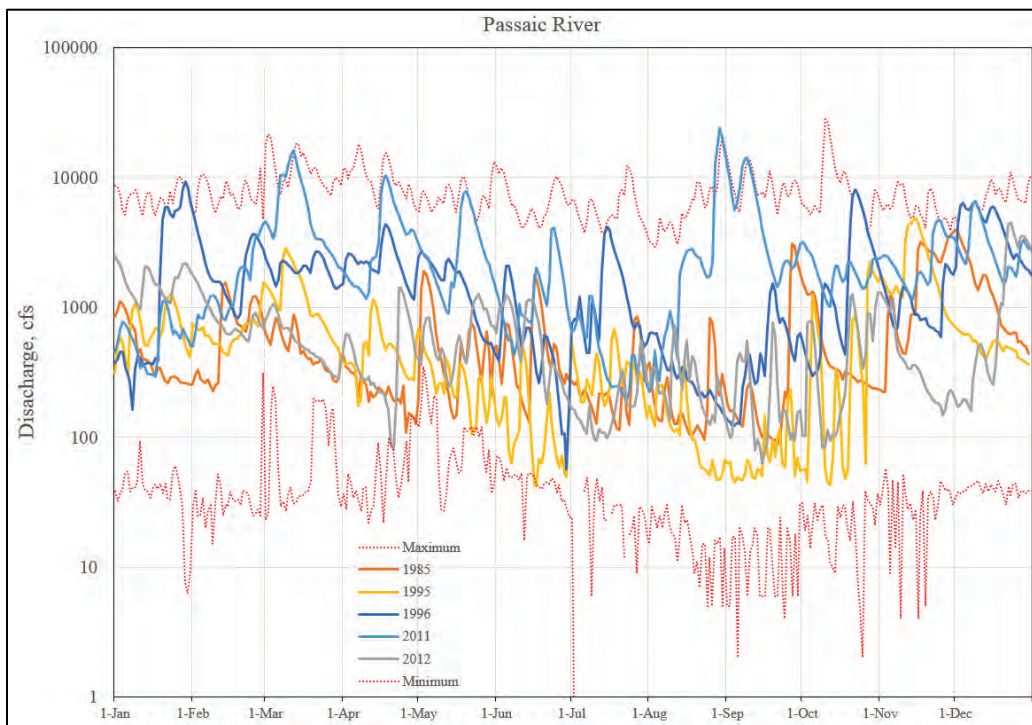




Figure 31. Annual river discharges for Saddle River for simulation years 1985, 1995, 1996, 2011, and 2012 compared to the minimum and maximum discharges.

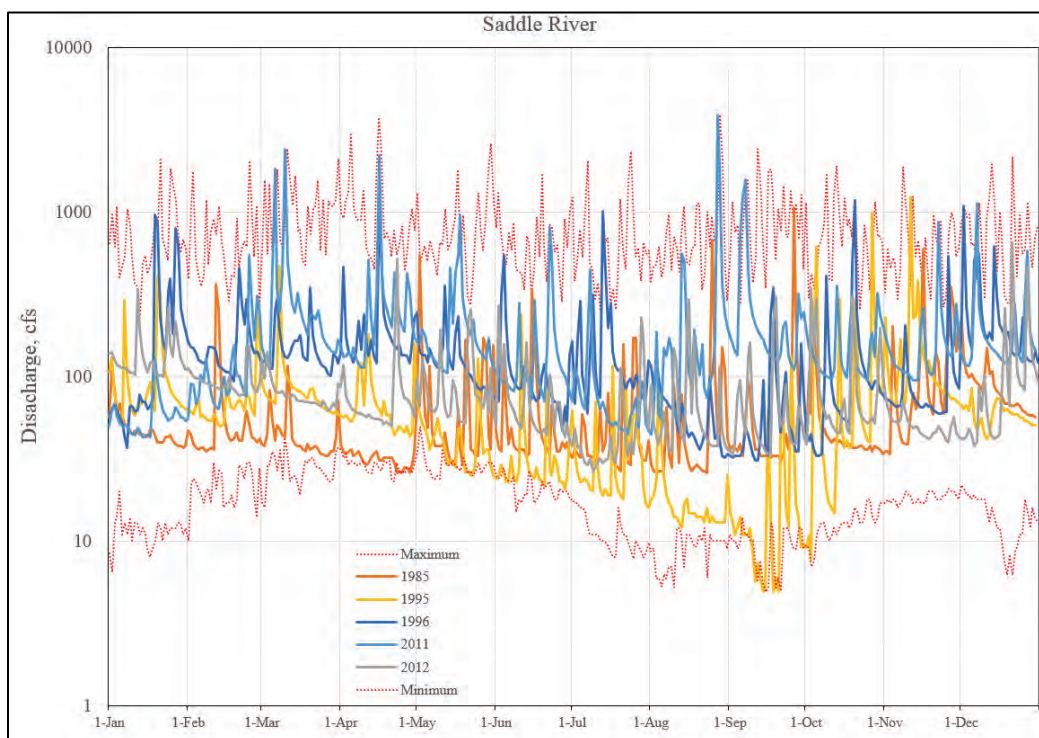


Figure 32. Annual river discharges for Third River for simulation years 1985, 1995, 1996, 2011, and 2012 compared to the minimum and maximum discharges.

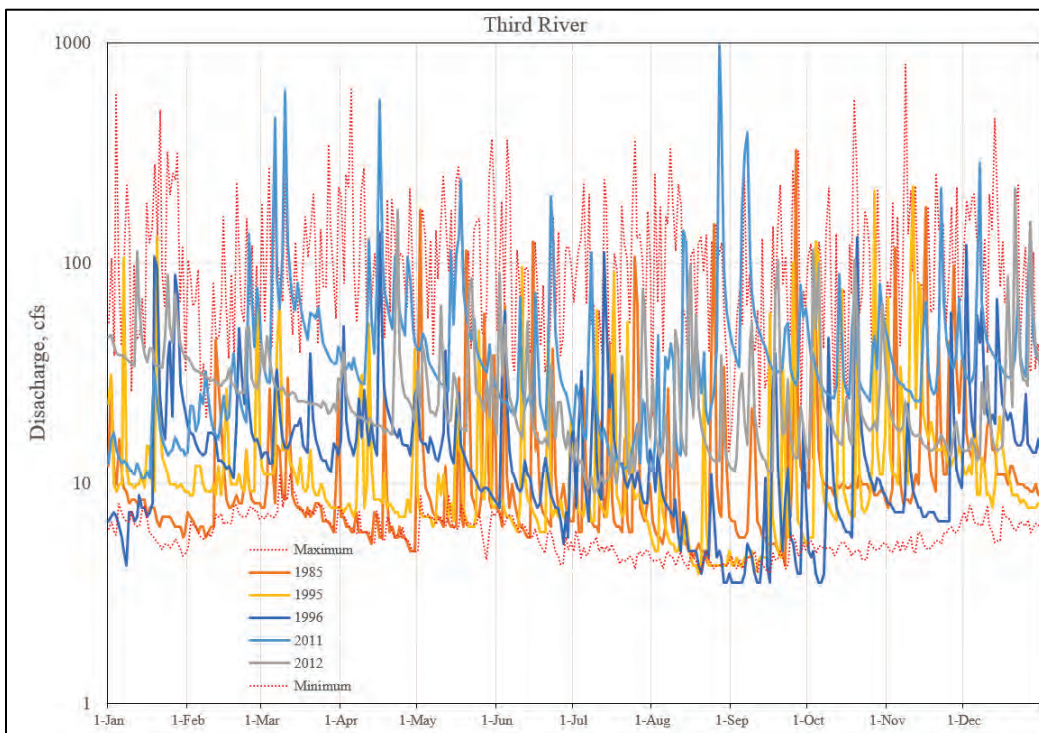


Figure 33. Annual river discharges for Rahway River for simulation years 1985, 1995, 1996, 2011, and 2012 compared to the minimum and maximum discharges.

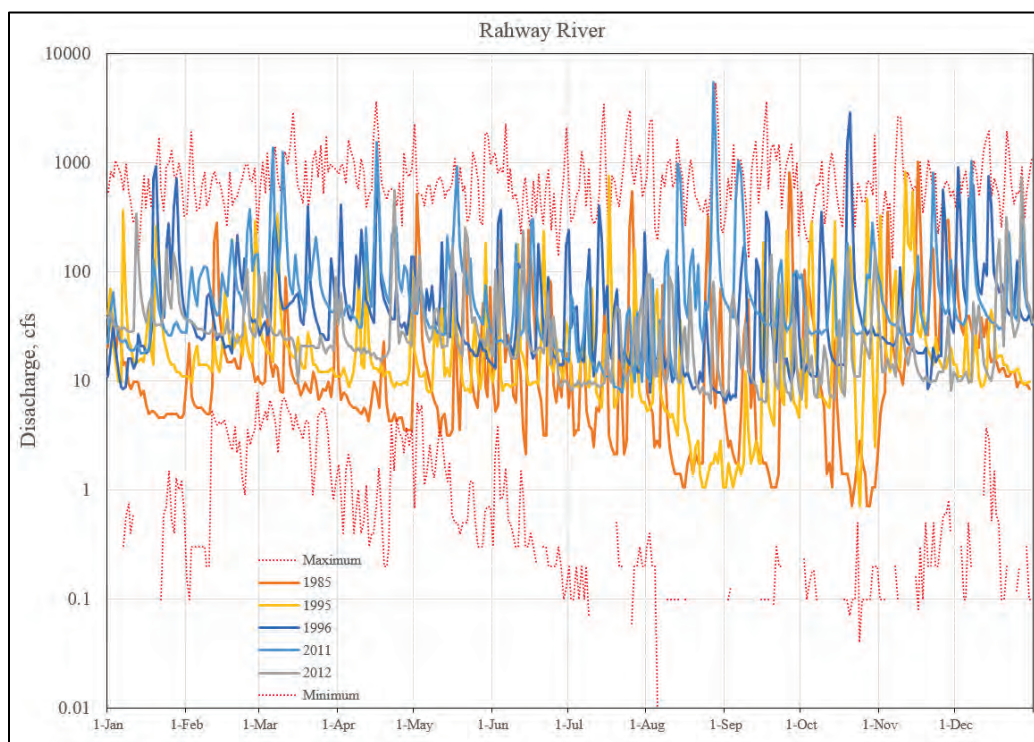


Figure 34. Annual river discharges for Raritan River for simulation years 1985, 1995, 1996, 2011, and 2012 compared to the minimum and maximum discharges.

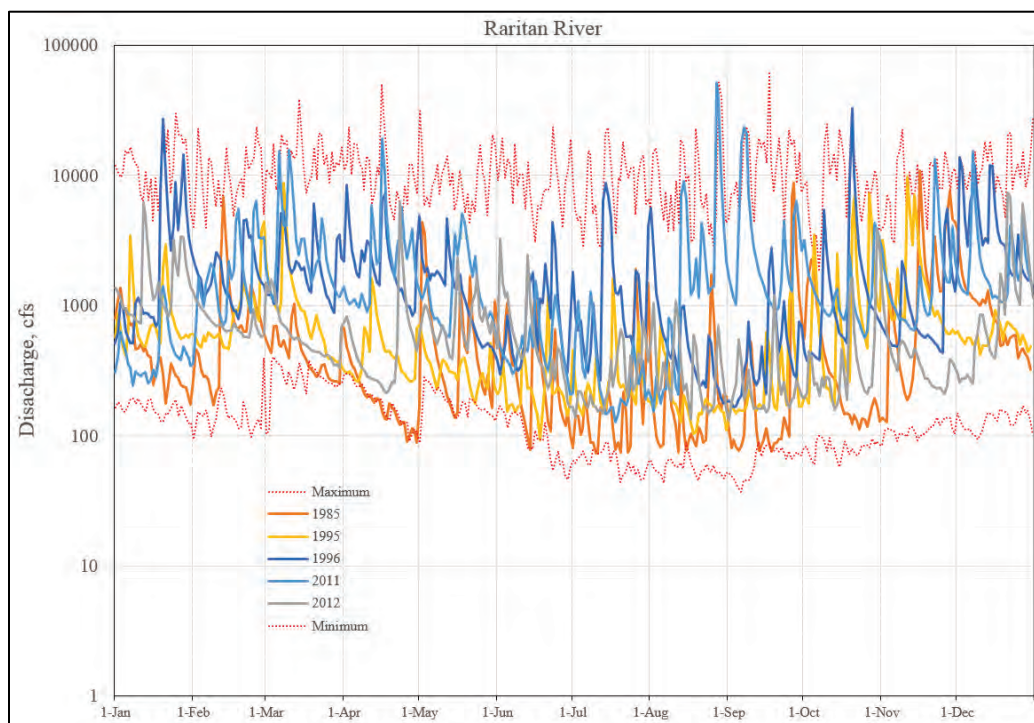




Figure 35. Annual river discharges for Lawrence Brook for simulation years 1985, 1995, 1996, 2011, and 2012 compared to the minimum and maximum discharges.

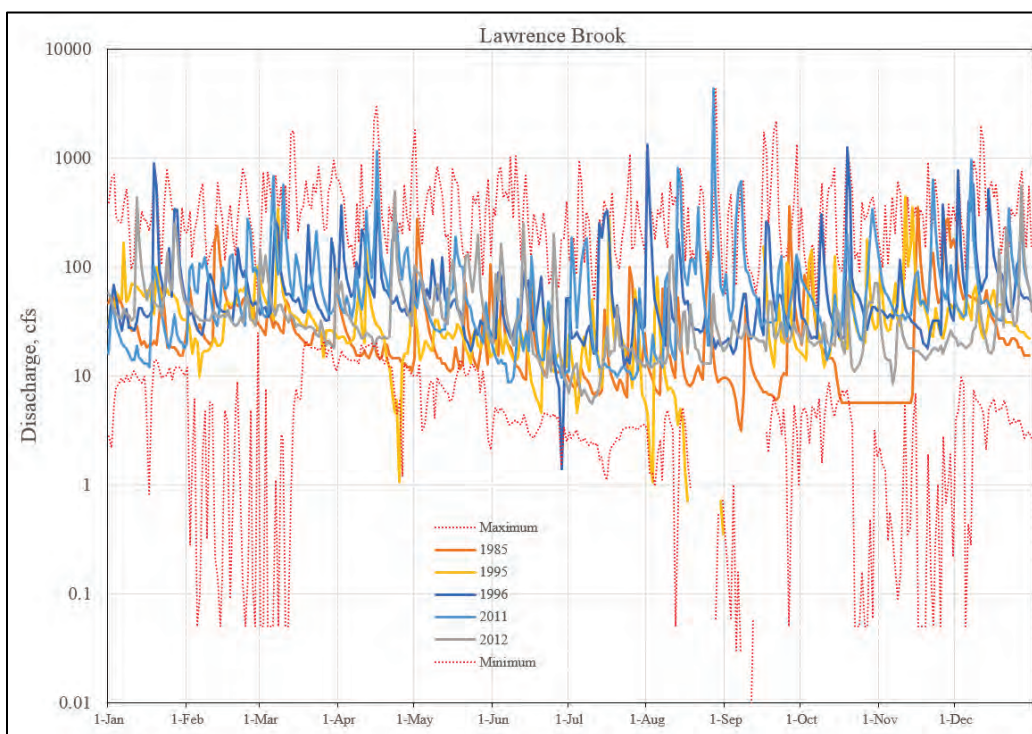


Figure 36. Annual river discharges for the South River for simulation years 1985, 1995, 1996, 2011, and 2012 compared to the minimum and maximum discharges.

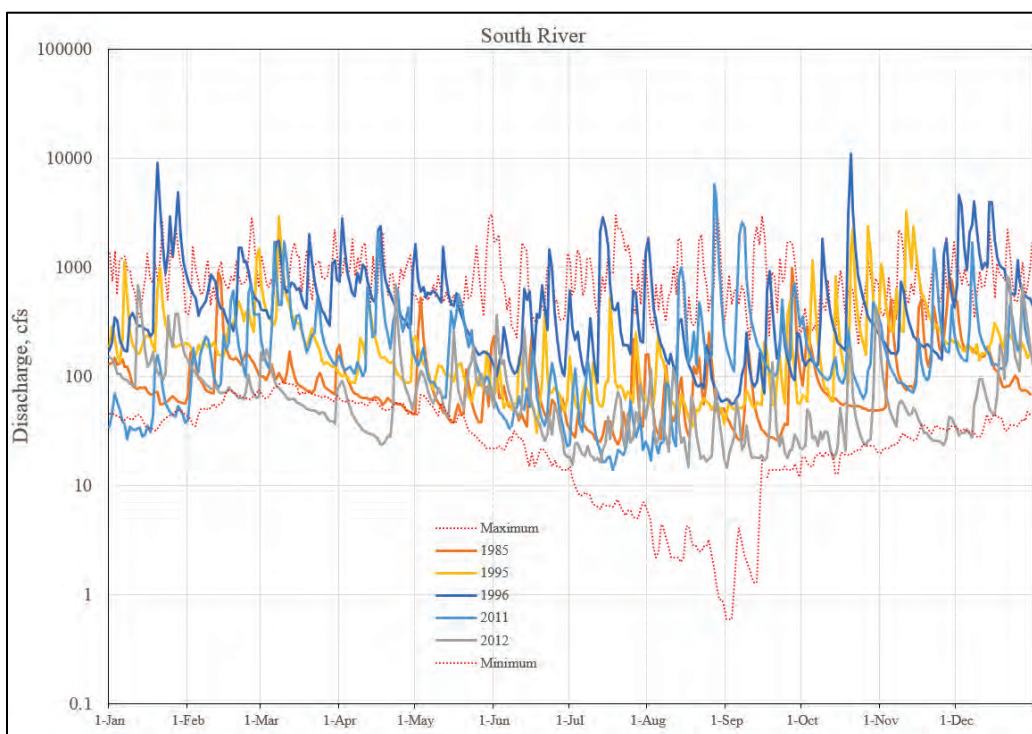


Figure 37. Cumulative frequency of average annual Hudson River discharge from 1947 through 2014 compared to model simulation years.

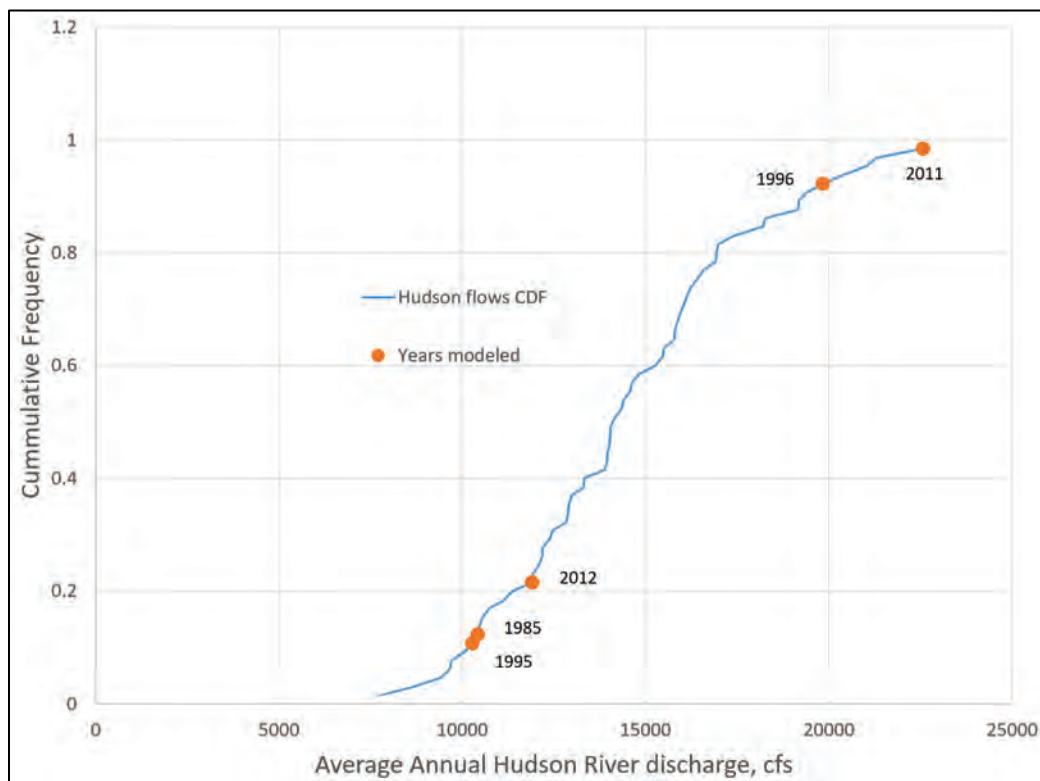


Table 2. Statistics of tributary inflows for simulation years (in cms)

Calendar Year	Statistic	Tributary								
		Hudson	Passaic	Raritan	Hackensack	South	Lawrence	Rahway	Saddle	Third
1985	Peak	1,869.0	111.8	305.8	14.24	27.52	10.28	28.60	30.30	9.20
	Minimum	63.4	2.5	2.1	0.00	0.68	0.09	0.02	0.74	0.12
	Average	296.8	18.4	18.9	0.19	3.06	0.91	0.97	1.86	0.42
	Std Dev	225.6	20.8	33.0	1.17	3.41	1.26	2.67	2.45	0.74
1995	Peak	1,667.9	137.6	277.8	14.67	92.60	12.54	23.22	35.11	6.34
	Minimum	53.8	1.2	2.6	0.00	0.87	0.00	0.02	0.14	0.11
	Average	290.6	17.2	21.1	0.29	7.04	1.00	1.01	1.96	0.43
	Std Dev	250.1	21.0	31.9	1.16	10.64	1.25	2.38	2.87	0.67
1996	Peak	3,879.6	262.5	926.0	47.86	308.66	37.38	81.84	35.11	3.90
	Minimum	127.4	1.6	4.7	0.03	1.58	0.04	0.18	0.88	0.10
	Average	560.9	50.9	57.5	2.89	19.16	2.24	2.46	4.14	0.46
	Std Dev	498.2	48.8	86.2	6.42	28.74	3.78	5.93	4.44	0.49
2011	Peak	4,474.2	674.0	1,461.2	152.35	162.36	122.90	154.05	110.72	27.68
	Minimum	100.0	5.3	3.6	0.27	0.40	0.25	0.22	1.22	0.30
	Average	638.4	81.3	63.9	5.99	7.10	2.64	3.25	5.74	1.43
	Std Dev	489.1	92.8	123.5	17.03	13.72	7.21	9.85	9.19	2.30
2012	Peak	1,452.7	127.7	209.3	6.12	23.25	15.66	20.50	18.58	6.19
	Minimum	87.2	1.8	3.7	0.25	0.41	0.16	0.18	0.76	0.25
	Average	337.8	19.1	20.8	0.56	2.31	1.20	1.06	2.41	0.80
	Std Dev	207.5	19.8	26.6	0.70	2.95	1.56	1.74	1.91	0.64

Table 3. Return periods for mean annual Hudson River inflows for simulation years

Calendar Year	Mean Annual Discharge		Return Period (years)
	cfs	cms	
1985	10,420	295.1	1.14
1995	10,270	290.8	1.12
1996	19,830	561.5	13
2011	22,570	639.1	65
2012	11,900	337.0	1.3

*River inflow sediment concentrations*

The data needs for the upstream sediment boundary conditions are based on the numerical approach used at the boundary. There are two general approaches that have been used in AdH for other sediment transport studies. The most direct is to specify the inflowing sediment concentrations by sediment size class, with the summation of all size classes being the total concentration. The primary problem with this method is insufficient data to specify either the size distribution or even the total concentration as a function of time. The second approach was developed to compensate for these data deficits.

This method is usually best applied to riverine conditions that are in relative equilibrium. The assumption of equilibrium in the transport is only applicable to sand transport. A section of the model adjacent to the boundary and some distance downstream is treated in a special way. The bottom bed surface elevation is fixed. The bed sediment distribution is initialized and the bed thickness set as a deep reservoir of sediment. The boundary concentration is set to a low value, commonly zero. As the flow enters, the model sediment entrainment occurs, providing enough sediment supply, until at the downstream end of this initialization section the sediment concentrations are near equilibrium based on the hydrodynamic conditions. This method does not work well for fines or wash load. Also, tidal rivers provide further complications. This study utilized a combination of the two aforementioned approaches. The specification of the inflowing concentrations was directly specified while the upstream riverine sections were specified with a fixed bottom bed surface elevation to allow the model to adjust to inconsistencies in the inflowing concentrations. The issues regarding data deficits in determining an accurate incoming sediment concentration at all times for each grain class is still present but reduced with this methodology.



### *Hudson River*

The primary source of sediment for the estuary is the Hudson River for the inner harbor and littoral beach sands for Ambrose Channel. The upstream limit of the numerical model was chosen as the Troy Lock and Dam. The gaging station used for the Hudson River inflows is primarily at Green Island, which is approximately a mile downstream of Troy Lock and Dam. There are only limited measurements of suspended sediment at the Green Island gaging station and none for the simulated time periods.

Upstream of Troy Lock and Dam on the Hudson River is the Waterford gaging station with suspended sediment concentrations (SSC) available for 2011 and 2012, but not for the other 3 years (1985, 1995, and 1996). Between the Waterford gaging station and the Green Island station, the Mohawk River enters the Hudson from the west, approximately 0.8 mi above Troy Lock and Dam. A schematic of this confluence is provided in Figure 38. An aerial image of the confluence is provided in Figure 39. Suspended sediment and discharge data are available for the Mohawk River at Cohoes, NY, for some years but not others. When no suspended sediment concentration data were available for the Hudson River at Green Island, an estimate could be made, provided there were SSC data at both the Mohawk River at Cohoes and for the Hudson at Waterford.

Figure 38. Schematic of confluence of Mohawk River and Hudson River.

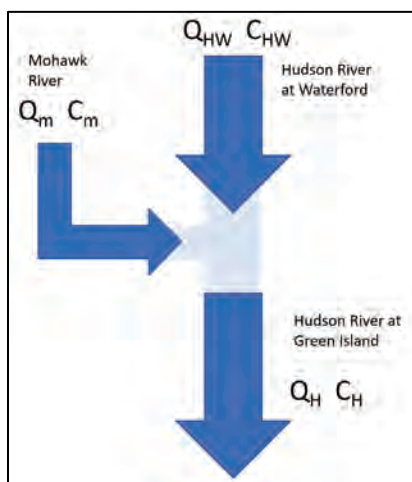


Figure 39. Aerial Image of confluence of Mohawk and Hudson Rivers.



The estimate (Equation 5) was made assuming that the SSC does not interact with the bed between the upstream gaging station and the station at Troy (which is aliased as Green Island data).

$$C_H = \frac{C_M Q_M + C_{HW} Q_{HW}}{Q_H} \quad (5)$$

where

- $C_H$  = SSC at Green Island
- $C_M$  = SSC of Mohawk River at Cohoes
- $C_{HW}$  = SSC of Hudson River at Waterford
- $Q_H$  = Hudson River discharge at Green Island
- $Q_M$  = Mohawk River discharge at Cohoes
- $Q_{HW}$  = Hudson River discharge at Waterford.

The percentiles of available SSC data for the Hudson River at Waterford are presented in Figure 40. The peak SSC was approximately 800 ppm by weight. The percentiles of SSC for the Mohawk River at Cohoes are presented in Figure 41. The maximum SSC for the Mohawk River was approximately 2,500 ppm. The sediment concentrations on the Mohawk are generally higher than on the Hudson.

The Hudson River also has ungauged flows that enter below Troy Lock and Dam. This modeling effort neglected these flows as they were not deemed significant and would have minimal impact on the model results. Appendix A details the magnitude of these additional flows.

Figure 40. Percentiles of sediment concentration for Hudson River at Waterford.

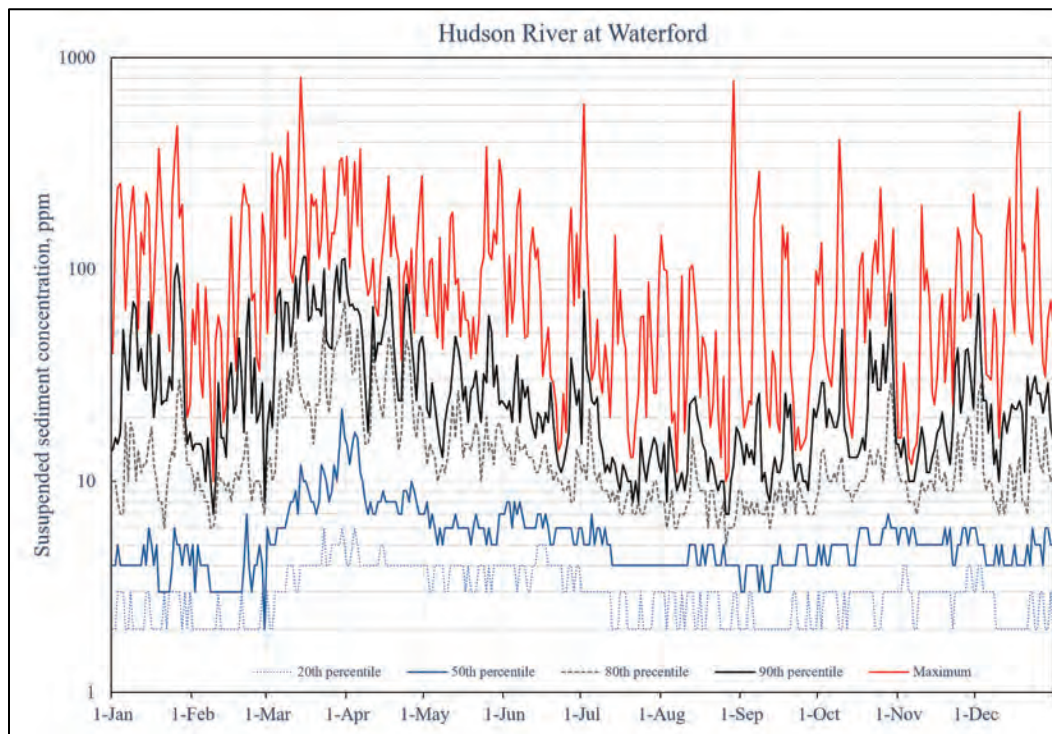
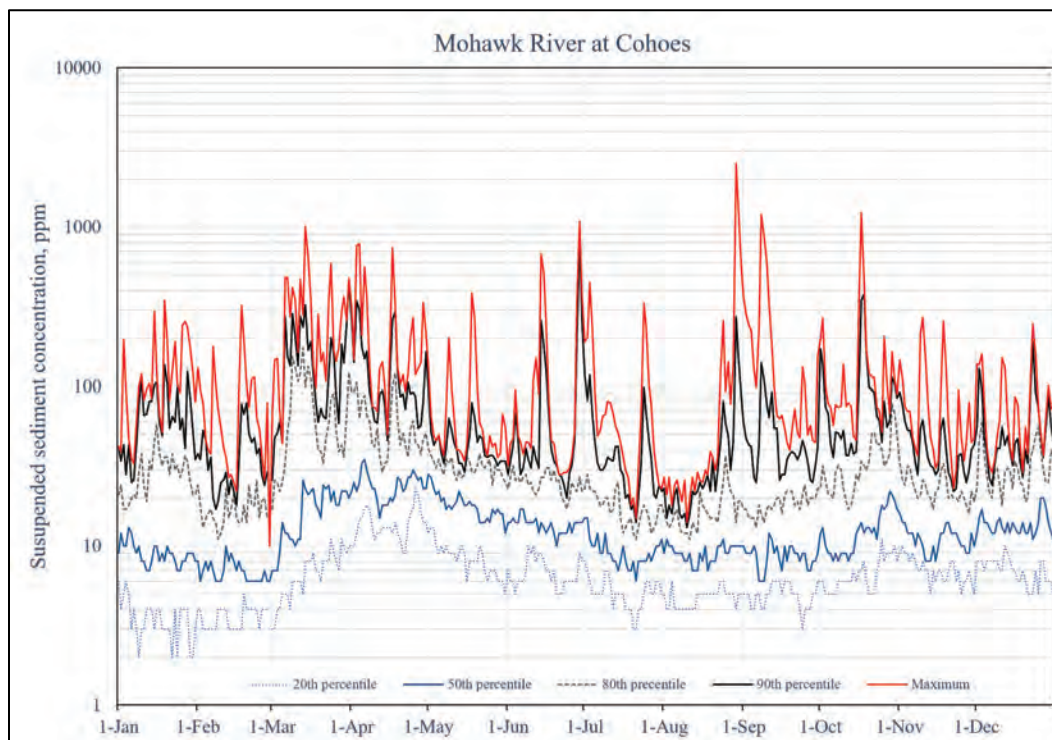


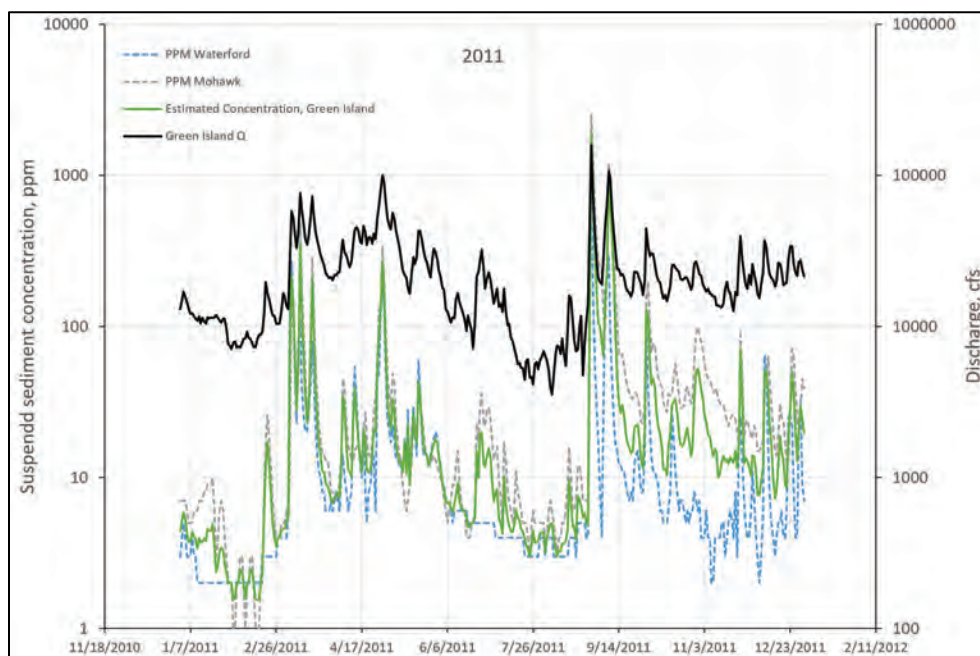
Figure 41. Percentiles of sediment concentration for Mohawk River at Cohoes, NY.



For calendar year 2011, the approximation technique of Equation 5 for the SSC of the Hudson River at Green Island is presented in Figure 42 and compared to the SSC data for the Mohawk at Cohoes and the Hudson River at Waterford. The maximum concentrations in early September are associated with the heavy rains of Hurricane Irene, which produced significant sediment load on the Mohawk River. As expected, because Equation 5 is essentially a weighted averaging, the estimated SSC for Green Island lies between the values at Waterford and Cohoes. The maximum SSC for 2011 at Green Island was estimated to be 1,841 ppm.

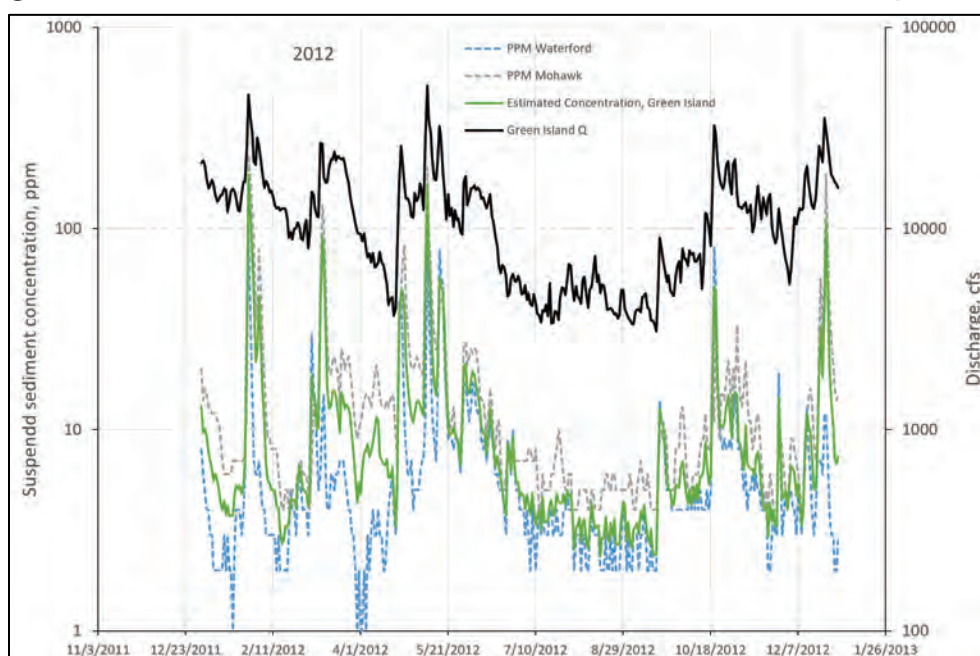


Figure 42. Estimation of 2011 SSC at Hudson River at Green Island via Equation 5.



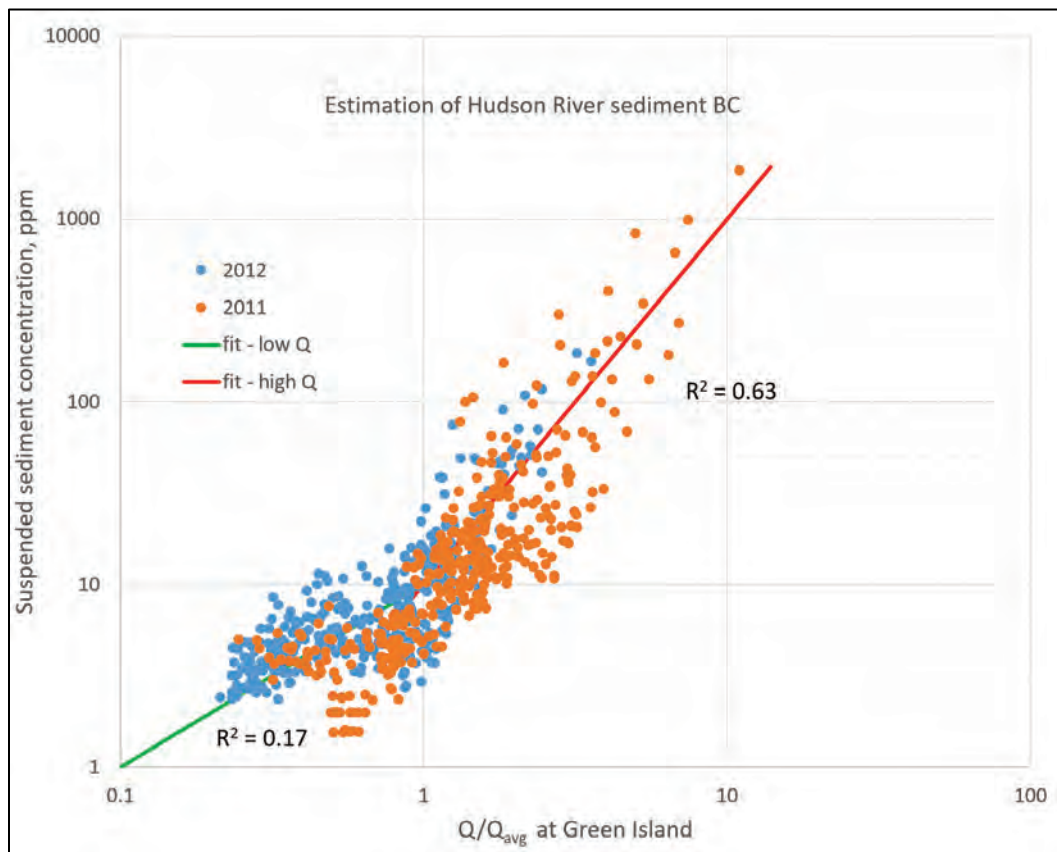
The estimation for calendar year 2012 is presented in Figure 43. Similar averaging of results is seen for 2012. The maximum SSC at Green Island was estimated at 185 ppm for 2012.

Figure 43. Estimation of 2012 SSC at Hudson River at Green Island via Equation 5.



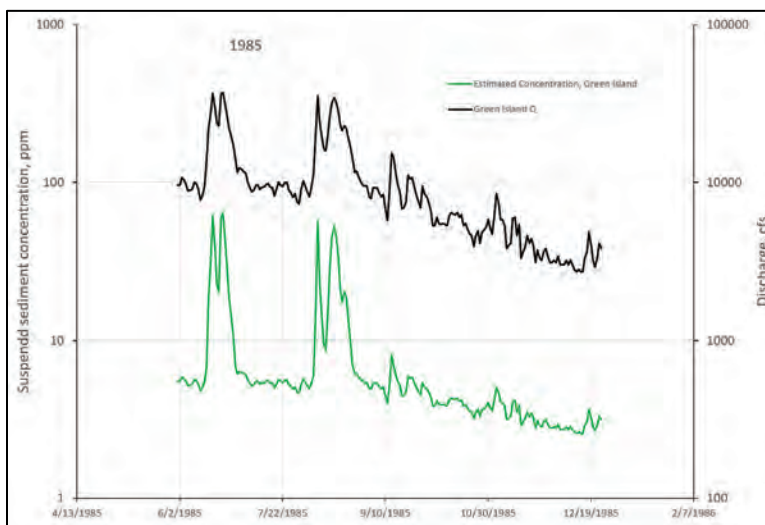
For calendar years 1985, 1995, and 1996, SSC data were not available for both the Mohawk River at Cohoes and the Hudson River at Waterford; therefore, making use of Equation 5 was not an option. Also, SSC data were not available at the Hudson River at Green Island. As an alternative, a relationship was sought between the Hudson River discharge at Green Island and the estimated SSC for 2011 and 2012. It was found that an effective independent variable for the SSC is the nondimensional discharge ( $Q/Q_{avg}$ ). A plot of the SSC versus the nondimensional discharge is shown in Figure 44 for the estimated SSC for years 2011 and 2012. A regression was performed for the nondimensional discharges above and below 1.0. The upper data showed the SSC to be dependent on the square of the discharge and the lower data linear with discharge. At higher flood flows (nondimensional discharge  $> 1$ ), the SSC is transport capacity controlled. At lower flows the SSC may be sediment supply limited.

Figure 44. Relationship of flow-weighted suspended sediment concentration with nondimensional river discharge for the Hudson River at Green Island.



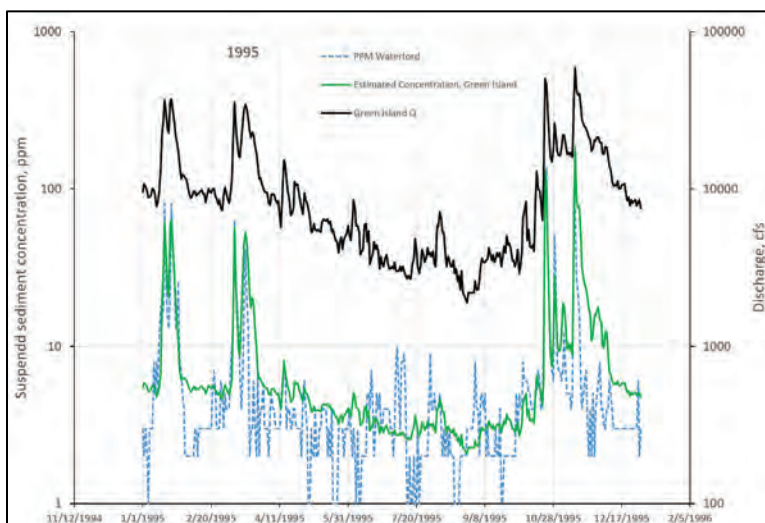
Using the regression fits shown in Figure 44, the SSC for the Hudson River at Green Island were estimated for the calendar year 1985 (Figure 45). The correlation is clear, showing the trends in SSC directly following the variation in the river discharge.

Figure 45. Estimation of the SSC for 1985 using the regression shown in Figure 44.



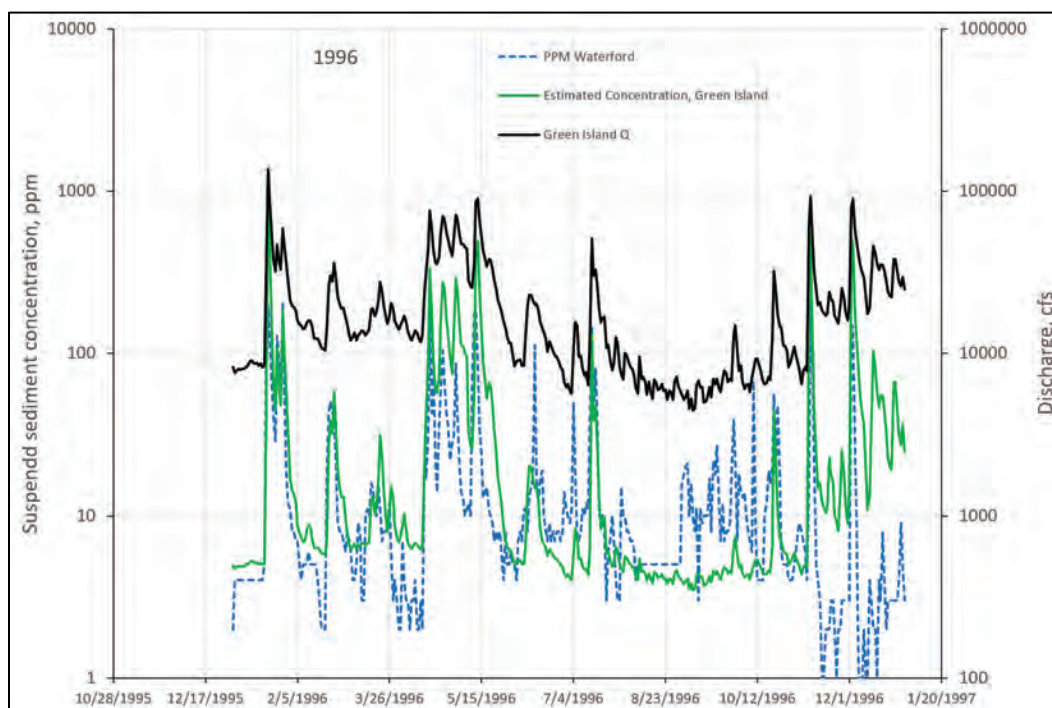
The application of the relationship of Figure 44 for calendar year 1995 is presented in Figure 46. For 1995, SSC data were available at Waterford on the Hudson, which follows very closely the regression-estimated sediment concentrations for Green Island.

Figure 46. Estimation of the SSC for 1995 using the regression shown in Figure 44.



The estimated SSC for calendar year 1996 is shown in Figure 47. For 1996, data were again available at Waterford. The estimated Green Island SSC follows the trends of the Waterford SSC very well through August but shows some deviation in the fall.

Figure 47. Estimation of the SSC for 1996 using the regression shown in Figure 44.

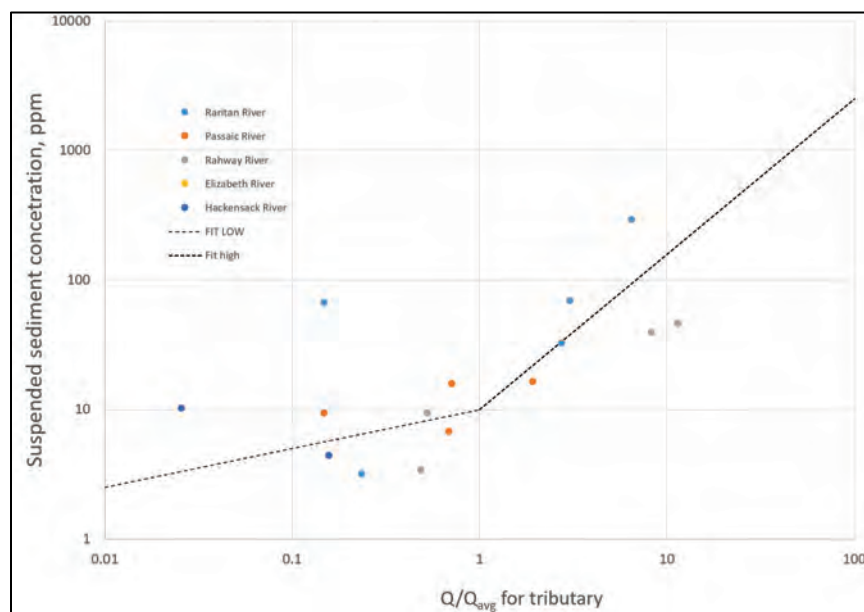


### *Remaining tributaries*

For the secondary tributaries discharging into the harbor, there are very limited SSC data. Many of these tributaries are regulated, and there is not significant sediment load. Taking all of the limited measurements of SSC from these tributaries and plotting them against the nondimensional discharges for each tributary yields the relationship shown in Figure 48.



Figure 48. Secondary tributary SSC data as a function of the nondimensional river discharge.



Applying the relationship of Figure 48 to the individual river flows on the secondary tributaries gives the overall estimated SSC time series for 2012 as shown in Figure 49. Comparable time series were developed for the remaining years of simulation. The sediment inflows from the smaller tributaries are small primarily because the discharges are relatively small. However, each sediment inflow can have localized impact on the sedimentation environment. Note that the uncertainty in these inflow concentrations is significant and could result in increased uncertainty in the model results. The data fit shown in Figure 48 exhibits a scatter of approximately an order of magnitude for a given non-dimensional discharge.

The estimated grain size distribution of the inflows is shown in Figure 50. The development of the distribution curves for sediment concentrations was based on the fact that as the river discharge increases, the shear stresses will increase and the range of grain sizes that can be mobilized from the bed and entrained will become coarser. The use of relative river flows includes an assumption that each of the tributary systems has reached some sort of equilibrium in the balance between the morphology of the river channels and the hydrology. Therefore, doubling the discharge from the mean flow would have a similar impact on each tributary in terms of entrainment of coarser material. Note that as the relative discharge increases, the finest fraction is fixed, and the other percentiles become progressively coarser.

The coarsest grain size that is in suspension increases in response to increases in the shear stresses associated with increased discharge. Below the mean flow, the flows are confined to the river channel, so the increase in velocities are more linear with the ratio of the discharge. At flood flows, the response is less dramatic on the flow velocities due to increased water depths and flows in the overbanks. The grain size distributions in Figure 50 reflect this sensitivity. For flows less than the mean, the proportion was linear while above the mean flows, the coarsest grain size ratio was assumed proportional to the flow ratio to the one-third.

Also note that the actual distribution curve used is interpolated between the plotted curves based on the actual nondimensional discharge. The curve for a nondimensional discharge of 100 is very rarely used because for the majority of tributaries the peak nondimensional discharge is below 10. The only tributaries with high nondimensional discharges tend to be the small tributaries.

Because most of the tributaries have long river channel reaches before entering the estuary, it is assumed that the bed interaction along the tributaries within the model domain will make adjustments to the sediment distribution.

Figure 49. Time series of suspended sediment inflow boundary conditions for the 2012 simulation year.

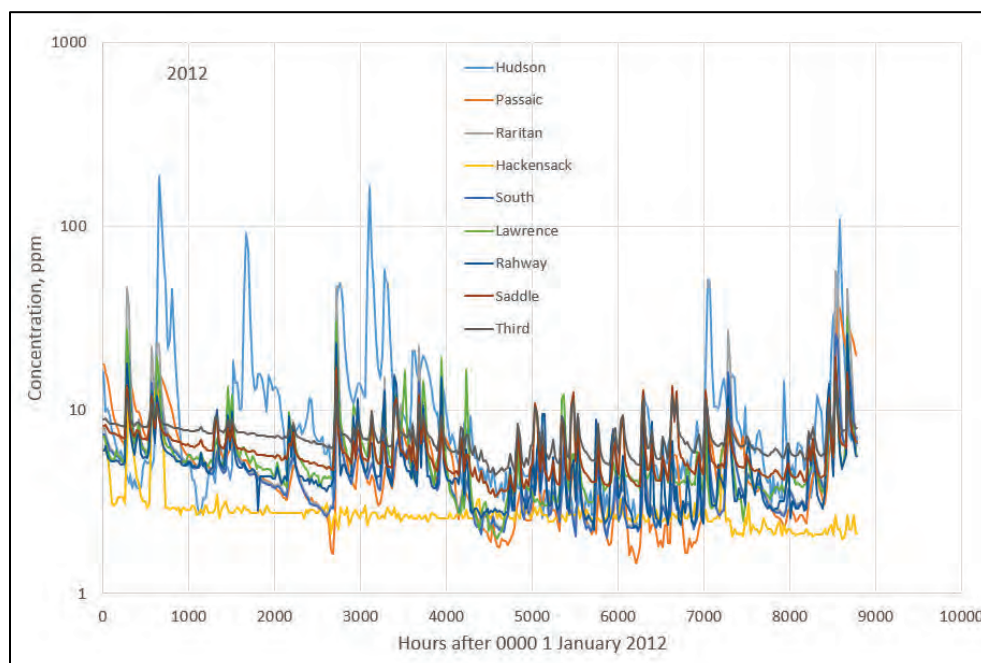
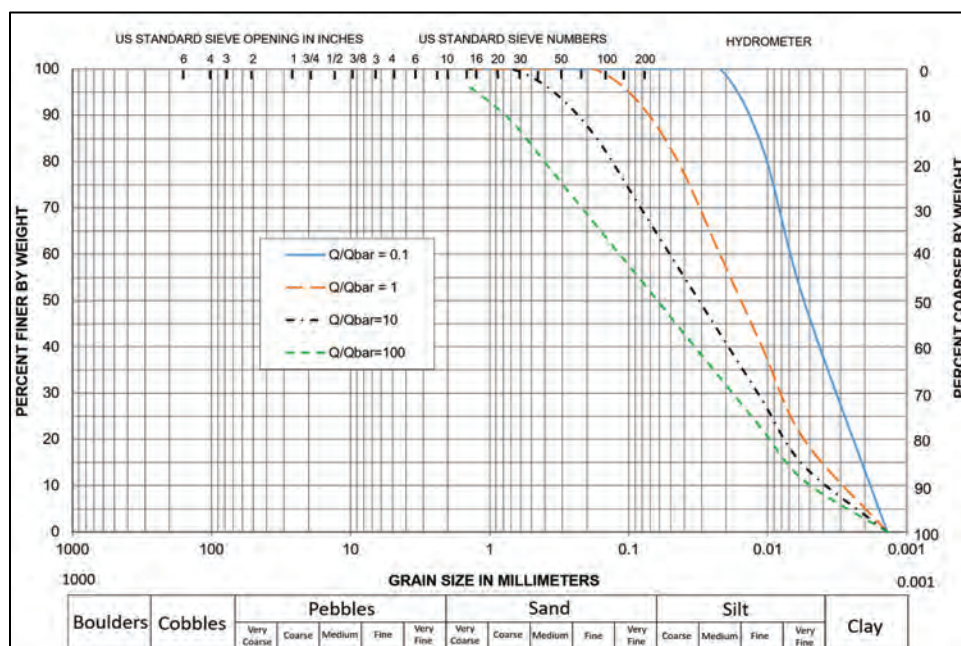


Figure 50. Grain size distribution used in the tributary inflows as a function of the nondimensional discharge.



### Wastewater treatment facility flows

NYNJH Estuary Program, 2008, details the New Jersey wastewater treatment facilities along with approximate flowrates. This consisted of 12 facilities with a total flowrate of 612.7 MGD or 26.84 cms. The New York City Department of Environmental Protection (n.d.) details the New York wastewater treatment facilities along with approximate flowrates. This consisted of 14 facilities with a total flowrate of 1,805 MGD or 79.1 cms. At times, the cumulative flow of wastewater treatment facilities can rival the riverine freshwater flows (see Table 4 and Figure 28 to Figure 36). The locations of all the New York and New Jersey MWWTs are shown in Figure 51. The locations and flowrates are provided in Table 4.

Figure 51. Wastewater facility discharge locations.

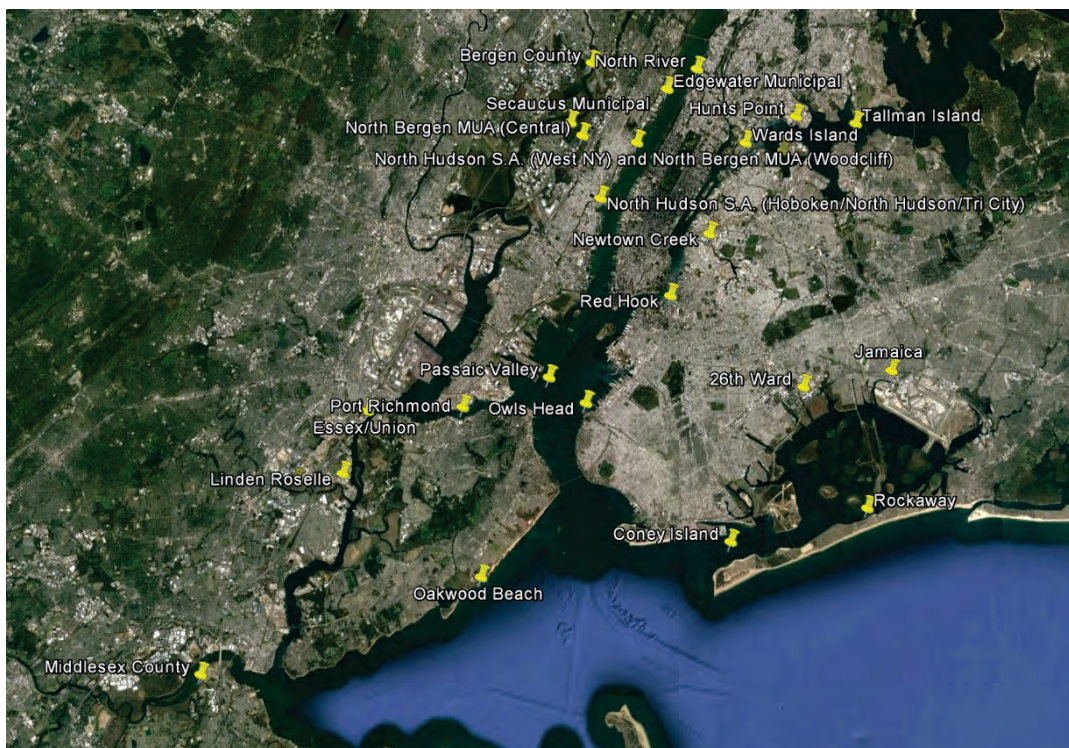


Table 4. Wastewater treatment discharge locations and flow rates.

Wastewater Treatment Locations and Discharges			
Wastewater Treatment Facility	Location (decimal degrees)		Discharge (cms)
	Latitude	Longitude	
Passaic Valley (NJ)	40.7084	74.1209	12.4
Middlesex County (NJ)	40.4922	74.3177	5.0
Bergen County (NJ)	40.8314	74.0320	3.0
Essex/Union (NJ)	40.6386	74.1961	2.6
Rahway Valley (NJ)	40.5999	74.2482	1.1
Linden Roselle (NJ)	40.6038	74.2141	0.6
North Hudson S.A. (Hoboken/North Hudson/Tri City) (NJ)	40.7565	74.0257	0.9
North Bergen MUA (Central) (NJ)	40.7913	74.0389	0.3
North Hudson S.A. (West NY) and North Bergen MUA (Woodcliff) (NJ)	40.7874	73.9991	0.6
Secaucus Municipal (NJ)	40.7985	74.0477	0.1

Wastewater Treatment Locations and Discharges			
Wastewater Treatment Facility	Location (decimal degrees)		Discharge (cms)
	Latitude	Longitude	
Edgewater Municipal (NJ)	40.8170	73.9769	0.1
Bowery Bay (NY)	40.7827	73.8919	6.6
Hunts Point (NY)	40.8017	73.8825	8.8
Tallman Island (NY)	40.7977	73.8388	3.5
Wards Island (NY)	40.7871	73.9195	12.0
Newtown Creek (NY)	40.7366	73.9461	13.6
North River (NY)	40.8281	73.9550	7.4
Oakwood Beach (NY)	40.5466	74.1130	1.8
Port Richmond (NY)	40.6408	74.1265	2.6
Red Hook (NY)	40.7024	73.9747	2.6
26th Ward (NY)	40.6518	73.8774	3.7
Coney Island (NY)	40.5898	73.9308	4.8
Jamaica (NY)	40.6607	73.8131	4.4
Owls Head (NY)	40.6430	74.0364	5.3
Rockaway (NY)	40.5846	73.8309	2.0

## Tidal specification

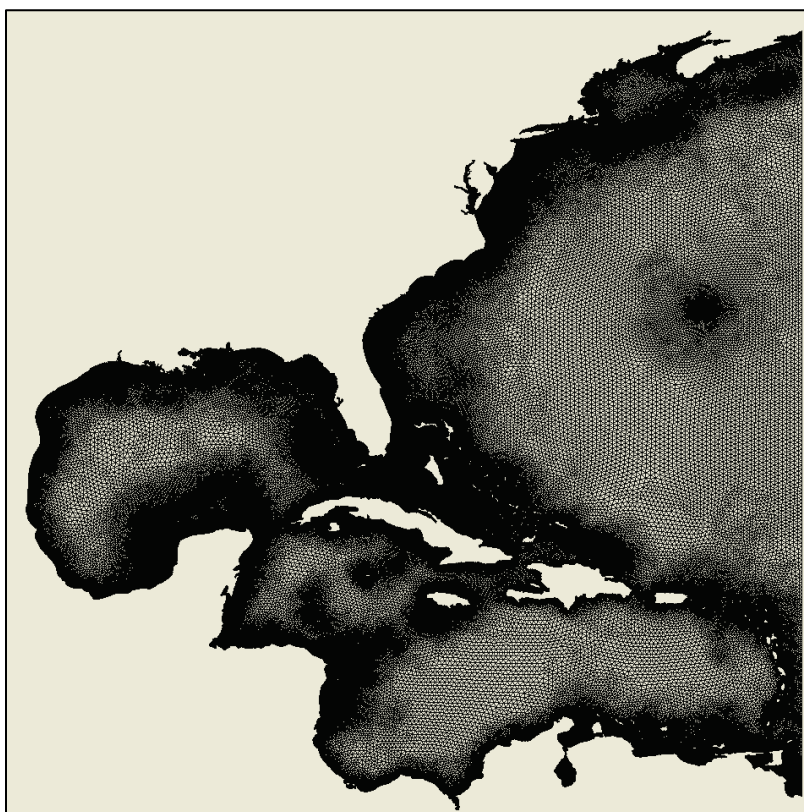
### *Tidal harmonics*

The development of tidal boundary conditions along the ocean boundary was conducted so that the model can be simulated both with and without meteorological forcing. The limits of the AdH model were previously shown in Figure 14. The southern limit of the ocean boundary is approximately at Atlantic City, NJ, and extends perpendicular to the New Jersey shore offshore to the edge of the continental shelf at a depth of approximately 75 m (250 ft). The offshore boundary then follows the edge of the shelf northeastward to south of Martha's Vineyard, then north to Martha's Vineyard.



The primary tidal harmonics (largest nine constituent amplitudes) have been modeled extensively and documented within the ADCIRC East Coast tidal harmonic database. The overall modeled domain for the ADCIRC tidal harmonic model is presented in Figure 52. The domain includes the western Atlantic Ocean and the Gulf of Mexico, covering all of the eastern shoreline of the United States. The AdH ocean boundary conditions are believed to be sufficiently posed to simulate extreme events and generally matches the previously shown NOAA model domain (Figure 15).

Figure 52. ADCIRC East Coast tidal database model grid.



The AdH ocean water surface elevation boundary conditions are enforced along each individual finite element face as represented by the 36 small black squares in Figure 53. The harmonic amplitudes extracted from the ADCIRC model were for the 37 nodes along the boundary with the edge values being a simple average of the two participating computational nodal water level values. The extracted harmonic amplitudes are presented in Figure 54 at each node from the southern end to the northern end of the model boundary. The greatest variability is in the over-tides ( $M_4$  and  $M_6$  harmonics). For the remaining constituents, the amplitudes are relatively uniform.

Figure 53. Boundary condition locations (squares) for extraction of tidal harmonics from ADCIRC Tidal Database.

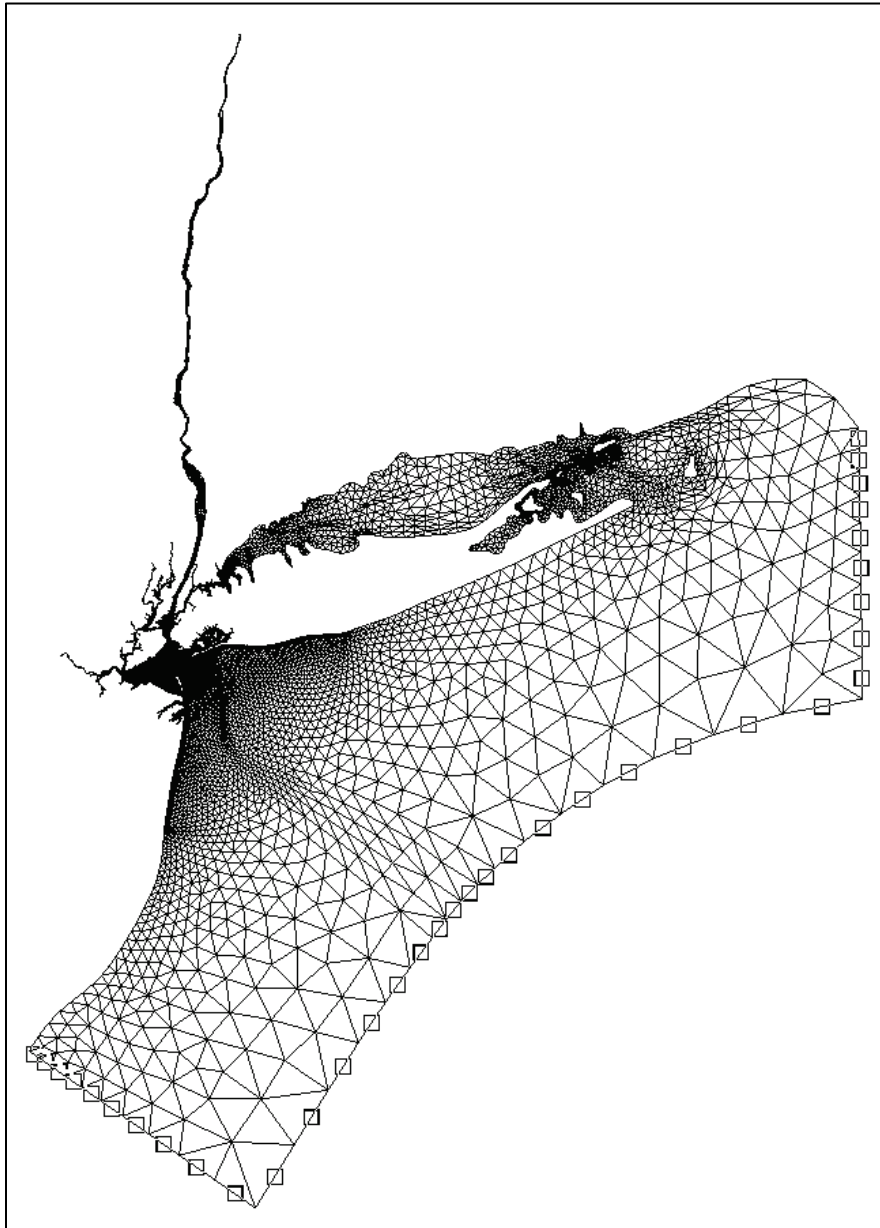
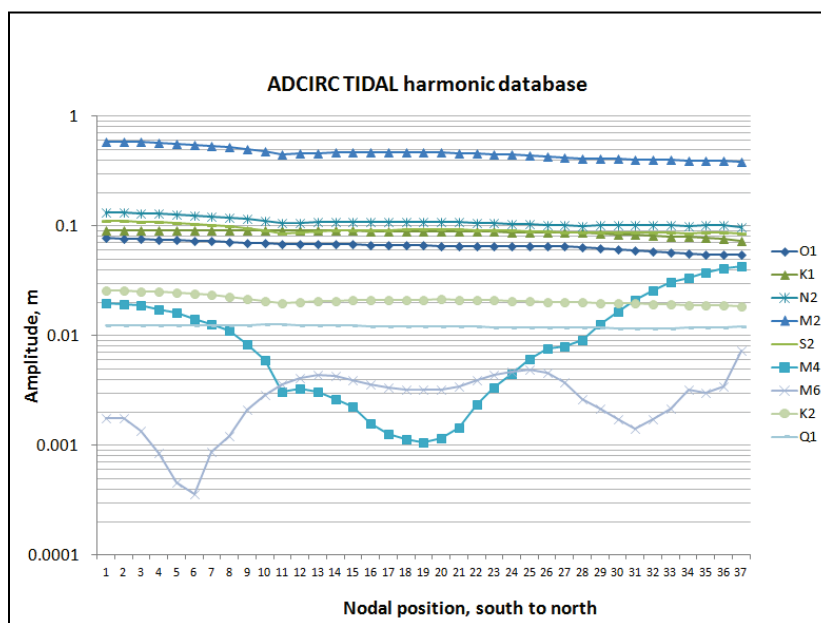
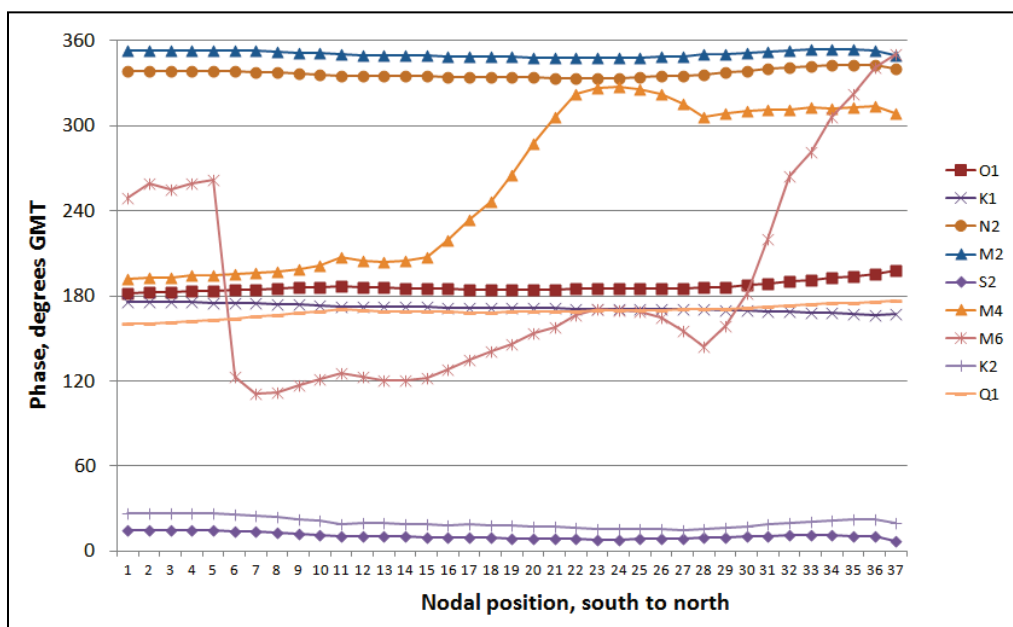


Figure 54. Variation of the nine ADCIRC tidal harmonic amplitudes along the AdH model boundary.



The tidal constituent phases along the AdH ocean boundary are presented in Figure 55. The phases are again most variable for the  $M_4$  and  $M_6$  over-tides, and the remainder have relatively uniform phases.

Figure 55. Variation in the nine ADCIRC tidal harmonic phases along the AdH ocean tidal boundary.





The NOAA standard 37 harmonic constituents were obtained at all of the available tide stations in the study area. The three primary gages of interest near the AdH model boundary are Atlantic City, Montauk Point, and Woods Hole. The remaining 28 constituents (9–37) not available from the ADCIRC database are presented in Figure 56 and Figure 57 for the amplitudes and phases, respectively. None of the remaining constituents have amplitudes greater than 0.07 m (0.23 ft) with the majority less than 0.01 m (0.03 ft). The phases of the 28 constituents are relatively constant, particularly between Atlantic City and Woods Hole. The large difference for the NU2 constituent is not as great when it is recognized that a 340 deg phase is the same as a -20 deg phase.

Figure 56. Variation in the NOAA tidal harmonic amplitudes for the tidal constituents not included in the ADCIRC database.

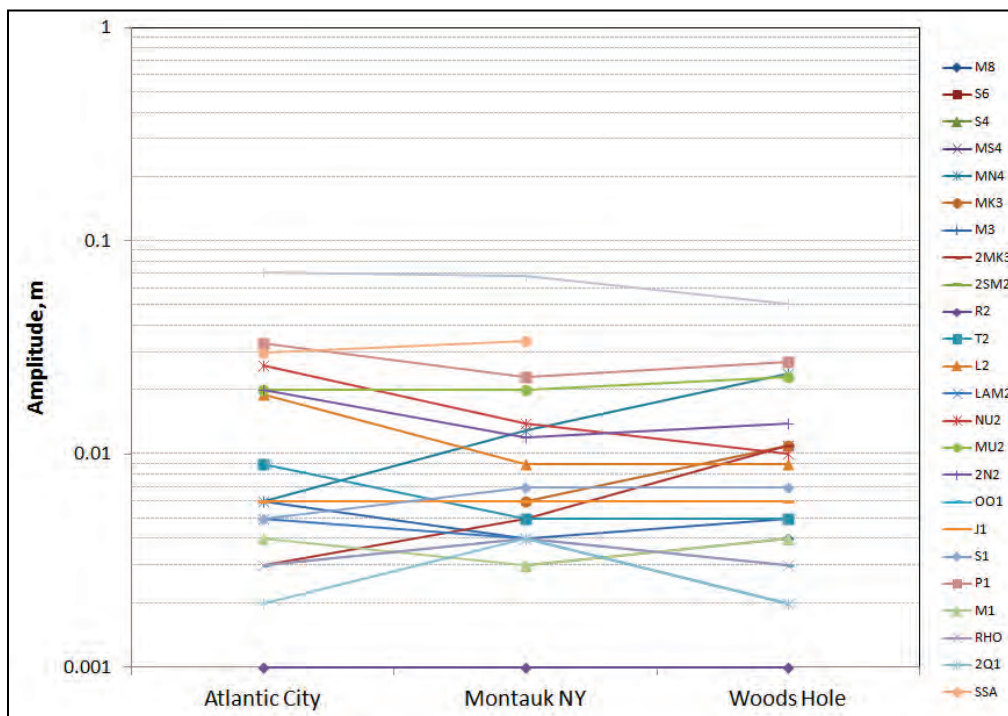
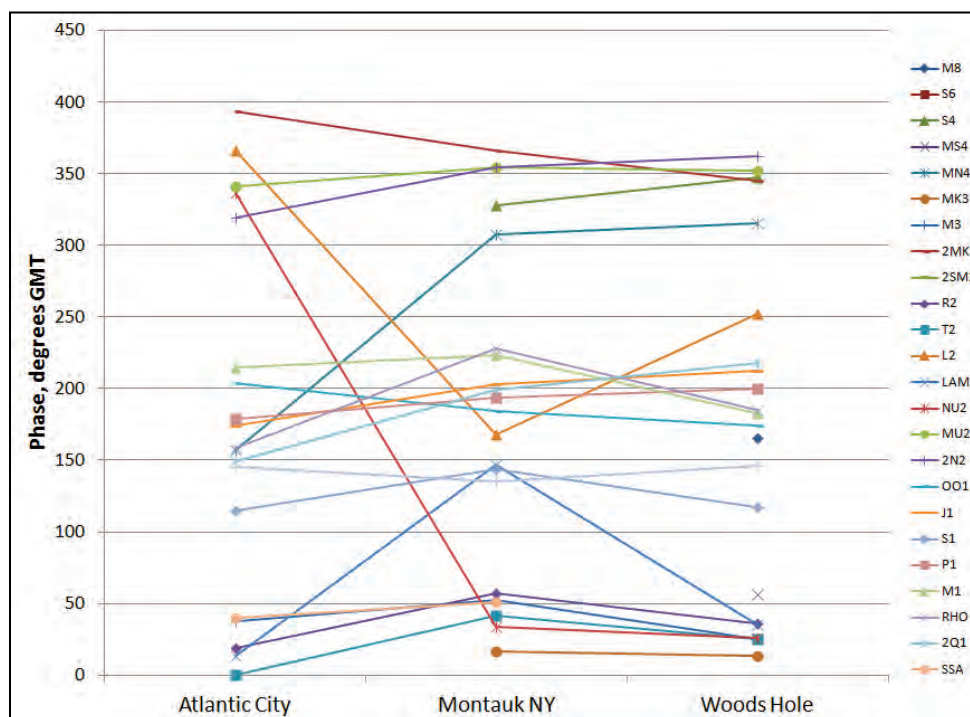


Figure 57. Variation in the NOAA tidal harmonic phases for the tidal constituents not included in the ADCIRC database.



For the purposes of developing tidal harmonic conditions along the ocean boundary, the average amplitudes and phases between Atlantic City and Woods Hole were used with constant amplitudes and phases along the 37 nodes of the AdH boundary for these minor harmonics. The nine harmonics included in the ADCIRC database vary along the boundary as appropriate in both amplitude and phase.

#### *Tidal/meteorological residuals*

For the second task of the AdH model tidal validation, the model was simulated for the period of 1995 with the meteorological influences included in the model boundary conditions. For that simulation, the observed tidal signals at Atlantic City and Nantucket were compared to the predicted harmonic tides to obtain a residual tidal signal representing the meteorological influence at each end of the model ocean boundary. The tidal comparison for the full year is presented in Figure 58 and for the month of January and early February in Figure 59. The meteorological residual tides follow the same general trends but have some localized differences that are significant.

Figure 58. Comparison of tidal elevation time series in 1995 between Atlantic City, NJ, and Nantucket Island, MA, for the purpose of extracting the tidal residual series.

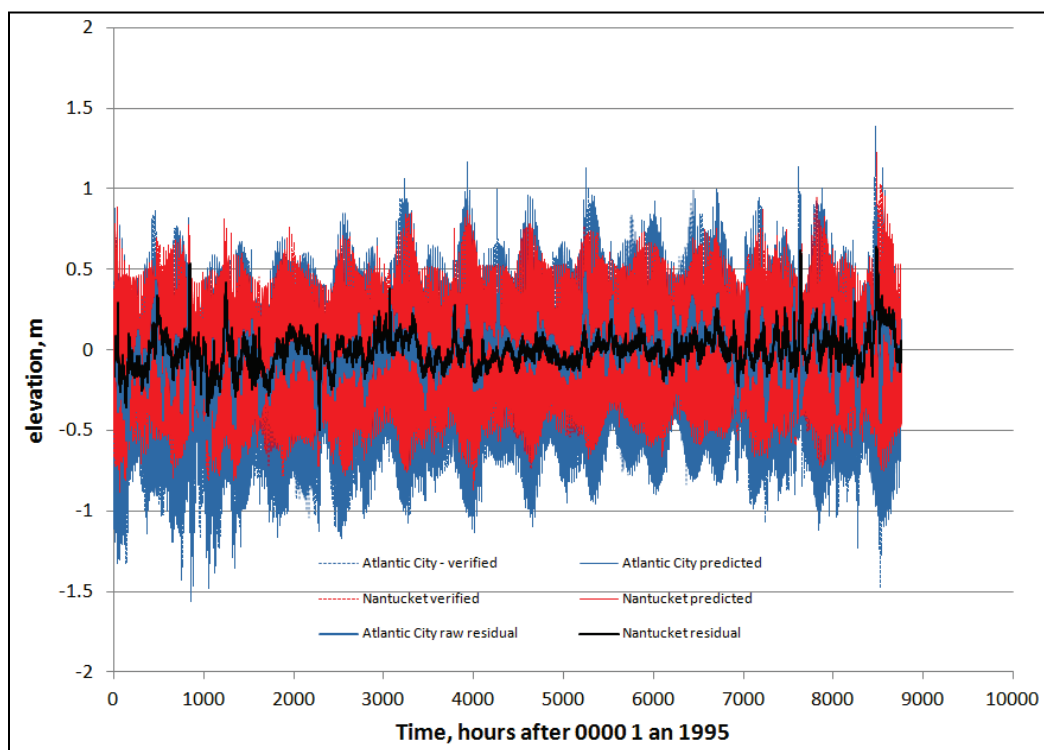
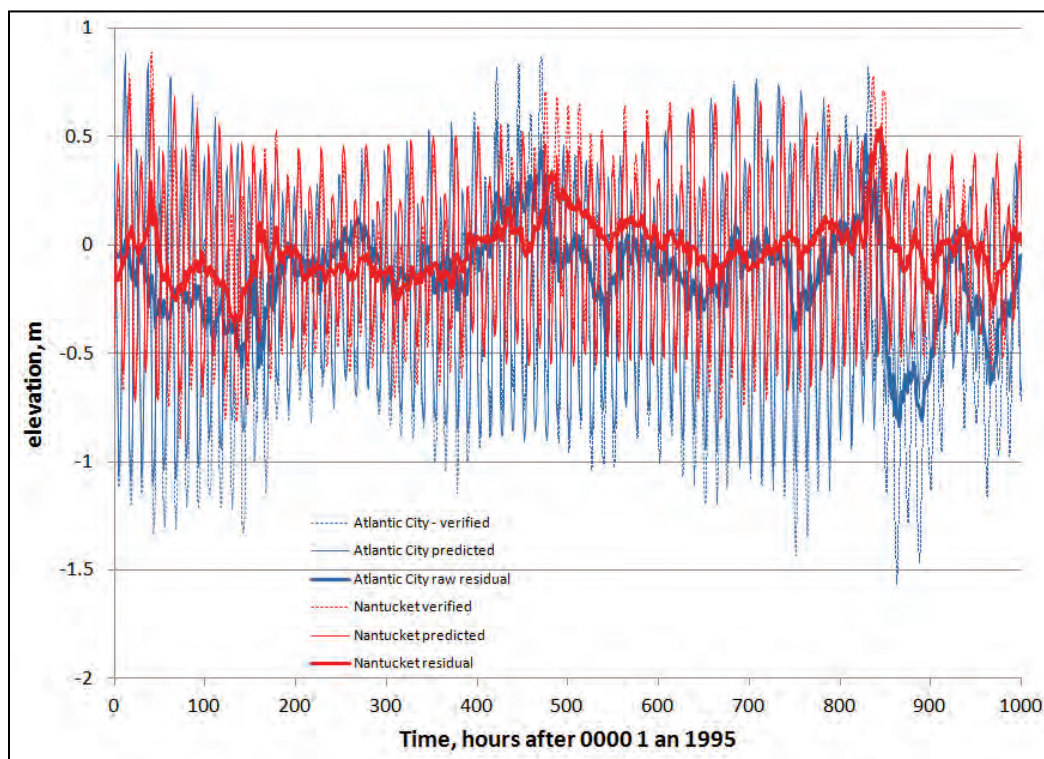
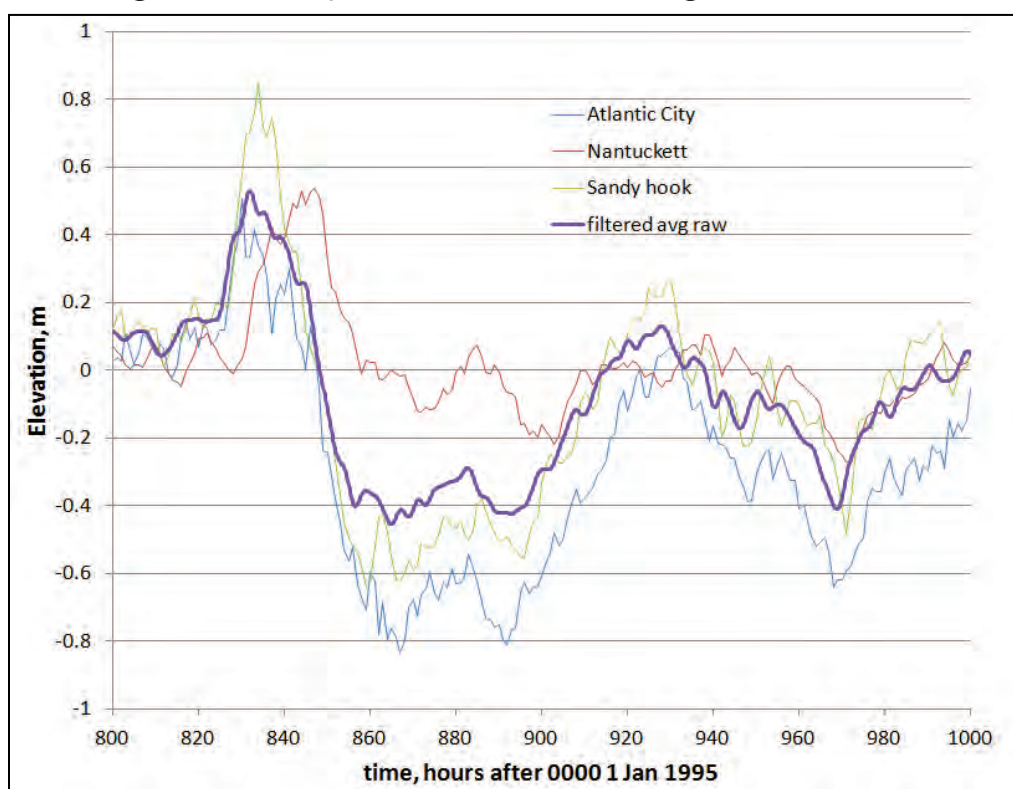


Figure 59. Details of the 1995 tidal time series for January.



The comparison of the meteorological residual tidal signals at Atlantic City, Sandy Hook, and Nantucket are presented in Figure 60. The Sandy Hook meteorological signal compares very well with the average of the Atlantic City and Nantucket residuals. The Atlantic City and Nantucket residuals were filtered using a low pass filter to filter out the high frequency noise with periods less than 3 hours. These filtered residuals were linearly interpolated along the offshore boundary and added to the reconstituted harmonic signal to create the offshore tidal signal with the appropriate meteorological component.

Figure 60. Development of the residual tidal signal for AdH model.



The results of simulating the AdH model with harmonics only is presented in Figure 61 for Sandy Hook for the month of January 1995. The results of simulating the AdH model with inclusion of the meteorological residual component are presented in Figure 62 for Sandy Hook for the entire year of 1995.



Figure 61. Result of using the combined ADCIRC and NOAA harmonics. The NOAA predicted tides at Sandy Hook are compared with the AdH model driven with harmonics only.

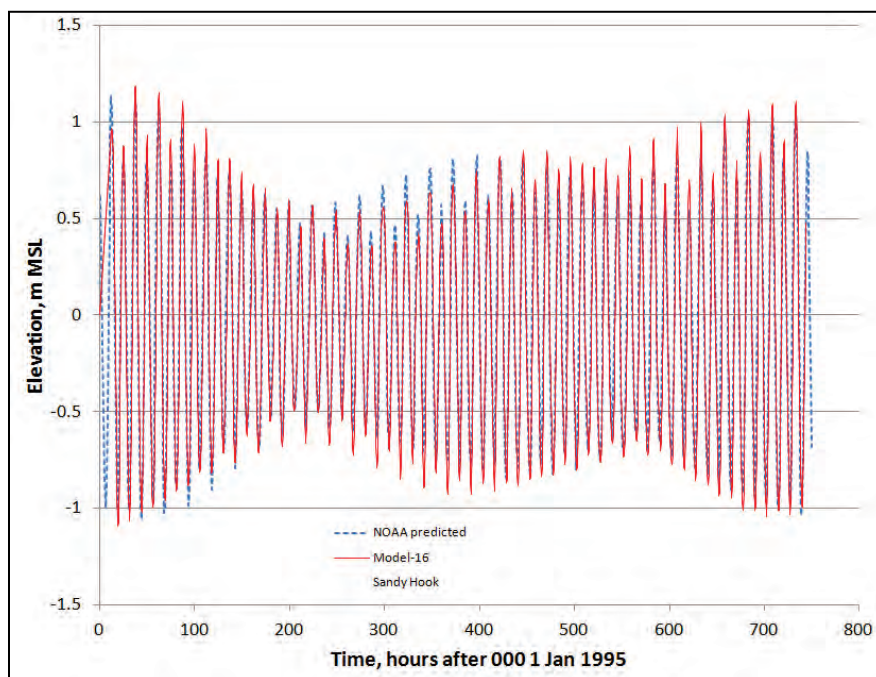
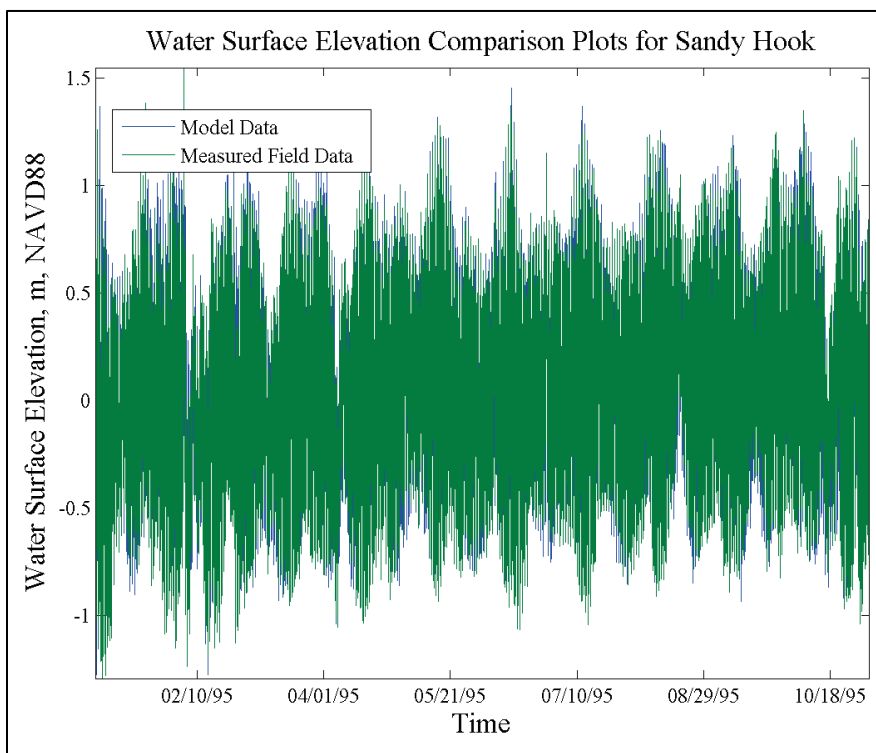


Figure 62. Comparison of modeled versus observed tidal signal at Sandy Hook when driving the model with tidal harmonics and meteorological residuals.



### *Summary of tidal boundary condition approach*

The steps that were used to develop the tidal boundary condition for the three-dimensional AdH model are the following:

1. For normal tidal conditions (no ocean storm influence)
  - a. Use the nine ADCIRC harmonic constituents as a spatially varying amplitude and phase along the AdH boundary.
  - b. Use the 28 remaining NOAA harmonics (9–37) specified as a uniform amplitude and phase along the AdH model boundary.
  - c. Apply (add to harmonics) the appropriate residual signal along the AdH boundary as a linearly interpolated time series along the AdH boundary to incorporate meteorological forcings.
2. For oceanic storm conditions
  - a. Extract from ADCIRC storm simulations completed as part of the NACCS that includes the astronomical tides time series of tide at each finite element face along the AdH boundary.

The storm conditions tidal boundary (number 2, above) was combined with the results for the normal tidal conditions (number 1, above) to obtain a single time series at each tidal boundary location that included both the normal tidal conditions with meteorological residuals and ADCIRC generated storm surge boundary during storm events.

### *Salinity specification at the tidal boundary*

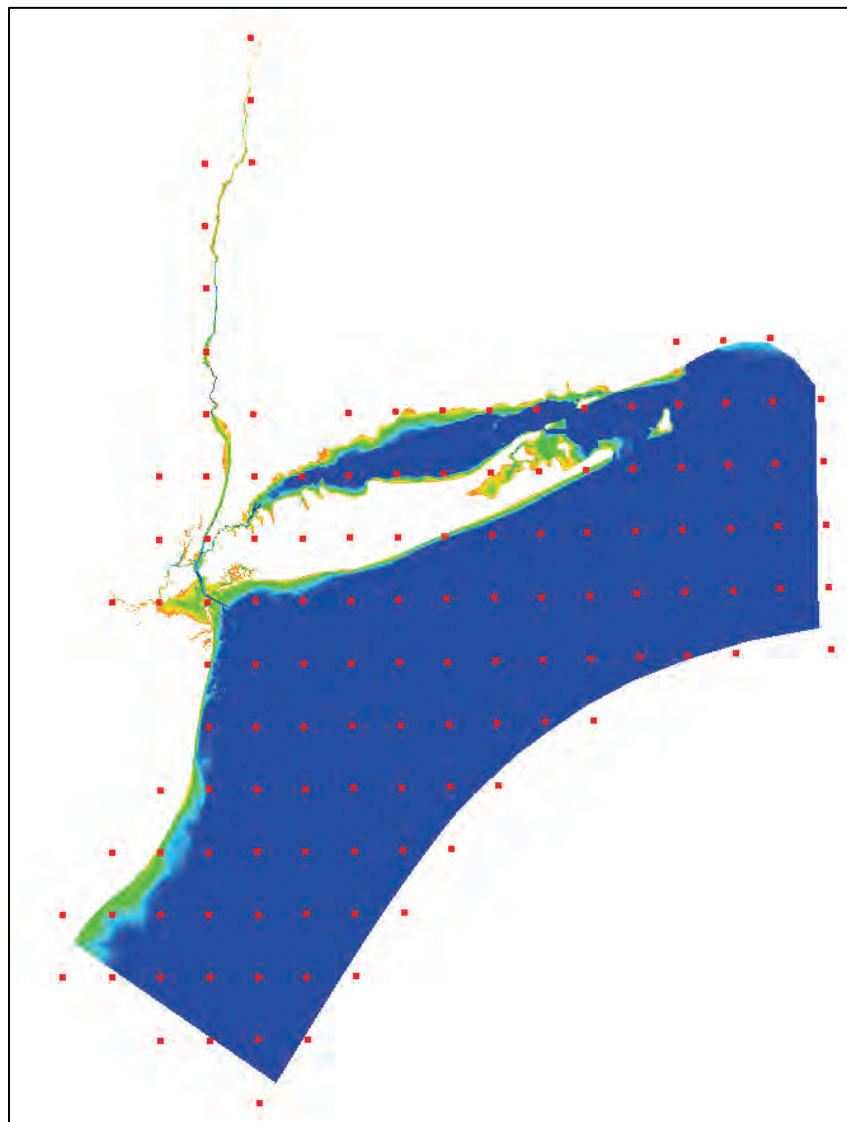
The salinity specification at the tidal boundary was set to 33 ppt for the entire model simulation time period and was held constant along the entire tidal boundary. This specification was utilized for all five simulated years. The salinity at the offshore boundary was approximately 33 ppt with negligible temporal variation as observed in HydroQual, Inc (2008). Chen and He (2010) modeled New York Bight shelf dynamics and showed that 33 ppt was representative.

## **Wind and pressure specification**

The wind and pressure fields generated as part of the WIS (<http://wis.usace.army.mil/>) were utilized for this modeling effort. The WIS research effort consists of hindcasting wave characteristics for much of the Atlantic and Pacific Oceans. As part of this hindcasting effort, wind and pressure fields are generated to use as input to the wave model. These

wind/pressure datasets consist of wind/pressure fields with discrete locations that are consistent between years and are available as far back as the early 1980s. This dataset provides a consistent wind/pressure forcing method that is consistent for all of the time periods simulated and removes difficulty in obtaining consistent forcing conditions for various time periods. The WIS study includes wind/pressure values over the majority of the Atlantic Ocean. Since this study was limited to the NYNJH area, the WIS values were reduced to only the locations impacting the numerical model domain. Figure 63 shows the WIS wind/pressure data locations over the numerical model domain.

Figure 63. Locations of WIS wind/pressure values in relation to the AdH model domain.



### Wave model offshore boundary spectra

The years modeled were 1985, 1995, 1996, 2011, and 2012. These years are associated with the following historical storm events: Hurricane Gloria (1985), the Blizzard of 1996 (Nor'easter), Hurricane Irene (2011), and Hurricane Sandy (2012). The 2D spectra mined from National Data Buoy Center (NDBC) 44025 served to force STWAVE. When historical observations were not available, hindcast model data from WIS served as a supplement. The location of NDBC 44025 is 40.251°N and 73.164°W and is shown in Figure 64. Although slightly shoreward of the offshore boundary, NDBC 44025 is found in a water depth similar to that of the offshore STWAVE boundary and is the closest buoy with historical data. To force STWAVE, the location of NDBC 44025 was moved to State Plane coordinates (265431.44, 140129.39) to lie along the offshore boundary.

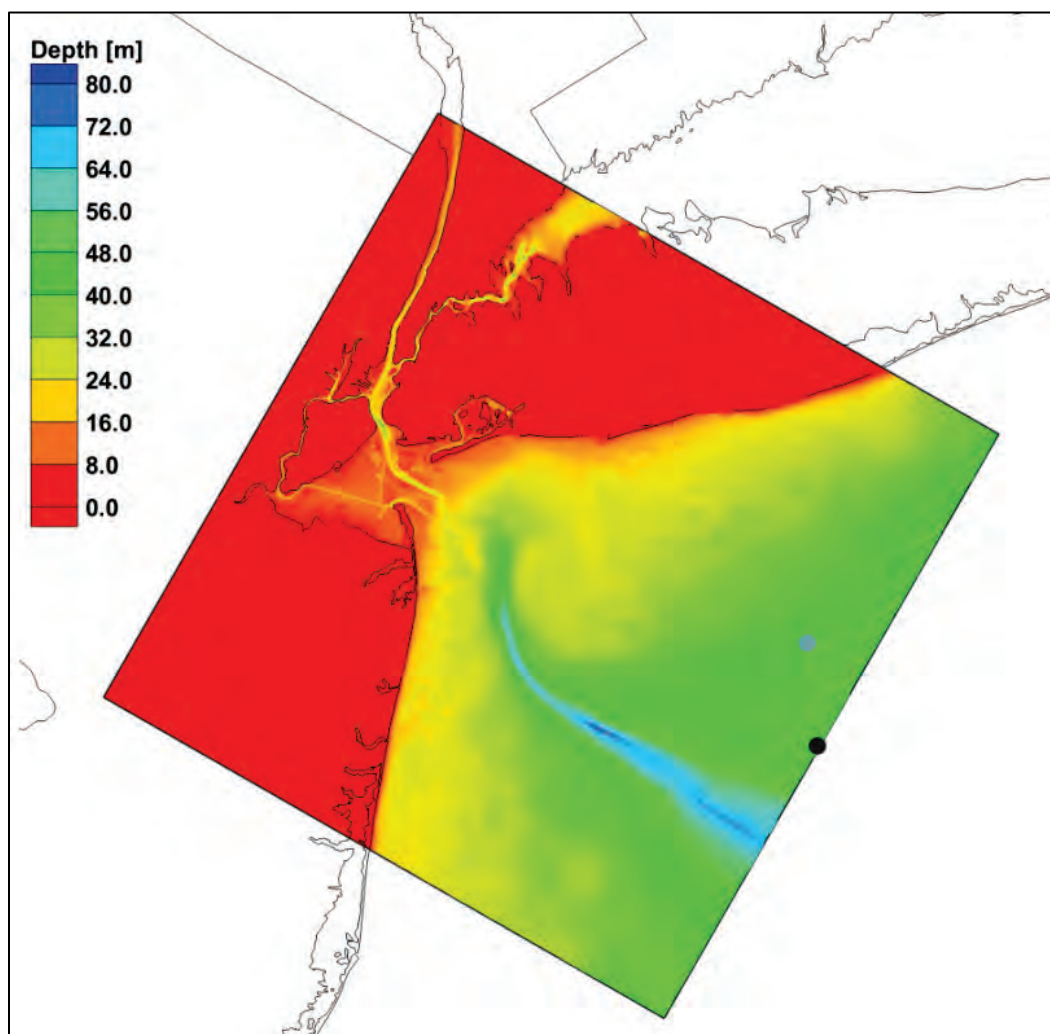
The number and value of the discrete frequency bands were the following:

$$f(n + 1) = 1.1 * f(n) \text{ where } n = 1, 29 \quad (6)$$

and the starting and ending bands were 0.035 Hz ( $T = 28.6$  s) and 0.505 Hz ( $T = 1.98$  s), respectively. The angular resolution was 5 deg, beginning at 0 deg and increasing to 355 deg. A one-dimensional transformation was performed along the lateral boundaries, and a constant spectrum was applied along the offshore boundary. Offshore forcing was applied every 3 hours, beginning 1 January 01:00 of the modeled year.



Figure 64. Location of NDBC 44025. The gray point is the actual buoy location whereas the black point is the assigned location for the STWAVE model.



### Simulated sediment classes

The sediment transport model for the NYNJH estuary needs to address a wide range of sediment classes, from littoral sands in the bar channel to fine sediments within the inner pier slips of Newark Bay. The approach taken balanced the wide range of size classes within the model domain with the computational requirements of simulating a large number of size classes, based on the specific sizes of significance to the navigation channel maintenance. Consequently, sediment sizes equal to and coarser than pebbles were excluded from analysis. The model was developed using five noncohesive sand classes and five cohesive sediment classes. These 10 size classes are defined in Table 5, based on the Wentworth size classification. The mineral specific gravity for all 10 sediment classes was set to 2.65.

Table 5. Sediment classes used in sedimentation model.

Wentworth Sediment Size Class	Type	Particle size ( $\mu\text{m}$ )	Specific Gravity
Clay	Cohesive	1.38	2.65
Very Fine Silt	Cohesive	5.5	2.65
Fine Silt	Cohesive	11.0	2.65
Medium Silt	Cohesive	22.1	2.65
Coarse Silt	Cohesive	44.2	2.65
Very Fine Sand	Noncohesive	88.0	2.65
Fine Sand	Noncohesive	177.0	2.65
Medium Sand	Noncohesive	354.0	2.65
Coarse Sand	Noncohesive	707.0	2.65
Very Coarse Sand	Noncohesive	1414.0	2.65

The cohesive classes are *clay*, *very fine silt*, *fine silt*, *medium silt*, and *coarse silt*. The cohesive properties for these five classes are shown in Table 6. The settling velocity for the cohesive sediments was calculated based on Stokes Law (Equation 7) and is required to be specified.

$$w_s = \sqrt{\frac{4g}{3C_D} \frac{\Delta\rho}{\rho}} \sqrt{d_p} \quad (7)$$

where

$W_s$  = settling velocity

$g$  = acceleration of gravity

$C_D$  = drag coefficient

$\Delta\rho = \rho_s - \rho_f$  = density difference between sediment and fluid

$\rho_s$  = density of sediment particles

$\rho_f$  = density of the fluid

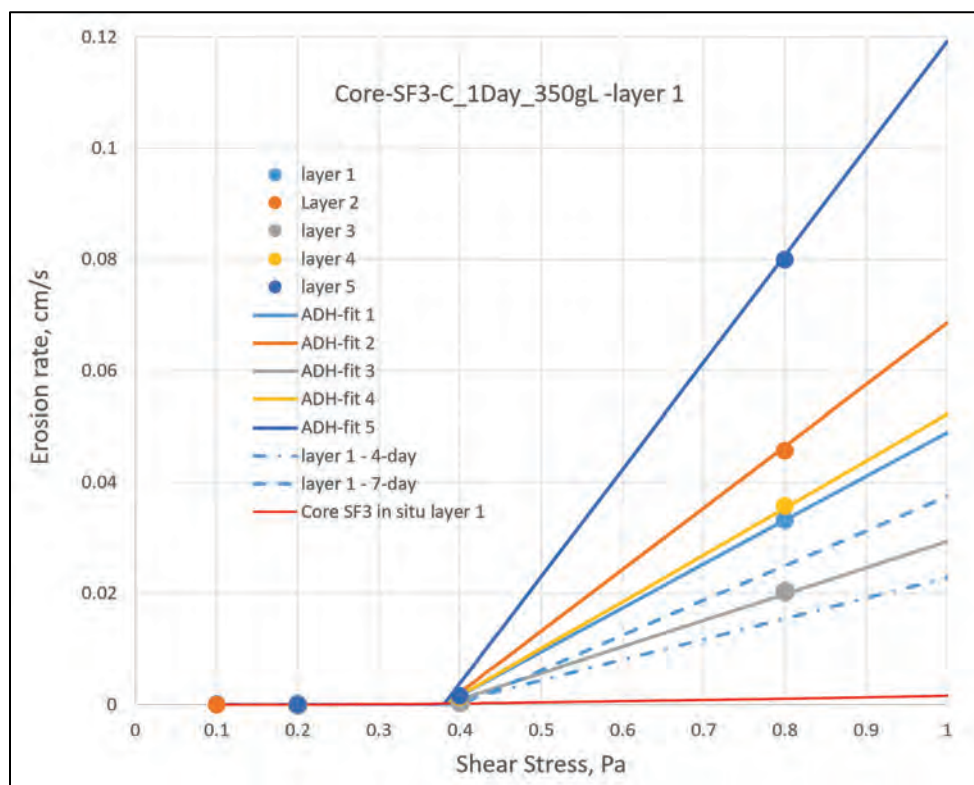
$d_p$  = diameter of the sediment particle.

Table 6. Cohesive sediment class properties.

Wentworth Sediment Size Class	Particle Size ( $\mu\text{m}$ )	Settling Velocity (mm/sec)	Critical Shear Stress for Erosion (Pa)	Erosion Rate Constant (mm/sec)	Critical Shear Stress for Deposition (Pa)	Bulk Density ( $\text{kg/m}^3$ )
Clay	1.38	0.007	0.38	0.7	0.02	1425
Very Fine Silt	5.5	0.027	0.38	0.7	0.02	1425
Fine Silt	11.0	0.110	0.38	0.7	0.02	1425
Medium Silt	22.1	0.440	0.38	0.7	0.04	1425
Coarse Silt	44.2	1.760	0.38	0.7	0.075	1425

The critical shear stress for erosion was specified based in part on the analysis of SEDFlume cores (Figure 65) collected within Newark Bay (Sea Engineering 2008 and 2013). The values are consistent with previous investigators and experimental work (Partheniades 1962; Mehta 1973; Teeter 2001a; Teeter 2001b; Letter 2009). The critical shear stresses for erosion are set uniformly across the cohesive grain sizes because erosion rates are based on bulk samples. Critical shear stresses for deposition are based on experimental data (Krone 1962; Mehta 1973). The three finest classes are set to the same value because the current AdH model does not include a flocculation model that allows for the finer particles to combine into larger effective sizes and deposit at higher shear stresses. The bulk density was assigned based on an average of the sediment cores (Sea Engineering 2013).

Figure 65. SEDFLUME results for core sample in Newark Bay.



Noncohesive size classes used are *very fine sand*, *fine sand*, *medium sand*, *coarse sand*, and *very coarse sand*. The properties of the noncohesive sand classes are presented in Table 7. The grain porosity was set at 0.3 for all sand classes. The settling velocities in Table 7 are approximate for free settling in clear water (Graf 1971). The settling velocity for noncohesive sediment is computed internally within the numerical model taking the local fluid density into account.

Table 7. Noncohesive sediment class properties.

Wentworth Sediment Size Class	Particle Size ( $\mu\text{m}$ )	Settling Velocity (m/sec)*	Grain Porosity
Very Fine Sand	88.0	0.006	0.3
Fine Sand	177.0	0.02	0.3
Medium Sand	354.0	0.05	0.3
Coarse Sand	707.0	0.1	0.3
Very Coarse Sand	1414.0	0.2	0.3

\* Computed internally within model, not specified.

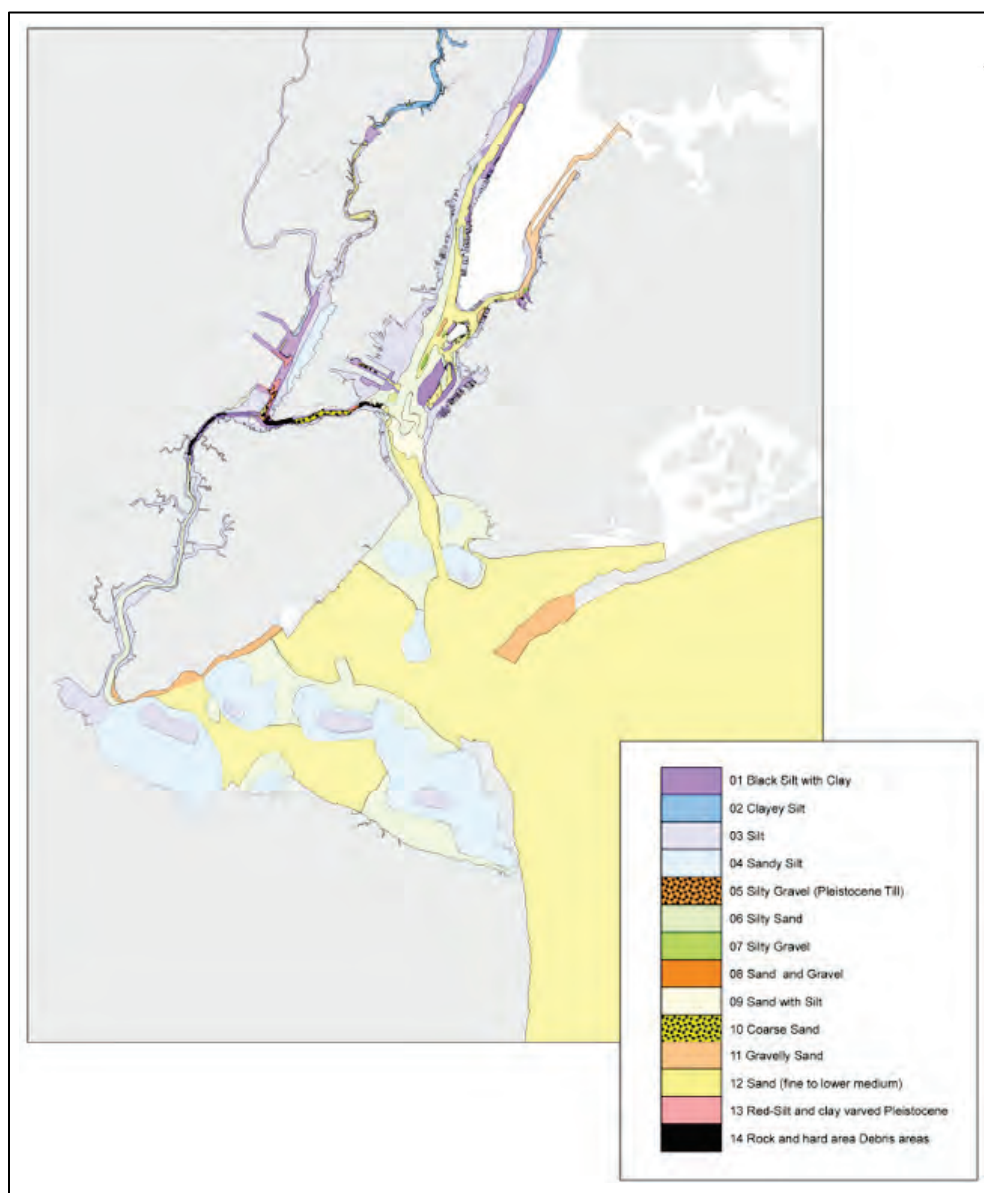
## **Sediment bed initialization**

The development of the sediment transport model requires the specification of the characteristics of the sediment in the bottom surface of the estuary, the vertical structure of the subsurface layers within the bed, and the sediment size class concentration distribution in tributary inflows.

The sediment distribution within the bed of the model specifies the sediments available for entrainment into the water column during erosion events. Armoring of finer sediments by larger fractions is included in the model. The domain required for sediment property specification is the entire domain of the model. The inflowing size distribution within the tributary inflows will control the characteristics of much of the deposition that occurs within the estuary.

The sediment bed characteristics at the bottom of the water column over the model domain were estimated from several data sources. The primary study area was evaluated as a separate task for this study by a contractor to the US Army Corps of Engineers, New York District (e4sciences). The summary of the sediment classification performed by e4sciences for the New York Harbor and vicinity is shown in Figure 66.

Figure 66. Sediment classifications developed by e4sciences and spatial variability within the harbor.



Sediments in Ambrose Channel through the Narrows are dominated by fine to medium sand. Sediments in Upper Bay are primarily fine sand and silt. Kill van Kull has coarse sand and hard pan that required blasting to deepen. Newark Bay and Arthur Kill are dominated by fine sediments.

The sediment categories delineated by e4sciences represent a general description of sediment grain size distributions, which is comprised of sediments from a variety of size classes, some of which are represented explicitly within the model. These characterizations are presented in

Table 8. A specific sediment characterization class defined by e4sciences was developed as a composite of a group of bottom surficial samples. Consequently, the percent of sediment size classes (e.g., silt) is reported within Table 8 as a percentage range.

Table 8. Preliminary particle size of New York Harbor sediments (e4sciences 2018).

Class No.	Sediment Type		Clay	Silt	Fine Sand to Lower Medium Sand	Upper Medium Sand	Coarse Sand	Fine Gravel	Coarse Gravel
1	Black Silt with Clay	wet and soft	~30%	60%					
2	Clayey Silt	soft/loose	~38%	50 to 60%	<10%	<10%		<10%	<10%
3	Silt	soft/loose	<10%	>85%	<10%	<10%		<10%	<10%
4	Sandy Silt	loose	<10%	55-85	45-15%	<10%		<10%	<10%
5	Silty Gravel (Pleistocene Till)	dense	5-15%	10 to 30%	<10%	<10%	<10%	60 to 90%	<10%
6	Silty Sand	loose	5-10%	10 to 30%	60 to 90%	<10%	<10%	<10%	<10%
7	Silty Gravel	dense	5-10%	10 to 30%	<10%	<10%	<10%	60 to 90%	<10%
8	Sand and Gravel	dense	<10%	<10%	<10%	<10%	80 to 50%	20-50%	<10%
9	Sand with Silt	loose	<10%	10 to 20%	70-90%	<10%		<10%	<10%
10	Coarse Sand	loose	<10%	<10%	<10%	<10%	80 to 90%	5 to 20%	
11	Gravelly Sand	dense	<10%	<10%	30%	50%		5 to 20%	5 to 20%
12	Sand (fine to lower medium)	loose	<10%	<10%	80-90%	<10%		<10%	<10%
13	Red-Silt and clay varved Pleistocene	compact/cohesive	30-40	30-40	<10%	<5%		<5%	<1%
14	Rock and hard debris areas								

To use the sediment categories from e4sciences, these needed to be converted into distinct grain size distributions that sum to 100%. By taking the lower and upper percentage reported for each size class in Table 8, percent finer cumulative curves as lower and upper bounds were developed. These curves for clayey silt are presented in Figure 67 as an example. The cumulative percentage through coarse gravel (assumed

76 mm) was bounded between 88% and 134% (Figure 67). Forcing that cumulative percentage to 100% places the corrected curve 26% from the lower bound to the upper bound for that size class. This adjustment was applied for each size class reported as shown in Figure 67 as the curve weighted to sum to 100%. This procedure was applied to all of the sediment categories defined by e4sciences to yield the grain size distribution curves shown in Figure 68.

Figure 67. Example of the methodology used to approximate particle size distribution classifications provided by e4sciences (class number 2, clayey silt).

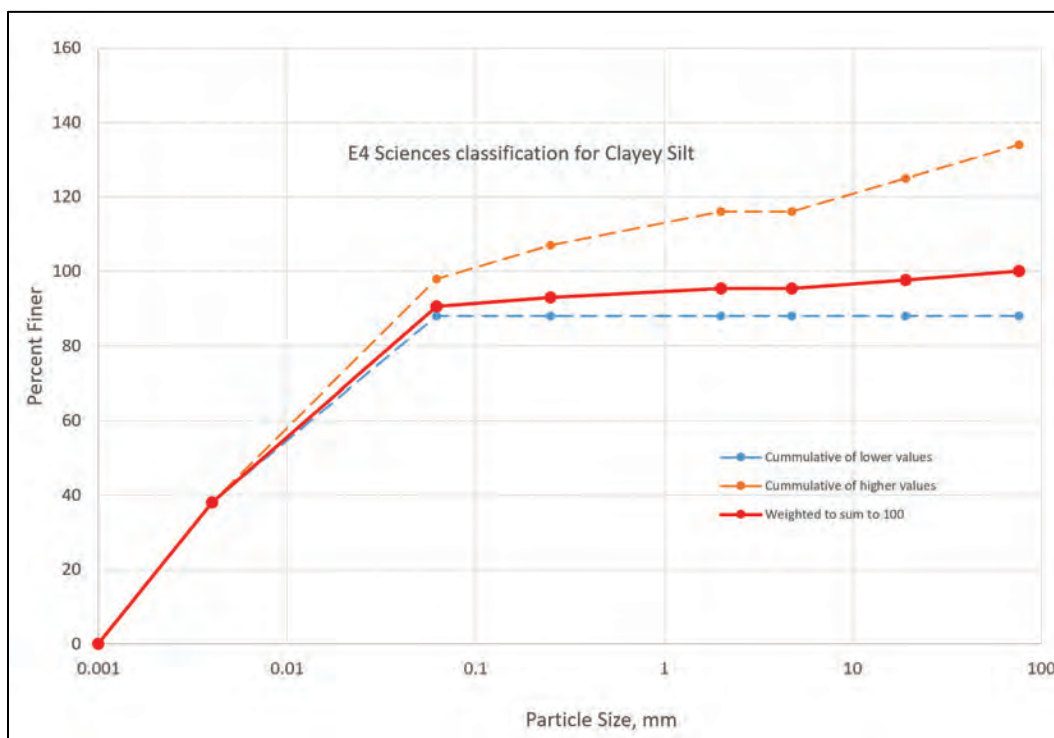
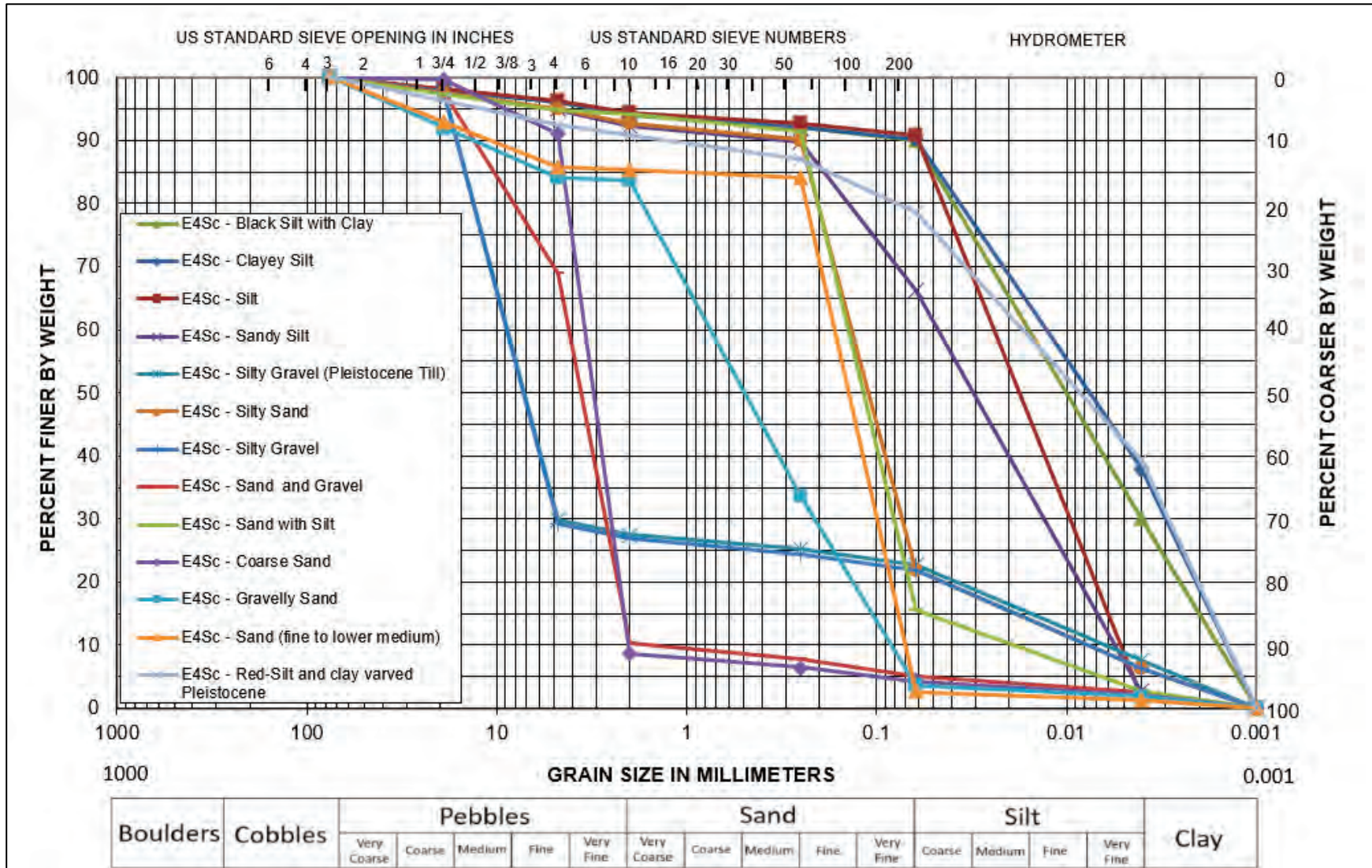


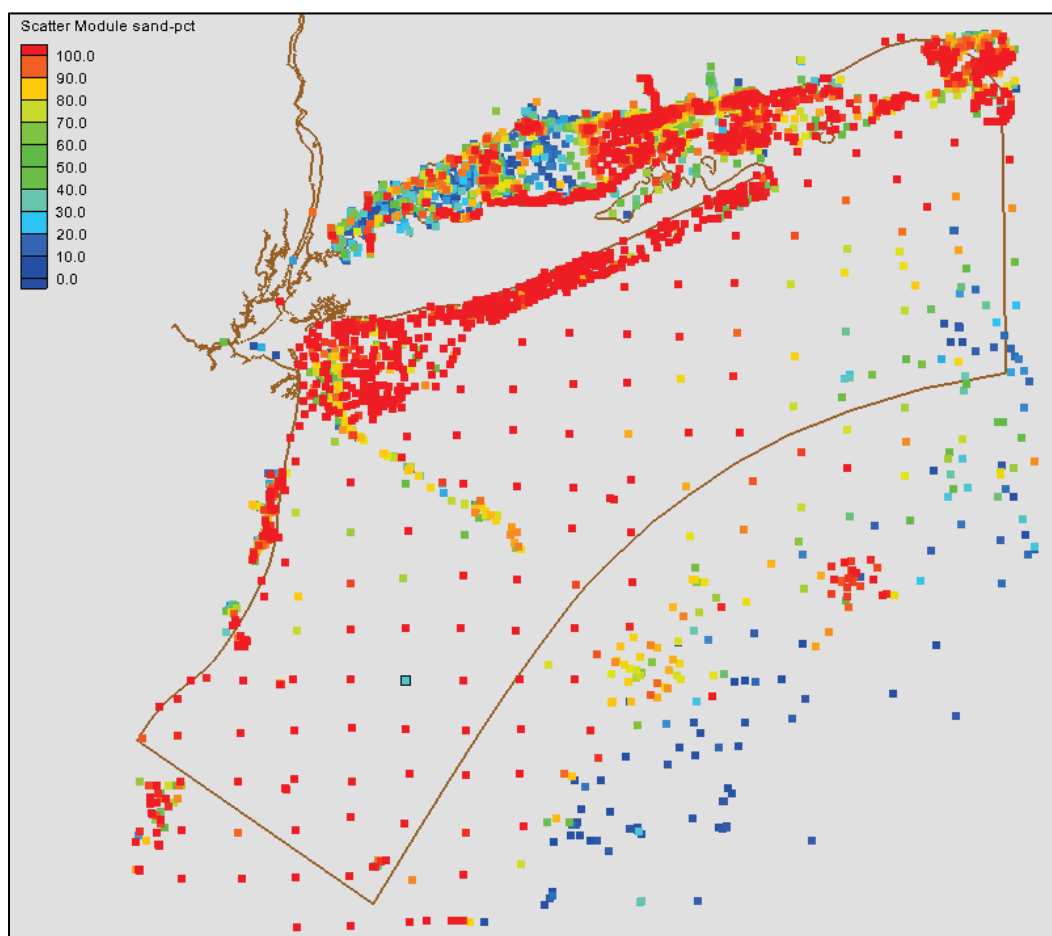


Figure 68. Particle size distribution approximations for all classifications developed by e4sciences.



The numerical model domain includes large areas outside of the coverage analyzed by e4sciences (Figure 66). Additional sediment bottom surficial samples were available from the USGS, Woods Hole, MA. Two separate databases were used: the Long Island Sound Sediment Database (LISSDB) and the East Coast Sediment Texture Database (ECSTDB). These two databases were combined, and the locations of samples are presented relative to the numerical model domain in Figure 69. The location markers are colored based on the percent sand of the samples, from blue for 0% to red for 100%.

Figure 69. Location of sediment characterization sampling from the combined LISSDB and ECSTDB sediment databases. The percent sand is color coded for each station.



The sediment classification types within the LISSDB and ECSTDB were different than those developed by e4sciences. For consistency in the specification over the full domain of the model, the classifications from e4sciences were compared with the classifications from the LIS and ECSTDB and refinements were made for each category of grain size

distribution for use within the numerical model. These refinements are illustrated in Figure 70 through Figure 82 for the sediment categories 1 through 13, respectively. A summary of defined sediment classification distributions used in the AdH numerical model is presented in Figure 83 for all of the 13 sediment characterizations.

Figure 70. Refinement of sediment class 1 for consistency between e4sciences and LISSDB/ECSTDB.

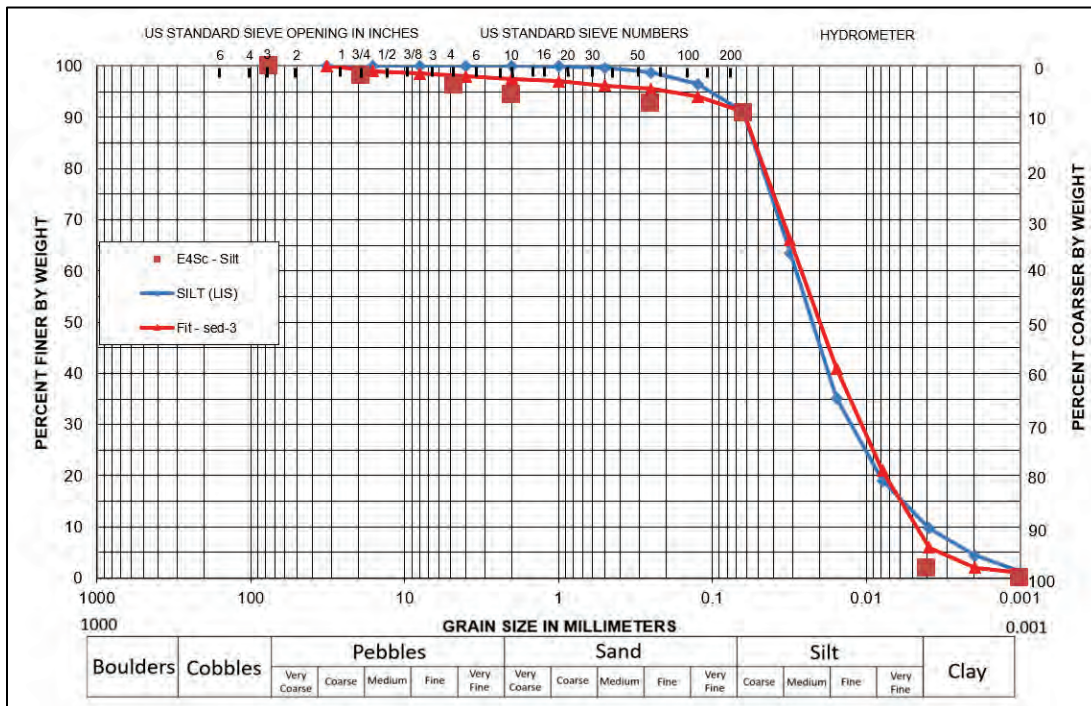
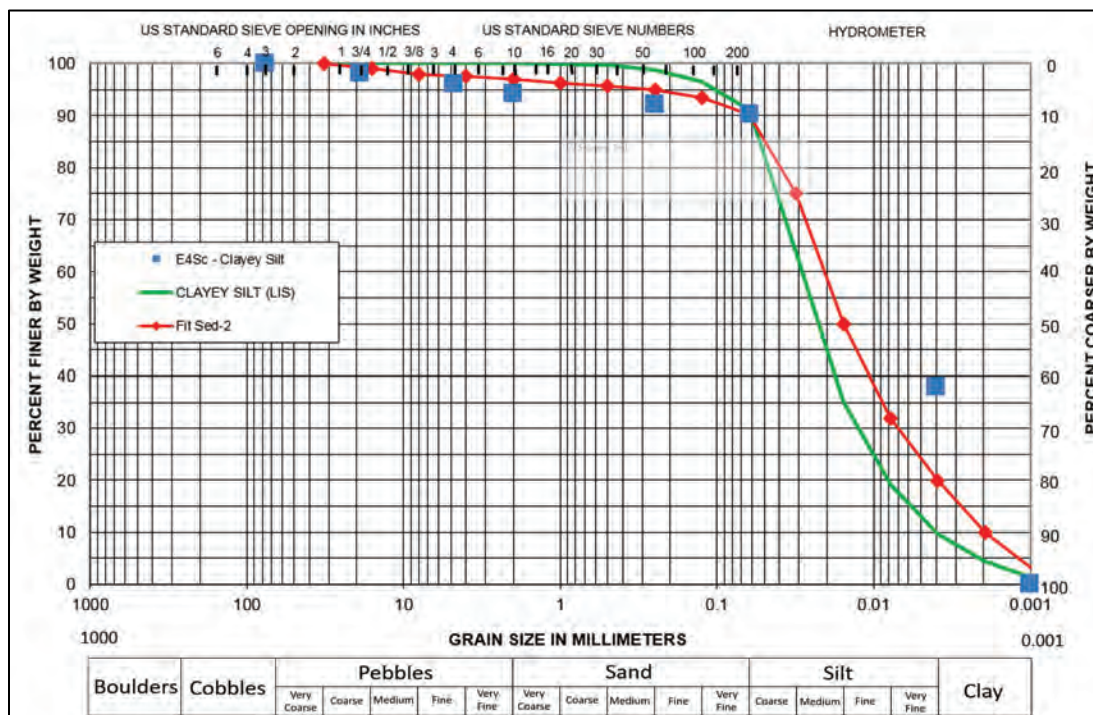




Figure 71. Refinement of sediment class 2 for consistency between e4sciences and LIS/ECST databases.



**Figure 72. Refinement of sediment class 3 for consistency between e4sciences and LIS/ECST databases.**

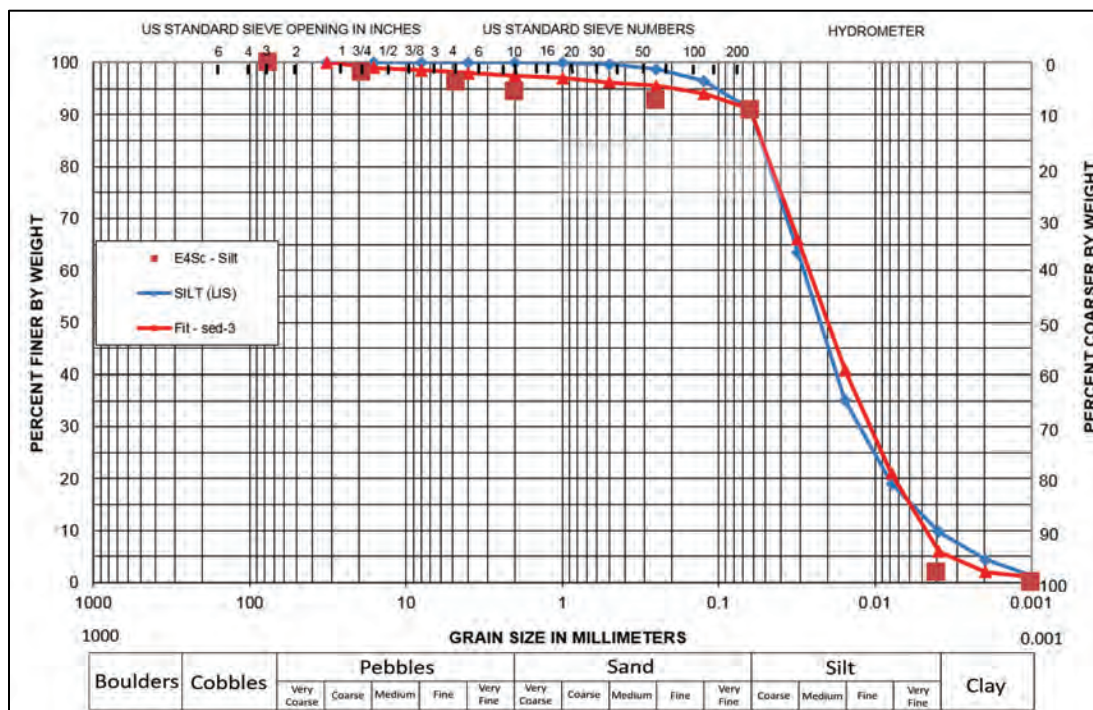


Figure 73. Refinement of sediment class 4 for consistency between e4sciences and LIS/ECST databases.

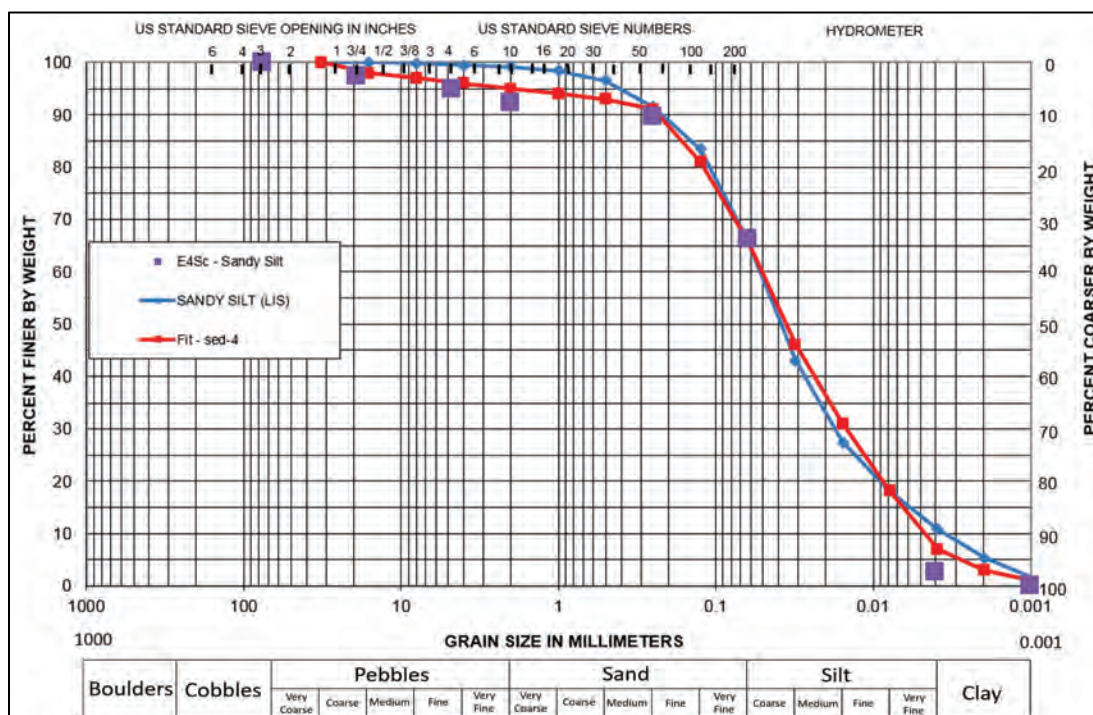


Figure 74. Refinement of sediment class 5 for consistency between e4sciences and LIS/ECST databases.

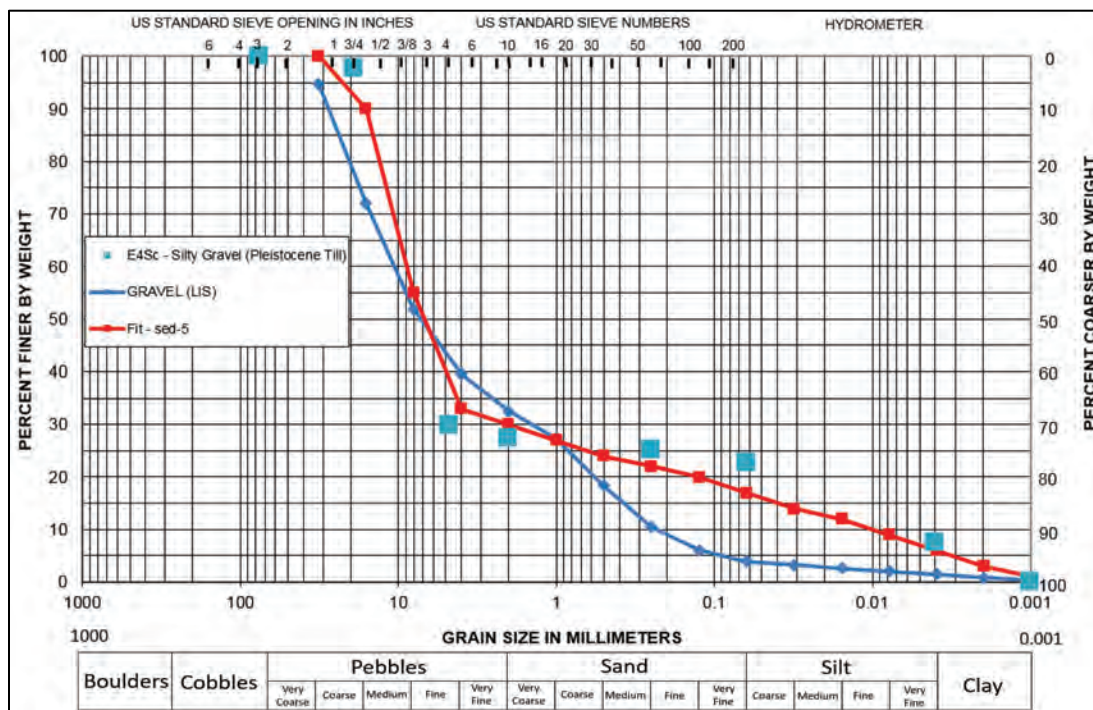




Figure 75. Refinement of sediment class 6 for consistency between e4sciences and LIS/ECST databases.

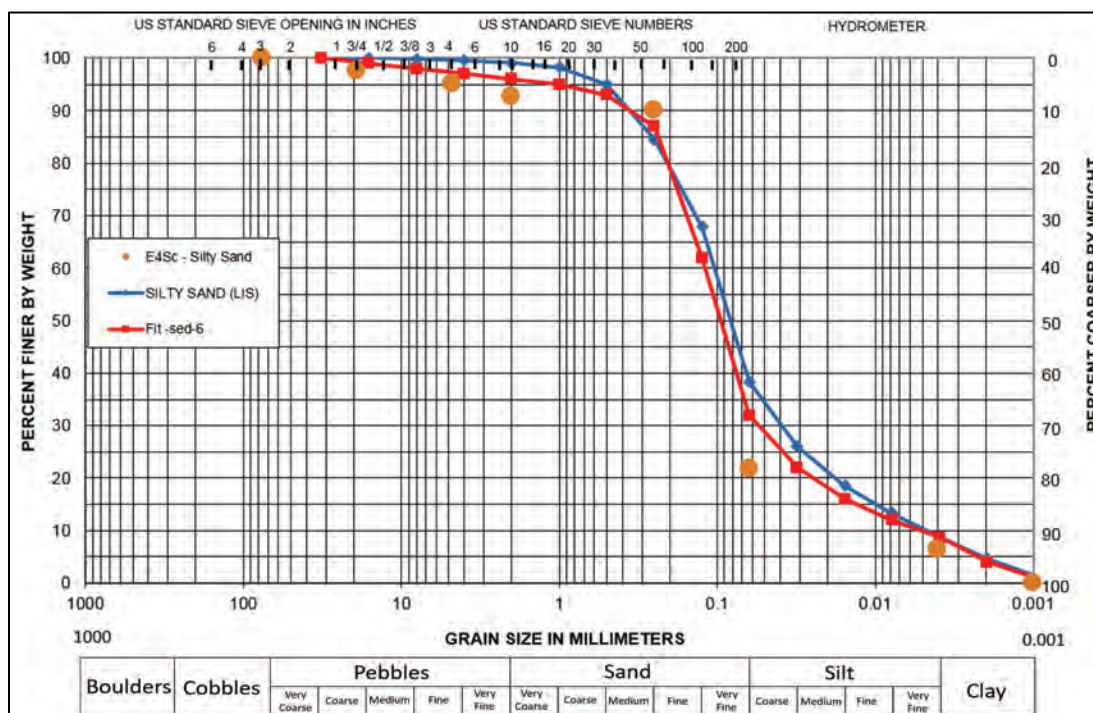


Figure 77. Refinement of sediment class 8 for consistency between e4sciences and LIS/ECST databases.

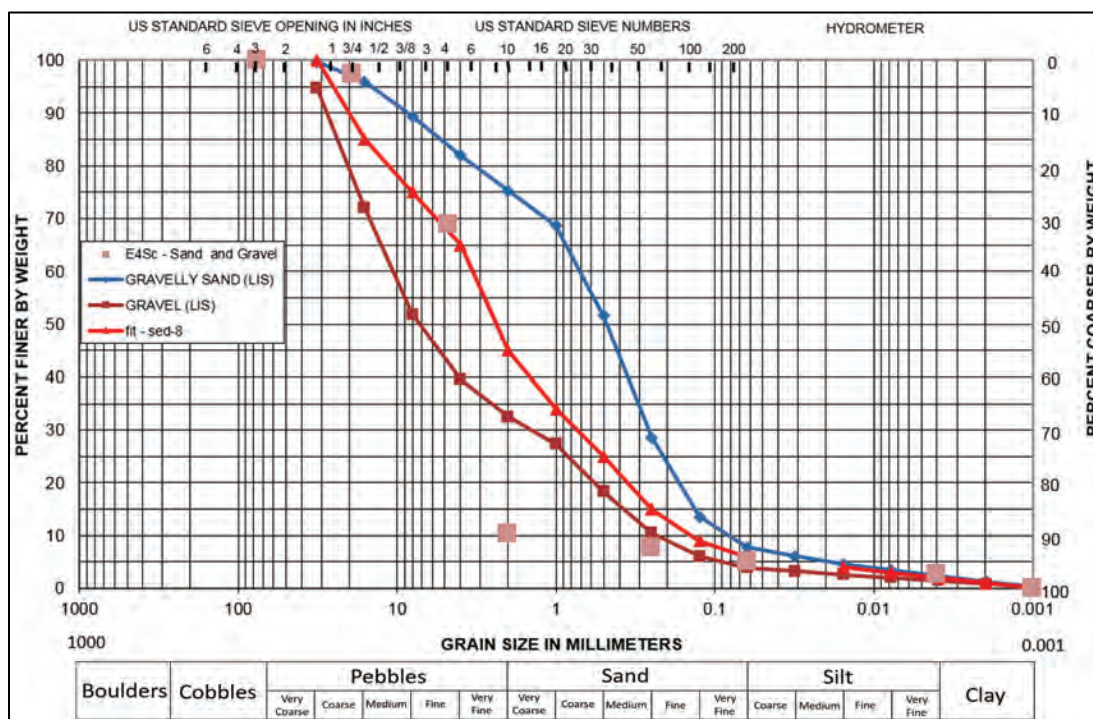




Figure 79. Refinement of sediment class 10 for consistency between e4sciences and LIS/ECST databases.

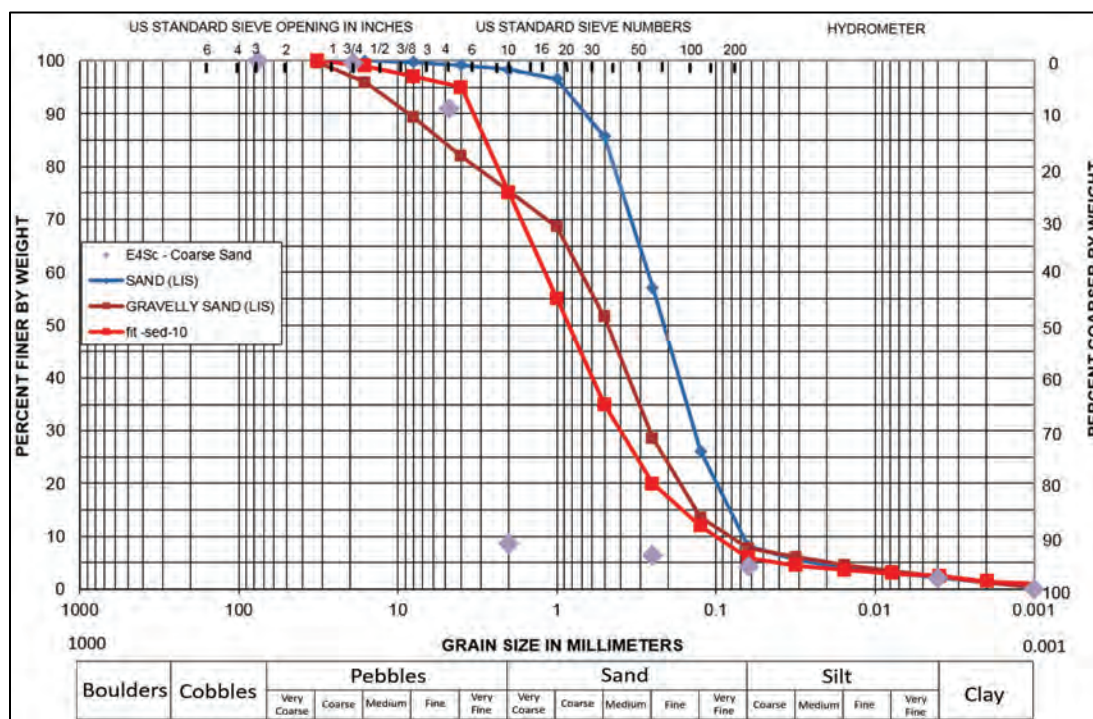


Figure 80. Refinement of sediment class 11 for consistency between e4sciences and LIS/ECST databases.

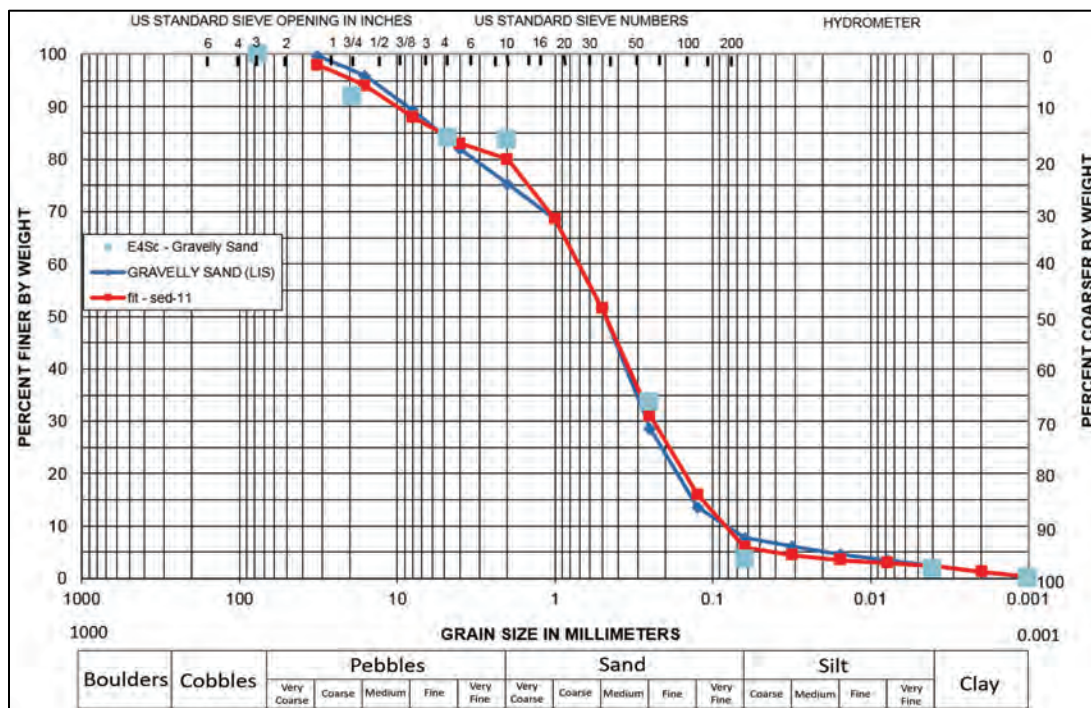




Figure 81. Refinement of sediment class 12 for consistency between e4sciences and LIS/ECST databases.

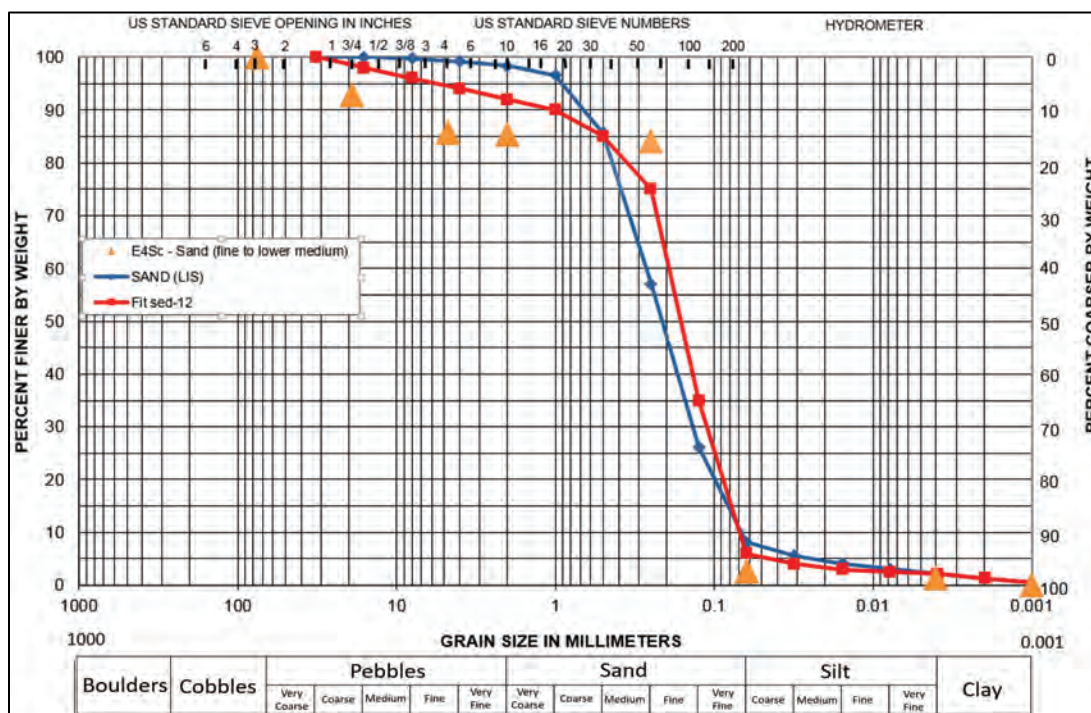
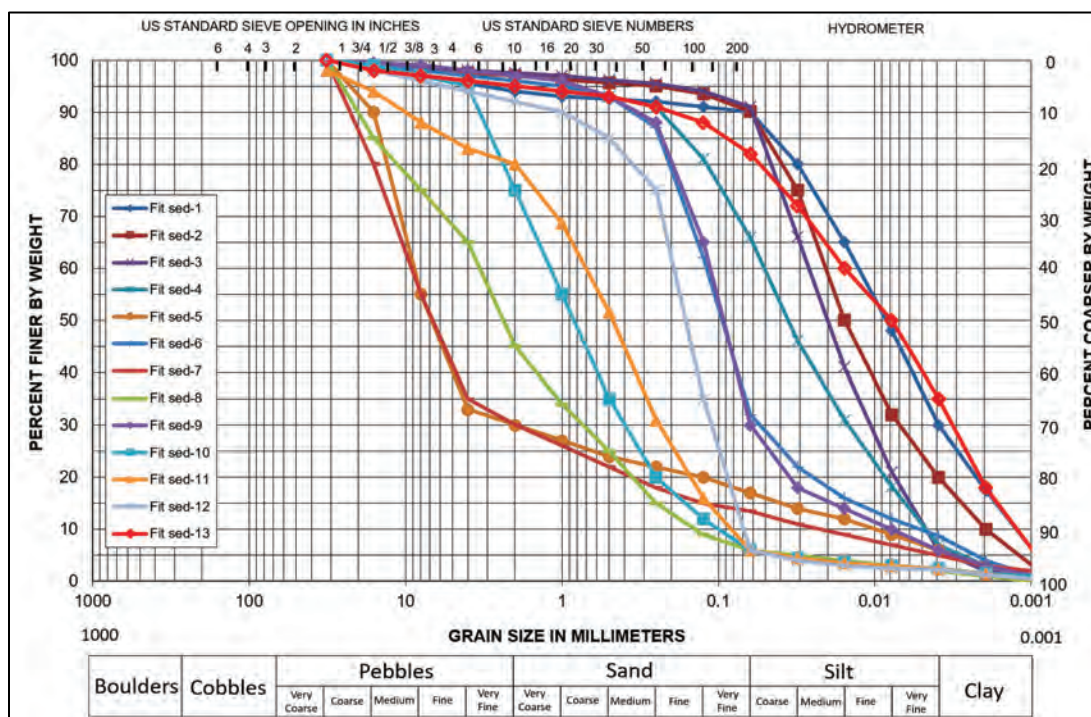


Figure 83. Summary of defined sediment classification distributions used in AdH numerical model.



The sediment characteristics within the domain of the numerical model vary dramatically. The trends of greatest interest to the model specification are the broad trends over scales associated with the dimensions of the estuary water bodies. Local heterogeneity at the scale of the numerical model mesh resolution is not within the capability of the model to resolve.

The specification of the initial bottom sediment gradations was made through the assignment of material types, which vary over the horizontal domain of the model. Fourteen material types were defined which corresponded to the fourteen characterizations developed by e4sciences and the refinements made for consistency with the LIS and ECSTDB. The material specifications within the harbor are presented in Figure 84. These are presented so that the color coding corresponds to the e4sciences delineation shown in Figure 66. The material specifications over Long Island Sound and offshore are presented in Figure 85.

Figure 84. Sediment classifications used in the AdH numerical sediment transport model within the harbor (see color bars in Figure 66 and Figure 85).

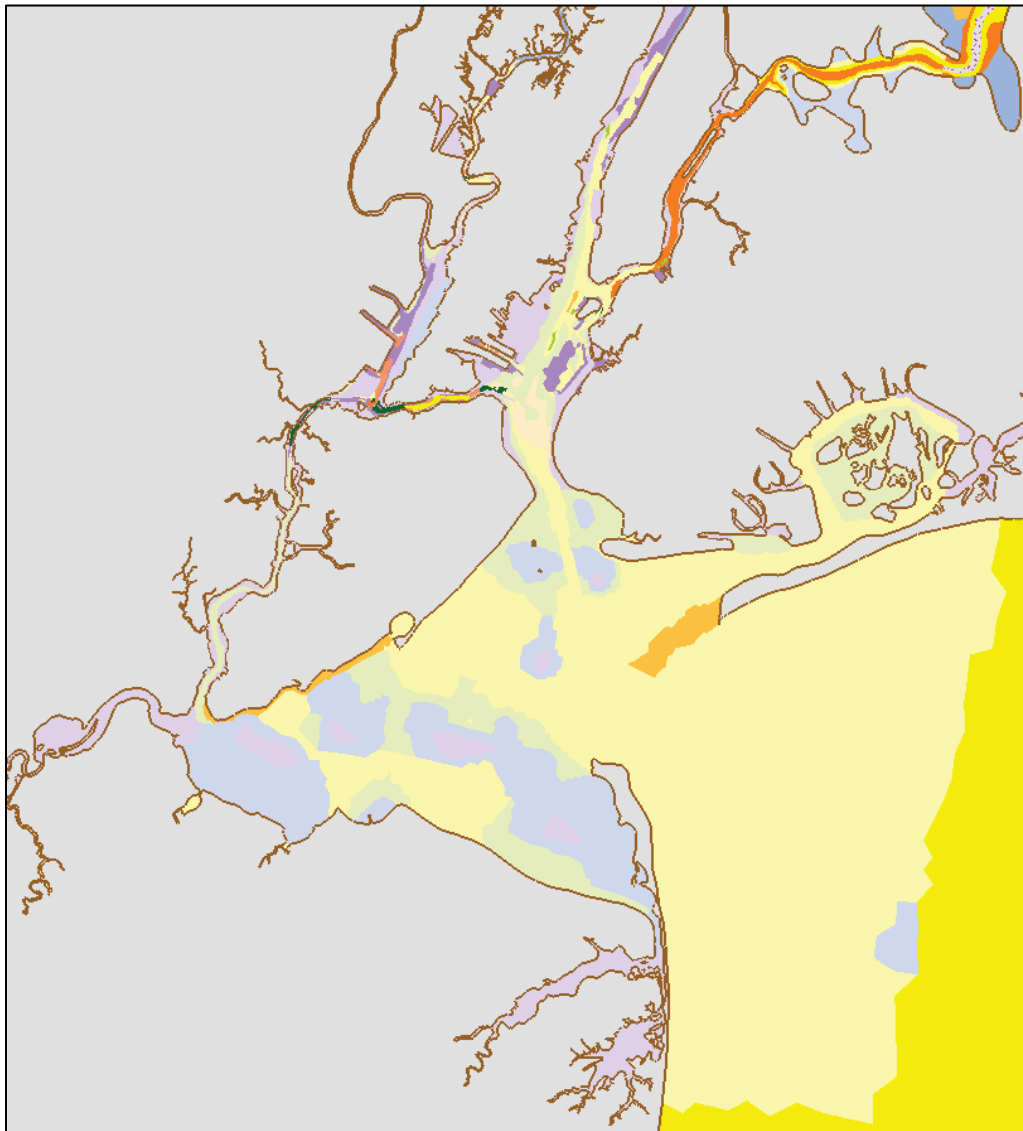
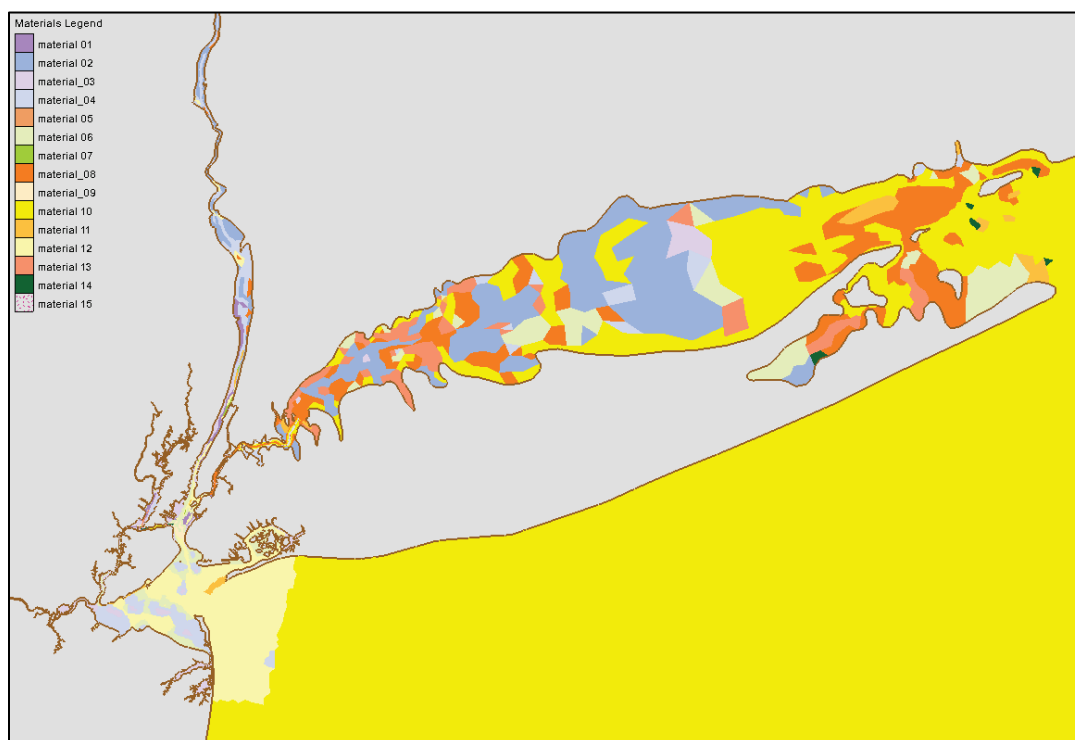


Figure 85. Sediment classifications used in the AdH numerical sediment transport model within the harbor and Long Island Sound.



A 1-year model simulation (2012 forcings) was completed to *spin up* the bed composition without allowing the bed elevations to change. This process initializes the bed by allowing the grain size distribution to vary spatially in a manner consistent with the local bed shear stresses. This procedure was deemed necessary to minimize the impacts of discontinuous specification and localized discrepancies between the specifications and the local hydrodynamic conditions. The data used to develop the bed specification were collected over a variety of hydrodynamic conditions, and there is no way to determine *accuracy* of the initialization of the bed. This process was repeated for both the with-project and without-project configurations. This adjusted bed distribution was utilized as the initial bed (with- or without-project as appropriate) for all subsequent sediment transport model simulations in this report. Note that the five simulated years were completed independently. Therefore, the model forcings/results from 1995 have no impact on 1996, and the same is true for 2011 and 2012.

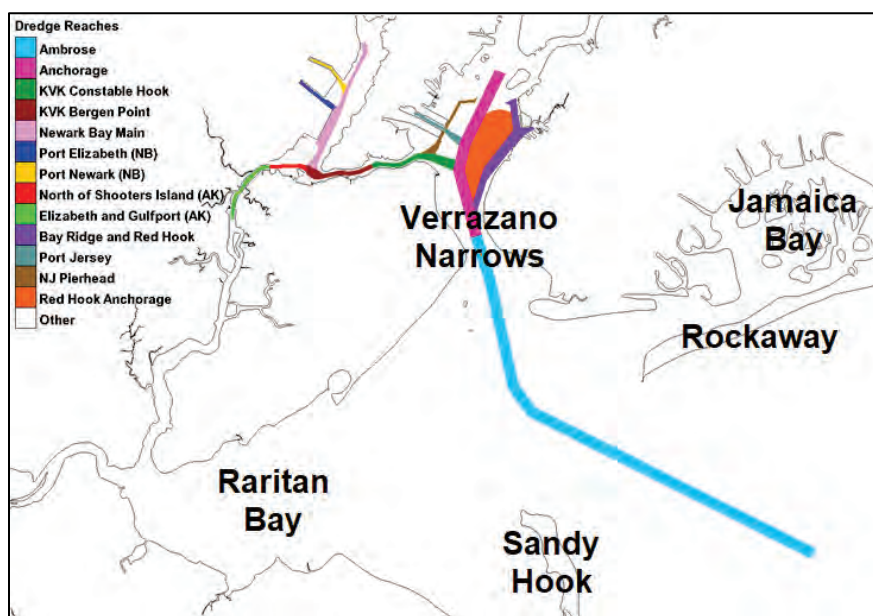


## 6 Dredging History

### Dredging for the 45 ft project

Malcolm-Pirnie\* reported a preliminary assessment on the proposed channel deepening for the harbor. In that report, a review of channel maintenance dredging was presented. They reported dredging in Ambrose Channel that occurred between the completion of the 45 ft channel in 1940 and 1982. They estimated that non-federal maintenance dredging totals approximately 24% of the total dredging requirement in the harbor. Figure 86 illustrates the locations of the commonly dredged channels discussed in this chapter.

Figure 86. Commonly dredged channels for NYNJH.



### Lower New York Harbor

The spit on the northern end of Sandy Hook has been migrating northward consistently between 1857 and 1976\* at an average rate of 20 m per year. The migration has been stopped by the trapping of sediment either within the Sandy Hook channel or by transport of littoral sediments offshore and inshore by the tidal currents within the channel. The

\* Malcolm-Pirnie. 1983. Unpublished report. *New York Harbor Navigation Study: Preliminary Assessment of Channel Deepening on Coastal Hydraulics*. Special Study Report prepared for U.S. Army Corps of Engineers, New York District, White Plains, NY.

maintenance dredging was reported to be approximately 249,000 cy/year in 1983. The estimated maintenance dredging for the Raritan Bay reaches was 865,000 cy/year.

### **Upper Bay**

Malcolm-Pirnie\* reported that data were limited for estimation of the dredging requirements in Upper Bay. They reported limited shoaling in the Anchorage Channel, which tends to be kept relatively deep because of the conveyance from the Hudson River. They reported an average annual maintenance of 33,000 cy. For the period of 1966 to 1976, maintenance of Red Hook Flats was 50,000 cy/year. The Buttermilk Channel maintenance was 253,000 cy/year. The Red Hook and Bay Ridge channels required 910,000 cy/year.

### **Ambrose Channel**

Malcolm-Pirnie\* performed a more thorough analysis of the maintenance dredging within Ambrose Channel. They compared maps obtained from the US Army Corps of Engineers (USACE) with the dredged quantities removed. The resulting average annual dredging requirements by channel reach, broken down further into the south, north, and center of the channel, are presented in Table 9. The locations of the navigation buoys are shown in Figure 87 for the 45 ft project. The annual average total maintenance for the 45 ft Ambrose Channel was 272,000 cy. The bulk of that dredging was performed on the north side of the channel (157,000 cy), with the lowest accumulation in the center of the channel.

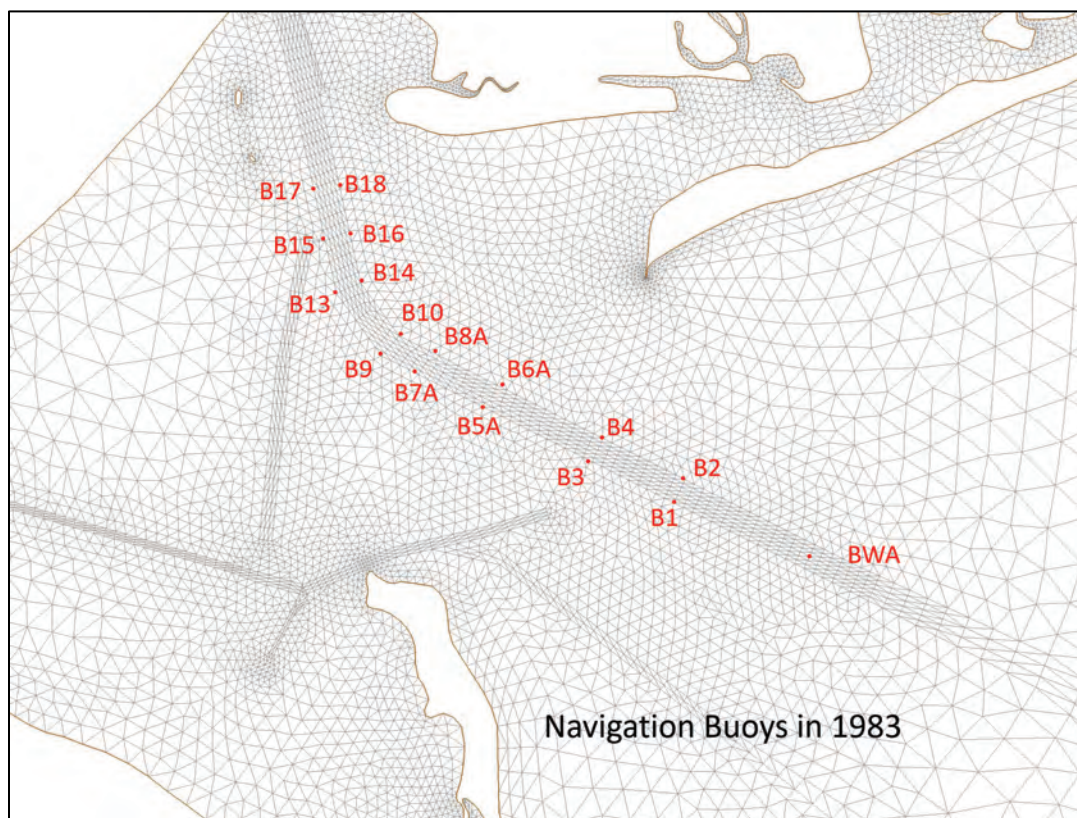
---

\* Malcolm-Pirnie. 1983. Unpublished report. *New York Harbor Navigation Study: Preliminary Assessment of Channel Deepening on Coastal Hydraulics*. Special Study Report prepared for U.S. Army Corps of Engineers, New York District, White Plains, NY.

**Table 9. Ambrose Channel maintenance for 45 ft channel (1940–1982) in thousands of cy/year.**

Reach	Distance (mi)	South	Center	North	Total
BWA to 0.5	0.25	7.8	18	10.2	36
0.5 to B2	1.2	0.9	0	26.9	27.8
B2 to B4	2.5	8.3	0	20.7	29
B4 to B6A	3.8	17.6	0	50	67.6
B6A to B8A	5.0	8.1	0	0	8.1
B8A to B10	5.7	5.4	0	2.5	7.9
B10 to B14	6.4	7.1	0.8	23.3	31.2
B14 to B16	7.2	3.4	13.6	10.9	27.9
B16 to B18	7.9	16.9	7.3	12.2	36.4
Total		75.5	39.7	156.7	271.9

**Figure 87. Navigation buoys for the 45 ft project\*.**



\* Malcolm-Pirnie. 1983. Unpublished report. *New York Harbor Navigation Study: Preliminary Assessment of Channel Deepening on Coastal Hydraulics*. Special Study Report prepared for U.S. Army Corps of Engineers, New York District, White Plains, NY.



The distribution of the dredging for each of the reaches is presented in Figure 88 for the channel reaches between buoys. These volumes of dredging were divided by the surface areas of the reaches to convert the dredging maintenance to an average sedimentation rate for the channel. These are presented in Figure 89. These figures show average sedimentation rates up to 7 cm per year over a portion of the channel and across-channel averages of up to 5 cm per year.

Figure 88. Distribution of Ambrose Channel dredging for the 45 ft project (1940–1982).

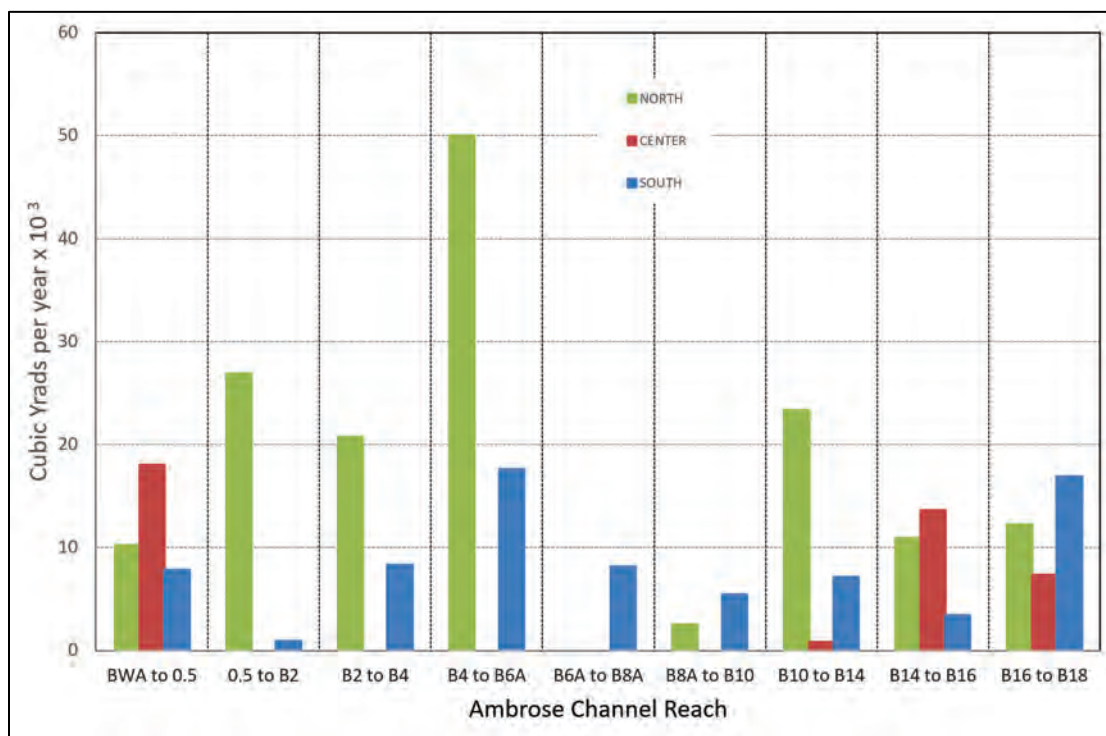
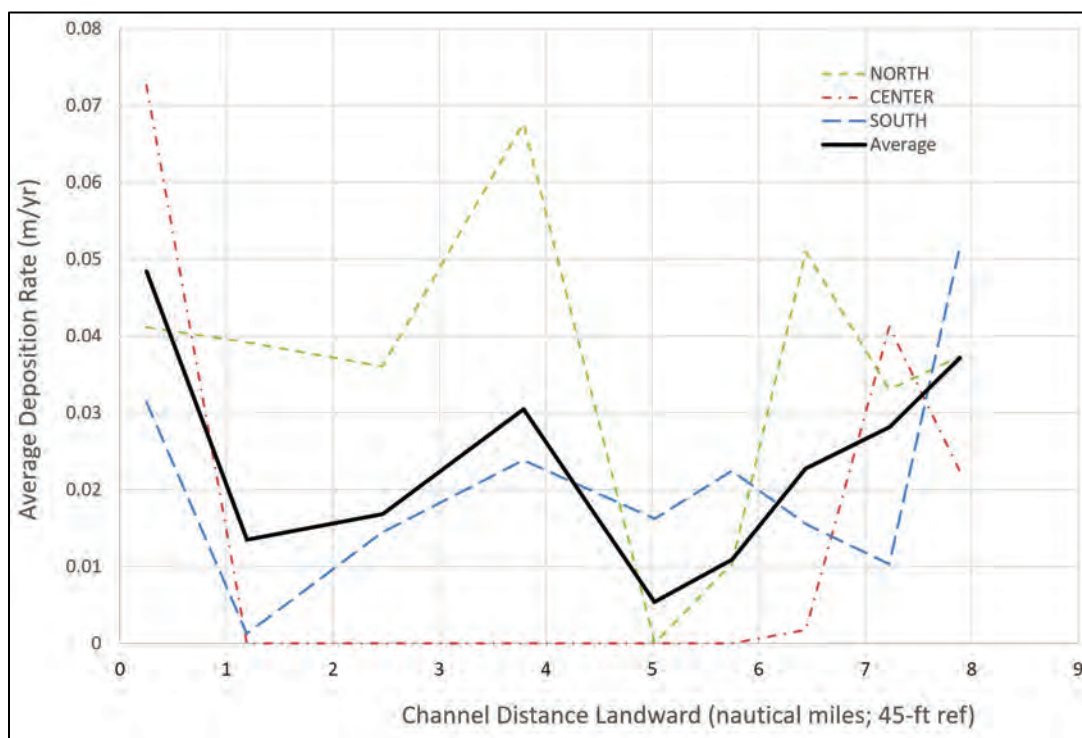


Figure 89. Average annual sedimentation rate derived from dredging volumes for 45 ft project



Malcolm-Pirnie\* warned about the uncertainty in these numbers due to variability in the actual dredged depth over different reaches and the nonuniformity of dredging within specific contract limits. However, the data are generally representative of the trends in maintenance requirements. The reach between buoys B4 (B3) and B6A(B5A) is the peak of the dredging requirement, which lies on the transect between Rockaway Point and Sandy Hook. This is the area of the greatest littoral transport of sediment.

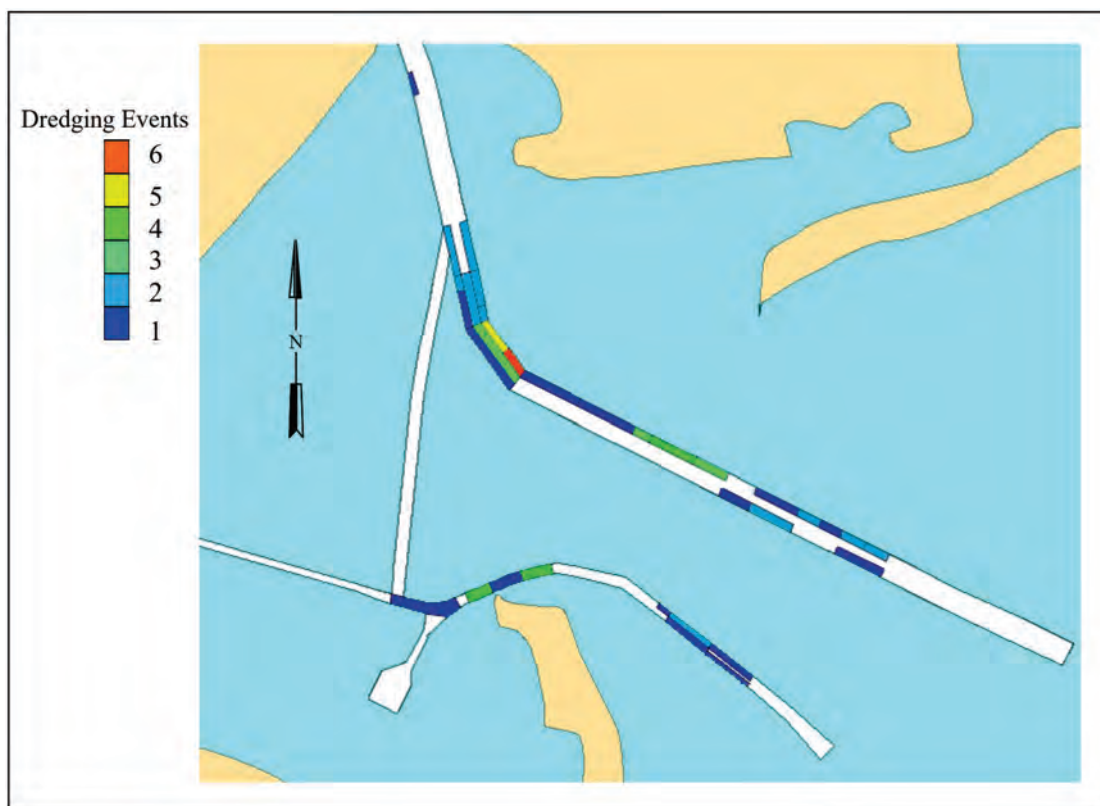
The temporal variability of the dredging requirement for the 45 ft project is illustrated by the range of reported dredging requirements for differing periods by a variety of investigators. The 1940 to 1982 average for Ambrose Channel was reported as 272,000 cy/year\*. The Mitre Corporation (1979) reported that the period 1966 to 1976 required 307,000 cy/year. Malcolm-Pirnie\* reported 900,000 cy/year for the period 1976 to 1980. This is a

\* Malcolm-Pirnie. 1983. Unpublished report. *New York Harbor Navigation Study: Preliminary Assessment of Channel Deepening on Coastal Hydraulics*. Special Study Report prepared for U.S. Army Corps of Engineers, New York District, White Plains, NY.

range of over a factor of three for Ambrose Channel, which shows that long-term trends must cover a variety of conditions.

For evaluation of the spatial distribution of dredging requirements, ERDC investigated the dredging records of Operations Division of the U.S. Army Corps of Engineers, New York, for the period 1961 through 1984 to estimate the general trends in dredging. The coverage of the specific dredging contracts was overlaid to define a frequency of dredging, defined as the number of dredging events during the 24-year period. The results of this analysis are presented in Figure 90. The peak frequency was six events at the first inbound bend in the navigation channel. There are areas of four dredging events on the north side of Ambrose Channel at the crossing of the Rockaway-Sandy Hook transect, as well as the Sandy Hook Channel just off Sandy Hook. These results are very similar to the maintenance dredging distribution reported by Malcolm-Pirnie\*.

Figure 90. Prototype dredging frequencies, 1961–1984.



## Development of maintenance volumes by e4sciences

The average annual dredging volumes were evaluated and summarized by e4sciences, under contract with US Army Corps of Engineers, New York District (CENAN) (e4sciences 2018). e4sciences compiled the data from CENAN dredging records. The data provided included estimates of dredging for the following periods:

1. Pre-1999 dredging volumes and annual rates
2. 1999 – 2007 dredging volumes and annual rates
3. Post-2007 dredging volumes and annual rates.

The dredging volumes developed by e4sciences are summarized for these periods in Table 10. The pre-1999 volumes were taken from the New York and New Jersey Harbor Deepening re-evaluation report (USACE 2004). The dredging volumes for the 1999 to 2007 period were reported with a low and a high range of annual dredging volumes based on the uncertainty in the dredging records for the duration of time between dredging activities.

The post-2007 dredging volumes are shown as those volumes reported as purely maintenance dredging in the fourth and fifth columns of Table 10. However, a portion of the dredging reported as new work included material that was unacceptable for open water disposal at the Historic Area Remediation Site (HARS) dump site. That material required special upland disposal. Those volumes could be assumed to be the result of recent deposition and therefore a component of the maintenance volumes. The two final columns include those volumes in the post-2007 volume estimates for both the low and high ranges of the dredging estimates.

The variability in the annual rate of dredging estimates over the differing periods and channel depths suggest that natural variability due to different river flows and meteorological conditions is more significant than the navigation channel depth. This observation is the primary motivation for the current numerical model study, which can isolate the navigation channel depth impacts by simulating the exact same conditions for both pre- and post-deepening channel conditions.

Table 10. Dredging volume distributions by channel reach in cy (e4sciences 2015).

Channel	pre-1999	1999–2007		post 2007		post 2007+ non-HARS	
		Low range	High range	Low range	High range	Low range	High range
Ambrose	400,000			57,175	133,408	134,209	313,153
Anchorage				12,565	29,317	186,623	435,454
Kill van Kull Constable Hook	28,000	0	0	11,710	27,324	11,710	27,324
Kill van Kull Bergen Point	4,000	14,591	10,228	11,710	27,324	11,710	27,324
Newark Bay (NB) Main	211,000	92,137	65,812			160,528	374,566
NB Port Elizabeth	121,700	64,358	48,269	18,441	43,029	63,545	148,271
NB Port Newark	226,200			14,780	34,487	14,780	34,487
AK north of Shooters Island	115,000	99,725	62,328	4,888	11,404	4,888	11,404
AK Elizabeth and Gulfport	7,000	96,205	60,128	20,641	48,163	20,641	48,163
Bay Ridge and Red Hook	520,000						
Port Jersey	58,000	160,220	112,089	11,368	26,525	106,299	248,031
Claremont	25,000						
NJ Pierhead	40,000						
Red Hook Anchorage	145,000						
Gravesend Anchorage	28,000						
Stapleton Anchorage	0						

## 7 Description of Project

The purpose of this study is to determine an approximate impact to the NYNJH system due to the channel deepening with particular emphasis on the impact to dredge volumes. To accomplish this goal, an appropriate without-project mesh configuration was determined and then altered to incorporate the project deepening. As previously discussed, the without-project bathymetry was created by taking the bathymetry dataset compiled by e4sciences and removing any components of the project already constructed in 2004. The with-project mesh configuration was then developed by modifying the without-project configuration to create a new mesh where the only differences were associated with the project. The deepening project increased the authorized depth from 45 ft (13.72 m mean lower low water [MLLW]) to 50 ft (15.24 m MLLW) with the Ambrose Channel further deepened to 53 ft (16.16 m MLLW). These channel elevations were decreased by 0.78 m) to correct from MLLW to MSL datum (based on Sandy Hook) in the numerical model mesh. The with-project bathymetry dataset is shown in Figure 91, and the without-project bathymetry dataset is shown in Figure 92.

Areas in the channel deeper than the new authorized depth were left unchanged and are equivalent in both mesh configurations. The Verrazano Narrows is an example of this. Prior to the channel deepening project, the depth in the Verrazano Narrows was approximately 90 ft, and therefore no channel deepening was required in this location.

Figure 91. Without-project bathymetry.

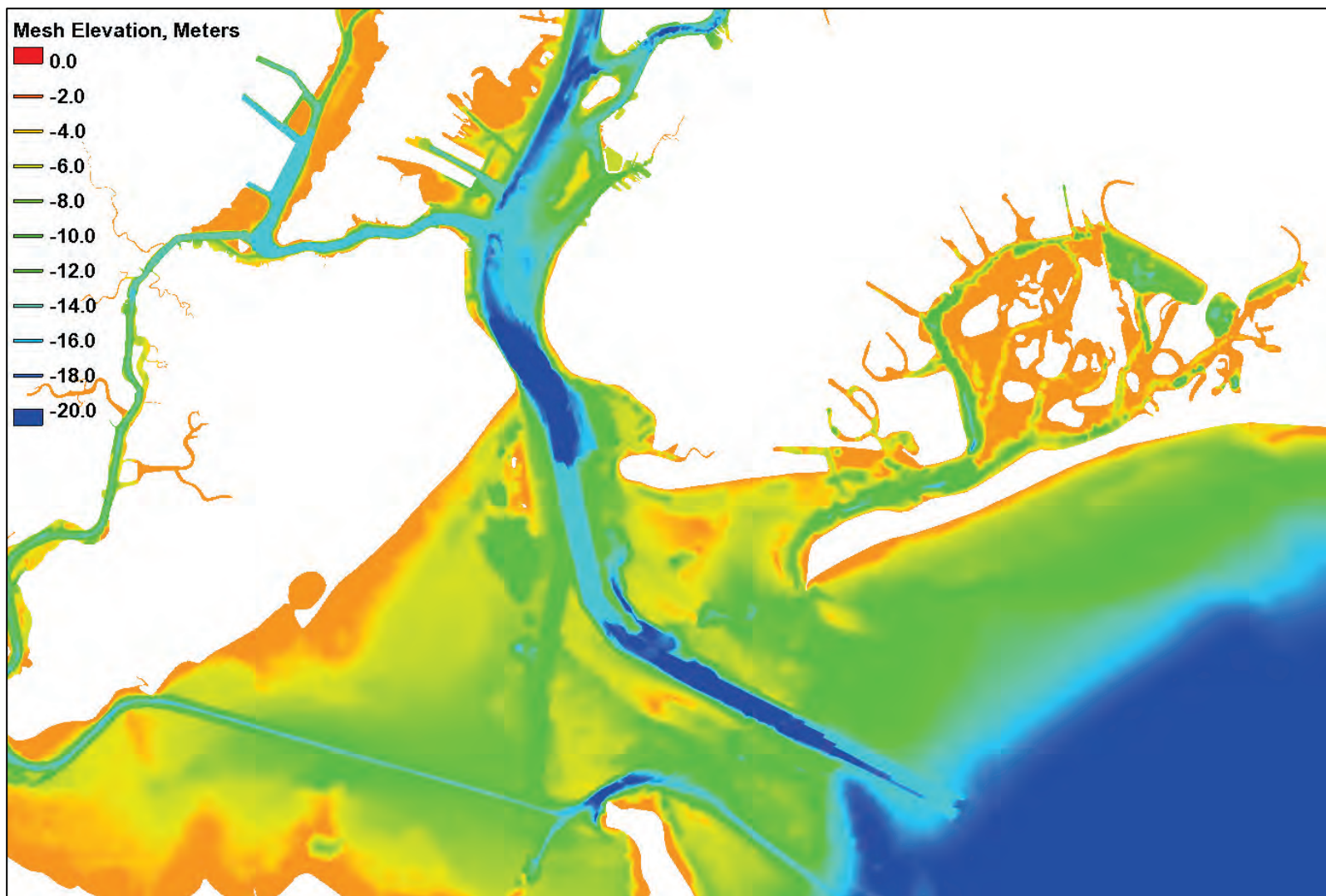
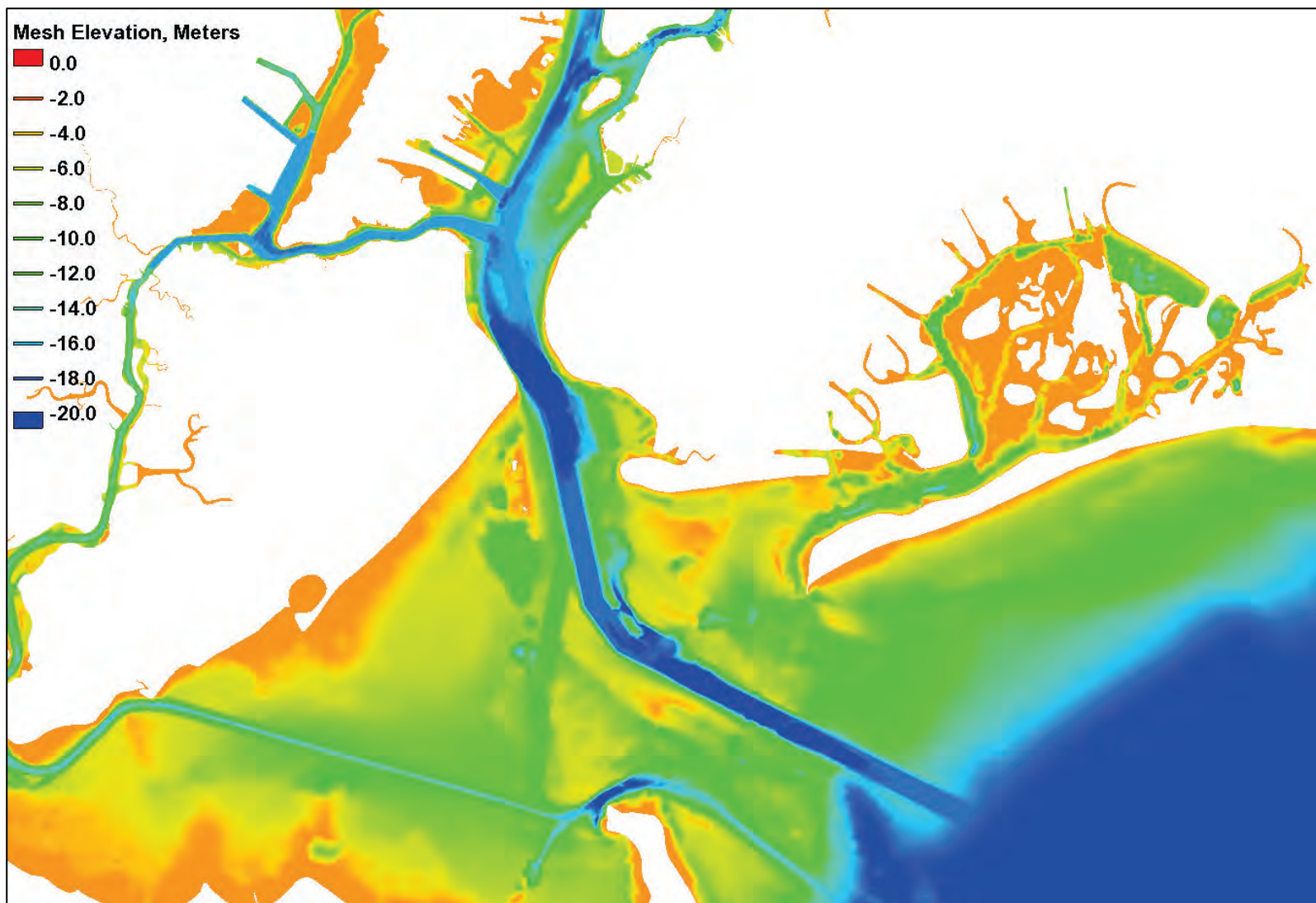




Figure 92. With-project (channel deepening) bathymetry.



## 8 Model Validation

The model validation was a multistep process that continuously expanded the complexity of the model. A 3D hydrodynamic and salinity and sediment transport model has numerous components that individually could negatively impact the model results. This step-by-step approach allowed for the isolation of particular components to prevent unknowingly propagating a hydrodynamic error through the process all the way to the sediment transport results. The steps followed in the model validation were as follows:

1. 2D model validation to NOAA (2005) tidal harmonics and phases
2. 3D model validation of hydrodynamics to observed NOAA water level data
3. 3D salinity transport validation to observed salinity measurements
4. 3D sediment transport validation to historical dredging volumes.

The final simulations were 3D simulations with hydrodynamics, salinity and sediment transport that also include the impact of local wind generated waves using the CSTORM-MS system to link the AdH hydrodynamic, salinity and sediment transport model to the STWAVE model. This chapter details the validation process and comparisons to the observed data.

Before performing sedimentation simulations, the salinity model was validated to the salinity distribution within the estuary. The primary calibration parameters for the salinity validation are the turbulent mixing coefficients (Harleman 1966). These mixing coefficients within the salinity transport equation are the same coefficients used in the sediment transport governing equations (advection/diffusion equation). The only difference in the basic equations is that the sediment transport equation includes a settling velocity for the particles and a source/sink term at the bottom for deposition/erosion. Other terms in the equations are the same between the salinity and sediment transport. Of course, the initial conditions are different, and there are 10 separate sediment transport equations, one for each sediment size class.

After salinity validation, the model incorporated sediment transport by adding specific sediment size classes and the associated sediment properties for each size class. The sediment properties included the settling velocities of the sediment when in suspension and boundary conditions, which include the sediment size distribution within the bed sediment layers and the sediment suspended concentrations by size class within the river inflows (previously discussed in Chapter 4).

This study is essentially a hindcast project whereby the validation of the numerical model consisted of comparing observations to both the with- and without-project model results. Some observations were prior to the construction of the project, some were during construction, and some were post construction. The model-to-field comparisons in this chapter were compared to the most appropriate mesh configuration based on the time the data were collected. As such, this project, as opposed to most projects, includes model to field comparisons for the with-project model results.

## **Model simulations**

The model simulations consisted of simulating five calendar years (1985, 1995, 1996, 2011, and 2012) with both the without-project conditions and the with-project conditions and analyzing the model results to quantify the variation between the two sets of simulations. The primary point of focus was on the dredge volumes but additional analysis was also completed to investigate the overall impact of the channel deepening project.

## **Sources of model uncertainty and consequences**

Uncertainty can, in general, be classified as either natural uncertainty or epistemic uncertainty (Merz and Thielen 2005). Natural uncertainty arises from the stochastic nature of the forcing conditions that lead to the processes being studied. Epistemic uncertainty arises from a variety of sources, including measurement error, a limited period of record, modeling limitations, and other factors related to imperfect knowledge or measurement of the processes of interest. Epistemic uncertainty can be reduced by careful design of the analysis while the natural uncertainty cannot be reduced.

In numerical modeling, the high-fidelity results (both temporally and spatially) can sometimes mislead the user into assuming an unrealistic level of accuracy in the model results. For complex models such as the one

utilized in this study, there are numerous forcing conditions and model input parameters that are uncertain, each of which impact the model results. For the hydrodynamic model results, the bathymetry, tidal boundary, river inflows, wind and pressure fields, and frictional specification are just a few of the parameters specified in the model that possess uncertainty. While it is extremely difficult to determine an exact level of uncertainty in the model results, some indication of the accuracy of the model can be inferred from the accuracy of the model in replicating the observed data. It is also beneficial to analyze the variation in the model results across a wide range of forcing conditions and through the completion of sensitivity simulations to investigate the impact of certain parameters. By simulating 5 years with a wide range of forcing conditions, an uncertainty due to the boundary conditions can be inferred from the model results. The absolute dredge volume results can vary significantly with these differing boundary conditions, but the with-project versus without-project comparisons will be more consistent as the impact of some of these variations between years will be negated by comparing the model results in this manner.

For the salinity transport, the uncertainty is primarily attributed to any inaccuracies in the hydrodynamics, the initial salinity field specified in the model, offshore salinity boundary specification and the mixing values utilized for model stability. The initial salinity field can sometimes impact the salinity results for long periods of time depending on the residence time for the particular estuary. That is why it is important to choose a reasonable beginning salinity field. For this study, 2D salinity transport baroclinic simulations were performed to obtain a realistic spatially varying salinity field. Then this 2D (constant over depth) salinity field was simulated in the 3D model for 1 month leading up to the year being simulated. Therefore, the last month of the preceding year was utilized as an initialization time period for the hydrodynamics and salinity for each yearly simulation. This initialization was performed separately for the with- and without-project conditions.

As expected the sediment transport results have the largest degree of uncertainty as the previously discussed sources of uncertainty for the hydrodynamic and salinity transport results are propagated to the sediment transport results. There is also significant uncertainty in the specification of the sediment parameters themselves. A model can never be more accurate than the data used to develop said model and with

sediment transport modeling the observed input data commonly includes a wide range of uncertainty. An example of this would be the data utilized in Table 8; the observed data have a range of approximately 20% in some locations and/or sediment classes, and as such, expecting the numerical model to be more accurate than these observed values is unlikely.

Considering the previously discussed model uncertainties, some could ask “what is the use of such a model rife with uncertainties?”, but the model is useful for gaining insight into the behavior of the system. When considering the model results across the wide range of forcing conditions in this study, consistent results across simulations reinforce the confidence in those results. There is also a tiered expectation level in terms of model accuracy. The absolute value provided by the model is expected to have the largest degree of uncertainty, with base-versus-plan differences expected to be an order of magnitude more accurate, and overall trends are expected to be the most accurate (increasing in location A and decreasing in location B). In essence, the value of the numerical model is to minimize as much as possible epistemic uncertainty by simulating both with- and without-project conditions under the same forcing conditions.

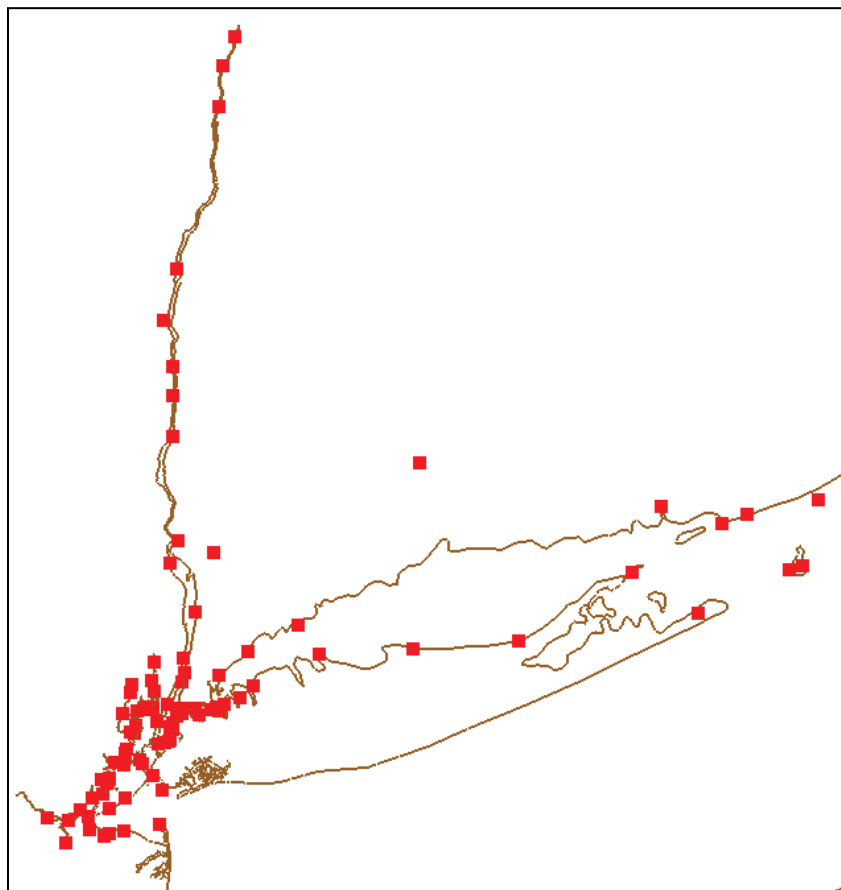
This section of the report serves as an introduction to the topic of uncertainty in the model results but additional discussion is provided in subsequent sections whereby the variation in the model results across years and mesh configurations is utilized to infer some expected level of accuracy in the model results.

## **Two-dimensional (2D) tidal harmonic comparisons**

The first step in the AdH model validation was to simulate the harmonic tidal signal within the 2D depth-averaged module of AdH. This approach was performed as a preliminary model adjustment to get general agreement of basic harmonic tidal propagation within the harbor. There is a large database of historic tidal data throughout the harbor that supports the NOAA-predicted tidal analyses. This preliminary step was for qualitative comparisons. The detailed quantitative verification is deferred to the full 3D model with full meteorological and hydrologic forcing. The harmonic tidal simulations included no meteorological forcing and were compared with the long-term NOAA-tabulated mean tides and average spring tides along with the tidal progression as documented in the lunar intervals, tidal phases relative to Sandy Hook time of mean high water.

The 2D model horizontal mesh (previously shown in Figure 17, Figure 18, and Figure 19) is the same resolution mesh utilized for the 3D model. The tidal harmonic boundary condition used for the harmonic validation was previously discussed in Chapter 4. The data for the calibration of the model to purely harmonic propagation are provided in Appendix B from NOAA (2005). The locations of the tide stations are shown in Figure 93.

Figure 93. Location of NOAA tide stations with general tidal characteristics defined.



The AdH model was simulated with very low flow on all rivers to represent the periods used by NOAA to develop their tidal characteristics. This strategy generally gives a greater tidal influence up the rivers than when normal flows of the Hudson River are included.

### Hudson River

Tidal amplitudes and high/low water arrival times relative to Sandy Hook were compared for the Hudson River locations shown in Figure 94. Some location names are omitted from the points in Figure 94 (and future

location figures) due to the abundance of points. The locations in the plot figures are all represented by points in the location figures, but some locations are not explicitly named. The orders in the location figures and amplitude/arrival time plots are also consistent. The profile of the time of high and low waters up the Hudson River relative to the time of high water at Sandy Hook is presented in Figure 95 for both the NOAA data and the model results. The profile comparison of the tide range is presented in Figure 96. The progression of the wave up the river is in phase with the predicted NOAA tides, but the tide range is lower at the farthest upstream end of the profile outside of the dredging project. This underestimation of the tide range in the upper reaches of the Hudson River should have negligible impacts on the sedimentation in the harbor.

Figure 94. Hudson River analysis locations.

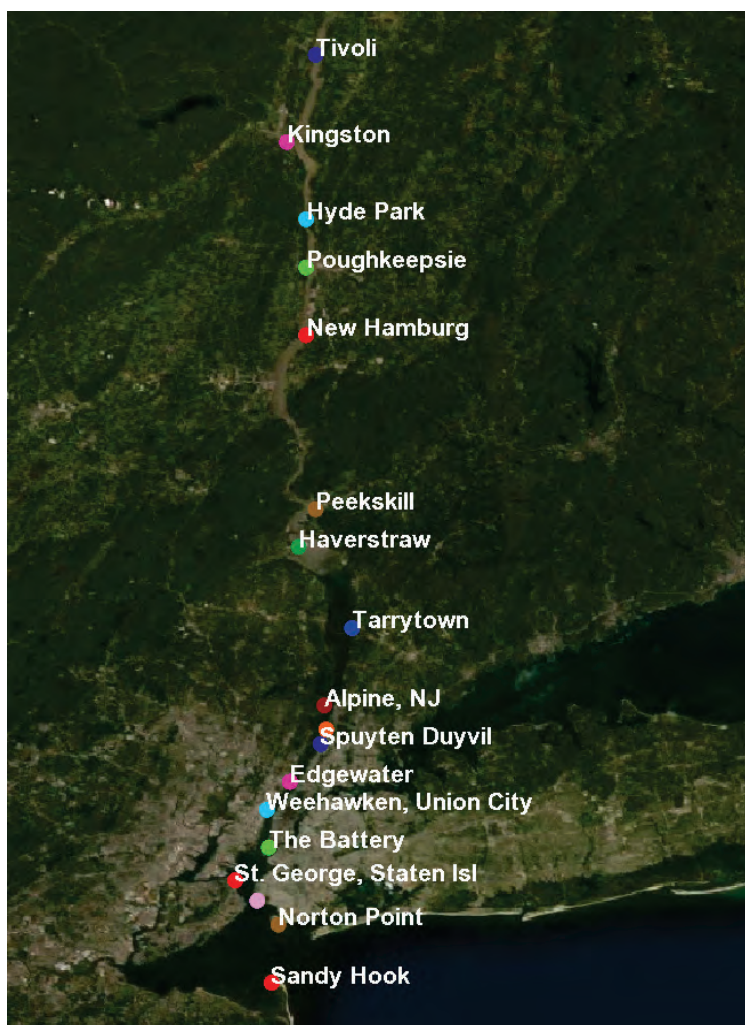




Figure 95. Tidal propagation for the times of high and low waters up the Hudson River for the low-flow tidal harmonic simulation.

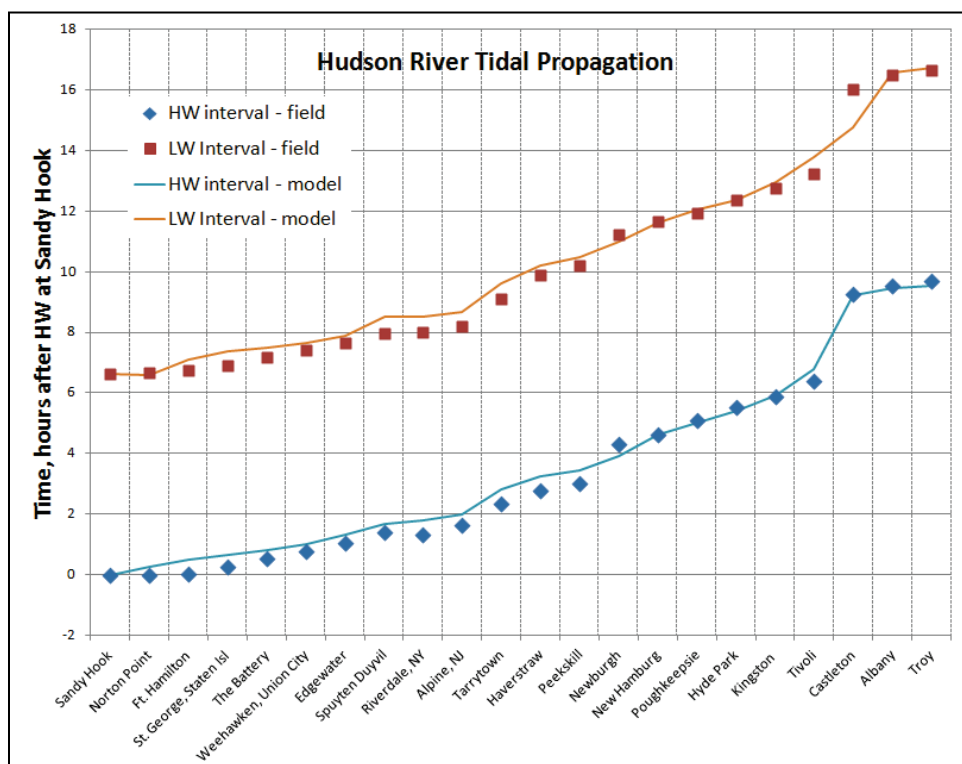
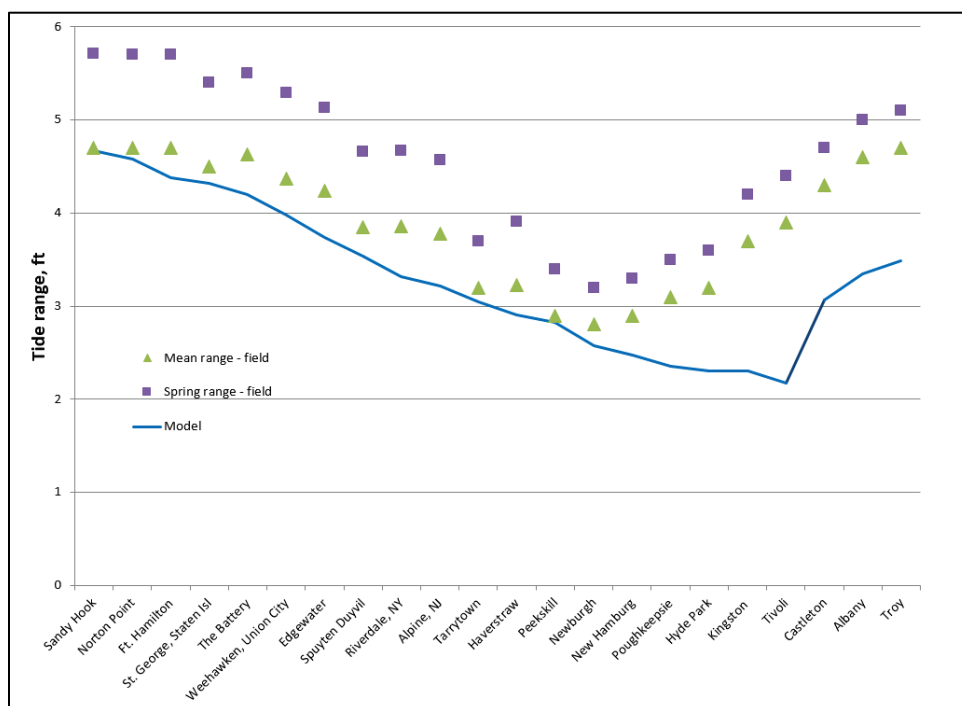


Figure 96. Tidal range propagation up the Hudson River for the low-flow tidal harmonic simulation.



## East River and Long Island Sound

The profile of the time of high and low waters relative to the time of high water at Sandy Hook for a transect from Sandy Hook, through Upper Bay and then up the East River and eastward through Long Island Sound (analysis locations shown in Figure 97 and Figure 98) is presented in Figure 99. Tides propagate through Lower Bay and northward up the East River. Tides also propagate westward through Long Island Sound into the East River. The inner East River between Hell's Gate and the western end of Long Island Sound behave as a standing wave, with little phase difference. Consequently, the tide range is dramatically increased in that reach. The profile comparison of tide range through this transect is shown in Figure 100. The tidal characteristics show that the model tides arrive as much as an hour early in the eastern end of East River. Low waters are in better agreement. The high water enters Long Island Sound at the eastern end and then propagates west. The tides are in relatively good phase in the western end of East River. The tide range, which is slightly higher than a mean tide at Sandy Hook, propagates through the East River with relatively good magnitude with the exception of around Hell's Gate.

Figure 97. East River analysis locations.



Figure 98. Long Island sound analysis locations.

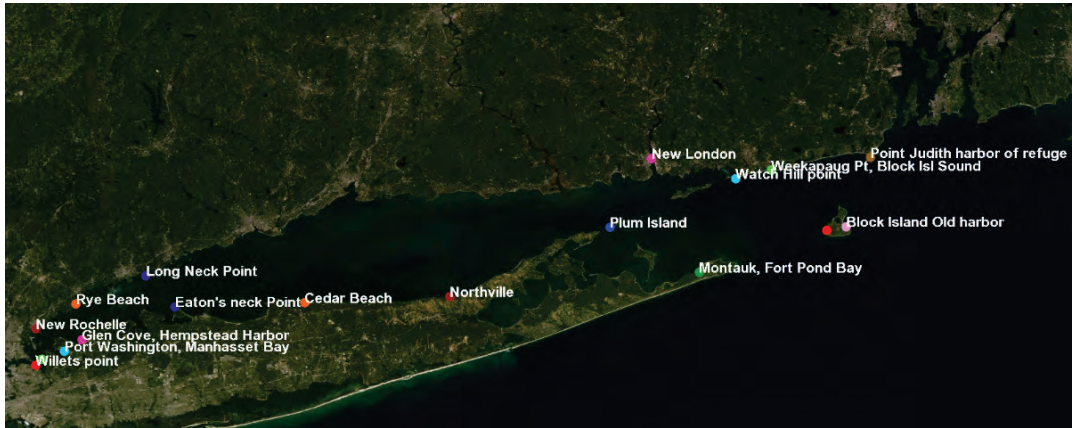


Figure 99. Tidal propagation for the times of high and low waters up the East River and through Long Island Sound for the low-flow tidal harmonic simulation.

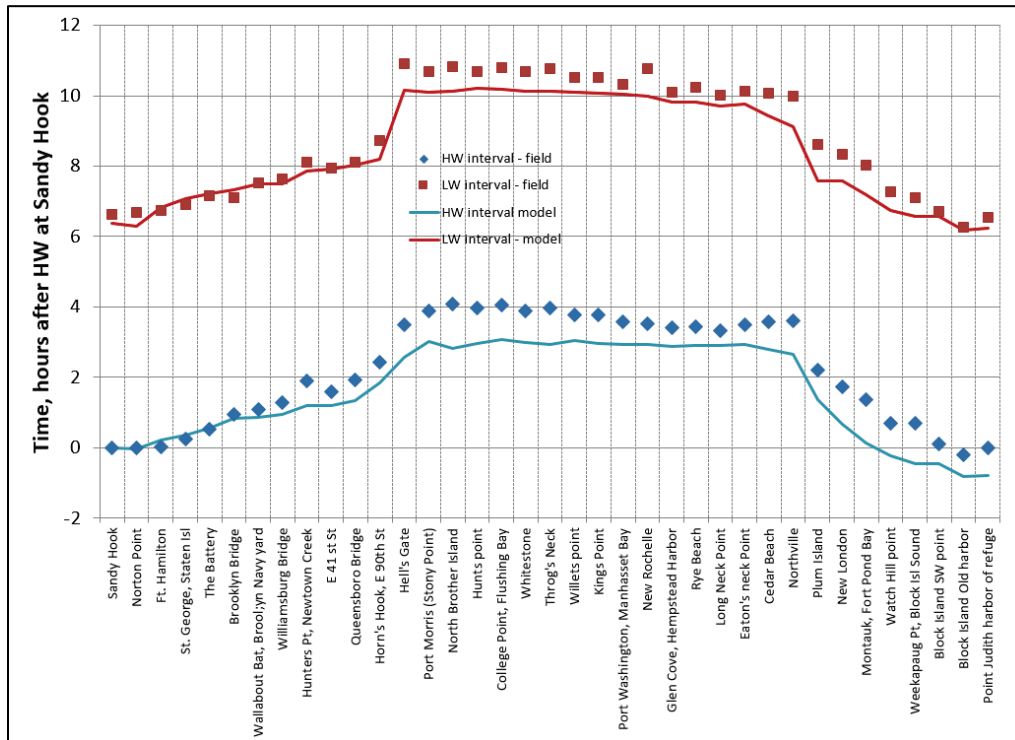
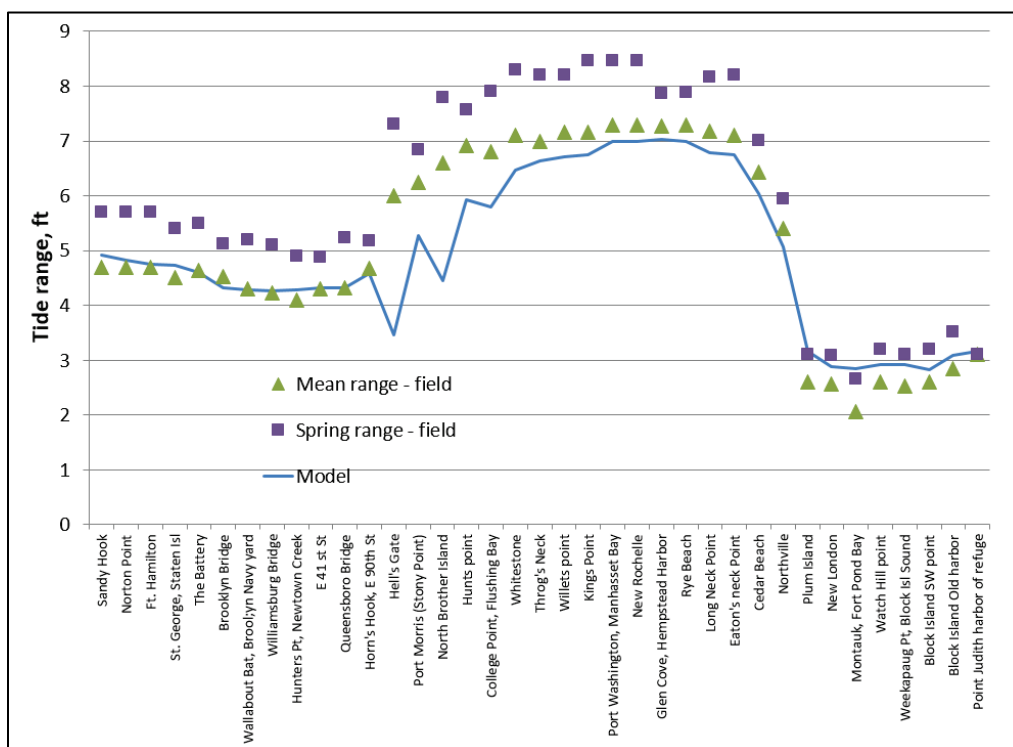


Figure 100. Tidal range propagation up the East River and through Long Island Sound for the low-flow tidal harmonic simulation.



## Staten Island

The profile of the times of high and low waters relative to the time of high water at Sandy Hook for the loop around Staten Island (locations shown in Figure 101) is presented in Figure 102 for both the NOAA data and the model results. The profile comparison of the tide range is presented in Figure 103. The high and low water intervals around Staten Island are in very good agreement for both high and low waters. The comparison of tide range variation around Staten Island is also in good agreement.



Figure 101. Staten Island analysis locations.



Figure 102. Tidal propagation for the times of high and low waters around Staten Island through Kill van Kull and Arthur Kill for the low-flow tidal harmonic simulation.

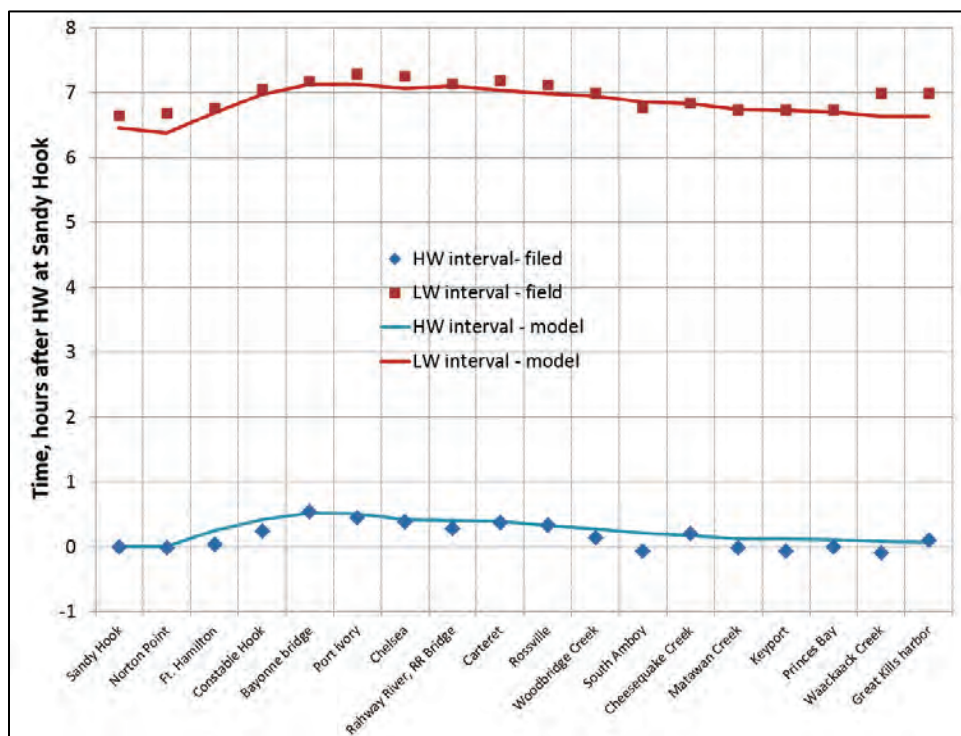
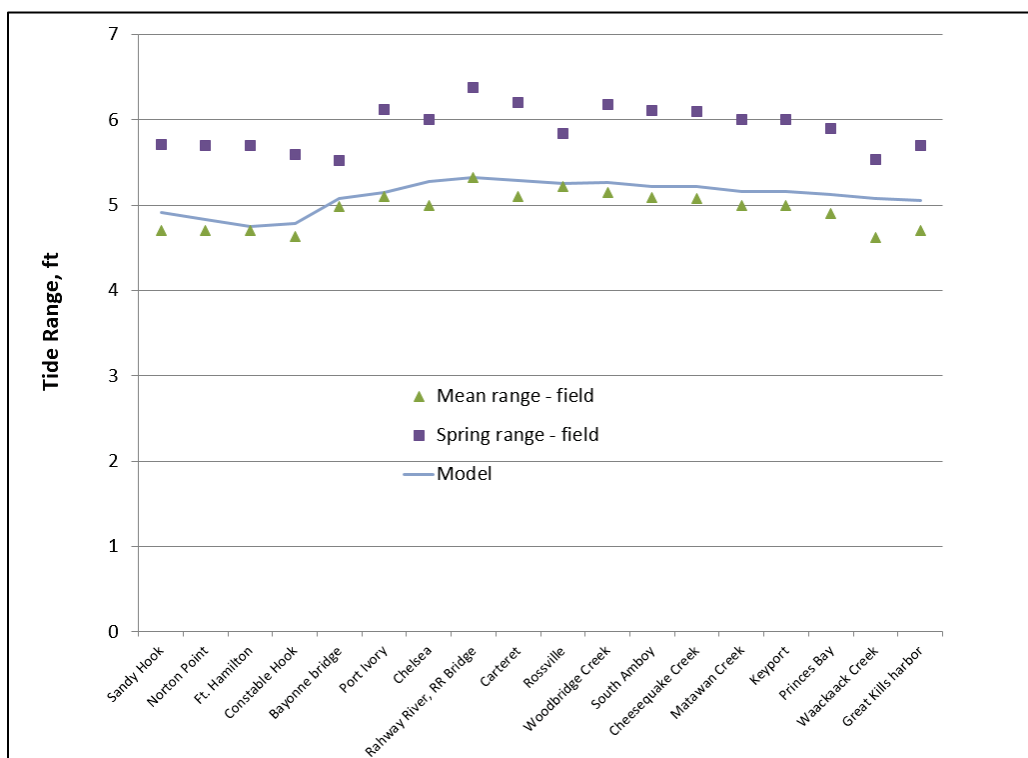


Figure 103. Tidal range propagation around Staten Island through Kill van Kull and Arthur Kill for the low-flow tidal harmonic simulation.



## Hackensack River

The profile comparison of the model to the observed NOAA times of high and low waters relative to the time of high water at Sandy Hook through the harbor and up the Hackensack River (locations shown in Figure 104) is presented in Figure 105. The Hackensack River stations are above (to the right on the plot) of Kearny Point. The profile for the tide range up the Hackensack River is presented in Figure 106. The propagation of high and low waters up the Hackensack River is generally in agreement, but the times of high water are slightly early in the Hackensack River itself. Low waters are in very good agreement except for the low water at New Milford, which exhibits a drastic phase lag in the NOAA data. The tide profile comparison between the model and NOAA is good up the Hackensack, again with the exception of New Milford, which has approximately a 20% drop in range compared to Hackensack.

Figure 104. Hackensack River analysis locations.

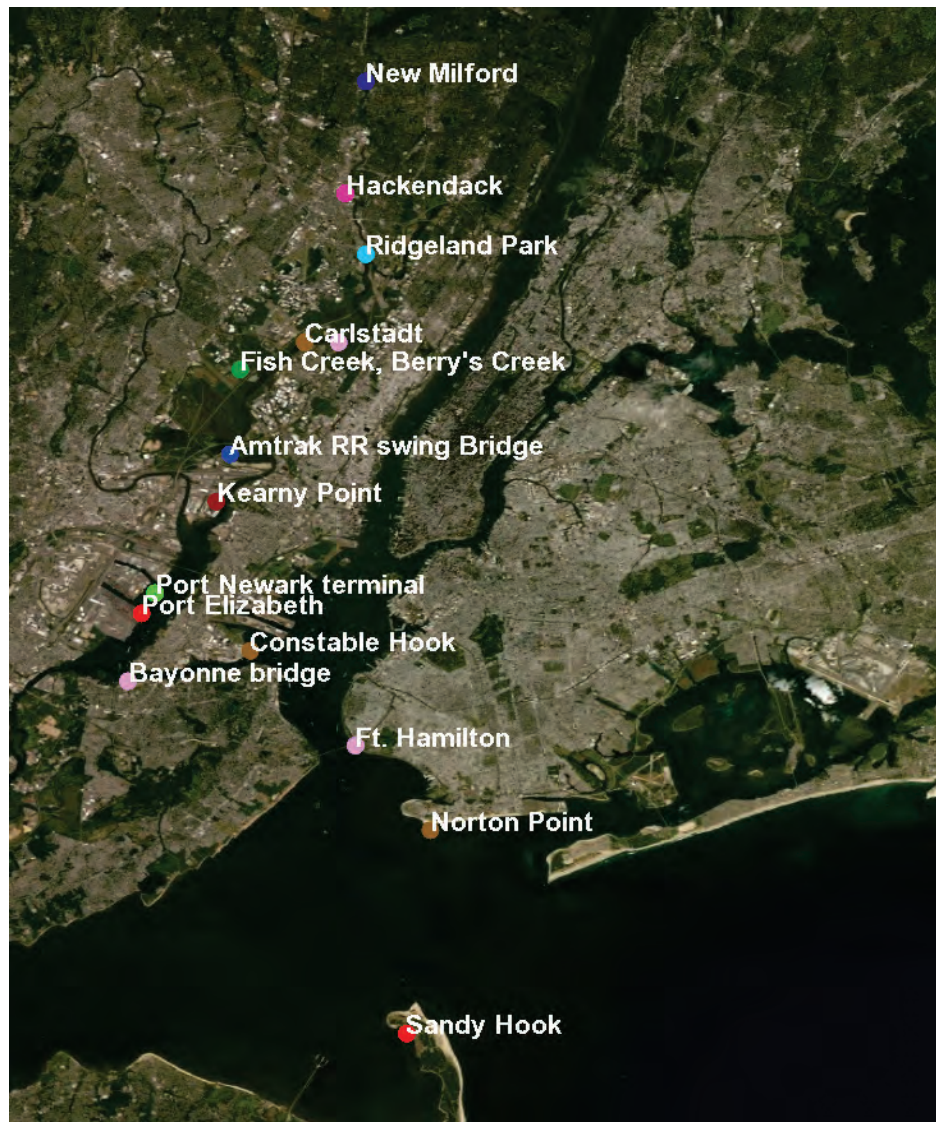




Figure 105. Tidal propagation for the times of high and low waters from Sandy Hook through Kill van Kull and up the Hackensack River for the low-flow tidal harmonic simulation.

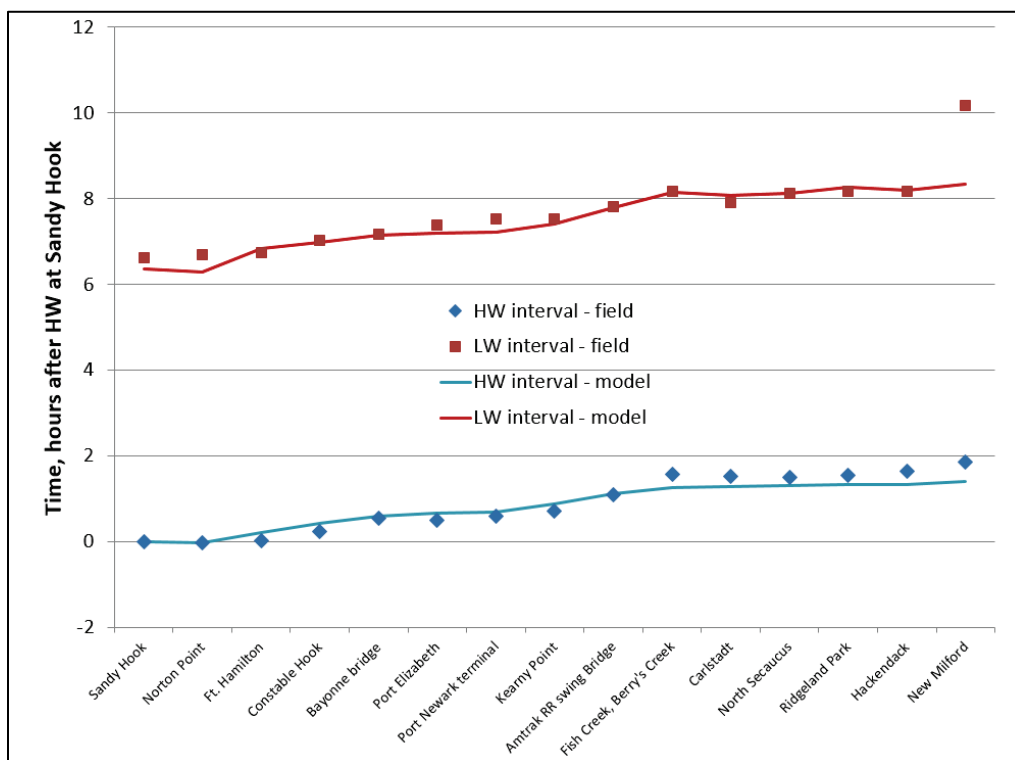
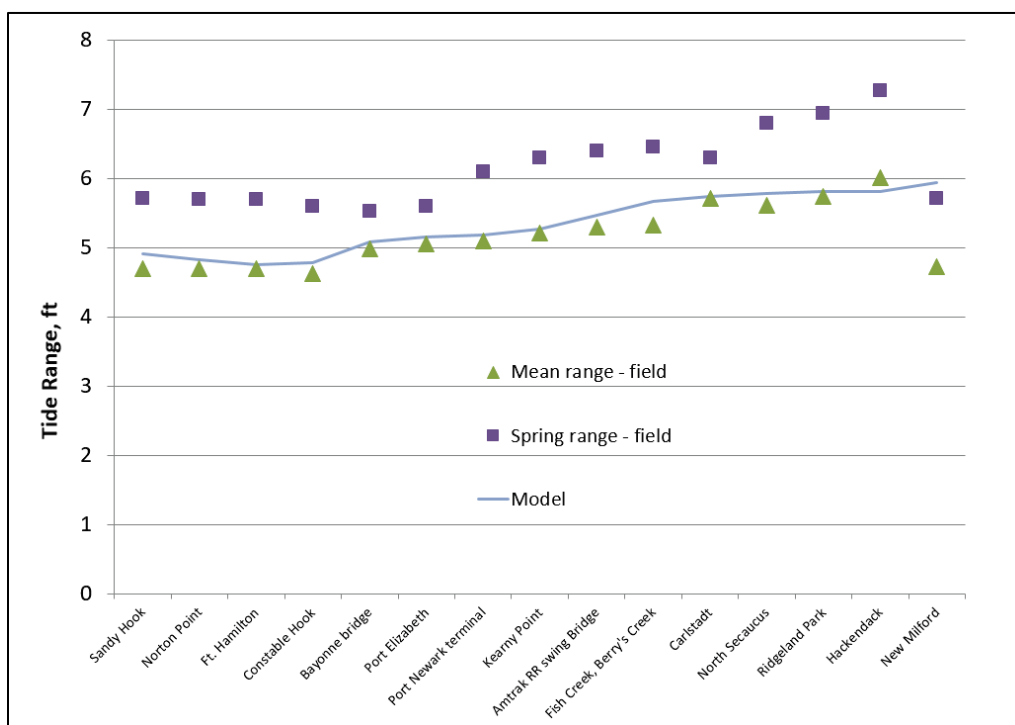


Figure 106. Tide range profile from Sandy Hook through Kill van Kull and up the Hackensack River for the low-flow tidal harmonic simulation.



## Passaic River

The profile comparison of the model to the observed NOAA times of high and low waters relative to the time of high water at Sandy Hook through the harbor and up the Passaic River (locations shown in Figure 107) is presented in Figure 108. The Passaic River stations are the last three points in the profile. The profile for the tide range up the Passaic River is presented in Figure 109. The tidal propagation up the Passaic River is in good agreement both in tidal phases and in tide range.

Figure 107. Passaic River analysis locations.



Figure 108. Tidal propagation for the times of high and low waters from Sandy Hook through Kill van Kull and up the Passaic River for the low-flow tidal harmonic simulation.

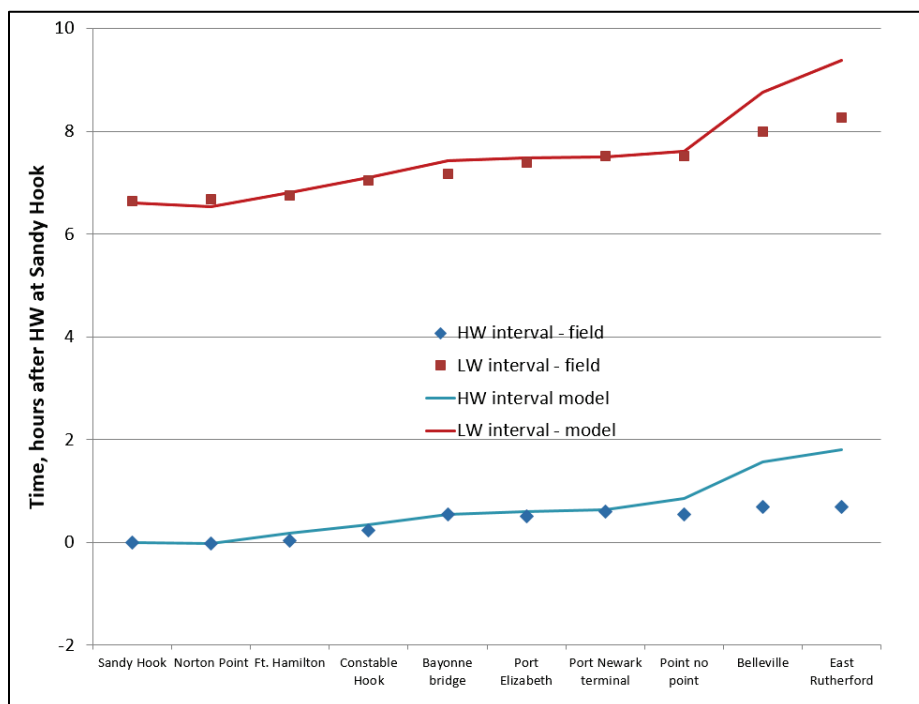
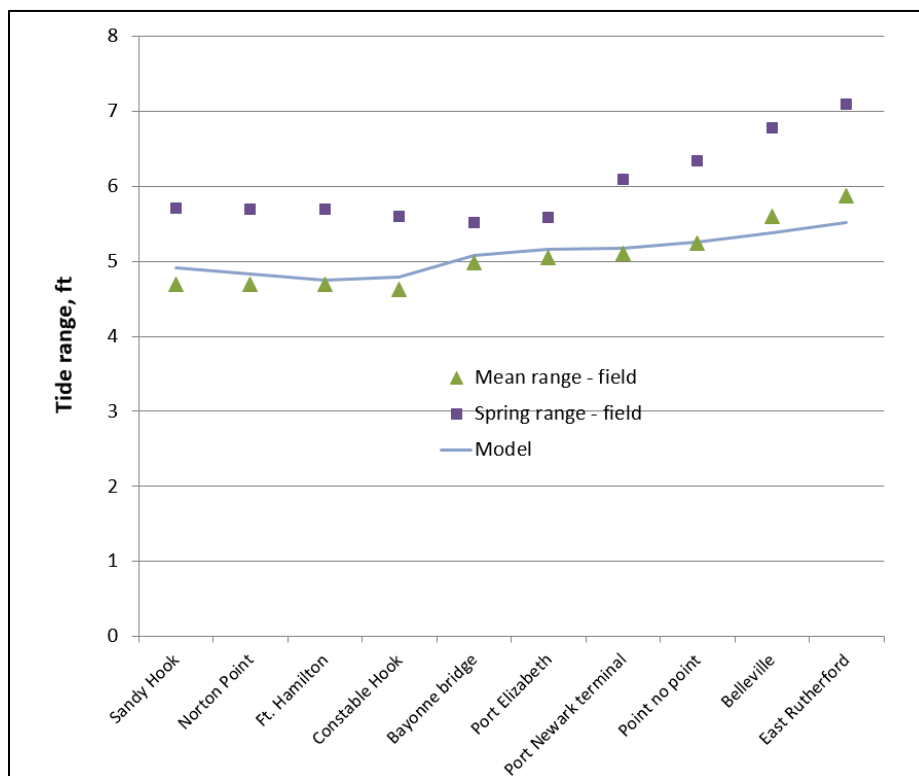


Figure 109. Tide range profile from Sandy Hook through Kill van Kull and up the Passaic River for the low-flow tidal harmonic simulation.



## Raritan River

The profile comparison of the model to the observed NOAA times of high and low waters relative to the time of high water at Sandy Hook through the harbor and up the Raritan River (locations shown in Figure 110) is presented in Figure 111. The Raritan River stations are the last four points in the profile. The profile for the tide range up the Raritan River is presented in Figure 112. The tidal propagation up the Raritan River is in good agreement both in tidal phases and in tide range with the exception of the extreme upstream at New Brunswick, where the model tides slow down and drop in tide range.

Figure 110. Raritan Bay/River analysis locations.



Figure 111. Tidal propagation for the times of high and low waters from Sandy Hook through Raritan Bay and up the Raritan River for the low-flow tidal harmonic simulation.

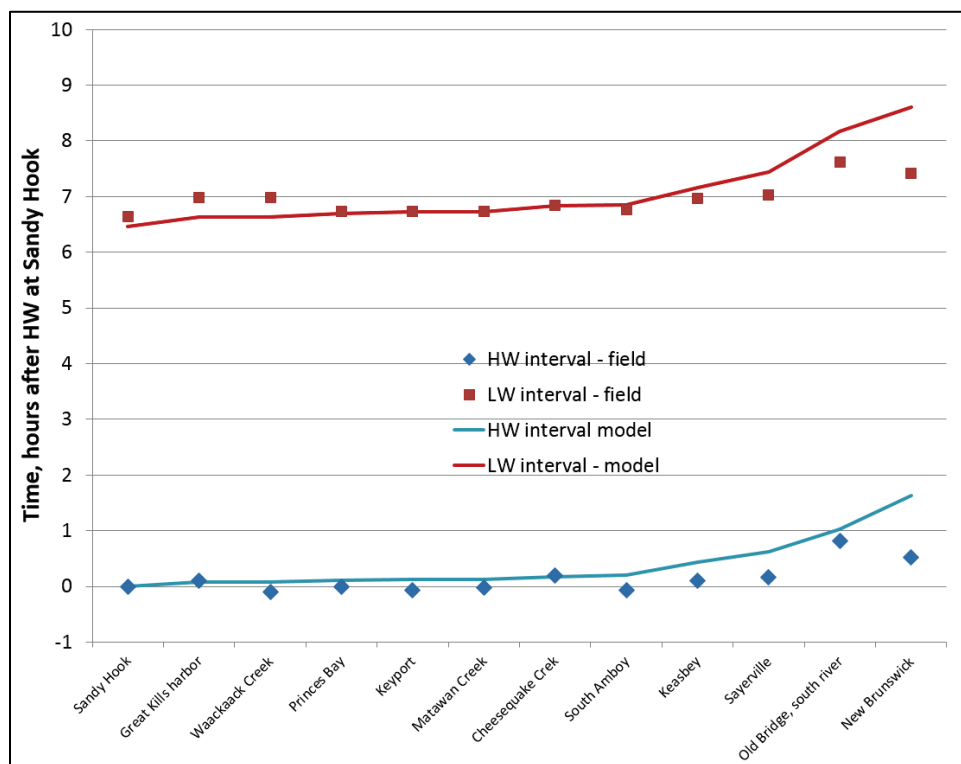
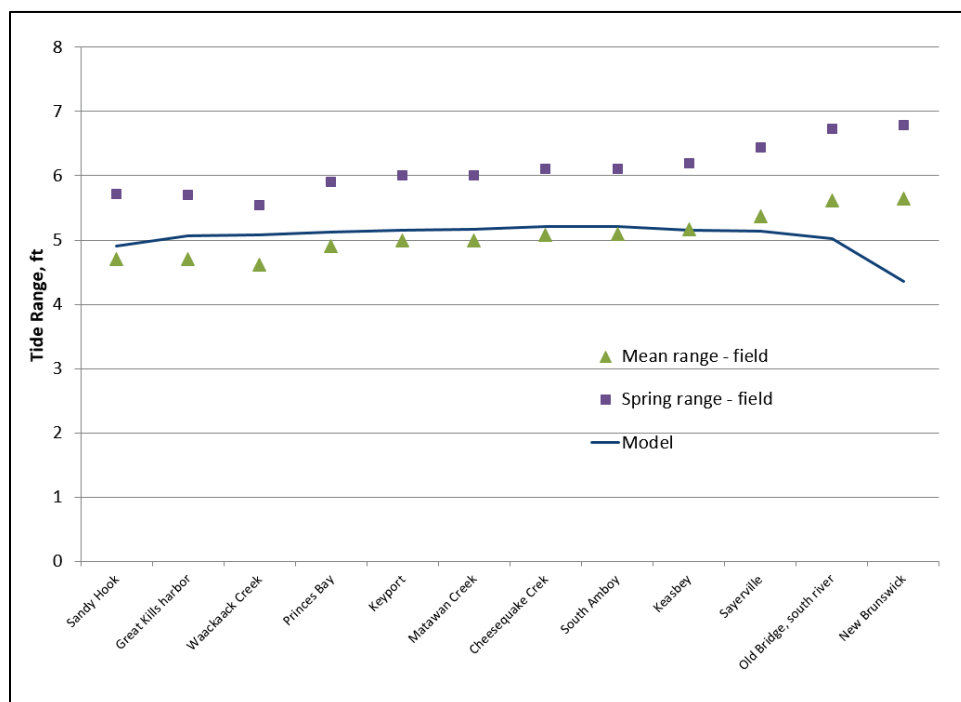


Figure 112. Tide range profile from Sandy Hook through Raritan Bay and up the Raritan River for the low-flow tidal harmonic simulation.



### **Conclusion for tidal harmonic verification**

The general characteristics of the tidal propagation in the 2D version of AdH adequately replicate the NOAA data to warrant proceeding to the 3D model development.

### **Three-dimensional (3D) hydrodynamic comparisons**

The 3D hydrodynamic comparisons consisted primarily of comparing the NOAA-observed water levels to the model results. As opposed to the previous section with 2D harmonic comparisons, this section details comparisons to observed data impacted by winds, pressure fields, inflows, and tidal conditions. All of these forcings were previously discussed in Chapter 4 and were included in the boundary conditions for these simulations.

### **Quantitative comparisons**

NOAA maintains several water level gauges within the model domain of this study. The gauges are shown in Figure 113. Time-series comparison plots (1 May to 1 June) and box plots for the entire 1995 year (black line is equality line) are provided in Figure 114 to Figure 123. Error metrics were computed for all five simulated years and are provided in Table 11. The error metric values reported in Table 11 are similar in magnitude to those reported in HydroQual (2008) and Blumberg et al. (1999).



Figure 113. Hydrodynamic validation locations.



Figure 114. Water surface elevation comparison plot for Atlantic City (1995).

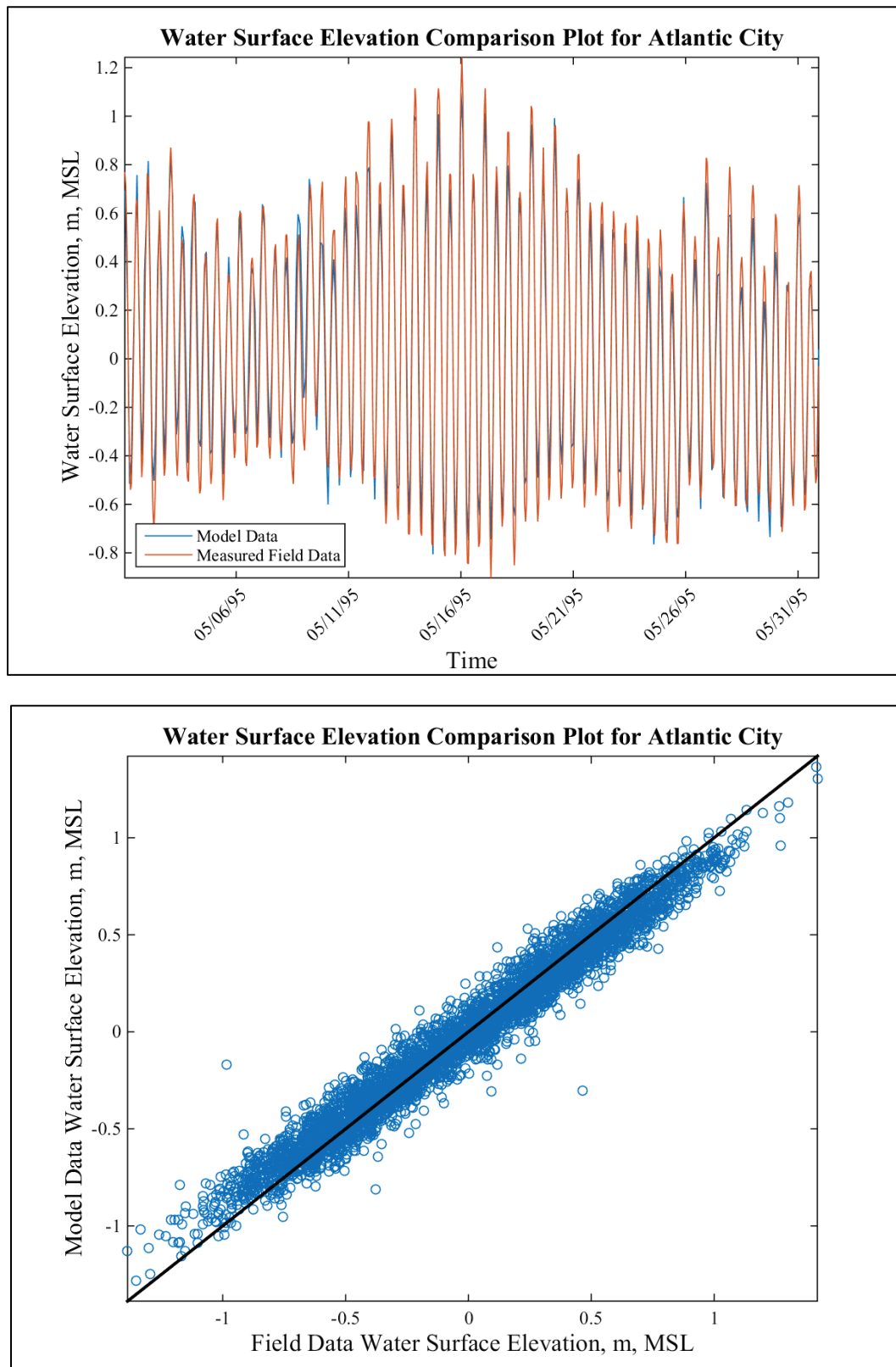


Figure 115. Water surface elevation comparison plot for Bergen Point (1995).

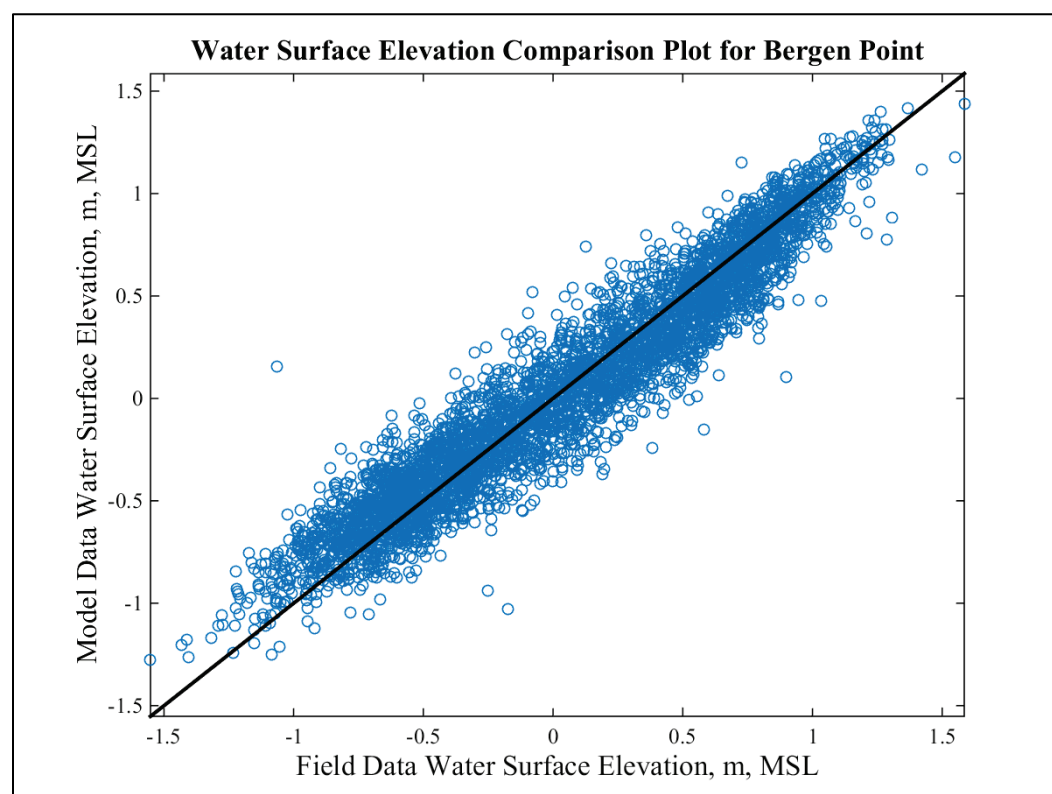
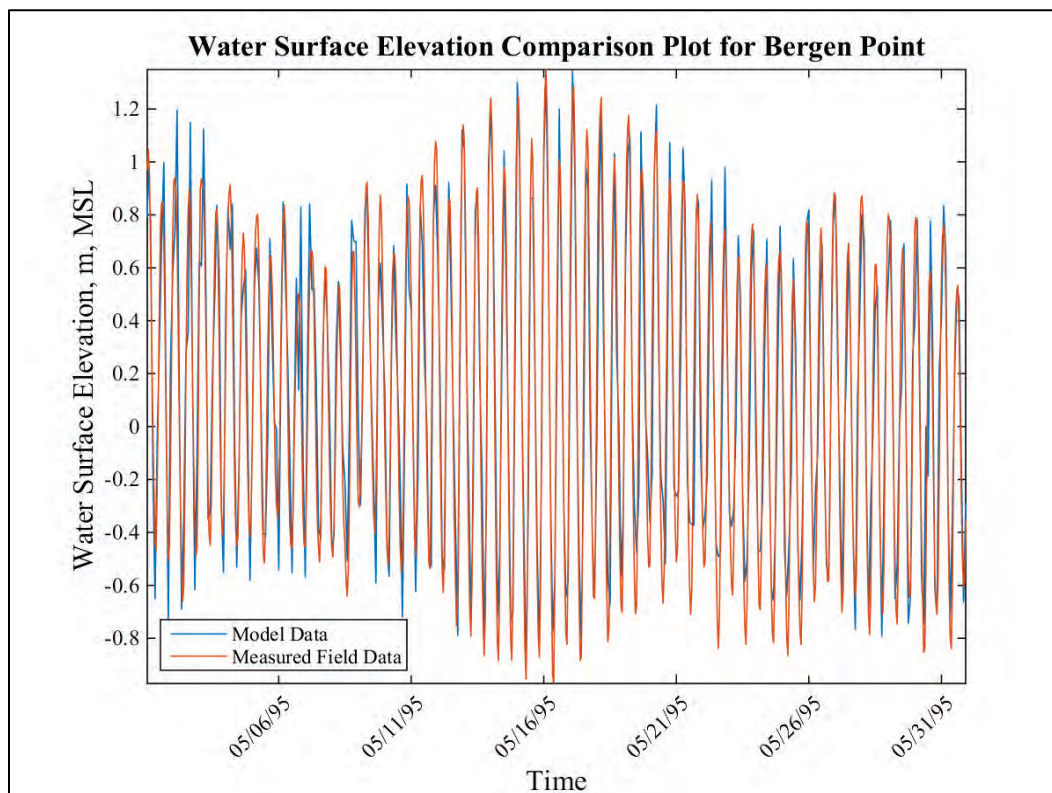


Figure 116. Water surface elevation comparison plot for Bridgeport (1995).

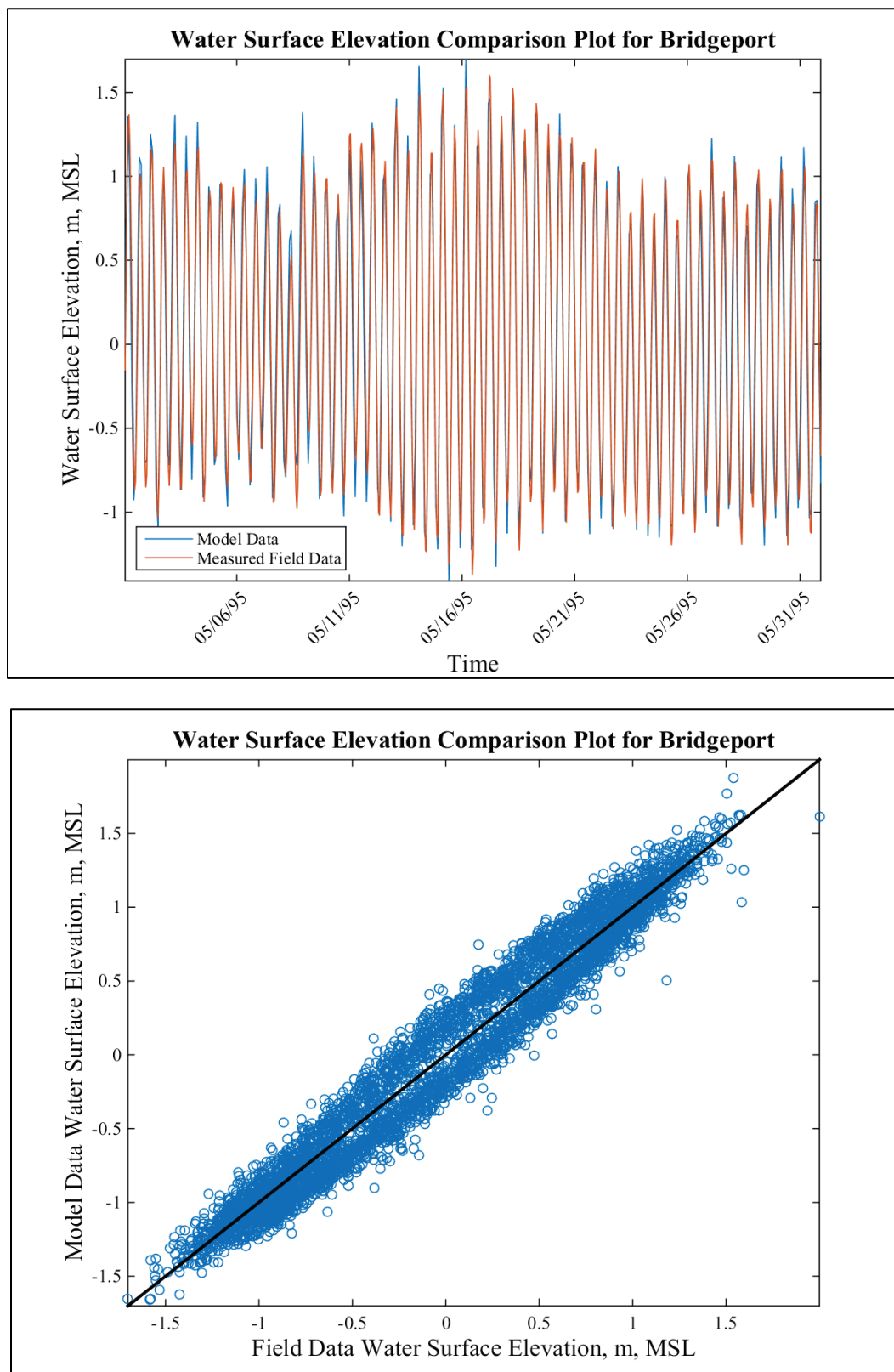


Figure 117. Water surface elevation comparison plot for Eatons Neck (1995).

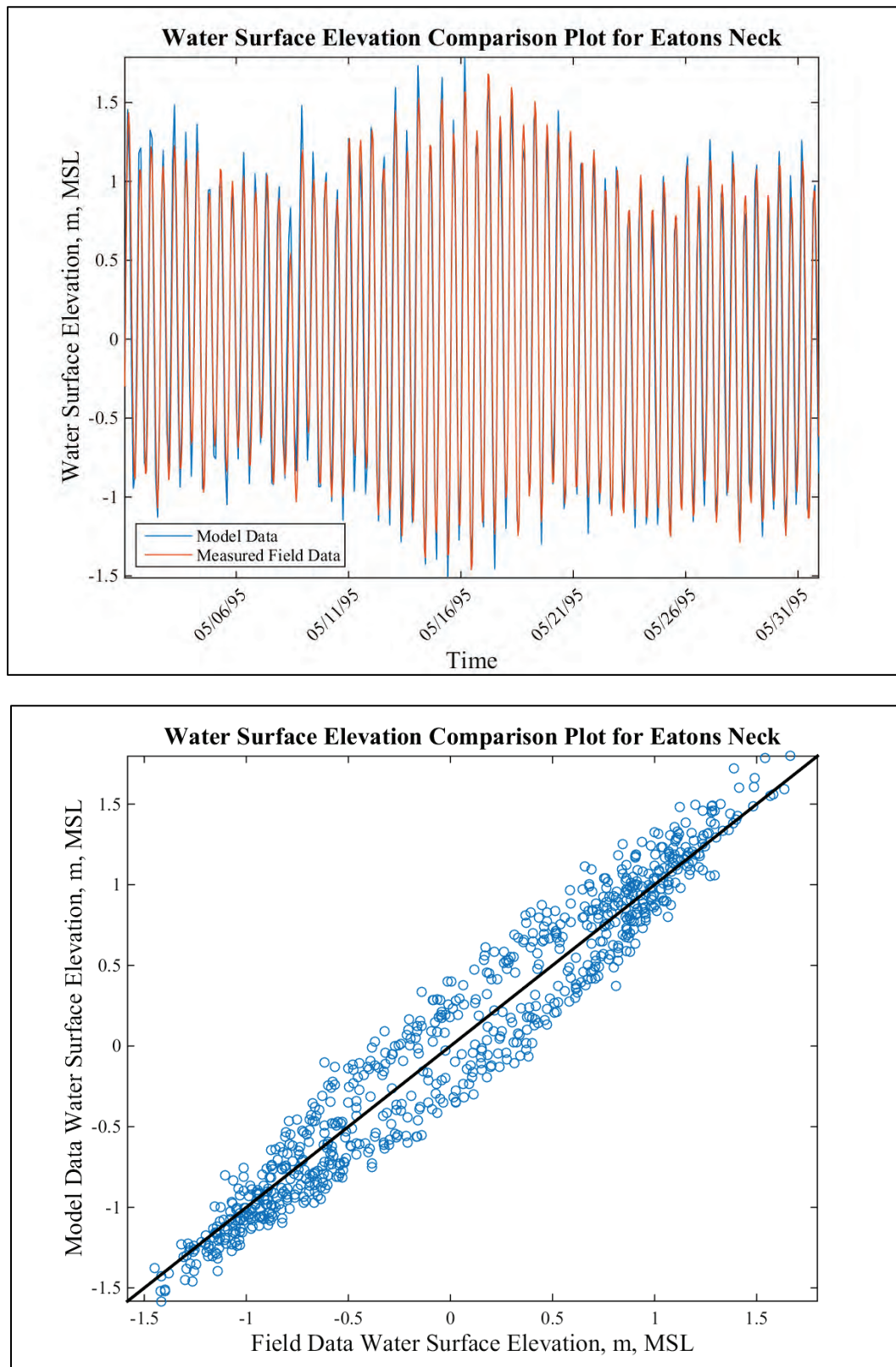




Figure 118. Water surface elevation comparison plot for Long Neck Point (1995).

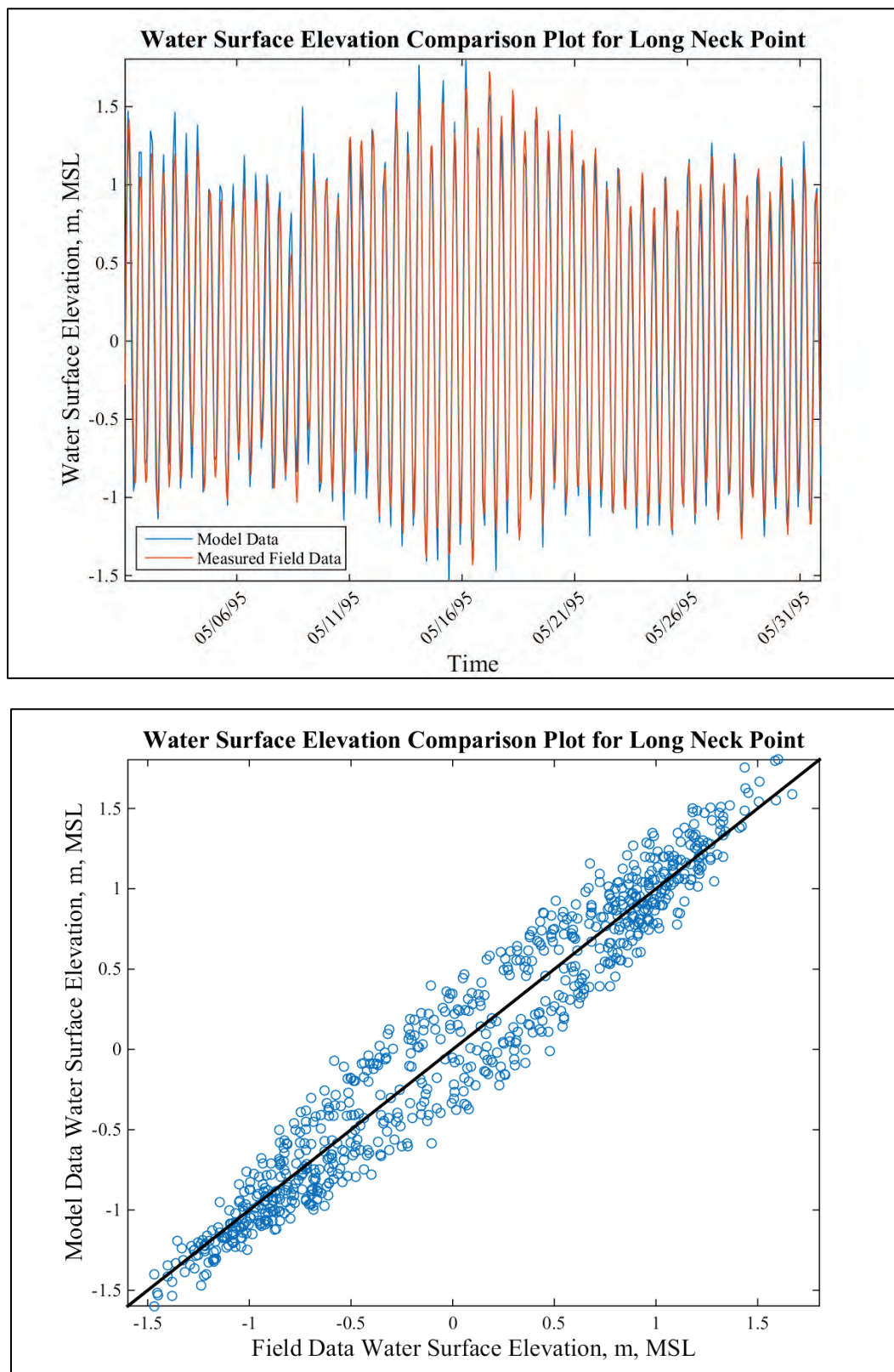




Figure 119. Water surface elevation comparison plot for Montauk (1995).

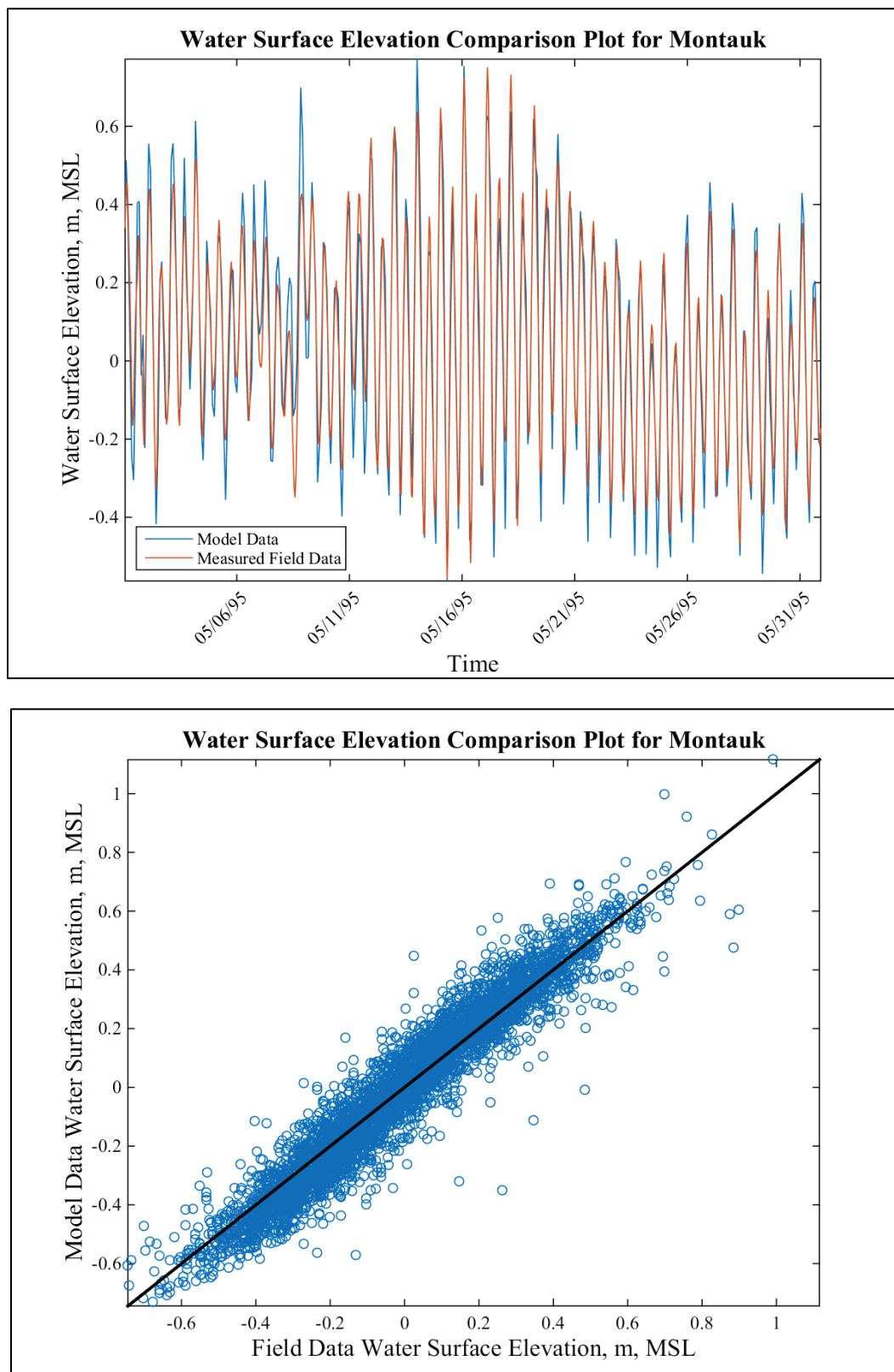


Figure 120. Water surface elevation comparison plot for New London (1995).

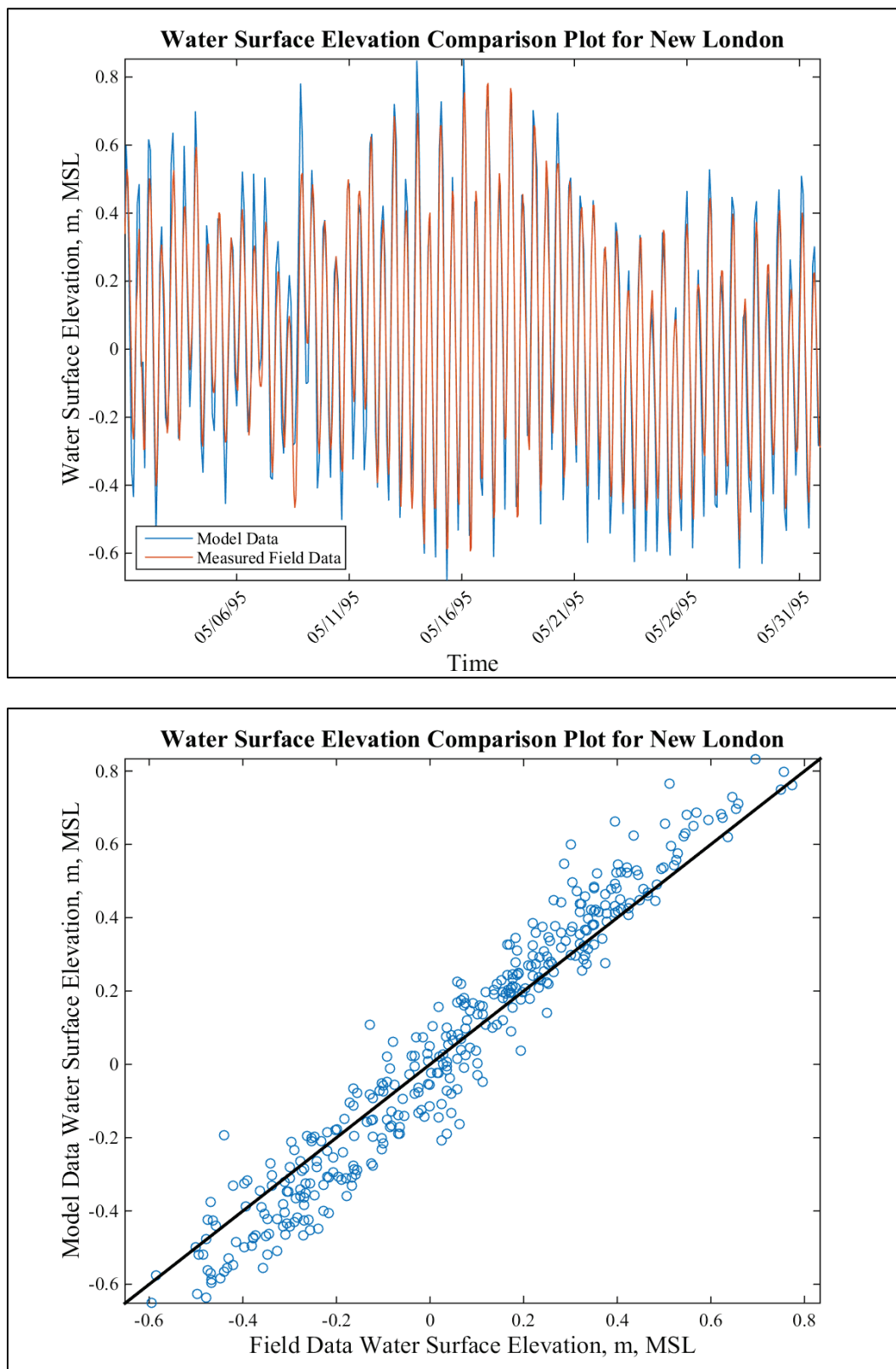


Figure 121. Water surface elevation comparison plot for Sandy Hook (1995).

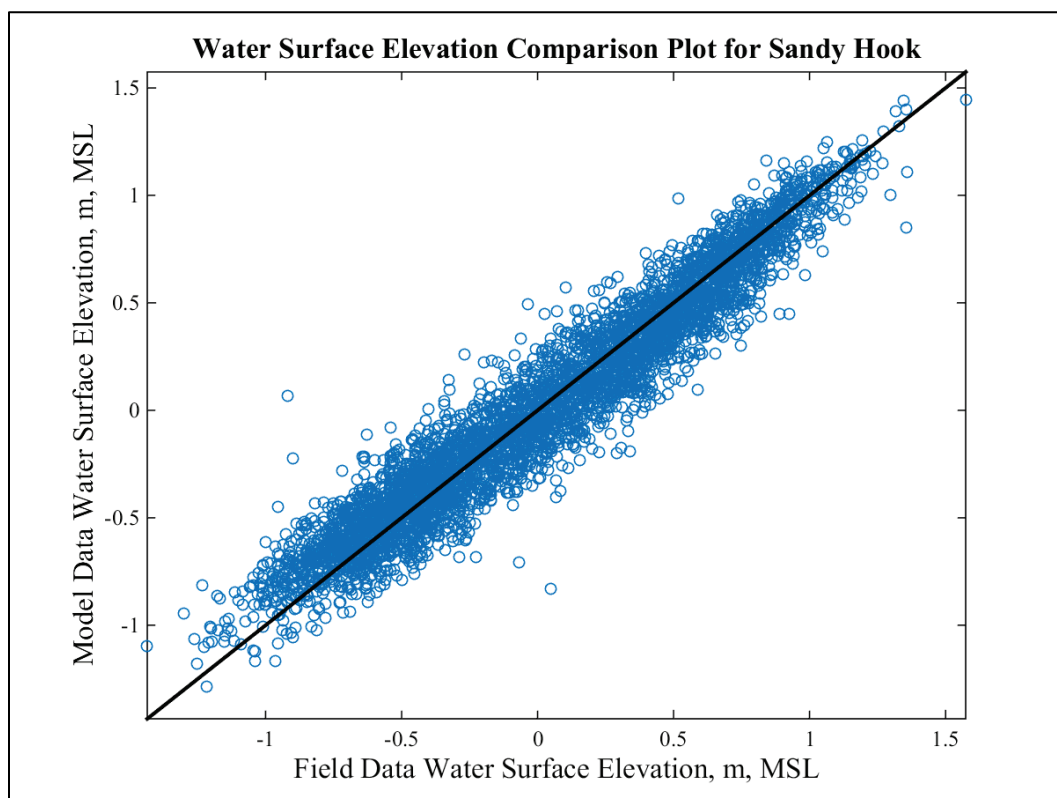
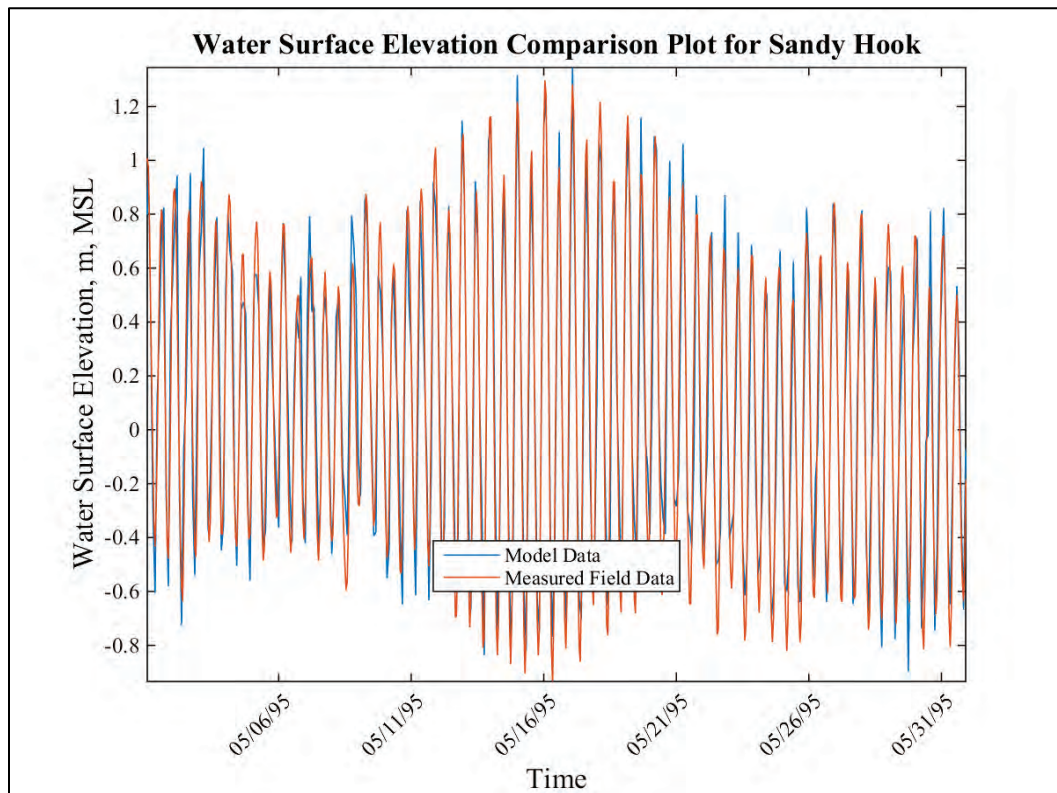


Figure 122. Water surface elevation comparison plot for The Battery (1995).

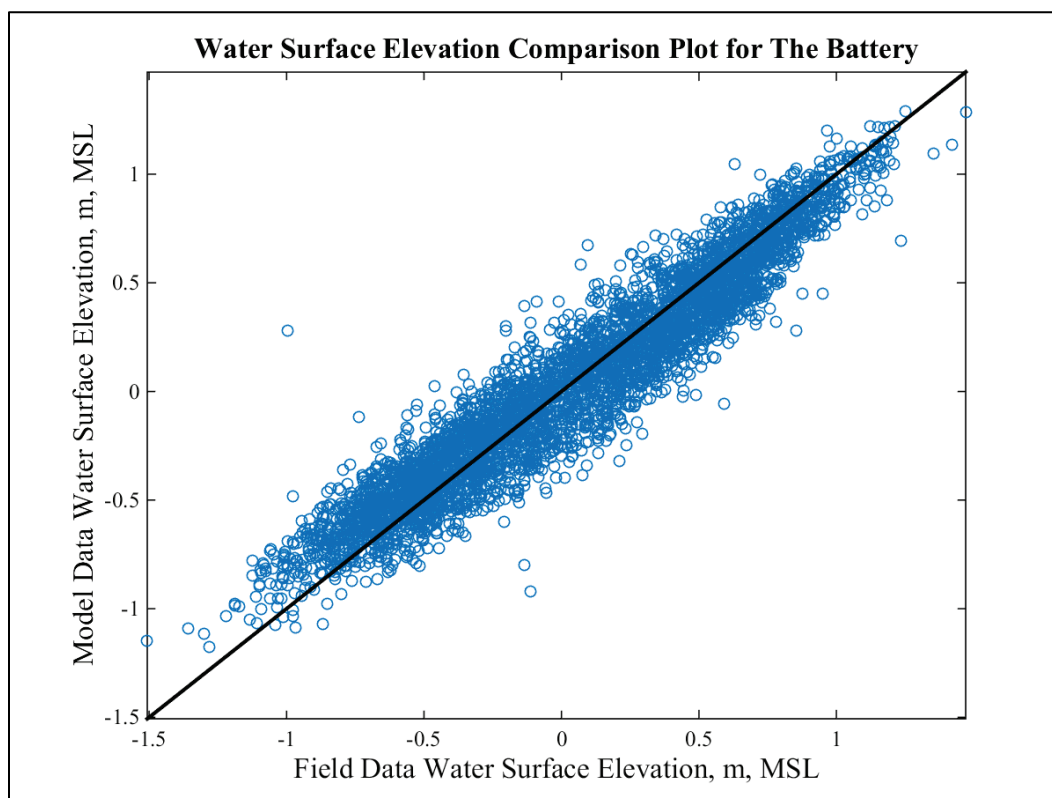
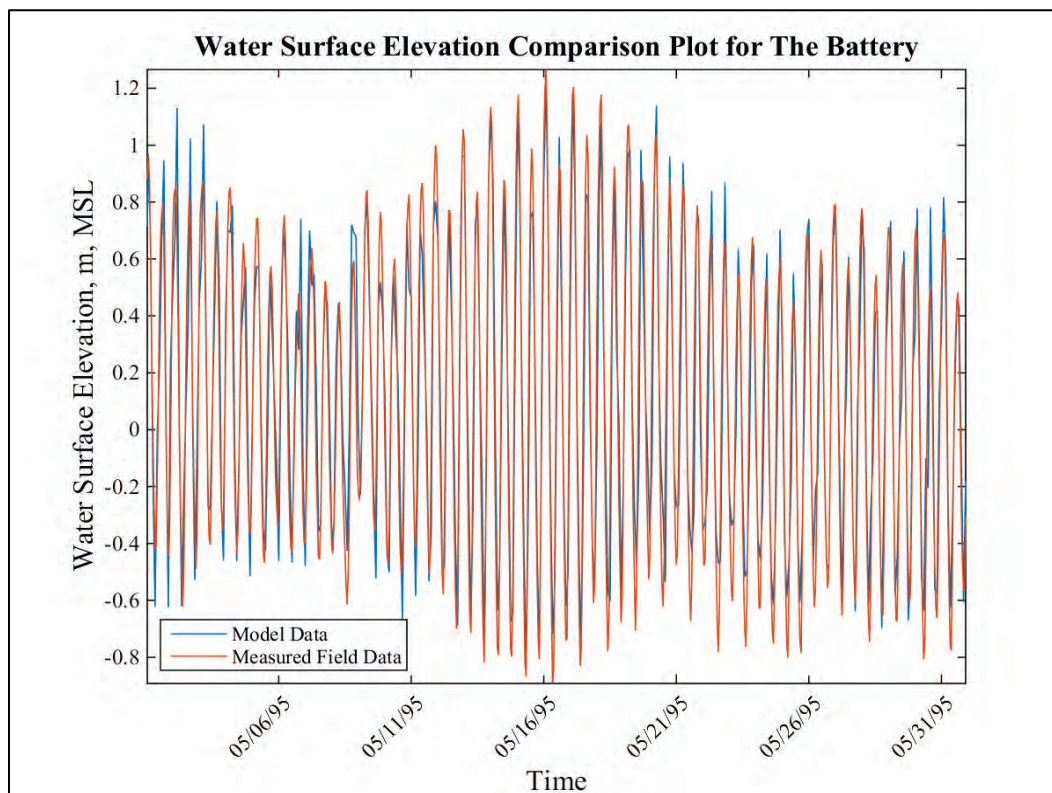


Figure 123. Water surface elevation comparison plot for Willets Point.

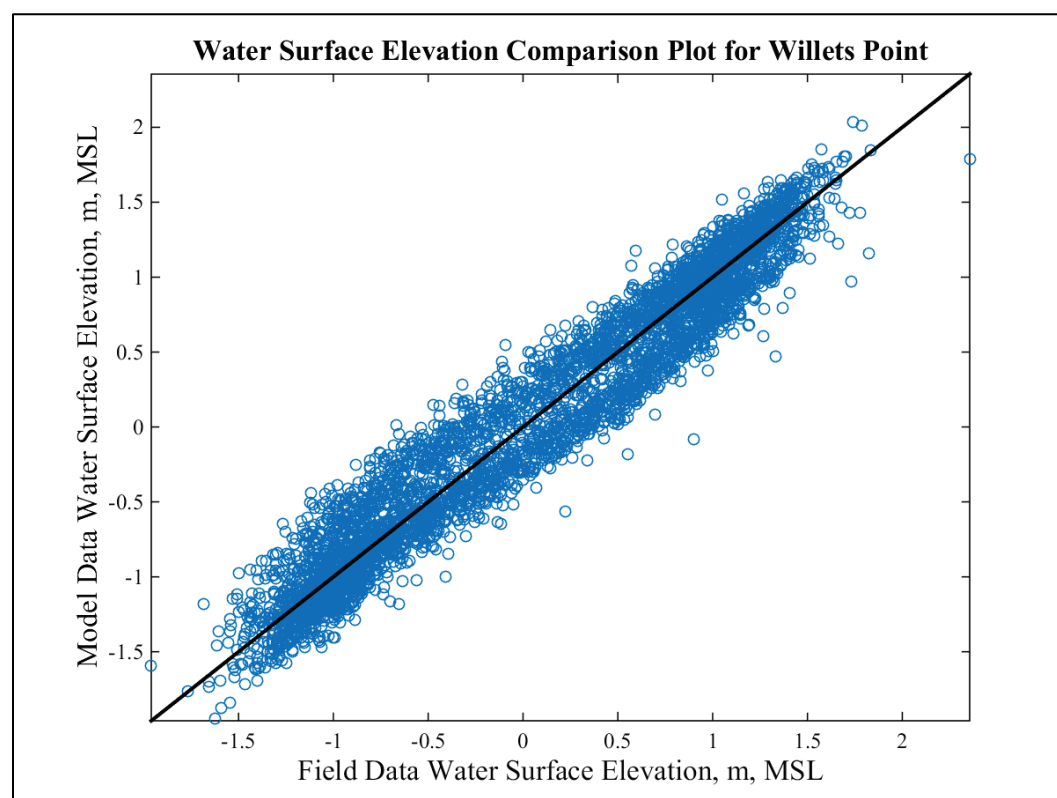
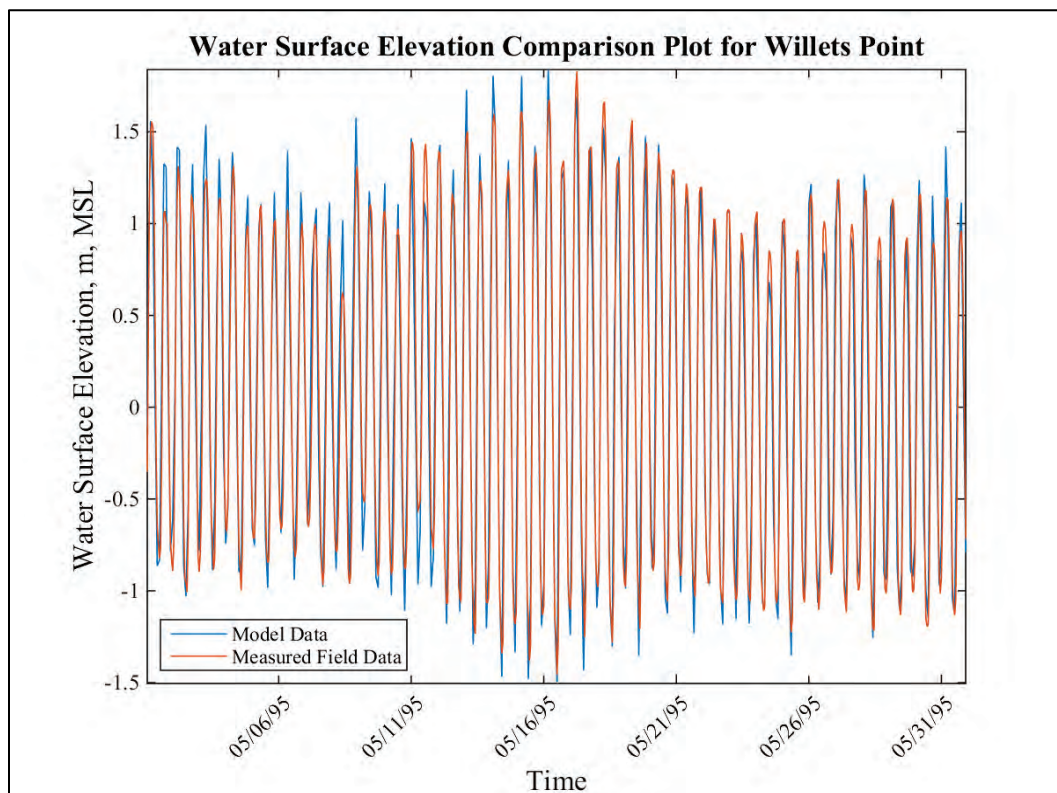




Table 11. Error metrics for water level comparisons.

Comparisons to NOAA observed water levels (1985, 1995, and 1996 were compared to the without-project and 2011 and 2012 were compared to the with-project configuration). N/A indicates data were not available for that particular year and location.															
NOAA Gauge	RMSE (m)					Correlation Coefficient					Nash-Sutcliffe Coefficient				
	1985	1995	1996	2011	2012	1985	1995	1996	2011	2012	1985	1995	1996	2011	2012
Atlantic City (Station 8534720)	0.11	0.10	0.09	0.08	0.08	0.98	0.98	0.98	0.99	0.99	0.95	0.96	0.97	0.97	0.97
Sandy Hook (Station 8531680)	0.16	0.15	0.16	0.14	0.14	0.96	0.96	0.96	0.96	0.97	0.91	0.93	0.92	0.93	0.94
Bergen Point (Station 8519483)	0.18	0.17	0.17	0.17	0.16	0.95	0.96	0.96	0.96	0.96	0.90	0.92	0.92	0.91	0.92
The Battery (Station 8518750)	0.17	0.16	0.16	0.16	0.15	0.95	0.96	0.96	0.96	0.96	0.90	0.91	0.91	0.91	0.92
Willeys Point (Station 8516990)	0.22	0.22	N/A	N/A	N/A	0.97	0.97	N/A	N/A	N/A	0.93	0.94	N/A	N/A	N/A
Eatons Neck (Station 8515786)	N/A	0.20	N/A	N/A	N/A	N/A	0.97	N/A	N/A	N/A	N/A	0.94	N/A	N/A	N/A
Long Neck Point (Station 8468799)	N/A	0.20	N/A	N/A	N/A	N/A	0.97	N/A	N/A	N/A	N/A	0.94	N/A	N/A	N/A
Bridgeport (Station 8467150)	0.17	0.17	0.18	0.16	0.16	0.97	0.98	0.97	0.98	0.98	0.94	0.95	0.94	0.95	0.95
Montauk (Station 8510560)	0.08	0.08	0.09	0.08	0.08	0.95	0.96	0.96	0.96	0.96	0.90	0.90	0.90	0.90	0.91
New London (Station 8461490)	0.11	0.09	N/A	0.09	0.09	0.95	0.97	N/A	0.97	0.97	0.87	0.92	N/A	0.91	0.92
Kings Point (Station 8516945)	N/A	N/A	N/A	0.21	0.22	N/A	N/A	N/A	0.97	0.97	N/A	N/A	N/A	0.94	0.94
New Haven (Station 8465705)	N/A	N/A	N/A	0.15	0.16	N/A	N/A	N/A	0.98	0.98	N/A	N/A	N/A	0.95	0.95



The water level comparisons show a phase difference between the model results and the observations in the Long Island Sound. This is consistent with the 2D analysis discussed in the preceding section and as such was not created in the conversion of the model from two to three dimensions.

### Qualitative comparisons

Qualitative comparisons of the 3D hydrodynamics consisted of comparing to velocity ranges reported in the literature in addition to net annual discharges for the Kill van Kull channel. Since either the raw data were unavailable and/or the data were for time periods not simulated, these are qualitative comparisons that should be viewed simply as a *general* agreement between observations in the field and model results. Exact comparisons should not be expected.

#### *Velocity point comparisons*

While velocity observations were not readily available to compare directly to the simulated time periods for quantitative comparisons, some velocity data are available in the literature for qualitative comparisons. Blumberg et al. (1999) reports velocity ranges for a variety of locations. Blumberg et al. (1999) does not provide the coordinate locations of these observations but does include a map of their locations. From Figure 5 in Blumberg et al. (1999), the approximate locations of the observations were determined, and the velocities in Table 12 compare the observations and the model results. Pecchioli et al. (2006) reported velocities for the Kill van Kull, Arthur Kill, and Newark Bay. Again, the exact locations are unknown, but the approximate locations are determined from Figure 2 in Pecchioli et al. (2006). The locations utilized for the model comparisons are shown in Figure 124.

Velocity point observations are impacted by several factors, and as such are difficult to replicate in a numerical model. Uncertainties in the forcing conditions, model parameters, and bathymetry can easily impact the velocities in the model to improve/worsen the comparisons. Given these uncertainties, these comparisons are only to provide an indication if the model is in general agreement with the approximate velocities reported in the literature.

Figure 124. Velocity comparison locations.



Table 12. Velocity comparisons in m/s. Parenthesis indicates with-project values.

Locations	Data Range	1985	1995	1996	2011	2012
College Point (Near Surface) <sup>1</sup>	1.79-1.87	1.59 (1.60)	1.63 (1.64)	1.61 (1.62)	1.66 (1.67)	1.76 (1.77)
College Point (Middepth) <sup>1</sup>	1.577-1.931	1.38 (1.39)	1.40 (1.41)	1.41 (1.42)	1.44 (1.45)	1.52 (1.52)
College Point (Near Bed) <sup>1</sup>	1.317-1.485	1.18 (1.20)	1.20 (1.19)	1.24 (1.26)	1.24 (1.24)	1.15 (1.20)
South Clason (Near Surface) <sup>1</sup>	1.437	1.53 (1.54)	1.53 (1.53)	1.59 (1.60)	1.62 (1.64)	1.60 (1.61)
South Clason (Middepth) <sup>1</sup>	1.723	1.24 (1.25)	1.25 (1.25)	1.27 (1.28)	1.28 (1.29)	1.26 (1.27)

Locations	Data Range	1985	1995	1996	2011	2012
South Clason (Near Bed) <sup>1</sup>	1.524	1.03 (1.07)	1.01 (1.02)	1.12 (1.10)	1.18 (1.21)	1.25 (1.15)
Red Hook (Near Surface) <sup>1</sup>	3.739	2.85 (2.86)	2.89 (2.90)	2.98 (2.95)	3.01 (3.02)	2.99 (3.00)
Red Hook (Middepth) <sup>1</sup>	3.363	2.55 (2.55)	2.57 (2.58)	2.66 (2.66)	2.72 (2.72)	2.69 (2.70)
Red Hook (Near Bed) <sup>1</sup>	3.035	1.89 (1.88)	1.85 (1.84)	1.97 (2.03)	1.94 (1.96)	1.85 (1.90)
Harlem River (Near Surface) <sup>1</sup>	2.03	1.63 (1.63)	1.50 (1.53)	1.62 (1.60)	1.59 (1.59)	1.82 (1.82)
Harlem River (Middepth) <sup>1</sup>	1.97	1.66 (1.67)	1.50 (1.51)	1.60 (1.60)	1.61 (1.62)	1.74 (1.74)
Harlem River (Near Bed) <sup>1</sup>	1.761	1.28 (1.29)	1.25 (1.26)	1.27 (1.28)	1.35 (1.36)	1.29 (1.30)
Upper Bay (Near Bed) <sup>1</sup>	1.169	0.77 (0.71)	0.73 (0.69)	0.76 (0.69)	0.76 (0.69)	0.77 (0.77)
The Battery (Near Bed) <sup>1</sup>	0.953	0.81 (0.81)	0.78 (0.77)	0.74 (0.74)	0.81 (0.80)	0.75 (0.76)
Weehawken (Near Bed) <sup>1</sup>	1.139	1.05 (1.06)	1.02 (1.04)	1.12 (1.12)	1.15 (1.14)	1.16 (1.16)
Spuyten Duyvil (Near Bed) <sup>1</sup>	1.363	0.93 (0.94)	0.93 (0.94)	0.97 (0.99)	0.91 (0.91)	0.95 (0.96)
Kill van Kull <sup>2</sup>	>0.70	2.15 (2.02)	2.21 (2.09)	3.08 (3.00)	1.91 (1.88)	2.03 (1.93)
Newark Bay 1 <sup>2</sup>	<0.5	1.21 (1.26)	1.39 (1.40)	1.15 (1.18)	1.39 (1.38)	1.20 (1.20)
Newark Bay 2 <sup>2</sup>	<0.5	1.04 (1.02)	1.09 (1.05)	1.06 (1.05)	0.95 (0.97)	1.19 (1.11)
Arthur Kill <sup>2</sup>	0.55-0.60	0.89 (0.91)	1.03 (1.07)	1.12 (1.18)	0.89 (0.99)	0.78 (0.78)

<sup>1</sup>Blumberg et al. (1999)<sup>2</sup>Pecchioli et al. (2006)

Pecchioli et al. (2006) did not specify if the currents were surface, bottom, or depth averaged. The model results presented in Table 12 are surface, and as such are expected to be higher than those reported by Pecchioli et al. (2006).

While the model velocities are in general slightly below the values reported in Blumberg et al. (1999), they are not significantly lower and could easily be due to variations in the bathymetry, frictional specification, and/or boundary forcings between the observational time periods and the time periods simulated in this study. These comparisons indicate the velocities in the model are reasonable in comparison to the values reported in the literature.

#### *Kill van Kull discharge comparisons*

Blumberg et al. (1999) and Sommerfield and Chant (2010) report average flowrates through the Kill van Kull channel. These observations were over a limited amount of time (not included in the model simulated times) and utilized to report approximate yearly average flowrates. Therefore, a model yearly average flowrate for the Kill van Kull was calculated and compared to the values reported in the literature. Blumberg et al. (1999) reported a mean water flux of 95 cms and Sommerfield and Chant (2010) reported a mean water flux of 120 cms. Blumberg et al. (1999) should equate closer to the without-project conditions, and Sommerfield and Chant (2010) is between the start and finish of the with-project expansion. The model results for the simulated years are presented in Table 13. These results indicate the model may be somewhat overpredicting the net flow through the Kill van Kull by approximately 30 cms for the without-project configuration and approximately 50 cms for the with-project configuration. The model appears to be relatively accurate in predicting the percent change between the with- and without-project flowrates with the field indicating an increase of approximately 26% and the model indicating an increase of approximately 36%.

Table 13. Kill van Kull flow comparisons.

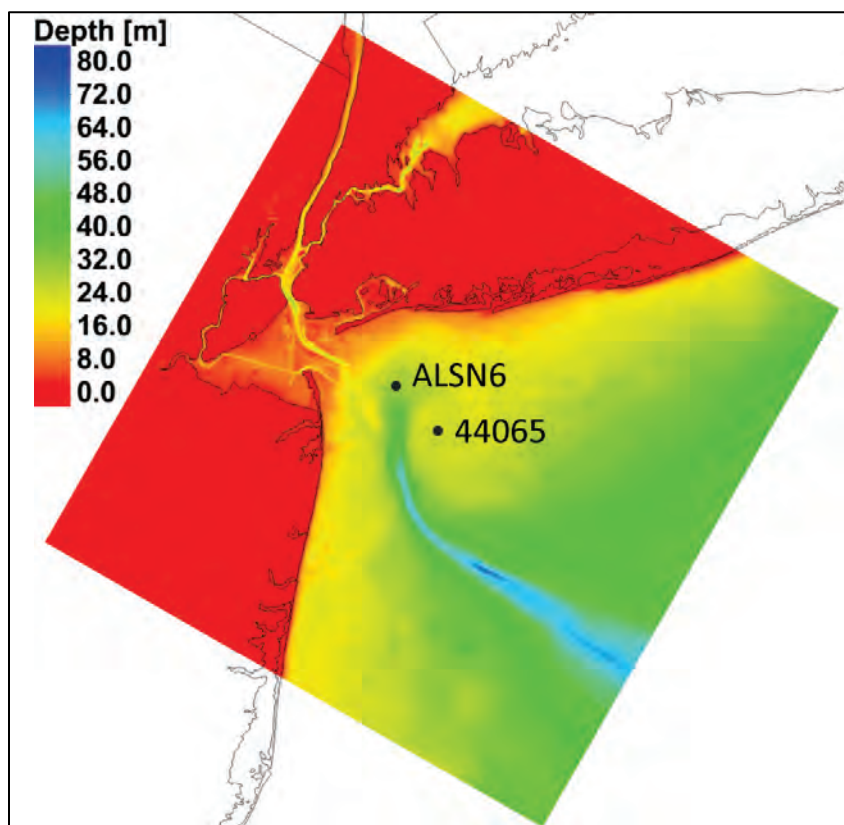
Blumberg et al. (1999) – 95 cms Sommerfield and Chant (2010) - 120 cms		
Year	Without-project average flow, cms compare to 95 cms	With-project average flow, cms compare to 120 cms
1985	122	162
1995	115	154
1996	123	170
2011	125	177
2012	129	170

## Wave model validation

The accuracy of the STWAVE model results is influenced by forcing parameters (e.g., wind, water levels, and offshore spectra), representation of the geographic area (e.g., bathymetry and bottom roughness), and inherent model physics and assumptions. Comparisons between measurements and model results were undertaken to assess the STWAVE model performance in replicating the nearshore wave climate of the study area.

Only two nearshore buoys were found within the STWAVE domain, ALSN6 at the Ambrose Light Tower in New York and NDBC 44065 at the approach to New York Harbor. ALSN6 is located at 40.45°N, 73.80°W, and NDBC 44065 is located at 40.369°N and 73.703°W. The locations of these buoys are shown in Figure 125. Measurements are available at ALSN6 for 1995 and 1996 and at NDBC 44065 for 2011 and 2012.

Figure 125. Location of ALSN6 and NDBC 44065.



STWAVE results were compared to measurements both graphically and statistically. Graphical products included time-paired histories and scatter plots. Statistical calculations included bias (modeled – measured), root-mean-square error (RMSE), and linear regression (slope and correlation coefficient) (Bryant et al. 2016).

Figure 126 compares time series of measured and modeled significant wave height ( $H_s$  or  $H_{mo}$ ), peak wave period ( $T_p$ ), and mean wave period from 1 January 1995 00:00 to 31 December 1995 22:00. ALSN6 did not collect data from 17 February 18:00 until 03 August 15:00. The largest waves of the year occurred on 12 November and exceeded 4 m. The average significant wave height was 1.03 m, the average peak period was 8.08 s, and the average mean period was 6.9 s for 1995. Although STWAVE underestimates larger wave heights near the beginning of February and mid-November, the evolution of the significant wave height, peak wave period, and mean wave period is estimated reasonably well throughout the year.



Figure 126. Time series of STWAVE results versus measurements at ALSN6 for 1995.

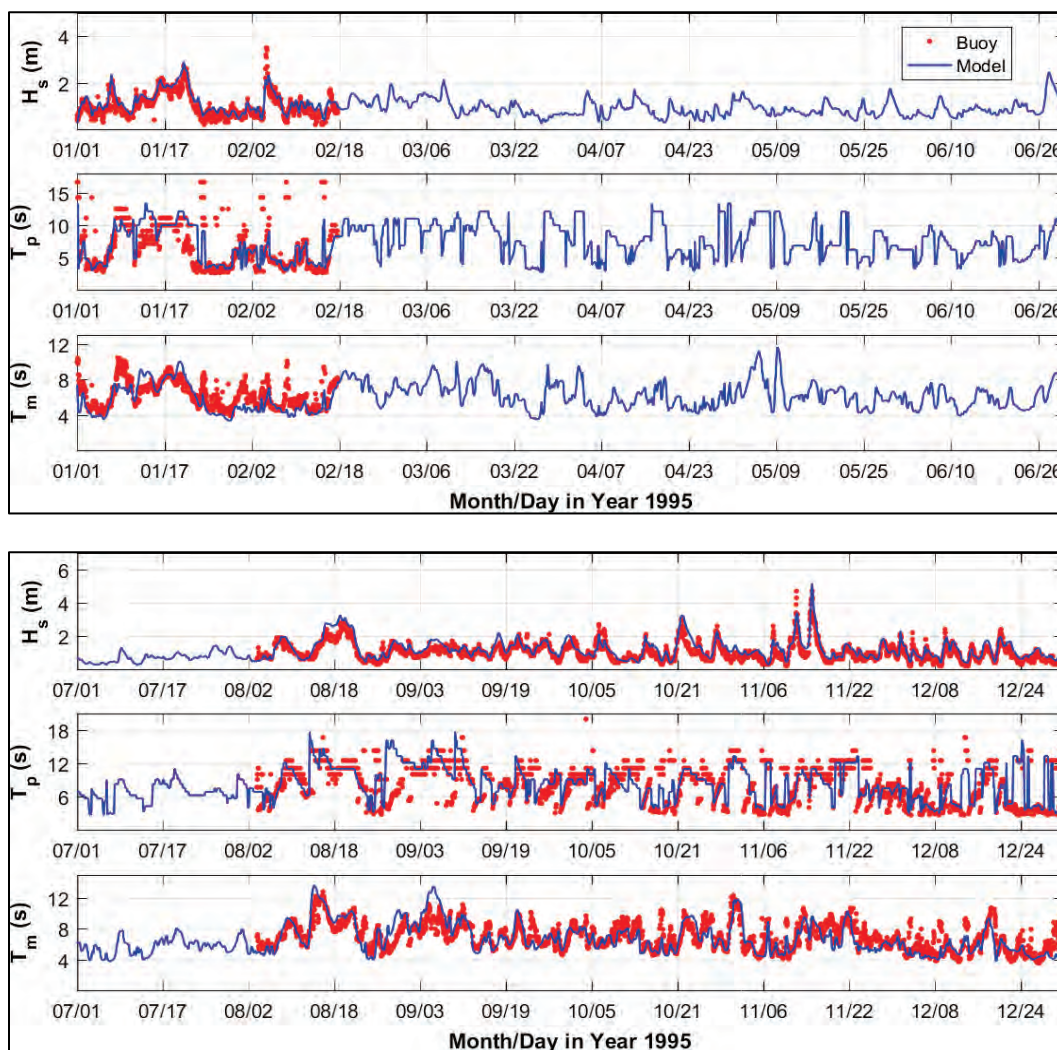


Figure 127 presents scatter plots of time-paired observed and modeled significant wave height and mean period for 1995. The blue line is a 1-to-1 line of equality plotted for visualization purposes. As observations of peak period  $T_p$  are highly variable and model results are limited to defined wave frequency bins, mean period  $T_m$  is considered a more stable parameter for comparison. The number of paired observations for 1995 was 1,291. Looking at the upper panel, there is clear binning of the wave height data. This binning is due to the resolution of the measurements being limited to one significant digit. Most of the wave height population was less than 2.5 m. STWAVE systematically overestimated wave heights at ALSN6 for 1995 as indicated by the distribution of data above the line of the best of fit and the positive bias of 0.19 m. The RMSE and Scatter Index (SI) with respect to wave height were 0.27 m and 26, respectively. A correlation of 0.89 indicates STWAVE demonstrated good association with wave height

observations. Based on the regression analysis, STWAVE showed an average positive error of 16% with respect to significant wave height. Unlike significant wave height, STWAVE underestimated the mean wave period as indicated by the distribution of scatter, a negative bias of -0.28 s, and a regression slope (Sym r) of 0.97. The RMSE with respect to mean wave period was 1.4 s. STWAVE demonstrated greater association with wave height than mean wave period; the correlation for mean wave period was 0.75, lower than that for wave height.

Figure 127. Scatter plots for 1995 of significant wave height (top) and mean period (bottom).

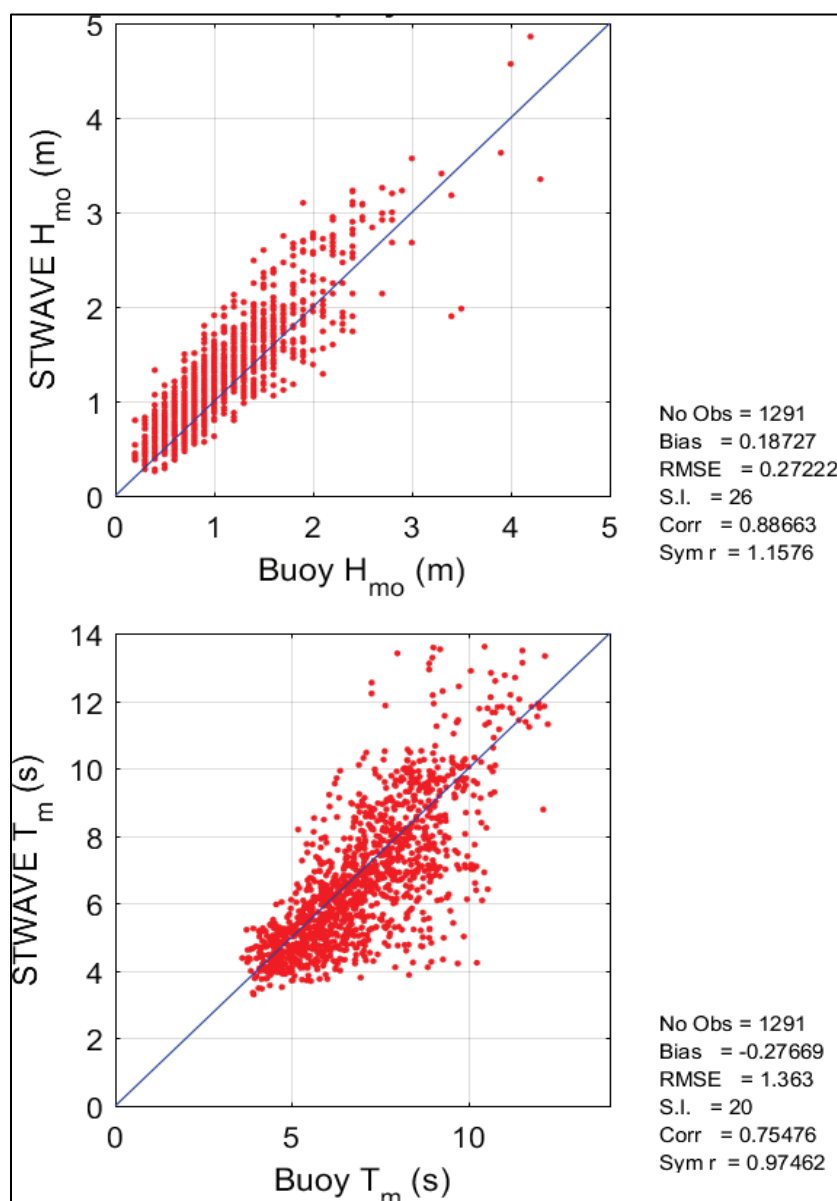


Figure 128 presents time series of measured and modeled significant wave height, peak wave period, and mean wave period from 1 January 1996 00:00 to 31 December 1996 22:00 for ALSN6. The largest wave height of approximately 5.0 m occurred on 8 January, which corresponds with the Blizzard of '96. The average significant wave height, peak period, and mean wave period measured by ALSN6 for 1996 is 0.96 m, 8.27 s, and 7.03 s, respectively. The model results follow the evolution of the wave observations well, particularly for significant wave height and mean period.

Figure 128. Time series of STWAVE results versus measurements at ALSN6 for 1996.

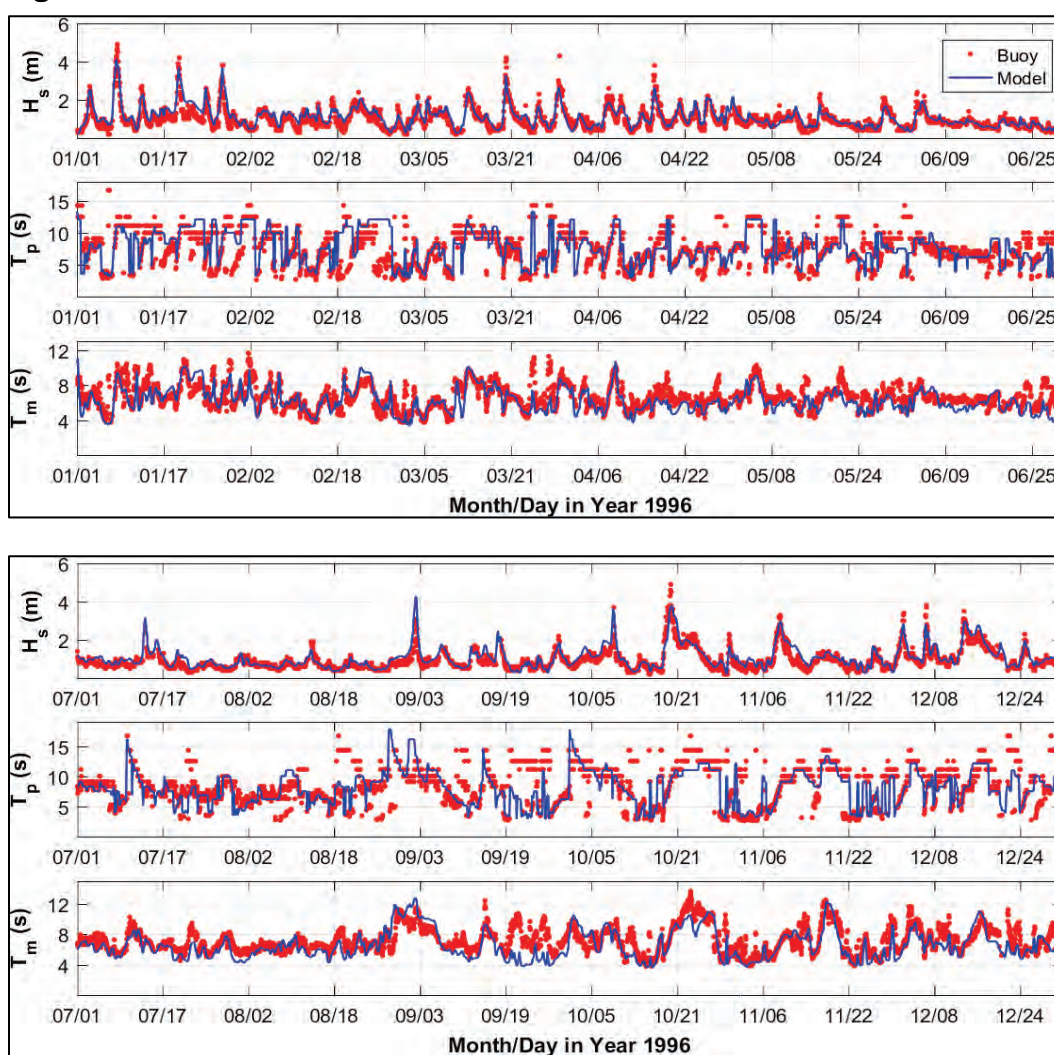


Figure 129 shows a scatter plot of time-paired measurements and models results for ALSN6 for 1996. The total number of paired observations was 2,337. The trends and statistics for 1996 are similar to those of 1995. STWAVE systematically overestimated the significant wave height (bias of 0.12 m, regression slope of 1.09) and systematically underestimated the

mean wave period (bias of -0.51 s, regression slope of 0.94). The RMSE errors for significant wave height (0.25 m) and mean wave period (1.26 s) are also similar to 1995. Again, STWAVE results were better associated with respect to wave height (correlation of 0.90) compared to mean wave period (correlation of 0.71).

Figure 129. Scatter plots for 1996 of significant wave height (top) and mean period (bottom).

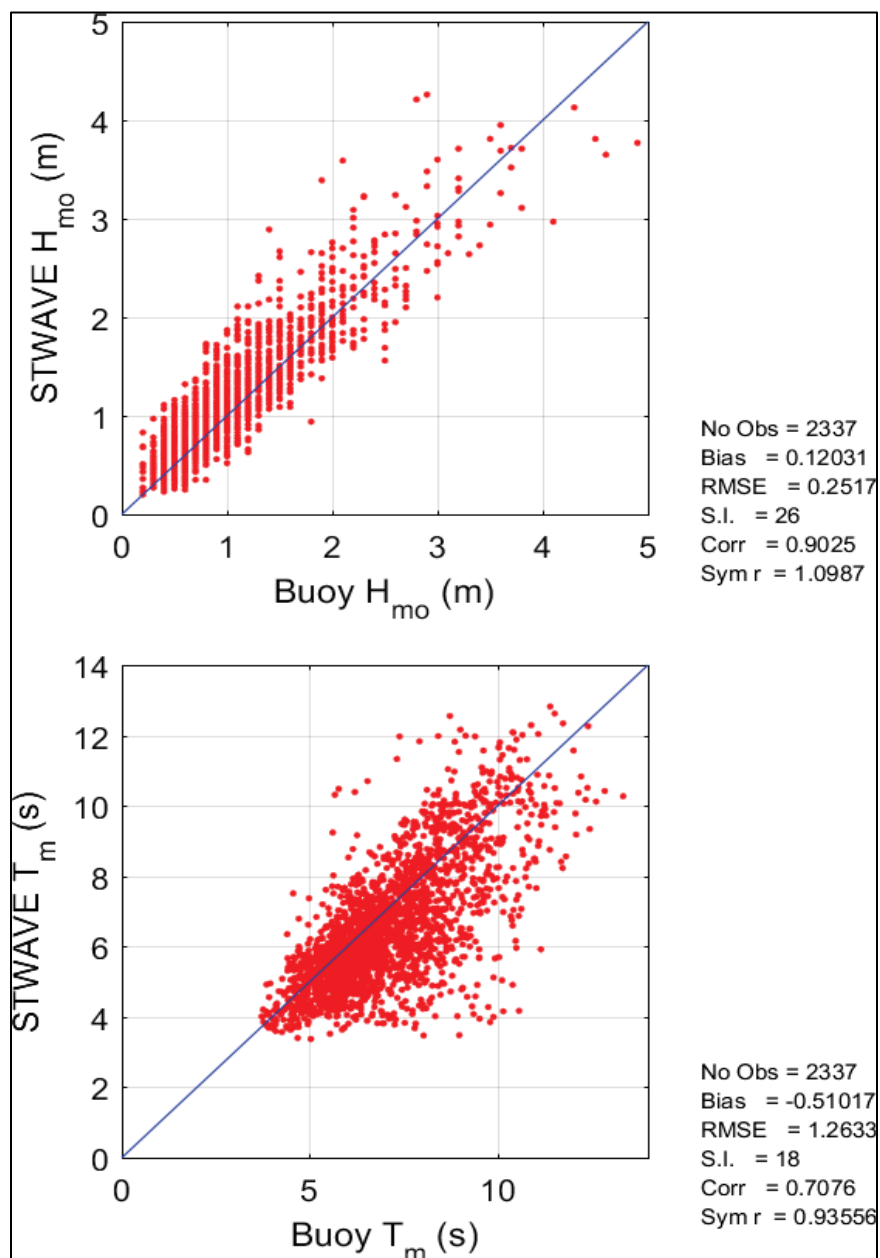




Figure 130 presents time series of measured and modeled significant wave height, peak wave period, mean wave period, and mean wave direction ( $\theta_{\text{wave}}$ ) from 1 January 2011 00:00 to 31 December 2011 22:00. The largest waves of the year were measured during Hurricane Irene on 28 August and exceeded 5 m. NDBC 44065 failed to collect data between 5 September and 8 October. For 2011, the average significant wave height was 1.0 m, the average peak period was 7.5 s, and the average mean wave period was 6.2 s. In general, STWAVE demonstrates good agreement with measured integral wave parameters throughout the year.

Figure 130. Time series of STWAVE results versus measurements at NDBC 44065 for 2011.

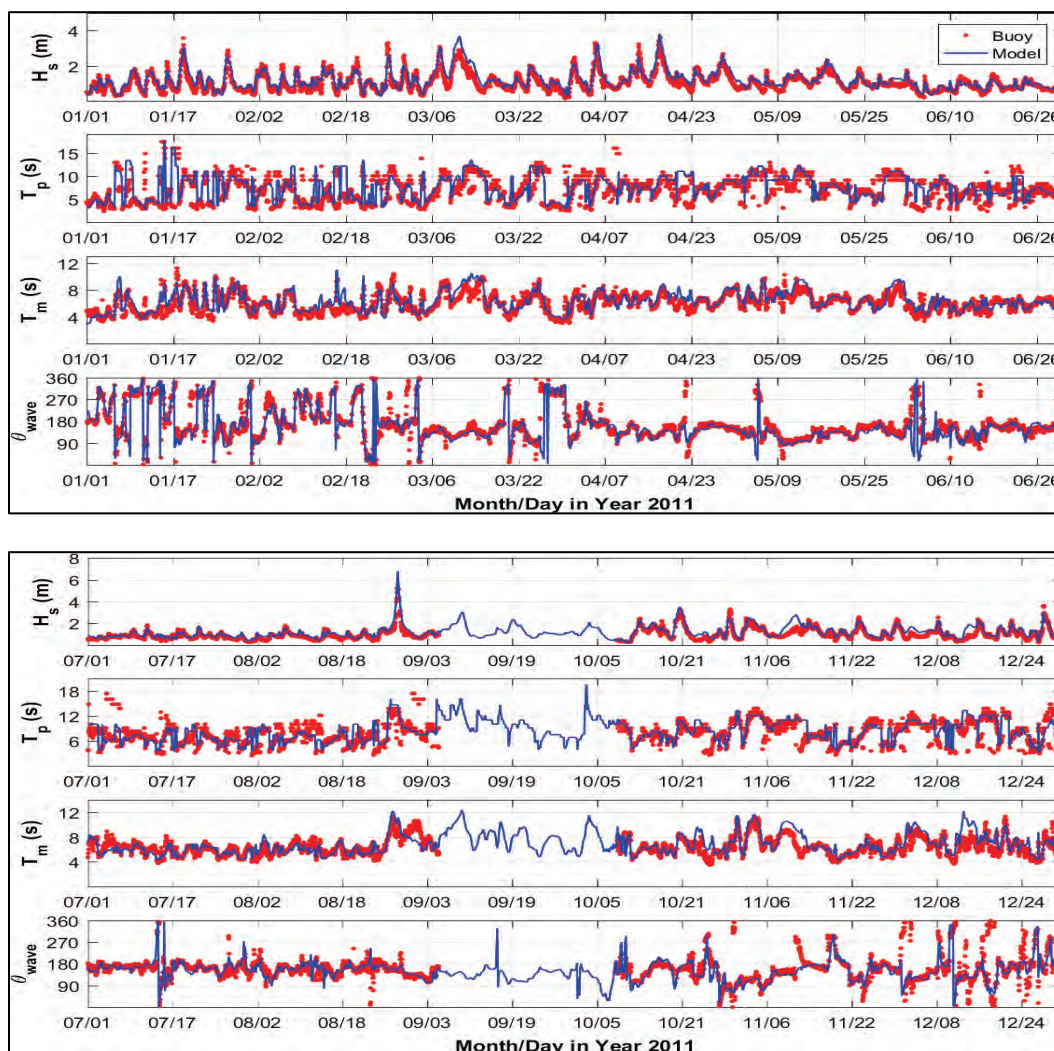


Figure 131 presents scatter plots of time-paired measured and modeled significant wave height and mean period for 2011. The total number of records compared for 2011 was 2,616. Looking at the upper panel, more scatter lies above the line of best fit than below, indicating a model trend of overestimating significant wave heights. This is supported by the slightly positive bias of 0.17 m. There is a noticeable overestimation of the largest wave heights associated with Hurricane Irene. The RMSE was 0.24 m and the SI was 24 for 2011. The correlation coefficient was about 0.90, and the symmetric slope indicated an average positive error of 14% in modeled significant wave height. Compared to significant wave height, the scatter for mean wave period is more equally distributed above and below the line of best fit. The bias and RMSE for mean period was approximately 0.25 s and 1.0 s, respectively. The correlation coefficient was 0.78, lower than that for the significant wave height, with an average positive error of 4% in modeled mean wave period with respect to measured mean wave period.

Figure 131. Scatter plots for 2011 of significant wave height (top) and mean period (bottom).

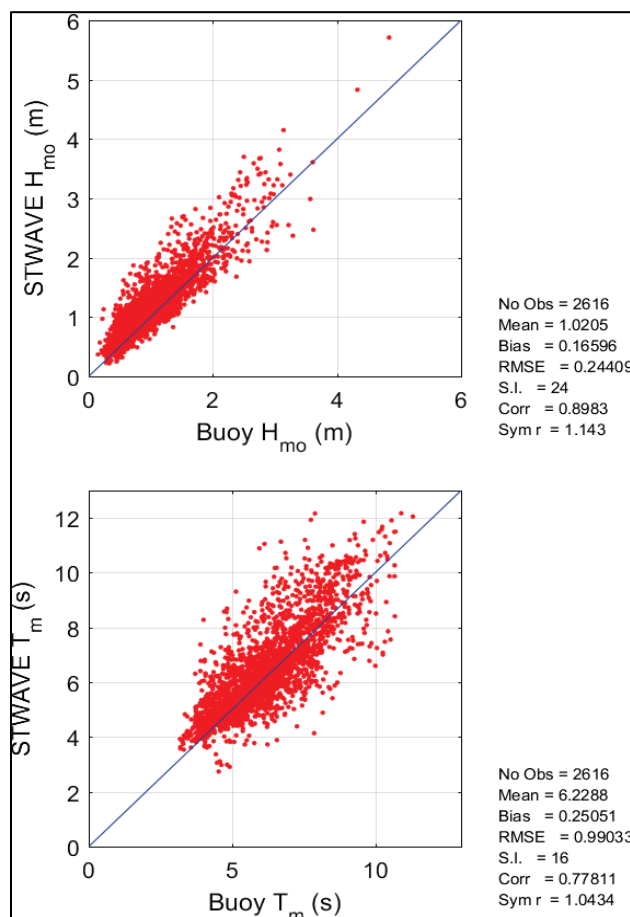
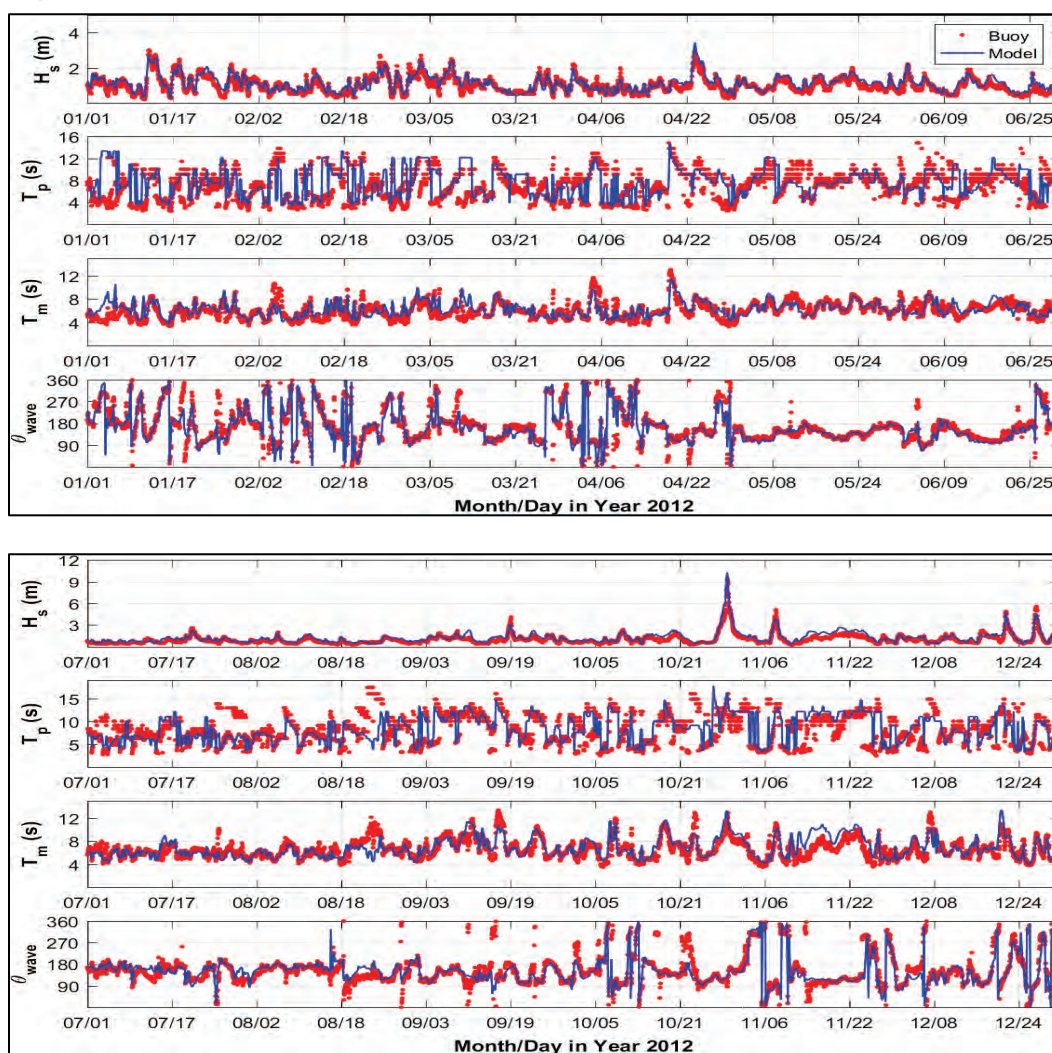




Figure 132 presents time series of modeled and measured significant wave height, peak wave period, mean wave period, and mean wave direction from 1 January 2012 00:00 to 31 December 2012 22:00. The largest waves of the year were associated with Hurricane Sandy and exceeded 9 m on 29 October. For 2012, the average significant wave height was 1.0 m, the average peak period was 7.6 s, and the average mean wave period was 6.3 s. Again, STWAVE adequately replicates the wave climate at NDBC 44065 for 2012 for the purposes of this study.

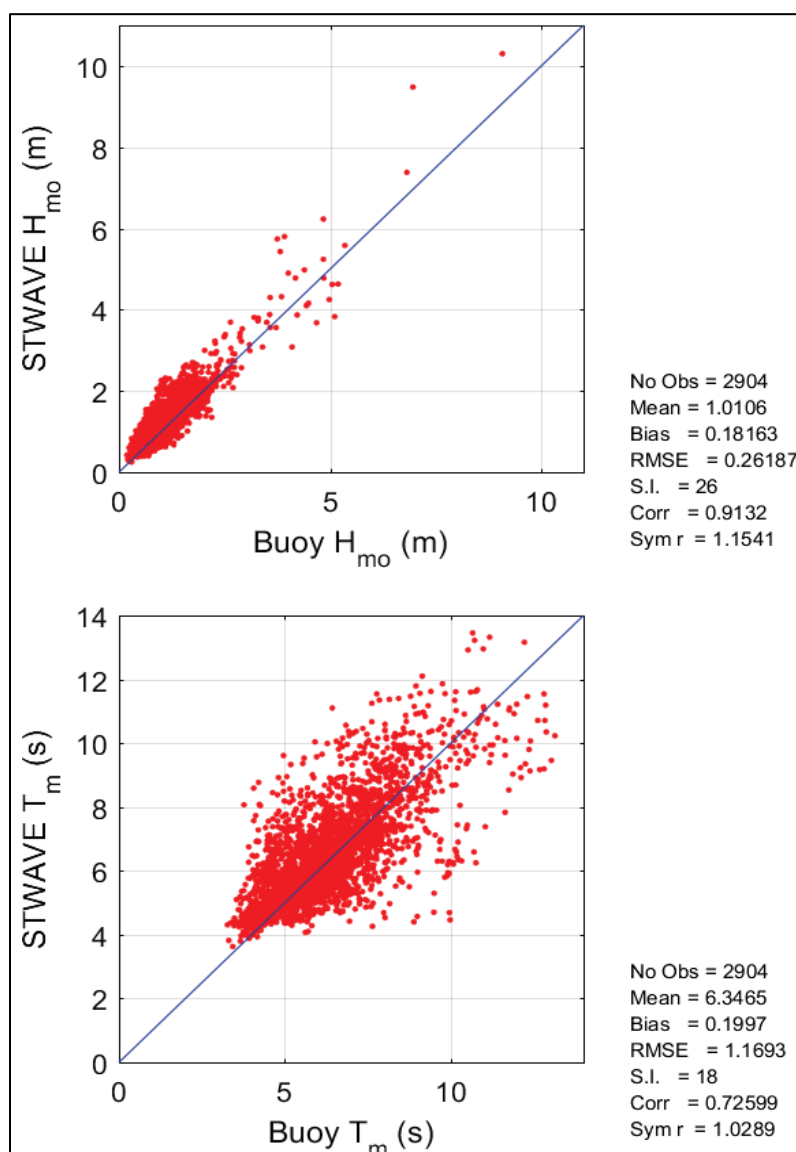
Figure 132. Time series of STWAVE results versus measurements at 44065 for 2012.



The number of time-paired records for 2012 is 2,904. Overall, results for 2012 are comparable to those of 2011 for both significant wave height and mean period. Again, STWAVE overestimated the largest waves associated with Hurricane Sandy. The bias, RMSE, and SI for the significant wave height for 2012 was slightly higher than for 2011 with values of 0.18 m,

0.26 m, and 26, respectively. The linear regression produced a correlation coefficient of 0.91 and a symmetric slope of 1.15, indicating an average positive error of 15% in modeled significant wave height. More scatter is evident for the mean wave period than for the significant wave height as seen in Figure 133. The bias and RMSE for mean wave period were 0.20 s and 1.17 s, respectively. The SI was slightly higher than in 2011 with a value of 18. The correlation coefficient was 0.73 with the symmetric slope indicating an average positive error of 3% in modeled mean wave period with respect to measured wave period.

Figure 133. Scatter plots for 2012 of significant wave height (top) and mean period (bottom).



### **3D salinity transport comparisons**

The 3D salinity comparisons consisted primarily of comparing model results to observed surface and bottom salinity measurements from 1995. Comparisons also consisted of comparing to qualitative behavior reported in the literature.

#### **Quantitative comparisons**

In 1995, a comprehensive data collection effort was performed whereby numerous salinity measurements were collected at various times and locations in the NYNJH system. Figure 134 shows the locations where data were collected. The time-series comparisons are provided in Figure 135 to Figure 175. The lines are model data, and the stars are observations (Blue – Surface; Red – Bottom; Green – Stratification [Bottom – Surface]).



Figure 134. Salinity observation locations.

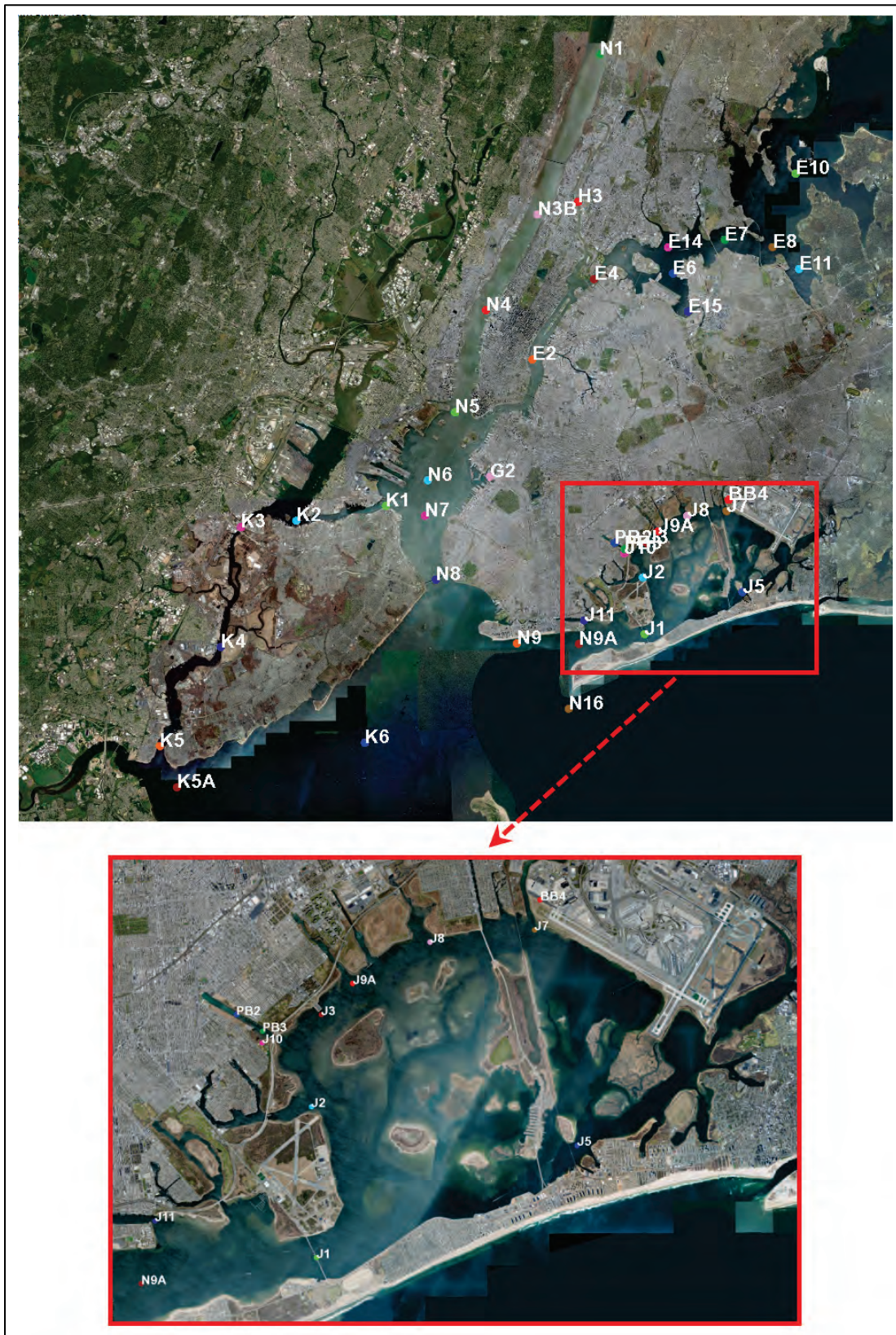


Figure 135. Salinity distribution at BB4.

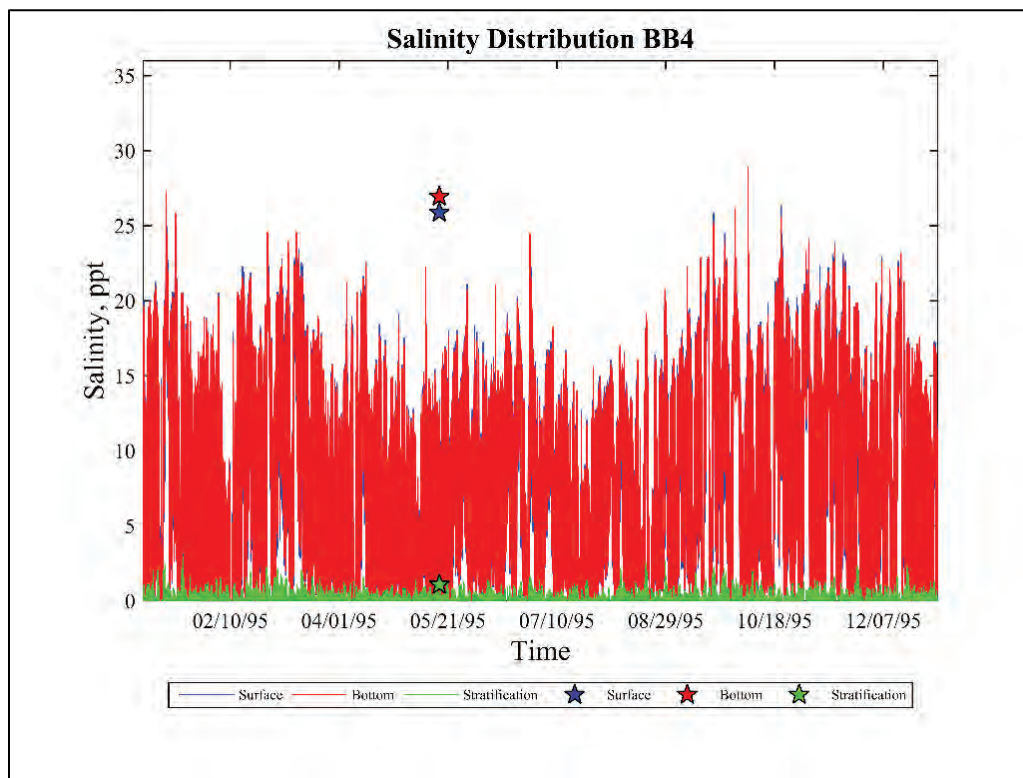


Figure 136. Salinity distribution at E2.

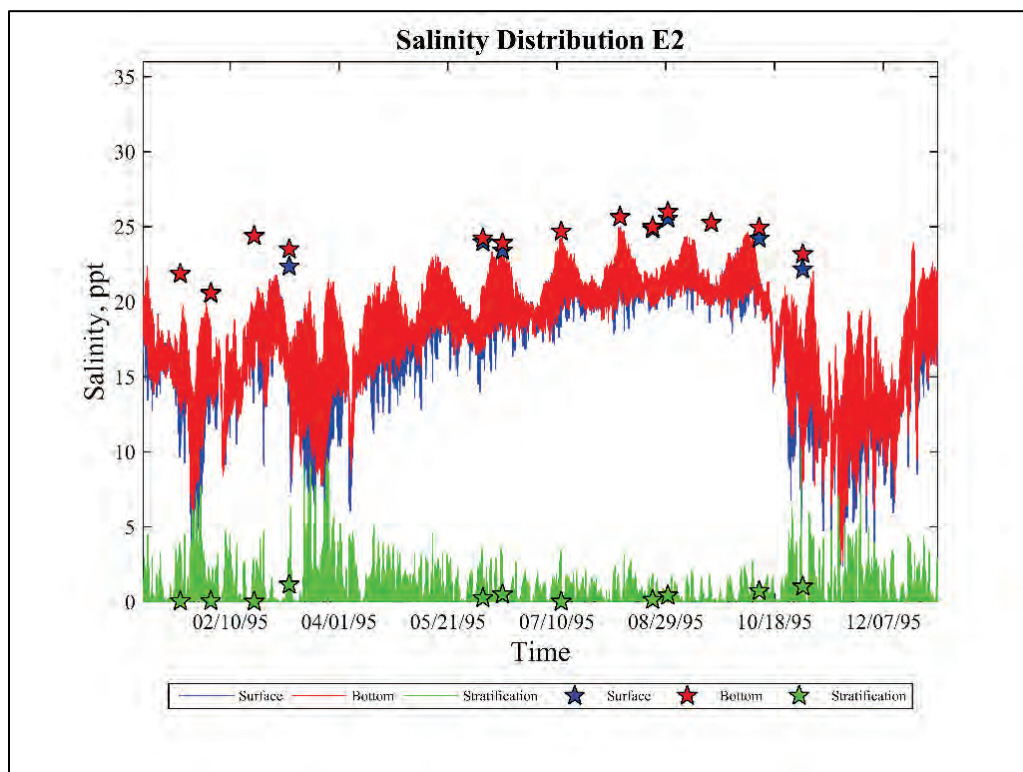




Figure 137. Salinity distribution at E4.

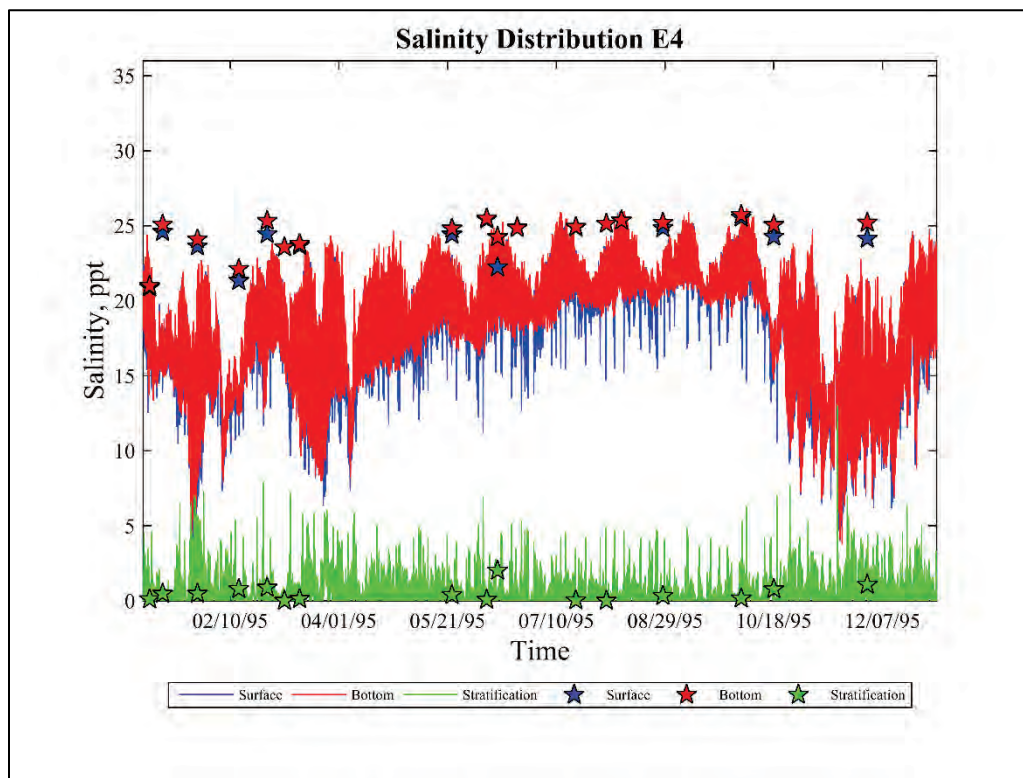


Figure 138. Salinity distribution at E6.

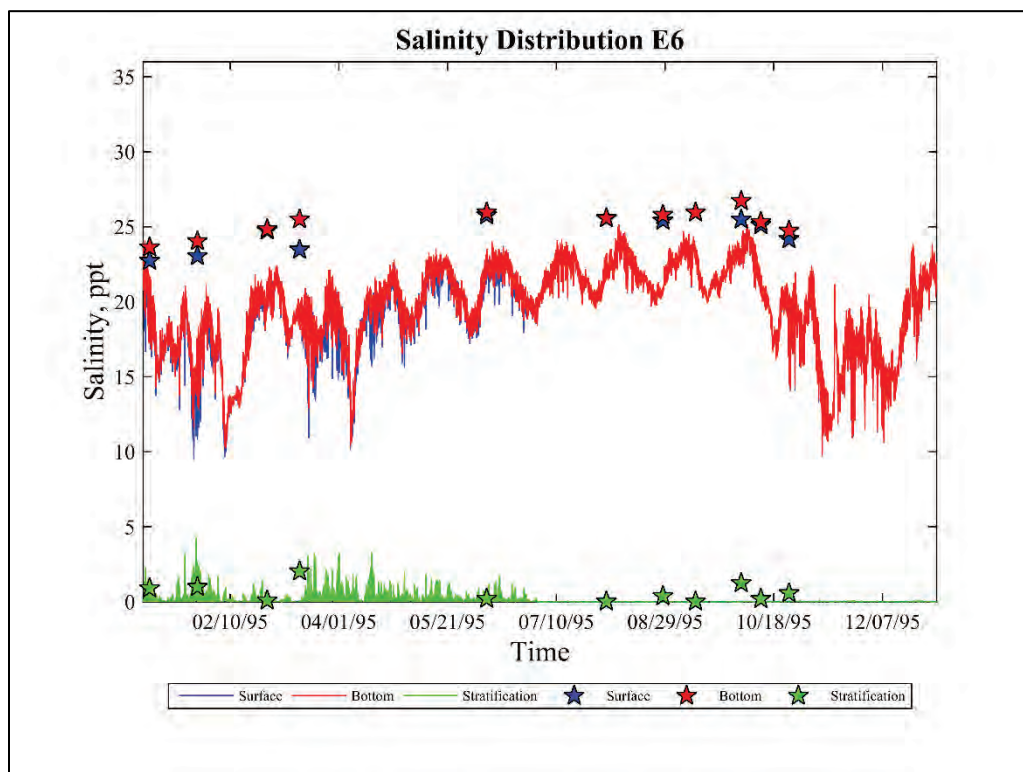




Figure 139. Salinity distribution at E7.

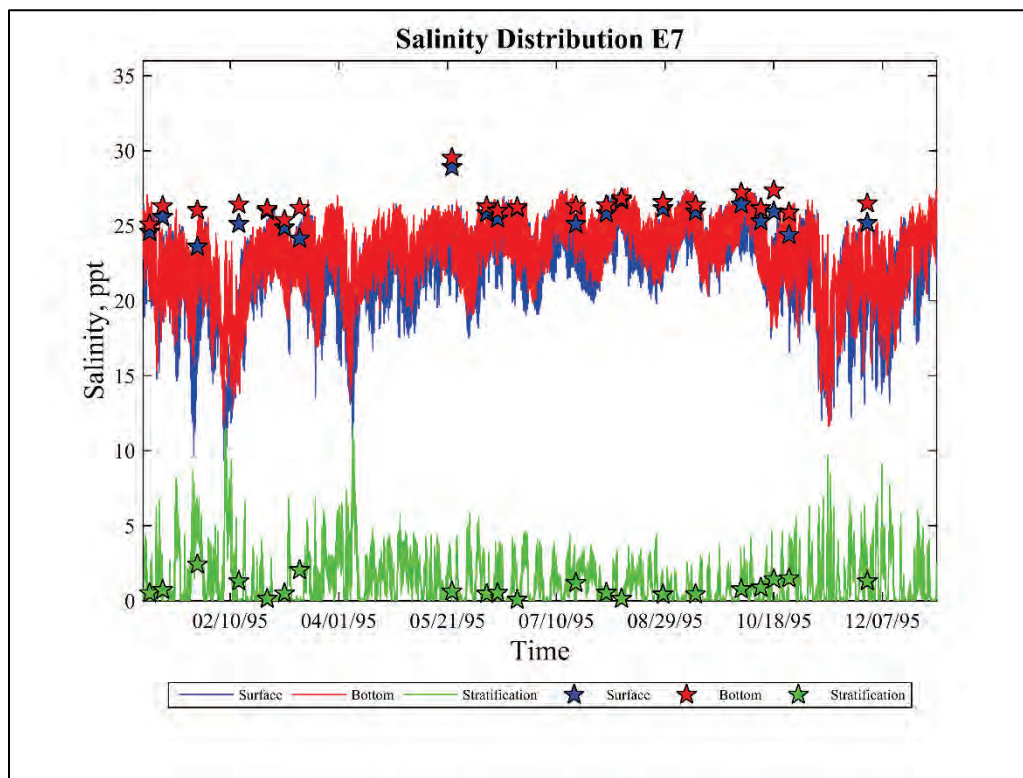


Figure 140. Salinity distribution at E8.

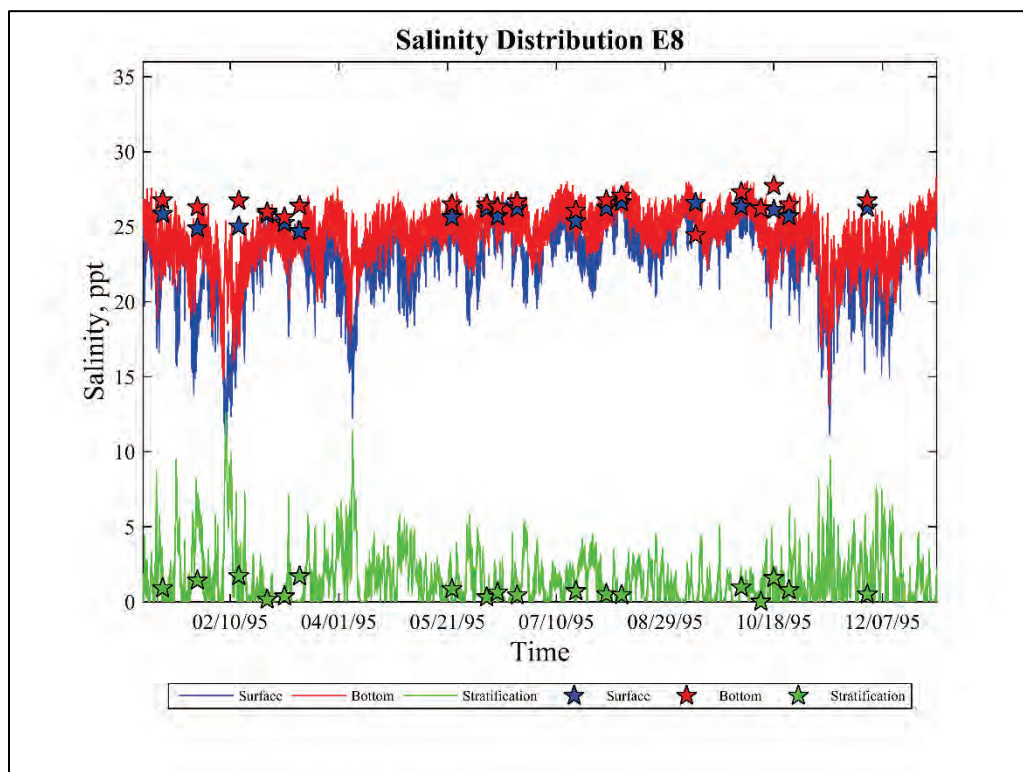


Figure 141 Salinity distribution at E10.

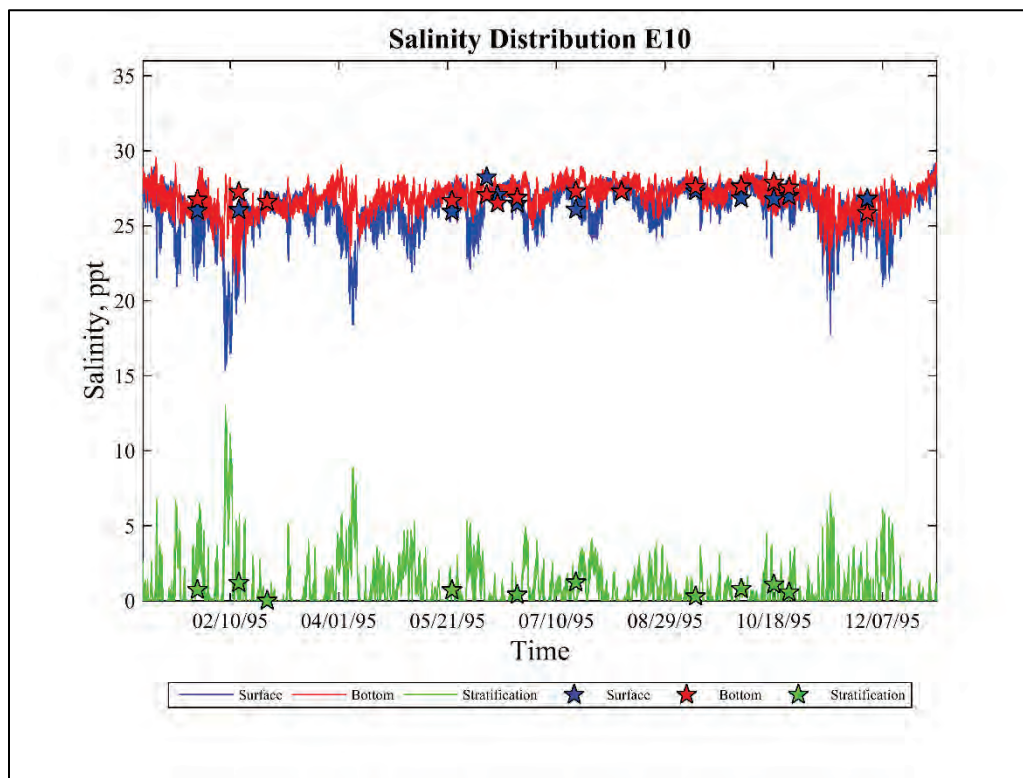


Figure 142. Salinity distribution at E11.

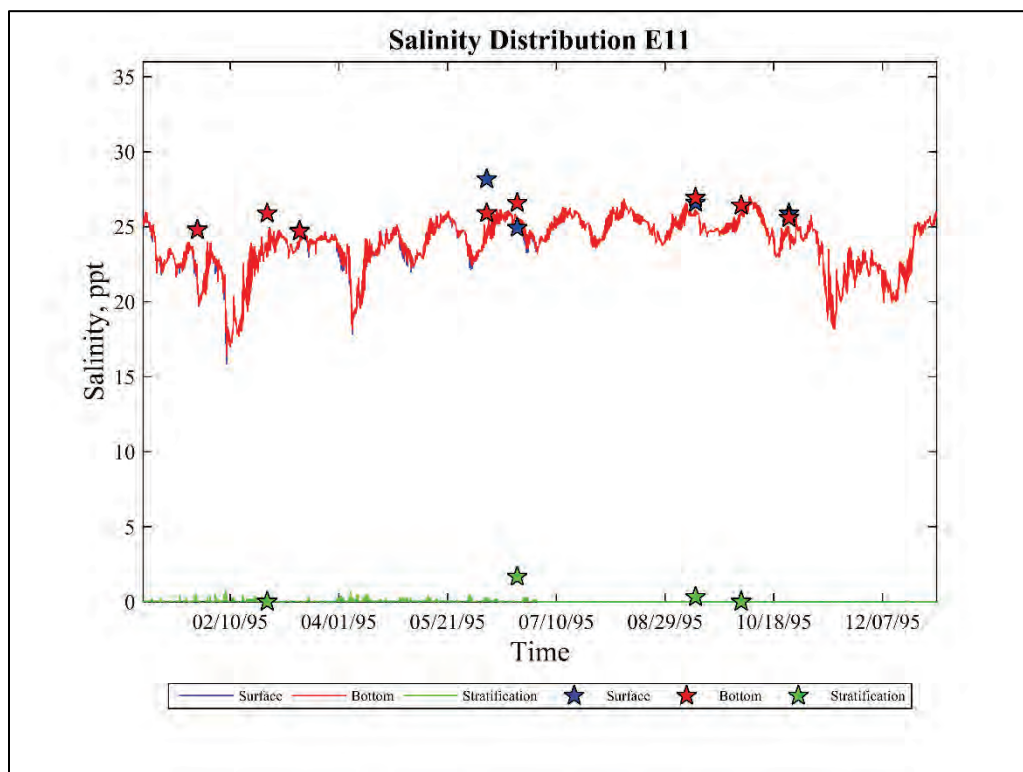


Figure 143. Salinity distribution at E14.

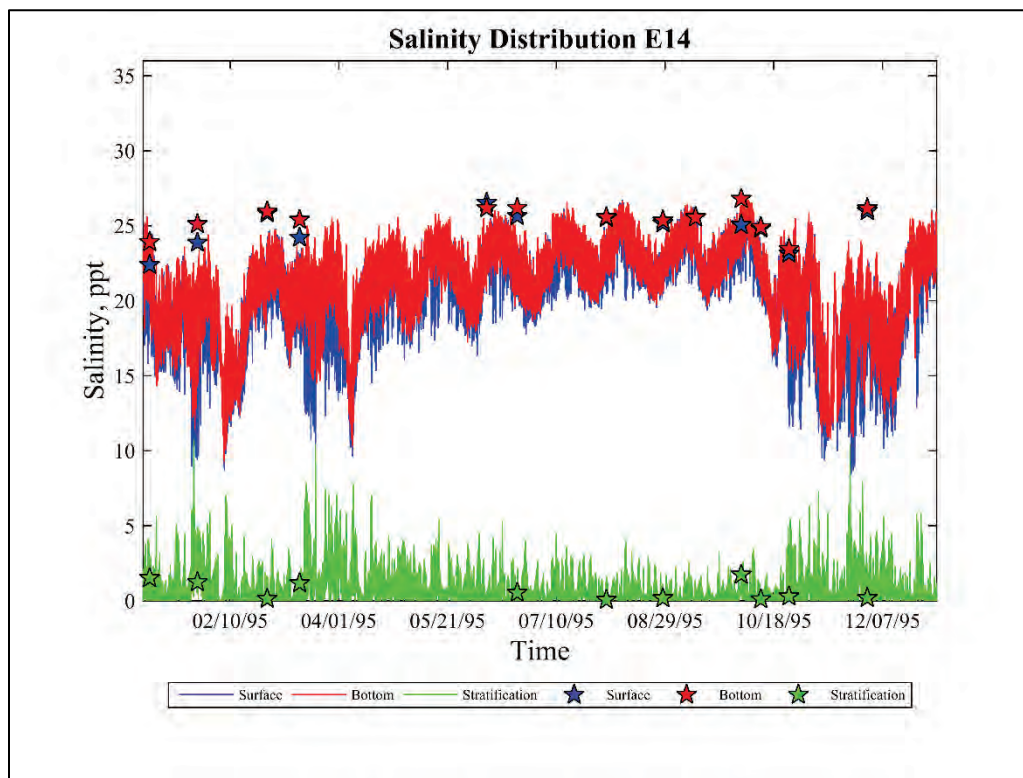


Figure 144. Salinity distribution at E15.

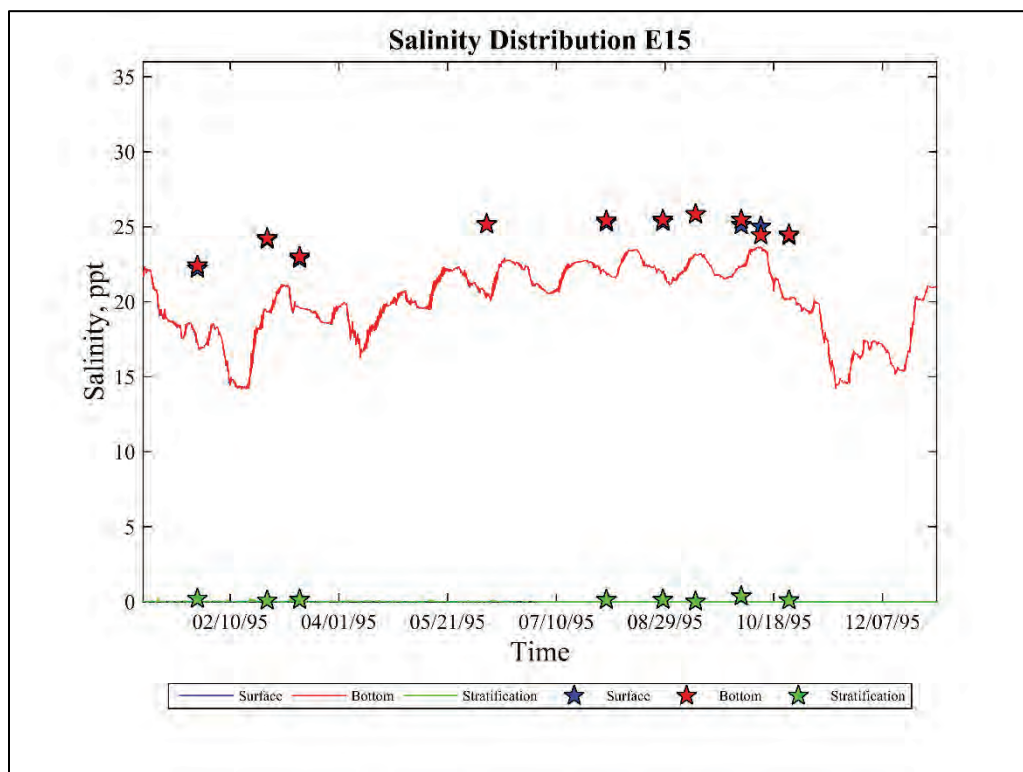




Figure 145. Salinity distribution at G2.

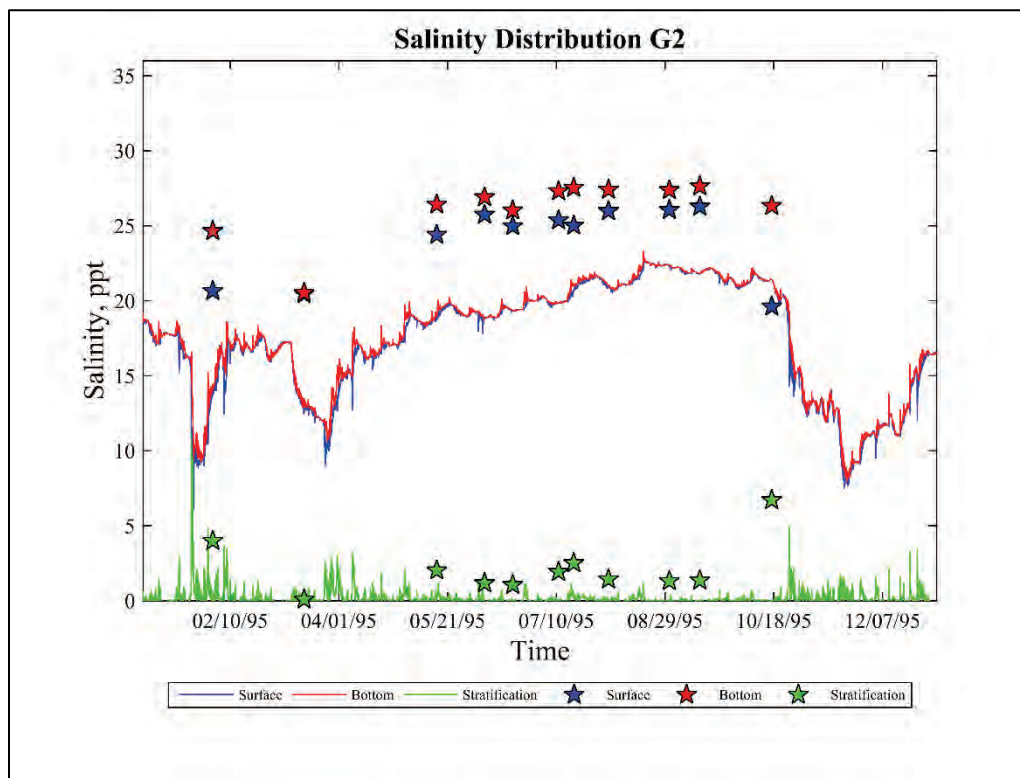


Figure 146. Salinity distribution at H3.

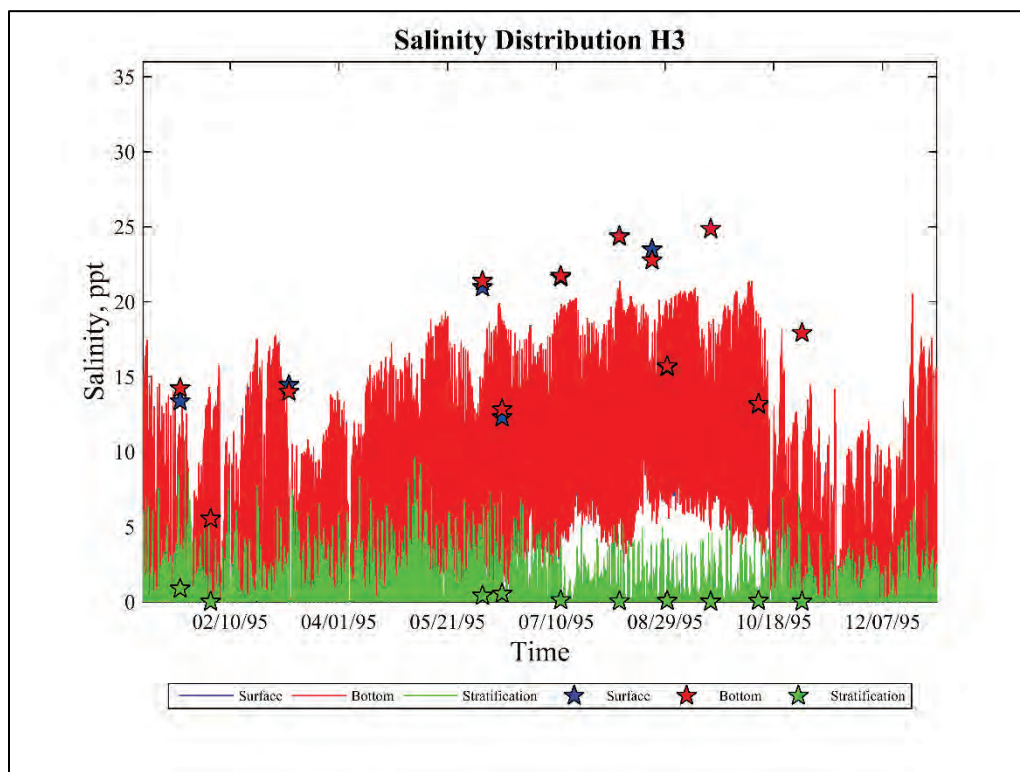


Figure 147. Salinity distribution at J1.

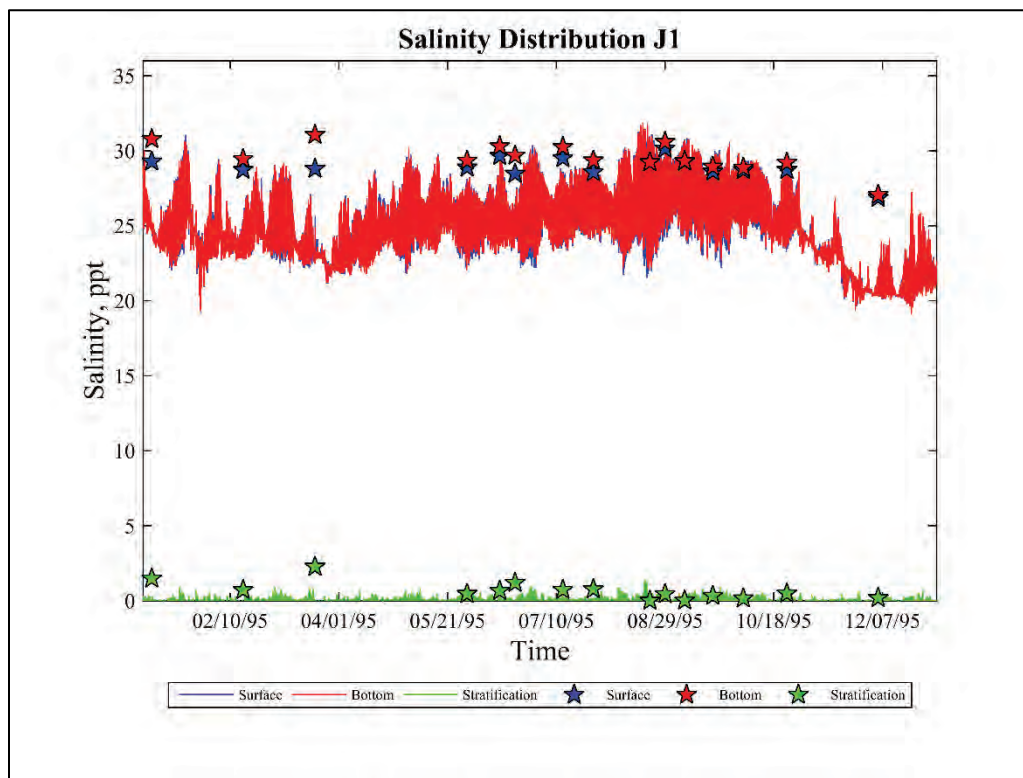


Figure 148. Salinity distribution at J2.

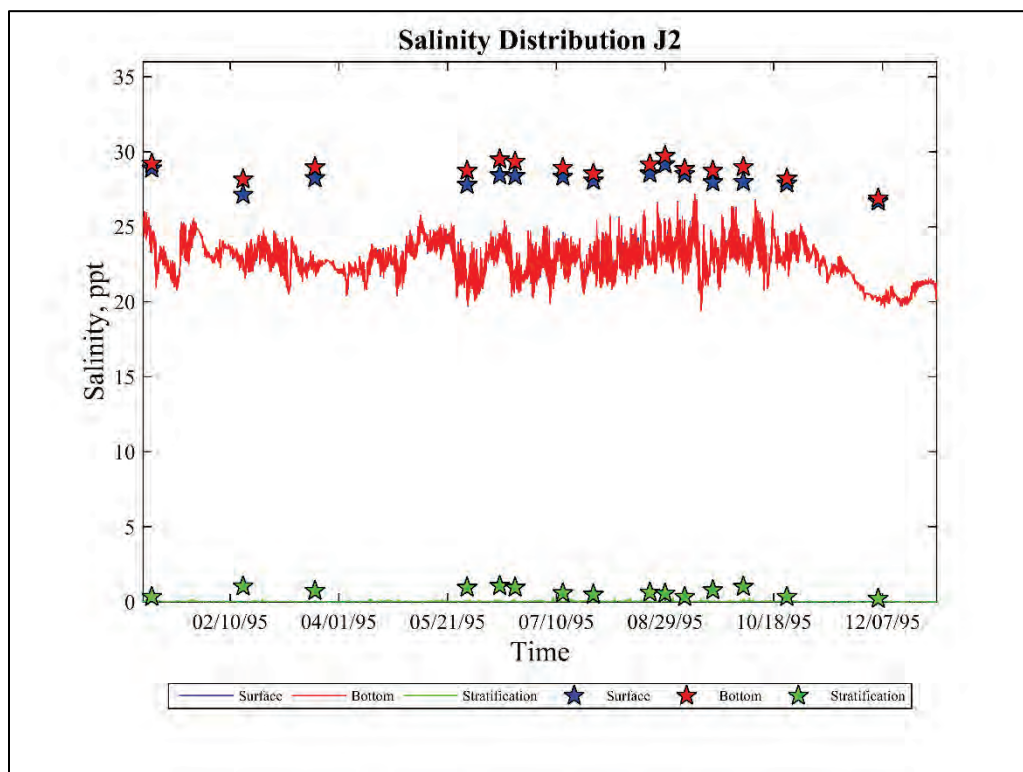


Figure 149. Salinity distribution at J3.

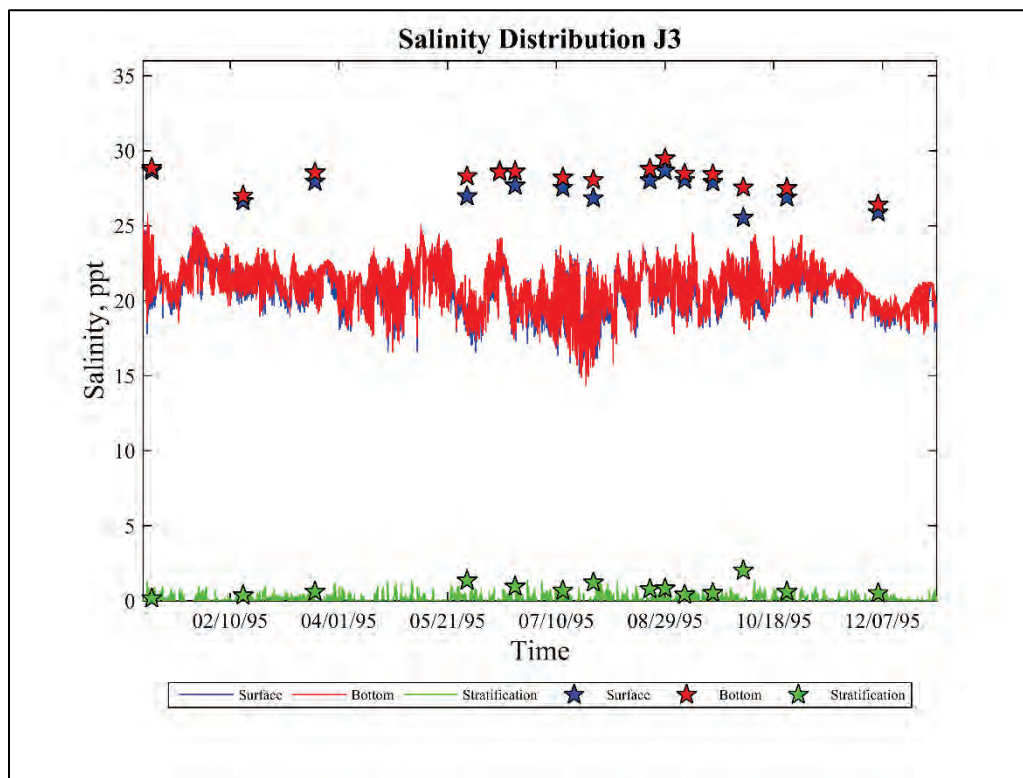


Figure 150. Salinity distribution at J5.

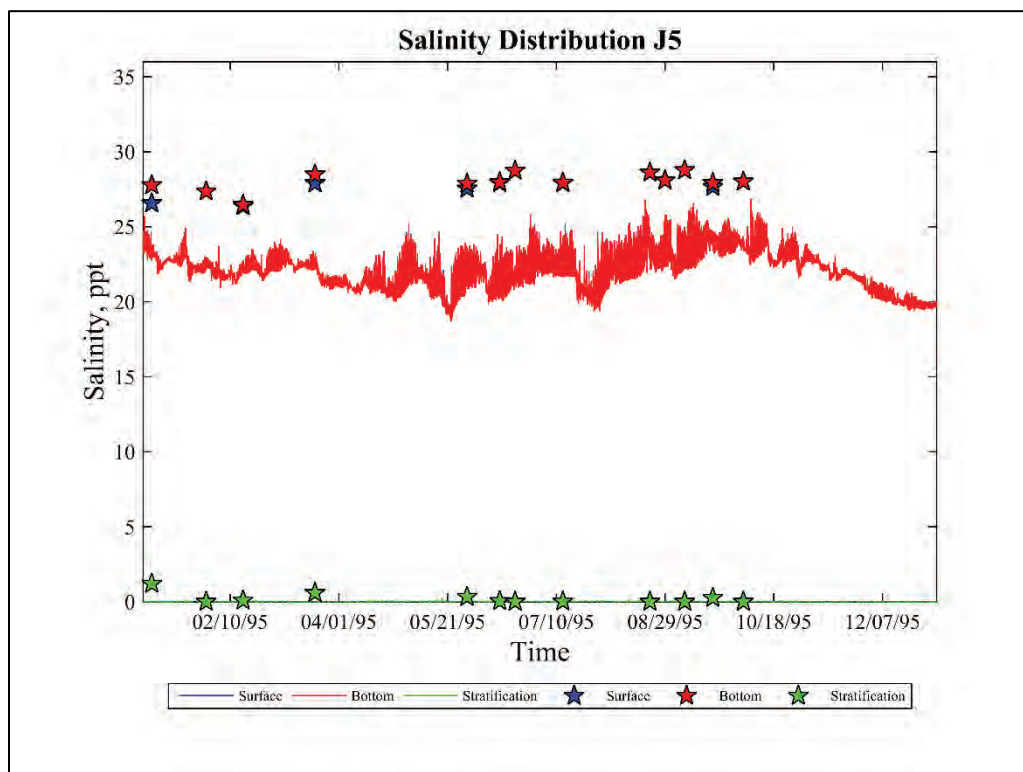




Figure 151. Salinity distribution at J5D.

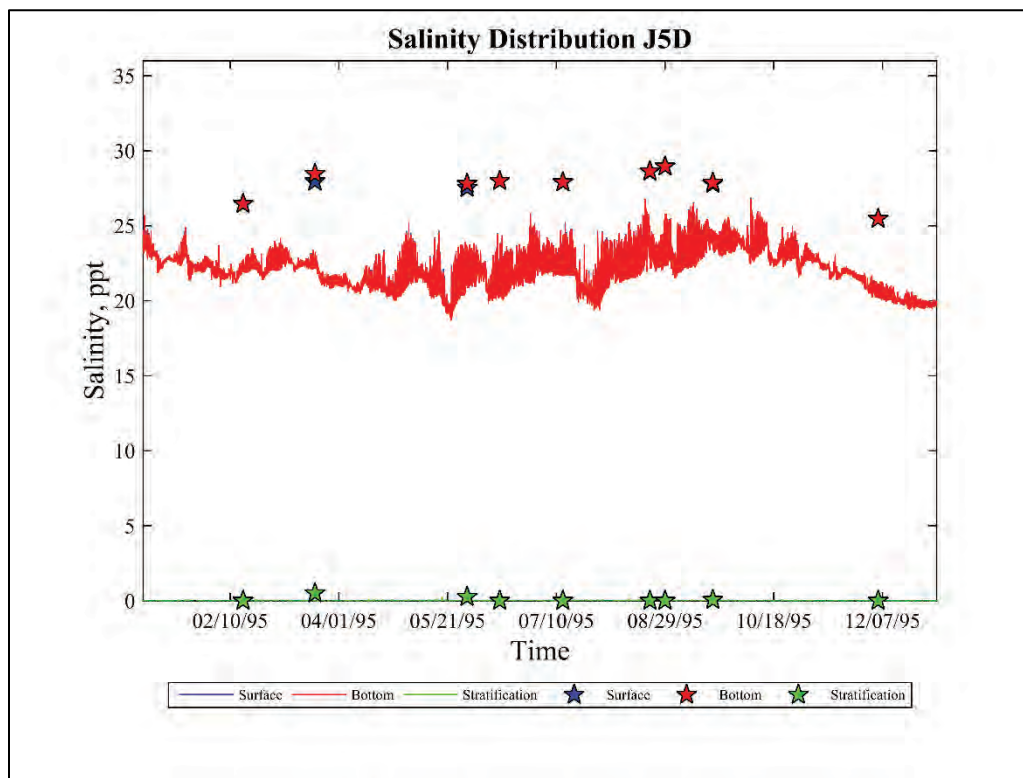


Figure 152. Salinity distribution at J7.

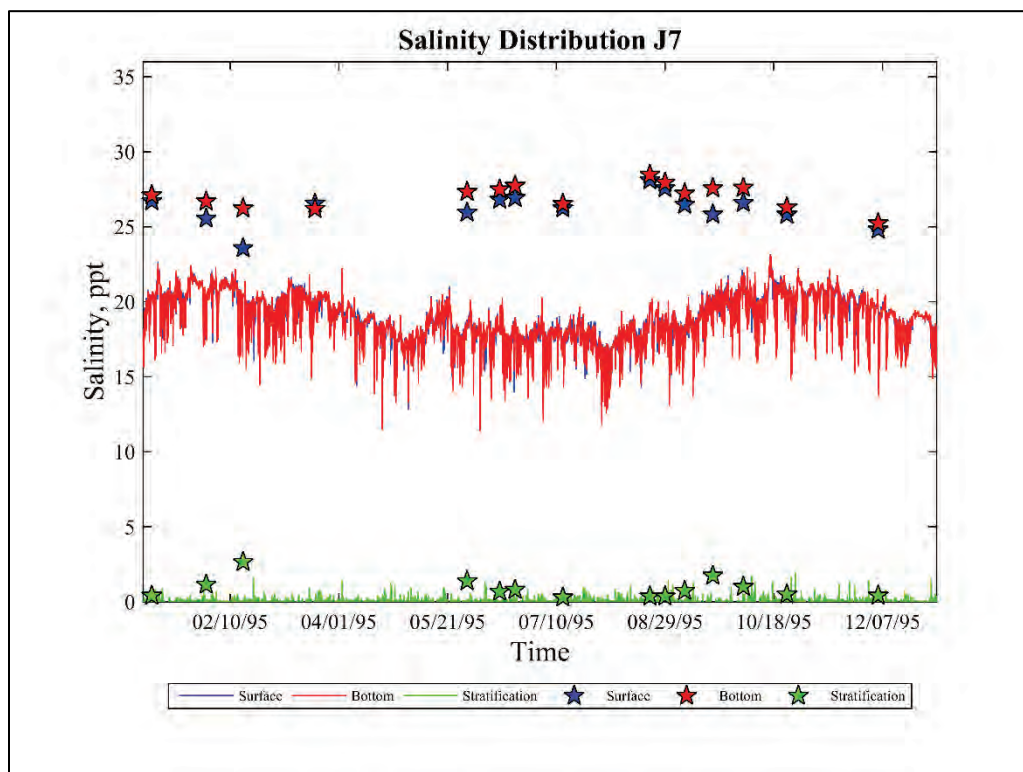


Figure 153. Salinity distribution at J8.

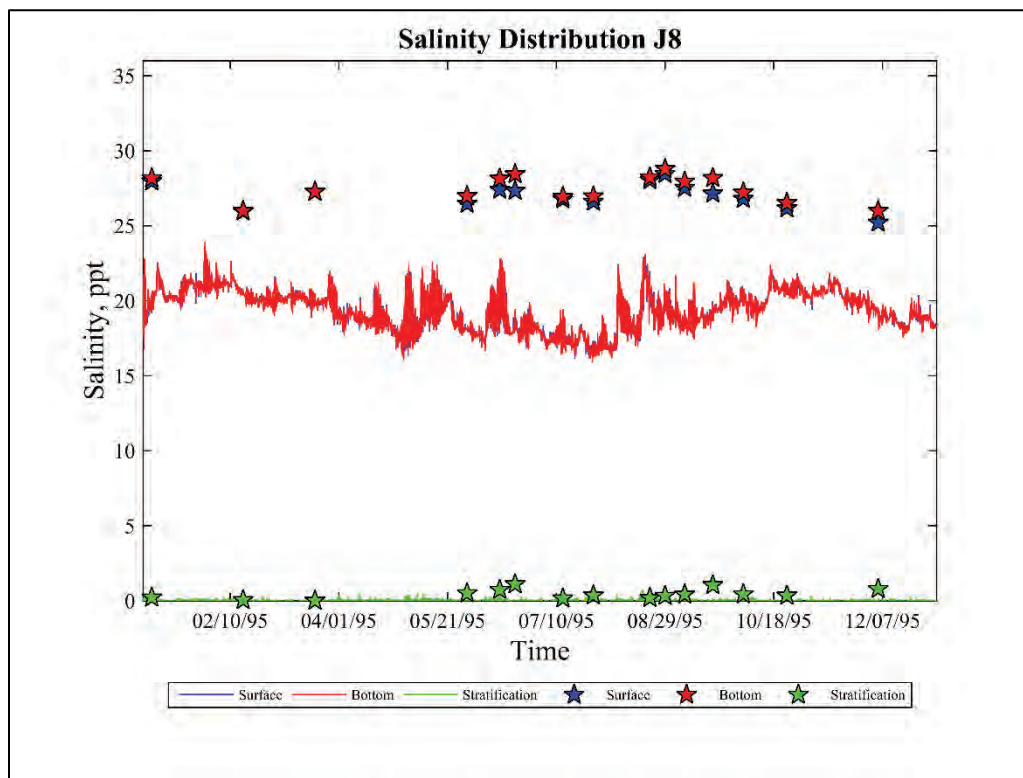


Figure 154. Salinity distribution J9A.

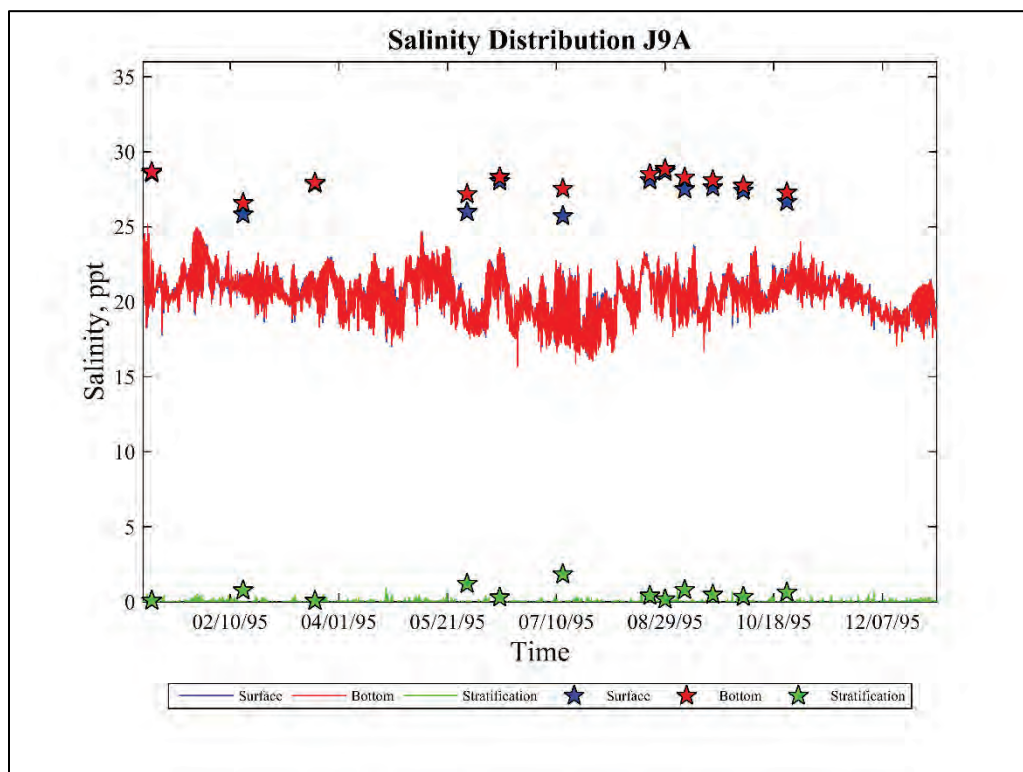


Figure 155. Salinity distribution at J10.

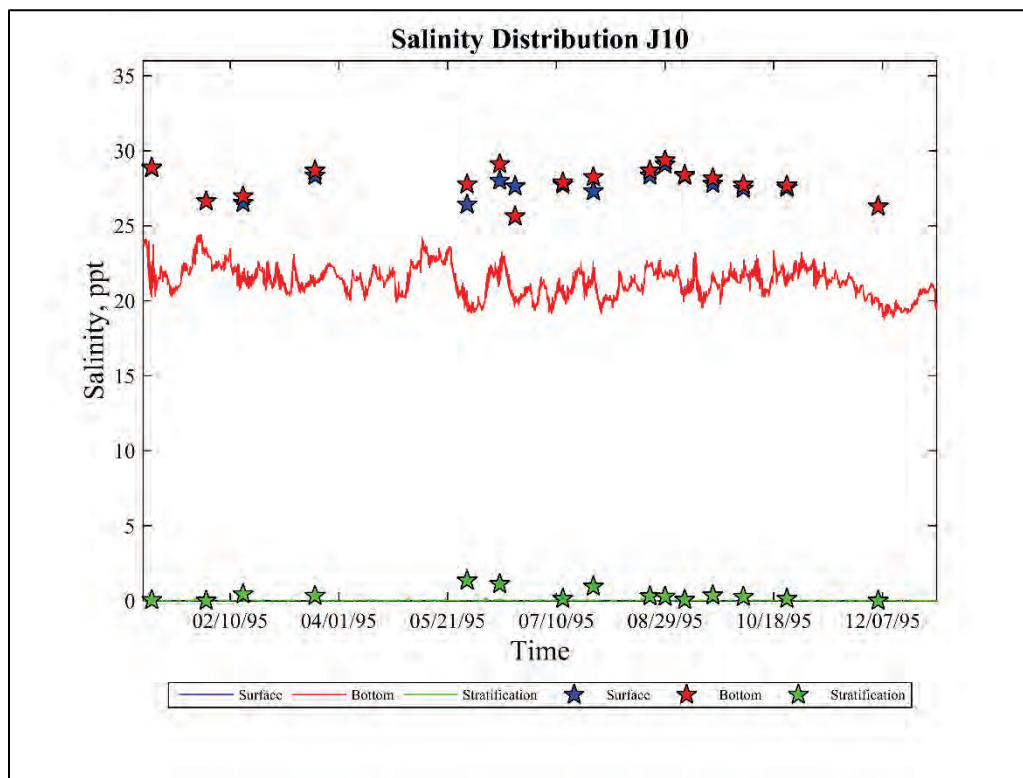


Figure 156. Salinity distribution at J11.

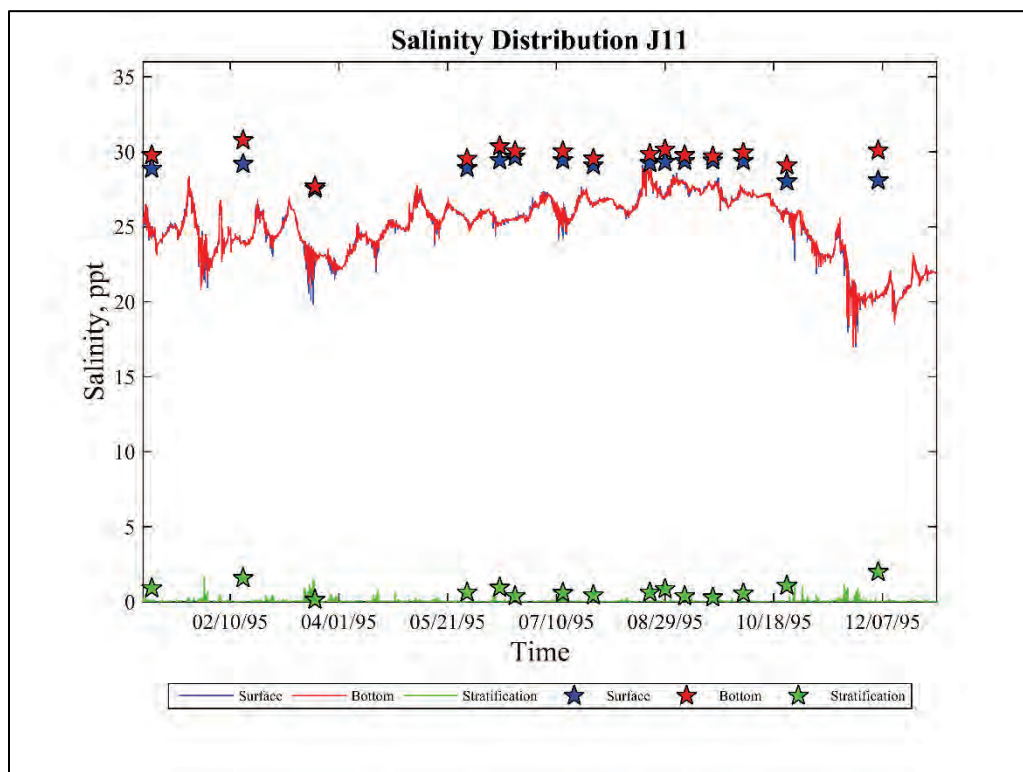


Figure 157. Salinity distribution at K1.

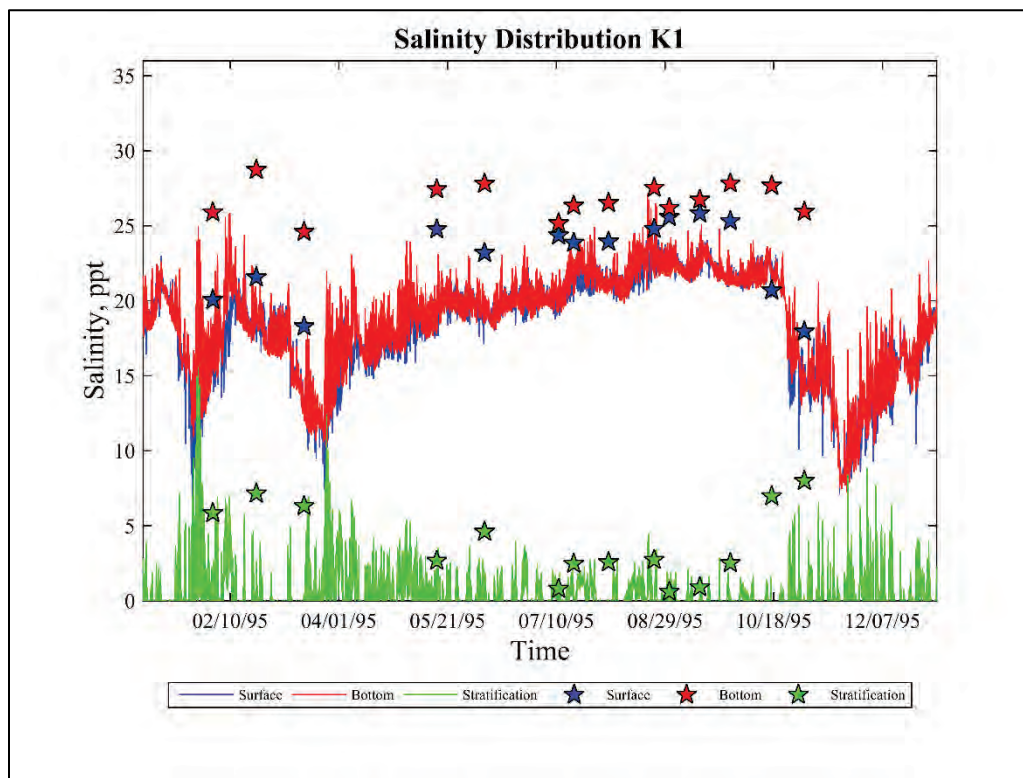


Figure 158. Salinity distribution at K2.

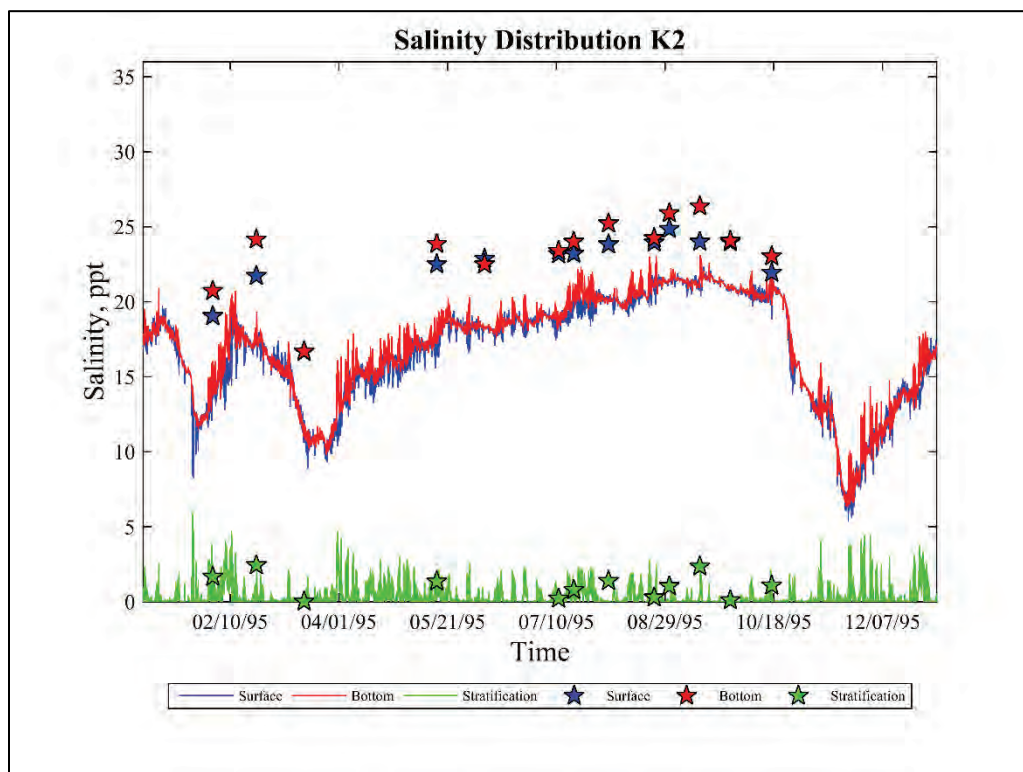




Figure 159. Salinity distribution at K3.

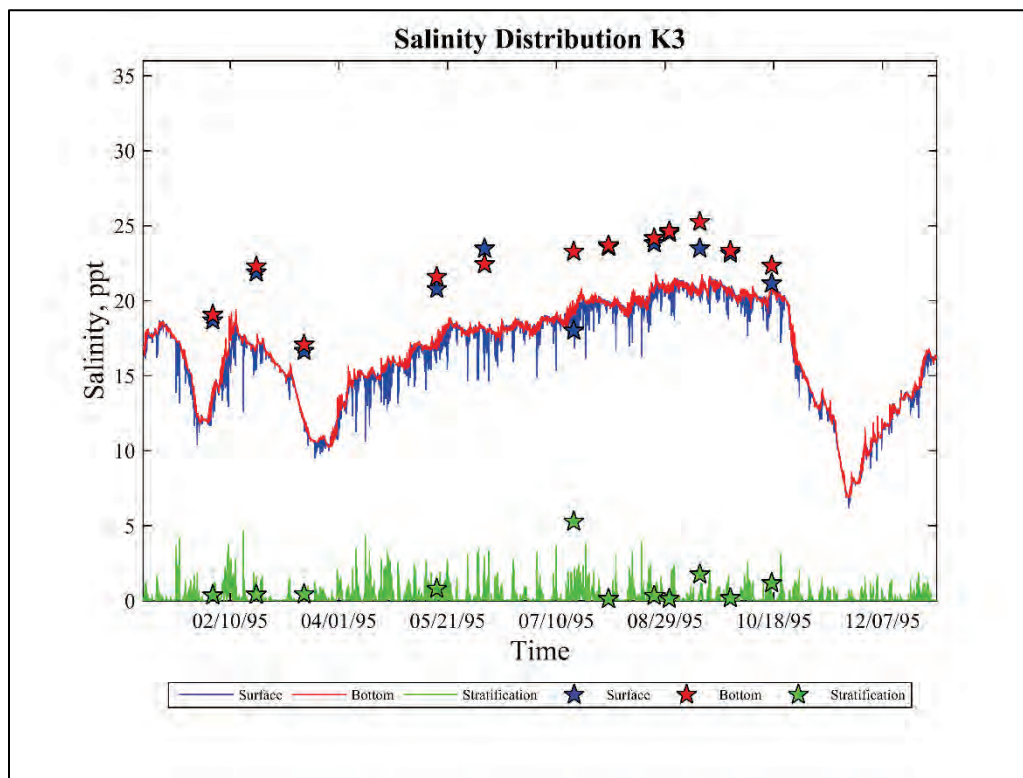


Figure 160. Salinity distribution at K4.

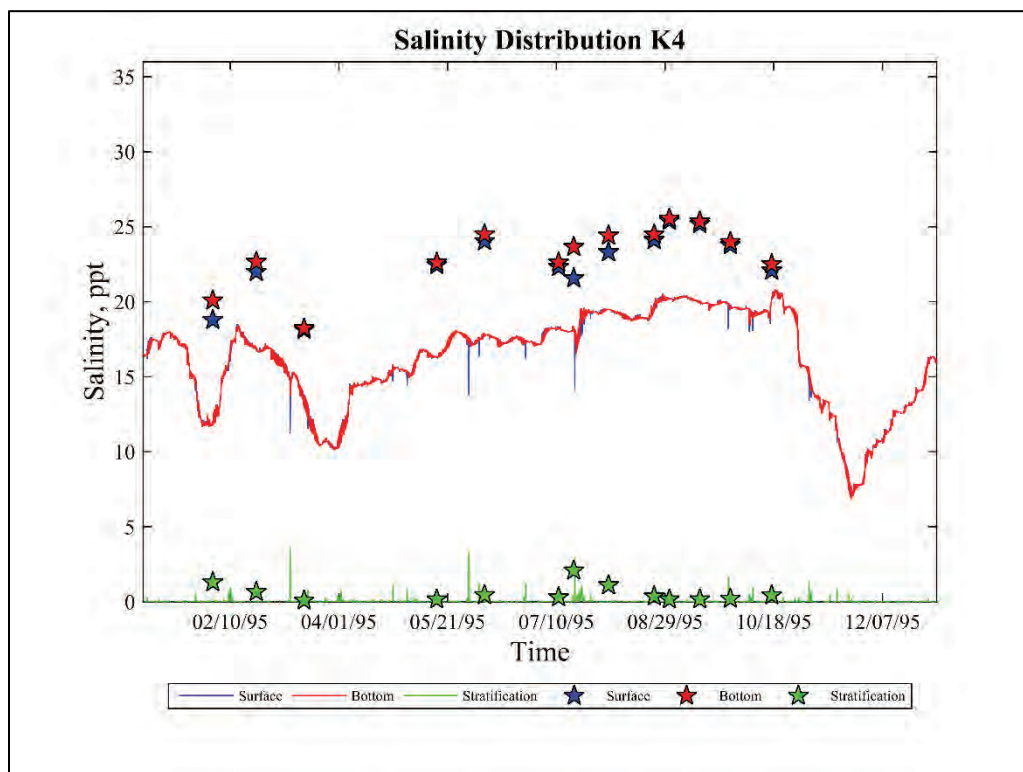


Figure 161. Salinity distribution at K5.

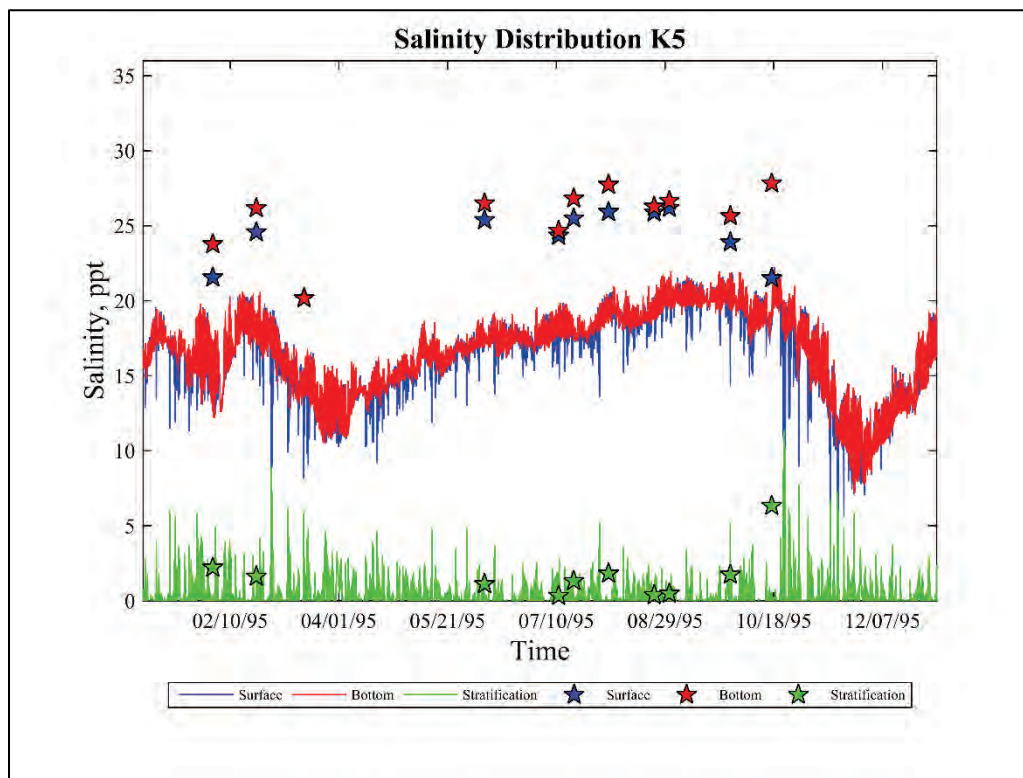


Figure 162. Salinity distribution at K5A.

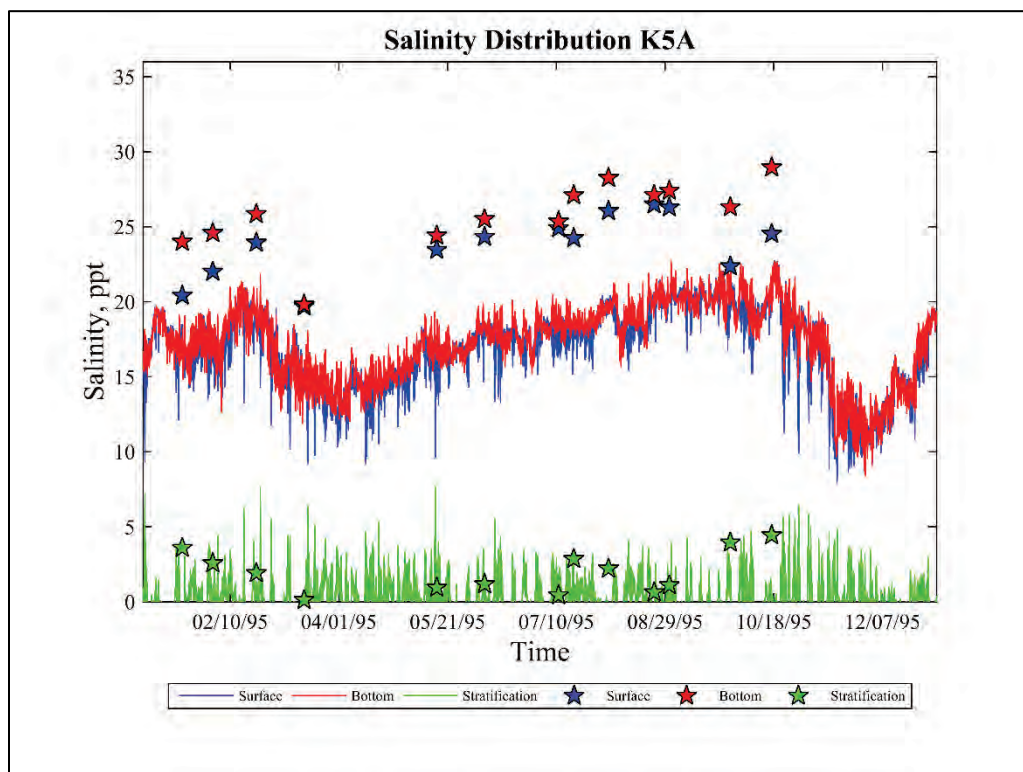




Figure 163. Salinity distribution at K6.

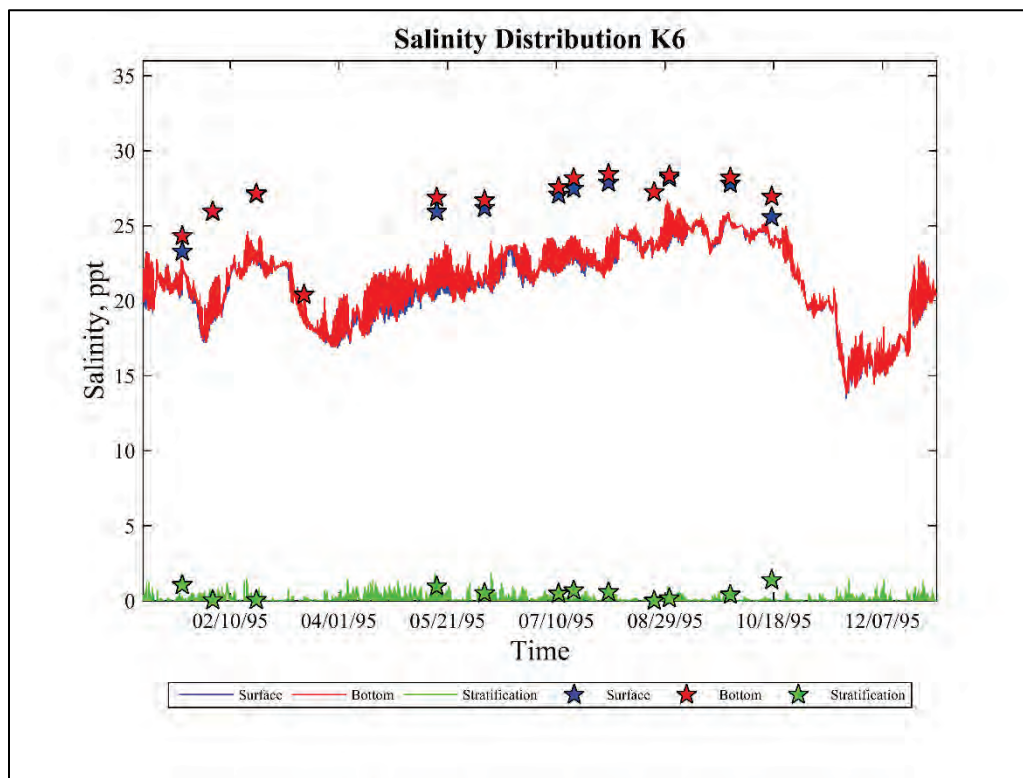


Figure 164. Salinity distribution at N1.

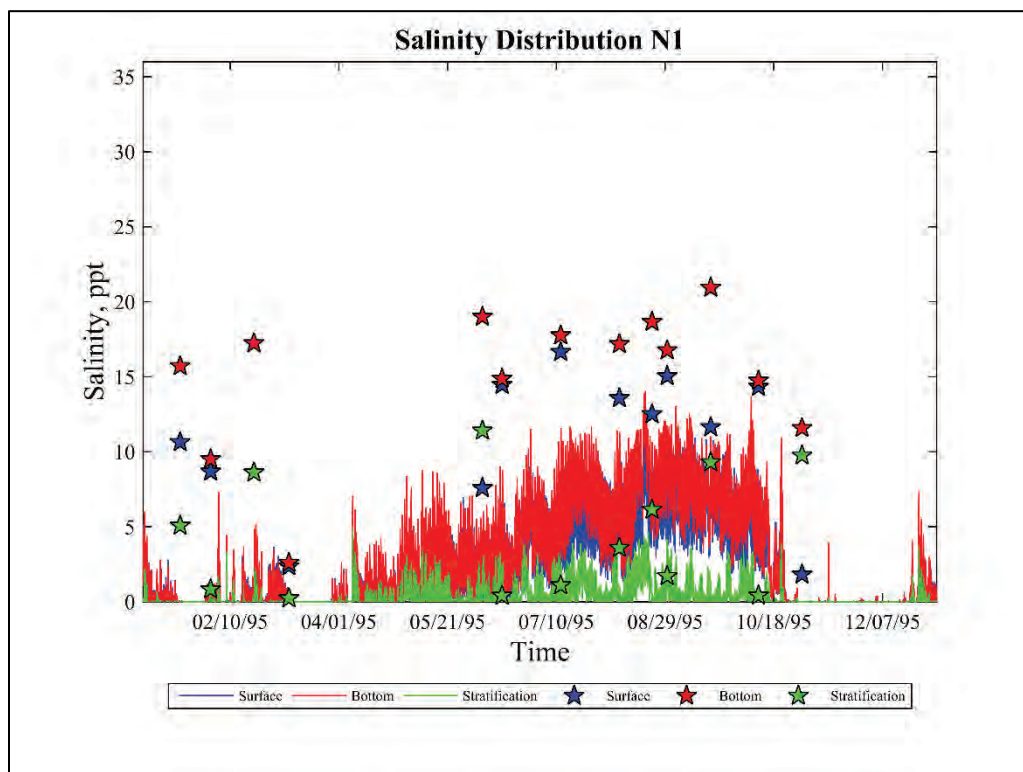


Figure 165. Salinity distribution at N3B.

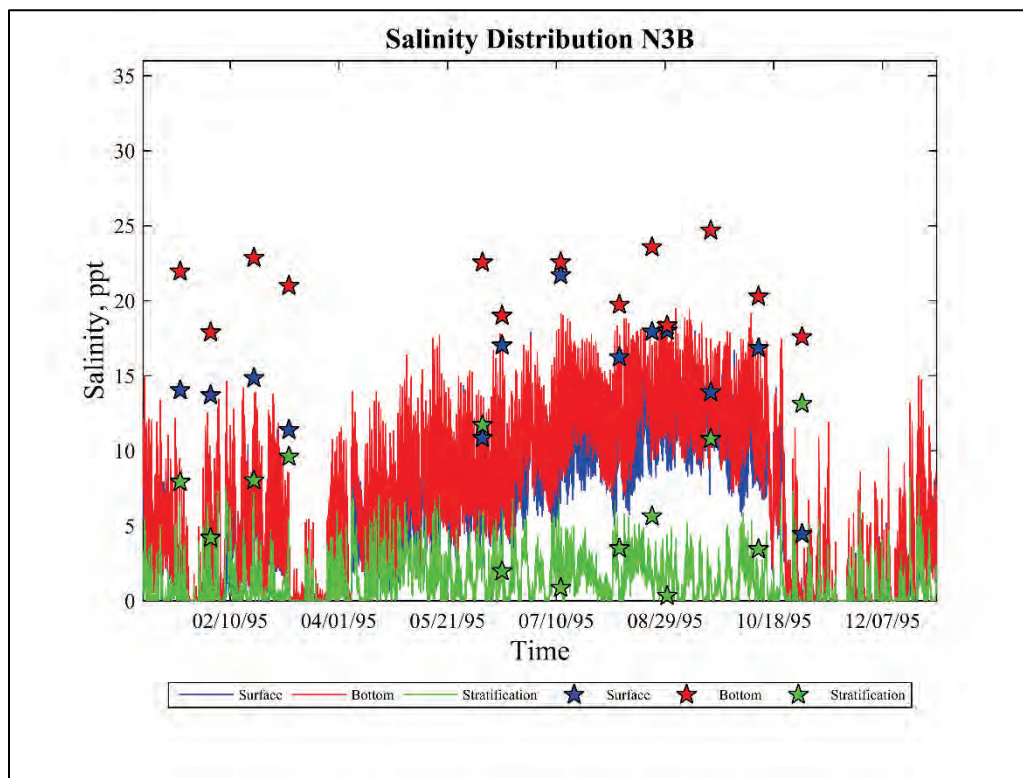


Figure 166. Salinity distribution at N4.

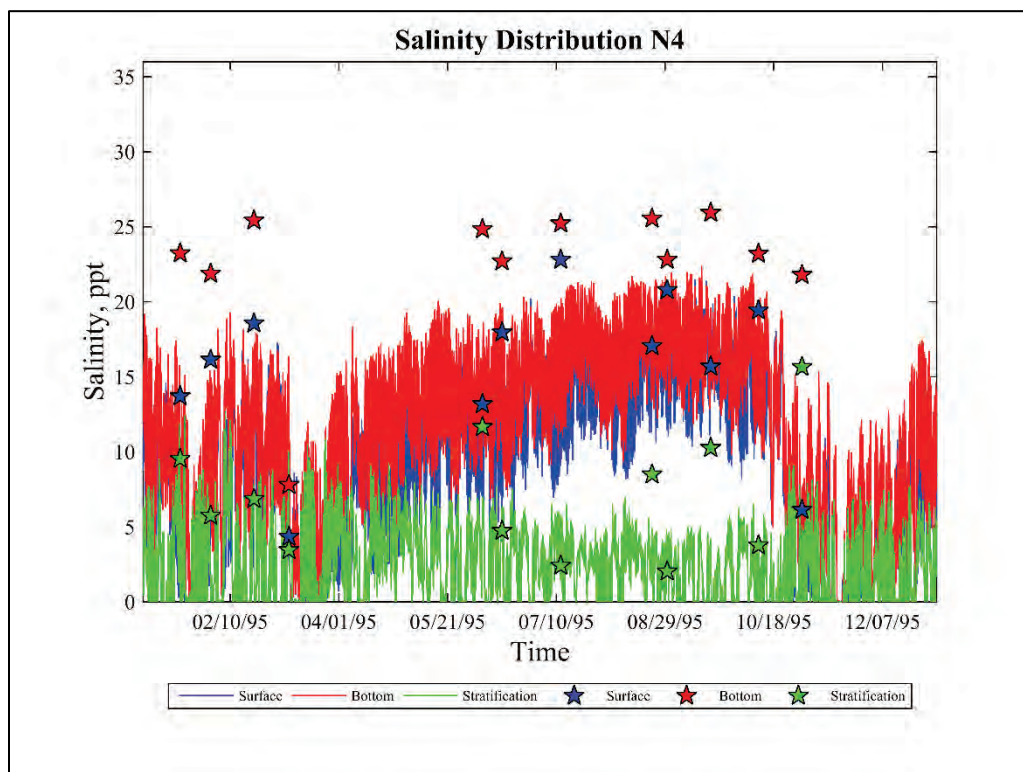


Figure 167. Salinity distribution at N5.

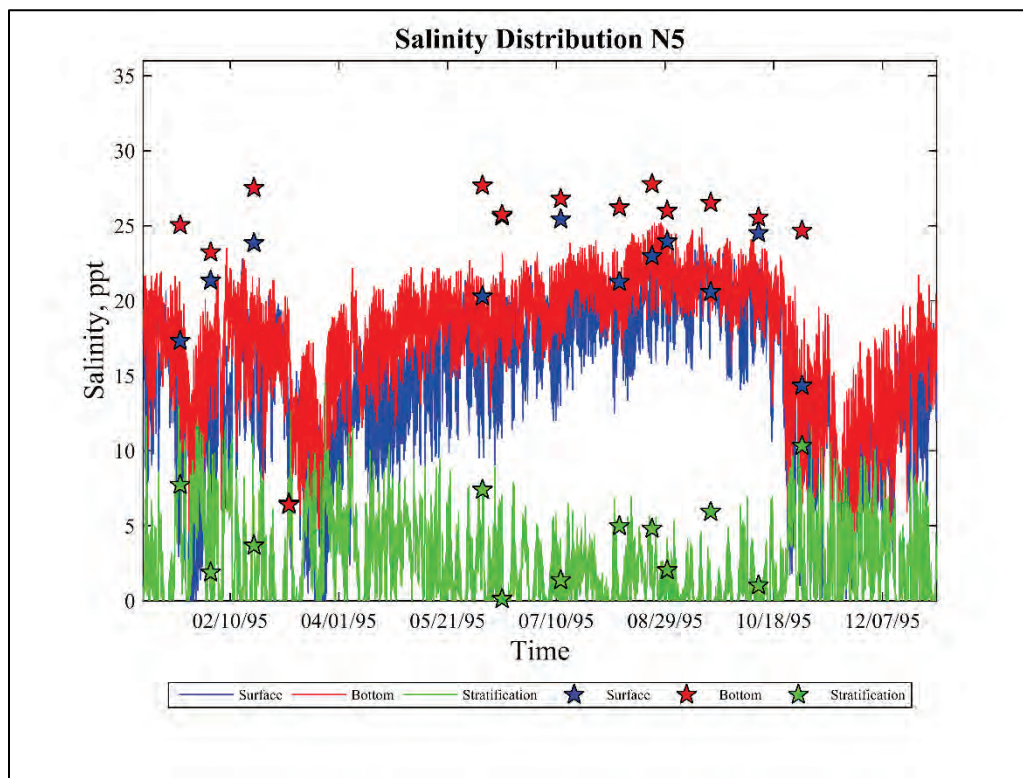


Figure 168. Salinity distribution at N6.

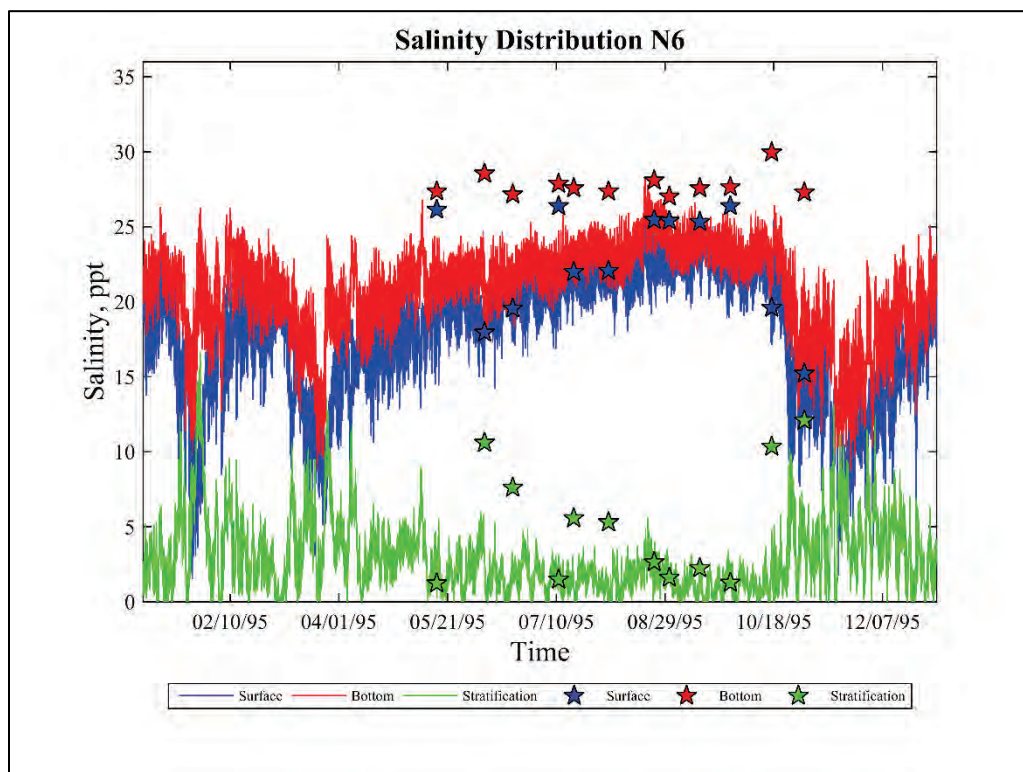




Figure 169. Salinity distribution at N7.

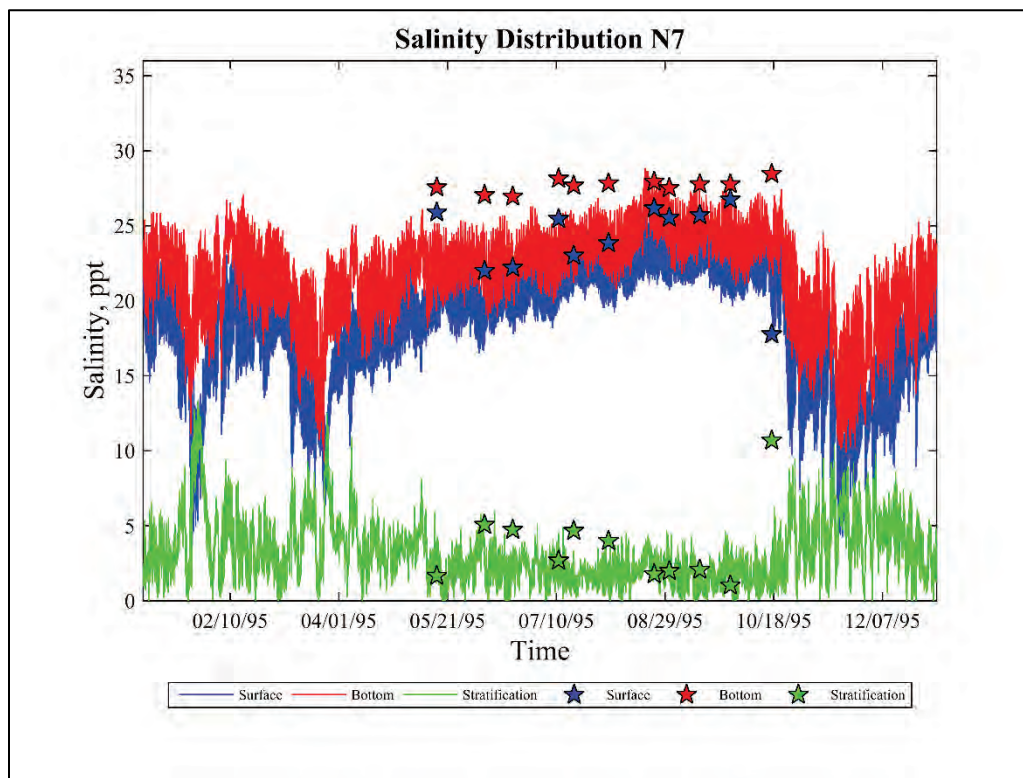


Figure 170. Salinity distribution at N8.

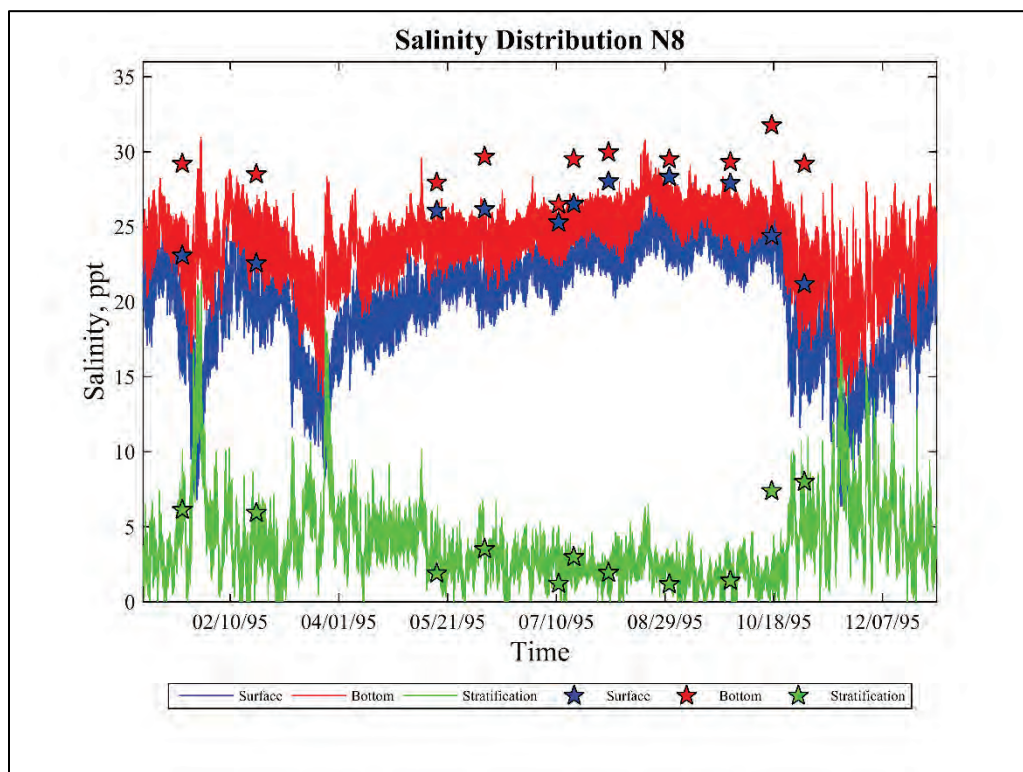


Figure 171. Salinity distribution at N9.

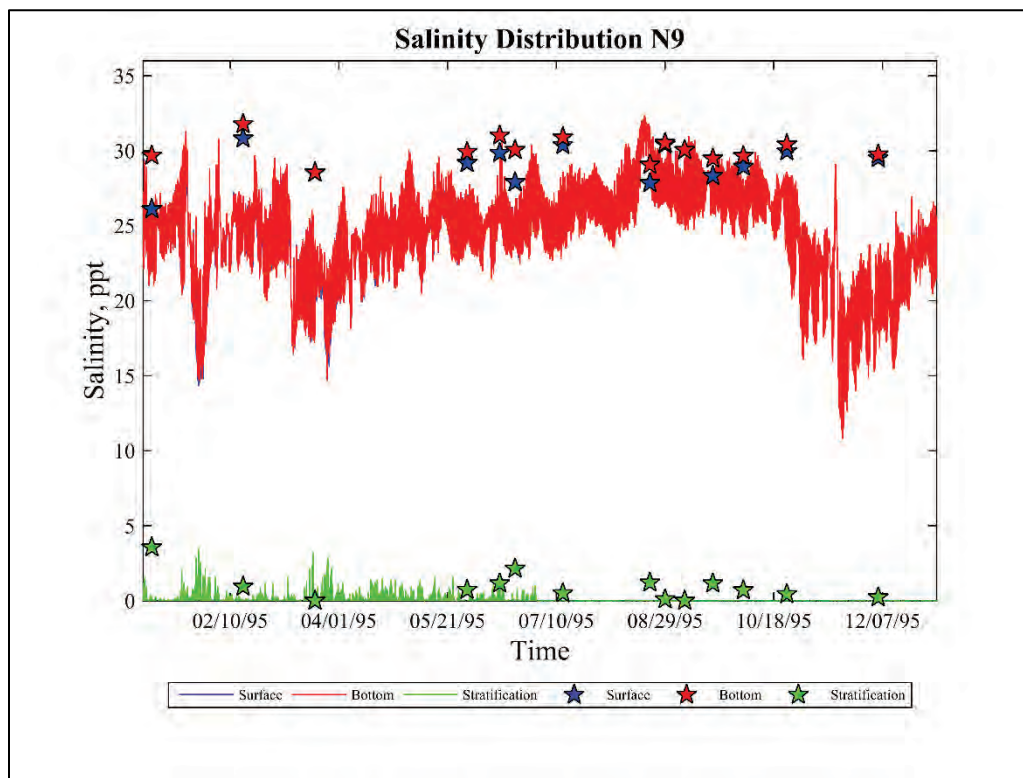


Figure 172. Salinity distribution at N9A.

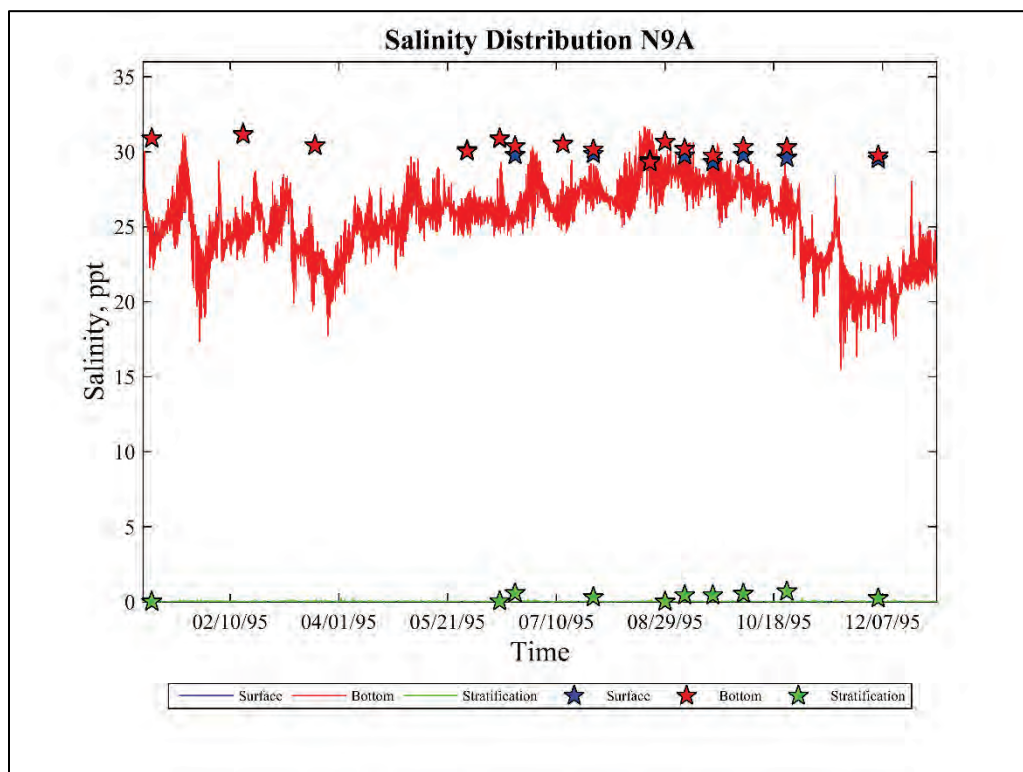


Figure 173. Salinity distribution at N16.

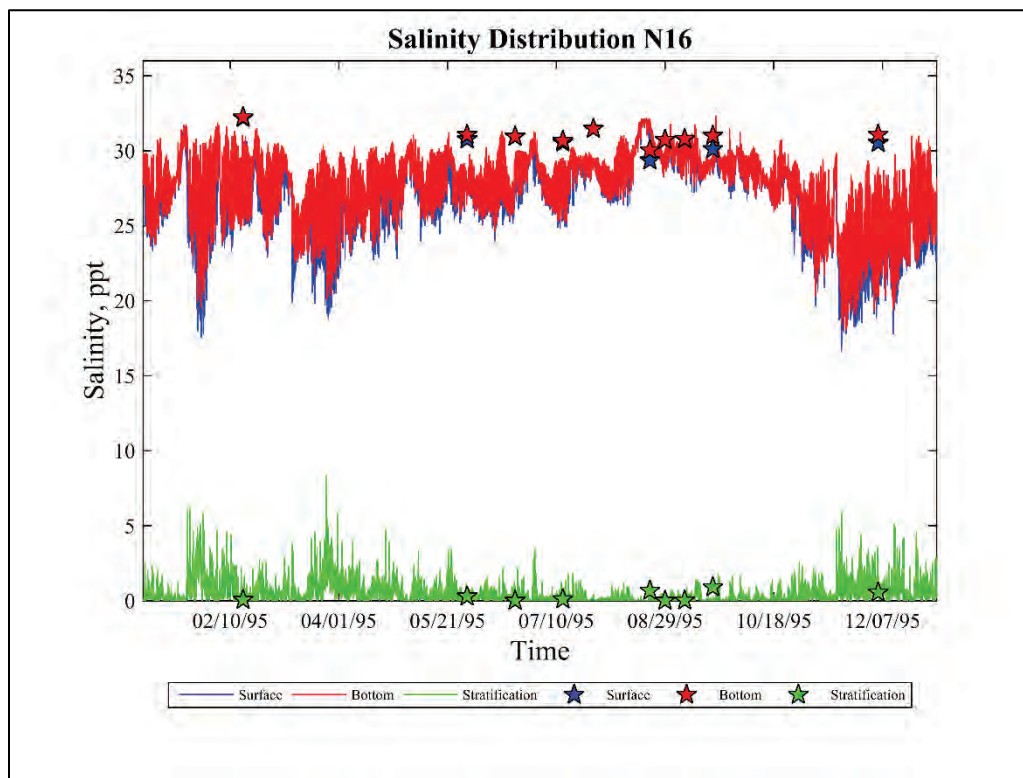


Figure 174. Salinity distribution at PB2.

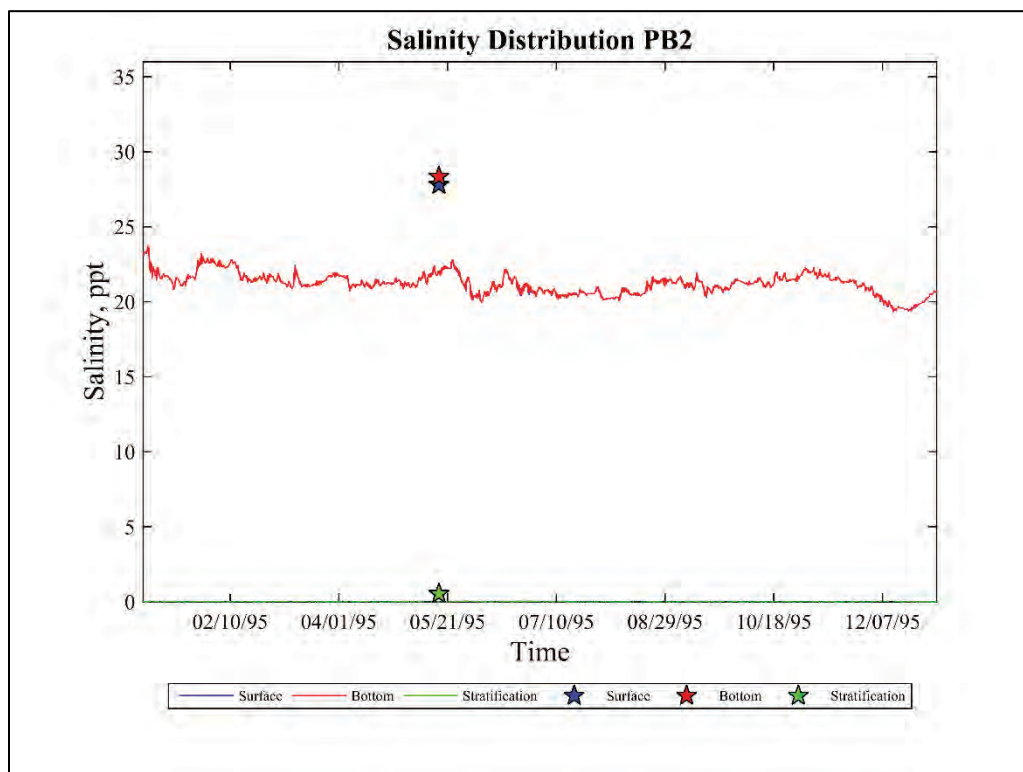
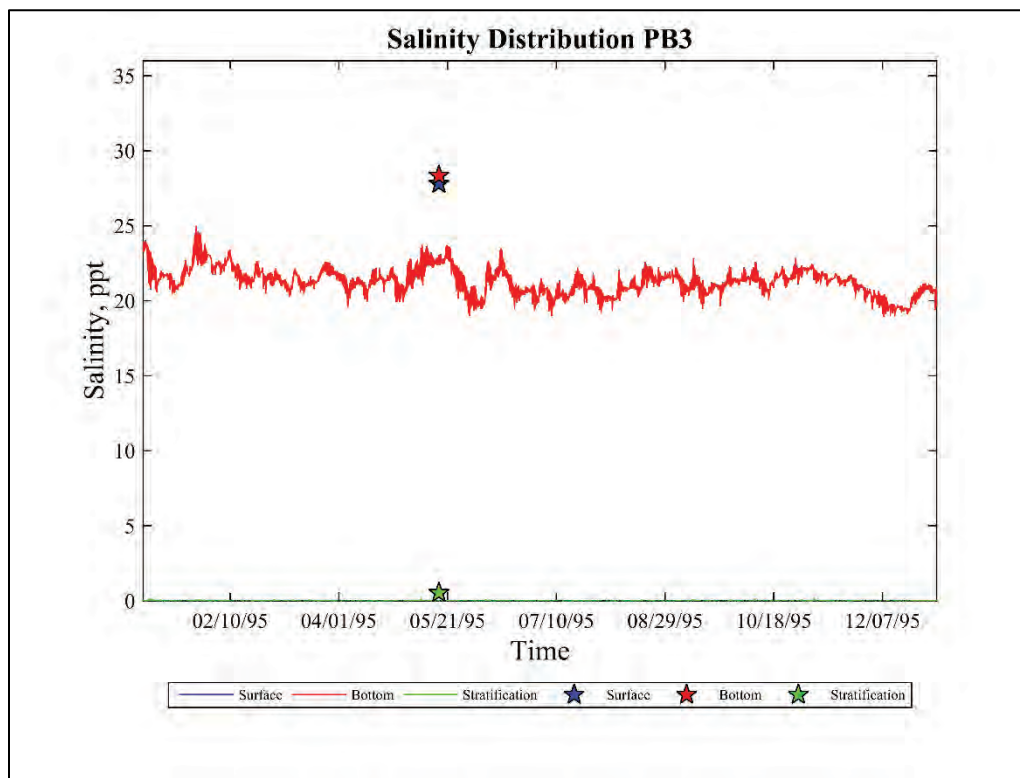




Figure 175. Salinity distribution at PB3.

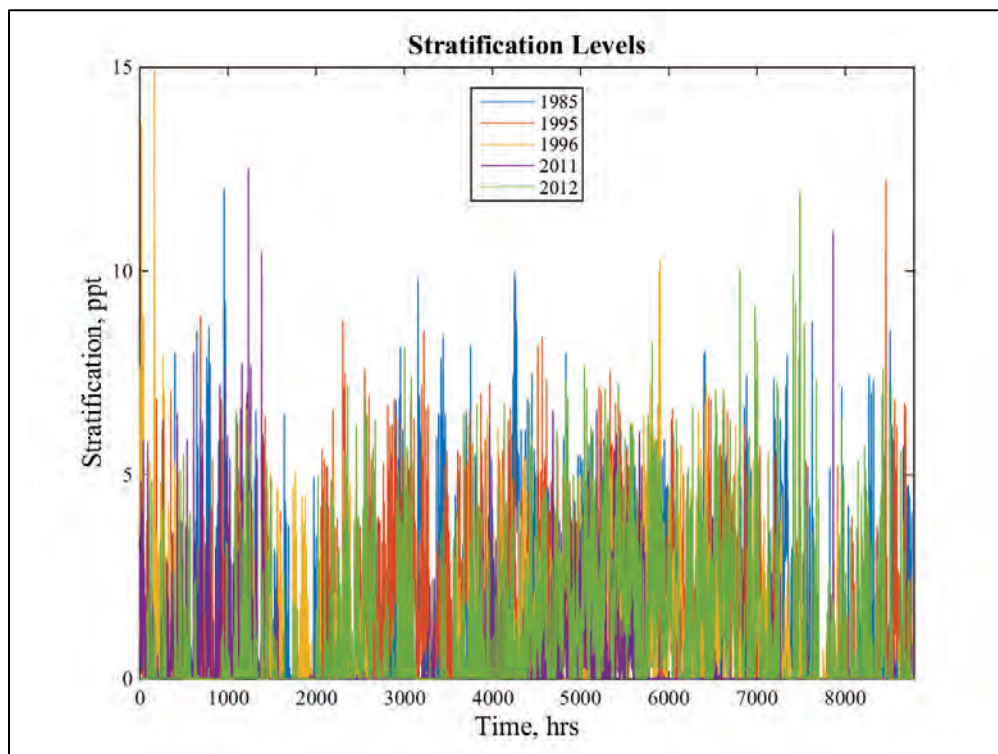


While the absolute surface and bottom salinity values are low in the model as compared to the observations, the stratification levels are adequately replicated. For the purposes of this study, the stratification levels are the primary driver of the density driven circulation that is important for the sediment transport calculations. Therefore the salinity transport results are adequate for the purposes of this study.

### Qualitative comparisons

Geyer et al. (2001) reported the Estuarine Turbidity Maximum (ETM) zone is in the lower Hudson River estuary 10–25 km north of The Battery with stratification levels of 0 to 17 ppt at the ETM location. The plot in Figure 176 shows the stratification levels (bottom – surface salinity) values for the five simulated years at a distance of 18 km north of The Battery for the without-project results. While the salinity stratification never reaches 17 ppt, it does occasionally exceed 10 ppt. These stratification levels could possibly be improved with added resolution going up the Hudson River, but since this was not the purpose of this study, the added resolution and associated computational burden was not justified.

Figure 176. Stratification levels on the Hudson River.



### 3D sediment transport comparisons

Validation of sediment transport models is extremely challenging due to the large uncertainty in the observed results in conjunction with the limited availability of data, both temporally and spatially. It is also highly dependent on previous forcing conditions. As such, sediment transport comparisons are commonly more qualitative in nature.

### Dredge volume comparisons

The primary validation metric for the sediment transport model was to ensure the model adequately reproduced the dredge volumes observed in the field. As previously discussed, the average dredge volumes for particular channel reaches were determined based on historical dredge records. Since the purpose of this study is to determine changes in dredge volumes for the with-project and without-project conditions, comparisons to these dredge volumes is a key component in determining the applicability of this model to address the goals of the study. The assumption was made that any deposition in the navigation channel in a given reach would be dredged even if said deposition did not result in channel bed elevations that exceeded the authorized depths.

The five simulated years were averaged to obtain a single *average* dredge volume for each of the reaches and compared to the historical dredge volumes as shown in Figure 177. The without-project mesh was used for the comparisons to the historical data as it was considered more representative of the conditions during these time periods than the with-project mesh. Figure 86 previously shown in Chapter 6 shows the extents of the reaches utilized in the comparisons in Figure 177.

The model computed variation in dredge volumes for the five simulated years for each of these reaches is shown in Figure 178. Year 2011 possesses extremely high dredge volumes for the Newark Bay reaches. This is due to the high Passaic River flows for that year primarily due to Hurricane Irene, which resulted in the entire system experiencing significantly higher flow rates. The Passaic River in particular experienced a flow of almost 24,000 cfs (675 cms), which was the largest flow since the early 1900s. The specification of the Passaic River bed composition allowed for significant erosion along the river due to the extreme flood event resulting in the extreme sediment supply to Newark Bay for that year. The Hudson River flow during Hurricane Irene was almost 160,000 cfs (4,500 cms), which is also one of the largest flowrates of record for the Hudson River. The accuracy of these results is somewhat suspect given the extreme conditions associated with this event (largest Passaic River discharge since the early 1900s and one of the larger Hudson River discharges) and the already discussed uncertainties in the inflowing sediment concentrations and bed characteristics.

The statistics for the annual model dredging estimates for each channel reach are presented in Figure 179 and Table 14. The minimum, maximum, average, average plus one standard deviation and average minus one standard deviation are included in the figure. The variability is defined as the standard deviation divided by the average, expressed as a percent. The variability ranges from 8% to 88% and averages 42% over all the channel reaches.

Figure 177. Dredge volume comparisons (without project versus historical rates).

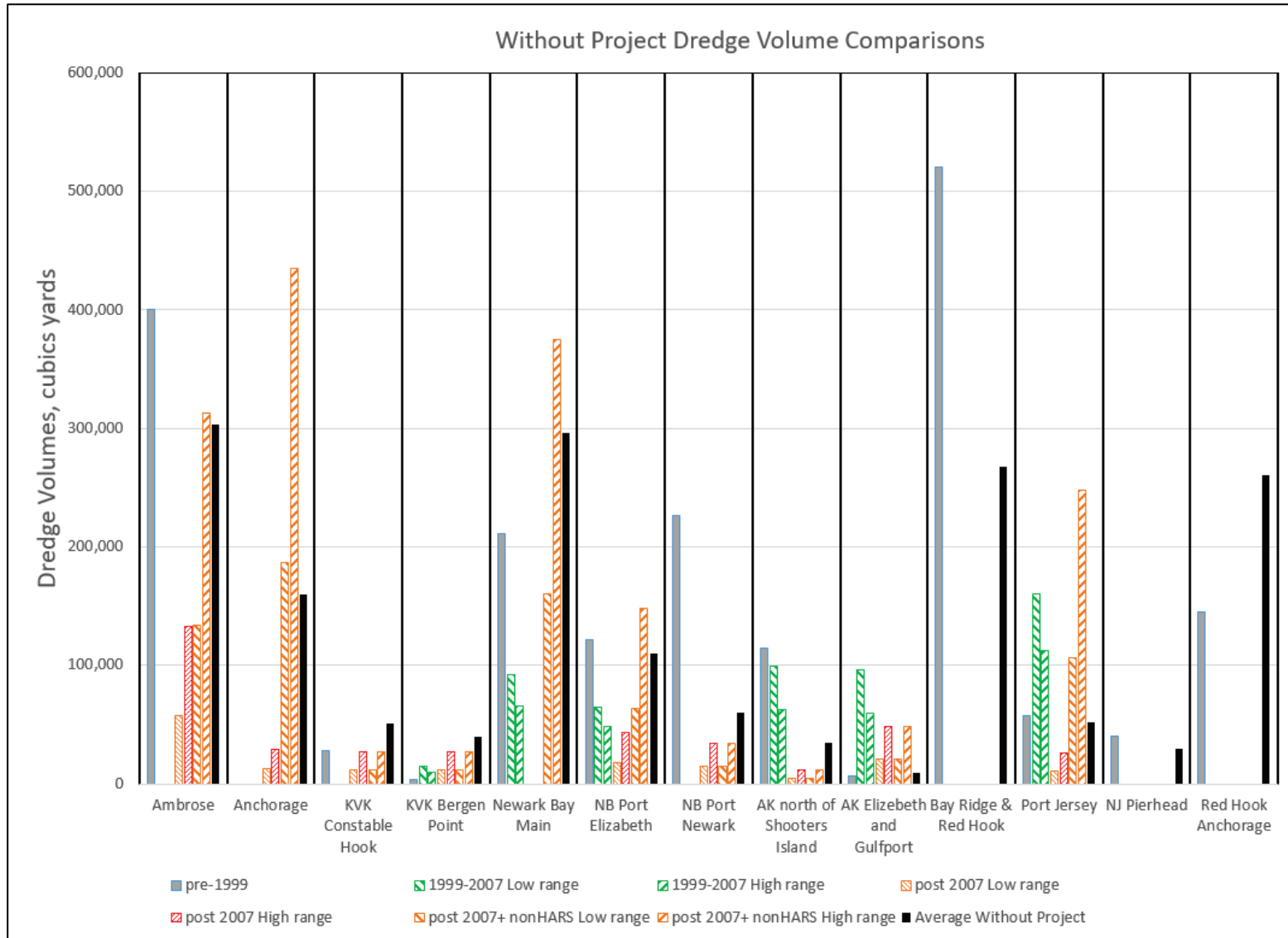


Figure 178. Variation in dredge volumes for the five simulated years (model results).

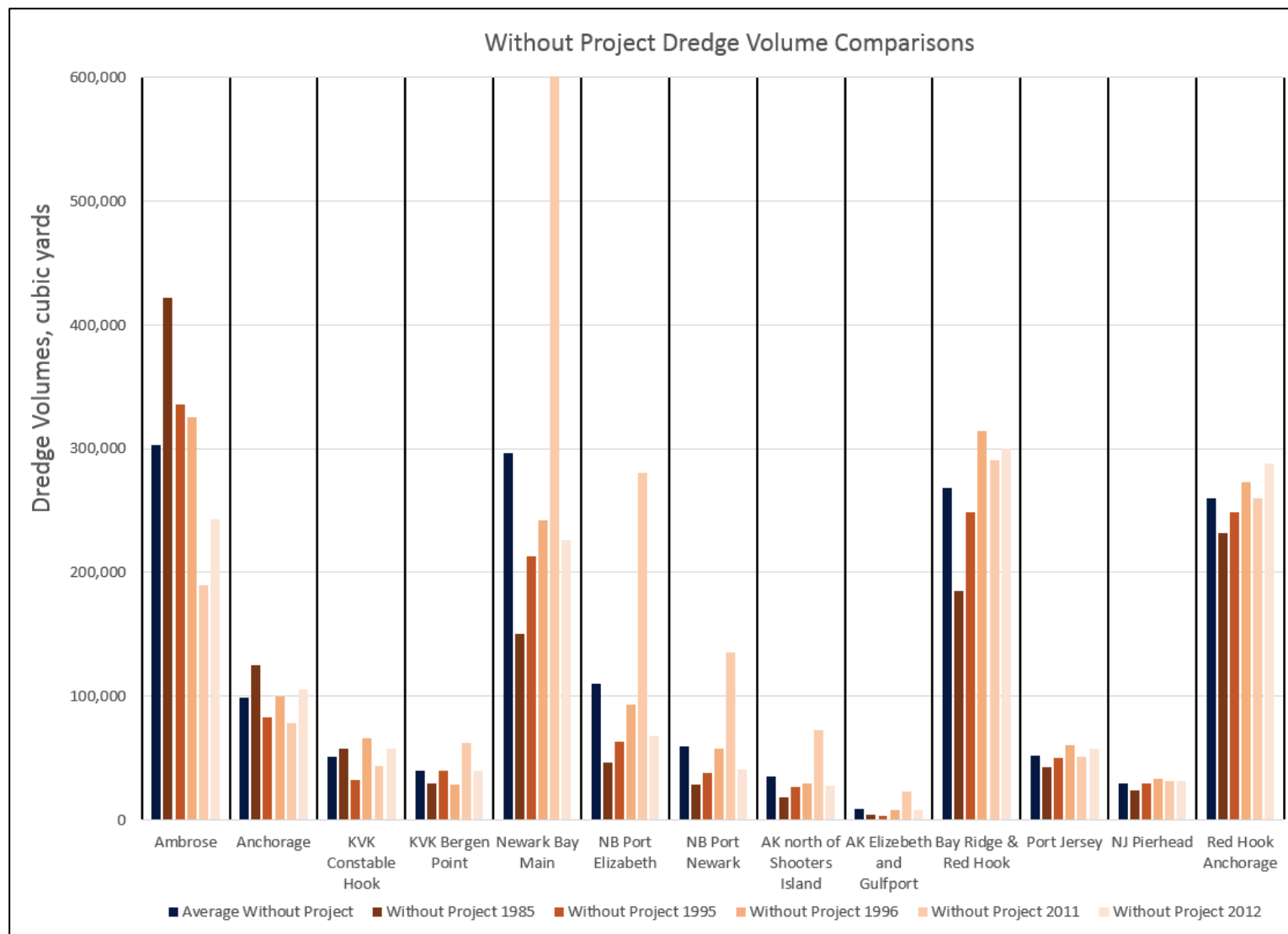


Figure 179. Statistics for the model range of dredging estimates.

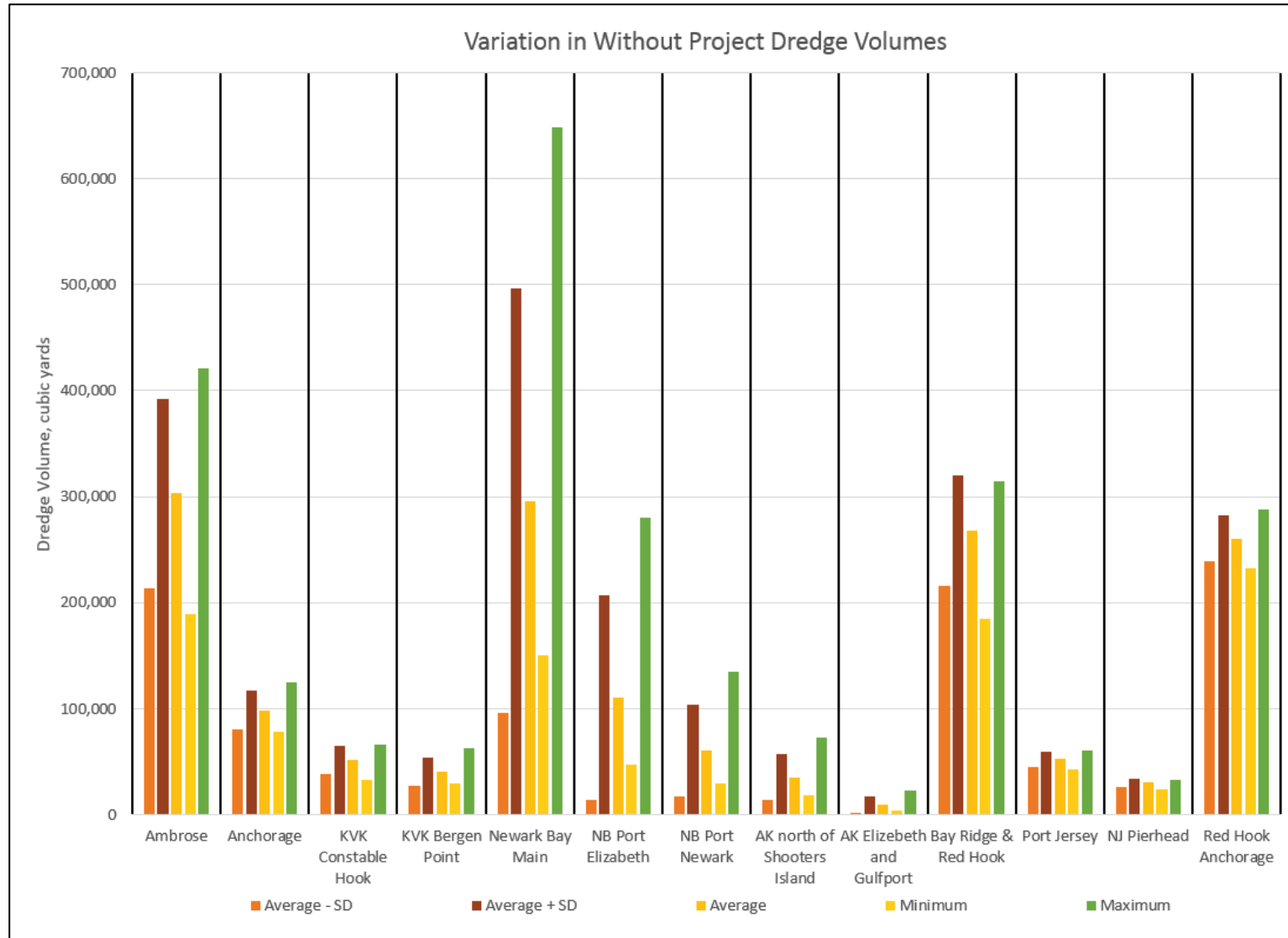




Table 14. Statistics for model estimations of annual dredging volumes in cy.

Channel	Minimum	Maximum	Average	Standard Deviation	Average - Std. Dev.	Average + Std. Dev.	Percent Variability
Ambrose	189,231	421,499	302,938	89,629	213,309	392,567	30
Anchorage	78,489	124,655	98,259	18,588	79,670	116,847	19
Kill van Kull Constable Hook	31,926	65,632	51,302	13,394	37,909	64,696	26
Kill van Kull Bergen Point	28,599	61,998	39,840	13,407	26,433	53,247	34
Newark Bay (NB) Main	150,510	648,677	296,064	200,147	95,917	496,211	68
NB Port Elizabeth	46,599	280,325	110,043	96,618	13,425	206,661	88
NB Port Newark	28,605	134,982	59,791	43,275	16,516	103,066	72
AK north of Shooters Island	18,194	72,937	35,082	21,624	13,458	56,706	62
AK Elizabeth and Gulfport	3,625	22,958	9,198	7,958	1,240	17,156	87
Bay Ridge & Red Hook	184,952	314,602	267,907	52,482	215,425	320,389	20
Port Jersey	42,073	60,549	52,147	7,124	45,024	59,271	14
NJ Pierhead	23,844	32,828	29,843	3,556	26,287	33,399	12
Red Hook Anchorage	231,985	287,755	260,258	21,558	238,700	281,816	8

## Sediment core comparisons

The New York District collected some sediment cores during 2012. These are point location data and as such are less likely to provide favorable model to field comparisons due to the model being inherently less accurate at a particular spatial and temporal point. Since the sediment results at a location can be very dependent on the previous forcing conditions in the system, these observations were compared to both the 2011 and 2012 model simulations. The sediment breakdown (fines versus sands) for the entire 2011 and 2012 years are plotted versus the single core observation at the points in Figure 180 (comparisons in Figure 181 to Figure 183), Figure 184 (comparisons in Figure 185 to Figure 187), Figure 188 (comparisons in Figure 189 to Figure 191), and Figure 192 (comparisons in Figure 193 and Figure 194). Comparisons for the remaining locations are provided in Appendix C.

The figures include a breakdown of the accumulated sediment (labeled “Model Fines” and “Model Sands” along with the distribution of the superficial bed sediment composition (“Model Fines (Top)” and “Model Sands (Top)”). The superficial results would be equivalent to a surface grab comparison and are included to illustrate the variability in the surface sediment distributions. The “sediment ratio” is defined as the percentage of the size fraction for the fines and the sands.

There is a distinct difference in the model results for 2011 as opposed to 2012. This is due to 2011 being a much higher flow year than 2012. In reality, the higher-than-normal 2011 flows impacted the 2012 bed distributions, but in these model results, 2011 had no impact on the 2012 results and as such could explain why 2011 compares much better to the observations in Newark Bay. Note that extreme events can significantly alter the bed composition at a location. This is evident in the model results for Hurricane Irene in 2011 and Hurricane Sandy in 2012.

For times/locations that possess no deposited sediment, the sediment ratio is set to 50%.

Figure 180. Sediment core locations in Upper Bay.

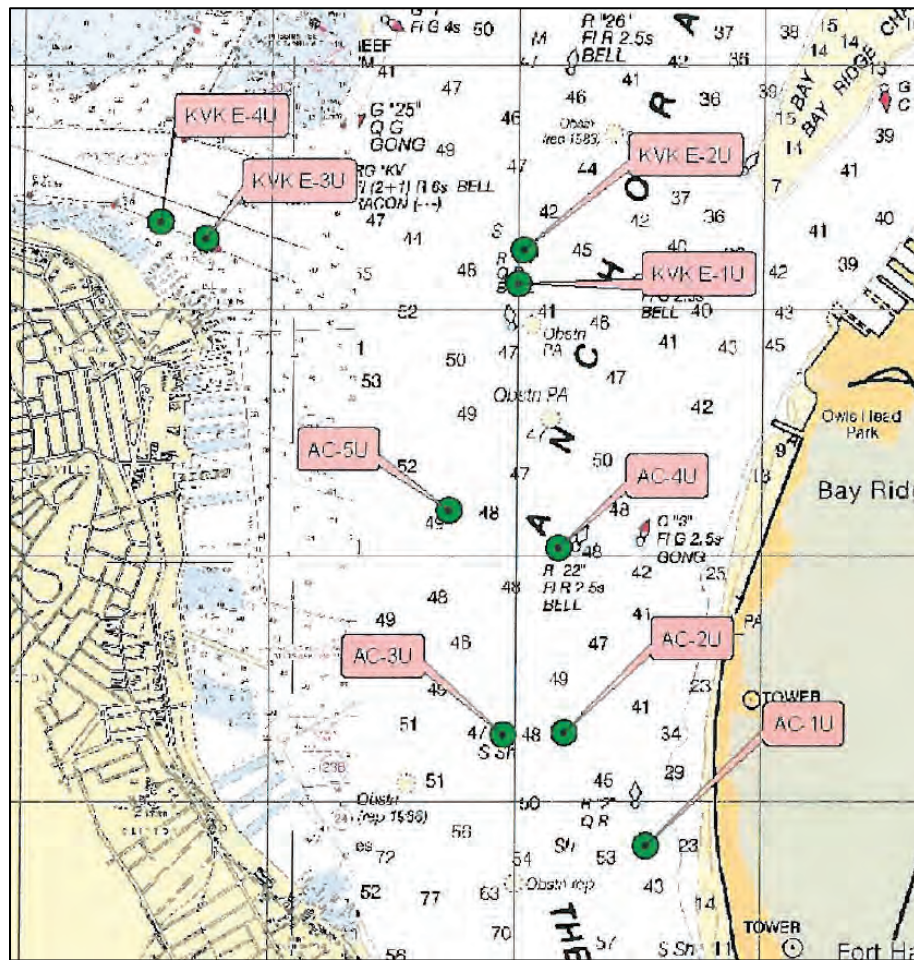


Figure 181. Sediment bed composition comparisons at Location A-2U for 2011 (top) and 2012 (bottom).

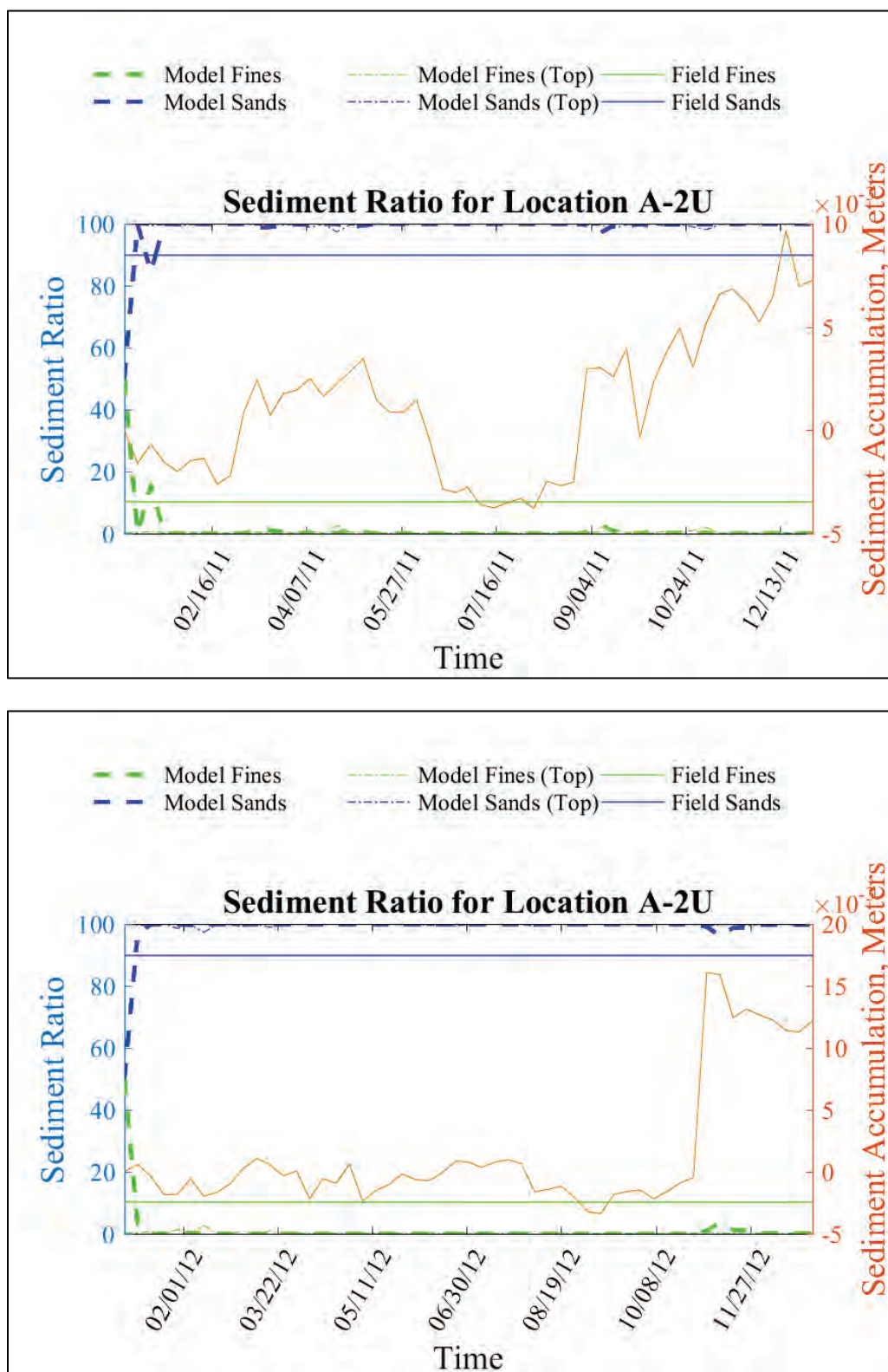


Figure 182. Sediment bed composition comparisons at Location E-1U for 2011 (top) and 2012 (bottom).

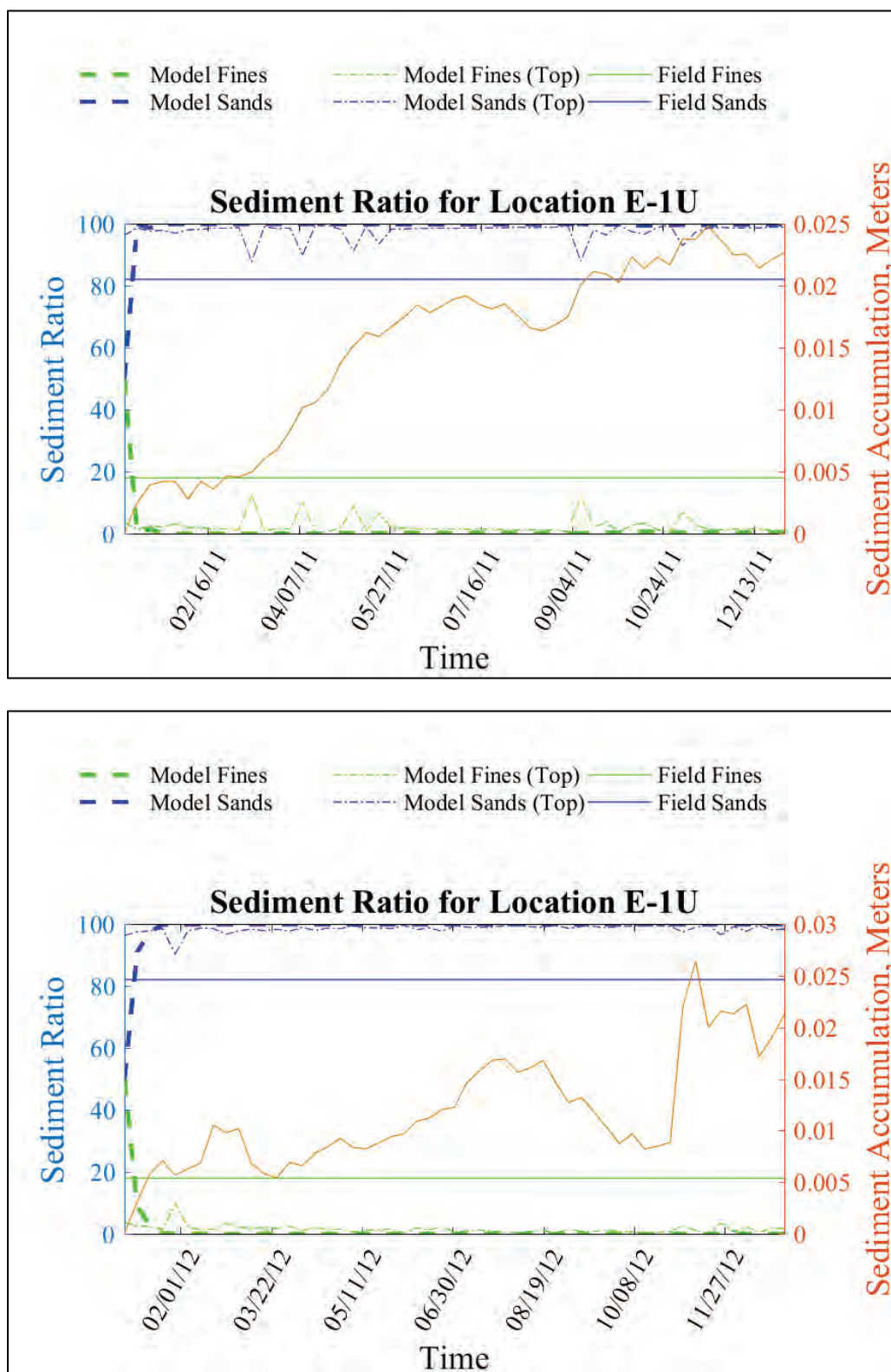
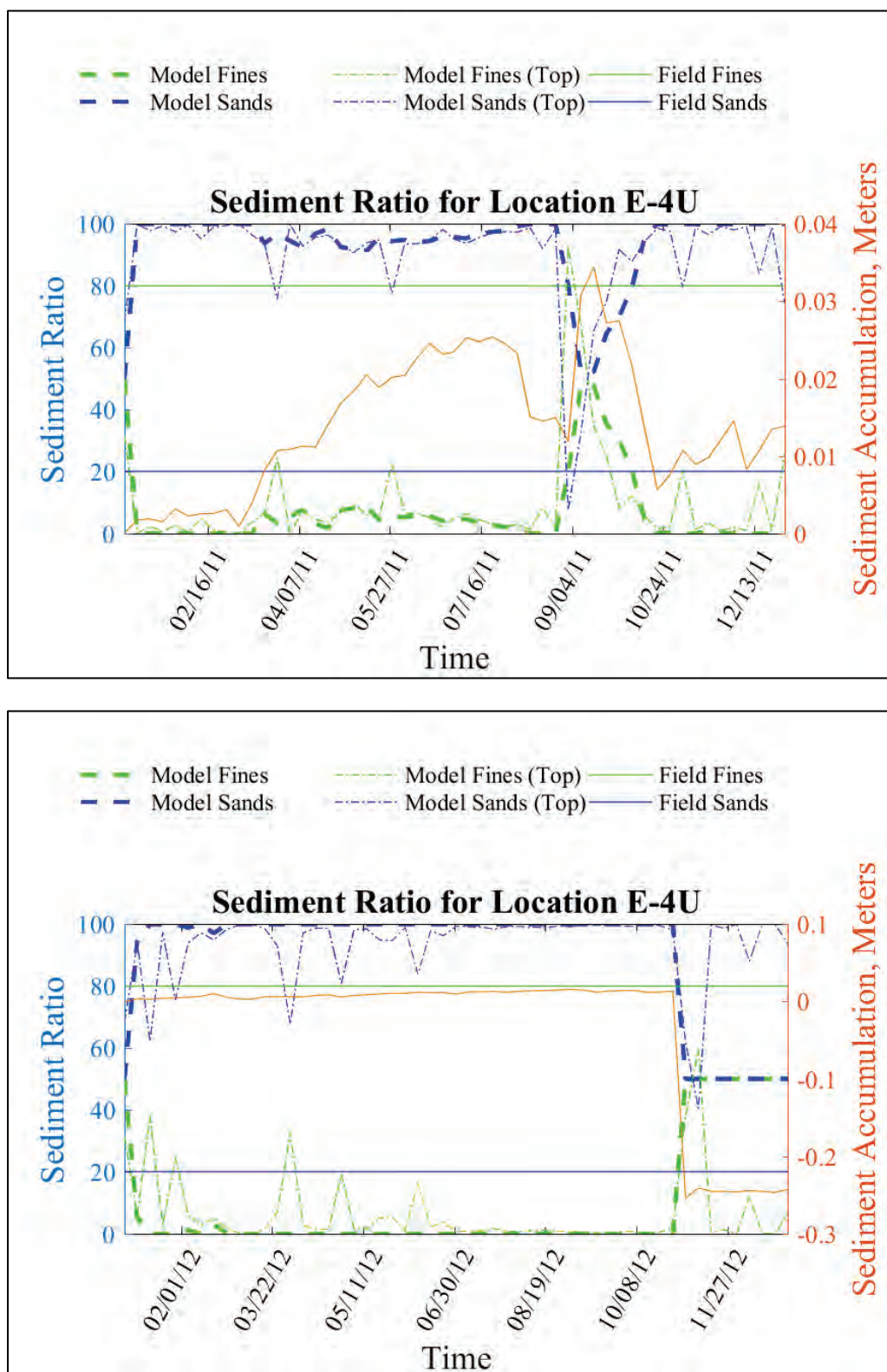




Figure 183. Sediment bed composition comparisons at Location E-4U for 2011 (top) and 2012 (bottom).





**Figure 184. Sediment core locations in western Kill van Kull and southern Newark Bay.**

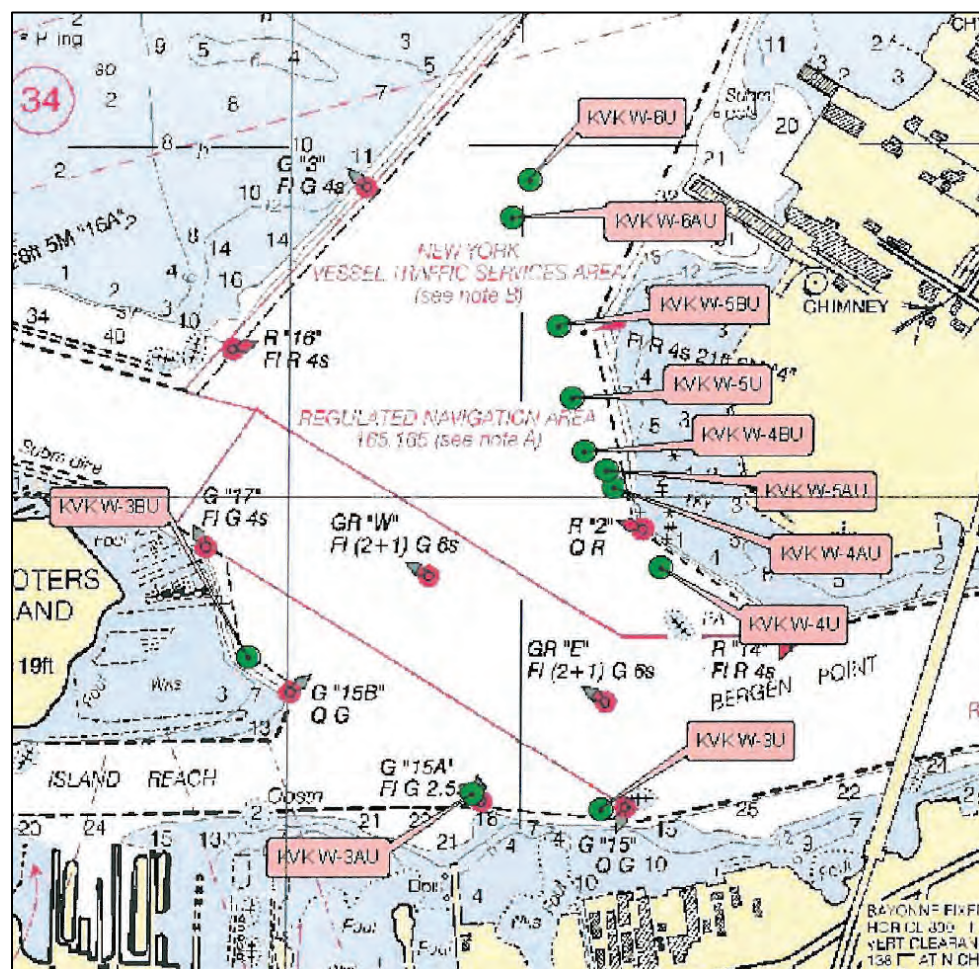


Figure 185. Sediment bed composition comparisons at Location W-4BU for 2011 (top) and 2012 (bottom).

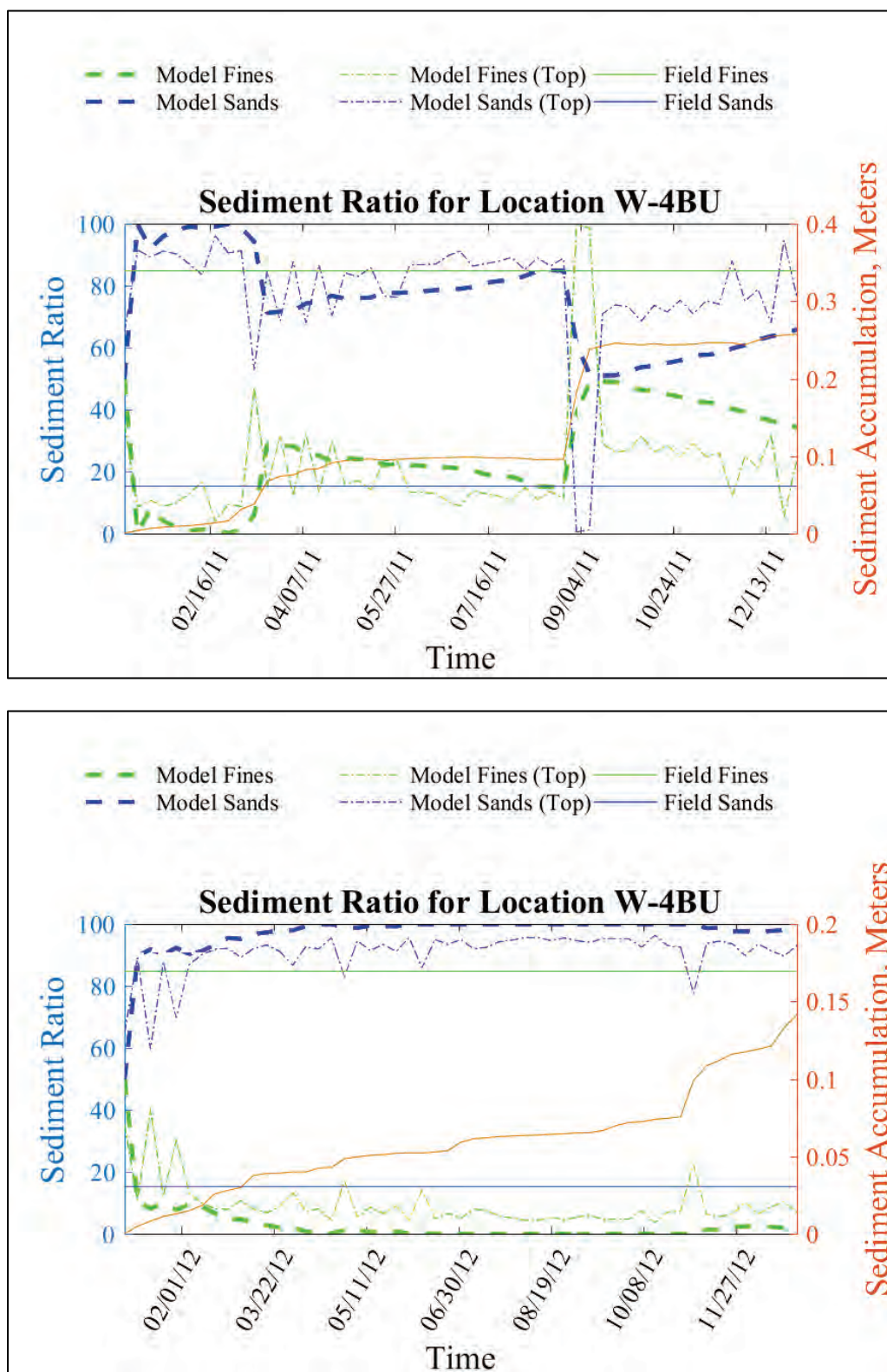


Figure 186. Sediment bed composition comparisons at Location W-6AU for 2011 (top) and 2012 (bottom).

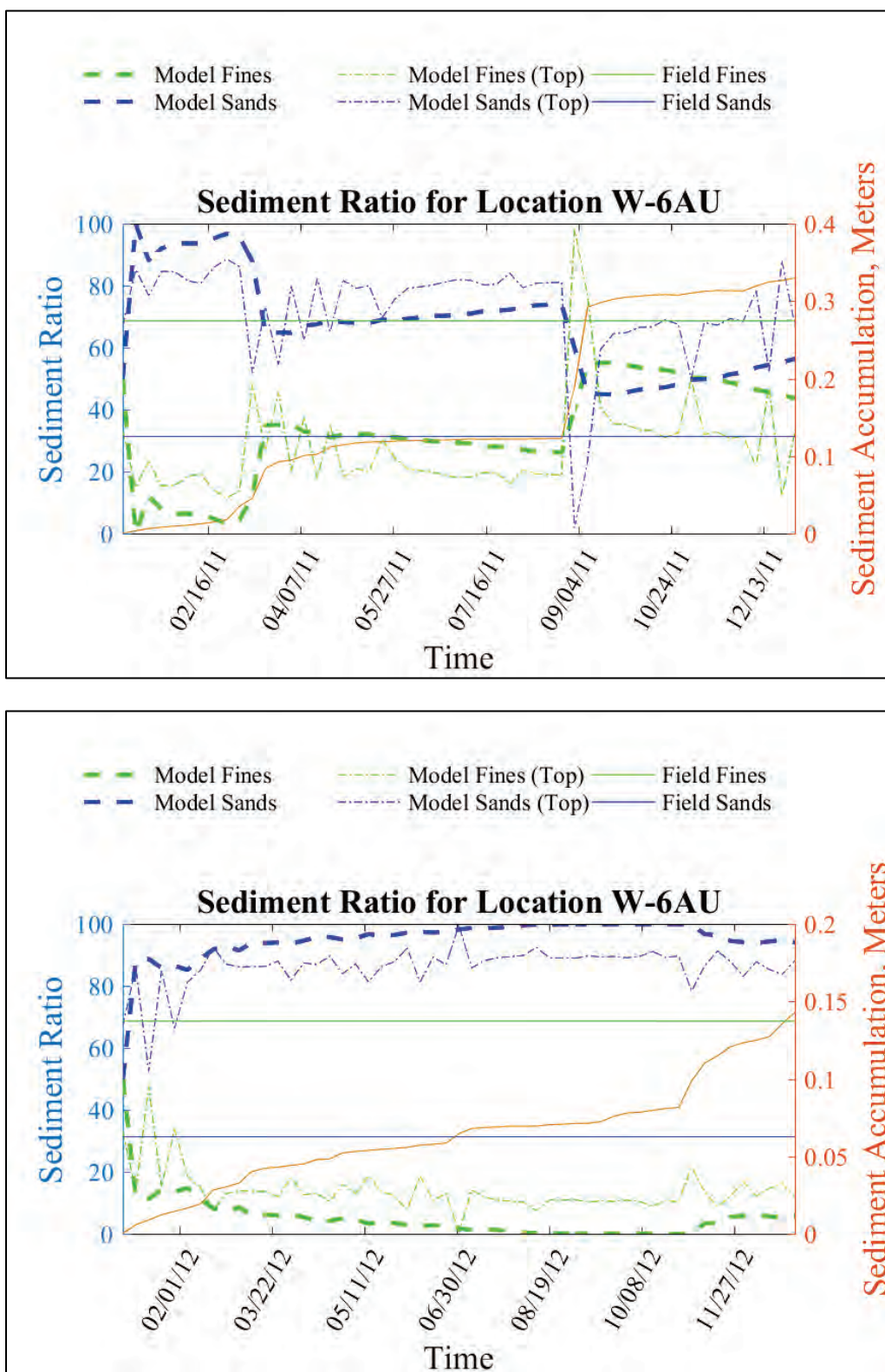




Figure 187. Sediment bed composition comparisons at Location W-3AU for 2011 (top) and 2012 (bottom).

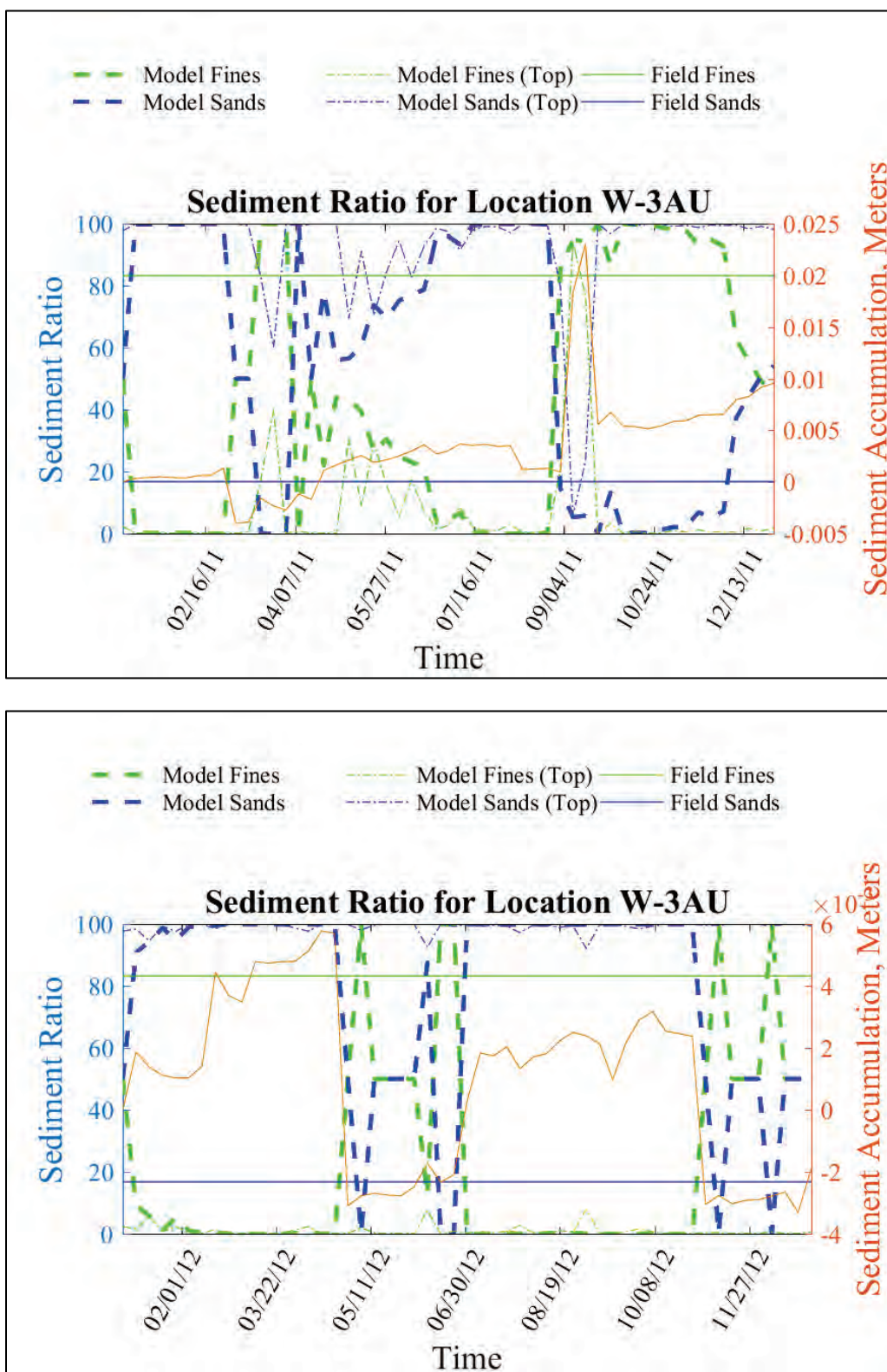


Figure 188. Sediment core locations in Newark Bay.

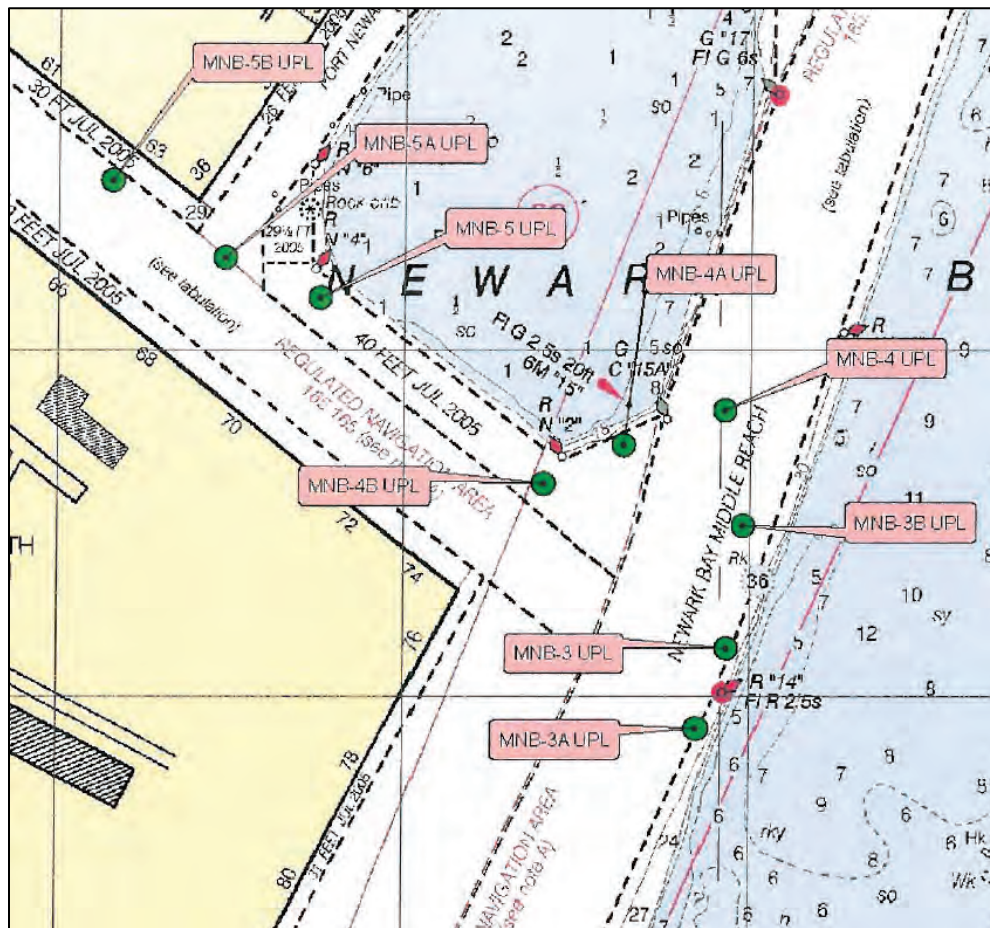


Figure 189. Sediment bed composition comparisons at Location MNB-3 for 2011 (top) and 2012 (bottom).

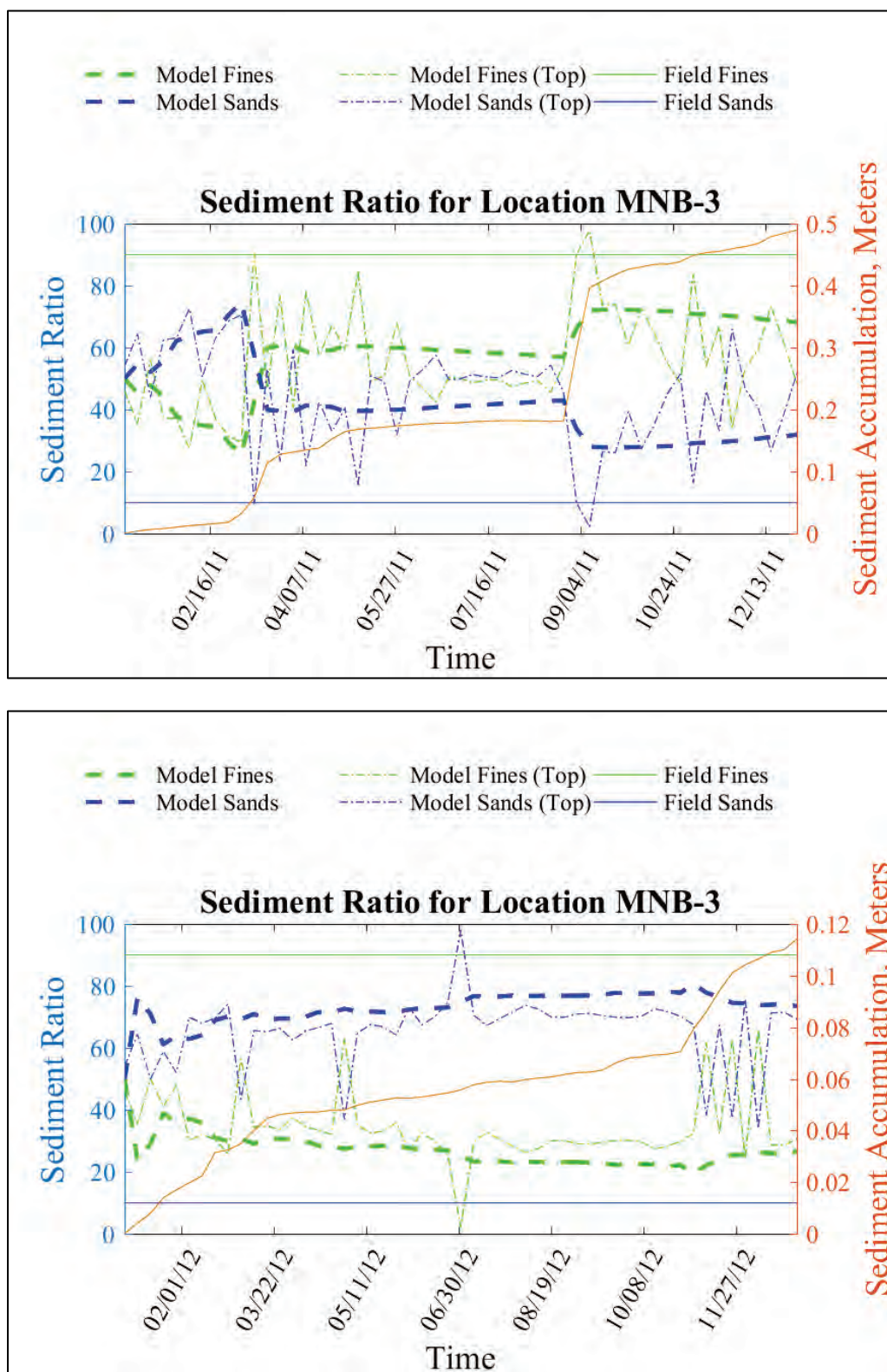




Figure 190. Sediment bed composition comparisons at Location MNB-4B for 2011 (top) and 2012 (bottom).

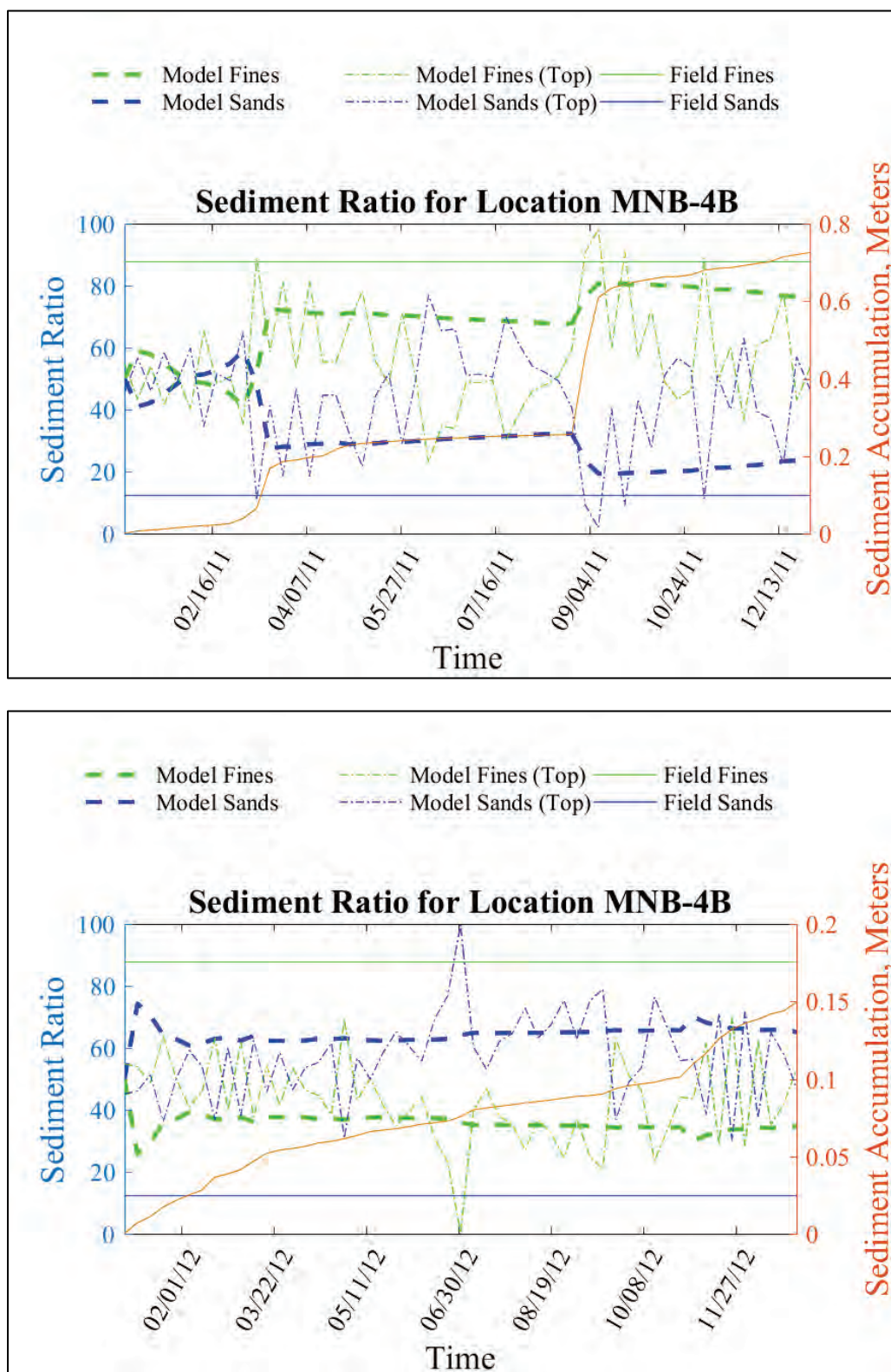


Figure 191. Sediment bed composition comparisons at Location MNB-5A for 2011 (top) and 2012 (bottom).

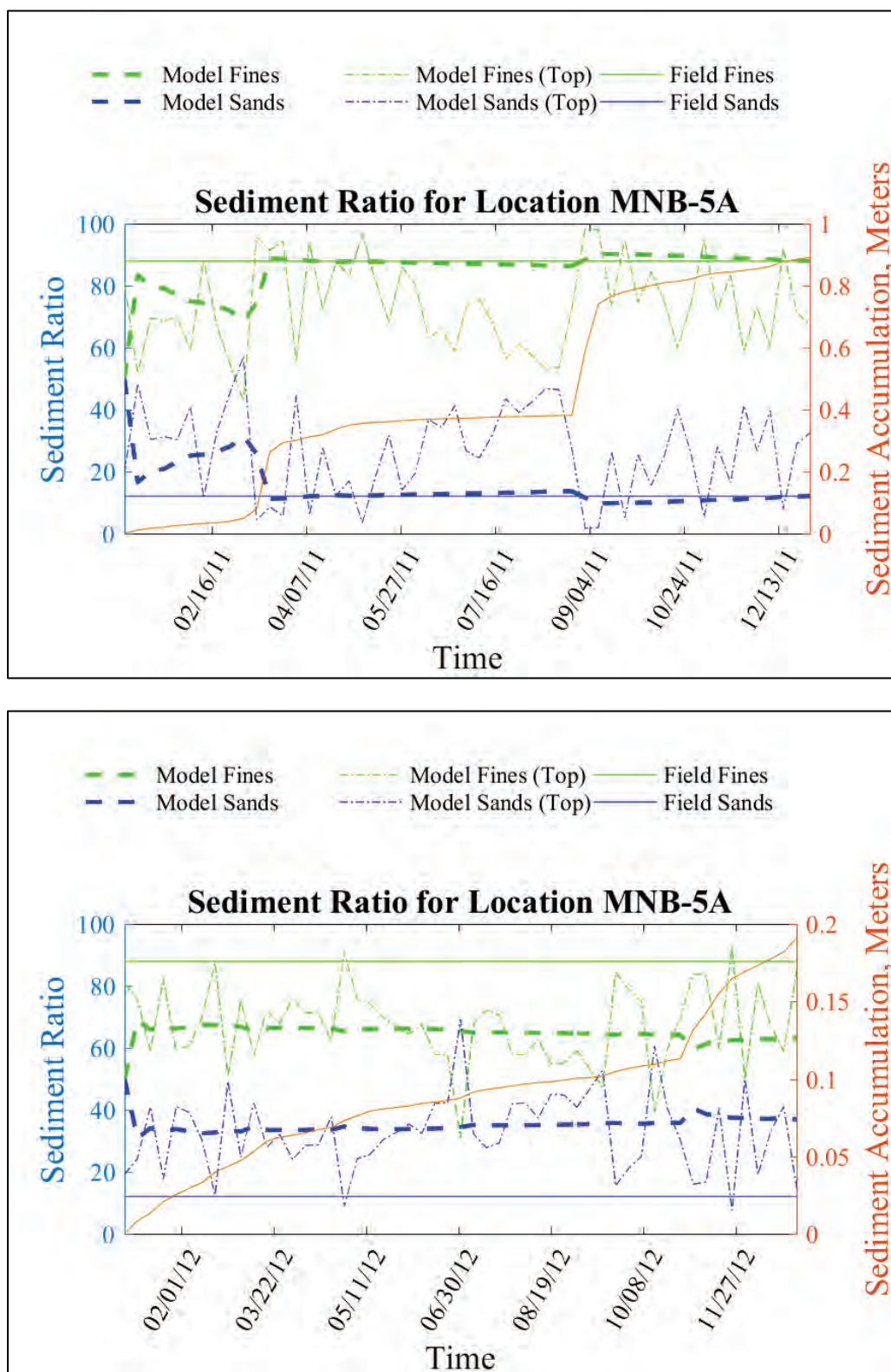






Figure 193. Sediment bed composition comparisons at Location PJ-1 for 2011 (top) and 2012 (bottom).

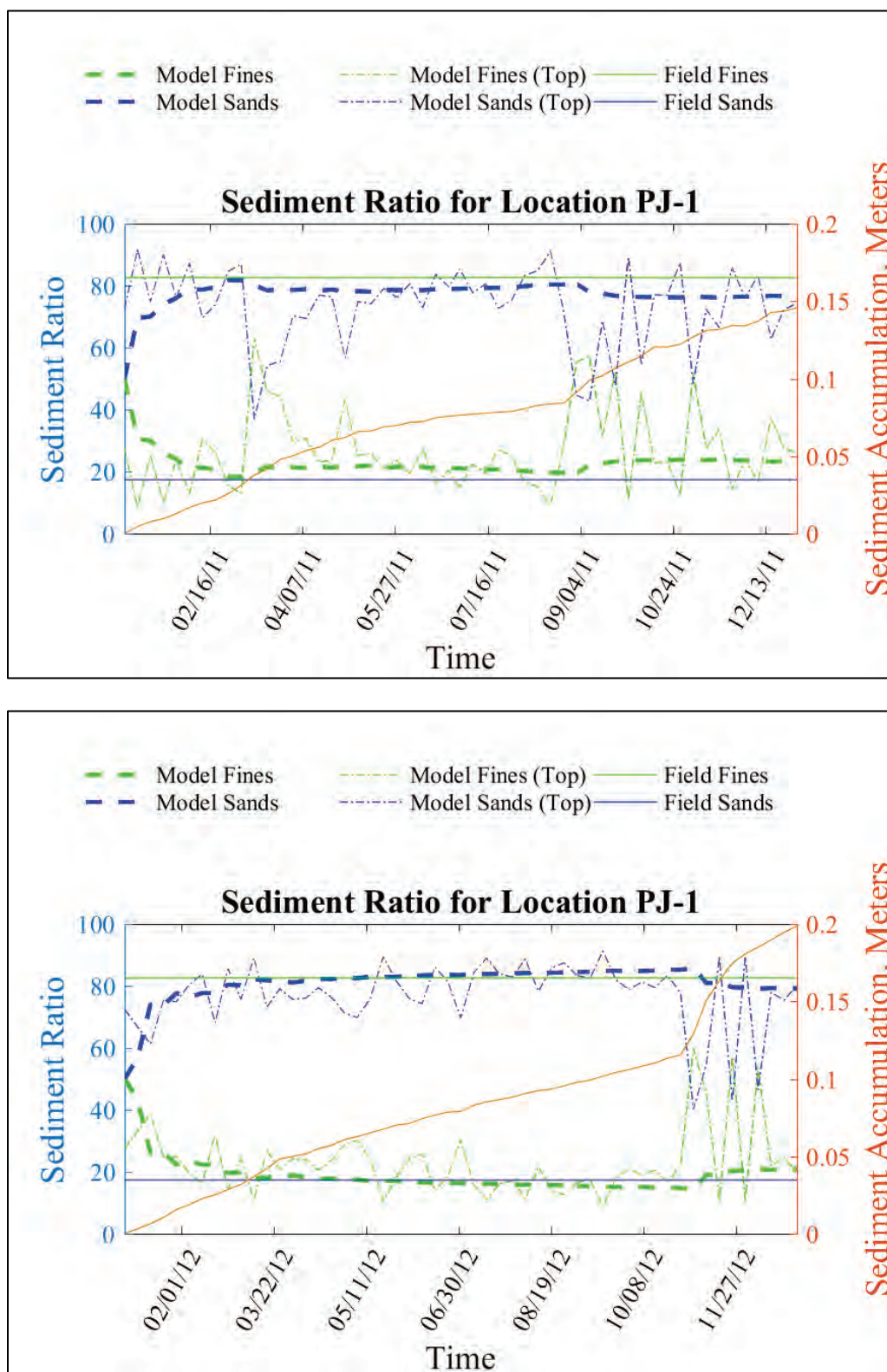
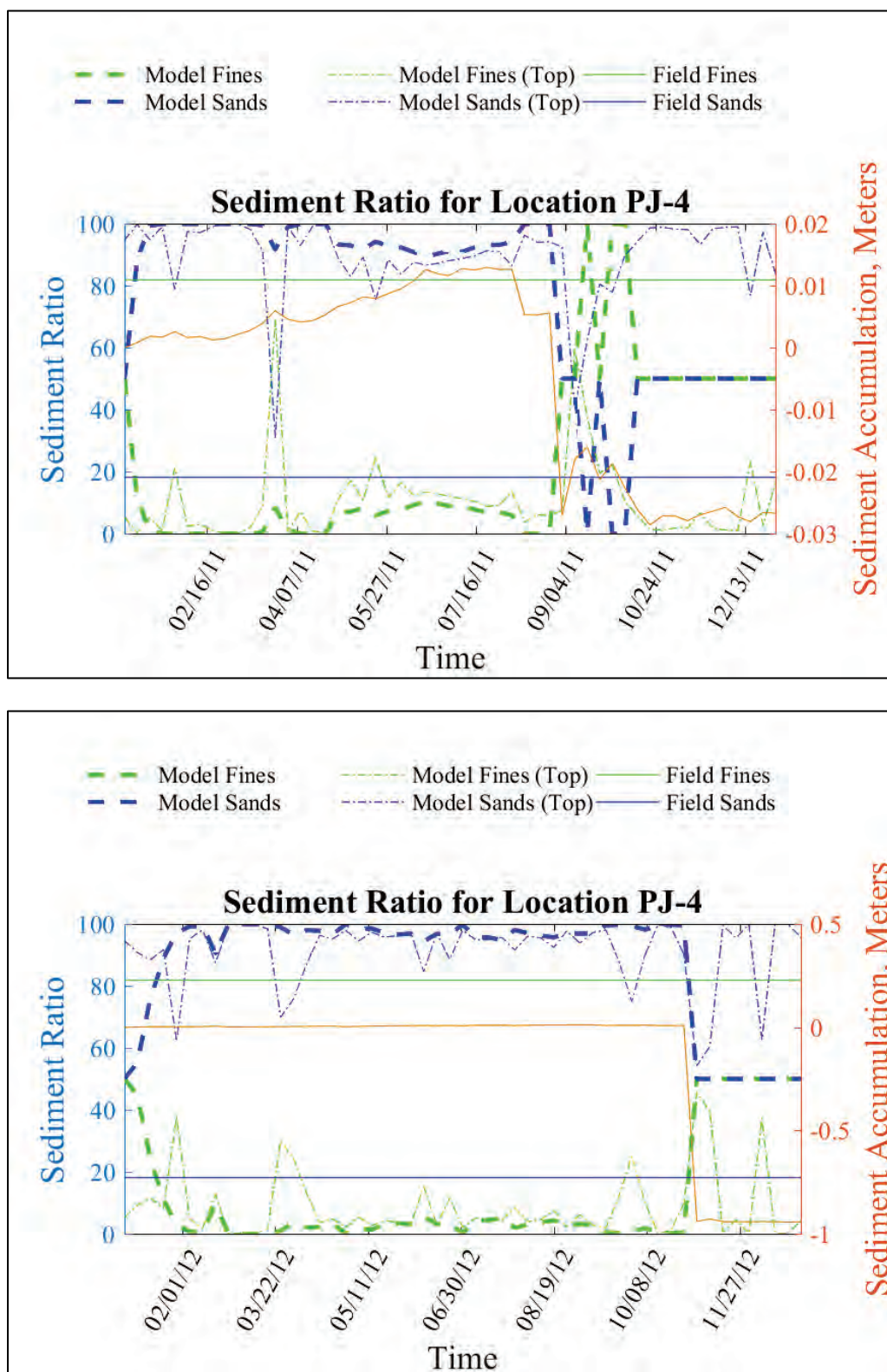


Figure 194. Sediment bed composition comparisons at Location PJ-4 for 2011 (top) and 2012 (bottom).





### Qualitative sediment flux comparisons

From the literature, there are several reports of various sediment fluxes up and down the Hudson River, through the Kill van Kull, and through the Narrows. While these values are not for the periods simulated in the model, comparisons can be performed to determine if the results are consistent with the simulated results.

#### *Hudson River sediment loads*

There are various sediment transport estimates for the Hudson River. Panuzio (1965), Olsen (1979), and Wall et al. (2008) estimated ranges of Hudson River sediment loads of 0.2 to 1.0 Megatons (1 million metric tons). Woodruff et al. (2001) estimated 560,000 metric tons delivered by the Hudson River in 1998 and 120,000 metric tons in 1999. Obviously, this provides a very wide range of estimates and the model values in Table 15 indicate a similarly broad range of values over the five simulated years. The majority of the Hudson River sediment load is fine sediment, but the values reported in Table 15 include sand transport as well.

Table 15. Hudson River sediment loads for the simulated years.

Year	Without-Project Sediment Load, metric tons	With-Project Sediment Load, metric tons
1985	83,000	85,000
1995	111,000	111,000
1996	647,000	645,000
2011	932,000	927,000
2012	170,000	168,000

The literature also discusses sand moving up the Hudson River on the east side of the Hudson River while fine sediment moves down the river (Coch, 2016). Geyer and Chant (2006) have shown that this up-estuary transport (sands) extends northward at least to the George Washington Bridge. The sand load was extracted from the model results for the two locations shown in Figure 195. The bottom line represents the location of the George Washington Bridge. The sand transport values up the Hudson River are provided in Table 16. Calendar years 1996 and 2011 have a net export of sand from the Hudson River. This is not unexpected as these 2 years were



above-average flow years (see Figure 37). The remaining 3 years are consistent with the reported behavior in the literature.

Figure 195. The black lines represent extracted sand transport locations. The lower black line is at the George Washington Bridge.

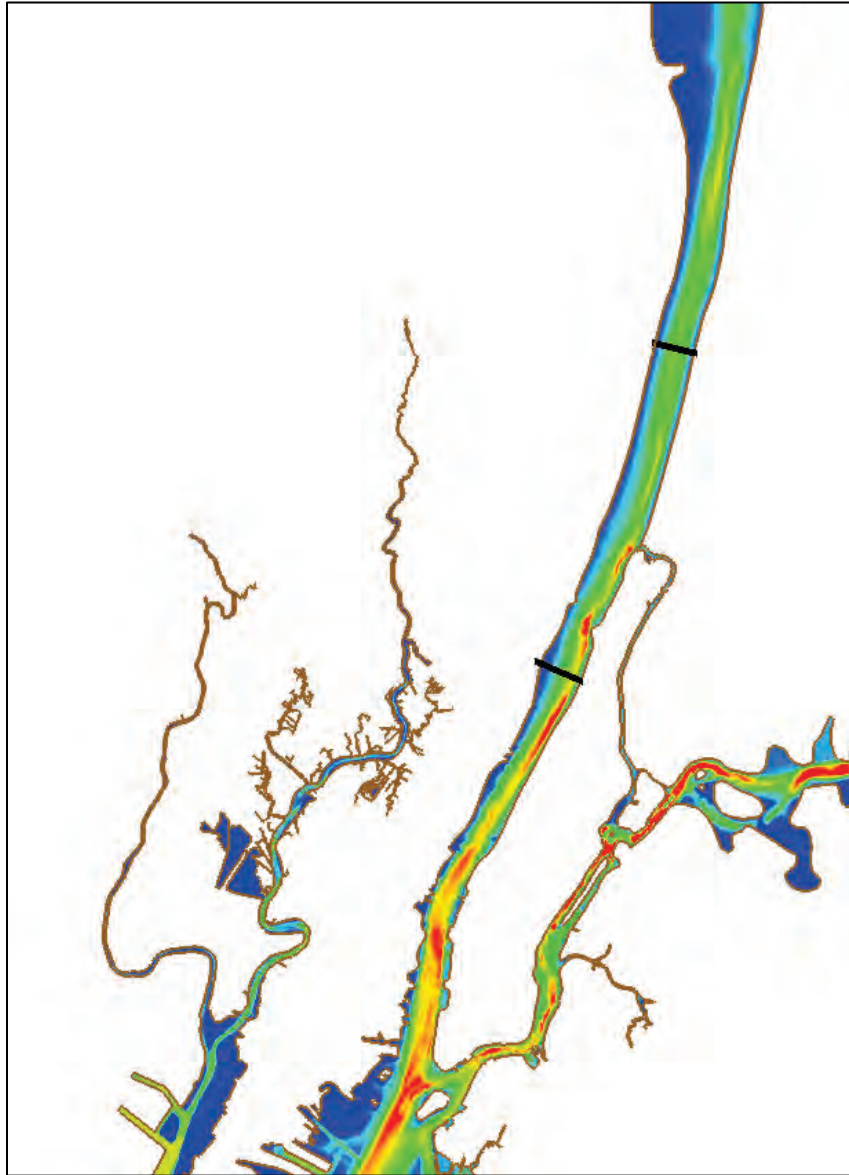


**Table 16. Sand transport up the Hudson River Estuary (negative indicates downward transport).**

Sand Transport in the Hudson River at the George Washington Bridge. Values in parentheses are the location farther upstream.		
Year	Without-Project Sand Load, metric tons	With-Project Sand Load, metric tons
1985	29,000(26,000)	29,000(25,000)
1995	12,000(19,000)	13,000(19,000)
1996	-2,600(1,200)	-3,100(1,900)
2011	-7,600(-3,000)	-7,900(90)
2012	21,000(15,000)	23,000(16,000)

#### *Kill van Kull sediment loads*

Several studies have been completed attempting to quantify the sediment load traveling through Kill van Kull (from Upper Bay toward Newark Bay). Pecchioli et al. (2006) estimated approximately 100,000 MT/year of suspended sediment through Kill van Kull. Chant (2006) reported transport of between 120,000 and 200,000 MT/year using data collected in 2002, and Shrestha et al. (2014) reported Kill van Kull transport of 140,000 MT/year. This indicates an acceptable range of approximately 100,000 MT/year to 200,000 MT/year, although this would vary depending on the Hudson River flow conditions. These yearly transport rates are also based on shorter-term observations providing some level of uncertainty in the reported values.

The total sediment load through Kill van Kull in the numerical model results is provided in Table 17. These results indicate 1985, 1995, and 2012 as slightly below the reported values with 1996 and 2011 in the range of the reported values. This is not unexpected as 1985, 1995, and 2012 are below average flow years for the Hudson River (Figure 37). It is also assumed the Pecchioli et al. (2006) and Chant (2006) data are more applicable for comparing to the without-project results and the Shrestha et al. (2014) would be more appropriate to compare to the with-project results as the majority of the project had been completed prior to 2014. The majority of the sediment load traveling through the Kill van Kull is fine sediment, but there is a sand component as well.

Table 17. Kill van Kull total sediment load for the simulated years.

Year	Without-Project Total Sediment Load, metric tons	With-Project Total Sediment Load, metric tons
1985	48,000	67,000
1995	60,000	78,000
1996	110,000	144,000
2011	54,000	121,000
2012	73,000	96,000

*Passaic and Hackensack sediment loads*

Shrestha et al. (2014) compiled a table of sediment load values for the Passaic and Hackensack Rivers from other sources in the literature that ranged from a low of 7,440 MT/year to as high as 47,456 MT/year with an average of 25,661 MT/year. The total model sediment load being delivered to Newark Bay from the Passaic and Hackensack Rivers is provided in Table 18. The 2011 results are extremely high and would appear to be somewhat unrealistic. From further analysis of the results for the 2011 calendar year, the inflow specification included approximately 175,000 MT with the remaining being sourced from the bed. This large bed sourced load indicates the model bed specification in the Passaic and Hackensack Rivers may not have been appropriate for such an extreme event but currently it is unknown if the model is greatly overestimating the sediment delivery for 2011 or if this year was actually that extreme in relation to the other four simulated years. This model definition also explains the large variation in the previously shown dredge volumes in Newark Bay for 2011 (Figure 178).

Table 18. Passaic and Hackensack River total sediment load into Newark Bay for the simulated years.

Year	Without-Project Total Sediment Load, metric tons	With-Project Total Sediment Load, metric tons
1985	31,000	31,000
1995	41,000	43,000
1996	87,000	87,000
2011	444,000	438,000
2012	33,000	33,000

## **9 With-Project and Without-Project Comparisons**

The with-project versus without-project comparisons were broken up into areas consisting of Lower Bay (Figure 196 to Figure 203 and Table 19); Newark Bay, Kill van Kull and Upper Bay (Figure 204 to Figure 211 and Table 20); and Arthur Kill and Raritan Bay (Figure 212 to Figure 219 and Table 21). The analysis consisted primarily of comparing the yearly averages for shear stresses, salinities, sediment concentrations, bed change, and dredge volumes for the channel reaches provided by CENAN. The results provided in Chapter 9 are the average values for the 1995 calendar year. The results for the remaining years are provided in Appendix D (1985), Appendix E (1996), Appendix F (2011), and Appendix G (2012). Difference plots of the shear stresses, salinities, and sediment concentrations for all years are provided in Appendix H. The black lines in the images represent the channel reaches as supplied by CENAN. While comparisons of the absolute values across multiple years do indicate variations in the results, the patterns tend to be consistent.

## Lower Bay results

Figure 196. Without-project (top) and with-project (bottom) average shear stresses, Pa (1995).

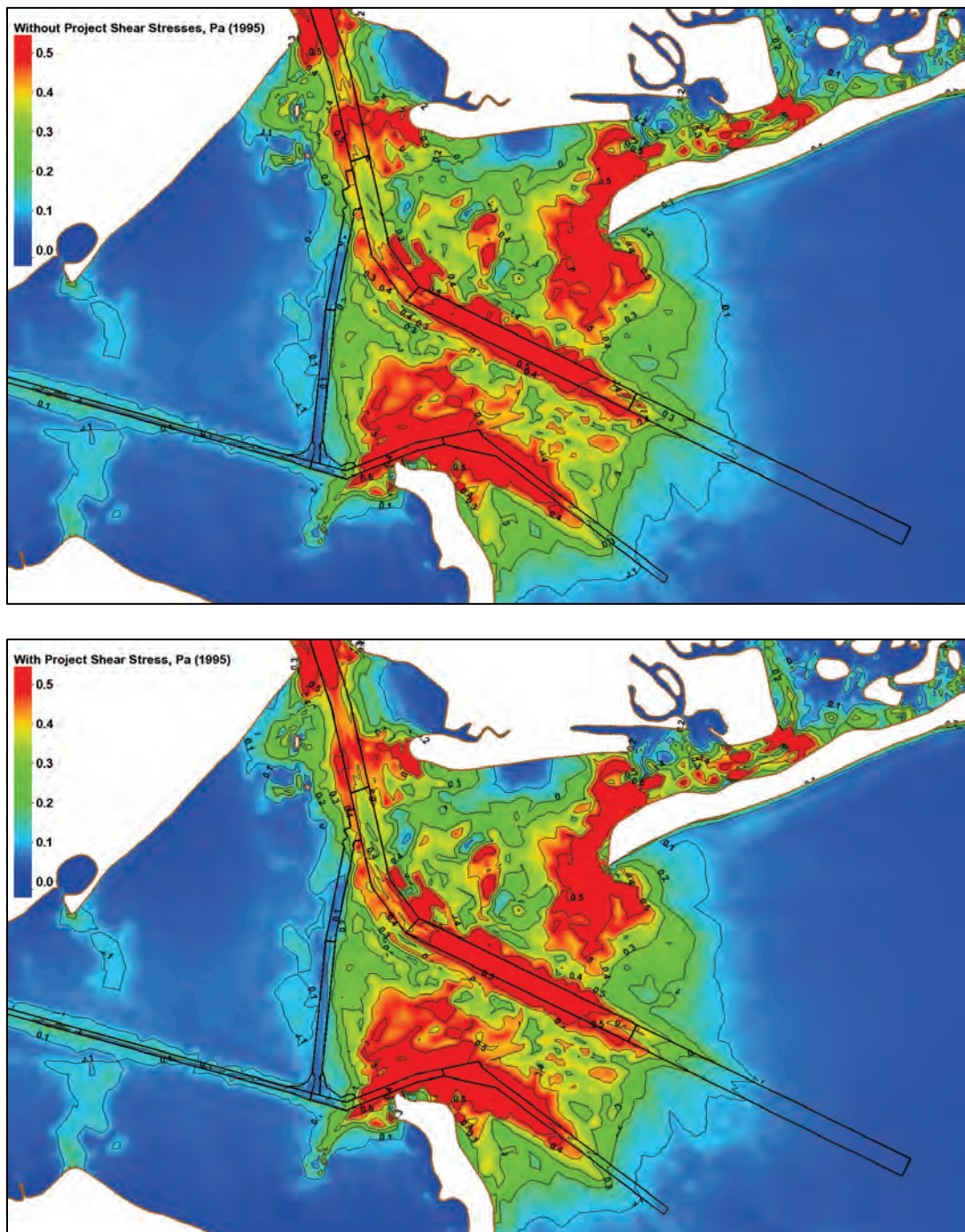




Figure 197. Without-project (top) and with-project (bottom) average bottom salinity, ppt (1995).

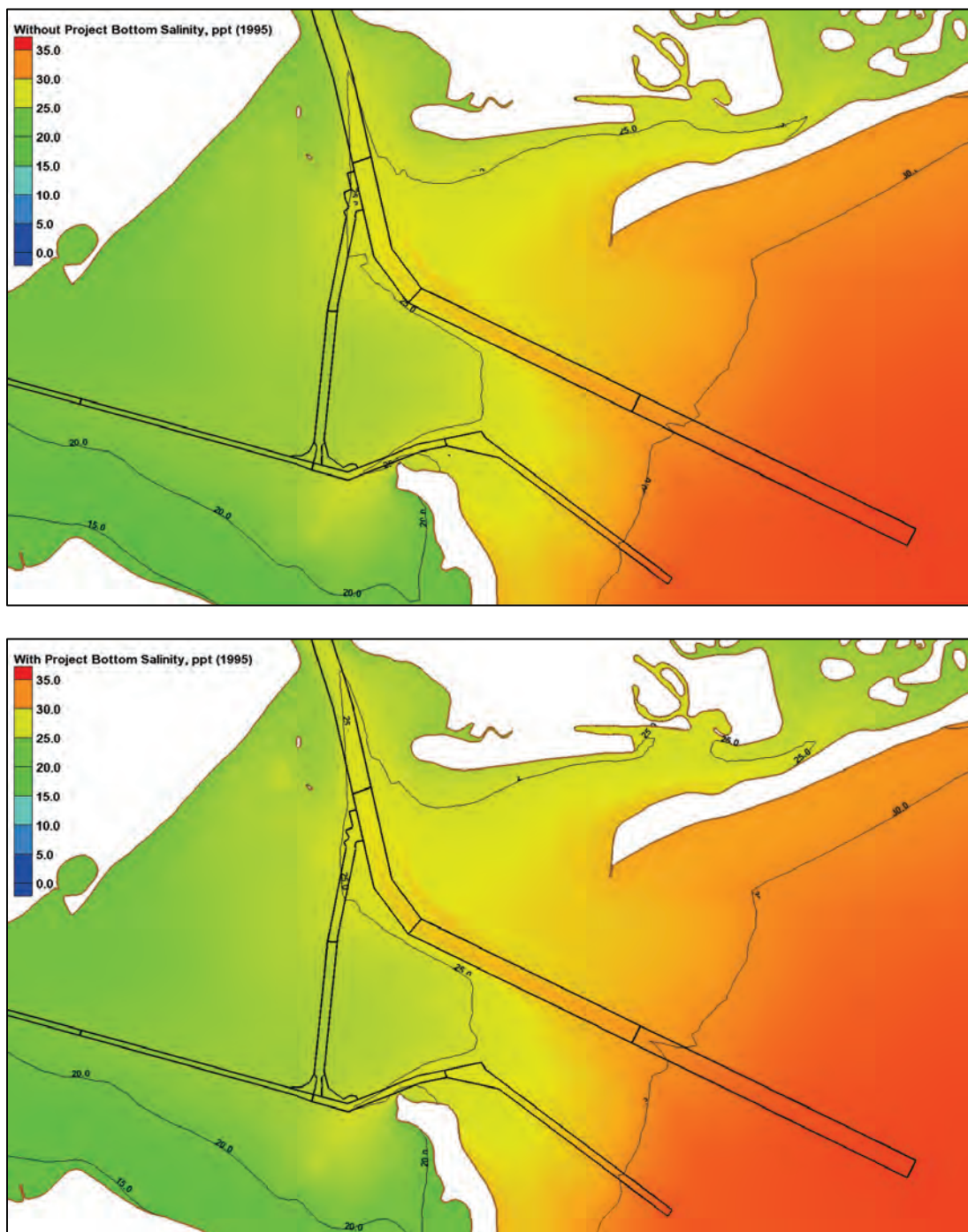




Figure 198. Without-project (top) and with-project (bottom) average fine sediment bottom concentrations, ppm (1995).

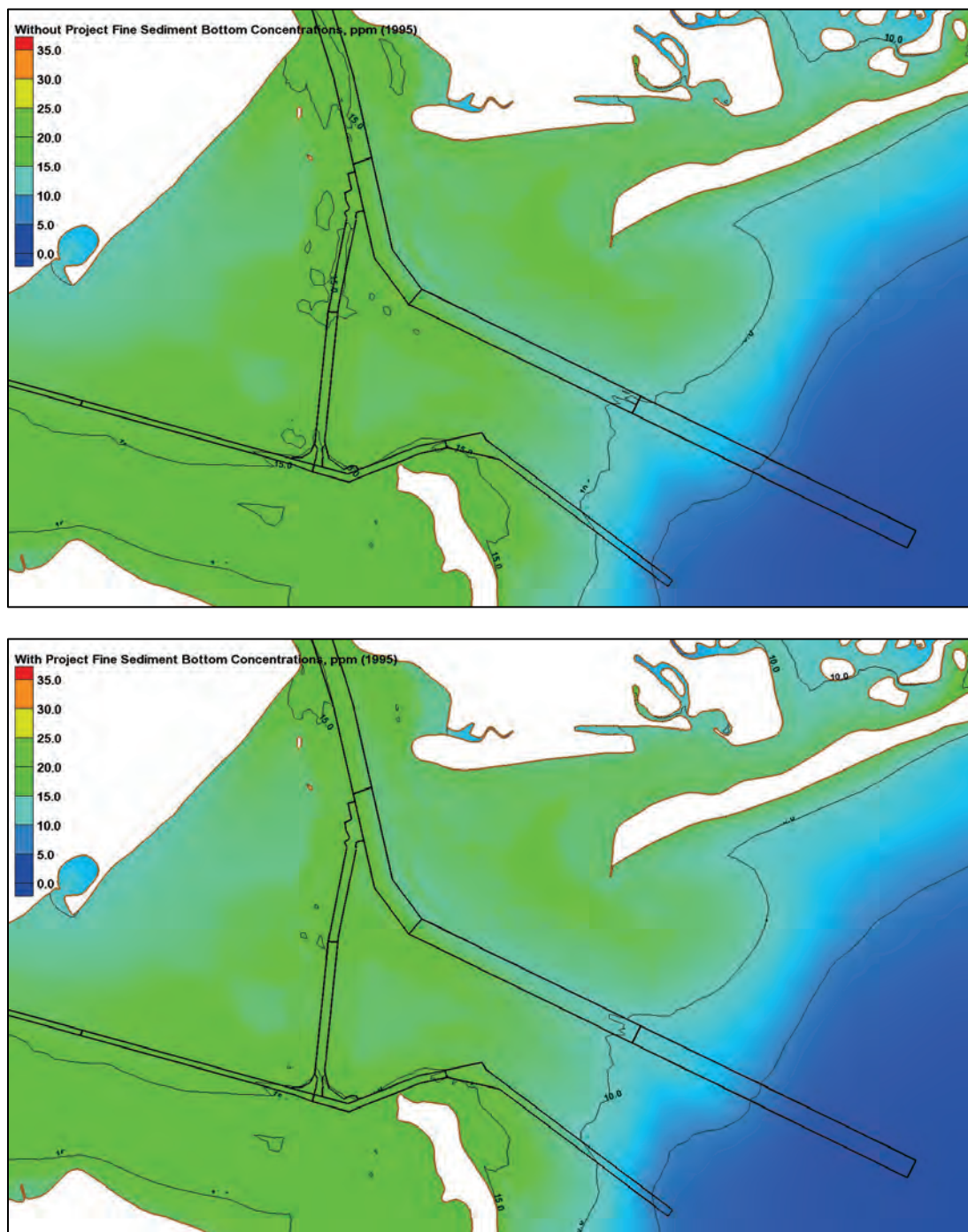


Figure 199. Without-project (top) and with-project (bottom) average sand bottom concentrations, ppm (1995).

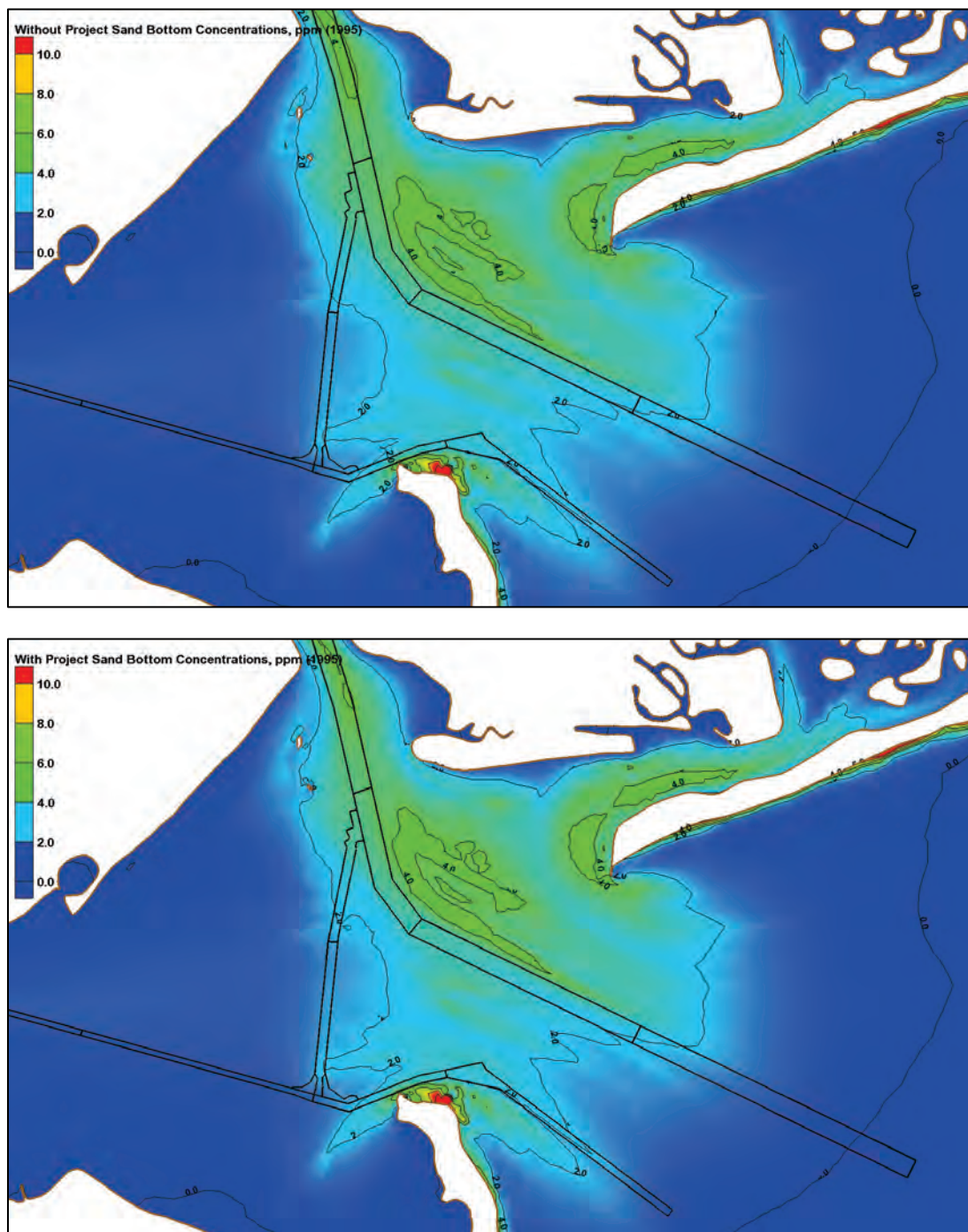




Figure 200. Without-project (top) and with-project (bottom) bed displacement, m (1995).

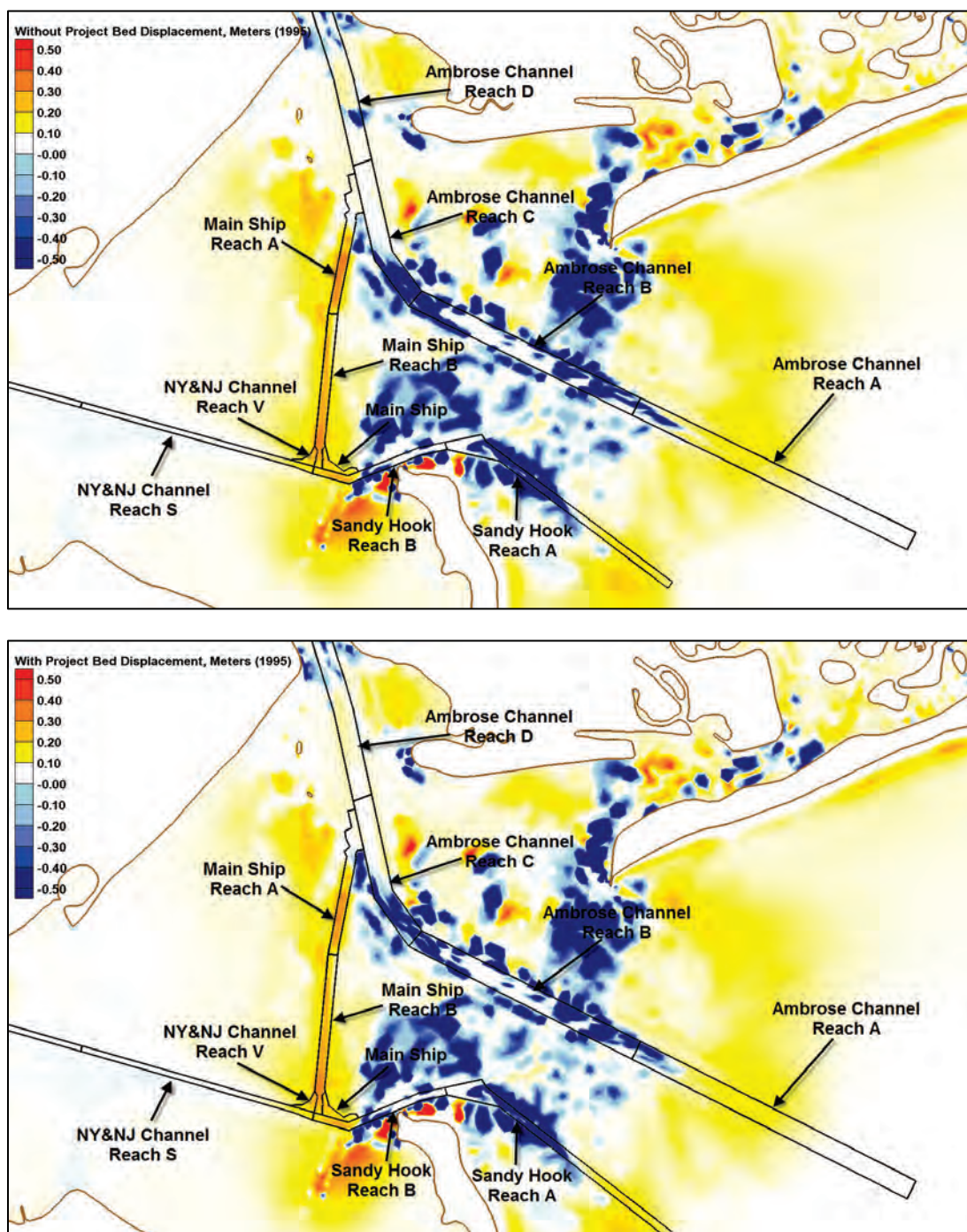


Figure 201. Without-project (top) and with-project (bottom) fine-sediment accumulation,  $\text{kg/m}^2$  (1995),

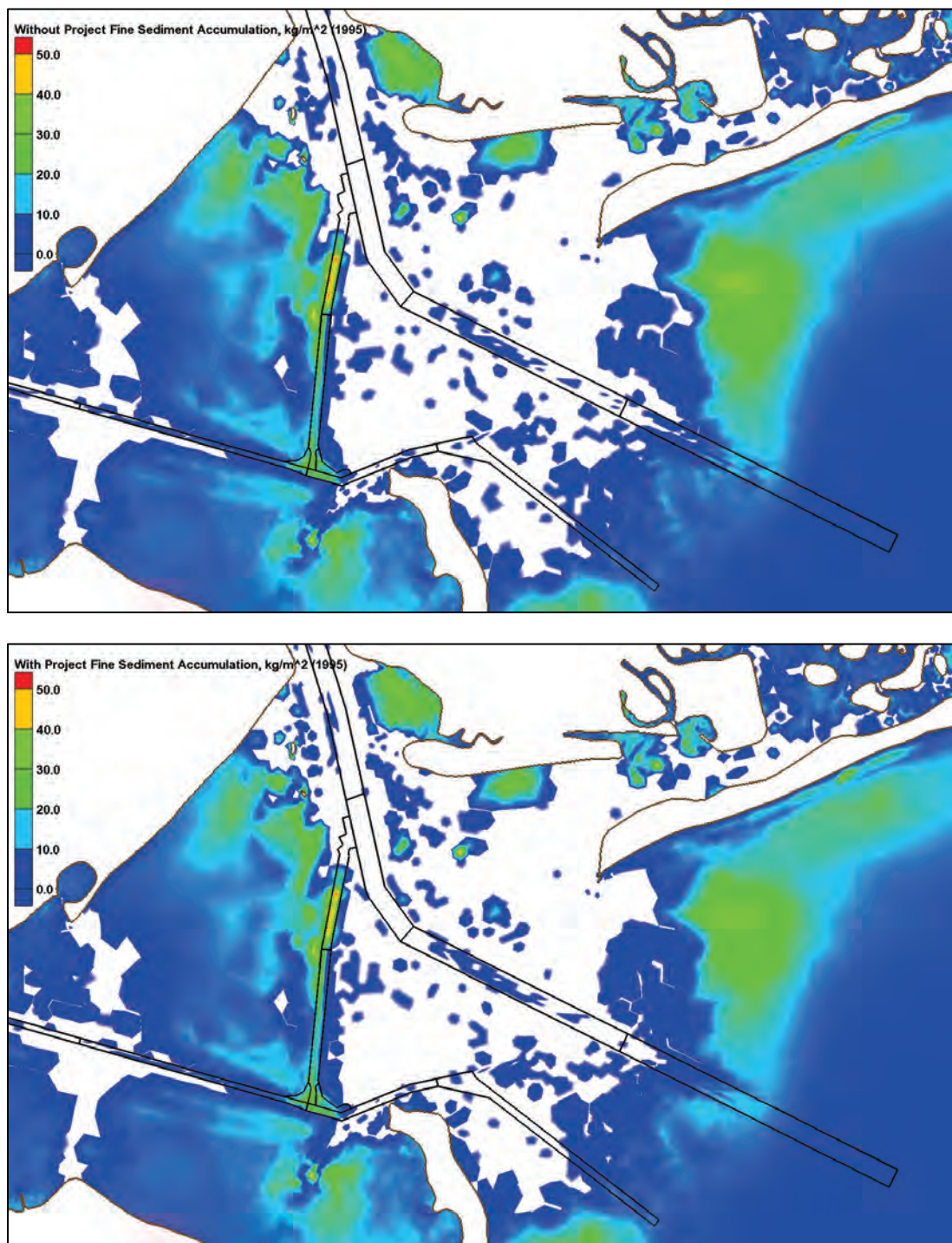




Figure 202. Without-project (top) and with-project (bottom) sand accumulation,  $\text{kg}/\text{m}^2$  (1995).

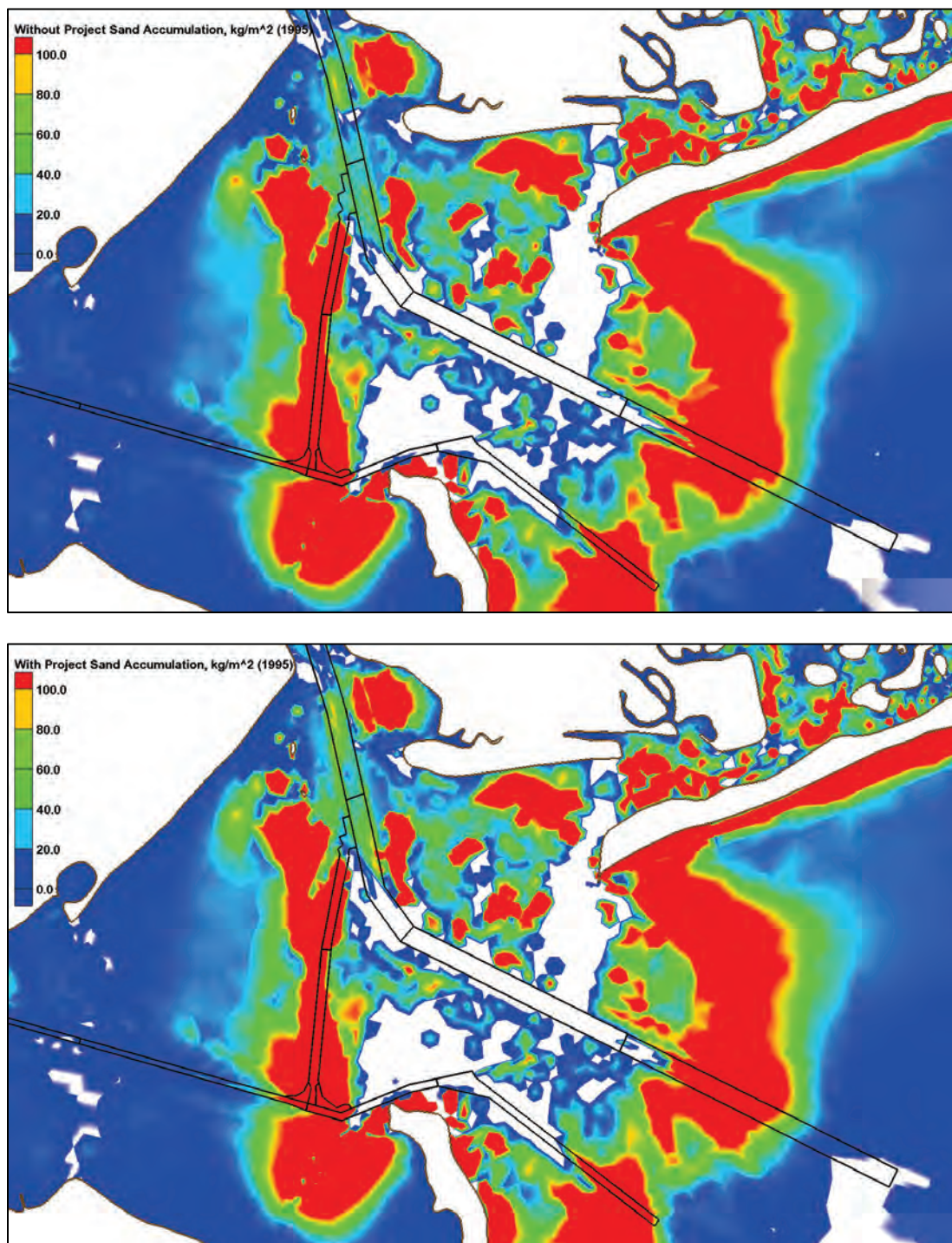




Figure 203. Dredge with-project/without-project percent differences (1995).



Table 19. Dredge volumes in Lower Bay (1995).

Depositional Volumes in Lower Bay, cy (1995)			
Reach	Without Project	With Project	With/Without Dredge Percentage
Ambrose Channel Reach A	273,941	292,521	107
Ambrose Channel Reach B	1,244	409	33
Ambrose Channel Reach C	13,675	23,399	171
Ambrose Channel Reach D	46,413	54,319	117
Main Ship	58,291	58,040	100
Main Ship Reach A	229,342	205,294	90
Main Ship Reach B	329,731	327,078	99
Sandy Hook Reach A	103,013	105,135	102
Sandy Hook Reach B	76,755	76,396	100
NY&NJ Channels Reach S	32,595	32,299	99
NY&NJ Channels Reach V	39,217	39,081	100

As would be expected, the salinity intrusion up the Ambrose ship channel is increased. This is expected due to a combination of the channel deepening and the redistribution of flow through Kill van Kull. The dredge volume for the Ambrose Channel Reach B was reduced. This is expected due to the increased salinity intrusion up the channel thereby resulting in increased dredging requirements in reaches C and D. Overall, the Ambrose channel experienced an increase in dredging of approximately 35,000 cy or approximately 10% for 1995. The Main Ship Reach A experienced a decrease of approximately 24,000 cy. This channel was not deepened as part of the with-project configuration. The deepened Ambrose channel results in more sediment farther down in the water column resulting in less transport of sediment into the adjacent Main Ship Reach A channel possessing a higher bed elevation. This reduces the Main Ship Reach A dredge volumes while increasing the Ambrose channel requirements.

## Newark Bay, Kill van Kull, and Upper Bay results

Figure 204. Without-project (top) and with-project (bottom) average shear stresses, Pa (1995).

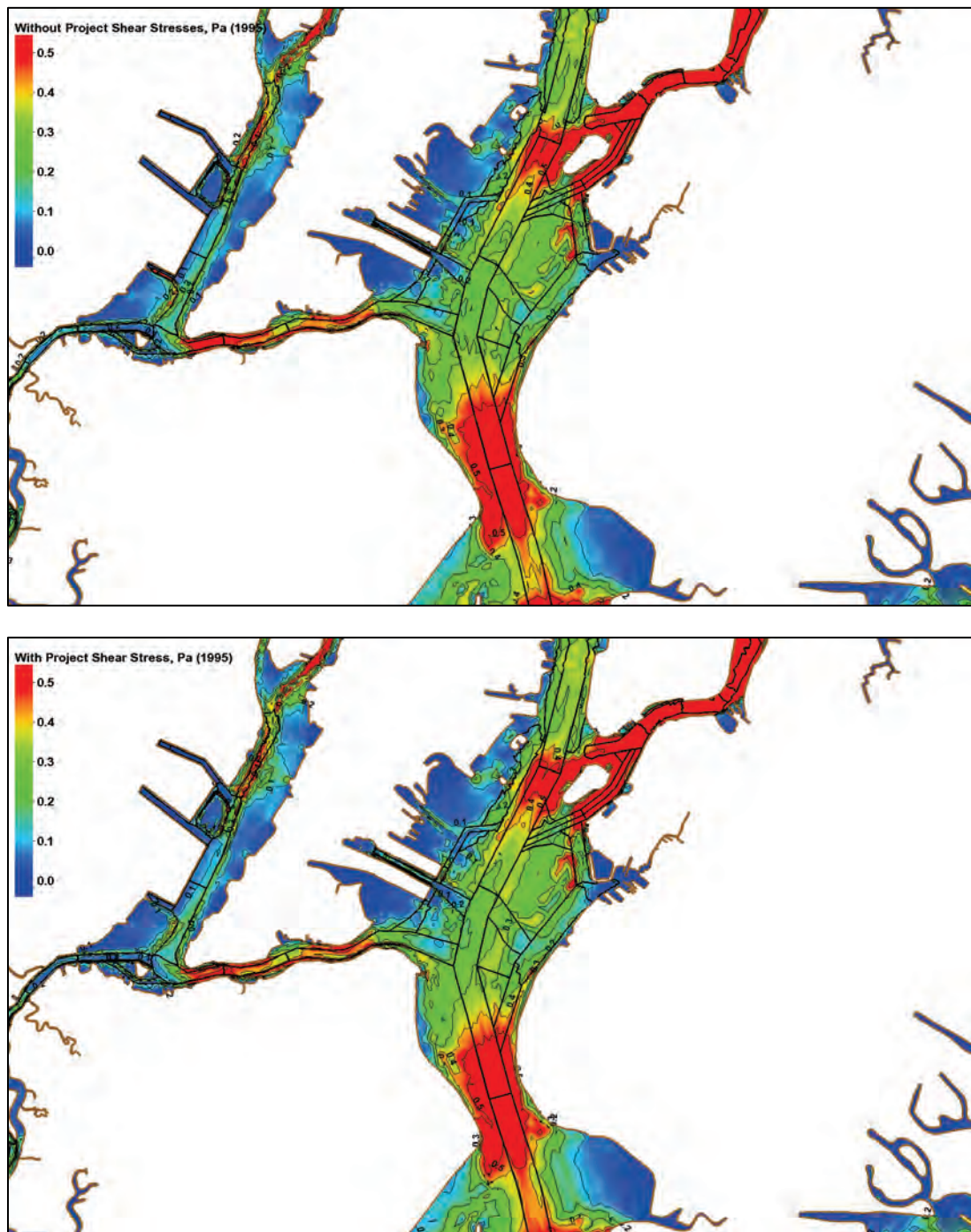


Figure 205. Without-project (top) and with-project (bottom) average bottom salinity, ppt (1995).

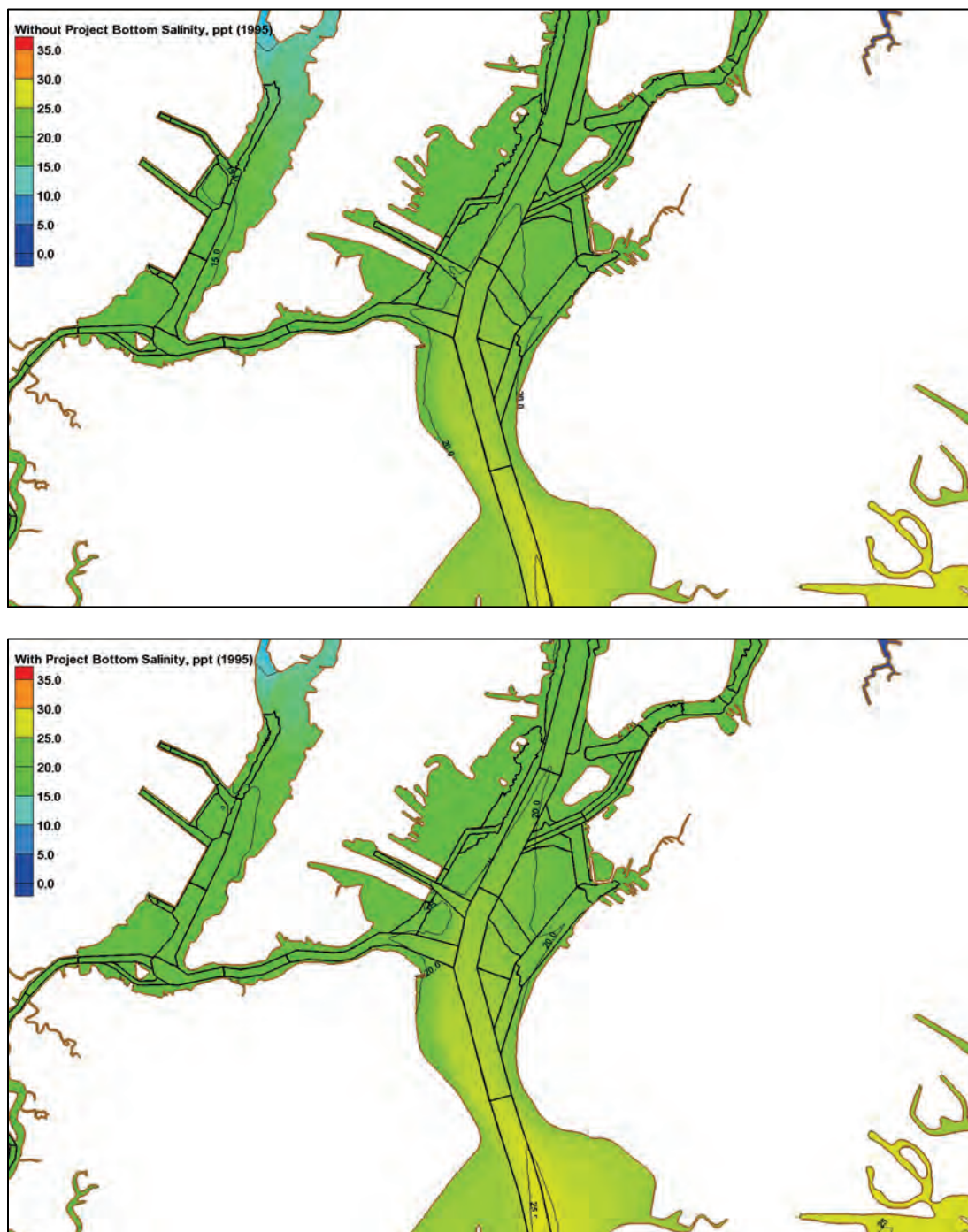




Figure 206. Without-project (top) and with-project (bottom) average fine bottom sediment concentrations, ppm (1995).

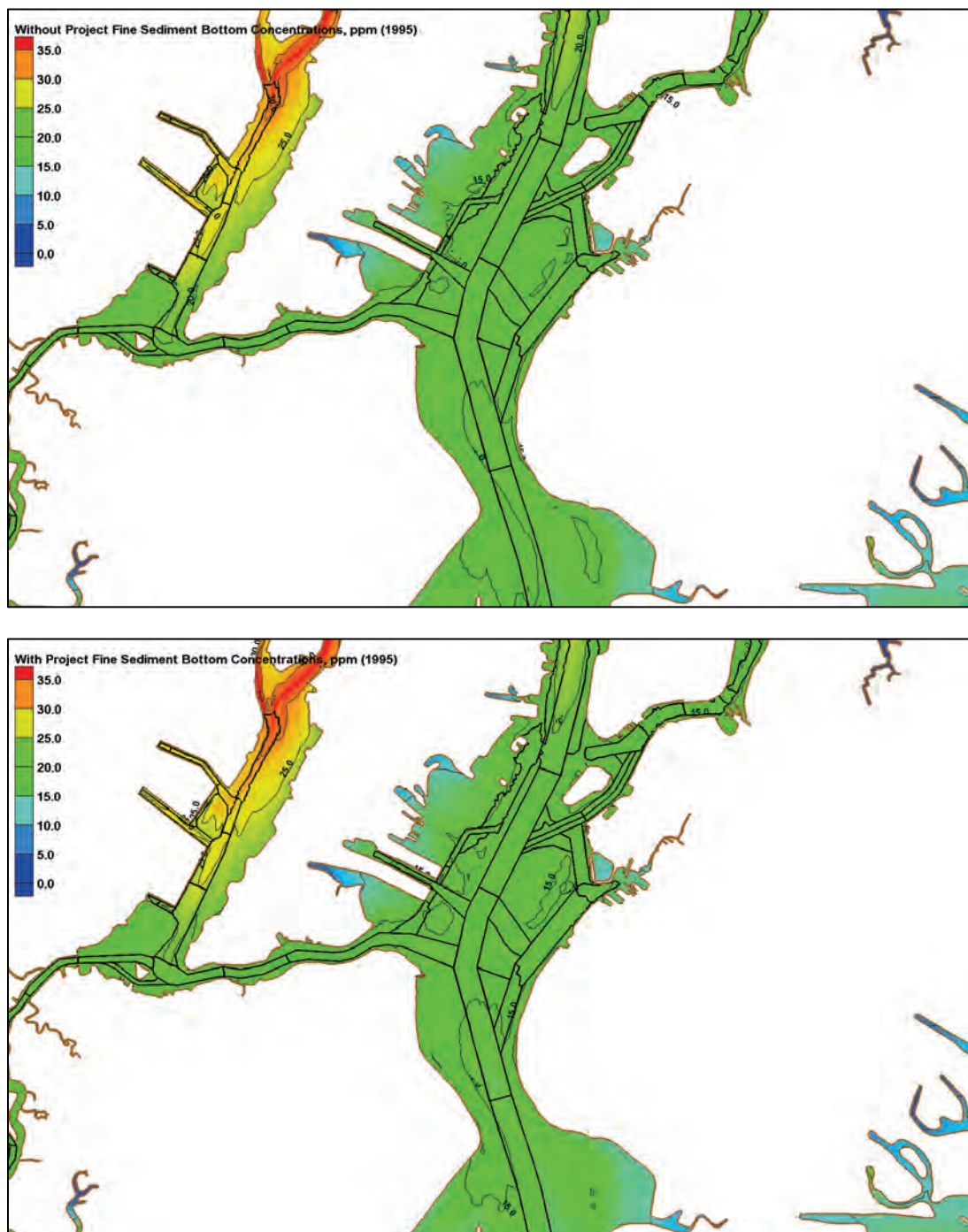




Figure 207. Without-project (top) and with-project (bottom) average sand bottom concentrations, ppm (1995).

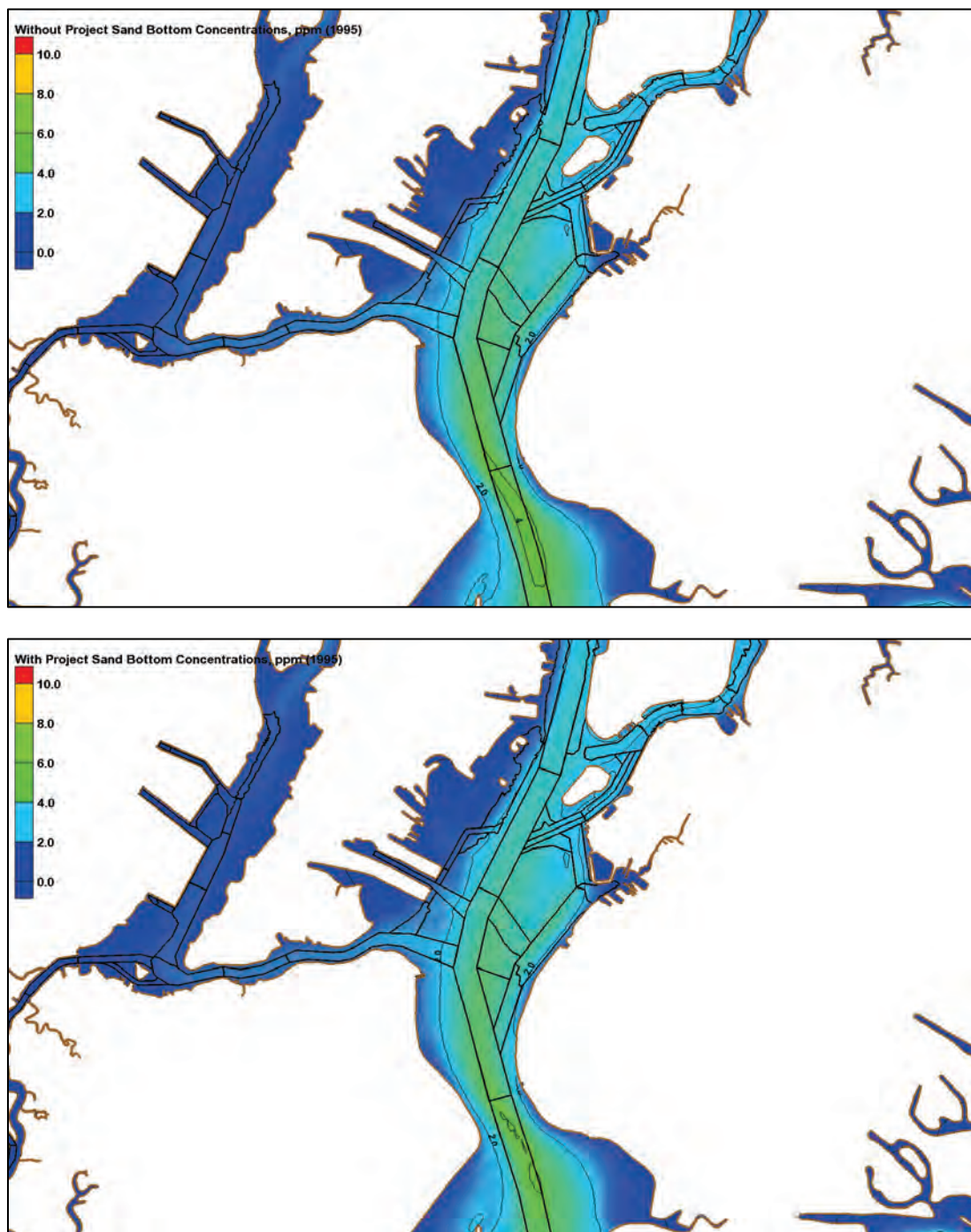


Figure 208. Without-project (top) and with-project (bottom) bed displacement, m (1995).

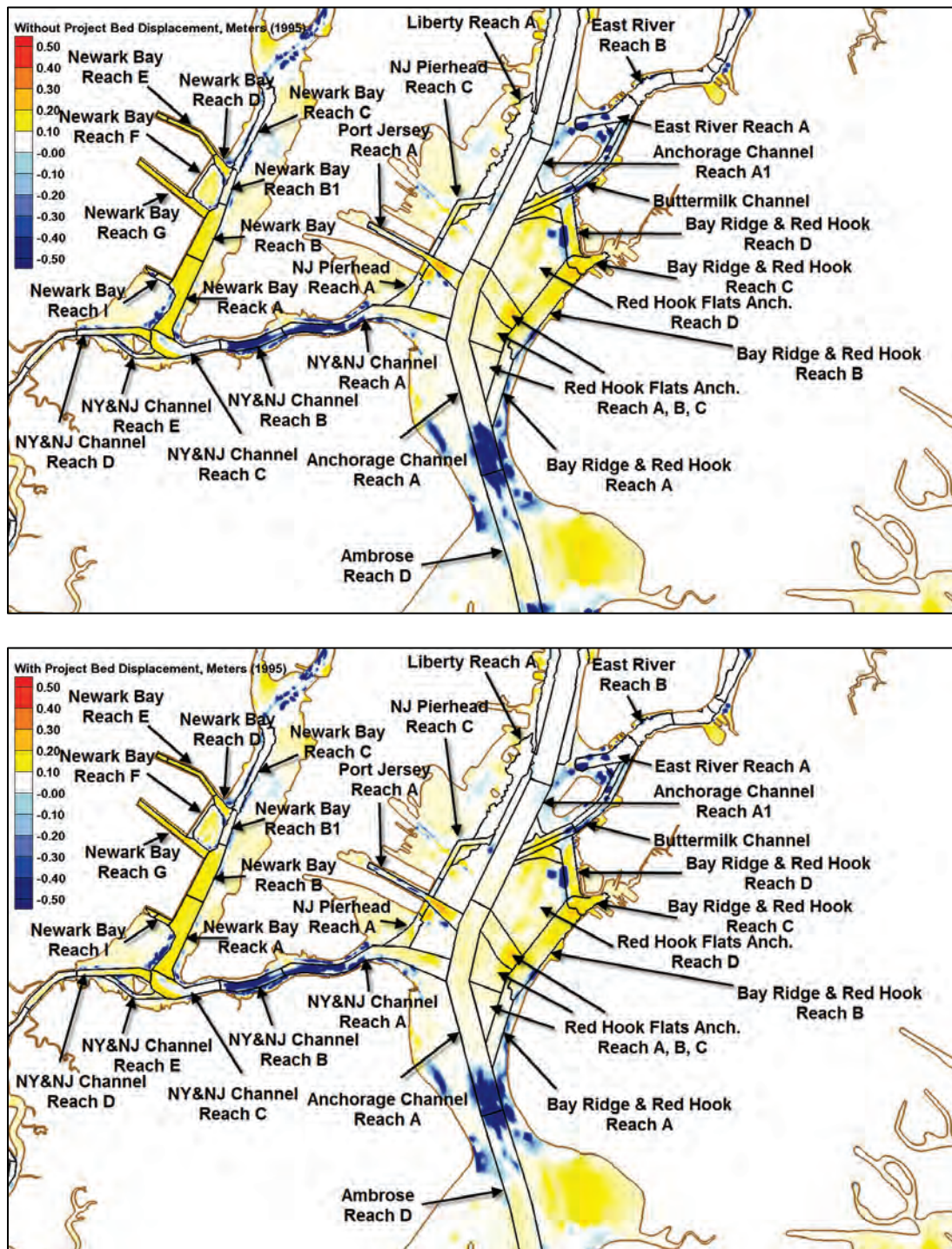




Figure 209. Without-project (top) and with-project (bottom) fine sediment accumulation,  $\text{kg}/\text{m}^2$  (1995).

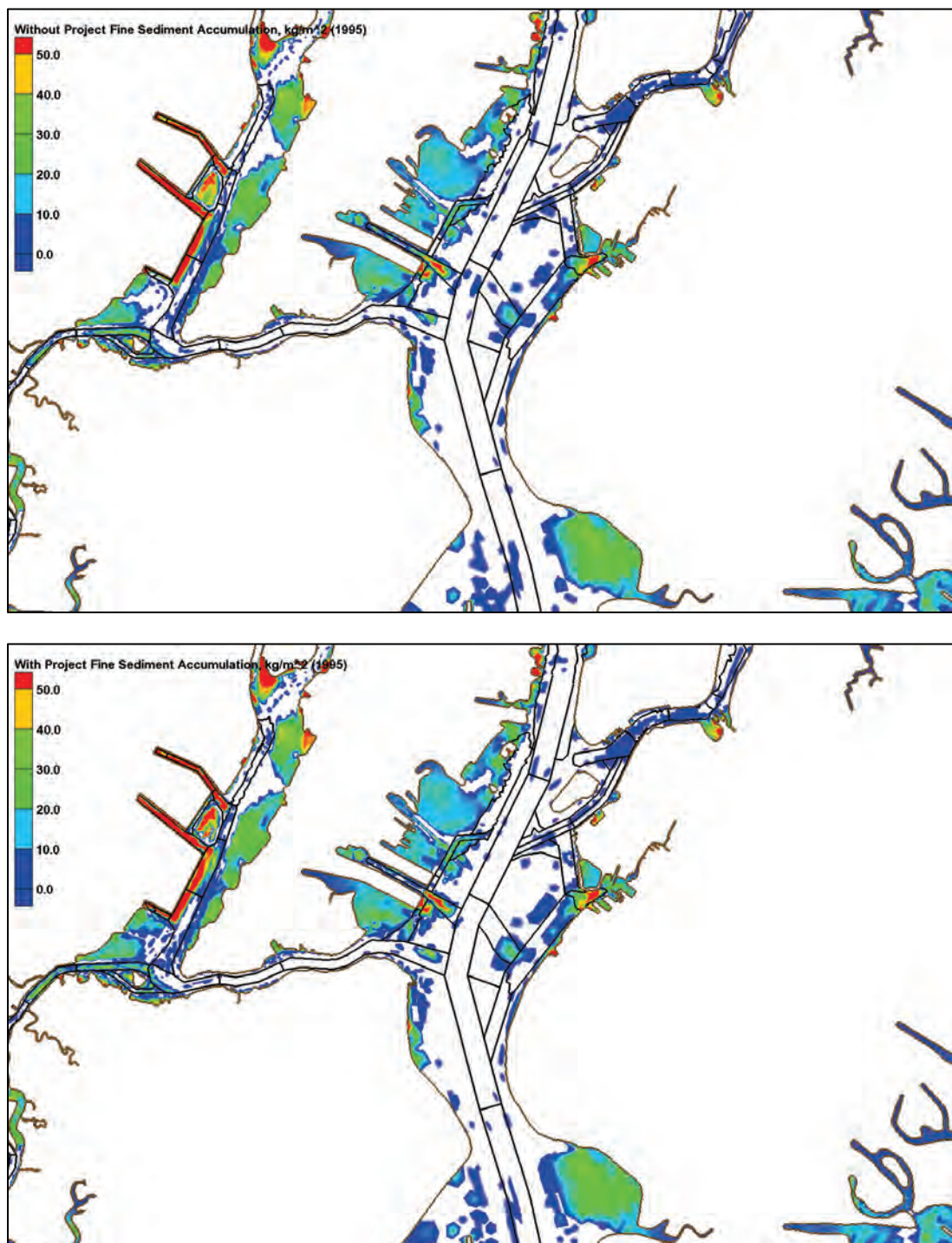


Figure 210. Without-project (top) and with-project (bottom) sand accumulation,  $\text{kg/m}^2$  (1995).

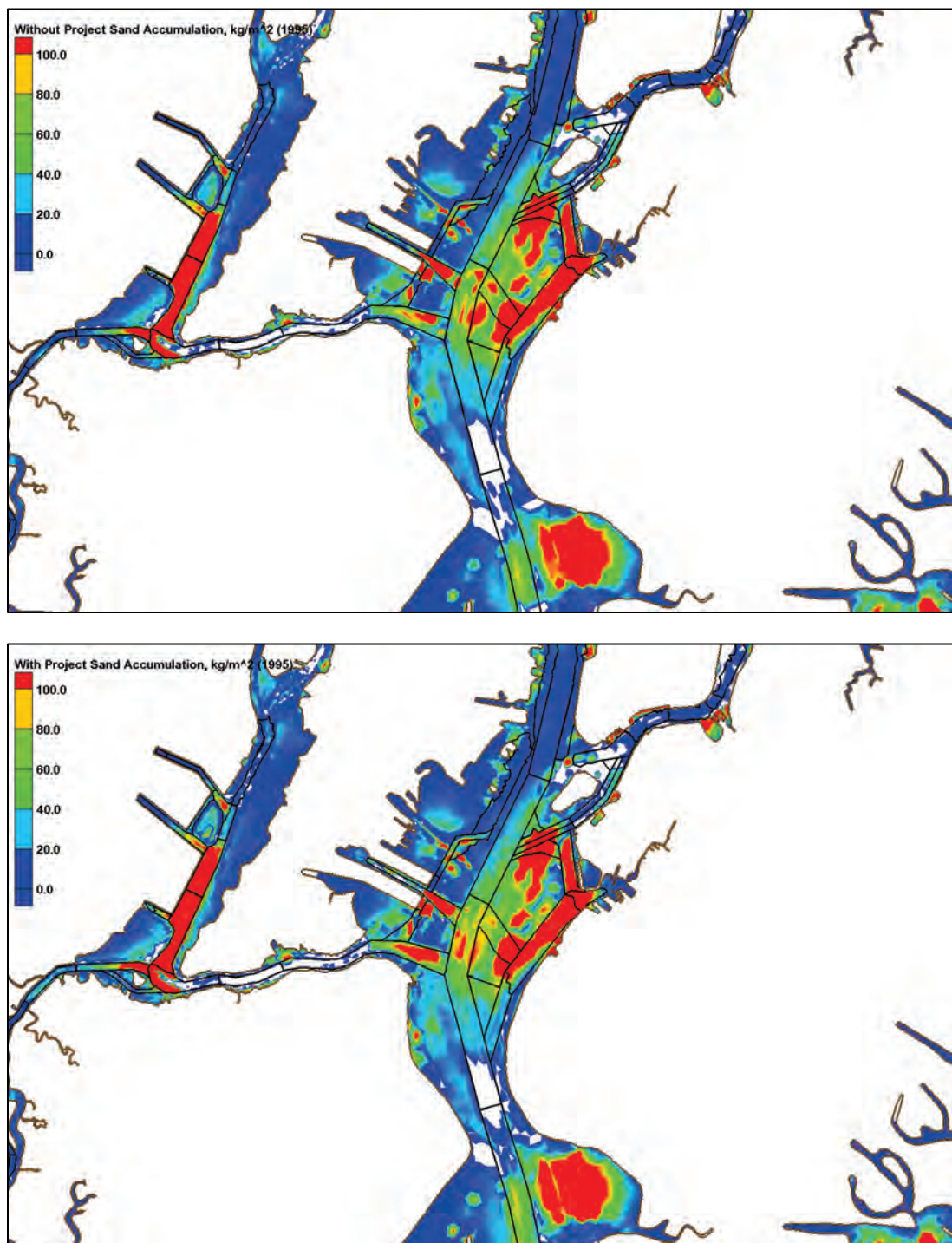


Figure 211. Dredge with-project/without-project percent differences (1995).



As would be expected, the salinity intrusion into Upper Bay and Newark Bay is increased for the with-project configuration. Overall, the Upper Bay channels experience a reduction in the dredge volumes with the Newark Bay and Kill van Kull having increases in dredge volumes of approximately 18,000 cy each or percentages of approximately 6% and 20%, respectively, for 1995. Newark Bay and Kill van Kull are the locations possessing the largest influences in terms of dredge volumes due to the with-project configuration.



Table 20. Dredge volumes in Newark Bay, Kill van Kull, and Upper Bay (1995).

Depositional Volumes in Newark Bay, Kill van Kull, and Upper Bay, cy (1995)			
Reach	Without Project	With Project	With/Without Dredge Percentage
<b>Newark Bay</b>			
Newark Bay Reach A	132,068	140,462	106
Newark Bay Reach B	77,020	87,119	113
Newark Bay Reach B1	2,483	2,437	98
Newark Bay Reach C	1,616	1,480	92
Newark Bay Reach D	14,550	15,802	109
Newark Bay Reach E	20,048	22,459	112
Newark Bay Reach E1	3,171	3,679	116
Newark Bay Reach F	2,749	3,042	111
Newark Bay Reach G	62,719	54,405	87
Newark Bay Reach I	2,621	6,131	234
Newark Bay Reach I1	2,025	2,662	131
<b>Kill van Kull</b>			
NY&NJ Channels Reach A	31,926	39,636	124
NY&NJ Channels Reach B	658	154	23
NY&NJ Channels Reach C	38,689	49,546	128
<b>Upper Bay</b>			
Anchorage Channel Reach A	62,733	61,232	98
Anchorage Channel Reach A1	20,061	19,179	96
Anchorage Reach C1	7,863	7,551	96
Bay Ridge & Red Hook Reach A	11,193	10,706	96
Bay Ridge & Red Hook Reach B	139,254	143,855	103
Bay Ridge & Red Hook Reach C	49,066	42,861	87
Bay Ridge & Red Hook Reach D	49,098	49,637	101
Red Hook Flats Anch. Reach A	12,849	12,689	99
Red Hook Flats Anch. Reach B	41,718	40,729	98
Red Hook Flats Anch. Reach C	67,621	67,428	100
Red Hook Flats Anch. Reach D	126,276	117,560	93
Port Jersey Reach A	49,730	47,978	96
NJ Pierhead Ch. Reach A	11,819	12,715	108
NJ Pierhead Ch. Reach B	6,963	8,532	123
NJ Pierhead Reach C	10,749	10,467	97
Liberty Reach A	6,105	4,953	81

## Arthur Kill and Raritan Bay results

Figure 212. Without-project (top) and with-project (bottom) average shear stresses, Pa (1995).

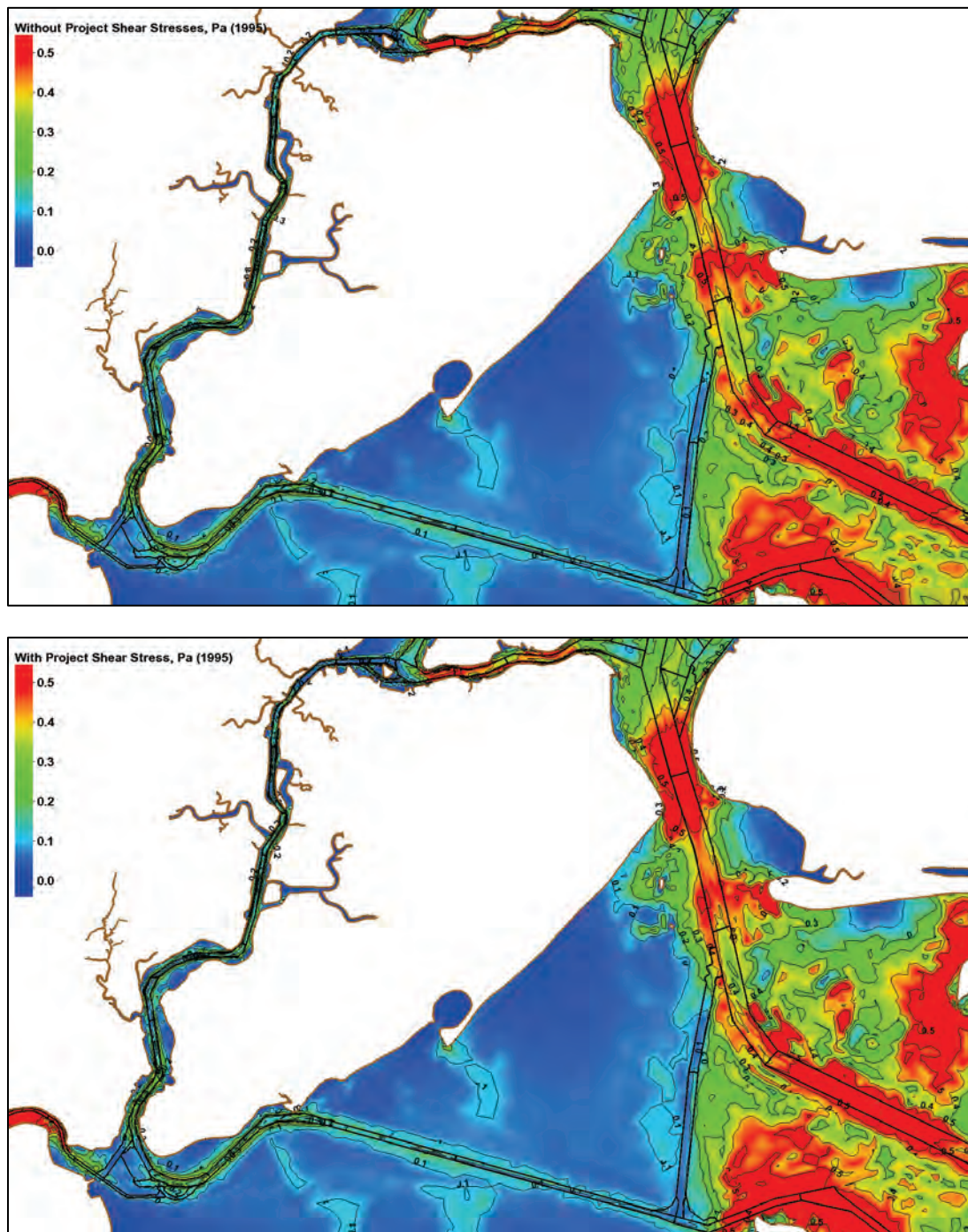


Figure 213. Without-project (top) and with-project (bottom) average bottom salinity, ppt (1995).

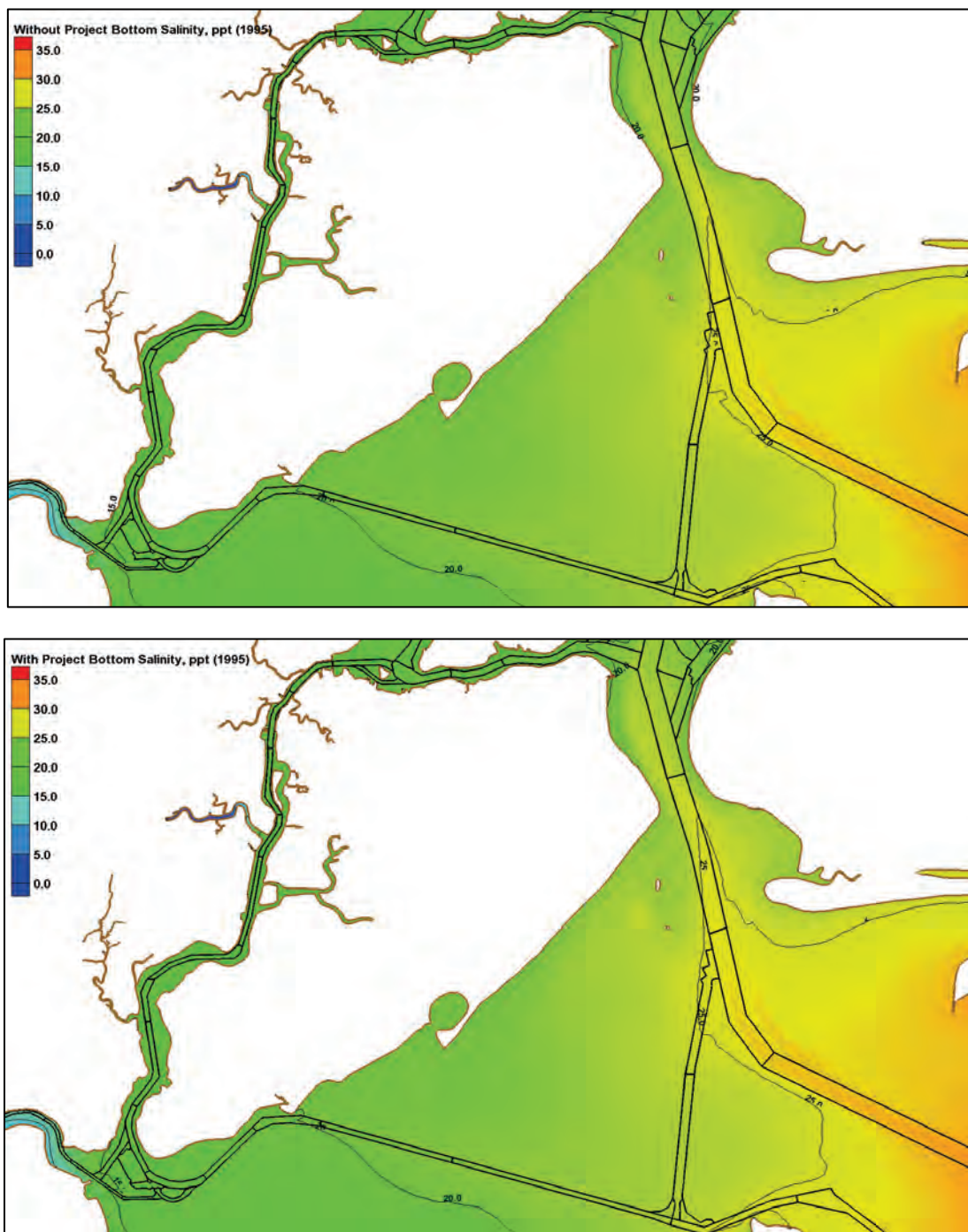




Figure 214. Without-project (top) and with-project (bottom) average fine sediment bottom concentrations, ppm (1995).

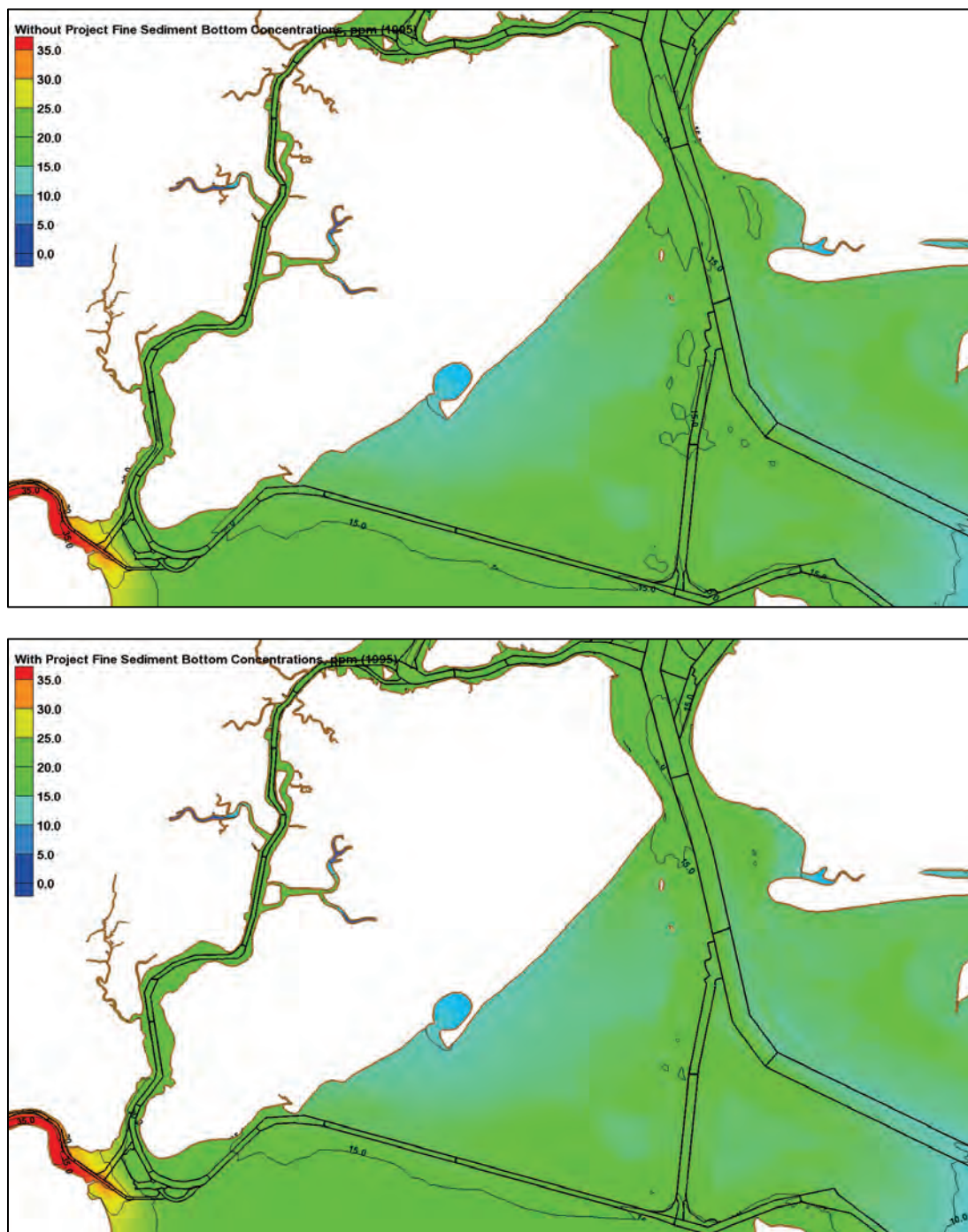


Figure 215. Without-project (top) and with-project (bottom) average sand bottom concentrations, ppm (1995).

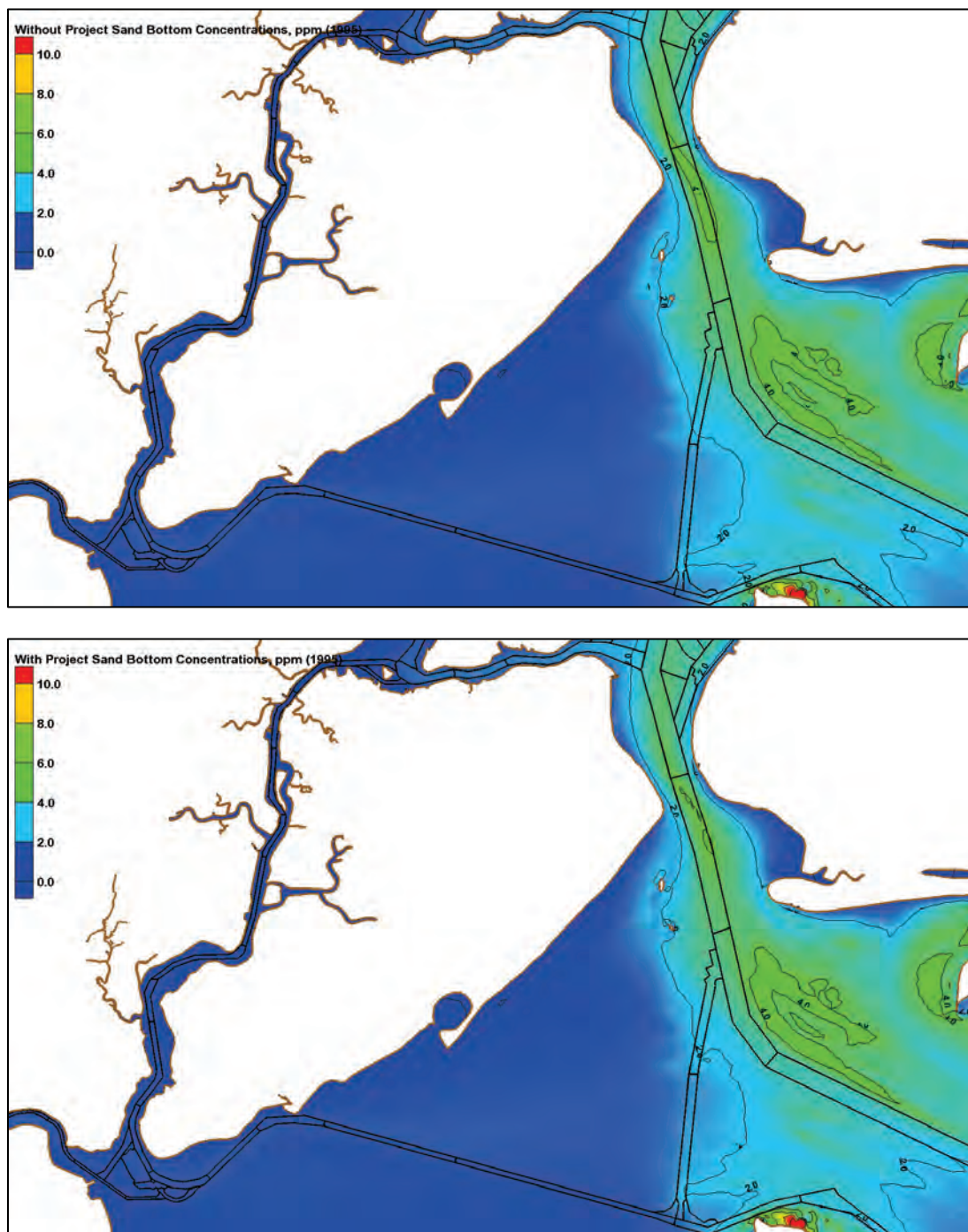




Figure 216. Without-project (top) and with-project (bottom) bed displacement, m (1995).

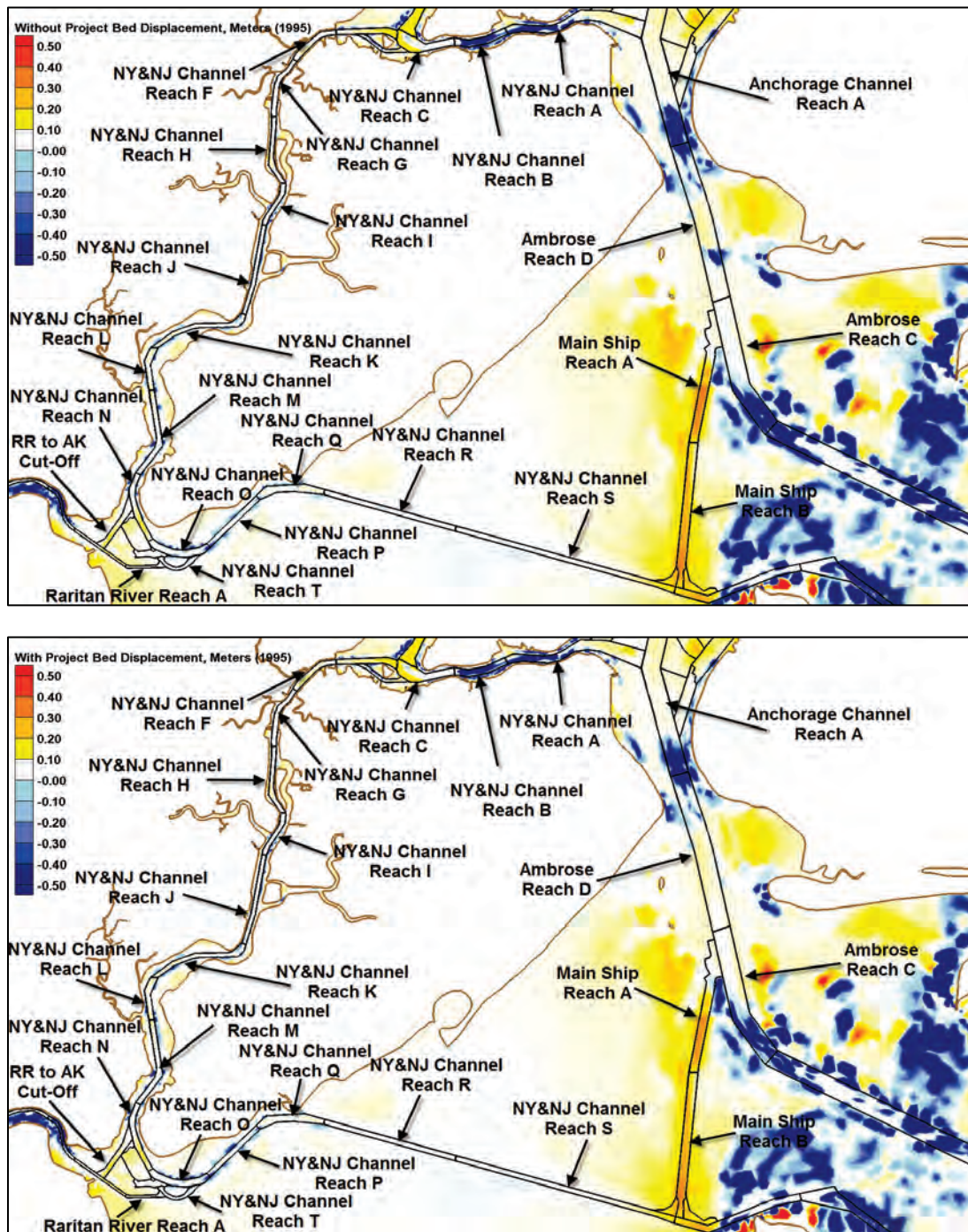


Figure 217. Without-project (top) and with-project (bottom) fine sediment accumulation,  $\text{kg}/\text{m}^2$  (1995).

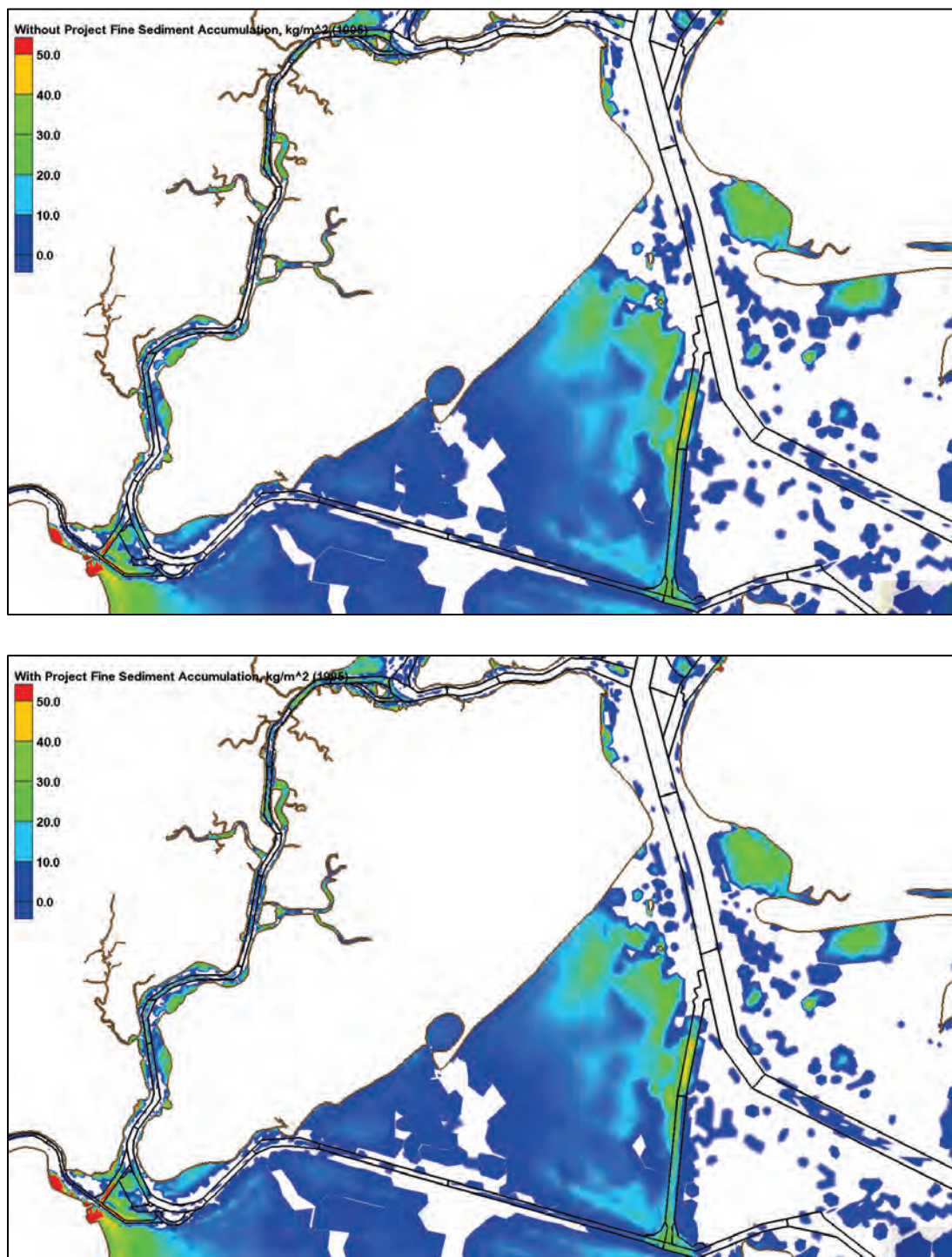




Figure 218. Without-project (top) and with-project (bottom) sand accumulation,  $\text{kg/m}^2$  (1995).

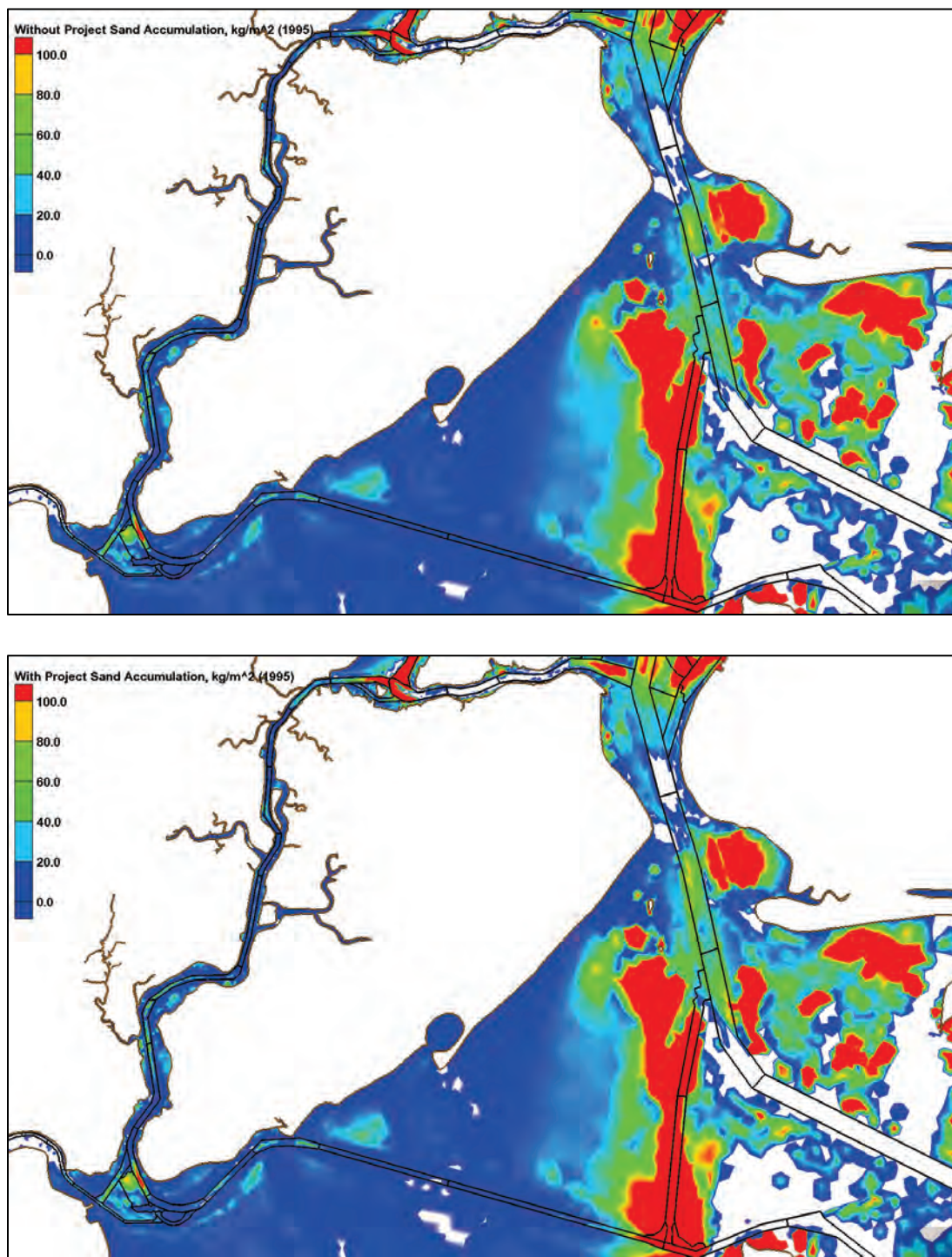
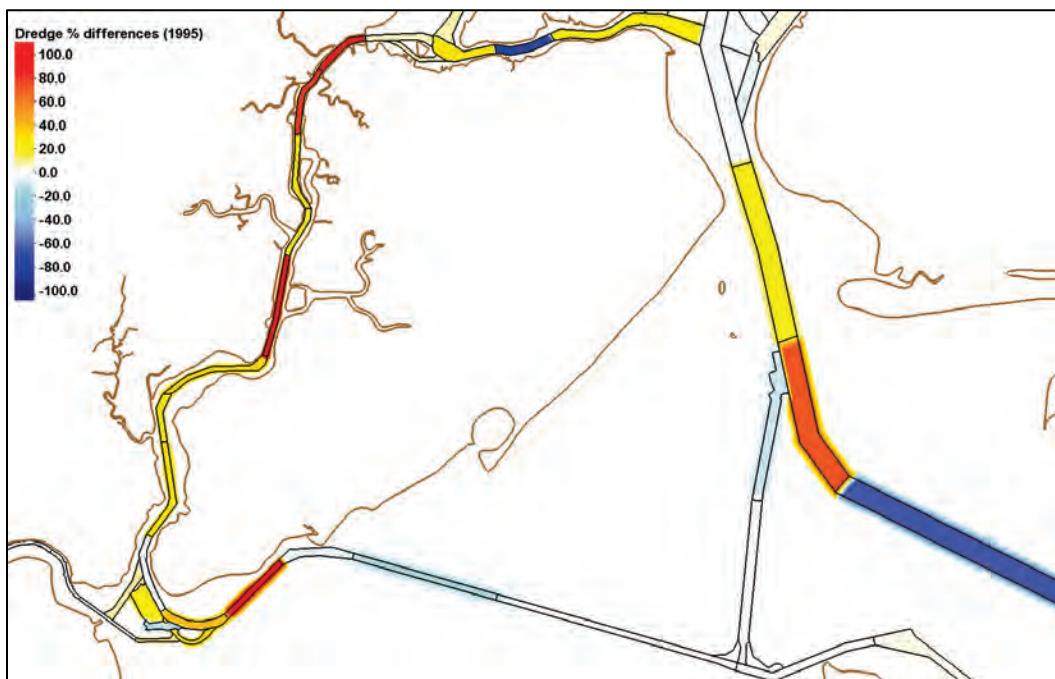


Figure 219. Dredge with-project/without-project percent differences (1995).



In general, the with-project impacts to the Arthur Kill and Raritan Bay areas are relatively minor. Some dredge volumes are redistributed among reaches, but the overall dredging requirements are similar. The redistribution of deposition across the reaches is to be expected due to the increased net flowrate through the Kill van Kull. This increased net flow rate also impacts the amount of water and sediment moving up the Arthur Kill from the Raritan River and Raritan Bay. Some of the dredge volume changes in Table 21 create large percentage changes, but these volumes are relatively small, so small changes in the dredge volumes can appear to be significant when in actuality the dredge volume (and change) is relatively small.

Table 21. Dredge volumes for Arthur Kill and Raritan Bay (1995).

Depositional Volumes in Arthur Kill and Raritan Bay, cy (1995)			
Reach	Without Project	With Project	With/Without Dredge Percentage
<b>Arthur Kill</b>			
NY&NJ Channels Reach D	26,484	27,844	105
NY&NJ Channels Reach E	4,555	4,874	107
NY&NJ Channels Reach F	3,240	6,977	215
NY&NJ Channels Reach G	385	687	179
NY&NJ Channels Reach H	2,477	2,959	119
NY&NJ Channels Reach I	146	170	117
NY&NJ Channels Reach J	230	741	322
NY&NJ Channels Reach K	3,587	4,716	131
NY&NJ Channels Reach L	4,269	4,991	117
NY&NJ Channels Reach M	2,513	3,237	129
NY&NJ Channels Reach N	12,141	11,589	95
<b>Raritan Bay</b>			
NY&NJ Channels Reach O	1,147	1,598	139
NY&NJ Channels Reach P	920	1,917	208
NY&NJ Channels Reach Q	4,617	4,395	95
NY&NJ Channels Reach R	935	758	81
NY&NJ Channels Reach T	586	778	133
RR to AK Cut-Off Reach A	12,243	13,164	108
Raritan River Reach A	2,390	2,624	110
Raritan River Reach B	6,517	6,603	101
Raritan River Reach C	764	772	101
Raritan River Reach D	277	274	99

### Average dredge volumes for all reaches

The average annual dredge volumes over the five simulated years for each channel reach are provided in Table 22. These results indicate an increase in the Ambrose Channel, but that is almost offset by the decrease in the Main Ship Reach A channel. This offset appears to be somewhat of a trend with the primary deepened channels showing increases in dredging



requirements with some other adjacent channels actually showing decreases in dredge volumes. The Kill van Kull and Newark Bay are the primary channels with increased dredging requirements.

**Table 22. Average annual dredge volumes in cy by reach over the five simulated years.**

Reaches	Average Without Dredge Volumes	Average With Dredge Volumes	Percentage Change
<b>Lower Bay</b>			
Ambrose Channel Reach A	255,407	271,730	6
Ambrose Channel Reach B	1,717	1,158	-33
Ambrose Channel Reach C	12,512	22,008	76
Ambrose Channel Reach D	33,303	39,313	18
Main Ship Reach A	216,092	191,440	-11
Total	519,030	525,649	1
<b>Sandy Hook/Raritan Bay Channels</b>			
Sandy Hook Reach A	104,664	104,970	0
Sandy Hook Reach B	85,669	85,920	0
Main Ship Reach B	277,208	271,402	-2
Main Ship	54,797	54,191	-1
NY&NJ Channels Reach O	3,072	3,558	16
NY&NJ Channels Reach P	6,471	6,361	-2
NY&NJ Channels Reach Q	10,580	10,069	-5
NY&NJ Channels Reach R	993	918	-8
NY&NJ Channels Reach S	30,872	30,917	0
NY&NJ Channels Reach T	1,727	1,895	10
NY&NJ Channels Reach V	36,948	36,507	-1
NY&NJ Channels Reach U Area 1	31,703	35,191	11
NY&NJ Channels Reach U Area 2	2,467	2,189	-11
NY&NJ Channels Reach U Area 3	49	50	2

NY&NJ Channels Reach U Area 4	1,175	1,163	-1
RR to AK Cut-Off Reach A	19,191	20,208	5
Raritan River Reach A	4,655	4,914	6
Raritan River Reach B	8,449	8,607	2
Raritan River Reach C	876	859	-2
Raritan River Reach D	146	133	-8
Total	681,713	680,023	0
<b>Upper Bay Channels</b>			
Anchorage Channel Reach A	68,020	64,656	-5
Anchorage Channel Reach A1	30,238	26,903	-11
Port Jersey Reach A	52,147	47,224	-9
NJ Pierhead Ch. Reach A	11,661	12,565	8
NJ Pierhead Ch. Reach B	7,699	9,266	20
NJ Pierhead Reach C	10,483	10,373	-1
Bay Ridge & Red Hook Reach A	14,946	14,337	-4
Bay Ridge & Red Hook Reach B	145,143	149,670	3
Bay Ridge & Red Hook Reach C	53,230	47,338	-11
Bay Ridge & Red Hook Reach D	54,588	53,925	-1
Red Hook Flats Anch. Reach A	17,373	16,793	-3
Red Hook Flats Anch. Reach B	43,684	39,127	-10
Red Hook Flats Anch. Reach C	133,715	125,352	-6
Red Hook Flats Anch. Reach C	65,486	63,389	-3
Anchorage Reach C1	7,814	7,637	-2
Liberty Id. Reach A	7,622	6,268	-18
Buttermilk Ch. Reach A	23,871	23,048	-3
Buttermilk Ch. Reach B	785	748	-5
Buttermilk Ch. Reach C	30,474	29,574	-3
Buttermilk Ch. Reach D	14,475	13,707	-5

Buttermilk Ch. Reach E	286	260	-9
Buttermilk Ch. Reach F	1,978	1,756	-11
Buttermilk Ch. Reach G	1	1	-31
Total	795,721	763,917	-4
<b>Kill van Kull Channels</b>			
NY&NJ Channels Reach A	51,302	61,571	20
NY&NJ Channels Reach B	643	383	-41
NY&NJ Channels Reach C	39,196	45,597	16
Total	91,142	107,551	18
<b>Arthur Kill Channels</b>			
NY&NJ Channels Reach D	35,082	31,860	-9
NY&NJ Channels Reach E	5,664	5,850	3
NY&NJ Channels Reach F	7,489	12,111	62
NY&NJ Channels Reach G	1,709	2,203	29
NY&NJ Channels Reach H	5,956	6,908	16
NY&NJ Channels Reach I	553	710	28
NY&NJ Channels Reach J	2,210	2,975	35
NY&NJ Channels Reach K	10,248	10,597	3
NY&NJ Channels Reach L	9,022	8,977	0
NY&NJ Channels Reach M	7,467	7,588	2
NY&NJ Channels Reach N	16,597	15,077	-9
Total	101,998	104,855	3
<b>East River Channels</b>			
East River Reach A	2,526	2,281	-10
East River Reach B	651	754	16
East River Reach C	229	254	11
East River Reach C1	0	0	33
East River Reach D	10	14	33

East River Reach E	32	33	2
East River Reach F	582	576	-1
East River Reach G	253	252	0
East River Reach H	85,432	76,992	-10
East River Reach I	109,929	109,671	0
East River Reach J	1,276	788	-38
East River Reach K	186	157	-16
Total	201,106	191,770	-5
<b>Newark Bay</b>			
Newark Bay Reach A	160,379	177,079	10
Newark Bay Reach B	129,822	157,190	21
Newark Bay Reach B1	3,190	3,124	-2
Newark Bay Reach C	2,674	2,718	2
Newark Bay Reach D	25,026	29,129	16
Newark Bay Reach E	30,636	37,599	23
Newark Bay Reach E1	4,129	5,429	31
Newark Bay Reach F	7,612	8,958	18
Newark Bay Reach G	110,043	100,850	-8
Newark Bay Reach I	3,530	8,333	136
Newark Bay Reach I1	3,226	4,393	36
Total	480,267	534,801	11
<b>All Reaches</b>	<b>2,870,977</b>	<b>2,908,566</b>	<b>1</b>

When considering all channel reaches, the increase in dredging is estimated at 1% as shown in Table 22. For the locations shown in Figure 86, the percentage increases in overall dredging were 6% (1985), 4% (1995), 3% (1996), 7% (2011), and 0% (2012) with an average annual increase in dredging of 4%. This would indicate the non-project channels experienced less increase and even some decreases in dredging as compared to the deepened project channels.

### **Variation in dredge volumes for the simulated years**

By simulating five different years, the variability in dredge volumes could be approximated. The total dredge volumes for all reaches ranged from approximately 2.5 million cy (1985) to approximately 3.4 million cy (2011) for the without project and approximately 2.5 million cy (1985) to approximately 3.6 million cy (2011) for the with project. From these results, it can be inferred the forcing conditions across years can result in a variation in the dredge volumes of as much as 1.1 million cy with larger yearly variations possible. The total average dredge volumes were approximately 2.9 million cy for both configurations and the with-project conditions has an increase in dredging of approximately 40,000 cy equating to a 1% increase over the without-project configuration (see Table 22).

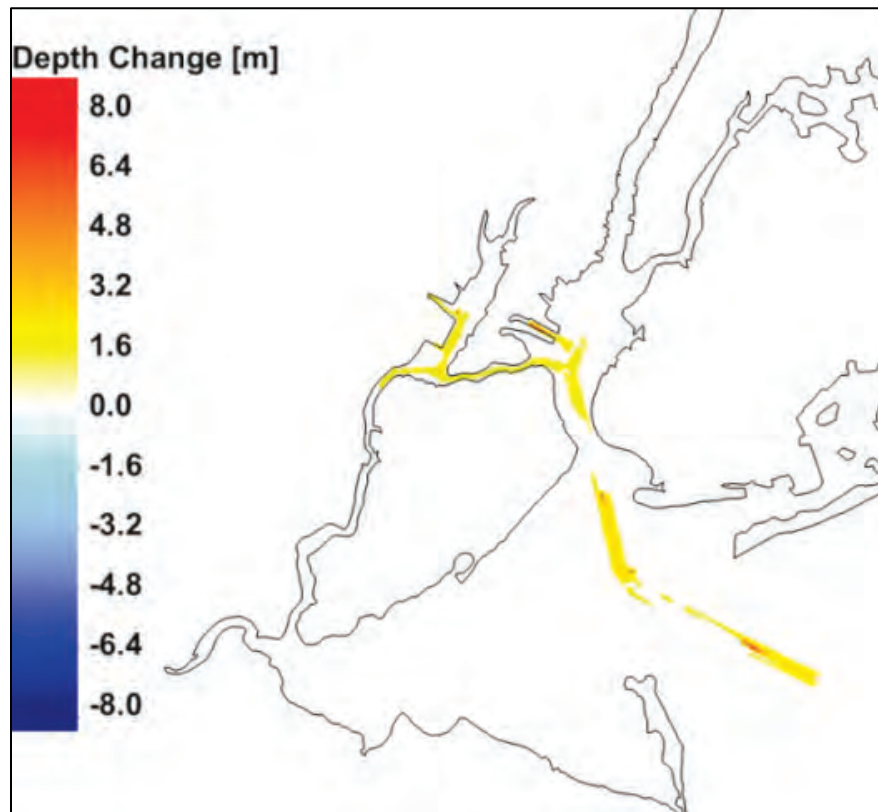
The dredge volumes for the five simulated years for the commonly dredged locations shown in Figure 86 ranged from approximately 1.3 million cy (1985) to a high of 2.3 million cy (2011). The variation in the annual dredge volumes for these locations (~1 million cy) is an order of magnitude larger than the changes due to the project (~70,000 cy).

### **Wave impacts due to channel deepening**

Like the AdH model, the STWAVE bathymetry was updated to reflect the deepening of the navigation channel. The extent of the channel deepening is indicated by the warm colors in Figure 220.



Figure 220. Channel deepening in STWAVE domain.



The impact of channel deepening on the mean wave climate is summarized below by comparing the mean significant wave height envelope for each year-long simulation. The left panels of Figure 221 through Figure 225 show the average significant wave height for each grid cell, and the right panel shows the difference in average significant wave height due to the channel deepening project. In the difference plots, warm colors indicated larger wave heights whereas cool colors indicate smaller wave heights.

Figure 221. Effect of channel deepening on mean significant wave height for 1985.

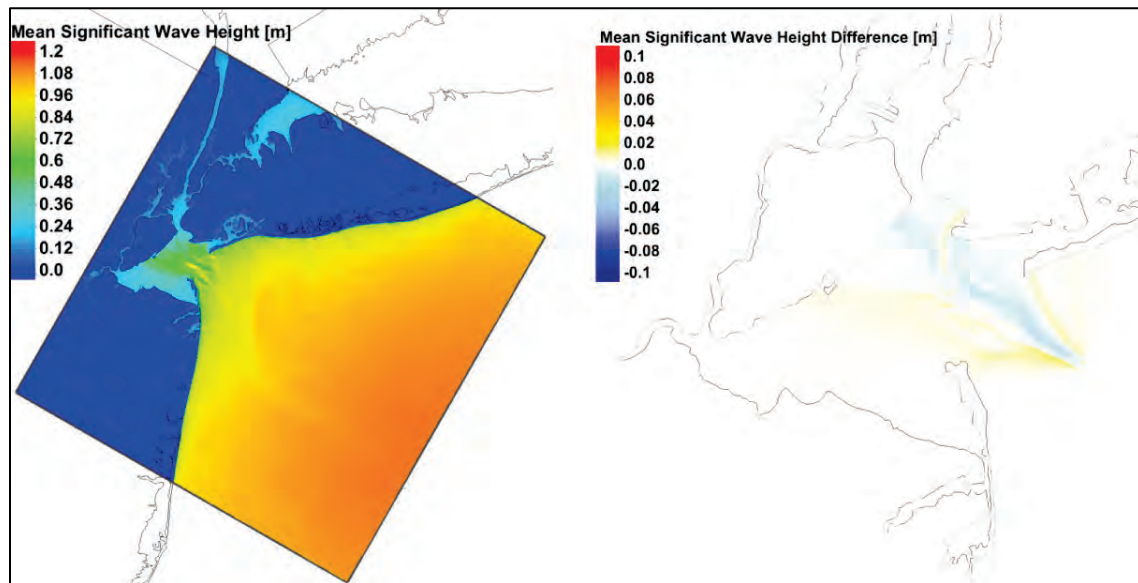


Figure 222. Effect of channel deepening on mean significant wave height for 1995.

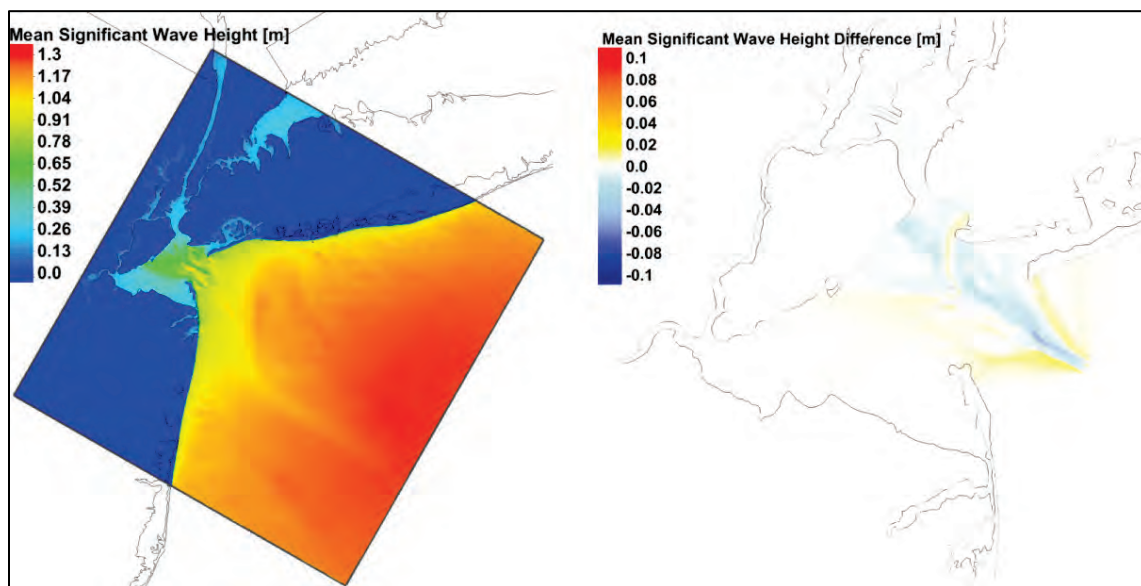


Figure 223. Effect of channel deepening on mean significant wave height for 1996.

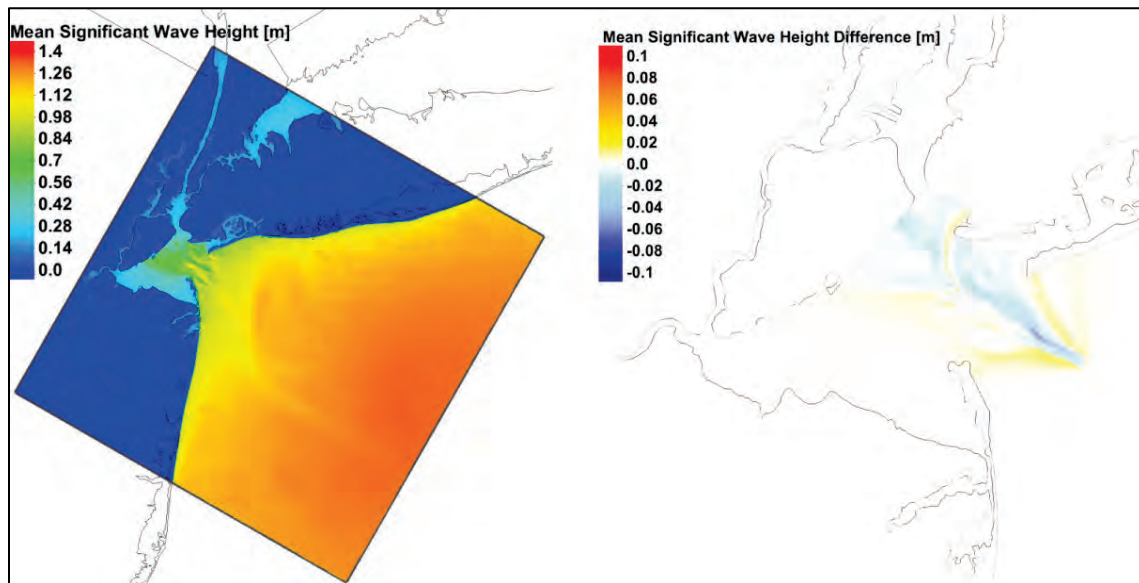


Figure 224. Effect of channel deepening on mean significant wave height for 2011.

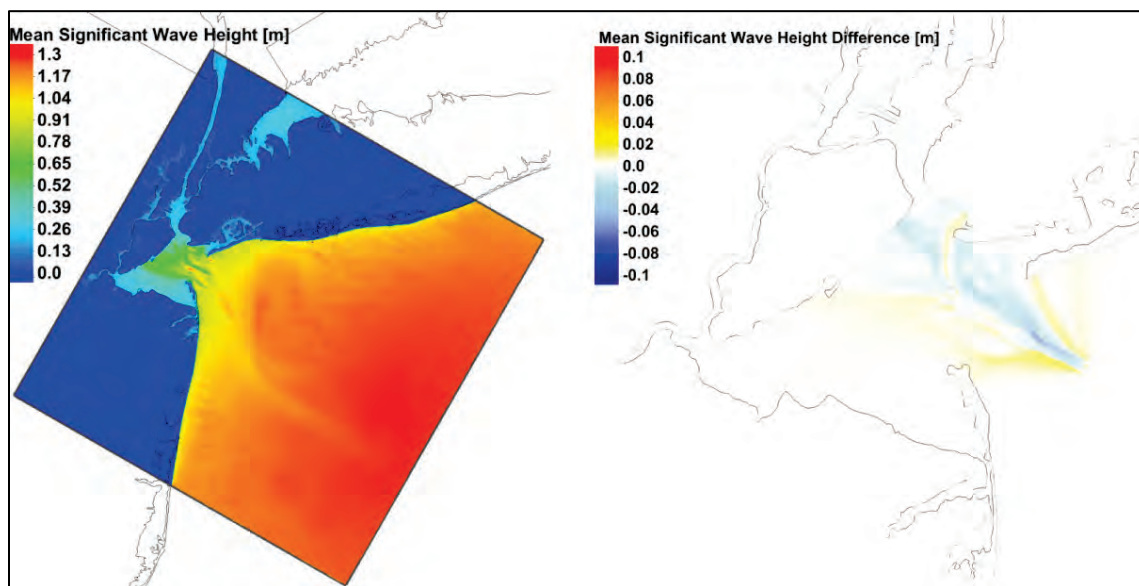
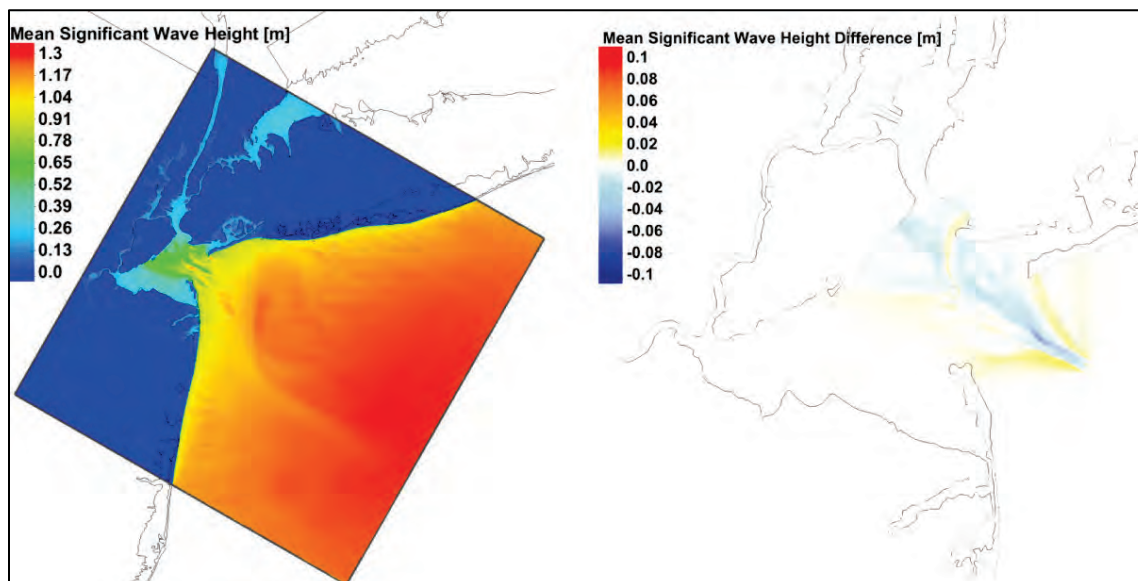


Figure 225. Effect of channel deepening on mean significant wave height for 2012.



The mean significant wave height envelope for all modeled timeframes is similar. The maximum average wave height ranges from 1.2 m in 1985 to 1.4 m in 1996. For all modeled timeframes, average significant wave heights within the Ambrose Navigation Channel are slightly smaller whereas waves adjacent to the channel are slightly larger. This pattern results from changes in the shoaling location of propagating waves due to the deeper channel (e.g., waves are influenced less by the deeper bathymetry). The effect of the channel deepening on the mean significant wave height is marginal, with differences on the order of 10 cm or less.

In addition to mean wave climate, it is important to look at the storm wave climate since larger waves can result in more sediment transport. The effect of channel deepening on the storm wave climate is generalized below by comparing the maximum wave envelope for each year-long simulation. As in the previous figures, the left panels of Figure 226 through Figure 230 show the maximum significant wave height and the right panel shows the difference in maximum significant wave height due to the channel deepening project. Note that the maximum wave height envelope is a single instance of the entire year-long simulation and may not occur at the same time-step for each grid cell.



Figure 226. Effect of channel deepening on max significant wave height for 1985.

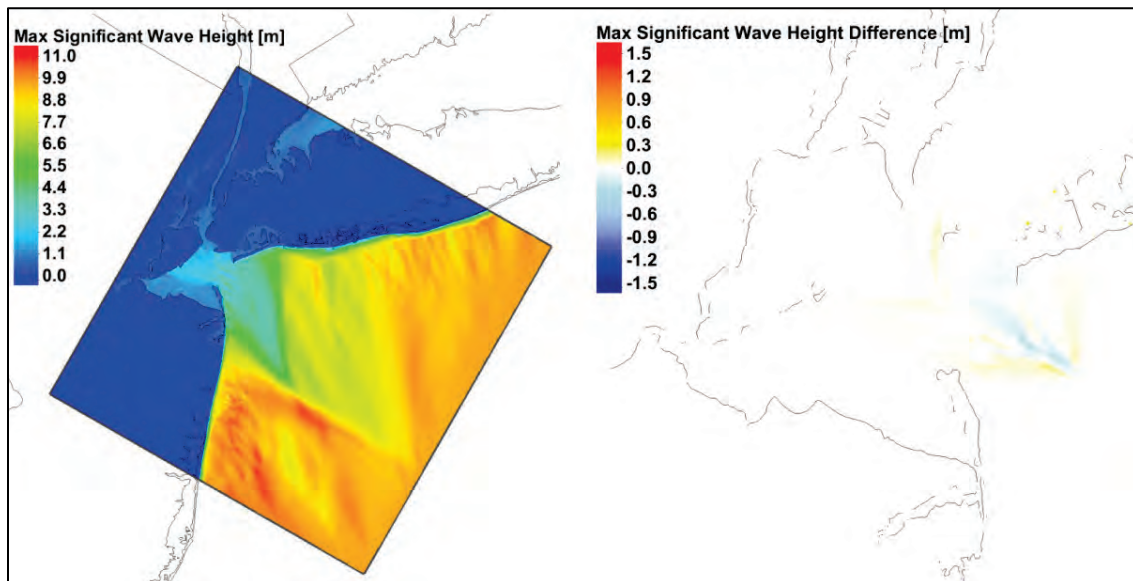


Figure 227. Effect of channel deepening on max significant wave height for 1995.

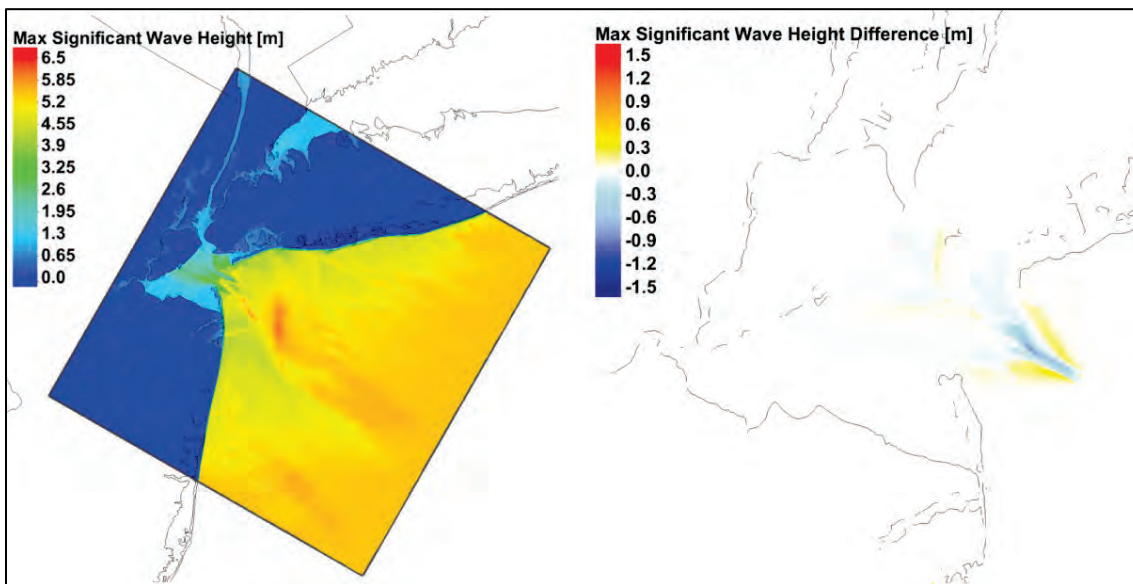




Figure 228. Effect of channel deepening on max significant wave height for 1996.

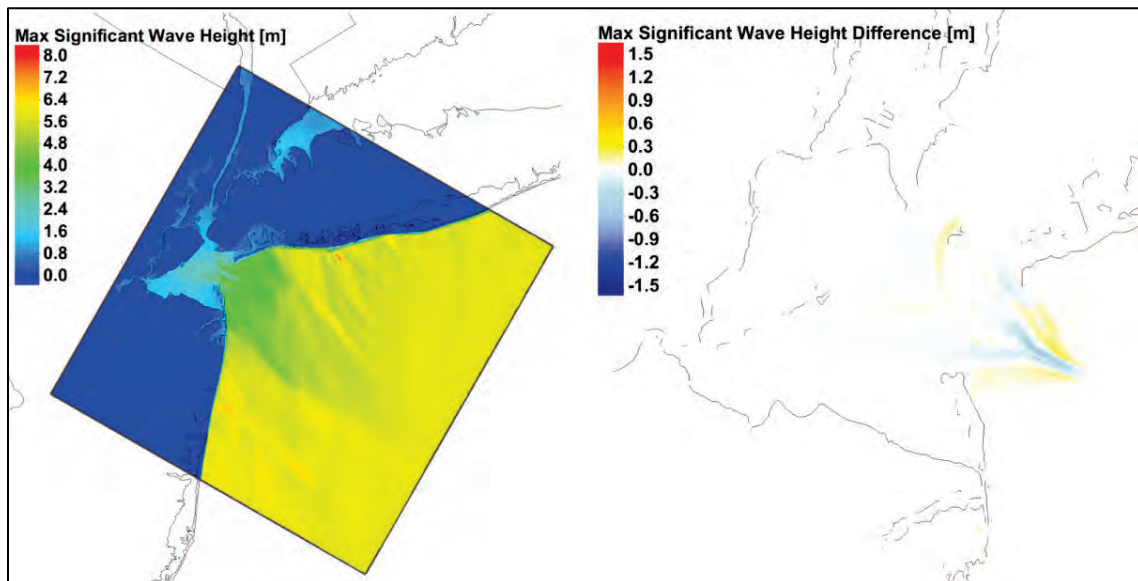


Figure 229. Effect of channel deepening on max significant wave height for 2011.

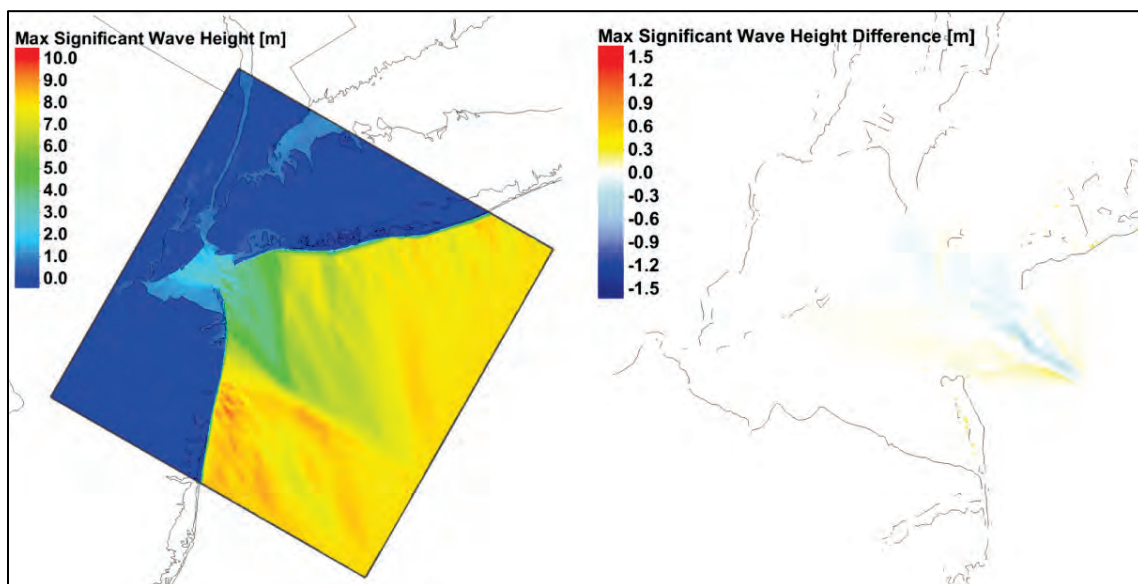
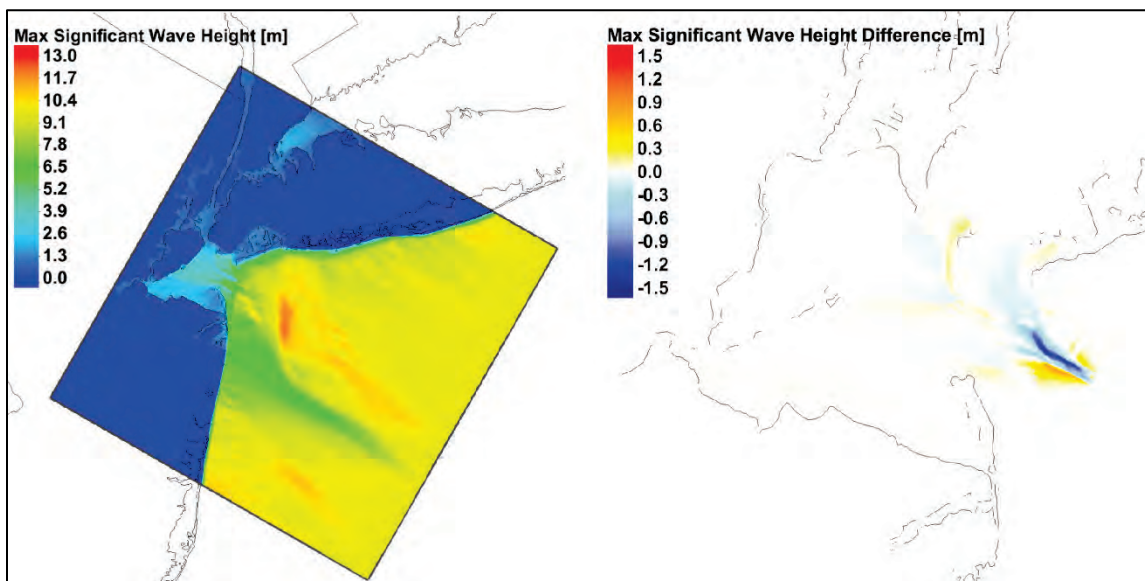


Figure 230. Effect of channel deepening on max significant wave height for 2012.



The smallest and largest significant wave height was found in 1995 and 2012, respectively. The greatest differences are localized within the entrance of the Ambrose Navigation Channel, and the magnitude of the difference is much larger than the mean wave climate of the same year. Except for 2011, the difference in maximum wave height exceeds 0.5 m. The largest differences, up to 1.5 m, are seen for 2012. The difference plots look similar to that of the mean wave climate analysis in that waves for the with-project configuration are again generally smaller within the channel and larger adjacent to the channel as compared to the without-project configuration. Like the mean wave climate, this pattern is a result of the channel deepening altering the transformation of the waves.

## 10 Extreme Event Analysis

Extreme events (primarily hurricanes) can have a significant impact on an estuarine system. This impact extends to the dredge volumes analyzed as part of this study. The 5 years simulated for this study included 3 years with major hurricanes — Hurricane Gloria (1985), Hurricane Irene (2011), and Hurricane Sandy (2012). While the actual events are relatively short in duration, the impacts in terms of inflows and/or sediment concentrations can linger for several weeks and even months. The modeled fine sediment bottom (water) concentrations were analyzed at the three locations in Figure 231 in an attempt to determine an approximate duration of influence due to these extreme events. From analysis of the results shown in Figures 232, 233, and 234, the start and stop times for these events were determined as provided in Table 23.

Also note that in 2011, there were two very large flows on the Passaic River that dominated the sediment concentrations in Newark Bay. These events were two to three times larger than any other event simulated for the remaining four years and as such resulted in very large impacts on the sediment concentrations and associated dredge volumes.

Figure 231. Three points to analyze for the duration of storm impacts on sediment concentrations.

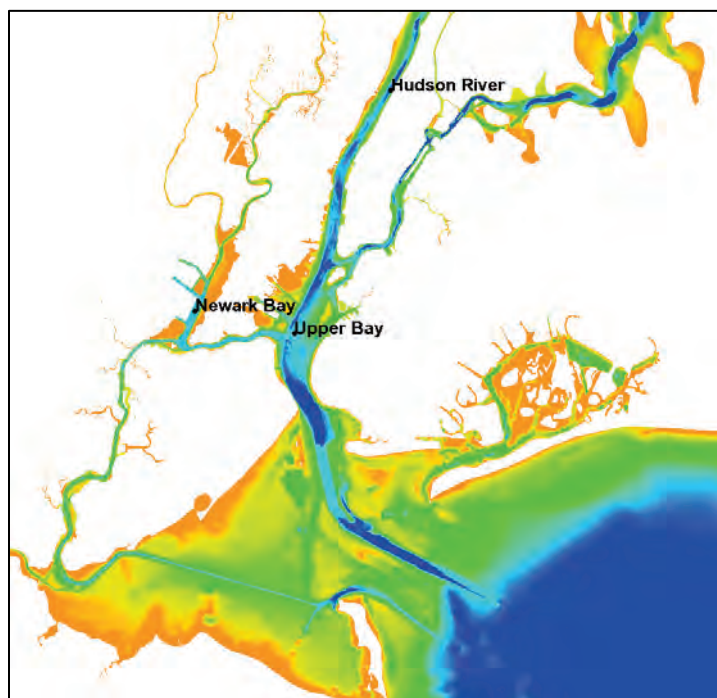


Figure 232. Hudson River bottom water layer fine sediment concentrations.

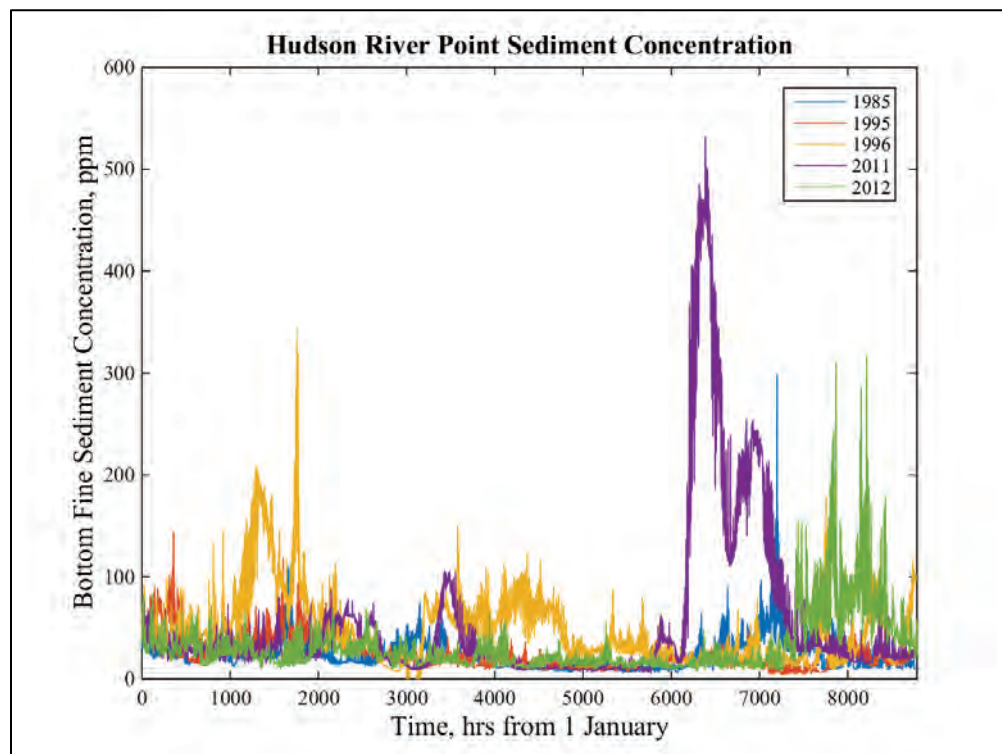


Figure 233. Upper Bay bottom water layer fine sediment concentrations.

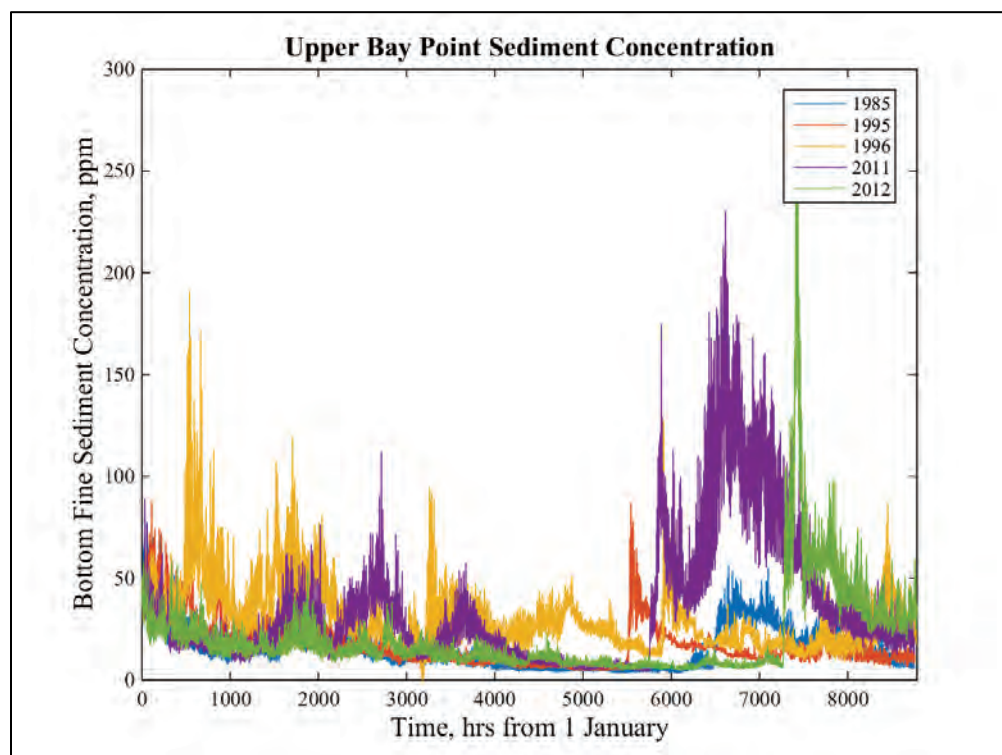


Figure 234. Newark Bay bottom water layer fine sediment concentrations.

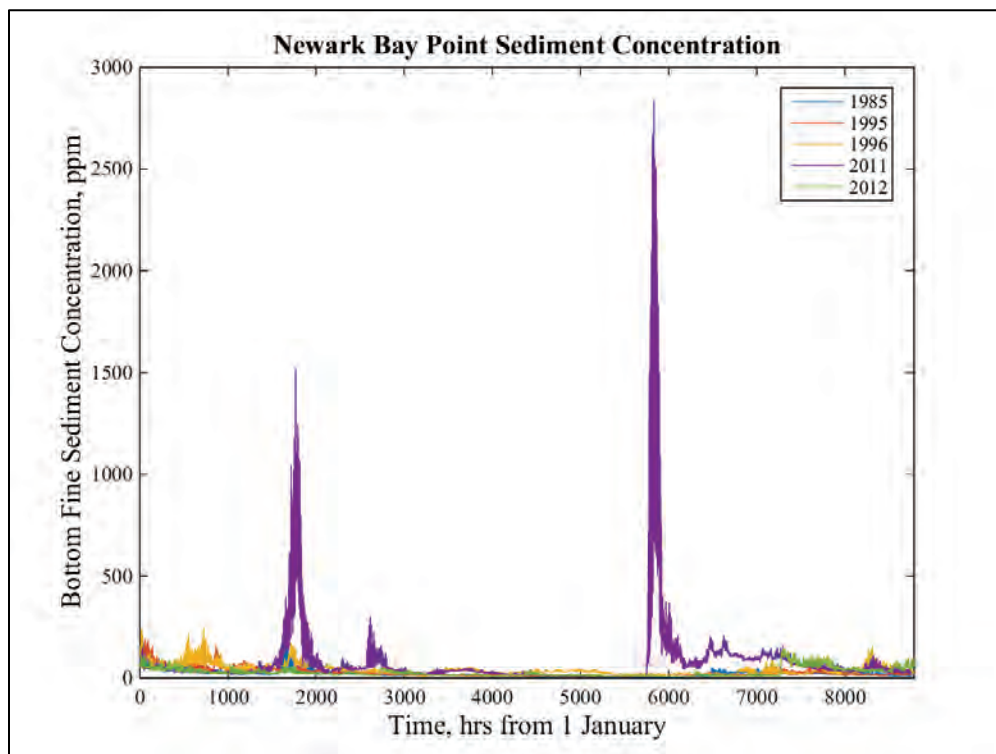


Table 23. Storm duration of influence on sediment transport.

Hurricane	Start Time (hours)	Stop Time (hours)
Gloria	09/27/1985 (6456)	11/07/1985 (7450)
Irene	08/27/2011 (5712)	11/30/2011 (8000)
Sandy	10/29/2012 (7248)	12/21/2012 (8500)

The reaches previously analyzed as part of the validation process (see Figure 86) were analyzed to determine an approximate percentage of dredging associated with the previously discussed hurricanes. A comparison of the dredge volumes due to hurricanes is presented in Figure 235 and Figure 236 and Table 24. Figure 237 shows a comparison of the impact of the hurricanes in the with-project and without-project configurations. These dredge volumes represent the deposition that occurred in the model between the start and stop times in Table 23. Deposition prior to or after this time period is not represented in the Hurricane-attributed values presented in Figure 235, Figure 236, and Figure 237.



Figure 235. Hurricane impacts of dredge volumes in the without-project configuration.

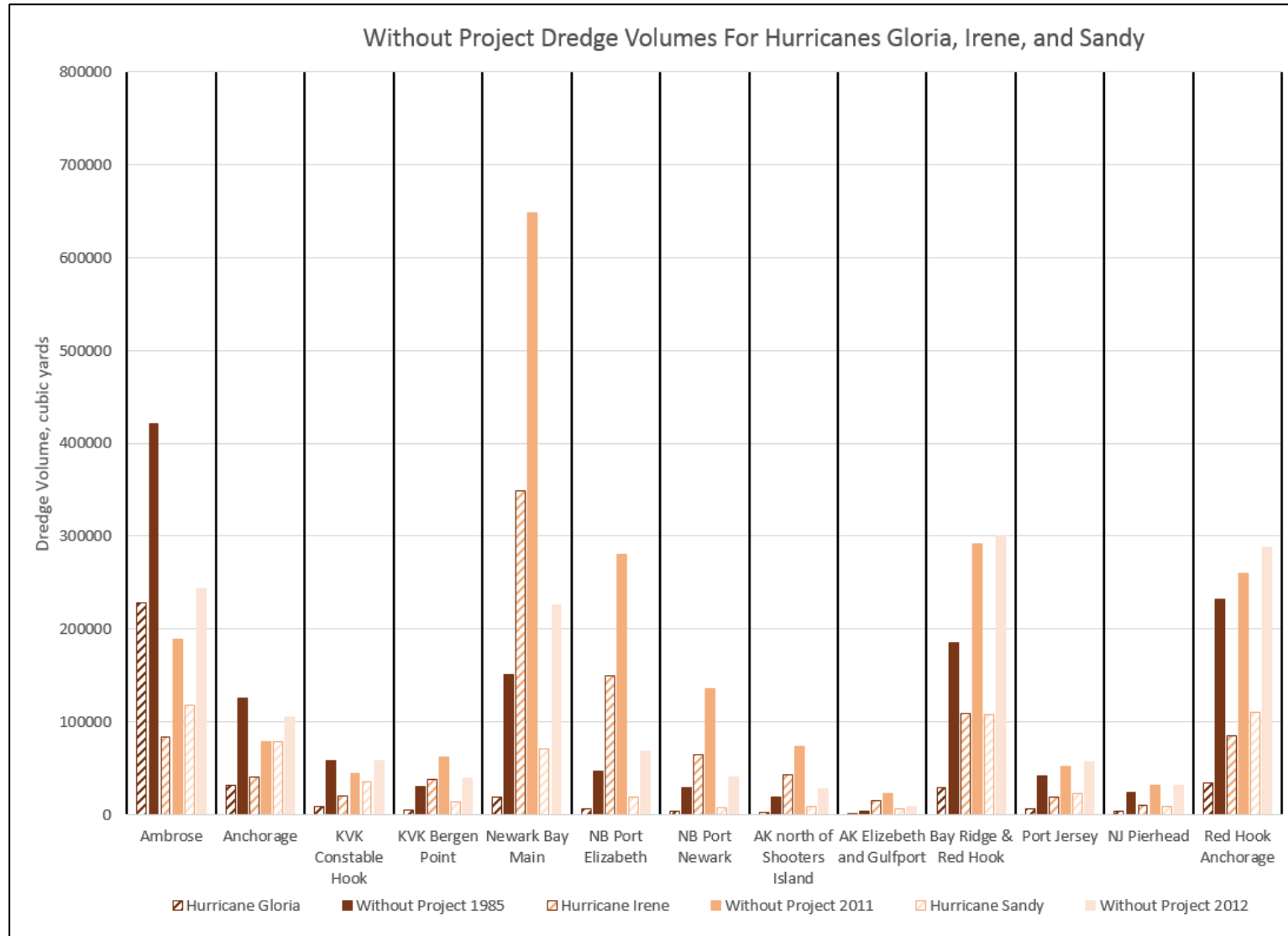


Figure 236. Hurricane impacts of dredge volumes in the with-project configuration.

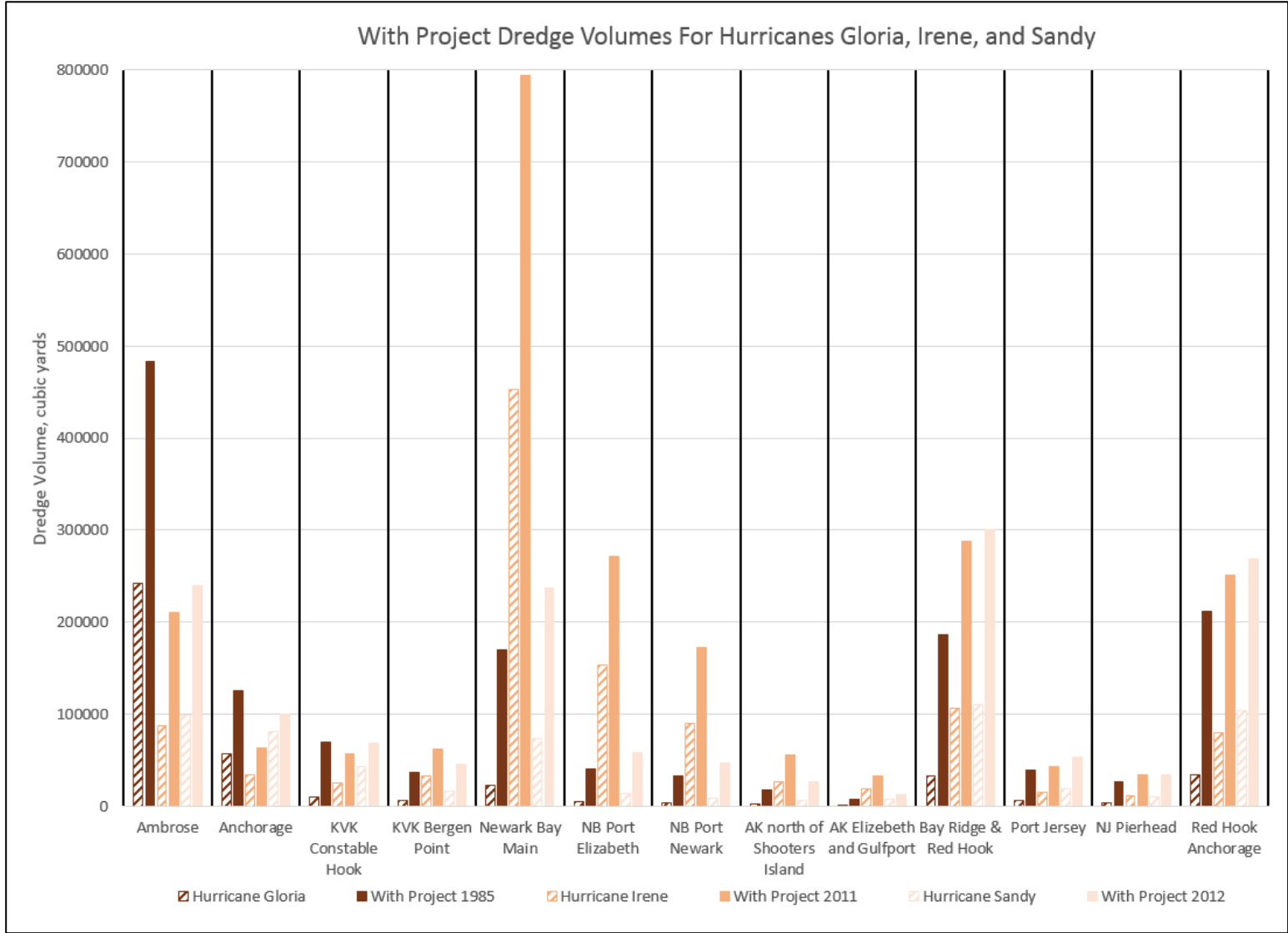


Figure 237. With-project versus without-project hurricane impacts.

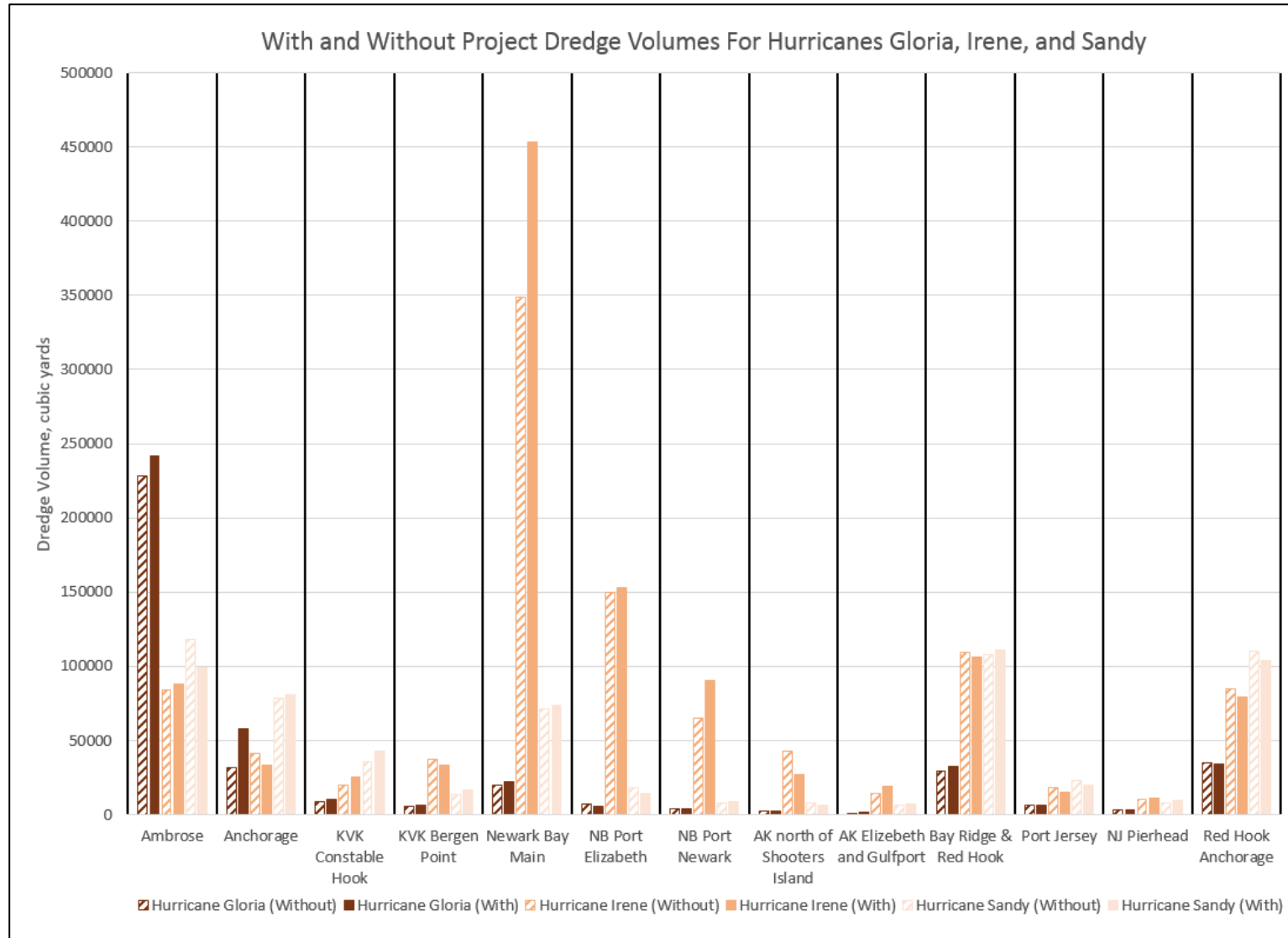


Table 24. Hurricanes Gloria, Irene, and Sandy dredge volumes, cy.

Channel Reach	Gloria (without project)	Gloria (with project)	Irene (without project)	Irene (with project)	Sandy (without project)	Sandy (with project)
Ambrose	228,133	241,961	83,628	87,807	117,810	98,672
Anchorage	31,521	57,350	40,663	33,480	78,029	80,444
Kill van Kull Constable Hook	8,560	9,946	19,498	24,768	35,376	42,578
Kill van Kull Bergen Point	5,162	6,258	37,444	33,084	13,613	16,145
Newark Bay Main	19,293	21,963	348,677	453,186	71,178	73,833
NB Port Elizabeth	6,601	5,346	149,384	152,811	18,045	13,733
NB Port Newark	3,502	4,079	64,759	89,907	7,741	8,853
AK north of Shooters Island	2,315	2,360	42,698	26,879	8,068	5,913

It is evident from these model results that extreme tropical hurricanes can have a significant impact on the dredging requirements in NYNJH. While the resulting dredge volumes due to hurricanes can vary over an order of magnitude, it is imperative any estimate of dredging requirements consider these factors. While the occurrences of such events are unpredictable, neglecting these events could result in a significant underprediction of long-term dredging requirements

Hurricane Gloria was responsible for approximately 28% of the dredging for 1985. Hurricane Irene was responsible for approximately 48% of the dredge volumes for 2011. The dredge volumes induced by Hurricane Irene were over 70% of the total dredge volumes for 1985 (78%), 1995 (77%), and 2012 (76%), illustrating the severity of this event and 2011 in general. Hurricane Sandy was responsible for approximately 40% of the dredge volumes for 2012.

Considering the variation in dredge volumes for the with-project and without-project configurations (Figure 237), it is apparent the increase/decrease in dredging varies both by event and location and does not appear to be consistent across storm events. This variation is to be expected. While all these events are hurricanes, they possess varying characteristics (forward speed, pressure, wind field, etc.) and therefore are expected to result in differing system impacts. For these particular reaches (Figure 86), it appears for Gloria and Irene that the with-project configuration results in increases in dredge volumes of 12% and 10%, respectively. However, Sandy produces a slight decrease (2%) for these reaches. Note these numbers change if a different start/stop time was chosen beyond those listed in Table 23. The previously shown comparisons of the without-project to with-project configurations over the entire year indicated increases of 6% for 1985, 7.5% for 2011, and 0% for 2012.



## **11 Sensitivity Simulations**

In an effort to investigate the uncertainty in the numerical model results, sensitivity simulations were completed to quantify the impact of specific model parameters, inputs, and processes. A brief description is provided for each of the sensitivity simulations with a comparison of the model results compiled. Performing these sensitivity simulations over each of the 5 years would have been a significant computational effort. Therefore, a single year was chosen, and the sensitivity simulations were completed by modifying the individual parameters with the forcings from 1995. The 1995 calendar year was a median year in terms of the dredge volume increase due to the project and as such deemed the most appropriate for this endeavor. The sensitivity simulations were completed by making single, independent modifications to the model input to investigate the impact of the various parameters. These sensitivity simulations were simulated for both the with-project and without-project configurations to evaluate both the impact to the absolute numbers and the implied impact due to the system modifications.

### **Sewage flow sensitivity**

In the previously shown results, the sewage flows were held constant for the entirety of the simulations due to a lack of time-series data for all the wastewater treatment facilities which is not representative of the true system. A sensitivity simulation was completed whereby the sewage flows were removed completely from the boundary conditions file to investigate the impact of the wastewater treatment facility flows on the dredge volumes. Completely removing these freshwater inflows is the extreme case but was utilized to bracket the impact of wastewater treatment flows.

### **Diffusion specification sensitivity**

Vertical turbulent diffusion is handled by Mellor-Yamada 2.0 (Mellor and Yamada 1982) closure with vertical mixing reduced based on Richardson number for cases of stratification (Savant 2015). For stability purposes, a minimum diffusion value is specified in the boundary conditions file. This sensitivity simulation doubled that minimum value to investigate the impact of this model input parameter on the dredge volumes.

## **Friction specification sensitivity**

The bed friction was implemented using a Manning's  $n$  value for the entire model domain. A specification of 0.025 produced reasonable water levels as compared to the observations (see Chapter 8 for model to field comparisons). This sensitivity increased the 0.025 Manning's  $n$  value to 0.030. This was deemed the higher limit of reasonable Manning's  $n$  values for this system.

## **Wind wave sensitivity**

In an effort to quantify the impact of the wind wave generation and propagation on the sedimentation, simulations were performed without linking to STWAVE. These simulations included no wind-wave generation or propagation.

## **Inflow sensitivity**

The inflows were observations obtained from the USGS, but uncertainty exists in these measurements. This set of sensitivity simulations investigates the impact of varying the riverine inflows by increasing each of the riverine inflows by 20%. Note that the boundary sediment concentrations were not updated to represent the higher flows. This approach was utilized to prevent changes of multiple parameters in a single set of simulations.

## **Sea level rise sensitivity**

A common concern is the impact of climate change on coastal systems and the impact any proposed alternatives have in conjunction with sea level rise. This set of simulations increased the sea level value by 6 ft. This set of simulations required the 1-month hydrodynamic spinups be re-done to allow the hydrodynamics and salinity transport to adjust to this new water level. All other input and model parameters were left unchanged.

## **Initial bed specification**

The initial bed specification can have a significant impact on the sediment erosion and transport. As previously discussed, the initial bed was specified based on available data with a 1-year spin-up time period being simulated to allow the bed to adjust to the hydrodynamics. This step was completed for both the with- and without- project configurations. The impact of this

change is the reported sediment transport is more representative of the longer-term behavior. This sensitivity utilized the without-project bed spinup for the with-project simulations. This would be more representative of an instantaneous creation of the with-project configuration while also assuming no change to the bed composition. For this study, this sensitivity is an attempt to quantify the impact of the bed specification on the dredge volumes.

## Model results

A brief discussion of the results of these sensitivity simulations is provided for the locations shown in Figure 86. The dredge volume results are provided in Figure 238 and Figure 239 with the actual numbers provided in Table 25 and Table 26. These results indicate the largest sensitivity is associated with the sea level rise (6 ft) which is to be expected given this is a large change in the mean water level and could be considered more a representation of future conditions than a true sensitivity test. The friction changes provided the next largest impact on the absolute dredge volumes. The total dredge volumes for these channel reaches were analyzed to determine the impact of these parameters on the with- versus without-project percentage differences. As expected, all simulations showed an increase in the dredge volumes for the with-project configuration. The results are as follows:

1. Original 1995 comparisons of with- versus without-project indicated an increase of approximately 4%.
2. The sewage sensitivity simulations indicate an increase of approximately 5%.
3. The diffusion sensitivity simulations indicate an increase of approximately 2.5%.
4. The friction sensitivity simulations indicate an increase of approximately 6.5%.
5. The wave sensitivity simulations indicate an increase of approximately 3.5%.
6. The inflow sensitivity simulations indicate an increase of approximately 3%.
7. The sea level rise sensitivity simulations indicate an increase of approximately 1.5% but has a large redistribution of sedimentation (see Figure 238 and Figure 239).
8. The initial bed sediment sensitivity simulations indicate an increase of approximately 10.5%.

While these results illustrate the uncertainty in the results of this model study, these sensitivity simulations reinforce the previously reported 4% increase for 1995 is a reasonable value since the sensitivity results tended to be slightly higher and lower than the reported value. These values are also within the range of values obtained for varying meteorological conditions (yearly variation).

Note that the sea level rise sensitivity of 6 ft is more of a future prediction of impacts than a true sensitivity due to the large change, but it provides an indication of the expected impact of sea level rise and brackets the changes. The initial bed sediment sensitivity is also somewhat unrealistic in that the bed utilized was initialized based on the without-project spinup. As shown in previous results the flow is redistributed due to the alternative and as such this is a somewhat unrealistic scenario. It was completed to bracket the results.

Table 25. With-project sensitivity simulation results.

Channel	With Project 1995, cy							
	Base	Sewage	Diffusion	Friction	Waves	Inflow	Sea Level Rise	Initial Bed Sediment
Ambrose	370,648	400,229	340,691	368,952	321,254	353,135	213,908	398,968
Anchorage	80,410	79,329	58,511	89,581	76,159	81,200	107,576	102,381
Kill van Kull Constable Hook	39,636	39,189	33,571	53,807	37,021	40,752	34,850	50,627
Kill van Kull Bergen Point	49,700	50,287	45,870	57,959	49,582	50,303	43,367	49,454
Newark Bay Main	231,498	226,829	194,784	218,948	232,301	238,706	205,369	236,549
NB Port Elizabeth	54,405	54,872	45,646	54,821	53,764	57,458	59,625	54,276
NB Port Newark	41,940	42,604	35,027	46,199	41,668	44,559	50,068	42,873
AK north of Shooters Island	27,844	26,918	26,628	27,452	27,876	28,707	23,818	26,720
AK Elizebeth and Gulfport	7,664	7,098	7,275	20,022	7,287	7,872	3,548	8,783
Bay Ridge & Red Hook	247,059	245,448	231,640	141,995	240,636	249,939	461,572	258,073
Port Jersey	47,978	50,570	42,089	36,766	46,294	48,001	49,824	62,294
NJ Pierhead	31,714	32,855	31,996	29,225	30,644	32,322	42,923	35,114
Red Hook Anchorage	238,406	226,638	191,592	141,095	229,187	243,081	367,173	232,018



**Table 26. Without-project sensitivity simulation results.**

Channel	Without Project 1995, cy						
	Base	Sewage	Diffusion	Friction	Waves	Inflow	Sea Level Rise
Ambrose	335,272	361,111	322,328	326,423	298,025	324,667	189,876
Anchorage	82,794	78,107	64,352	91,674	79,131	86,450	118,302
Kill van Kull Constable Hook	31,926	30,651	27,812	44,440	30,421	32,356	29,522
Kill van Kull Bergen Point	39,347	39,921	36,280	47,690	39,762	39,491	35,847
Newark Bay Main	213,186	207,841	178,638	190,805	213,800	219,159	196,644
NB Port Elizabeth	62,719	62,506	51,846	63,106	61,176	65,343	69,059
NB Port Newark	37,770	38,362	31,785	39,816	37,013	39,342	46,026
AK north of Shooters Island	26,484	25,765	25,548	28,770	26,738	27,103	23,880
AK Elizebeth and Gulfport	3,625	3,072	3,204	16,227	3,354	3,603	772
Bay Ridge & Red Hook	248,612	245,973	235,786	142,689	243,812	256,378	468,551
Port Jersey	49,730	52,345	45,040	40,175	47,478	49,828	50,277
NJ Pierhead	29,532	30,556	29,535	25,954	28,261	29,727	40,748
Red Hook Anchorage	248,463	232,301	202,469	149,125	237,463	259,850	370,370

Figure 238. Sensitivity simulation results for 1995 for the without-project configuration.

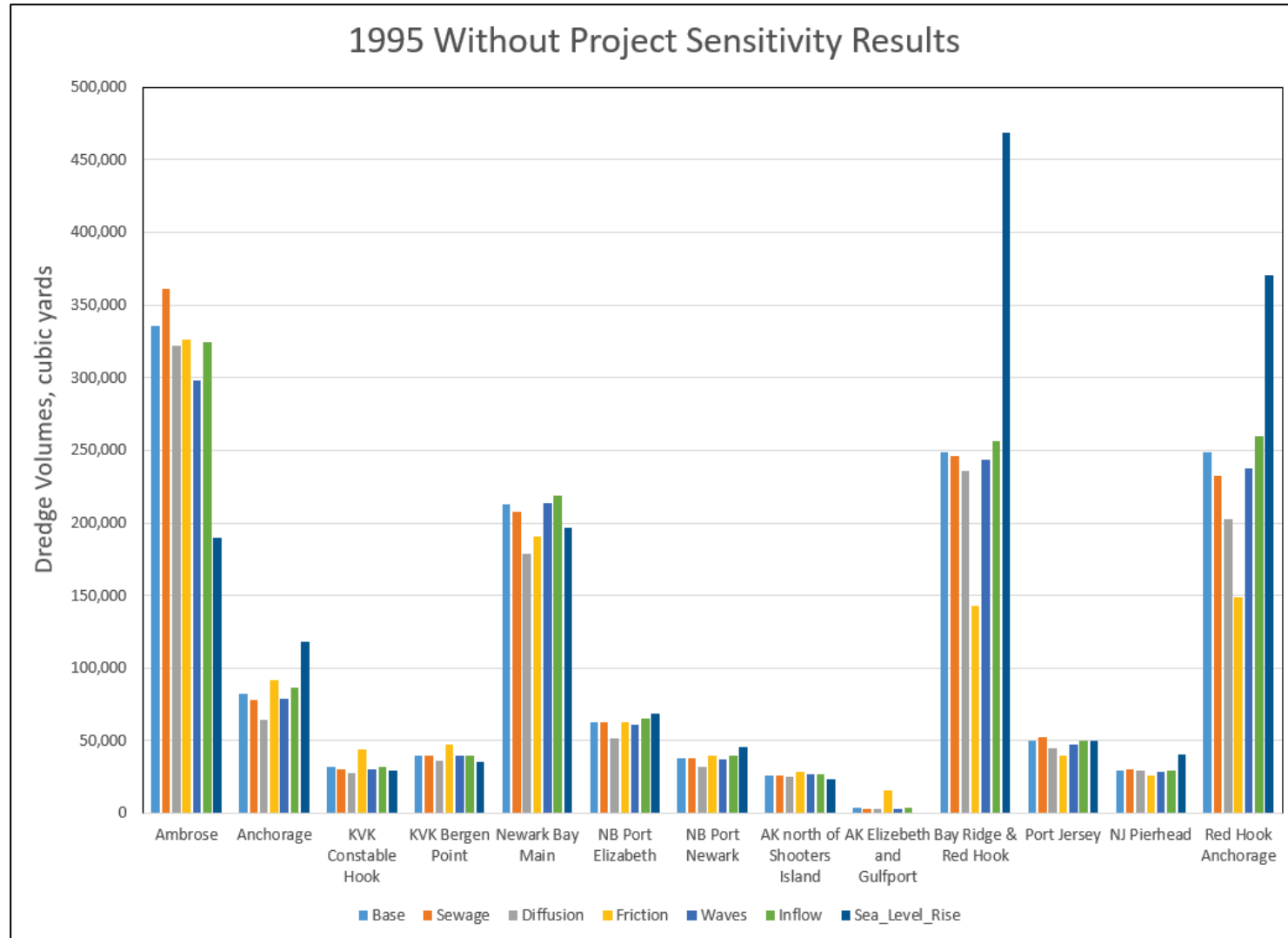
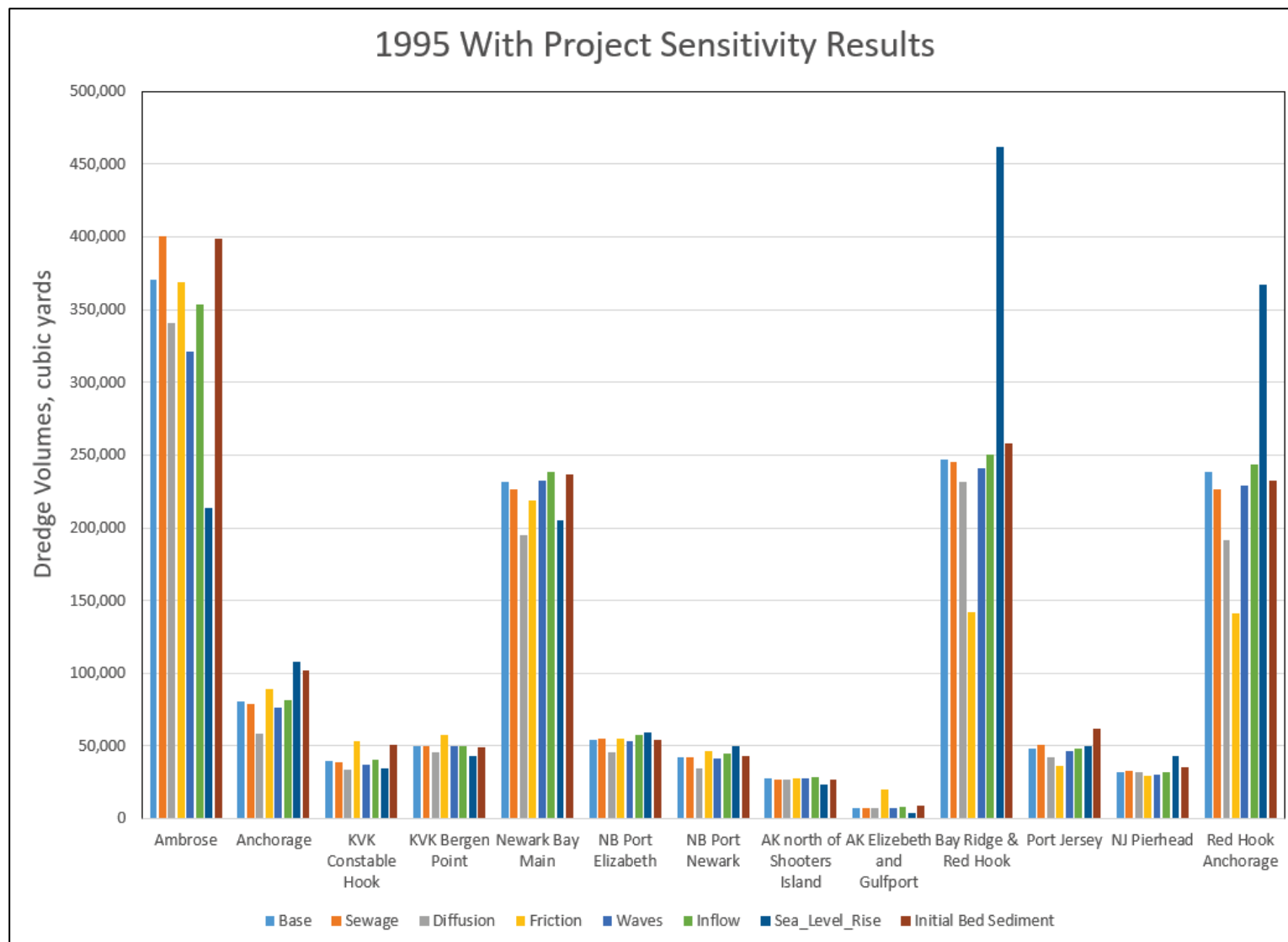


Figure 239. Sensitivity simulation results for 1995 for the with-project configuration.



## 12 Conclusions

Analysis of the model results provides insight into several impacts associated with the channel deepening. The primary impacts are as follows:

1. The flow through the Kill van Kull is increased by approximately 36% with increased flow of salinity and sediment as well.
2. As would be expected, the salinity intrusion up the Ambrose ship channel is increased. This is expected to be due to a combination of the channel deepening and the redistribution of flow through Kill van Kull.
3. The Kill van Kull and Newark Bay are the primary channels with increased dredging requirements with expected increases of 18% and 11% respectively. This equates to increases in the dredge volumes of approximately 16,500 cy (Kill van Kull) and 54,500 cy (Newark Bay).
4. The variation in the total annual dredge volumes of 1.1 million cy is an order of magnitude larger than the changes due to the project (approximately 40,000 cy).
5. The dredge volumes for the five simulated years for the commonly dredged locations shown in Figure 86 ranged from approximately 1.3 million cy (1985) to a high of 2.3 million cy (2011) indicating a possible variation across years of approximately 1 million cy. The average dredge volume was approximately 1.61 million cy for the without project and approximately 1.68 million cy for the with project indicating an increase of approximately 70,000 cy or 4%.
6. For the locations shown in Figure 86, the yearly percentage increases (with project compared to without project) in overall dredging were 6% (1985), 4% (1995), 3% (1996), 7% (2011), and 0% (2012) with an average annual increase in dredging of 4%.
7. When considering all channel reaches, the increase in dredging is only 1% as shown in Table 22. This would indicate the non-project channels experienced less increase and even some decreases in dredging as compared to the deepened project channels.
8. Sensitivity simulations were performed to evaluate the variability in the results due to certain input parameters using the 1995 forcing conditions. These results reinforced the previously reported increase of approximately 4% for the with-project configuration as it was in the median range of the sensitivity simulations. All of the sensitivity

- simulations indicated the same direction of change for the project condition (increased dredging) with some of the results indicating larger increases and some indicating smaller increases.
9. Extreme events like Hurricanes Irene and Sandy can have significant impacts on the dredging requirements. Simulations of Hurricanes Gloria (1985), Irene (2011), and Sandy (2012) accounted for approximately 28% (1985), 48% (2011), and 40% (2012) of the dredge volumes for the given years.

One limitation of this study is the exclusion of ship traffic impacts. While the model appears to replicate the historical dredge volumes adequately, larger ships traveling at higher speeds create large bow waves that can increase shoreline erosion and erosion of surrounding shallow bays. Any impact associated with these larger/faster ships would not be captured in this modeling effort.



## References

- Bender, C., J. M. Smith, A. Kennedy, and R. Jensen. 2013. "STWAVE Simulation of Hurricane Ike: Model Results and Comparison to Data." *Coastal Engineering* 73: 58–70.
- Blumberg, A. F., L. A. Khan, and J. P. St. John. 1999. "Three Dimensional Hydrodynamic Model of New York Harbor." *J. Hyd. Engr.*, ASCE 125(8): 799–816.
- Brown, Gary L. 2012a. "A Quasi-3D Suspended Sediment Model Using a Set of Correction Factors Applied to a Depth Averaged Advection Diffusion Equation." Proceedings, *IIHR 3rd International Shallow Flows Symposium*, University of Iowa, 2012.
- Brown, Gary L. 2012b. "Modification of the Bed Sediment Equations of Spasojevic and Holly (1993) to Account for Variable Porosity, Variable Grain Specific Gravity, and Nonerodable Boundaries." Proceedings, *IIHR 3rd International Shallow Flows Symposium*, University of Iowa, 2012.
- Bryant, Mary A., Tyler J. Hesser, and Robert E. Jensen. 2016. *Evaluation statistics computed for the Wave Information Studies (WIS)*. ERDC/CHL CHETN-1-91. Vicksburg, MS: US Army Engineer Research and Development Center.
- Bunya, S., J. Westerink, J. C. Dietrich, H. J. Westerink, L. G. Westerink, J. Atkinson, B. Ebersole, J. M. Smith, D. Resio, R. Jensen, M. A. Cialone, R. Luettich, C. Dawson, H. J. Roberts, and J. Ratcliff. 2010. "A High-Resolution Coupled Riverine Flow, Tide, Wind, Wind Wave and Storm Surge Model for Southern Louisiana and Mississippi: Part I-Model Development and Validation." *Monthly Weather Review* 138: 345–377.
- Caplow, Theodore, Peter Schlosser, David T. Ho, and Nicholas Santella. 2003. "Transport Dynamics in a Sheltered Estuary and Connecting Tidal Straits: SF<sub>6</sub> Tracer Study in New York Harbor." *Environmental Science and Technology* 37(22): 5116–5126.
- CENAN (US Army Engineer New York District). 2007. *Final Environmental Assessment: Effects of the NY/NJ Harbor Deepening Project on the Remedial Investigation/Feasibility Study of the Newark Bay Study Area*. New York, NY.
- Chant, R. J. 2006. *Hydrodynamics of the Newark Bay/Kills System: The New Jersey Toxics Reduction Workplan for New York-New Jersey Harbor – Study I-E*. April 2006. Prepared for NJ Department of Environmental Protection.
- Chant, Robert J., David Fugate, and Ed Garvey 2011. "The Shaping of an Estuarine Superfund Site: Roles of Evolving Dynamics and Geomorphology." *Estuaries and Coasts* 34: 90–105.
- Chen, Ke, and Ruoying He. 2010. "Numerical Investigation of the Middle Atlantic Bight Shelfbreak Frontal Circulation Using a High-Resolution Ocean Hindcast Model." *Journal of Physical Oceanography* 40(May 2010): 949–964.

- Cialone, M. A., C. T. Massey, M. E. Anderson, A. S. Grzegorzewski, R. E. Jensen, A. Cialone, D. J. Mark, K. C. Pevey, B. L. Gunkel, T. O. McAlpin, N. N. Nadal-Caraballo, J. A. Melby, and J. J. Ratcliff. 2015. *North Atlantic Coast Comprehensive Study (NACCS) Coastal Storm Model Simulations: Waves and Water Levels*. ERDC-CHL TR-15-14. Vicksburg, MS: U.S. Army Engineer Research and Development Center.
- Clarke, D., S. Zappala, K. J. Reine, C. Dickerson, C. Alcoba, J. Gallo, and B. Wisemiller. 2015. *Sediment Resuspension by Ship Traffic in Newark Bay, New Jersey*. ERDC/EL TR-15-1. Vicksburg, MS: U.S. Army Engineer Research and Development Center.
- Coch, Nicholas K. 2016. "Sediment Dynamics in the Upper and Lower Bays of New York Harbor." *Journal of Coastal Research* 32(4): 756–767.
- Dietrich, J. C., S. Bunya, J. J. Westerink, B. A. Ebersole, J. M. Smith, J. H. Atkinson, R. Jensen, D. T. Resio, R. A. Luettich, C. Dawson, V. J. Cardone, A. T. Cox, M. D. Powell, H. J. Westerink, and H. J. Roberts. 2010. "A High-Resolution Coupled Riverine Flow, Tide, Wind, Wind Wave, and Storm Surge Model for Southern Louisiana and Mississippi. Part II: Synoptic Description and Analysis of Hurricanes Katrina and Rita." *Monthly Weather Review* 138: 378–404.
- Dietrich, J. C., M. Zijlema, J. J. Westerink, L. H. Holthuijsen, C. Dawson, R. A. Luettich Jr., R. E. Jensen, J. M. Smith, G. S. Stelling, and G. W. Stone. 2011. "Modeling Hurricane Waves and Storm Surge Using Integrally-Coupled Scalable Computations." *Coastal Engineering* 58(2011): 45–65.
- Geyer, W. R., and R. Chant. 2006. "The Physical Oceanography Processes in the Hudson River Estuary." *Hudson River Estuary*. Edited by J. S. Levinton and J. R. Waldman. New York City: Cambridge University Press.
- Geyer, W. R., J. D. Woodruff, and P. Tyrrakovski. 2001. "Sediment Transport and Trapping in the Hudson River Estuary." *Estuaries* 24(5): 670–679.
- Graf, W. H. 1971. *Hydraulics of Sediment Transport*. New York, NY: McGraw-Hill.
- Harleman, Donald R. F. 1966. "Diffusion Processes in Stratified Flow." *Estuary and Coastline Hydrodynamics*. Edited by Arthur T. Ippen. Chapter 12. New York, NY: McGraw-Hill.
- Hasselmann, K., T. P. Barnett, E. Bouws, H. Carlson, D. E. Cartwright, K. Enke, J. A. Ewing, H. Gienapp, D. E. Hasselmann, P. Kruseman, A. Meerburg, P. Muller, D. J. Olbers, K. Richter, W. Sell, and H. Walden. 1973. "Measurement of Wind-Wave Growth and Swell Decay during the Joint North Sea Wave Project (JONSWAP)." *Deutsches Hydrographisches Institut Suppl. A* 8(12): 1–95.
- Hellweger, F. L., A. B. Blumberg, P. Schlosser, D. T. Ho, T. Caplow, U. Lall, and H. Li. 2004. "Transport in the Hudson Estuary: A Model Study of Estuarine Circulation and Tidal Trapping." *Estuaries* 27(3): 527–538.
- Holthuijsen, L. H. 2007. *Waves in Ocean and Coastal Waters*. United Kingdom: Cambridge University Press.

- Hope, M. E., J. J. Westerink, A. B. Kennedy, P. C. Kerr, J. C. Dietrich, C. Dawson, C. Bender, J. M. Smith, R. E. Jensen, M. Zijlema, L. H. Holthuijsen, R. A. Luettich, M. D. Powell, V. J. Cardone, A. T. Cox, H. Pourtaheri, H. J. Roberts, J. H. Atkinson, S. Tanaka, H. J. Westerink, and L. G. Westerink. 2013. "Hindcast and Validation of Hurricane Ike (2008) Waves, Forerunner, and Storm Surge." *Journal of Geophysical Research* 118(9): 4424–4460.
- HydroQual, Inc. 2008. *Lower Passaic River Restoration Project and Newark Bay Study: Final Hydrodynamic Modeling Report*. US Environmental Protection Agency, Region 2.
- Jonsson, I. G. 1990. "Wave-Current Interactions." *The Sea*. Chapter 3, Vol. 9, Part A, Edited by B. LeMehaute and D. M. Hanes. New York: John Wiley & Sons, Inc.
- Krone, R. B. 1962. *Flume Studies of Transport of Sediment in Estuarial Shoaling Processes*. Final Report. Berkeley, CA Hydraulics Engineering Research Laboratory, University of California.
- Letter, J. V., Jr. 2009. *Significance of Probabilistic Parameterization in Cohesive Sediment Bed Exchange*. Dissertation. Gainesville, FL: Coastal and Oceanographic Engineering, University of Florida.
- Martin, S. K., G. Savant, and D. C. McVan. 2011. "Two-Dimensional Numerical Model of the Gulf Intracoastal Waterway near New Orleans." *Journal of Waterway, Port, Coastal and Ocean Engineering* 138(3): 236–245.
- Massey, T. C., M. E. Anderson, J. M. Smith, J. Gomez, and R. Jones. 2011a. *STWAVE: Steady-State Spectral Wave Model User's Manual for STWAVE, Version 6.0*. ERDC/CHL SR-11-1. Vicksburg, MS: US Army Engineer Research and Development Center.
- Massey, T. C., T. V. Wamsley, and M. A. Cialone. 2011b. "Coastal Storm Modeling-System Integrations." *Proc., 2011 Solutions to Coastal Disasters Conf.*, ASCE, Reston, VA.
- McAlpin, T. O., G. Savant, G. L. Brown, J. Smith, and R. S. Chapman. 2013. "Hydrodynamics of Knik Arm: Modeling Study." *Journal of Waterway, Port, Coastal and Ocean Engineering* 139(3): 232–246.
- Mehta, A. J. 1973. *Depositional Behavior of Cohesive Sediments*. Dissertation. Gainesville, FL: University of Florida, Coastal and Oceanographic Engineering.
- Mellor, G. L., and T. Yamada. 1982. "Development of a Turbulence Closure Model for Geophysical Fluid Problems." *Reviews of Geophysics and Space Science* 20(4): 851–875.
- Merz, Bruno, and A. H. Thielen. 2005. "Separating Natural and Epistemic Uncertainty in Flood Frequency Analysis." *Journal of Hydrology* 309: 114–132.
- Miche, M. 1951. *Le Pouvoir Reflechissant des Ouvrages Maritimes Exposes a L'action de la Houle*. *Annals des Ponts et Chaussées* 121e Annee, 285–319. Translated by Lincoln and Chevron. University of California, Berkeley: Wave Research Laboratory, Series 3, Issue 363, June 1954.

- New York City's Wastewater Treatment System. n.d. *Cleaning the Water We Use: Protecting the Environment We Live In*. New York City Department of Environmental Protection. <https://semspub.epa.gov/work/02/206372.pdf>
- New York-New Jersey Harbor Estuary Program. 2008. *New Jersey Toxics Reduction Work Plan Study I-G Project Report*. Great Lakes Environmental Center.
- NOAA (National Ocean and Atmospheric Administration). 2005. *Tide Tables 2006, High and Low Water Predictions, East Coast of North and South America, Including Greenland*. National Imagery and Mapping Agency.
- NOAA. 2008. *VDATUM for the Long Island Sound, Narragansett Bay, and New York Bight: Tidal Datums, Marine Grids, and Sea Surface Topography*. NOAA Technical Memorandum NOS CS 16. Silver Spring, MD.
- Olsen, C. R. 1979. *Radionuclides, Sedimentation and the Accumulation of Pollutants in the Hudson River Estuary*. PhD Thesis. New York, New York: Columbia University.
- Padilla-Hernandez, R., and J. Monbaliu. 2001. "Energy Balance of Wind Waves as a Function of the Bottom Friction Formulations." *Coast. Engrg.* 43: 131–148.
- Panuzio, F. L. 1965. "Lower Hudson River Siltation." *Proceedings of the 2nd Federal Interagency Sedimentation Conference*. Agricultural Research Service, Misc. Publication 970.
- Parkman, Aubrey. 1983. *History of the Waterways of the Atlantic Coast of the United States*. NWS-83-10. US Army Engineer Water Resources Support Center. Institute for Water Resources.
- Partheniades, E. 1962. *A Study of Erosion and Deposition of Cohesive Soils in Salt Water*. PhD Dissertation. Berkeley, CA: University of California.
- Pecchioli, Joel A., Michael S. Bruno, Robert Chant, Anne Marie Pence, Alan F. Blumberg, David Fugate, Brian J. Fulerton, Scott Glenn, Chip Haldeman, Eli Hunter, and Kelly Rankin. 2006. *The New Jersey Toxics Reduction Workplan for New York – New Jersey Harbor: Study I-E – Hydrodynamic Studies in the Newark Bay Complex*. Division of Science, Research and Technology. Research Project Summary.
- PANYNJ (Port Authority of New York and New Jersey). 2010. *The Economic Impact of the New York-New Jersey Port/Maritime Industry 2010*. New York Shipping Association, Inc. October 2011.
- Ralston, D. K., and W. R. Geyer. 2009. "Episodic and Long-Term Sediment Transport Capacity in the Hudson River Estuary." *Estuaries and Coasts* 32: 1130–1151. doi:10.1007/s12237-009-9206-4
- Resio, D. T. 1987. "Shallow-Water Waves. I: Theory." *Journal of Waterway, Port, Coastal, and Ocean Engineering* 113(3): 264–281.
- Resio, D. T. 1988. "Shallow-Water Waves. II: Data Comparisons." *Journal of Waterway, Port, Coastal, and Ocean Engineering* 114(1):50–65.

- Resio, D. T., and W. Perrie. 1989. "Implications of An f-4 Equilibrium Range for Wind-Generated Waves." *Journal of Physical Oceanography* 19: 193–204.
- Rodrigue, Jean-Paul. 2004. "The Port Authority of New York and New Jersey: Global Changes, Regional Gains and Local Challenges in Port Development." *Les Cahiers Scientifiques du Transport* 44(2003): 55–75.
- Savant, G., and C. Berger. 2012. "Adaptive Time Stepping-Operator Splitting Strategy to Couple Implicit Numerical Hydrodynamic and Water Quality Codes." *Journal of Environmental Engineering* 138(9): 979–984.
- Savant, G., C. Berger, T. O. McAlpin, and J. N. Tate. 2011. "Efficient Implicit Finite-Element Hydrodynamic Model for Dam and Levee Breach." *Journal of Hydraulic Engineering* 137(9): 1005–1018.
- Savant, Gaurav, R. Charlie Berger, Tate O. McAlpin, and Corey J. Trahan. 2014. *Three-Dimensional Shallow Water Adaptive Hydraulics (AdH-SW3): Hydrodynamic Verification and Validation*. ERDC/CHL TR-14-7. Vicksburg, MS: US Army Engineer Research and Development Center.
- Savant, Gaurav. 2015. *Three-Dimensional Shallow Water Adaptive Hydraulics (ADH-SW3): Turbulence Closure*. ERDC/CHL TR-15-1. Vicksburg, MS: US Army Engineer Research and Development Center.
- Savant, G., and R. C. Berger. 2015. *Three-Dimensional Shallow Water Adaptive Hydraulics (ADH-SW3) Validation: Galveston Bay Hydrodynamics and salinity Transport*. ERDC/CHL TR-15-3. Vicksburg, MS: US Army Engineer Research and Development Center.
- Savant, G., C. J. Trahan, C. Berger, J. T. McAlpin, and T. O. McAlpin. "Refinement Indicator for Dynamic Mesh Adaption in Three-Dimensional Shallow-Water Equation Modeling." *Journal of Hydraulic Engineering* 144(2).
- Sea Engineering. 2008. *Sedflume Consolidation Analysis, Passaic River, New Jersey*. Prepared for Hydroqual, Inc. and US EPA, Santa Cruz, CA. <https://semspub.epa.gov/work/02/212973.pdf>
- Sea Engineering, Inc. 2013. *FINAL: SEDFlume Analysis Data Report, Newark Bay, New Jersey*. Prepared for US Environmental Protection Agency, Santa Cruz, CA.
- Scheffner, Norman W., S. Rao Vemulakonda, David J. Mark, H. Lee Butler, Keu W. Kim. 1994. *New York Bight Study, Report 1: Hydrodynamic Modeling*. Technical Report CERC-94-4. Vicksburg, MS: US Army Corps of Engineers, Waterways Experiment Station.
- Shrestha, P. L., S. H. Su, S. C. James, P. J. Shaller, M. Doroudian, C. E. Firstenberg and C. T. Thompson., 2014. "Conceptual Site Model for Newark Bay—Hydrodynamics and Sediment Transport." *Journal of Marine Science and Engineering* 2: 123–139.
- Sommerfield, C. K., and R. J. Chant. 2010. *Mechanisms of Sediment Trapping and Accumulation in Newark Bay, New Jersey: An Engineered Estuarine Basin*. HRF 008/07A. Final Report to the Hudson River Foundation.



- Suszkowski, D. J. 1978. *Sedimentology of Newark Bay, New Jersey: An Urban Estuarine Bay*. PhD dissertation, University of Delaware, Newark, 222 pp.
- Tate, Jennifer N., Brittany Gunkel, Julie Rosati, Eric Wood, Alejandro Sanchez, Rob Thomas, Naveen Ganesh, and Thad Pratt. 2014. *Monitoring Completed Navigation Projects Program; Houston-Galveston Navigation Channel Shoaling Study*. ERCD/CHL TR-14-14. Vicksburg, MS: US Army Engineer Research and Development Center.
- Tate, J. N., G. Savant, and D. McVan. 2012. "Rapid Response Numerical Modeling of the 2010 Pakistan Flooding." *Leadership and Management in Engineering* 12(4): 315–323.
- Teeter, A. M. 2001a. "Clay-Silt Sediment Modeling Using Multiple Grain Classes. Part I: Settling and Deposition." *Proceeding in Marine Science, Coastal and Estuarine Fine Sediment Processes*. Edited by A. J. Mehta and W. H. McAnally. Amsterdam, The Netherlands: Elsevier.
- Teeter, A. M. 2001b. "Clay-Silt Sediment Modeling Using Multiple Grain Classes. Part II: Application to Shallow-Water Resuspension and Deposition." *Proceeding in Marine Science, Coastal and Estuarine Fine Sediment Processes*. Edited by A. J. Mehta and W. H. McAnally. Amsterdam, The Netherlands: Elsevier.
- The MITRE Corporation. 1979. *Disposal of Dredged Material Within the New York District: Volume I Present Practices and Candidate Alternatives*. [file:///C:/Users/RDCHLTOM/Downloads/rutgers-lib-32136\\_PDF-1.pdf](file:///C:/Users/RDCHLTOM/Downloads/rutgers-lib-32136_PDF-1.pdf)
- USACE CENAN (US Army Corps of Engineers, New York District). 2004. *Consolidated Implementation of the New York & New Jersey Harbor Deepening Project: Re-evaluation Report*. New York, NY.
- USACE (US Army Corps of Engineers). 2016. *Hudson-Raritan Estuary Comprehensive Restoration Plan*. Version 1.0 Volume I. US Army Corps of Engineers and the Port Authority of New York and New Jersey.
- USGS DOI (US Geological Survey, US Department of the Interior). 2020. *USGS Surface-Water Data for USA*. Accessed 02 June. <https://waterdata.usgs.gov/nwis/sw?>
- Wakeman, Thomas H., Alan F. Blumberg, Dov B. Kruger, and Anne M. Fullerton. 2007. "Sediment Movement and Dredging in Newark Bay, NJ." *Ports 2007: 30 Years of Sharing Ideas, 1977-2007*.
- Wall, G. R., E. A. Nystrom, and S. Litten. 2008. "Suspended Sediment Transport in the Freshwater Reach of the Hudson River Estuary in Eastern New York." *Estuaries and Coasts* 31: 542–553.
- Woodruff, Jonathan D., W. Rockwell Geyer, Christopher K. Sommerfield, and Neal W. Driscoll. 2001. "Seasonal Variation of Sediment Deposition in the Hudson River Estuary." *Marine Geology* 179(2001): 105–119.

## **Appendix A: Ungauged Flows on the Hudson River**

There are numerous secondary tributaries that discharge into the Hudson River below Troy Lock and Dam. There were four of these tributaries that had USGS discharge data during the 5 years simulated for this study. These four tributaries are the following:

1. Rondout Creek at Rosendale, NY (USGS station 01367500)
2. Croton River at New Croton, Dam (USGS station 01375000)
3. Esopus Creek at Mount Marion, NY (USGS station 01364500)
4. Wappinger Creek near Wappinger Falls, NY (USGS station 01372500).

These four creeks have a collective drainage area of 1,361 mi<sup>2</sup>, which is approximately 17% of the drainage basin area above Green Island on the Hudson (8,070 mi<sup>2</sup>). There are no sediment concentration data for these smaller tributaries, and they enter the Hudson in the tidal zone, minimizing their influence. The local ungauged drainage area along the Hudson was estimated to add an additional 24% to the drainage area. The local ungauged contribution is also within the tidal zone.

The contributions of these added inflows are presented in Figure 240 through Figure 244 for the five simulated years. Adding the additional tributaries explicitly into the model computational mesh would require a considerable increase in mesh resolution and computer requirements. Sensitivity tests were performed using the full estimated Hudson flows as inflow at Green Island. This bulking of the flow also increased the sediment load by the implied assumption that the suspended sediment concentrations were the same for the added flows as what passes Green Island. The results of the sensitivity simulations were that there was no discernable difference in the sedimentation results in the harbor for the additional flow volume.

In addition, this numerical model study ignored tributary inflows into Long Island Sound. Those flows were assumed to have no significant impact on the sedimentation environment in the vicinity of the proposed channel deepening.

Figure 240. Additional tributary inflows below the Hudson River at Green Island for 1985.

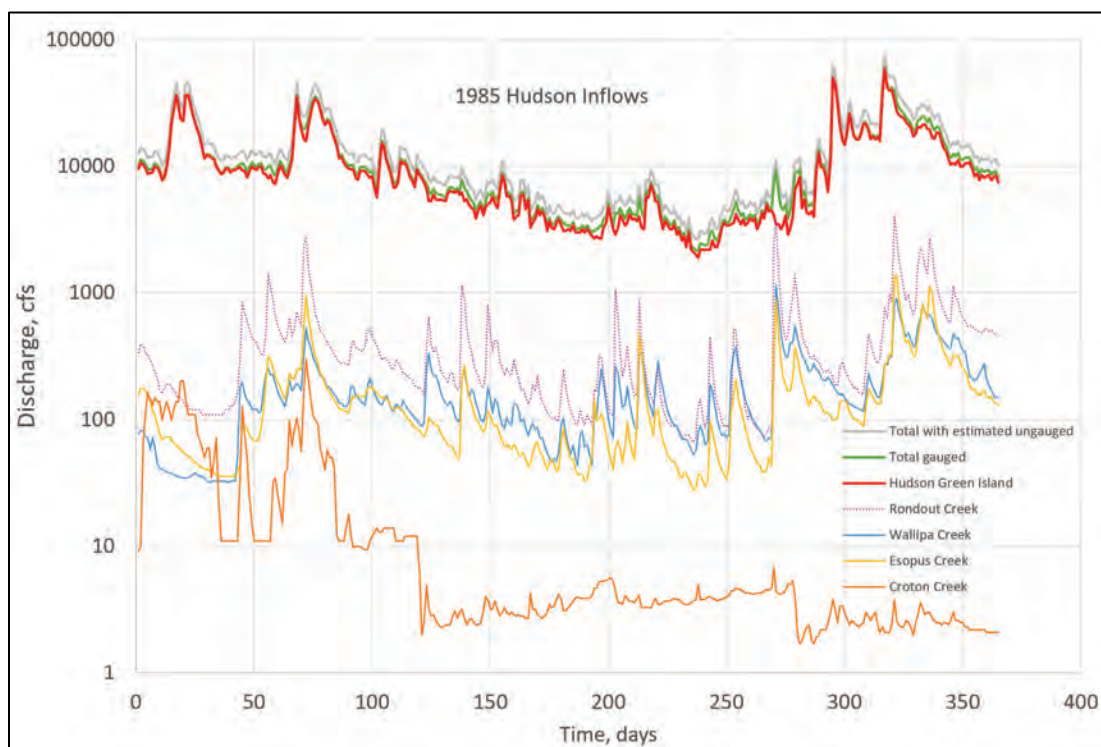


Figure 241. Additional tributary inflows below the Hudson River at Green Island for 1995.

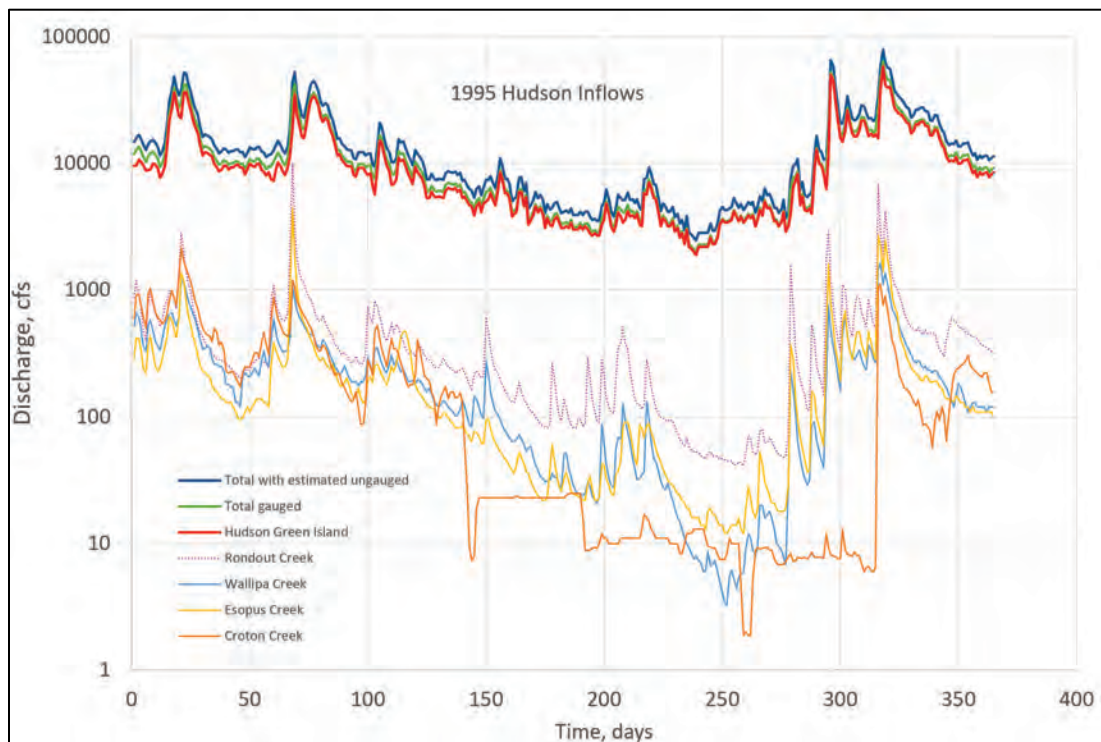


Figure 242. Additional tributary inflows below the Hudson River at Green Island for 1996.

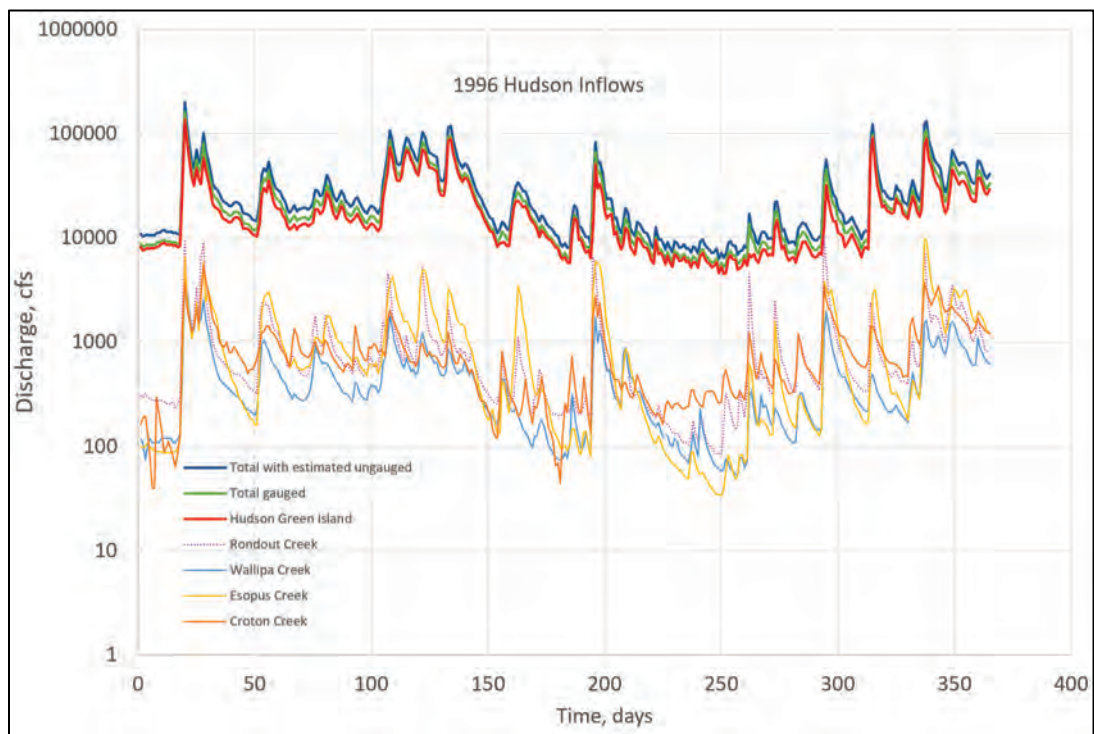


Figure 243. Additional tributary inflows below the Hudson River at Green Island for 2011.

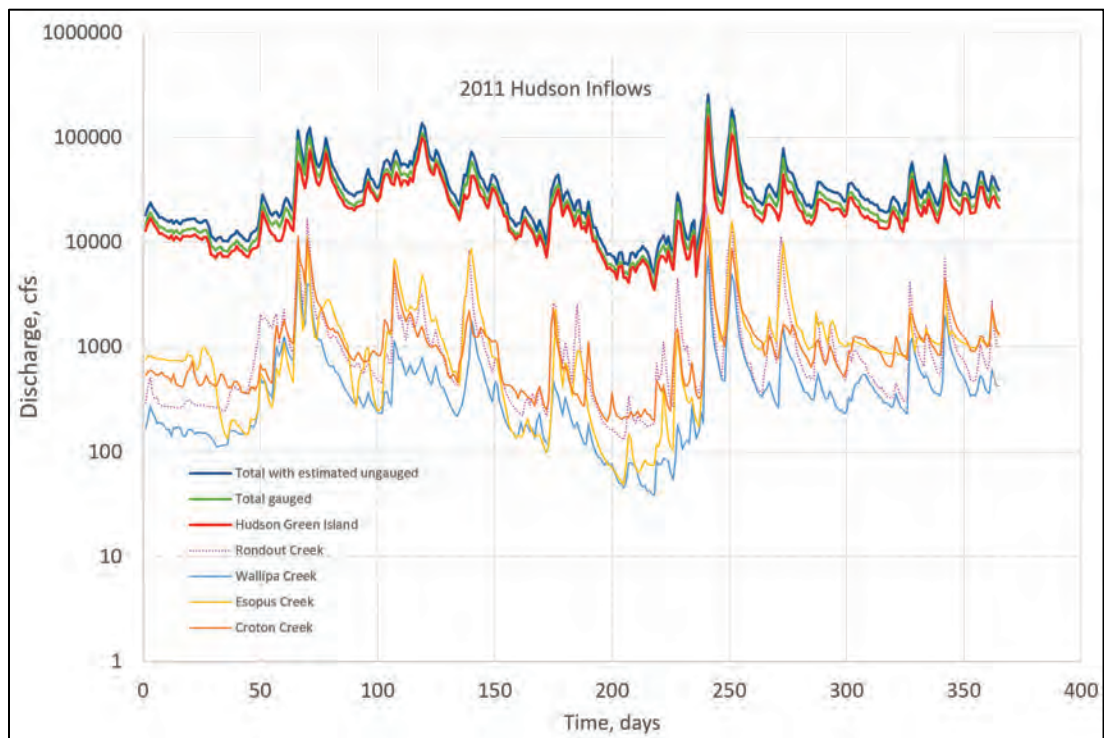
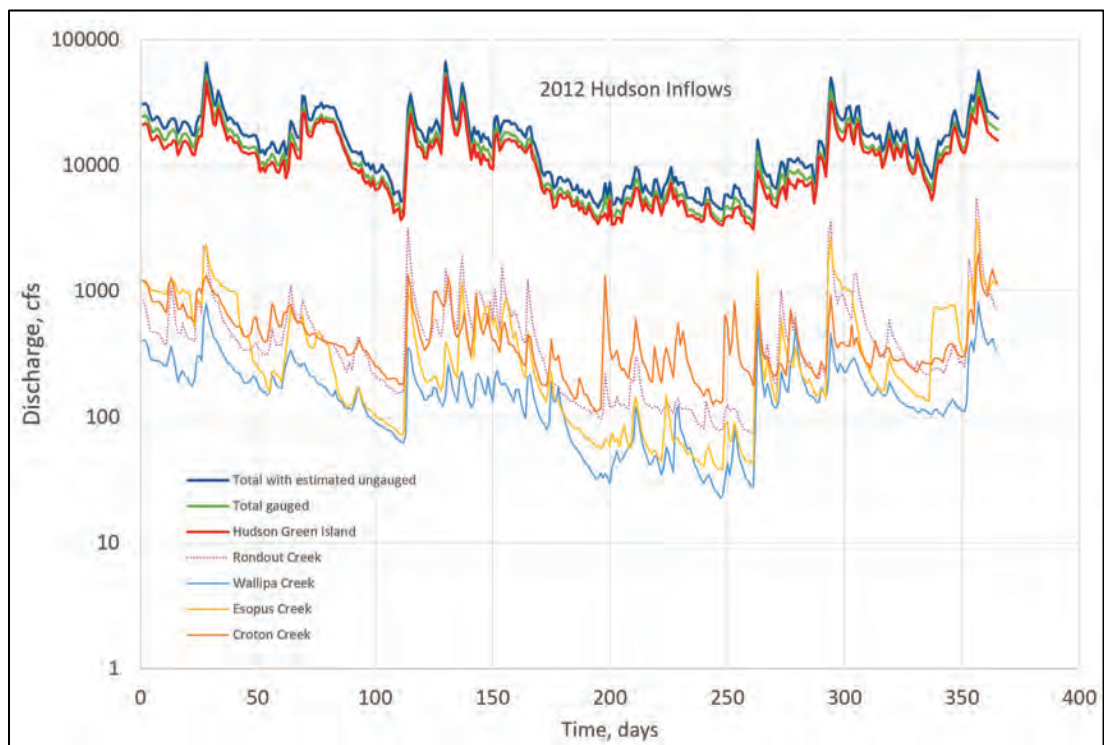


Figure 244. Additional tributary inflows below the Hudson River at Green Island for 2012.





## Appendix B: NOAA Tide Gauge Information

Table 27 shows the tidal information for the NOAA gauges analyzed as part of this project taken from NOAA (2005).

Table 27. NOAA tidal data.

Locations	Latitude		Longitude		Lag to SH		HW ratio	LW ratio	Tide Range (ft)		MTL (ft MLLW)
	deg	min	deg	min	HW	LW			mean	spring	
Point Judith harbor of refuge	41	21.8	71	29.4	0.0	6.1	0.87	0.54	3.10	3.10	1.70
Block Island Old harbor	41	10.4	71	33.4	-0.2	5.8	0.82	0.86	2.85	3.51	1.54
Block Island SW point	41	9.8	71	36.6	0.1	6.3	0.75	0.79	2.60	3.20	1.41
Weekapaug Pt, Block Isl Sound	41	19.7	71	45.7	0.7	6.7	0.74	0.93	2.53	3.11	1.39
Watch Hill point	41	18.3	71	51.6	0.7	6.8	0.74	0.71	2.60	3.20	1.40
New London	41	21.6	72	5.5	1.7	7.9	1.00	1.00	2.56	3.09	1.47
Long Neck Point	41	2.3	73	28.8	3.3	9.6	1.06	0.96	7.17	8.17	3.82
Rye Beach	40	57.7	73	40.3	3.4	9.8	1.00	0.93	7.29	7.89	3.88
New Rochelle	40	53.6	73	46.9	3.5	10.4	1.01	1.11	7.29	8.46	3.90
Throg's Neck	40	48.3	73	47.7	4.0	10.4	0.98	0.96	7.00	8.20	3.80
Whitestone	40	47.9	73	48.8	3.9	10.3	1.00	1.04	7.10	8.30	3.80
College Point, Flushing Bay	40	47	73	51.4	4.1	10.4	0.95	1.04	6.80	7.90	3.70
Hunts point	40	48	73	52.4	4.0	10.3	0.97	1.07	6.92	7.57	3.75
North Brother Island	40	48.1	73	54	4.1	10.4	0.93	1.11	6.60	7.80	3.60
Port Morris (Stony Point)	40	48.1	73	54.4	3.9	10.3	0.87	0.96	6.24	6.85	3.39
He3II Gate	40	47.2	73	55.3	3.5	10.5	1.33	1.59	6.00	7.30	3.40
Horn's Hook, E 90th St	40	46.6	73	56.5	2.4	8.3	1.03	0.90	4.68	5.18	2.53
Queensboro Bridge	40	45.5	73	57.5	1.9	7.7	0.96	1.00	4.33	5.24	2.38
E 41st St	40	44.8	73	58.1	1.6	7.5	0.95	1.09	4.31	4.89	2.40

Locations	Latitude		Longitude		Lag to SH		HW ratio	LW ratio	Tide Range (ft)		MTL (ft MLLW)
	deg	min	deg	min	HW	LW			mean	spring	
Hunters Pt, Newtown Creek	40	44.4	73	57.7	1.9	7.7	0.89	0.90	4.10	4.90	2.20
Williamsburg Bridge	40	42.7	73	58.1	1.3	7.2	0.93	0.95	4.22	5.11	2.31
Wallabout Bat, Brooklyn Navy yard	40	42.4	73	58.5	1.1	7.1	0.94	1.05	4.30	5.20	2.40
Brooklyn Bridge	40	42.2	73	59.3	0.9	6.7	0.99	1.00	4.53	5.13	2.48
Harlem River, Randals Island	40	48	73	55.7	2.2	8.2	1.02	1.09	4.60	5.60	2.50
Willets point	40	47.6	73	46.9	3.8	10.1	1.00	1.04	7.15	8.21	3.88
Kings Point	40	48.6	73	45.9	3.8	10.1		1.00	7.16	8.46	3.86
Port Washington, Manhasset Bay	40	49.9	73	42.2	3.6	9.9	1.02	0.96	7.29	8.46	3.92
Glen Cove, Hempstead Harbor	40	51.8	73	39.3	3.4	9.7	1.01	0.82	7.27	7.87	3.87
Eaton's neck Point	40	57.2	73	24	3.5	9.7	1.05	1.04	7.10	8.20	3.90
Cedar Beach	40	57.9	73	2.6	3.6	9.7	0.96	1.00	6.43	7.01	3.46
Northville	40	58.9	72	38.7	3.6	9.6	0.81	0.96	5.40	5.95	2.94
Plum Island	41	10.3	72	12.3	2.2	8.2	1.01	1.01	2.60	3.10	1.50
Montauk, Fort Pond Bay	41	2.9	71	57.6	1.4	7.6			2.07	2.66	1.21
Norton Point	40	34	73	59.9	0.0	6.3	1.02	1.15	4.70	5.70	2.60
Ft. Hamilton	40	36.5	74	2.1	0.0	6.3	1.01	1.00	4.70	5.70	2.50
St. George, Staten Island	40	38.6	74	4.4	0.3	6.5	0.99	0.99	4.50	5.40	2.40
The Battery	40	42	74	0.9	0.5	6.7			4.63	5.50	2.47
Weehawken, Union City	40	45.9	74	1.1	0.8	7.0	0.96	0.96	4.37	5.29	2.41
Edgewater	40	48.8	73	58.7	1.1	7.2	0.93	0.93	4.24	5.13	2.33
Spuyten Duyvil	40	52.7	73	55.5	1.4	7.5	0.84	0.84	3.85	4.66	2.20
Riverdale, NY	40	54.2	73	54.9	1.3	7.6	0.85	0.85	3.86	4.67	2.13
Alpine, NJ	40	56.7	73	55.1	1.6	7.8	0.83	0.83	3.78	4.57	2.09
Tarrytown	41	4.7	73	52.2	2.4	8.7	0.70	0.70	3.20	3.70	1.80

Locations	Latitude		Longitude		Lag to SH		HW ratio	LW ratio	Tide Range (ft)		MTL (ft MLLW)
	deg	min	deg	min	HW	LW			mean	spring	
Haverstraw	41	13.1	73	57.8	2.8	9.4	0.72	0.81	3.23	3.91	1.78
Peekskill	41	17	73	56	3.0	9.8	0.64	0.64	2.90	3.40	1.80
Newburgh	41	30	74	0.4	4.3	10.8	0.62	0.64	2.80	3.20	1.50
New Hamburg	41	35	73	57	4.6	11.2	0.64	0.64	2.90	3.30	1.60
Poughkeepsie	41	42	73	57	5.1	11.5	0.68	0.68	3.10	3.50	1.70
Hyde Park	41	47	73	57	5.5	11.9	0.70	0.68	3.20	3.60	1.80
Kingston	41	55	73	59	5.9	12.3	0.81	0.82	3.70	4.20	2.00
Tivoli	42	4	73	56	6.4	12.8	0.86	0.86	3.90	4.40	1.90
Hudson	41	15	73	48	7.5	13.9	0.88	0.86	4.00	4.40	2.20
Castleton	42	32	73	46	9.3	15.6			4.30	4.70	2.20
Albany	42	39	73	44.8	9.5	16.1			4.60	5.00	2.50
Troy	42	44	73	42	9.7	16.2	1.00	1.00	4.70	5.10	2.30
Constable Hook	40	39.3	74	5.2	0.2	6.6	1.02	1.02	4.63	5.60	2.54
Bayonne bridge	40	38.4	74	8.8	0.5	6.7	1.00	1.00	4.98	5.52	2.70
Port Elizabeth	40	40.4	74	8.4	0.5	7.0	1.11	0.95	5.05	5.59	2.73
Port Newark terminal	40	41	74	8	0.6	7.1	1.12	1.12	5.10	6.10	2.70
Point No Point	40	43.9	74	7	0.5	7.1	1.15	1.15	5.24	6.34	2.86
Belleville	40	47.2	74	8.8	0.7	7.6	1.23	1.19	5.60	6.78	3.08
East Rutherford	40	50.8	74	7.2	0.7	7.8	1.29	1.29	5.87	7.10	3.20
Garfield	40	52.1	74	6.7	0.7		na	na	na	na	na
Kearny Point	40	43.7	74	6.2	0.7	7.1	1.15	1.14	5.21	6.30	2.85
Amtrak RR swing Bridge	40	45.1	74	5.8	1.1	7.4	1.16	1.16	5.29	6.40	2.89
Fish Creek, Berry's Creek	40	47.6	74	5.5	1.6	7.7	1.17	1.17	5.33	6.45	2.90
Carlstadt	40	48.4	74	3.6	1.5	7.5	1.26	1.29	5.71	6.29	3.12
North Secaucus	40	48.4	74	2.6	1.5	7.7	1.23	1.23	5.61	6.79	3.06
Mill Creek	40	47.9	74	3	2.1		na	na	na	na	na
Cromakill Creek	40	48.2	74	2	1.5		na	na	na	na	na
Ridgeland Park	40	51	74	1.8	1.5	7.7	1.26	1.26	5.73	6.93	

Locations	Latitude		Longitude		Lag to SH		HW ratio	LW ratio	Tide Range (ft)		MTL (ft MLLW)
	deg	min	deg	min	HW	LW			mean	spring	
Hackendack	40	52.8	74	2.4	1.6	7.7	1.33	1.33	6.01	7.27	3.29
New Milford	40	56.1	74	1.8	1.9	9.7	1.04	1.04	4.72	5.71	2.44
Port Ivory	40	38.7	74	10.8	0.5	6.9	1.09	1.09	5.10	6.12	2.78
Rahway River, RR Bridge	40	35.9	74	13.9	0.3	6.7	1.14	1.14	5.32	6.38	2.89
Chelsea	40	36	74	12	0.4	6.8	1.07	1.05	5.00	6.00	2.70
Carteret	40	35.2	74	12.6	0.4	6.8	1.09	1.09	5.10	6.20	2.80
Rossville	40	33.3	74	13.4	0.3	6.7	1.12	1.12	5.22	5.84	2.89
Woodbridge Creek	40	32.7	74	15.9	0.1	6.6	1.11	1.11	5.15	6.18	2.78
Great Kills harbor	40	32.6	74	8.4	0.1	6.6	1.01	1.00	4.70	5.70	2.60
Princes Bay	40	30.7	74	12	0.0	6.3	1.05	1.05	4.90	5.90	2.60
South Amboy	40	29.5	74	16.9	-0.1	6.3	1.09	1.09	5.09	6.11	2.77
Keasbey	40	30.5	74	18.7	0.1	6.5	1.11	1.11	5.16	6.19	2.81
Sayerville	40	28.7	74	21.4	0.2	6.6	1.15	1.15	5.37	6.44	2.92
Old Bridge, south river	40	25	74	21.8	0.8	7.2	1.20	1.20	5.61	6.73	3.05
New Brunswick	40	29.3	74	26.1	0.5	7.0	1.21	1.21	5.65	6.78	3.06
Cheesequake Creek	40	27.2	74	16.4	0.2	6.4	1.09	1.09	5.08	6.10	2.76
Keyport	40	26.4	74	11.9	-0.1	6.3	1.07	1.07	5.00	6.00	2.72
Matawan Creek	40	26	74	13.1	0.0	6.3	1.07	1.07	5.00	6.00	2.75
Waackaack Creek	40	26.9	74	8.6	-0.1	6.6	0.99	0.99	4.62	5.54	2.47
Sandy Hook	40	28	74	0.6	0.0	6.2			4.70	5.71	2.54

## Appendix C: Sediment Core Comparisons

Figure 245. Sediment bed composition comparisons at location A-1U for 2011 (top) and 2012 (bottom).

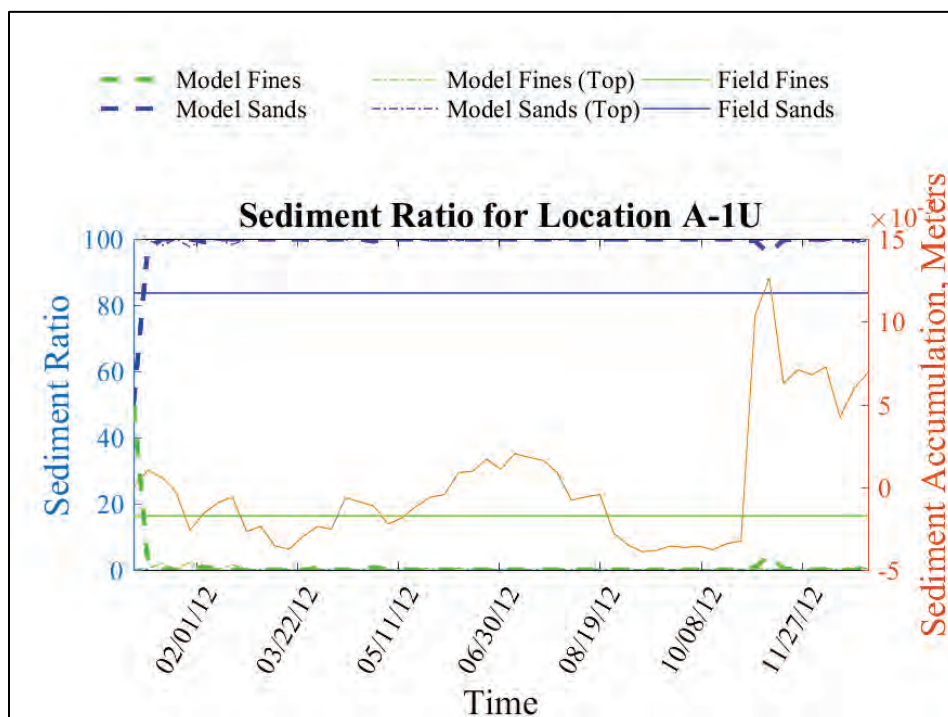
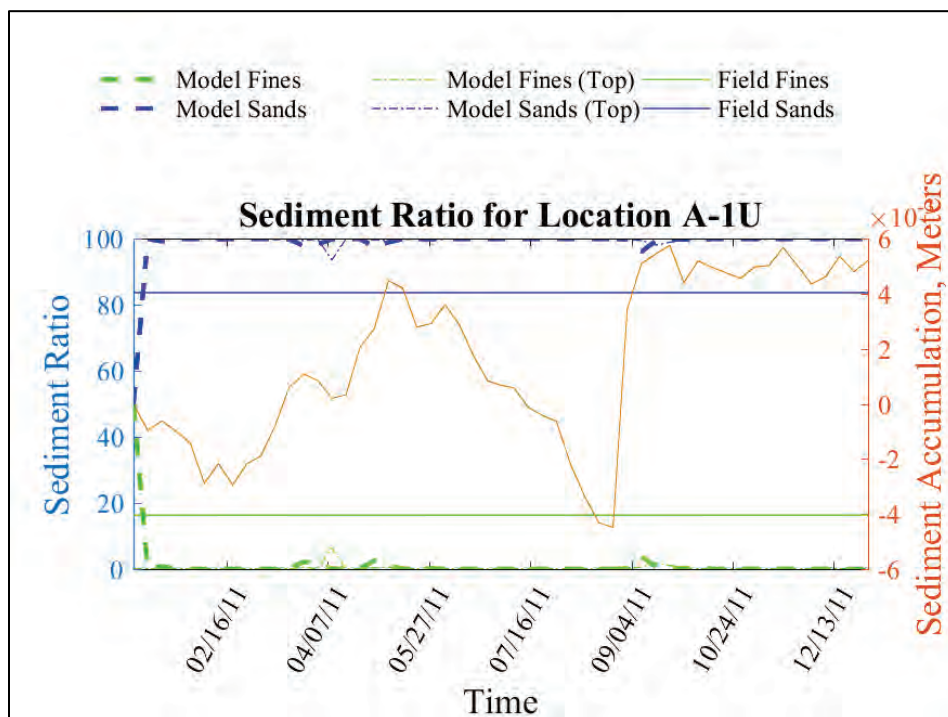




Figure 246. Sediment bed composition comparisons at location A-3U for 2011 (top) and 2012 (bottom).

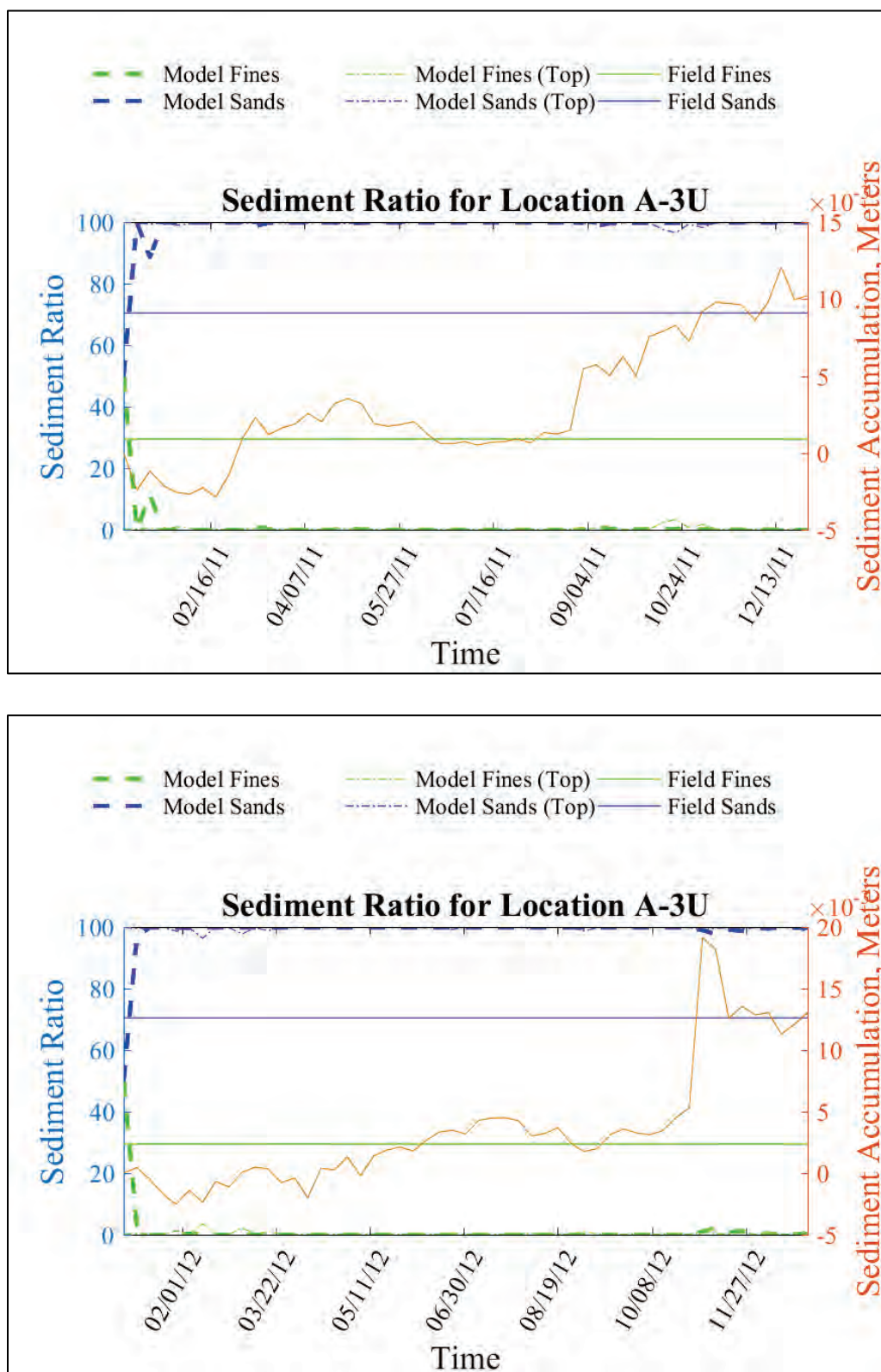


Figure 247. Sediment bed composition comparisons at Location A-4U for 2011 (top) and 2012 (bottom).

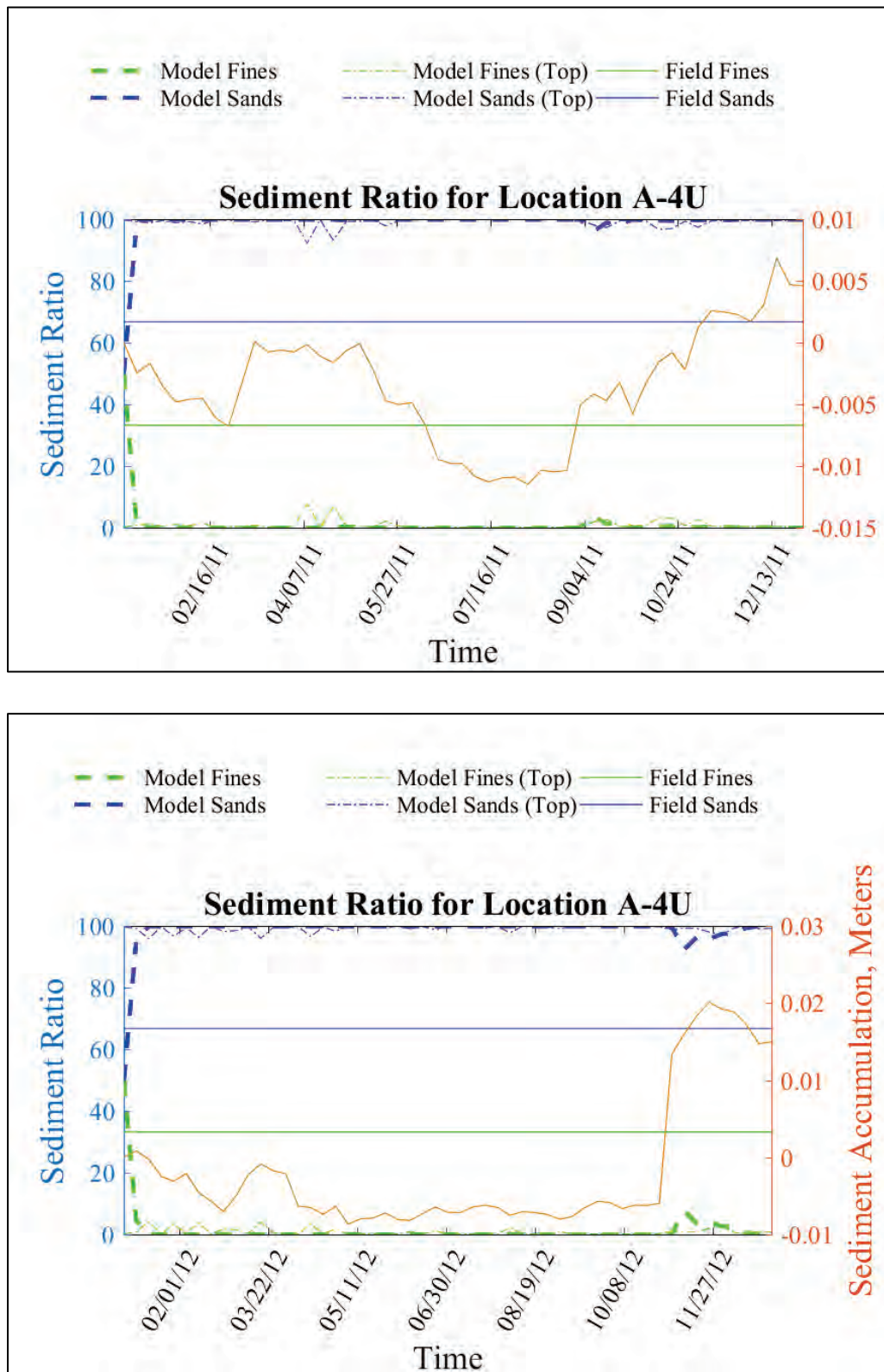


Figure 248. Sediment bed composition comparisons at location A-5U for 2011 (top) and 2012 (bottom).

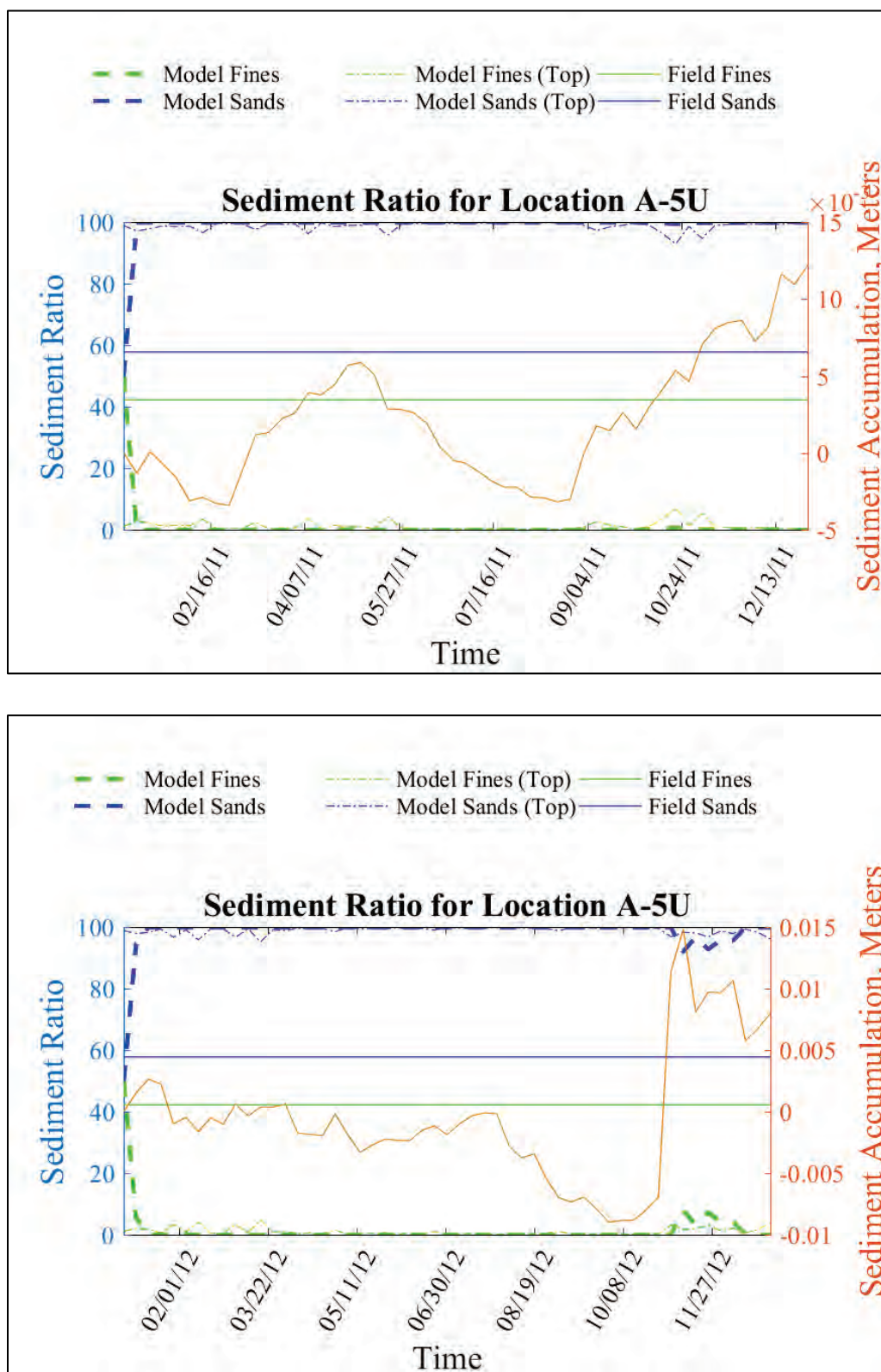




Figure 249. Sediment bed composition comparisons at location E-2U for 2011 (top) and 2012 (bottom).

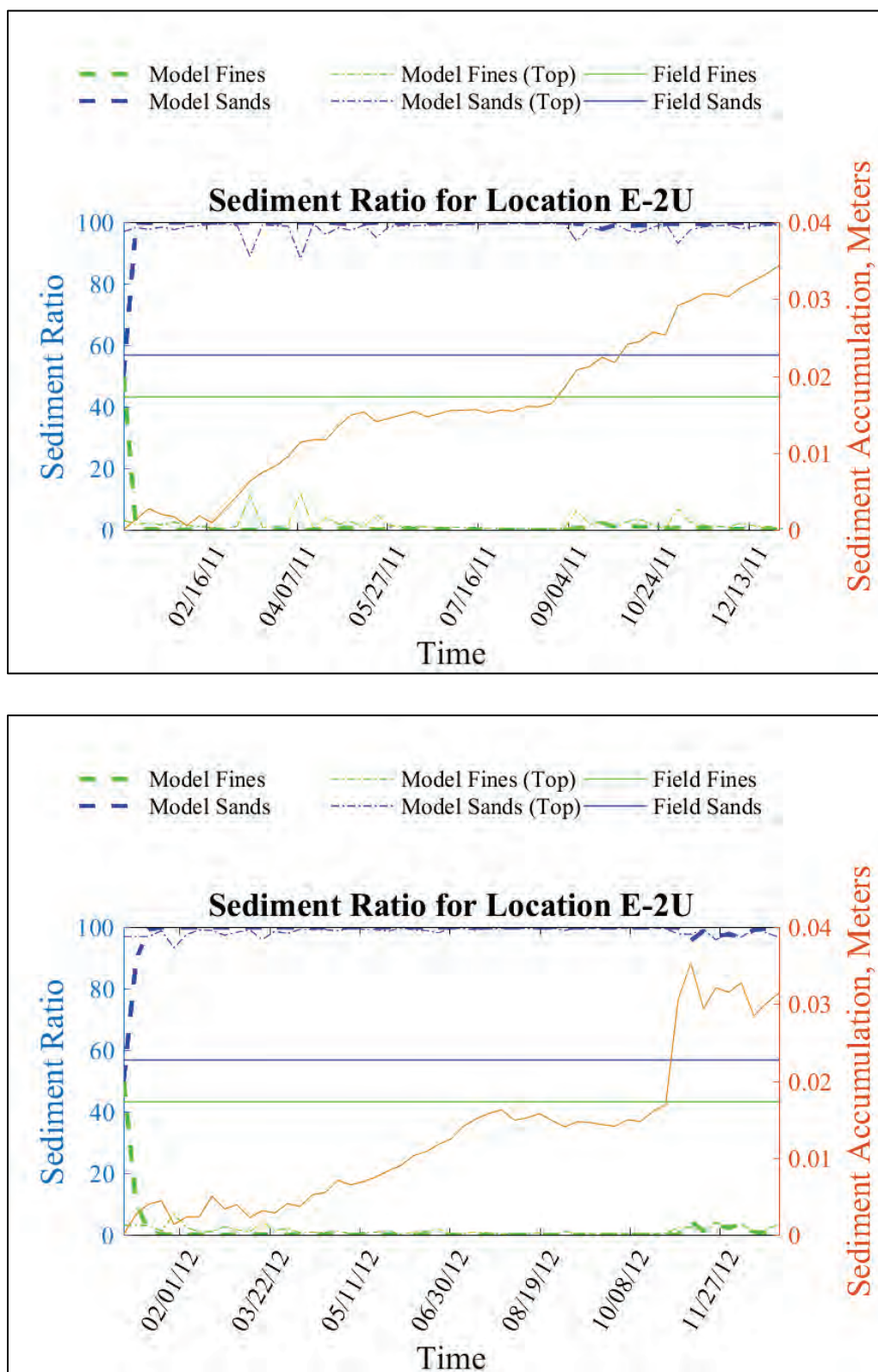


Figure 250. Sediment bed composition comparisons at location E-3U for 2011 (top) and 2012 (bottom).

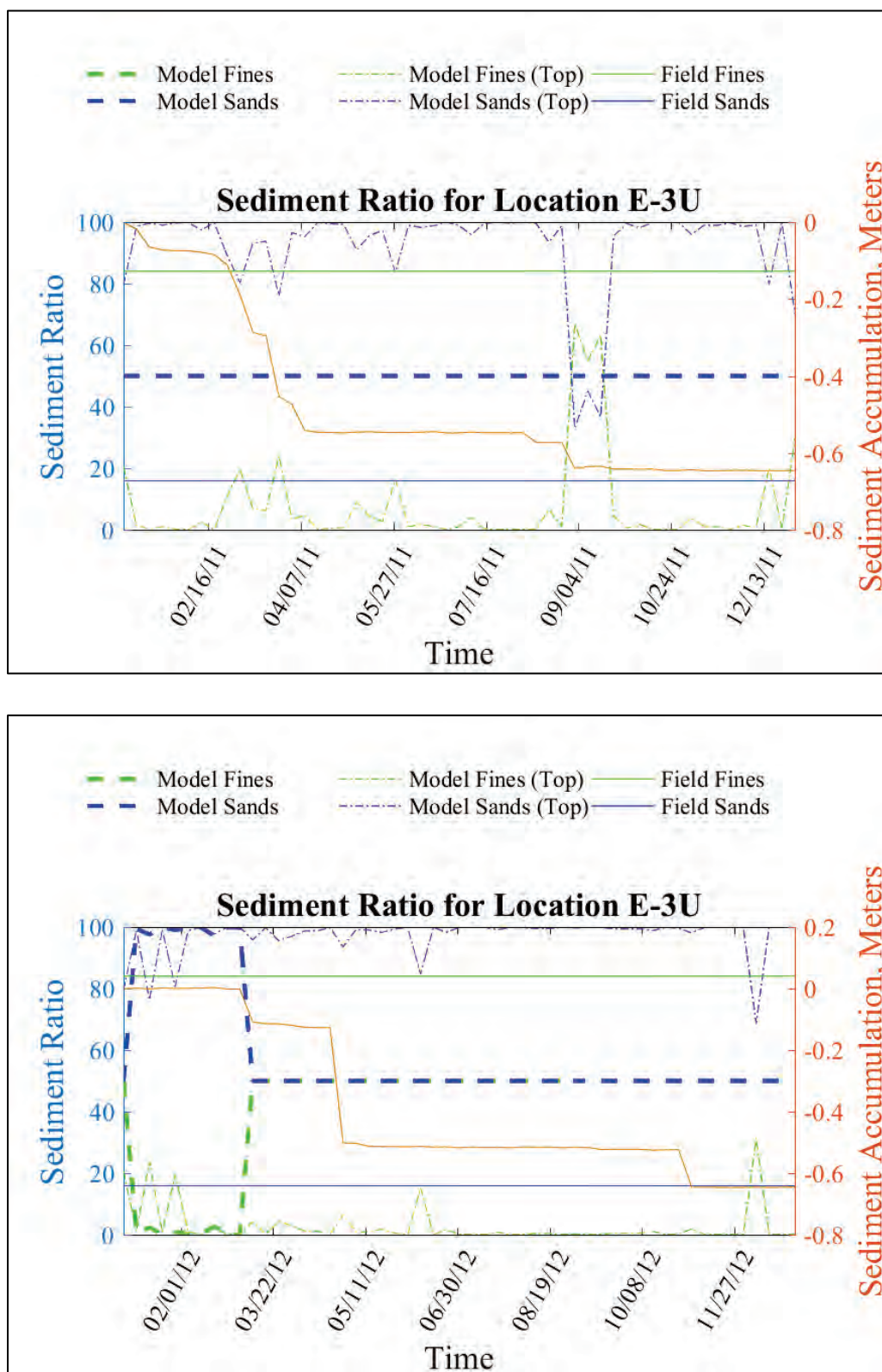




Figure 251. Sediment bed composition comparisons at location W-3BU for 2011 (top) and 2012 (bottom).

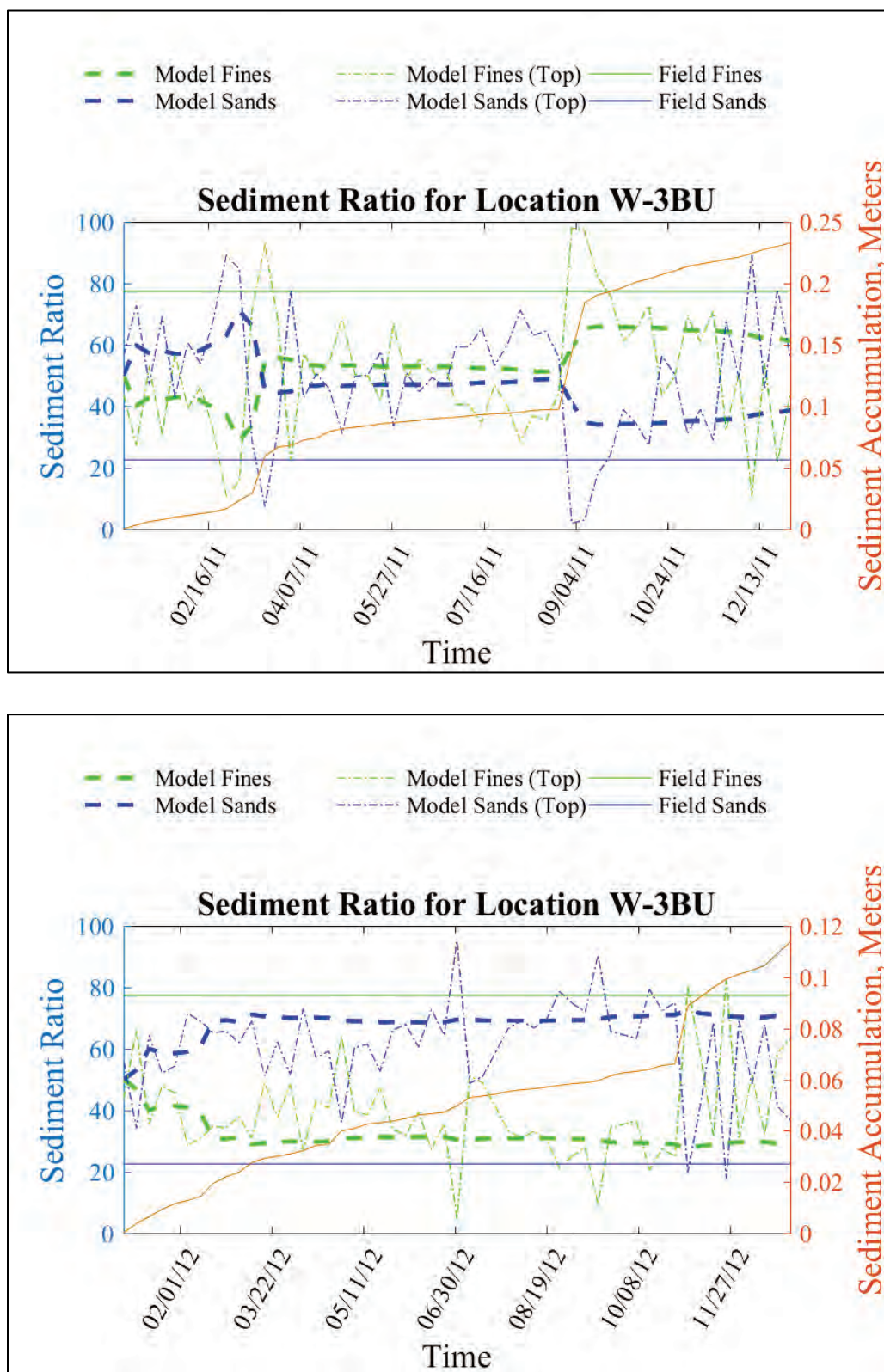


Figure 252. Sediment bed composition comparisons at location W-3U for 2011 (top) and 2012 (bottom).

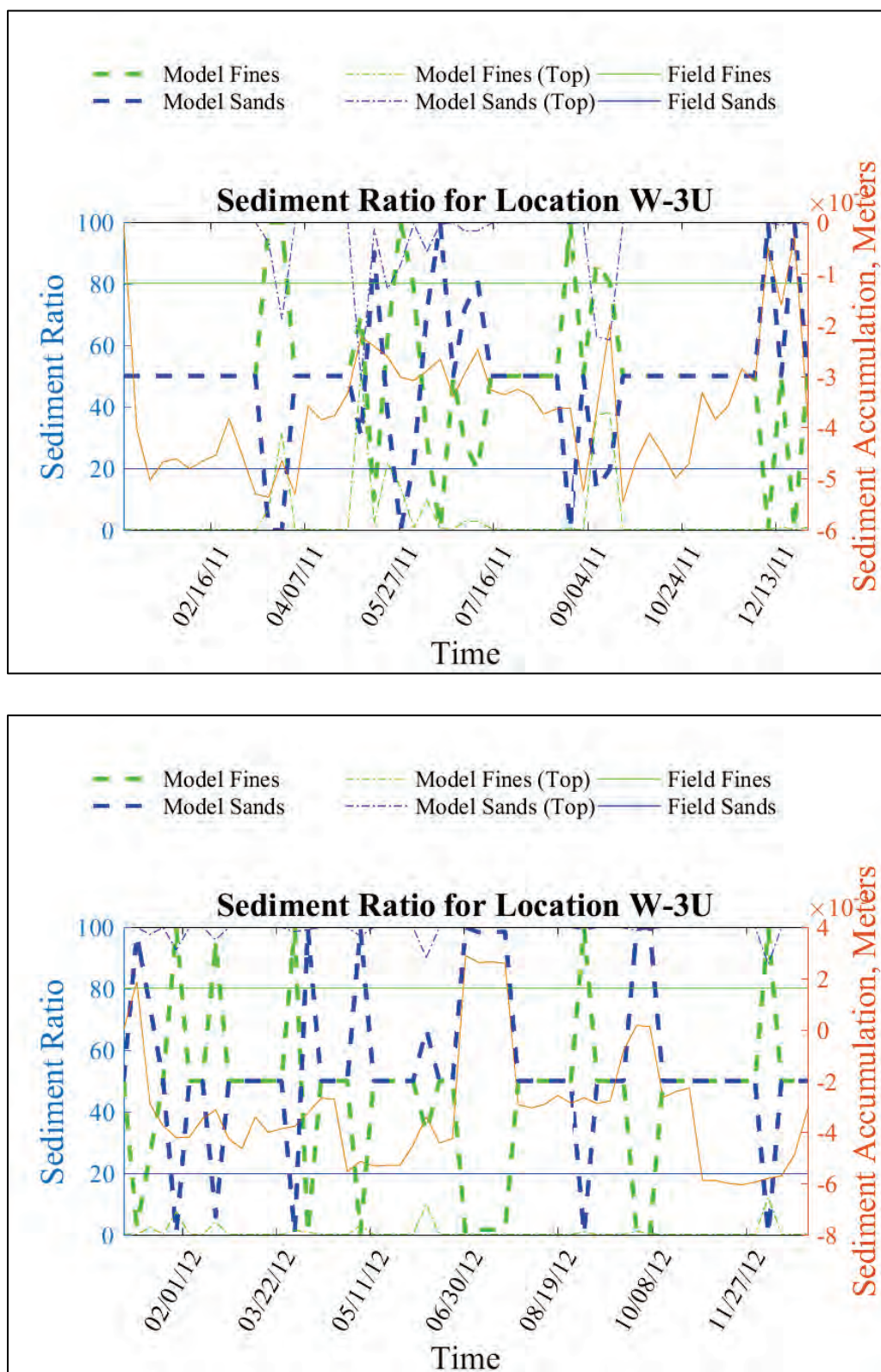


Figure 253. Sediment bed composition comparisons at location W-4AU for 2011 (top) and 2012 (bottom).

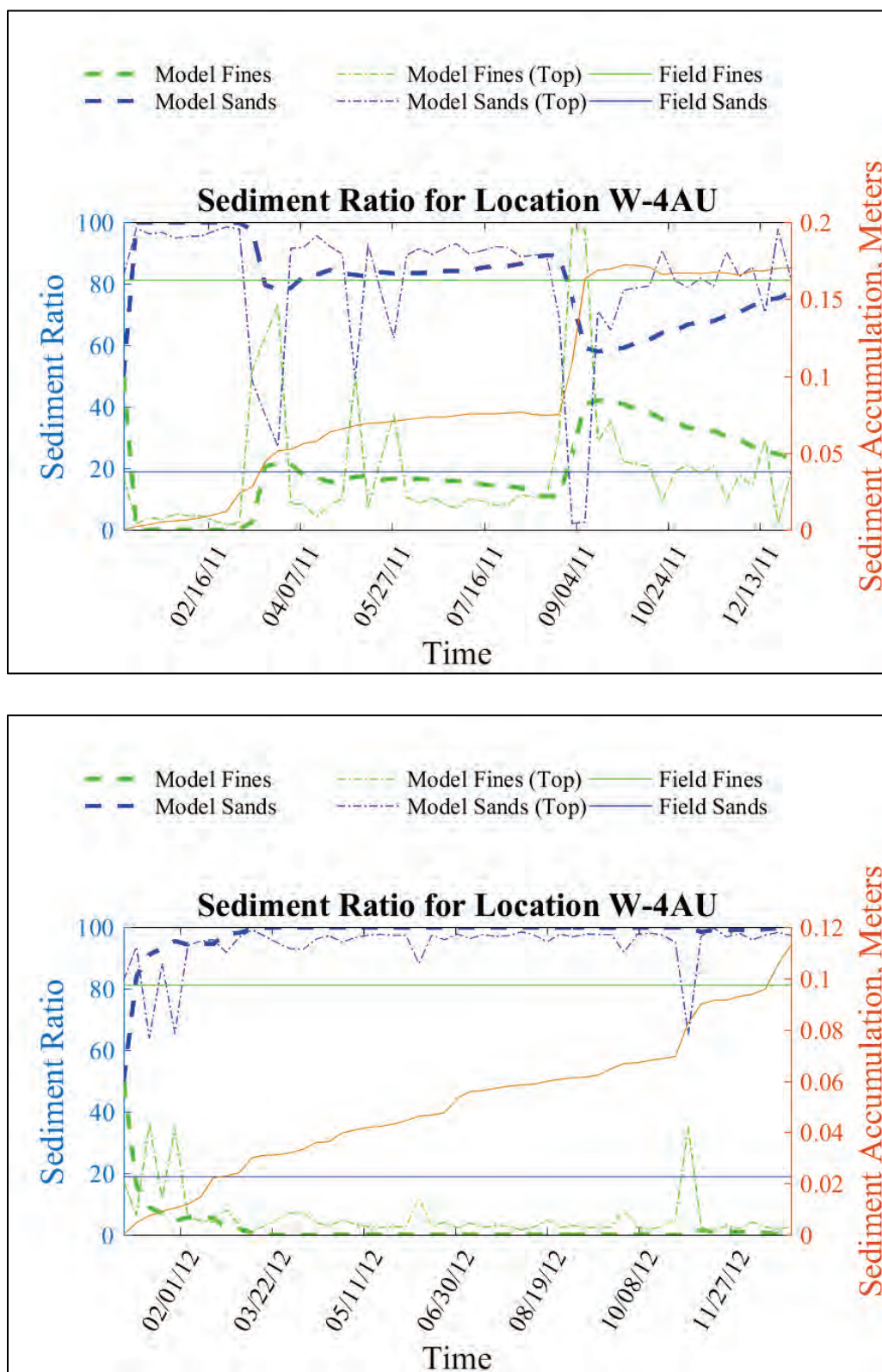




Figure 254. Sediment bed composition comparisons at location W-4U for 2011 (top) and 2012 (bottom).

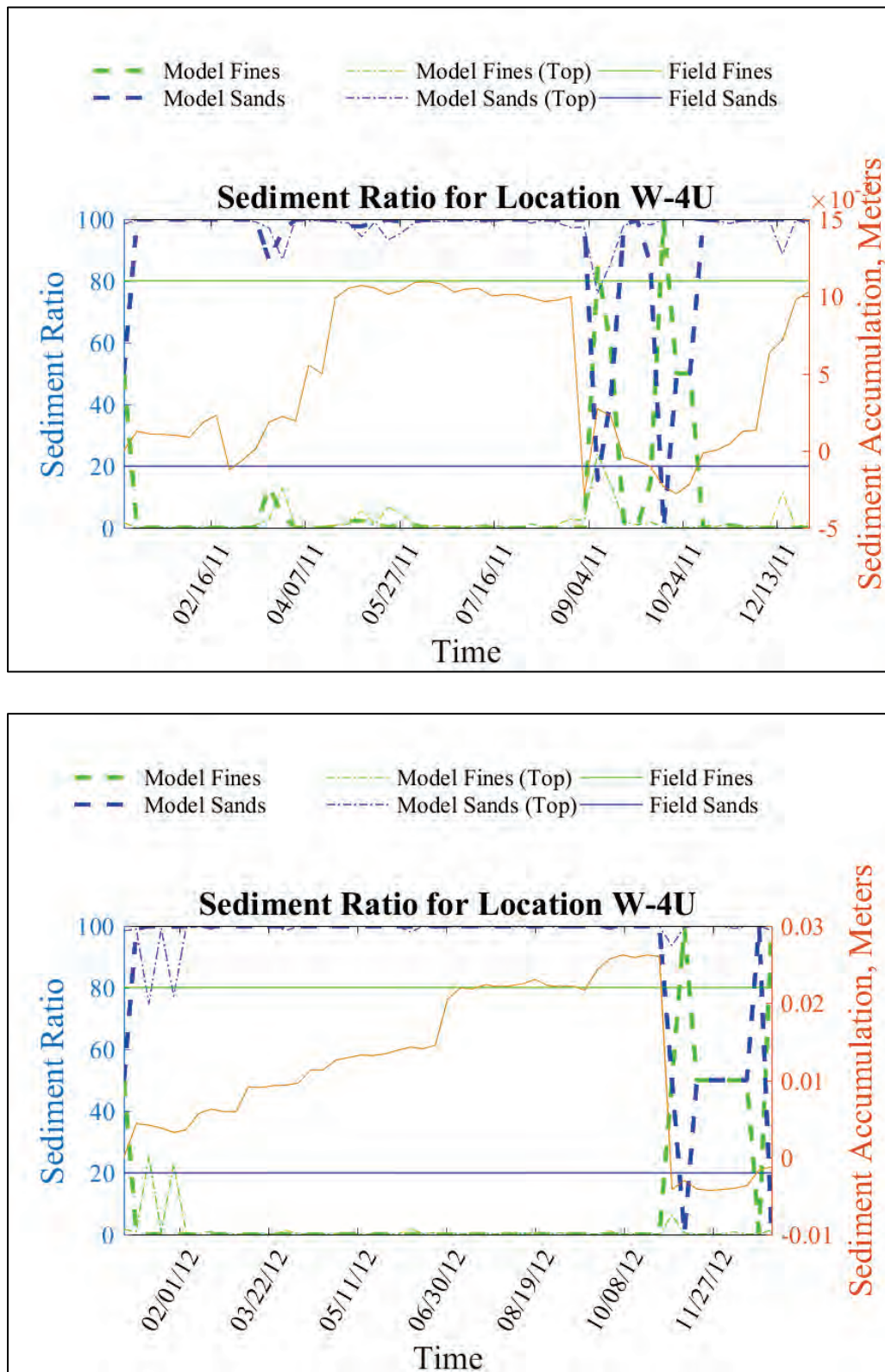


Figure 255. Sediment bed composition comparisons at location W-5AU for 2011 (top) and 2012 (bottom).

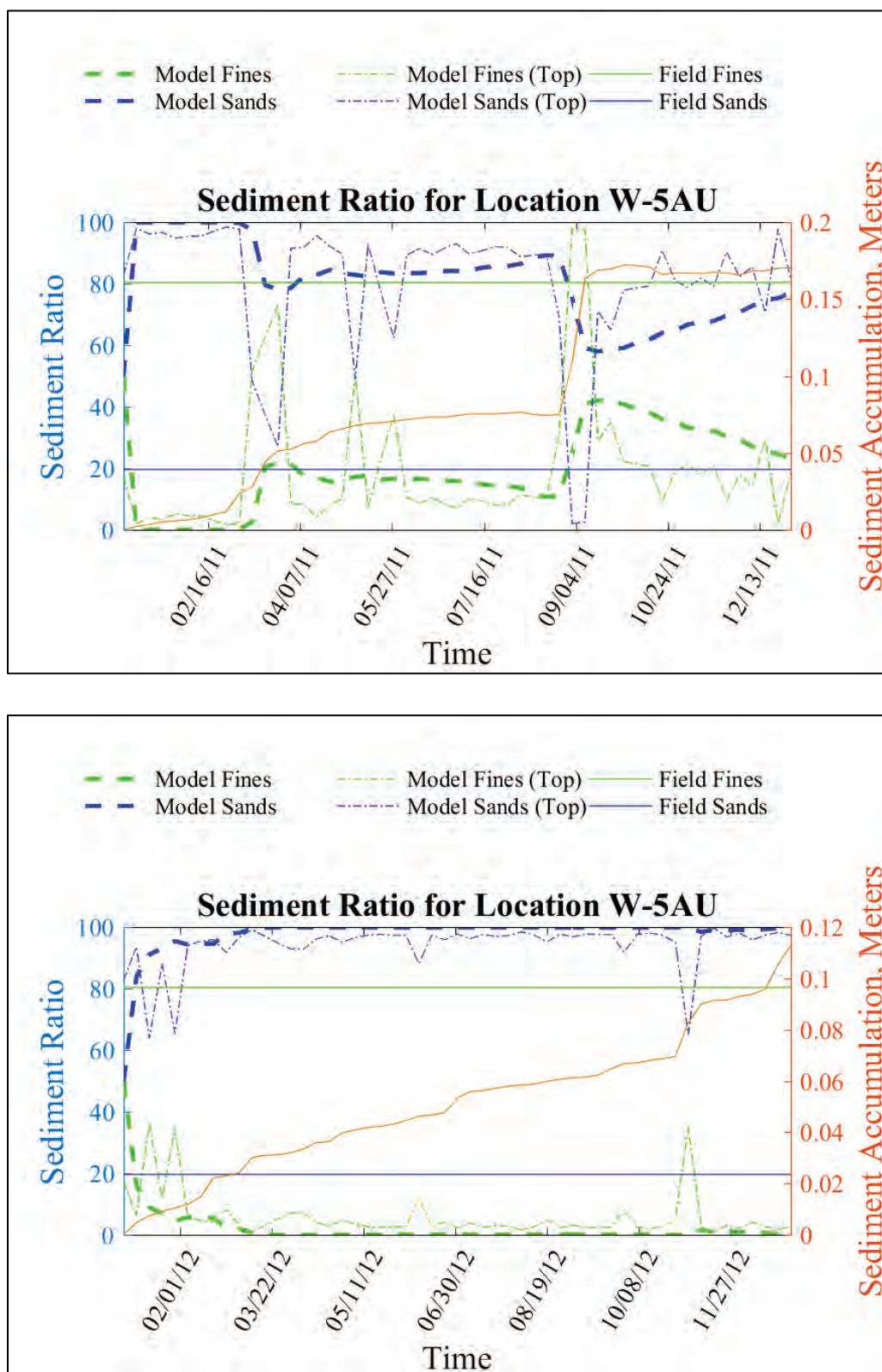




Figure 256. Sediment bed composition comparisons at location W-5BU for 2011 (top) and 2012 (bottom).

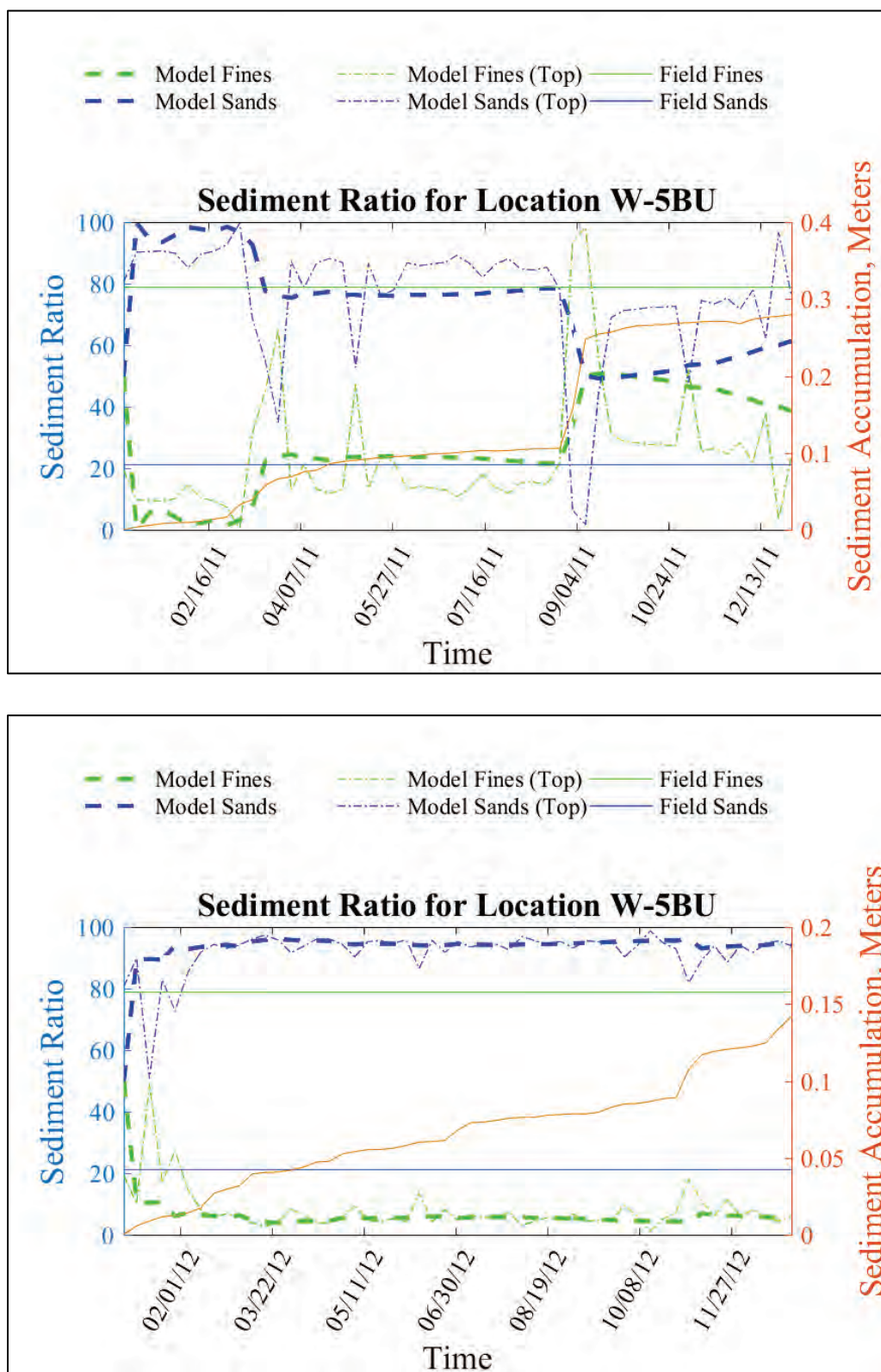


Figure 257. Sediment bed composition comparisons at location W-5U for 2011 (top) and 2012 (bottom).

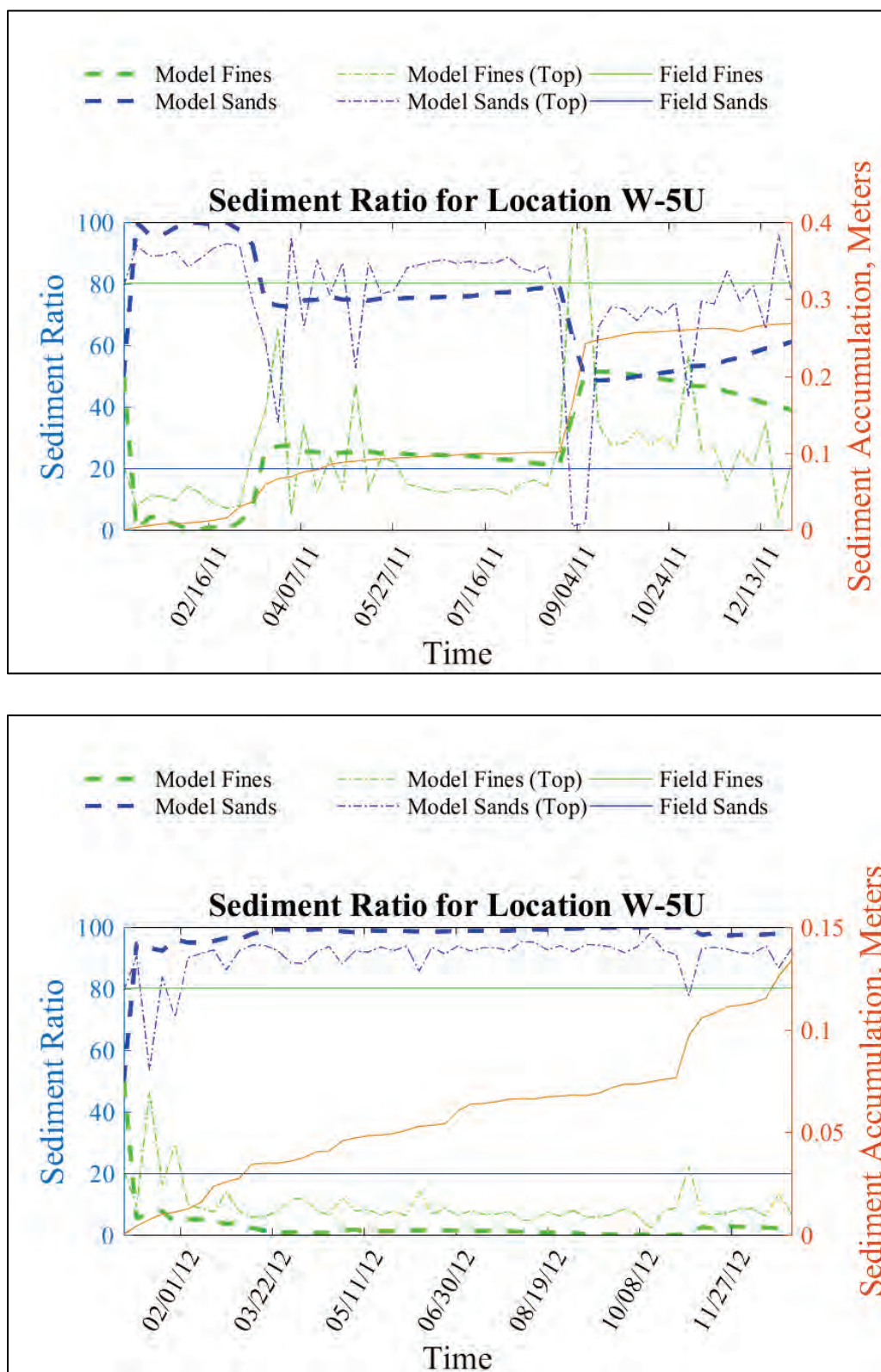
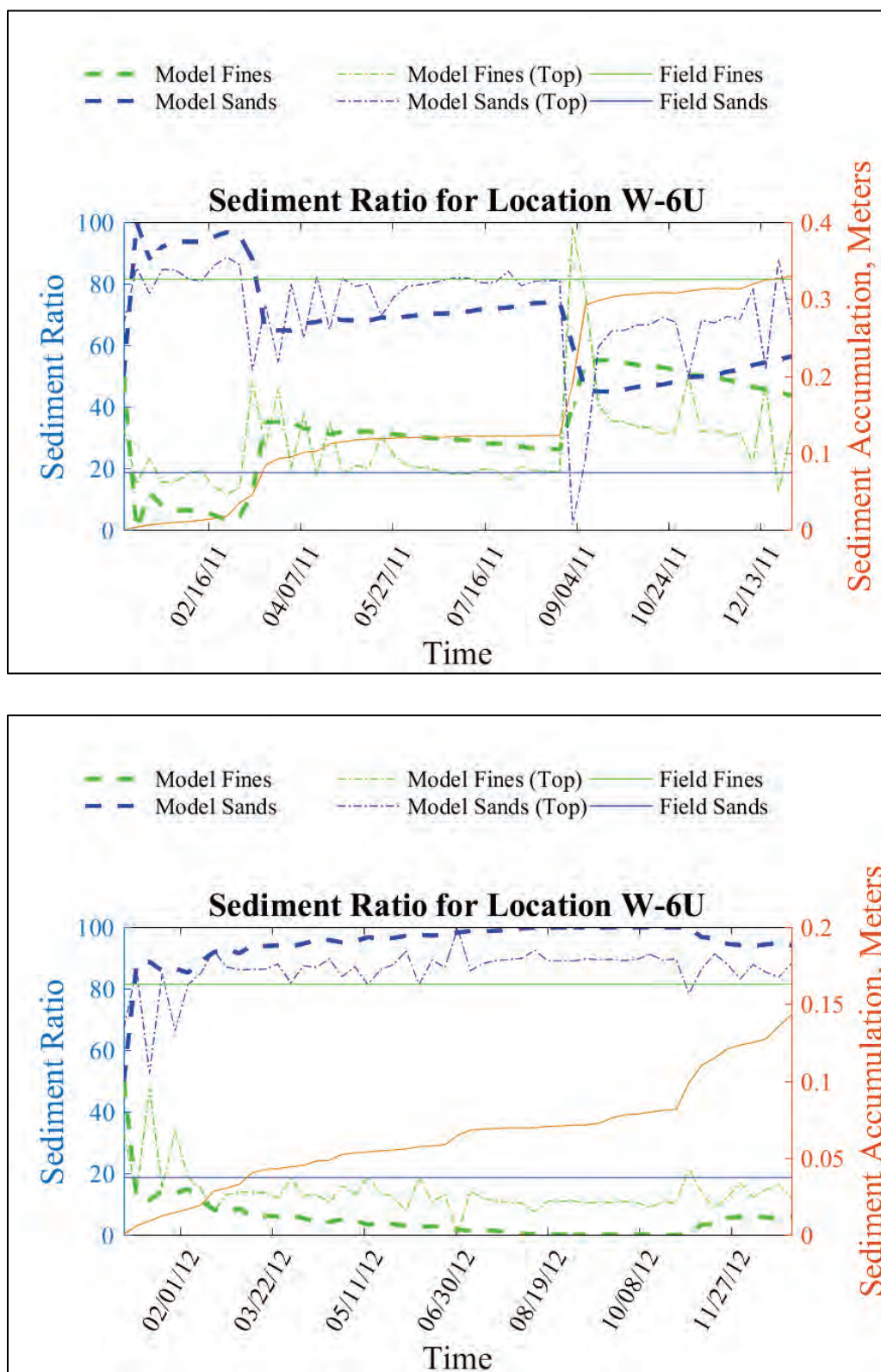


Figure 258. Sediment bed composition comparisons at location W-6U for 2011 (top) and 2012 (bottom).





## Appendix D: Results for 1985

### Lower Bay results

Figure 259. Without-project (top) and with-project (bottom) average shear stresses, Pa (1985).

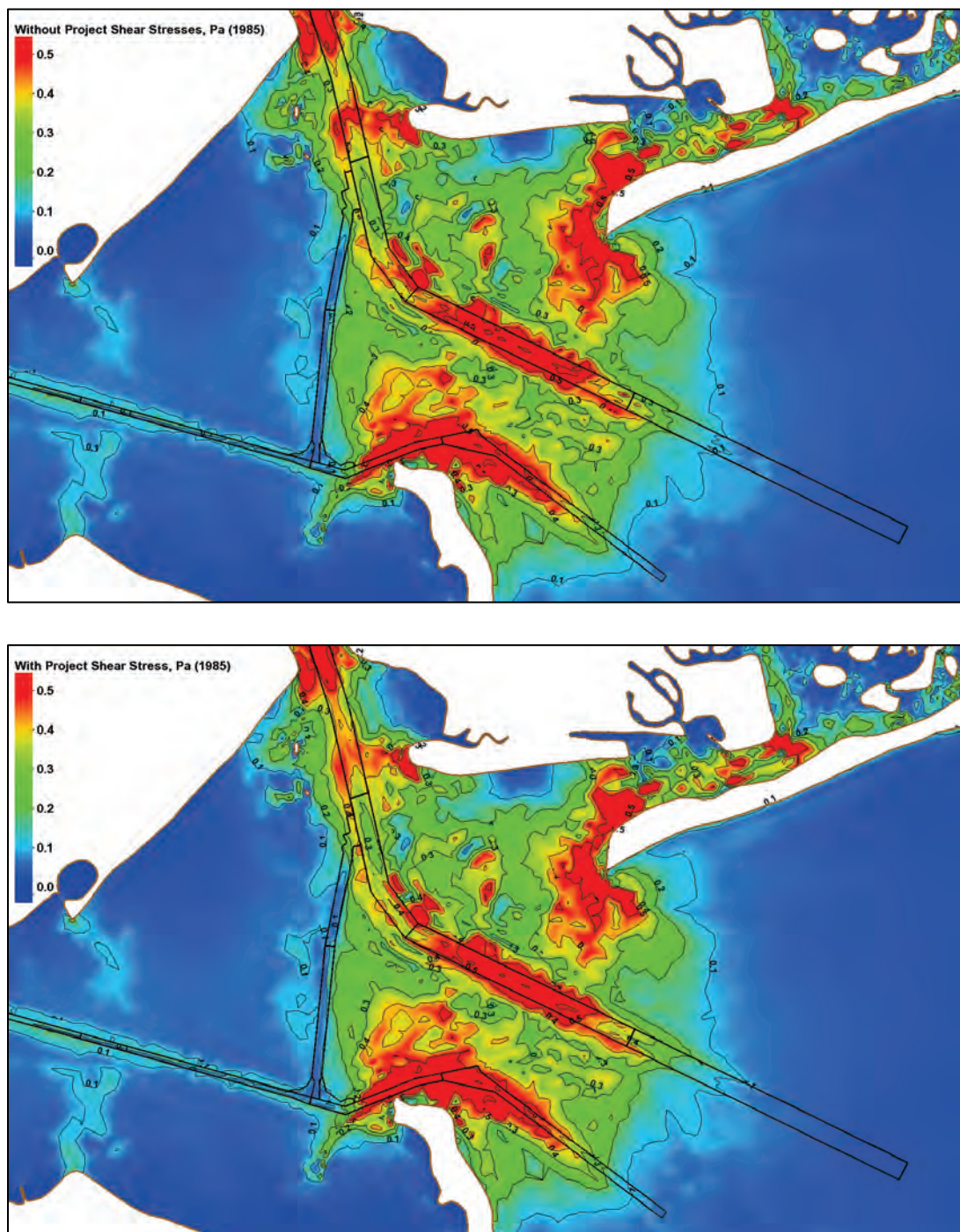


Figure 260. Without-project (top) and with-project (bottom) average bottom salinity, ppt (1985).

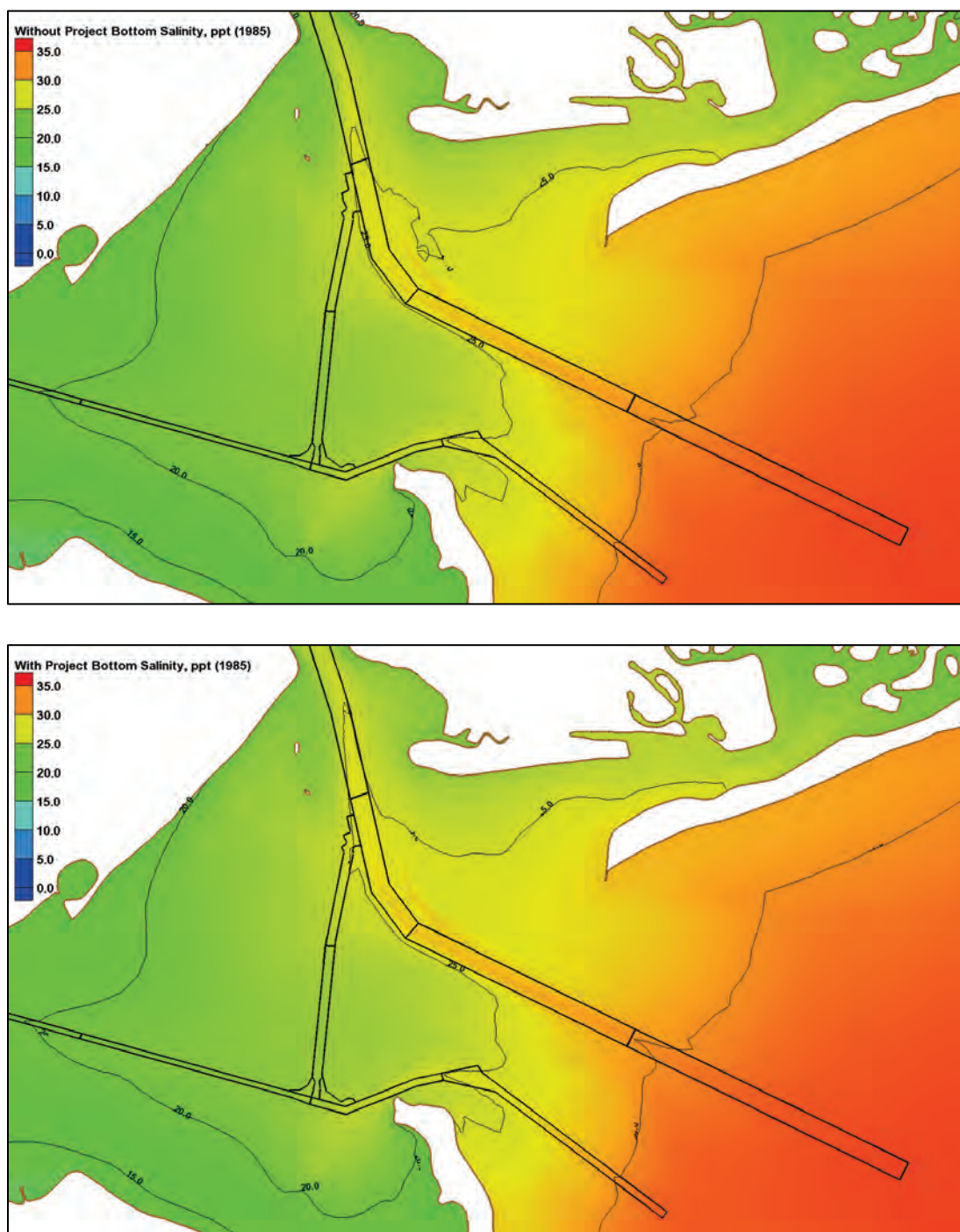




Figure 261. Without-project (top) and with-project (bottom) average fine sediment bottom concentrations, ppm (1985).

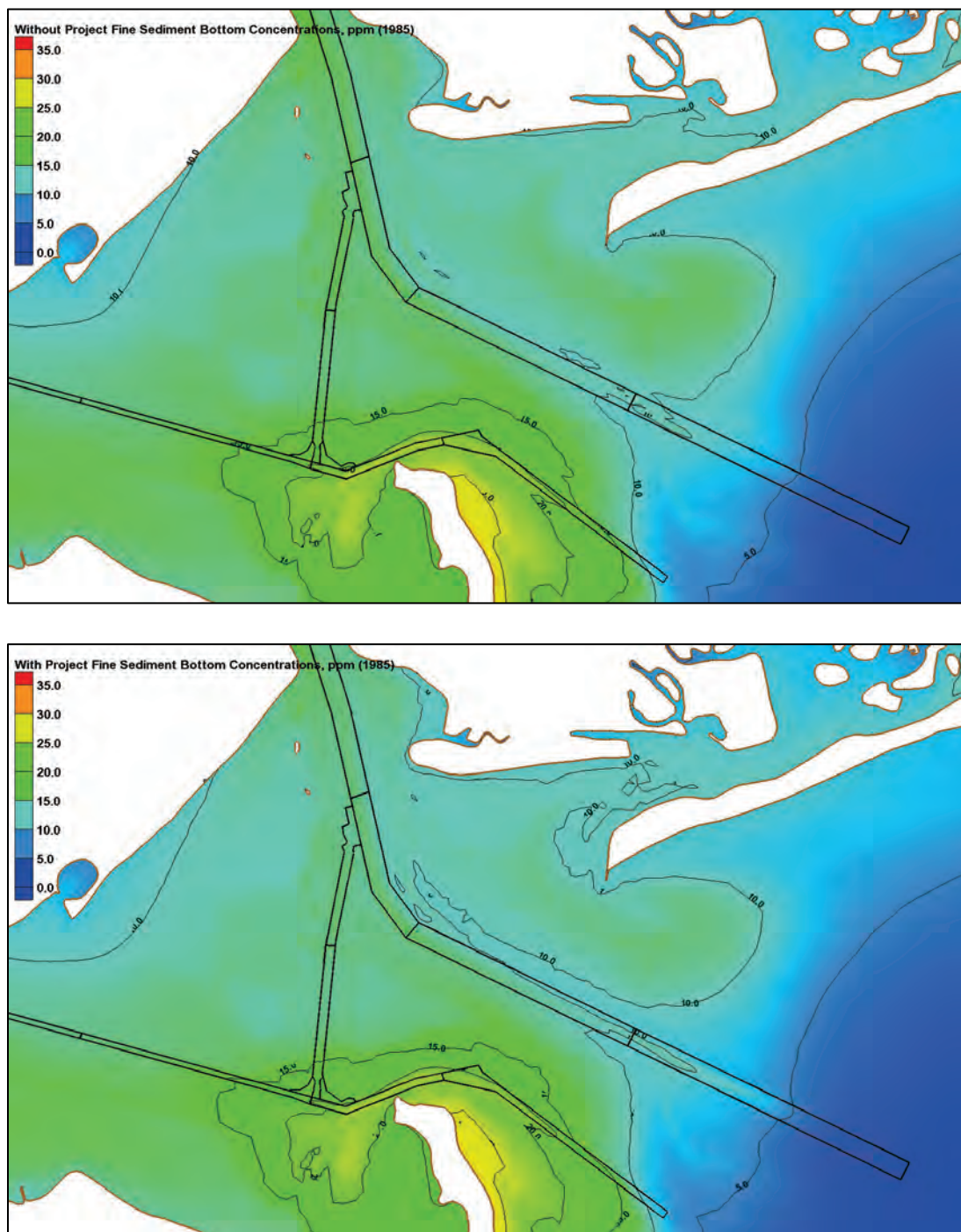


Figure 262. Without-project (top) and with-project (bottom) average sand bottom concentrations, ppm (1985).

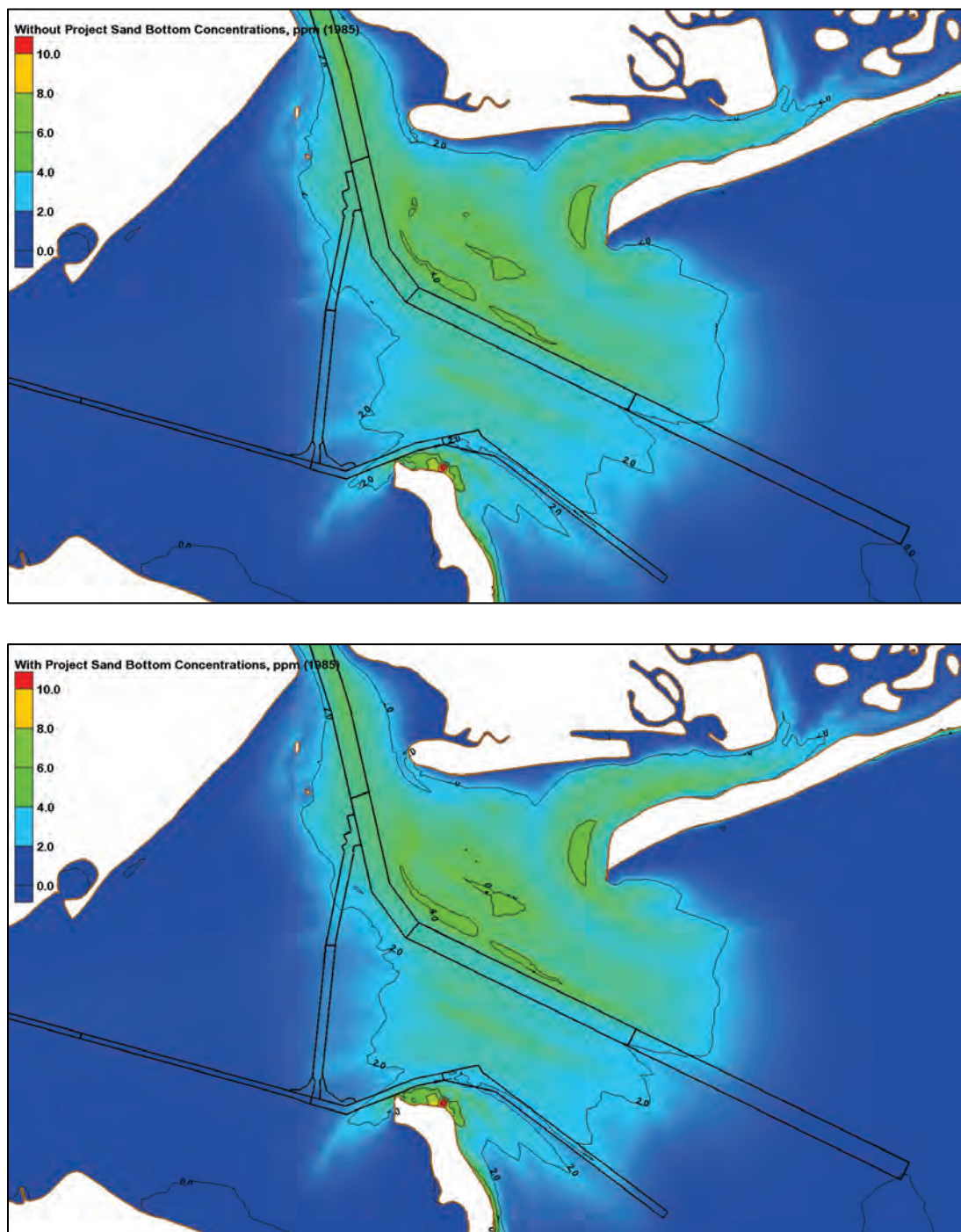




Figure 263. Without-project (top) and with-project (bottom) bed displacement, m (1985).

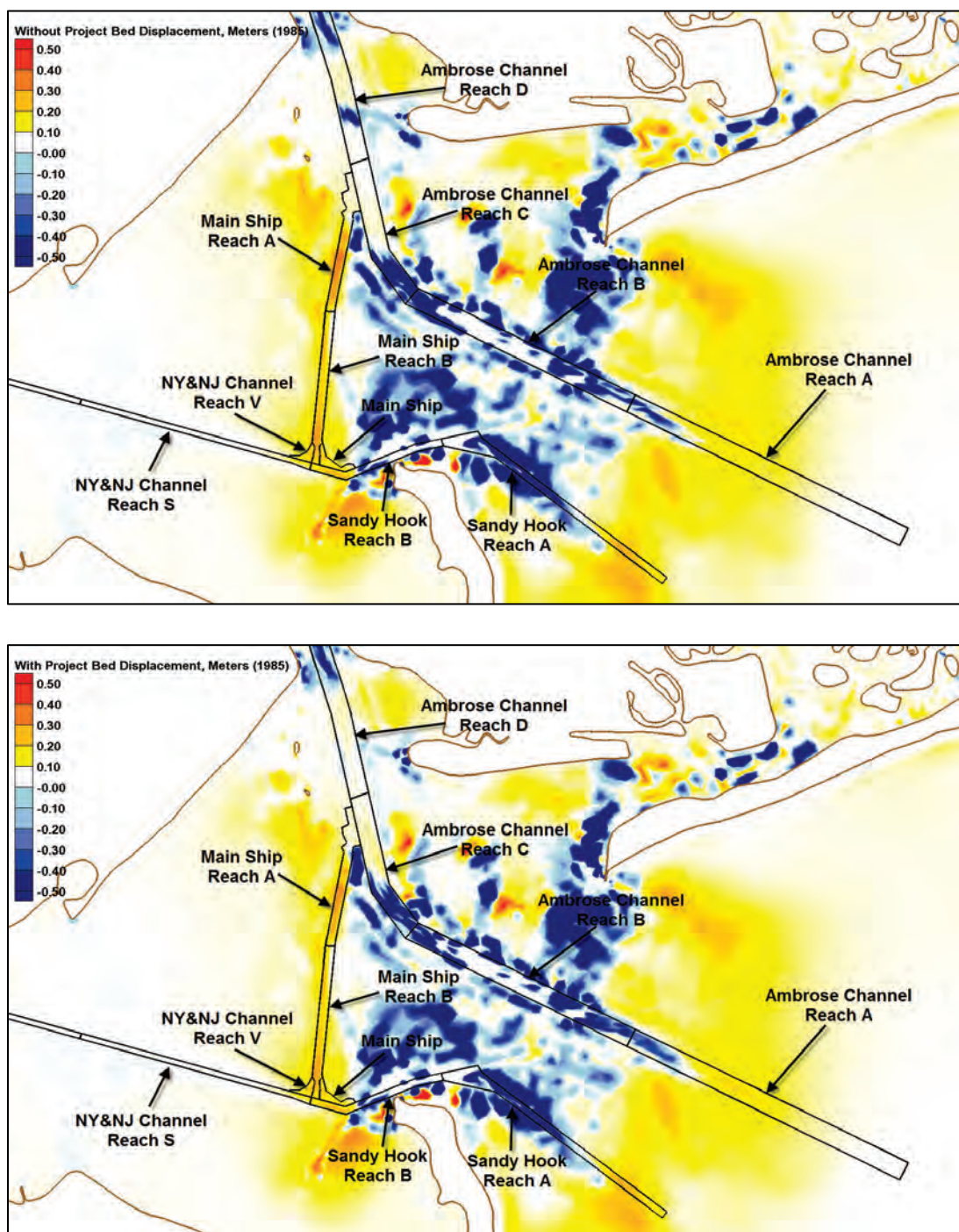


Figure 264. Without-project (top) and with-project (bottom) fine sediment accumulation,  $\text{kg/m}^2$  (1985).

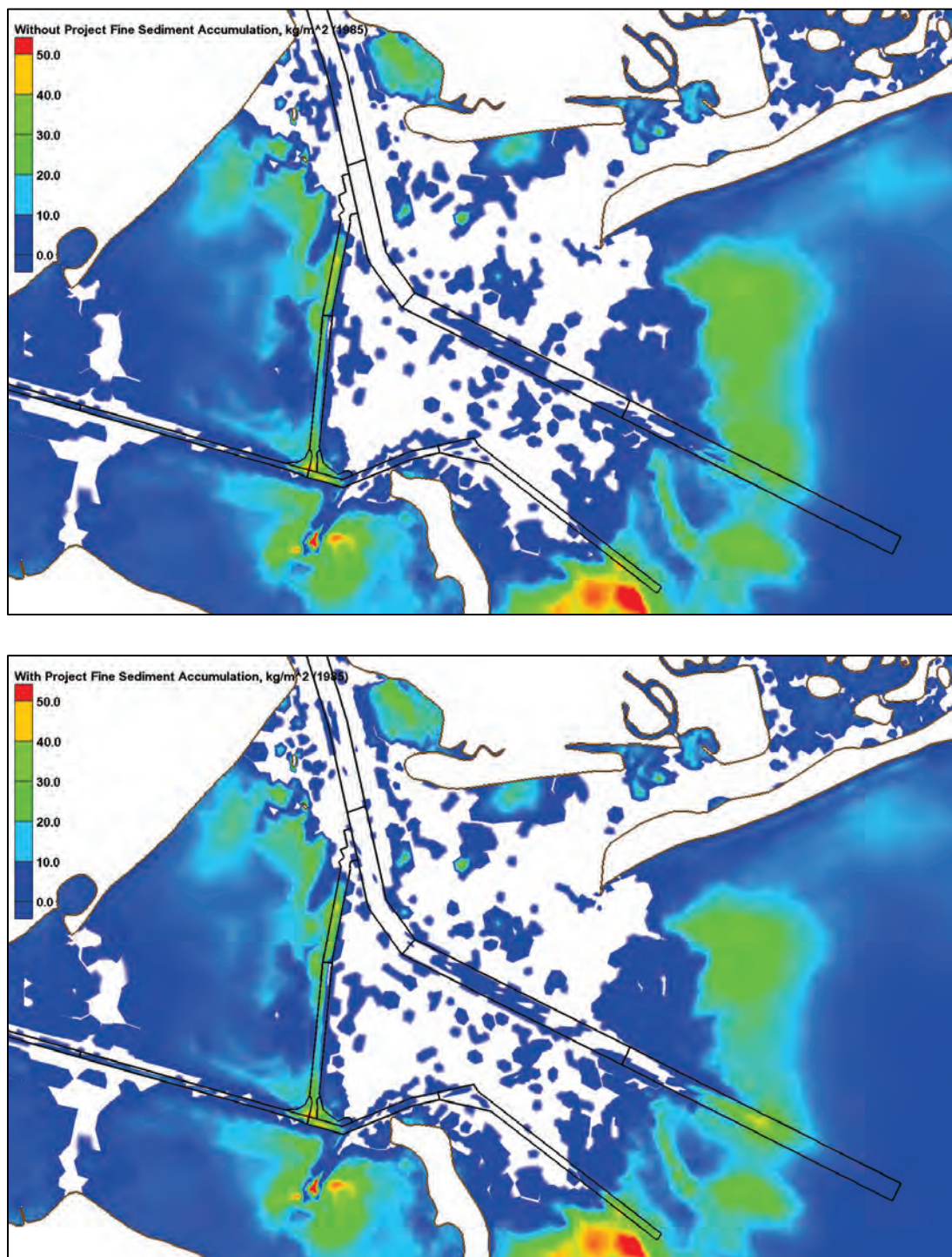




Figure 265. Without-project (top) and with-project (bottom) sand accumulation, kg/m<sup>2</sup> (1985).

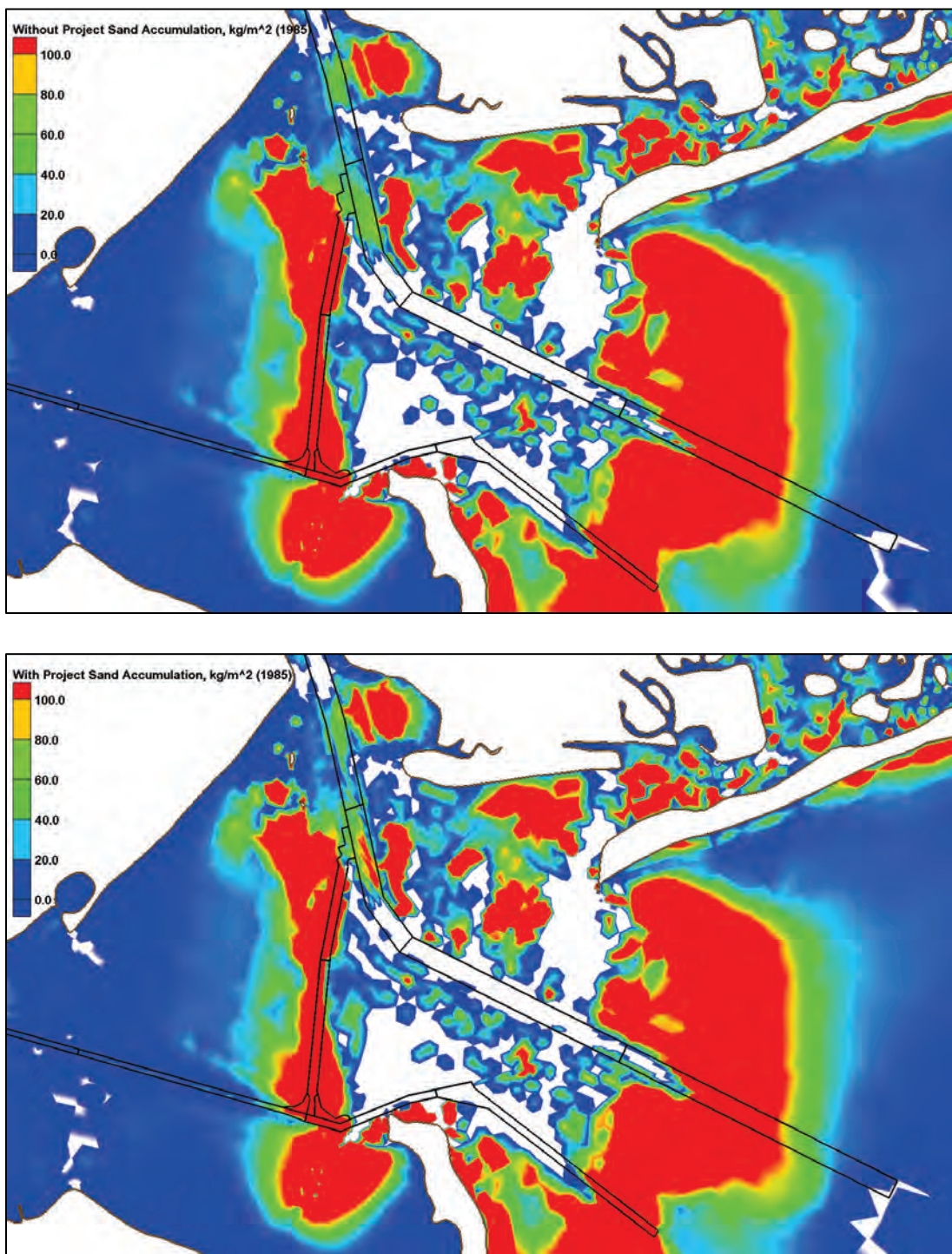




Figure 266. Dredge with-project/without-project percent differences (1985).

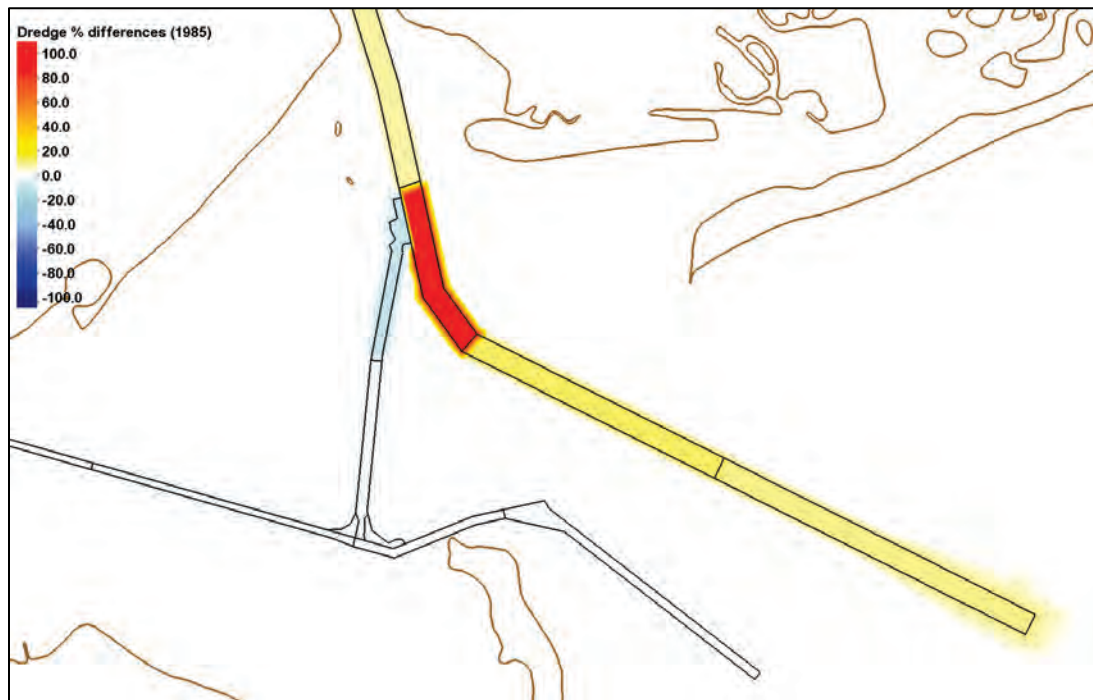


Table 28. Dredge volumes for Lower Bay (1985).

Depositional Volumes in Lower Bay, cy (1985)			
Reach	Without Project	With Project	With/Without Dredge Percentage
Ambrose Channel Reach A	356,513	390,125	109
Ambrose Channel Reach B	3,730	4,185	112
Ambrose Channel Reach C	28,854	53,873	187
Ambrose Channel Reach D	32,401	34,763	107
Main Ship	47,779	46,348	97
Main Ship Reach A	231,922	203,453	88
Main Ship Reach B	263,941	256,636	97
Sandy Hook Reach A	134,405	131,859	98
Sandy Hook Reach B	65,695	65,491	100
NY&NJ Channels Reach S	25,414	24,447	96
NY&NJ Channels Reach V	34,131	32,647	96

## Newark Bay, Kill van Kull, and Upper Bay results

Figure 267. Without-project (top) and with-project (bottom) average shear stresses, Pa (1985).

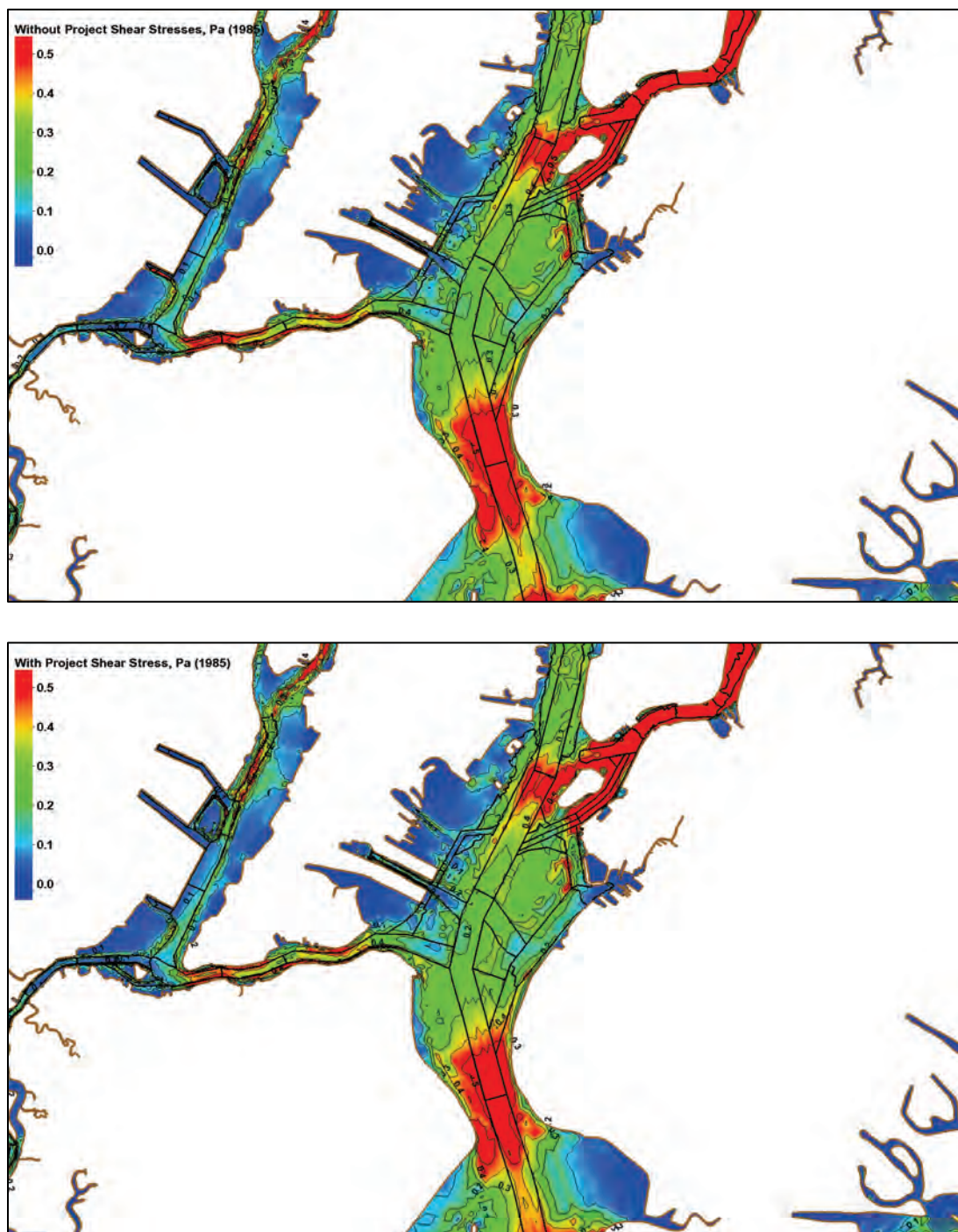


Figure 268. Without-project (top) and with-project (bottom) average bottom salinity, ppt (1985).

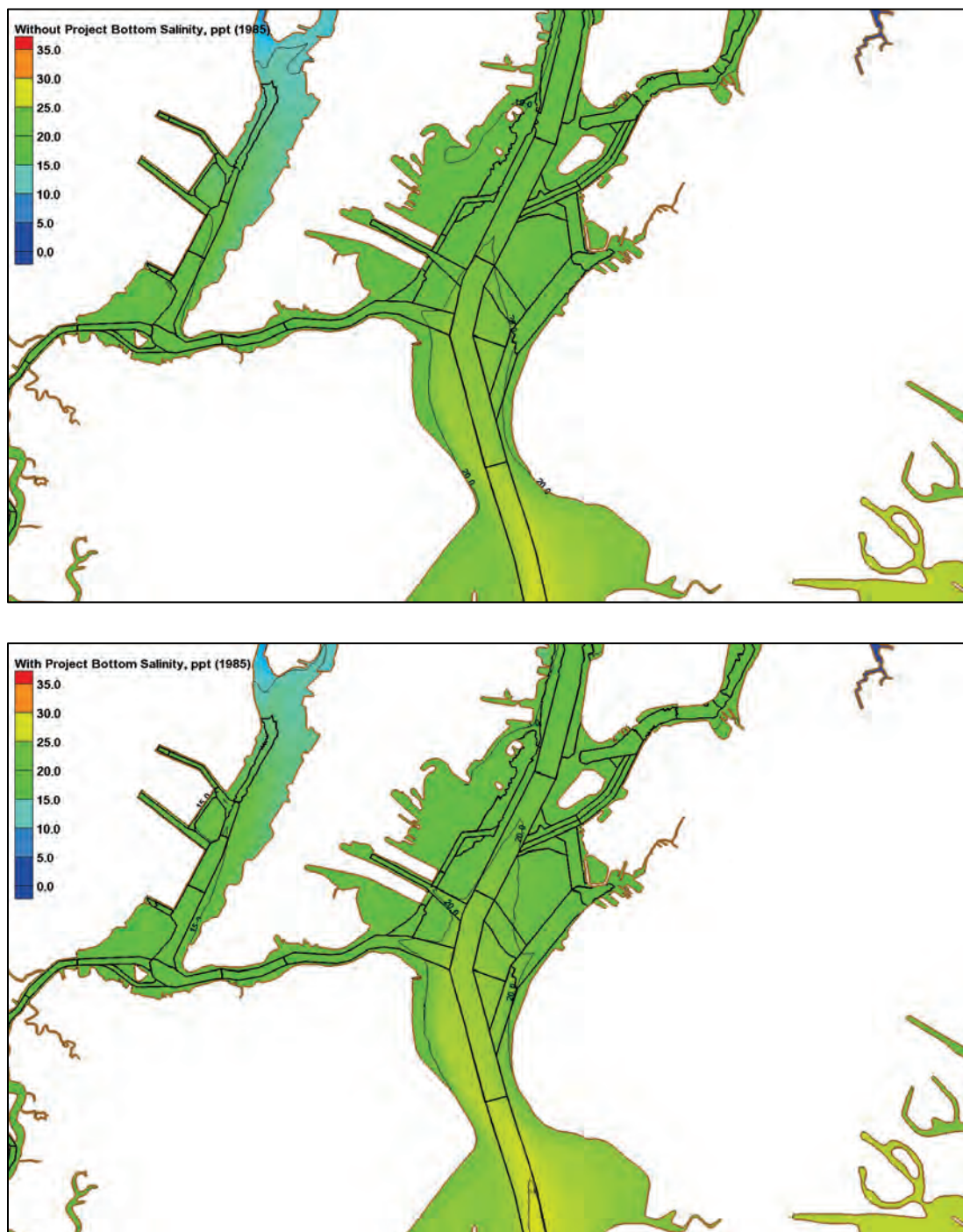




Figure 269. Without-project (top) and with-project (bottom) average fine sediment bottom concentrations, ppm (1985).

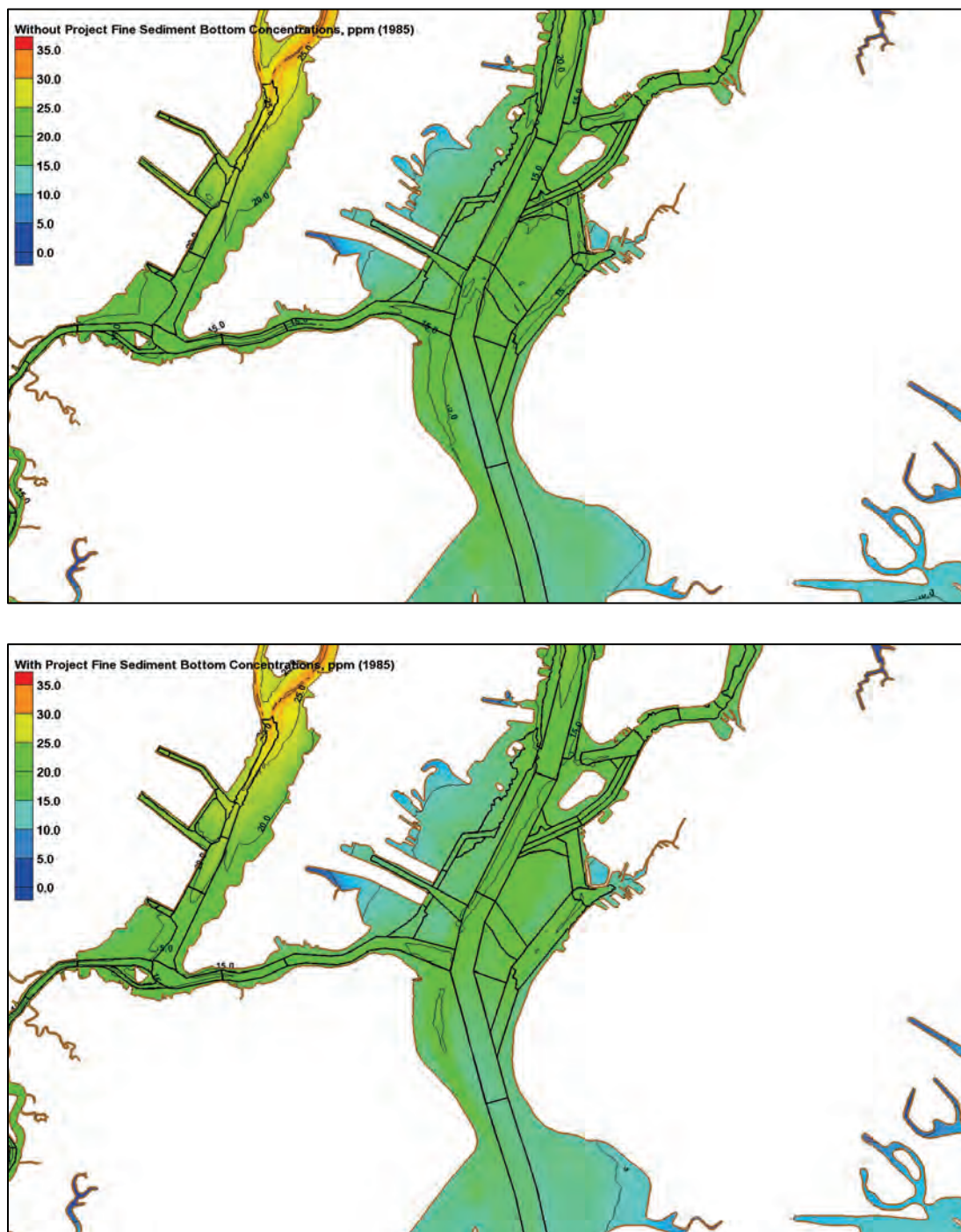


Figure 270. Without-project (top) and with-project (bottom) average sand bottom concentrations, ppm (1985).

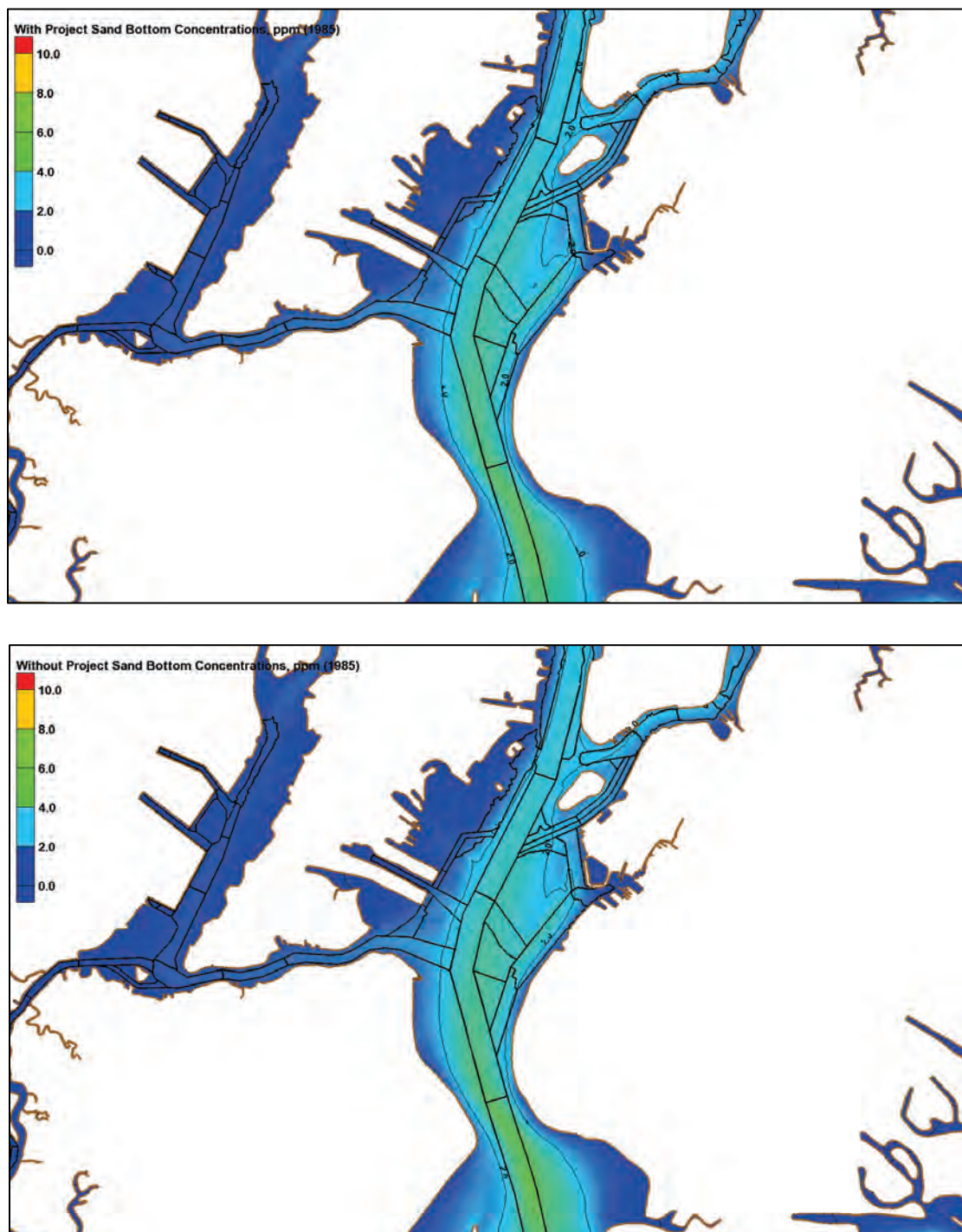




Figure 271. Without-project (top) and with-project (bottom) bed displacement, m (1985).

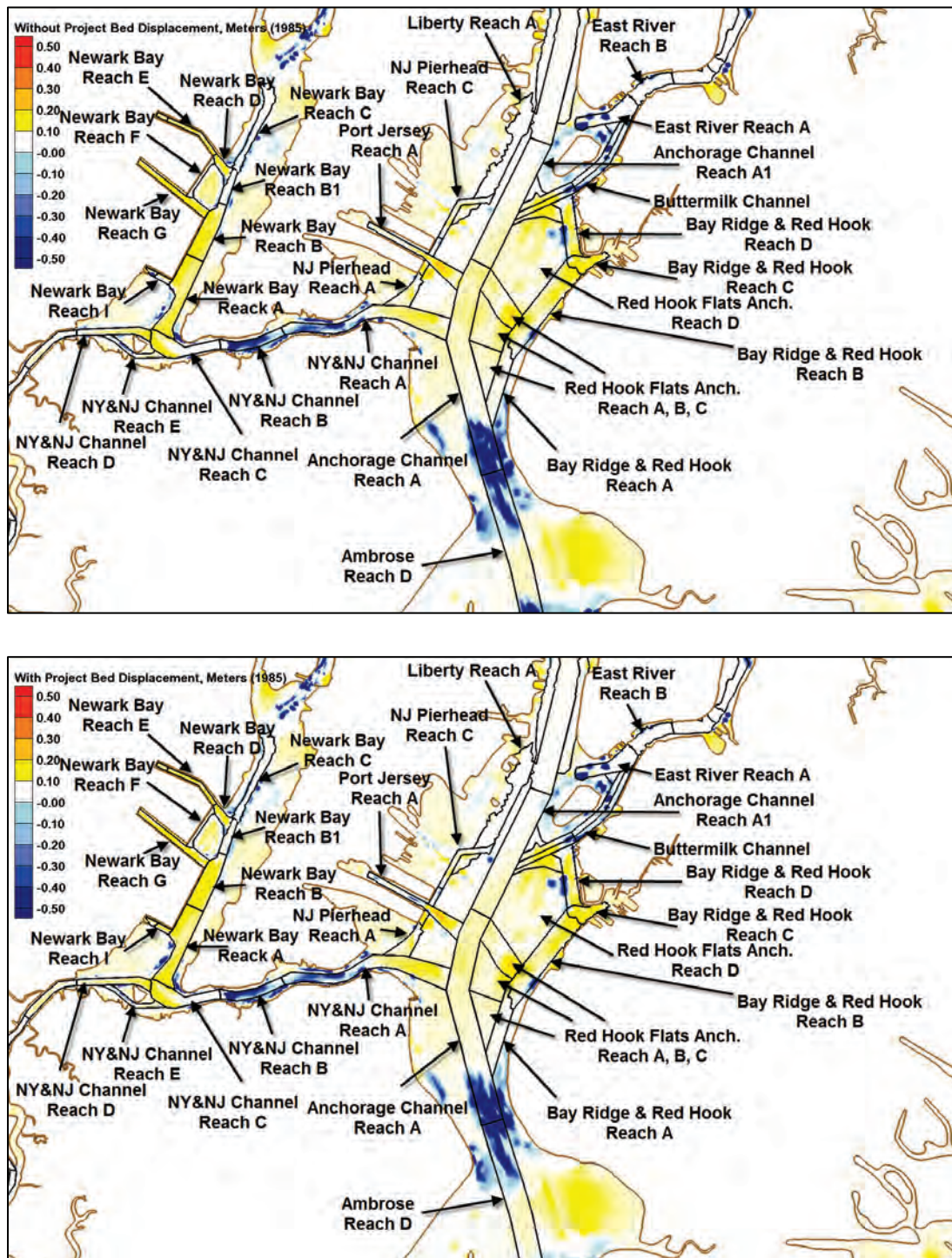


Figure 272. Without-project (top) and with-project (bottom) fine sediment accumulation,  $\text{kg}/\text{m}^2$  (1985).

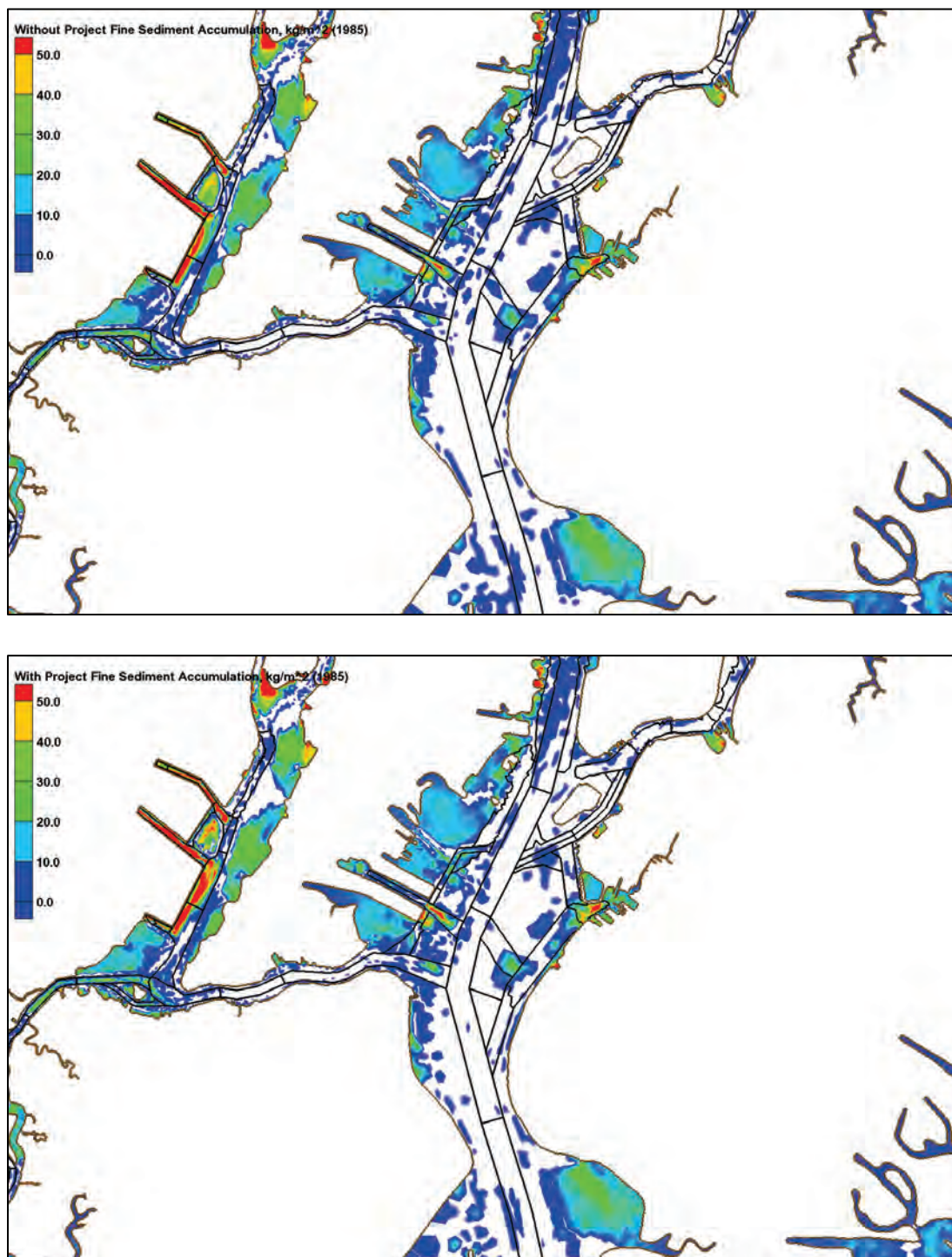




Figure 273. Without-project (top) and with-project (bottom) sand accumulation,  $\text{kg/m}^2$  (1985).

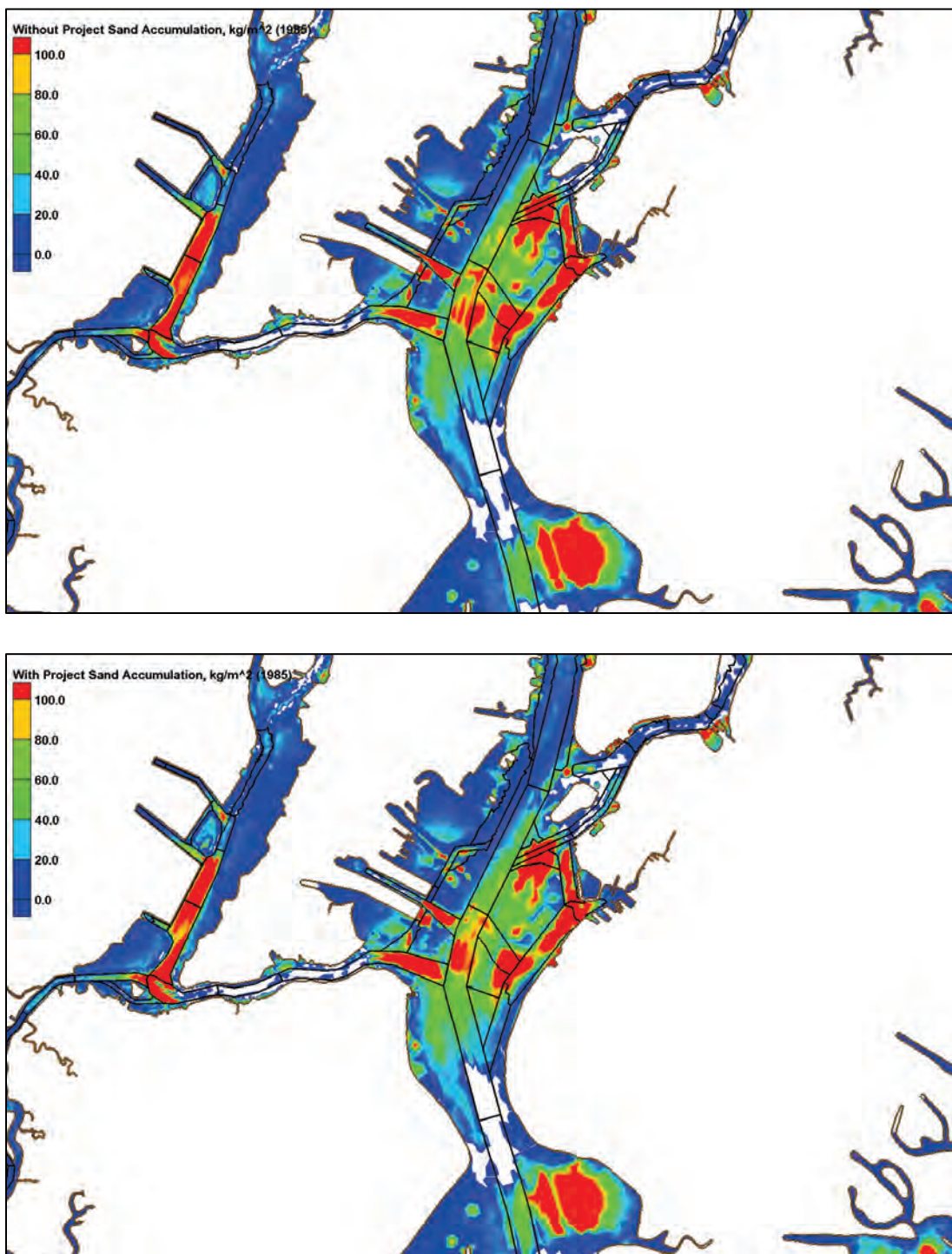


Figure 274. Dredge with-project/without-project percent differences (1985).



Table 29. Dredge Volumes for Newark Bay, Kill van Kull, and Upper Bay (1985).

Depositional Volumes in Newark Bay, Kill van Kull, and Upper Bay, cy (1985)			
Reach	Without Project	With Project	With/Without Dredge Percentage
<b>Newark Bay</b>			
Newark Bay Reach A	83,633	90,229	108
Newark Bay Reach B	63,839	76,130	119
Newark Bay Reach B1	1,298	1,606	124
Newark Bay Reach C	1,741	2,012	116
Newark Bay Reach D	11,322	12,840	113
Newark Bay Reach E	15,131	16,915	112
Newark Bay Reach E1	2,152	2,461	114
Newark Bay Reach F	2,107	2,558	121
Newark Bay Reach G	46,599	40,565	87
Newark Bay Reach I	1,727	3,731	216
Newark Bay Reach I1	1,573	1,741	108
<b>Kill van Kull</b>			
NY&NJ Channels Reach A	57,569	68,980	120
NY&NJ Channels Reach B	112	6	5
NY&NJ Channels Reach C	29,663	36,588	123
<b>Upper Bay</b>			
Anchorage Channel Reach A	84,791	89,554	106
Anchorage Channel Reach A1	39,864	35,324	89
Anchorage Reach C1	5,777	5,725	99
Bay Ridge & Red Hook Reach A	9,670	8,908	92
Bay Ridge & Red Hook Reach B	96,808	102,447	106
Bay Ridge & Red Hook Reach C	38,422	35,095	91
Bay Ridge & Red Hook Reach D	40,052	39,790	99
Red Hook Flats Anch. Reach A	17,103	16,515	97
Red Hook Flats Anch. Reach B	48,438	41,589	86
Red Hook Flats Anch. Reach C	59,992	57,640	96
Red Hook Flats Anch. Reach D	106,452	95,808	90
Port Jersey Reach A	42,073	39,577	94
NJ Pierhead Ch. Reach A	10,531	11,387	108
NJ Pierhead Ch. Reach B	5,832	6,993	120
NJ Pierhead Reach C	7,481	7,508	100
Liberty Reach A	4,327	3,600	83



## Arthur Kill and Raritan Bay results

Figure 275. Without-project (top) and with-project (bottom) average shear stresses, Pa (1985).

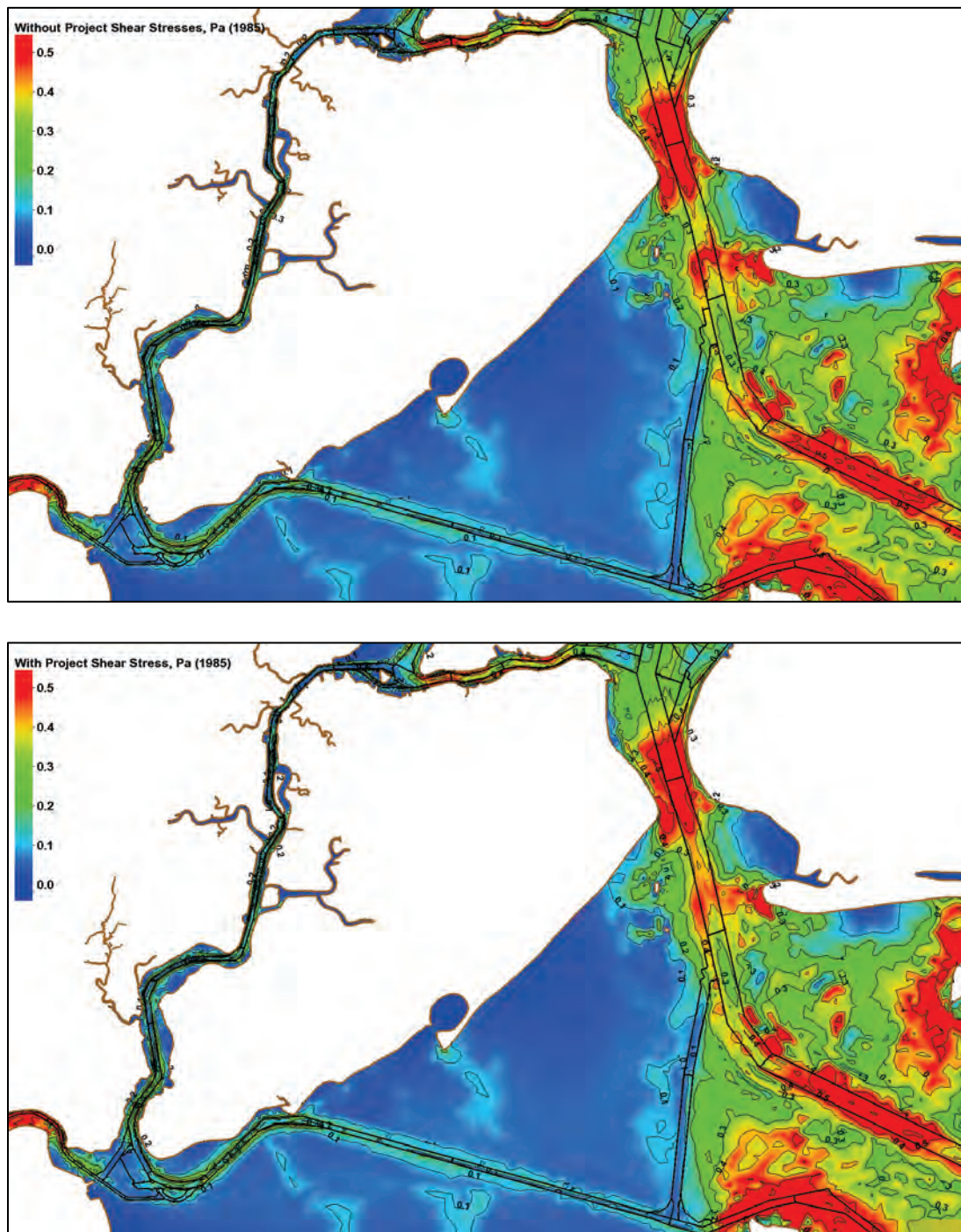


Figure 276. Without-project (top) and with-project (bottom) average bottom salinity, ppt (1985).

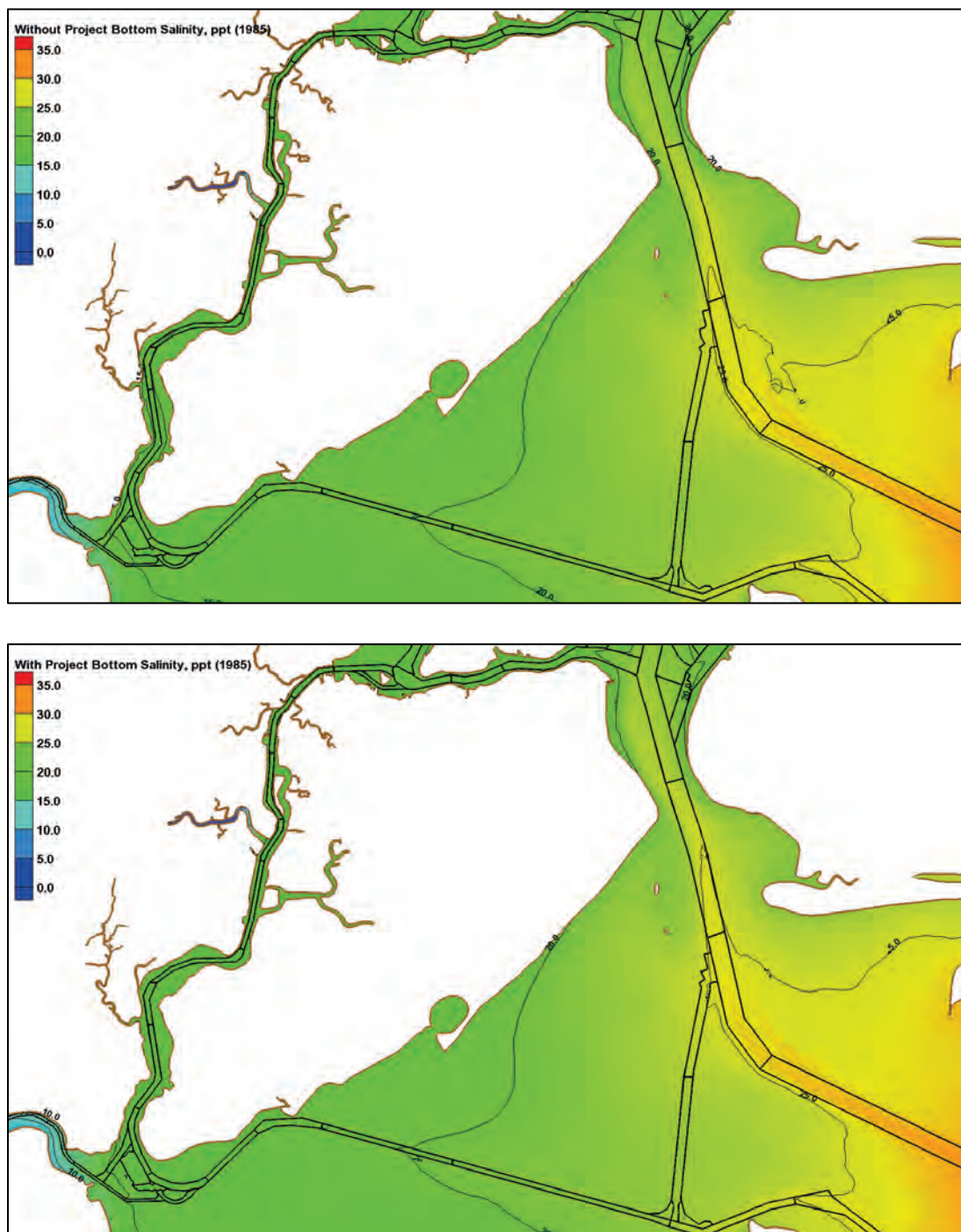


Figure 277. Without-project (top) and with-project (bottom) average fine sediment bottom concentrations, ppm (1985).

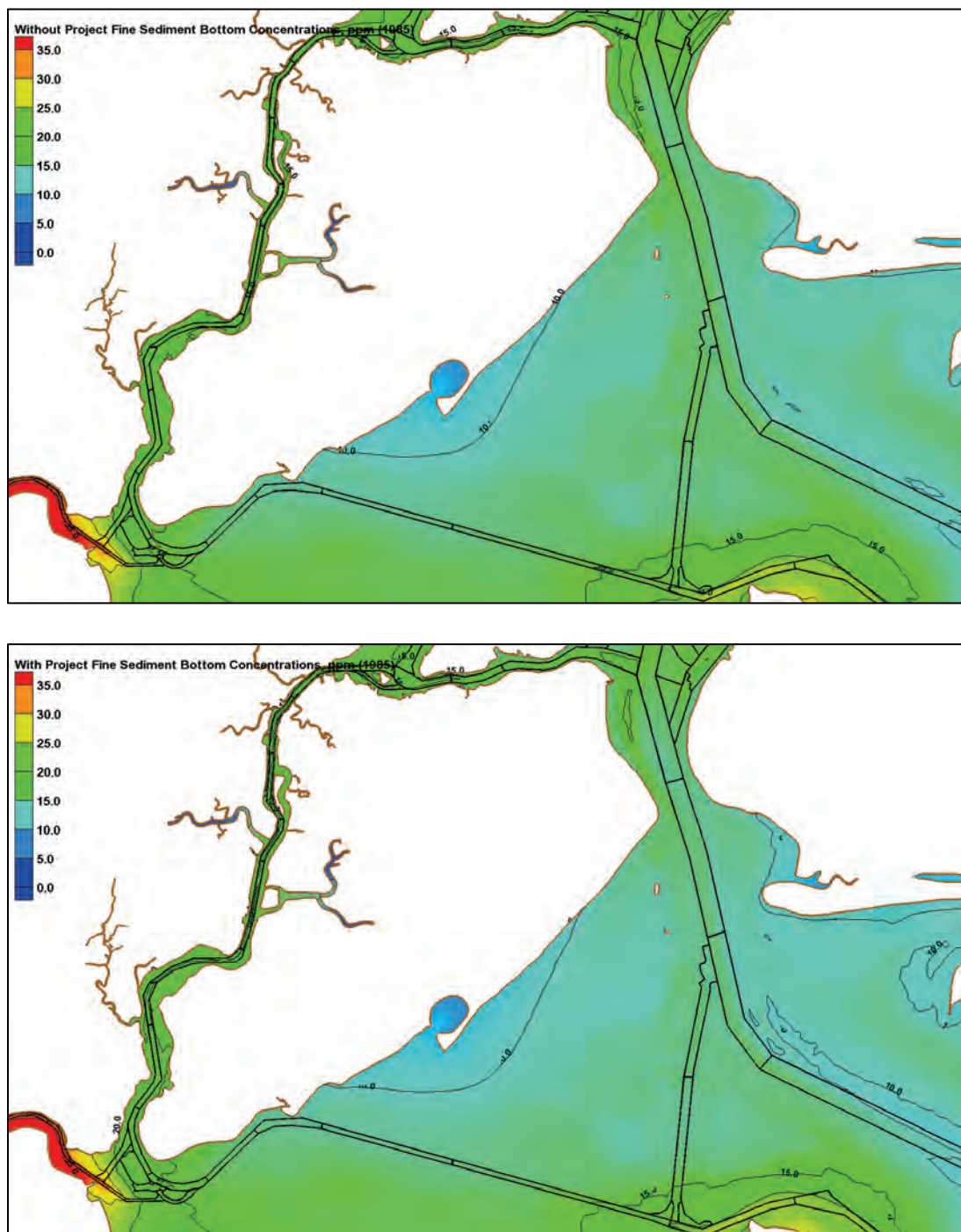




Figure 278. Without-project (top) and with-project (bottom) average sand bottom concentrations, ppm (1985).

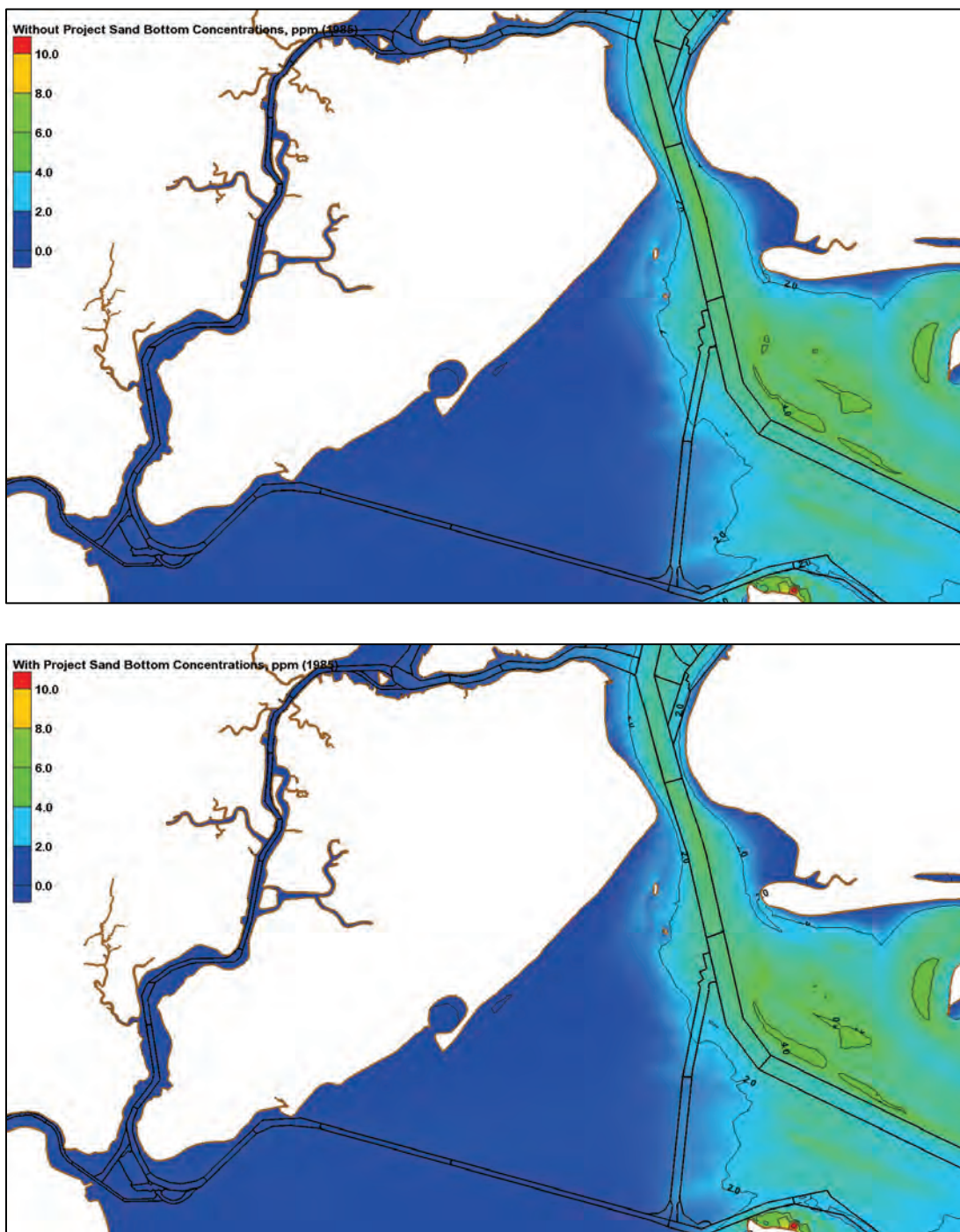


Figure 279. Without-project (top) and with-project (bottom) bed displacement, m (1985).

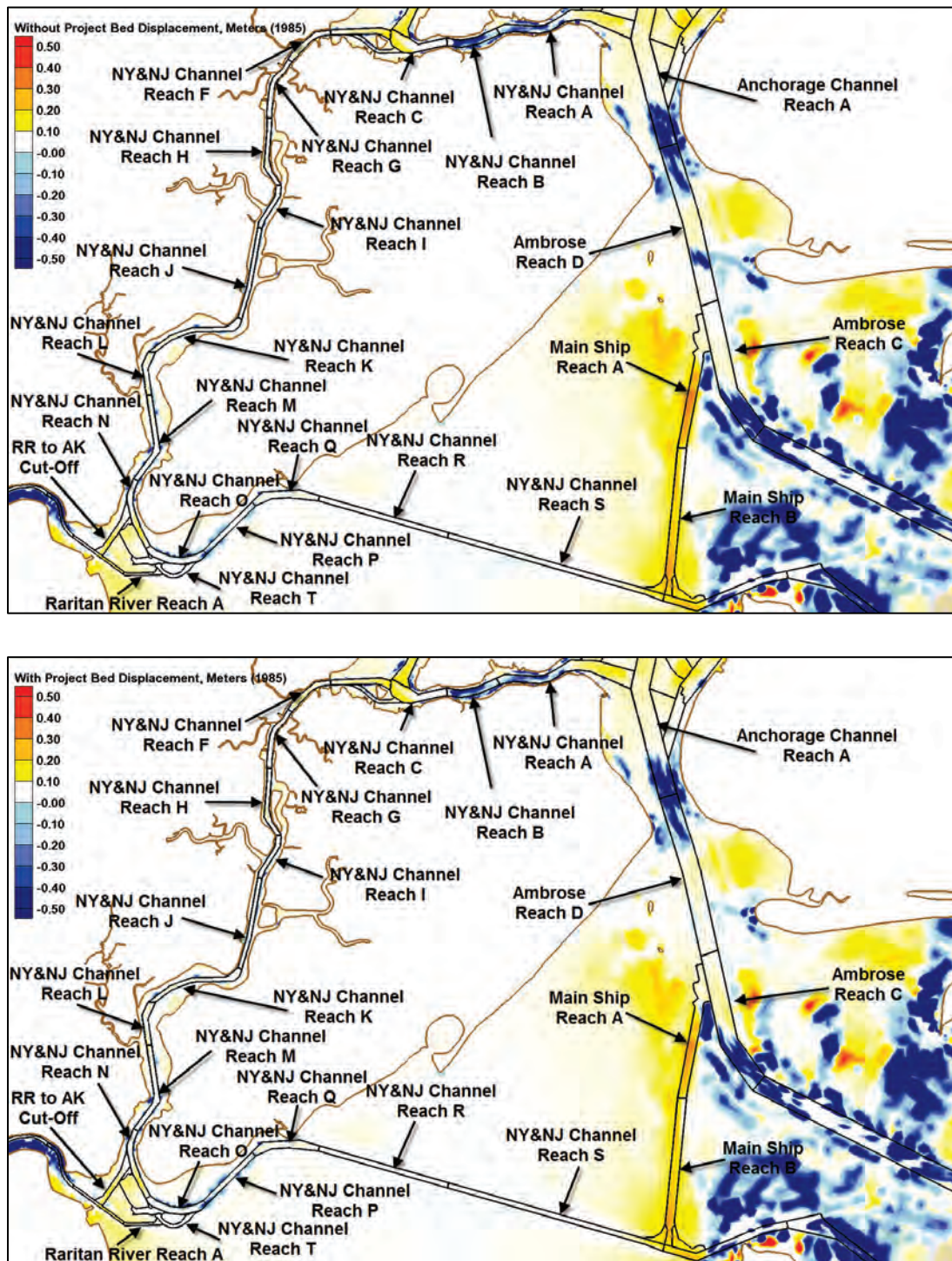




Figure 280. Without-project (top) and with-project (bottom) fine sediment accumulation,  $\text{kg}/\text{m}^2$  (1985).

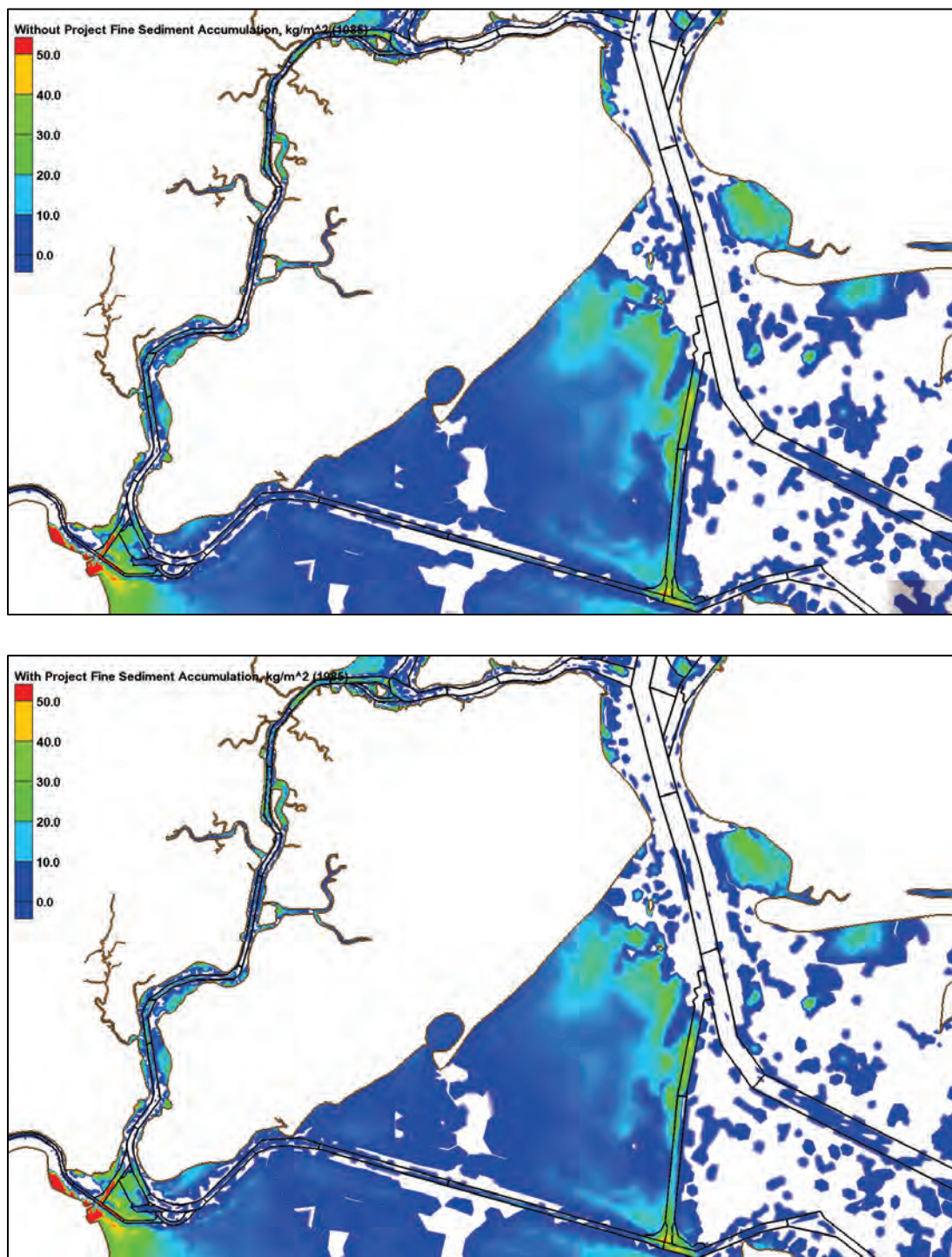


Figure 281. Without-project (top) and with-project (bottom) sand accumulation,  $\text{kg/m}^2$  (1985).

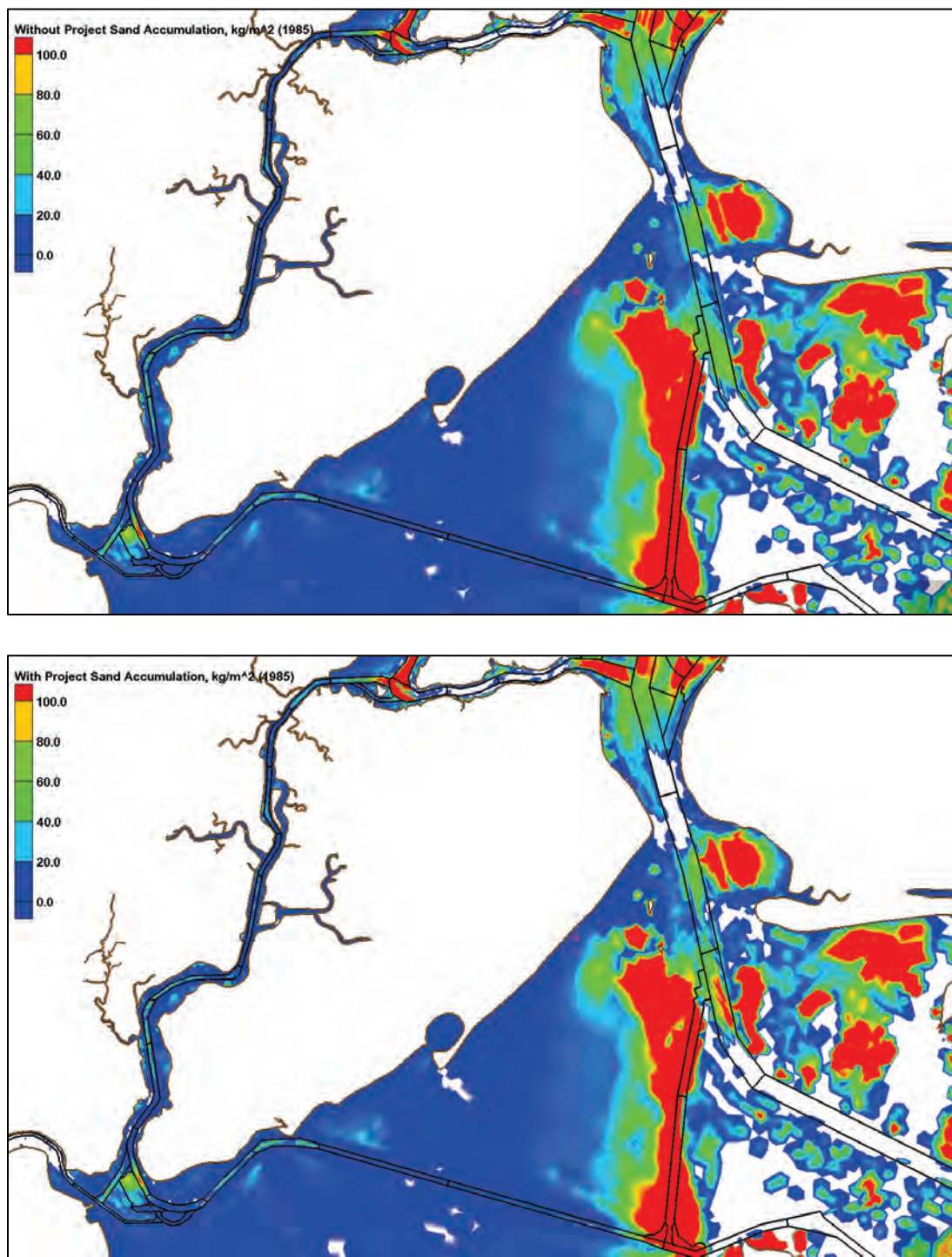


Figure 282. Dredge with-project/without-project percent differences (1985).

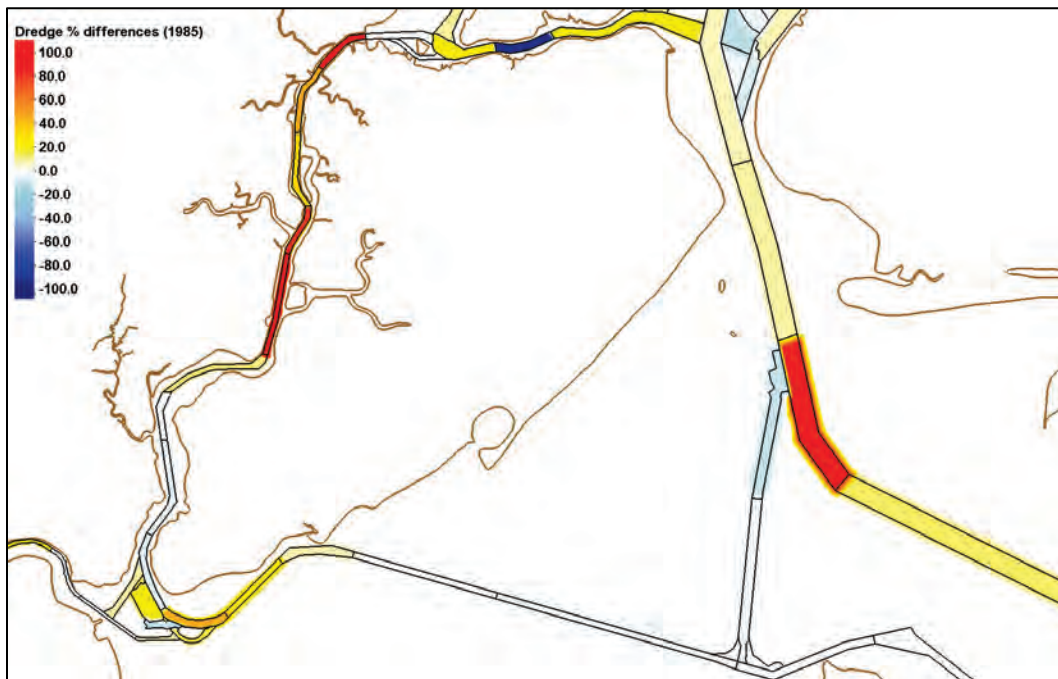


Table 30. Dredge Volumes for Arthur Kill (1985).

Depositional Volumes in Arthur Kill and Raritan Bay, cy (1985)			
Reach	Without Project	With Project	With/Without Dredge Percentage
<b>Arthur Kill</b>			
NY&NJ Channels Reach D	18,194	17,866	98
NY&NJ Channels Reach E	2,933	2,953	101
NY&NJ Channels Reach F	3,254	6,357	195
NY&NJ Channels Reach G	575	836	145
NY&NJ Channels Reach H	2,092	2,759	132
NY&NJ Channels Reach I	95	170	179
NY&NJ Channels Reach J	176	856	487
NY&NJ Channels Reach K	3,626	4,004	110
NY&NJ Channels Reach L	4,157	4,098	99
NY&NJ Channels Reach M	2,936	2,796	95
NY&NJ Channels Reach N	11,151	10,378	93
<b>Raritan Bay</b>			
NY&NJ Channels Reach O	975	1,411	145
NY&NJ Channels Reach P	1,918	2,419	126
NY&NJ Channels Reach Q	4,468	4,747	106
NY&NJ Channels Reach R	1,137	1,134	100
NY&NJ Channels Reach T	336	386	115
RR to AK Cut-Off Reach A	14,154	15,191	107
Raritan River Reach A	2,808	2,973	106
Raritan River Reach B	8,227	8,201	100
Raritan River Reach C	622	618	99
Raritan River Reach D	39	48	123



## Appendix E: Results for 1996

### Lower Bay results

Figure 283. Without-project (top) and with-project (bottom) average shear stresses, Pa (1996).

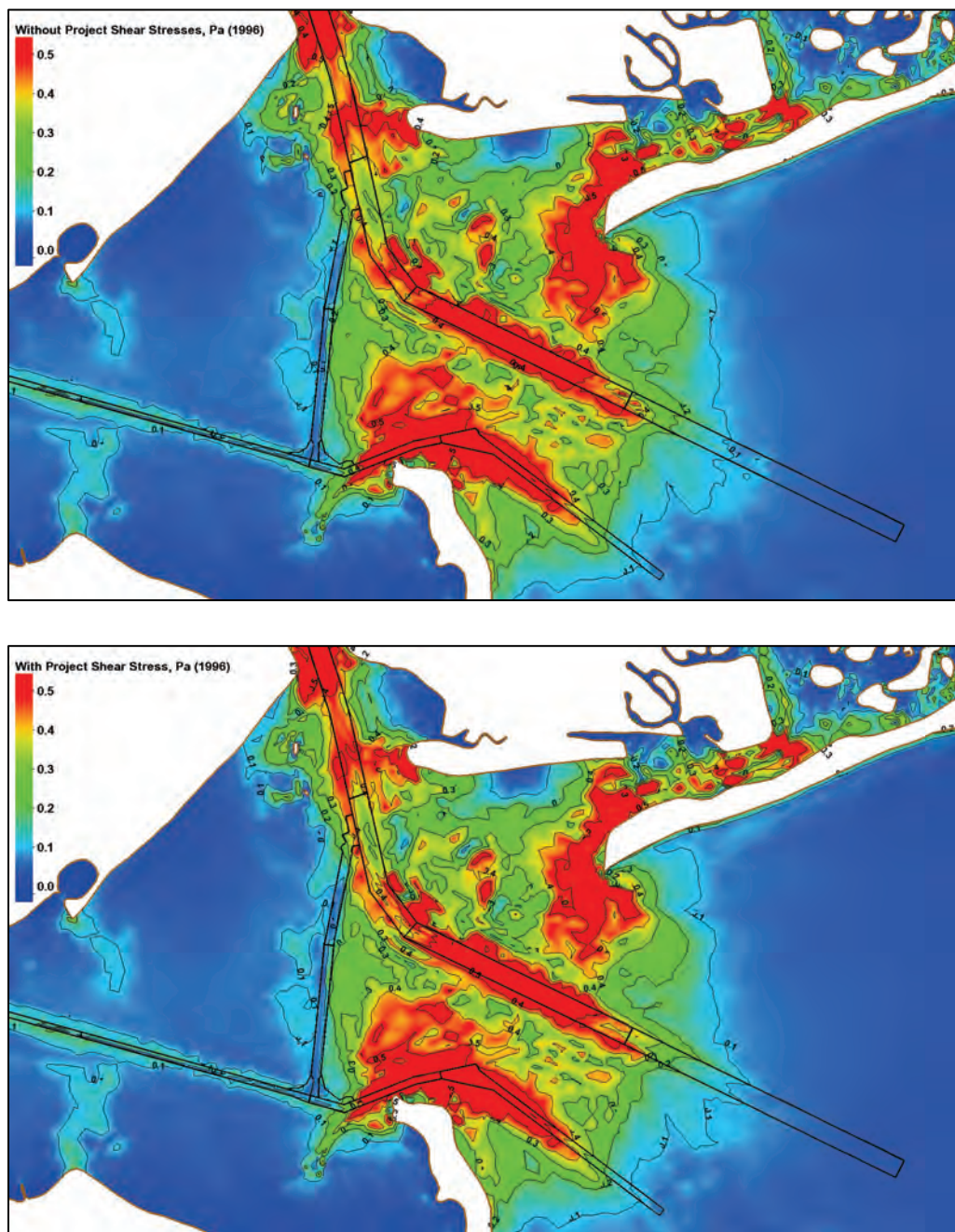




Figure 284. Without-project (top) and with-project (bottom) average bottom salinity, ppt (1996).

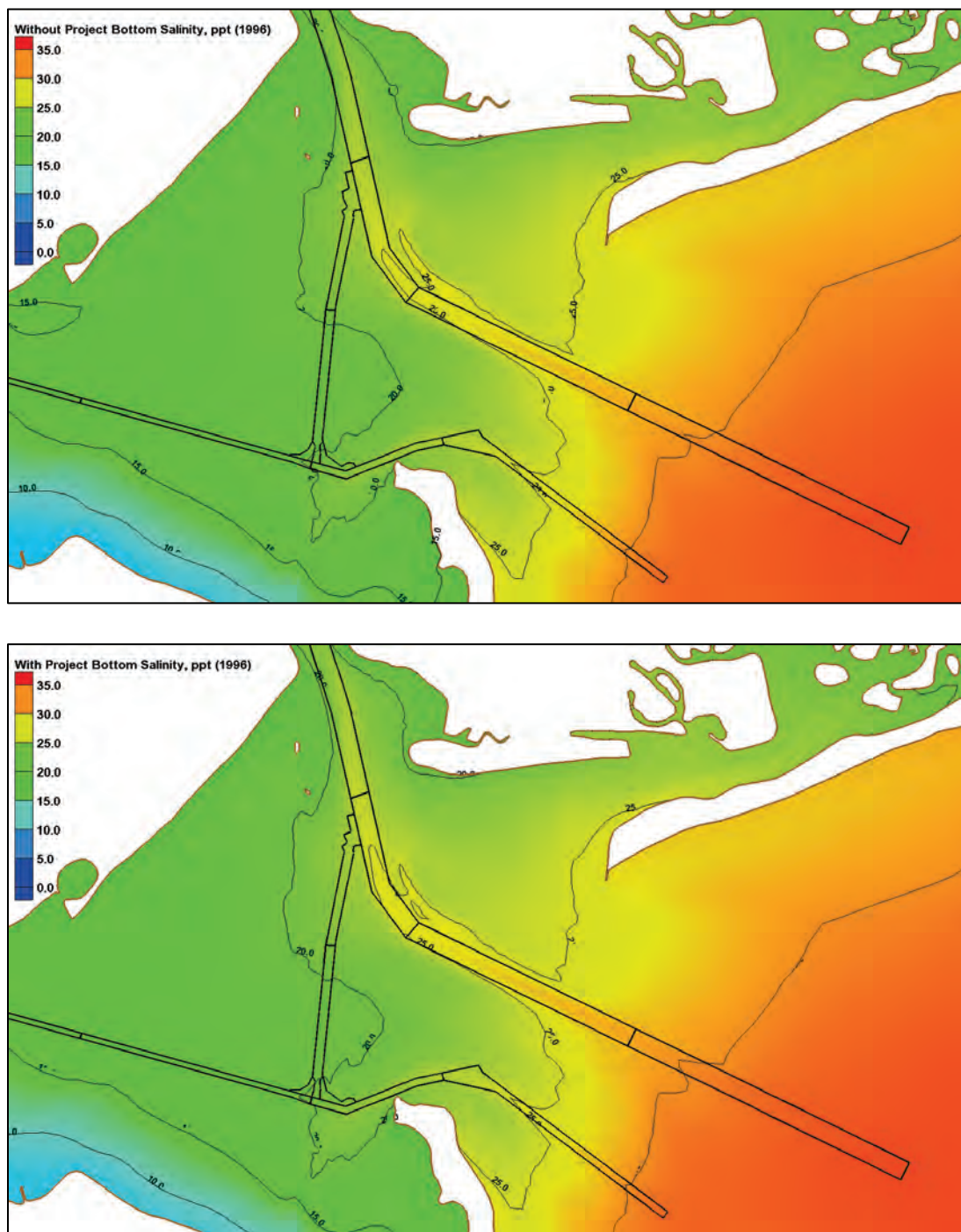


Figure 285. Without-project (top) and with-project (bottom) average fine sediment bottom concentrations, ppm (1996).

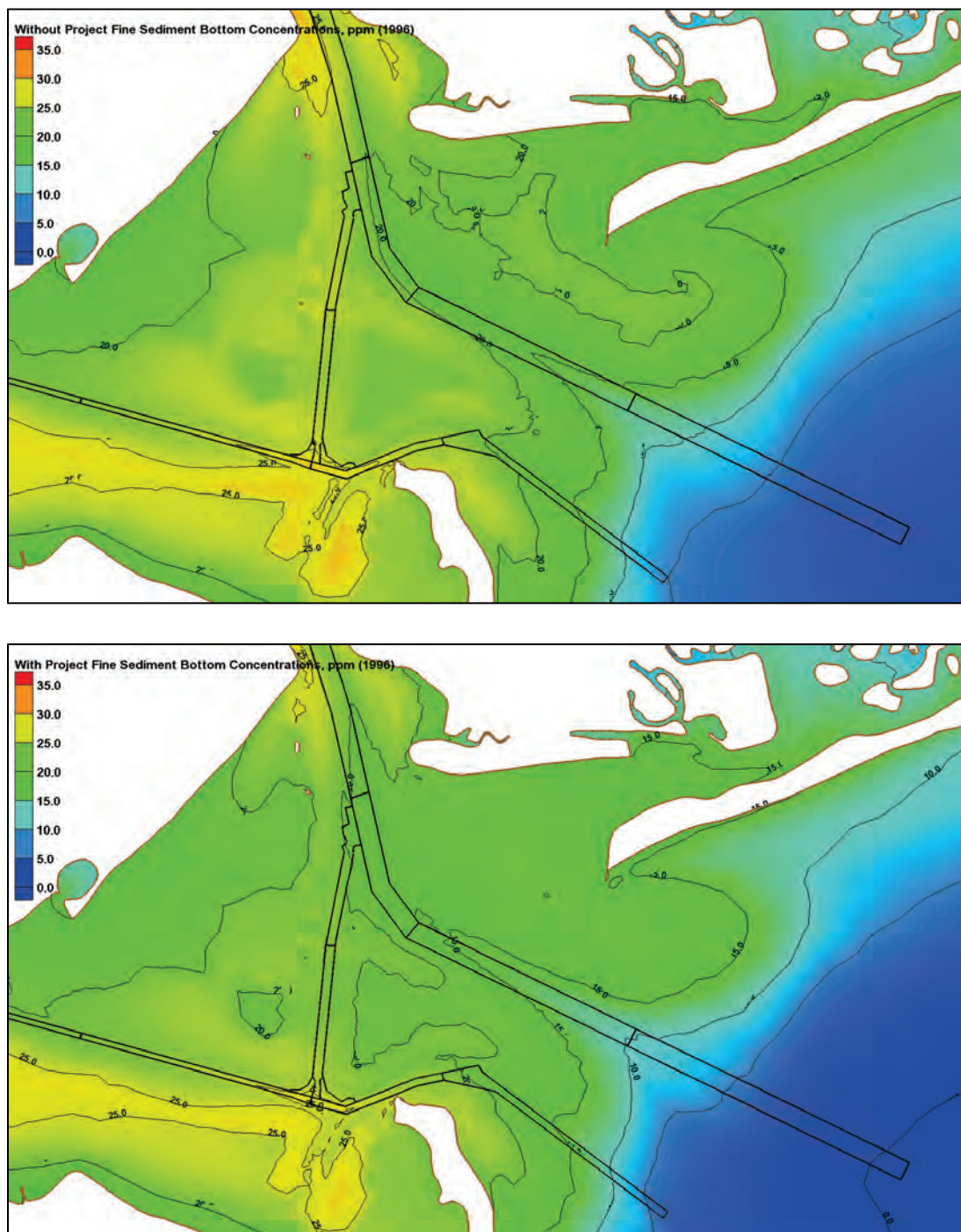




Figure 286. Without-project (top) and with-project (bottom) average sand bottom concentrations, ppm (1996).

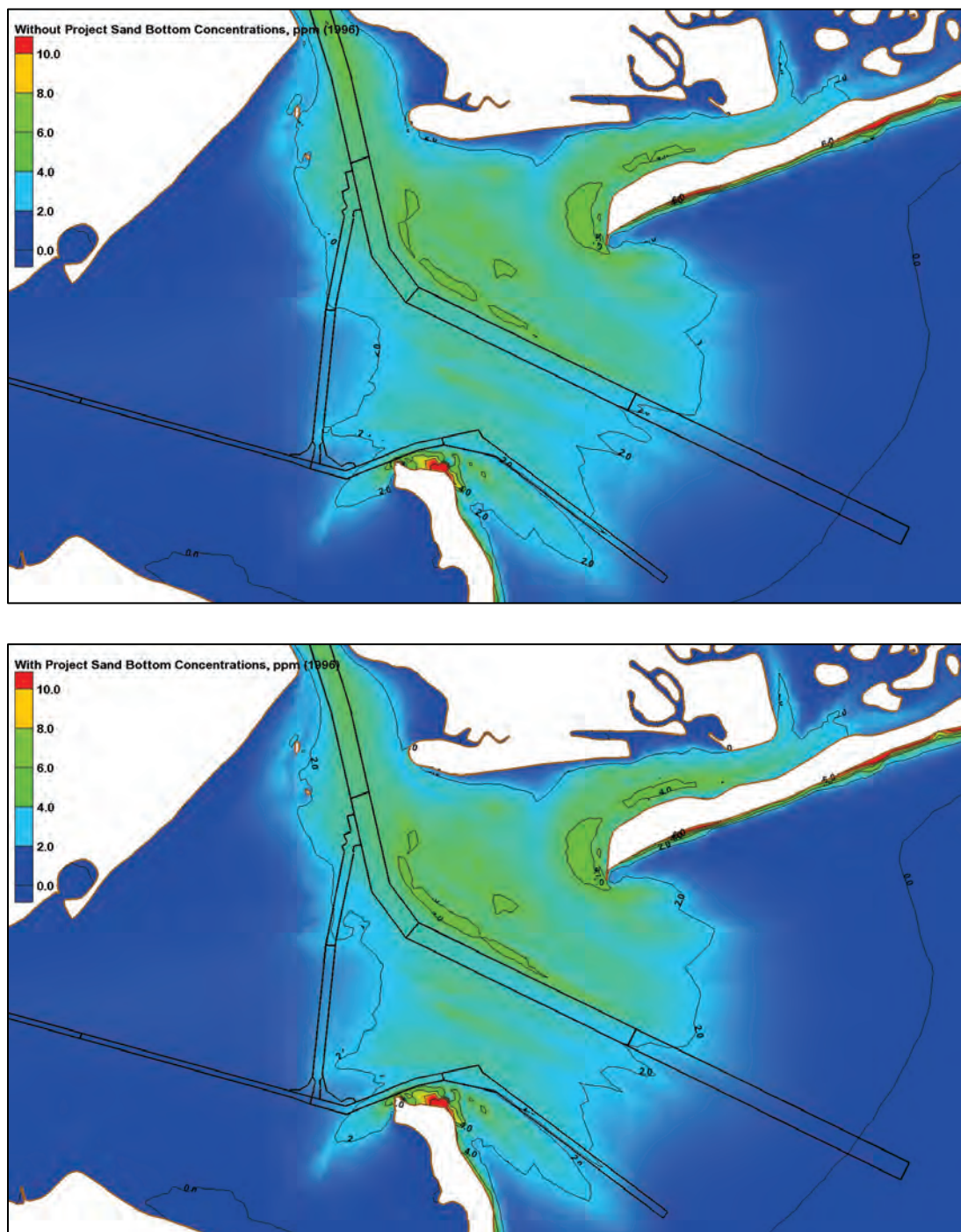


Figure 287. Without-project (top) and with-project (bottom) bed displacement, m (1996).

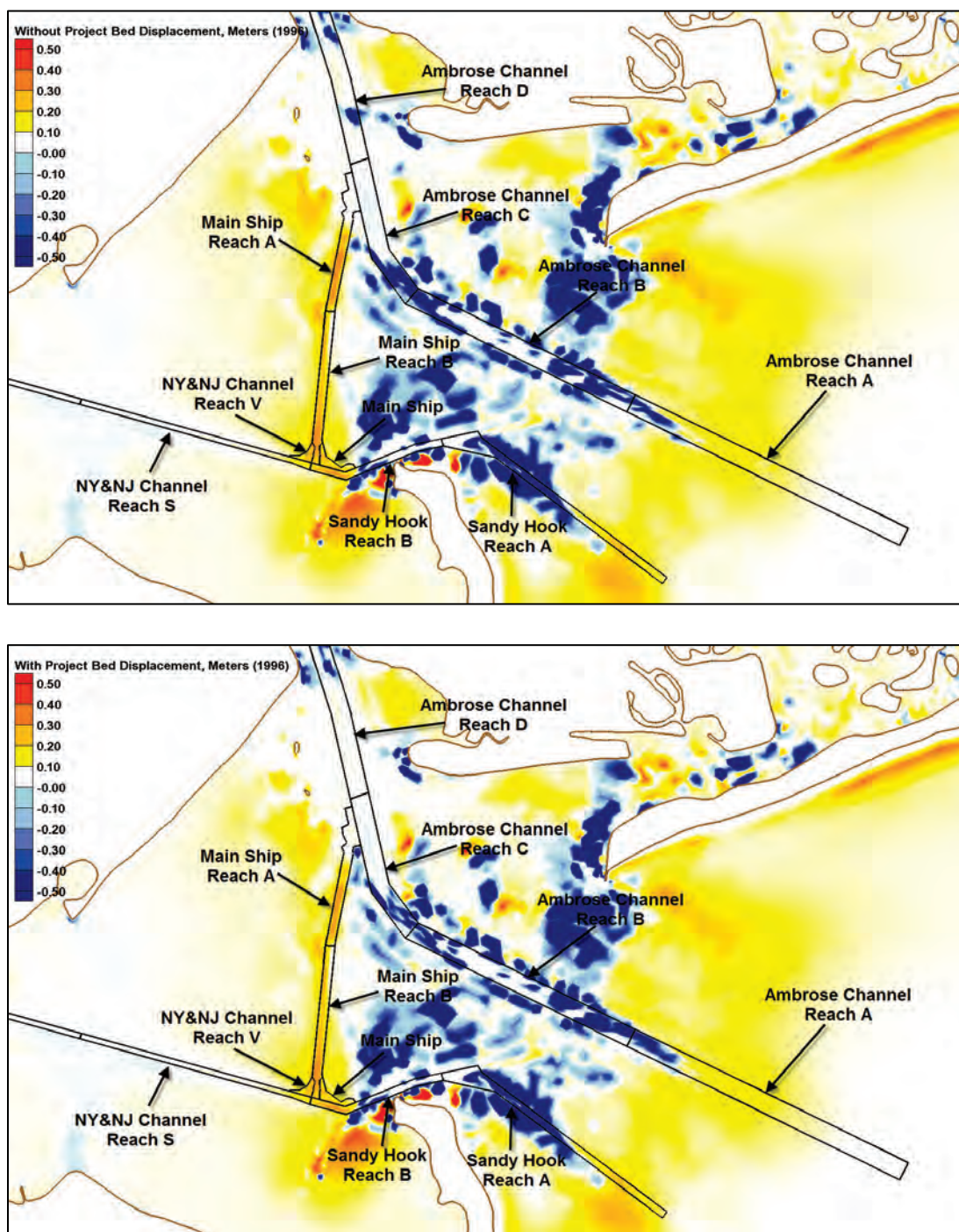




Figure 288. Without-project (top) and with-project (bottom) fine sediment accumulation,  $\text{kg}/\text{m}^2$  (1996).

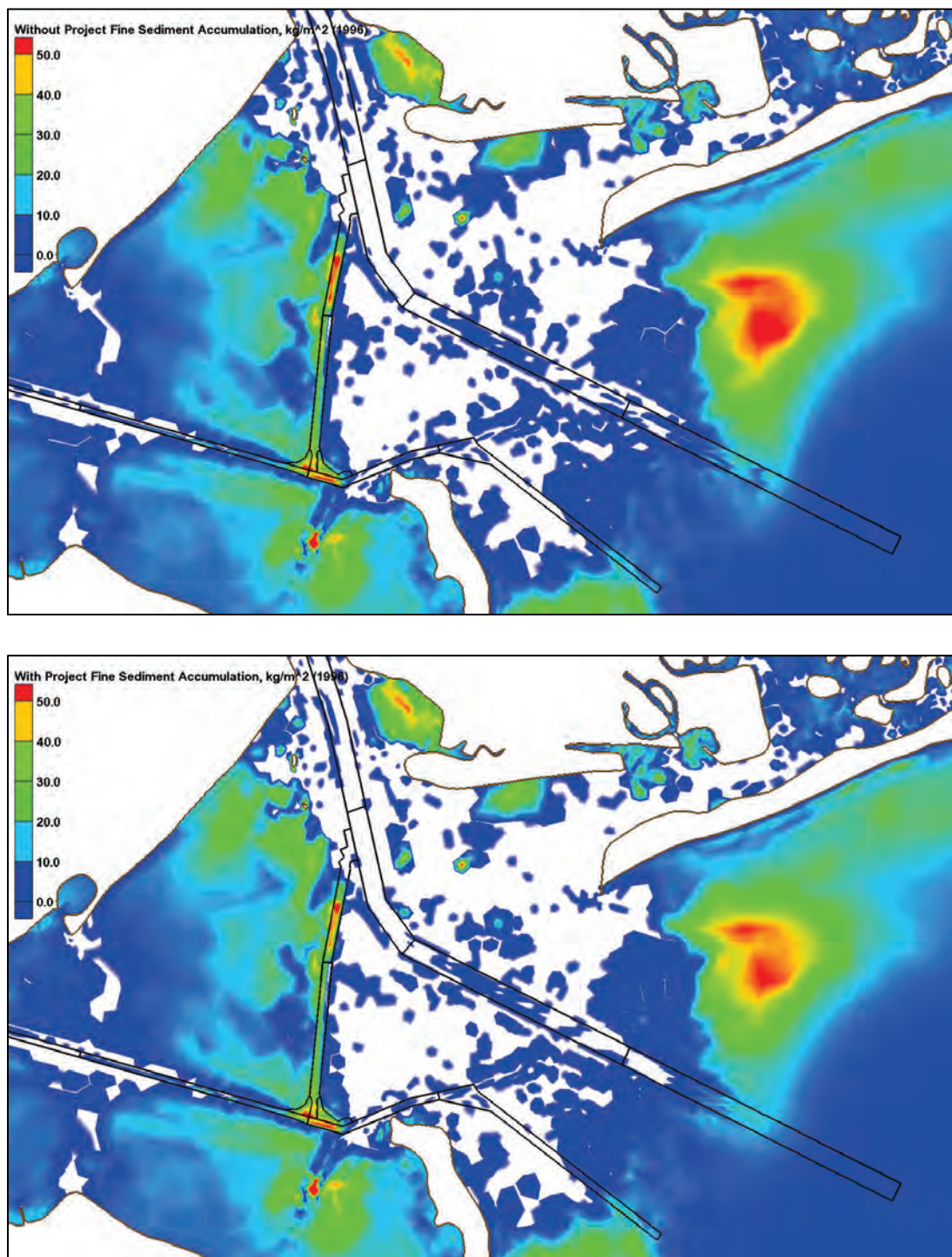




Figure 289. Without-project (top) and with-project (bottom) sand accumulation, kg/m<sup>2</sup> (1996).

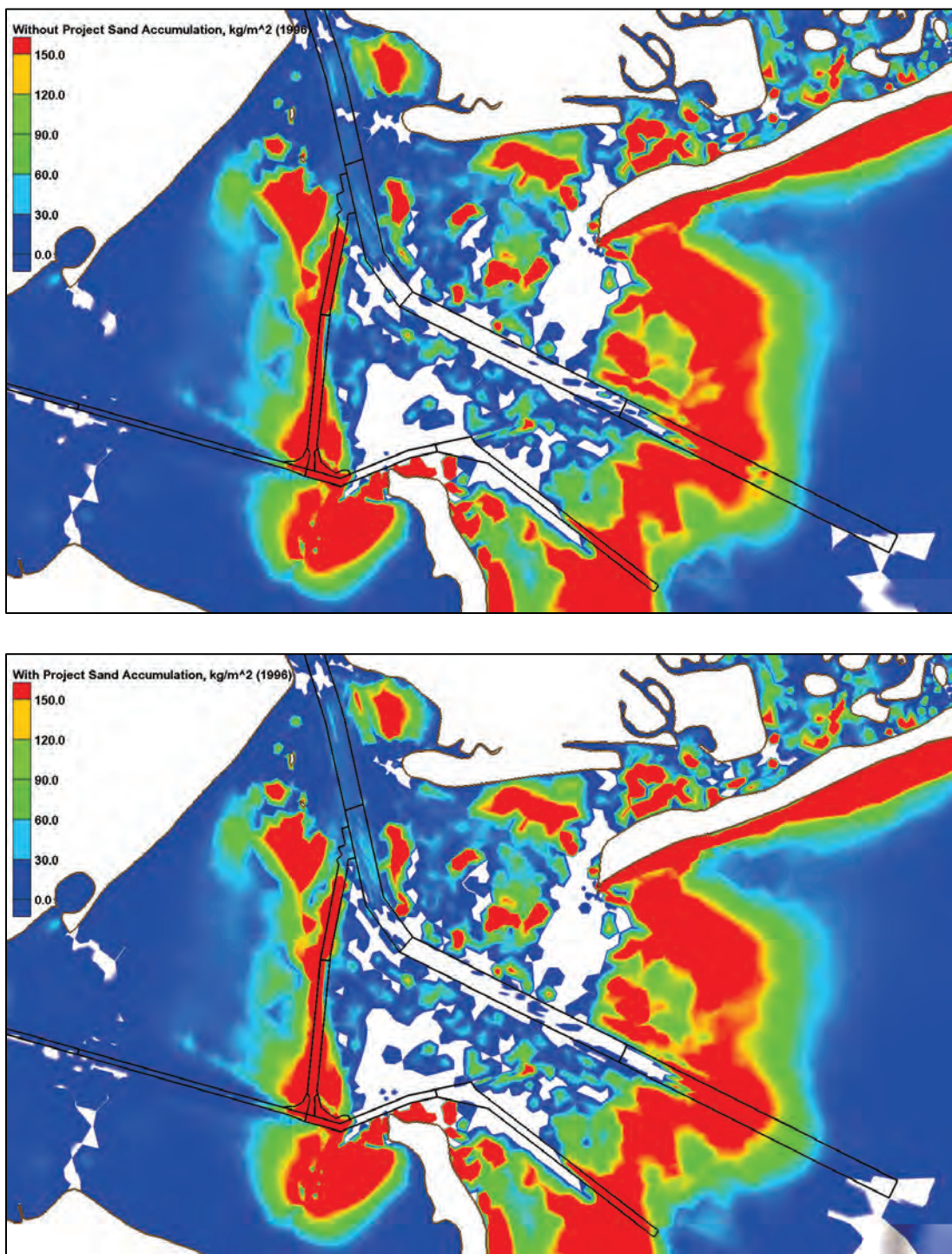


Figure 290. Dredge with-project/without-project percent differences (1996).

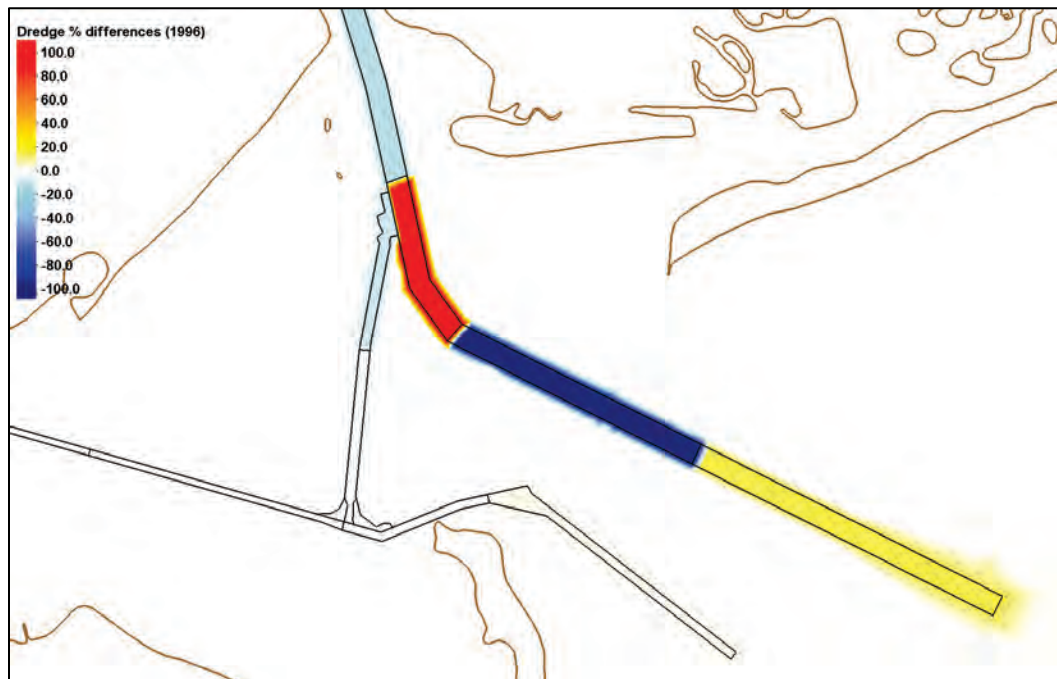


Table 31. Dredge volumes for Lower Bay (1996).

Depositional Volumes in Lower Bay, cy (1996)			
Reach	Without Project	With Project	With/Without Dredge Percentage
Ambrose Channel Reach A	302,560	344,359	114
Ambrose Channel Reach B	2,611	12	0
Ambrose Channel Reach C	4,012	8,774	219
Ambrose Channel Reach D	16,457	13,966	85
Main Ship	55,294	54,680	99
Main Ship Reach A	203,061	182,102	90
Main Ship Reach B	284,896	280,059	98
Sandy Hook Reach A	131,610	133,995	102
Sandy Hook Reach B	80,436	80,864	101
NY&NJ Channels Reach S	34,242	34,111	100
NY&NJ Channels Reach V	39,236	39,121	100

## Newark Bay, Kill van Kull, and Upper Bay results

Figure 291. Without-project (top) and with-project (bottom) average shear stresses, Pa (1996).

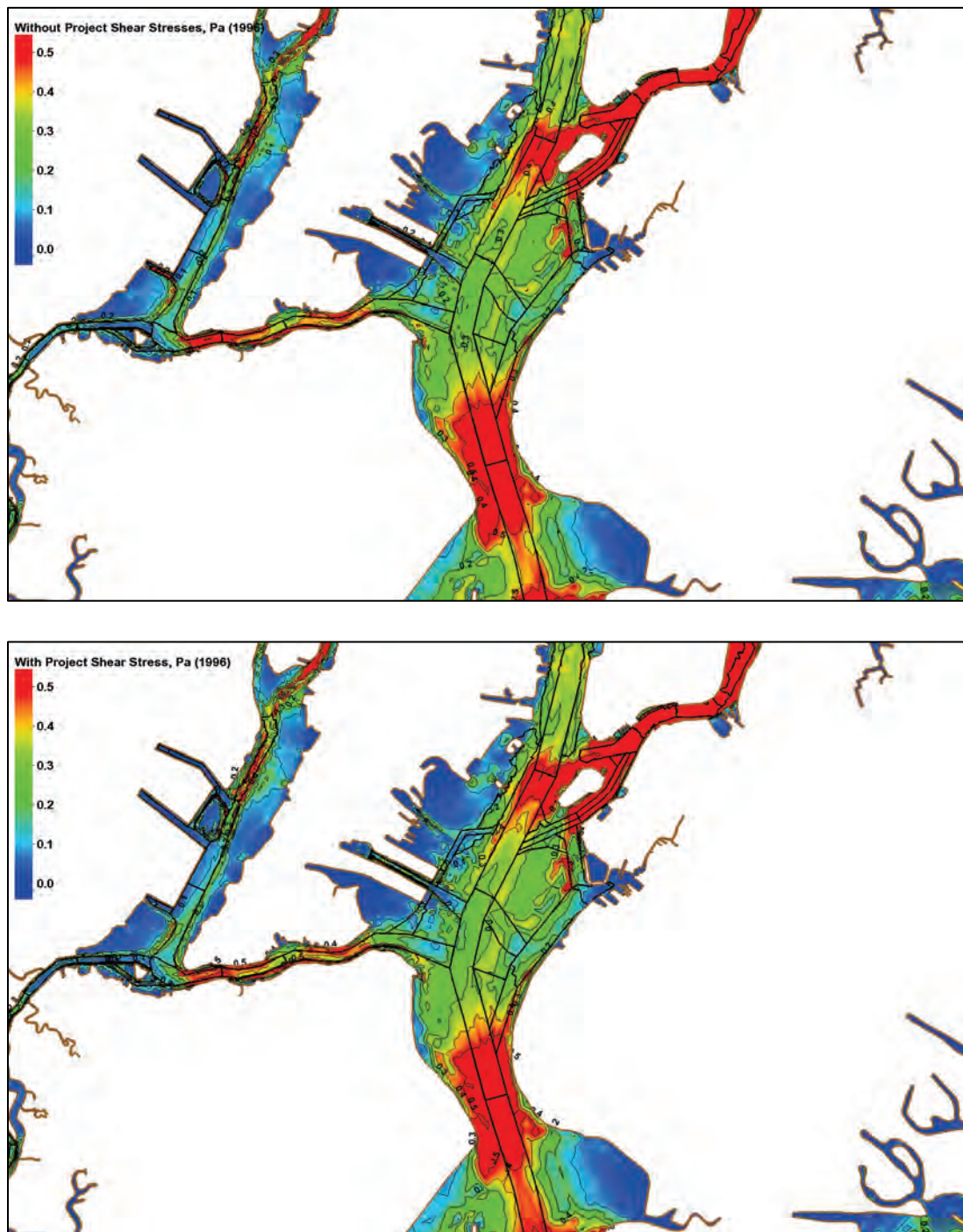




Figure 292. Without-project (top) and with-project (bottom) average bottom salinity, ppt (1996).

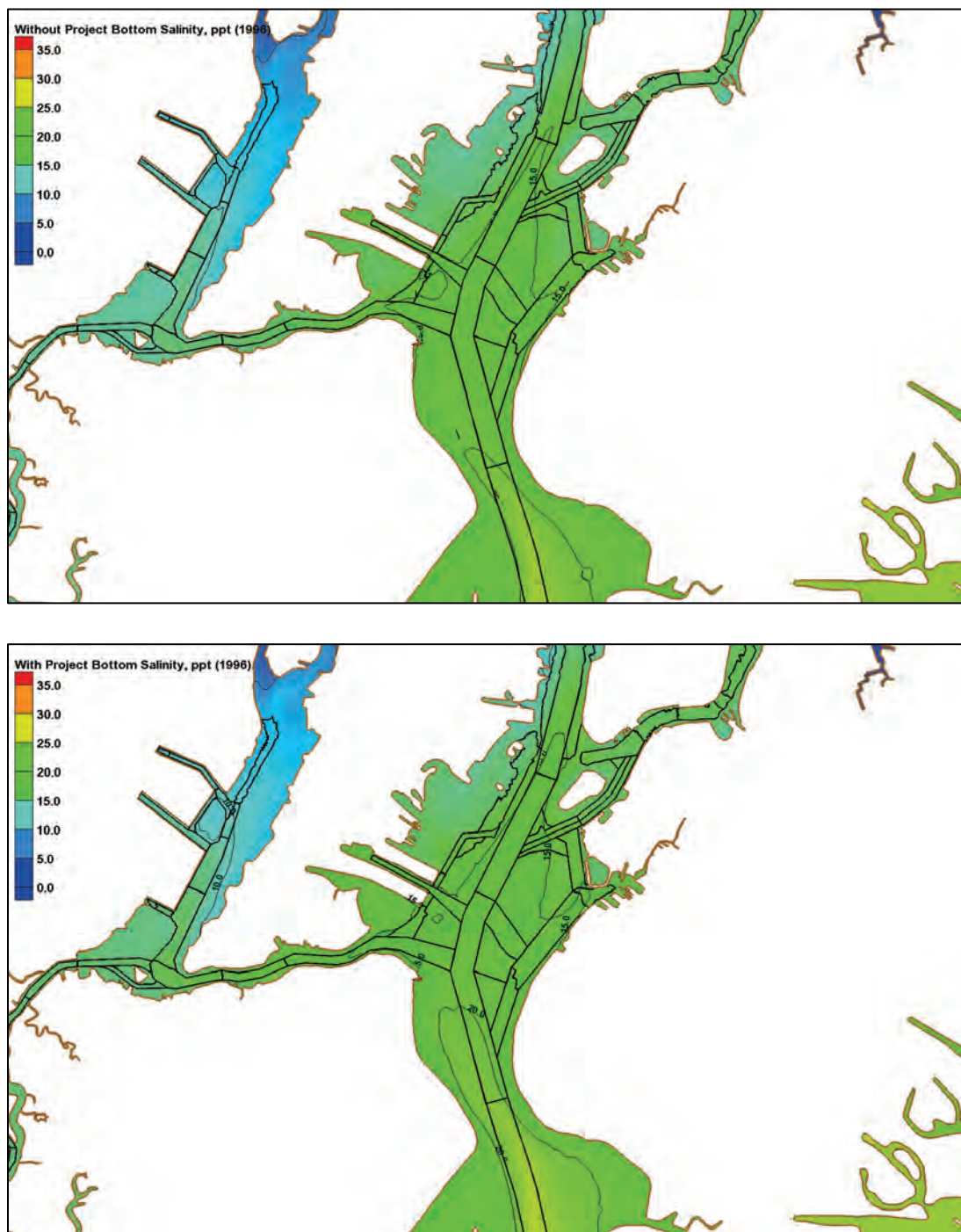


Figure 293. Without-project (top) and with-project (bottom) average fine sediment bottom concentrations, ppm (1996).

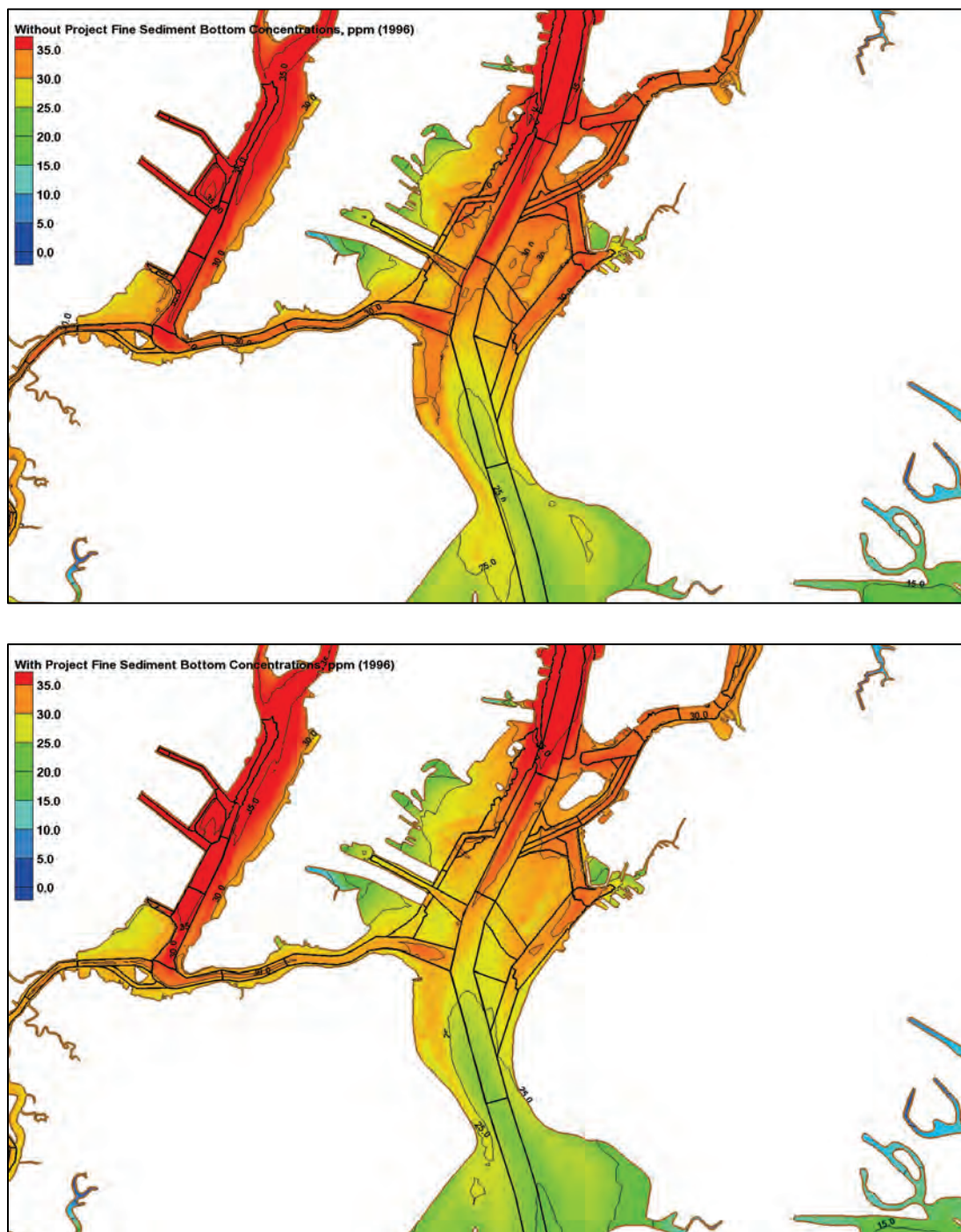




Figure 294. Without-project (top) and with-project (bottom) average sand bottom concentrations, ppm (1996).

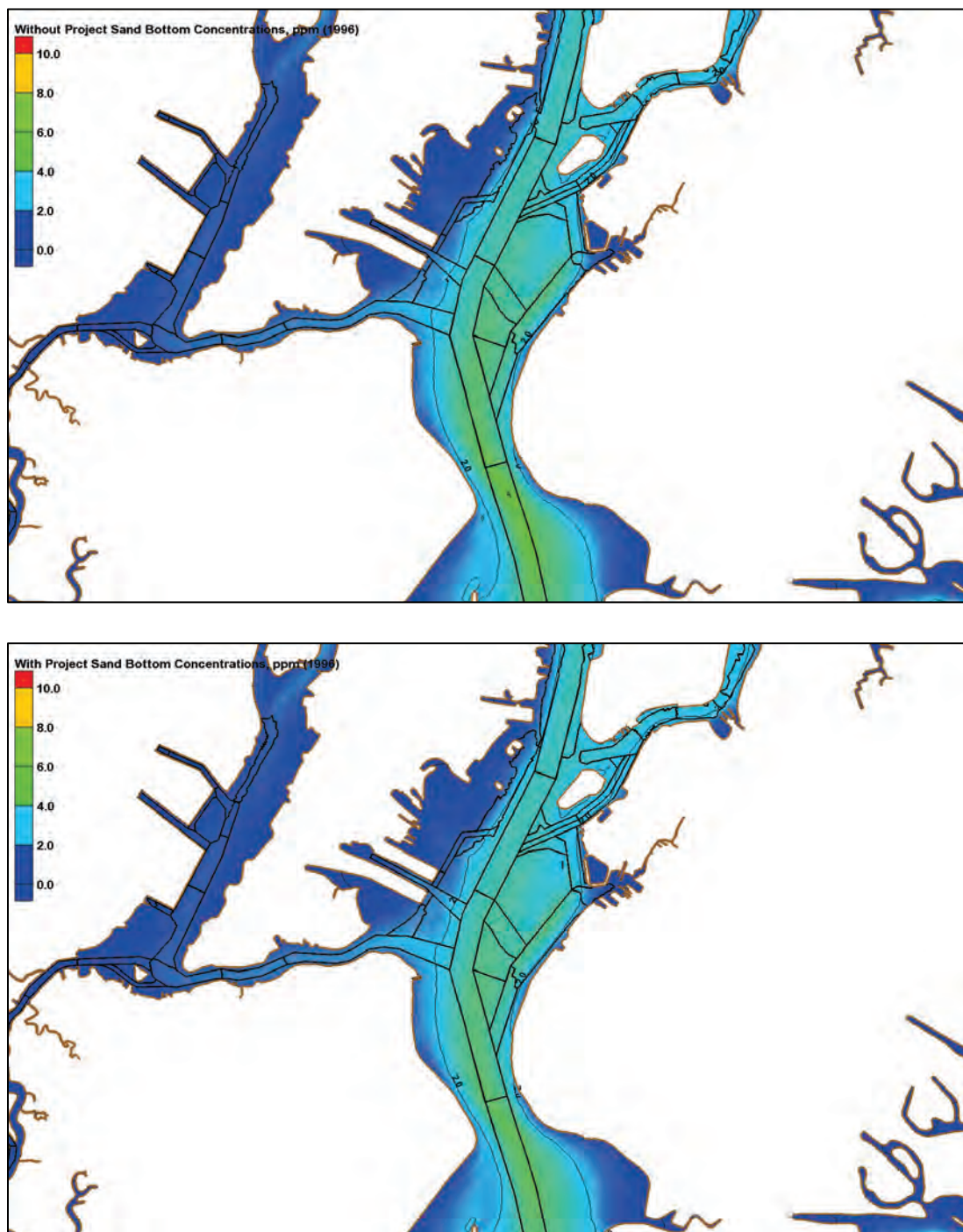


Figure 295. Without-project (top) and with-project (bottom) bed displacement, m (1996).

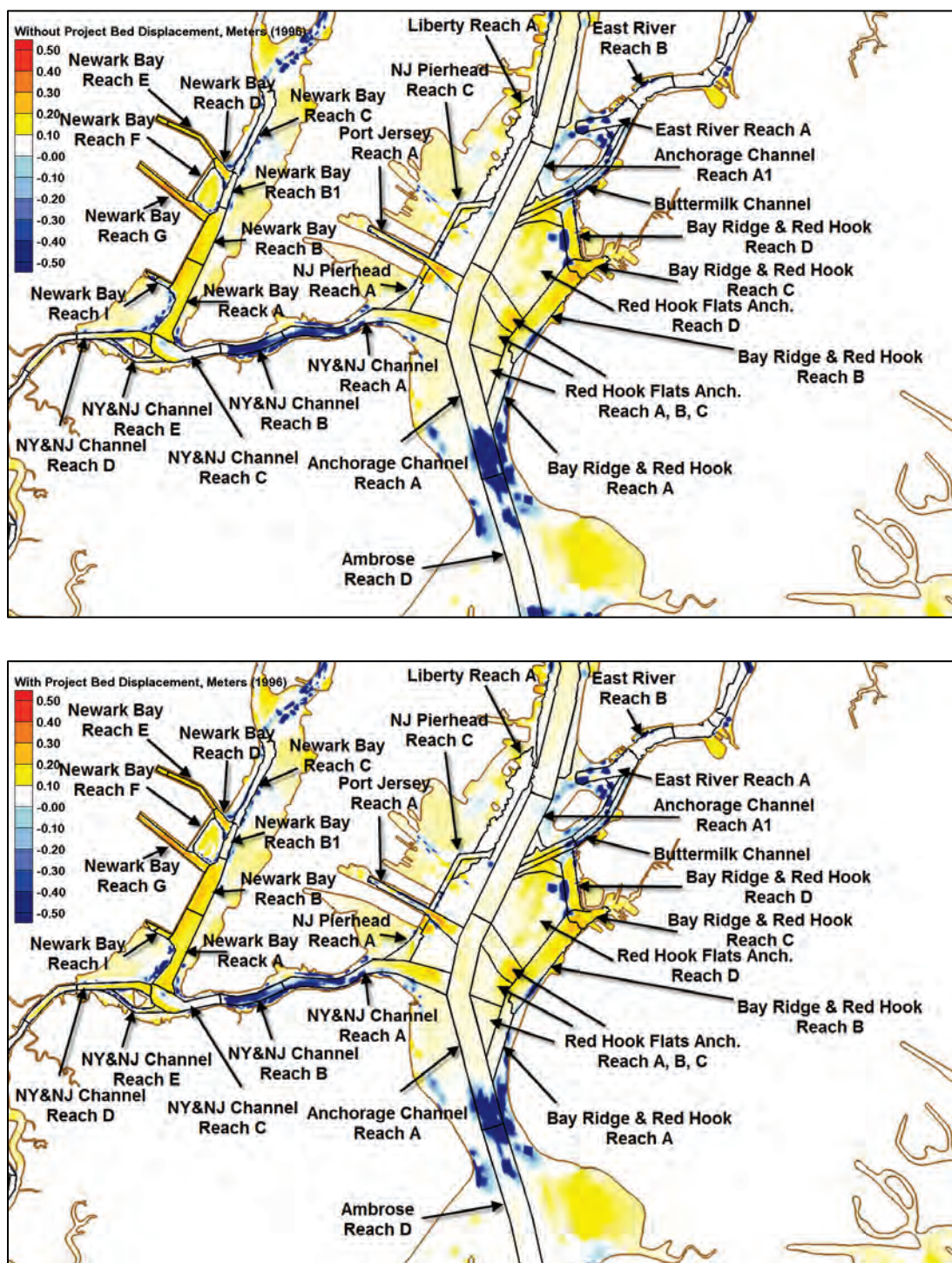




Figure 296. Without-project (top) and with-project (bottom) fine sediment accumulation,  $\text{kg}/\text{m}^2$  (1996).

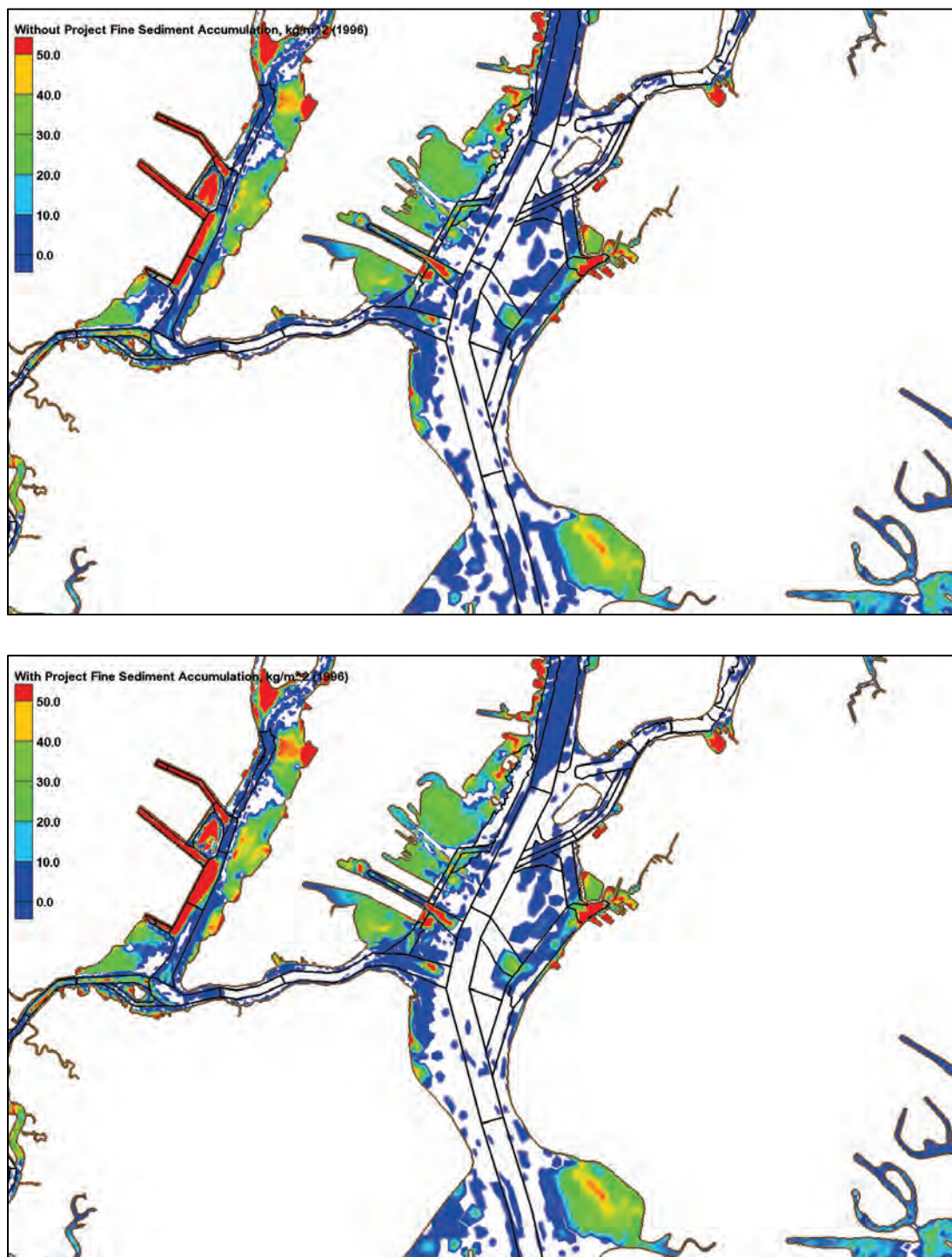


Figure 297. Without-project (top) and with-project (bottom) sand Accumulation,  $\text{kg/m}^2$  (1996).

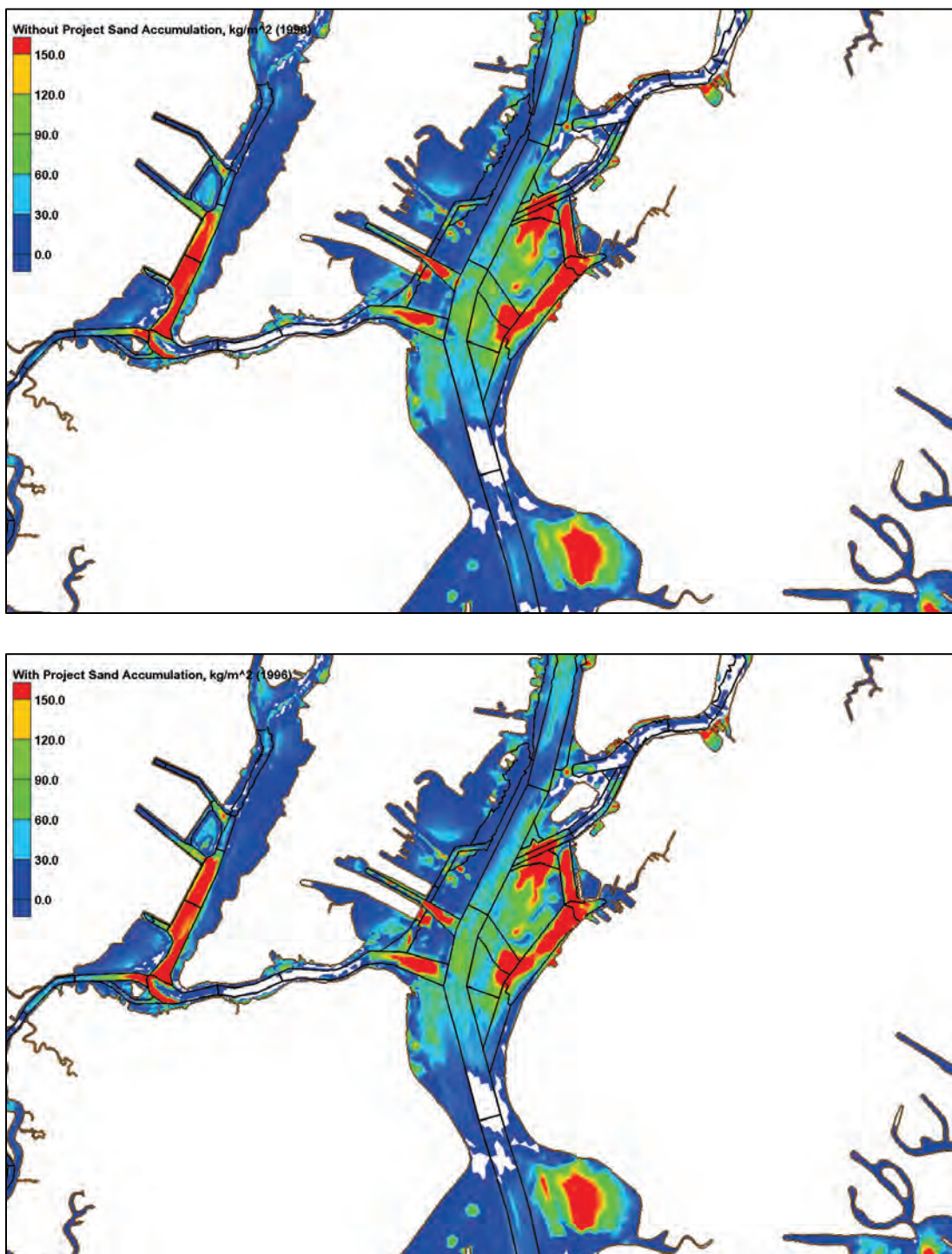
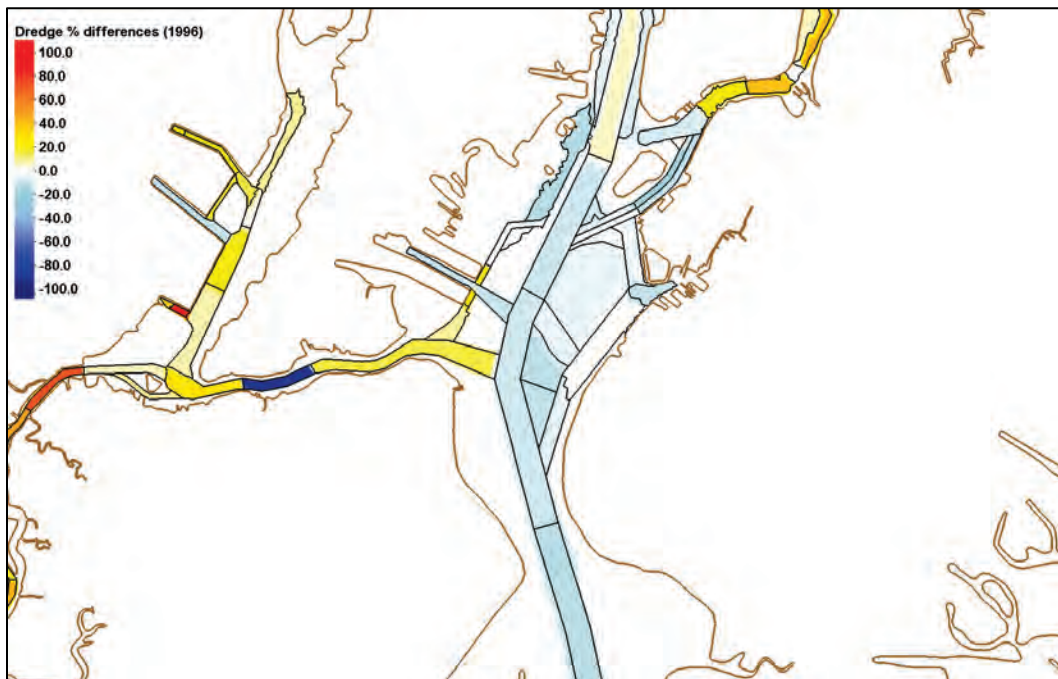


Figure 298. Dredge with-project/without-project percent differences (1996).





**Table 32. Dredge volumes in Newark Bay, Kill van Kull, and Upper Bay (1996).**

<b>Depositional Volumes in Newark Bay, Kill van Kull, and Upper Bay, cy (1996)</b>			
<b>Reach</b>	<b>Without Project</b>	<b>With Project</b>	<b>With/Without Dredge Percentage</b>
<b>Newark Bay</b>			
Newark Bay Reach A	136,294	145,056	106
Newark Bay Reach B	99,412	116,990	118
Newark Bay Reach B1	3,050	3,097	102
Newark Bay Reach C	3,410	3,688	108
Newark Bay Reach D	18,907	21,526	114
Newark Bay Reach E	33,334	39,977	120
Newark Bay Reach E1	4,863	6,329	130
Newark Bay Reach F	4,276	4,929	115
Newark Bay Reach G	92,711	80,746	87
Newark Bay Reach I	3,253	7,382	227
Newark Bay Reach I1	2,792	3,744	134
<b>Kill van Kull</b>			
NY&NJ Channels Reach A	65,632	74,980	114
NY&NJ Channels Reach B	333	25	8
NY&NJ Channels Reach C	28,266	36,447	129
<b>Upper Bay</b>			
Anchorage Channel Reach A	67,492	60,638	90
Anchorage Channel Reach A1	32,334	28,965	90
Anchorage Reach C1	8,384	8,288	99
Bay Ridge & Red Hook Reach A	15,468	14,493	94
Bay Ridge & Red Hook Reach B	165,306	166,247	101
Bay Ridge & Red Hook Reach C	62,815	55,605	89
Bay Ridge & Red Hook Reach D	71,013	68,688	97
Red Hook Flats Anch. Reach A	21,331	18,616	87
Red Hook Flats Anch. Reach B	45,732	39,074	85
Red Hook Flats Anch. Reach C	67,751	64,100	95
Red Hook Flats Anch. Reach D	138,264	131,511	95
Port Jersey Reach A	60,549	53,491	88
NJ Pierhead Ch. Reach A	12,760	13,741	108
NJ Pierhead Ch. Reach B	9,137	10,999	120
NJ Pierhead Reach C	10,930	10,886	100
Liberty Reach A	8,227	6,908	99

## Arthur Kill and Raritan Bay results

Figure 299. Without-project (top) and with-project (bottom) average shear stresses, Pa (1996).

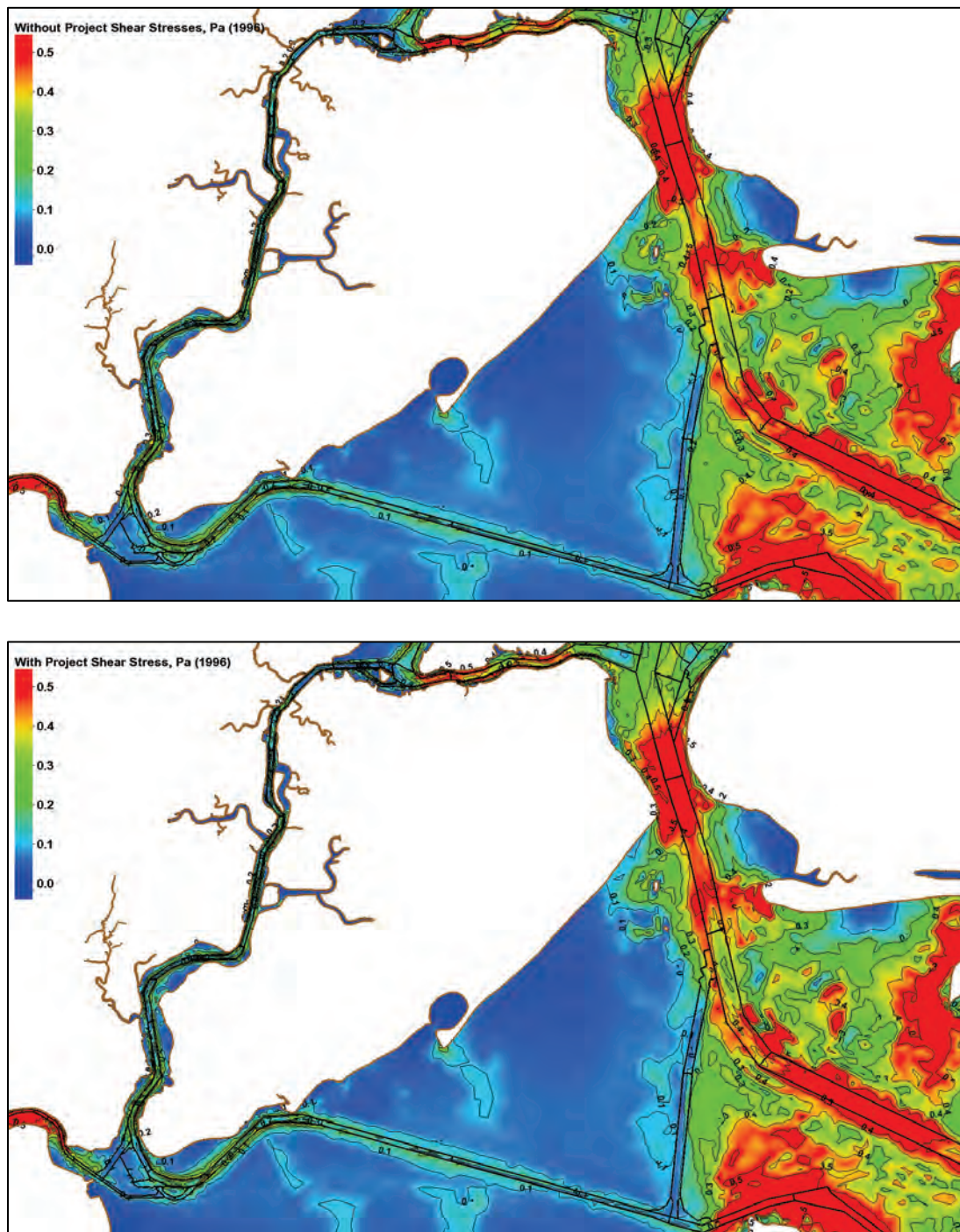


Figure 300. Without-project (top) and with-project (bottom) average bottom salinity, ppt (1996).

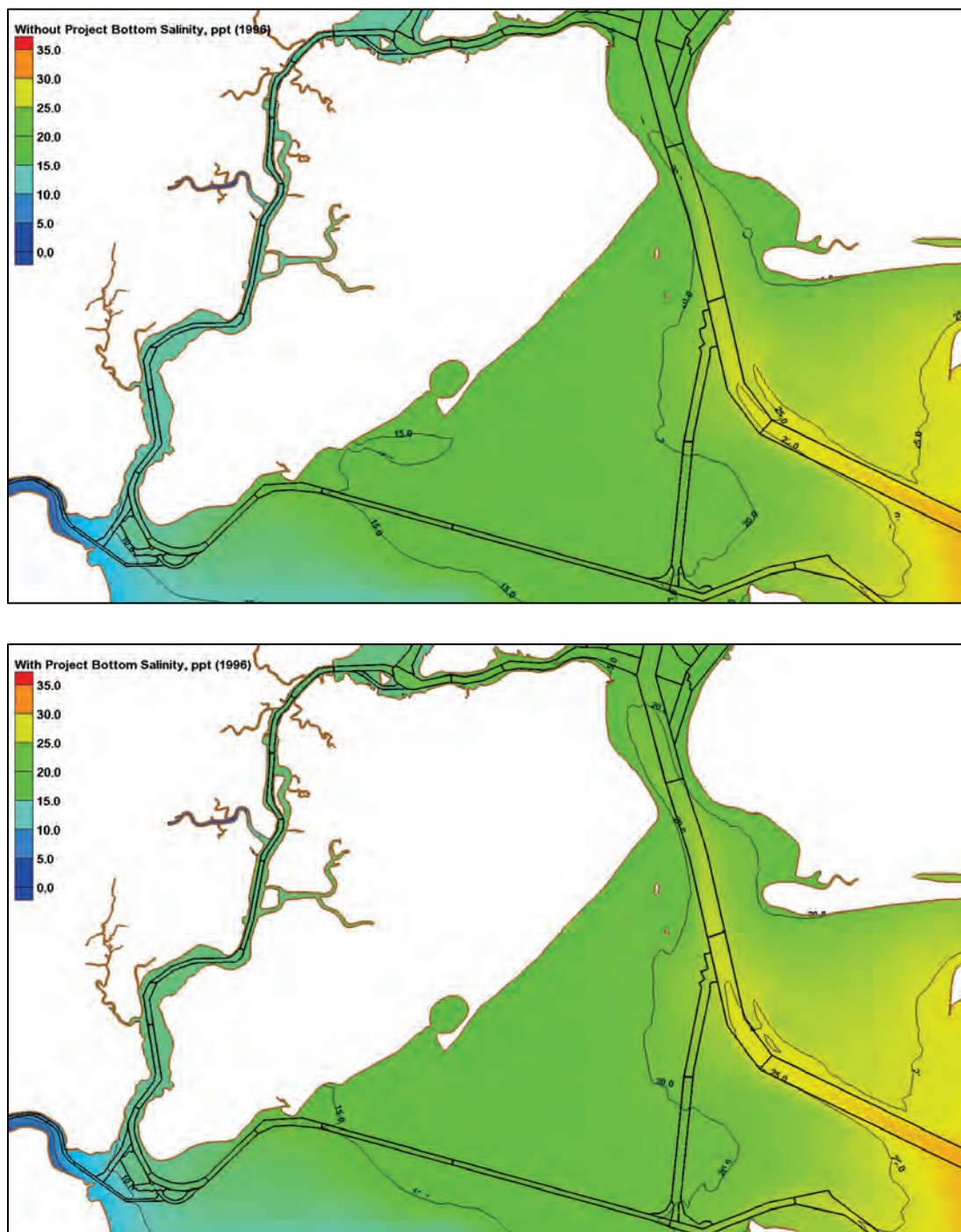




Figure 301. Without-project (top) and with-project (bottom) average fine sediment bottom concentrations, ppm (1996).

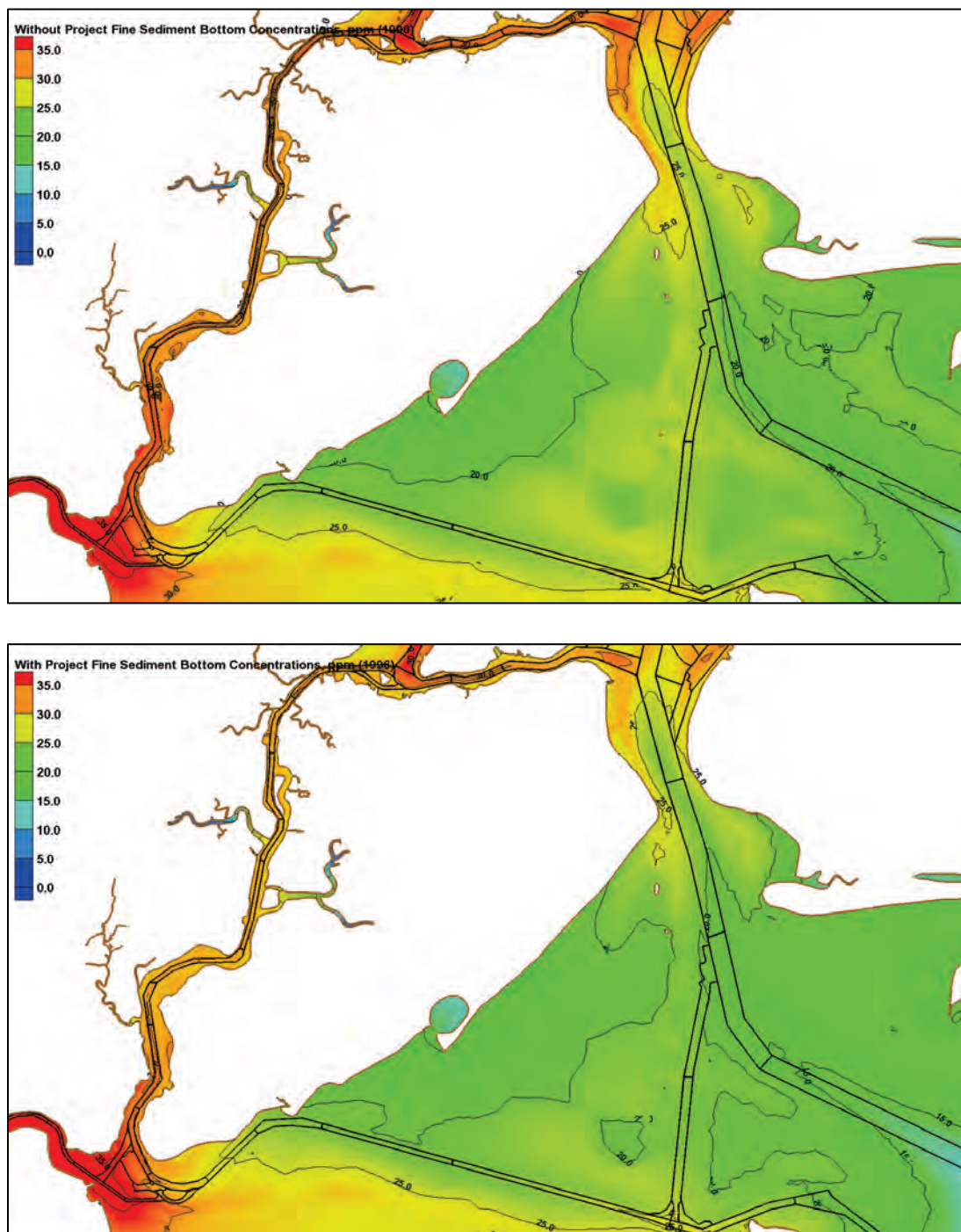


Figure 302. Without-project (top) and with-project (bottom) average sand bottom concentrations, ppm (1996).

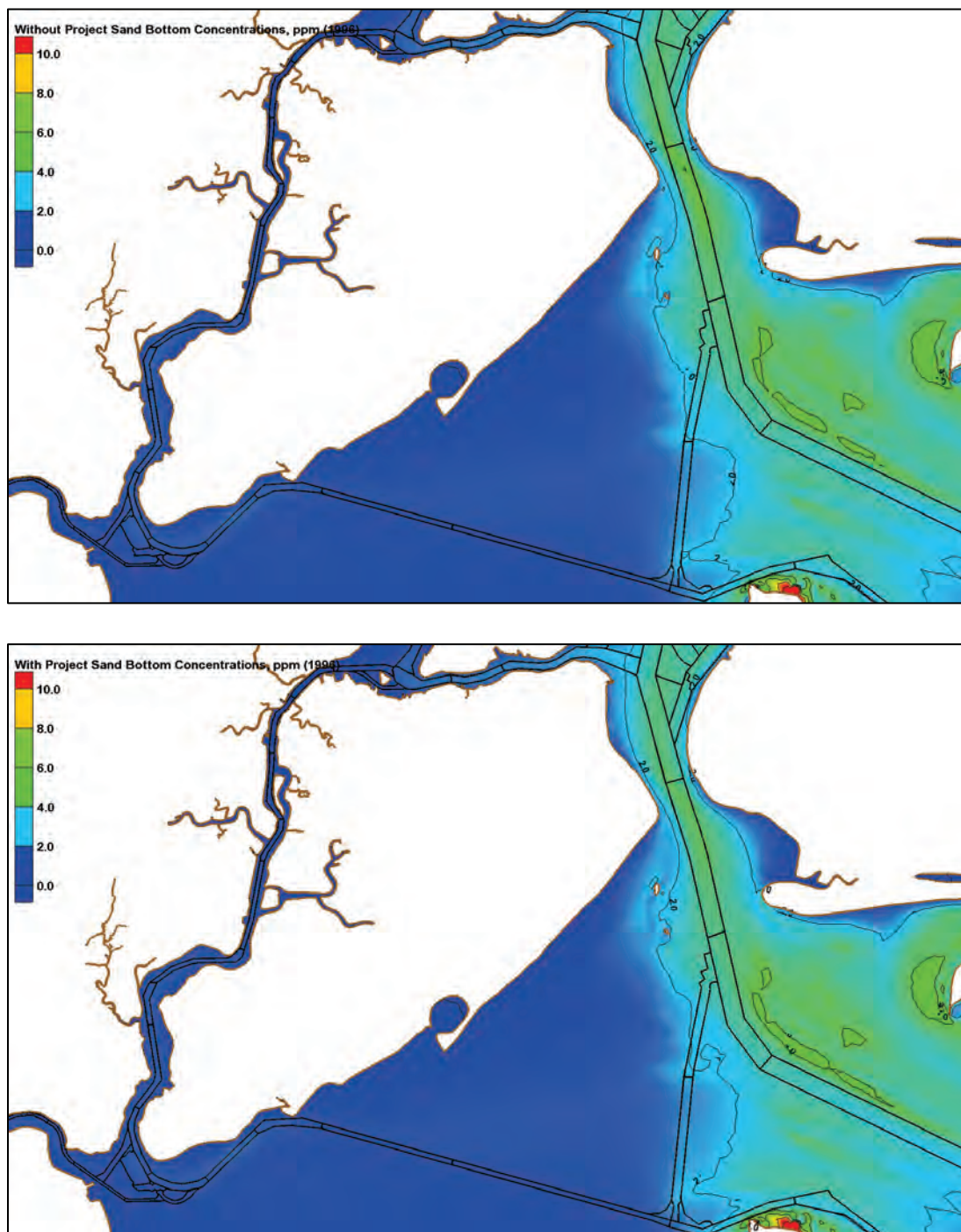




Figure 303. Without-project (top) and with-project (bottom) bed displacement, m (1996).

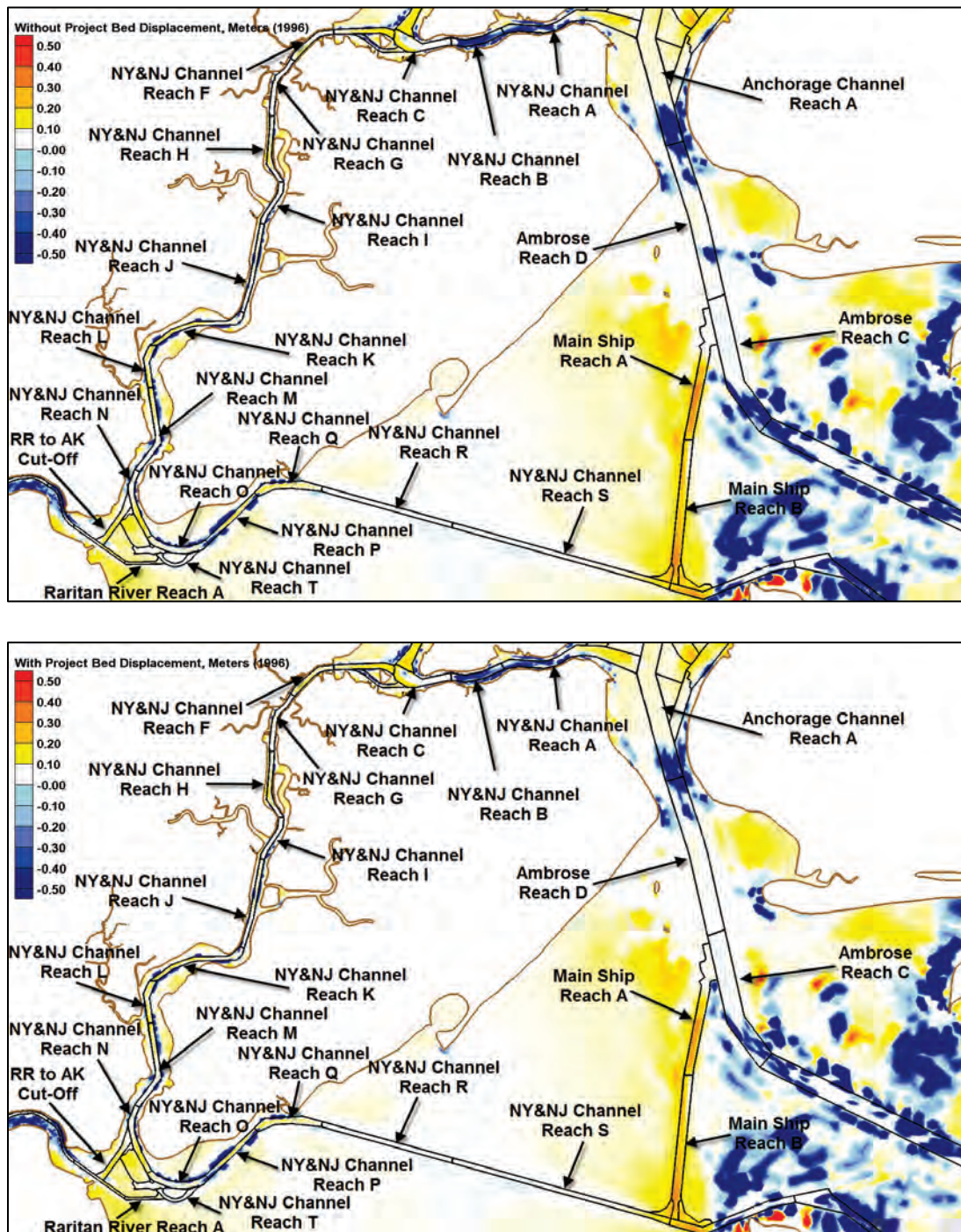


Figure 304. Without-project (top) and with-project (bottom) fine sediment accumulation,  $\text{kg}/\text{m}^2$  (1996).

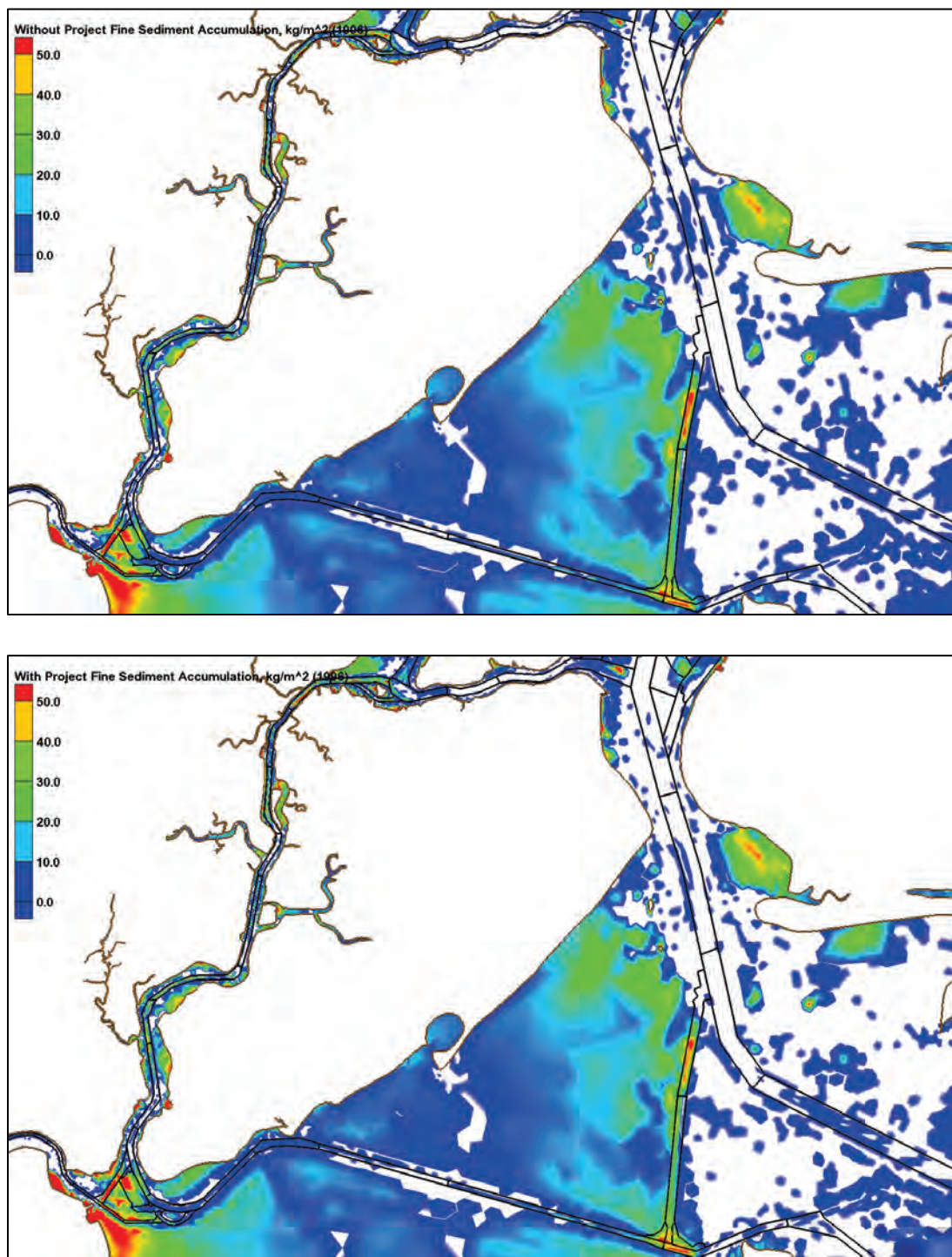




Figure 305. Without-project (top) and with-project (bottom) sand Accumulation,  $\text{kg/m}^2$  (1996).

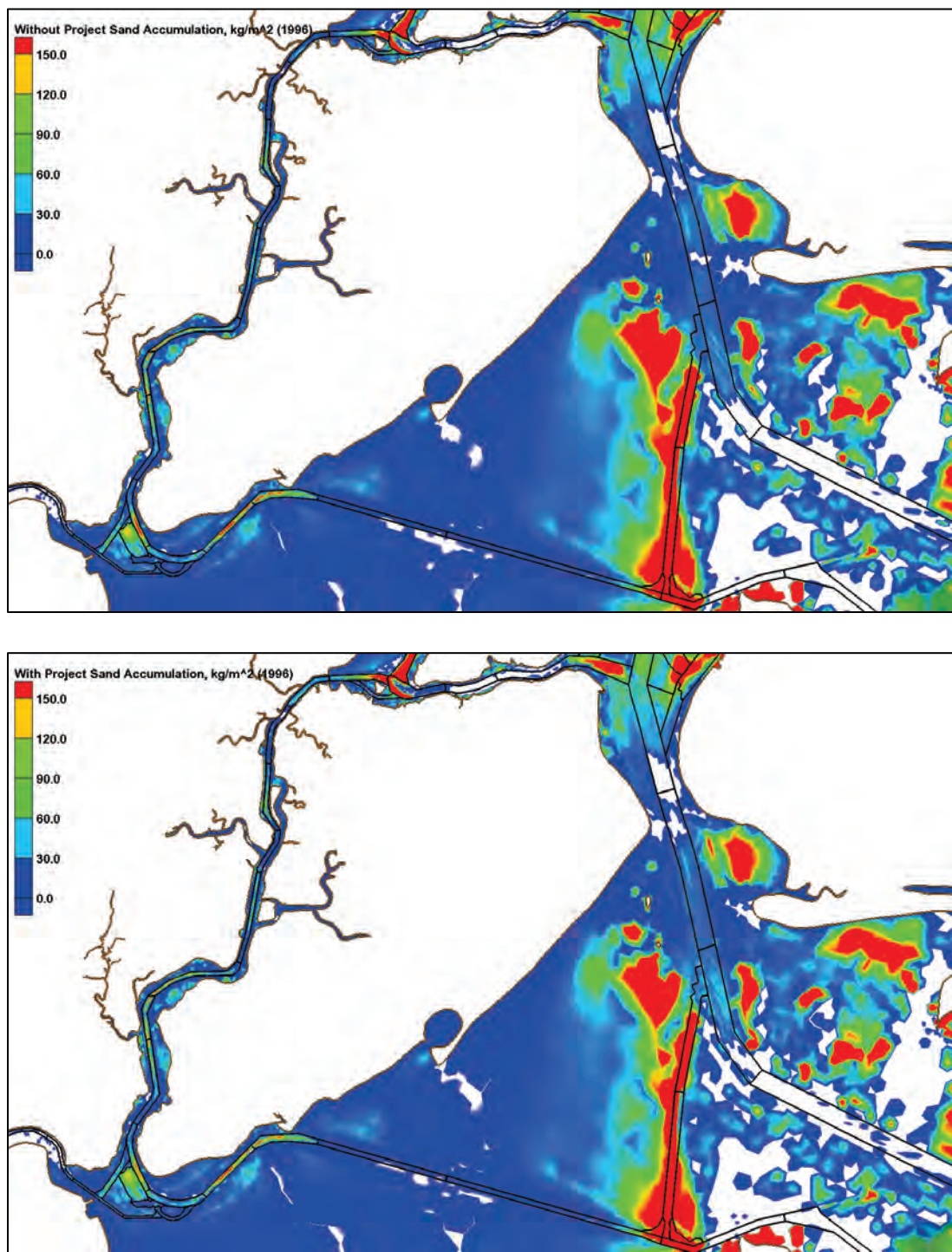


Figure 306. Dredge with-project/without-project percent differences (1996).

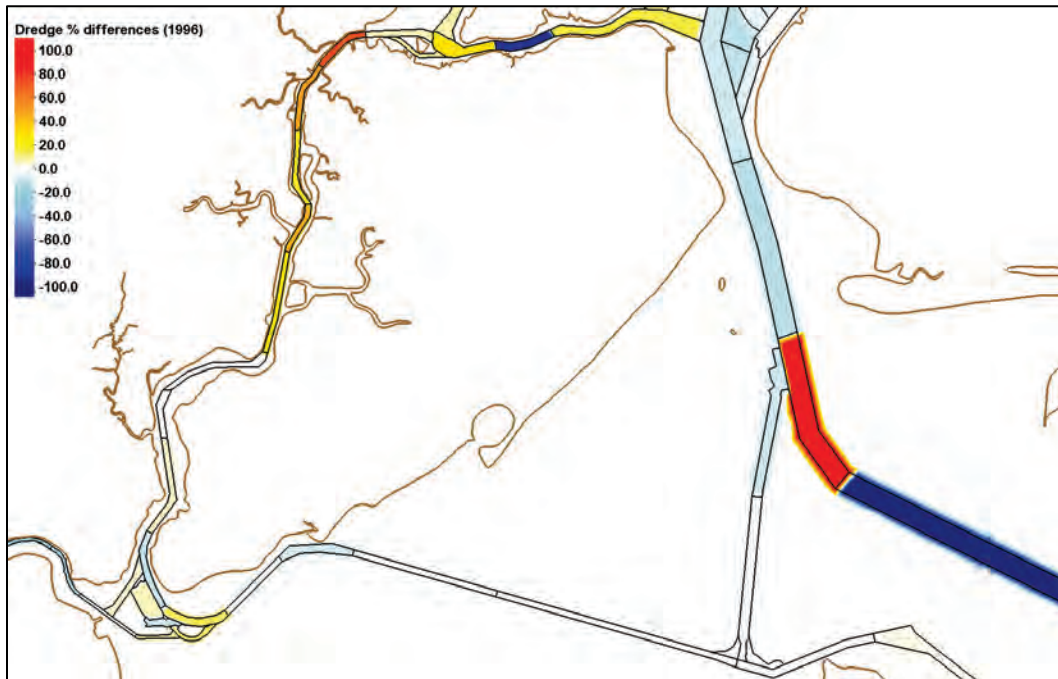


Table 33. Dredge volumes for Arthur Kill and Raritan Bay (1996).

Depositional Volumes in Arthur Kill and Raritan Bay, cy (1996)			
Reach	Without Project	With Project	With/Without Dredge Percentage
<b>Arthur Kill</b>			
NY&NJ Channels Reach D	29,861	31,464	105
NY&NJ Channels Reach E	4,849	5,254	108
NY&NJ Channels Reach F	6,318	10,796	171
NY&NJ Channels Reach G	1,233	1,822	148
NY&NJ Channels Reach H	7,968	9,236	116
NY&NJ Channels Reach I	654	932	143
NY&NJ Channels Reach J	4,340	5,390	124
NY&NJ Channels Reach K	17,380	17,483	101
NY&NJ Channels Reach L	13,453	13,539	101
NY&NJ Channels Reach M	11,776	12,305	104
NY&NJ Channels Reach N	20,672	18,124	88
<b>Raritan Bay</b>			
NY&NJ Channels Reach O	7,308	8,214	112
NY&NJ Channels Reach P	20,621	19,739	96
NY&NJ Channels Reach Q	22,607	20,663	91
NY&NJ Channels Reach R	392	392	100
NY&NJ Channels Reach T	1,452	1,618	111
RR to AK Cut-Off Reach A	19,628	20,478	104
Raritan River Reach A	4,206	4,525	108
Raritan River Reach B	7,098	7,184	101
Raritan River Reach C	617	511	83
Raritan River Reach D	105	82	78



## Appendix F: Results for 2011

### Lower Bay results

Figure 307. Without-project (top) and with-project (bottom) average shear stresses, Pa (2011).

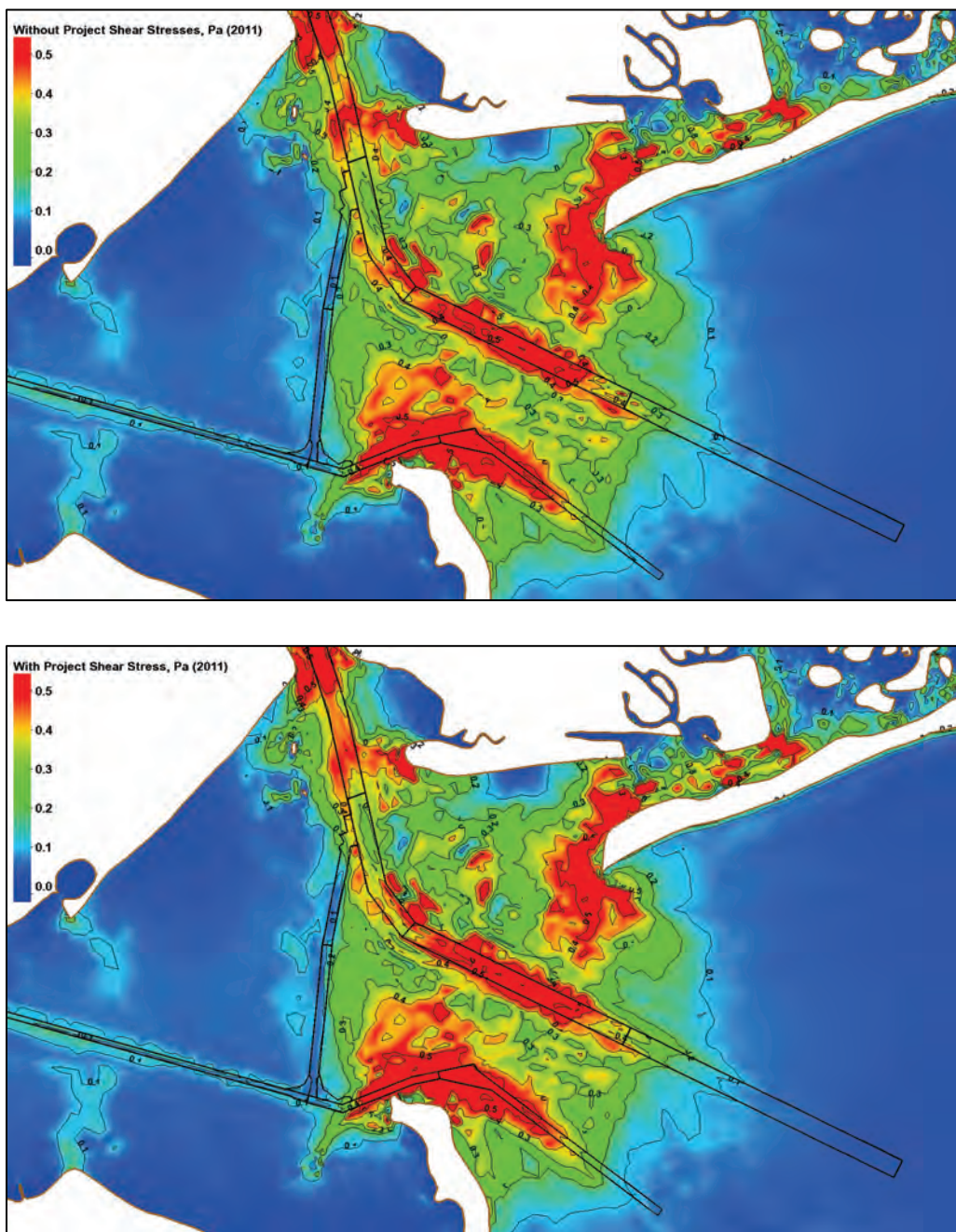


Figure 308. Without-project (top) and with-project (bottom) average bottom salinity, ppt (2011).

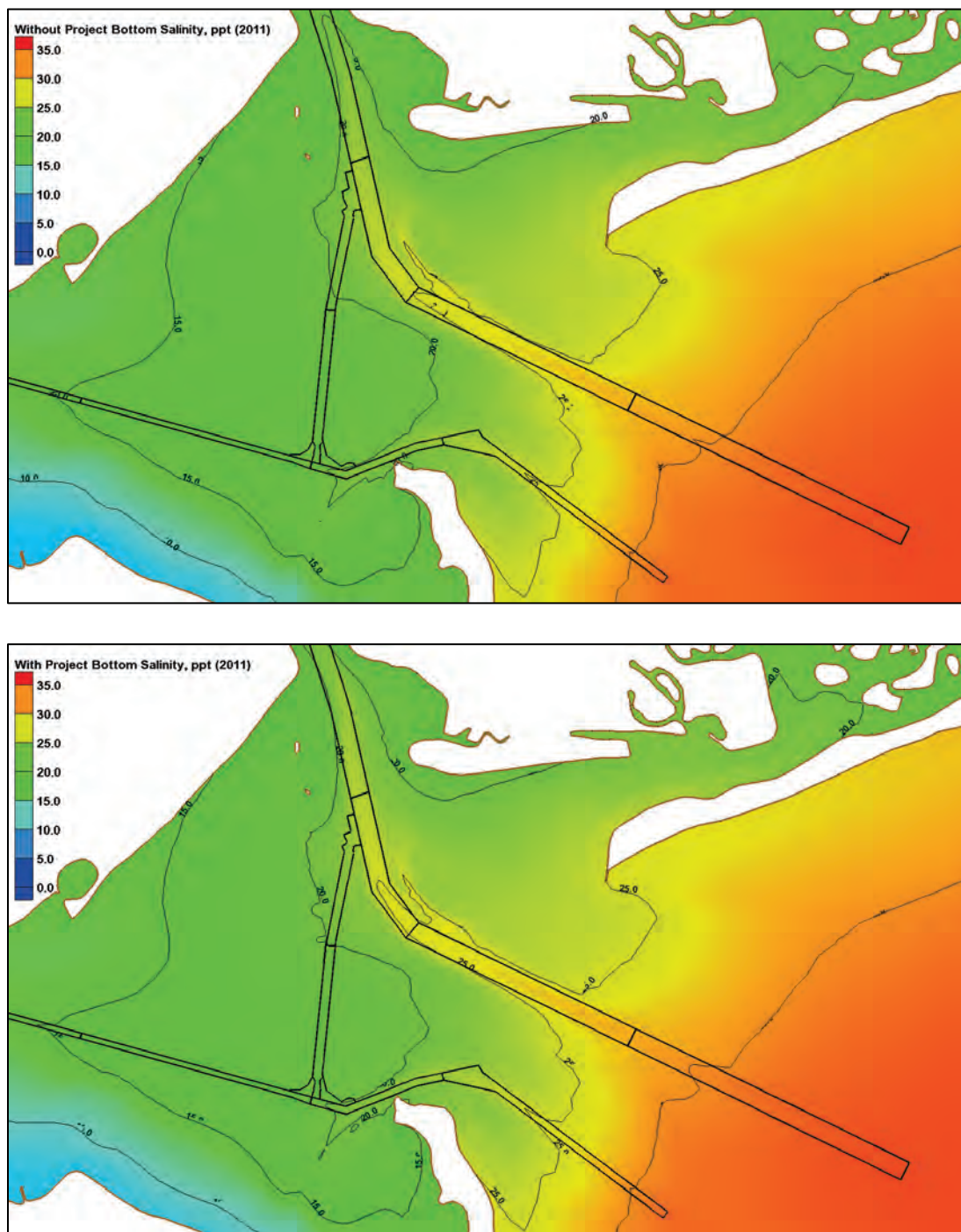




Figure 309. Without-project (top) and with-project (bottom) average fine sediment bottom concentrations, ppm (2011).

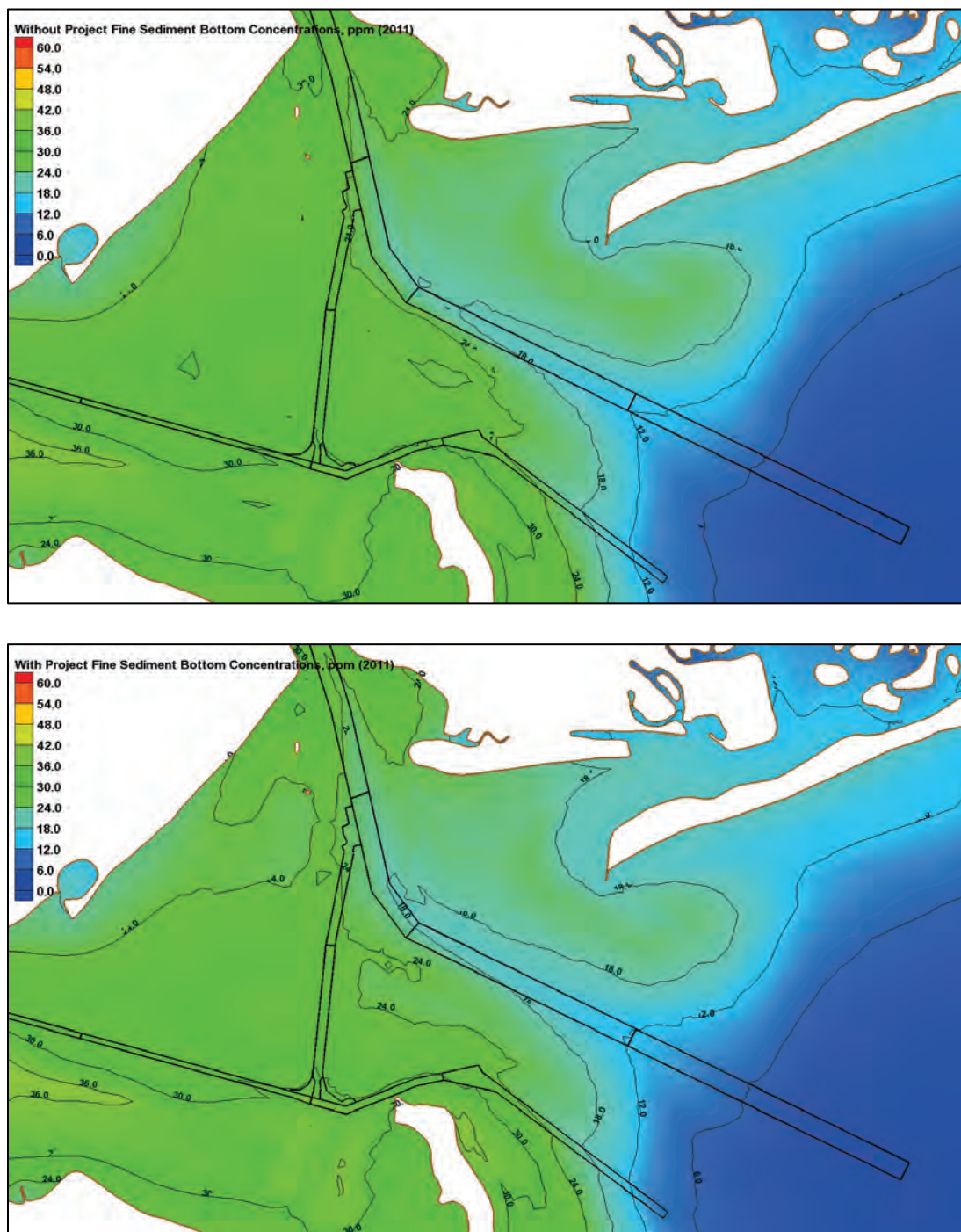


Figure 310. Without-project (top) and with-project (bottom) average sand bottom concentrations, ppm (2011).

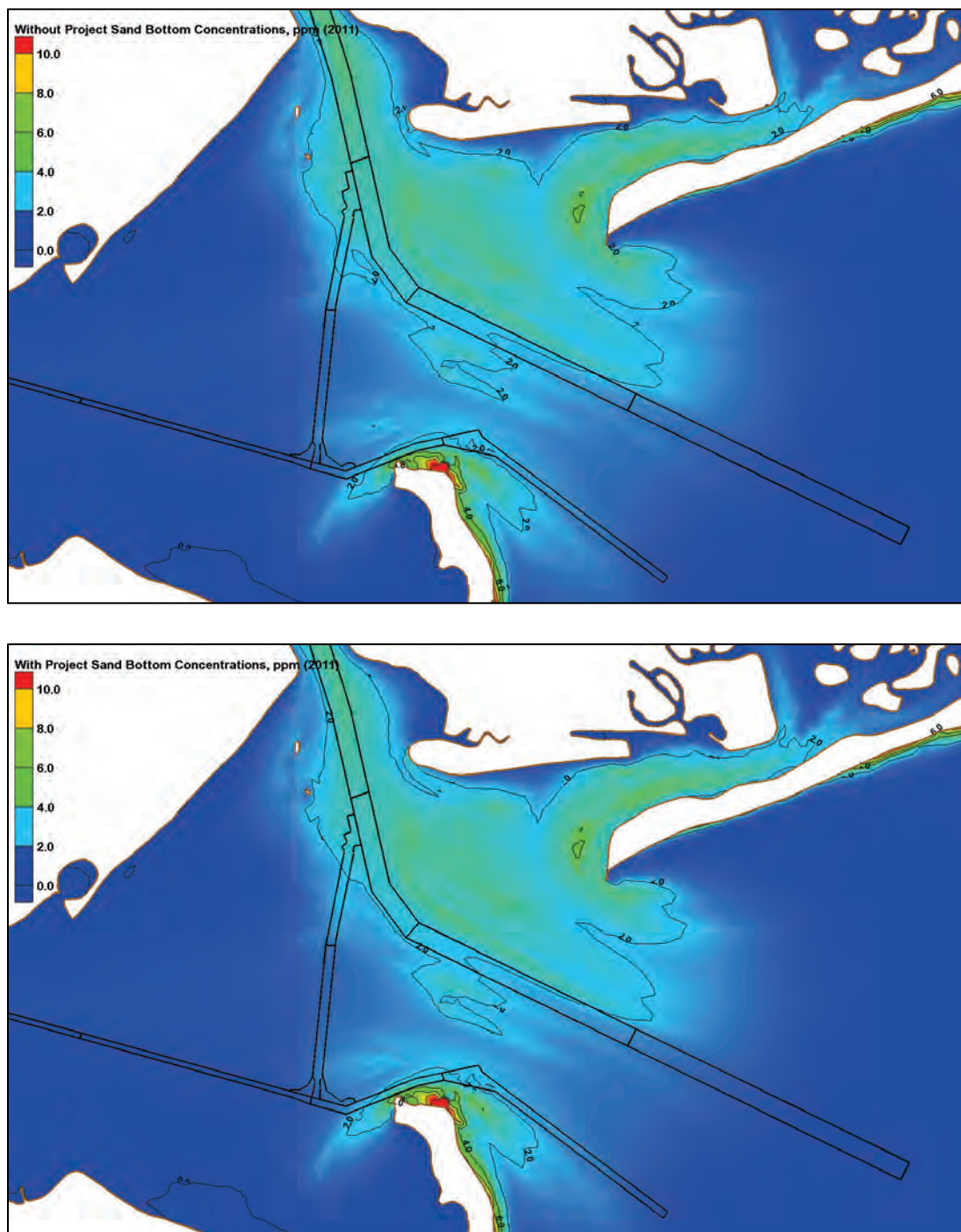




Figure 311. Without-project (top) and with-project (bottom) bed displacement, m (2011).

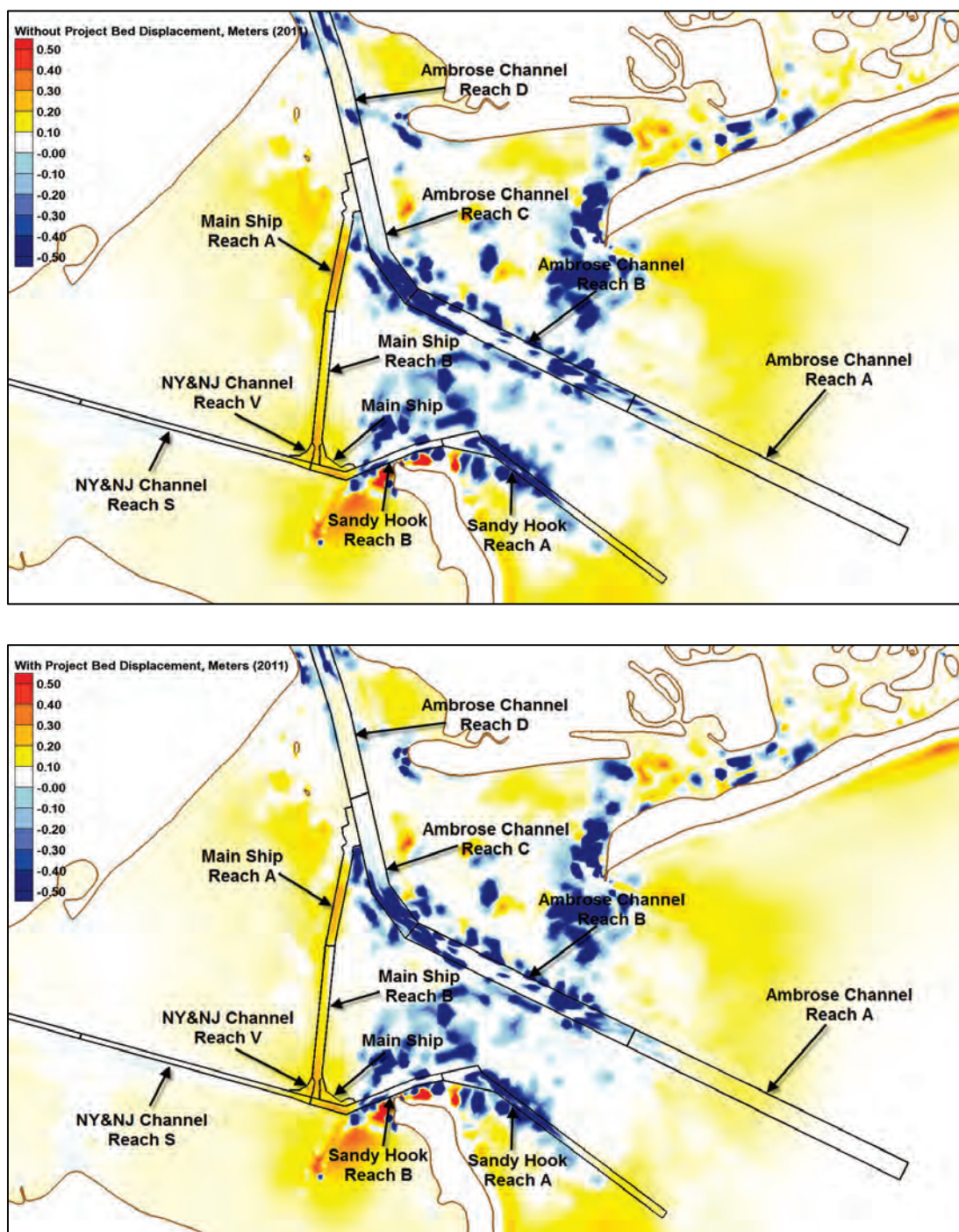




Figure 312. Without-project (top) and with-project (bottom) fine sediment accumulation,  $\text{kg}/\text{m}^2$  (2011).

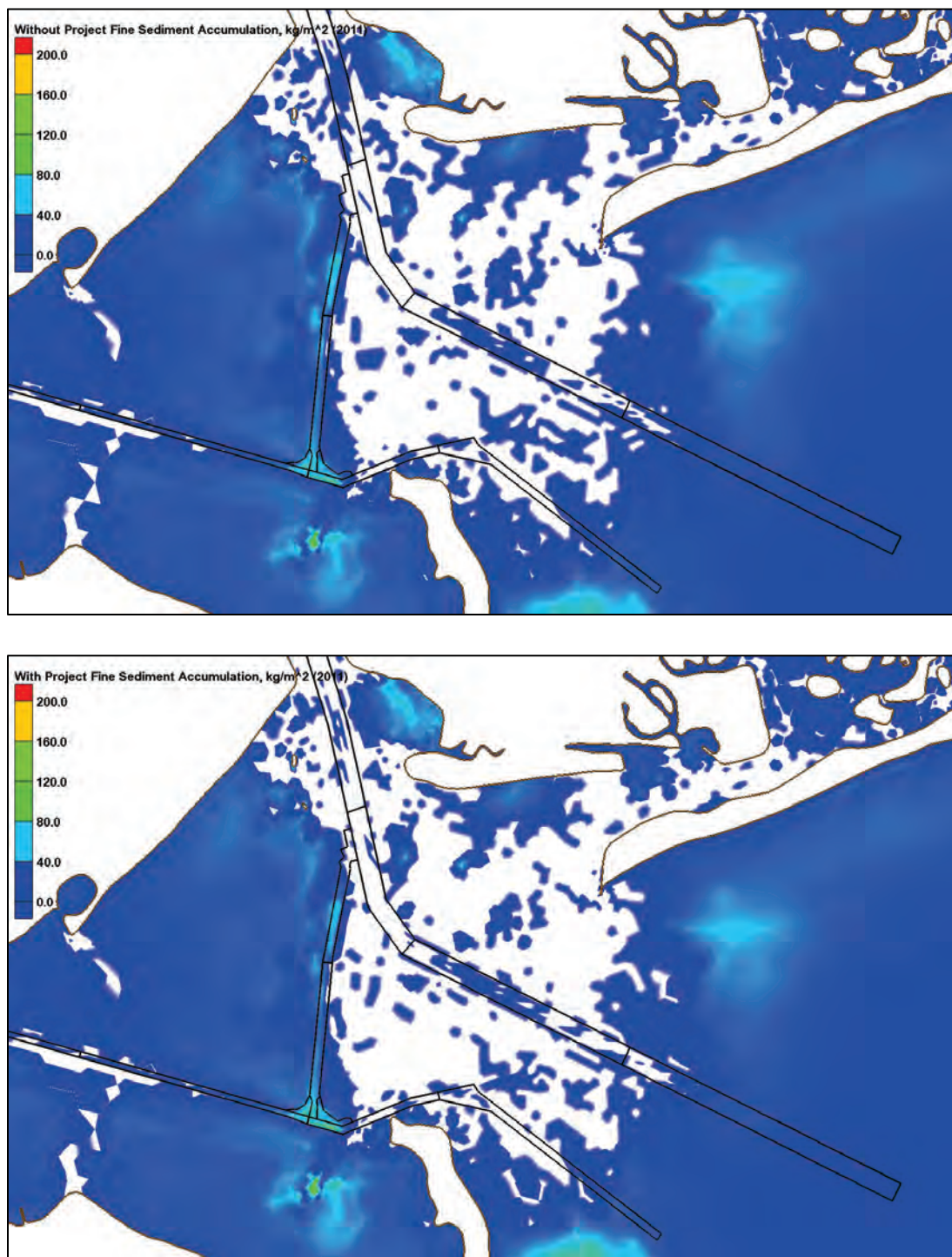


Figure 313. Without-project (top) and with-project (bottom) sand accumulation, kg/m<sup>2</sup> (2011).

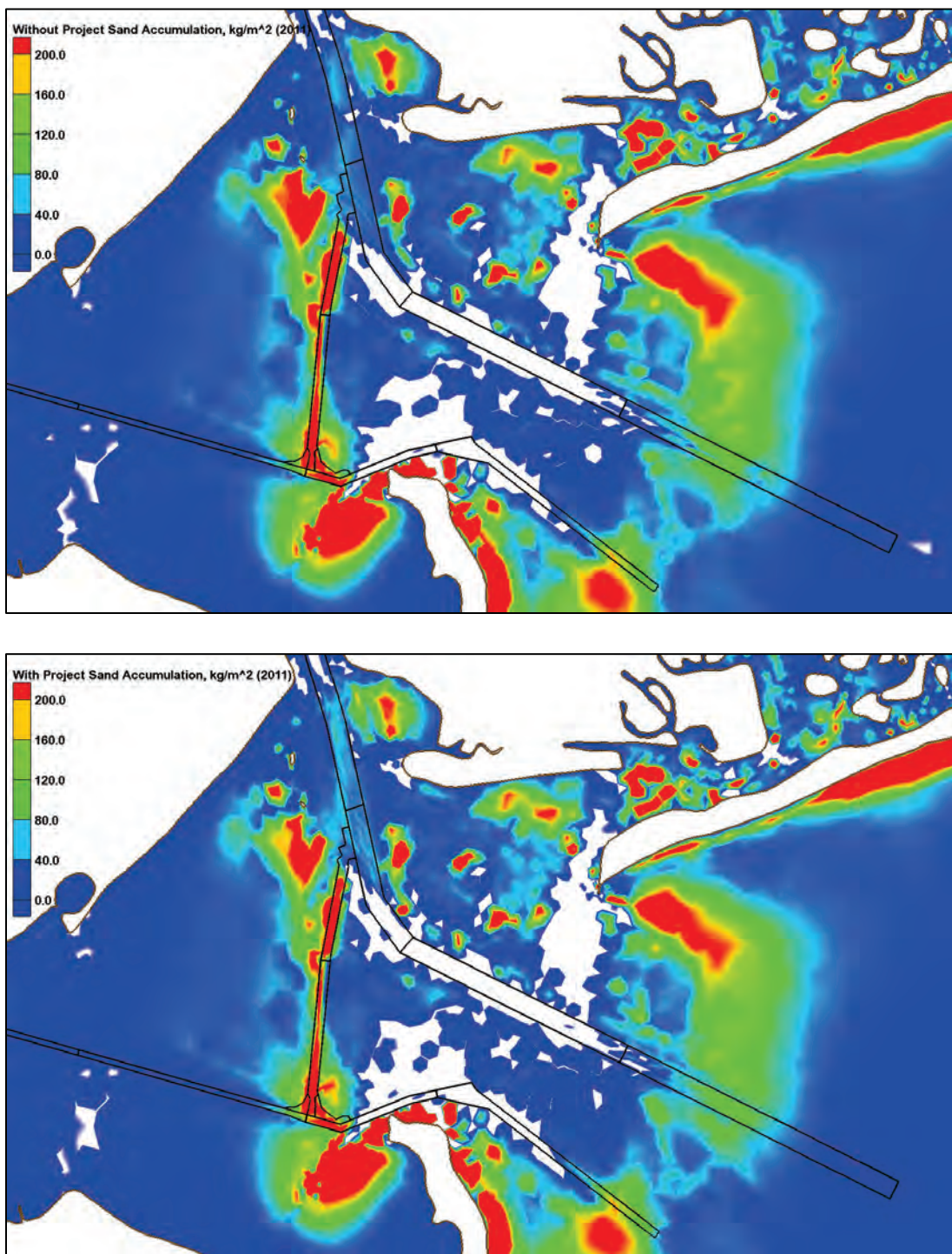


Figure 314. Dredge with-project/without-project percent differences (2011).

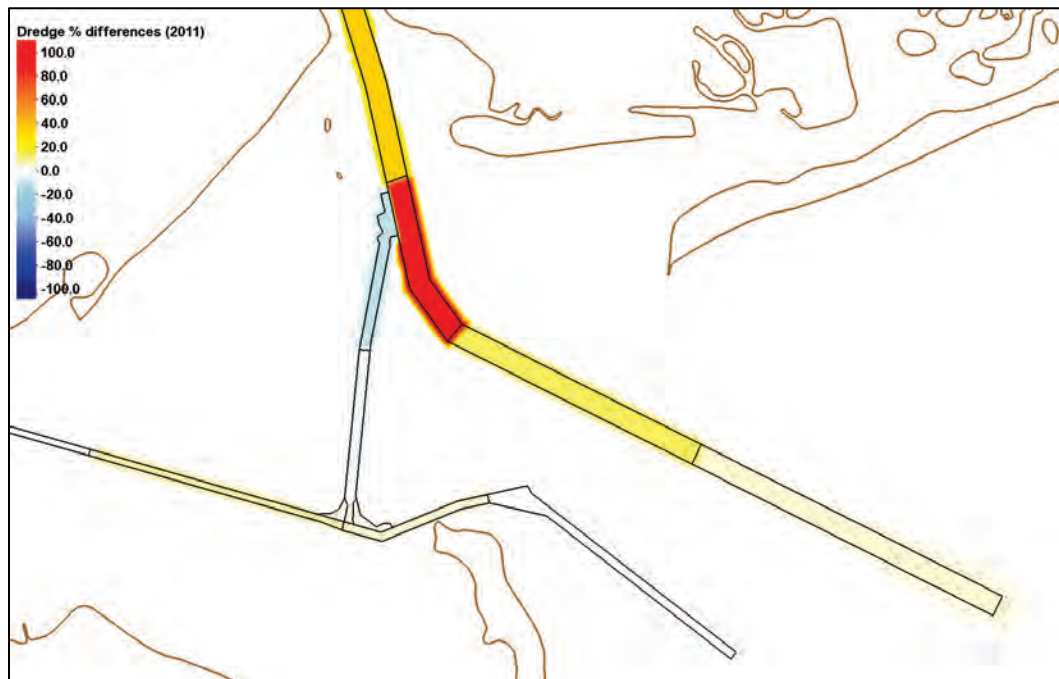


Table 34. Dredge volumes for Lower Bay (2011).

Depositional Volumes in Lower Bay, cy (2011)			
Reach	Without Project	With Project	With/Without Dredge Percentage
Ambrose Channel Reach A	152,305	157,665	104
Ambrose Channel Reach B	1,001	1,127	113
Ambrose Channel Reach C	3,931	8,697	221
Ambrose Channel Reach D	31,994	42,913	134
Main Ship	48,581	49,581	102
Main Ship Reach A	190,973	165,876	87
Main Ship Reach B	214,019	208,308	97
Sandy Hook Reach A	64,444	64,138	100
Sandy Hook Reach B	71,399	74,062	104
NY&NJ Channels Reach S	33,129	35,503	107
NY&NJ Channels Reach V	33,479	34,242	102



## Newark Bay, Kill van Kull, and Upper Bay results

Figure 315. Without-project (top) and with-project (bottom) average shear stresses, Pa (2011).

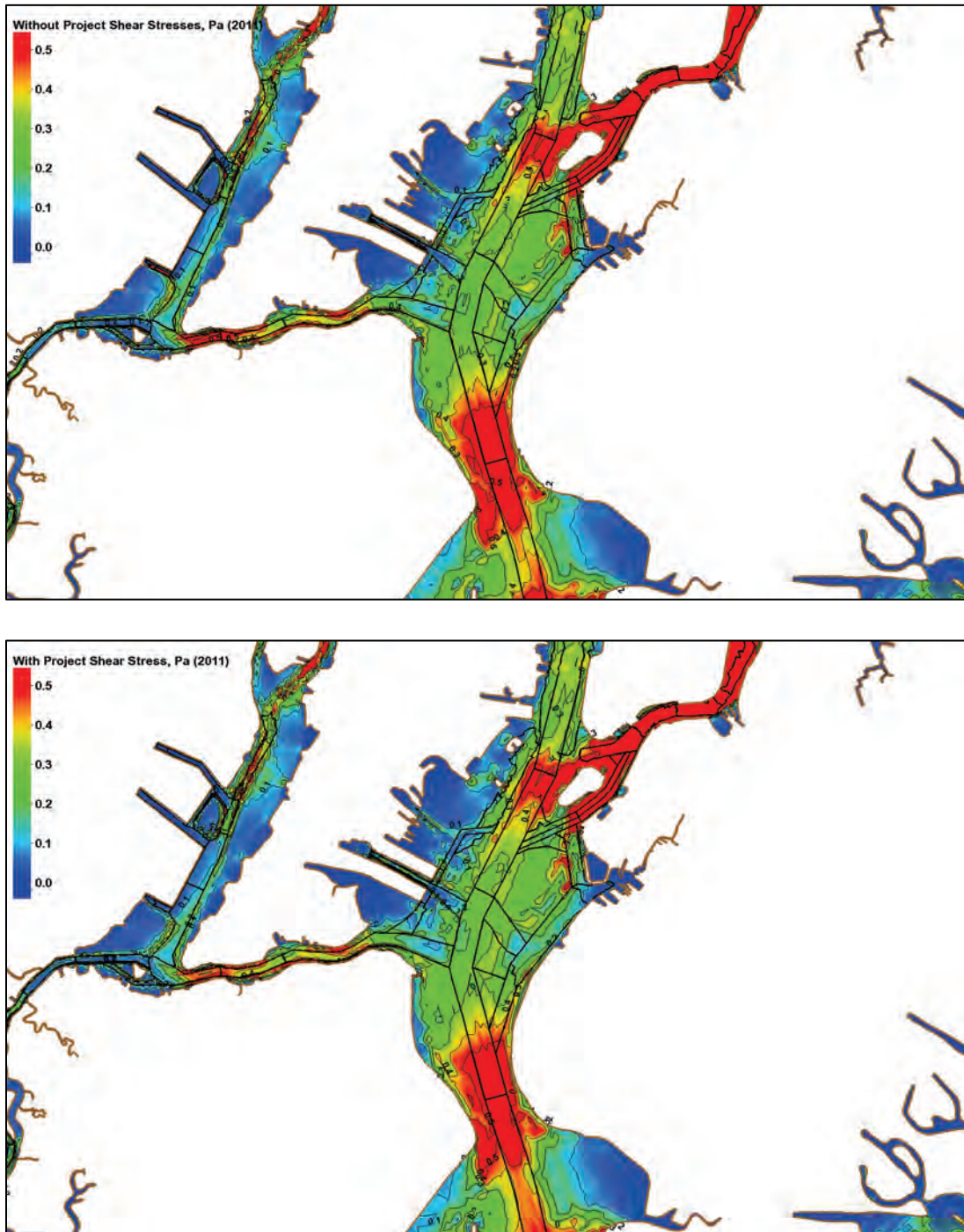


Figure 316. Without-project (top) and with-project (bottom) average bottom salinity, ppt (2011).

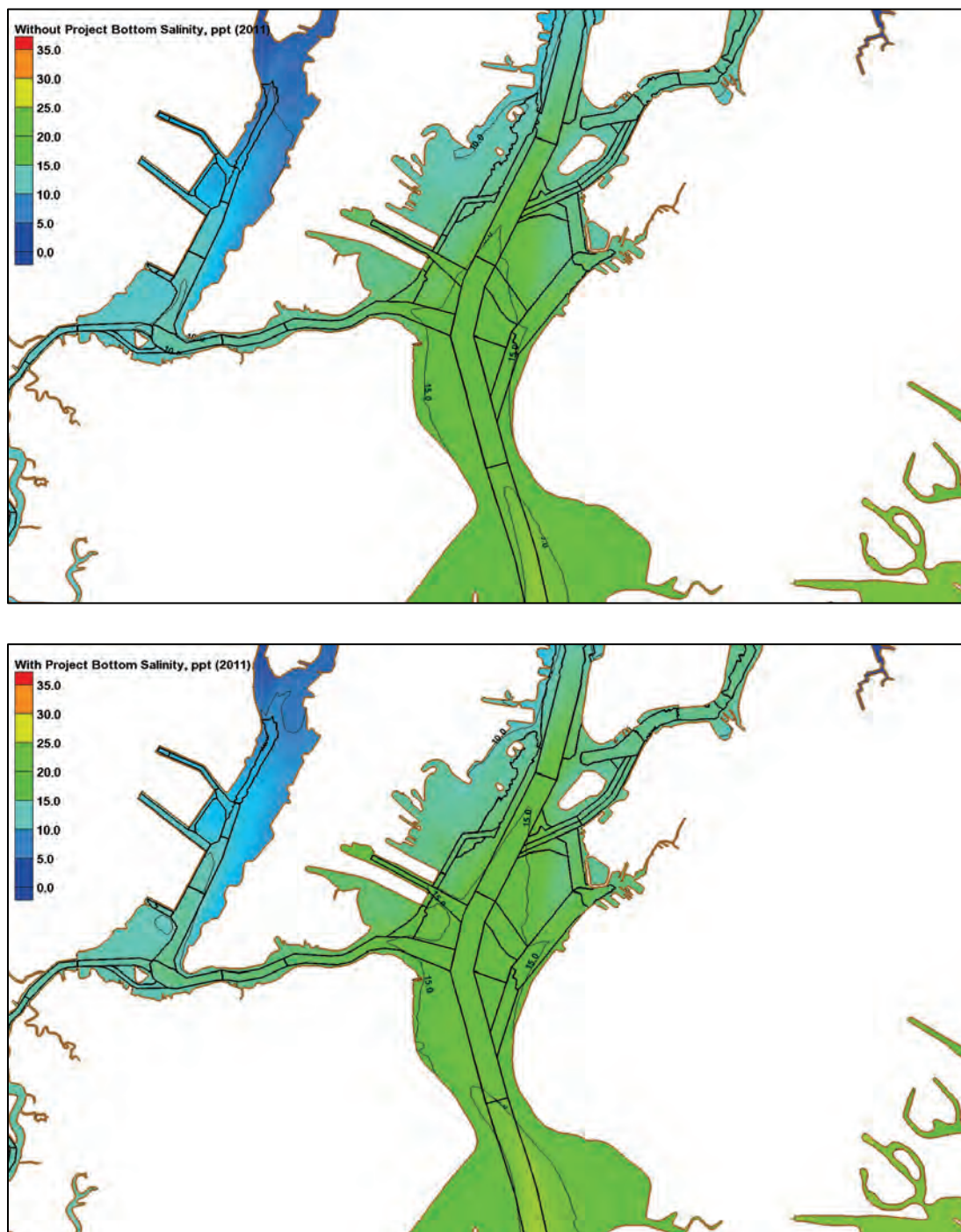




Figure 317. Without-project (top) and with-project (bottom) average fine sediment bottom concentrations, ppm (2011).

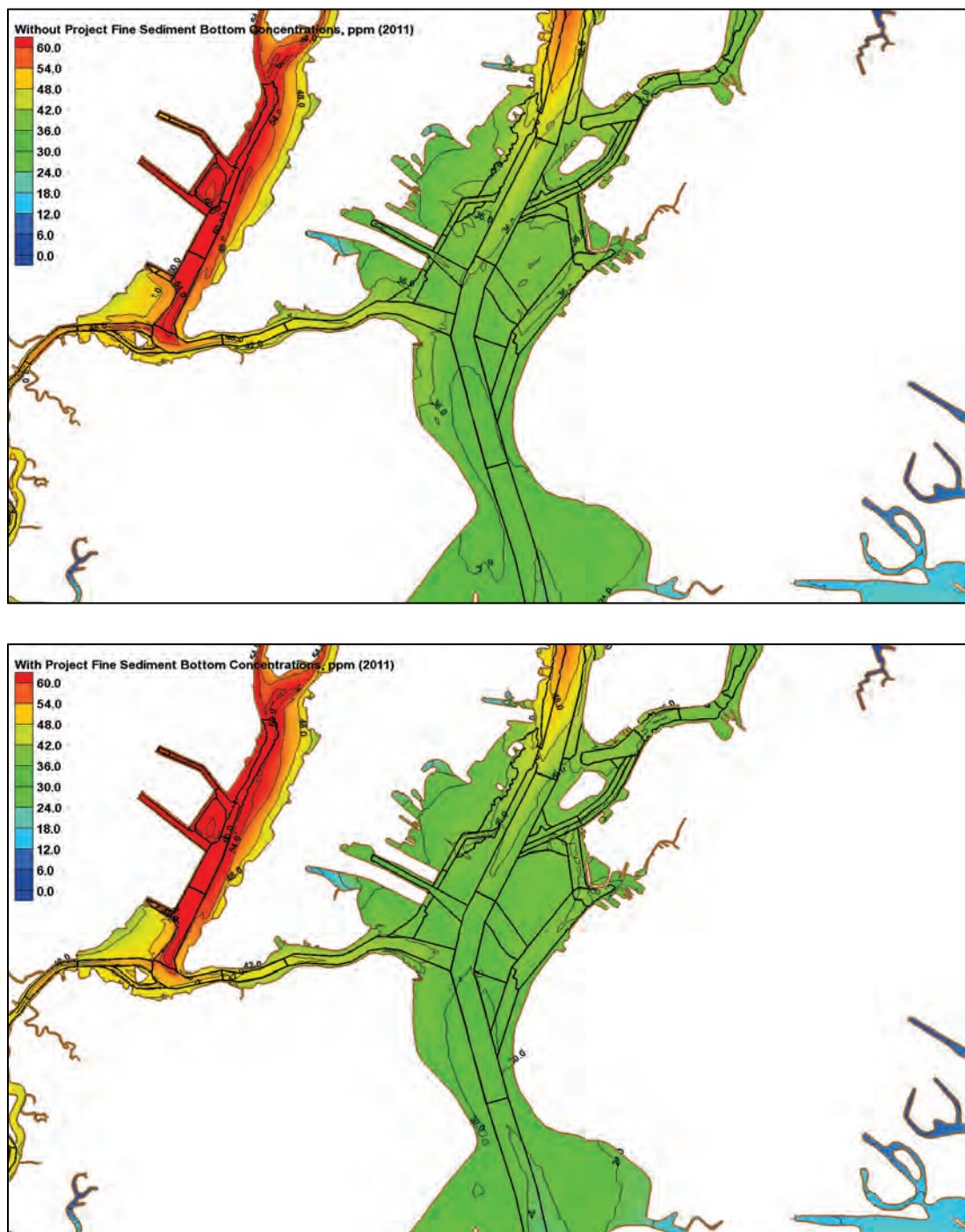


Figure 318. Without-project (top) and with-project (bottom) average sand bottom concentrations, ppm (2011).

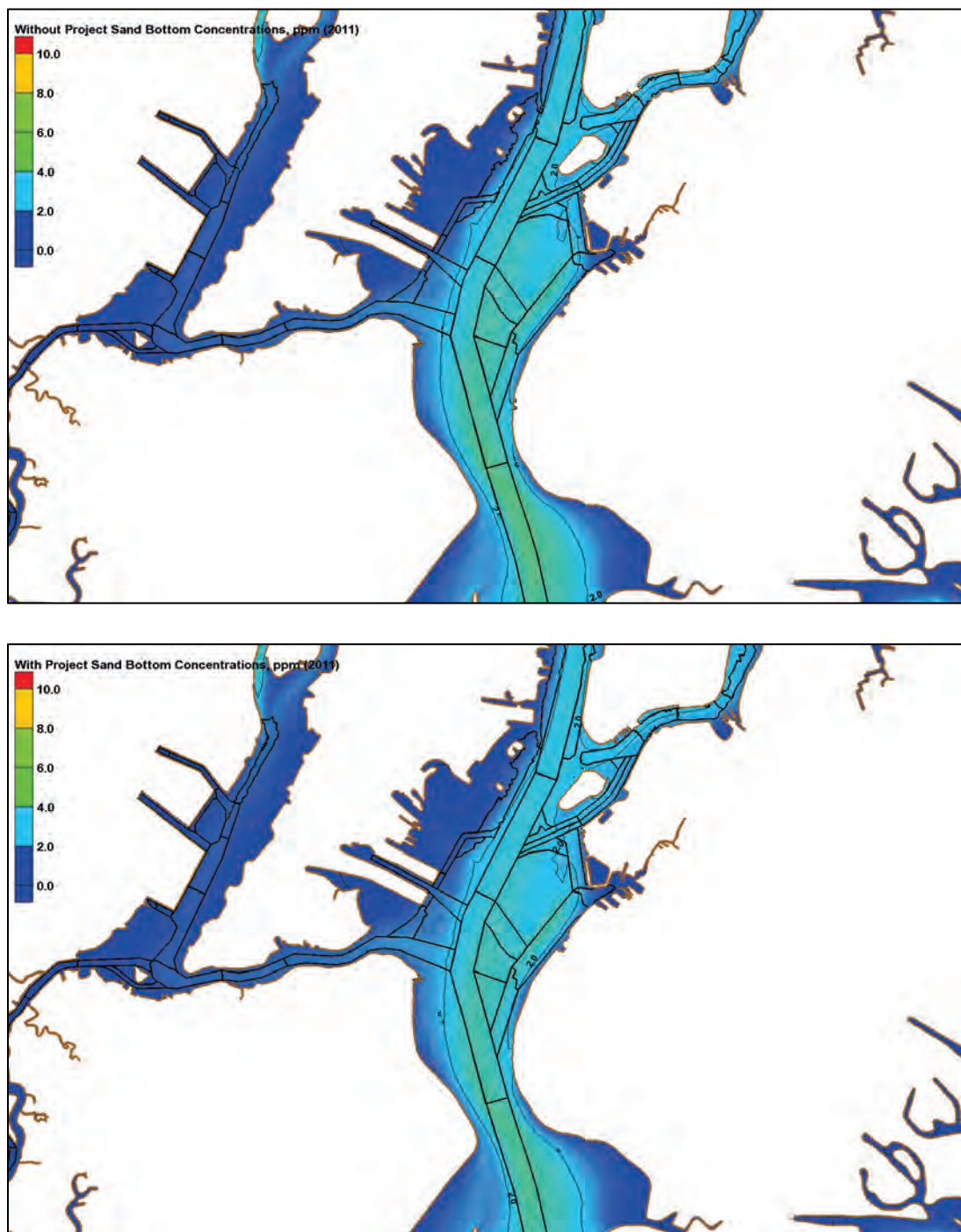




Figure 319. Without-project (top) and with-project (bottom) bed displacement, m (2011).

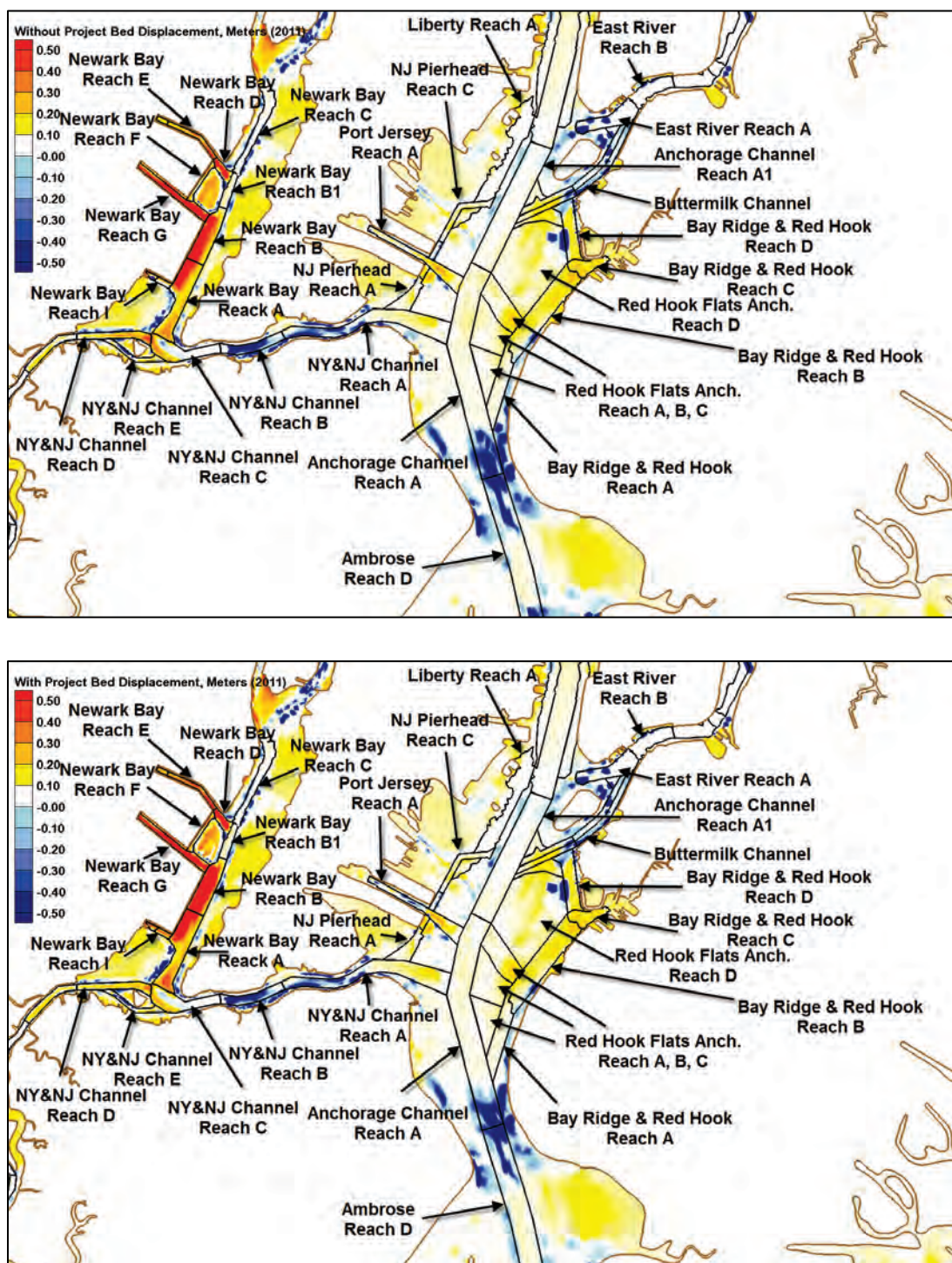


Figure 320. Without-project (top) and with-project (bottom) fine sediment accumulation,  $\text{kg}/\text{m}^2$  (2011).

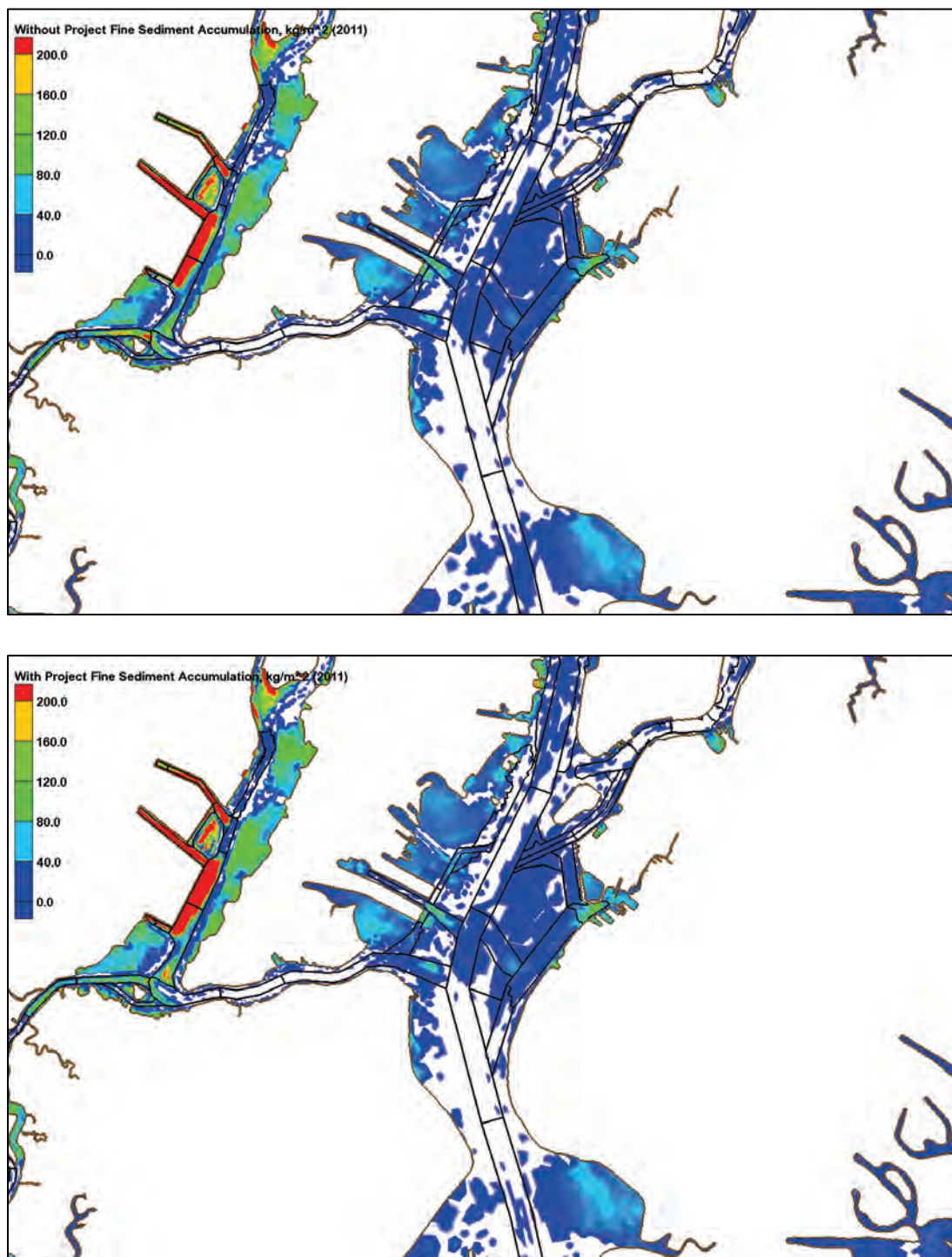




Figure 321. Without-project (top) and with-project (bottom) sand accumulation,  $\text{kg}/\text{m}^2$  (2011).

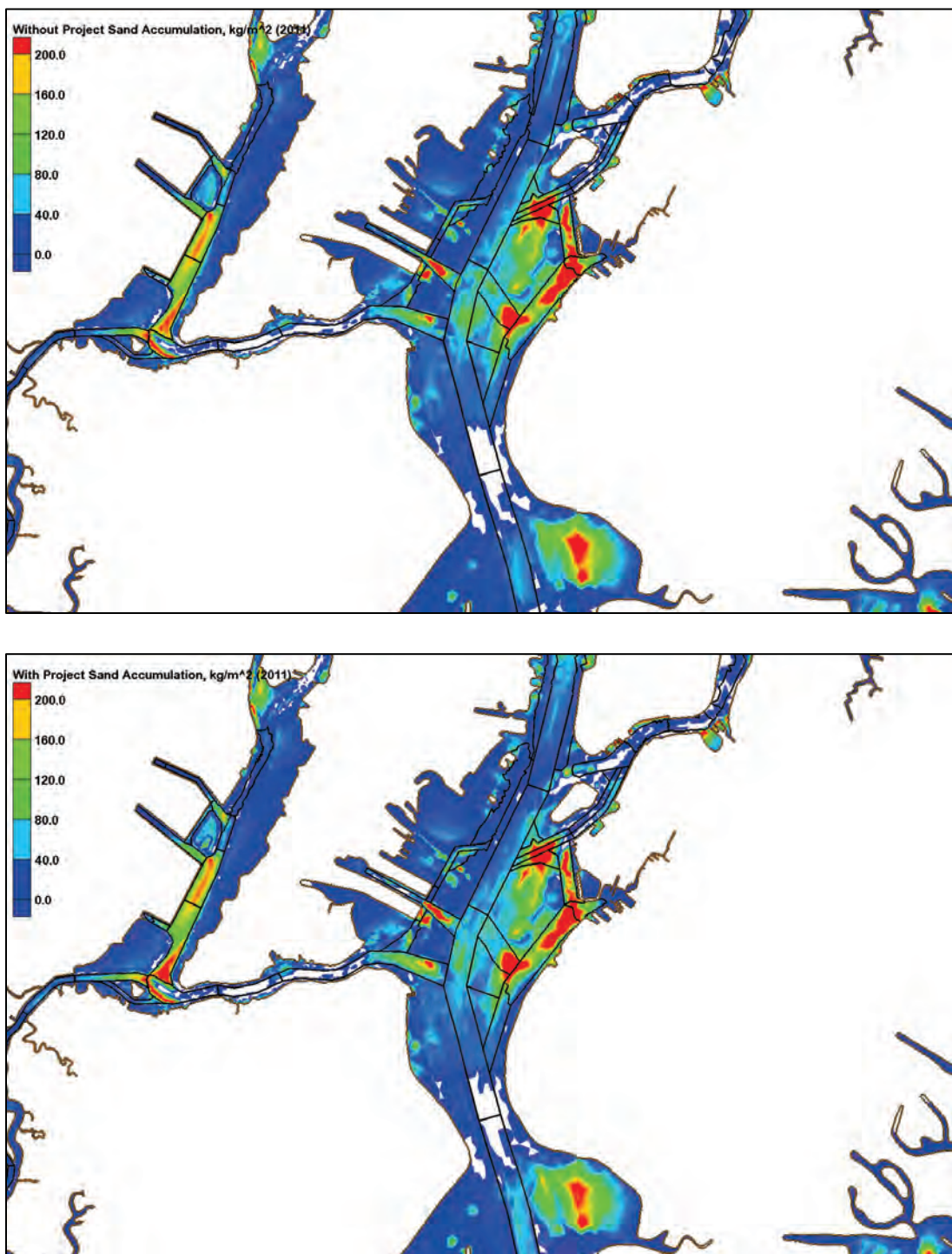




Figure 322. Dredge with-project/without-project percent differences (2011).



**Table 35. Dredge volumes for Newark Bay, Kill van Kull, and Upper Bay (2011).**

<b>Depositional Volumes in Newark Bay, Kill van Kull, and Upper Bay, cy (2011)</b>			
<b>Reach</b>	<b>Without Project</b>	<b>With Project</b>	<b>With/Without Dredge Percentage</b>
<b>Newark Bay</b>			
Newark Bay Reach A	317,327	372,027	117
Newark Bay Reach B	321,599	411,907	128
Newark Bay Reach B1	5,279	5,391	102
Newark Bay Reach C	4,471	4,376	98
Newark Bay Reach D	65,904	79,366	120
Newark Bay Reach E	61,929	82,445	133
Newark Bay Reach E1	7,150	10,801	151
Newark Bay Reach F	25,474	30,355	119
Newark Bay Reach G	280,325	270,799	97
Newark Bay Reach I	7,229	18,029	249
Newark Bay Reach I1	7,480	10,813	145
<b>Kill van Kull</b>			
NY&NJ Channels Reach A	43,736	56,159	128
NY&NJ Channels Reach B	601	593	99
NY&NJ Channels Reach C	61,398	60,702	99
<b>Upper Bay</b>			
Anchorage Channel Reach A	56,696	45,424	80
Anchorage Channel Reach A1	21,793	17,564	81
Anchorage Reach C1	8,752	8,652	99
Bay Ridge & Red Hook Reach A	16,723	15,909	95
Bay Ridge & Red Hook Reach B	158,204	162,998	103
Bay Ridge & Red Hook Reach C	58,923	52,727	89
Bay Ridge & Red Hook Reach D	57,356	55,795	97
Red Hook Flats Anch. Reach A	13,116	14,446	110
Red Hook Flats Anch. Reach B	34,266	30,210	88
Red Hook Flats Anch. Reach C	61,788	59,765	97
Red Hook Flats Anch. Reach D	150,840	146,815	97
Port Jersey Reach A	51,303	42,639	83
NJ Pierhead Ch. Reach A	11,058	11,882	107
NJ Pierhead Ch. Reach B	8,190	9,669	118
NJ Pierhead Reach C	12,430	12,257	99
Liberty Reach A	8,764	7,058	81

## Arthur Kill and Raritan Bay results

Figure 323. Without-project (top) and with-project (bottom) average shear stresses, Pa (2011).

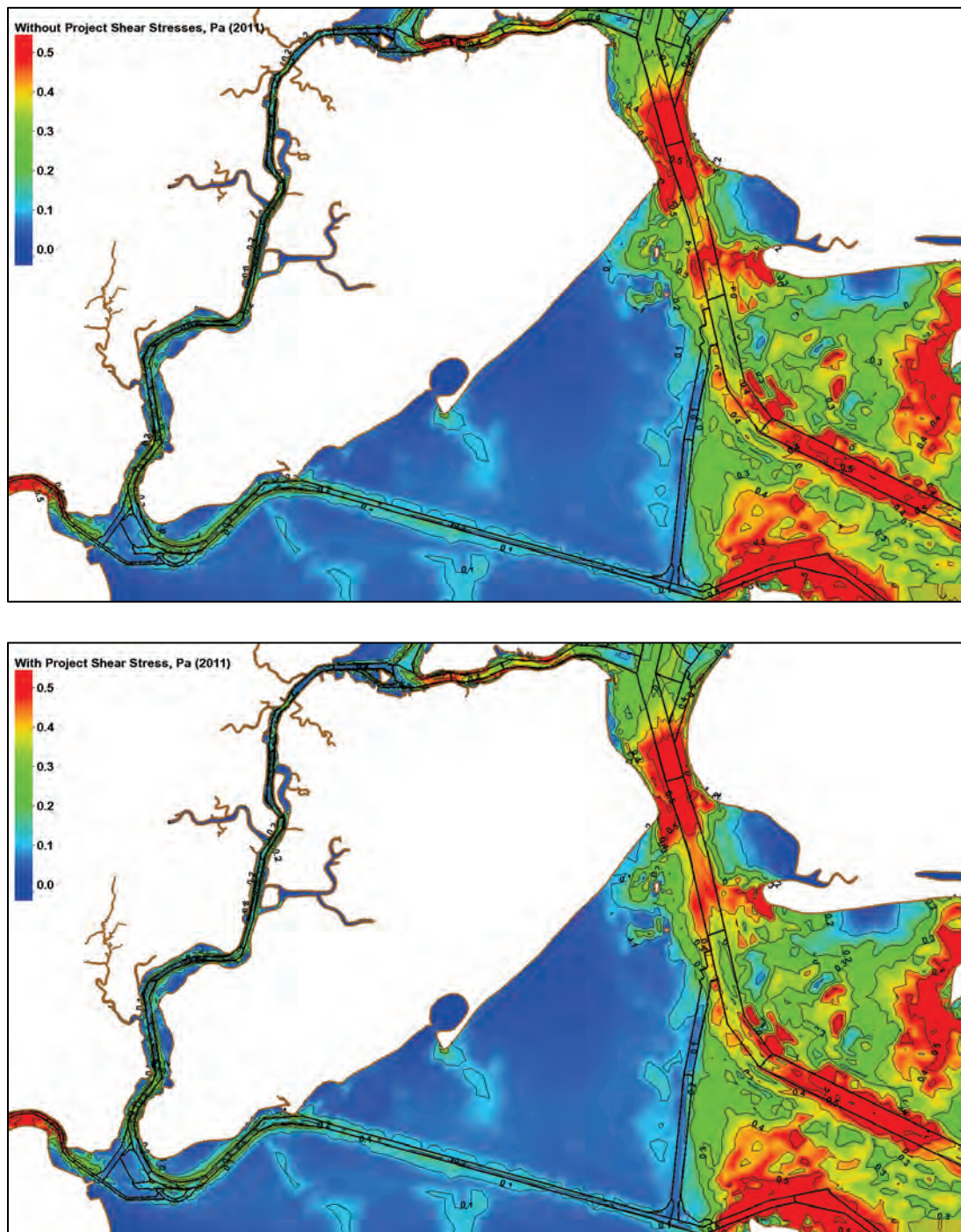


Figure 324. Without-project (top) and with-project (bottom) average bottom salinity, ppt (2011).

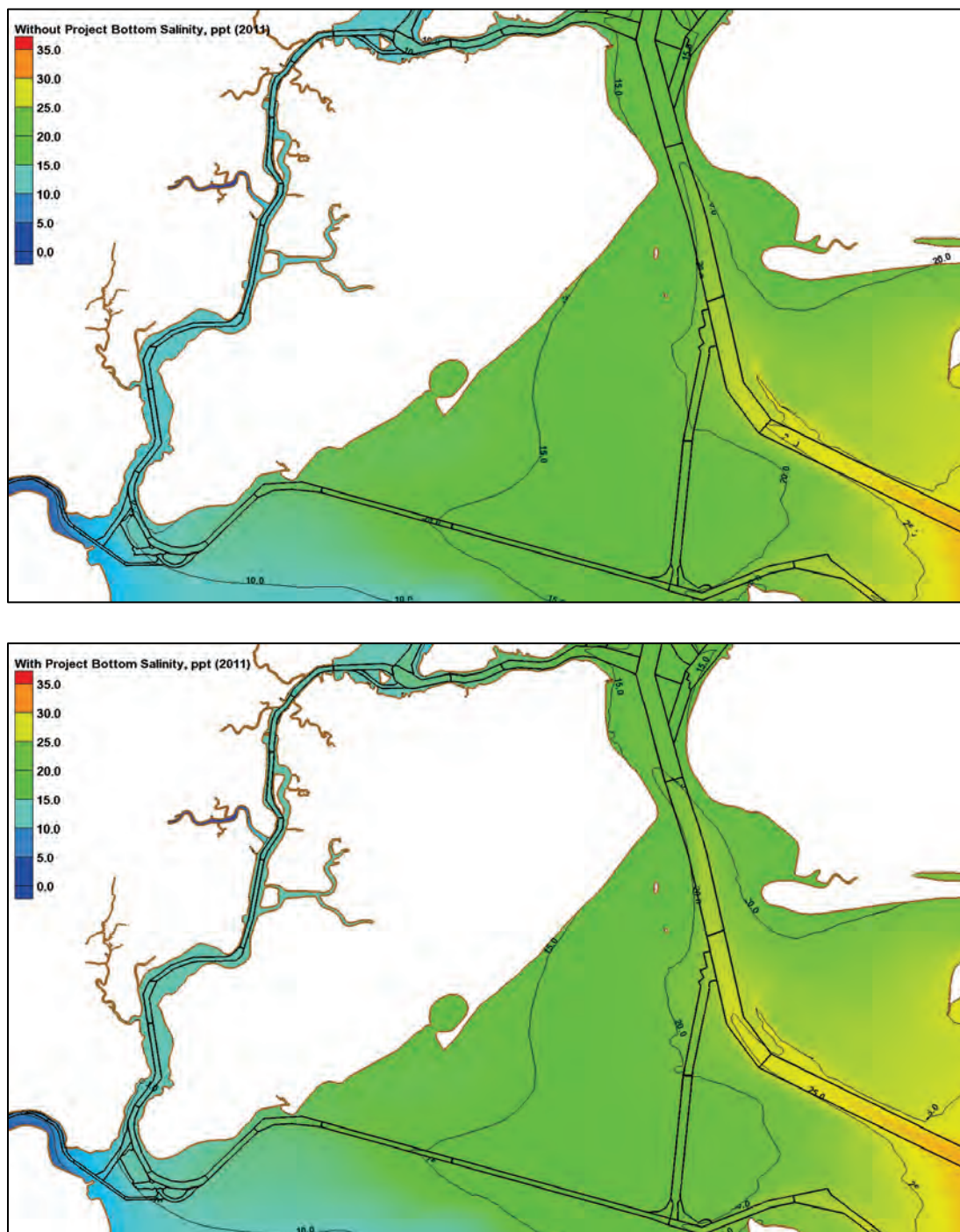




Figure 325. Without-project (top) and with-project (bottom) average fine sediment bottom concentrations, ppm (2011).

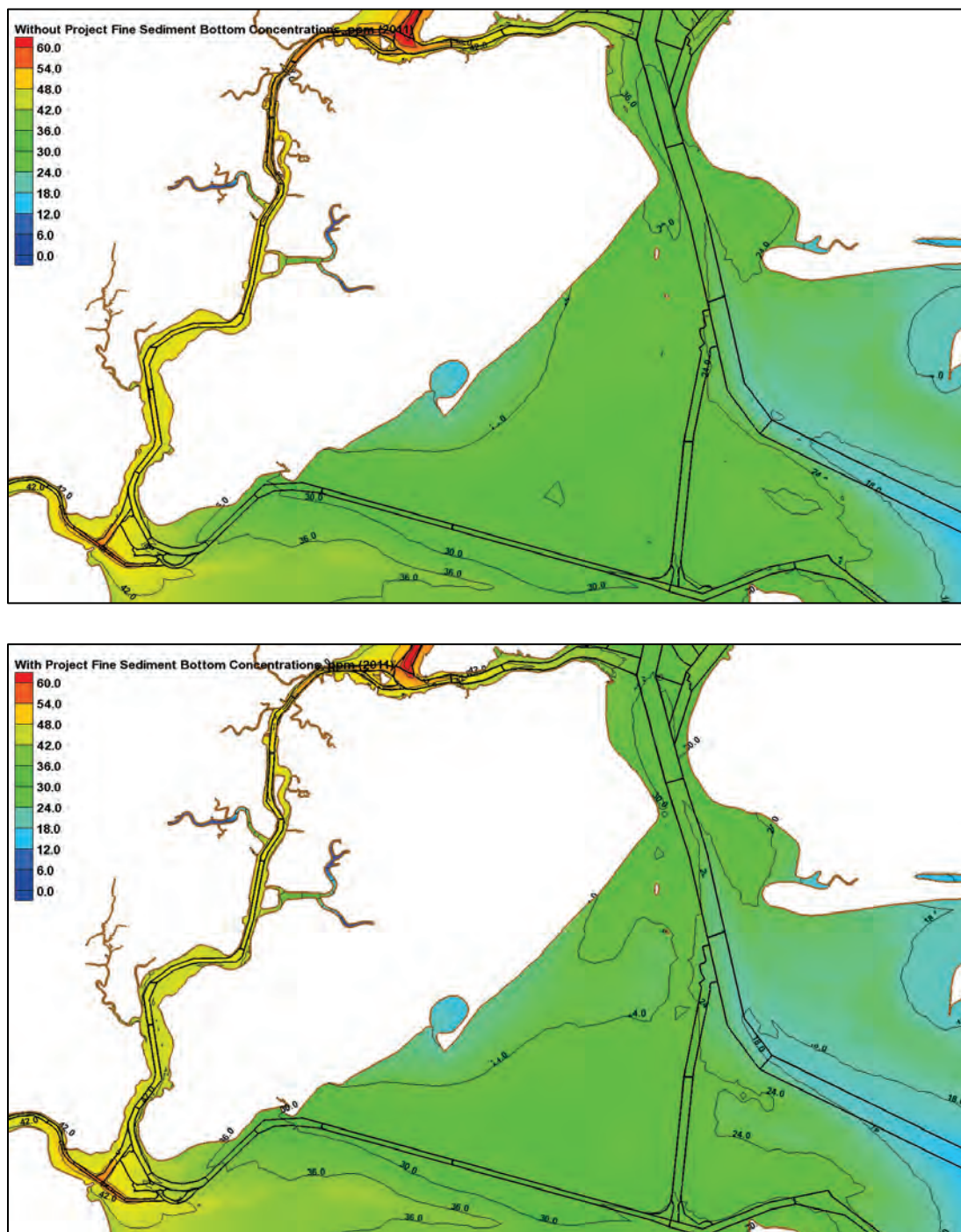




Figure 326. Without-project (top) and with-project (bottom) average sand bottom concentrations, ppm (2011).

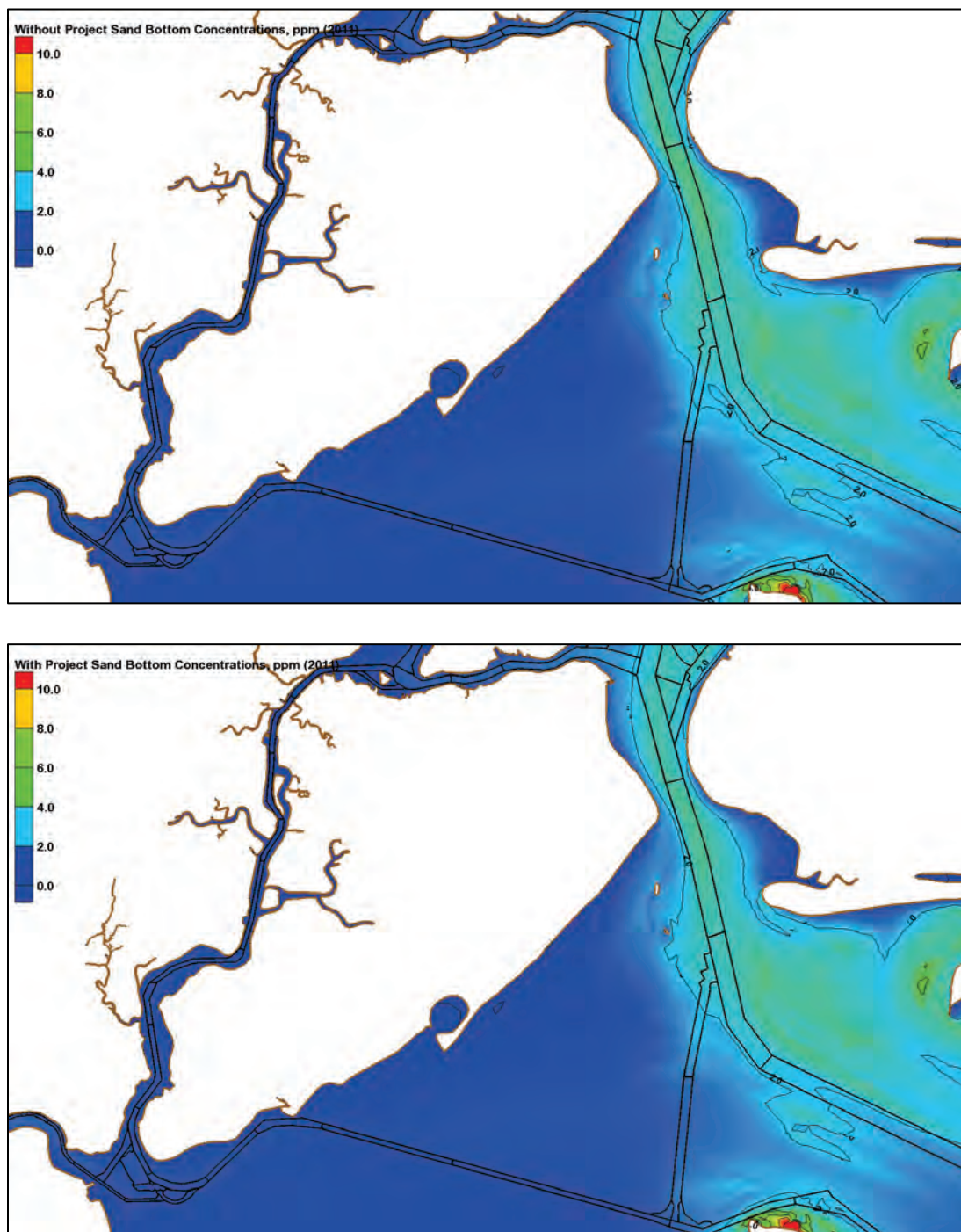


Figure 327. Without-project (top) and with-project (bottom) bed displacement, m (2011).

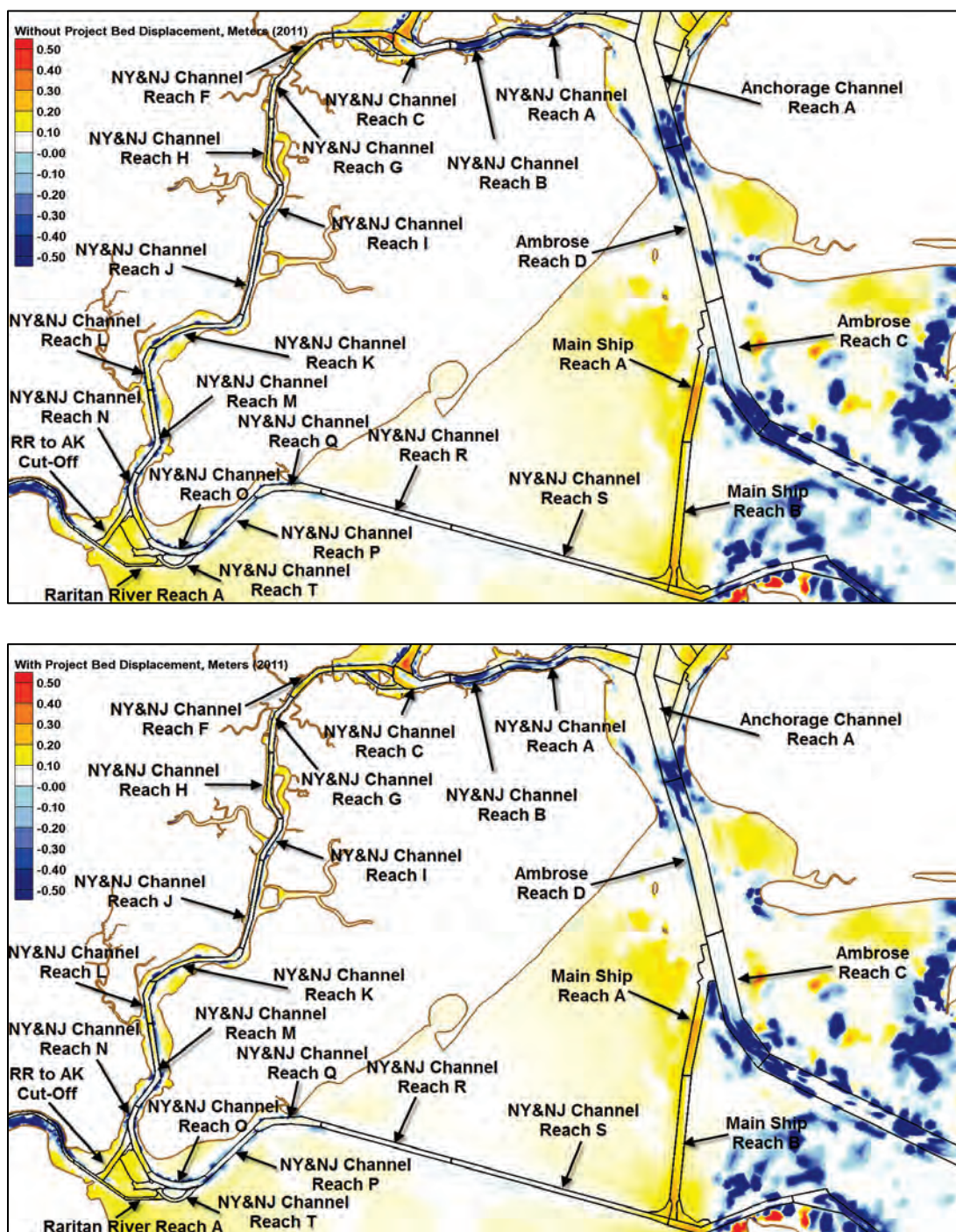




Figure 328. . Without-project (top) and with-project (bottom) fine sediment accumulation,  $\text{kg/m}^2$  (2011).

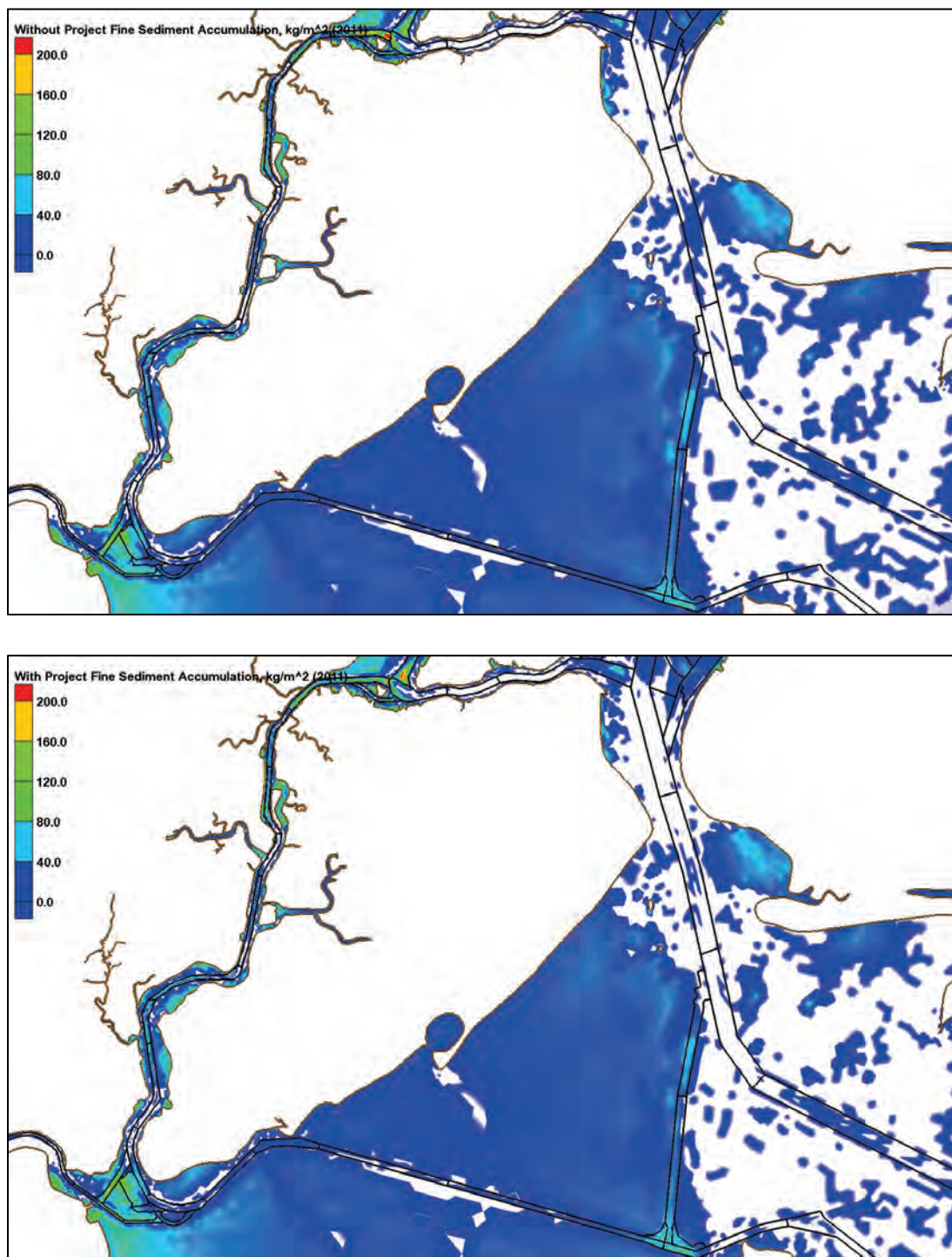


Figure 329. Without-project (top) and with-project (bottom) sand accumulation,  $\text{kg/m}^2$  (2011).

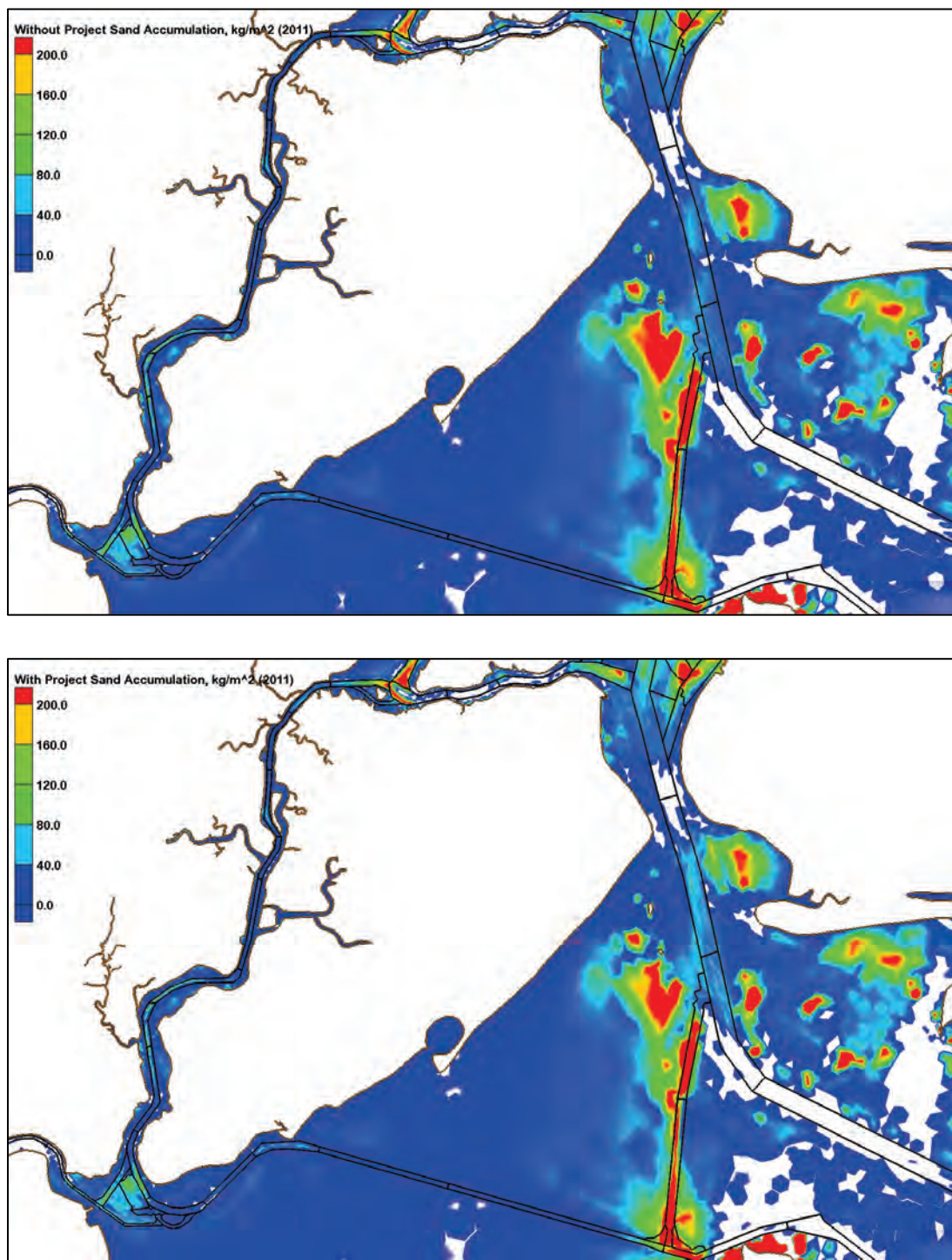


Figure 330. Dredge With-project/without-project percent differences (2011).

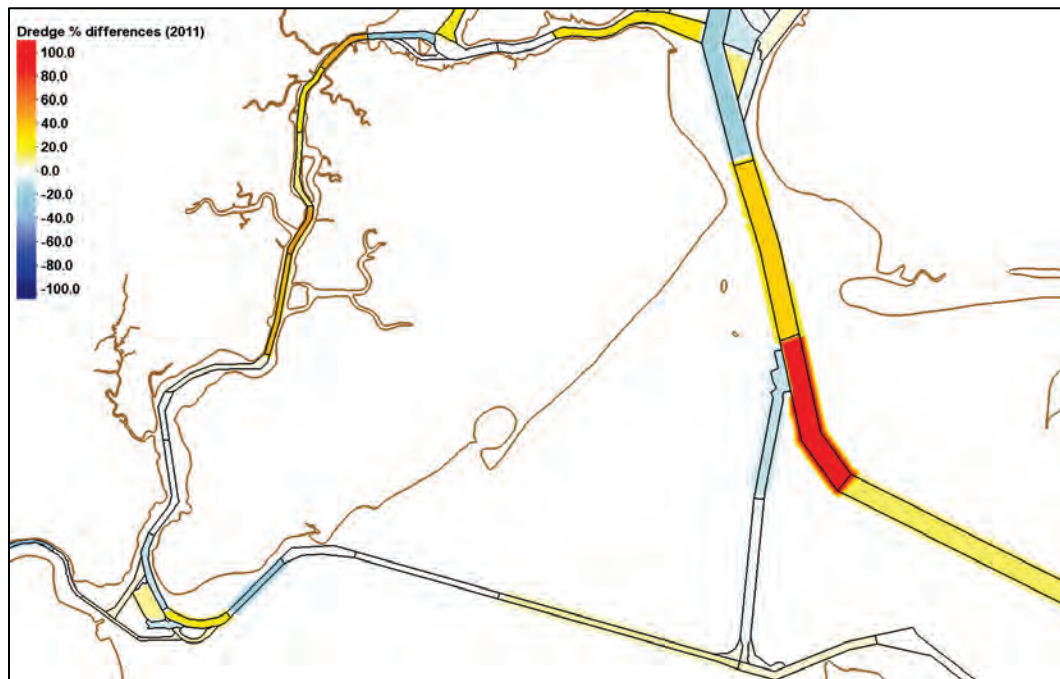




Table 36. Dredge volumes for Arthur Kill and Raritan Bay (2011).

Depositional Volumes in Arthur Kill and Raritan Bay, cy (2011)			
Reach	Without Project	With Project	With/Without Dredge Percentage
<b>Arthur Kill</b>			
NY&NJ Channels Reach D	72,937	55,311	76
NY&NJ Channels Reach E	11,094	11,005	99
NY&NJ Channels Reach F	18,510	26,534	143
NY&NJ Channels Reach G	4,449	5,488	123
NY&NJ Channels Reach H	11,359	12,523	110
NY&NJ Channels Reach I	739	1,101	149
NY&NJ Channels Reach J	2,526	3,532	140
NY&NJ Channels Reach K	15,998	16,462	103
NY&NJ Channels Reach L	13,819	13,219	96
NY&NJ Channels Reach M	10,957	11,026	101
NY&NJ Channels Reach N	21,943	19,196	87
<b>Raritan Bay</b>			
NY&NJ Channels Reach O	3,307	3,890	118
NY&NJ Channels Reach P	2,812	2,077	74
NY&NJ Channels Reach Q	6,151	6,075	99
NY&NJ Channels Reach R	423	418	99
NY&NJ Channels Reach T	5,401	5,756	107
RR to AK Cut-Off Reach A	35,173	36,563	104
Raritan River Reach A	10,663	10,985	103
Raritan River Reach B	12,104	12,623	104
Raritan River Reach C	2,009	2,018	100
Raritan River Reach D	86	54	63

## Appendix G: Results for 2012

### Lower Bay results

Figure 331. Without-project (top) and with-project (bottom) average shear stresses, Pa (2012).

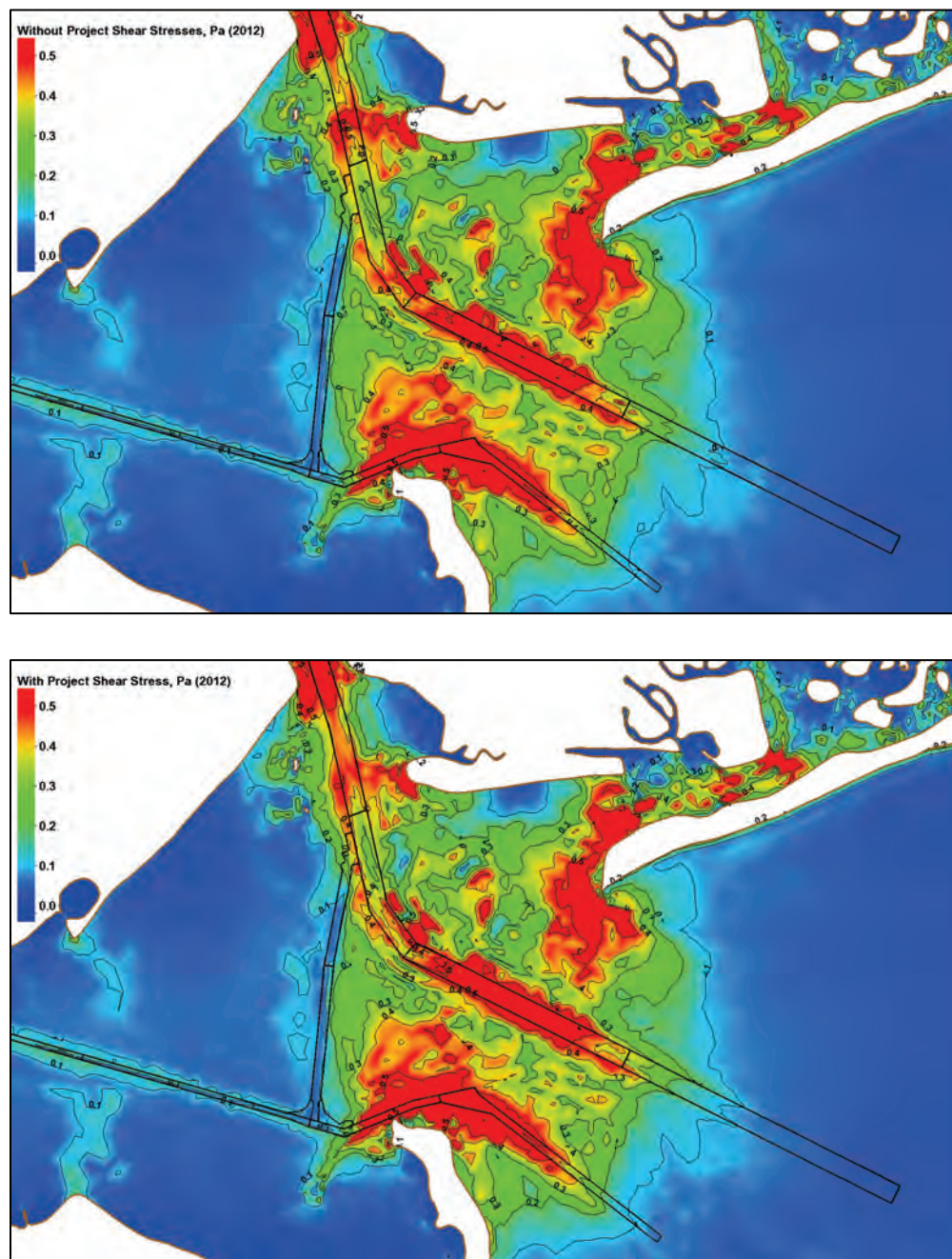


Figure 332. Without-project (top) and with-project (bottom) average bottom salinity, ppt (2012).

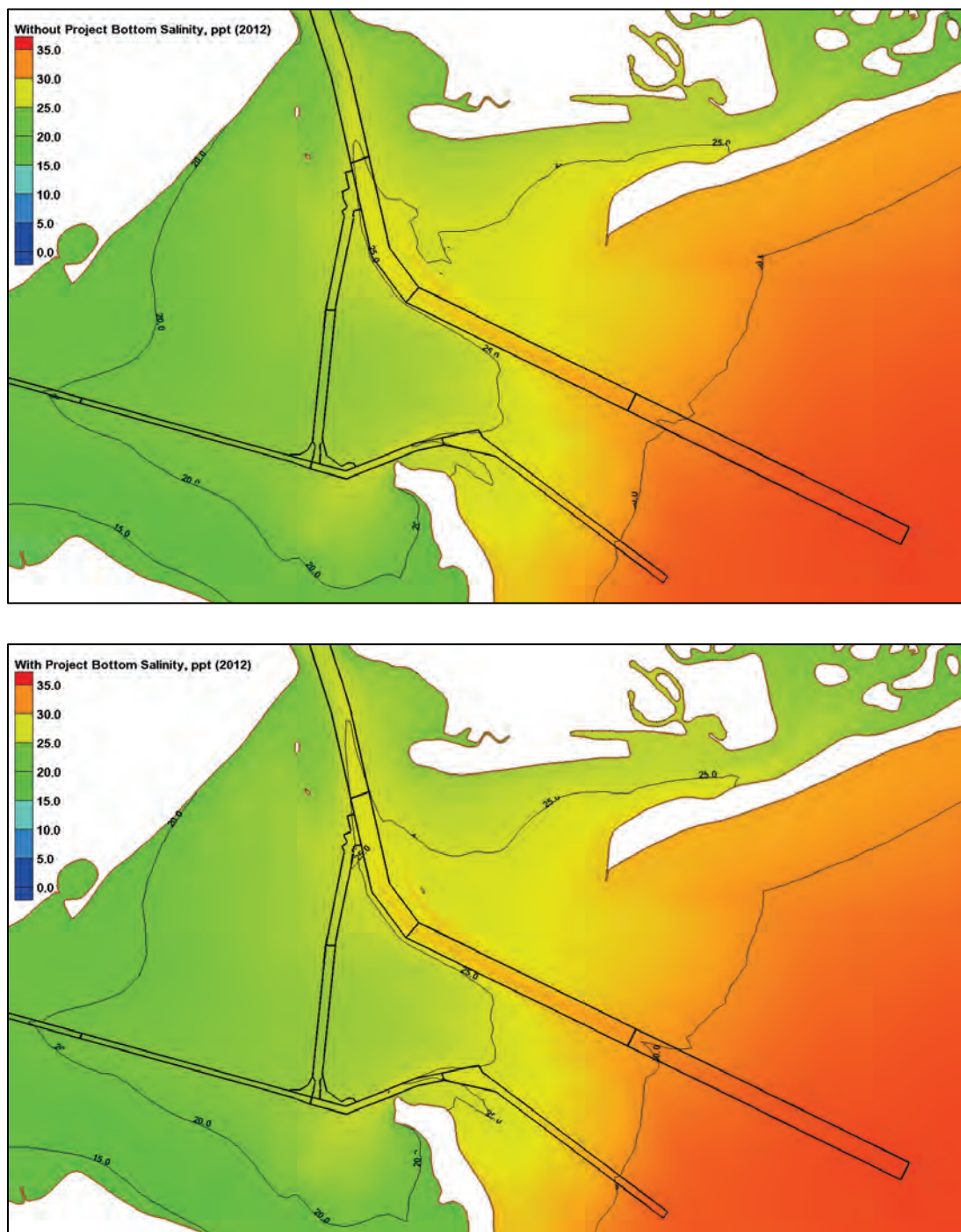




Figure 333. Without-project (top) and with-project (bottom) average fine sediment bottom concentrations, ppm (2012),

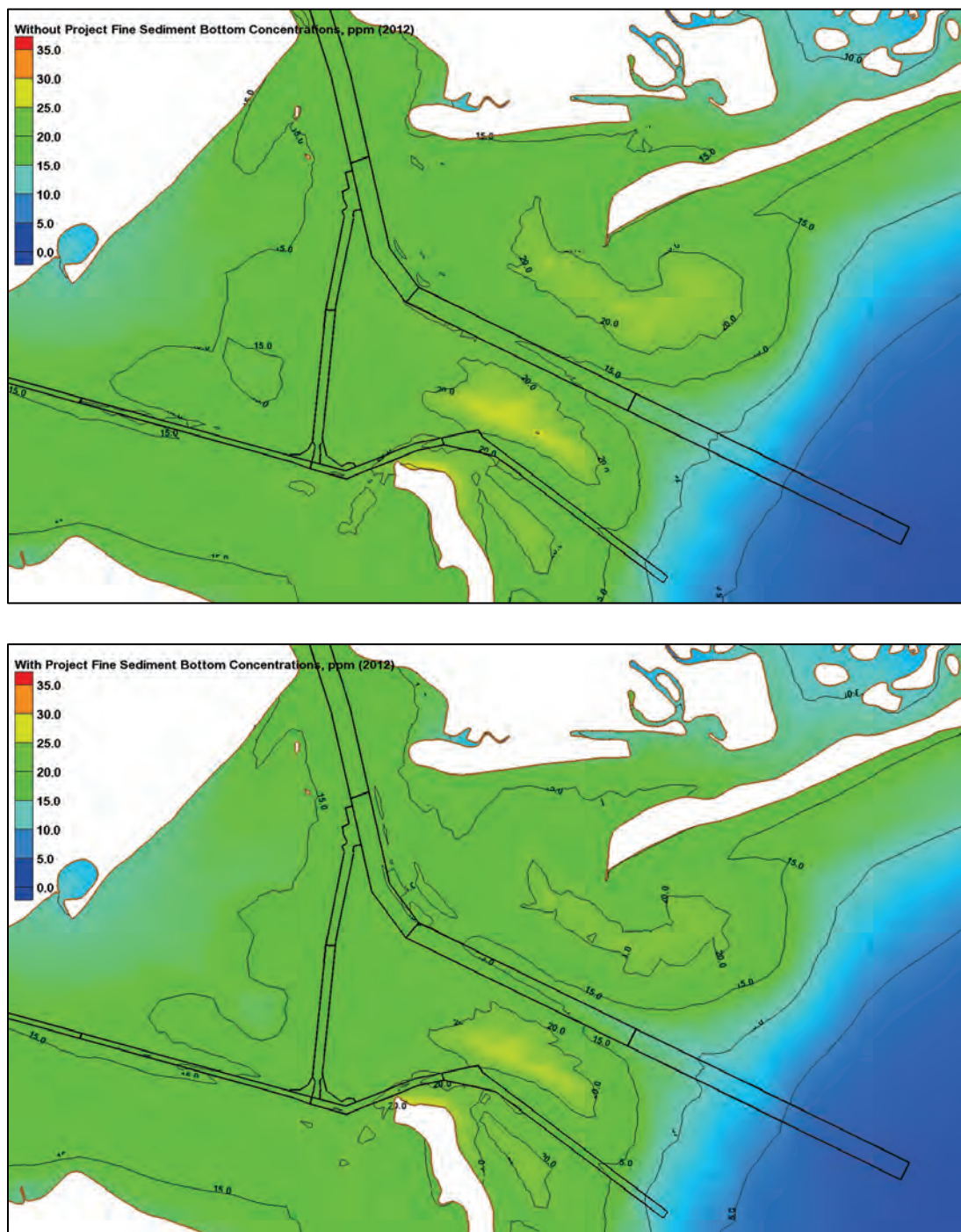


Figure 334. Without-project (top) and with-project (bottom) average sand bottom concentrations, ppm (2012).

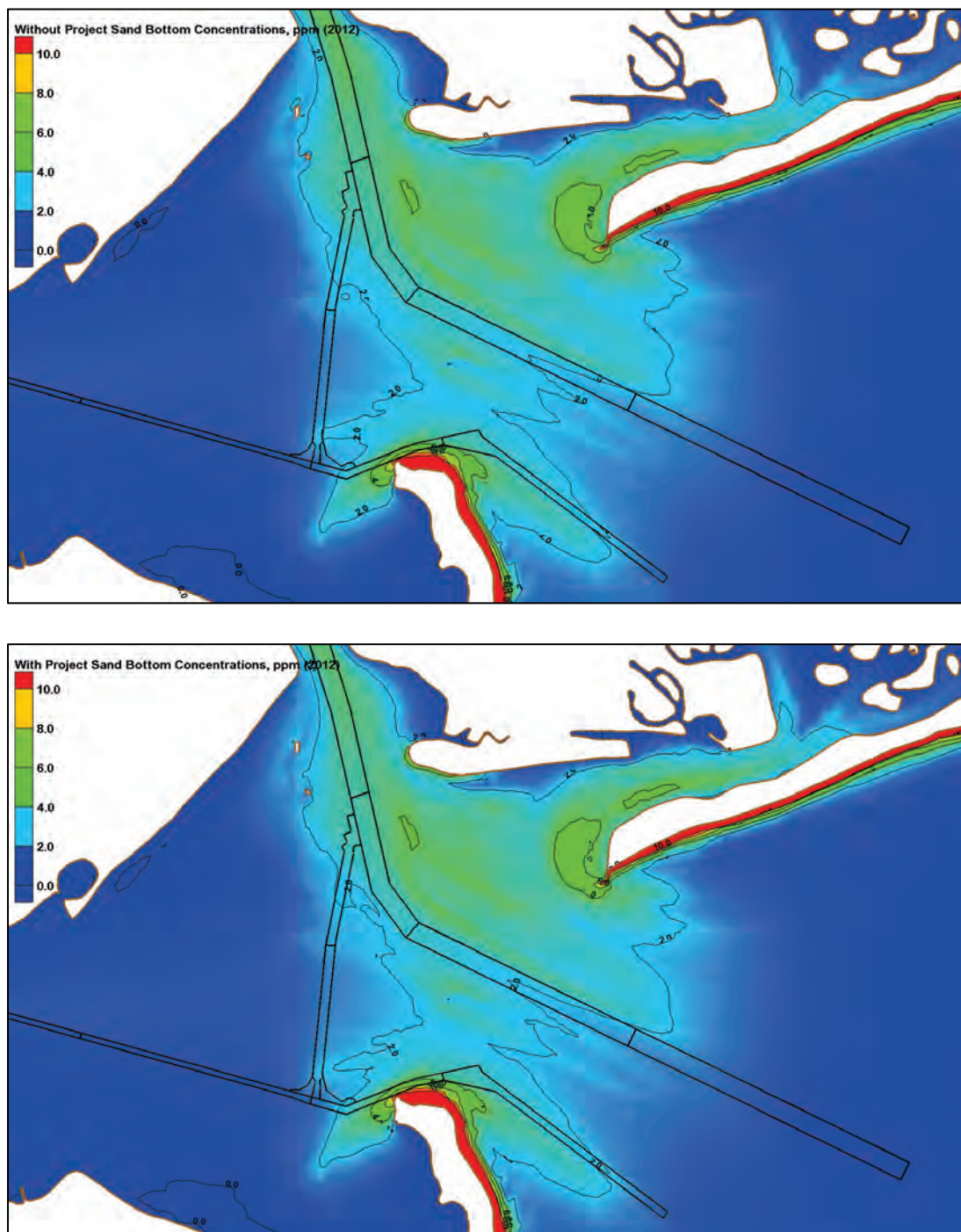




Figure 335. Without-project (top) and with-project (bottom) bed displacement, m (2012).

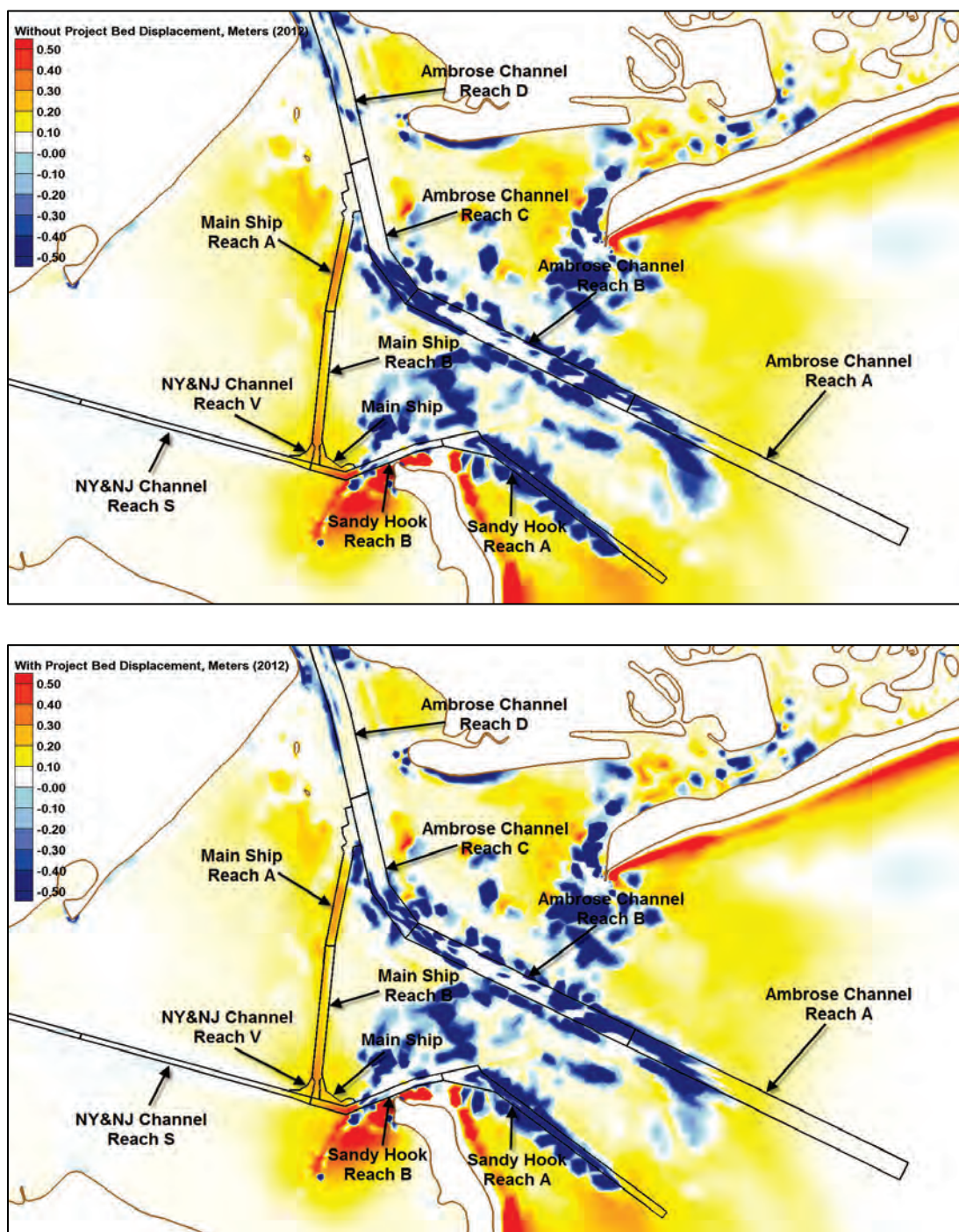


Figure 336. Without-project (top) and with-project (bottom) fine sediment accumulation,  $\text{kg}/\text{m}^2$  (2012).

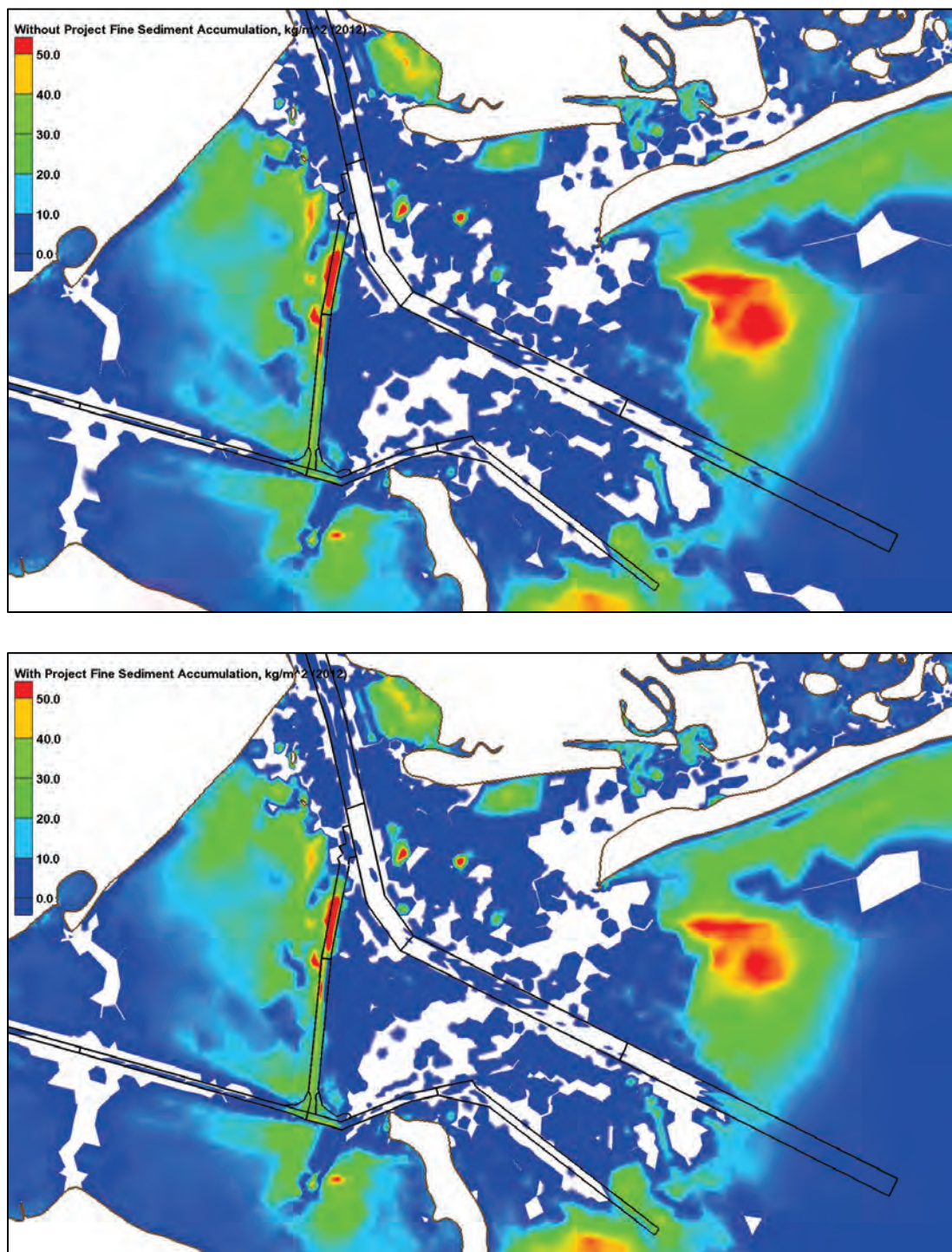




Figure 337. Without-project (top) and with-project (bottom) sand accumulation,  $\text{kg/m}^2$  (2012).

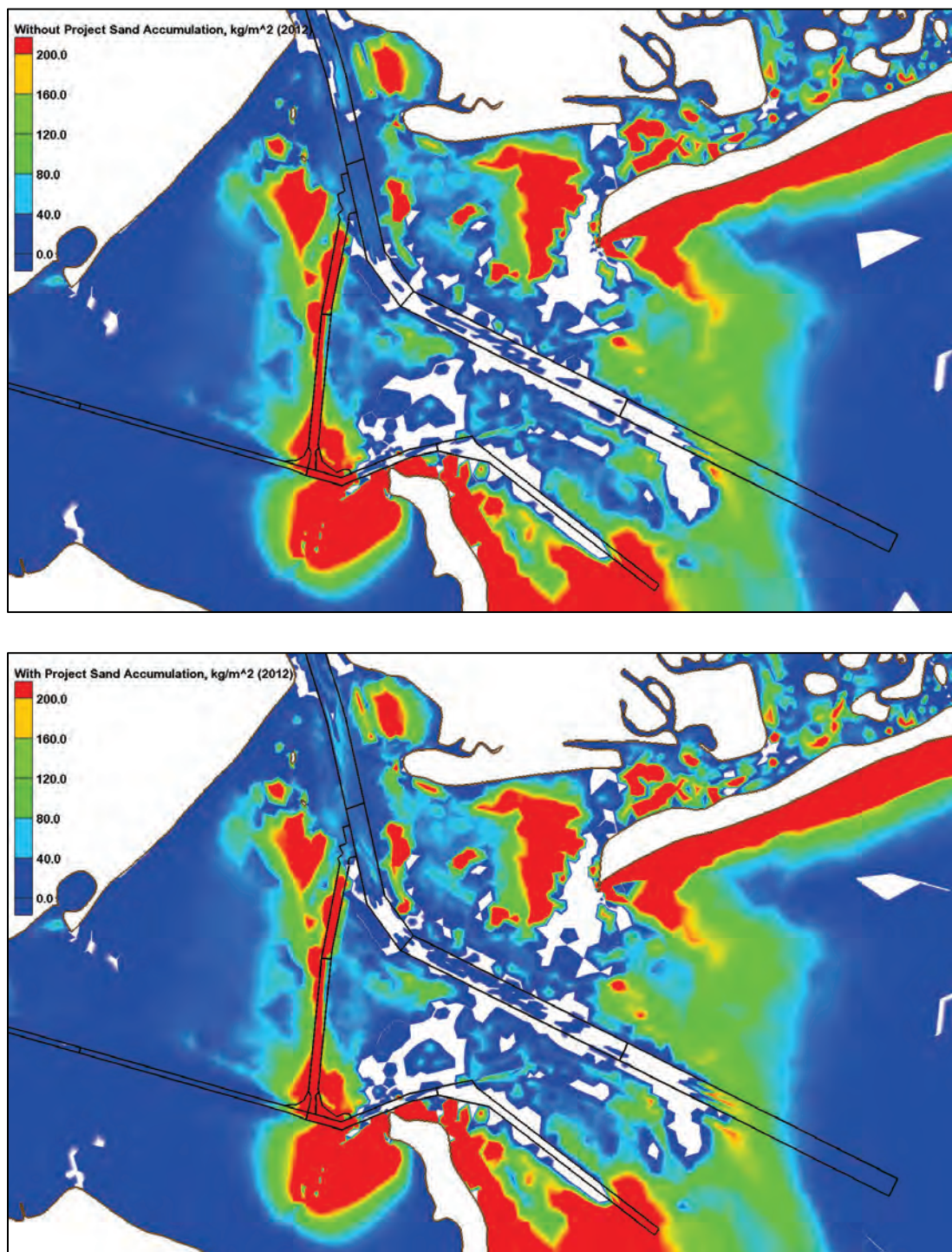


Figure 338. Dredge with-project/without-project percent differences (2012).

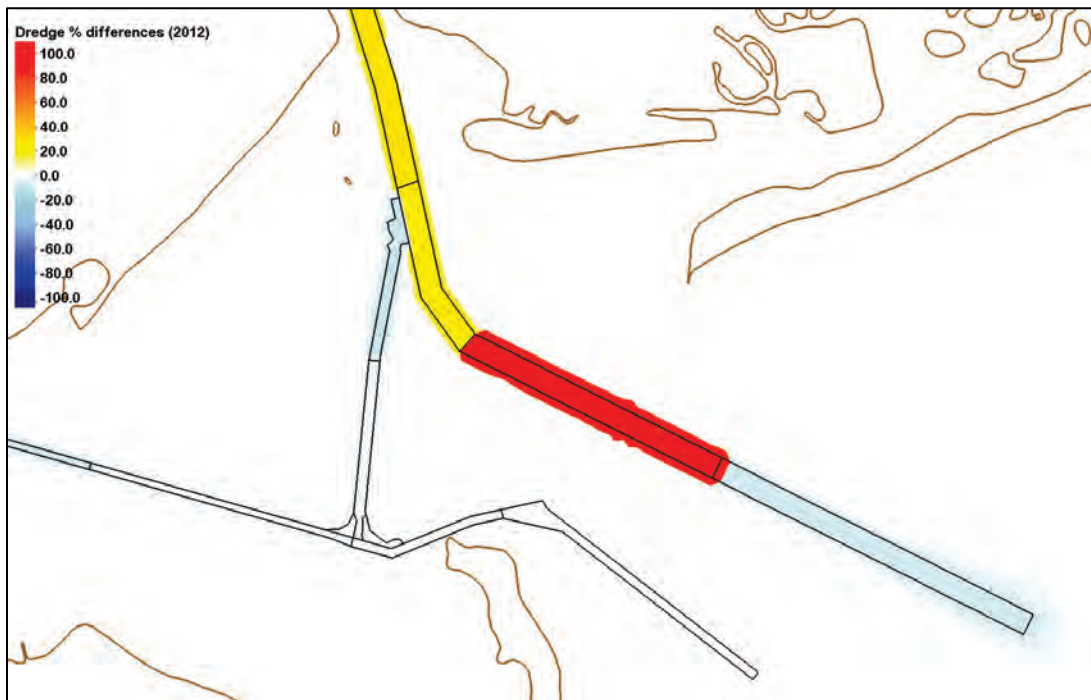


Table 37. Dredge volumes in Lower Bay (2012).

Depositional Volumes in Lower Bay, cy (2012)			
Reach	Without Project	With Project	With/Without Dredge Percentage
Ambrose Channel Reach A	191,714	173,980	91
Ambrose Channel Reach B	0	55	N/A
Ambrose Channel Reach C	12,088	15,297	127
Ambrose Channel Reach D	39,248	50,605	129
Main Ship	64,042	62,307	97
Main Ship Reach A	225,162	200,474	89
Main Ship Reach B	293,451	284,928	97
Sandy Hook Reach A	89,848	89,724	100
Sandy Hook Reach B	134,060	132,788	99
NY&NJ Channels Reach S	28,982	28,225	97
NY&NJ Channels Reach V	38,676	37,442	97



## Newark Bay, Kill van Kull, and Upper Bay results

Figure 339. Without-project (top) and with-project (bottom) average shear stresses, Pa (2012).

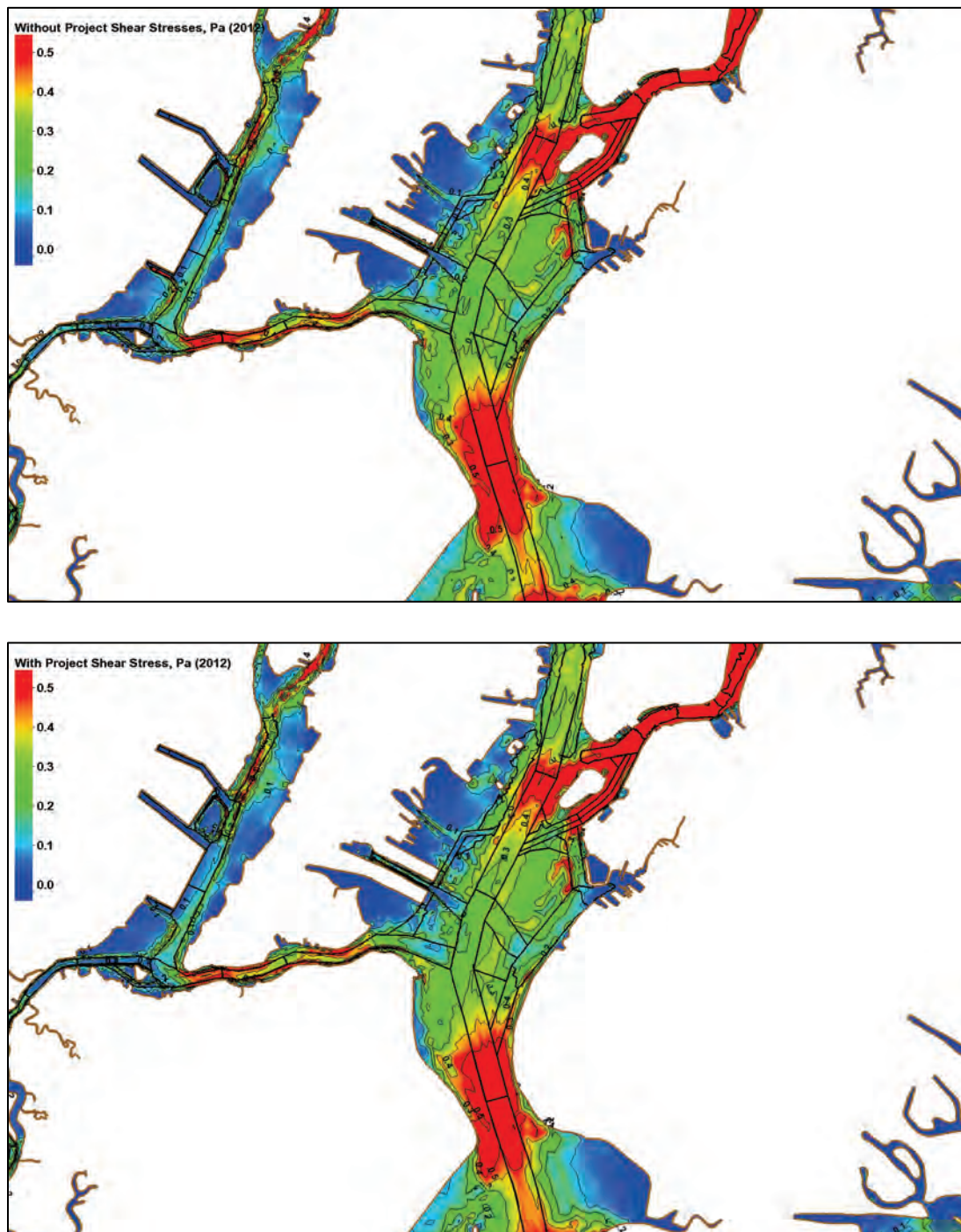


Figure 340. Without-project (top) and with-project (bottom) average bottom salinity, ppt (2012).

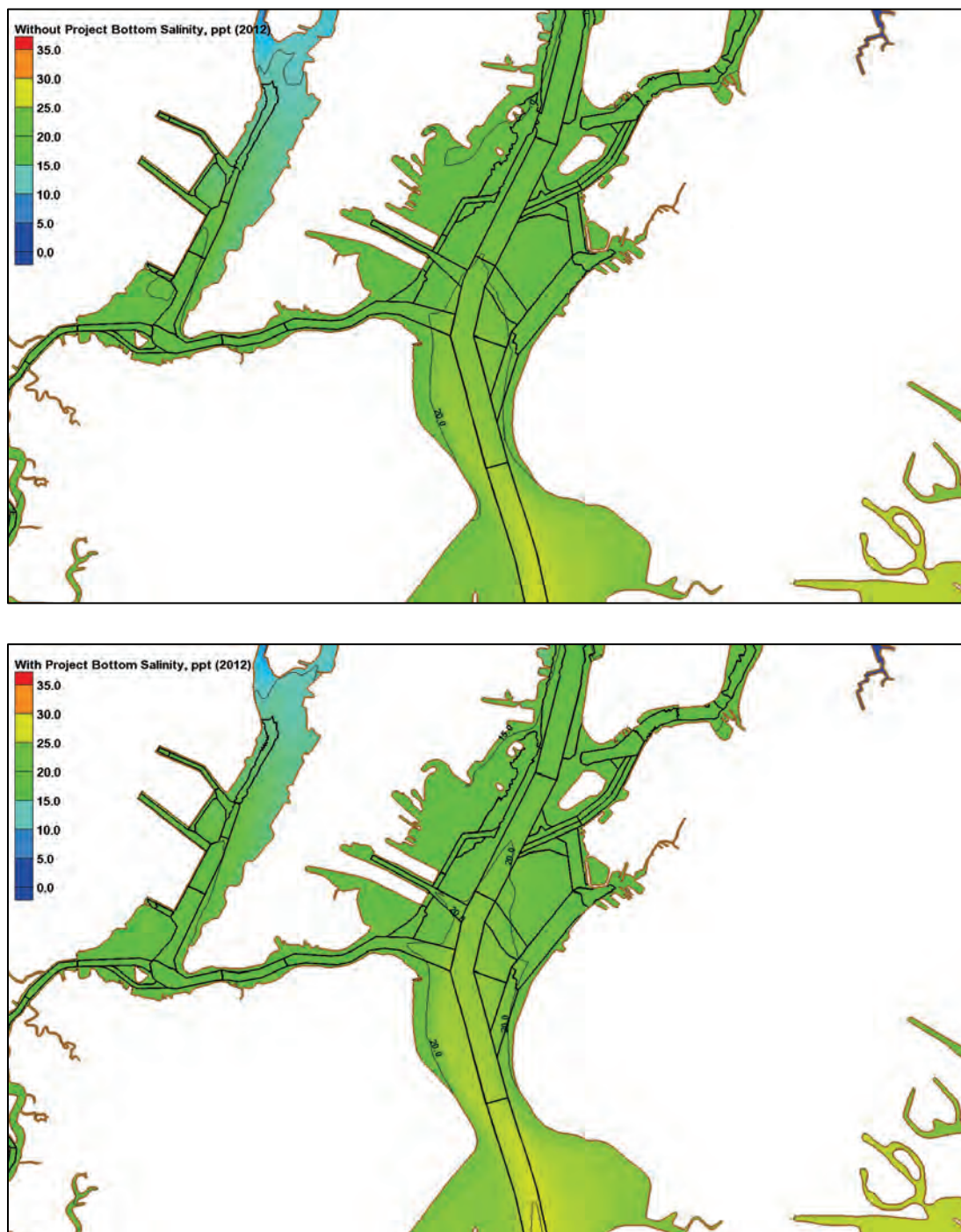


Figure 341. Without-project (top) and with-project (bottom) average fine sediment bottom concentrations, ppm (2012).

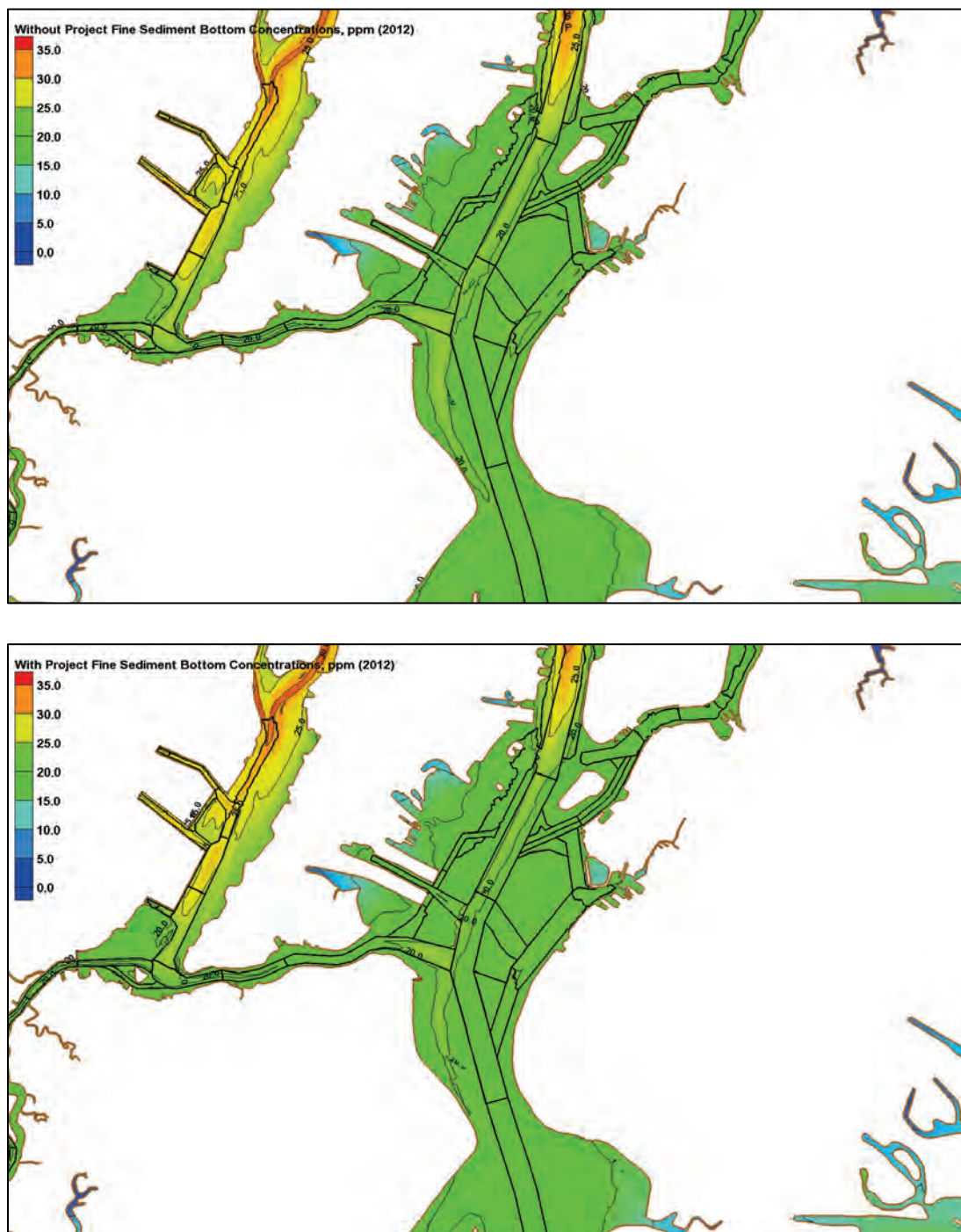




Figure 342. Without-project (top) and with-project (bottom) average sand bottom concentrations, ppm (2012).

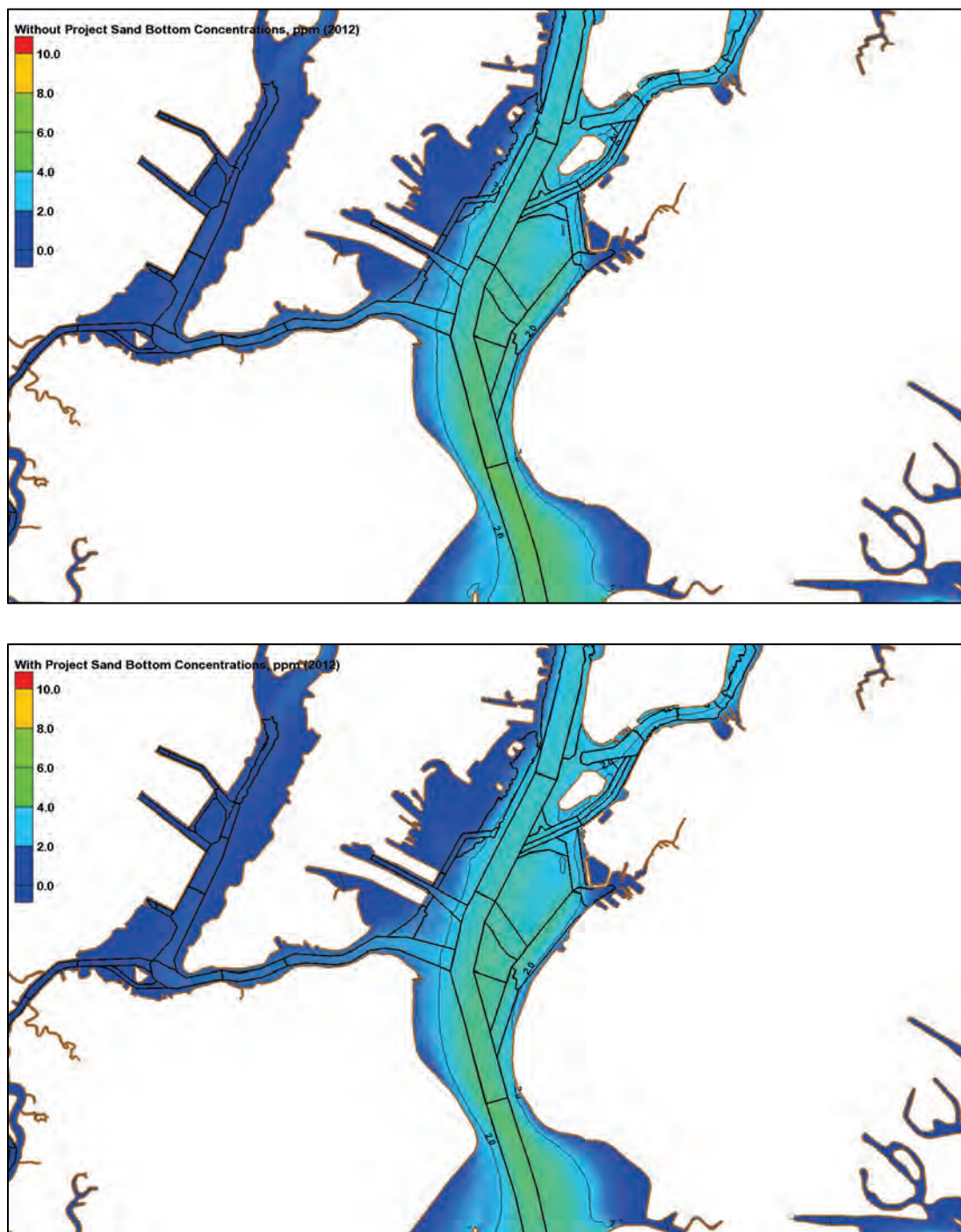




Figure 343. Without-project (top) and with-project (bottom) bed displacement, m (2012).

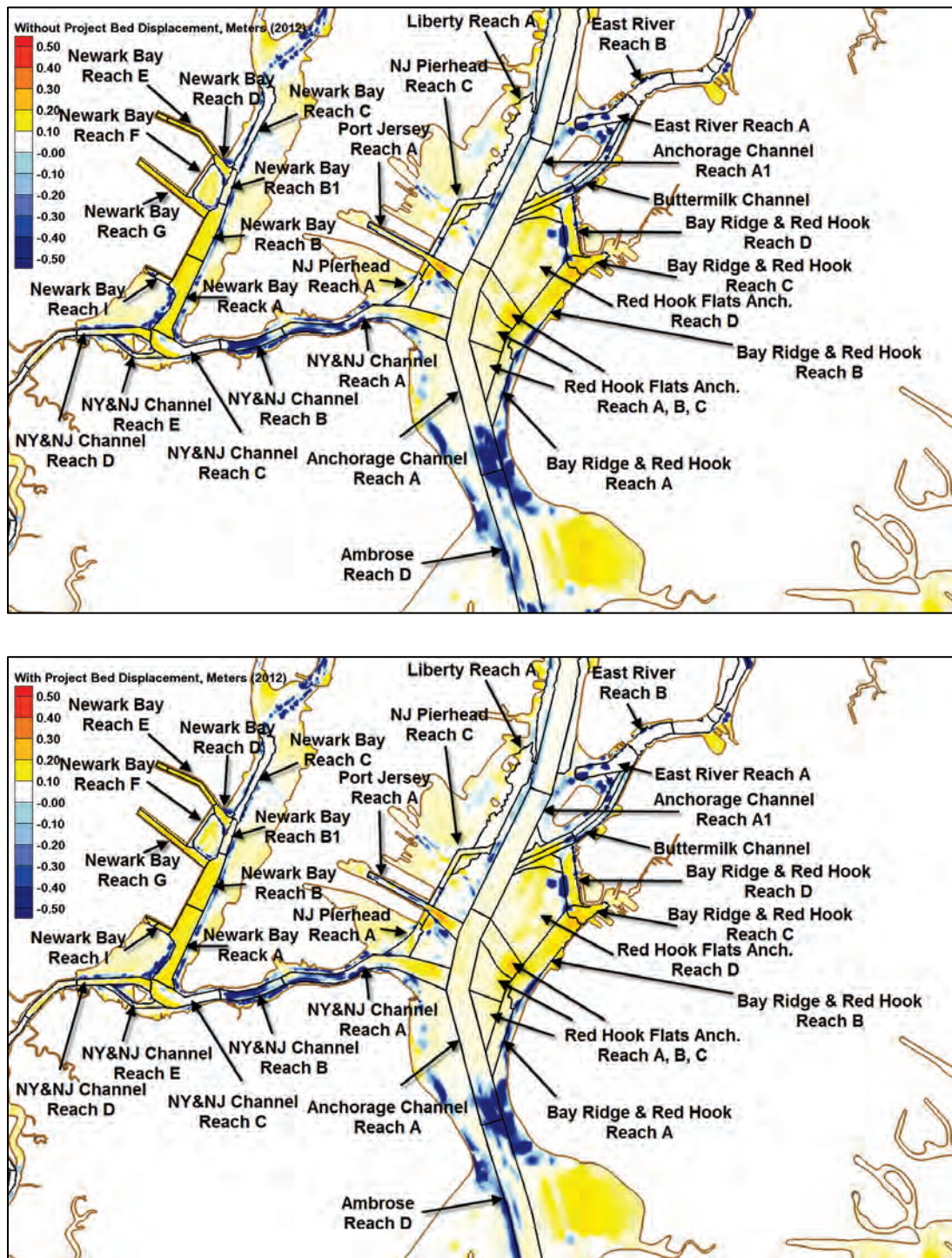


Figure 344. Without-project (top) and with-project (bottom) fine sediment accumulation,  $\text{kg}/\text{m}^2$  (2012).

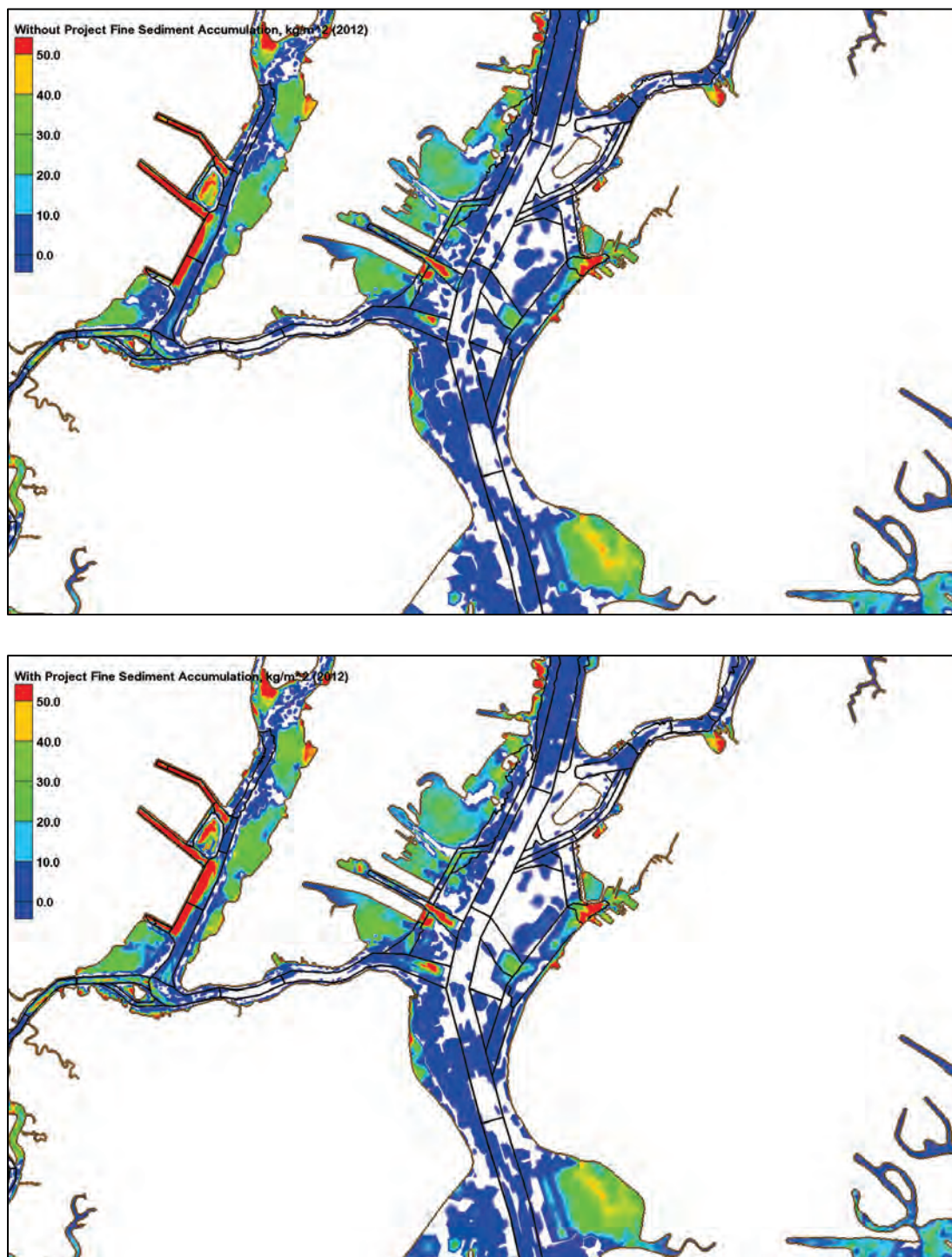




Figure 345. Without-project (top) and with-project (bottom) sand accumulation,  $\text{kg/m}^2$  (2012).

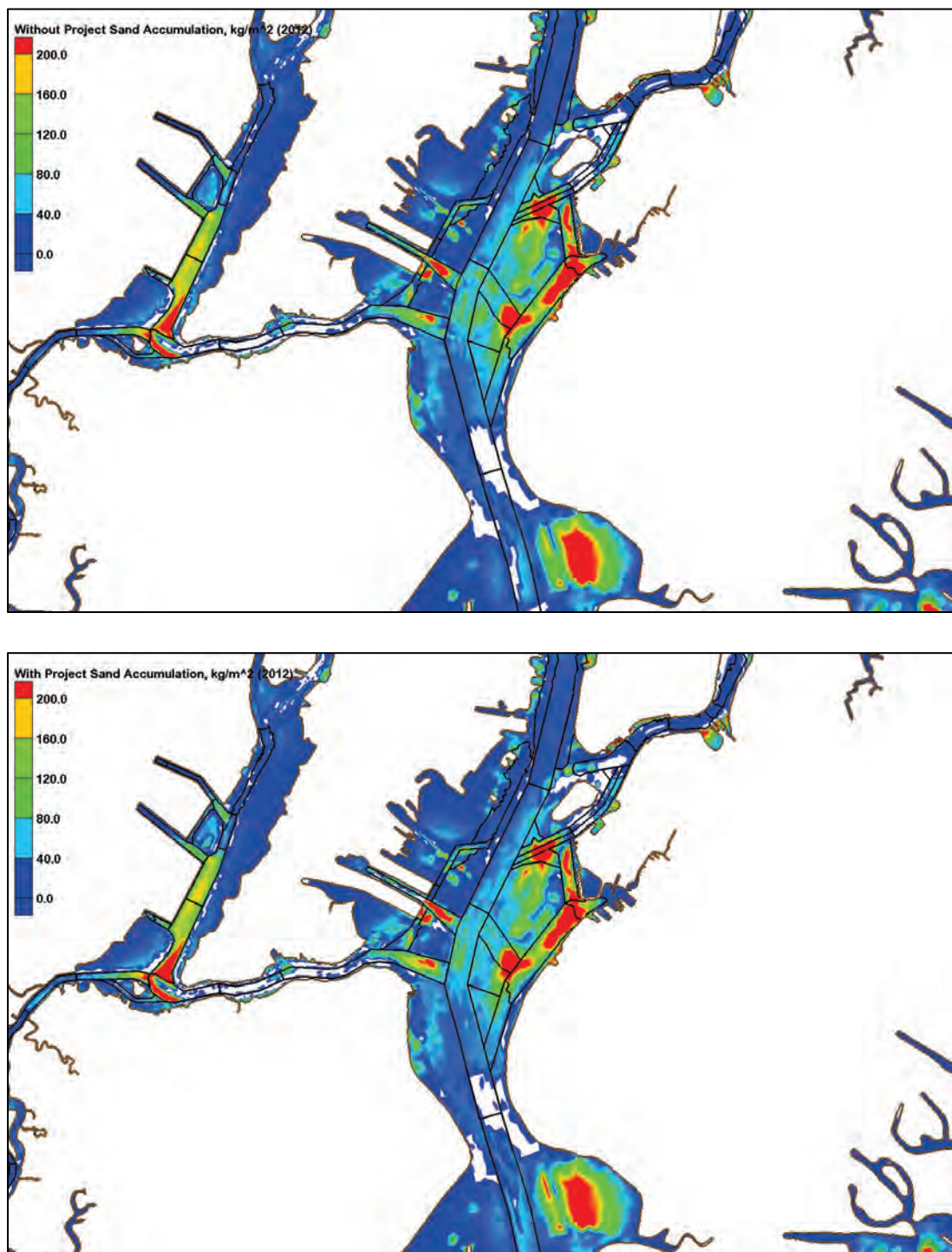
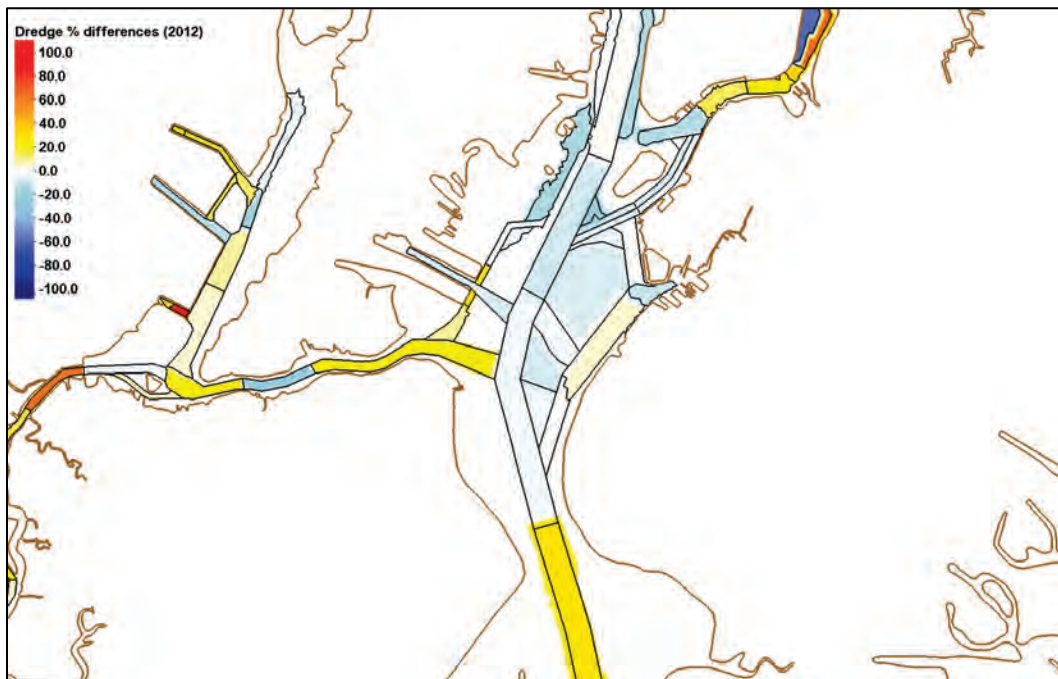


Figure 346. Dredge with-project/without-project percent differences (2012).





**Table 38. Dredge volumes in Newark Bay, Kill van Kull, and Upper Bay (2012).**

<b>Depositional Volumes in Newark Bay, Kill van Kull, and Upper Bay, cy (2012)</b>			
<b>Reach</b>	<b>Without Project</b>	<b>With Project</b>	<b>With/Without Dredge Percentage</b>
<b>Newark Bay</b>			
Newark Bay Reach A	132,574	137,619	104
Newark Bay Reach B	87,238	93,803	108
Newark Bay Reach B1	3,839	3,088	80
Newark Bay Reach C	2,131	2,034	95
Newark Bay Reach D	14,445	16,109	112
Newark Bay Reach E	22,738	26,199	115
Newark Bay Reach E1	3,310	3,875	117
Newark Bay Reach F	3,453	3,904	113
Newark Bay Reach G	67,863	57,735	85
Newark Bay Reach I	2,821	6,395	227
Newark Bay Reach I1	2,262	3,006	102
<b>Kill van Kull</b>			
NY&NJ Channels Reach A	57,649	68,101	118
NY&NJ Channels Reach B	1,513	1,136	75
NY&NJ Channels Reach C	37,967	44,703	118
<b>Upper Bay</b>			
Anchorage Channel Reach A	68,389	66,433	97
Anchorage Channel Reach A1	37,139	33,485	90
Anchorage Reach C1	8,295	7,970	96
Bay Ridge & Red Hook Reach A	21,676	21,668	100
Bay Ridge & Red Hook Reach B	166,141	172,801	104
Bay Ridge & Red Hook Reach C	56,922	50,402	89
Bay Ridge & Red Hook Reach D	55,422	55,717	101
Red Hook Flats Anch. Reach A	22,465	21,700	97
Red Hook Flats Anch. Reach B	48,265	44,034	91
Red Hook Flats Anch. Reach C	70,280	68,015	97
Red Hook Flats Anch. Reach D	146,744	135,065	92
Port Jersey Reach A	57,080	52,435	92
NJ Pierhead Ch. Reach A	12,135	13,100	108
NJ Pierhead Ch. Reach B	8,371	10,139	121
NJ Pierhead Reach C	10,827	10,746	99
Liberty Reach A	10,687	8,821	83

## Arthur Kill and Raritan Bay results

Figure 347. Without-project (top) and with-project (bottom) average shear stresses, Pa (2012).

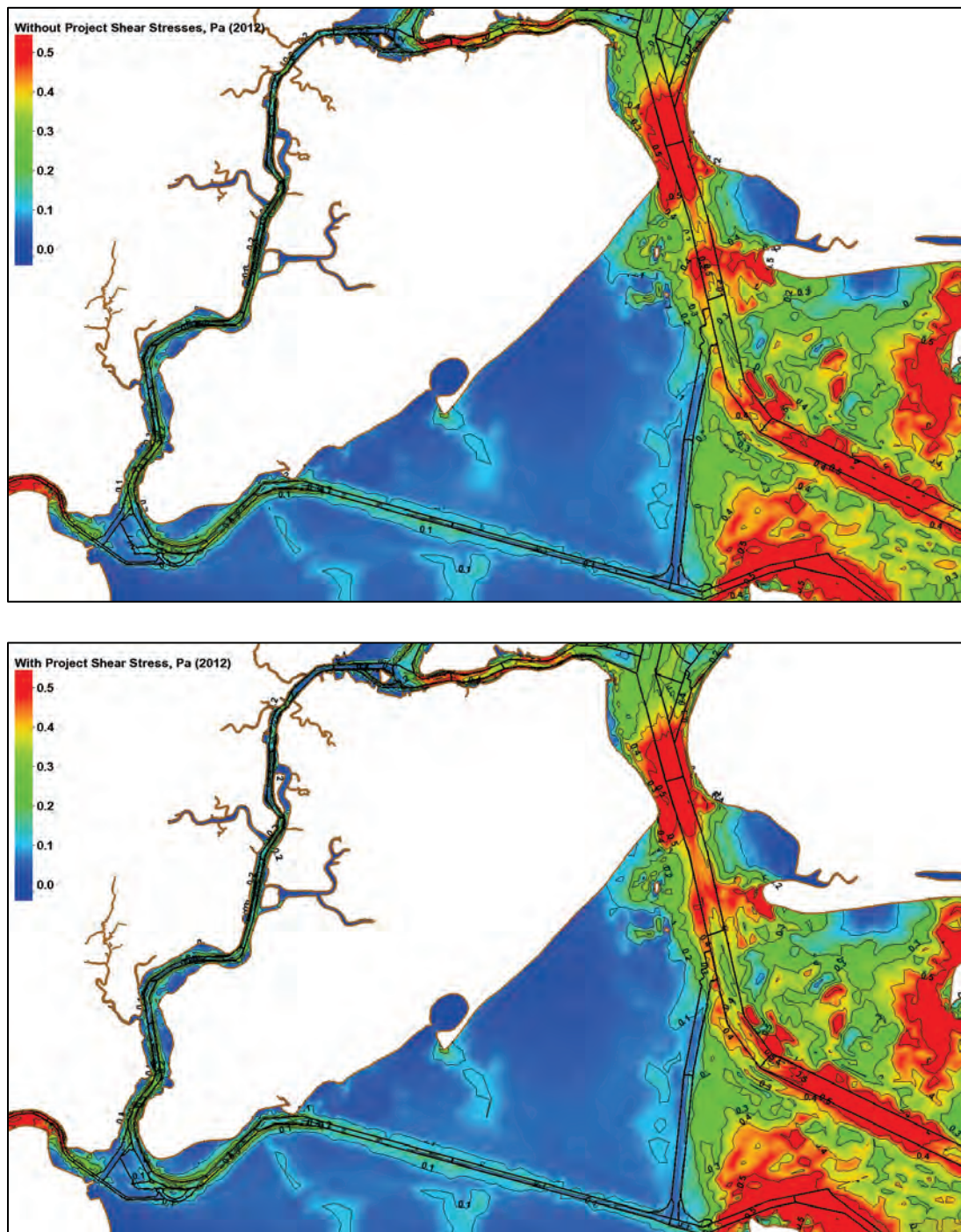


Figure 348. Without-project (top) and with-project (bottom) average bottom salinity, ppt (2012).

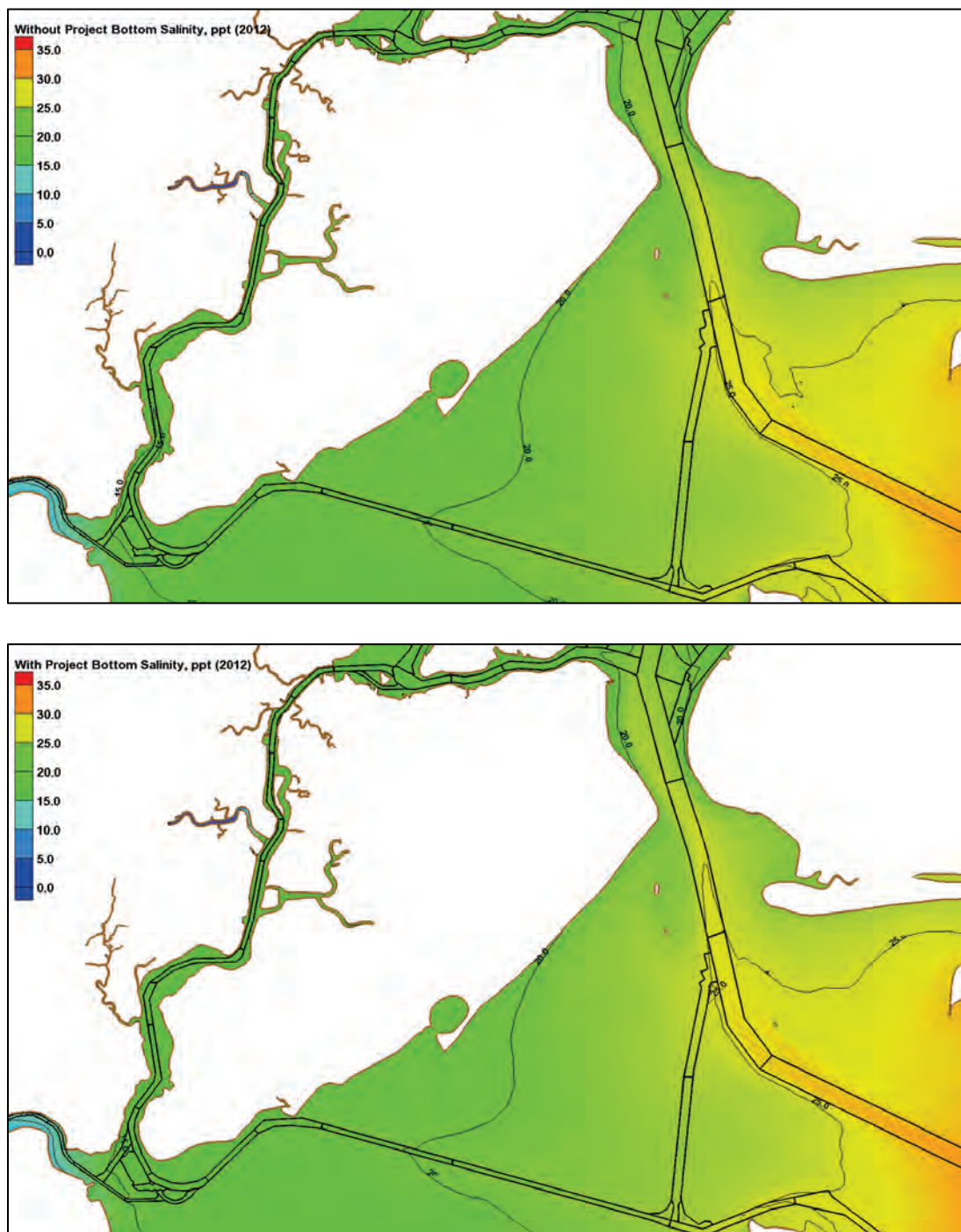




Figure 349. Without-project (top) and with-project (bottom) average fine sediment bottom concentrations, ppm (2012).

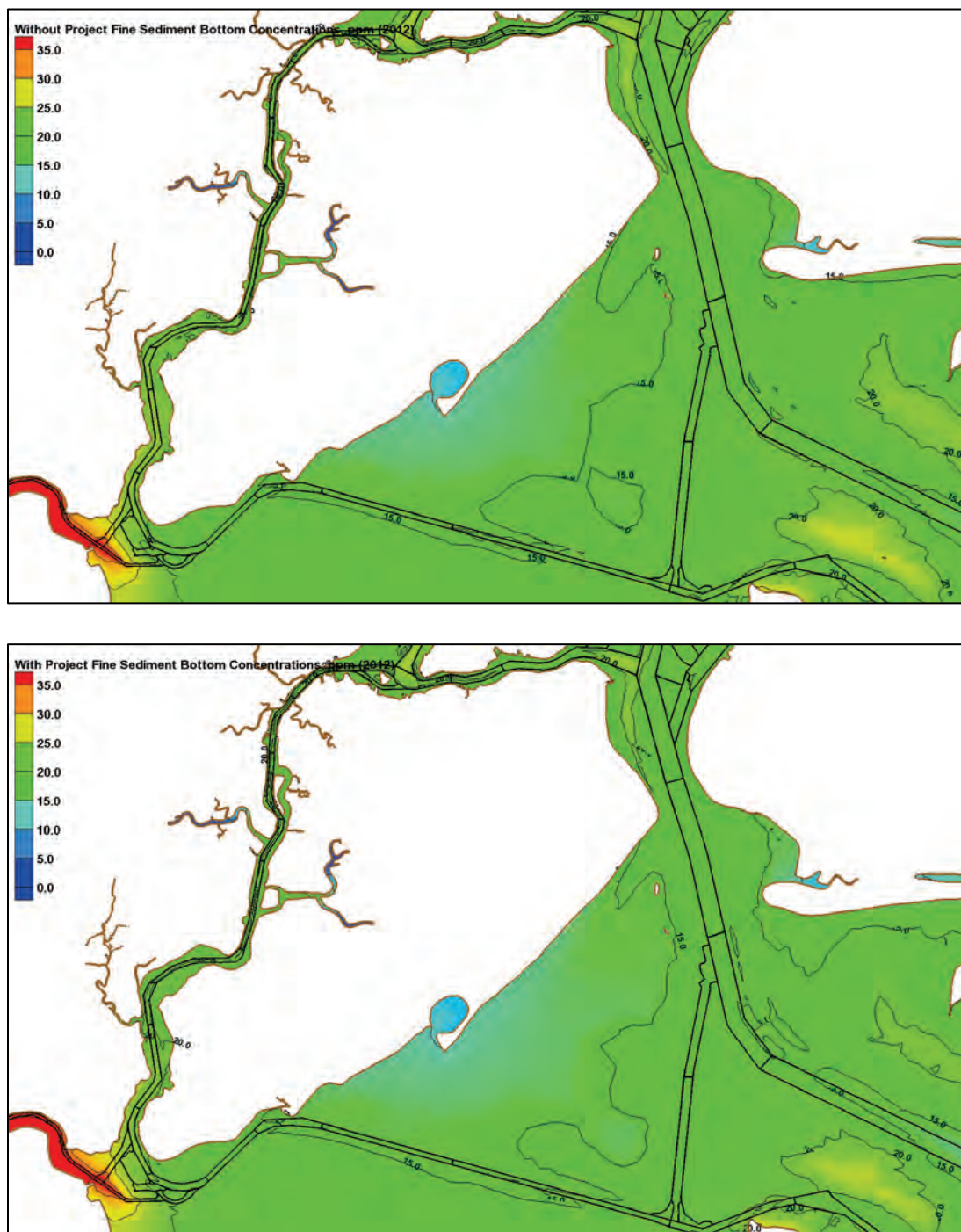




Figure 350. Without-project (top) and with-project (bottom) average sand bottom concentrations, ppm (2012).

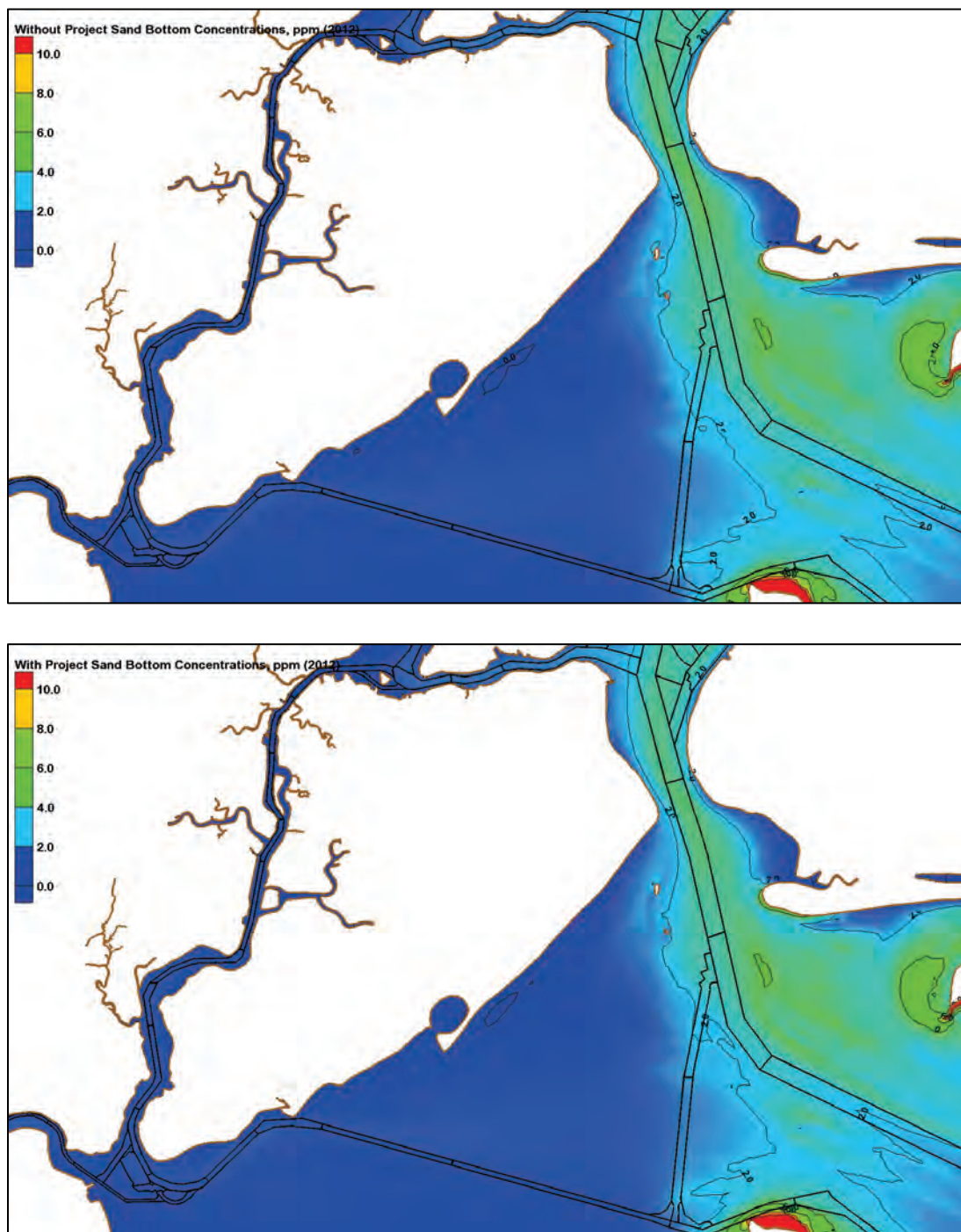


Figure 351. Without-project (top) and with-project (bottom) bed displacement, m (2012).

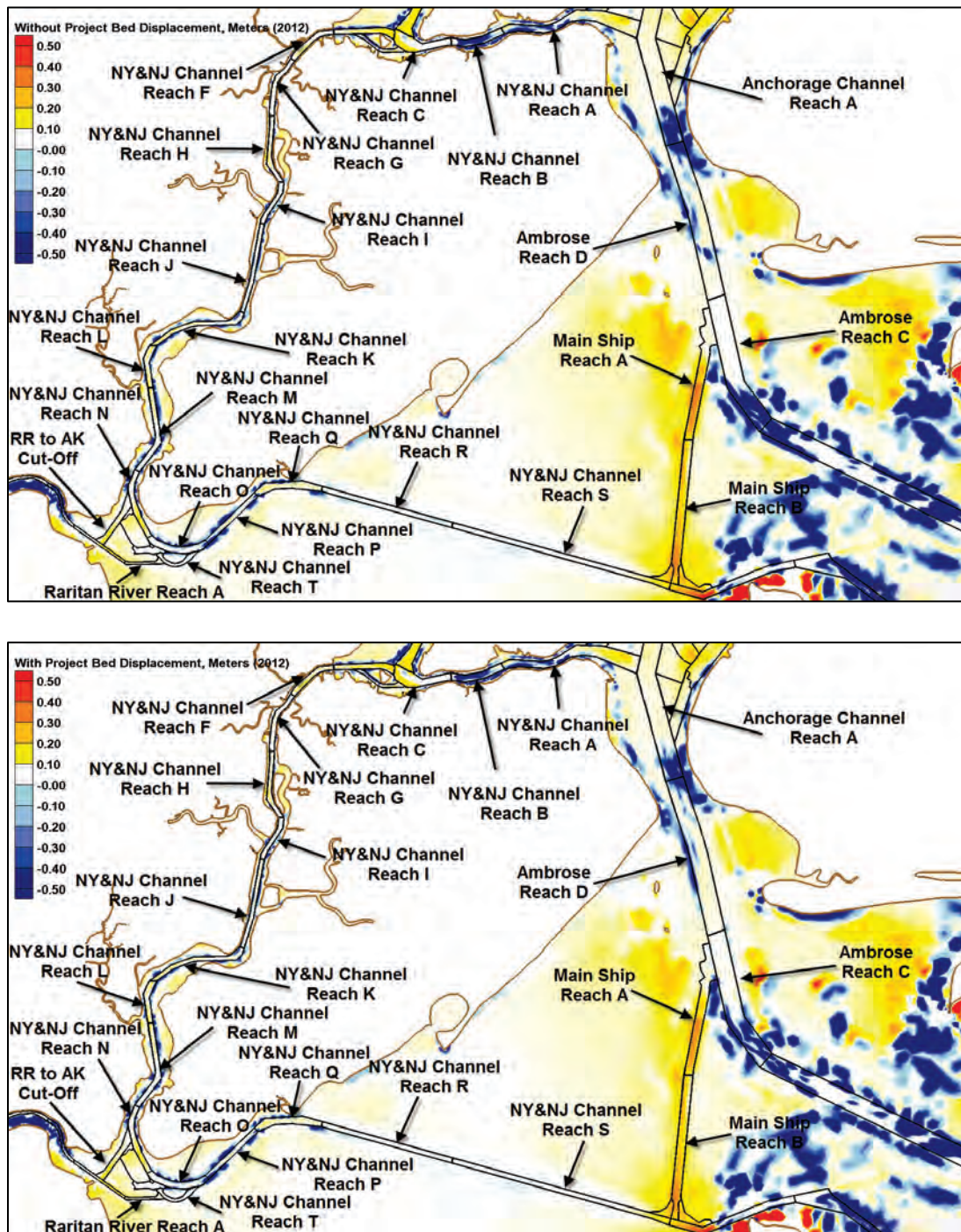




Figure 352. Without-project (top) and with-project (bottom) fine sediment accumulation,  $\text{kg/m}^2$  (2012).

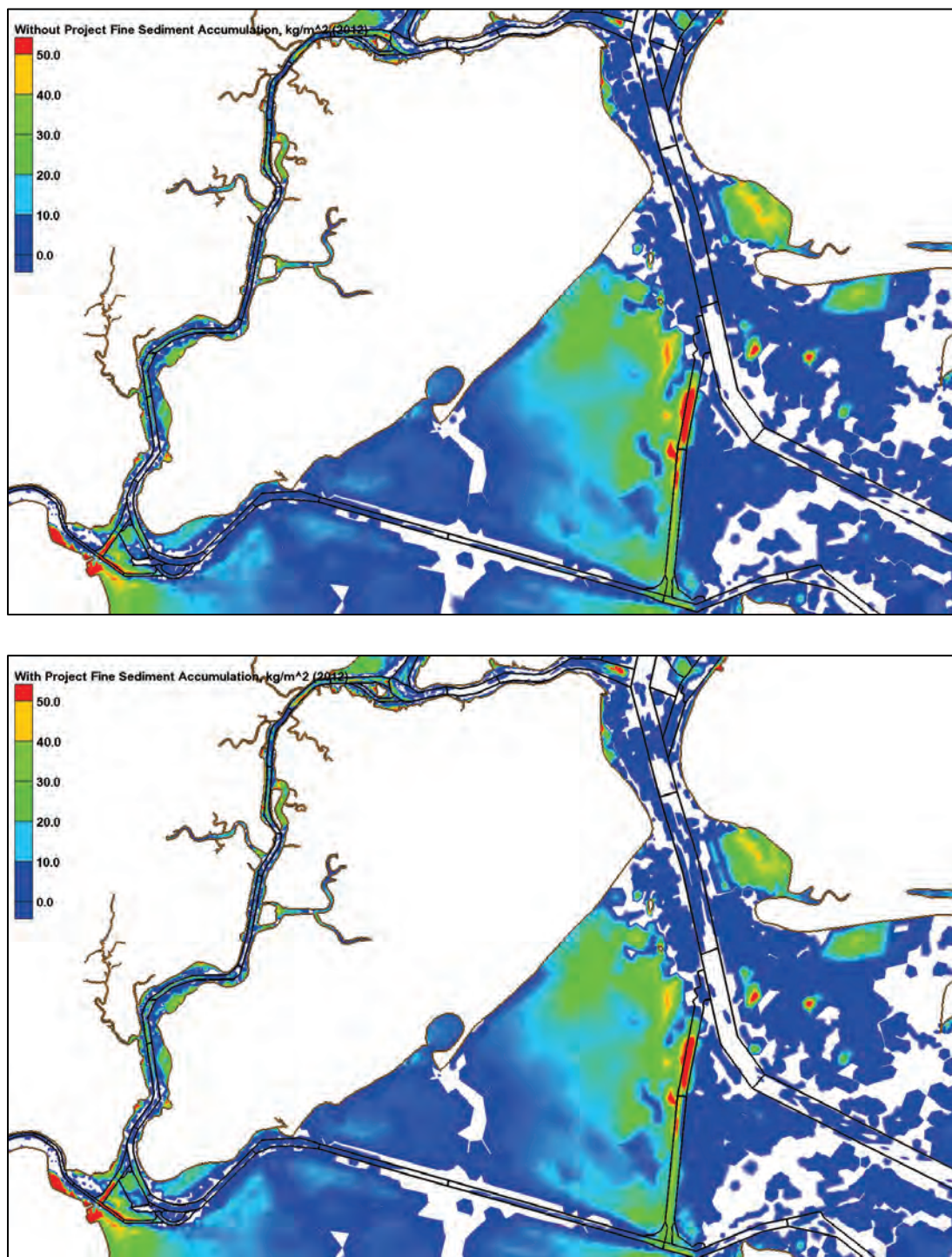


Figure 353. Without-project (top) and with-project (bottom) sand accumulation,  $\text{kg}/\text{m}^2$  (2012).

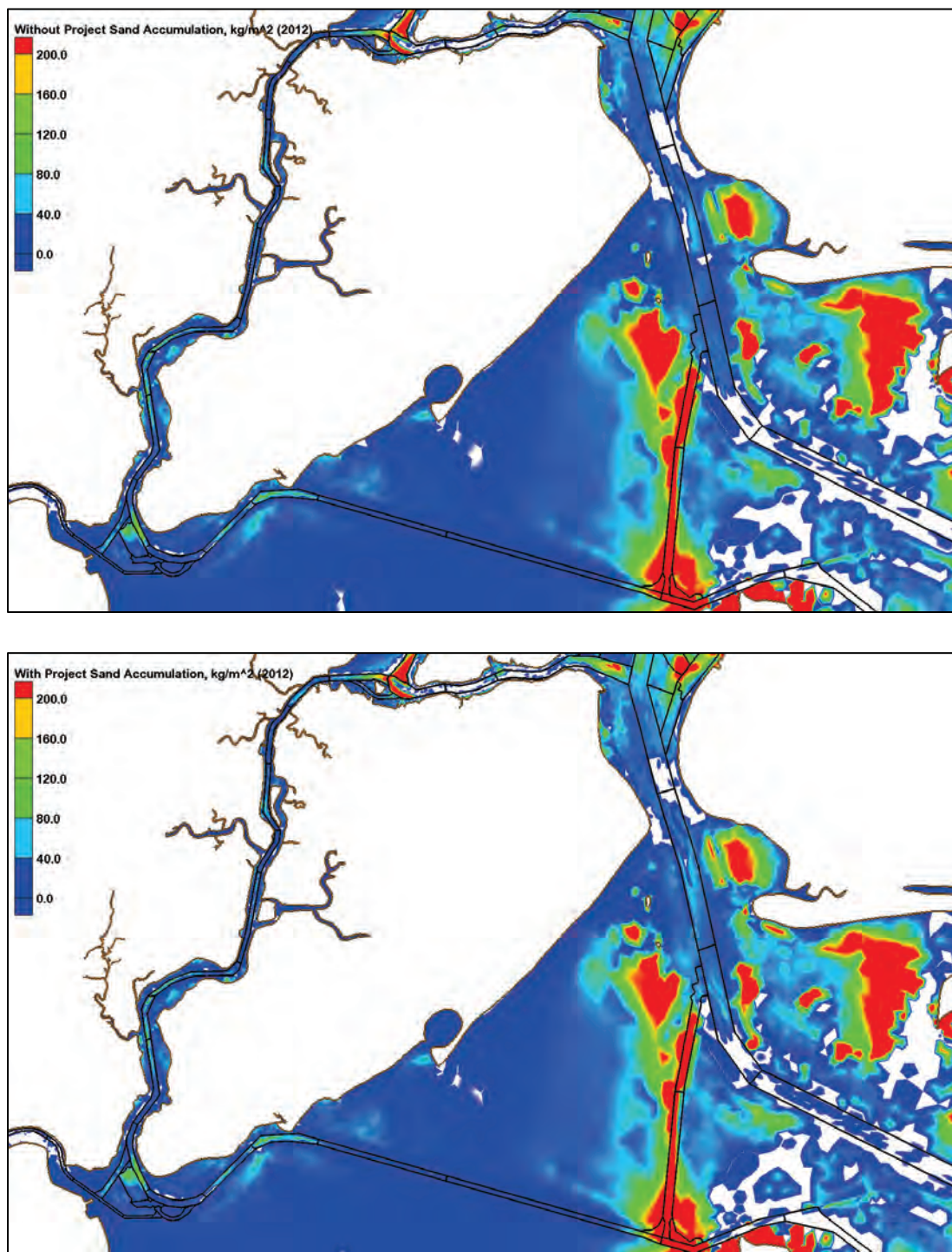




Figure 354. Dredge with-project/without-project percent differences (2012).

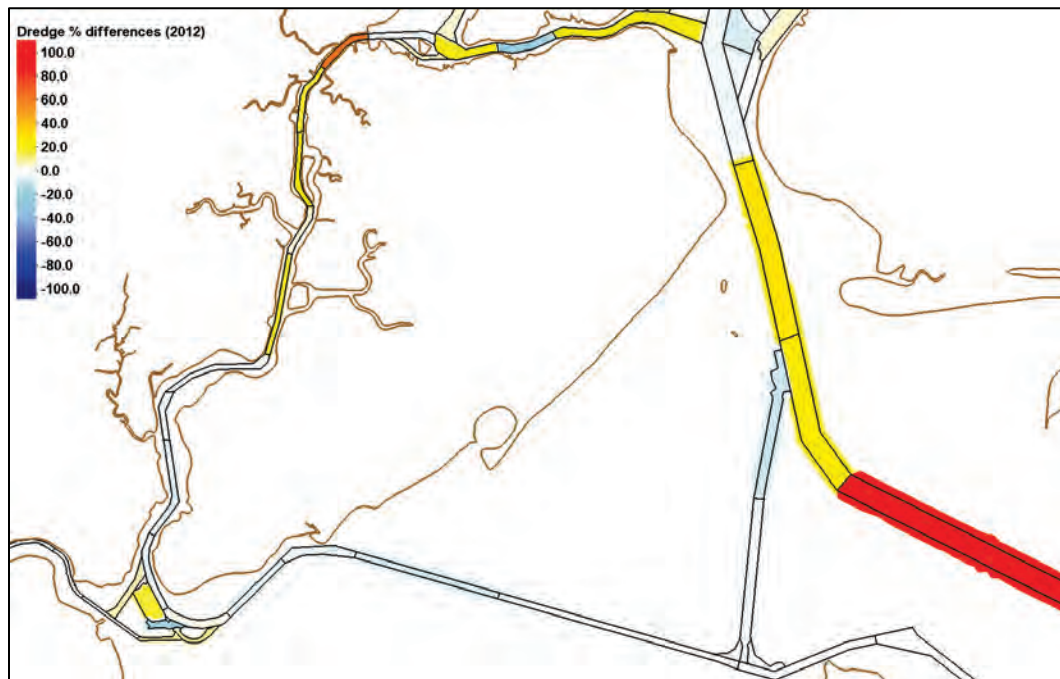


Table 39. Dredge volumes for Arthur Kill and Raritan Bay (2012).

Depositional Volumes in Arthur Kill and Raritan Bay, cy (2012)			
Reach	Without Project	With Project	With/Without Dredge Percentage
<b>Arthur Kill</b>			
NY&NJ Channels Reach D	27,935	26,814	96
NY&NJ Channels Reach E	4,892	5,162	106
NY&NJ Channels Reach F	6,126	9,889	161
NY&NJ Channels Reach G	1,902	2,179	115
NY&NJ Channels Reach H	5,886	7,066	120
NY&NJ Channels Reach I	1,131	1,174	104
NY&NJ Channels Reach J	3,778	4,357	115
NY&NJ Channels Reach K	10,650	10,322	97
NY&NJ Channels Reach L	9,412	9,038	96
NY&NJ Channels Reach M	9,150	8,577	94
NY&NJ Channels Reach N	17,080	16,097	94
<b>Raritan Bay</b>			
NY&NJ Channels Reach O	2,621	2,675	102
NY&NJ Channels Reach P	6,085	5,653	93
NY&NJ Channels Reach Q	15,060	14,467	96
NY&NJ Channels Reach R	2,078	1,889	91
NY&NJ Channels Reach T	862	938	109
RR to AK Cut-Off Reach A	14,758	15,646	106
Raritan River Reach A	3,210	3,464	108
Raritan River Reach B	8,301	8,423	101
Raritan River Reach C	369	375	102
Raritan River Reach D	220	209	95

## Appendix H: Difference Plots for the With- and Without-Project Bed Shears, Bottom Layer Salinity, Bottom Layer Fine Sediment Concentrations, and Bottom Layer Sand Concentrations

### Lower Bay results

Figure 355. With-minus without-project average bed shear stresses ( $\text{N/m}^2$ ) for 1985.

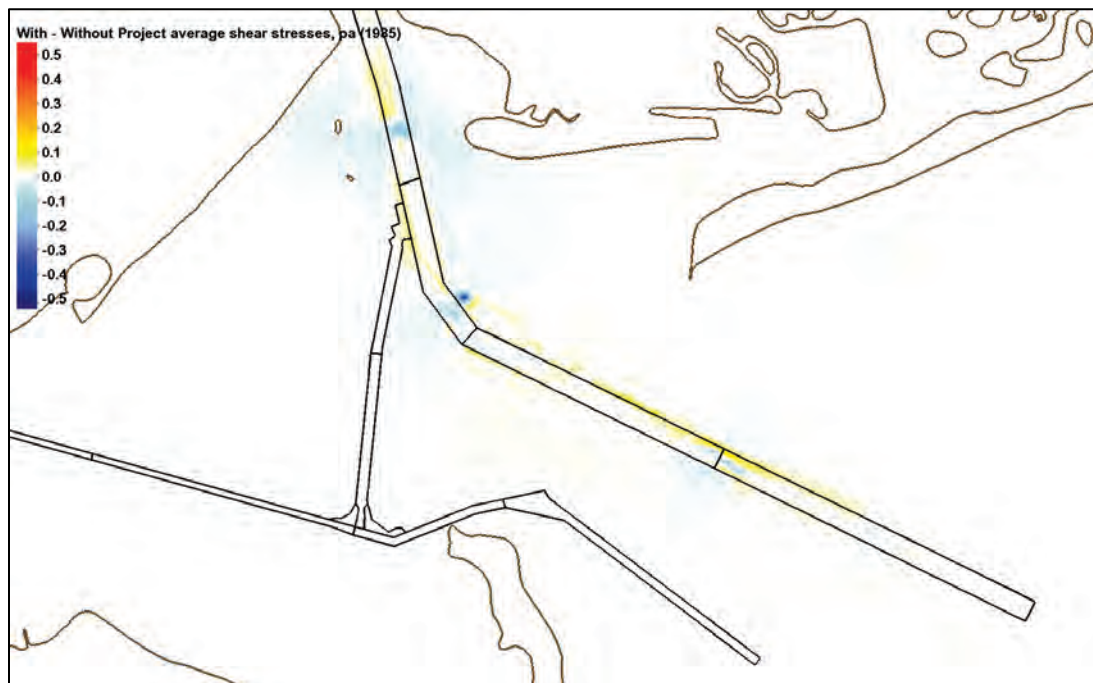


Figure 356. With- minus without-project average bed shear stresses ( $\text{N/m}^2$ ) for 1995.

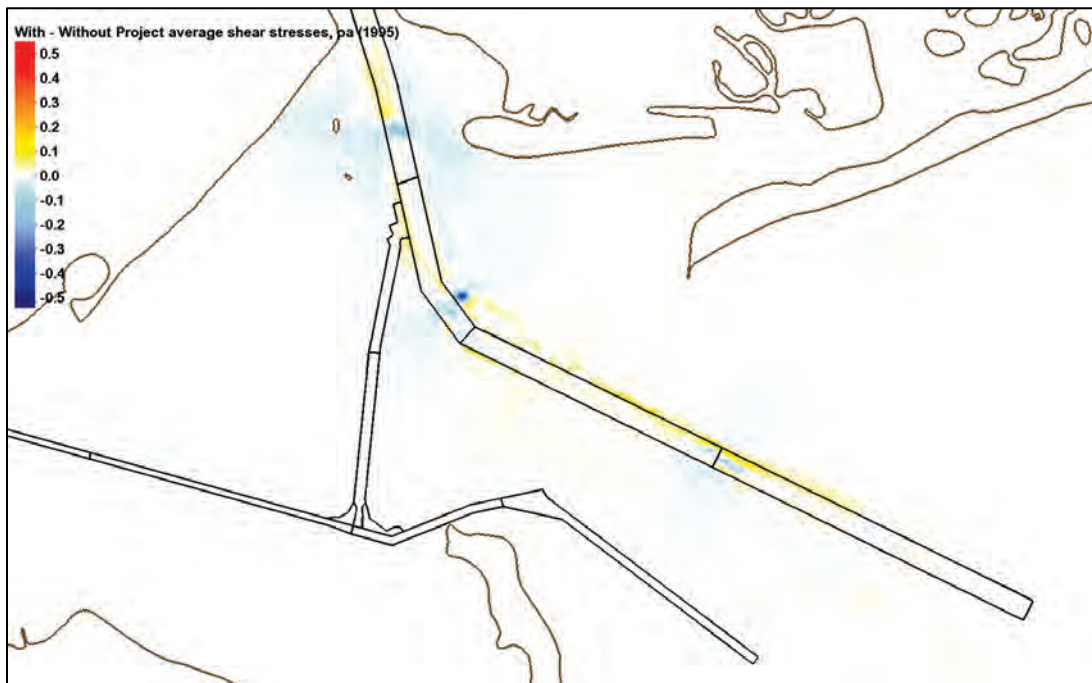


Figure 357. With- minus without-project average bed shear stresses ( $\text{N/m}^2$ ) for 1996.

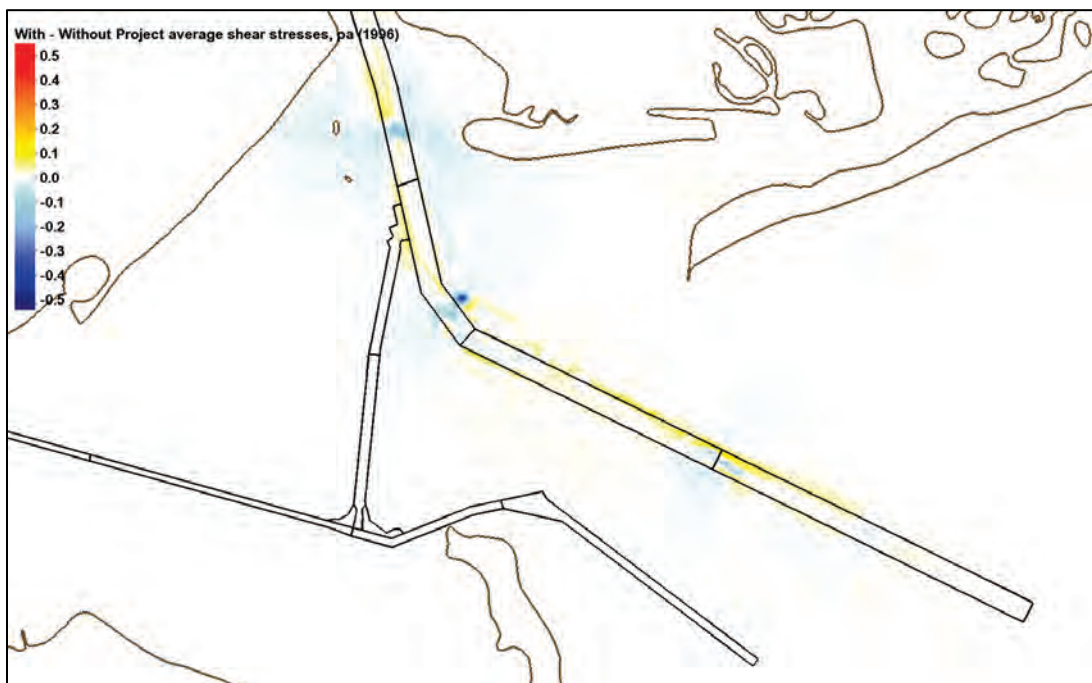




Figure 358. With- minus without-project average bed shear stresses ( $\text{N/m}^2$ ) for 2011.

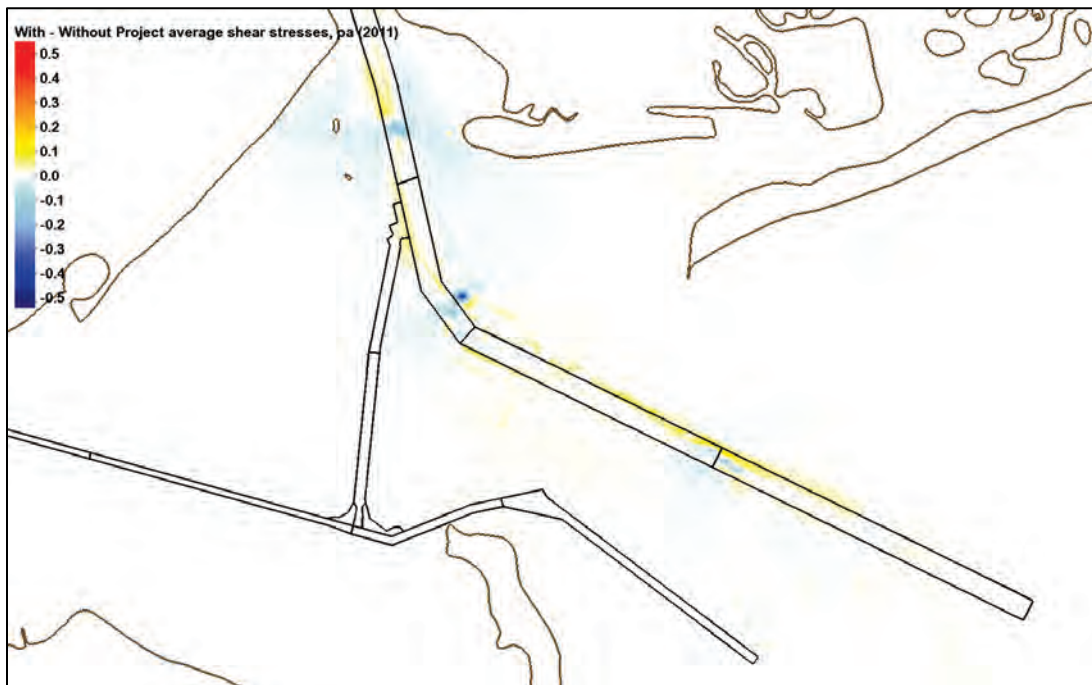


Figure 359. With- minus without-project average bed shear stresses ( $\text{N/m}^2$ ) for 2012.

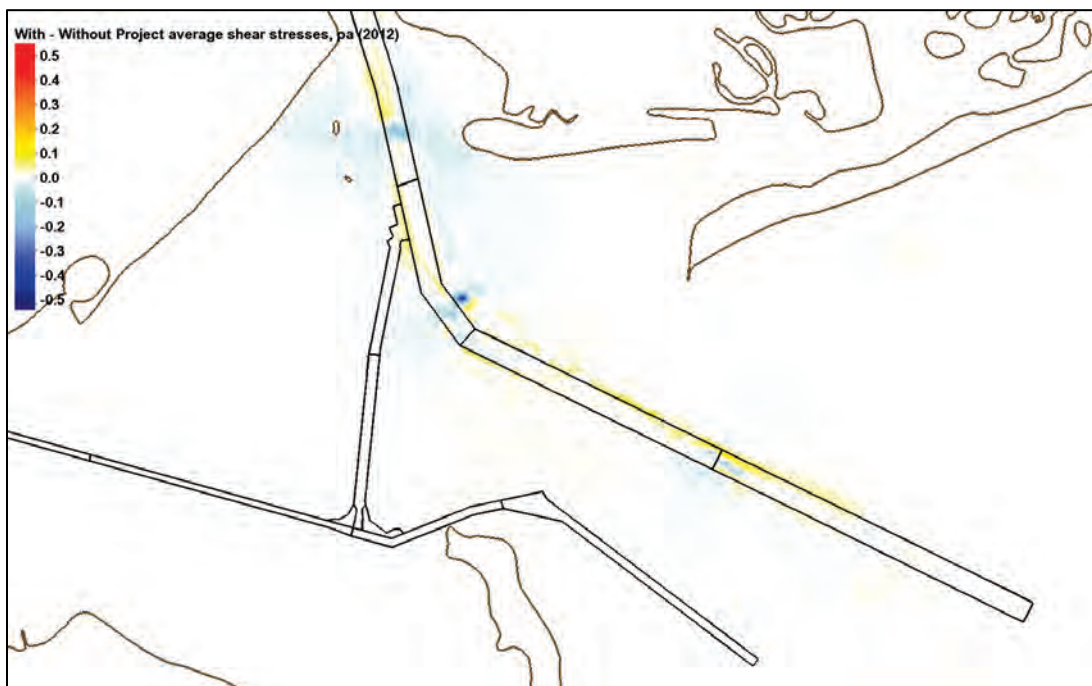


Figure 360. With- minus without-project average bottom layer salinity values (ppt) for 1985.

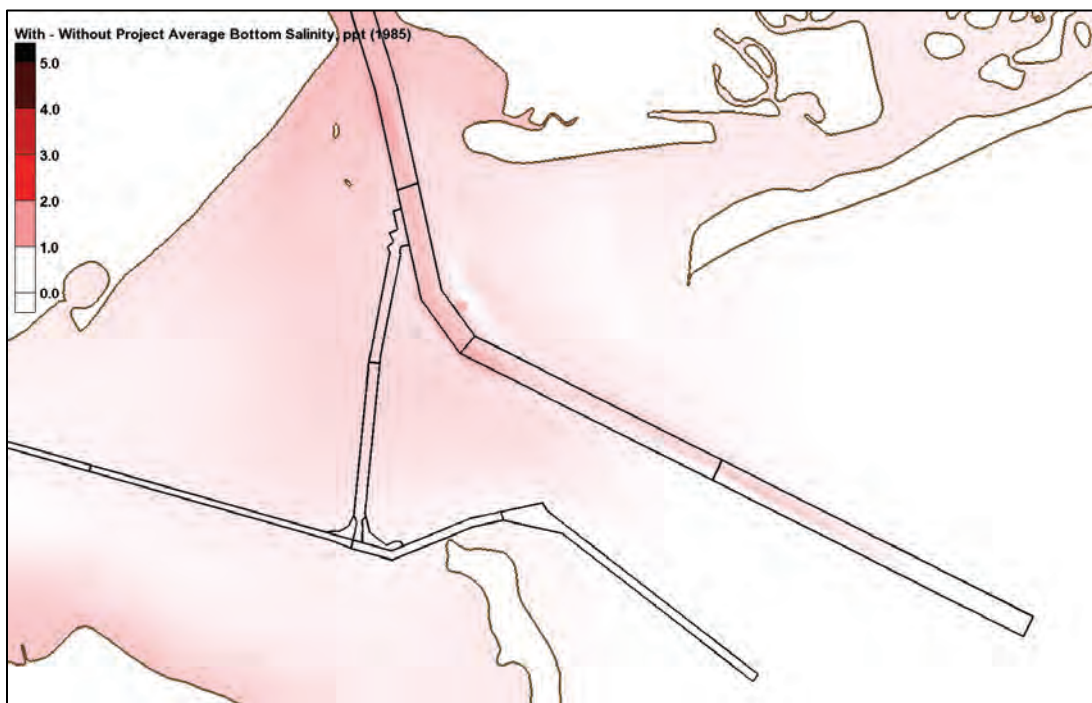


Figure 361. With- minus without-project average bottom layer salinity values (ppt) for 1995.

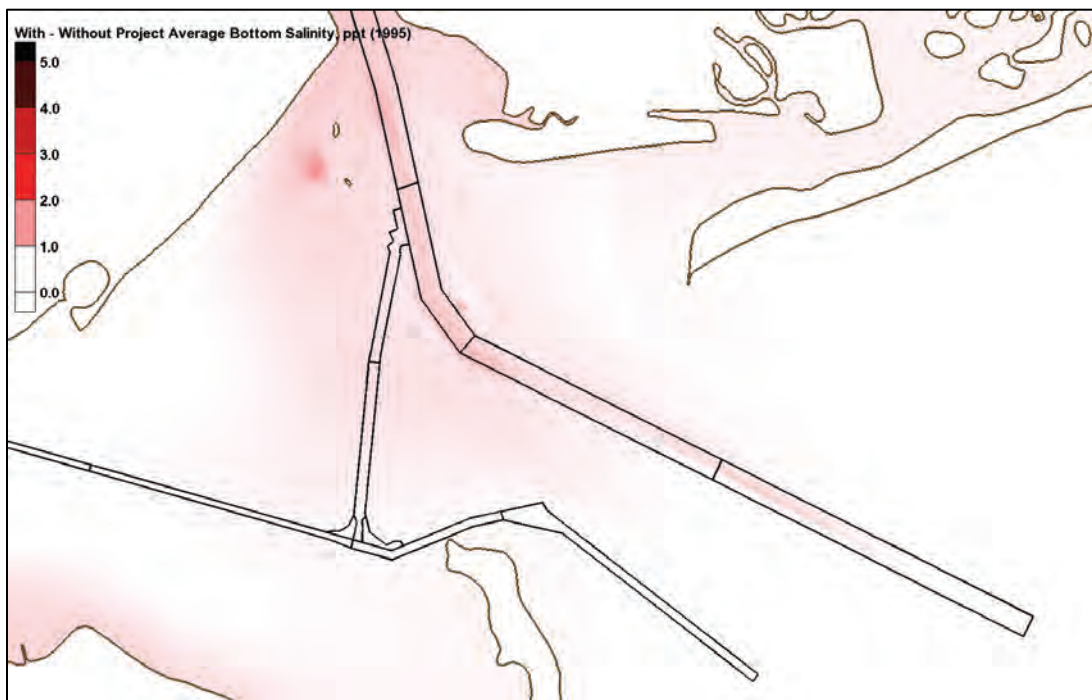


Figure 362. With- minus without-project average bottom layer salinity values (ppt) for 1996.

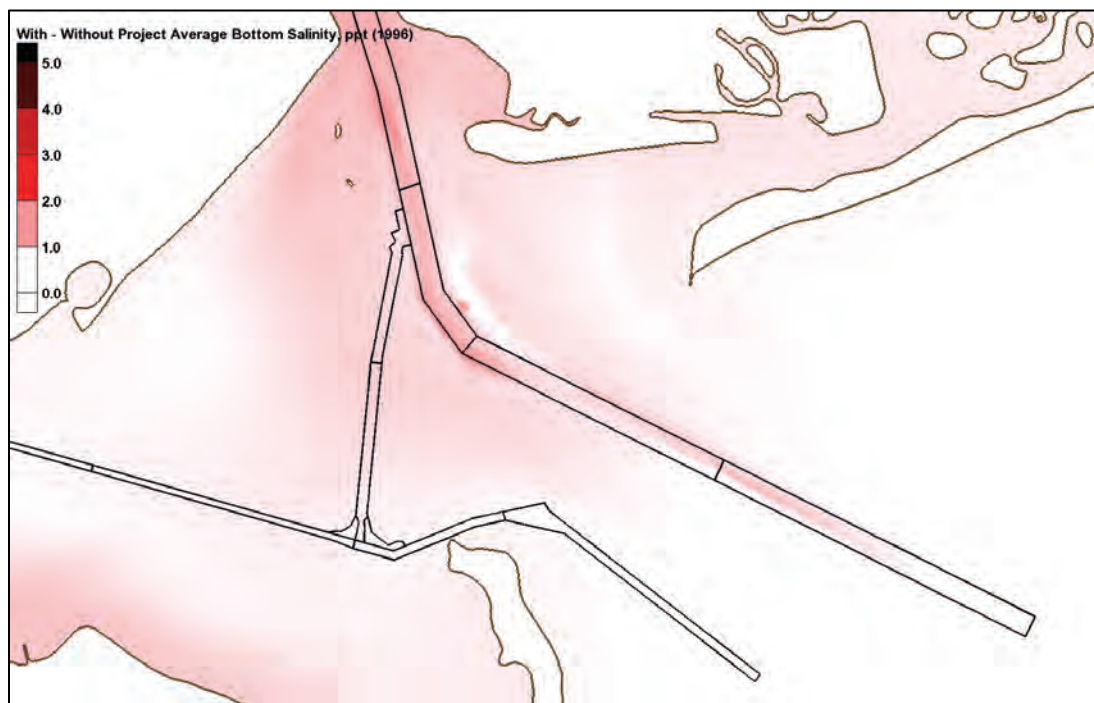


Figure 363. With- minus without-project average bottom layer salinity values (ppt) for 2011.

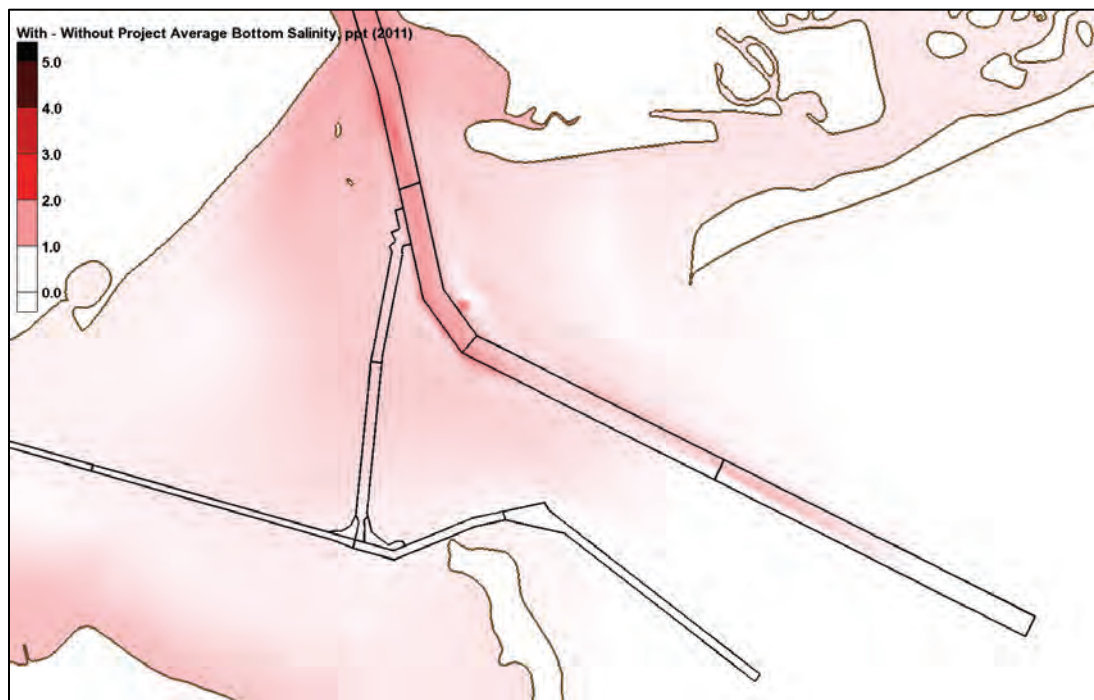




Figure 364. With- minus without-project average bottom layer salinity values (ppt) for 2012.

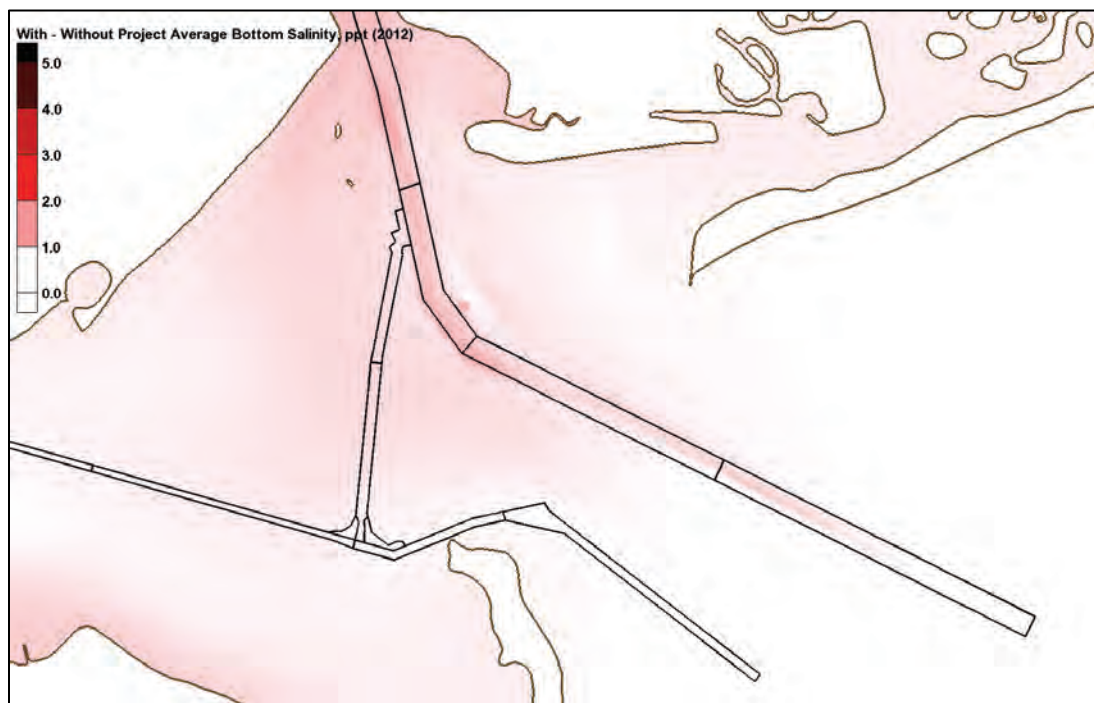


Figure 365. With- minus without-project average bottom layer fine sediment concentrations (ppm) for 1985.

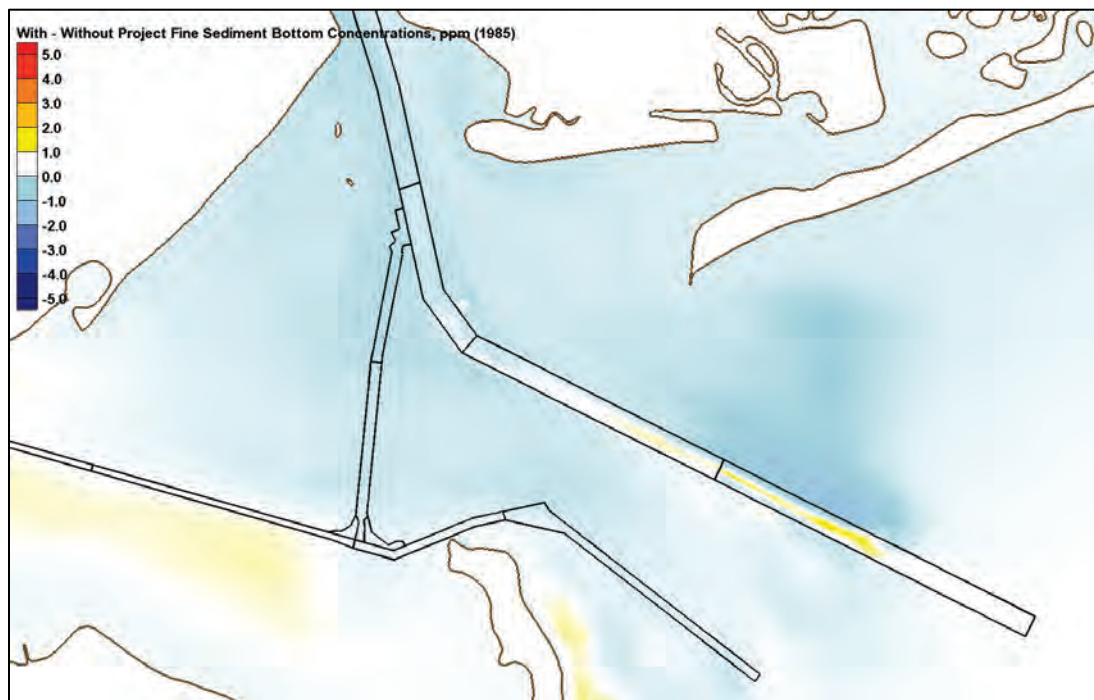




Figure 366. With- minus without-project average bottom layer fine sediment concentrations (ppm) for 1995.

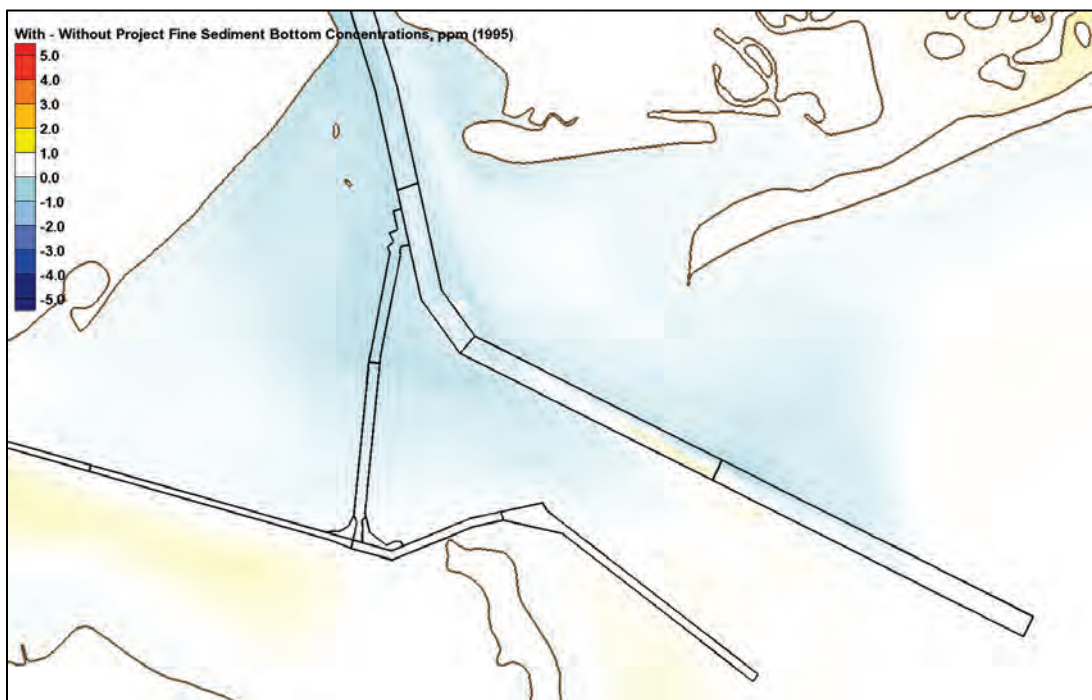


Figure 367. With- minus without-project average bottom layer fine sediment concentrations (ppm) for 1996.

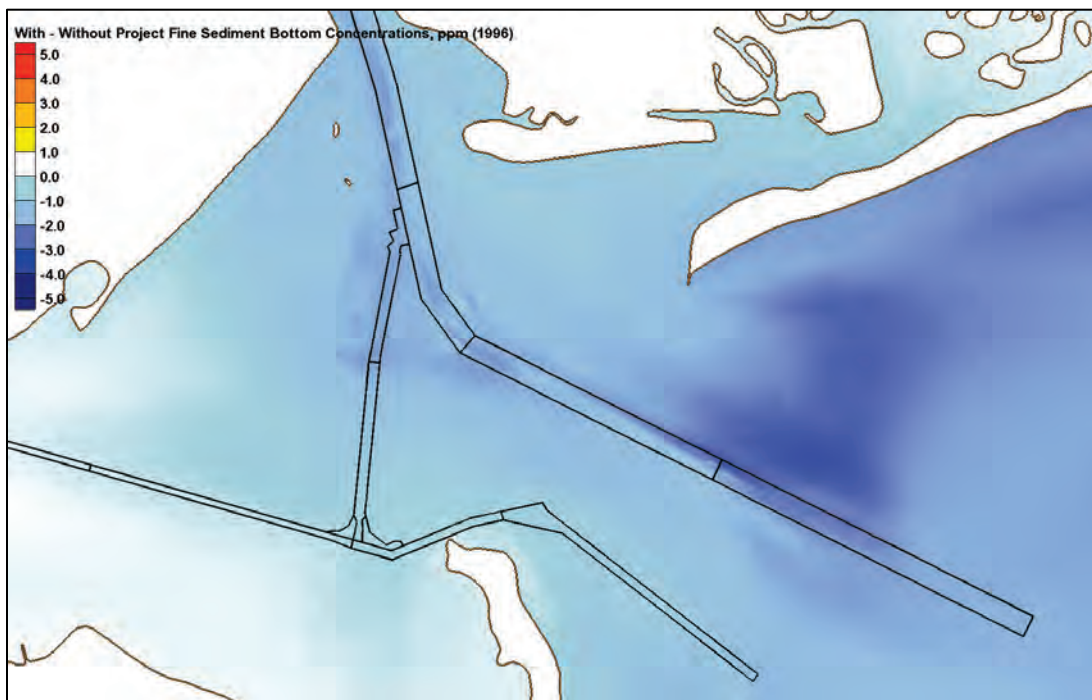


Figure 368. With- minus without-project average bottom layer fine sediment concentrations (ppm) for 2011.

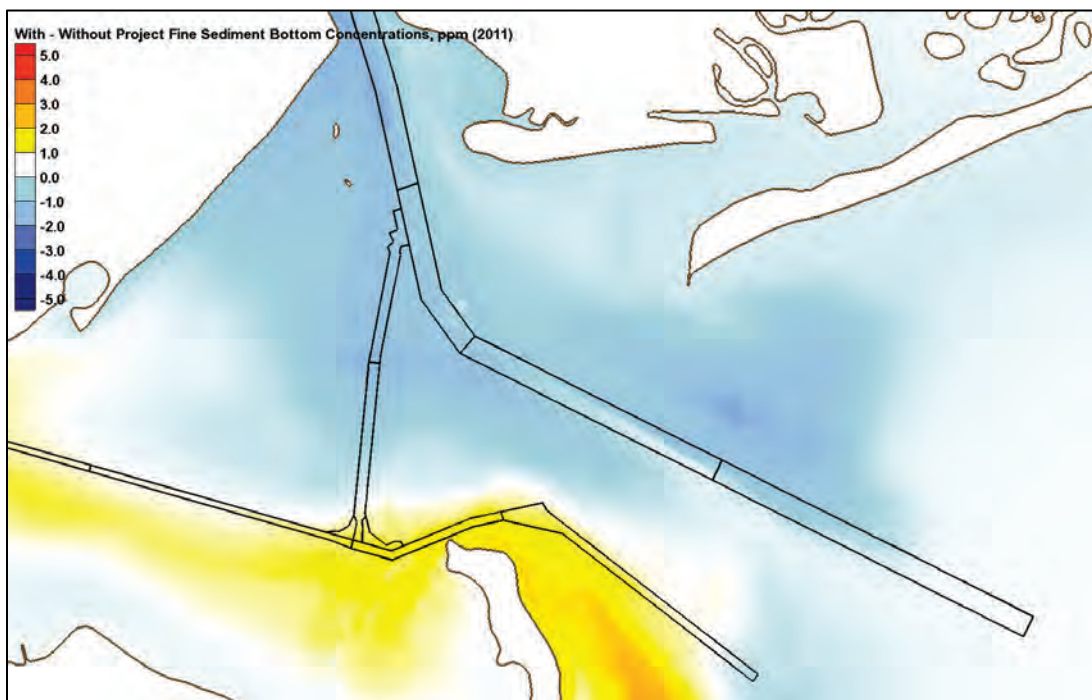


Figure 369. With- minus without-project average bottom layer fine sediment concentrations (ppm) for 2012.

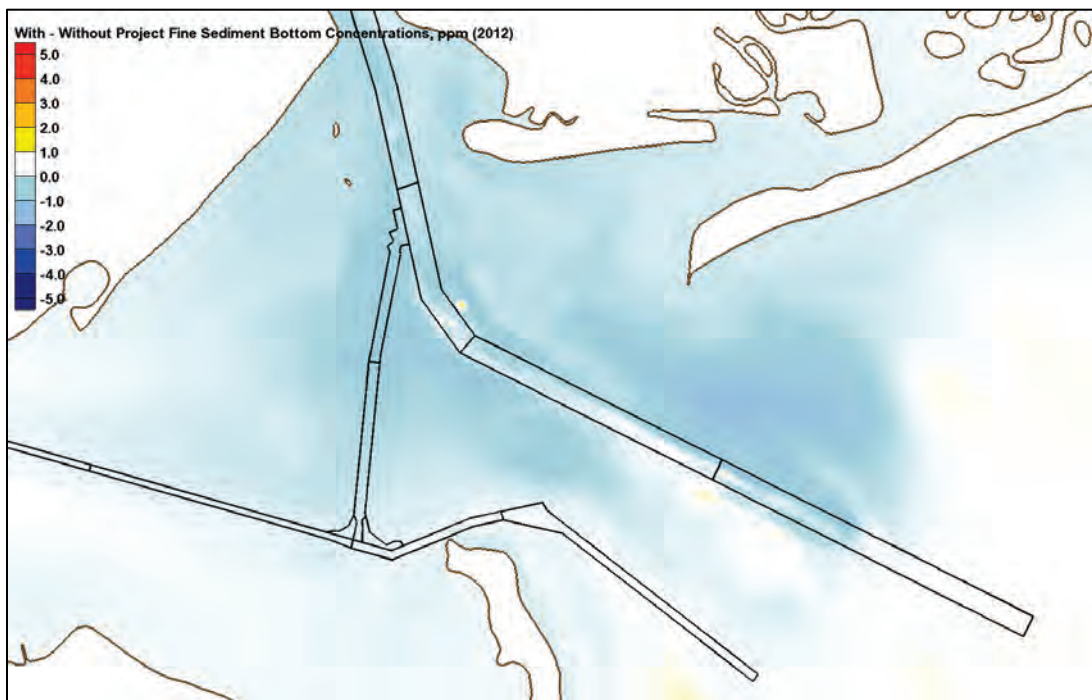


Figure 370. With- minus without-project average bottom layer sand concentrations (ppm) for 1985.



Figure 371. With- minus without-project average bottom layer sand concentrations (ppm) for 1995.





Figure 372. With- minus without-project average bottom layer sand concentrations (ppm) for 1996.

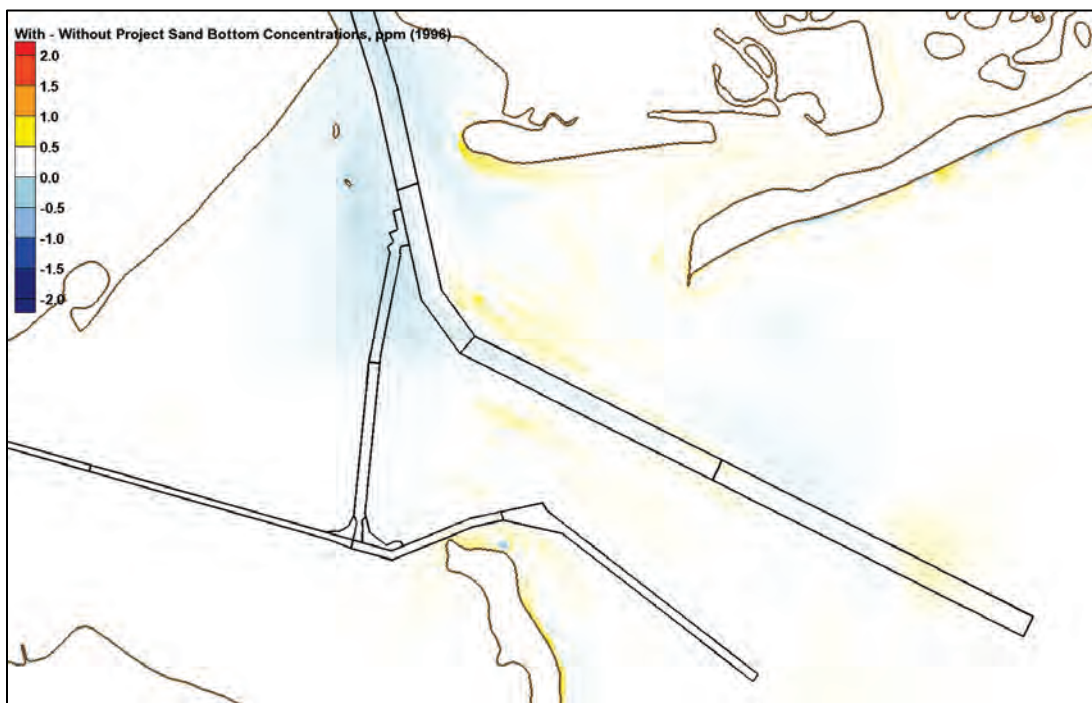


Figure 373. With- minus without-project average bottom layer sand concentrations (ppm) for 2011.





Figure 374. With- minus without-project average bottom layer sand concentrations (ppm) for 2012.



## Newark Bay, Kill van Kull, and Upper Bay

Figure 375. With- minus without-project average bed shear stresses ( $\text{N/m}^2$ ) for 1985.



Figure 376. With- minus without-project average bed shear stresses ( $\text{N/m}^2$ ) for 1995.



Figure 377. With- minus without-project average bed shear stresses ( $\text{N/m}^2$ ) for 1996.



Figure 378. With- minus without-project average bed shear stresses ( $\text{N/m}^2$ ) for 2011.





Figure 379. With- minus without-project average bed shear stresses ( $\text{N/m}^2$ ) for 2012.



Figure 380. With- minus without-project average bottom layer salinity values (ppt) for 1985.





Figure 381. With- minus without-project average bottom layer salinity values (ppt) for 1995.



Figure 382. With- minus without-project average bottom layer salinity values (ppt) for 1996.



Figure 383. With- minus without-project average bottom layer salinity values (ppt) for 2011.



Figure 384. With- minus without-project average bottom layer salinity values (ppt) for 2012.



Figure 385. With- minus without-project average bottom layer fine sediment concentrations (ppm) for 1985.



Figure 386. With- minus without-project average bottom layer fine sediment concentrations (ppm) for 1995.





Figure 387. With- minus without-project average bottom layer fine sediment concentrations (ppm) for 1996.



Figure 388. With- minus without-project average bottom layer fine sediment concentrations (ppm) for 2011.

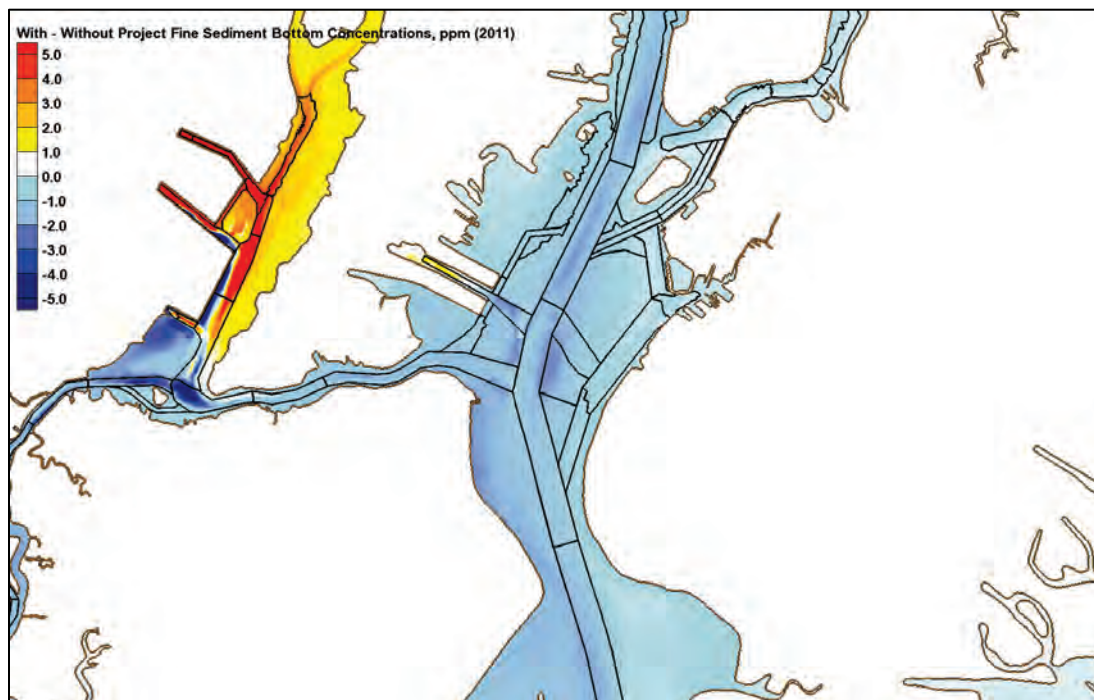




Figure 389. With- minus without-project average bottom layer fine sediment concentrations (ppm) for 2012.



Figure 390. With- minus without-project average bottom layer sand concentrations (ppm) for 1985.

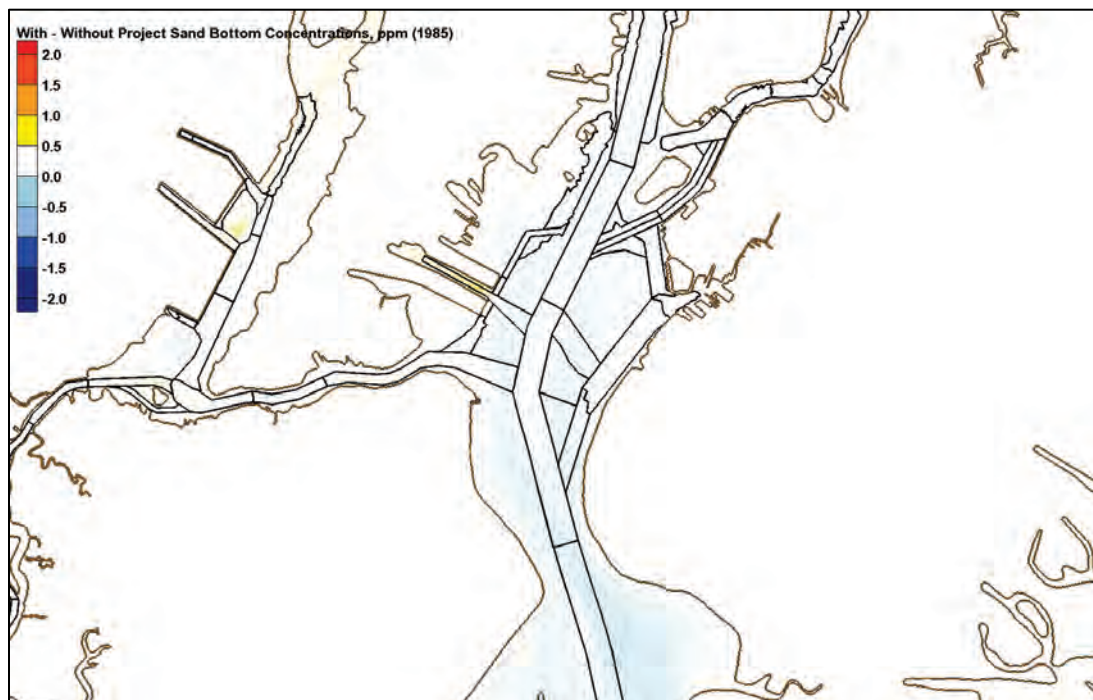


Figure 391. With- minus without-project average bottom layer sand concentrations (ppm) for 1995.



Figure 392. With- minus without-project average bottom layer sand concentrations (ppm) for 1996.



Figure 393. With- minus without-project average bottom layer sand concentrations (ppm) for 2011.

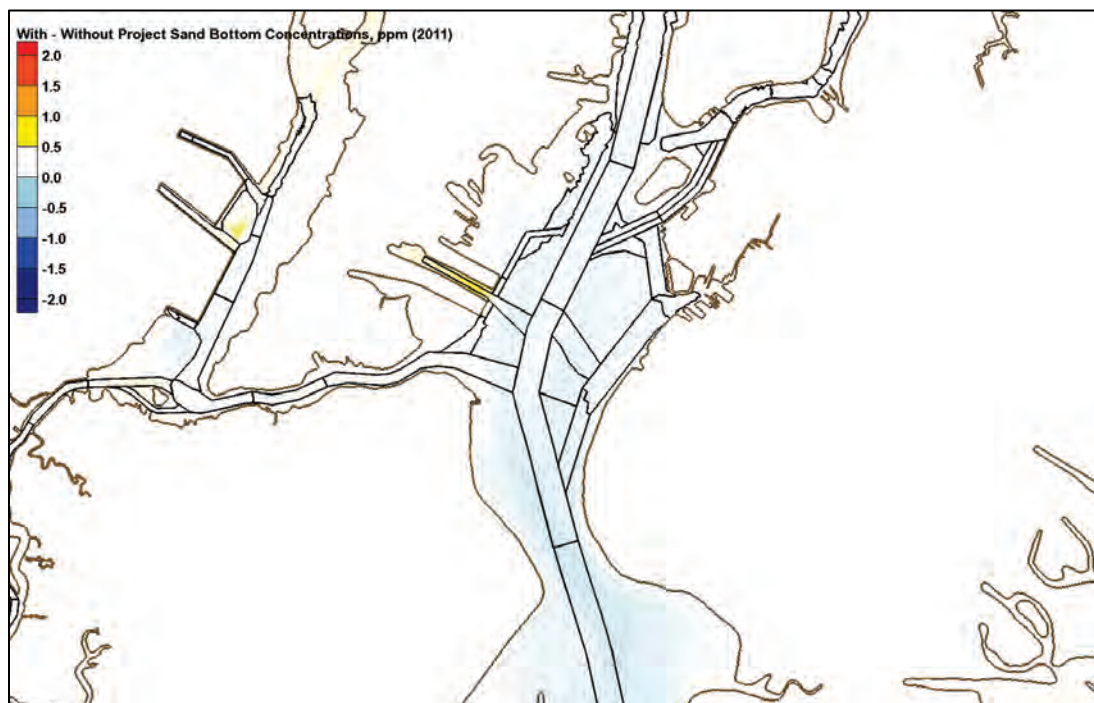
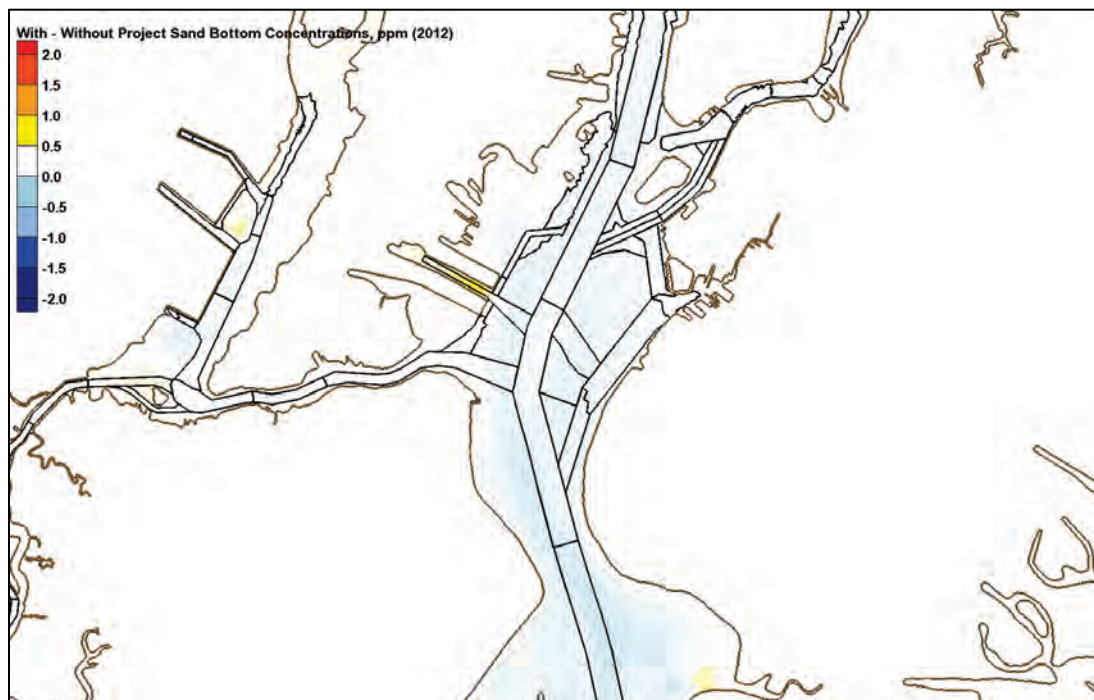


Figure 394. With- minus without-project average bottom layer sand concentrations (ppm) for 2012.





## Arthur Kill and Raritan Bay results

Figure 395. With- minus without-project average bed shear stresses ( $\text{N/m}^2$ ) for 1985.



Figure 396. With- minus without-project average bed shear stresses ( $\text{N/m}^2$ ) for 1995.

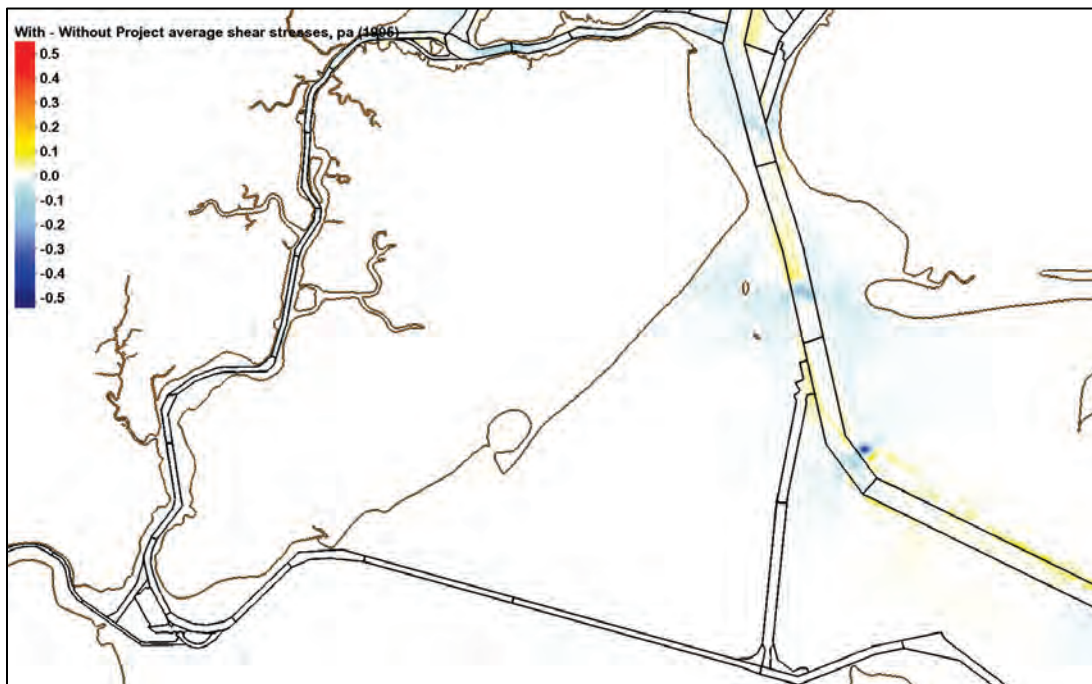




Figure 397. With- minus without-project average bed shear stresses ( $\text{N/m}^2$ ) for 1996.

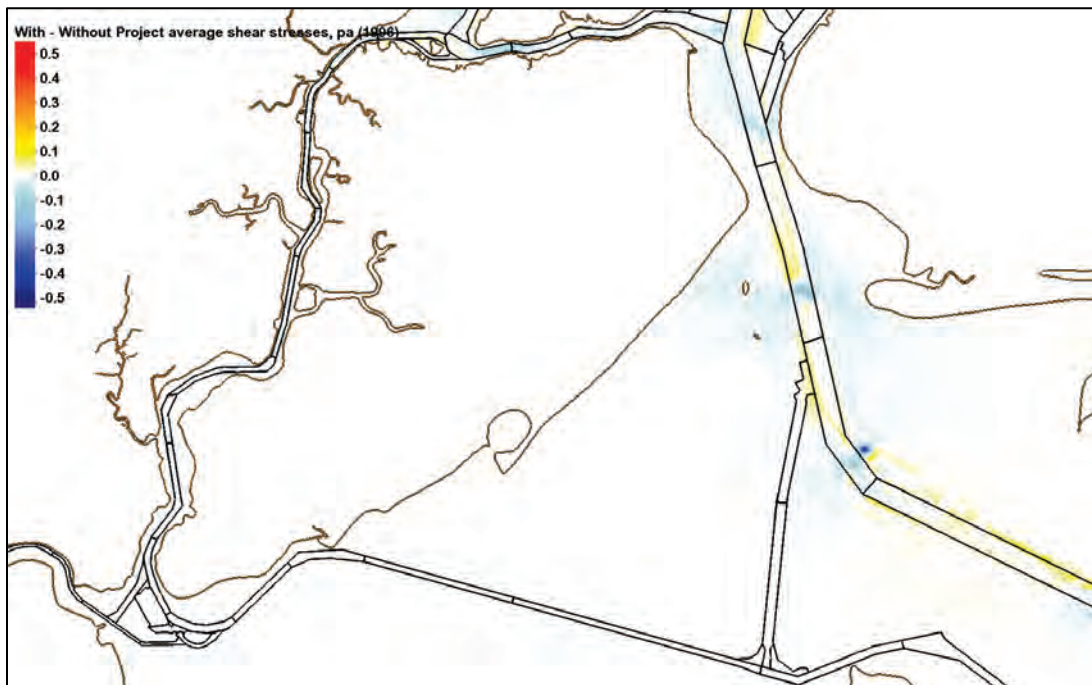


Figure 398. With- minus without-project average bed shear stresses ( $\text{N/m}^2$ ) for 2011.

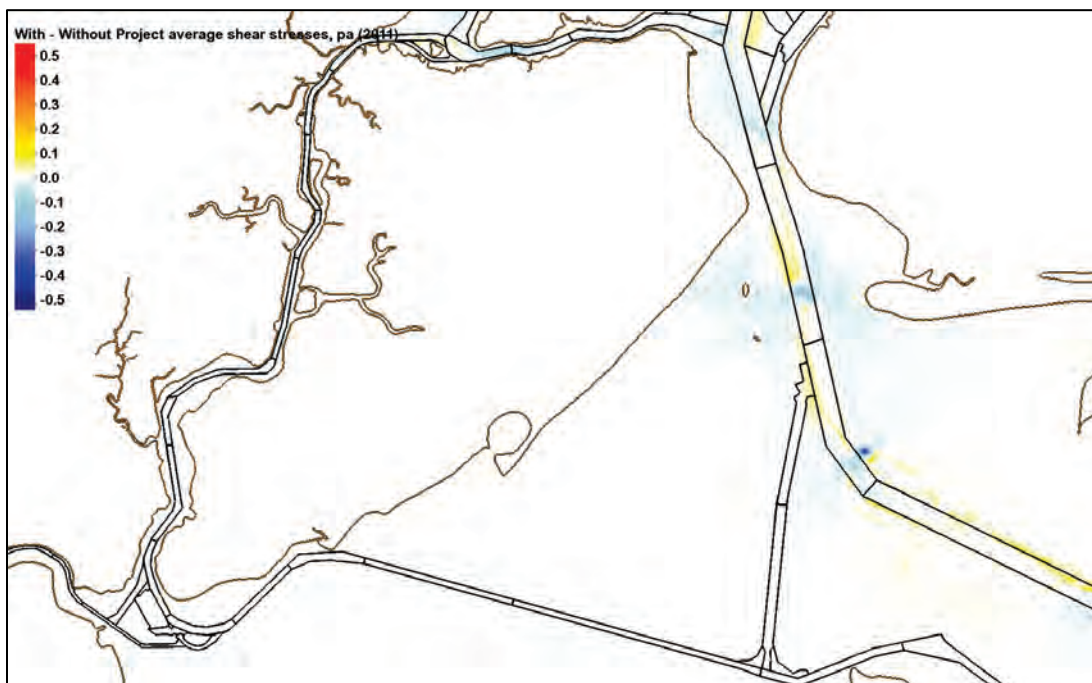


Figure 399. With- minus without-project average bed shear stresses ( $\text{N/m}^2$ ) for 2012.

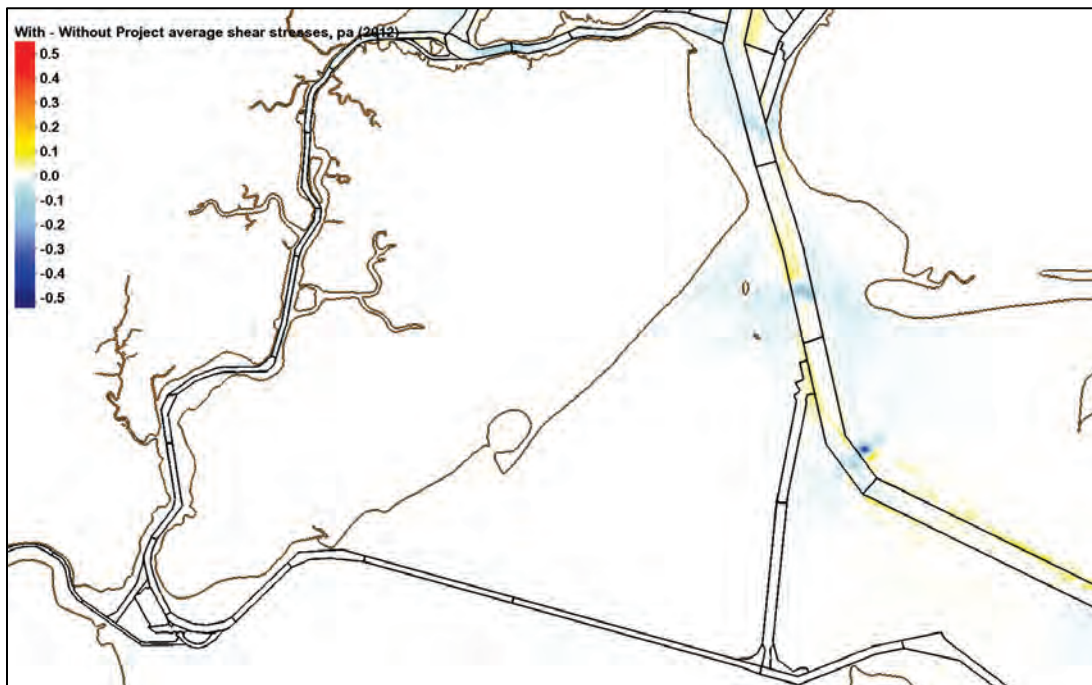


Figure 400. With- minus without-project average bottom layer salinity values (ppt) for 1985.

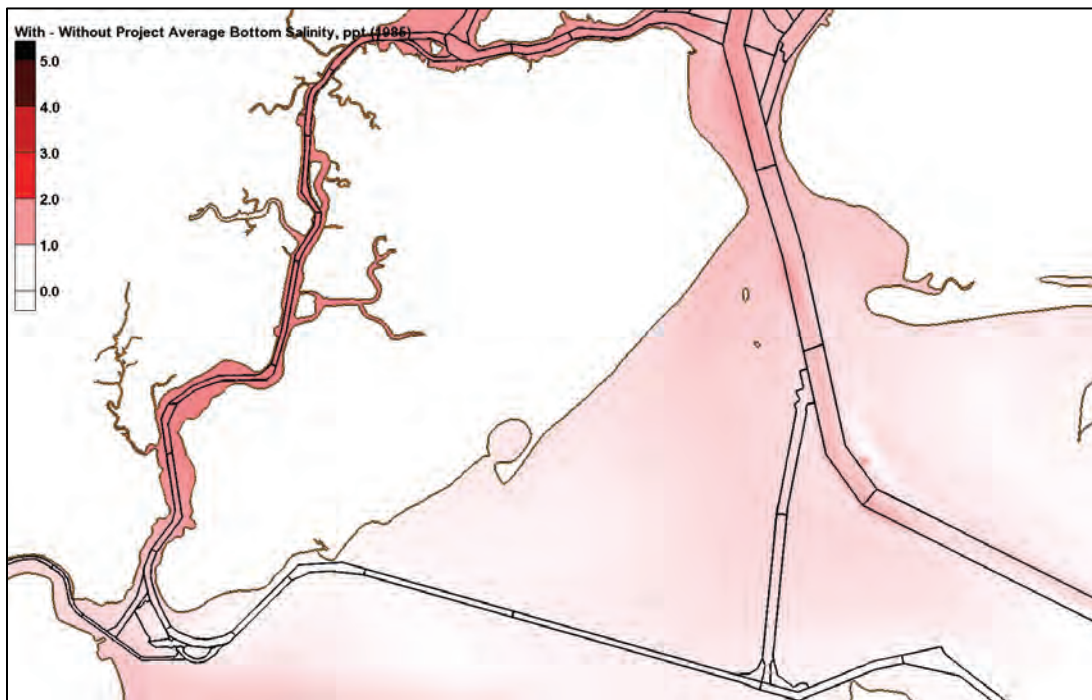


Figure 401. With- minus without-project average bottom layer salinity values (ppt) for 1995.

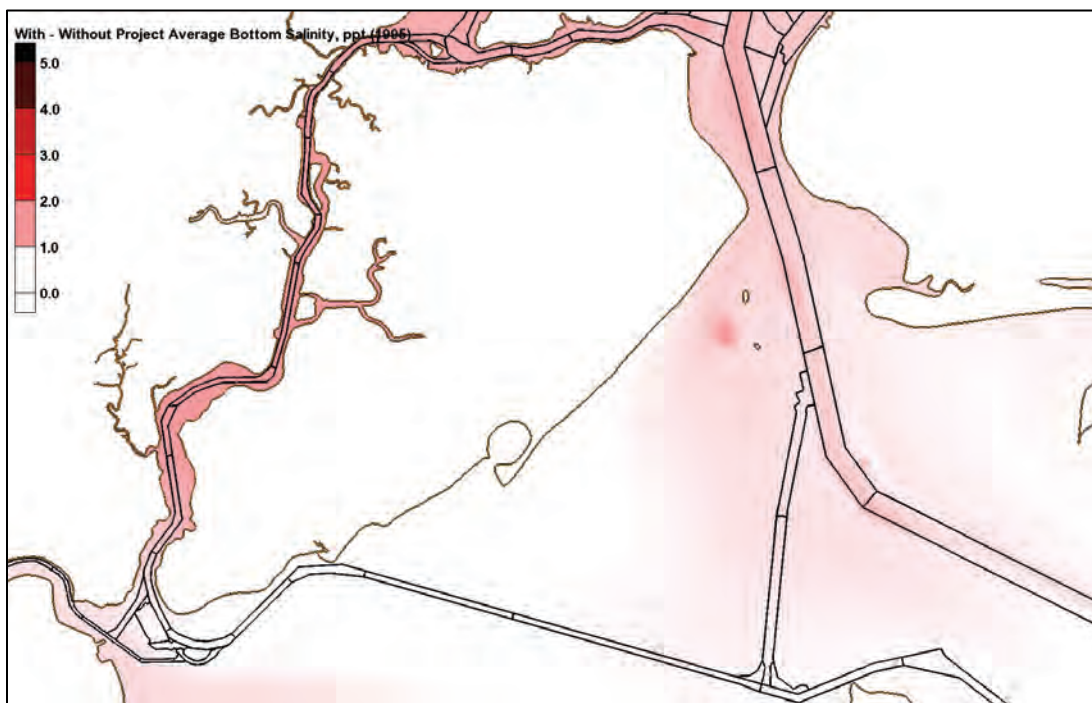


Figure 402. With- minus without-project average bottom layer salinity values (ppt) for 1996.

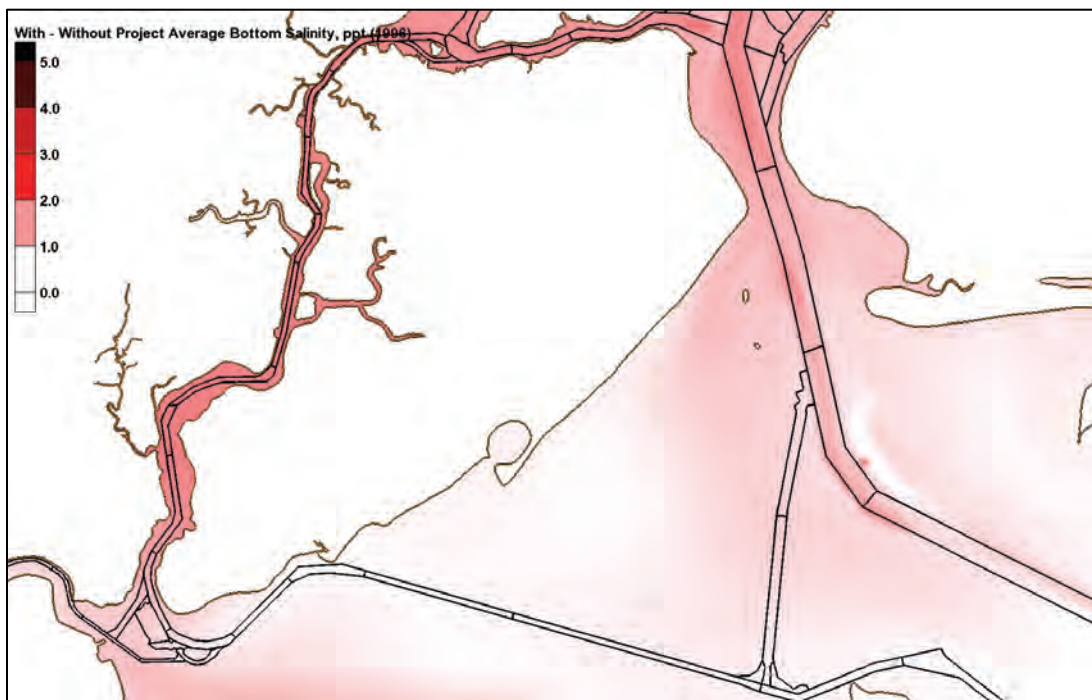




Figure 403. With- minus without-project average bottom layer salinity values (ppt) for 2011.

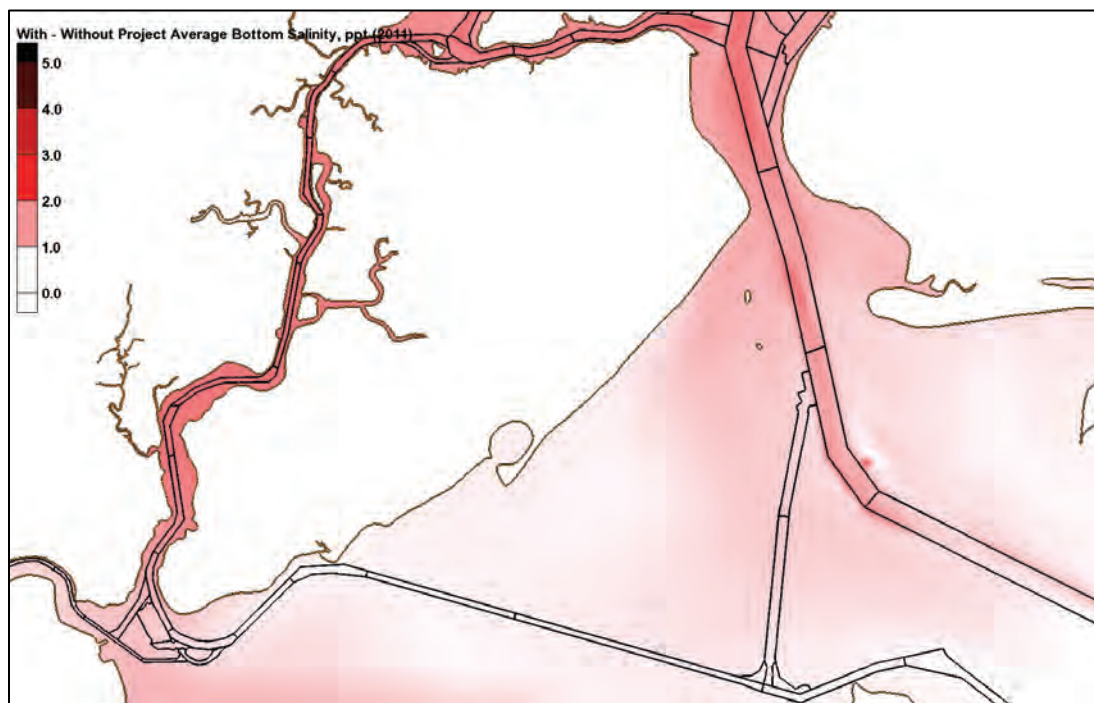


Figure 404. With- minus without-project average bottom layer salinity values (ppt) for 2012.

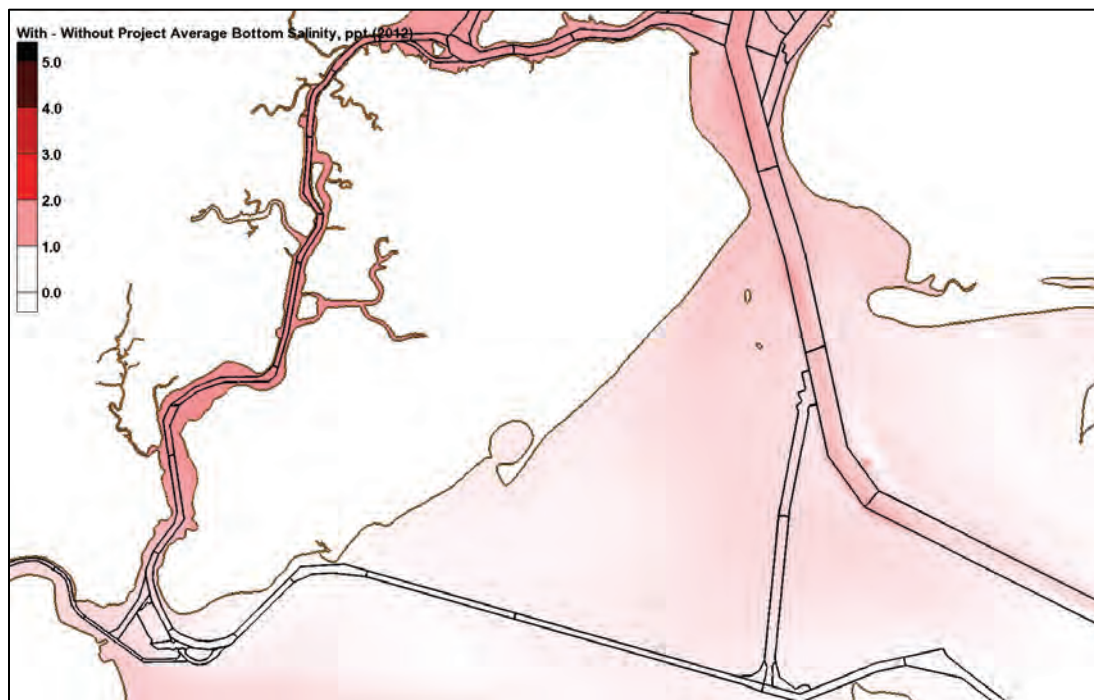




Figure 405. With- minus without-project average bottom layer fine sediment concentrations (ppm) for 1985.

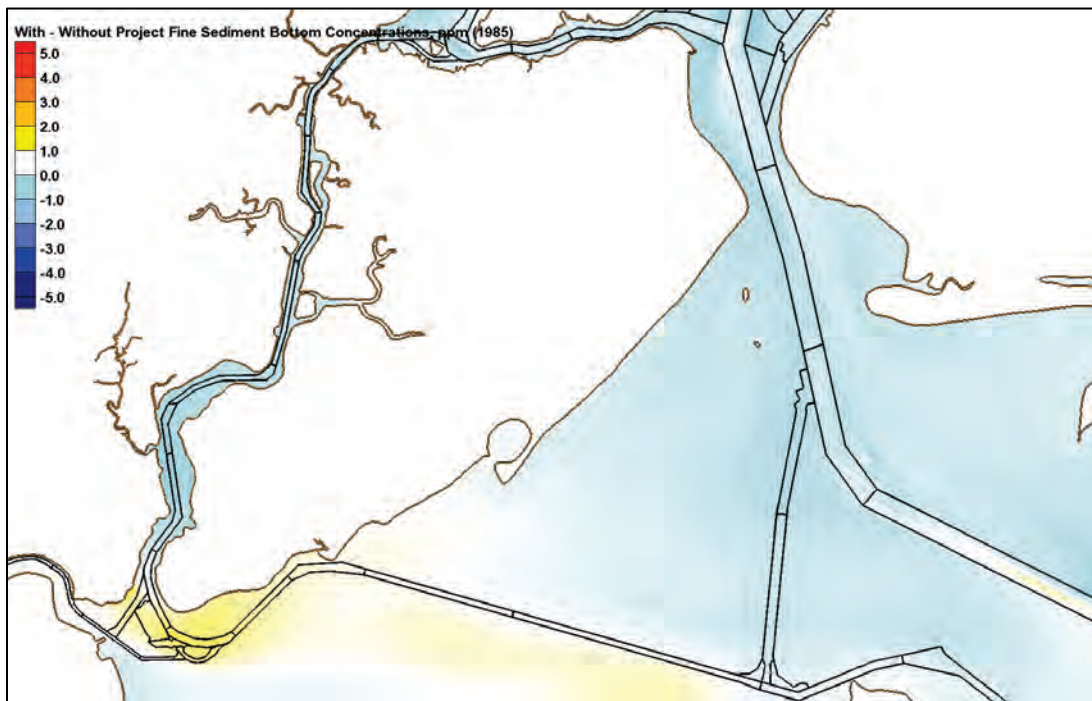


Figure 406. With- minus without-project average bottom layer fine sediment concentrations (ppm) for 1995.

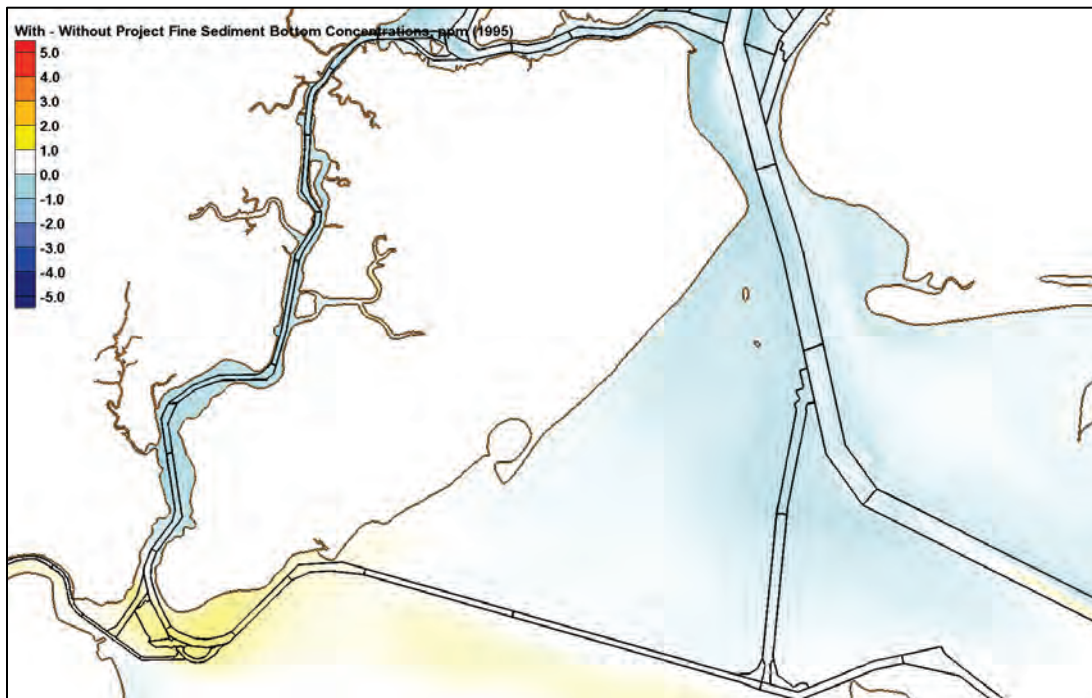


Figure 407. With- minus without-project average bottom layer fine sediment concentrations (ppm) for 1996.

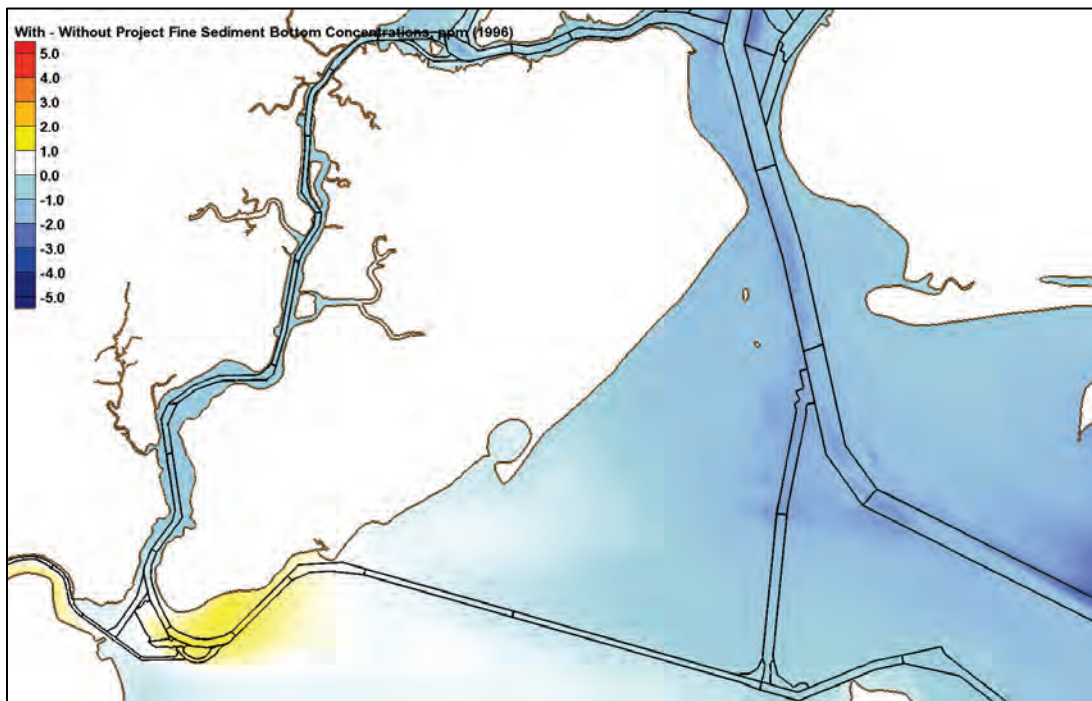


Figure 408. With- minus without-project average bottom layer fine sediment concentrations (ppm) for 2011.

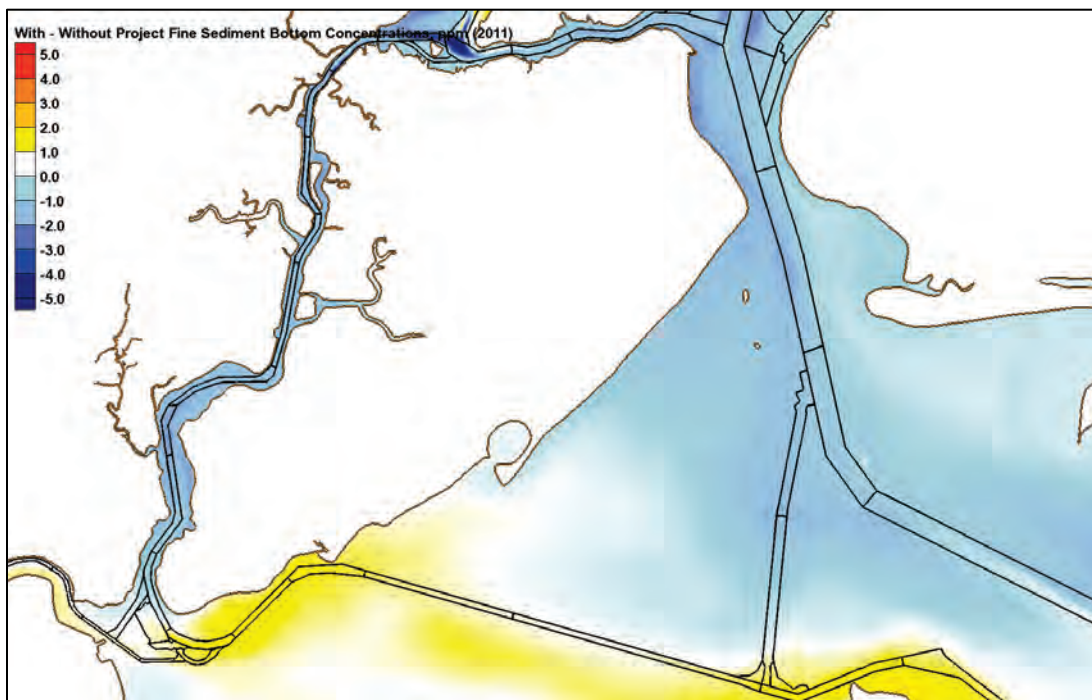


Figure 409. With- minus without-project average bottom layer fine sediment concentrations (ppm) for 2012.



Figure 410. With- minus without-project average bottom layer sand concentrations (ppm) for 1985.

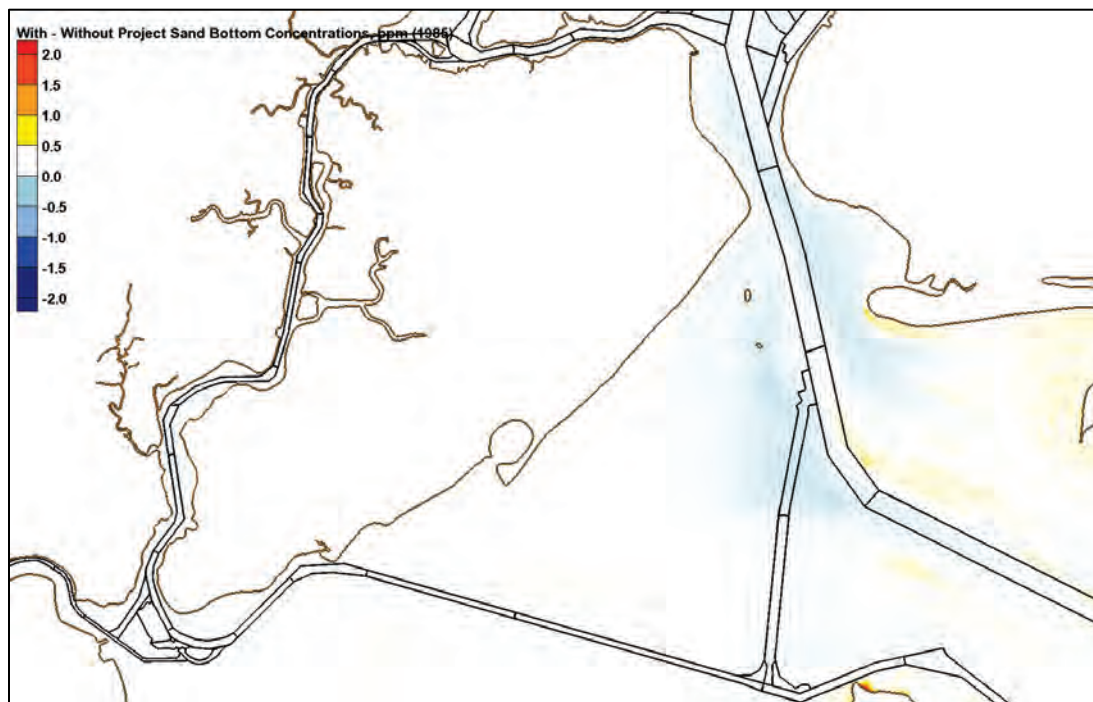




Figure 411. With- minus without-project average bottom layer sand concentrations (ppm) for 1995.

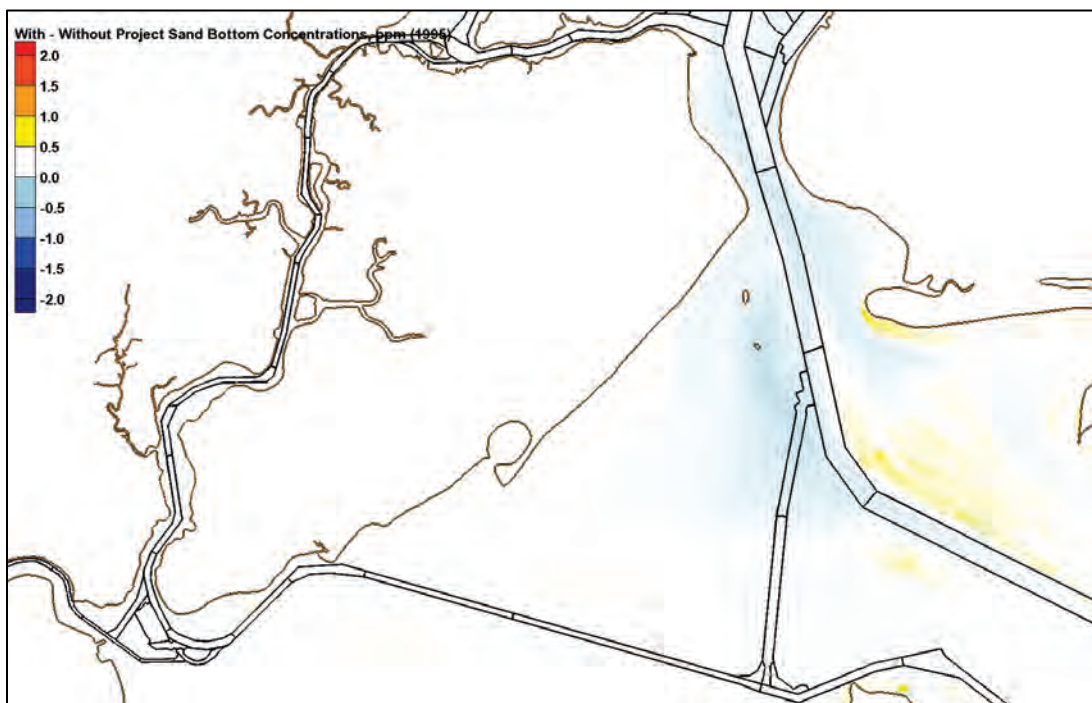


Figure 412. With- minus without-project average bottom layer sand concentrations (ppm) for 1996.





Figure 413. With- minus without-project average bottom layer sand concentrations (ppm) for 2011.

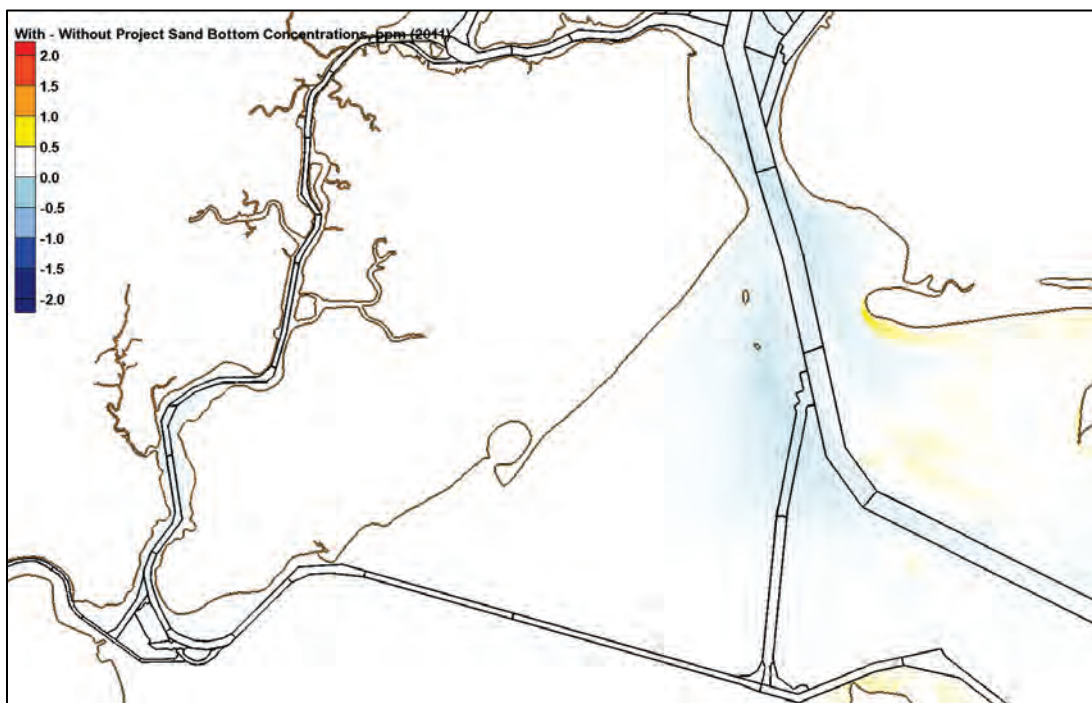
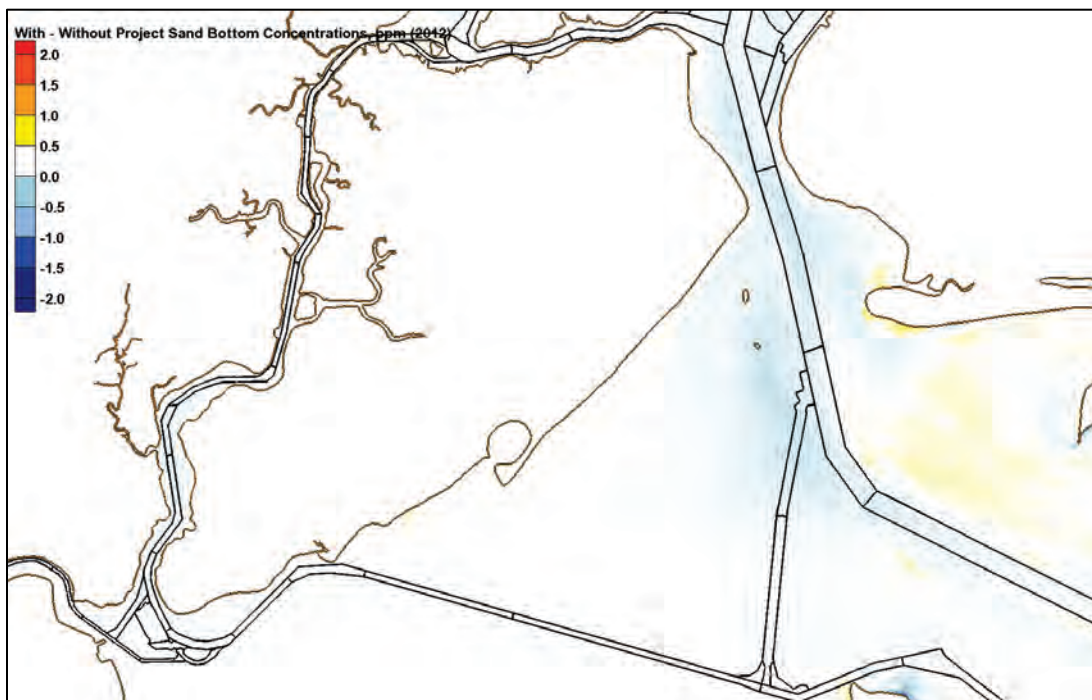


Figure 414. With- minus without-project average bottom layer sand concentrations (ppm) for 2012.



## Unit Conversion Factors

Multiply	By	To Obtain
acres	4,046.873	square meters
acre-feet	1,233.5	cubic meters
angstroms	0.1	nanometers
atmosphere (standard)	101.325	kilopascals
bars	100	kilopascals
cubic feet	0.02831685	cubic meters
cubic inches	1.6387064 E-05	cubic meters
cubic yards	0.7645549	cubic meters
feet	0.3048	meters
foot-pounds force	1.355818	joules
inches	0.0254	meters
knots	0.5144444	meters per second
microns	1.0 E-06	meters
miles (nautical)	1,852	meters
miles (US statute)	1,609.347	meters
miles per hour	0.44704	meters per second
pounds (force)	4.448222	newtons
pounds (force) per square foot	47.88026	pascals
pounds (mass)	0.45359237	kilograms
quarts (US liquid)	9.463529 E-04	cubic meters
slugs	14.59390	kilograms
square feet	0.09290304	square meters
square inches	6.4516 E-04	square meters
square miles	2.589998 E+06	square meters
square yards	0.8361274	square meters
tons (2,000 pounds, mass)	907.1847	kilograms
tons (2,000 pounds, mass) per square foot	9,764.856	kilograms per square meter
yards	0.9144	meters

## Acronyms and Abbreviations

2D	two-dimensional
3D	three-dimensional
AdH	Adaptive Hydraulics
CENAN	US Army Corps of Engineers, New York District
ECSTDB	East Coast Sediment Texture Database
ERDC	US Army Engineer Research and Development Center
ETM	Estuarine Turbidity Maximum
HARS	Historic Area Remediation Site
LISSDB	Long Island Sound Sediment Database
MLLW	mean lower low water
MSL	mean sea level
MWTF	Municipal Wastewater Treatment Facilitie
NACCS	North Atlantic Coast Comprehensive Study
NDBC	National Data Buoy Center
NOAA	National Oceanic and Atmospheric Administration
NYNJH	New York/New Jersey Harbor
RMSE	root-mean-square error
SEDLIB	Sediment transport library
SI	Scatter Index
SSC	suspended sediment concentrations
STWAVE	Steady-State spectral WAVE
SW	Shallow Water
USGS	US Geological Survey
WIS	Wave Information Study

REPORT DOCUMENTATION PAGE					Form Approved OMB No. 0704-0188	
<p>The public reporting burden for this collection of information is estimated to average 1 hour per response, including the time for reviewing instructions, searching existing data sources, gathering and maintaining the data needed, and completing and reviewing the collection of information. Send comments regarding this burden estimate or any other aspect of this collection of information, including suggestions for reducing the burden, to Department of Defense, Washington Headquarters Services, Directorate for Information Operations and Reports (0704-0188), 1215 Jefferson Davis Highway, Suite 1204, Arlington, VA 22202-4302. Respondents should be aware that notwithstanding any other provision of law, no person shall be subject to any penalty for failing to comply with a collection of information if it does not display a currently valid OMB control number.</p> <p><b>PLEASE DO NOT RETURN YOUR FORM TO THE ABOVE ADDRESS.</b></p>						
1. REPORT DATE August 2020		2. REPORT TYPE Final Report		3. DATES COVERED (From - To)		
4. TITLE AND SUBTITLE New York/New Jersey Harbor Sedimentation Study: Numerical Modeling of Hydrodynamics and Sediment Transport				5a. CONTRACT NUMBER		
				5b. GRANT NUMBER		
				5c. PROGRAM ELEMENT NUMBER		
6. AUTHOR(S)  Tate O. McAlpin, Joseph V. Letter, Jr., Mary Bryant, Anthony G. Emiren, Gary L. Brown, Gaurav Savant, Bryce W. Wisemiller, Jamal A. Sulayman, and Corey J. Trahan				5d. PROJECT NUMBER		
				5e. TASK NUMBER		
				5f. WORK UNIT NUMBER		
7. PERFORMING ORGANIZATION NAME(S) AND ADDRESS(ES) (see reverse)				8. PERFORMING ORGANIZATION REPORT NUMBER ERDC TR-20-15		
9. SPONSORING/MONITORING AGENCY NAME(S) AND ADDRESS(ES) US Army Corps of Engineers, New York District New York, NY 10278				10. SPONSOR/MONITOR'S ACRONYM(S) USACE NAN		
				11. SPONSOR/MONITOR'S REPORT NUMBER(S)		
12. DISTRIBUTION/AVAILABILITY STATEMENT Approved for public release; distribution is unlimited.						
13. SUPPLEMENTARY NOTES Work Item Code 1J186F, "ERDC Sedimentation Modeling"						
14. ABSTRACT <p>The New York/New Jersey Harbor (NYNJH) is a vital economic resource for both the local economy and the entire US economy due to the vast quantity of imports and exports handled by the numerous ports in this waterway. As with most ports, there is a significant, recurring expense associated with dredging the navigation channels to the authorized depths. In an effort to determine the impact of channel enlargements ("the project") on dredging volumes, a numerical model study was performed. The advantage of a numerical model study is the ability to isolate individual system modifications and associated impacts in terms of dredging volumes. Five years (1985, 1995, 1996, 2011, and 2012) were simulated for both the with- and without-project conditions to determine the impact of the channel deepening on the dredging requirements for a wide range of meteorological conditions including storm events. The numerical model results were analyzed to provide insight into which locations will experience increased/decreased deposition and quantify the amount of increase/decrease for a given channel reach. The model results indicate a relatively minor increase in the total dredge volumes for the NYNJH with the increase being insignificant in comparison to the natural variability in dredge volumes across years.</p>						
15. SUBJECT TERMS <p>Channels (Hydraulic engineering), Dredging, Hydrodynamics, New York Harbor (N.Y. and N.J.), Numerical analysis, Salinity, Sedimentation and deposition, Sediment transport</p>						
16. SECURITY CLASSIFICATION OF:			17. LIMITATION OF ABSTRACT  SAR	18. NUMBER OF PAGES  448	19a. NAME OF RESPONSIBLE PERSON Tate O. McAlpin	
a. REPORT Unclassified	b. ABSTRACT Unclassified	c. THIS PAGE Unclassified			19b. TELEPHONE NUMBER (Include area code) 601-634-3249	



**7. PERFORMING ORGANIZATION NAME(S) AND ADDRESS(ES) (continued)**

Coastal and Hydraulics Laboratory  
US Army Research and Development Center  
3909 Halls Ferry Road  
Vicksburg, MS 39180-6199

Information Technology Laboratory  
US Army Engineer Research and Development Center  
3909 Halls Ferry Road  
Vicksburg, MS 39180-6199

Dynamic Solutions LLC  
6421 Deane Hill Dr., Suite 1  
Knoxville, TN 37919

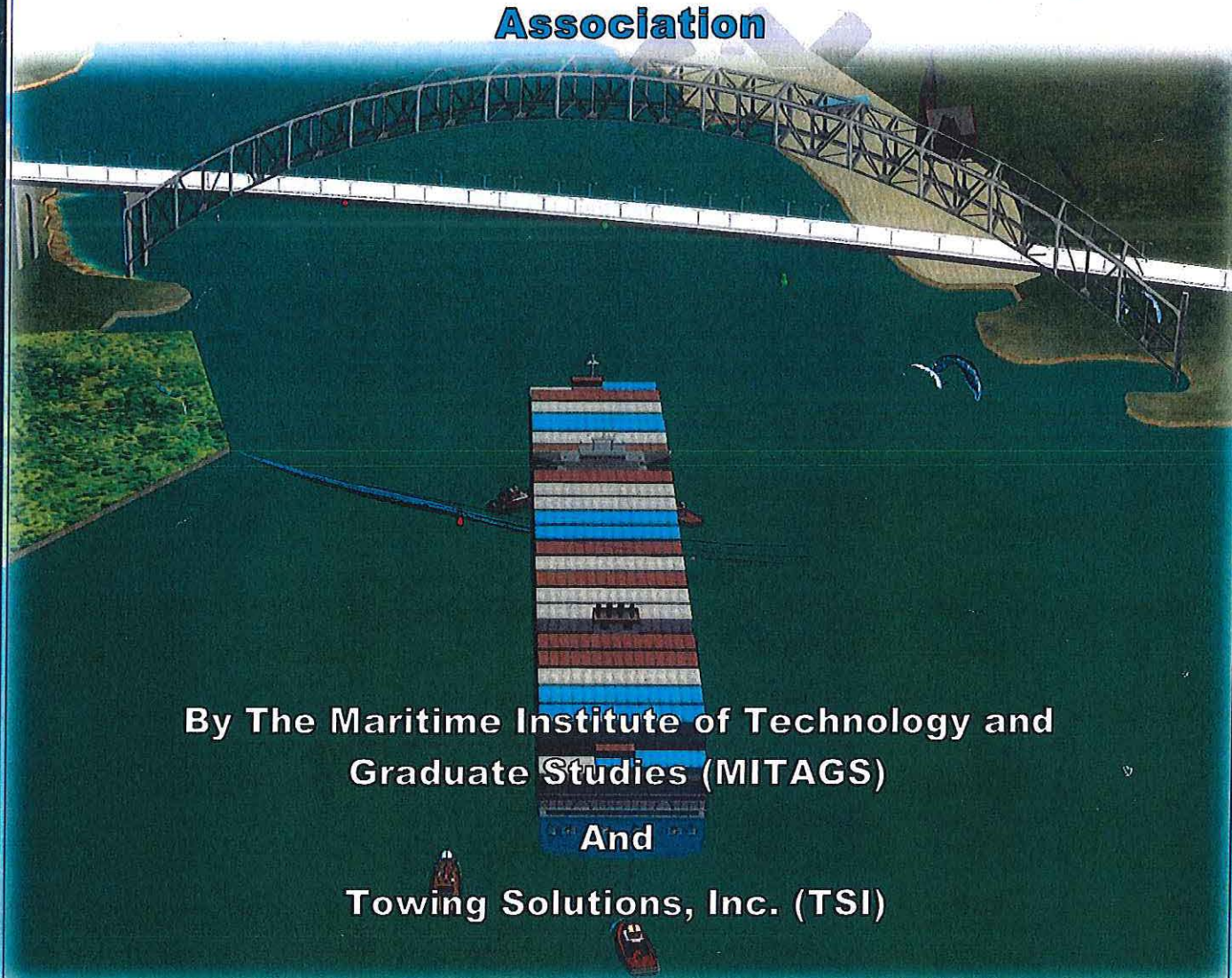
US Army Corps of Engineers  
New York District  
26 Federal Plaza  
New York, NY 10278

THIS PAGE INTENTIONALLY  
LEFT BLANK

## ATTACHMENT 5

### MITAGS STUDY

# **Preliminary 18,000 TEU Full Mission Ship Simulation Study Report For The Port of New York / New Jersey Shipping Association**



**By The Maritime Institute of Technology and  
Graduate Studies (MITAGS)**

**And**

**Towing Solutions, Inc. (TSI)**

**MITAGS** 692 MARITIME BOULEVARD  
LINTHICUM HEIGHTS, MARYLAND 21090  
TOLL-FREE: 866-656-5569  
WEBSITE: WWW.MITAGS.ORG

**PMI** 1729 ALASKAN WAY SOUTH  
SEATTLE, WASHINGTON 98134  
TOLL-FREE: 888-893-7829  
WEBSITE: WWW.MATES.ORG



MITAGS is internationally certified as a  
Maritime Simulation & Training Center  
by Det Norske Veritas



Study Name	Preliminary 18,000 TEU ULCV Full-Mission Ship Simulation Study for the Port of NY/NJ
<b>Note</b>	<i>The companion report is 14,000 TEU ULCV Study.</i>
Project Location	Port of New York and New Jersey
Purpose	Development of best practices for the navigational transits of 18,000 TEU Ultra Large Containerships (ULCV) in the Port of NY/NJ
Customer	Port of New York / New Jersey Shipping Association
Bidder Legal Name and Location	The MMP MATES Program, DBA the Maritime Institute of Technology & Graduate Studies, and the Pacific Maritime Institute (MITAGS-PMI). 692 Maritime Boulevard Linthicum Heights, MD 21090-1952 Tel: 410-859-5700 Fax: 410-859-8416 Email: <a href="mailto:exdir@mitags.org">exdir@mitags.org</a> Web: <a href="http://www.mitags-pmi.org">http://www.mitags-pmi.org</a>
Bidder Description	The MM&P Mates Program is a 501(c)9 VEBA Non-profit Trusteeship. The "MATES Program" was founded by the International Organizations of Masters, Mates and Pilots and the leading U.S. Flag ship operators in 1968. Its mission is to enhance professionalism through the development and presentation of internationally recognized programs in leadership, education, training and safety for the maritime industry. MITAGS and PMI are the primary training and simulation centers for the MMP professional deck officers and pilots.  Tax ID Number: 13-2577386. MD Tax Exemption Number: 31000665 Dun and Bradstreet Number: 010094977
Draft Release Date	
Project Leader	Mr. Glen Paine, Executive Director, MMP MATES Program
Authorized Signature	

MITAGS-PMI accepts no liability for the use of the findings, conclusions and recommendations provided by the conning pilots in this simulation study. Additionally, MITAGS-PMI cannot be held responsible for errors in the data provided by the client and other third parties used for the programming of the simulator hydrodynamic ship / tug models, and databases.



## TABLE OF CONTENTS

Table of Figures .....	5
Table of Tables .....	6
1. Background and Purpose .....	7
1.1 Simulation Study Objectives .....	8
1.2 Scope of Work.....	8
Deliverables – Parts A & B Phase I Studies .....	8
1.3 Assumptions.....	9
1.4 Assumptions and Limitations.....	10
1.5 Project Team and Simulation Facilities .....	10
1.6 Time Line and Test Location .....	11
2. Hydrodynamic Ship Modeling.....	13
3. Databases' Development.....	15
3.1 Underwater Contours .....	17
3.2 Water Currents .....	18
3.3 Wind Directions and Speeds .....	20
3.4 Visibility; Day Night Scenes .....	20
4. Waterway Simulation Technology (WST) Support Studies.....	21
5. Maneuvering Study Methodology.....	22
5.1 Exercise Scenarios.....	22
6. Towsings Solutions Observations – 18,000 TEU.....	23
6.1 Full Length Runs - in or outbound – Con Hook to Port Elizabeth .....	24
Run 1 Kalina Meeting Tanker in KVK.....	24
Run 2 Kalina Meeting Tanker in the KVK .....	25
Alternate Meeting Solution .....	25
Run 3 Inbound Run through KVK to South Reach .....	26
Run 15 Kalina Meeting Traffic in KVK.....	27
Run 16 Triple E Inbound KVK .....	28
Run 17 Triple E Inbound to KVK .....	29
Run 18 Triple E Inbound to KVK.....	30
6.2 Rounding Bergen Point Inbound Bergen Point East Reach to Buoy 3 .....	31
Run 4 Bergen Point Turn Inbound.....	31
Run 5 Triple E Inbound Bergen Point .....	32
6.3 Bergen Point Outbound Buoy 3 to Bergen Point East Reach. ....	33
Run 6 Outbound Bergen Point.....	33
Run 7 Outbound Bergen Point .....	34
6.4 Inbound from Buoy 10 Newark Bay to Port Elizabeth .....	35
Run 8 Inbound to Port Elizabeth Branch Reach .....	35



Run 9	Inbound to Port Elizabeth .....	36
Run 12	Inbound Port Elizabeth .....	37
Run 13	Inbound Port Elizabeth .....	38
Run 25	Demonstration Run.....	39
6.5	Outbound from Port Elizabeth to Buoy 10 Newark Bay .....	40
Run 10	Outbound from Port Elizabeth to Newark Bay .....	40
Run 14	Outbound from Port Elizabeth to Newark Bay .....	41
Run 11	.....	42
Run 26	Demonstration Run.....	43
6.6	Inbound from Upper Bay Buoy 30 to Global Terminal .....	44
Run 19	.....	44
Run 20	Inbound Global Marine Terminal.....	45
Run 27	Demonstration Run.....	46
6.7	Outbound from Global Terminal to Upper Bay Buoy 30 .....	47
Run 21	.....	47
Run 22	.....	48
6.8	Emergency Turns above and below the Verrazano Narrows Bridge .....	49
Run 23	Emergency Turn South of Verrazano Bridge.....	49
Run 24	Emergency Turn South of Verrazano Bridge.....	50
7.	Pilot Findings, Conclusions and Recommendations .....	51
7.1	Final Questionnaire Graphs and Comments.....	54
	Realism of Ship and Tug Models Ratings Graph .....	54
	Realism of Environmental Conditions Ratings Graph .....	55
	Realism of Visual Database Ratings Graph .....	56
	Overall Final Evaluation Comments.....	56
7.2	MITAGS Observations and Comments.....	58
	ULCV Meeting Situations in the KVK.....	58
	18,000 TEU Turn into Con Hook Range (Runs 3, 16 -18) .....	59
	18,000 TEU Turn at Bergen Point (Runs 4-7) .....	59
	Port Elizabeth Branch Reach (8 – 14).....	59
	Global Marine Terminal (Runs 19 – 22, 27) .....	59
	General Information on the Maneuverability of the Triple E Class ULCV .....	63
	Future Considerations.....	63
8.	Final Test Marix.....	65
APPENDIX A:	Pilot Cards.....	70
	Container Triple E_3.0.55.2 * 42' draft.....	70
	Container Triple E_3.0.52.1 * 49' Draft .....	71
	Tanker OH (Disp 57575t)_CPP_FL_8 v03.17.VSY .....	72
	Tanker Memphis 3.0.26.0 * .....	73



Container Kalina_NewYork 3.0.45.1 * 42' Draft .....	74
Container Kalina_NewYork 3.0.46.1 * 49' Draft .....	75
Conventional Twin Screw Tug 4 (bp 46.3t) TRANSAS 2.31.17.0 * .....	76
Tug Brian McAllister (85t bp) 3.0.57.1 * .....	77
Tug Edward Moran 3.0.63.0 * .....	78
APPENDIX B: Container Kalina and Container Triple E Swept Path Calculations .....	79
APPENDIX C: Description of Water Current Model Development by Waterway Simulation Technology .....	80
APPENDIX D: Introduction to MITAGS and PMI .....	88
MITAGS Location and General Facility Description .....	88
PMI Location and General Facility Description .....	88
MITAGS DNV Class A Full-Mission Ship Simulator #1 (Bridge for Phase I and II Tests) ...	89
MITAGS Tug Bridge Simulator (Bridge for Phase I and II Tests) .....	89
Aerial Photograph of MITAGS Campus and Location Diagram .....	90

#### Table of Figures

Figure 1: Layout of NJ/NY Terminal Area .....	7
Figure 2: Port Elizabeth / Newark, NJ .....	7
Figure 3: Kalina Meeting in KVK .....	12
Figure 4: Model Motion .....	13
Figure 5: Profile Views of the Triple E and Kalina Models .....	14
Figure 6: Sample Visual Graphics .....	15
Figure 7: Depth Areas of 45 feet or More at MLLW .....	17
Figure 8: Depth Areas of 52 Feet or More at MLLW .....	17
Figure 9: WST Water Current File Names .....	18
Figure 10: Sample Flood Current Data Points .....	18
Figure 11: Excerpt of Surge Forces vs. Speed by Vessel Class in the KVK from the WST Report .....	21
Figure 12: Triple E entering Port Elizabeth Branch Reach .....	22
Figure 13: Run 1 – Kalina - Meeting in Kill Van Kull .....	24
Figure 14: Run 2 – Kalina – Meeting in Kill Van Kull .....	25
Figure 15: Run 3 – Triple E – Approach & Turn at Bergen Pt. ....	26
Figure 16: Run 15 - Kalina meeting Tanker Memphis .....	27
Figure 17: Run 16 – Triple E grounding as it entered Con Hook Reach .....	28
Figure 18: Run 16 Screen Shot .....	<b>Error! Bookmark not defined.</b>
Figure 19: Run 17 – Triple E Entering & Transiting Con Hook Reach – Ebb .....	29
Figure 20: Run 17 Screen Shot .....	29
Figure 21: Run 18 – Triple E Entering & Transiting Con Hook Reach - Flood .....	30
Figure 22: Run 18 Screen Shot .....	<b>Error! Bookmark not defined.</b>
Figure 23: Run 4 – Triple E @ 49' .....	31
Figure 24: Run 5 - Triple E – Inbound at Bergen Point .....	32
Figure 25: Run 6 – Triple E Southbound to Bayonne Bridge .....	33
Figure 26: Run 7 – Triple E Close to the Channel Edge .....	34
Figure 27: Run 8 – Triple E Turing too early at Port Elizabeth .....	35



Figure 28: Run 9 – Triple E entering Port Elizabeth Chanel .....	36
Figure 29: Run 12 – Triple E turning into Port Elizabeth Channel .....	37
Figure 30: Run 13 AMAersk passing between two Triple E's at Port Elizabeth .....	38
Figure 31: Run 13 Screen Shot .....	38
Figure 32: Run 25 Inbound between berthed Kalina Classes. ....	39
Figure 33: Run 10 Triple E – Control Issues.....	40
Figure 34: Run 14 Screen Shot .....	41
Figure 35: Run 14 – AMAersk slipping between two, Triple E models.....	41
Figure 36: Run 11 – Triple E backing out of Port Elizabeth .....	42
Figure 37: Run 26 – Triple E Backing out of Port Elizabeth Branch Reach .....	43
Figure 38: Run 19 – Triple E Entering Port Jersey Channel .....	44
Figure 39: Run 20 – Triple E Entering Port Jersey Channel .....	45
Figure 40: Triple E entering Global Marine Terminal.....	46
Figure 41: Run 21- Triple E backing out of Port Jersey Channel .....	47
Figure 42: Run 22 - Triple E backing out of Port Jersey Channel .....	48
Figure 43: Emergency Turn in the Narrows .....	49
Figure 44: Emergency Turn .....	50
Figure 45: View from the Tanker Meeting the Kalina in the KVK .....	58
Figure 46: Triple E Inbound Constable Hook Reach .....	59
Figure 47: Triple E Inbound at Bergen Point .....	60
Figure 48: Triple E Inbound into Port Elizabeth Branch Reach .....	60
Figure 49: Triple E Inbound to Global Marine Terminal Past Cruise Ship Terminal .....	61

#### Table of Tables

Table 1: Table of Abbreviations .....	6
Table 2: 18,000 TEU (Part B, Phase I) Support Team for August 23-26, 2016 Tests .....	11
Table 3: Ship Models Used in the Study .....	13
Table 4: Electronic Chart Data Used for Developing Visual Databases .....	16
Table 5: Swept Path: Kalina (meters) .....	79
Table 6: Swept Path: Container Triple E (meters) .....	79

Table 1: Table of Abbreviations			
A	Aft	P	Port
CL	Center Lead	Q	Quarter
COG	Course of ground	S	Starboard
DM	Docking Master	SH	Shoulder
F	Forward	SOG	Speed over the ground
KVK	Kill Van Kull Waterway	STW	Speed through the water
NBD	Newark Bay Draw		



## 1. BACKGROUND AND PURPOSE

The Port of New York and New Jersey has completed a major navigational channel deepening and improvement project. The controlling depths of the channels have been increased to 50 feet at mean low, lower, water. Additionally, the project includes raising the Bayonne Bridge to allow passage of higher ultra large container vessel (ULCV) air drafts. The bridge project is expected to be completed in 2017.

The Port of NY/NJ, through the Deep Draft Working Group of the Harbor Operations Committee, desired to conduct a full-mission ship simulation study to develop the “best practices” for ULCV transits to the major container terminals within the area. This includes APM / Maher Terminals in Port Elizabeth, Port Newark Container Terminal, GCT New York LP Terminal (Howland Hook), and GCT Bayonne LP Terminal (Global Marine).

The Maritime Institute of Technology and Graduate Studies (MITAGS) provided this service in two Parts.

**Part A, Phase I** evaluated 14,000 TEU ULCV MSC Kalina Class (max LOA 366 x beam 51 meters). Phase I used full-mission ship simulation (FMSS) to assist in the development of “best practices” for handling ULCV. (Phase II sessions will occur at later dates to familiarize the other pilots and tug masters on the what was learned in Part A, Phase I.) *The results of these tests are contained in a separate report.*

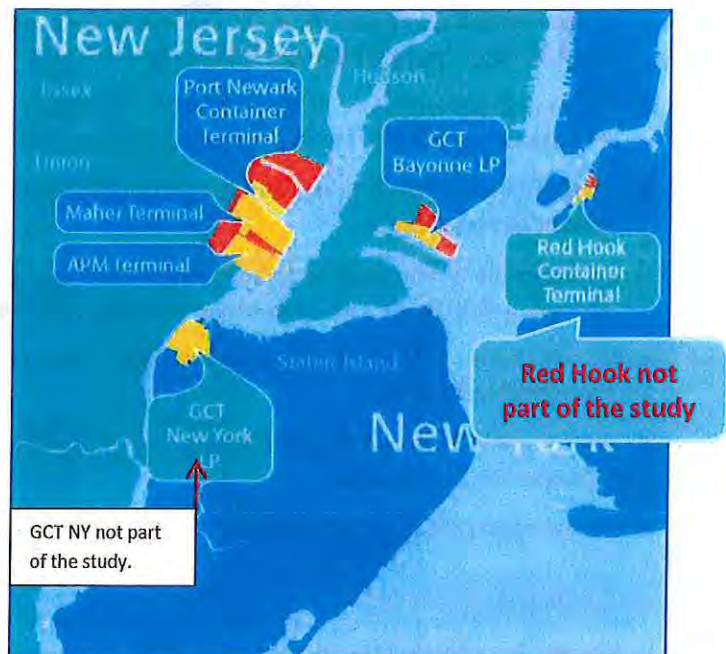


**Figure 1: Layout of NJ/NY Terminal Area**

**Part B, Phase I** evaluation was similar, but used the 18,000 TEU Maersk Triple E ULCV Class (max LOA 399 x beam 59 meters) instead of the Kalina Class. The goal was to determine the feasibility and challenges to address for this vessel class. **This report contains the results of Triple E Tests.**

The MITAGS simulators are capable of providing the most realistic presentation in the world. The theater projection area is over twenty-four meters wide and twelve meters in height. This provides unsurpassed depth perception and visual accuracy. The FMSS simulator, operated by the Sandy Hook and docking pilot(s), was integrated with one assist-tug simulator operated by an experienced tug master. Additional tugs were operated from the console.



**Figure 2: Port Elizabeth / Newark, NJ**



For more information on MITAGS, please visit [www.mitags-pmi.org](http://www.mitags-pmi.org), and our YouTube® site for video excerpts of previous simulation projects: <http://www.youtube.com/user/MaritimeInstitute>.

## 1.1 SIMULATION STUDY OBJECTIVES

The 18,000 TEU ULCV Simulation Study provides preliminary findings, conclusions, recommendations for the following objectives:

1. Recommendations on “best practices” for ULCV inbound / outbound transits and berthing evolutions to / from APM/Maher/PNCT (Port Elizabeth/Port Newark) with similar sized ULCVs berthed on both sides of the channel.
2. ~~Recommendations on “best practices” for ULCV inbound / outbound transits and berthing evolutions to / from GCT New York LP (Howland Hook).~~ **Note: In the interest of time, the pilots’ removed this objective since the Terminal does not have cranes capable of handling the larger ULCVs and no immediate plans for replacements.**
3. Recommendations on “best practices” for ULCV inbound / outbound transits and berthing evolutions to GCT Bayonne LP (Bayonne Marine Terminal / Port Jersey).
4. Identification of environmental operational limits for wind directions / speed, and water current velocities / directions.
5. Assessment of limitations of the existing assist tug capabilities (number, type, and power) needed for safe handling of ULCV Class under various environmental conditions.
6. Feasibility of ULCV meeting Panamax Class size vessels at selected channel reaches in order to expedite traffic flow.
7. Recommendations on “best practices” for responding to propulsion, rudder, and / or tug failures at selected channel reaches.
8. Recommendations for future pilot / tug master familiarization training.

## 1.2 SCOPE OF WORK

Part B, Phase I modeled the 18,000 TEU ULCV Class entering and departing Port Elizabeth / Port Newark, and Bayonne Terminals to / from the Verrazano Bridge. The environmental conditions evaluated started from slack water up to maximum flood / ebb, and wind conditions from calm up to 20 knots.

### Deliverables – Parts A & B Phase I Studies

The following services were provided to meet the study’s objectives:

- ♦ Updated the existing MITAGS visual New York Harbor database to include the heightened Bayonne Bridge and changes to Port Elizabeth, Port Newark, Howland Hook, and Global Marine Container Terminal Berths capable of handling the ULCVs.
- ♦ Updated the depth contours based on the ACOE soundings. This enhanced the simulation of the “bank effect” experienced by a deep-draft vessel transiting in a restricted channel.
- ♦ Modified USACOE water current data to be uploaded into the simulator for exercises. Waterway Simulation Technology (WST) programmed 48 different water current models that covered two different Hudson River flow conditions, and multiple times. Each model is a single point in time.
- ♦ Modified the MITAGS library’s hydrodynamic ship model of the *Maersk Triple E* Class to drafts of 42’-00” and 49’-00.” The models were even keel. The models represented ULCV with maximum LOA of 1,308’ x 193.5’ beam.



- ◆ Provided the MITAGS library's ASD "Edward J. Moran" tug model.
- ◆ Provided MITAGS library Transas Conventional #4 tug model to represent the class of conventional tugs that are currently used for post panamax vessels.
- ◆ Programmed the "Brian McAllister" ASD model.
- ◆ Assisted in the development of the test matrix with client.
- ◆ Pre-validated database and models with Sandy Hook Pilots and Docking Masters on May 3 – 6, 2016. Also contracted with a United Kingdom pilot to assist in the model validation process.
- ◆ Provided pilot plug interface for the pilots' portable navigation system.
- ◆ Provided one FMSS and one tug bridge for one-way traffic simulation tests, and two, FMSS and one tug bridges for two-way traffic tests.
- ◆ Conducted simulation tests with appropriate support staff of shiphandling expert, simulator operator, and engineering support.
- ◆ Contracted with Towing Solutions, Inc. to observe tests and make recommendations related to the use of assist tugs.
- ◆ Provided report of simulation tests with findings, conclusions, recommendations, and supporting data.
- ◆ Contracted with Waterway Simulation Technology (WST) to complete a surge study to calculate the approximate forces and moments a 9,000 TEU Containership, and Aframax tanker, moving at speeds from 4 to 8 knots, would exert on a tanker moored parallel to the ship channel in still water at select distances off the moored vessel. This was compared against the forces and moments generated by models of the *MSC Kalina Class* and *Maersk Triple E* transiting at the same speeds and distances. (A separate report.)

### 1.3 ASSUMPTIONS

MITAGS used the following assumptions in developing this study:

1. The Port Authority provided accurate data of the areas not depicted on existing NOAA for programming the terminals. This included location of berths, bulkheads, dimensions of container cranes, and depth soundings alongside.
2. The Port Authority provided accurate electronic pictures of the facilities.
3. The Pilots provided the climatological data on the environmental conditions simulated and included in the test matrix. This included prevailing wind directions / strengths.
4. The Port Authority provided accurate illumination guides for terminal lights for night visuals.
5. MITAGS test matrix assumed one-way traffic for most exercises. Select meeting situations in the Kill Van Kull were conducted using two bridges integrated together. This allowed pilots to conn both bridges.
6. Made four tugs available for each exercise. The assist tugs included two, 46-ton BP conventional, and two, ASDs with bollard pull between 80 to 85 tons.
7. The Pilots provided information on the size of target vessels placed alongside the berths at 5c-IMTT, Buckeye Bayonne, Gordon's Terminal, Pier A-IMTT.



## 1.4 ASSUMPTIONS AND LIMITATIONS

Inherent in any simulation is the accuracy of the data programmed into the simulator. MITAGS simulation exercises are based on the information provided by the client. The accuracy of this data will have a major impact on the validity of the test results.

The hydrodynamic models used in the simulation were vetted by experienced pilots, MITAGS staff, and company representatives. The model behaviors are based on the pilot card, windage, general arrangement plans, squat table, and other data provided by client or other sources. The model behaviors, as calculated by the simulator, are adjusted based on the consensus opinion of the MITAGS staff and the pilots. Since the adjustments are “subjective,” the recommended model adjustments may vary depending on the collective experience of the testing captains and pilots at each session. The models were a good approximation of the particular classes of vessels. Specific vessels in “real-world” situations may handle significantly different from those programmed into the simulator.

The MITAGS simulator provides a close approximation of vessel squat in shallow water. However, an adequate safety margin needs to be used in order to account for changes in squat due to vessel speeds, displacements, channel shoaling, and tidal actions. In this study, squat was generally not a significant factor due to the water depths and slow speeds.

Due to the underwater volume of these vessels, substantial surge forces may occur in confined waters even at low speeds. *Port Elizabeth Reach* and *Port Jersey* warrant special attention due to restricted configurations. This analysis is beyond the capabilities of full-mission ship simulation.

Model behavior is highly dependent on the accuracy of depth contours (shape), the current and wind flows. In “real world” situations, such forces could vary significantly over the operating area. In addition, the models used in these tests were representative of “vessel classes” similar in size and displacement. Vessels of the same class may have significant differences in handling characteristics in real-world conditions.

Water currents were based on U.S. Army Corps. Engineers’ models. However, at the time of simulation, there were no field measurements available at Bergen Point for validation purposes. (Additional current meters are being installed at Bergen Point and other areas. Once installed the simulated current models should be compared.)

The “auto-tug” feature of the simulator provides a more realistic simulation of the assist tug than vector forces, but is not as accurate as having a tug bridge integrated with the full-mission simulator. Auto-tugs and one integrated tug bridge was used in these tests.

The test recommendations assume experienced pilots and tug masters operating vessels with the current technology. Operational limits should take into account the real-world tug capabilities, and the need for all local pilots and tug masters to gain experience. Limitations can be gradually reduced as the pilots and tug masters gain experience.

## 1.5 PROJECT TEAM AND SIMULATION FACILITIES

Project team members are listed below. The team members are highly experienced in channel design / modeling, simulation and shiphandling. The full-mission shiphandling simulator meets or exceeds the Det Norske Veritas (DNV) standards. MITAGS-PMI is DNV certified as a “Maritime Training and



Simulation Center.” Please refer to the MITAGS-PMI Simulation Capability & Facilities Guide for further details on team member qualifications and simulation capabilities.

<b>Table 2: 18,000 TEU (Part B, Phase I) Support Team for August 23-26, 2016 Tests</b>	
<b>MITAGS Team Member</b>	<b>Position and Duties</b>
Mr. Glen Paine Executive Director	Responsible for overall coordination with client representatives and ensured the necessary resources were allocated to the project.
Mr. Hao Cheong Ship Modeler	Responsible for the overall simulation technical support of project. Assisted in collecting the data for modeling the terminals and vessels. Served as liaison with MITAGS Simulation Engineering Staff.
Mr. Robert Weiner, Naval Architect Ship Modeler	Responsible for the programming of the ship models, databases, and underwater depth contours. Also provides support for simulator projection system and maintenance during tests.
Captain Curtis Fitzgerald SHS Consultant	Responsible for validating the ship model with Capt. Michael.
Captain Larry Bergin Shiphandling Consultant Project Leader	Responsible for providing on-bridge support to pilots conning the simulated vessels, and expertise in the handling of large deep-draft vessels in pilotage waters.
Captain Greg Brooks, TSI Assist Tug Consultant	Provided comments and suggestions on the use of assist tugs during transits and berthing evolutions. Co-author of Final Report.
Capt. Ken Kujala Simulator Operator	Responsible for the overall operation of the simulator during the tests. Reports to MITAGS SHS Project Leader.
<b>Sandy Hook, Docking Masters, and Tug Captains</b>	
Captain R. J. Schoenlank	Senior Pilot and President, Sandy Hook Pilots
Captain John J. DeCruz	Sandy Hook and President, Sandy Hook Pilots
Captain Robert J. Blake	Sandy Hook Conning Pilot
Captain John Oldmixon	Sandy Hook Conning Pilot
Capt. Jack Olthuis	Executive Director, Sandy Hook Pilots
Capt. Bobby Flannery	Moran Docking Master and Conning Pilot
Capt. Robert Ellis	McAllister Docking Master and Conning Pilot
Capt. Nathan Oliveira (6/29 to 7/1)	Moran Tug Master and operator of tug bridge
<b>Observers</b>	
Captain Michael Day	Captain of the Port – New York. United States Coast Guard (24 <sup>th</sup> )
Mr. Gregory Hitchen	Director, Vessel Traffic Service. United States Coast Guard. (24 <sup>th</sup> )
Ms. Bethann Rooney	Assistant Director, Port Development, The Port Authority of NY & NJ.

## 1.6 TIME LINE AND TEST LOCATION

The Study took place at the Linthicum Heights, Maryland Campus of the Maritime Institute of Technology and Graduate Studies. This campus is located near the Baltimore / Washington



International Airport (BWI) and has easy access to the AMTRAK® BWI Baltimore Station as well as Interstate I-95. Hotel accommodations were made available on the 40-acre campus.

**Part B, Phase I (18,000 TEU ULCV)** took four days to complete (Tuesday, August 23, 2016 to Friday, August 26, 2016). Monday, August 22, 2016 was used for pre-validation review.

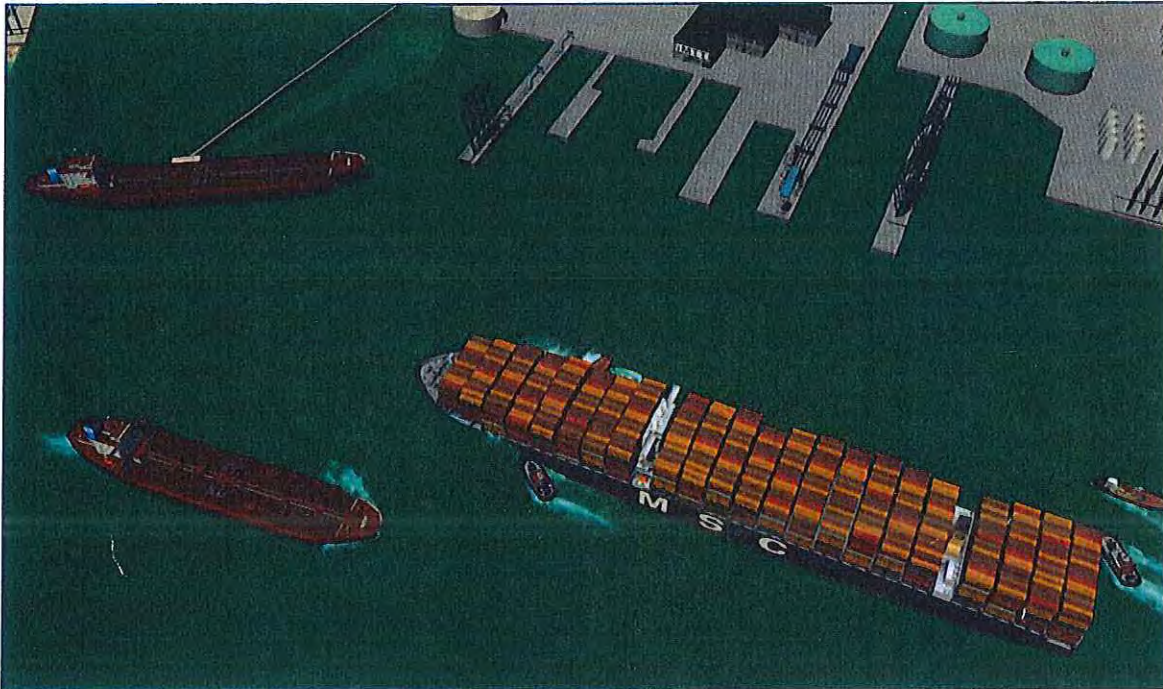


**Figure 3: Kalina Meeting in KVK**



## 2. HYDRODYNAMIC SHIP MODELING

The ship models, used in the study included two load conditions. Each hydrodynamic model was pre-validated by the MITAGS-PMI shiphandling experts comparing to sea trial data, tank tests (if available), pilot / captain reports, and vessels of similar class and size. The models were also validated by pilots that had experience handling these vessel classes. The models used data provided by MSC and Maersk Lines. Please refer to Appendices for more detailed information on the handling characteristics of each model.

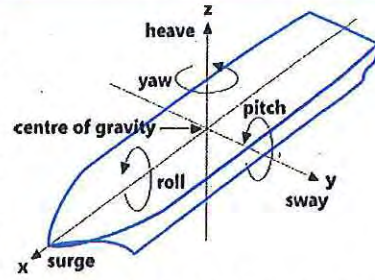


Figure 4: Model Motion

Table 3: Ship Models Used in the Study

Ship Models	Parts A & B 14,000 TEU ULCV MSC Kalina Class	Part B 18,000 TEU Maersk Triple E	Assist Tug	Assist Tug*	Assist Tug*
			Transas Conventional #4	Brian A. McAllister	Edward J. Moran
Bridge Location	Forward	Forward	n/a	n/a	n/a
Maximum Container Load	14,000 TEU	18,000	n/a	n/a	n/a
Displacement at 42' Draft	172,769	206,397	n/a	n/a	n/a
Displacement at 49' Draft	198,160	240,905	n/a	n/a	n/a
Wind Area with Max Deck Load in Load & Ballasted (sq. meters)	14526m <sup>2</sup> at 42' draft 14,000m <sup>2</sup> at 49'draft	15,633m <sup>2</sup> at 42' draft 16,555m <sup>2</sup> at 49'draft	n/a	n/a	n/a
Length (meters)	366 (1,201')	399 (1,308')	126 feet	99.1 feet	100 feet
Beam	51.2 (168')	59 (193.5')	34 feet	40 feet	37.1'
Trim	even	even	even	even	even
Load Draft	14.9 (49')	14.9 (49')	12'-06"	18.9 feet	16 feet
Mid Load Draft	12.8 (42')	12.8 (42')	n/a	n/a	n/a
Engine kW and Propeller	Low Speed Diesel, Single Screw FPP	Low Speed Diesel, Twin Screw FPP	Conventional twin screw	6,770 BHP	6,000 BHP
Rudder Type	1, Semi suspended	2, Semi suspended		ASD	ASD
Bow Thrusters	2, at 1,700kW	2 at 2,500kW each	n/a	n/a	n/a
Stern Thrusters	n/a	n/a	n/a	n/a	n/a
Chock and Bitt SWL/Bollard Pulls	75 metric tons	75/ 150	46 metric tons	85 metric tons +	83 tons
Chock and Bitt Locations	Fwd. / Aft	Fwd. / Aft	n/a	n/a	n/a
Tug Location Restrictions	TBD	TBD	n/a	n/a	n/a

\*The model Edward J. Moran was programmed for the Savannah River Pilots ULCV Tests. It should have similar horsepower and bollard pull as the Moran boats being built at Washburn & Doughty. The Brian McAllister was programmed using design parameters since the vessel is still under construction.



The test matrix used assessed the impact of the following forces on the handling of these simulated vessels:

- ◆ Prevalent local environmental conditions (waves, wind, currents, and tides).
- ◆ Forces created by tugs.
- ◆ The reduction in under keel clearance due to squat and interaction.
- ◆ Bank effects depending on the channel conditions and ship operating speed.
- ◆ Drift angles created by wind forces from various directions.
- ◆ Acceleration and deceleration of model.
- ◆ Rudder / propulsion forces needed to maintain track line.

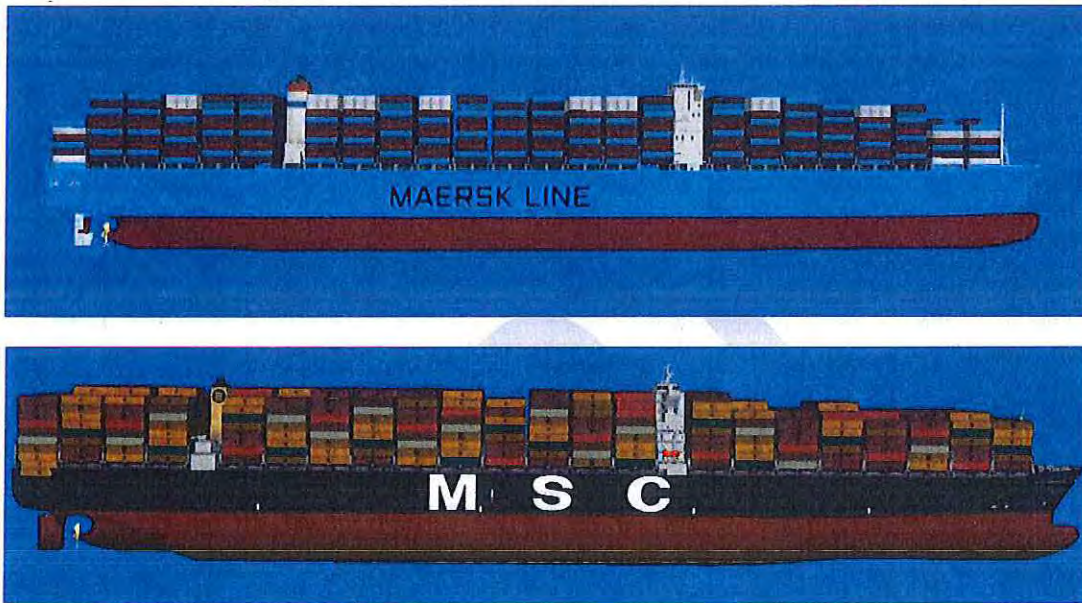


**Figure 5: Profile Views of the Triple E and Kalina Models**

### 3. DATABASES' DEVELOPMENT

The MITAGS Simulation Engineering Department used proprietary Transas® database modeling software to import the electronic chart display information system (ECDIS) data. This software automatically transferred the information from ECDIS into simulator database elements, and links the visual and radar databases. The ECDIS data included:

- ◆ Hydrographic: depth points, depth lines, depth contours, drying areas, three dimensional (3D) channel bottom.
- ◆ Landmass: 3D terrain, DEM data, coastlines, islands, pier structures, etc.
- ◆ Navigation Aids: buoys, ranges, and lighthouses.
- ◆ Navigation Signals: color, light timing, light sector, etc.

The database was then overlaid with the terminal design(s), approach channels, and any other navigationally significant feature that was available. The database included ECDIS and RADAR displays.



**Figure 6: Sample Visual Graphics<sup>1</sup>**

---

<sup>1</sup> The visual depicts the existing Bayonne Bridge raised in height for the purposes of the simulation study. It does not reflect the image bridge after construction. The pilots did not evaluate placement for maximum air draft for maneuvering at Bergen Point. The bridge visuals can be updated at a later date for future training requirements.



Table 4: Electronic Chart Data Used for Developing Visual Databases			
New York_F Database Information			
Database version: 6.40.000.24062.55			
Build data: 7/1/2016			
Exercise area size: 47.9 x 43.0 nautical miles			
Number of lighthouses: 75			
Number of buoys: 384			
<b>Database purposes</b>			
New York_F exercise area is designed for the purposes of navigational training.			
<b>Database bounds</b>			
New York_F exercise area exists within the rectangle with following coordinates:			
SW corner: 40°09.00N 74°13.99W			
NE corner: 40°51.99N 73°11.00W			
<b>List of used electronic nautical charts</b>			
NM	Number	Scale	Date of last correction
1	u12339	10000	08.04.2004
2	u12334	10000	03.03.2004
3	u12335	10000	08.04.2004
4	u12333	15000	08.04.2004
5	u12401	15000	08.04.2004
6	u12402	15000	08.04.2004
7	u12366	20000	08.04.2004
8	u12326	80000	08.04.2004
Created by			
6/29/2016			
<b>The following updates have been added in the database.</b>			
1. Updated all of the navigational aids to NOAA ENC charts dated March 2016			
> US4NY1AM			
> US5NJ11M			
> US5NJ13M			
> US5NJ14M			
> US5NY1BM			
> US5NY1CM			
> US5NY1DM			
> US5NY1IM			
> US5NY12M			
> US5NY19M			
2. Imported the depth survey of 2015 from the Army Corp			
3. Imported the depth survey of 2014 and 2016 from NOAA			
4. Added more visual details around Port Elizabeth, Global Marine Terminal, Howland Hook Terminal and also along the coastline.			
5. Raised the Bayonne Bridge to meet the specified clearance			



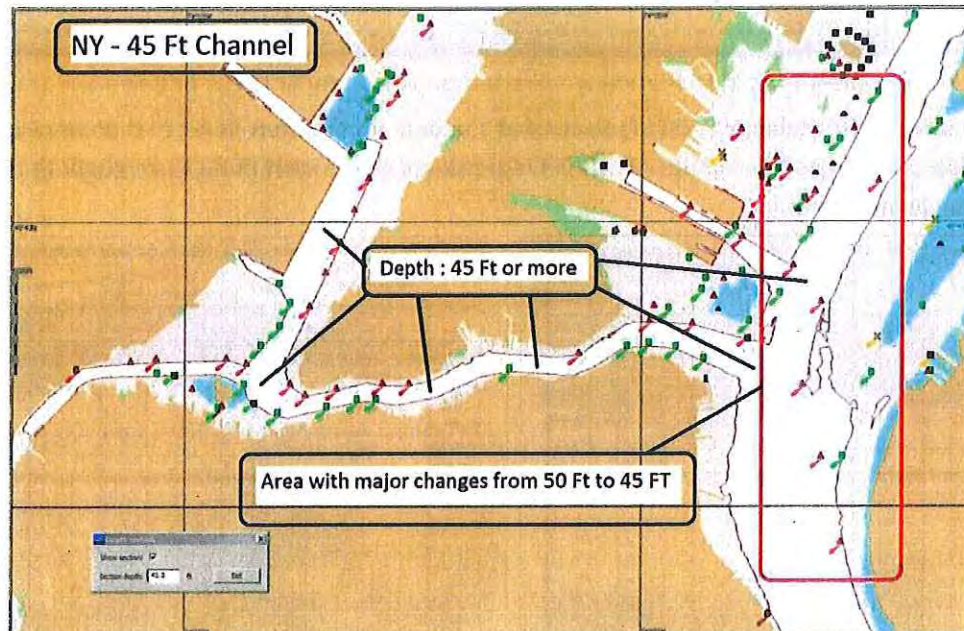


**Figure 7: Depth Areas of 45 feet or More at MLLW**

### 3.1 UNDERWATER CONTOURS

The first stage of the programming used the underwater contours based on the NOAA electronic chart for that area from the Transas® World Library. It was then enhanced with bathymetric data provided by the Army Corps of Engineers for the navigation channel, and NOAA for deep water adjacent to the channels. This created more realistic bank slopes and contours. The bathymetric data coordinates were in latitude and longitude and referenced to WGS-84 datum. Coordinate format was degrees and decimal degrees to six places. Isolated shallow spots were removed from the channels, and alongside the berths at Global Marine Terminal, Port Elizabeth, and Howland Hook.

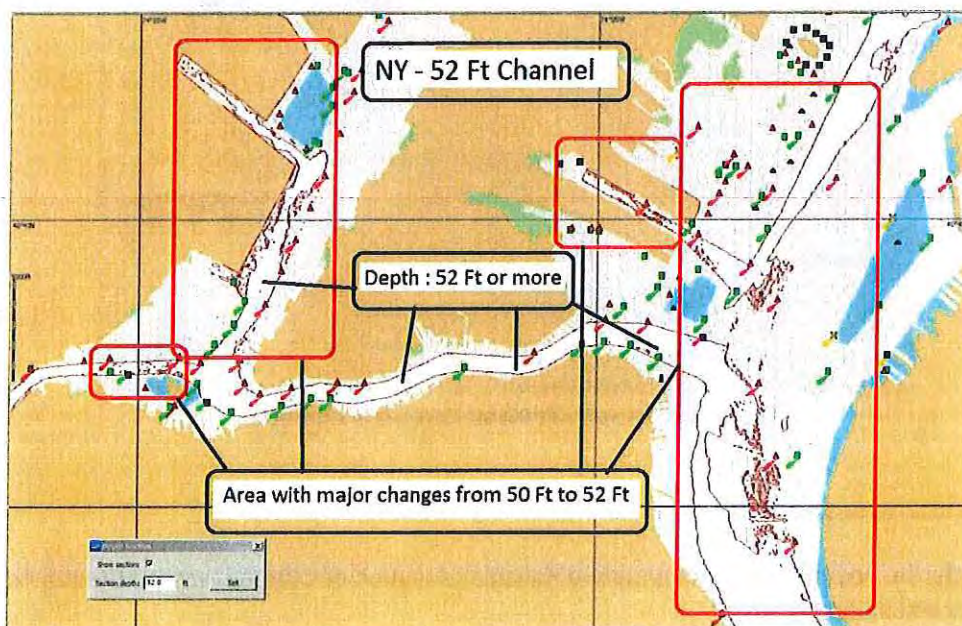


**Figure 8: Depth Areas of 52 Feet or More at MLLW**



### 3.2 WATER CURRENTS

The water current models used in the Study were based on U.S. Army Corps of Engineers (ACOE) data. Waterway Simulation Technology (WST) formatted the data in 48 different files<sup>2</sup> that were capable of being loaded into the Transas Simulator. Each file represented the current flows throughout the testing area at a single point in time.

May 10, 2012 - After Spring Tide - 51,300 cfs on Hudson River (Magnitude in Knots)							
File	Goethals Bridge	Bergen Pt.	Port Elizabeth	Constable Hook Range	Port Jersey	Verrazano Bridge N	Verrazano Bridge S
NY-3120	0.31	1.28	0.29	0.60	0.08	0.50	0.29
NY-3121	0.16	1.44	0.39	0.70	0.39	1.26	0.91
NY-3122	0.54	1.57	0.50	0.85	0.81	1.73	1.40
NY-3123	1.03	1.36	0.49	0.76	1.01	1.98	1.59
NY-3124	1.18	0.60	0.31	0.23	0.97	1.67	1.26
NY-3125	0.78	0.54	0.04	0.43	0.58	0.62	0.60
NY-3126	0.12	1.03	0.58	0.70	0.00	0.70	0.21
NY-3126(1.25)	0.15	1.29	0.73	0.88	0.00	0.88	0.26
NY-3127	0.60	0.76	0.80	0.70	0.64	1.46	0.85
NY-3128	0.87	0.35	0.62	0.52	0.91	1.77	1.14
NY-3129	0.95	0.10	0.47	0.27	0.99	1.78	1.20
NY-3130	0.89	0.04	0.37	0.19	0.93	1.59	1.09
NY-3131	0.85	0.12	0.25	0.06	0.74	1.16	0.83
NY-3132	0.68	0.37	0.08	0.19	0.50	0.64	0.49
NY-3133	0.47	0.76	0.10	0.45	0.14	0.23	0.16
NY-3134	0.12	1.67	0.37	0.85	0.43	1.46	1.09
NY-3135	0.49	2.04	0.62	1.05	0.89	2.00	1.61
NY-3135(1.25)	0.61	2.55	0.78	1.31	1.11	2.50	2.01
NY-3135(1.5)	0.74	3.80	0.93	1.60	1.34	3.00	2.42
NY-3136	1.38	1.32	0.54	0.66	0.97	1.80	1.47
NY-3137	1.13	0.37	0.04	0.45	0.62	0.70	0.76
NY-3138	0.31	1.09	0.70	0.58	0.12	0.35	0.21
NY-3139	0.74	0.50	0.74	0.41	0.29	0.95	0.14
NY-3140	0.72	0.16	0.37	0.21	0.64	1.09	0.66
NY-3141	0.72	0.06	0.31	0.25	0.87	1.63	1.13
NY-3142	0.91	0.16	0.43	0.37	0.95	1.75	1.16
NY-3143	1.01	0.19	0.49	0.25	0.76	1.28	0.89
Flood Tide							
Ebb Tide							

April 8, 2012 - Spring Tide - 7,062 cfs on Hudson River (Magnitude in Knots)							
File	Goethals Bridge	Bergen Pt.	Port Elizabeth	Constable Hook Range	Port Jersey	Verrazano Bridge N	Verrazano Bridge S
NY-2352	0.97	1.78	0.62	0.95	1.03	2.19	1.77
NY-2353	1.40	1.18	0.52	0.62	1.14	2.21	1.83
NY-2353(1.5)	2.10	1.77	0.83	0.93	1.71	3.32	2.45
NY-2354	1.24	0.31	0.29	0.10	0.95	1.51	1.16
NY-2355	0.58	0.70	0.14	0.62	0.45	0.27	0.45
NY-2356	0.31	1.05	0.72	0.76	0.19	1.01	0.39
NY-2357	0.68	0.80	0.83	0.78	0.83	1.61	1.01
NY-2357(1.25)	0.85	1.00	1.04	0.98	1.04	2.01	1.26
NY-2357(1.8)	1.22	1.44	1.49	1.75	1.50	2.90	1.82
NY-2358	0.93	0.43	0.66	0.52	1.01	2.00	1.34
NY-2359	0.55	0.31	0.54	0.33	1.09	1.98	1.36
NY-2359(1.5)	1.43	0.47	0.81	0.50	1.64	2.97	2.04
NY-2359(2.3)	2.19	0.71	1.25	0.76	2.50	4.55	3.12
NY-2360	0.91	0.23	0.50	0.33	0.97	1.69	1.16
NY-2361	0.87	0.10	0.35	0.12	0.74	1.09	0.78
NY-2362	0.74	0.78	0.04	0.49	0.37	0.12	0.14
NY-2363	0.31	1.86	0.33	0.91	0.23	1.34	0.99
NY-2364	0.35	2.15	0.60	1.05	0.80	1.94	1.55
NY-2365	1.18	1.73	0.60	0.83	1.01	2.08	1.63
NY-2366	1.26	0.43	0.25	0.08	0.91	1.53	1.28
NY-2367	0.52	0.43	0.17	0.49	0.58	0.70	0.70
NY-2368	0.23	0.80	0.52	0.58	0.17	0.19	0.17
NY-2369	0.43	0.50	0.54	0.47	0.43	1.16	0.47
NY-2370	0.72	0.43	0.50	0.54	0.89	1.73	1.18
NY-2371	0.91	0.45	0.56	0.52	1.03	2.02	1.38
NY-2372	0.59	0.41	0.60	0.41	0.99	1.77	1.24
NY-2373	1.01	0.19	0.37	0.10	0.70	0.91	0.64
NY-2374	0.64	1.28	0.12	0.70	0.33	0.19	0.14
NY-2375	0.64	1.63	0.39	0.74	0.16	1.09	0.81
Flood Tide							
Ebb Tide							

Figure 9: WST Water Current File Names

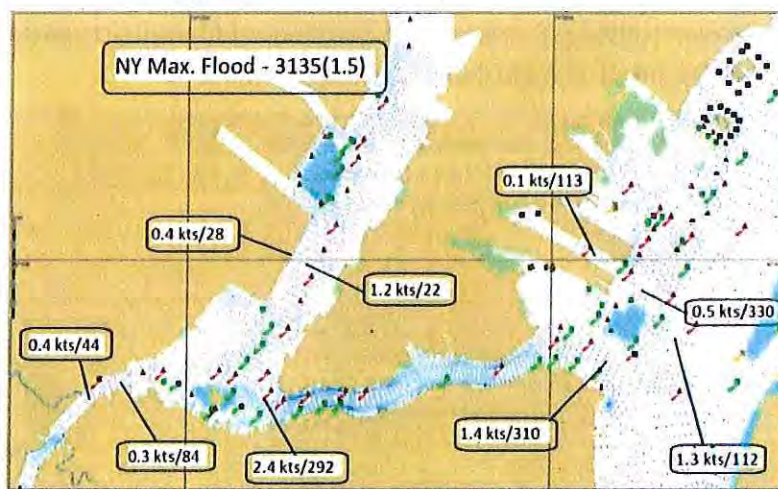


Figure 10: Sample Flood Current Data Points

<sup>2</sup> Please refer to the Appendices for a more detailed explanation of how the water current models were developed and programmed.



During the pre-validation exercises, the pilots noted that the directions of flows were accurate, but the velocities were less than they expect to experience in real-world situations in the Bergen Point area. WST increased the velocities of each data point by a certain percentage (see file names highlighted in yellow in the table above). After the changes, the pilots felt the ship model reaction was more realistic. However, it did raise some concern about the accuracy of the velocities and the model responses to the current forces.

Transiting through Bergen Point (inbound / outbound) was determined to be the controlling factor of the transit. The ULCVs would have to time their transits to make the turn at Bergen Point when the tidal currents velocities were low. This meant determining time "windows" on either side of slack water-high, and slack water-low that the velocities would be low enough for safe transits. Theoretically, there would be four different time windows per twenty-four hour tidal cycles (two highs, two lows). However, the Triple E at 49' draft would be limited to the periods before / after slack water-high in order to have enough under keel clearance.

To determine which current model files to use, the pilots analyzed the NOAA predicted current tables for the Bayonne Bridge KVK location (the closest reference to Bergen Point). They were able to determine that, on average, the change in current velocity on either side of slack waters over time can be roughly calculated as a percentage of the max current velocity during a particular tide cycle. The relationship determined was as follows:

**Flood to High Water Slack (High Water)**

- ◆ 1.5 hours before the end of the flood-high water, the current strength was approximately 60% of the predicted max flood current.
- ◆ 1 hour before the end of flood-high water, the current strength was approximately 43% of the predicted max flood current.

**High Water Slack Ebb Begins**

- ◆ 1 hour into the ebb, the current strength was approximately 40% of the predicted max flood current.
- ◆ 1.5 hours into the ebb, the current strength was approximately 54% of the predicted max flood current.

**Ebb to Slack Low Water**

- ◆ 1.5 hours before the end of ebb-low water, the current strength was approximately 60% of the predicted max flood.
- ◆ 1 hour before the end of the ebb-low water, the current strength was approximately 40% of the predicted max flood.

**Slack Flood Begins (Low Water)**

- ◆ 0.5 hour (30 minutes) into the flood, the current strength was approximately 30% of the predicted max flood.
- ◆ 1 hour into the flood, the current strength was approximately 60% of the predicted max flood.
- ◆ 1.5 hours into the flood, the current strength was approximately 85% of the predicted max flood.

Assuming 2.55 knots as the average maximum flood current at Bergen Point, the following current velocities were calculated based on percentages:

**Flood to High Water Slack (High Water)**

- ◆ 1.5 hours before the end of flood-high water, 60% of 2.55 knots: 1.53 knots flood
- ◆ 1 hour before the end of flood-high-water, 43% of 2.55 knots: 1.09 knots flood

**High Water Slack Ebb Begins**

- ◆ 1 hour into the ebb, after high water, 40% of 2.55 knots: 1.02 knots ebb
- ◆ 1.5 hours into the ebb, after high water, 54% of 2.55 knots: 1.38 knots ebb

**Ebb to Slack Low Water**

- ◆ 1.5 hours before end of ebb-low water, 60% of 2.55 knots: 1.53 knots ebb
- ◆ 1 hour before the end of ebb-low water, 40% of 2.55 knots: 1.02 knots ebb

**Slack Flood Begins (Low Water)**

- ◆ 0.5 hour into the flood after low water, 30% of 2.55 knots: 0.77 knots flood
- ◆ 1 hour into the flood after low water, 60% of 2.55 knots: 1.53 knots flood
- ◆ 1.5 hours into the flood after low water 80% of 2.55 knots: 2.1 knots flood

From this information, the pilots went back to the WST current model files and selected models where the maximum currents at Bergen Point were the closest to the following values:

1. 1.02 knots to represent 40% of ebb.
2. 1.53 knots to represent 60% of ebb.
3. 1.09 knots to represent 43% of flood.
4. 1.53 knots to represent 60% of flood.

**Approximate Bergen Point Transit Time Windows**

Based on above, the ULCV should have the following time windows where, on average, the maximum predicated current at Bergen point would be the following percentage less than max current:

- ◆ 60% or less: 1.5 before to 2.0 hours after high-water slack; 1.5 hours before to 1.0 after low-water slack.
- ◆ 40% or less: 1.0 before either side of high-water slack; 1.0 hour before to 45 minutes after low-water slack.

Again, note that the ULCV at 49' draft can only use the time windows around slack high water to ensure enough under keel clearance.

### 3.3 WIND DIRECTIONS AND SPEEDS

Wind directions and speeds were controlled from the operator console. The directions, and speeds (including gusts), were provided by the local pilots. In most cases, the wind directions and velocities selected were the most challenging. Maximum wind speed tested was 30 knots.

### 3.4 VISIBILITY; DAY NIGHT SCENES

Tests were conducted with clear visibility during daylight hours. However, the simulator operator was capable of simulating rain squalls, fog, low-altitude clouds, and night visuals.



#### 4. WATERWAY SIMULATION TECHNOLOGY (WST) SUPPORT STUDIES

WST generated a separate “Memo for the Record of Passing Effects on Moored Vessels in Kill Van Kull 6-4-16.” The Study placed a target vessel in the approximate position of the Hess (Buckeye) – Bayonne Terminal berths. It then calculated the theoretical forces each vessel class would generate on the berth when transiting along the centerline of the channel at various speeds. The *Kalina*, at 5 knots, generated the same forces as the *AMaersk* (9,000 TEU) at 6 knots. The *Triple E*, at 4 knots, generated the same forces as 9,000 TEU at 6 knots. The pilots used this as guidance for the maximum speed to transit in the KVK where the theoretical forces would be no greater than currently produced by current vessel transits. Note that the forces’ calculations were based on maintaining position on the center line of the channel. Forces rapidly increase as distance between the transiting ship and berth decreases.

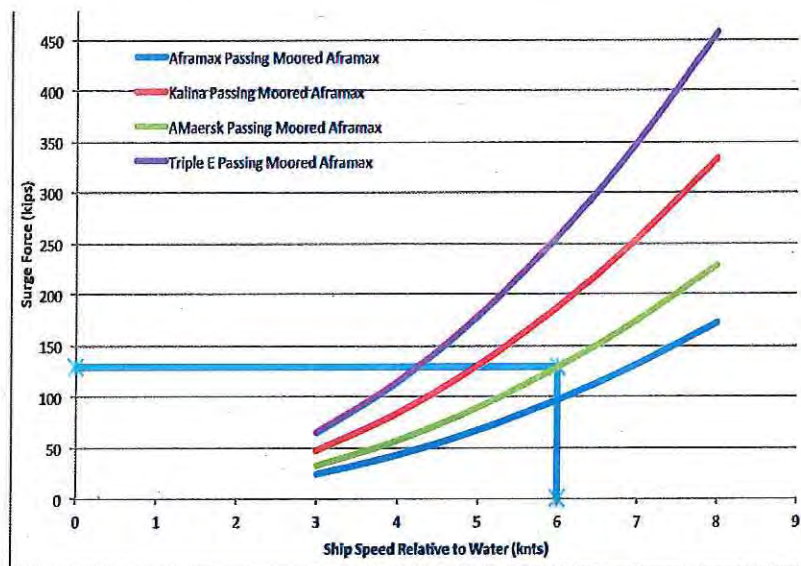


Figure 6: Moored Aframax Forward Surge Forces

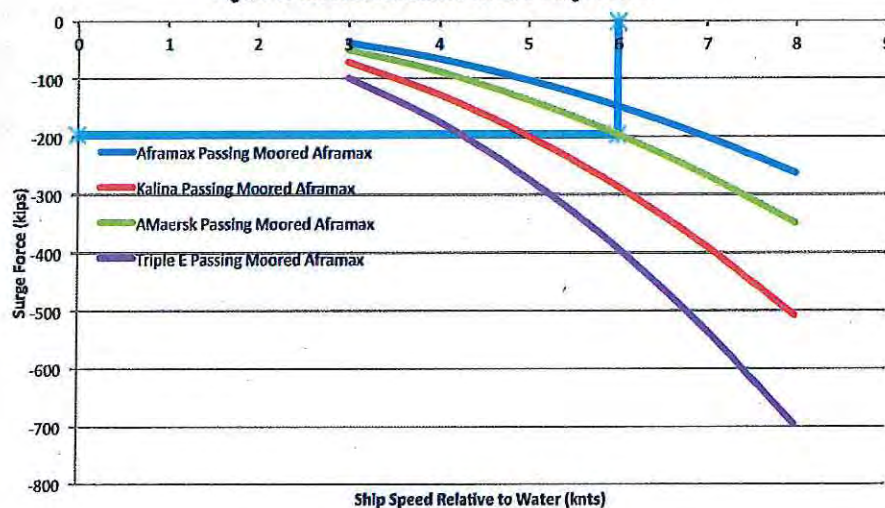


Figure 7: Moored Aframax Aft Surge Forces

Figure 11: Excerpt of Surge Forces vs. Speed by Vessel Class in the KVK from the WST Report.



## 5. MANEUVERING STUDY METHODOLOGY

MITAGS programmed the deepened navigation channels, turning basin, and container berths. MITAGS modified the *Maersk Triple E Class* hydrodynamic ship models to the requested drafts (42' and 49'). The tide was set at mean lower, low water (MLLW) unless otherwise specified by the conning pilot. All models used the maximum deck load profile for windage area.

The test matrix was developed by the pilots to formulate the "best practices for handling 18,000 ULCVs to the specific container terminals, suggested environmental limits (wind, current, tide, and visibility), and assist tug requirements. The exercises used the *Triple E Class* Models at the 42' and 49' drafts. Target ships were placed on the container berths to better simulate the expected restrictions. All simulation exercises were run in "real time." This meant that it took close to the same amount of time in the simulator as in the real world. To maximize the simulator time, the exercises were stopped when the objectives were achieved. In order to make better use of the simulator time, the pilots decided not to evaluate Howland Hook, Staten Island Terminal since these berths are not equipped to handle the 14,000 TEU Class of containership ships. In four days, the pilots completed twenty-seven runs.

### 5.1 EXERCISE SCENARIOS

After each run, the coning pilot and tug operator were debriefed and requested to fill out a run questionnaire. At the end of the simulation, final evaluations were requested from all participants and a consensus on the parameters needed to handle this class of ship on a routine basis.

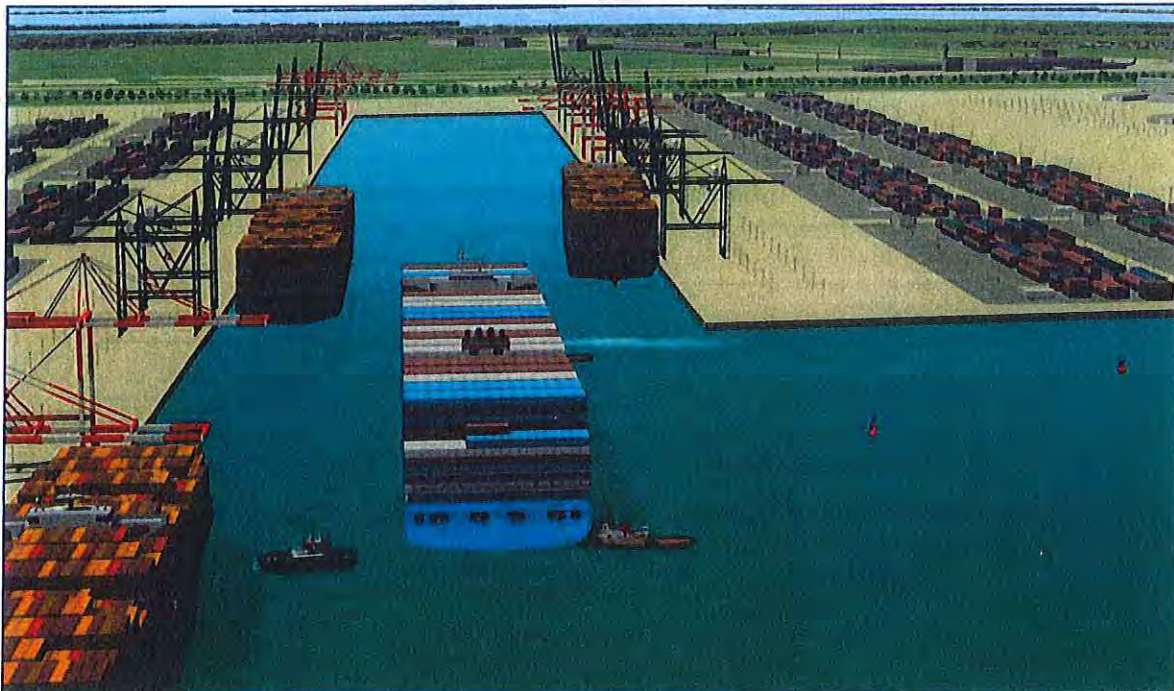


**Figure 12: Triple E entering Port Elizabeth Branch Reach**



## 6. TOWINGS SOLUTIONS OBSERVATIONS – 18,000 TEU

Towing Solutions, Inc., is a recognized expert in the use of assist tugs. MITAGS contracted with TSI to observe the simulation and provide suggestions on ways maximize the efficiencies of the assist tugs, and comments on the feasibility of handling Ultra Large Container Vessels (ULCVs) in the Port of New York/New Jersey.

This Study was a preliminary review of the feasibility of handling 18,000 TEU ULCVs. It was a follow-up to the 14,000 TEU Study conducted in June 27 – July 1, 2016). Both classes of vessels are in service, and are significantly larger than the current ULCVs calling on the Port of NY / NJ. The Study completed 27 research simulation runs of various lengths to develop procedures, if possible, to safely and consistently bring these large ships into both Port Elizabeth and Global Terminal in Port Jersey. To facilitate the review, the runs are categorized as follows:

1. Full (or near full) runs inbound or outbound from Stapleton Anchorage to Port Elizabeth.
2. Rounding Bergen Point inbound from Bergen Point East Reach to Buoy 3 in Newark Bay.
3. Rounding Bergen Point Outbound from Buoy 3 in Newark Bay to Bergen Point East Reach.
4. Inbound from Buoy 10 Newark Bay to Port Elizabeth.
5. Outbound from Port Elizabeth to Buoy 10 Newark Bay.
6. Inbound from Upper Bay Buoy 30 to Global Terminal.
7. Outbound from Global Terminal to Upper Bay Buoy 30.
8. Emergency Turns above and below the Verrazano Narrows Bridge.

The Feasibility Evaluation Team met with the MITAGS staff on the afternoon of Monday, August 22, 2016, to review the data that they had gathered and developed on the Maersk "Triple E" 18,000 TEU ULCV. Additionally, time was allotted to run additional exercises with the *Kalina model* meeting a smaller tanker (600'x10'x41') in the Kill Van Kull.

With the exception of the meeting runs previously mentioned and some demonstration runs, The Maersk "Triple E" class model was used at 42' and 49' drafts. The tug packages consisted of a mix of up to four tugs. The newly modeled *Brian McAllister* was used to model a 6,000 hp. ASD with a bollard pull rating of approximately 85 (metric) tons. This *Edward J. Moran* model was also used (an 82 ton, 6,000 hp. ASD). In addition to the two tractors, the Docking Masters (DMs) had the option of adding up to two, 4,000 Hp. 46 ton bollard pull conventional boats (*Brendan McAllister* and *McAllister Sisters*). During these sessions, one of the ASDs was operated by Captain Nathan Oliveira of Moran. The other boats were controlled by the simulator operator with advice provided by Captain Brooks if there was a question as to the DM's order(s).

## 6.1 FULL LENGTH RUNS - IN OR OUTBOUND – CON HOOK TO PORT ELIZABETH

### Run 1 *Kalina* Meeting a Tanker (600'x 105' x 41') in KVK

Pilot: Robert Flannery

*Kalina*, 49' Draft

Pilot: Robert Blake

600'x 106' CPP Tanker

Wind/Current: 40% Flood, S 20

Start: Con Hook Reach

Finish: Con Hook & Bergen Point Reaches

Tugs: *Kenny* Port Bow, *Brian* Starboard Bow, *Edward* C/L aft, *Miriam* port bow

#### Description:

Initially the Docking Master (DM) used the *Edward* at half astern to slow the *Kalina*, and then increased the *Edward's* power to  $\frac{3}{4}$ . The DM then used the *Edward* at a port 45° to slow his swing into the KVK. The ship was making 4.0 knots passing Hess, Bayonne, with the *Edward* stopped. The *Edward* was then used at a 45° angle to port at half power to slow the ship and induce a starboard turn on the ship. Several of the tugs were used to turn to starboard and then arrest the turn as the ship was still making only 4.0 knots as the ship passed the red lighted buoy. The ships met by design just before the intersection of Con Hook Reach and the Bergen Point East Reach. The ships safely passed each other with a separation of 354' (the *Kalina* was making 4.5 knots). However, as is usual with the *Kalina*, her stern swung wide in the turn and the stern was closer to the tanker berth on the north side of the channel.

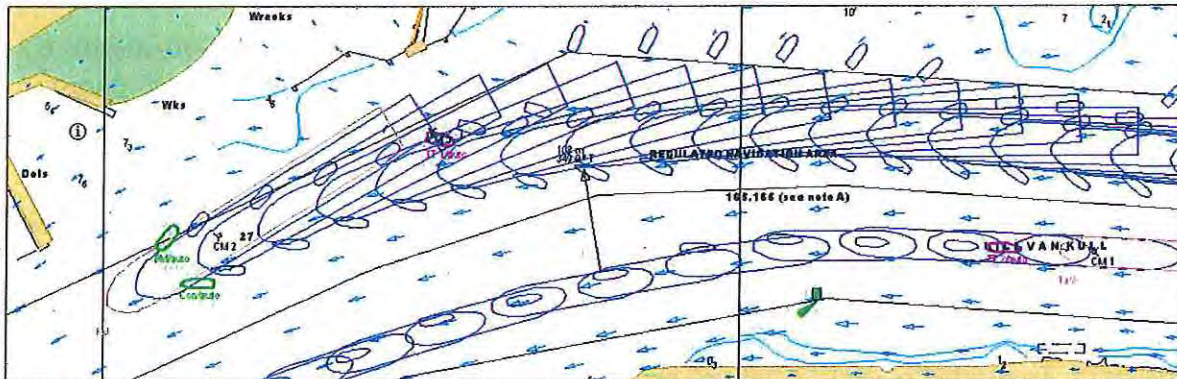


Figure 13: Run 1 – *Kalina* - Meeting in Kill Van Kull



## Run 2 Kalina Meeting Tanker in the KVK

Pilot: Robert Flannery      *Kalina*, [Inbound] 49' Draft      Wind/Current: 40% Flood, S 20  
Pilot: John Oldmixon      *Memphis*, [outbound]  
Start: Buoy 26      Finish: Intersection of Con Hook and Bergen Point East Reaches  
Tugs: Kenny Port Bow, Brian Starboard Bow, Edward C/L aft, Miriam Free

### Description:

The DM was not satisfied with the results of Run 1, and asked to repeat it. The *Kalina* started on the Con Hook Reach making 7.4 knots. The pilot used the *Edward* in the direct pull mode at a starboard 45°, at  $\frac{3}{4}$  power to slow the ship and to begin his turn to port off the range. The pilot also used the bow tugs backing alongside the ship's hull at half astern to further assist slowing the ship. The ship was making 3.8 knots off Hess, Bayonne. The DM continued to use the tugs to maintain a modest speed on the ship as it proceeded up the KVK. The *Kalina* passed the other ship at the intersection of the Con Hook Reach and the Bergen Point East Reach at 4.7 knots, and cleared the ship at Pier A. Unfortunately, in order for the *Kalina* to make this turn she needs to be turned hard and this makes the stern swing in a very wide swath. Because of this the DM felt that he ended up "too close to the ship at Pier A" and "could have sucked the berth ship off the dock". Another issue with this large turn is getting the required swing rate off of the ship, so that she can then begin the turn to starboard towards the Bayonne Bridge.

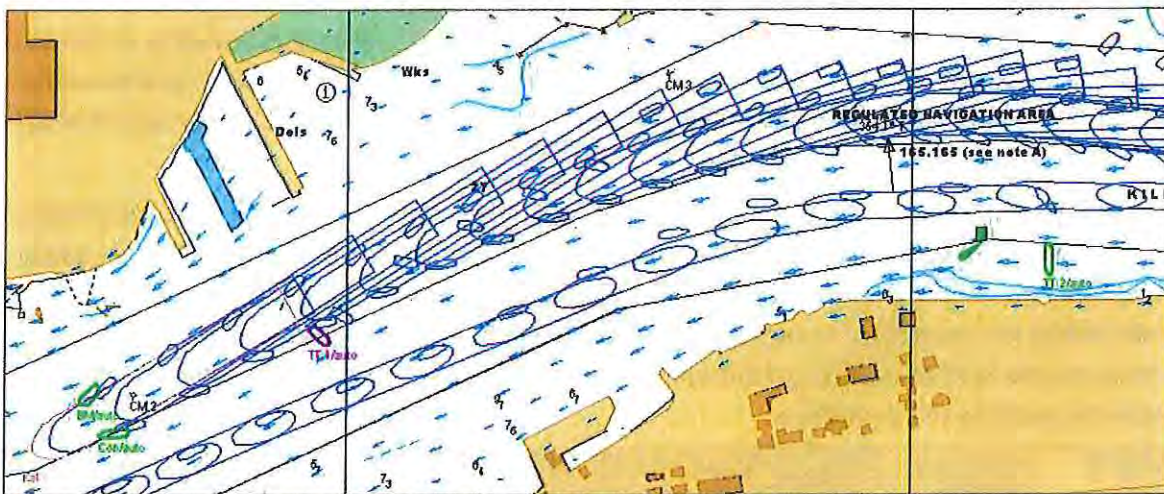


Figure 14: Run 2 – Kalina – Meeting in Kill Van Kull

### Alternate Meeting Solution

The pilots and docking master were concerned about their ability to safely maneuver this class of vessel, and meet a small vessel in the KVK. If they were unable to resolve this issue, the KVK would have to be closed to all traffic during the 14,000 TEU ULCV transits to Port Elizabeth. In Runs #1 and #2, and the runs made in the initial 14,000 TEU Study, the *Kalina* was operated on her side of the channel and met the opposing traffic port to port. This is the norm, but requires the *Kalina* to negotiate some very sharp turns. In discussing this, the pilots and docking masters noted that if instead of passing port to port, if they were to pass starboard to starboard they could minimize these large turns as seen above. Further, if the *Kalina* class were to enter the KVK favoring the southern side of the channel, they would be creating a maximum clearance to all of the tankers berthed in this waterway, as all of the berths are located on the north side of the channel. *Because of the importance of keeping the KVK open to smaller traffic, this starboard to starboard passing should be explored in more depth.*



### Run 3 Inbound Run through KVK to South Reach

Pilot: Robert Flannery

Triple E, Draft 42'

Current/Wind: Slack, N-5

Start: Stapleton

Finish: Newark Bay Draw (NBD)

Tugs: C/L aft *Edward*, Starboard bow *Brian*, Port bow *Miriam*, Light Boat *McAllister Sisters*

#### Description:

The DM used the *Edward* indirect to starboard at full power, then reduced quickly to half power, as the ship responded well to the tug forces. The ship developed an 11°/m turn rate to port and the pilot stopped the *Edward*. Passing the St. George Ferry Terminal, the ship was just slightly to port of the Con Hook range making 5.6 knots (SOG) with a 4°/m turn rate to port (using 10° port rudder). The DM used the *Edward* in transverse arrest slow to ease the ship's speed down (the DM changed to inline slow on the *Edward* at 4.8 knots, then went up to half power in the tug). At 4.6 knots the rudder was placed hard to port and the *Miriam* ordered to pull full alongside. With the ship off buoy 5 making 4.5 knots and headed 270° the *Edward* and *Miriam* were stopped. From this position to buoy 8 the DM ordered the *Edward* indirect to port (initially the tug produced only 28t but Captain Oliveira eventually was able to work the boat up to the mid 50'st). The ship made the turn at buoy 8 very nicely at 4.5 knots.

Off of Cadell's Shipyard, the DM used the tugs to slow the ship as its speed had increased to 5.4 knots. Turning on to the west end of the East Bayonne Reach, the DM used the stern tug in the indirect mode to create a 6°/m turn rate to starboard. The speed was reduced to 3.5 knots. Both bow tugs were used to retard the ship on half bells, then up to full.

When the ship's bow reached Bergen Point buoy 16, the *Edward* was used in the powered indirect mode, full to port, then down to half, as the DM used the tug at various speeds to maintain the DM's desired turn rate. The ship was making 3.9 knots with the stern moving sideways to port at 2.8 knots and the bow to starboard at 0.7 knots. Halfway around the turn the pilot stopped the tug but had to use the boat again to keep the ship's turn rate up. The DM did a very good job keeping this *Triple E* model safely in the center of the channel.



Figure 15: Run 3 – Triple E – Approach & Turn at Bergen Pt.



## Run 15 Kalina Meeting Traffic in KVK

Pilot: Robert Flannery *Kalina*, Inbound

Pilot: John DeCruz *Memphis*, Outbound

Wind/Current: S 20, 1.5 Flood

Start: Con Hook Range Finish: After passing

Tugs: C/LA *Brian*, Starboard Bow *Miriam*, Port bow *Edward*, Free - *Sisters*

### Description:

At the start of the exercise the *Kalina* was being set to the north as it entered the Con Hook Reach by the flood current and wind. Once the set had been controlled by getting the *Kalina* fully into the current flooding into the Kills, the ship passes up the channel in the middle of the channel. As the *Kalina* was passing Buoy 8 in the Kills, the *Brian* was ordered into the powered indirect maneuver, full to port. Unfortunately, this maneuver was conducted late and the *Kalina* finished its turn back to starboard when the ship was fully on the port side of the channel. This missed turn required another hard turn to starboard in order to miss the oncoming *Memphis* which was accomplished. However, the model was heading for the tanker moored at Berth A. Another hard turn to port was required to miss the moored tanker. The two models passed safely with a 152' of clearance. The next turn was successfully executed and the *Kalina* cleared the moored tanker by 171'. While this run was successful, it is one that we would not want to repeat. It should also be noted that this run took place at the end of a busy day.

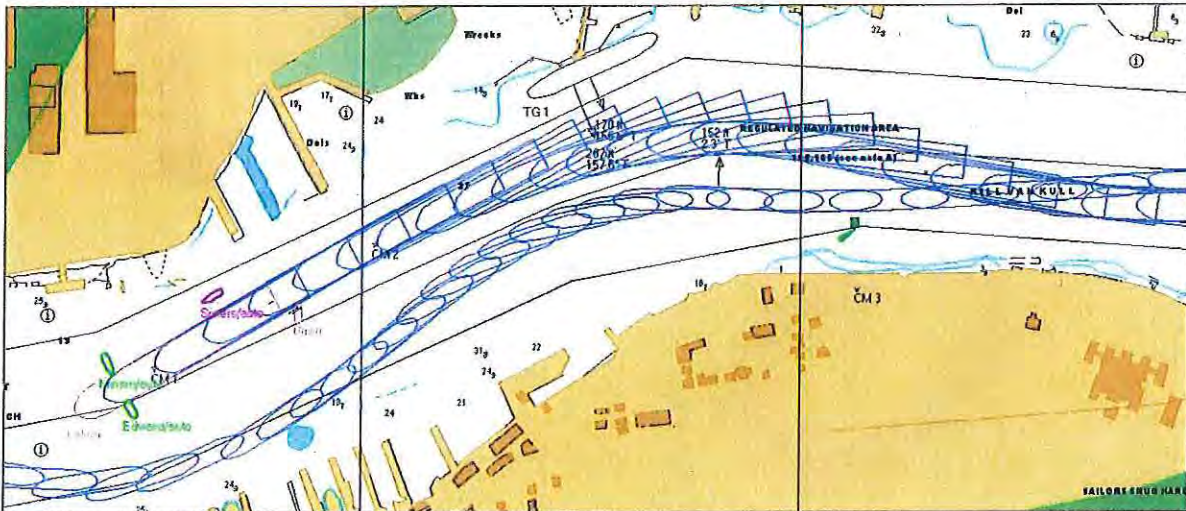


Figure 16: Run 15 - Kalina meeting Tanker Memphis

## Run 16 Triple E Inbound KVK

Pilot: Robert Ellis

*Triple E*, Draft: 49'

Wind/Current: S 20, 1.5 Flood +3' Tide

Start: Con Hook Range

Finish: Grounded

Tugs: CLA *Brian*, Starboard Bow *Sisters*, Port Bow *Edward*, Free: *Miriam*

### Description:

The DM was late turning the ship onto the Constable Hook Reach and the ship grounded on the north side of the channel into the KVK. Captain Ellis felt the 3.3 knot northerly current was not representative of real-world conditions.

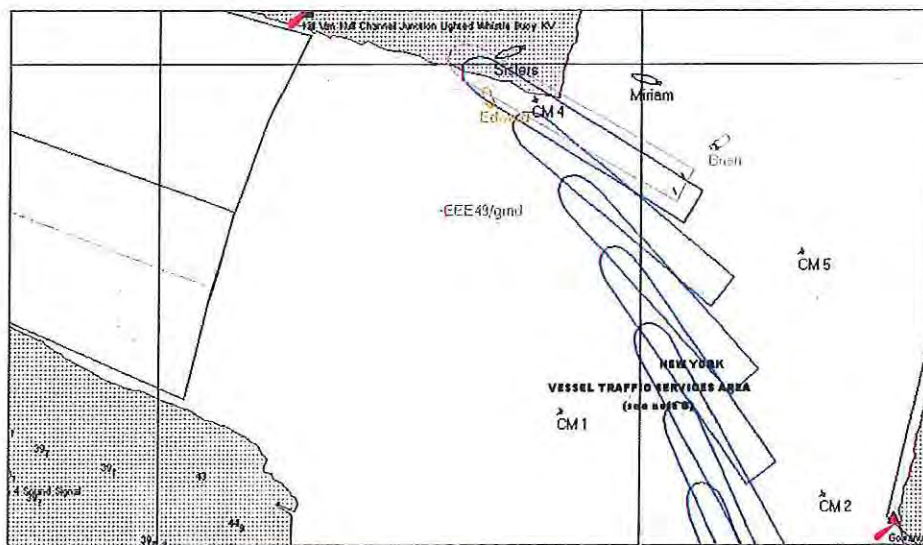


Figure 17: Run 16 – *Triple E* grounding as it entered Con Hook Reach



## Run 17 Triple E Inbound to KVK

Pilot: Robert Flannery Triple E, Draft 49'

Wind/Current: S 20, 1.25 Flood +3' Tide

Start: Stapleton Anchorage Finish: KVK

Tugs: CLA Brian, Starboard bow, Miriam, Port Bow Edward, Free Sisters

### Description:

As the model passed Stapleton Anchorage, it had the two bow tugs and the tug C/L aft backing to slow the ship down. Reaching 4.5 knots (SOG) the DM slowed the three boats to slow bells. Passing the St. George Ferry Terminal, the DM had the model lined up on the Con Hook Range with a 16° drift angle on the ship. Later, the DM ordered the two bow tugs to pull at half astern alongside of the ship.

When the bow of the model was abeam of buoy 5, the speed had been reduced to 4.1 knots and the DM stopped the *Edward* and asked the *Miriam* to back alongside at full power to reduce the ship's turn to port. Passing Buoy 7, the DM asked the *Brian* to perform a powered indirect to port, easy. In order to keep the speed of the ship moderate as it passed a series of tankers moored on the Bayonne shore, the *Brian* was eased up to half. The ship passed the second ship at Hess Bayonne making 4.1 knots (STW). Passing buoy 8 the model was making 4.3 knots (STW). A nice run with complete control.

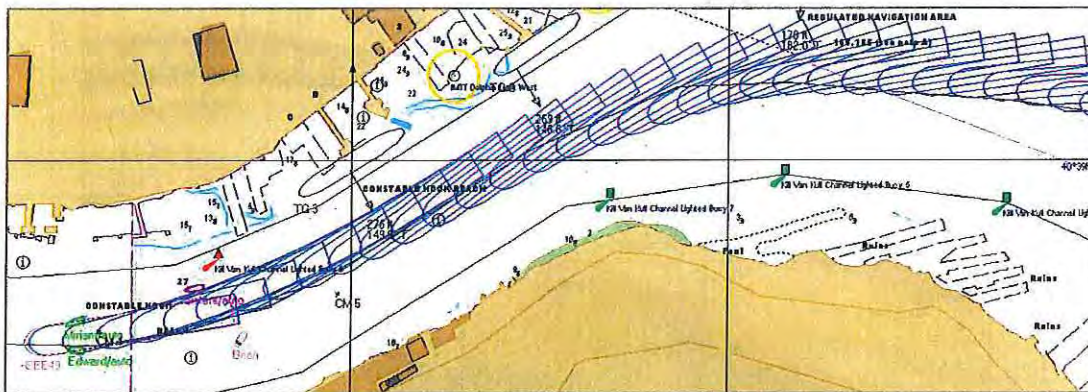


Figure 18: Run 17 – Triple E Entering & Transiting Con Hook Reach – Ebb



Figure 19: Run 17 Screen Shot



## Run 18 Triple E Inbound to KVK

Pilot: Robert Ellis

Triple E, Draft 49'

Start: Stapleton

Finish Bergen Pt. E Reach

Current/Wind: S 20, 1 knot flood

Tugs: C/L Aft *Brian*, Starboard Bow *Miriam*, Port bow *Edward*, Free *Sisters*

### Description:

This a repeat of Run 17 but with the wind and current reversed. The DM turned into the Con Hook Reach a bit late but was able to establish the model on the port side of the channel rounding the green buoys north of the Staten Island Ferry Terminal. With the bow of the ship passing Buoy 3, the model was making 4.7 knots (STW). The *Brian* was used to create the turn to port using the powered indirect maneuver to starboard with the ship making 15°/m rate of turn. The *Triple E* passed the second ship moored on the Bayonne waterfront at 3.1 knots (STW), and safely made the turn at the red Lashing buoy 8.

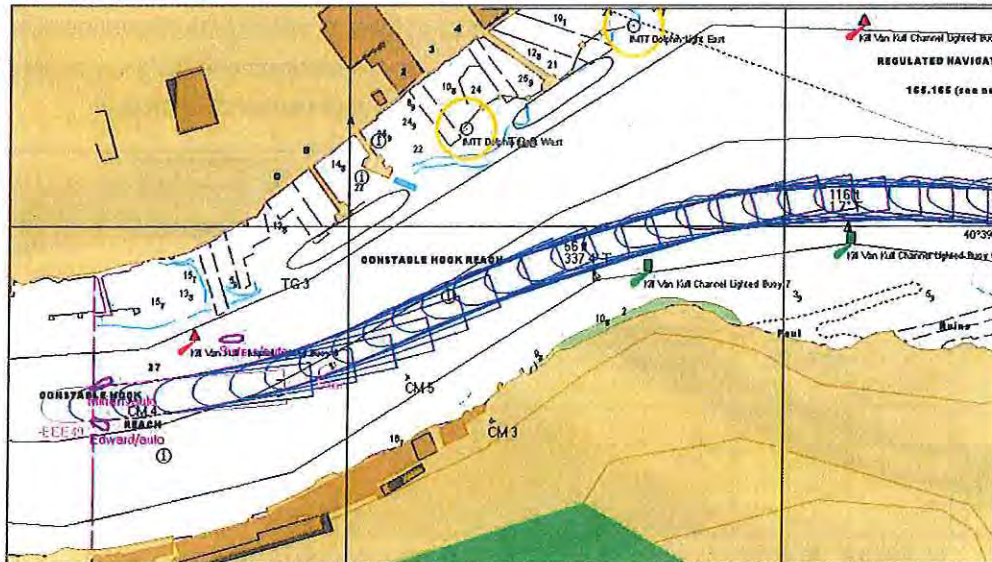


Figure 20: Run 18 –Triple E Entering & Transiting Con Hook Reach – Flood



## 6.2 ROUNDING BERGEN POINT INBOUND BERGEN POINT EAST REACH TO BUOY 3

The following runs focused on the sharp turn at Bergen Point into South Reach, Port Elizabeth

### Run 4 Bergen Point Turn Inbound

Pilot: Robert Ellis *Triple E*, Draft 49'

Current/Wind: 40% Ebb, NE-20 +3' Tide

Start: Bayonne City Dock Finish: NBD

Tugs: C/L aft *Edward*, Starboard Bow *Brian*, Port bow *Miriam*, Light Boat *Sisters*

#### Description:

At the start of the exercise the model was making 3.7 knots (STW). Passing Buoy 12 the DM asked the Tug *Sisters* to come up and lay on the starboard quarter. Passing under the bridge the DM ordered the *Edward* to direct pull mode at 45° full; the *Sisters* push full; and *Brian* back easy alongside. The *Edward*, in the direct pull could only get to about a 45° angle on his towline and the pilot DM stopped him as he was headed to the green buoy. *Edward*, 45° to port full (indirect – 75t). *Sisters* push half and then full. *Brian* backed half at a 45. Using the assist tugs, the DM made a very nice turn round Bergen Point. The *Triple E* model handled quite well.

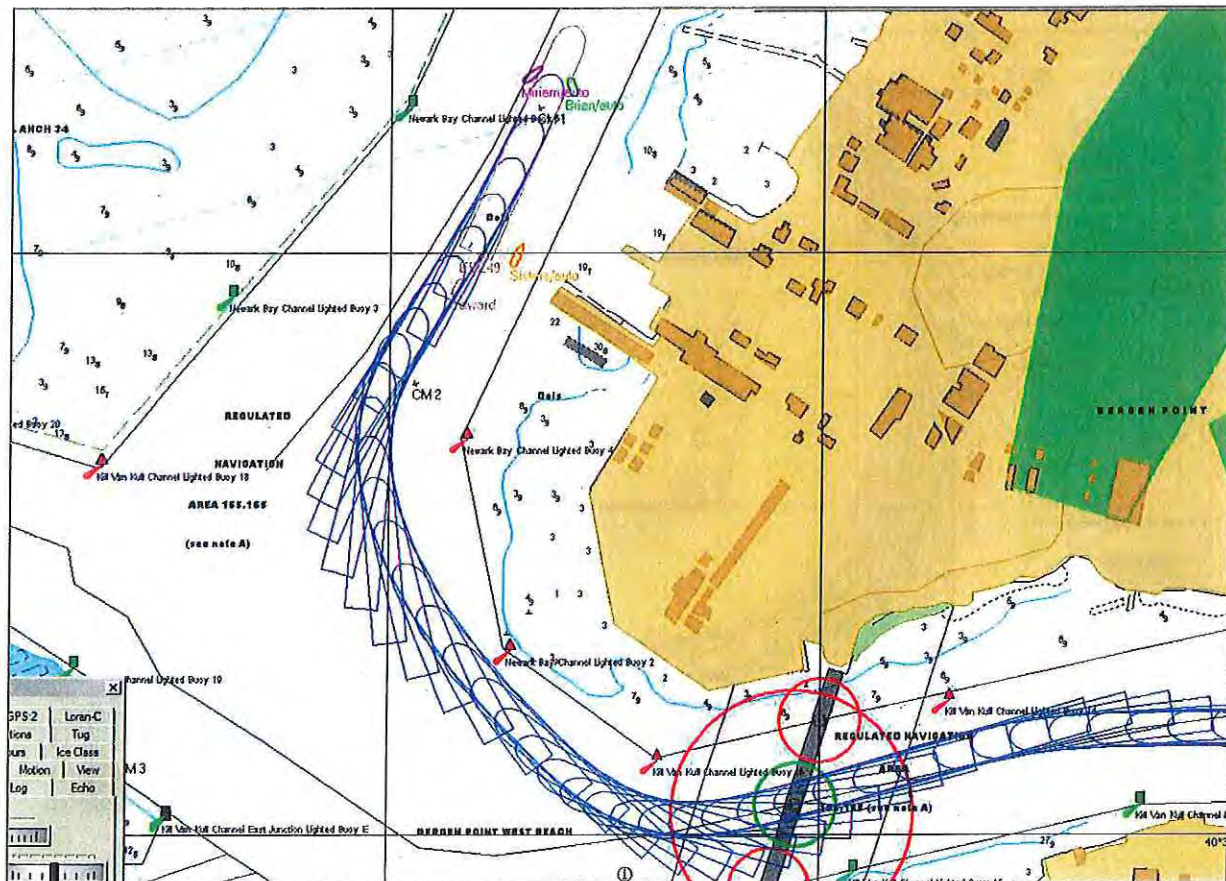


Figure 21: Run 4 – Triple E @ 49'



## Run 5 Triple E Inbound Bergen Point

Pilot: Robert Flannery

Triple E, Draft - 49' +3' Tide

Current/Wind: 1.8 knots Flood, NE - 20

Start: Stapleton

Finish: Buoy South Reach, Buoy 5

Tugs: C/L aft *Edward*, Starboard Bow *Brian*, Port bow *Miriam*, Light Boat *Sisters*

### Description:

The DM used the tugs to minimize the ship's speed in the Kills which allowed him to make controlled turns as the channel weaved its way to Bergen Point. With the flood current, the DM passed under the Bayonne Bridge on the north side of the channel. Passing buoy 16, the DM placed the rudder hard to starboard and ordered the *Edward* to conduct the powered indirect maneuver to port at half power and then ordered the *Edward* up to  $\frac{3}{4}$  power. The DM made a very controlled turn around Bergen Point and ended up exactly on the centerline of the channel heading north to Port Elizabeth.

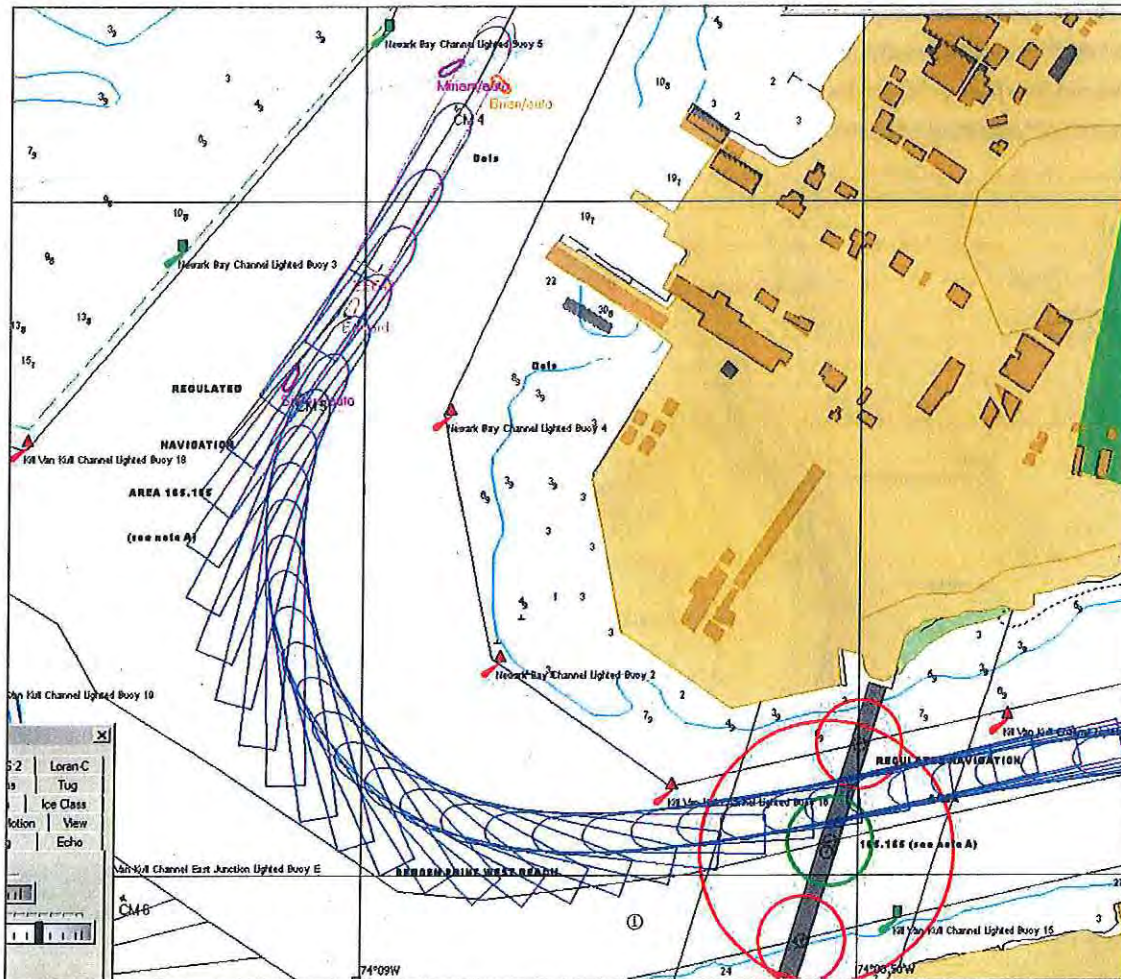


Figure 22: Run 5 - Triple E - Inbound at Bergen Point



### 6.3 BERGEN POINT OUTBOUND BUOY 3 TO BERGEN POINT EAST REACH.

The following exercises focused on the outbound turn at Bergen Point.

#### Run 6 Outbound Bergen Point

Pilot: Robert Ellis

Triple E, Draft 49'

Current/Wind: 40% Flood, NW - 20

+ 3' Tide

Start: NBD

Finish: Bergen Point East Reach

Tugs: C/L aft *Edward*, Starboard Bow *Miriam*, Port bow *Brian*, Light Boat *Sisters*

#### Description:

The model approached the Bergen Point turn at 3.9 Knots (STW). Prior to starting his turn, the DM ordered the *Sisters* red to the port quarter. Once the DM wanted to begin his turn, he ordered the *Sisters* to push easy, the *Brian* was ordered to conduct a direct pull at port 45° easy. Finally, the *Edward* was ordered into the powered indirect at  $\frac{3}{4}$  power and then up to full. Later, the *Brian* was ordered up to  $\frac{3}{4}$  and then to full power. Of note, during this maneuver, the *Edward* lost 15 tons of towline force by jackknifing to the direct pull too soon. The DM maintained a 12°/m turn rate throughout the turn and passed under the Bayonne Bridge slightly to the north side of the channel. A very pretty run!

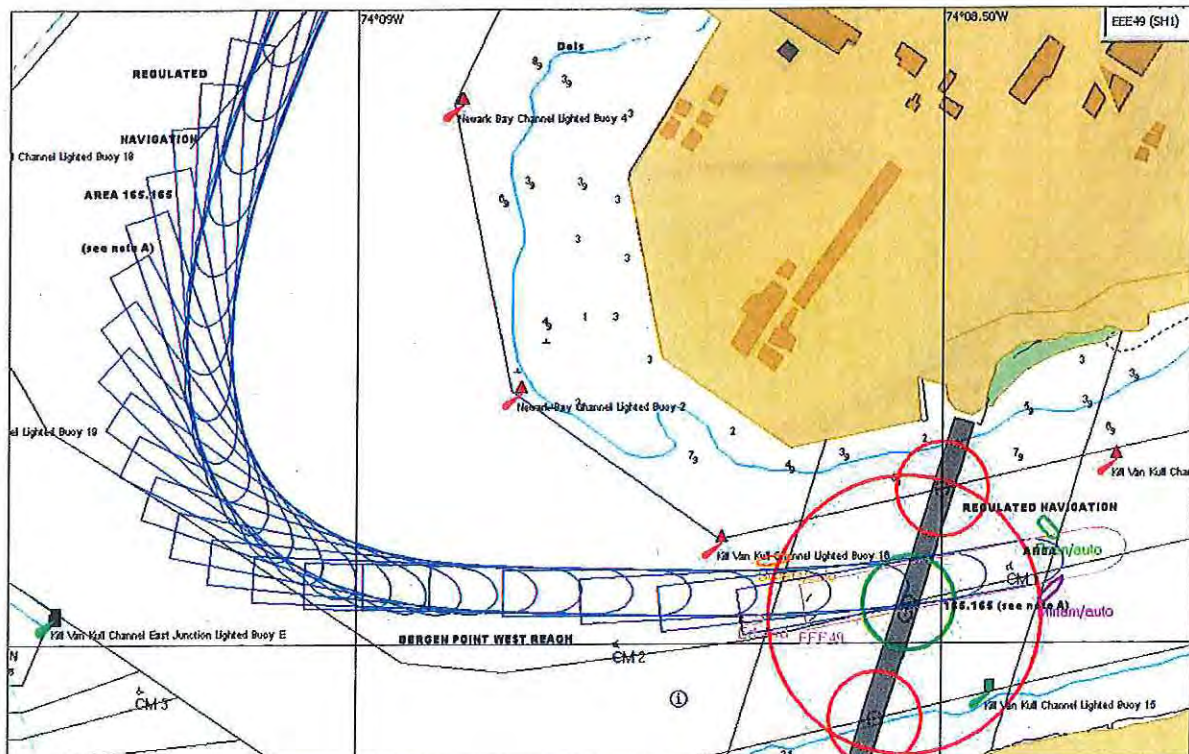


Figure 23: Run 6 – Triple E Southbound to Bayonne Bridge



## Run 7 Outbound Bergen Point

Pilot: Robert Flannery

Triple E, Draft 49'

Current/Wind: 40% Ebb, NW - 20

+3' Tide

Start: NBD

Finish: Off Moran's Yard

Tugs: C/L aft *Edward*, Starboard Bow *Miriam*, Port bow *Brian*, Light Boat *Sisters*

### Description:

At the start of the exercise the model was making 7.4 knots (STW). The docking master ordered the *Edward* to pull direct inline half, and then increased this order to  $\frac{3}{4}$  power. The *Brian* was backing at half alongside and then the DM increased him to  $\frac{3}{4}$  power. Approaching the turn to the bridge, the *Edward* was ordered to conduct a direct pull to starboard at full power. The *Brian* was also ordered to pull at full power. At the start of this turn the ship was making 5.0 knots (STW). The DM established a  $15^\circ/\text{m}$  turn rate and used the tugs to maintain this turn rate. On completing the turn, the ship was to the south of the bridge's centerline (eventually the ship's main deck aft came to within 43' of the edge of the channel) and the DM ordered both bow boats to drag at half power. The bow boats were stopped and the *Edward* ordered to perform a direct pull to port half power. Very quickly the DM had the ship back on the centerline of the channel.

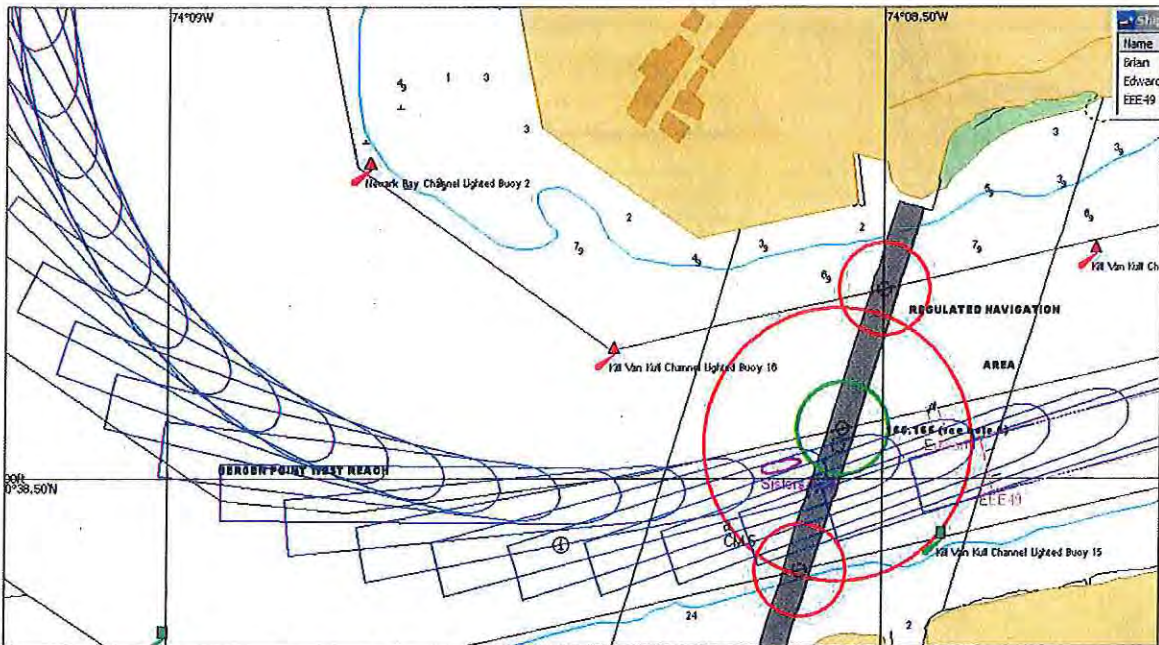


Figure 24: Run 7 – Triple E Close to the Channel Edge





## Run 9 Inbound to Port Elizabeth

Pilot: Robert Flannery

Triple E, Draft 49'

Current/Wind: 1.8 Knots Flood, S - 20 + 3' Tide

Start: NBD

Finish: Port Elizabeth

Tugs: CLA Brian McAllister, Starboard Bow Miriam, CLF Edward, Starboard Quarter Sisters

### Description:

The ship was making 2.9 knots (SOG) turning into the Port Elizabeth Channel. The DM started his turn into the PE channel a bit too early using the *Edward* (C/L Forward) to initially pull to port at a "45" easy, while he ordered the *Miriam* to push full on the starboard bow. The DM then brought the *Edward* to a 90° angle to port at half power and then up to full. In the meantime, the ship's stern was falling to the north and he had to work the tugs hard to regain control and begin heading into the Port. Eventually the DM regained control, but then came within 45' of the ship on the south side of the channel.

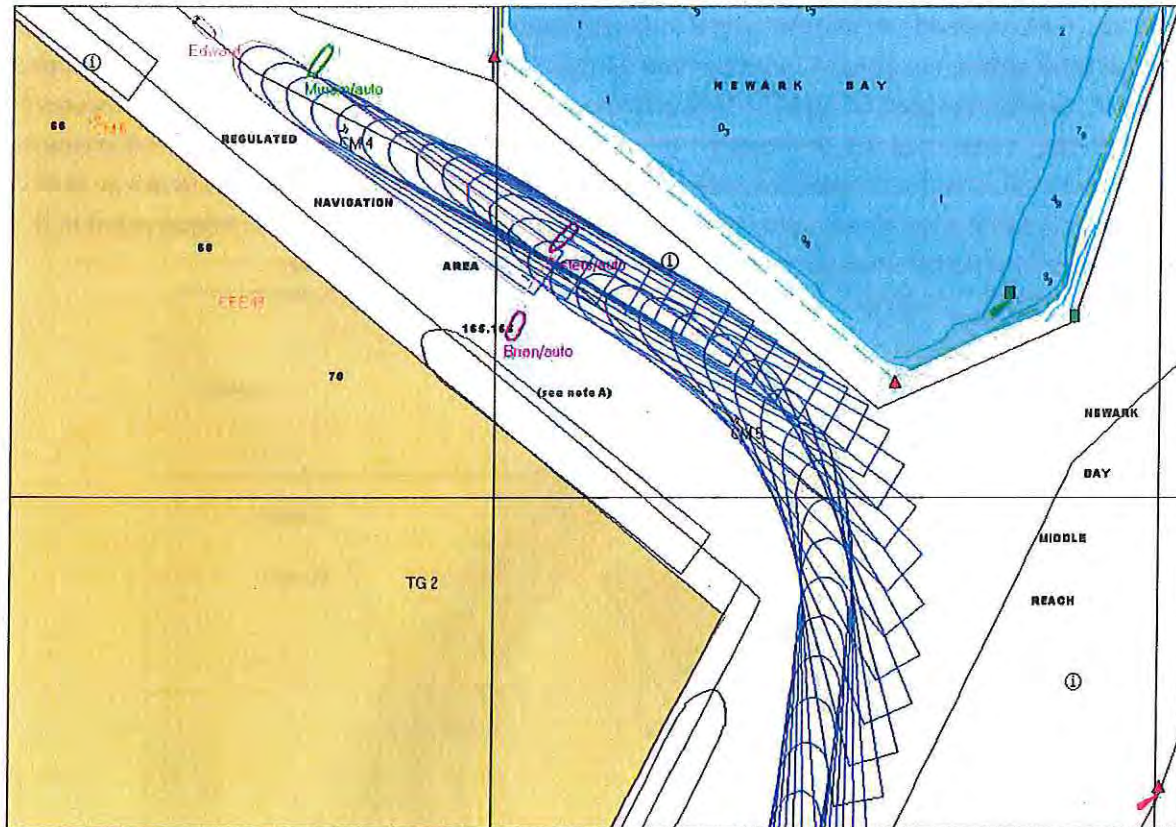


Figure 26: Run 9 – Triple E entering Port Elizabeth Channel

## Run 12 Inbound Port Elizabeth

Pilot: Robert Ellis Triple E, Draft 49'

Current/Wind: 1.5 Ebb, NE - 20 +3' tide

Start: Newark Bay Buoy 10 Finish: Port Elizabeth

Tugs: CLA Brian McAllister, Starboard Bow Miriam, Edward Port Bow, Free Sisters

### Description:

The model was making 6.1 knots at the start of the exercise. The *Sisters* was ordered to make fast on the port side just aft of the bridge. The *Sisters* dropped back to the quarter and was ordered to push half. The *Brian* performed a powered indirect to starboard at half power. Finally, the *Edward* backed half at a "45" to port. Using the tugs, the DM made a very nice turn into the Port Elizabeth channel and then smoothly moved up to her berth (ships were only moored on the south side of the channel).

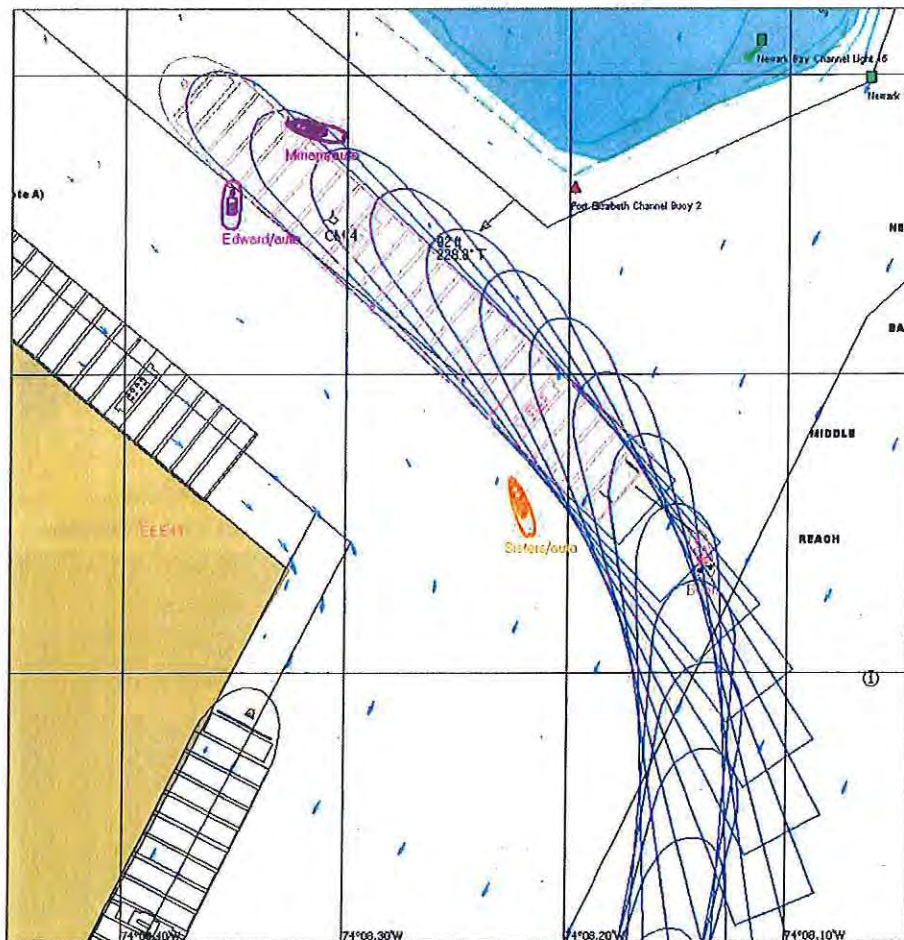


Figure 27: Run 12 – Triple E turning into Port Elizabeth Channel



### Run 13 Inbound Port Elizabeth

Pilot: Robert Flannery *AMAersk*, Draft 46'

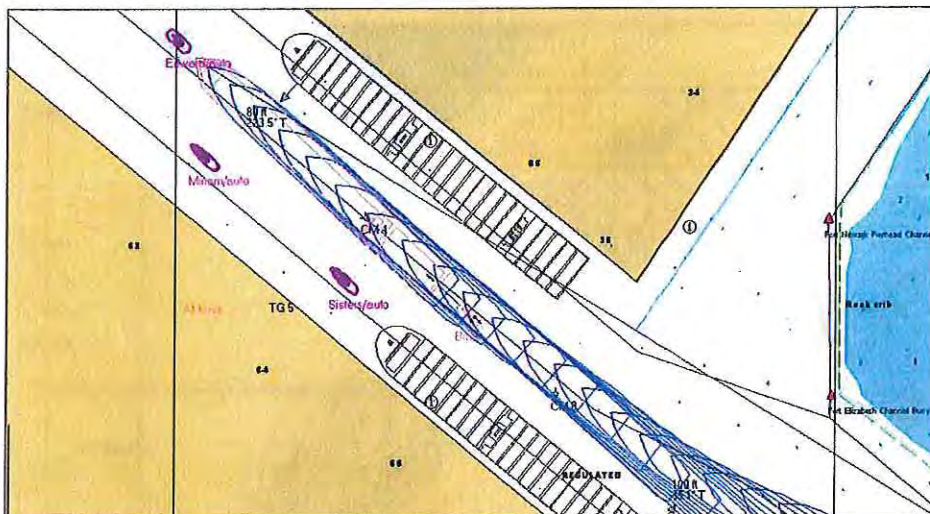
Current/Wind: 1.5 Ebb, NE - 20 +3' Tide

Start: Newark Bay Buoy 10 Finish: Port Elizabeth

Tugs: CLA *Brian McAllister*, Port Bow *Miriam*, *Edward CLF*, Free - *Sisters*

#### Description:

This exercise began to explore whether ULCVs could safely transit between two ULCVs at their berths. On this run, the 9,000 TEU *AMAersk* (140' Beam) transited with a *Triple E* Class on either side of the Elisabeth Branch Reach. The DM did a very nice job of turning the *AMAersk* into the Port Elizabeth channel. The *AMAersk* easily passed between the two *Triple E* clearing the *Triple E* at berth on the north side by 80'.





## Run 25 Demonstration Run

Pilot Robert Flannery

*Kalina*, Draft 49'

Current/Wind: 40% Flood, S - 20 +3' Tide

Start: Newark Bay Buoy 10

Finish: Port Elizabeth

Tugs: CLA Brian McAllister, Starboard Bow Edward, Starboard Quarter Miriam, Port Bow Sisters

### Description:

This was a demonstration run for the NY/NJ Port Authority. With the wind and current pushing the ship to the north, Captain Flannery cut the corner at the southern edge of the Port Elizabeth Channel in order to get the ship lined up on the Port Elizabeth Channel centerline. He finished his turn almost a ship width north of the centerline but well clear of the shoaling to the north. Later in the run when the DM attempted to take the ship between two *Kalina* class ships berthed on either side of the channel, he came within 40' of the moored model on the south side.

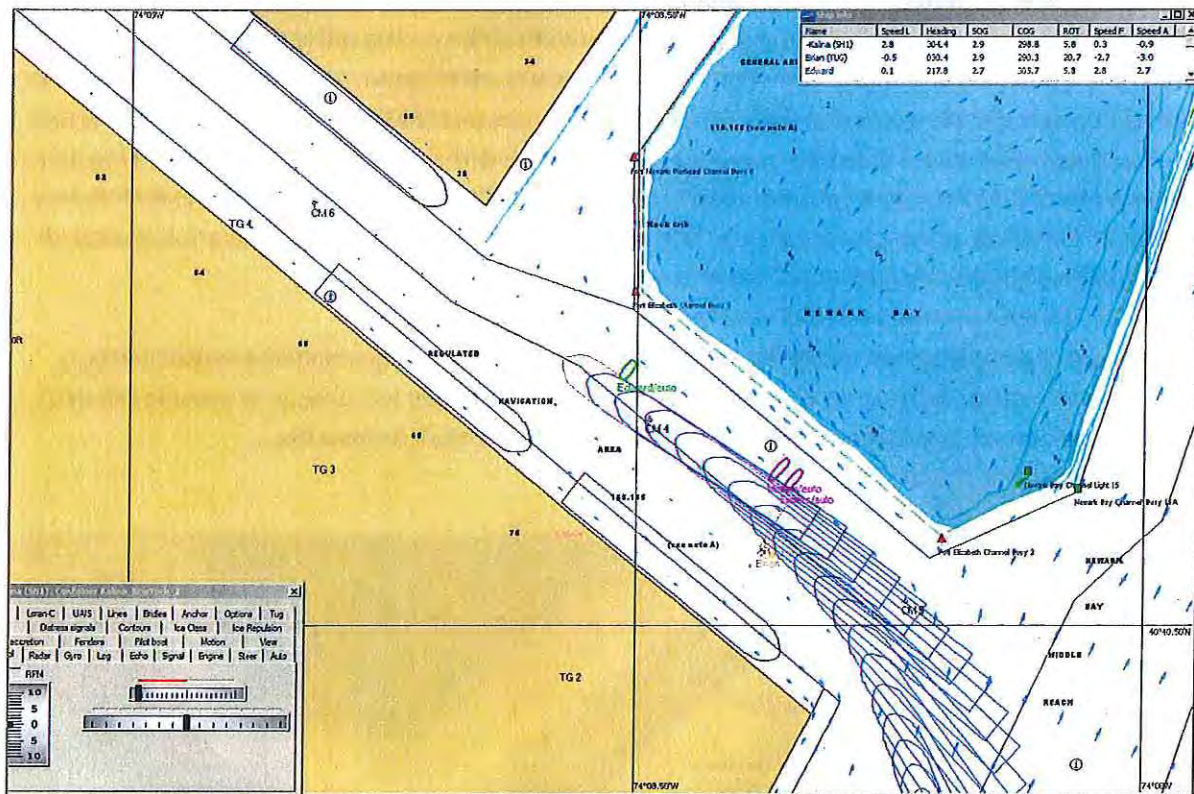


Figure 30: Run 25 Inbound between berthed Kalina Classes.



## 6.5 OUTBOUND FROM PORT ELIZABETH TO BUOY 10 NEWARK BAY

The following runs focused on outbound from the Port Elizabeth Branch Reach.

### Run 10 Outbound from Port Elizabeth to Newark Bay

Pilot: Robert Ellis Triple E, Draft – 49'

Current/Wind: 1.5 Knots Flood, S - 20 +3' Tide

Start: Port Elizabeth Finish: Newark Bay buoy 10

Tugs: CLA *Brian McAllister*, Port Quarter *Miriam*, CLF *Edward*, Starboard Quarter *Sisters* (no line)

#### Description:

The pilot used the three tugs placed near the ship's wheelhouse aft to control the model. Initially, this did not work very well as the DM was overpowering the ship by using too much tug power from too many tugs to control the ship (1<sup>st</sup> plot below). Once the DM got the ship settled down he made a controlled exit backing smoothly between two other Triple E's. The DM maintained great control over the ship all the way out of the Port Elizabeth channel. Approaching the Newark Bay main channel the DM had the *Sisters* pushing full at the starboard bow and the *Brian* pulling full to port at a 45° angle to port as the DM swung the ship's stern into the Newark Bay main channel. The ship's bow cleared the other ship moored at the corner by 160'. When the ship's bow cleared the other ship, the DM ordered the ship slow ahead and worked his way up to full ahead, but the ship did not realistically slow her sternway and the ship's stern went aground at the edge of the 50' dredging line in the channel. This was a run that identified many new issues that the DMs are going to have to get their arms around to successfully handle these large ships. They are as follows:

1. Do not over control the ship when leaving or coming on to a berth,
2. Keep the transit speed within the DM's ability to control the ship based on the assigned tugs,
3. When backing the ship down a waterway use the C/L aft tug in line only, to provide the desired transit speed, and control the heading of the ship using the C/L forward tug.

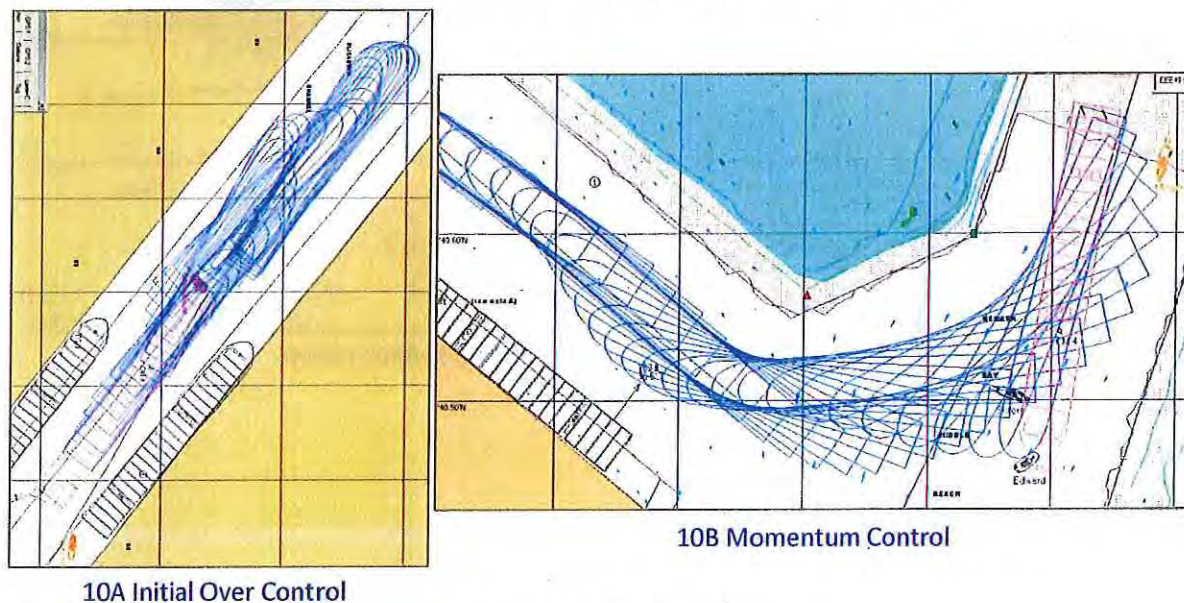


**Figure 31: Run 10 Triple E – Control Issues**



## Run 14 Outbound from Port Elizabeth to Newark Bay

Pilot: Robert Ellis                      *AMaersk*, Draft 46'

Current/Wind: 1.5 Ebb, NE - 20    +3' Tide

Start: Port Elizabeth                      Finish: Newark Bay Buoy 10

Tugs: *CLA Brian McAllister*, *Free Miriam*, *CLF Edward*, *Free Sisters*

### Description:

Similar to Run 13, the DM was determining the feasibility of a smaller container ship transiting between two, 18,000 TEU containerships berthed in Port Elizabeth Branch Reach. In this exercise Captain Ellis set up the two conventional tugs at the quarters (*Sisters* – port, *Miriam* – starboard) and used them to initially steer the ship. Having conventional tugs working on both sides of the ship greatly reduces the room in which the tugs have to work. (The *Sisters* came within 25' of the ship.) This run came close to the *Triple E* berthed on the north side, but was safe.

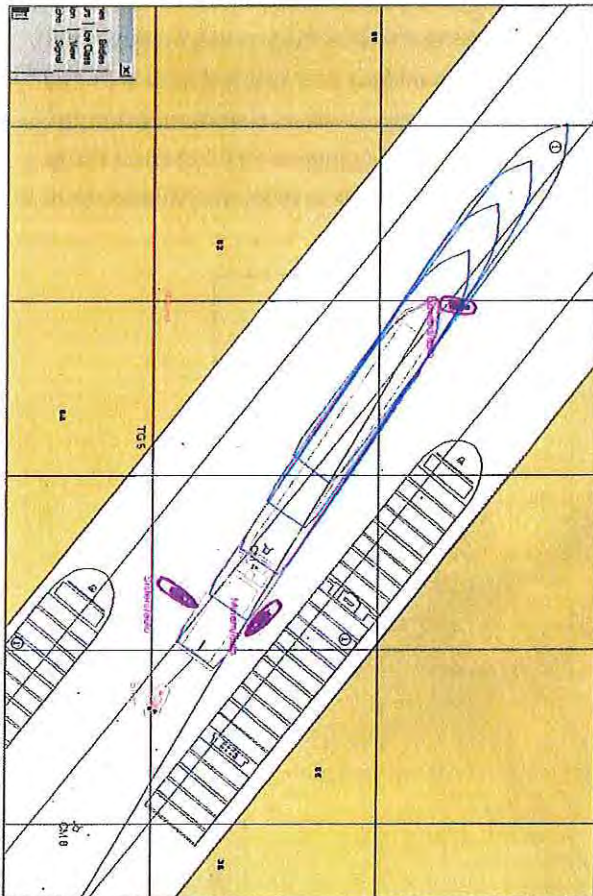


Figure 33: Run 14 – *AMaersk* slipping between two, *Triple E* models



Figure 32: Run 14 Screen Shot



## Run 11

Pilot: Robert Flannery

Triple E Draft 49'

Current/Wind: 1.5 Knots Ebb, N - 20

Start: Port Elizabeth

Finish: Newark Bay buoy 10

Tugs: CLA *Brian McAllister*, Port Quarter *Miriam*, *Edward* at bow (no line), Port Quarter *Sisters*

### Description:

To save time, this exercise started with the ship in the middle of the channel. The DM backed the model out to Middle Reach. To accelerate the model speed, the *Brian* was used in line at half power. The DM then started to steer the ship using the *Brian* and the two conventional boats at the port quarter. This may not be the most optimum configuration since the ship's pivot point will move towards the stern making it more difficult for the stern and quarter boats to move the ship's stern laterally. A better approach would be to use the *Brian* simply to tow the ship by pulling in line and letting the *Edward* provide the steering control. As the ship squeezed between the two Triple E ships moored on the north and south bank of the channel, the two conventional tugs cleared the ship on the south bank by 30'. The DM is still steering the ship with the stern tug. With the ship making 3 knots, the ship was neatly controlled by the DM, but he used a lot of tug orders to get the job done. With the stern entering the main channel, the ship was proceeding at 1.32 knots. Stopping the ship's engine the DM used the tugs to turn the ship fair with the channel, and then the ship's engine was engaged to move the ship south in the waterway.

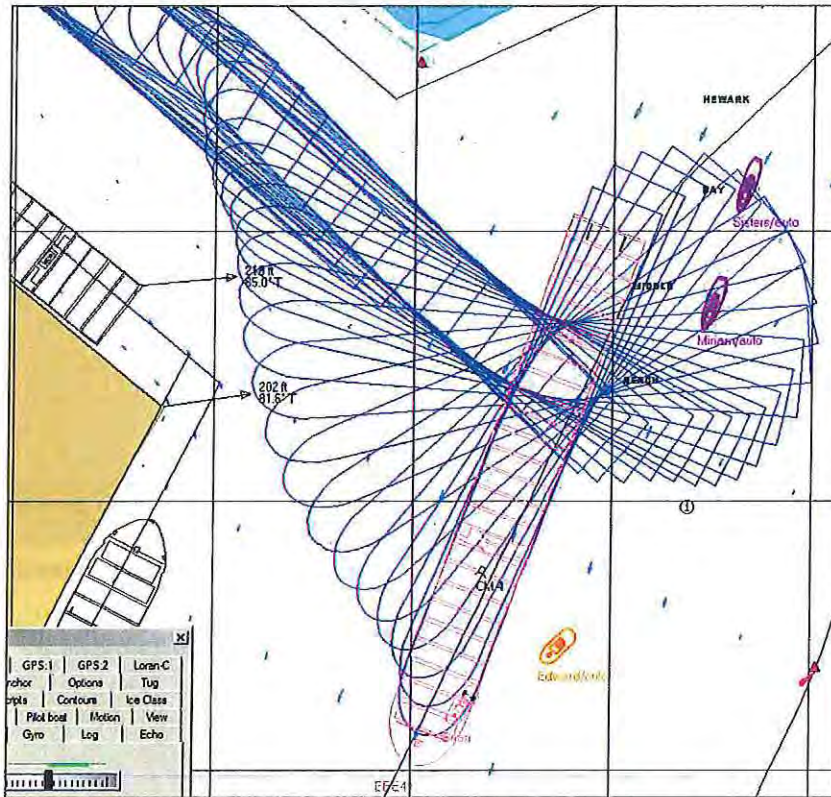


Figure 34: Run 11 – Triple E backing out of Port Elizabeth



## Run 26 Demonstration Run

Pilot: Robert Ellis

Triple E, Draft 49'

Current/Wind: 40% Flood, N – 20 +3' Tide

Start: Newark Bay Buoy 10

Finish: Port Elizabeth

Tugs: CLA *Brian McAllister*, Bow (no line) *Edward*, Starboard Quarter *Miriam*, Port Quarter *Sisters*

### Description:

This run was a demonstration for the NY/NJ Port Authority. The run was conducted at modest speeds and modest use of the assisting tugs. When the ship's stern was being turned into the main Newark Bay channel the ship's bow came within 85' of the berthed ship moored on the outer southern berth of Port Elizabeth Cannel, but there was no danger of collision as the ship was under very good control.

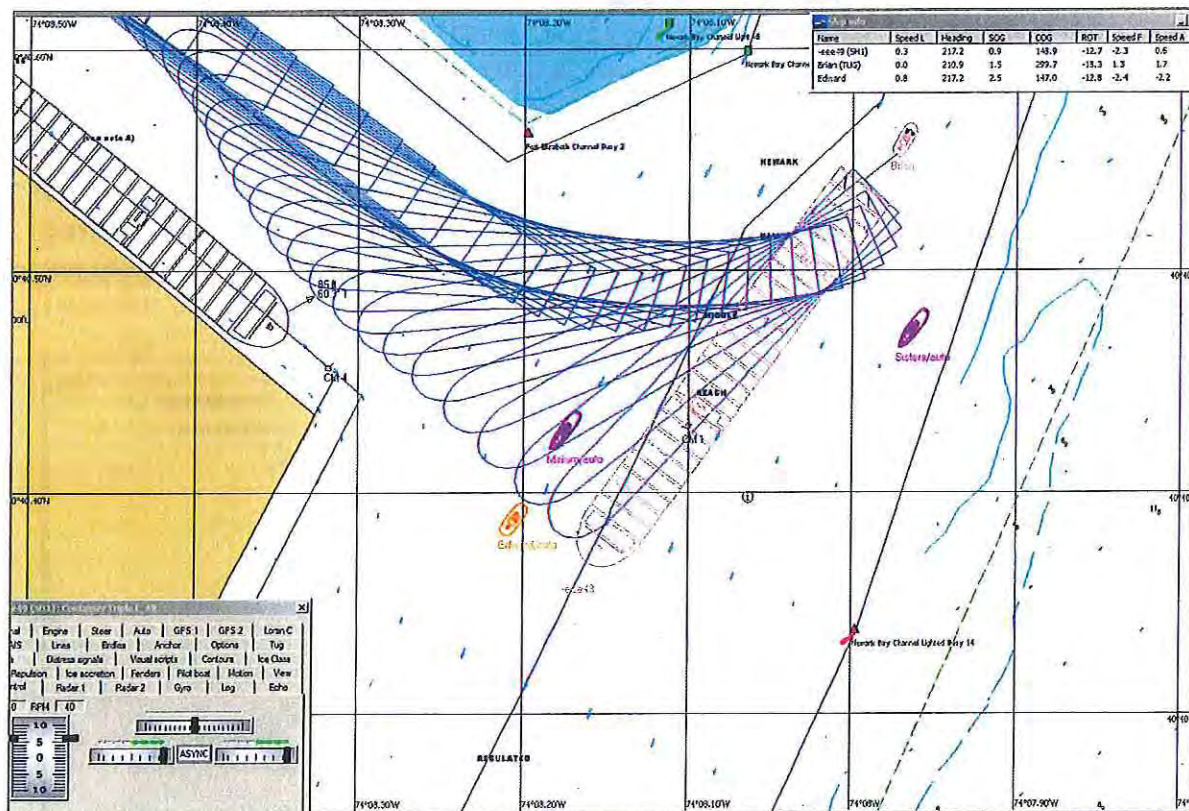


Figure 35: Run 26 – Triple E Backing out of Port Elizabeth Branch Reach

## 6.6 INBOUND FROM UPPER BAY BUOY 30 TO GLOBAL TERMINAL

These exercises focused on the Global Marine Terminal

### Run 19

Pilot: Robert Flannery      *Triple E*, Draft 49'  
Current/Wind: Slack, S 20      +3' Tide.  
Start: Robbins Reef      Finish: Global Term.  
Tugs: *CLA Brian*, Starboard bow *Edward*, Port Bow *Miriam*, Free Sisters

#### Description:

The ship started out at six knots. The *Edward* was initially backed at half power alongside the ship to bleed off some speed. Approaching the entrance channel, the *Brian* was ordered into the powered indirect mode to starboard at half power and then quickly increased to full. Simultaneously, the *Edward* was ordered to push full. Later in the turn the *Brian* was reduced to half. The *Edward* was now pushing half ahead at a "90" when the ship's bow was just passing the entrance buoy to Port Jersey. The DM continued to use various tugs as he lined up the ship for the Port Jersey channel. At the opening of the Port Jersey channel, the ship was making 3.9 knots. When passing the *Quantum of the Seas* the Triple E was making 3.8 knots (STW). The pilot had been attempting to slow the ship after he made his turn into the Port Jersey Channel, so as to pass the passenger ship at a more modest speed, but could not successfully slow the ship.

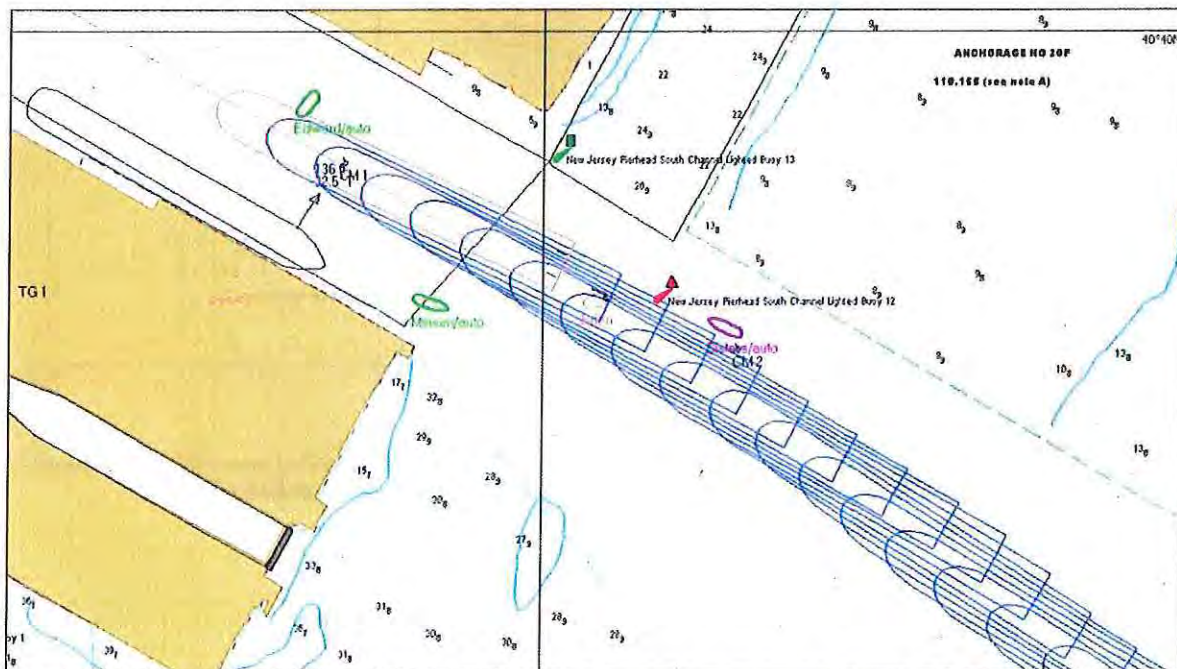


**Figure 36: Run 19 – Triple E Entering Port Jersey Channel**



## Run 20 Inbound Global Marine Terminal

Pilot: Robert Ellis

Triple E, Draft 49'

Start: Robbins Reef

Finish: Global Terminal

Current/Wind: Slack, N 20

+3' Tide

Tugs: CLA *Brian*, Starboard bow *Edward*, Port Bow *Miriam*, Free Sisters

### Description:

The DM turned into the Port Jersey Channel early to allow room for the wind to set the ship to the north as he completed his turn. During this turn the DM used the *Brian* with the powered indirect maneuver to assist the ship's rudder and to slow the ship. He also used the *Edward* and the *Miriam* to assist slowing the ship down as he approached the passenger ship. In making his approach to the Port Jersey Channel, the DM kept the ship to the north of the channel's centerline to allow more clearance with the Passenger ship.

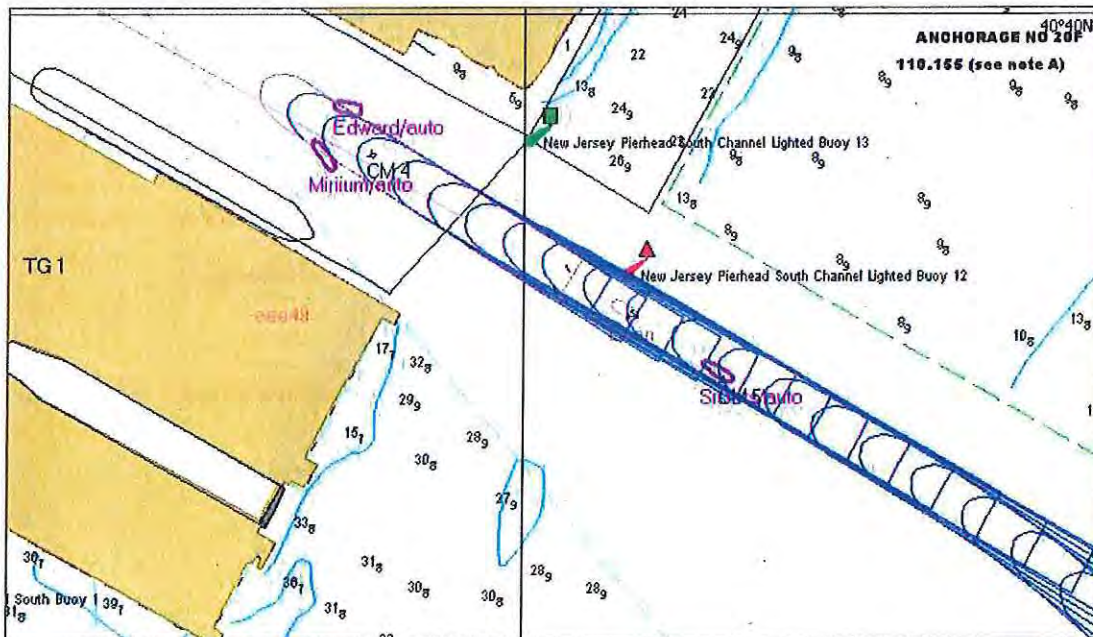


Figure 37: Run 20 – Triple E Entering Port Jersey Channel



## Run 27 Demonstration Run

Pilot: Robert Flannery Triple E Draft 49'

Current/Wind: Slack, N - 20 +3' Tide

Start: Robbins Reef Finish: Global Terminal

Tugs: CLA Brian McAllister, Port Bow Edward, Port Quarter Miriam, Free Sisters

### Description:

This was another demonstration run for the NY/NJ Port Authority. The DM started his turn before reaching the Port Jersey Channel buoy #1 and then eased the ship around using the tugs. He entered the enclosed channel where the passenger ship was berthed slightly to the north of the channel's centerline.

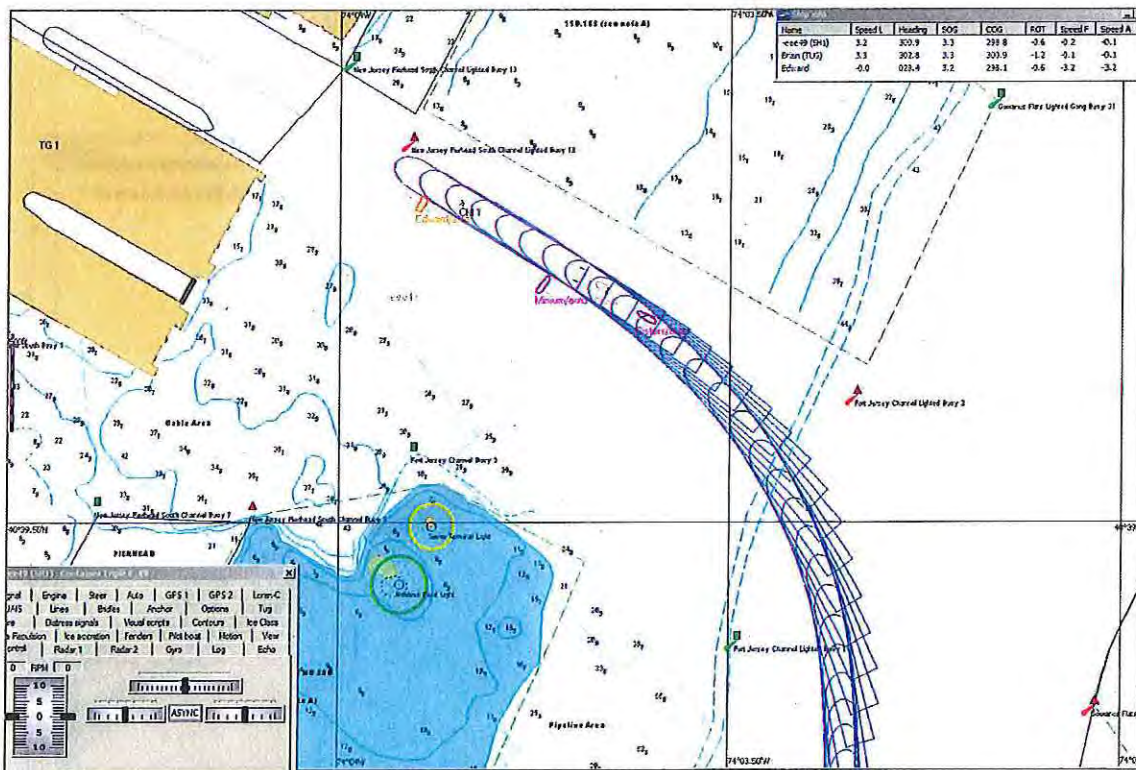


Figure 38: Triple E entering Global Marine Terminal

## 6.7 OUTBOUND FROM GLOBAL TERMINAL TO UPPER BAY BUOY 30

### Run 21

Pilot: Robert Flannery

Triple E Draft 49'

Start: Global Term.

Finish: Robbins Reef

Current/ Wind: N 20, Slack

+3' Tide

Tugs: CLA *Brian*, CLF *Edward*, Port Bow *Miriam*, Port Quarter *Sisters*

#### Description:

To save time, the model was started off of her berth and in mid-channel. Initially the *Brian* was ordered to pull in-line at half power to accelerate the ship. During the transit out of the Port Jersey Channel, the *Miriam* and *Sisters* were used to keep the ship headed down the channel on the desired course of the DM. At times, the *Brian* was also used pulling at a 45° angle to port and to starboard to keep the ship lined up and the DM used the *Edward* to push at the port bow to assist in holding the ship up against the wind. The ship was making 2.4 knots when the ship passed the passenger ship and she was north of the channel centerline for maximum clearance (181'). The DM continued to back the ship until it entered New York Upper Bay proper at Buoy 2 where Captain Flannery began his turn with the ship to head south in the Upper Bay.

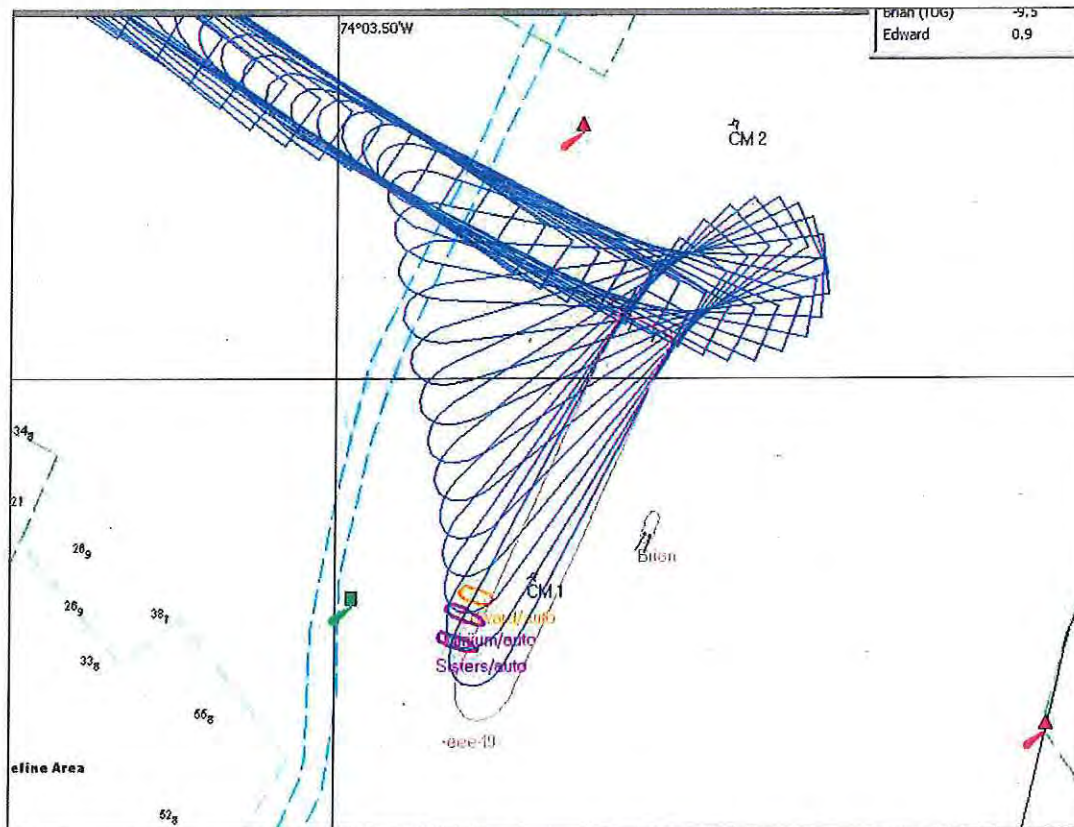


Figure 39: Run 21- Triple E backing out of Port Jersey Channel



## Run 22

Pilot: Robert Ellis

Triple E, Draft 49'

Start: Global Terminal

Finish: Robbins Reef

Current /Wind: S 20, Slack

+3' Tide

Tugs: CLA *Brian*, Starboard Quarter *Miriam*, CLF *Edward*, Port Quarter *Sisters*

### Description:

The DM did a very nice job backing the ship out of the Port Jersey Channel using the *Brian* to accelerate the ship and then maintain the ship in the center of the channel. The other two boats aft were used to hold the ship up against the wind. The *Edward* was used as necessary at the ship's bow to keep the ship tracking properly down the channel. When passing the passenger ship, the Triple E was on the channel centerline and cleared the ship by 111'. After clearing the ship, the DM took the ship further to the south to give the ship more room to turn which worked very well.

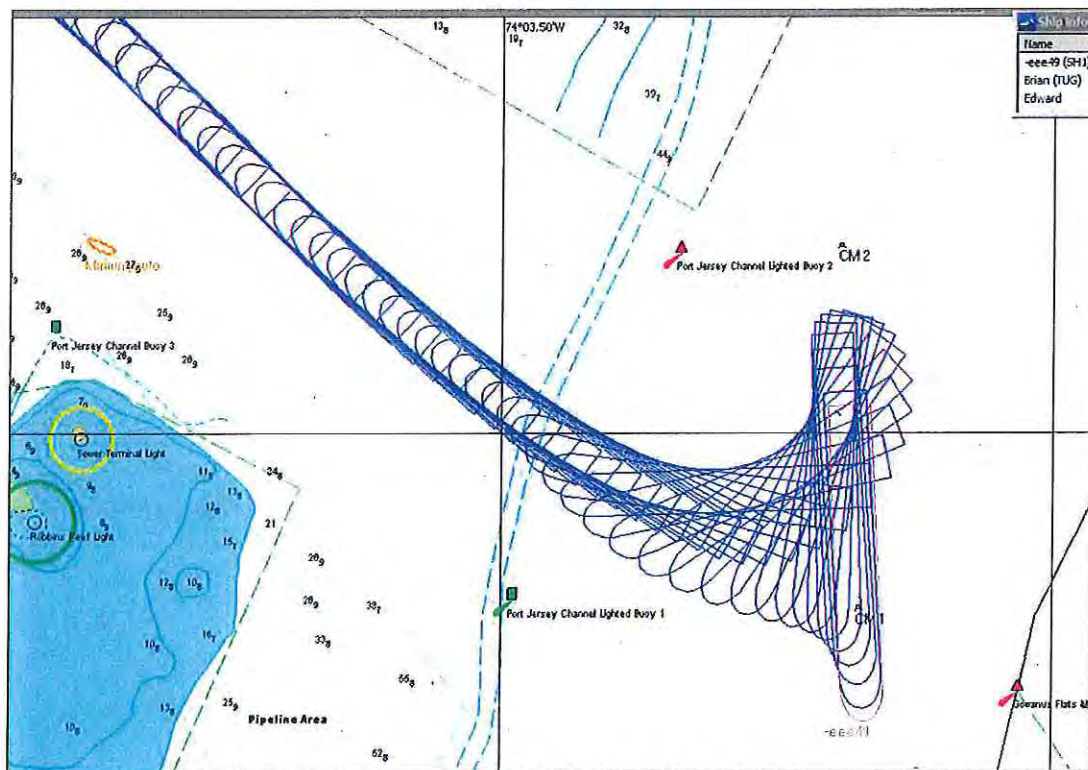


Figure 40: Run 22 - Triple E backing out of Port Jersey Channel

## 6.8 EMERGENCY TURNS ABOVE AND BELOW THE VERRAZANO NARROWS BRIDGE

These runs focused on the ability of the pilot to abort the transit, and turn the ship around above and below the Verrazano Bridge.

### Run 23 Emergency Turn South of Verrazano Bridge

Pilot: Richard Schoenlank      *Triple E*, Draft 49'

Start: Norton Point      Finish: Below VN Bridge

Current/Wind: S 20, 2 kn. Flood    +3' Tide

Tugs: *CLA Brian*, Port Bow *Sisters*

#### Description:

Once the tugs joined the ship, the pilot ordered the *Brian* (positioned center lead aft) into the transverse arrest mode, and then direct pull inline to reduce the speed of the ship. Once the speed had been reduced, the *Brian* pulled at a port "90" full and the *Sisters* pushed at the bow until the ship was turned 180°.

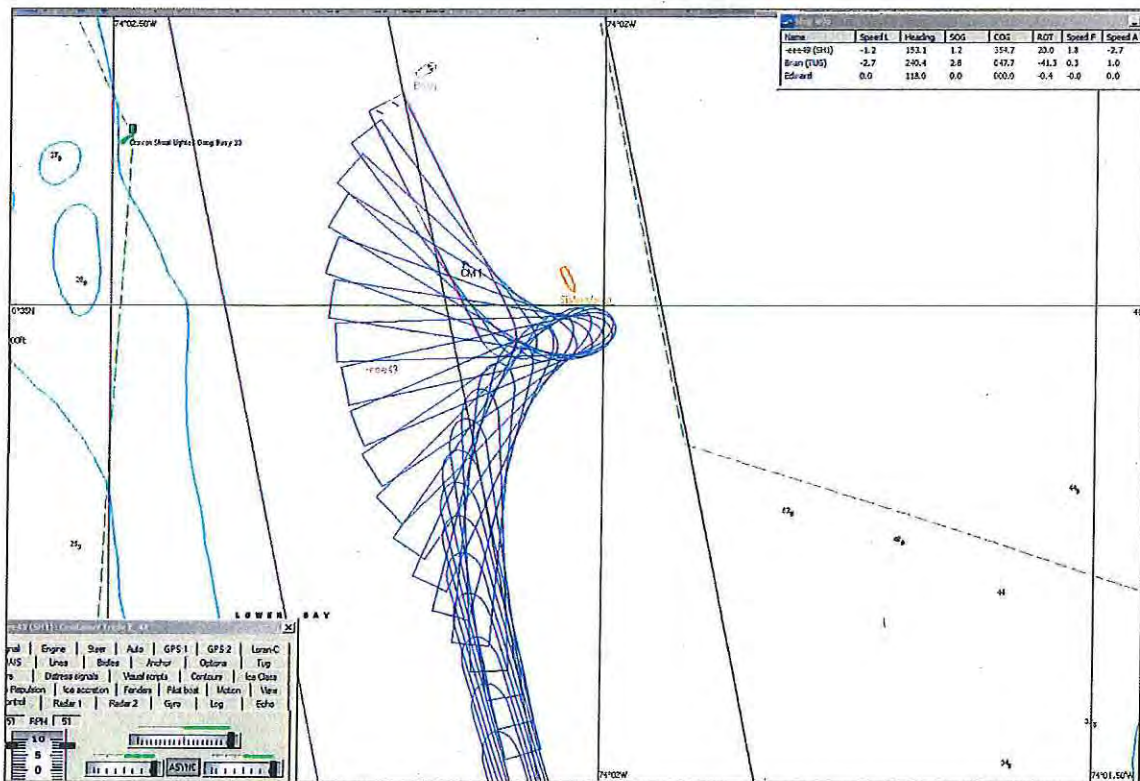


Figure 41: Emergency Turn in the Narrows



## Run 24 Emergency Turn South of Verrazano Bridge

Pilot: John Oldmixon

Triple E, Draft 49'

Start: Off Caven Shoals

Current/Wind: S 20, 2 knots Flood +3' Tide

Tugs: CLA Brian, Port Bow Sisters

### Description:

In this run, the ship was almost stopped when the tugs joined and the pilot immediately ordered the *Sisters* to push at the port bow full and the *Brian* to pull full at the transom, Port "90" full. The round turn was quickly performed.

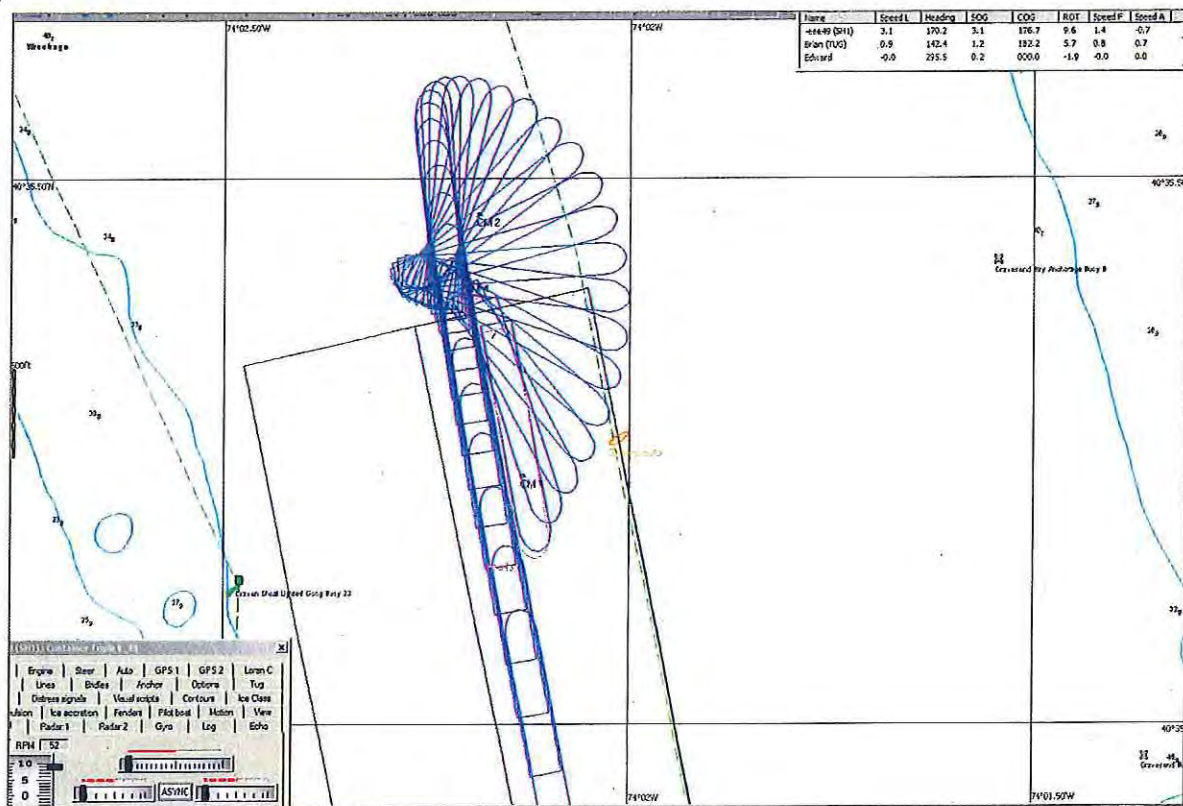
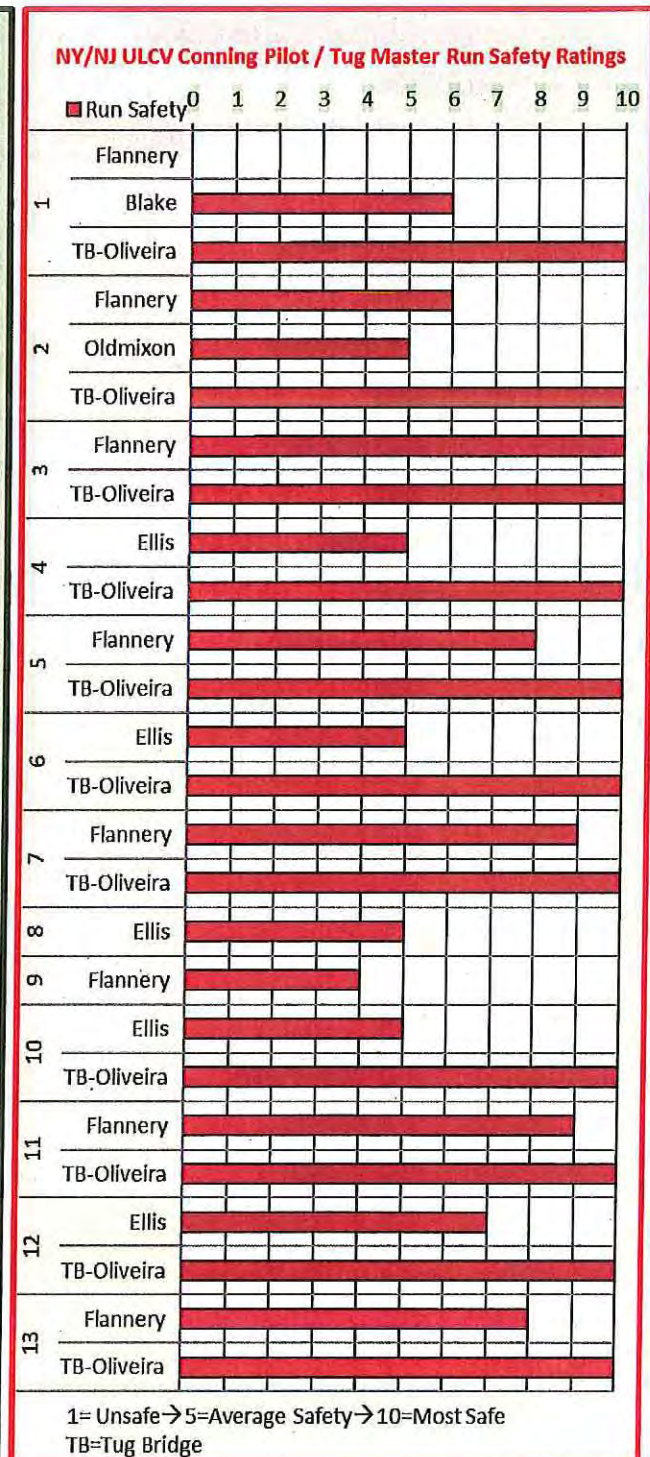
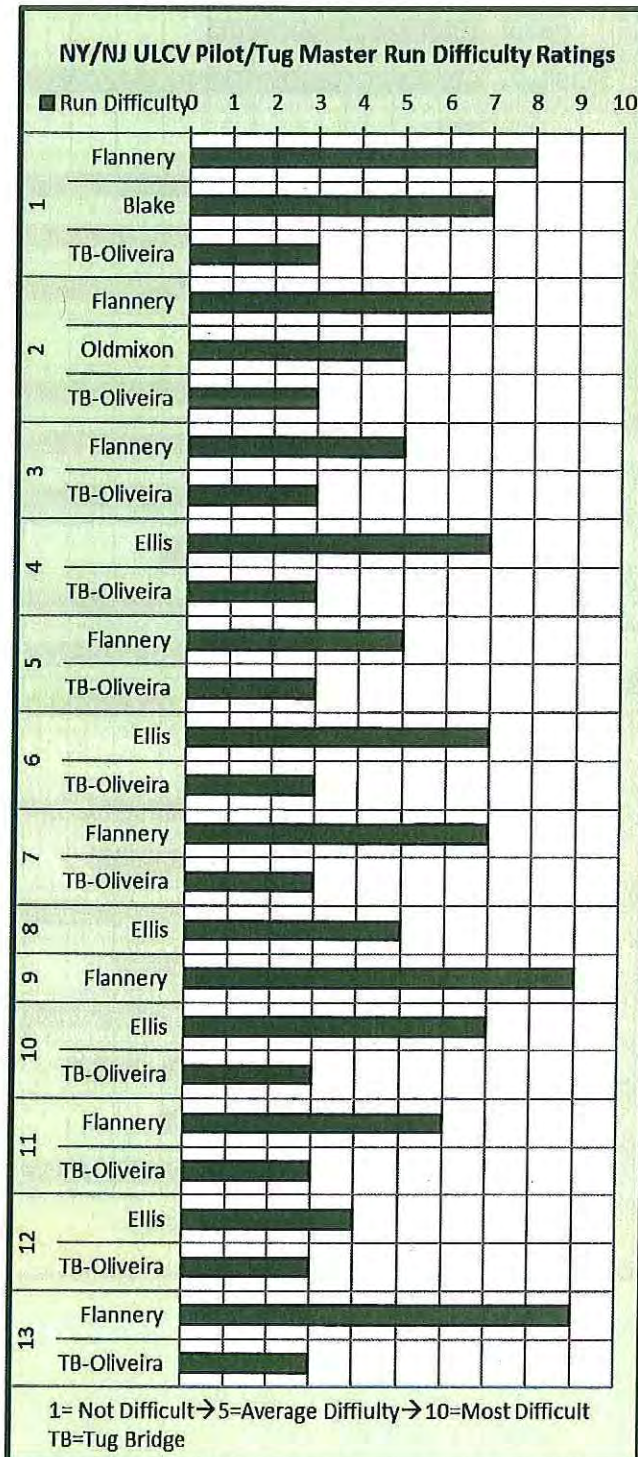


Figure 42: Emergency Turn

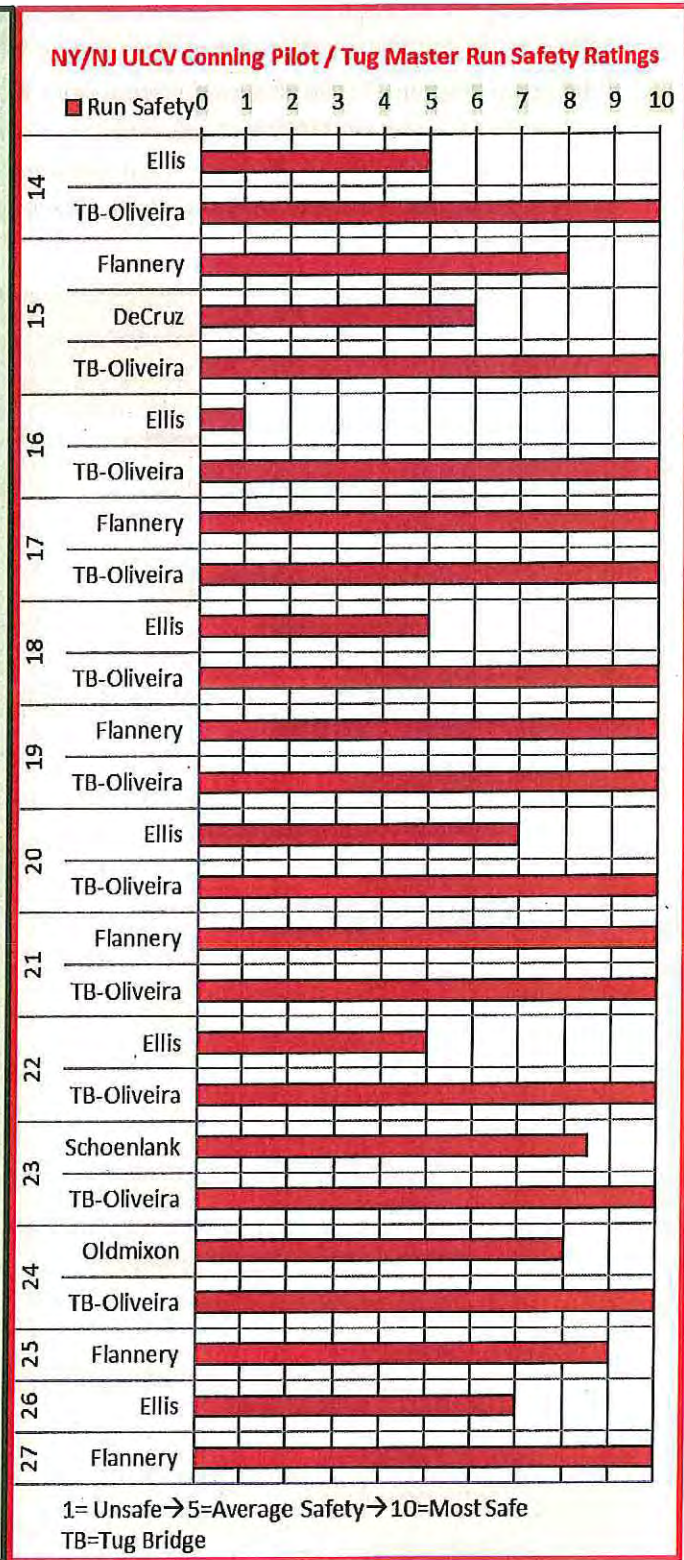
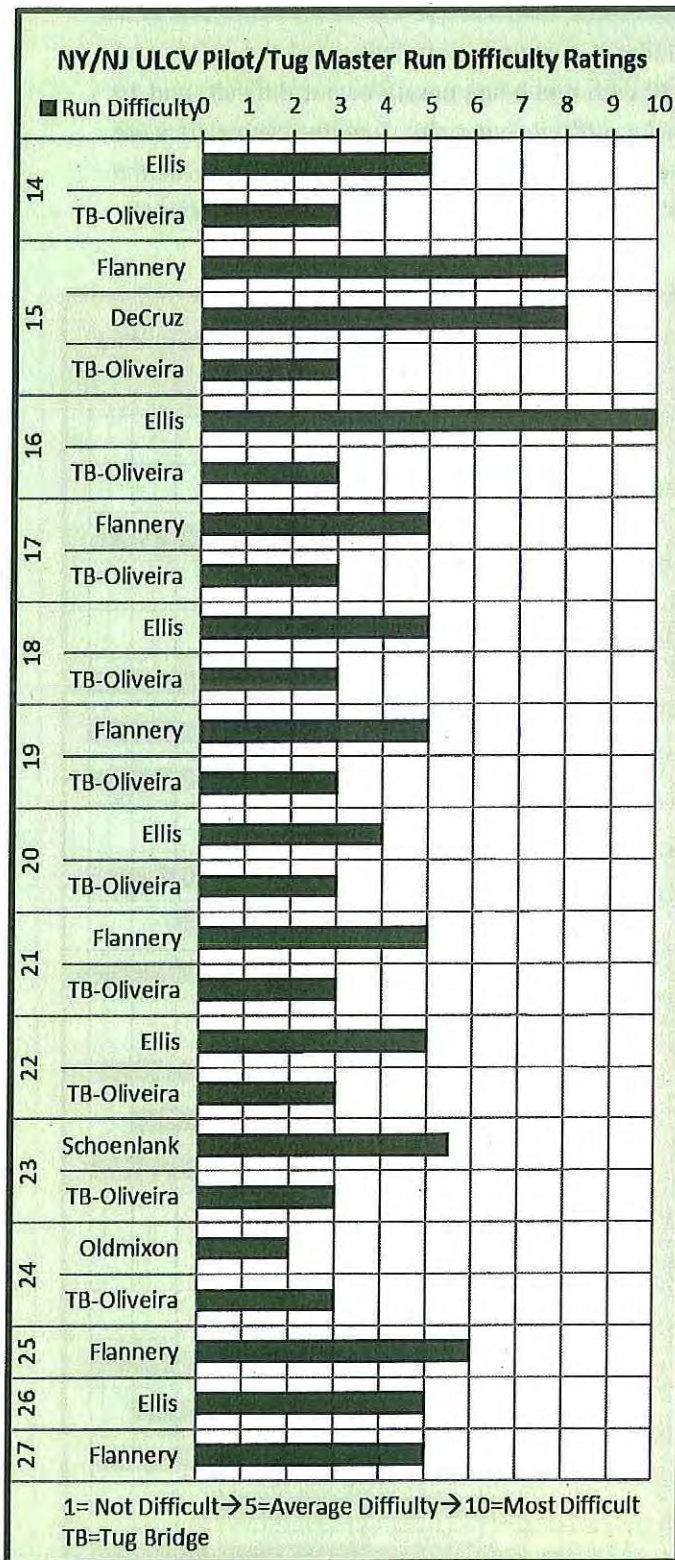


## 7. PILOT FINDINGS, CONCLUSIONS AND RECOMMENDATIONS

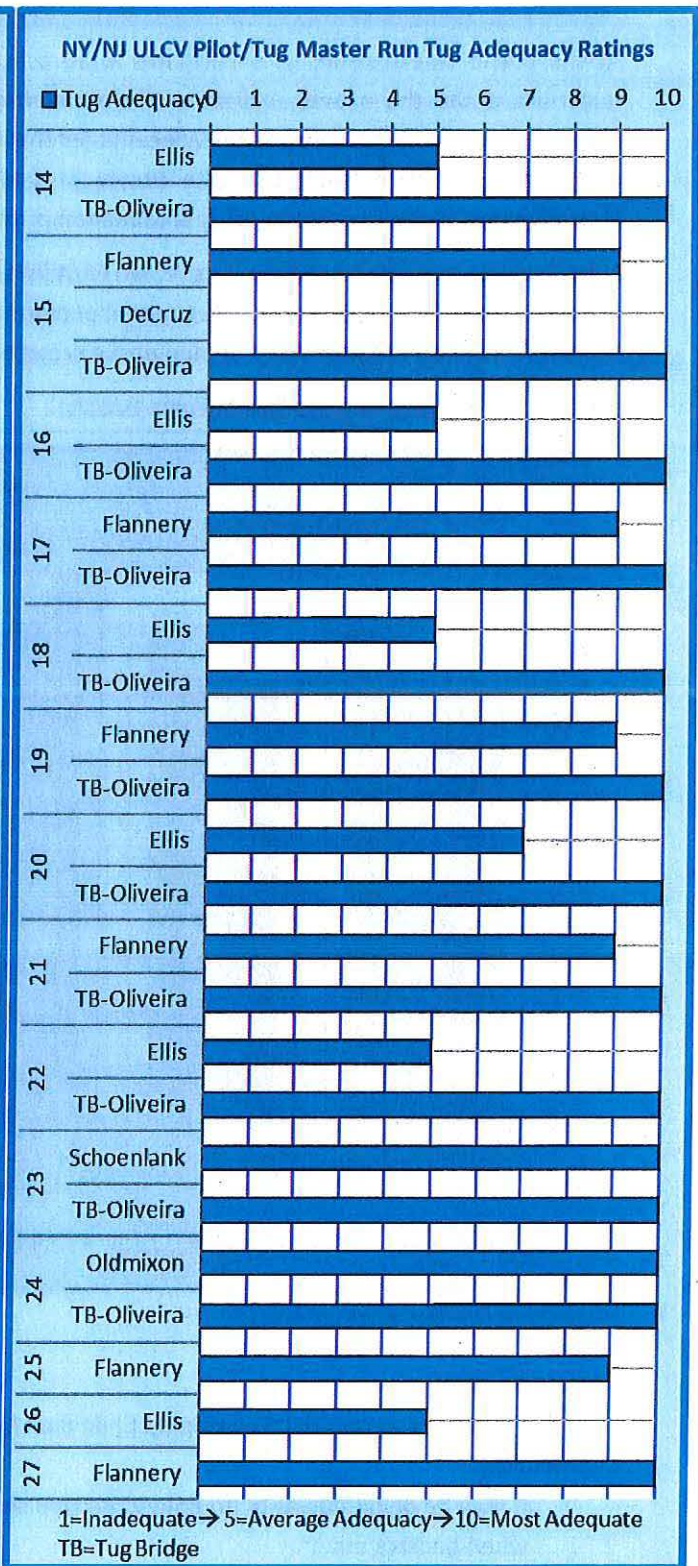
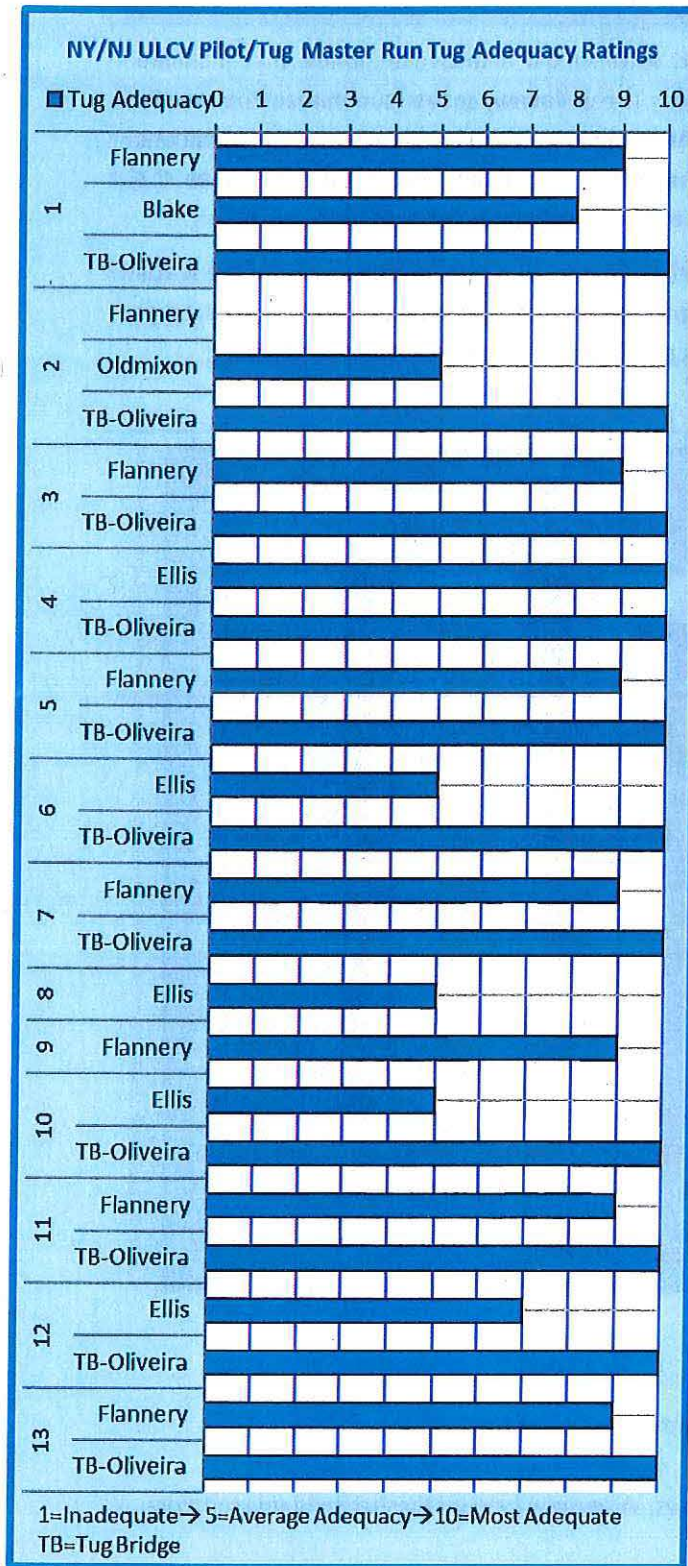
After each run, the conning pilot and tug operator filled out questionnaires that rated the safety and difficulty of the run. The scales used were from 1 to 10 with one being unsafe or not difficult, and 10 being very safe or very difficult. Note that a run can be difficult, but safe. Twenty-seven runs were completed in the August 2016 tests. The following graphs display side by side comparisons of the difficulty and safety ratings of the runs. "Tug Adequacy" graphs follow the difficulty and safety ratings.











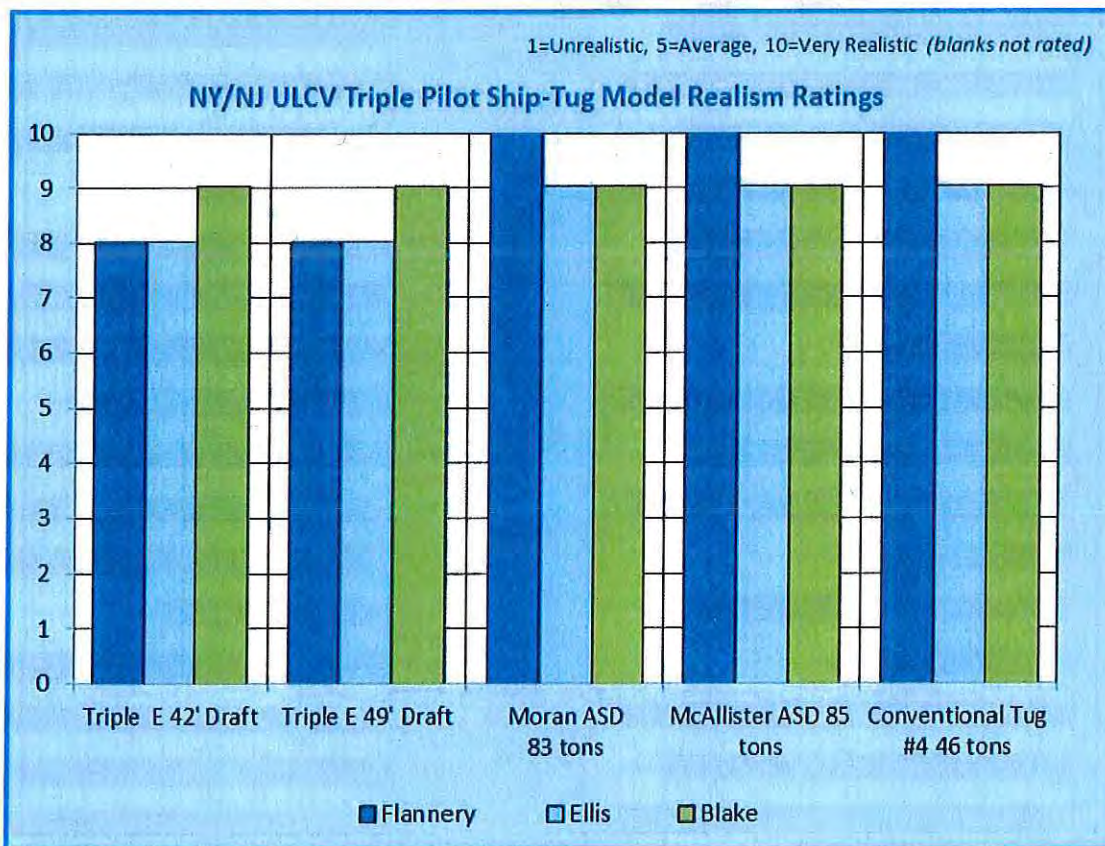


## 7.1 FINAL QUESTIONNAIRE GRAPHS AND COMMENTS

At the end of the session, all participants were asked to fill out a final questionnaire that included questions about the overall realism of the simulation. The following tables summarize the results followed by the written comments. We can infer that the higher "realism" ratings are good indications of higher confidence levels in the accuracy of the results. The below ratings indicate that the hydrodynamic models were a good approximation of the handling characteristics of these vessels.

Note that sea trial information on the "Brian McAllister" tug model was unavailable since the tug is still under construction. However, the tug model performed as expected for a tug of that class. The other models have been routinely used on numerous projects and found to be performed as expected.

### Realism of Ship and Tug Models Ratings Graph



Comments regarding model realism:

Captain Flannery

- > I think it is correct that the ship (EEE) doesn't back.

Captain Ellis

- > It may be debatable as to how slow the ship stops. Also, how long it takes to build up sternway when backing out.

Captain Schoenlank

- > The models were excellent – concern about lack of astern power, but perhaps that is accurate!
- > It was great having a live tug operator – believe it to be valuable for all involved.



## Realism of Environmental Conditions Ratings Graph



### Comments regarding Environmental Forces Realism

Captain Ellis

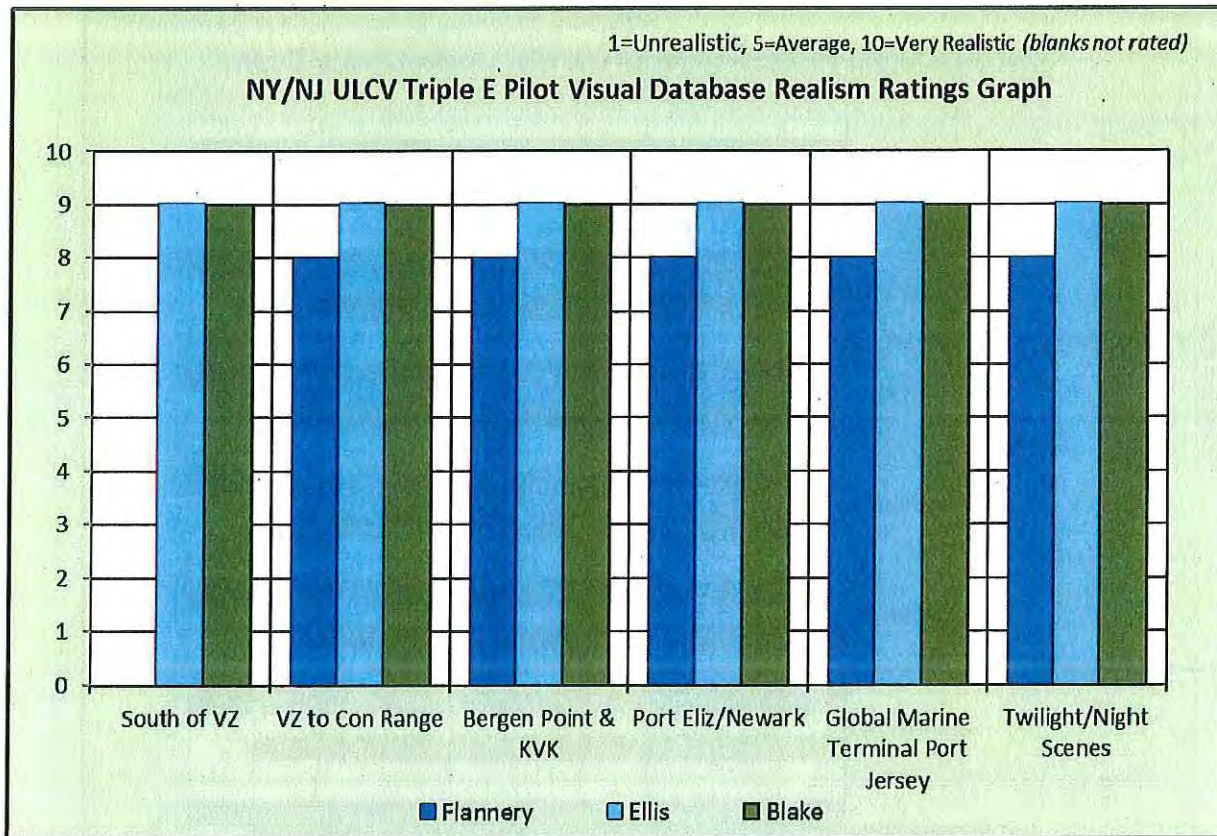
- > A 3.5 flood current at the approach to KV buoy was not realistic. It was modified later.

Captain Schoenlank

- > Believe the forces were good – would still like a visual of wind on water effect if possible.



## Realism of Visual Database Ratings Graph



Comments regarding Visual Database Realism

Captain Schoenlank

- > The database served the purpose – no problems.

### Overall Final Evaluation Comments

1. Based on the simulation exercises, were you able to make the turn at Con Hook Range, transit the KVK, and make the turn at Bergen Point? Additionally, what are the environmental limits, and issues that should be resolved prior to making the final determination on whether this class of ULCV should be allowed to call NY/NJ?

Captain Flannery

- > Visibility, 40% Current.
- > No more than 20 (knots) wind.

Captain Ellis

- > One hour either side of SW at Bergen Point.
- > 20 knot wind limit.
- > Meeting other commercial vessels not recommended.

Captain Schoenlank

- > As experienced and discussed, once the familiarization of the models took place and experienced gained, the transits met with success at the higher level. Believe the parameters on tide and wind are valid at this point. 18K TEU ships are one-way traffic situations.

Captain Blake

- > Yes. One hour either side of slack water at Bergen Point.
- > 20 knot wind limit.
- > No meeting / no overtaking except light boats.

2. Based on the simulation exercises, were you able to safely make the turn into Port Elizabeth Reach? Additionally, what are the environmental limits, and issues that should be resolved prior to making the final determination on whether this class of ULCV should be allowed to call on these terminals?

Captain Flannery

- > Can't go between 2 side by side EEE class.

Captain Ellis

- > One hour either side of SW at Bergen Point.
- > 20 knot wind limit.
- > Meeting other commercial vessels not recommended.

Captain Schoenlank

- > Yes, but thought as to other ships berthed needs to be considered – unrealistic to think an 18k TEU should go deep into Port Liz Channel past other vessels.

Captain Blake

- > Yes, 20 knot wind limit.
- > Cranes up.
- > Ships in berth with lines out.
- > No backing out between two Triple E class ships.

3. Based on the simulation exercises, were you able to transit in / out of Global Marine Terminal? Additionally, what are the environmental limits, and issues that should be resolved prior to making the final determination on whether this class of ULCV should be allowed to call on this terminal?

Captain Flannery

- > Visibility.
- > Slack Current.
- > No more than 20 (knots) wind.
- > One ship at NEAT or Cruise Terminal.
- > No two ships same time.

Captain Ellis

- > SW and 20 knots max wind.
- > Only one moored vessel slowed at the entrance.

Captain Schoenlank

- > Yes – again, only one ship should be berthed at either NEAT or Cape Liberty – not both!

Captain Blake

- > 20 knot wind limit.
- > Only one ship alongside at either Cape Liberty or NEAT.
- > Passengers off the gangways while ship is passing because of interaction.



4. Please list any other issue / challenges that should be resolved prior to allowing this class of vessel to call on NY/NJ?

Captain Flannery

- › Lot of communication.
- › Ships must leave on time.
- › Closing of KVK.
- › There's a lot of work to be done.
- › My thanks to the MITAGS group – par excellent. Professional and fun to work with.

Captain Blake

- › There should be a four tug, two tractor, two conventional limit minimum.

Captain Schoenlank

- › Strongly believe experience shall be gained first on smaller vessels (14k TEU's).
- › Surge issues, traffic arrangements, logistics of tidal parameters, and interaction with other ship transits that need to take place, must be allowed to get worked through. Believe 18k TEU's will further exacerbate this, need gradual experience – not sudden and dramatic.

## 7.2 MITAGS OBSERVATIONS AND COMMENTS

Overall, the docking masters, the pilots, and tug operators provided a consistent assessment of the difficulty and safety of each run.

### ULCV Meeting Situations in the KVK

In addition to the June tests, the pilot ran three more meeting situations in the KVK. For Runs 1, 2, and 15, the exercises used the *Kalina* meeting a smaller tanker. Although successful, the stern of the *Kalina* swept uncomfortably closed to the moored tanker models on the North side of the KVK. Discussions indicated that a "starboard to starboard" meeting may generate more favorable outcome, but due to time constraints they were not tested. Until further tests can be completed, 14,000 TEU and larger classes should avoid meeting traffic in the KVK.



**Figure 43: View from the Tanker Meeting the Kalina in the KVK**



#### 18,000 TEU Turn into Con Hook Range (Runs 3, 16 -18)

After the grounding on the run into Con Hook Range, the pilots adjusted their techniques and did remarkably well in controlling the turn, and getting the speed down below 5 knots by the time they turned into Constable Hook Reach. Additionally, the “difficulty” rating dropped to a “5” by Run 18.

In some respects, the Triple E model handling characteristics were superior to the *Kalina* model. This is something that will need to be validated over time.



**Figure 44: Triple E Inbound Constable Hook Reach**

#### 18,000 TEU Turn at Bergen Point (Runs 3, 4-7)

The DM executed nearly textbook turning maneuvers at Bergen Point inbound and outbound directions. The DM rated the runs as having high difficulty levels, but with above average safety levels. The DM and the tug master provided above average adequacy ratings for the tugs. They appear to have adapted and applied the “lessons learned” from the *Kalina* tests to the larger 18,000 TEU model.

#### Port Elizabeth Branch Reach (8 – 14)

A good portion of the runs focused on inbound and outbound maneuvers. The exercises had high difficulty ratings and above average safety ratings. The critical challenges include the very limited space for the assist tugs to maneuver when the container berths are filled with other ULCVs. The general consensus, at this time, is the Port should avoid putting two Triple E class vessel across from each other.

#### Global Marine Terminal (Runs 19 – 22, 27)

The DM generally gave above average difficulty and safety ratings for these maneuvers. The most critical challenge appeared to be the ability to get the way off the model in a timely manner. This may or may not be a function of the model.



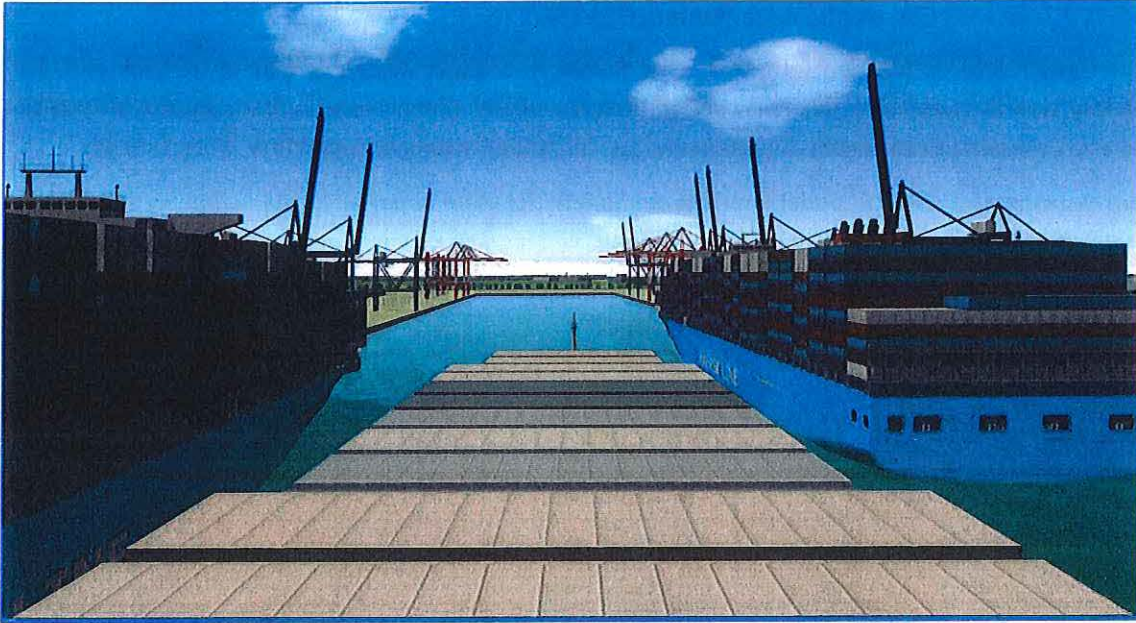


**Figure 45: Triple E Inbound into Port Elizabeth Branch Reach**



**Figure 46: Triple E Inbound at Bergen Point**





**Figure 47: Triple E Inbound to Global Marine Terminal Past Cruise Ship Terminal**

The follow tables provide an estimate on the amount of tug forces needed to offset beam wind and currents.

	Load Condition	Wind Velocity (knots)	Wind Force (N)	Wind Force (t)	Current Velocity (knots)	Current Force (N)	Current Force (t)	Required Effective Bollard Pull (t)
<b>Container Maersk Triple E</b>	Loaded (12.8 m)	15	395710.3	44.48	0	0.00	0.00	69.4
Displacement (t)	206397				1	462805.52	52.02	137.0
Length Over All (m)	399				2	1851222.07	208.10	339.9
Length Between Perps (m)	376.21				3	4165249.65	468.22	678.1
beam (m)	59	20	703485.0	79.08	0	0.00	0.00	123.4
draft (m)	12.8				1	462805.52	52.02	191.0
Lateral Wind Coefficient	0.75				2	1851222.07	208.10	393.9
Lateral Sway Coefficient	1				3	4165249.65	468.22	732.0
Windage Area (m <sup>2</sup> )	15633	25	1099195.3	123.56	0	0.00	0.00	192.8
Underwater Profile Area (m <sup>2</sup> )	3412.7				1	462805.52	52.02	260.4
Block Coefficient	0.7087				2	1851222.07	208.10	463.3
Disp/Power (LT/hp)	3.48				3	4165249.65	468.22	801.4
(399 x 59 meters)		30	1582841.3	177.93	0	0.00	0.00	277.6
					1	462805.52	52.02	345.2
					2	1851222.07	208.10	548.1
					3	4165249.65	468.22	886.2

**\*\*Formulas Used**

Thoresen, C. (2003). Tugboat Assistance. In *Port designer's handbook recommendations and guidelines*. London: Thomas Telford.

Zubaly, R. (1996). *Applied Naval Architecture*.

Wind Force =  $0.5 \times C_{y_{wind}} \times 1.2$  (air density)  $\times$  Wind Velocity<sup>2</sup>  $\times$  Windage Area

$C_{y_{wind}}$  range from 0.60 to 0.75 for containerships. 0.75 used for safety factor.

Current Force =  $0.5 \times C_{y_{current}} \times 1,025$  (seawater density)  $\times$  Current Velocity<sup>2</sup>  $\times$  Underwater Profile Area

Required Effective Bollard Pull =  $S_f \times [(Wind\ Force \times F_g) + Current\ Force]$ , where  $S_f$  = Tugboat bollard pull factor = 1.3,  $F_g$  = gust factor = 1.2

Newton-to-Ton Conversion Factor = 1 ton/8896 Newton



	Load Condition	Wind Velocity (knots)	Wind Force (N)	Wind Force (t)	Current Velocity (knots)	Current Force (N)	Current Force (t)	Required Effective Bollard Pull (t)
Container Maersk Triple E	Loaded (14.94 m)	15	419048.4	47.11	0	0.00	0.00	73.5
Displacement (t)	240904.9				1	540180.81	60.72	152.4
Length Over All (m)	399				2	2160723.26	242.89	389.2
Length Between Perps (m)	376.21				3	4861627.33	546.50	783.9
beam (m)	59	20	744975.0	83.74	0	0.00	0.00	130.6
draft (m)	14.94				1	540180.81	60.72	209.6
Lateral Wind Coefficient	0.75				2	2160723.26	242.89	446.4
Lateral Sway Coefficient	1				3	4861627.33	546.50	841.1
Windage Area (m <sup>2</sup> )	16555	25	1164023.4	130.85	0	0.00	0.00	204.1
Underwater Profile Area (m <sup>2</sup> )	3983.3				1	540180.81	60.72	283.1
Block Coefficient	0.7087				2	2160723.26	242.89	519.9
Disp/Power (LT/hp)	4.06				3	4861627.33	546.50	914.6
(399 x 59 meters)		30	1676193.8	188.42	0	0.00	0.00	293.9
					1	540180.81	60.72	372.9
					2	2160723.26	242.89	609.7
					3	4861627.33	546.50	1004.4

**\*\*Formulas Used**

Thoresen, C. (2003). Tugboat Assistance. In *Port designer's handbook recommendations and guidelines*. London: Thomas Telford.

Zubaly, R. (1996). *Applied Naval Architecture*.

Wind Force =  $0.5 \times C_{y_{wind}} \times 1.2$  (air density)  $\times$  Wind Velocity<sup>2</sup>  $\times$  Windage Area

$C_{y_{wind}}$  range from 0.60 to 0.75 for container ships. 0.75 used for safety factor.

Current Force =  $0.5 \times C_{y_{current}} \times 1,025$  (seawater density)  $\times$  Current Velocity<sup>2</sup>  $\times$  Underwater Profile Area

Required Effective Bollard Pull =  $S_f \times [(Wind\ Force \times F_g) + Current\ Force]$ , where  $S_f$  = Tugboat bollard pull factor = 1.3,  $F_g$  = gust factor = 1.2

Newton-to-Ton Conversion Factor = 1 ton/8896 Newton

For safety purposes, the hydrodynamic model used a full deck load profile for wind area calculations. When the actual pro-forma load profiles are established, there may be value in updating the models to more accurately simulate the wind effects. For example, of the forces created by wind and currents, please review the table below. The figure in the last column is the wind and current forces total plus a 20% safety factor for wind gusts and 30% factor for variabilities of the tugs<sup>3</sup>.

Note there are exponential increases in the forces exerted on the vessel as wind and current increase. A doubling of the wind speed (15 to 30 knots) increases the forces by more than three times. Also note the large forces generated by beam water currents. Maneuver outside of near slack water conditions will be a challenge. Accurate real-time wind and current information will be very important components of the pilot's assessment of the situation. Additional assist power may be needed to counteract unexpected conditions.

The tug design and placement are also important factors. The ASD propulsion systems allow the tug to provide more power when alongside. This could be significant when transiting between ULCVs berthed on either side of the channel, and there is not enough room to go out perpendicular to the ship's hull. Making fast on the ships' center leads forward and aft ensures the maximum safe working loads, and

<sup>3</sup> Thoresen, C. (2003). Tugboat Assistance. In *Port designer's handbook recommendations and guidelines*. London: Thomas Telford, and Zubaly, R. (1996). *Applied Naval Architecture*.



provides additional leverage. Tugs capable of safely performing “power indirect” commands with short leads add an additional layer of safety.

### **General Information on the Maneuverability of the Triple E Class ULCV**

---

From simulation studies and observations from conning pilots, we can make some general comments about the expected maneuvering characteristics of the *18,000 TEU Triple E Class* in the real-world.

In general, the design characteristics and anecdotal evidence indicates the Triple E Class handles well for a ship of its size, but does have difficulty in taking way off quickly. The large deck load obstructs the pilot’s view, and makes the use of electronic navigation systems critically important. The model and field evidence<sup>4</sup> indicates the vessel takes longer than expected to slow down in confined waters. This condition maybe exacerbated for the under keel clearances of less than 10% of draft.

### **Future Considerations**

---

The study used water current models originally developed by the Army Corps of Engineers and modified by the Waterway Simulation Technology (WST) Study for loading into the Transas ship simulator. At the time of the Study, there were no current meters at Bergen Point (the most critical area) to validate the velocities. In order to achieve the proper ship model behavior at Bergen Point the current velocities were increased over the original algorithms. Once the water current meters have been installed at Bergen Point, the data should be compared against current models used in this study, and select exercises should be re-run to validate the accuracy of the current velocities used in the study.

The large underwater volume of the ULCVs relative to the channel volume could create significant surge forces on moored vessels in confined waters. Keeping the speed off these vessels will be critical to managing the surge forces<sup>5</sup>. However, even at very slow speeds, surge may still be a significant factor in areas such as Global Marine Terminal, and / or Port Elizabeth Channel Reach where the water flow is restricted by the berths and other vessels. Suggest further study of the water flows created by a ULCV entering and departing these areas, to determine maximum safe speed of approach. These studies may indicate a need for changes in the mooring line configurations and stronger bollard and fendering arrangements.

The numbers, locations and sizes of the vessels at the berths in the Port Elizabeth / Global Marine Terminals will be significant factors in determining whether it is safe to transit. Various combinations of berth ships were evaluated and some had assist tug clearances of less than twenty feet. Suggest further study to develop guidelines for maximum beam combinations. Other suggestions include requiring the container crane booms in the up position, and berth vessels fully secured until the ULCV docking / undocking evolutions have been completed.

---

<sup>4</sup> From Capt. Ian Love, Pilot, Flexistowe, UK, and SHS Consultant. Capt. Love was brought over from the UK to assist in the pre-validation of the Kalina and Triple models.

<sup>5</sup> Please refer to the separate Waterway Simulation Technology Study mentioned in Section 4 of this report.

Even within the same ULCV Class, vessel maneuvering behavior can be different. Suggest the pilots consider simulating other classes of ULCV that are expected to call on NY/NJ.

ULCV transit restrictions will be a significant factor in managing the vessel traffic through the Kill Van Kull. Suggest the Port consider mechanisms for coordinating the activities of the various stake holders that use this waterway.

Due to time constraints, only a limited number of "emergency exercises" were run in the vicinity of the Verrazano Bridge. Suggest further simulation to develop "best practices" for handling emergencies (propulsion / tug failures, etc.) at other points along the transit.

On behalf of the MITAGS-PMI team, we thank the participants and Port Authority, and the NY/NJ Shipping Association for their confidence in our simulation capabilities. We hope the lessons learned will contribute, in a small way, to the safe and efficient handling of the next generation of containerships. We wish the pilots and the Port every success in this new endeavor. Additionally, we look forward to the pilots' feedback on the simulation after they have handled the ULCVs under real-world conditions.



### 8. FINAL TEST MARIX

Run No. & Direction	1 Inbound Meeting				1 Outbound Meeting				2 Inbound Meeting				2 Outbound Meeting			
Pilot Name(s)	Flannery (Docking)				Blake				Flannery (Docking)				Oldmixon			
Starting Location	Con Hook Range				Shooters Island				Con Hook Range				Bergen Point			
Initial Heading & Speed	345° @ 8 Knots				112° @ 6.3 knots				291° @ 6.7 knots				111° @ 7.1 knots			
Database Used	New York_F								New York_F							
Ship Model & Condition	49' Kalina Loaded				Tanker_OH_CPP_R				49' Kalina				Tanker_OH_Memphis			
Current File Name, Tide	2353 (1.5) Flood 1.8 knots @ Bergen								2353 (1.5) Flood 1.8 knots @ Bergen, Tide + 3'							
Wind Dir. "From" Speed	S @ 20 knots								S @ 20 Knots							
Visibility	Clear – Day								Clear – Day							
Tugs	McAllister	Moran	Edward	Brian	Conv.	Conv.				Conv.	Brian	Edward	Conv.			
Bollard Pull	80	85	46			46				46	85	80	46			
Live or Auto	Live	Auto	Auto			Auto				Auto	Auto	Live	Auto			
Tug Initial Position	CLA	SB.	PB			PB				PB	SB	CLA	Escort Aft			
All Fast Order																
CPA to Meeting Ship	354'								204'							
Ending Location	Buoy 9				IMIT Dock				Con Hook @ Bergen Point E				Con Hook Range			
Simulation Time	30.5 Minutes								34 minutes							

Run No. & Direction			3 Inbound				4 Inbound				5 Outbound			
Pilot Name(s)			Flannery (Docking)				Ellis (Docking)				Flannery (Docking)			
Starting Location			Stapleton Anchorage				Pier A Bayonne City Dock				Bayonne City Dock			
Initial Heading & Speed			351° @ 6.6 knots				246° @ 6.5 knots				246° @ 6.5 knots			
Database Used			New York_F				New York_F				New York_F			
Ship Model & Condition			42' Triple E				49' Triple E				49' Triple E			
Current File Name, Tide			None				3126 (1.25) Ebb: 0.8 knots @ Bergen, Tide + 3'				2353(1.5) Flood: 1.8 knots @ Bergen, Tide + 3'			
Wind Dir. "From" Speed			N @ 5 Knots				NE @ 20 Knots				NE @ 20 Knots			
Wave/Swell Dir. "From" Height (meters); Model							Height: 1.3' NE Pierson-Moskowitz				Height: 1.3' NE Pierson-Moskowitz			
Visibility			Clear – Day				Clear – Day				Clear – Day			
Tugs	McAllister	Moran	Edward	Brian	Miriam	Sisters	Edward	Brian	Miriam	Sisters	Edward	Brian	Miriam	Sisters
Bollard Pull			80	85	46	46	80	85	46	46	80	85	46	46
Live or Auto			Live	Auto	Auto	Auto	Live	Auto	Auto	Auto	Live	Auto	Auto	Auto
Tug Initial Position			CLA	SSB	PB	STBY	CLA	SB	PB	Escort Aft	CLA	SB	PB	Escort
All Fast Order			1	3	2		2	1	3					
Ending Location			Newark Buoy 5				Port Eliz / Newark Buoy 5				Old Bay Draw Newark Buoy 5			
Simulation Time			1 hour 12 minutes				30:5 minutes				28 Minutes			



Run No. & Direction			6 Outbound				7 Outbound				8 Inbound			
Pilot Name(s)			Ellis (Docking)				Flannery (Docking)				Ellis (Docking)			
Starting Location			Old Bay Draw Port Eliz / Newark				Port Eliz / Newark				Bayonne City Dock			
Initial Heading & Speed			205° @ 6.5 knots				205° @ 6.5 knots				216° @ 6.5 knots			
Database Used			New York_F				New York_F				New York_F			
Ship Model & Condition			49' Triple E				49' Triple E				49' Triple E			
Current File Name, Tide			2353 Flood: 1.2 knots @ Bergen, Tide + 3'				3126 (1.25) Ebb: 1.3 knots @ Bergen, Tide + 3'				2359 (1.5) Ebb, Tide +3'			
Wind Dir. "From" Speed			NW @ 20 Knots				NW @ 20 Knots				N @ 20 Knots			
Wave/Swell Dir. "From" Height (meters); Model			Height: 1.3' NE Pierson-Moskowitz				Height: 1.3' NE Pierson-Moskowitz				Height: 1.3' N Pierson-Moskowitz			
Visibility			Clear – Day				Clear – Day				Clear – Day			
Tugs	McAllister	Moran	Edward	Brian	Miriam	Sisters	Edward	Brian	Miriam	Sisters	Brian	Edward	Miriam	Sisters
Bollard Pull			80	85	46	46	80	85	46	46	85	80	46	46
Live or Auto			Live	Auto	Auto	Auto	Live	Auto	Auto	Auto	Live	Auto	Auto	Auto
Tug Initial Position			CLA	PB	SB	Escort	CLA	PB	SB	Escort	CLA	PB	SB	Escort
All Fast Order			3	1	2		3	2	1		1	2	3	
CPA in Kills							43' South Side Channel @ Bridge							
Ending Location			KVK Buoy 13				KVK Buoy 22				Port Elizabeth			
Simulation Time			27 minutes				29 minutes				60 Minutes			

Run No. & Direction			Run 9 Inbound				Run 10 Outbound				11 Outbound			
Pilot Name(s)			Flannery (Docking)				Ellis (Docking)				Flannery (Docking)			
Starting Location			Newark Bay				Berth 59 Port Newark				Berth 59			
Initial Heading & Speed			025° @ 6.5 knots				309° @ 0 knots				309° @ 0 knots			
Database Used			New York_F				New York_F				New York_F			
Ship Model & Condition			49' Triple E				49' Triple E				49' Triple E			
Current File Name, Tide			2353 (1.5) Flood: 1..8 @ Bergen, Tide +3'				2353 (1.5) Flood: 1..8 @ Bergen, Tide +3'				2359 (1.5), Tide +3'			
Wind Dir. "From" Speed			S @ 20 Knots				S @ 20 Knots				N @ 20 Knots			
Wave/Swell Dir. "From" Height (meters); Model			Height: 1.3' S Pierson-Moskowitz				Height: 1.3' S Pierson-Moskowitz				Height: 1.3' N Pierson-Moskowitz			
Visibility			Clear – Day				Clear – Day				Clear – Day			
Tugs	McAllister	Moran	Edward	Brian	Miriam	Sisters	Brian	Edward	Miriam	Sisters	Brian	Edward	Miriam	Sisters
Bollard Pull			80	85	46	46	85	80	46	46	85	80	46	46
Live or Auto			Live	Auto	Auto	Auto	Live	Auto	Auto	Auto	Live	Auto	Auto	Auto
Tug Initial Position			CLF	CLA	SB	SQ	CLA	CLF	PQ	SQ	CLA	Bow	PQ	PQ
All Fast Order			4	1	2	3	3	1	2	4				
CPA Other											66' to ship on starboard			
Ending Location			Berth 59 Port Newark				Newark Bay				Newark Bay			
Simulation Time			45 minutes				42 minutes				40 Minutes			



Run No. & Direction			12 Inbound				13 Inbound				14 Outbound			
Pilot Name(s)			Ellis (Docking)				Flannery (Docking)				Ellis (Docking)			
Starting Location			Newark Bay Buoy 10				Newark Bay Buoy 10				Berth 59 Port Newark			
Initial Heading & Speed			027° @ 6.5 knots				027° @ 6.2 knots				310° @ 0 knots			
Database Used			New York_F				New York_F				New York_F			
Ship Model & Condition			49' Triple E				45.9' AMAersk				45.9' AMAersk			
Current File Name, Tide			2359 (1.5) Ebb, Tide +3'				2359 (1.5) Ebb, Tide +3'				2359 (1.5) Ebb, Tide +3'			
Wind Dir. "From" Speed			NE @ 20 Knots				NE @ 20 Knots				NE @ 20 Knots			
Wave/Swell Dir. "From" Height (meters); Model			Height: 1.3' NE Pierson-Moskowitz				Height: 1.3' NE Pierson-Moskowitz				Height: 1.3' NE Pierson-Moskowitz			
Visibility			Clear – Day				Clear – Day				Clear – Day			
Tugs	McAllister	Moran	Brian	Edward	Miriam	Sisters	Brian	Edward	Miriam	Sisters	Brian	Edward	Miriam	Sisters
Bollard Pull			85	80	46	46	85	80	46	46	85	80	46	46
Live or Auto			Live	Auto	Auto	Auto	Live	Auto	Auto	Auto	Live	Auto	Auto	Auto
Tug Initial Position			CLA	PB	SB	Escort	CLA	CLF	PB	Escort	CLA	CLF	Escort	Escort
All Fast Order			3	1	2						3	4	1	2
CPA Other											Sterns of 46t tugs 25' to ships both sides			
Ending Location			Berth 61 Port Newark				Berth 59 Port Newark				Newark Bay Buoy 10			
Simulation Time			28 minutes				33 minutes				25 Minutes			

Run No. & Direction			15 Inbound Meeting				15 Outbound Meeting		16 Inbound			
Pilot Name(s)			Flannery (Docking)				DeCruz		Ellis (Docking)			
Starting Location			Con Hook Range				Shooters Island Reach		Buoy 2 Bay Ridge			
Initial Heading & Speed			000° @ 6.7 knots				103° @ 6.9 knots		346° @ 6.5 knots			
Database Used			New York_F						New York_F			
Ship Model & Condition			49' Kalina				Tanker Memphis		49' Triple E			
Current File Name, Tide			Flood 2353(1.5) Flood: 1.8 @ Bergen, Tide + 3'						2353 (1.5) Flood: 1.8 @ Bergen, Tide + 3'			
Wind Dir. "From" Speed			S @ 20 Knots						S @ 20 Knots			
Wave/Swell Dir. "From" Height (meters); Model			Height: Pierson-Moskowitz						Height: 1.3' S Pierson-Moskowitz			
Visibility			Clear – Day						Clear – Day			
Tugs	McAllister	Moran	Brian	Edward	Miriam	Sisters	None		Brian	Edward	Miriam	Sisters
Bollard Pull			85	80	46	46			85	80	46	46
Live or Auto			Live	Auto	Auto	Auto			Live	Auto	Auto	Auto
Tug Initial Position			CLA	PB	SB	Escort			CLA	PB	Escort	SB
All Fast Order			3	1	2				1	2	3	3
CPA in Kills			270' to ship at berth to starboard									
CPA to meeting ship			152'						0' @ buoy 2 Port Elizabeth			
Ending Location			KVK Buoy 10						Con Range			
Simulation Time			33 minutes						12.5 Minutes			



Run No. & Direction			17 inbound				18 Inbound				19 Inbound			
Pilot Name(s)			Flannery (Docking)				Ellis (Docking)				Flannery (Docking)			
Starting Location			Buoy 2				Bay Ridge Buoy 2				Upper Bay Buoy 28			
Initial Heading & Speed			346° @ 6.5 knots				346° @ 6.5 knots				000° @ 6.5 knots			
Database Used			New York_F				New York_F				New York_F			
Ship Model & Condition			49' Triple E				49' Triple E				49' Triple E			
Current File Name, Tide			3135 (1.25) Flood, Tide +3'				Ebb 2357 (1.25)				Slack, Tide +3'			
Wind Dir. "From" Speed			S @ 20 Knots				N @ 20 Knots				NW @ 20 Knots			
Wave/Swell Dir. "From" Height (meters); Model			Height: 1.3' S Pierson-Moskowitz				Height: 1.3' N Pierson-Moskowitz				Height: 1.3' S Pierson-Moskowitz			
Visibility			Clear – Day				Clear – Day				Clear – Day			
Tugs	McAllister	Moran	Brian	Edward	Miriam	Sisters	Brian	Edward	Miriam	Sisters	Brian	Edward	Miriam	Sisters
Bollard Pull			85	80	46	46	85	80	46	46	85	80	46	46
Live or Auto			Live	Auto	Auto	Auto	Live	Auto	Auto	Auto	Live	Auto	Auto	Auto
Tug Initial Position			CLA	PB	SB	Escort	CLA	PB	SB	Escort	CLA	SB	PB	Escort
All Fast Order			1	2	3		3	2	1		3	1	2	
CPA to Chan. toe line during transit							56' at KVK 7							
CPA Other			276' to ship at berth on starboard											
Ending Location			KVK Buoy 8				KVK 8				Port Jersey Buoy 2			
Simulation Time			37 minutes				40 minutes				29 Minutes			

Run No. & Direction			20 Inbound				21 Outbound				22 Outbound			
Pilot Name(s)			Ellis(Docking)				Flannery (Docking)				Ellis (Docking)			
Starting Location			Buoy 28				Port Jersey				Port Jersey			
Initial Heading & Speed			000° @ 6.5 knots				299° @ 0 knots				299° @ 0 knots			
Database Used			New York_F				New York_F				New York_F			
Ship Model & Condition			49' Triple E				49' Triple E				49' Triple E			
Current File Name, Tide			Slack, Tide + 3'				Slack, Tide + 3'				Slack, Tide + 3'			
Wind Dir. "From" Speed			N @ 20 Knots				N @ 20 Knots				S @ 20 Knots			
Wave/Swell Dir. "From" Height (meters); Model			Height: 1.3' N Pierson-Moskowitz				Height: 1.3' N Pierson-Moskowitz				Height: 1.3' S Pierson-Moskowitz			
Visibility			Clear – Day				Clear – Day				Clear – Day			
Tugs	McAllister	Moran	Brian	Edward	Miriam	Sisters	Brian	Edward	Miriam	Sisters	Brian	Edward	Miriam	Sisters
Bollard Pull			85	80	46	46	85	80	46	46	85	80	46	46
Live or Auto			Live	Auto	Auto	Auto	Live	Auto	Auto	Auto	Live	Auto	Auto	Auto
Tug Initial Position			CLA	SB	PB	Escort	CLA	CLF	PB	PQ	CLA	CLF	SQ	PQ
All Fast Order			2	1	2		2	1	3	4	3	1	2	4
CPA Other							191 to ship on port at dock				111' to Cruise Ship			
Ending Location			Port Jersey				KVK Buoy				Port Jersey Buoy 1			
Simulation Time			29.5 minutes				50 Minutes				50 minutes			



Run No. & Direction	23 Inbound				24 Inbound				25 Inbound			
Pilot Name(s)	Schoenlank				Oldmixon				Flannery (Docking)			
Starting Location	VZ Bridge Buoy 20				VZ Bridge Buoy 20				Newark Bay Buoy 10			
Initial Heading & Speed	349° @ 6.4 knots				349° @ 6.5 knots				027° @ 6.7 knots			
Database Used	New York_F				New York_F				New York_F			
Ship Model & Condition	49' Triple E				49' Triple E				49' Triple E			
Current File Name, Tide	3135 (1.5) Flood: 3.8 knots at Bergen, Tide +3'				2359 (1.5) Ebb, Tide +3'				2352 (1.5) Flood: 1.8 @ Bergen, Tide + 3'			
Wind Dir. "From" Speed	S @ 20 Knots				N @ 20 Knots				S @ 20 Knots			
Wave/Swell Dir. "From" Height (meters); Model	Height: 1.3' S Pierson-Moskowitz				Height: 1.3' @ 000° Pierson-Moskowitz				Height: 1.3' S Pierson-Moskowitz			
Visibility	Clear – Day				Clear – Day				Clear – Day			
Tugs	McAllister	Moran	Brian	Sisters	Brian	Sisters	Brian	Edward	Miriam	Sisters		
Bollard Pull			85	46	85	46	85	80	46	46		
Live or Auto			Live	Auto	Live	Auto	Live	Auto	Auto	Auto		
Tug Initial Position			CLA	PB	CLA	PB	CLA	SB	Escort	PB		
All Fast Order			2	1	1	2	3	2		3		
CPA Other									46' to Ship on port side			
Ending Location	Craven Shoal Buoy 23				Craven Shoal Buoy 23				Port Elizabeth Berth 59			
Simulation Time	28 minutes				18 minutes				25 Minutes			

Run No. & Direction			26 Outbound				27 Inbound			
Pilot Name(s)			Ellis				Flannery			
Starting Location			Port Elizabeth Berth 61				Gowanus Buoy 28			
Initial Heading & Speed			306° @ 10 knots				000° @ 6.5 knots			
Database Used			New York_F				New York_F			
Ship Model & Condition			49' Triple E				49' Triple E			
Current File Name, Tide			2359 (1.5) Tide +3'				Slack, Tide + 3'`			
Wind Dir. "From" Speed			N @ 20 Knots				N @ 20 Knots			
Wave/Swell Dir. "From" Height (meters); Model			Height: 1.3 N Pierson-Moskowitz				Height: 1.3 @ 000° Pierson-Moskowitz			
Visibility			Clear – Day				Clear – Day			
Tugs	McAllister	Moran	Brian	Edward	Sisters	Miriam	Brian	Edward	Miriam	Sisters
Bollard Pull			85	80	46	46	85	80	46	46
Live or Auto			Live	Auto	Auto	Auto	Live	Auto	Auto	Auto
Tug Initial Position			CLA	CLF	PQ	Escort SQ	CLA	PB	PQ	SB
All Fast Order			2	1	3	4	4	1	3	2
CPA Other			85' to ship at port during swing							
Ending Location			Port Newark				Port Jersey Global			
Simulation Time			27 minutes				25 minutes			



**APPENDIX A: Pilot Cards**

**Container Triple E\_3.0.55.2 \* 42' draft**

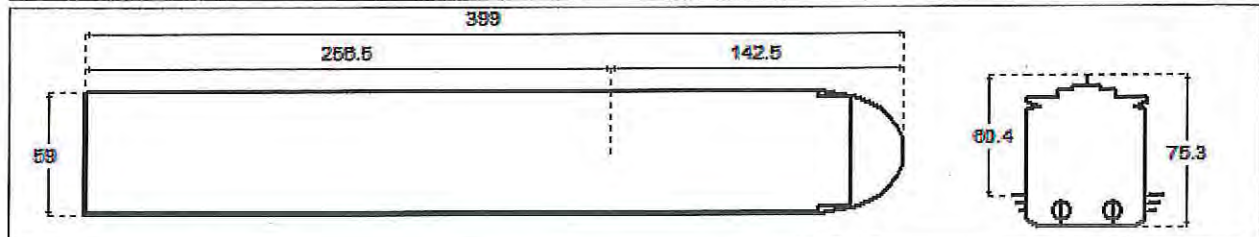
PILOT CARD					
Ship name	Container Triple E 42 3.0.55.2 *			Date	19.04.2016
IMO Number	N/A	Call Sign	N/A	Year built	N/A
Load Condition	Loaded				
Displacement	206397 tons		Draft forward	12.8 m / 42 ft 1 in	
Deadweight	171310 tons		Draft forward extreme	12.8 m / 42 ft 1 in	
Capacity			Draft after	12.8 m / 42 ft 1 in	
Air draft	62.54 m / 205 ft 8 in		Draft after extreme	12.8 m / 42 ft 1 in	
Ship's Particulars					
Length overall	399 m	Type of bow	Bulbous		
Breadth	59 m	Type of stern	Transom		
Anchor(s) (No./types)	2 ( PortBow / StbdBow )				
No. of shackles	14 / 14	(1 shackle =27.5 m / 15 fathoms)			
Max. rate of heaving, m/min	15 / 15				
Steering characteristics					
Steering device(s) (type/No.)	Semisuspended / 2	Number of bow thrusters	2		
Maximum angle	35	Power	2500 kW / 2500 kW		
Rudder angle for neutral effect	0 degrees	Number of stern thrusters	N/A		
Hard over to over(2 pumps)	12 seconds	Power	N/A		
Flanking Rudder(s)	0	Auxiliary Steering Device(s)	N/A		
Stopping			Turning circle		
Description	Full Time	Head reach	Ordered Engine: 100%, Ordered rudder: 35 degrees		
FAH to FAS	1039 s	18.02 cbls	Advance	5.63 cbls	
HAH to HAS	1322.8 s	17.9 cbls	Transfer	2.06 cbls	
SAH to SAS	1761.7 s	17.83 cbls	Tactical diameter	5.34 cbls	
Main Engine(s)					
Type of Main Engine	Low speed diesel		Number of propellers	2	
Number of Main Engine(s)	2		Propeller rotation	Right/Left	
Maximum power per shaft	2 x 29680 kW		Propeller type	FPP	
Astern power	85 % ahead		Min. RPM	9.99	
Time limit astern	N/A		Emergency FAH to FAS	37.2 seconds	
Engine Telegraph Table					
Engine Order	Speed, knots	Engine power, kW	RPM	Pitch ratio	
"FSAH"	23.4	56392	70.6	1.04	
"FAH"	16.9	21258	51	1.04	
"HAH"	13.3	10256	40	1.04	
"SAH"	10	4327	30	1.04	
"DSA H"	6.7	1282	20	1.04	
"DSAS"	-3.4	3043	-20	1.04	
"SAS"	-5.1	10270	-30	1.04	
"HAS"	-6.8	24343	-40	1.04	
"FAS"	-8.6	50456	-51	1.04	
"FSAS"	-8.6	50456	-51	1.04	



**Container Triple E\_ 3.0.52.1 \* 49' Draft**

PILOT CARD				
Ship name	Container Triple E 49 3.0.52.1 *			Date
IMO Number	N/A	Call Sign	N/A	Year built
Load Condition	Loaded			
Displacement	240904.9 tons	Draft forward	14.94 m / 49 ft 1 in	
Deadweight	194153.4 tons	Draft forward extreme	14.94 m / 49 ft 1 in	
Capacity		Draft after	14.94 m / 49 ft 1 in	
Air draft	60.4 m / 198 ft 8 in	Draft after extreme	14.94 m / 49 ft 1 in	

Ship's Particulars			
Length overall	399 m	Type of bow	Bulbous
Breadth	59 m	Type of stern	Transom
Anchor(s) (No./types)	2 ( PortBow / StbdBow )		
No. of shackles	14 / 14		(1 shackle =27.5 m / 15 fathoms)
Max. rate of heaving, m/min	15 / 15		



Steering characteristics			
Steering device(s) (type/No.)	Semisuspended / 2	Number of bow thrusters	2
Maximum angle	35	Power	2500 kW / 2500 kW
Rudder angle for neutral effect	0 degrees	Number of stern thrusters	N/A
Hard over to over(2 pumps)	12 seconds	Power	N/A
Flanking Rudder(s)	0	Auxiliary Steering Device(s)	N/A

Stopping			Turning circle	
Description	Full Time	Head reach	Ordered Engine: 100%, Ordered rudder: 35 degrees	
FAH to FAS	1422.9 s	22.04 cbfs	Advance	5.23 cbfs
HAH to HAS	1811.2 s	21.94 cbfs	Transfer	1.75 cbfs
SAH to SAS	2414 s	21.87 cbfs	Tactical diameter	4.35 cbfs

Main Engine(s)			
Type of Main Engine	Low speed diesel	Number of propellers	2
Number of Main Engine(s)	2	Propeller rotation	Right/Left
Maximum power per shaft	2 x 29680 kW	Propeller type	FPP
Astern power	85 % ahead	Min. RPM	9.99
Time limit astern	N/A	Emergency FAH to FAS	37.2 seconds

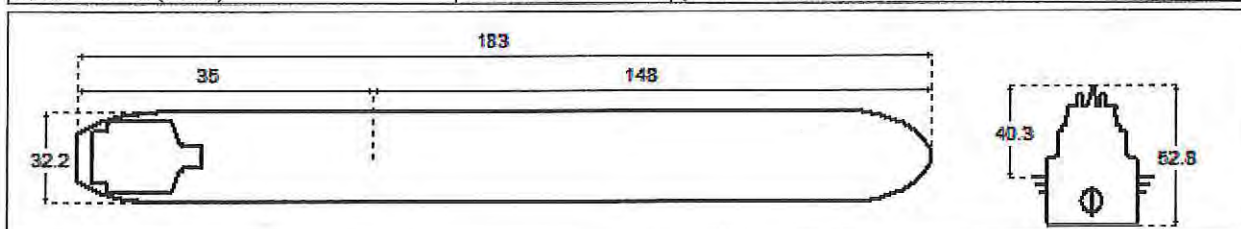
Engine Telegraph Table				
Engine Order	Speed, knots	Engine power, kW	RPM	Pitch ratio
"FSAH"	23	56392	70.6	1.04
"FAH"	16.6	21258	51	1.04
"HAH"	13	10256	40	1.04
"SAH"	9.8	4327	30	1.04
"DSAH"	6.5	1282	20	1.04
"DSAS"	-2.6	3043	-20	1.04
"SAS"	-3.8	10270	-30	1.04
"HAS"	-5.1	24343	-40	1.04
"FAS"	-6.5	50456	-51	1.04
"FSAS"	-6.5	50456	-51	1.04



**Tanker OH (Disp 57575t)\_CPP\_FL\_8 v03.17.VSY**

PILOT CARD				
Ship name	Tanker OH(Disp 57575t) CPP FL 8 v03.17.VSY			Date 01.09.16
IMO Number	N/A	Call Sign	N/A	Year built N/A
Load Condition	Full load			
Displacement	57575 tons	Draft forward	12.5 m / 41 ft 1 in	
Deadweight	49500 tons	Draft forward extreme	12.5 m / 41 ft 1 in	
Capacity		Draft after	12.5 m / 41 ft 1 in	
Air draft	40.34 m / 132 ft 8 in	Draft after extreme	12.5 m / 41 ft 1 in	

Ship's Particulars			
Length overall	183 m	Type of bow	Bulbous
Breadth	32.2 m	Type of stern	V-shaped
Anchor Chain(Port)	14 shackles		
Anchor Chain(Starboard)	9 shackles		
Anchor Chain(Stern)	4 shackles	(1 shackle =27.5 m / 15 fathoms)	



Steering characteristics			
Rudder(s) (type/No.)	Schilling rudder / 1	Number of bow thrusters	1
Maximum angle	35	Power	1550 kW
Rudder angle for neutral effect	1 degrees	Number of stern thrusters	N/A
Hard over to over(2 pumps)	26 seconds	Power	N/A
Flanking Rudder(s)		Auxiliary Steering Device(s)	

Stopping			Turning circle	
Description	Full Time	Head reach	Ordered Engine: 100%, Ordered rudder: 35 degrees	
FAH to FAS	390.5 s	7.89 cbls	Advance	3.25 cbls
HAH to HAS	305 s	3.66 cbls	Transfer	1.35 cbls
SAH to SAS	358.5 s	2.9 cbls	Tactical diameter	2.81 cbls

Main Engine(s)			
Type of Main Engine	Medium speed diesel	Number of propellers	1
Number of Main Engine(s)	1	Propeller rotation	Right
Maximum power per shaft	1 x 8647 kW	Propeller type	CPP
Astern power	50 % ahead	Min. RPM	87.2
Time limit astern	N/A	Emergency FAH to FAS	135 seconds

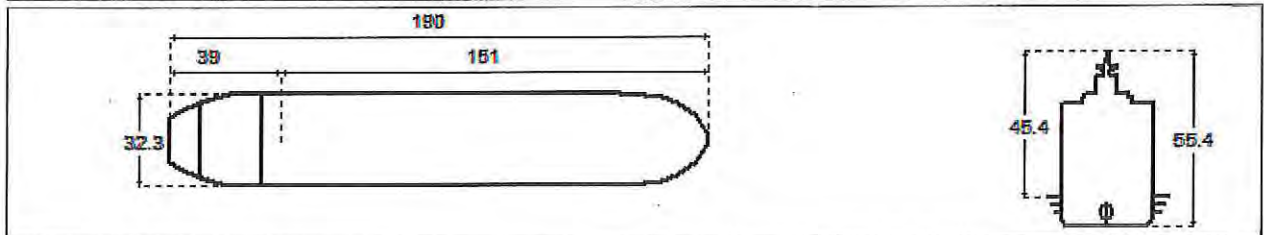
Engine Telegraph Table				
Engine order	Speed, knots	Engine power, kW	RPM	Pitch ratio
100 %	12	6200.3	120.01	1.15
80 %	12	6200.3	120.01	1.15
60 %	8.9	3200.1	120.01	0.81
40 %	6.3	1469.9	120	0.54
20 %	3.7	1199.9	120	0.34
-20 %	-2.3	1180	120.01	-0.18
-40 %	-3	1330	120.01	-0.28
-60 %	-4.1	2400.1	120.02	-0.42
-80 %	-4.7	4496.2	120.01	-0.56



**Tanker Memphis 3.0.26.0 \***

PILOT CARD				
Ship name	Tanker Memphis 3.0.26.0 *			Date 01.09.2016
IMO Number	N/A	Call Sign	N/A	Year built 2007
Load Condition	Partial Loaded 2			
Displacement	42000 tons	Draft forward	10 m / 32 ft 10 in	
Deadweight	32300 tons	Draft forward extreme	10 m / 32 ft 10 in	
Capacity		Draft after	10 m / 32 ft 10 in	
Air draft	45.4 m / 149 ft 4 in	Draft after extreme	10 m / 32 ft 10 in	

Ship's Particulars			
Length overall	190 m	Type of bow	Bulbous
Breadth	32.3 m	Type of stern	V-shaped
Anchor(s) (No./types)	2 ( PortBow / StbdBow )		
No. of shackles	14 / 14	(1 shackle =25 m / 13.7 fathoms)	
Max. rate of heaving, m/min	18 / 18		



Steering characteristics			
Steering device(s) (type/No.)	Semisuspended / 1	Number of bow thrusters	N/A
Maximum angle	35	Power	N/A
Rudder angle for neutral effect	0.22 degrees	Number of stern thrusters	N/A
Hard over to over(2 pumps)	20 seconds	Power	N/A
Flanking Rudder(s)	0	Auxiliary Steering Device(s)	N/A

Stopping			Turning circle	
Description	Full Time	Head reach	Ordered Engine: 100%, Ordered rudder: 35 degrees	
FAH to FAS	577.6 s	7.67 cbls	Advance	3.54 cbls
HAH to HAS	733.6 s	7.25 cbls	Transfer	1.67 cbls
SAH to SAS	1079.7 s	6.74 cbls	Tactical diameter	4.33 cbls

Main Engine(s)			
Type of Main Engine	Low speed diesel	Number of propellers	1
Number of Main Engine(s)	1	Propeller rotation	Right
Maximum power per shaft	1 x 9800 kW	Propeller type	FPP
Astern power	77.6 % ahead	Min. RPM	10
Time limit astern	N/A	Emergency FAH to FAS	35.2 seconds

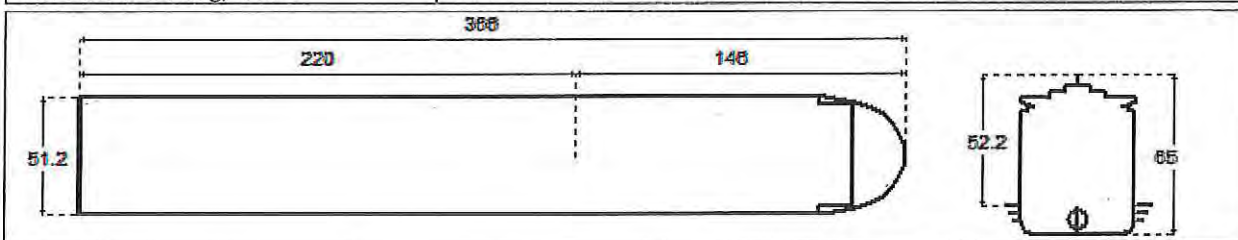
Engine Telegraph Table				
Engine Order	Speed, knots	Engine power, kW	RPM	Pitch ratio
"100%"	14.5	8330	90	0.74
"80%"	11.3	3919	70	0.74
"60%"	8.8	1901	55	0.74
"40%"	5.6	490	35	0.74
"20%"	3.2	91	20	0.74
"-20%"	-1.4	102	-19	0.74
"-40%"	-2.5	534	-33	0.74
"-60%"	-3.8	1857	-50	0.74
"-80%"	-4.9	4079	-65	0.74
"-100%"	-6	7605	-80	0.74



**Container Kalina\_NewYork 3.0.45.1 \* 42' Draft**

PILOT CARD					
Ship name	Container Kalina NewYork		3.0.46.1 *	Date	26.05.2016
IMO Number	N/A	Call Sign	N/A	Year built	1995
Load Condition	Partial Loaded 2				
Displacement	172769.22 tons		Draft forward	12.8 m / 42 ft 1 in	
Deadweight	135460 tons		Draft forward extreme	12.8 m / 42 ft 1 in	
Capacity			Draft after	12.8 m / 42 ft 1 in	
Air draft	52.2 m / 171 ft 8 in		Draft after extreme	12.8 m / 42 ft 1 in	

Ship's Particulars			
Length overall	366 m	Type of bow	Bulbous
Breadth	51.2 m	Type of stern	Transom
Anchor(s) (No./types)	2 ( PortBow / StbdBow )		
No. of shackles	14 / 14		(1 shackle =27.5 m / 15 fathoms)
Max. rate of heaving, m/min	15 / 15		



Steering characteristics			
Steering device(s) (type/No.)	Semisuspended / 1	Number of bow thrusters	2
Maximum angle	35	Power	1700 kW / 1700 kW
Rudder angle for neutral effect	0.2 degrees	Number of stern thrusters	N/A
Hard over to over(2 pumps)	21 seconds	Power	N/A
Flanking Rudder(s)	0	Auxiliary Steering Device(s)	N/A

Stopping			Turning circle	
Description	Full Time	Head reach	Ordered Engine: 100%, Ordered rudder: 35 degrees	
FAH to FAS	442.6 s	9.58 cbles	Advance	5.49 cbles
HAH to HAS	514.6 s	8.96 cbles	Transfer	2.08 cbles
SAH to SAS	619.6 s	9 cbles	Tactical diameter	5.1 cbles

Main Engine(s)			
Type of Main Engine	Low speed diesel	Number of propellers	1
Number of Main Engine(s)	1	Propeller rotation	Right
Maximum power per shaft	1 x 73340 kW	Propeller type	FPP
Astern power	82 % ahead	Min. RPM	21
Time limit astern	N/A	Emergency FAH to FAS	26.2 seconds

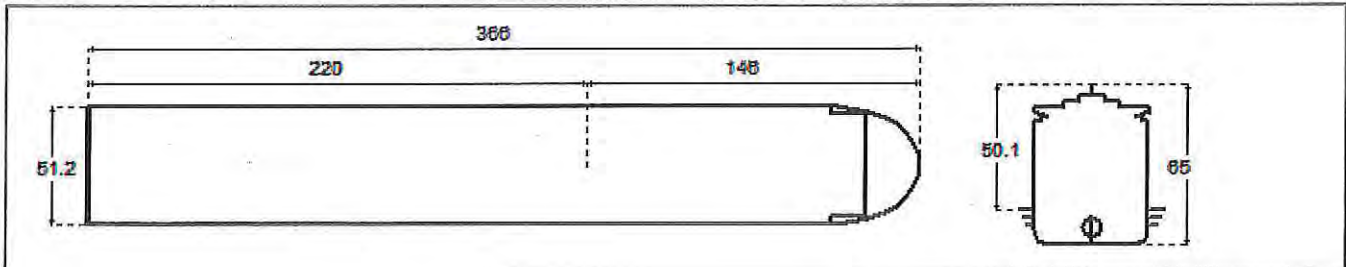
Engine Telegraph Table				
Engine Order	Speed, knots	Engine power, kW	RPM	Pitch ratio
"FSAH"	25.1	66723	100.7	1.03
"FAH"	17.6	23280	70.4	1.03
"HAH"	14.1	11337	55.4	1.03
"SAH"	11.8	6249	45.4	1.03
"DSAH"	7.9	1538	28.3	1.03
"DSAS"	-3.1	1856	-28	1.03
"SAS"	-5	7591	-45.1	1.03
"HAS"	-6.2	13810	-55.1	1.03
"FAS"	-7.3	22736	-65.1	1.03
"FSAS"	-9.9	60189	-90.2	1.03



**Container Kalina\_NewYork 3.0.46.1 \* 49' Draft**

PILOT CARD				
Ship name	Container Kalina NewYork 3.0.46.1 *			Date 26.05.2016
IMO Number	N/A	Call Sign	N/A	Year built 1995
Load Condition	Loaded			
Displacement	198160 tons	Draft forward	14.9 m / 49 ft 0 in	
Deadweight	135460 tons	Draft forward extreme	14.9 m / 49 ft 0 in	
Capacity		Draft after	14.9 m / 49 ft 0 in	
Air draft	50.1 m / 164 ft 9 in	Draft after extreme	14.9 m / 49 ft 0 in	

Ship's Particulars			
Length overall	366 m	Type of bow	Bulbous
Breadth	51.2 m	Type of stern	Transom
Anchor(s) (No./types)	2 ( PortBow / StbdBow )		
No. of shackles	14 / 14	(1 shackle =27.5 m / 15 fathoms)	
Max. rate of heaving, m/min	15 / 15		



Steering characteristics			
Steering device(s) (type/No.)	Semisuspended / 1	Number of bow thrusters	2
Maximum angle	35	Power	1700 kW / 1700 kW
Rudder angle for neutral effect	0.2 degrees	Number of stern thrusters	N/A
Hard over to over(2 pumps)	21 seconds	Power	N/A
Flanking Rudder(s)	0	Auxiliary Steering Device(s)	N/A

Stopping			Turning circle	
Description	Full Time	Head reach	Ordered Engine: 100%, Ordered rudder: 35 degrees	
FAH to FAS	475.6 s	9.97 cbles	Advance	5.6 cbles
HAH to HAS	555.6 s	9.39 cbles	Transfer	2.07 cbles
SAH to SAS	668.6 s	9.44 cbles	Tactical diameter	5.11 cbles

Main Engine(s)			
Type of Main Engine	Low speed diesel	Number of propellers	1
Number of Main Engine(s)	1	Propeller rotation	Right
Maximum power per shaft	1 x 73340 kW	Propeller type	FPP
Astern power	82 % ahead	Min. RPM	21
Time limit astern	N/A	Emergency FAH to FAS	26.2 seconds

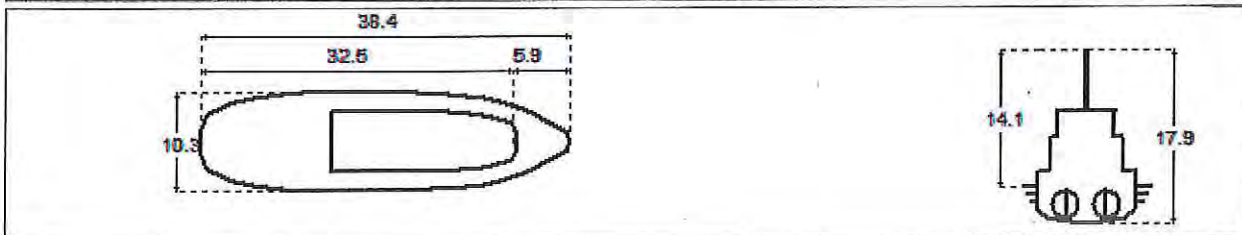
Engine Telegraph Table				
Engine Order	Speed, knots	Engine power, kW	RPM	Pitch ratio
"FSAH"	23.7	67444	99.9	1.03
"FAH"	16.8	23214	70	1.03
"HAH"	13.6	11310	55.1	1.03
"SAH"	11.4	6236	45.2	1.03
"DSAH"	7.6	1536	28.2	1.03
"DSAS"	-3	1855	-28	1.03
"SAS"	-4.8	7585	-45	1.03
"HAS"	-5.8	13797	-55	1.03
"FAS"	-6.9	22712	-65	1.03
"FSAS"	-9.3	60143	-90	1.03



**Conventional Twin Screw Tug 4 (bp 46.3t) TRANSAS 2.31.17.0 \***

PILOT CARD			
Ship name	Conventional twin screw tug 4 (bp 46.3t) TRANSAS 2.31.17.0 *		Date 06.06.2013
IMO Number	N/A	Call Sign	N/A
Load Condition	Full load		
Displacement	686 tons	Draft forward	3.8 m / 12 ft 6 in
Deadweight	N/A tons	Draft forward extreme	3.8 m / 12 ft 6 in
Capacity		Draft after	3.8 m / 12 ft 6 in
Air draft	14.11 m / 46 ft 4 in	Draft after extreme	3.8 m / 12 ft 6 in

Ship's Particulars			
Length overall	38.43 m	Type of bow	-
Breadth	10.37 m	Type of stern	Transom
Anchor(s) (No./types)	1 ( StbdBow )		
No. of shackles	9	(1 shackle =27.4 m / 15 fathoms)	
Max. rate of heaving, m/min	30		



Steering characteristics			
Steering device(s) (type/No.)	Suspended / 2	Number of bow thrusters	N/A
Maximum angle	35	Power	N/A
Rudder angle for neutral effect	0 degrees	Number of stern thrusters	N/A
Hard over to over(2 pumps)	7 seconds	Power	N/A
Flanking Rudder(s)	0	Auxiliary Steering Device(s)	N/A

Stopping			Turning circle	
Description	Full Time	Head reach	Ordered Engine: 100%, Ordered rudder: 35 degrees	
FAH to FAS	28.25 s	0.51 cbles	Advance	0.51 cbles
HAH to HAS	25.25 s	0.39 cbles	Transfer	0.18 cbles
SAH to SAS	24.25 s	0.27 cbles	Tactical diameter	0.46 cbles

Main Engine(s)			
Type of Main Engine	High speed diesel	Number of propellers	2
Number of Main Engine(s)	2	Propeller rotation	Inward
Maximum power per shaft	2 x 1840 kW	Propeller type	FPP
Astern power	80 % ahead	Min. RPM	5.83
Time limit astern	N/A	Emergency FAH to FAS	5.15 seconds

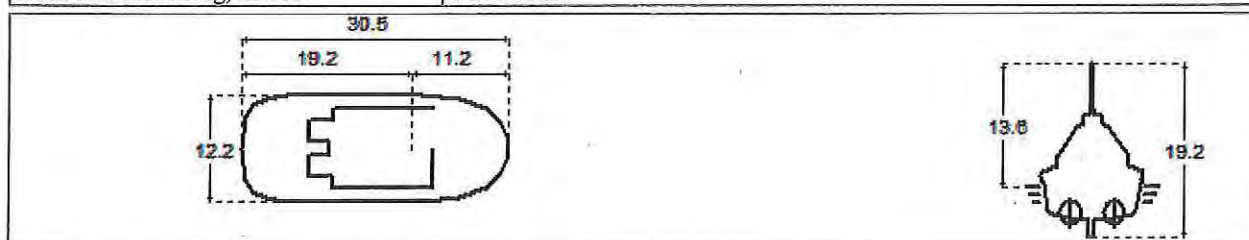
Engine Telegraph Table				
Engine order	Speed, knots	Engine power, kW	RPM	Pitch ratio
"FSAH"	13.2	3652	252	0.64
"FAH"	11.8	2389	219.1	0.64
"HAH"	10.3	1455	185.9	0.64
"SAH"	8.6	792	151.4	0.64
"DSAH"	6.8	397	119.3	0.64
"DSAS"	-3.6	739	-110.8	0.64
"SAS"	-4.2	1083	-126	0.64
"HAS"	-4.8	1595	-143.9	0.64
"FAS"	-5.4	2207	-160.6	0.64
"FSAS"	-5.9	2920	-176.3	0.64



**Tug Brian McAllister (85t bp) 3.0.57.1 \***

PILOT CARD				
Ship name	Tug Brian McAllister (85tbp) 3.0.57.1 *			Date 22.06.2016
IMO Number	N/A	Call Sign	N/A	Year built N/A
Load Condition	Full Load			
Displacement	763 tons	Draft forward	5.6 m / 18 ft 5 in	
Deadweight	343.35 tons	Draft forward extreme	5.6 m / 18 ft 5 in	
Capacity		Draft after	5.6 m / 18 ft 5 in	
Air draft	13.6 m / 44 ft 8 in	Draft after extreme	5.6 m / 18 ft 5 in	

Ship's Particulars			
Length overall	30.5 m	Type of bow	-
Breadth	12.2 m	Type of stern	U-shaped
Anchor(s) (No./types)	2 ( PortBow / StbdBow )		
No. of shackles	11 / 11		(1 shackle =25 m / 13.7 fathoms)
Max. rate of heaving, m/min	10.2 / 10.2		



Steering characteristics			
Steering device(s) (type/No.)	Z-Drive / 2	Number of bow thrusters	N/A
Maximum angle	180	Power	N/A
Rudder angle for neutral effect	0 degrees	Number of stern thrusters	N/A
Hard over to over(2 pumps)	2 seconds	Power	N/A
Flanking Rudder(s)	0	Auxiliary Steering Device(s)	N/A

Stopping			Turning circle	
Description	Full Time	Head reach	Ordered Engine: 100%, Ordered rudder: 35 degrees	
FAH to FAS	10.7 s	0.16 cbles	Advance	0.21 cbles
HAH to HAS	11.8 s	0.15 cbles	Transfer	0.06 cbles
SAH to SAS	12.9 s	0.13 cbles	Tactical diameter	0.16 cbles

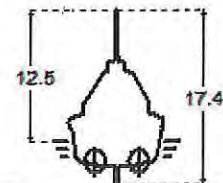
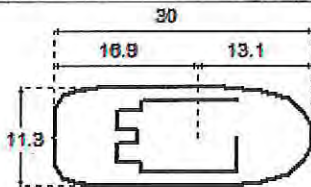
Main Engine(s)			
Type of Main Engine	High speed diesel	Number of propellers	2
Number of Main Engine(s)	2	Propeller rotation	Right/Left
Maximum power per shaft	2 x 2524 kW	Propeller type	Azimuth FPP
Astern power	0 % ahead	Min. RPM	84.86
Time limit astern	N/A	Emergency FAH to FAS	11.9 seconds

Engine Telegraph Table				
Engine Order	Speed, knots	Engine power, kW	RPM	Pitch ratio
"100%"	11.9	4226	235	1
"90%"	9.8	2446	195.8	1
"80%"	9.1	1988	182.8	1
"70%"	8.4	1592	169.7	1
"60%"	7.8	1252	156.7	1
"50%"	7.2	965	143.6	1
"40%"	6.5	725	130.6	1
"30%"	5.8	528	117.5	1
"20%"	4.6	249	91.4	1
"10%"	4.2	199	84.9	1

**Tug Edward Moran 3.0.63.0 \***

PILOT CARD				
Ship name	Tug Edward Moran 3.0.63.0 *			Date 21.06.2016
IMO Number	N/A	Call Sign	N/A	Year built N/A
Load Condition	Full Load			
Displacement	442.69 tons	Draft forward	4.88 m / 16 ft 0 in	
Deadweight	105 tons	Draft forward extreme	4.88 m / 16 ft 0 in	
Capacity		Draft after	4.88 m / 16 ft 0 in	
Air draft	12.52 m / 41 ft 2 in	Draft after extreme	4.88 m / 16 ft 0 in	

Ship's Particulars			
Length overall	30 m	Type of bow	-
Breadth	11.3 m	Type of stern	U-shaped
Anchor(s) (No./types)	2 ( PortBow / StbdBow )		
No. of shackles	11 / 11		(1 shackle =25 m / 13.7 fathoms)
Max. rate of heaving, m/min	10.2 / 10.2		



Steering characteristics				
Steering device(s) (type/No.)	Z-Drive / 2	Number of bow thrusters	N/A	
Maximum angle	180	Power	N/A	
Rudder angle for neutral effect	-1.67 degrees	Number of stern thrusters	N/A	
Hard over to over(2 pumps)	6 seconds	Power	N/A	
Flanking Rudder(s)	0	Auxiliary Steering Device(s)	N/A	

Stopping			Turning circle	
Description	Full Time	Head reach	Ordered Engine: 100%, Ordered rudder: 35 degrees	
FAH to FAS	10.7 s	0.2 cbles	Advance	0.22 cbles
HAH to HAS	10.7 s	0.18 cbles	Transfer	0.11 cbles
SAH to SAS	10.7 s	0.17 cbles	Tactical diameter	0.2 cbles

Main Engine(s)				
Type of Main Engine	High speed-diesel	Number of propellers	2	
Number of Main Engine(s)	2	Propeller rotation	Left/Right	
Maximum power per shaft	2 x 2424.5 kW	Propeller type	Azimuth FPP	
Astern power	0 % ahead	Min. RPM	84.86	
Time limit astern	N/A	Emergency FAH to FAS	15.6 seconds	

Engine Telegraph Table				
Engine Order	Speed, knots	Engine power, kW	RPM	Pitch ratio
"100%"	12.5	4607	235	1
"90%"	12.5	3548	215.4	1
"80%"	11.7	2774	198.5	1
"70%"	10.8	2167	182.8	1
"60%"	10.1	1735	169.7	1
"50%"	9.7	1365	156.7	1
"40%"	9.2	1201	150.1	1
"30%"	8.1	790	130.6	1
"20%"	6.7	404	104.5	1
"10%"	5.6	217	84.9	1



**APPENDIX B: Container Kalina and Container Triple E Swept Path Calculations**

<b>Table 5: Swept Path: Kalina (meters)</b>				
<b>Bearing</b>	<b>Length</b>	<b>Width</b>	<b>Total Swept Width</b>	<b>Percentage of Beam</b>
1	366	51.2	57.58	112.46%
2	366	51.2	63.94	124.89%
3	366	51.2	70.28	137.27%
4	366	51.2	76.61	149.62%
5	366	51.2	82.90	161.92%
6	366	51.2	89.18	174.17%
7	366	51.2	95.42	186.37%
8	366	51.2	101.64	198.51%
9	366	51.2	107.82	210.60%
10	366	51.2	113.98	222.61%
11	366	51.2	120.10	234.56%
12	366	51.2	126.18	246.44%

<b>Table 6: Swept Path: Container Triple E (meters)</b>				
<b>Bearing</b>	<b>Length</b>	<b>Width</b>	<b>Total Swept Width</b>	<b>Percentage of Beam</b>
1	399	59	65.95	111.79%
2	399	59	72.89	123.54%
3	399	59	79.80	135.26%
4	399	59	86.69	146.93%
5	399	59	93.55	158.56%
6	399	59	100.38	170.14%
7	399	59	107.19	181.67%
8	399	59	113.96	193.15%
9	399	59	120.69	204.56%
10	399	59	127.39	215.91%
11	399	59	134.05	227.20%
12	399	59	140.67	238.42%



APPENDIX C: Description of Water Current Model Development by Waterway Simulation Technology

MEMORANDUM FOR: Glen Paine, Maritime Institute of Technology & Graduate Studies

SUBJECT: Navigation Channel Deepening in New York/New Jersey Harbor

The purpose of this memorandum is to provide a summary of the development of the numerical model currents developed for use by MITAGS in navigation analysis of various channels in the New York/New Jersey Harbor.

The numerical model used for the development of these currents was the current Adaptive Hydraulics (ADH) model being applied to the ongoing *Shoaling Associated with Navigation Channel Deepening in New York/New Jersey Harbor Study*. The current model for the NY/NJ area was developed by hydraulic engineers at the U.S. Army Engineers Engineering Research and Development Center (ERDC) in Vicksburg, Mississippi.

The model was developed for project deepened conditions with a 50-ft depth for the navigation channels.

The numerical model simulation from which the data were extracted was the depth-averaged version of the study model. Therefore, the reported data are depth-averaged current velocities.

The numerical model resolution with bathymetric contours is shown in Figure 1 for the harbor area. Also shown in Figure 1 are the zones within which hydrodynamic data were extracted.

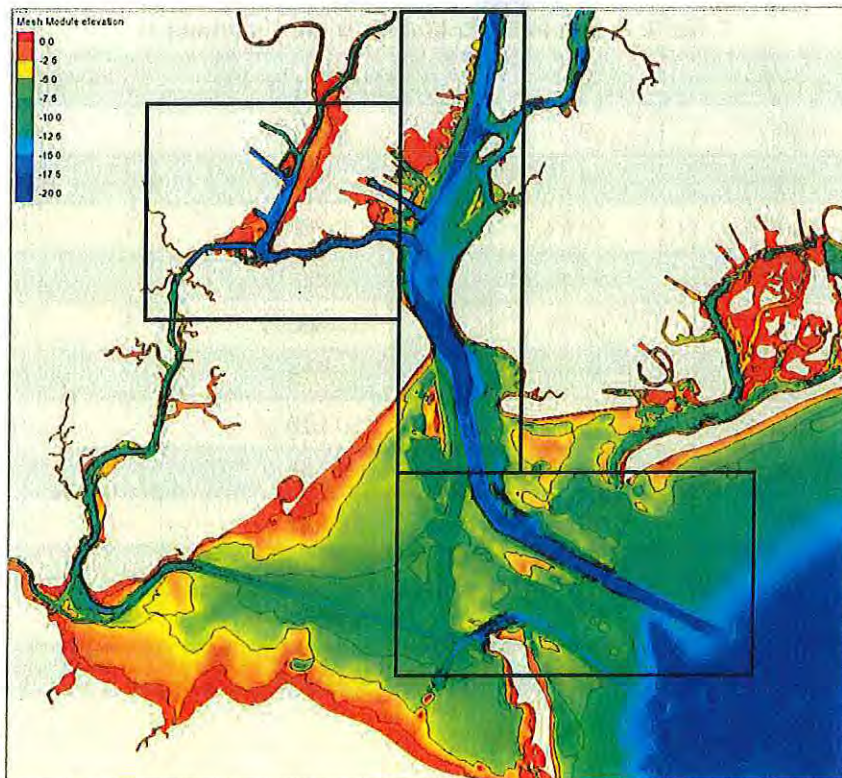


Figure 1. Numerical model bathymetric resolution and the extract windows for hydrodynamic data.

Details of tidal conditions and Hudson River discharge between hours 2000 (8AM 24 March) and 3500 (8PM 25 May) are presented in Figures 2 & 3. Two periods when data were extracted are highlighted in the figure. The two periods for extraction were 2352-2376 (8 April) and 3120-3144 (10 May). These two periods were selected because the first had full spring tides with a relatively low flow on the Hudson River of around 200 cms (7000 cfs). The second period was just following a spring tide with higher flows on the Hudson River, having just peaked on the previous day at 1453 cms (51300 cfs).

Current velocity patterns for the two periods are shown in Figures 4 through 9 for areas around the navigation channels.

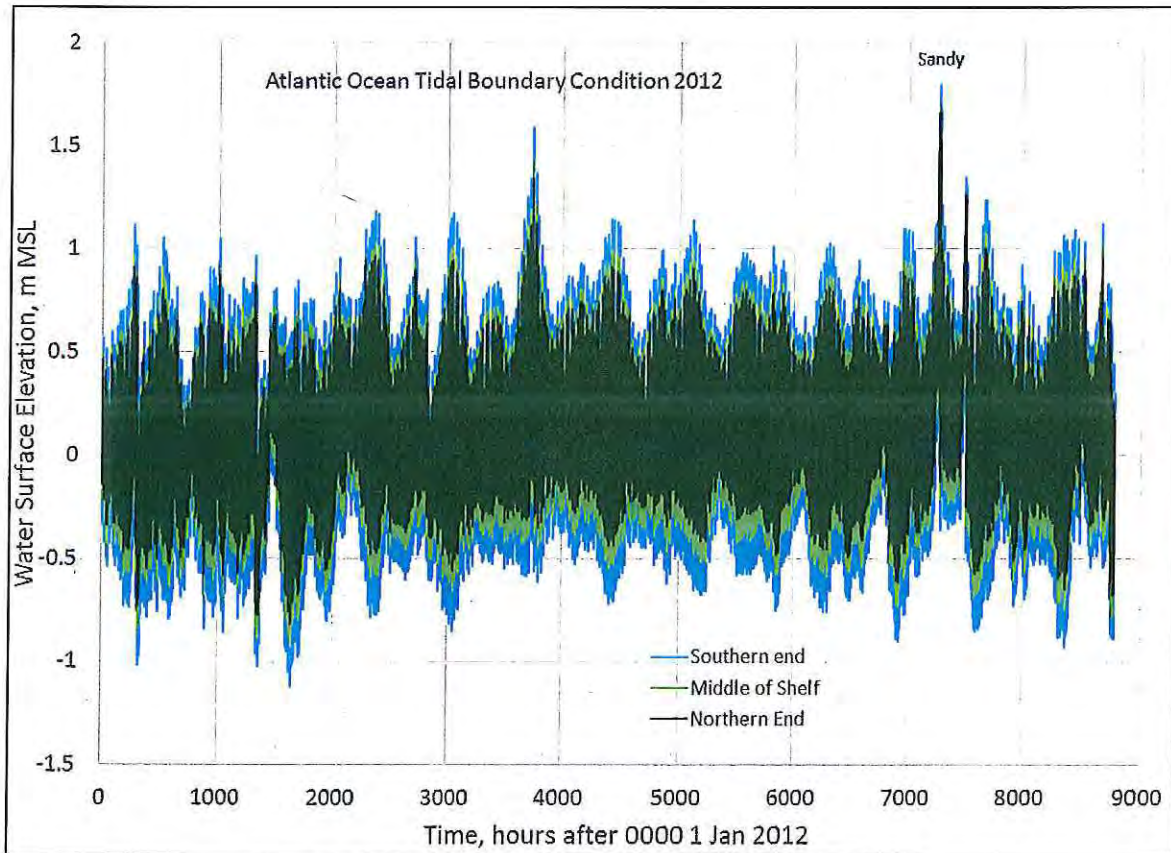


Figure 2. Tidal boundary conditions for the 2012 simulation.



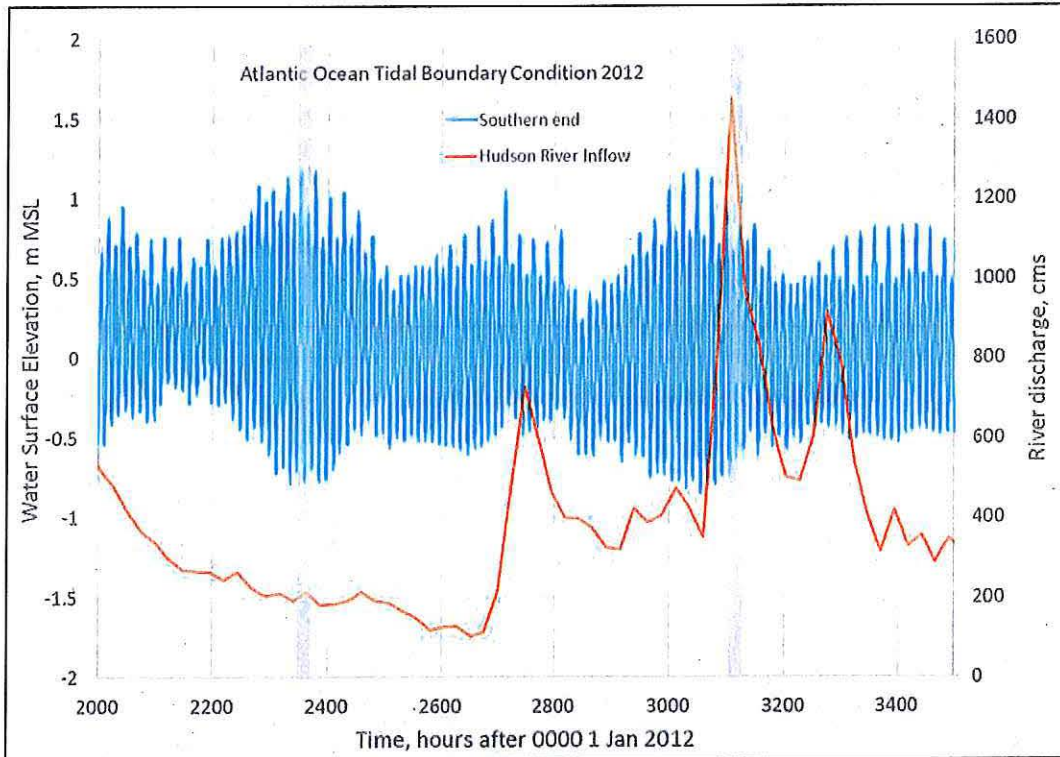


Figure 3. Details of tidal conditions and Hudson River discharge. The two periods when data were extracted are highlighted in the figure.

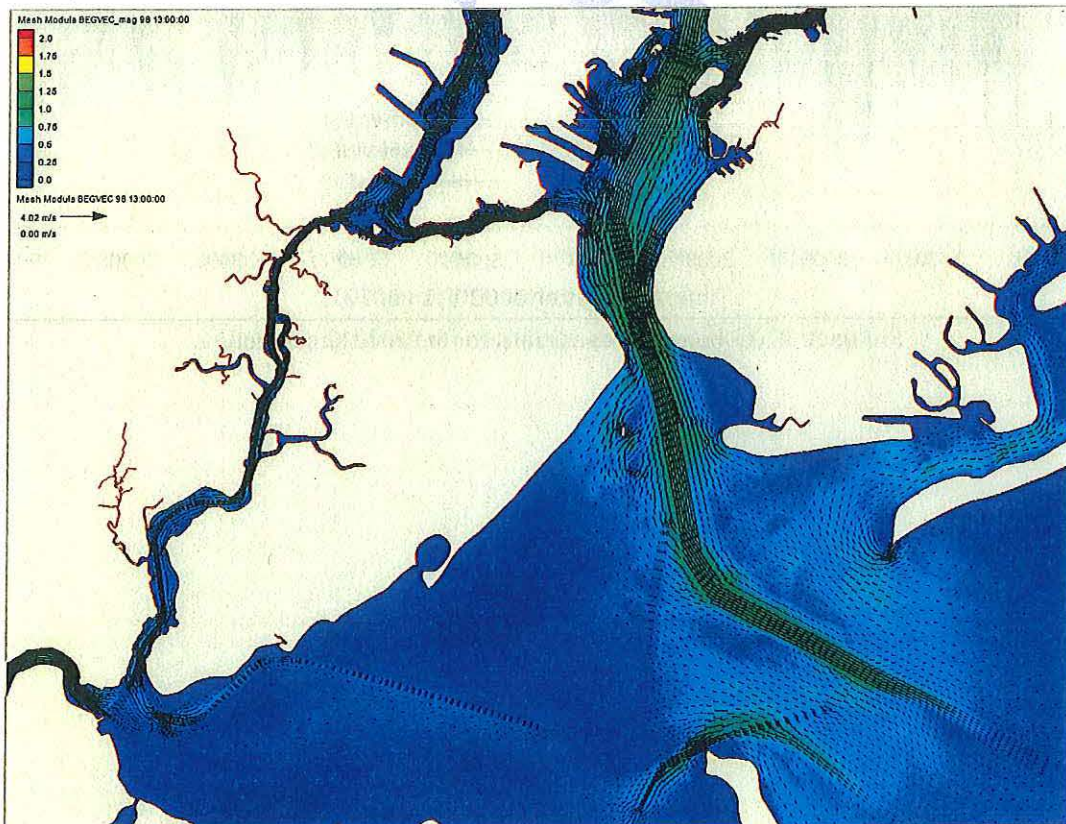


Figure 4. Flood currents over the navigation channel for time period 1, with low river flows



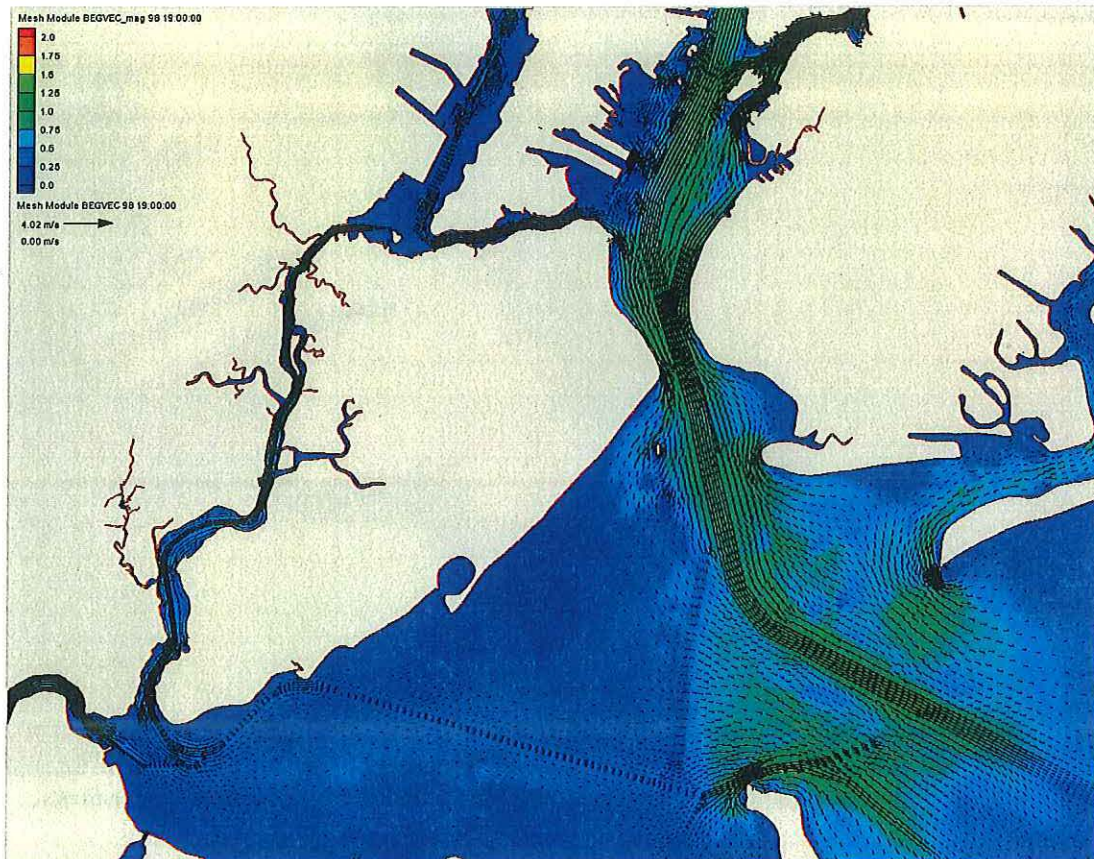


Figure 5. Ebb currents over the navigation channel for time period 1, with low river flows

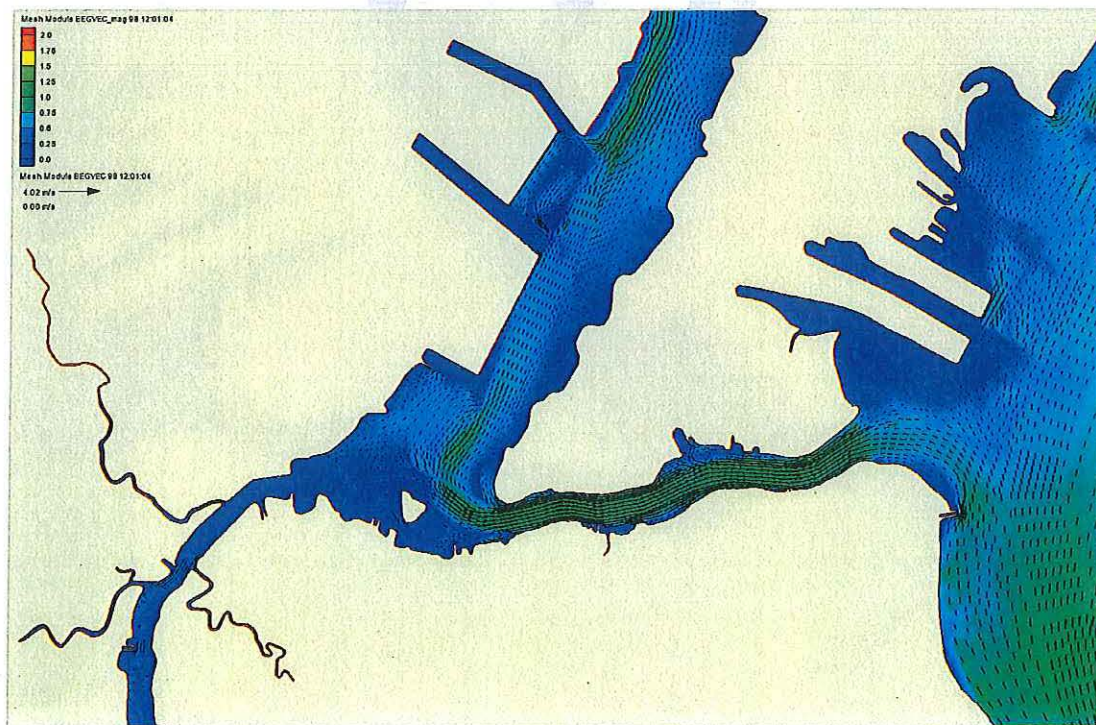


Figure 6. Flood currents in the inner navigation channel for time period 1, with low river flows



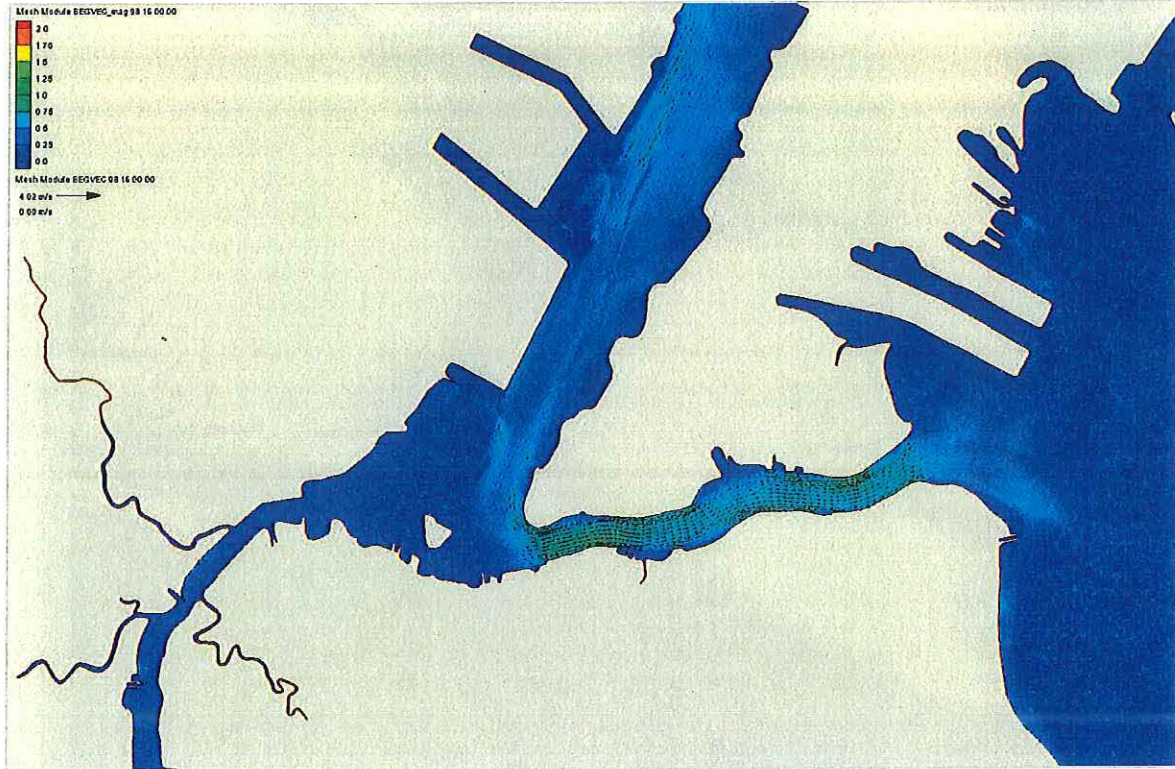


Figure 7. Ebb currents over the inner navigation channels for time period 1, with low river flows

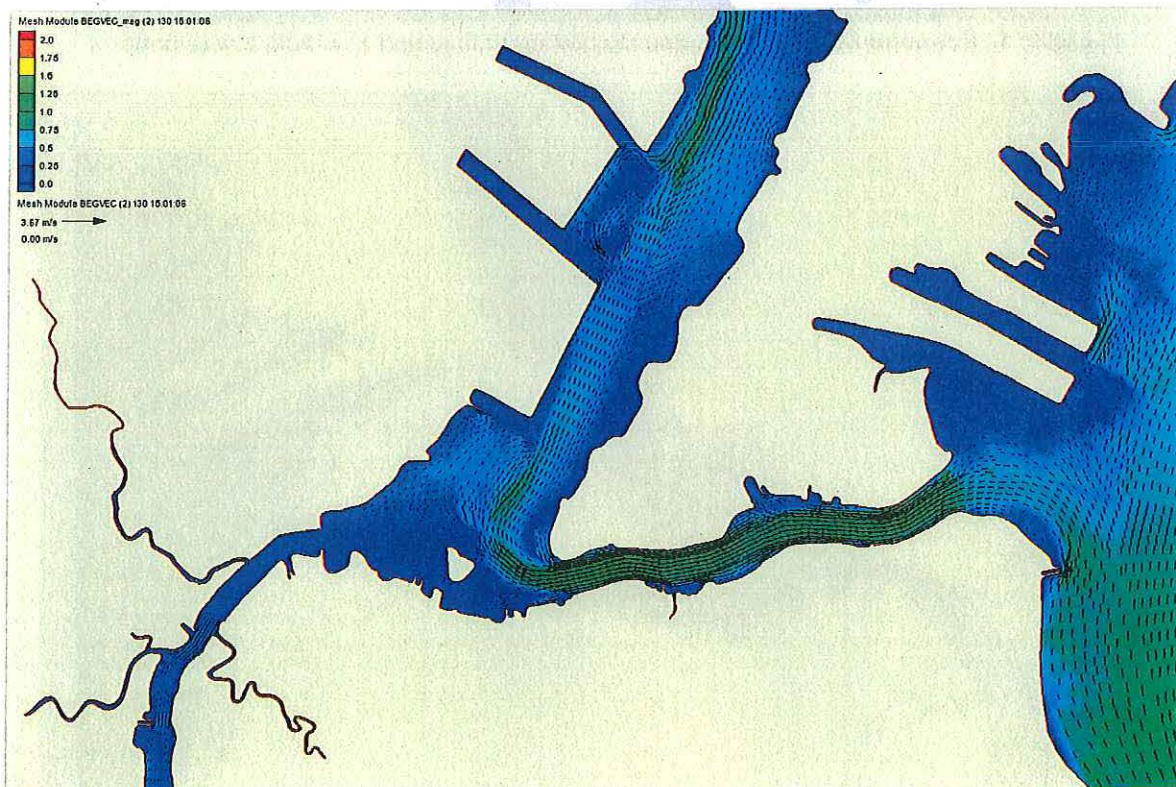


Figure 8. Flood currents over the inner navigation channel for time period 2, with high river flows



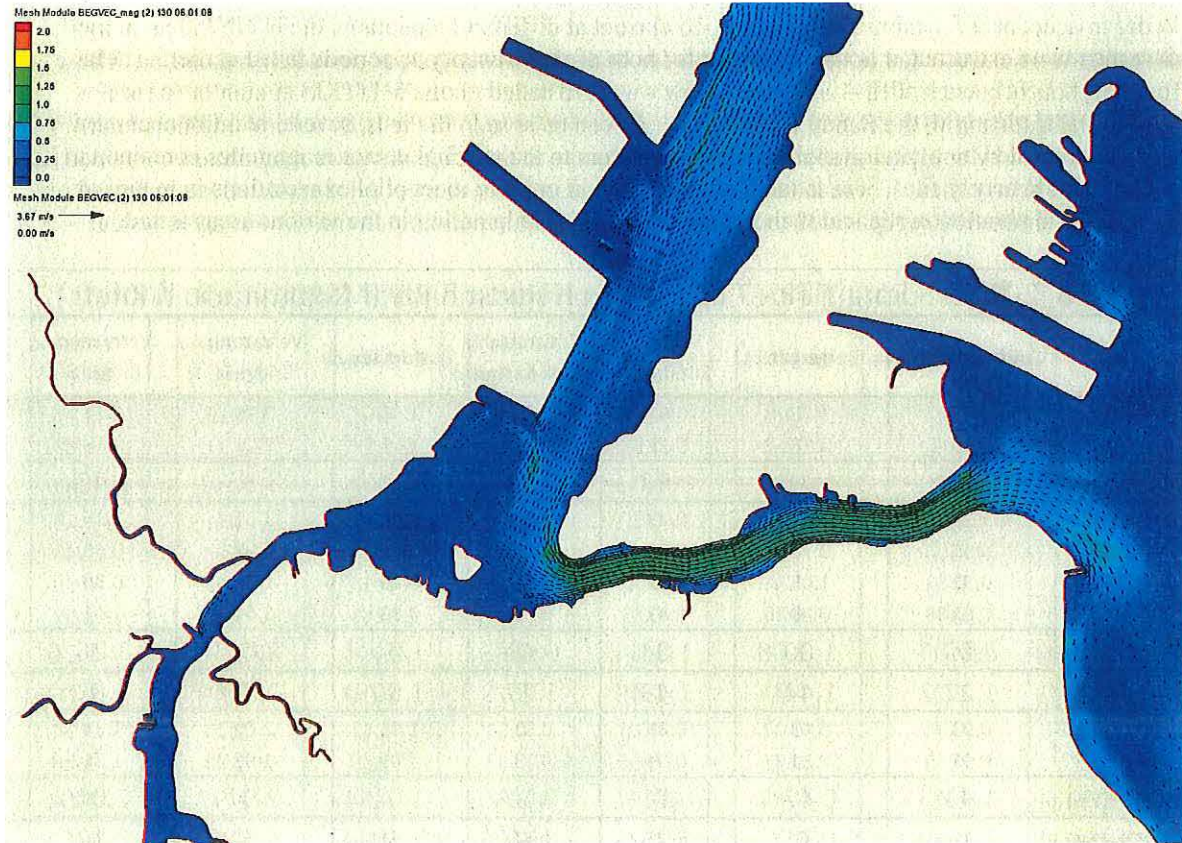


Figure 9. Ebb currents over the inner navigation channel for time period 2, with high river flows

In order to account for maximum ebb and flood current at different locations in the NY/NJ area, model data results were extracted at hourly intervals for both of the twenty-four periods listed earlier. These forty-eight hourly current files – tabulated below - were installed on the MITAGS simulator for use during initial testing with the Sandy Hook pilots. As can be seen in the lists, several additional current files were created by applying global multiplying factors to the original vector magnitudes contained in the individual hourly files. These latter files were used in order to meet pilot expectations in regard to how well the simulation replicated their experiences with ship handling in the various areas tested.

April 8, 2012 - Spring Tide - 7,062 cfs on Hudson River (Magnitude in Knots)							
File	Goethals Bridge	Bergen Pt.	Port Elizabeth	Constable Hook Range	Port Jersey	Verrazano Bridge N	Verrazano Bridge S
NY-2352	0.97	1.78	0.62	0.95	1.03	2.19	1.77
NY-2353	1.40	1.18	0.52	0.62	1.14	2.21	1.63
NY-2353(1.5)	2.10	1.77	0.83	0.93	1.71	3.32	2.45
NY-2354	1.24	0.31	0.29	0.10	0.95	1.51	1.16
NY-2355	0.58	0.70	0.14	0.62	0.45	0.27	0.45
NY-2356	0.31	1.05	0.72	0.76	0.19	1.01	0.39
NY-2357	0.68	0.80	0.83	0.78	0.83	1.61	1.01
NY-2357(1.25)	0.85	1.00	1.04	0.98	1.04	2.01	1.26
NY-2357(1.8)	1.22	1.44	1.49	1.75	1.50	2.90	1.82
NY-2358	0.93	0.43	0.66	0.52	1.01	2.00	1.34
NY-2359	0.95	0.31	0.54	0.33	1.09	1.98	1.36
NY-2359(1.5)	1.43	0.47	0.81	0.50	1.64	2.97	2.04
NY-2359(2.3)	2.19	0.71	1.25	0.76	2.50	4.55	3.12
NY-2360	0.91	0.23	0.50	0.31	0.97	1.69	1.16
NY-2361	0.87	0.10	0.35	0.12	0.74	1.09	0.78
NY-2362	0.74	0.78	0.04	0.49	0.37	0.12	0.14
NY-2363	0.31	1.86	0.33	0.91	0.23	1.34	0.99
NY-2364	0.35	2.15	0.60	1.05	0.80	1.94	1.55
NY-2365	1.18	1.73	0.60	0.83	1.01	2.08	1.63
NY-2366	1.26	0.43	0.25	0.08	0.91	1.53	1.28
NY-2367	0.52	0.43	0.17	0.49	0.58	0.70	0.70
NY-2368	0.23	0.80	0.52	0.58	0.17	0.19	0.17
NY-2369	0.43	0.50	0.54	0.47	0.43	1.16	0.47
NY-2370	0.72	0.43	0.50	0.54	0.89	1.73	1.18
NY-2371	0.91	0.45	0.56	0.52	1.03	2.02	1.38
NY-2372	0.99	0.41	0.60	0.41	0.99	1.77	1.24
NY-2373	1.01	0.19	0.37	0.10	0.70	0.91	0.64
NY-2374	0.64	1.28	0.12	0.70	0.33	0.19	0.14
NY-2375	0.04	1.63	0.39	0.74	0.16	1.09	0.81
Flood Tide							
Ebb Tide							



**May 10, 2012 - After Spring Tide - 51,300 cfs on Hudson River (Magnitude in Knots)**

File	Goethals Bridge	Bergen Pt.	Port Elizabeth	Constable Hook Range	Port Jersey	Verrazano Bridge N	Verrazano Bridge S
NY-3120	0.31	1.28	0.29	0.60	0.08	0.50	0.29
NY-3121	0.16	1.44	0.39	0.70	0.39	1.26	0.91
NY-3122	0.54	1.57	0.50	0.85	0.81	1.73	1.40
NY-3123	1.03	1.36	0.49	0.76	1.01	1.98	1.59
NY-3124	1.18	0.60	0.31	0.23	0.97	1.67	1.26
NY-3125	0.78	0.54	0.04	0.43	0.58	0.62	0.60
NY-3126	0.12	1.03	0.58	0.70	0.00	0.70	0.21
<b>NY-3126(1.25)</b>	<b>0.15</b>	<b>1.29</b>	<b>0.73</b>	<b>0.88</b>	<b>0.00</b>	<b>0.88</b>	<b>0.26</b>
NY-3127	0.60	0.76	0.80	0.70	0.64	1.46	0.85
NY-3128	0.87	0.35	0.62	0.52	0.91	1.77	1.14
NY-3129	0.95	0.10	0.47	0.27	0.99	1.78	1.20
NY-3130	0.89	0.04	0.37	0.19	0.93	1.59	1.09
NY-3131	0.85	0.12	0.25	0.06	0.74	1.16	0.83
NY-3132	0.68	0.37	0.08	0.19	0.50	0.64	0.49
NY-3133	0.47	0.76	0.10	0.45	0.14	0.23	0.16
NY-3134	0.12	1.67	0.37	0.85	0.43	1.46	1.09
NY-3135	0.49	2.04	0.62	1.05	0.89	2.00	1.61
<b>NY-3135(1.25)</b>	<b>0.61</b>	<b>2.55</b>	<b>0.78</b>	<b>1.31</b>	<b>1.11</b>	<b>2.50</b>	<b>2.01</b>
<b>NY-3135(1.5)</b>	<b>0.74</b>	<b>3.80</b>	<b>0.93</b>	<b>1.60</b>	<b>1.34</b>	<b>3.00</b>	<b>2.42</b>
NY-3136	1.38	1.32	0.54	0.66	0.97	1.80	1.47
NY-3137	1.13	0.37	0.04	0.45	0.62	0.70	0.76
NY-3138	0.31	1.09	0.70	0.58	0.12	0.35	0.21
NY-3139	0.74	0.50	0.74	0.41	0.29	0.95	0.14
NY-3140	0.72	0.16	0.37	0.21	0.64	1.09	0.66
NY-3141	0.72	0.06	0.31	0.25	0.87	1.63	1.13
NY-3142	0.91	0.16	0.43	0.37	0.95	1.75	1.16
NY-3143	1.01	0.19	0.49	0.25	0.76	1.28	0.89
		Flood Tide					
		Ebb Tide					



## APPENDIX D: Introduction to MITAGS and PMI

The Maritime Institute of Technology and Graduate Studies (MITAGS) and the Pacific Maritime Institutes (PMI) are non-profit, continuing education centers for professional mariners. The Institutes provide training for both civilian and military mariners at every level of their career.

### MITAGS Location and General Facility Description

MITAGS is located less than five (5) miles from the Baltimore-Washington International Thurgood Marshall Airport (BWI). Complimentary shuttle links the campus with the airport, BWI Amtrak Rail, Baltimore Light Rail, and regional bus services. It is also near major tourist destinations; including Baltimore, Annapolis, and Washington, DC.



The MITAGS campus encompasses over forty (40) acres. The 300,000 square-foot facilities include:

- ◆ On campus hotel with 232 hotel rooms (3-STAR equivalent). Hotel and conference facilities approved by the International Association of Conference Centers (IACC).
- ◆ 500-seat dining facility, 250-seat auditorium, pub, and store.
- ◆ Indoor swimming pool, Jogging / walking trails, Nautilus® Fitness Room.
- ◆ Maritime Museum.
- ◆ ECDIS, Stability, LNG Cargo and Engine Room Training Software.
- ◆ Emergency Medical Lab.
- ◆ 16-station networked computer Lab.
- ◆ Two, 360° Transas Full-Mission Shiphandling Simulator integrated with a 120° Bridge Tug and a 300° Bridge Tug Simulators.
- ◆ 8-Ship Radar, Automatic Radar Plotting Aids (ARPA), and Electronic Chart Display and Information Systems (ECDIS) Simulators.
- ◆ Global Maritime Distress and Safety Systems (GMDSS) Communications Lab.
- ◆ Vessel Traffic System (VTS) Watchstander Training Lab.



### PMI Location and General Facility Description

The Pacific Maritime Institute (PMI) is a subsidiary of MITAGS in Seattle, Washington. PMI is located approximately twenty (20) minutes from Seattle Tacoma (SEA-TAC) International Airport. Their waterfront facility is positioned directly within the Maritime Technology and Career Center. PMI offers the following onsite technology and training support facilities:

- ◆ 240° DNV Class A Full-Mission Bridge Simulator.
- ◆ Two 300° Full-Mission Tugboat Simulator.
- ◆ 6-Radar/Automatic Radar Plotting Aids (ARPA) Simulators.
- ◆ Two Electronic Chart Display and Information Systems (ECDIS)/Electronic Navigation Labs.
- ◆ Global Maritime Distress and Safety Systems (GMDSS) Communications Lab.
- ◆ 2-Simulation Debriefing Rooms and 12 conference / classrooms.
- ◆ Complimentary parking.





MITAGS DNV Class A Full-Mission Ship Simulator #1 (Bridge for Phase I and II Tests)

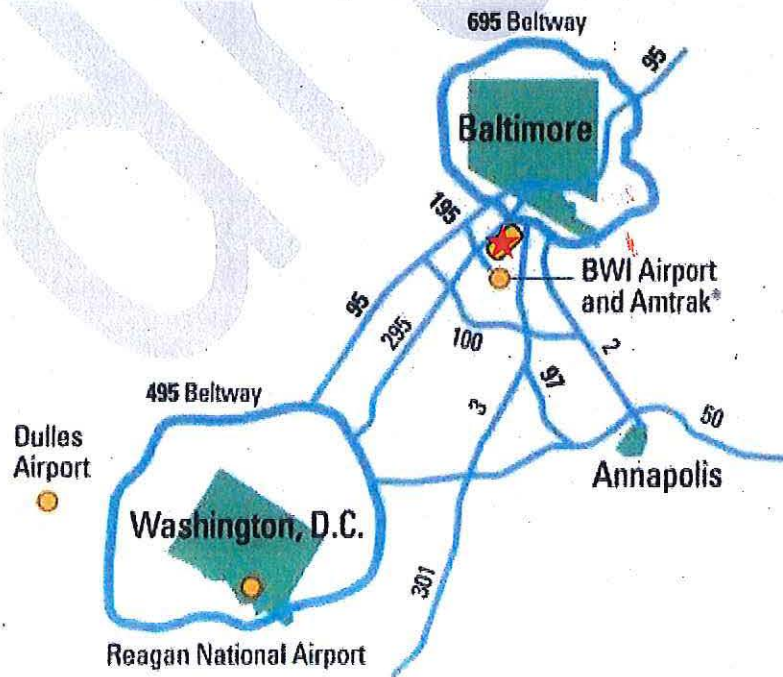


MITAGS Tug Bridge Simulator (Bridge for Phase I and II Tests)





Aerial Photograph of MITAGS Campus and Location Diagram





THIS PAGE INTENTIONALLY  
LEFT BLANK

## ATTACHMENT 6

### RELATIVE SEA LEVEL CHANGE TABLES

HDCI

8518750, The Battery, NY

NOAA's 2006 Published Rate: 0.00909 feet/yr

All values are expressed in feet relative to NAVD88

Year	USACE Low	USACE Int	USACE High	Year	USACE Low	USACE Int	USACE High
1992	-0.21	-0.21	-0.21	2065	0.45	0.93	2.43
1993	-0.2	-0.2	-0.2	2066	0.46	0.95	2.49
1994	-0.19	-0.19	-0.19	2067	0.47	0.97	2.56
1995	-0.18	-0.18	-0.18	2068	0.48	0.99	2.62
1996	-0.17	-0.17	-0.17	2069	0.49	1.02	2.69
1997	-0.17	-0.16	-0.16	2070	0.5	1.04	2.75
1998	-0.16	-0.15	-0.14	2071	0.51	1.06	2.82
1999	-0.15	-0.14	-0.13	2072	0.52	1.09	2.89
2000	-0.14	-0.13	-0.11	2073	0.53	1.11	2.96
2001	-0.13	-0.12	-0.1	2074	0.54	1.13	3.03
2002	-0.12	-0.11	-0.08	2075	0.54	1.16	3.1
2003	-0.11	-0.1	-0.07	2076	0.55	1.18	3.17
2004	-0.1	-0.09	-0.05	2077	0.56	1.21	3.24
2005	-0.09	-0.08	-0.03	2078	0.57	1.23	3.31
2006	-0.08	-0.07	-0.01	2079	0.58	1.25	3.39
2007	-0.07	-0.05	0.01	2080	0.59	1.28	3.46
2008	-0.07	-0.04	0.03	2081	0.6	1.3	3.54
2009	-0.06	-0.03	0.05	2082	0.61	1.33	3.61
2010	-0.05	-0.02	0.07	2083	0.62	1.35	3.69
2011	-0.04	-0.01	0.1	2084	0.63	1.38	3.76
2012	-0.03	0.01	0.12	2085	0.64	1.4	3.84
2013	-0.02	0.02	0.14	2086	0.64	1.43	3.92
2014	-0.01	0.03	0.17	2087	0.65	1.46	4
2015	0	0.05	0.2	2088	0.66	1.48	4.08
2016	0.01	0.06	0.22	2089	0.67	1.51	4.16
2017	0.02	0.07	0.25	2090	0.68	1.54	4.24
2018	0.03	0.09	0.28	2091	0.69	1.56	4.32
2019	0.04	0.1	0.31	2092	0.7	1.59	4.41
2020	0.04	0.11	0.34	2093	0.71	1.62	4.49
2021	0.05	0.13	0.37	2094	0.72	1.64	4.57
2022	0.06	0.14	0.4	2095	0.73	1.67	4.66
2023	0.07	0.16	0.43	2096	0.74	1.7	4.75
2024	0.08	0.17	0.46	2097	0.74	1.72	4.83
2025	0.09	0.19	0.49	2098	0.75	1.75	4.92
2026	0.1	0.2	0.53	2099	0.76	1.78	5.01
2027	0.11	0.22	0.56	2100	0.77	1.81	5.1
2028	0.12	0.23	0.6	2101	0.78	1.84	5.19
2029	0.13	0.25	0.63	2102	0.79	1.87	5.28
2030	0.14	0.26	0.67	2103	0.8	1.89	5.37
2031	0.14	0.28	0.71	2104	0.81	1.92	5.46
2032	0.15	0.3	0.75	2105	0.82	1.95	5.55
2033	0.16	0.31	0.79	2106	0.83	1.98	5.64
2034	0.17	0.33	0.83	2107	0.84	2.01	5.74
2035	0.18	0.35	0.87	2108	0.84	2.04	5.83
2036	0.19	0.36	0.91	2109	0.85	2.07	5.93
2037	0.2	0.38	0.95	2110	0.86	2.1	6.02
2038	0.21	0.4	0.99	2111	0.87	2.13	6.12
2039	0.22	0.41	1.04	2112	0.88	2.16	6.22
2040	0.23	0.43	1.08	2113	0.89	2.19	6.32
2041	0.24	0.45	1.13	2114	0.9	2.22	6.42
2042	0.24	0.47	1.17	2115	0.91	2.25	6.52
2043	0.25	0.49	1.22	2116	0.92	2.28	6.62
2044	0.26	0.5	1.26	2117	0.93	2.32	6.72
2045	0.27	0.52	1.31	2118	0.94	2.35	6.82
2046	0.28	0.54	1.36	2119	0.94	2.38	6.92
2047	0.29	0.56	1.41	2120	0.95	2.41	7.03
2048	0.3	0.58	1.46	2121	0.96	2.44	7.13
2049	0.31	0.6	1.51	2122	0.97	2.47	7.24
2050	0.32	0.62	1.56	2123	0.98	2.51	7.34
2051	0.33	0.64	1.62	2124	0.99	2.54	7.45
2052	0.34	0.66	1.67	2125	1	2.57	7.56
2053	0.34	0.68	1.72	2126	1.01	2.6	7.67
2054	0.35	0.7	1.78	2127	1.02	2.64	7.77
2055	0.36	0.72	1.83	2128	1.03	2.67	7.88
2056	0.37	0.74	1.89	2129	1.03	2.7	7.99
2057	0.38	0.76	1.95	2130	1.04	2.74	8.1
2058	0.39	0.78	2.01	2131	1.05	2.77	8.22
2059	0.4	0.8	2.06	2132	1.06	2.81	8.33
2060	0.41	0.82	2.12	2133	1.07	2.84	8.44
2061	0.42	0.84	2.18	2134	1.08	2.87	8.56
2062	0.43	0.86	2.24	2135	1.09	2.91	8.67
2063	0.44	0.88	2.3	2136	1.1	2.94	8.79
2064	0.44	0.91	2.37	2137	1.11	2.98	8.9
				2138	1.12	3.01	9.02



HDCI

8531680 Sandy Hook, NJ

NOAA's 2006 Published Rate: 0.01280 feet/yr

All values are expressed in feet relative to NAVD88

Year	USACE Low	USACE Int	USACE High	Year	USACE Low	USACE Int	USACE High
1992	-0.24	-0.24	-0.24	2065	0.69	1.17	2.67
1993	-0.23	-0.23	-0.23	2066	0.71	1.19	2.74
1994	-0.21	-0.21	-0.21	2067	0.72	1.22	2.81
1995	-0.2	-0.2	-0.2	2068	0.73	1.25	2.87
1996	-0.19	-0.19	-0.18	2069	0.75	1.27	2.94
1997	-0.18	-0.17	-0.17	2070	0.76	1.3	3.01
1998	-0.16	-0.16	-0.15	2071	0.77	1.33	3.09
1999	-0.15	-0.15	-0.13	2072	0.78	1.35	3.16
2000	-0.14	-0.13	-0.11	2073	0.8	1.38	3.23
2001	-0.13	-0.12	-0.1	2074	0.81	1.41	3.3
2002	-0.11	-0.1	-0.08	2075	0.82	1.44	3.38
2003	-0.1	-0.09	-0.05	2076	0.84	1.46	3.45
2004	-0.09	-0.07	-0.03	2077	0.85	1.49	3.53
2005	-0.07	-0.06	-0.01	2078	0.86	1.52	3.6
2006	-0.06	-0.04	0.01	2079	0.87	1.55	3.68
2007	-0.05	-0.03	0.04	2080	0.89	1.58	3.76
2008	-0.04	-0.01	0.06	2081	0.9	1.6	3.84
2009	-0.02	0	0.09	2082	0.91	1.63	3.92
2010	-0.01	0.02	0.11	2083	0.92	1.66	3.99
2011	0	0.04	0.14	2084	0.94	1.69	4.08
2012	0.02	0.05	0.16	2085	0.95	1.72	4.16
2013	0.03	0.07	0.19	2086	0.96	1.75	4.24
2014	0.04	0.09	0.22	2087	0.98	1.78	4.32
2015	0.05	0.1	0.25	2088	0.99	1.81	4.41
2016	0.07	0.12	0.28	2089	1	1.84	4.49
2017	0.08	0.14	0.31	2090	1.01	1.87	4.57
2018	0.09	0.15	0.34	2091	1.03	1.9	4.66
2019	0.11	0.17	0.38	2092	1.04	1.93	4.75
2020	0.12	0.19	0.41	2093	1.05	1.96	4.83
2021	0.13	0.21	0.44	2094	1.07	1.99	4.92
2022	0.14	0.22	0.48	2095	1.08	2.02	5.01
2023	0.16	0.24	0.51	2096	1.09	2.05	5.1
2024	0.17	0.26	0.55	2097	1.1	2.08	5.19
2025	0.18	0.28	0.59	2098	1.12	2.12	5.28
2026	0.2	0.3	0.62	2099	1.13	2.15	5.37
2027	0.21	0.32	0.66	2100	1.14	2.18	5.47
2028	0.22	0.34	0.7	2101	1.16	2.21	5.56
2029	0.23	0.36	0.74	2102	1.17	2.24	5.65
2030	0.25	0.38	0.78	2103	1.18	2.28	5.75
2031	0.26	0.39	0.82	2104	1.19	2.31	5.84
2032	0.27	0.41	0.87	2105	1.21	2.34	5.94
2033	0.28	0.43	0.91	2106	1.22	2.37	6.04
2034	0.3	0.45	0.95	2107	1.23	2.41	6.13
2035	0.31	0.48	1	2108	1.24	2.44	6.23
2036	0.32	0.5	1.04	2109	1.26	2.47	6.33
2037	0.34	0.52	1.09	2110	1.27	2.51	6.43
2038	0.35	0.54	1.13	2111	1.28	2.54	6.53
2039	0.36	0.56	1.18	2112	1.3	2.58	6.63
2040	0.37	0.58	1.23	2113	1.31	2.61	6.74
2041	0.39	0.6	1.28	2114	1.32	2.64	6.84
2042	0.4	0.62	1.33	2115	1.33	2.68	6.94
2043	0.41	0.64	1.38	2116	1.35	2.71	7.05
2044	0.43	0.67	1.43	2117	1.36	2.75	7.15
2045	0.44	0.69	1.48	2118	1.37	2.78	7.26
2046	0.45	0.71	1.53	2119	1.39	2.82	7.37
2047	0.46	0.73	1.59	2120	1.4	2.86	7.47
2048	0.48	0.76	1.64	2121	1.41	2.89	7.58
2049	0.49	0.78	1.69	2122	1.42	2.93	7.69
2050	0.5	0.8	1.75	2123	1.44	2.96	7.8
2051	0.52	0.82	1.81	2124	1.45	3	7.91
2052	0.53	0.85	1.86	2125	1.46	3.04	8.02
2053	0.54	0.87	1.92	2126	1.48	3.07	8.13
2054	0.55	0.9	1.98	2127	1.49	3.11	8.24
2055	0.57	0.92	2.04	2128	1.5	3.15	8.36
2056	0.58	0.94	2.1	2129	1.51	3.18	8.47
2057	0.59	0.97	2.16	2130	1.53	3.22	8.59
2058	0.6	0.99	2.22	2131	1.54	3.26	8.7
2059	0.62	1.02	2.28	2132	1.55	3.29	8.82
2060	0.63	1.04	2.34	2133	1.56	3.33	8.94
2061	0.64	1.07	2.41	2134	1.58	3.37	9.05
2062	0.66	1.09	2.47	2135	1.59	3.41	9.17
2063	0.67	1.12	2.54	2136	1.6	3.45	9.29
2064	0.68	1.14	2.6	2137	1.62	3.49	9.41
				2138	1.63	3.52	9.53